Structure-activity relationship of pyridinium oximes as therapeutics for organophosphorus nerve agent poisoning

by

Adriana Gambino

B.S. Biochemistry, Rowan University, 2016

Submitted to the Graduate Faculty of the

Dietrich School of Arts and Sciences in partial fulfillment

of the requirements for the degree of

Doctor of Philosophy

University of Pittsburgh

2021

UNIVERSITY OF PITTSBURGH

DIETRICH SCHOOL OF ARTS AND SCIENCES

This dissertation was presented

by

Adriana Gambino

It was defended on

February 18, 2021

and approved by

Peter Wipf, Distinguished University Professor, Department of Chemistry

W. Seth Horne, Associate Professor, Department of Chemistry

George D. Leikauf, Professor, Department of Environmental and Occupational Health

Dissertation Advisor: Kazunori Koide, Professor, Department of Chemistry

Structure-activity relationship of pyridinium oximes as therapeutics for organophosphorus nerve agent poisoning

Adriana Gambino, PhD

University of Pittsburgh, 2021

Organophosphorus nerve agents (OPNAs) are irreversible inhibitors of acetylcholinesterase and pose a threat to both military personnel and civilians. Despite providing limited protection, 2-pralidoxime (2-PAM) is the only United States Food and Drug Administration approved therapeutic for OPNA poisoning. Unfortunately, the spectrum of 2-PAM for a panel of OPNAs is narrow, necessitating further research. Herein, the design, synthesis, and in vitro activity of 2-PAM analogs is presented. Initial efforts used a methyl scan approach to identify ring positions of 2-PAM that could tolerate modification. Subsequently, structure-activity relationship (SAR)-guided molecular docking was used to rationalize feasible binding modes for 2-PAM and the reported methyl scan derivatives. Overall, the data in Section 2.1 provided new insights, e.g., that the 4-position of 2-PAM is tolerant of modifications. This information has proven to be useful in the rational design of new analogs.

In Section 2.2, a synthetic strategy for 4-alkyl and aryl ether and 4-alkyl and aryl sulfide analogs was developed. With these analogs and paraoxon as an OPNA mimic, SAR studies were performed. Through this study, 4-thiophenyl-2-PAM and 4-phenoxy-2-PAM were identified as efficient reactivators of inhibited acetylcholinesterase. Furthermore, the SAR study in Section 2.3 revealed that aryl sulfides were generally more tolerant of additional substituents in comparison to related ether analogs.

The final section of work (Section 2.4) details the design, synthesis, and in vitro evaluation of phenalkyl, phenalkyl ether, and phenethyl phenyl ether analogs. In vitro testing of these analogs revealed that 4-phenethyl-2-PAM was a superior reactivator of acetylcholinesterase inhibited by sarin, cyclosarin, VX, and tabun in comparison to 2-PAM.

Table of contents

Acknowledgements ..... **xv**

1.0 Introduction **1**

1.1 Acetylcholinesterase **1**

1.2 Organophosphorus nerve agents **6**

1.2.1 Organophosphorus pesticides **10**

1.2.2 Mechanism of inhibition **12**

1.3 Current treatments **14**

1.4 Previous studies **18**

1.4.1 Ellman's assay **20**

1.4.2 pK_a studies **22**

1.4.3 Alternative heterocycles **24**

1.4.4 Bispyridinium analogs **25**

1.4.5 *N*-alkyl analogs **26**

2.0 Results and discussion **30**

2.1 Methyl scan **30**

2.1.1 Synthesis **31**

2.1.2 In vitro reactivation **33**

2.1.3 Molecular modeling of methyl scan analogs **38**

2.1.4 Conclusions **41**

2.2 Ether and sulfide analogs **41**

2.2.1 Synthesis **42**

2.2.2 In vitro reactivation 46

2.2.3 Conclusions 53

2.3 Structure-activity relationship study of ADG3002 and ADG3003 54

2.3.1 Results 55

2.3.2 Conclusions 76

2.4 Aryl analogs 78

2.4.1 Results 78

2.4.2 Conclusions 98

3.0 Concluding remarks 99

Appendix A Supporting information 102

Appendix A.1 Assay experimental 102

Appendix A.2 Computational methods 110

Appendix A.3 Chemistry experimental 119

Appendix A.4 NMR spectra 312

Bibliography 702

List of tables

Table 1. Formation of C–O or C–S bonds 44

Table 2. One-pot deprotection and condensation 45

Table 3. *N*-methylation 46

Table 4. Example set up of 96-well plate using in the multi-agent screening assay..... 106

Table 5. Final quantitative HINT scores for active compounds 118

List of figures

Figure 1. Binding gorge of AChE. 2

Figure 2. Mechanism of acetylcholine hydrolysis. 4

Figure 3. Chemical weapons used during World War I. 6

Figure 4. Structures of OPNAs. 7

Figure 5. Novel scaffolds considered as Novichok agents. 8

Figure 6. Historical timeline of global events related to chemical weapons usage. 10

Figure 7. Organophosphorus pesticides. 11

Figure 8. Mechanism of inhibition and aging. 13

Figure 9. Structures of clinically used treatments. 15

Figure 10. Proposed mechanisms of oximate reactivation of OPNA-inhibited AChE. 17

Figure 11. Structures of compounds from the initial report of 2-PAM.[16] 19

Figure 12. Generic mechanism of Ellman's assay in the context of studying OPNA-inhibited AChE. 21

Figure 13. Analogs published by Renard et al.[77, 80] 23

Figure 14. Fluorinated analogs prepared by Timperley et al.[81] 24

Figure 15. Alternative heterocyclic AChE reactivators. 25

Figure 16. Bisquaternary analogs with xylene linkers. 26

Figure 17. Generic structures of analogs prepared by Kuča et al.[90] 26

Figure 18. Work presented by Chambers et al. 27

Figure 19. Analogs from Ohta et al.[93] 29

Figure 20. C-methylated 2-PAM analogs for the methyl scan study. 31

Figure 21. Reactivation of AChE by methyl scan analogs. 34

Figure 22. Reactivation of OPNA-inhibited *h*AChE 36

Figure 23. Inhibition data for C-methylated 2-PAM analogs at 12 min. 37

Figure 24. a) absorbance spectrum of 38 μM 4-Me-2-PAM in 100 mM phosphate pH 7.4 buffer. b) absorbance of varying concentrations of 4-Me-2-PAM at 290 nm. 38

Figure 25. The binding mode of 2-PAM and its methyl scan derivatives. 40

Figure 26. In vitro reactivation of *Ee*AChE inhibited with 2% v/v paraoxon in isopropanol by akyl ether and sulfide analogs. 48

Figure 27. Inhibition of *Ee*AChE by 600 μM oxime at 9 min. 49

Figure 28. In vitro reactivation of *Ee*AChE inhibited with 2% v/v paraoxon in isopropanol by by ADG3003 and ADG3002. 50

Figure 29. Inhibition of *Ee*AChE by 600 μM ADG3003 or ADG3002 at 9 min. 50

Figure 30. Reactivation of OPNA-inhibited *h*AChE using 52

Figure 31. X-ray structures. 53

Figure 32. In vitro activity of ADG3230. 57

Figure 33. In vitro reactivation of *Ee*AChE inhibited with 2% v/v paraoxon in isopropanol by fluoro-substituted analogs. 63

Figure 34. Inhibition of *Ee*AChE by 600 μM fluoro-substituted analogs at 9 min. 64

Figure 35. In vitro reactivation of *Ee*AChE inhibited with 2% v/v paraoxon in isopropanol by methyl-substituted analogs. 65

Figure 36. Inhibition of *Ee*AChE by 600 μM methyl-substituted analogs at 9 min. 66

Figure 37. In vitro reactivation of *Ee*AChE inhibited with 2% v/v paraoxon in isopropanol by methoxy-substituted analogs 68

Figure 38. Inhibition of *Ee*AChE by 600 μM methoxy-substituted analogs at 9 min. 69

Figure 39. In vitro reactivation of *Ee*AChE inhibited with 2% v/v paraoxon by isopropoxyphenyl ether-, diphenoxy-, and napthyl-substituted analogs. 74

Figure 40. Inhibition of *Ee*AChE by 600 μM isopropoxyphenyl ether-, diphenoxy-, and napthyl-substituted analogs at 9 min. 75

Figure 41. Passive permeability as determined by PAMPA assay 76

Figure 42. Summary of in vitro reactivation of paraoxon-inhibited *Ee*AChE by aryl ether and aryl sulfide analogs. 77

Figure 43. In vitro activity of ADG2173 and ADG2180. 80

Figure 44. Reactivation of OPNA-inhibited *h*AChE. 82

Figure 45. In vitro of *Ee*AChE inhibited with 2% v/v paraoxon in isopropanol by ADG4063 and ADG4111. 88

Figure 46. Inhibition of *Ee*AChE by ADG4063 or ADG4111 at 9 min. 88

Figure 47. In vitro reactivation of *Ee*AChE inhibited with 2% v/v paraoxon by phenalkyl and phenalkyl ether analogs. 93

Figure 48. Inhibition of *Ee*AChE by phenalkyl or phenalkyl ether analgos at 9 min. 94

Figure 49. In vitro reactivation of *Ee*AChE inhibited with 2% v/v paraoxon in isopropanol by phenethyl phenoxy analogs. 97

Figure 50. Inhibition of *Ee*AChE by phenethyl phenoxy analogs at 9 min. 98

Figure 51. Electrostatic surface potential maps for 2-PAM, 3-Me-2-PAM, 4-Me-2-PAM, 5-Me-2-PAM, and 6-Me-2-PAM. 111

Figure 52. The binding mode of 2-PAM taken directly from PDB entry code 5HFA102.. 112

Figure 53. Alignment of the X-ray co-crystal structures..... 115

Figure 54. Superimpositions of the highest available resolution apo-state X-ray structures of AChE from phylum *Chordata* species. 116

List of schemes

Scheme 1. Synthesis of C-methylated 2-PAM analogs. 32

Scheme 2. Synthesis of acetal 2-4. 43

Scheme 3. Synthesis of 3-5. 55

Scheme 4. Failed synthesis of 3-7. 56

Scheme 5. Synthesis of ADG3230. 56

Scheme 6. Failed synthesis of sulfoxide and sulfone analogs. 58

Scheme 7. Synthesis of fluoro-substituted analogs. 59

Scheme 8. Synthesis of methyl-substituted analogs. 60

Scheme 9. Synthesis of methoxy-substituted analogs. 61

Scheme 10. Synthesis of isopropoxy-substituted analogs. 70

Scheme 11. Synthesis of diphenoxy- and naphthyl-substituted analogs. 71

Scheme 12. Synthesis of ADG2173 and ADG2180. 79

Scheme 13. Failed synthesis of 4-8. 83

Scheme 14. Synthetic route for amido analog. 84

Scheme 15. Synthesis of ADG4063. 85

Scheme 16. Synthesis of 4-19. 86

Scheme 17. Synthesis of ADG4111. 87

Scheme 18. Synthesis of phenalkyl analogs. 90

Scheme 19. Synthesis of phenalkyl ether analogs. 91

Scheme 20. Synthesis of phenethyl phenoxy analogs. 96

List of equations

Equation 1..... 109

Equation 2..... 109

Acknowledgements

First and foremost, I thank God for His graces and blessings, especially the opportunity and character traits needed to complete a PhD. Secondly, I would like to thank my parents. My mom answered hundreds of panicked phone calls and provided never-ending, unwavering support and comforting words to ease all of my worries. My dad, the very reason I pursued a PhD in chemistry. Your memory and perseverance has served as an essential driving force throughout this process. I know you would be overjoyed to share this moment in my life. To the rest of my family and friends, especially my grandmother, brother, godmother, and best friend, your love and support has always been special to me, and I appreciate every one of you.

Of course, I must thank my PhD advisor, Prof. Kazunori Koide for accepting me into his laboratory, and thereafter trusting me with a new research project and the resources and freedom to pursue my own ideas. I would also like to thank Prof. Peter Wipf and Prof. W. Seth Horne for agreeing to be on my dissertation committee. Prof. George Leikauf is also gratefully acknowledged for agreeing to be my external committee member. I thank all of my committee members for being generous with their time and graciously providing advice and feedback on several occasions. I would be remiss if I did not acknowledge several collaborators. Namely, Dr. James Burnett for the molecular modeling work presented herein and the researchers evaluating the in vitro and in vivo activity of my analogs (United States Medical Research Institute of Chemical Defense and the members of the Leikauf group, respectively). The Defense Threat Reduction Agency and Southwest Research Institute are acknowledged for their financial support.

All of the past and current members of the Koide group are deserving of recognition. Specifically, I would like to acknowledge Dr. Wei Chuen Chan for years of continued mentorship

and friendship, long talks, and for making the lab an enjoyable place to be. I would not have wanted to sit next to anyone else! Dr. Robert Bressin and Dr. Dianne Pham are also recognized for their contributions to my training and the progression of my research. I would like to thank Ivanna Pohorilets, Jacob Beard, and Miho Naruse for reading the early draft of my dissertation. Additionally, I am grateful for the scientific discussions and friendships that I have shared with many past and present members of the Koide group and Department of Chemistry. Truly a source of light and very much appreciated.

My research progress would not have been possible without the NMR, MS, and X-ray crystallography directors (Dr. Damodaran Achary, Dr. Bhaskar Godugu, and Dr. Steve Geib, respectively). I wholeheartedly value the efforts required to maintain and provide these essential resources. Furthermore, I would like to thank all of the administrative and other staff members that made life easier and/or enriching and for maintaining a safe and clean work environment throughout the past five years, but especially during the last few months and the pandemic.

Despite four paragraphs of acknowledgement, it is likely that I am regretfully forgetting at least one person. I would like for it to be known that I could not have done this alone and I am grateful beyond words for the many people that have been a part of this chapter of my life.

1.0 Introduction

1.1 Acetylcholinesterase

Acetylcholine (ACh) is a cationic neurotransmitter that plays an essential role within the central and peripheral nervous systems.[1, 2] Once released from the presynaptic neuron, ACh binds to cholinergic receptors to transmit muscle contraction signals across nerve-nerve and neuromuscular synapses.[3] Given that ACh is one of the most abundant neurotransmitters in the human body, regulation of its release is vital for nervous system function.[1] Abnormalities in ACh transmission has been linked to various pathological conditions.[1] Acetylcholinesterase (AChE), a membrane-bound enzyme,[4] is responsible for the hydrolysis of ACh. The hydrolysis terminates neurotransmission and is essential for maintenance of homeostatic conditions within the cholinergic system.[4-6] For reviews on ACh and AChE, see Prado et al.[1] and Quinn[4] and/or Sussman et al.[7] respectively.

Early studies focused on hydrolytic power, isolation, and purification of AChE from members of the *Torpedo* genus and *Electrophorus electricus.*[8, 9] Efficient isolation and purification techniques allowed for the first sequence and crystal structure of AChE, isolated from *Torpedo californica* (*Tc*AChE), to be determined.[10, 11] Crystal structures for mouse AChE (*m*AChE) (complexed with snake toxin fasciculin), *Drosophila melanogaster* (*Dm*AChE), and human (*h*AChE) (complexed with snake toxin fasciculin) were published shortly thereafter.[12-14] The first crystal structure of recombinant *h*AChE in its apo state was reported in 2010.[7] Comparison of crystal structures revealed a large degree of sequence homology, especially in the active site, across vertebrate species.

The enzyme has a 20 Å deep gorge, lined with 14 aromatic residues, and contains four domains: an esteratic locus, an anionic locus, a hydrophobic region, and a peripheral anionic site (Figure 1).[4, 15] Esteratic loci are found in cholinesterases; the primary function of this site is to hydrolyze the ester of ACh.[16] In AChE, the esteratic locus is located at the bottom of the binding gorge and holds the active site: a catalytic triad consisting of Ser-203, Glu-334, and His-447 (human numbering). It is generally accepted that the Ser-203 and His-447 residues function as a nucleophilic attacking group and a general acid-base catalyst, respectively, during the hydrolysis of ACh (Figure 2).[17]

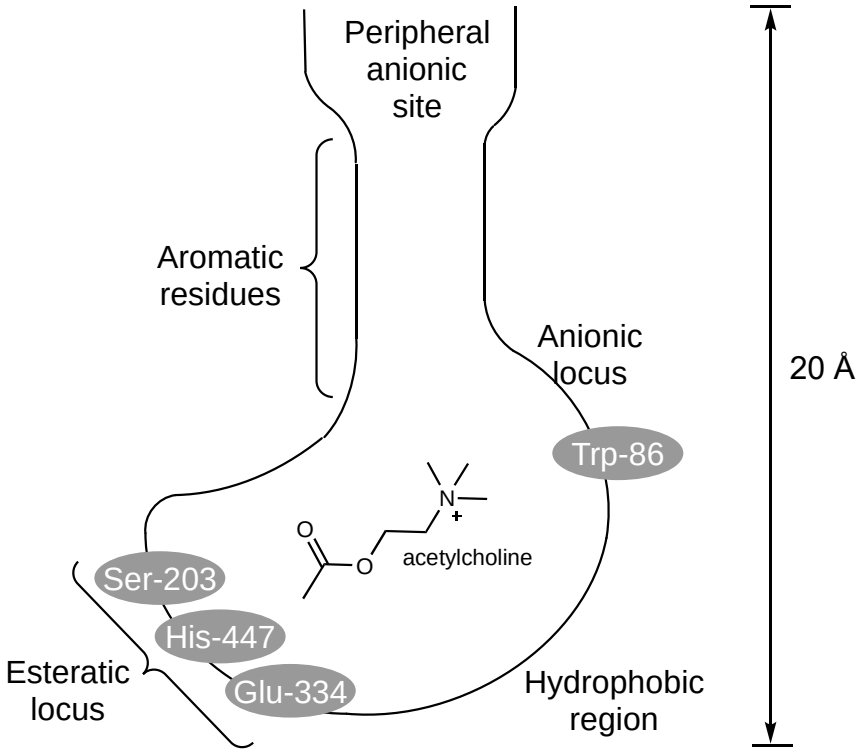

Figure 1. Binding gorge of AChE.

In the first stage of hydrolysis, Ser-203 becomes acetylated.[18] The turnover limiting step of this process is the formation of the enzyme-substrate complex **ES1** (Figure 2)[19] After the

complex forms, Ser-203 attacks the carbonyl carbon of ACh to form the tetrahedral intermediate **TI1**, while the imidazole moiety of the histidine residue functions as a general acid-base catalyst. There are numerous suggested roles of Glu-334 in the literature. It has been suggested that Glu-334 stabilizes the transition state and **TI1** through electrostatic interactions between the carboxylate of Glu-334 and the formed imidazolium cation.[20, 21] The carboxylate of Glu-334 has also been suggested to serve as a general acid-base catalyst, in which it is involved in the proton transfer between Glu-334 and His-447.[22, 23] The third possibility is the "low-barrier hydrogen bond" mechanism. This mechanism involves a the formation of a low-barrier hydrogen bond between the carboxylate of Glu-334 and the imidazolium cation of His-447, which stabilizes **TI1**.[17, 24] It is common for serine proteases to have an oxyanion hole; the oxyanion hole of AChE consists of Gly-121, Gly-122 and Ala-204. The residues of the oxyanion hole stabilize the high-energy intermediate **TI1** through the formation of up to three hydrogen bonds.[24] Unrestrained QM/MM MD simulations show that **TI1** is only stable for a few picoseconds before it collapses to form the acetylated enzyme **EA1** and release choline.[24]

The second stage describes the deacetylation of AChE and involves attack by a surrounding water molecule to generate a second tetrahedral intermediate **TI2**. This intermediate collapses to regenerate the active enzyme.[4, 24] AChE is highly efficient and has a turnover number (k_{cat}) of 10^4 s^{-1}.[4] The k_{cat}/K_M ratio for AChE and ACh is 10^8 s^{-1} M^{-1}, meaning that the catalytic velocity is near the diffusion-controlled limit.[4, 19, 25] Because of this high level of efficiency, AChE is considered

evolutionarily and kinetically perfect.[4] As a result, the intermediates are short-lived and difficult to characterize experimentally.[4, 24, 26]

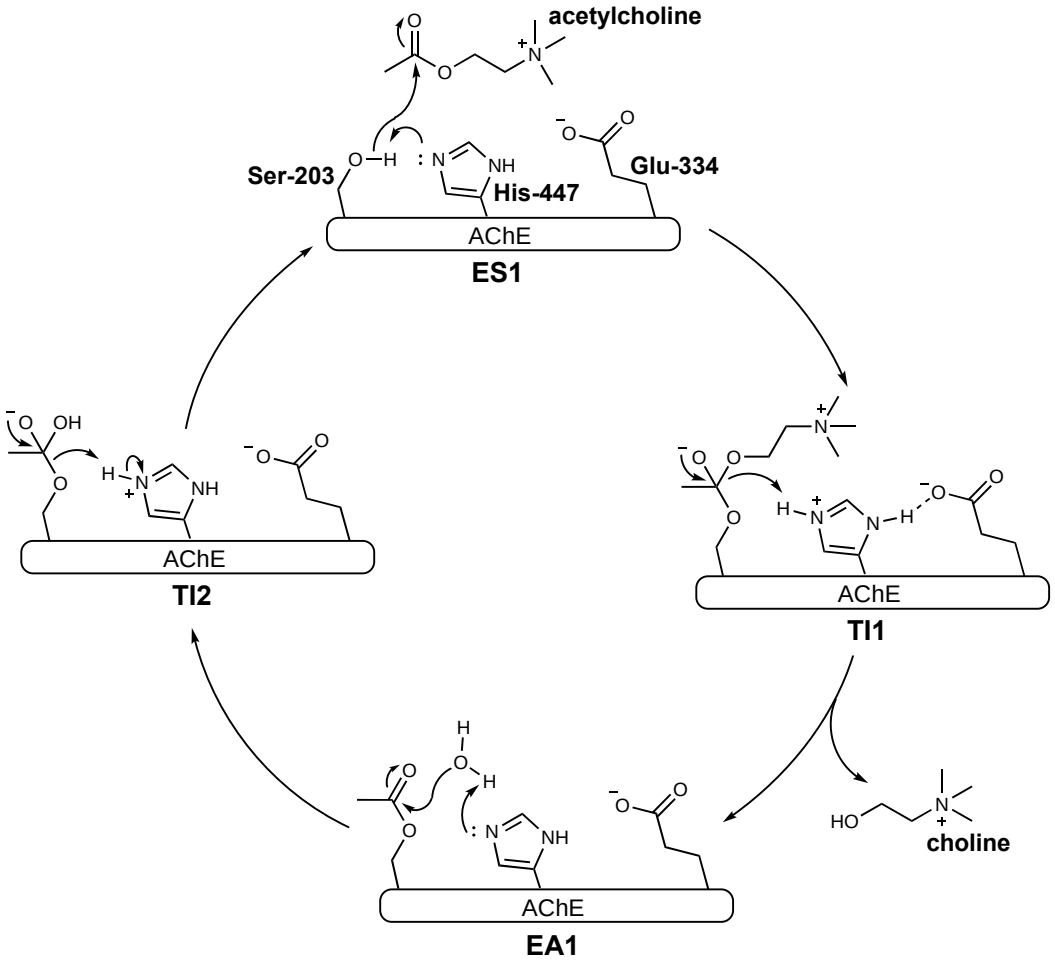

Figure 2. Mechanism of acetylcholine hydrolysis.

Trp-86 is located near the esteratic and anionic loci (Figure 1); this residue is essential for substrate binding.[27-29] Replacement of Trp-86 with Ala or Glu results in at least 100-fold reduction in enzyme activity.[28] Interestingly, cationic substrates are more sensitive to W86A mutations than isosteric substrates lacking the positive charge.[29] The hydrophobic region surrounding the esteratic

and anionic loci also aids in the binding of aryl or alkyl ligands (e.g., aromatic cations and *N*-alkyl quaternary ammonium ligands) (Figure 1).[4]

There is a fourth domain at the entrance of the binding gorge, which is often referred to as the peripheral anionic site (Figure 1). In this region, the peptide sequence contains multiple carboxylate groups, giving rise to the strong anionic character.[30] The negative charge attracts cationic ligands, which may be funneled into the active site, or remain bound to the peripheral anionic site.[31] Ligands binding to the peripheral anionic site can prevent substrates from reaching the active site by physically obstructing the entrance or by causing charge repulsion. Additionally, ligand binding to the peripheral anionic site may induce a conformation change within the active site, preventing normal enzymatic activity.[4, 32] Furthermore, the peripheral anionic site also facilitates heterologous protein association, mediating cell recognition and adhesion processes during synaptogenesis and nucleation of amyloid peptides during the onset of Alzheimer's disease.[33]

Kuča et al. published an extensive comparison of the structure of *h*AChE and AChE from other species by aligning the sequences of published crystal structures. The goal of this study was to classify regions as identical or similar. Amino acids were considered similar if they had the same properties, e.g., acidic, basic, polar, or aromatic. Vertebrate species, i.e., human, mouse, and *Torpedo californica*, were found to have 56% sequence identity, with especially high identity in the active site.[34] When the sequence identity is greater than 40%, approximately 90% of the main-chain atoms are likely to be within a root-mean-square error (RMSE) of about 1 Å.[35] When the RMSE of main-chain atoms was calculated, the values were found to be 1.20 Å, 0.87 Å and 0.57 Å for *Dm*AChE, *m*AChE, and *Tc*AChE, respectively. *m*AChE and *h*AChE were found to have the greatest degree of identity throughout the entire sequence and an active site identity of 100%.[34]

The high identity supports the use of non-human sources of AChE for future studies, especially molecular docking or other types of computational work. The sequence identity for *h*AChE and *Dm*AChE is 28%, which suggests that these two proteins may be folded differently. Additionally, there are some key mutations in the peripheral anionic site of *Dm*AChE; these mutations essentially remove the anionic character of this region.[34]

1.2 Organophosphorus nerve agents

Chemical weapons have been used for centuries and began with arrows, darts, and spears coated with poisons from various organic sources. Modern and large-scale chemical warfare emerged during World War I. Primarily, the use of pulmonary irritants, alkylating agents, and blistering agents, such as phosgene, chlorine gas, and sulfur mustard (Figure 3), led to millions of fatalities.[36]

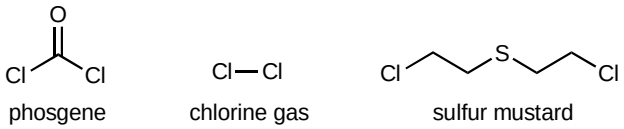

Figure 3. Chemical weapons used during World War I.

In 1941, Adrian et al. discovered that cholinesterases could be inhibited by organophosphorus esters. Simultaneously, Gerhard Schrader was attempting to develop novel pesticides for IG Farben. Synthetic efforts lead to the development of several pentavalent phosphorus compounds (Figure 4a); compounds with this generic structure are collectively referred to as organophosphorus nerve agents (OPNAs). Once the inherent toxicity became apparent, the potential for military usage was immediately reported. The compounds were

produced and stockpiled, but never used during World War II.[36] The volatile liquids that were discovered by Schrader are classified as the G-series (Figure 4b). Both liquid and vapor forms pose a threat to humans. The liquid form is absorbed dermally and can persist on clothing and other surfaces. Inhalation of the vapor leads to rapid absorption by mucous membranes and the lungs.[37]

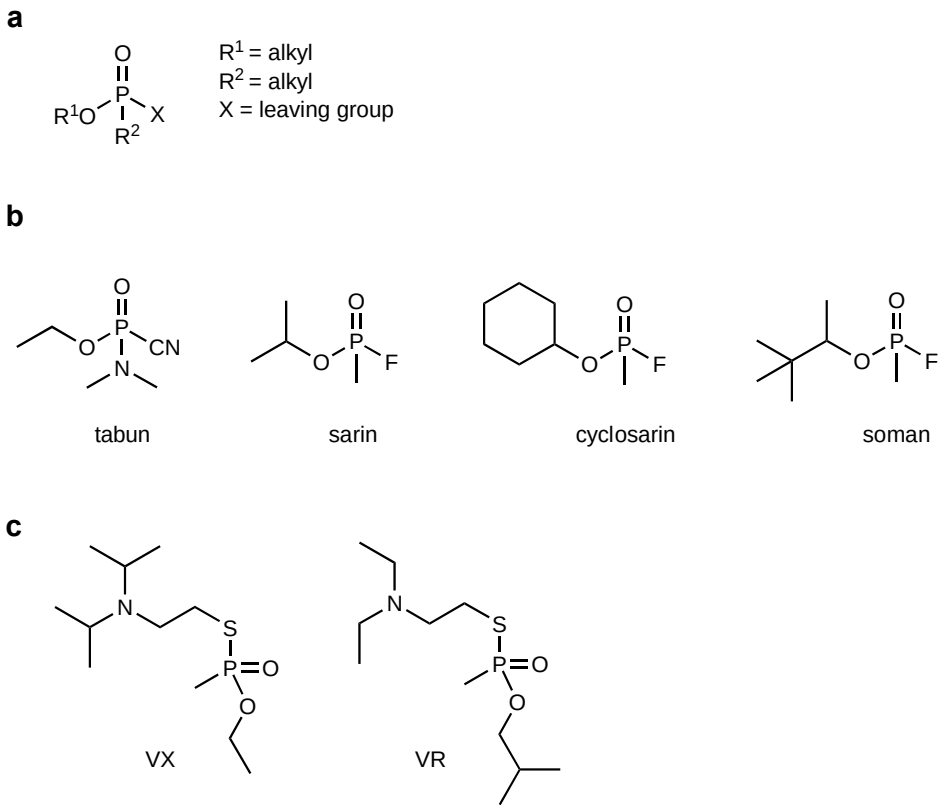

Figure 4. Structures of OPNAs. a) generic structure b) G-series c) V-series.

Structurally similar compounds were synthesized by the former Soviet Union and Great Britain during the 1950s, also while in pursuit of new pesticides. This series is classified as the V-series (Figure 4c). Of important note, these compounds are less volatile, i.e., more persistent, making neutralization efforts more difficult. As a result, these compounds, like sulfur mustard, are considered "area denial weapons" because dispersal of such compounds would prevent enemy

access to a given area. Significant concentrations of VX can last on the ground for 2–6 days; it is estimated that 90% of VX would dissipate from soil after 15 days.[38] For a review on OPNAs see Cavalcante et al.[36]

While the potential hazard of the G- and V-series was globally recognized, the compounds were unable to be classified as Weapons of Mass Destruction and outlawed because they had yet to be used in military conflicts. However, in the 1980s, sarin, tabun, and sulfur mustard were used to target civilians and military personnel during the Iran-Iraq war.[39] In 1993, the first draft of the Chemical Weapons Convention was written as a global effort to prevent future military usage of OPNAs. Before it could be enacted, Japan experienced two terrorist attacks in 1994 and 1995. In these attacks, sarin was responsible for causalities of civilians and first responders. The Chemical Weapons Convention established an international agreement to ban the use of OPNAs as weapons in 1997. The agreement is enforced by the Organization for the Prohibition of Chemical Weapons (OPCW). Despite these diplomatic efforts, multiple OPNAs attacks have occurred since the Chemical Weapons Convention was implemented. These events have involved a spectrum OPNAs and include extensive use during the Syrian civil war and the assassination of Kim Jun Nam.[36] Additionally, a new class of nerve agents, called Novichok agents (Figure 5) have been developed since the establishment of Chemical Weapons Convention.

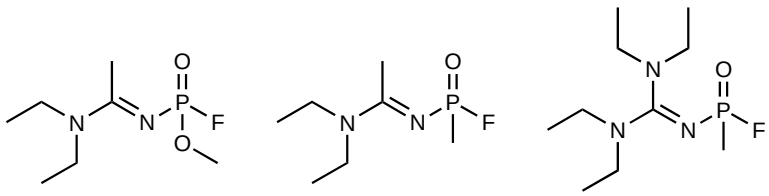

Figure 5. Novel scaffolds considered as Novichok agents.

Novichok agents have enhanced toxicity, despite being solids at room temperature. There remains a bit of mystery surrounding these novel chemical weapons, but generally, they are thought to act similarly to existing OPNAs. Novel scaffolds (Figure 5) will be acknowledged and added as an amendment to the Chemical Weapons Convention as Novichok agents.[36] The prohibition of use will be enforced after June 2020. The historical timeline of global events related to OPNAs is outlined in Figure 6.

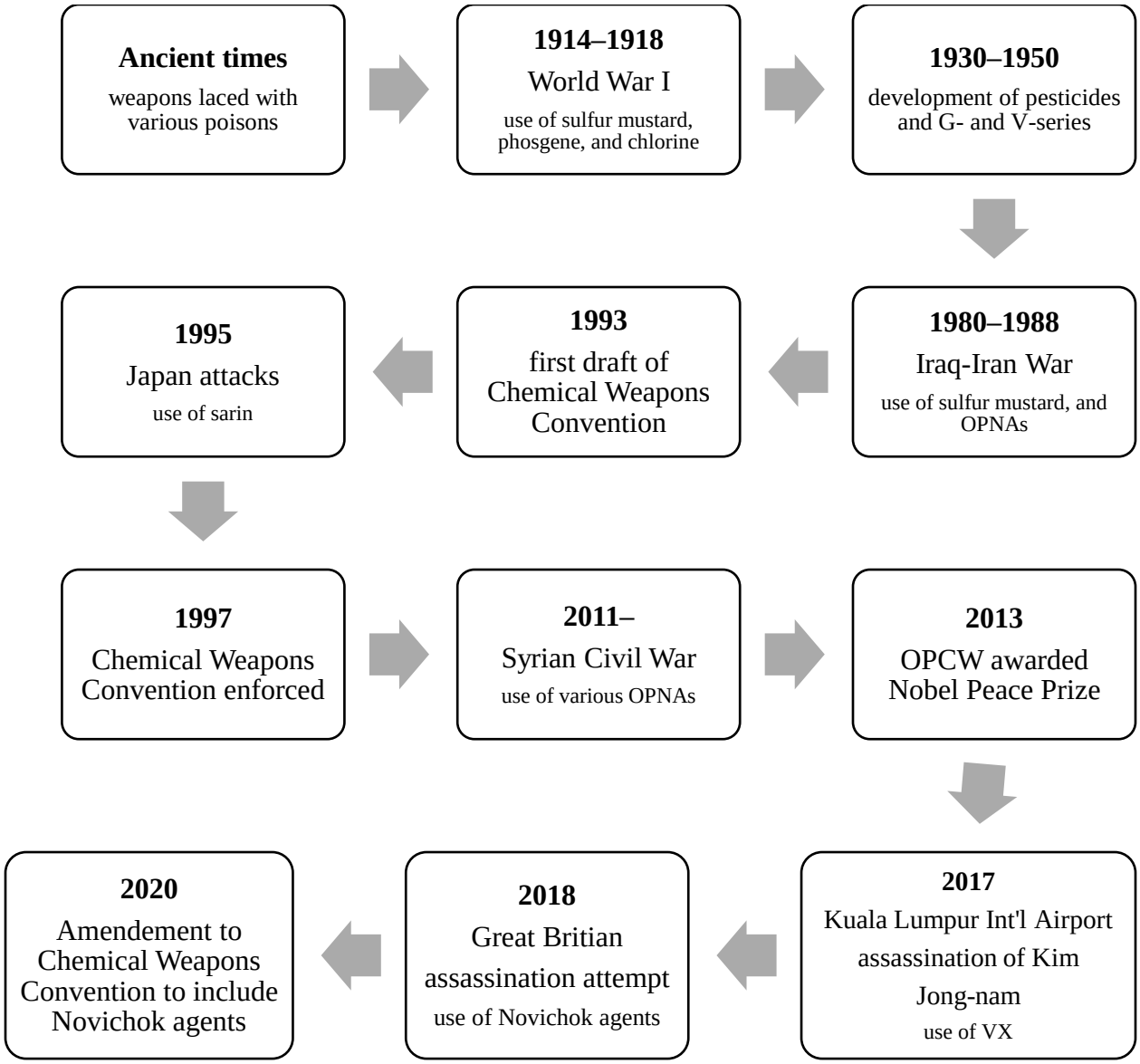

Figure 6. Historical timeline of global events related to chemical weapons usage (adapted from Cavalcante et al.[36]).

1.2.1 Organophosphorus pesticides

The danger and toxicity associated with OPNAs is apparent. However, related compounds have agricultural applications as pesticides. The structures of common organophosphorus pesticides are shown in Figure 7. The intrinsic toxicity of these compounds creates an occupational

hazard for workers.[40] In addition to the G-series, Schrader et al. synthesized parathion and paraoxon, which were used in pesticide industry. The active metabolite of parathion is paraoxon. Structure-activity relationship (SAR) studies on parathion were conducted in effort to increase the selectivity of organophosphorus pesticides for invertebrates, in turn reducing toxicity to mammals. The SAR study resulted in fenthion, clorthion, and fenitrothion. Concurrently, Saunders and Stacey synthesized diisopropyl phosphorofluoridate (DFP) in England. In 1950, American Cyanamide Co. developed malathion, an insecticide with relatively low mammalian toxicity.[41]

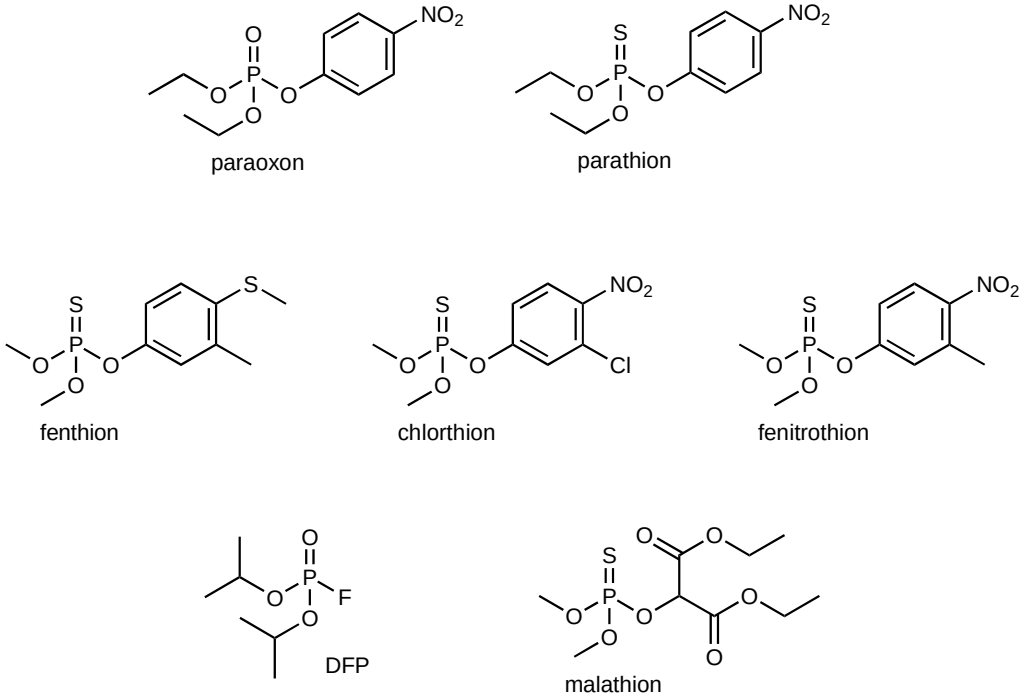

Figure 7. Organophosphorus pesticides.

1.2.2 Mechanism of inhibition

Studying the occurrence, impact, and long-term health effects of OPNAs and organophosphorus pesticides is challenging for epidemiologists because it primarily depends on hospital and poison control center data. This is problematic because occupational pesticide poisonings often has less severe effects and/or occurs in areas where such medical facilities may be inasscessible.[42] Data are also skewed due to a lack of objective evidence and in-depth investigations, which usually do not accurately discriminate between intentional, accidental, or occupational poisonings.[43] However, it is estimated that there are approximately 3 million cases of hospitalization and 220,000 deaths annually worldwide due to organophosphate poisoning, which would broadly include accidental over exposure to pesticides, suicides, and military usage.[40]

Chemical weapons, specifically OPNAs, are some of the most toxic synthetic substances. In small laboratory animals (e.g., rabbits, guinea pigs, and mice), the 24-h subcutaneous LD_{50} for OPNAs range from 10–165 µg/kg,[44] while the inhalation LCt_{50} range from 4–1040 mg-min/m^3.[45, 46] The toxicity is due to the irreversible, covalent inhibition of AChE throughout the central and peripheral nervous system. In 1949, Balls et al. discovered that the toxicity associated with organophosphorus inhibitors is due to the phosphylation of the esteratic site.[41] More specifically, these agents phosphylate the catalytic Ser-203 residue of AChE,[47] thereby blocking the hydrolysis of acetylcholine (Figure 8). Unlike the acetylated enzyme shown in Figure 2, the phosphylated species does not undergo spontaneous hydrolysis.[48] During inhibition, the active site histidine gets shifted into an orientation that blocks a water molecule from attacking the phosphorus atom.[49] As a result, toxic levels of ACh accumulate in the synaptic cleft and overstimulate postsynaptic muscarinic and nicotinic receptors.[50] Overstimulation induces an acute cholinergic crisis, which results in seizures, respiratory arrest, and potentially death.[51]

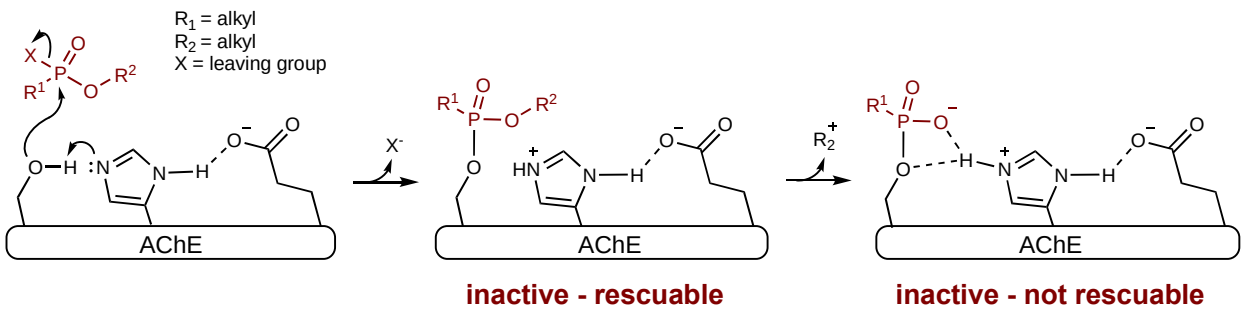

Figure 8. Mechanism of inhibition and aging.

Rescuing of the phosphylated enzyme by nucleophilic small molecule antidotes is possible if medical attention is sought out immediately. However, once the enzyme is inhibited by an OPNA, there is a time-dependent process, known as aging, that may occur. During the aging process, the phosphylated enzyme undergoes dealkylation (Figure 8).[52] There are several proposed mechanisms for this processes.[53-55] The aging half-life varies between OPNAs and ranges from minutes to several hours. Aging results in a truly irreversibly inhibited enzyme. The aged species is extremely stable because it displaces a water molecule and forms a hydrogen bond with neighboring and His-447.[48] The rate of aging is pH dependent, with rates increasing as pH is reduced from 8 to 6.[53] When the imidazolium moiety of His-447 is within hydrogen bond distance of aged-Ser-203, His-447 is also within 4.06 Å of the phenyl group of Phe-338, suggesting that the aged adduct is further stabilized by a cation-π interaction.[53] Additionally, His-447 is also within close proximity (3.15 Å) of the carboxylate of Glu-202.[53] Mutation of Phe-338 and Glu-202 slows the rate of aging.[53] Overall, the protonation of His-447 plays an essential role in aging.[53] Supplementary to stabilizing effects presented above, anionic phosphoesters are inherently resistant to nucleophilic attack, thus, leaving current treatment methods ineffective.[48] Efforts to rescue the aged adduct typically involve selective alkylating agents because alkylation of the anionic phosphoester would remove the formal negative charge, thus allowing for nucleophilic

attack and reactivation of the enzyme.[56-58] Despite these efforts, there is no publicly known compound that is capable of salvaging aged OPNA-inhibited AChE.

1.3 Current treatments

The general treatment strategy for organophosphorus poisoning includes administration of an AChE reactivator (Figure 9a and b) and atropine, a muscarinic receptor antagonist (Figure 9c). Initial treatment plans for humans involved administration of the AChE reactivator in high doses (1000–2000 mg) intravenously or intramuscularly over 30–40 min and 2-mg doses of atropine intravenously every 2–5 min as symptoms persist.[37] However, treatment has become more aggressive and administration methods have advanced. DuoDote ® is a dual-chamber autoinjector containing 2-PAM Cl (600 mg) and atropine (2.1 mg). The autoinjector delivers the combination therapy intramuscularly in seconds and is more convenient and efficient than previous autoinjectors containing 2-PAM Cl or atropine alone. First-responders and military personnel have been advised to administer up to three DuoDote ® injections (1800 mg 2-PAM Cl) before switching to atropine alone to prevent toxicities associated with doses in excess of 2000 mg 2-PAM Cl.[59] While atropine is effective in counteracting muscarinic overstimulation within the central and peripheral nervous system, it has no effect on nicotinic receptors within skeletal muscle and brain tissues.[60] Additionally, oxygen may be administered because well-oxygenated patients tend to experience fewer seizures. In some cases benzodiazepines are administered to further reduce seizing.[37]

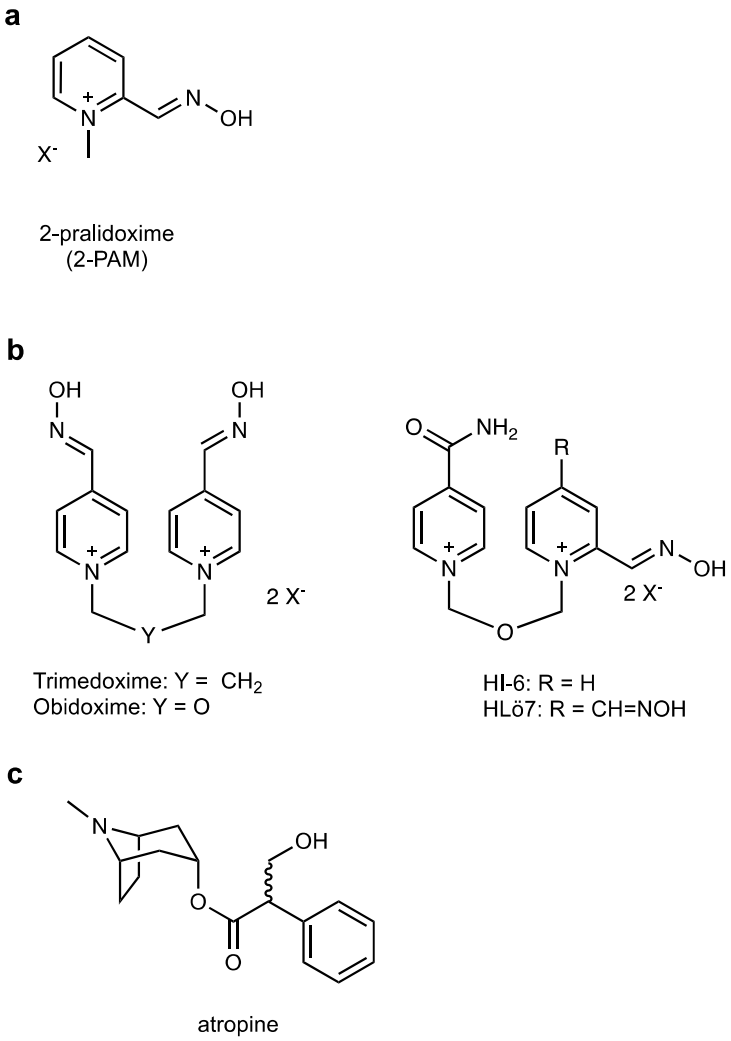

Figure 9. Structures of clinically used treatments. a) 2-PAM, AChE reactivator used in the Unites States b) AChE reactivators used in other countries c) muscarinic receptor antagonist.

The first reactivator of OPNA-inhibited AChE, 2-pralidoxime (2-PAM), was developed by Wilson and Ginsburg in 1955.[16] Today, 2-PAM remains the only antidote approved by the United States Food and Drug Administration for the treatment of OPNA poisoning. Additional antidotes have been developed after the initial discovery of 2-PAM; these subsequent reactivators feature the same pharmacophores, i.e., pyridinium and oxime moieties, as 2-PAM.[3] The positive charge of the pyridinium has been found to be essential for the activity of 2-PAM[16]; further studies

revealed that the pyridinium of clinically used reactivators engage in electrostatic attractions with the peripheral anionic site of AChE and cation-π interactions with Trp-86 near the active site,[61, 62] while also maintaining a reasonable orientation to attack the phosphylated enzyme.[3]

Oximes are α-nucleophiles, which are defined as a nucleophilic center that is adject to an atom with a lone pair of electrons and have nucleophilic reactivity that surpass predictions based on Brønsted basicity. Plausible explanations for the enhanced reactivity include ground-state destabilization of the nucleophile, transition-state stabilization, solvent effect differences in alpha and non-alpha nucleophiles, and thermodynamic product stability (as reviewed by Fina and Edwards).[63] Additionally, Brønsted plots for non-α-nucleophiles are generally linear with slopes ranging between 0.6–0.75 up to pK_a's ≈ 11.[64] The corresponding plots for oximes with $pK_a < 8$ are curved and eventually plateau as reactivity reaches the upper limit.[64] This is notable in the context of reactivators because at physiological pH, the reactivator exists partially as the oximate, which is sufficiently nucleophilic to attack and displace the phosphyl group as shown in Figure 10. The nucleophilic attack liberates the serine residue and restores the catalytic activity of AChE. It remains unclear whether phosphyl displacement occurs through an addition-elimination pathway or via bimolecular nucleophilic substitution.[65-67]

However, the hydrophilicity and positive charge of the current reactivators limit bioavailability and diffusion across the blood-brain barrier (BBB). For example, 2-PAM has a half-life of approximately 77 min; 2-PAM is rapidly excreted by the kidneys unchanged.[68] The prompt excretion may lead to several complications such as the dose being too low to reactivate a sufficient amount of AChE. Furthermore, organophosphorus pesticides and OPNAs may persist in lipophilic compartments throughout the body, leading to delayed inhibition and potentially a secondary crisis.[69] In regard to BBB permeability, it has been reported that only 10% of 2-PAM within the

blood crosses the BBB.[70] As a result, the extent of enzyme reactivation in the central nervous system (CNS) is limited.[60] Additionally, the structure of the inhibited enzyme, i.e., the phosphyl group on Ser-203, varies based on which inhibitor was used; the current antidotes reactivate the inhibited enzyme with a narrow spectrum.[3, 51, 71] Consequently, there remains the need for antidotes with improved pharmacokinetic profiles and BBB permeability, and a broader spectrum for OPNAs.

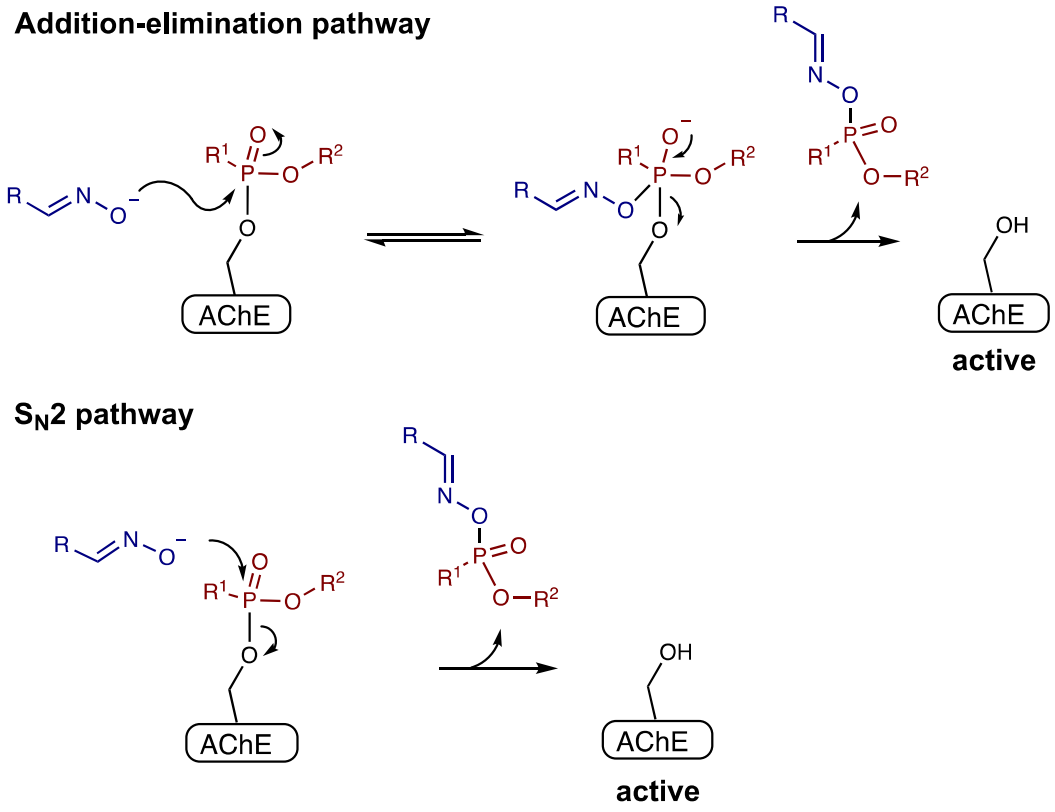

Figure 10. Proposed mechanisms of oximate reactivation of OPNA-inhibited AChE.

1.4 Previous studies

Researchers aim to develop antidotes with improved pharmacokinetic profiles, increased BBB permeability, and/or enhanced reactivity (i.e., development of an antidote that is effective against most, if not all, OPNAs). The brain microvasculature is composed of three cellular elements: endothelial cells, astrocytes end-feet, and pericytes. The endothelial cells of the BBB have extensive tight junctions, which form a diffusion barrier that prevents small molecules, especially ones of hydrophilic nature, from entering the brain. Transporters and receptor-mediated endocytosis allows for nutrients, such as glucose and amino acids, and larger molecules, e.g., insulin and iron transferrin, to enter the brain.[72] Endothelial cells are the primary cell type responsible for controlling permeability properties of the BBB.[73] Astrocyte end-feet and pericytes do not form a significant permeability barrier. However, these cells can modify endothelial cell characteristics and are considered essential components for the normal function and stability of the BBB.[73, 74]

There are several physicochemical properties known to influence passive BBB permeation. Pores, emerging from kinks in the fatty acyl-side chains of the phospholipid bilayer, are responsible for the passive diffusion of small molecules into the brain.[73] Because of the small size of the pores, the molecular weight of CNS targeted drugs is typically below 400 Da.[73, 74] Another generic rule is to limit the extent of hydrogen bonding. Typically, CNS targeted drugs have less than 8–10 total hydrogen bond donors and acceptors. This may facilitate in lowering the polar surface area, which is also commonly thought to improve BBB permeability.[74] Additionally, a large number of rotatable bonds and certain functional groups, e.g., quaternary ammonium and carboxyl groups, have been found to hinder passive diffusion of small molecules into the brain.[73]

Unfortunately, the quaternary ammonium of the currently used antidotes has been considered essential for effectiveness. In the initial report of 2-PAM, Wilson and Ginsburg demonstrate that 2-PAM is a million times more efficient at reactivating inhibited AChE in comparison to the non-methylated 2-pyridine aldoxime and 50,000 times better than picolinohydroxamic acid (Figure 11).[16] The combination of the pyridinium and oxime moieties appear to possesses the perfect balance of cation-π interactions as well as the basicity and nucleophilicity of the oxime to elicit the therapeutic response. This early result established a solid foundation and continues to influence the development of more recent works.

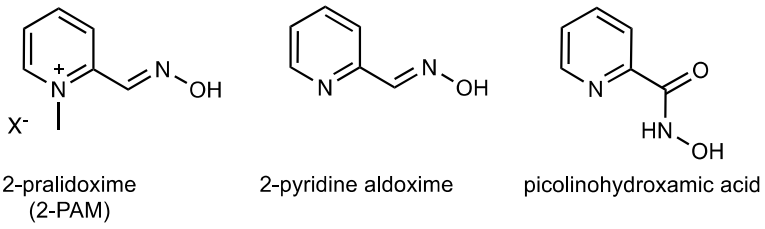

Figure 11. Structures of compounds from the initial report of 2-PAM.[16] 2-PAM was found to be one million and 50,000 more efficient than 2-pyridine aldoxime and picoline hydroxamic acid, respectively.

Although a new antidote has yet to be approved by the United States Food and Drug Administration for clinical use, there has been extensive efforts globally towards developing more efficient reactivators. However, these efforts often focus on dimeric derivatives of 2-PAM and/or involve multiple, simultaneous modifications, which makes it difficult to clearly establish a clear SAR. An additional challenge is deciphering the reported data as there has yet to be a standard method of collecting and reporting the data. This is in part due to the restricted access to OPNAs; some international research groups have access to OPNAs, while they are restricted for use in academic research labs in the United States. Reactivation efficiencies may be reported as relative

reactivation in comparison to 2-PAM or the uninhibited enzyme. Rate constants may be calculated and reported as a measure of efficiency. The enzyme source also varies. Despite the high sequence homology, there is evidence that the catalytic activities and response to OPNAs and/or reactivators may be differ slightly across vertebrate species.[75]

1.4.1 Ellman's assay

Perhaps the closest thing to a standard within the field is the use of some adaptation of a method developed by Ellman et al.[76] This assay is a colorimetric method that can be used to determine the catalytic activity of AChE. The reactivation efficiency can be extrapolated from the enzymatic activity. Minor variations are used and reported in the literature, but the general mechanism of the assay is outlined in Figure 12. In this context, AChE is incubated with an organophosphorus inhibitor. After a short period of time, a reactivator, acetylthiocholine and Ellman's reagent (5,5'-dithiobis-(2-nitrobenzoic acid) (DTNB) are introduced. Ideally the reactivator would react with the phosphylated enzyme and regenerate the functional enzyme. Once the functional enzyme is regenerated, Ser-203 would react with acetylthiocholine to form thiolate **1-1**, which will undergo disulfide exchange with DTNB. This liberates 2-nitro-5-sulfidobenzoate; the absorbance of 2-nitro-5-sulfidobenzoate (highlighted in yellow) can be measured at 405 nm and would reflect the enzyme's catalytic activity. The measured absorbance is then compared to samples containing uninhibited enzyme and/or an approved oxime (see Figure 9a and b) to determine the relative reactivation efficiency of the novel reactivator.

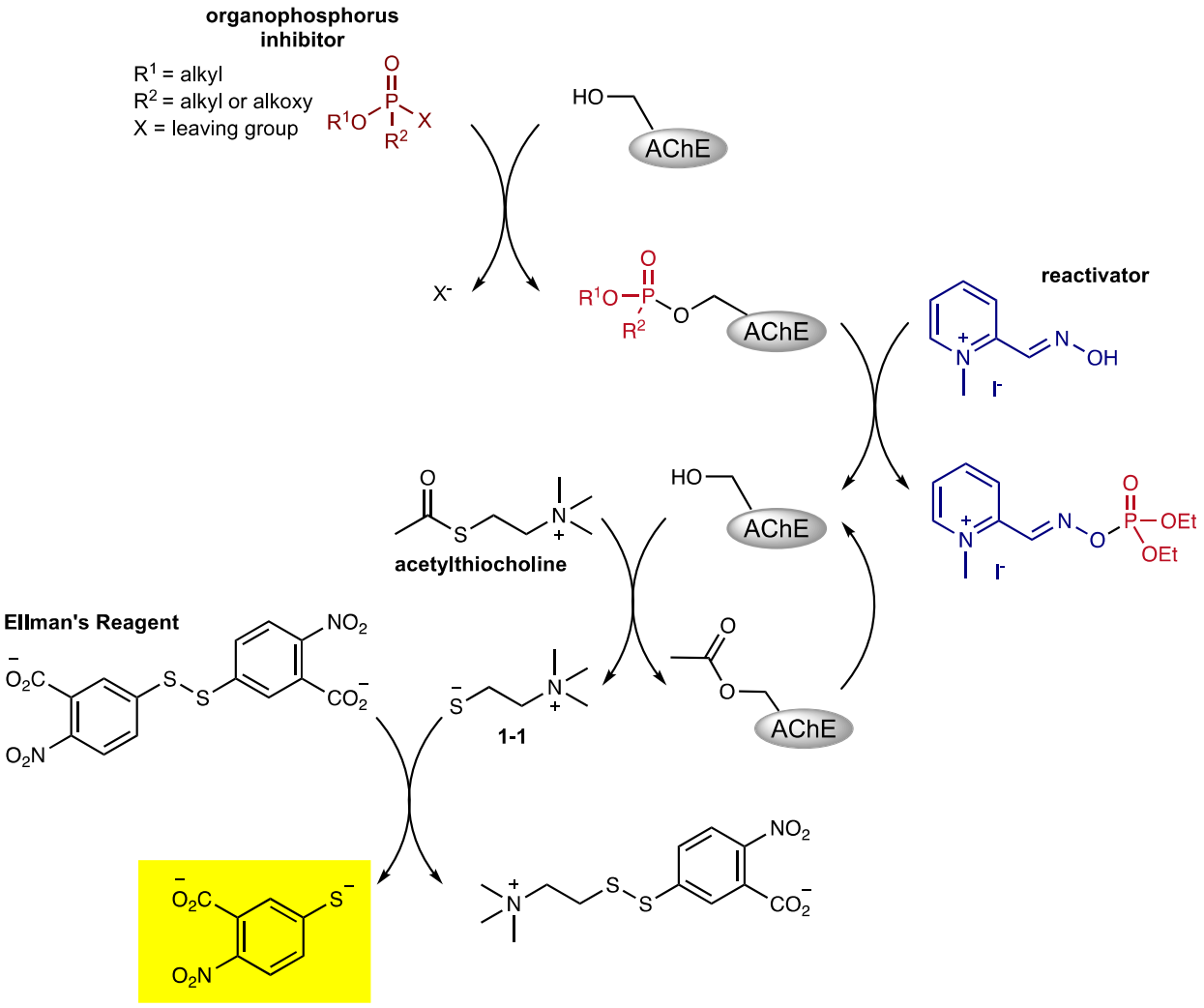

Figure 12. Generic mechanism of Ellman's assay in the context of studying OPNA-inhibited AChE. The inhibitor is incubated with AChE before the solution is added to the reactivator. If the reactivator is active, the P-O bond will be cleaved and AChE will be regenerated and will hydrolyze acetylthiocholine to produce thiolate 1-1. Ellman's reagent and thiolate 1-1 undergo disulfide exchange to yield 2-nitro-5-sulfidobenzoate (highlighted in yellow). The absorbance of 2-nitro-5-sulfidobenzoate is measured and is reflective of enzymatic activity.

1.4.2 pK_a studies

It is essential for new potential antidotes to have a moiety that is sufficiently nucleophilic to react with the inhibited enzyme. As a result, there is an interest in studying the pK_a of the oxime moiety. While the oximate is likely the active species, full deprotonation is undesirable because reactivity would be negatively impacted by the desolvation energy penalty. The pK_a allows the equilibrium concentrations of the active oximate to be calculated, which aids in designing analogs that would not become fully deprotonated at physiological pH. The pK_a values for the reactivators in Figure 9a and b range from 7.3– 8.0.[64] The pK_a of 2-PAM in water is 7.75, while non-methylated 2-pyridine aldoxime is 9.85.[64] As previously mentioned (see Section 1.4, paragraph 3), 2-PAM is a million times more efficient at reactivating inhibited AChE than the non-methylated 2-pyridine aldoxime.[16] However, the difference in reactivation efficiency is likely not solely the consequence of the difference in pK_a. Other contributing factors, e.g., lack of cation-π interactions or inherent differences in nucleophilicities, may also lead to the decrease in reactivation efficiency. There is evidence supporting that non-methylated 2-pyridine aldoxime is sufficiently nucleophilic to hydrolyze OPNA surrogates, albeit in the absence of AChE.[77]

There are several studies that explore alternative methods of lowering the pK_a, i.e., without *N*-alkylation. It is known that intramolecular hydrogen bonding between a hydrogen bond donor, such as a hydroxyl group, and the oxime nitrogen can reduce the pK_a.[78] As a result, several neutral compounds, have been synthesized and tested as reactivators of OPNA-inhibited AChE.[77, 79, 80] Initial efforts from Renard et al. identified a series of uncharged oximes with the ability to reactivate VX-inhibited *h*AChE. The most simple being 3-hydroxy-2-pyridinealdoxime **1-2** (Figure 13), which proved to be more efficient than 2-PAM at reactivating VX-inhibited *h*AChE in vitro. However, **1-2** had a much lower affinity for the inhibited enzyme and had a significantly

higher dissociation constant in comparison.[77] The decrease in affinity is likely due to the lack of cation-π interactions.

Renard et al. published a follow-up study in which **1-2** was modified to have to a peripheral anionic site ligand to circumvent the reduced enzyme binding affinity. In this study, seven novel reactivators were tested. The compounds were found to be 2–10 times more efficient at reactivating VX-inhibited *h*AChE in comparison to 2-PAM, but were less efficient than HI-6 or obidoxime (see Figure 9b). Of note, **1-3** (Figure 13) was equally efficient as 2-PAM at reactivating tabun-inhibited *h*AChE. However, the practicality of this result is questionable because it required incubation with 200 μM of **1-3** for 340 h and only 43% of the enzyme was reactivated.[80]

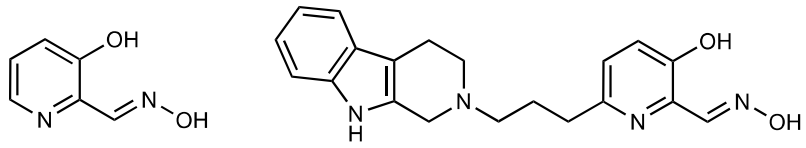

1-2 **1-3**

Figure 13. Analogs published by Renard et al.[77, 80]

Similarly, electron withdrawing groups, such as fluoro substituents, have been added to pyridine aldoximes in effort to lower the pK_a of the oxime so that it is within the optimal range without having a formal positive charge (Figure 14).[81] However, incorporation of a fluorine atom to the 3-position of the pyridine ring, as in **1-5**, only marginally decreased the pK_a of 4-pyridine aldoxime **1-4**. Inclusion of a fluorine atom at the 3-position of the pyridine ring, as in **1-6**, had no effect on the pK_a when the oxime is in the 2-postion. The pK_a of perfluoro-4-pyridine aldoxime **1-7** was 9.1, which remains outside of the optimal range for a reactivator.[81]

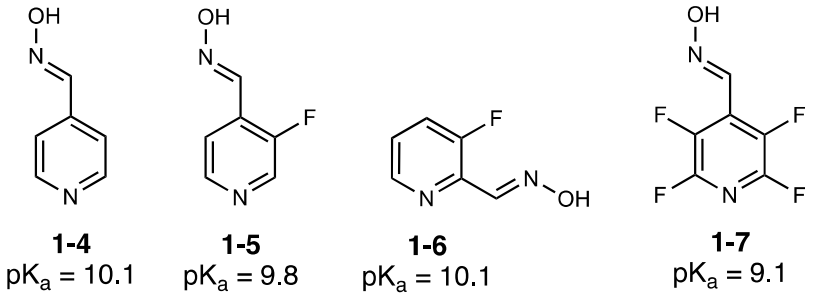

Figure 14. Fluorinated analogs prepared by Timperley et al.[81]

1.4.3 Alternative heterocycles

Several studies have replaced pyridine with other quaternary[82, 83] or non-quaternary[84-87] nitrogen heterocycles (Figure 15). Harris et al. published two studies exploring reactivators with the general imidazolium structure **1-8** (Figure 15a). While several compounds had encouraging in vitro results, there was no correlation between in vitro reactivation efficiency of soman-inhibited *h*AChE and in vivo survival in mice challenged with sublethal doses of soman.[82, 83] Of 134 novel compounds published by Palmer et al, imidazole aldoxime **1-9** (Figure 15b) was the most efficient reactivator of tabun-inhibited *h*AChE. The activity of **1-9** against VX was equivalent to that of 2-PAM. However, **1-9** was less effective than 2-PAM against other inhibitors, such as paraoxon, sarin or cyclosarin. Through this study, **1-10** (Figure 15b) was also identified as an effective reactivator. The conclusion of this work is that the oxime should be positioned further from the motif responsible for AChE recognition and binding; a five- or six-atom linker was the most effective in the reported structures.[87]

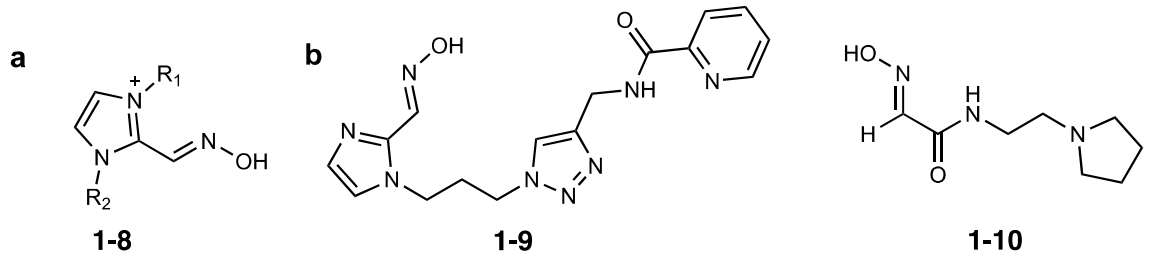

Figure 15. Alternative heterocyclic AChE reactivators. a) the generic structure of reactivators published by Harris et al.[82, 83] R_1 = Me, Et, *n*Pr. R_2 = alkyl chains substituted containing various functional groups, e.g., halo, nitro, sulfonyl, amino, aminosulfonyl. b) lead non-quaternary reactivators published by Palmer et al.[87]

1.4.4 Bispyridinium analogs

Additionally, studies have been conducted to determine the optimal linker for dimeric analogs. The monomeric pyridine subunits are most commonly joined via alkylation of the nitrogen. Xylene (*ortho, meta,* and *para*) linkers have been incorporated in effort to increase the antidotes' associative interactions with the inhibited enzyme (Figure 16).[51, 88] Several bisoxime reactivators were synthesized, but **1-11** (Figure 16a) was the most efficient reactivator of sarin-inhibited *h*AChE in vitro, surpassing 2-PAM and obidoxime.[51] A systematic study of 26 hetero-bispyridinium reactivators, resulted in the development of **1-12** (Figure 16b).[88] A carbamoyl moiety replaced the oxime functional group on one of the pyridinium subunits to decrease toxicity, which has been observed in bisoxime reactivators.[89] **1-12** displayed satisfactory reactivation of sarin-, paraoxon- and DFP-inhibited *h*AChE in vitro. Other analogs of this series yielded promising in vitro results, but were eliminated due to in vivo toxicity.[88]

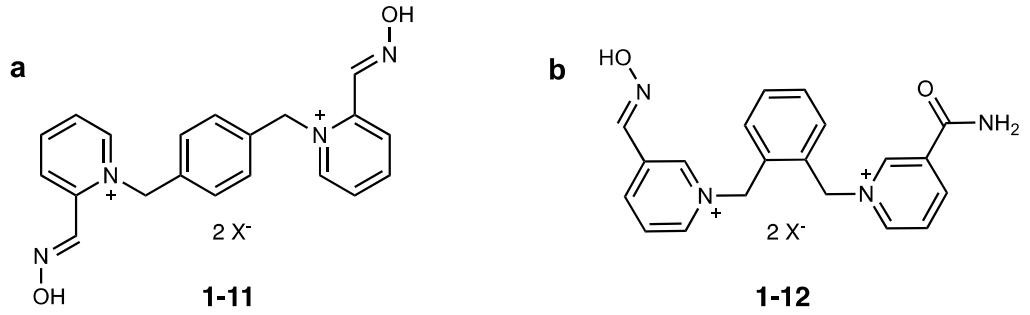

Figure 16. Bisquaternary analogs with xylene linkers a) bisoxime analog b) monooxime analog.

Additional work towards dimeric analogs containing non-aromatic linkers has also been conducted.[90, 91] Kuča et al. studied the length of the methylene bridge and/or changed the chemical structure of the methylene bridge (Figure 17).[90] Additionally, the optimal position of the second oxime group and other functional groups on the second ring were explored. Unfortunately, none of the modifications yielded a reactivator more efficient than trimedoxime (see Figure 9b) at reactivating tabun-inhibited *h*AChE.[90, 91]

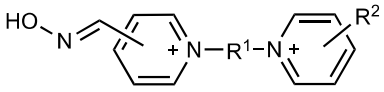

Figure 17. Generic structures of analogs prepared by Kuča et al.[90] $R_1 = (CH_2)_n$ (n = 1–6, 8, 10), alkyl sulfides, alkyl sulfones, alkyl sulfoxides, alkyl ethers, ketones. R_2 = hydrogen, oxime, carbamoyl.

1.4.5 *N*-alkyl analogs

Chambers et al. reported 35 novel oxime reactivators featuring lipophilic groups in effort to increase BBB permeability. The general structure **1-13** of reported reactivators is shown in Figure 18a; lead compound **1-14** and two additional compounds of interest (**1-15** and **1-16**) are also highlighted in Figure 18a. Rat brain homogenate was used as an AChE source. In this study,

phthalimidyl isopropyl methylphosphonate **1-17** and nitrophenyl isopropyl methylphosphonate **1-18** (Figure 18b) were used as sarin surrogates and nitrophenyl ethyl methylphosphonate **1-19** (Figure 18b) was used as a surrogate for VX. The novel oximes had in vitro reactivation efficiencies ranging from 14–76%, while 2-PAM achieved 91% reactivation. The octanol/water partition coefficients were experimentally determined as an index of lipophilicity and ranged from 0.011–2.244, which indicate that the modifications successfully increased lipophilicity because the octanol/water partition coefficient for 2-PAM was only 0.006. When tested in Sprague Dawley-derived rats, three compounds showed 15–25% brain AChE reactivation 30 min post-oxime injection, indicating that these compounds cross the BBB to at least some extent. In comparison, 2-PAM was reported to have 0% brain AChE reactivation.[92]

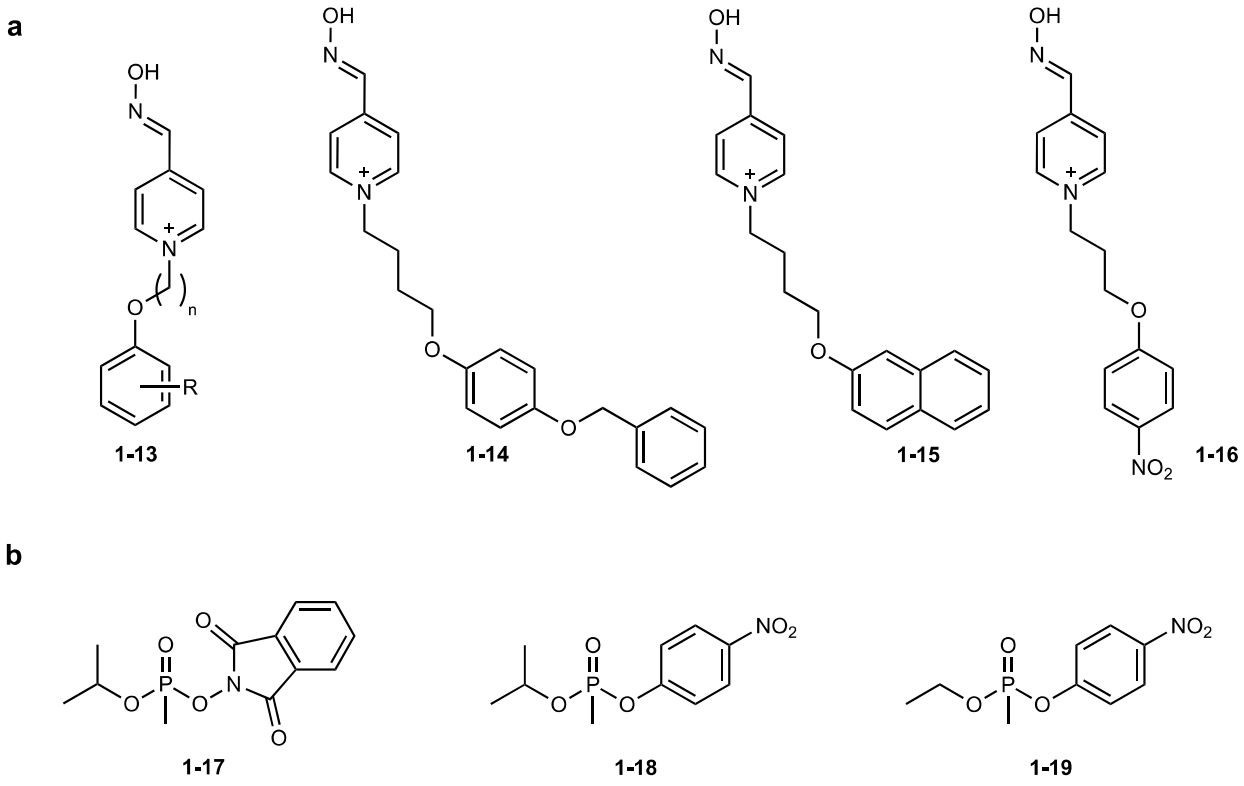

Figure 18. Work presented by Chambers et al. a) synthesized analogs n= 3–6, R = Cl, alkyl, nitro, ethers, ketones, and fused aromatic ring systems. b) OPNA surrogates used.

Some examples of systematic modifications do exist. For example, in 2006 Ohta et al. presented a comprehensive SAR study in which they added an oxime to different positions of the pyridinium ring and altered the length and bulkiness of the alkyl group attached to the pyridinium nitrogen (Figure 19). The results of this study showed that increasing the *N*-alkyl chain length of 2-PAM decreases reactivation efficiency. However, alkyl benzyl analogs of 2-PAM were moderate reactivators. Analogs of 3-pralidoxime showed little or no reactivation, regardless of the *N*-alkyl chain. Lastly, analogs of 4-pralidoxime showed enhanced reactivation efficiency as linear alkyl chain length increases. Benzyl analogs were modest reactivators. It is worth noting that none of the reactivators from this study were more active than 2-PAM.[93]

A follow-up study analyzed the BBB permeability of six analogs. The analogs were selected based on reactivity and lipophilicity. Determination of the LD_{50} of these analogs in Wistar rats ranged from 4.2–21.9 mg/kg. Rats were injected with a dose of 10% of the LD_{50}. After 1 hour, BBB penetration was determined by liquid chromatography-mass spectrometry (LC-MS/MS). The mean BBB penetration of the novel analogs was approximately 30%, while the BBB penetration of 2-PAM was 10%.[70, 94] However, further efforts are required to retain BBB permeability while reducing the toxicities of these compounds.

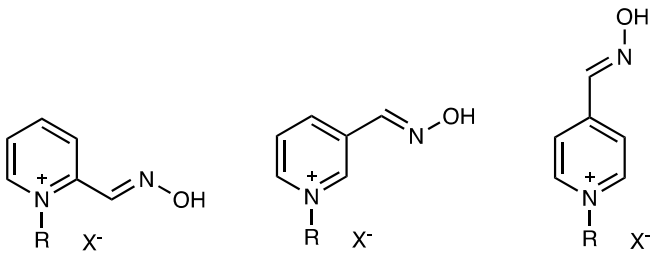

1-20 **1-21** **1-22**

Figure 19. Analogs from Ohta et al.[93] R = ethyl, n-butyl, n-hexyl, n-octyl, n-decyl, n-octadecyl, isoamyl, 2-ethylhexyl, benzyl, p-methylbenzyl, p-tert-butylbenzyl, 2-phenylethyl, 3-phenylpropyl, 4-phenylbutyl. X = Cl, Br, I.

To my knowledge, no studies to date have systematically explored the SAR for alkyl group substitution on the pyridinium ring of 2-PAM, i.e., with the position of the alkyl group being the only variable. This foundational study is the basis for the first section of my work.

2.0 Results and discussion

2.1 Methyl scan

In effort to find the optimal substitution pattern for new analogs, I conducted a methyl scan on the pyridinium ring of 2-PAM. This series of analogs serves two purposes: 1) the systematic addition of methyl groups to the pyridinium ring would directly probe the steric and electrostatic constraints of the AChE binding site, thereby providing a foundation for the rational design of new analogs, and 2) it was hypothesized that if a site on the pyridinium ring could tolerate an alkyl group, this might lead to a new therapeutic candidate that is more hydrophobic, and potentially more BBB permeable than 2-PAM.[95-97]

Methyl scanning involves synthesizing a series of compounds in which a methyl group is systematically added to each modifiable position of a parent structure. This is a viable experimental method to annotate regions of a drug that are important or unimportant for biological activity, affording opportunities for structural modifications to improve potency and/or modify bioavailablilty.[98] Specifically, I hypothesized that synthesizing the analogs shown in Figure 20 and subsequently testing their reactivation efficiencies against paraoxon- or OPNA-inhibited AChE would provide a better understanding of how such reactivators interact with surrounding AChE binding site residues and provide a rational basis future synthetic efforts.

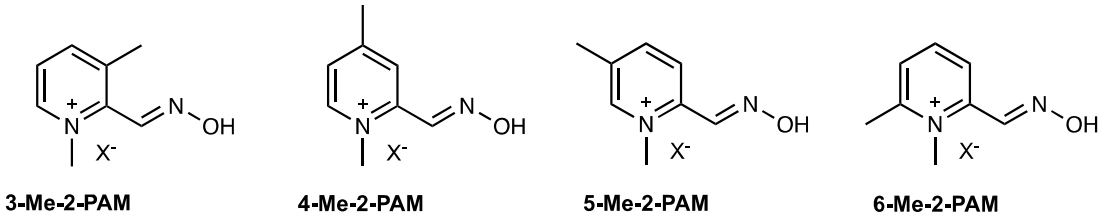

Figure 20. C-methylated 2-PAM analogs for the methyl scan study.

2.1.1 Synthesis

The compounds shown in Figure 20 were synthesized via the routes shown in Scheme 1. The first synthetic step involved the *N*-oxidation of commercially available dimethyl pyridines **1-23a–d** following a method reported by Limnios and Kokotos[99], which provided *N*-oxides **1-24a–d** in 54–69% yields. Subsequently, rearrangement[100] of the *N*-oxides **1-24a–d** afforded the corresponding hydroxymethyl pyridines **1-25a–d** in 40–96% yields. Oxidation of alcohols **1-25a–d** with MnO_2 generated aldehydes **1-26a–d** in 42–77% yields, and the thus formed aldehydes were then condensed with hydroxylamine to form oximes **1-27a–d** in 52–86% yields. Finally, *N*-methylation with MeI provided the final products in 21–77% yields. *N*-Methylation of the 3-, 4- and 5-methyl precursors was facile and went to completion in 15–20 h. The *N*-methylation of the 6-methyl precursor required longer reaction time and required more rigorous purification due to the formation of a side product.

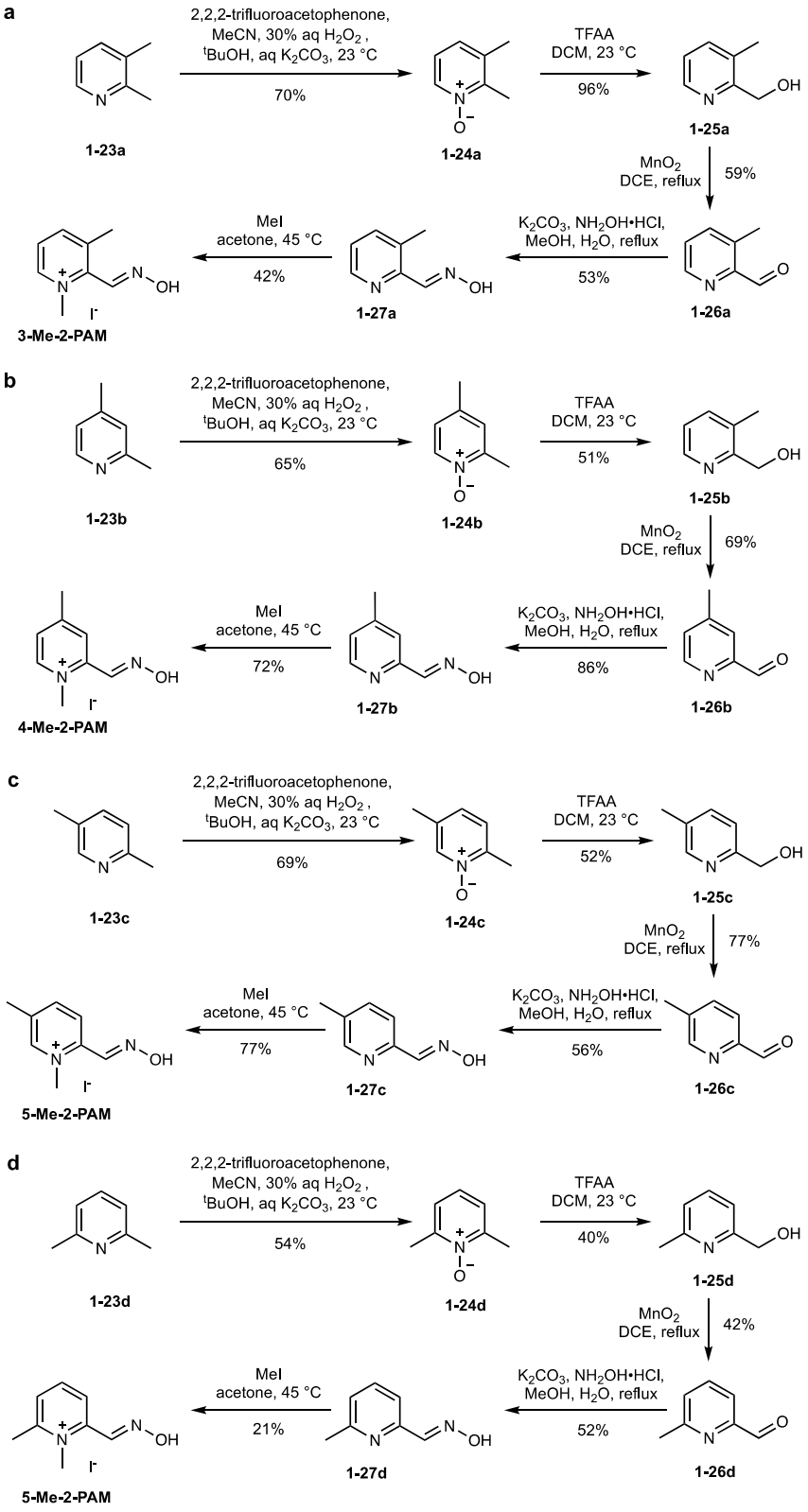

Scheme 1. Synthesis of C-methylated 2-PAM analogs. ^{t}Bu = tertiary butyl, TFAA = trifluoroacetic anhydride, Me = methyl, DCM = dichloromethane, DCE = 1,2-dichloroethane.

2.1.2 In vitro reactivation

With these four 2-PAM analogs in hand, Ellman's assay[76] was employed to determine their reactivation potencies. The enzyme, either *h*AChE or *Electrophorus electricus* AChE (*Ee*AChE), was incubated with paraoxon for 10 min before being added to a clear 96-well plate containing the oximes, Ellman's reagent, and acetylthiocholine. First, dose-dependent reactivation was determined by measuring the absorbance at 405 nm with *h*AChE (Figure 21a). At 18.8 μM, **3-Me-2-PAM** was approximately 13% as efficient as 2-PAM as a reactivator. The relative reactivation efficiencies for **4-Me-2-PAM**, **5-Me-2-PAM**, and **6-Me-2-PAM** were 67%, 34%, and 43%, respectively. When we compared the relative efficiency of reactivation at 75 μM, 3-, 4-, 5-, and **6-Me-2-PAM** were 20%, 85%, 37%, and 62%, respectively. The kinetic data with 18.8 μM oximes are shown in Figure 21b. Linear regression analysis suggests that the relative rates of **3-**, **4-**, **5-**, and **6-Me-2-PAM** (with 2-PAM being 100%) are 11%, 68%, 32%, and 45%, respectively. This is consistent with the above analysis with these oximes at 18.8 μM.

The dose response curve of the methyl scan analogs for *Ee*AChE (Figure 21c) showed that **4-Me-2-PAM** and **6-Me-2-PAM** were nearly equivalent to 2-PAM until approximately 150 μM concentrations. The reactivation efficiency decreased for both analogs at concentrations greater than 150 μM. **5-Me-2-PAM** showed moderate reactivation efficiency, while **3-Me-2-PAM** only slightly reactivated the inhibited enzyme at high concentrations. At 18.8 μM, both **4-Me-2-PAM** and **6-Me-2-PAM** reactivated paraoxon-inhibited *Ee*AChE (Figure 21d) and were found to be nearly equivalent to 2-PAM. Moreover, **5-Me-2-PAM** showed significantly reduced reactivation efficiency, while **3-Me-2-PAM** showed negligible reactivation (Figure 21d). At 18.8 μM, the

relative efficiencies of reactivation for 3-, 4-, 5-, and 6-Me-2-PAM in comparison to 2-PAM were 13%, 90%, 44%, and 87%, respectively.

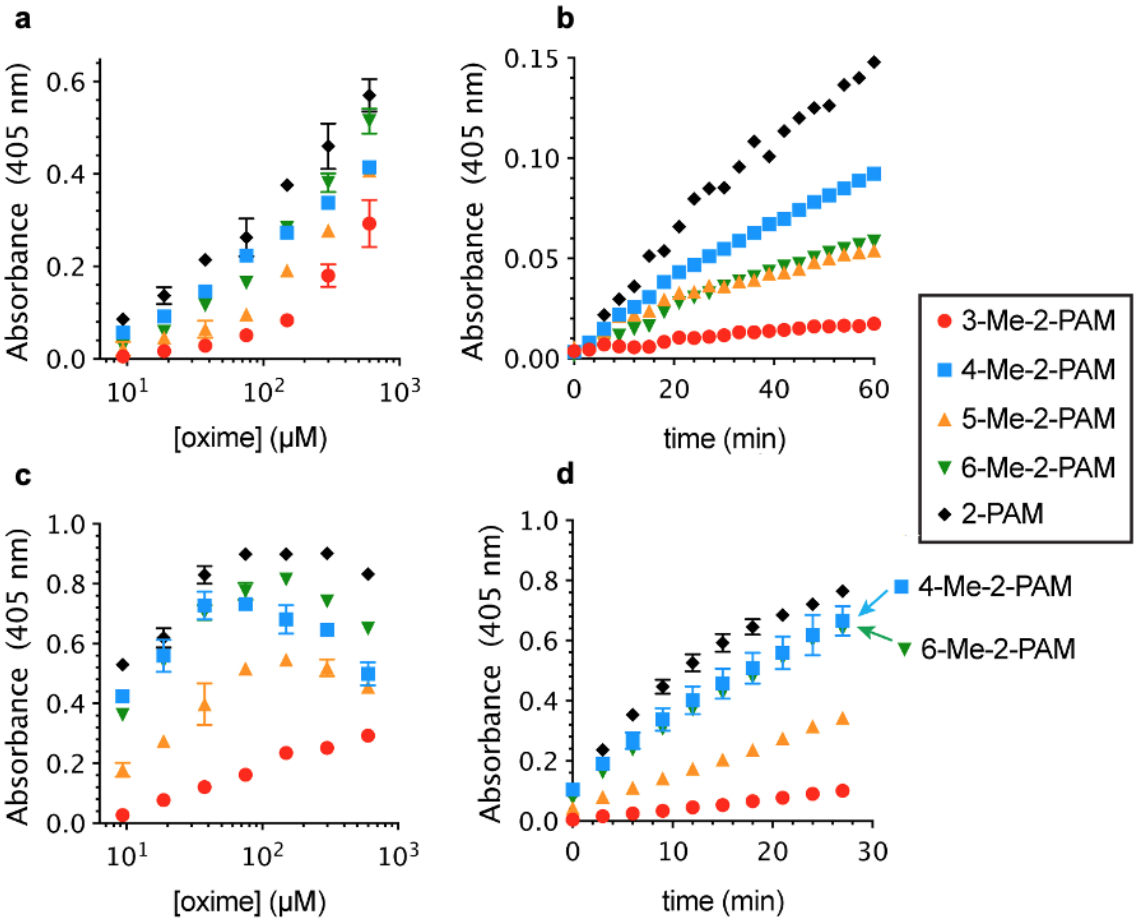

Figure 21. Reactivation of AChE by methyl scan analogs. (a) Dose response curve at 60 min with *h*AChE inhibited by 200 μM paraoxon in isopropanol. (b) 18.8 μM oxime with *h*AChE inhibited by 200 μM paraoxon in isopropanol. (c) Dose response curve at 20 min with *Ee*AChE inhibited 2% v/v paraoxon in isopropanol. (d) 18.8 μM oxime with *Ee*AChE inhibited 2% v/v paraoxon in isopropanol. Data are mean ± SD. n = 3.

Based on the reactivation data obtained, **4-Me-2-PAM** and **5-Me-2-PAM** were selected to be tested at the United States Medical Research Institute of Chemical Defense (USAMRICD) to determine the reactivation efficiencies against OPNAs. In this modified Ellman's assay,

recombinant *h*AChE was incubated with OPNAs for 10 min before excess OPNA was removed. Then, a solution containing either **4-Me-2-PAM** or **5-Me-2-PAM** was added and activity of the inhibited enzyme was measured periodically using acetylthiocholine and Ellman's reagent. Percent reactivation was computed by dividing the slope of the inhibited sample by the slope of the control enzyme.

The assay revealed that after 53 min, 10 μM **4-Me-2-PAM** was equally efficient at reactivating sarin-inhibited *h*AChE as 2-PAM. However, **5-Me-2-PAM** was only 27% as efficient as 2-PAM (Figure 22a). Between **4-Me-2-PAM, 5-Me-2-PAM**, and 2-PAM, there were indistinguishable differences in reactivation efficiencies against cyclosarin-inhibited *h*AChE. The most efficient reactivator of VX- and VR-inhibited *h*AChE was **4-Me-2-PAM**. In contrast, **5-Me-2-PAM** could reactivate approximately 4% of VX- and VR-inhibited *h*AChE, while 2-PAM only reactivated 6% of VX- and VR-inhibited *h*AChE. None of the oximes tested were able to reactivate tabun- or soman-inhibited *h*AChE. However, it is of note that tabun- and soman-inhibited AChE are especially difficult to reactivate for various reasons. A study by Carletti et al. used quantum mechanical computations at the BP86/TZVP level to show that the hybridization of the nitrogen in tabun-inhibited AChE is between sp^2 and sp^3-hybridized,[54] which indicates that the phosphorus atom less susceptible to nucleophilic attack and resistant toward reactivation. Poor reactivity of soman-inhibited AChE is largely because the aging of the inhibited enzyme, an irreversible process that results in an enzyme species that is currently unrescuable, occurs within minutes.[101]

Reactivation using 1000 μM doses (Figure 22b) was also studied. After 53 min, 2-PAM was the most efficient reactivator of sarin-inhibited *h*AChE while **4-Me-2-PAM** and **5-Me-2-PAM** were approximately 60% as efficient as 2-PAM. All three oximes were equally effective against cyclosarin-inhibited *h*AChE. Similarly, reactivation efficiencies of **4-Me-2-PAM, 5-Me-**

2-PAM, and 2-PAM against VX- and VR- inhibited *h*AChE were comparable. Increasing the dose did not result in appreciable reactivation of tabun- or soman-inhibited *h*AChE.

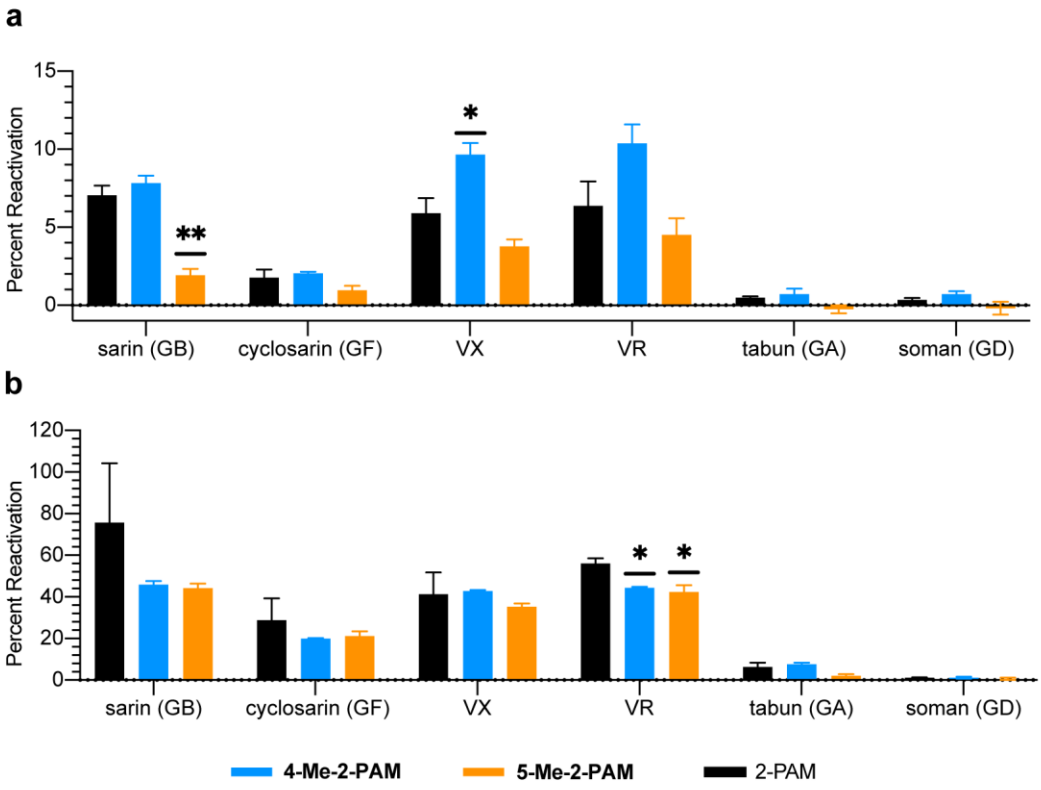

Figure 22. Reactivation of OPNA-inhibited *h*AChE using (a) 10 or (b) 1000 μM 2-PAM, 4-Me-2-PAM, and 5-Me-2-PAM at 53 min. (Acknowledgement to USAMRICD). *p < 0.05; **p < 0.01, as determined by an unpaired, two-tailed t-test. Data are mean ± SD. n = 2.

In effort to explain the lower reactivation efficiencies of **3-Me-2-PAM** and **5-Me-2-PAM** (Figure 21) and the bell-shaped curve observed for **4-Me-2-PAM** (Figure 21c), the four analogs were incubated with free *h*AChE and *Ee*AChE, i.e., in the absence of paraoxon, to determine whether any of them might directly inhibit the enzyme. As Figure 23 shows, the methyl scan compounds, with the exception of **6-Me-2-PAM**, result in a statistically significant reduction in

*h*AChE activity. However, none of the C-methylated analogs inhibit *Ee*AChE. The degree of inhibition if *h*AChE does not fully account for weaker reactivation efficiencies observed in Figure 21.

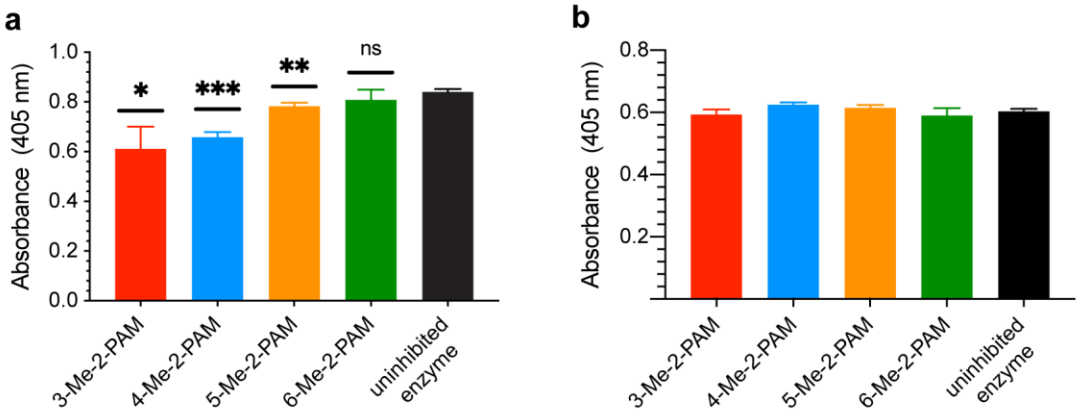

Figure 23. Inhibition data for 600 µM C-methylated 2-PAM analogs at 12 min. (a) *h*AChE (b) *Ee*AChE. *p < 0.05; **p < 0.01; ***p < 0.001, as determined by an unpaired, two-tailed t-test. Data are mean ± SD. n = 3.

The reproducibly observed bell-shaped for **4-Me-2-PAM** (Figure 21c) was further investigated. More specifically, to eliminate the possibility of aggregation, the absorbance of **4-Me-2-PAM** was measured. A 38 µM solution of **4-Me-2-PAM** in 100 mM phosphate pH 7.4 buffer was prepared. The solution was transferred to a quartz cuvette and the absorbance was measured (Figure 24a). This solution was diluted with 100 mM phosphate pH 7.4 buffer to 25, 19, and 9.5 µM. The absorbance of each solution was measured and plotted. Because the increase in absorbance was linearly proportional to the concentration (Figure 24b), aggregation was deemed not the source of reduced activity. At this stage, I am not able to account for the bell-shape trends. Regarding therapeutic viability, the downward trend may not be relevant, as the compound concentration in vivo, especially in the CNS, would unlikely exceed 100 µM.

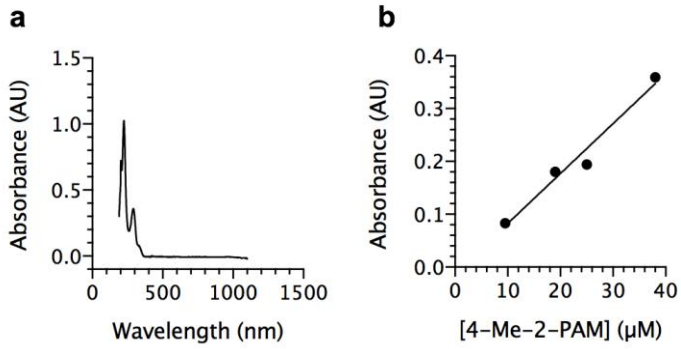

Figure 24. a) absorbance spectrum of 38 μM 4-Me-2-PAM in 100 mM phosphate pH 7.4 buffer. b) absorbance of varying concentrations of 4-Me-2-PAM at 290 nm.

2.1.3 Molecular modeling of methyl scan analogs

In collaboration with Dr. James Burnett (University of Pittsburgh), a new binding mode for 2-PAM was developed (Figure 25a and b). Subsequently, each methyl scan derivative was modeled in the binding site; the optimized 2-PAM binding mode and reactivation data shown in Figure 21 were taken into consideration. Figure 25c shows the predicted binding mode of **3-Me-2-PAM** derivative. Conformational analysis predicts that the 3-position methyl forces the oximate of this analog to adopt a twist-plane conformation with respect to the pyridinium. The resulting orientation prevents reactivation because the oximate is improperly positioned and distant from the phosphylated serine residue. When the oximate is oriented as observed for the optimized 2-PAM model (Figure 25b) the 3-methyl engages in highly unfavorable hydrophobic clashes with the hydroxy group of Tyr-124. On the other hand, if the pyridinium ring of **3-Me-2-PAM** is rotated to moderate this clash, the 3-methyl substituent then engages in a steric clash with the side chain of Tyr-337. In attempts to ameliorate both of these steric/electrostatic incompatibilities, the oxygen

of the oximate moiety remains in an orientation that is not suitable for phosphyl group displacement.

In contrast, the predicted binding mode of the efficient analog **4-Me-2-PAM** (Figure 25d) is promising. The model indicates that the 4-methyl substituent points out of the binding site and into sterically unhindered coordinate space that is surrounded by mainly aromatic residues of the enzyme's binding gorge. Hence, I hypothesize that the 4-position is an acceptable site for further modification. Further investigation of 4-position substitutions will be discussed in the following sections.

When oriented in a binding mode that mimics the optimized 2-PAM binding mode (Figure 25b), less efficient **5-Me-2-PAM** is predicted to have unfavorable hydrophobic-polar and steric clashes with the side chain of Tyr-337 (Figure 25e). When **6-Me-2-PAM** is placed in the optimized binding mode for 2-PAM, the new methyl substituent is predicted to point into a desolvated subsite of the enzyme. The additional methyl group can also engage in favorable hydrophobic contacts with the benzene component of the Trp-86 side chain indole (Figure 25f). In the case of paraoxon-inhibited AChE, the indole ring of Trp-86 is forced to rotate to fully accommodate **6-Me-2-PAM** (Figure 25f). As a result, the cation-π interaction with this analog is not as optimal as observed for 2-PAM, thereby rationalizing its decreased efficiency versus the parent compound in the Ellman assay with paraoxon.

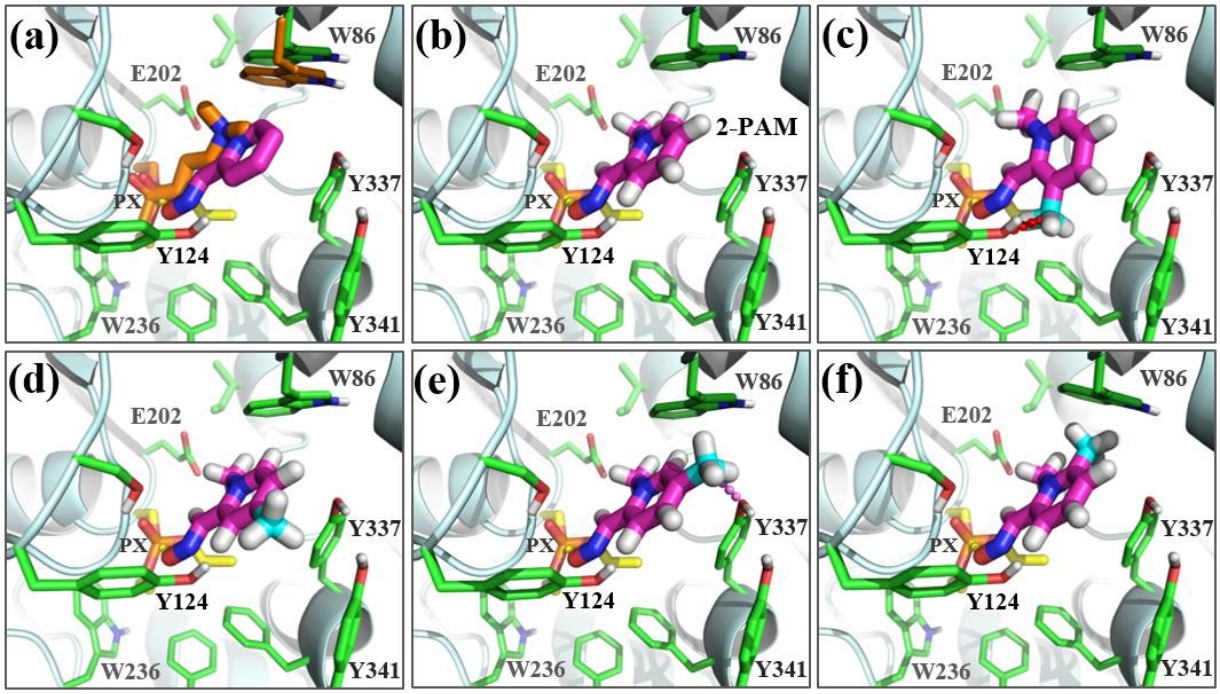

Figure 25. The binding mode of 2-PAM and its methyl scan derivatives. PDB entry 5HFA[102] was used for all modeling, and is shown in pale cyan cartoon. Select residues surrounding the active site are shown with green carbons, the carbons of both paraoxon-bound Ser-203 and paraoxon are shown in yellow carbons, and the paraoxon phosphorous is colored in orange in panels b–f. (a) A proposed 2-PAM (magenta carbons) binding mode that places the oximate group in an orientation that is relevant with respect to attack on the phosphorus atom of paraoxon when it is covalently bound to Ser-203. The proposed 2-PAM binding mode is superimposed on that of a covalently bound acetylcholine derivative KTA (orange carbons (both ligand and Trp-86), PDB entry 2HA0[103]). (b) The same binding mode of 2-PAM as shown in (a), but without KTA, and with 2-PAM hydrogens shown. (c) The 3-position methyl (cyan carbon) of 3-Me-2-PAM forces the oximate moiety to adopt a twist-plane with respect to the pyridinium component of the molecule. This conformation is predicted to significantly perturb the derivative's ability to achieve complimentary contacts and binding that allows for AChE reactivation. (d) The 4-methyl substituent (cyan carbon) of 4-Me-2-PAM points out of the AChE active site, and into the sterically unhindered binding gorge. (e) The 5-methyl (cyan carbon) of 5-Me-2-PAM is predicted to locate to a position that places it within 3.0 Å of the side chain phenol oxygen of Tyr-337, resulting in a hydrophobic-polar clash (pink dashes) and steric clashes that would perturb optimal binding. (f) The 6-position methyl (cyan carbon) of 6-Me-2-PAM points into a hydrophobic location in the AChE

binding site and engages in a favorable hydrophobic contact with the benzene ring of the side chain indole of Trp-86.

2.1.4 Conclusions

The first methyl scan of 2-PAM revealed that the 4- and 6-positions could tolerate methylation, while the 3-position cannot. **5-Me-2-PAM** showed appreciable reactivation of paraoxon-inhibited *h*AChE but was unimpressive in the multi-agent screen. In contrast, **4-Me-2-PAM** offered equivalent or superior reactivation in the multi-agent screening in comparison to 2-PAM. Computational analyses were used to provide and validate structure-based rationales for my experimental findings. Ultimately, all results obtained indicate that the 4-position of the 2-PAM pyridinium offered a promising site of derivation for future analogs. The methyl scan series provided foundational insights that could guide the rational and structure-based design of new derivatives in effort to improve binding affinity, AChE reactivation, and/or improved BBB permeability.

2.2 Ether and sulfide analogs

Therapeutics, including natural products and synthetic drugs, often contain heteroatoms and aromatic rings.[104-106] Functional groups containing oxygen and nitrogen introduce essential hydrogen-bond donor and acceptor properties, a critical attribute to consider in the drug development process as it affects target binding, absorption, water solubility, and permeability.[104] Ethers are found in nearly 40% of bioactive molecules.[107] Sulfur is less common in natural products

but is frequently introduced in synthetic bioactive compounds.[104] Sulfides are a common sulfur-containing functional group[105]; the prevalence of sulfides in drugs has increased recently.[107] Additionally, methoxy-substituted pyridiniums[108] and pyridinium aldoximes[109] have been developed as potential reactivators of aged and inhibited AChE, respectively.

In light of these literature findings and the results of the methyl scan study, the purpose of this work was to determine whether the installation of ethers or sulfides in 4-position of 2-PAM would enhance the reactivation efficiency and/or the spectrum of reactivation of OPNA-inhibited AChE. The systematic alteration of the alkyl group would provide insight into how much space is available within the binding pocket. In addition to alkyl groups, phenyl groups were included in effort to increase hydrophobicity and π-π stacking with residues lining the binding gorge of AChE.[4, 15] Additionally, aromatic rings are found in 55% of drug molecules; benzene is the most frequently incorporated ring.[106]

2.2.1 Synthesis

The starting material for this series of ether and sulfide analogs can be synthesized via the route shown in Scheme 2 and was selected based on literature precedents of nucleophilic aromatic substitution (S_NAr) of 4-nitropyridines.[110, 111] The first synthetic step involved a rearrangement[100] of commercially available 4-nitropicoline *N*-oxide **2-1** to afford hydroxymethyl pyridine **2-2** in 82% yield. Subsequently, oxidation with MnO_2 generated aldehyde **2-3** in 69% yield. In the third step, protection of the aldehyde **2-3** generated acetal **2-4** in 91% yield.

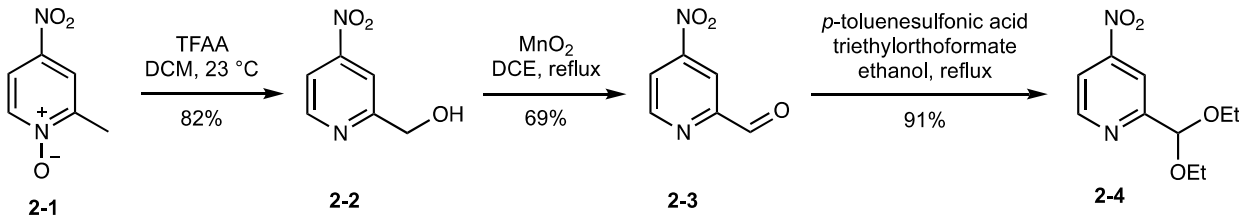

Scheme 2. Synthesis of acetal 2-4. TFAA = trifluoroacetic anhydride, DCM = dichloromethane, DCE = 1,2-dichloroethane.

Nitropyridine **2-4** was found to undergo S_NAr with the corresponding alcohol or thiol to make the carbon-heteroatom bond (Table 1). Two procedures were developed depending on the nucleophile. Alcohols (e.g., propanol, isopropanol, and *n*-butanol) were used as solvents with sodium hydride for deprotonation. Phenol and the thiols were used as reagents; their lower pK_a allowed potassium carbonate to be used as a base.

Table 1. Formation of C–O or C–S bonds

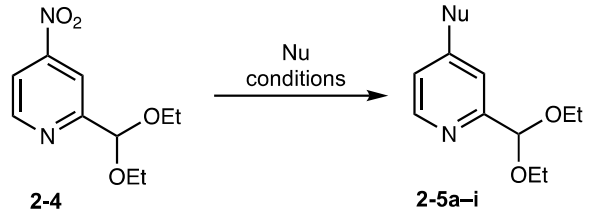

2-4 **2-5a–i**

Condition A

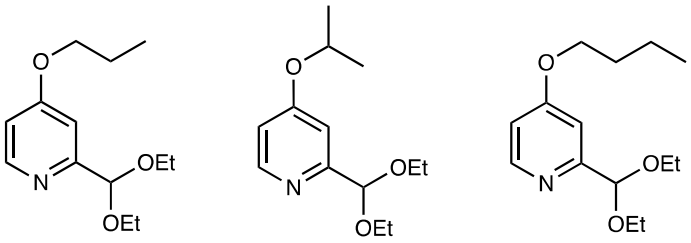

2-5a, 80% **2-5b,** 81% **2-5c,** 77%

Condition B

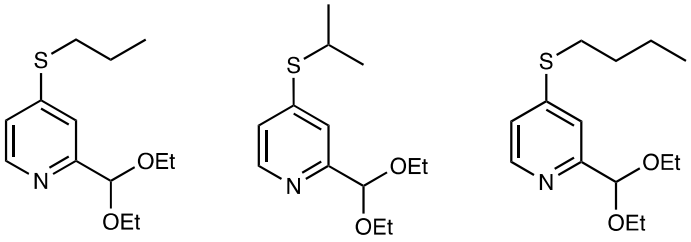

2-5d, 90% **2-5e**, 98% **2-5f**, 74%

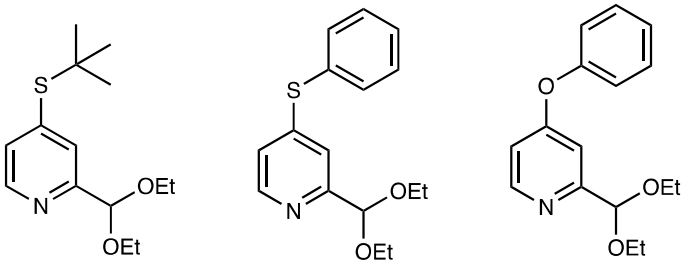

2-5g, 65% **2-5h**, 73% **2-5i**, 91%

Reagents and conditions: (A) NaH, ROH, reflux; (B) K_2CO_3, RSH or PhOH, DMSO, 85–95 °C; R = alkyl or aryl, Ph = phenyl, DMSO = dimethylsulfoxide

After generating the series in Table 1, a one-pot procedure for acetal deprotection and condensation with hydroxylamine could be used to afford the corresponding oximes **2-6a–i** (Table 2). Lastly, *N*-methylation with MeI afforded the final products in the yields shown in Table 3.

Table 2. One-pot deprotection and condensation

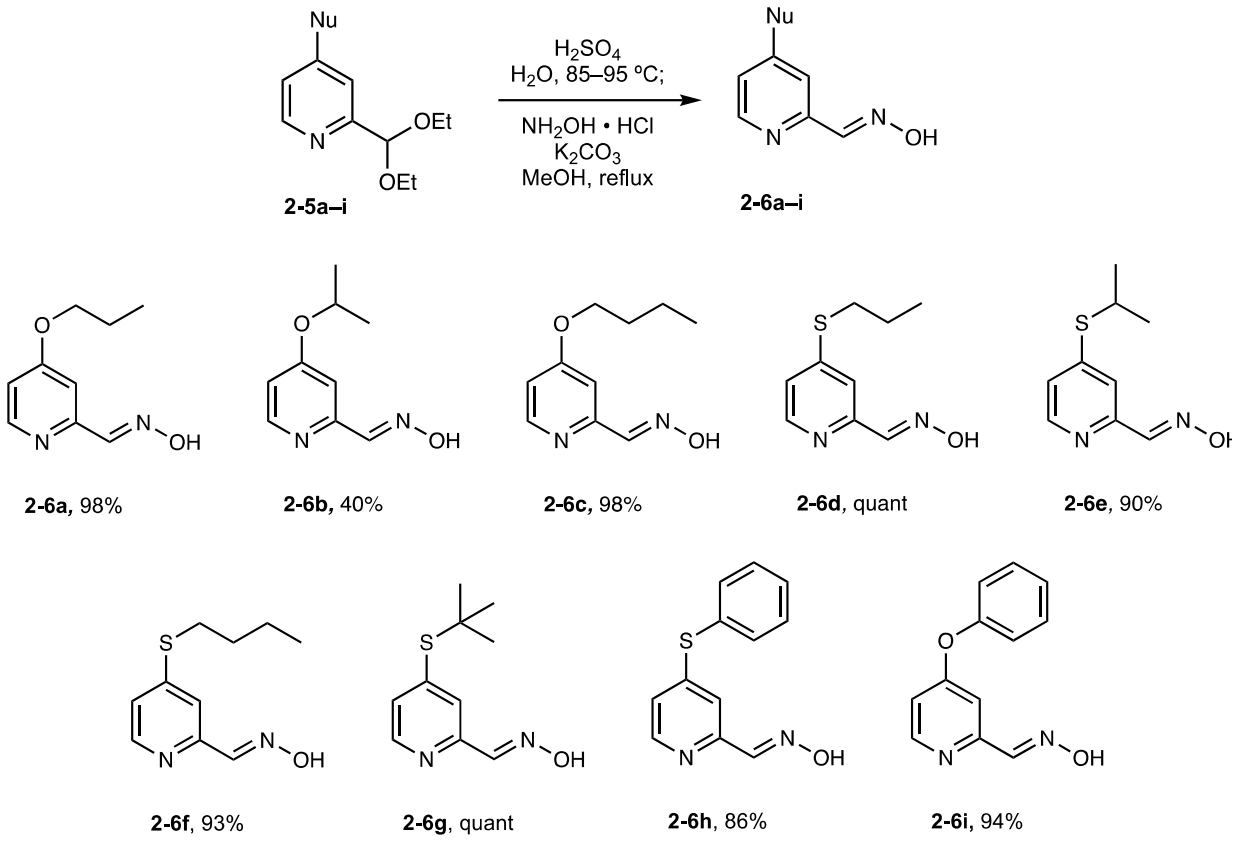

Table 3. *N*-methylation

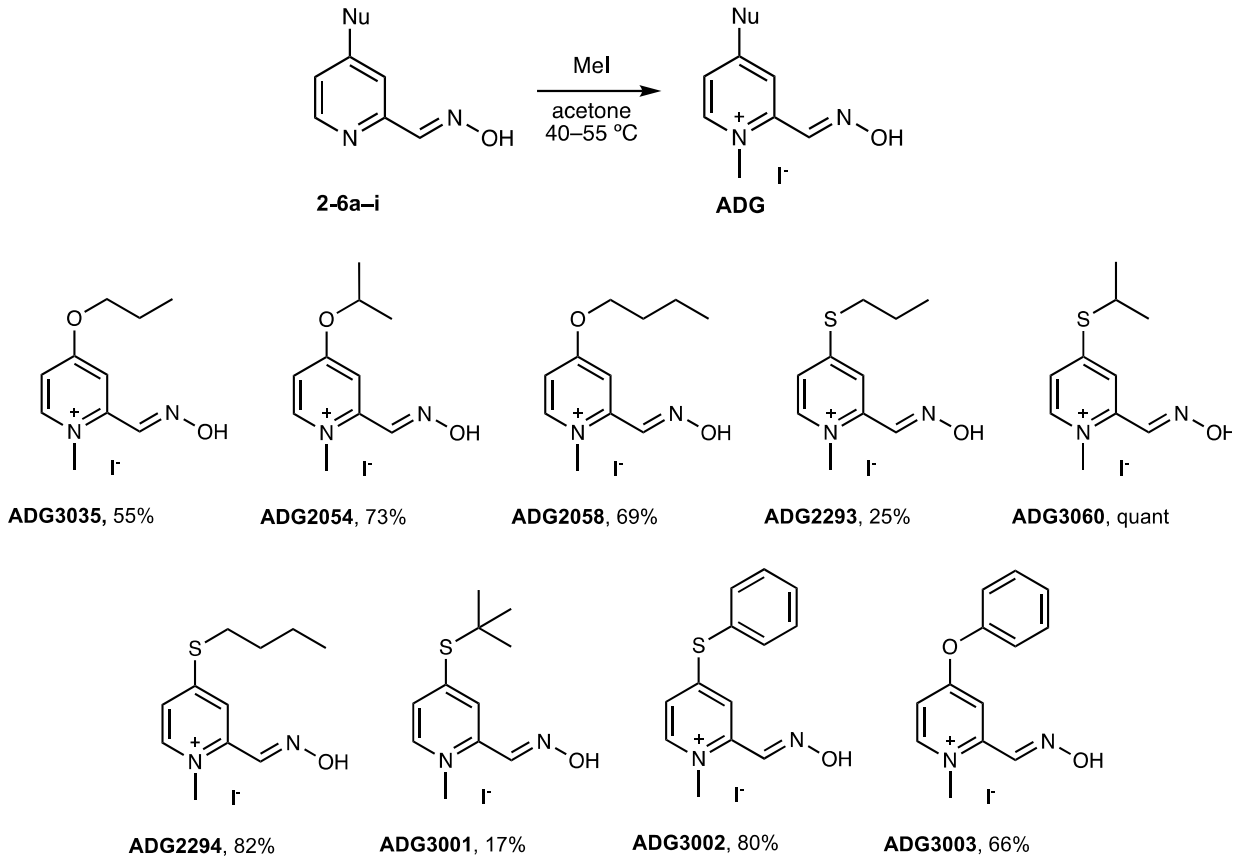

2.2.2 In vitro reactivation

With the ether and sulfide analogs shown in Table 3 in hand, a modified Ellman's assay was used to determine reactivation efficiency in vitro. Specifically, *Ee*AChE was incubated with paraoxon for 10 min before being added to a clear 96-well plate containing Ellman's reagent, acetylthiocholine, and varying concentrations of the ether or sulfide analogs or 2-PAM. The absorbance values at 405 nm are proportional to enzymatic activity.

I discovered alkyl ether analogs **ADG3035**, **ADG2054**, and **ADG2058** had identical reactivations efficiencies at 18 μM and were approximately 23% as efficient as 2-PAM (Figure

26a). The dose-response curves of alkyl ether analogs revealed that they were significantly less efficient than 2-PAM at all concentrations tested (Figure 26b). Interestingly, 4-propyl ether **ADG3035** had nearly the same activity at all concentrations tested, while 4-isopropyl ether **ADG2054**, and 4-butyl ether **ADG2058** had a dose-dependent increase in reactivation. Alkyl sulfides **ADG2293**, **ADG3060**, **ADG2294**, and **ADG3001** had identical reactivations efficiencies at 18 μM and were approximately 50% as efficient as 2-PAM (Figure 26c). The dose-response curves of the alkyl sulfide analogs showed that this series was less efficient than 2-PAM at all concentrations tested. Linear alkyl sulfides **ADG2293** and **ADG2294** had equivalent reactivation efficiencies at all concentrations tested (Figure 26d) and had a dose-dependent decrease in apparent enzyme activity. Branched alkyl sulfides **ADG3060** and **ADG3001** had equivalent reactivation efficiencies; apparently enzyme activity was independent of dose (Figure 26d). The heteroatom had a significant impact on reactivation efficiency; altering the alkyl chain had a negligible effect. Alkyl sulfides were more efficient than alkyl ethers at lower concentrations. None of the analogs in this series had impressive dose-response curves.

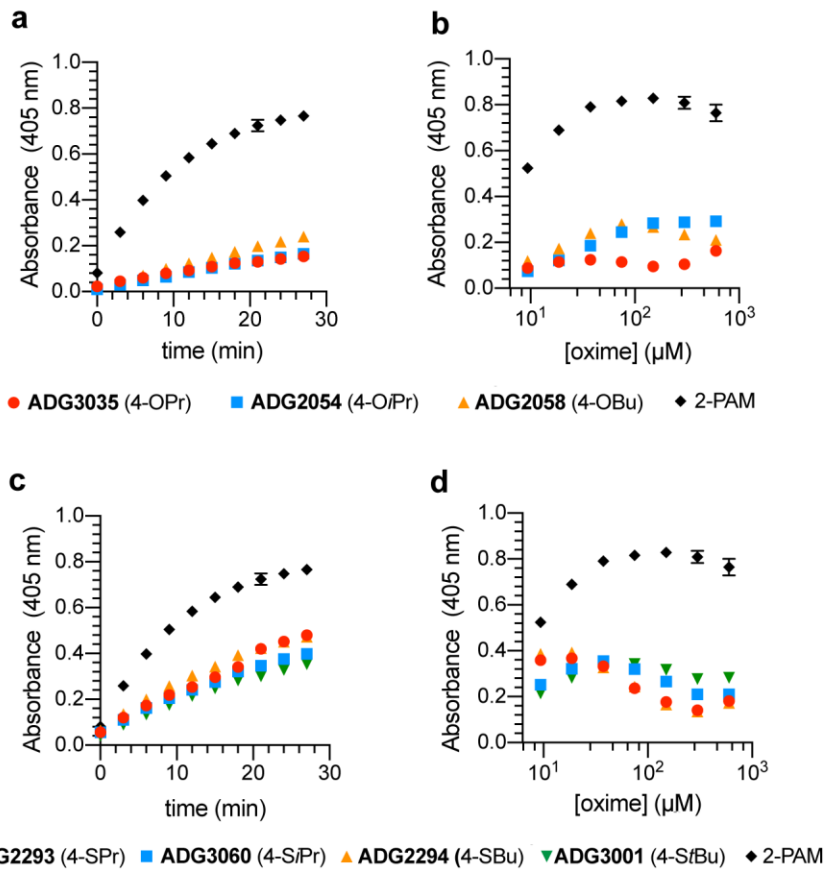

Figure 26. In vitro reactivation of *Ee*AChE inhibited with 2% v/v paraoxon in isopropanol by akyl ether and sulfide analogs. a) 18 μM alkyl ether analogs. b) dose-response of alkyl ether analogs at 18 min. c) 18 μM alkyl sulfide analogs. d) dose-response of alkyl sulfide analogs at 18 min. Data are mean ± SD. n = 3.

The alkyl ethers and sulfides were incubated with *Ee*AChE in the absence of paraoxon to determine whether the analogs inhibit the enzyme (Figure 27). Ether analogs with a three-carbon chain ADG3035 and ADG2054 have a minimal inhibitory effect on *Ee*AChE (Figure 27a) In contrast, *n*-butyl ether ADG2058 reduced enzyme activity by approximately 40% (Figure 27a). All of the alkyl sulfide analogs inhibited *Ee*AChE (Figure 27a). 4-Propyl sulfide **ADG2293** and 4-isopropyl sulfide **ADG3060** reduced enzyme activity by 50 and 40%, respectively. 4-Butyl sulfide **ADG224** exhibited the greatest inhibitory effect and reduced enzyme activity by 70%; 4-*tert*-butyl sulfide **ADG3001** had the least inhibitory effect, reducing enzyme activity by only 22%.

The overall poor reactivation of paraoxon-inhibited *Ee*AChE (Figure 26a and b) by alkyl ethers cannot solely be explained by enzyme inhibition. However, the observed decrease in reactivation at higher concentration of the alkyl sulfides (Figure 26d) is likely the result of enzyme inhibition.

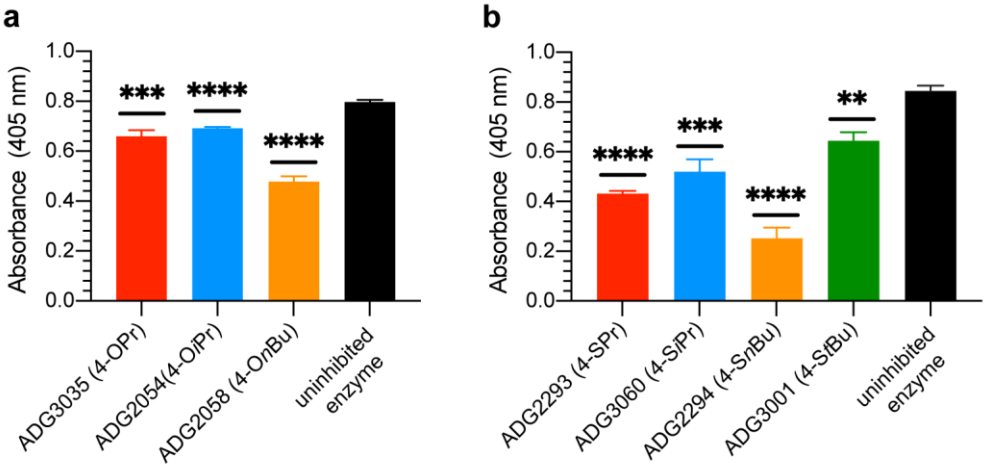

Figure 27. Inhibition of *Ee*AChE by 600 μM oxime at 9 min. (a) alkyl ether analogs. (b) alkyl sulfide analogs. **p < 0.01; *** p < 0.001; ****p < 0.0001, as determined by an unpaired, two-tailed t-test, Data are mean ± SD.

Phenyl ether **ADG3003** and phenyl sulfide **ADG3002** were also tested in the modified Ellman's assay reactivation of paraoxon-inhibition *Ee*AChE. I discovered that both analogs exhibited enhanced reactivation efficiencies compared to 2-PAM at 18 μM (Figure 28a). The analysis of the initial slopes indicates that sulfide **ADG3002** reactivated the paraoxon-bound *Ee*AChE 1.6 times faster than 2-PAM, while ether **ADG3003** was 1.4 times faster than 2-PAM. The dose-response curve of ether **ADG3003** revealed that the aryl ether has a reactivation efficiency equivalent to 2-PAM at all tested concentrations (Figure 28b). At concentrations less than or equal to 75 μM, sulfide **ADG3002** was superior or equivalent to 2-PAM. The reactivation

efficiency of the sulfide decreased when concentrations exceeded 75 μM, the concentration range unattainable in the CNS under physiological conditions. It is unlikely that the decrease is due to inhibition of AChE by **ADG3002** (Figure 29).

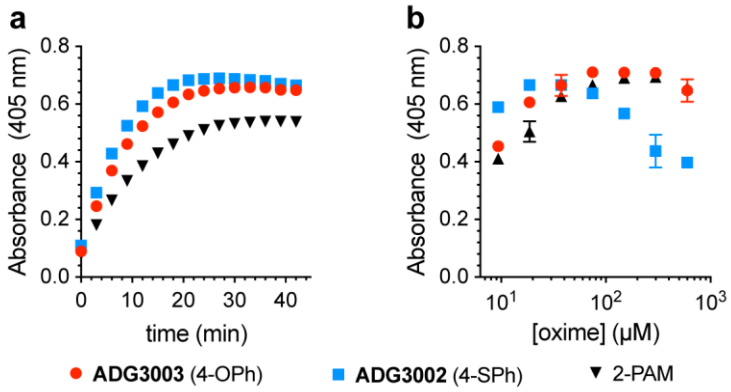

Figure 28. In vitro reactivation of *Ee*AChE inhibited with 2% v/v paraoxon in isopropanol by by ADG3003 and ADG3002. (a) 18 μM oxime. (b) dose-response at 18 min. Data are mean ± SD. n = 3.

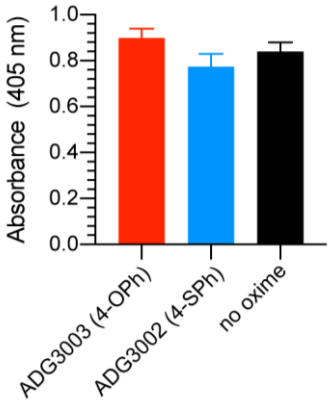

Figure 29. Inhibition of *Ee*AChE by 600 μM ADG3003 or ADG3002 at 9 min. Differences are not statistically significant as determined by an unpaired, two-tailed t-test. Data are mean ± SD. n = 3.

Encouraged by these results, ether **ADG3003** and sulfide **ADG3002** were tested at the USAMRICD to determine the reactivation efficiencies against nerve agents. In this modified Ellman's assay, recombinant *h*AChE was incubated with OPNAs for 10 min before excess OPNA was removed. Then, a solution containing either **ADG3003** or **ADG3002** was added and enzymatic activity was measured periodically using acetylthiocholine and Ellman's reagent. Percent reactivation was computed by dividing the slope of the inhibited sample by the slope of the control enzyme.

Pleasingly, the assay revealed that after 53 min, 10 μM ether **ADG3003** and sulfide **ADG3002** were both 1.5-fold better than 2-PAM at reactivating sarin-inhibited *h*AChE (Figure 30a). Against cyclosarin-inhibited *h*AChE, sulfide **ADG3002** reactivated 8% of the enzyme. In contrast, ether **ADG3003** and 2-PAM both had less than 2% reactivation. Sulfide **ADG3002** could reactivate nearly 20% of VX- and VR-inhibited *h*AChE. Ether **ADG3003** could reactivate 11% and 9% of VX- and VR-inhibited *h*AChE, respectively, while 2-PAM only reactivated 6% of VX- and VR-inhibited *h*AChE. Significantly, **ADG3002** efficiently reactivated VX-inhibited AChE at a presumably more physiologically relevant, low concentration. Unfortunately, 2-PAM, **ADG3003**, and **ADG3002** provided minimal or no protection against tabun and soman.

Higher doses of the antidotes were also examined. At 1000 μM doses, there is not a statistically significant difference in reactivation of sarin-inhibited *h*AChE by 2-PAM and ether **ADG3003**. At the same concentration, sulfide **ADG3002** reactivated 38% of the enzyme on average. Against cyclosarin-inhibited *h*AChE, the reactivation efficiency of the sulfide was nearly 2-fold that of 2-PAM. Ether **ADG3003** is approximately 70% as efficient as 2-PAM. The phenyl ether and phenyl sulfide analogs were equally efficient at reactivating VX-inhibited *h*AChE and were more efficient than 2-PAM. Against VR-inhibited *h*AChE, 2-PAM, sulfide **ADG3002**, and

ether **ADG3003** have equivalent reactivation efficiencies. Even at 1000 μM concentrations, none of antidotes were able to elicit significant reactivation of tabun- or soman-inhibited *h*AChE.

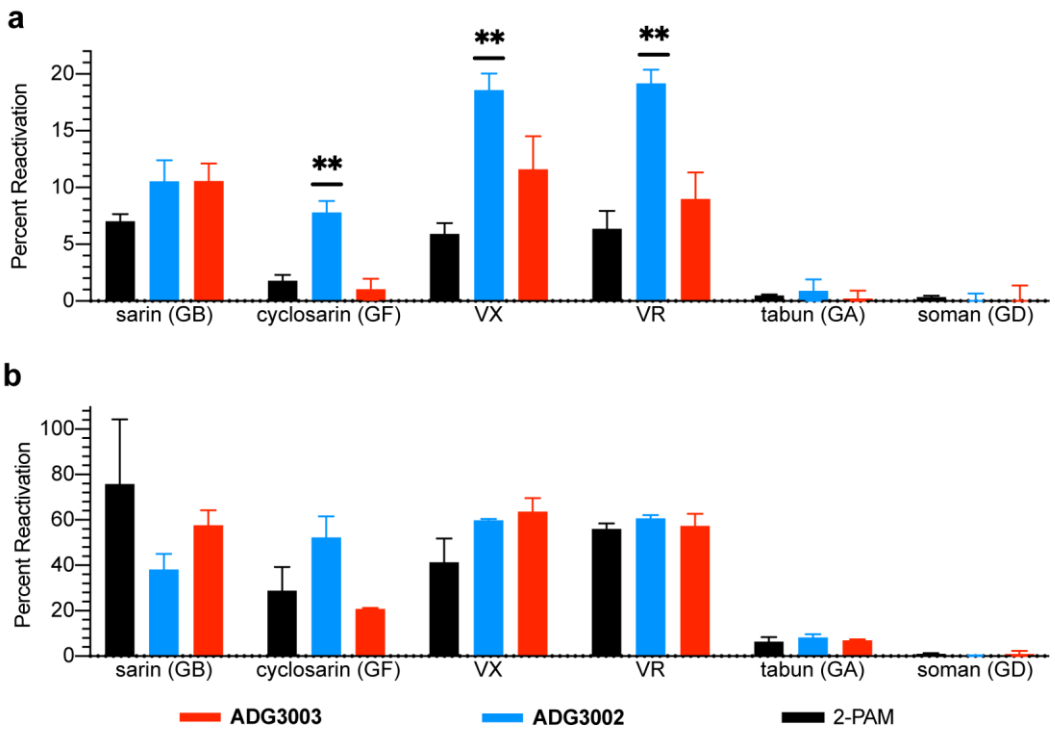

Figure 30. Reactivation of OPNA-inhibited *h*AChE using (a) 10 or (b) 1000 μM 2-PAM, ADG3002, and ADG3003 at 53 min. **p < 0.01, as determined by an unpaired, two-tailed t-test. Data are mean ± SD. n = 2

The X-ray crystal structures of ether **ADG3003** and sulfide **ADG3002** (Figure 31) were obtained in effort to understand the marked differences in biological activity. The C–O–C bond angle of ether **ADG3003** was found to be 117.1°, which is comparable with literature reports of related compounds.[112] The phenyl C–O bond was 1.40 Å; this is consistent with reported C–O single bond lengths.[113] However, there is slight shortening of the pyridinyl C–O bond, which was found to be 1.35 Å. This suggests that there may be π-electron contribution from the oxygen atom to the pyridinium. In contrast, the C–S–C bond angle of sulfide **ADG3002** was found to be 103.8°.

Neither of the C–S bonds were shortened; both were found to be 1.77 Å. The bond angles and lengths of sulfide **ADG3002** are consistent with those reported for related and uncharged biaryl sulfides.[112, 114] Because there is no detectable bond shortening of the C–S bonds, any possible π-electron contribution from the sulfur atom appears negligible.

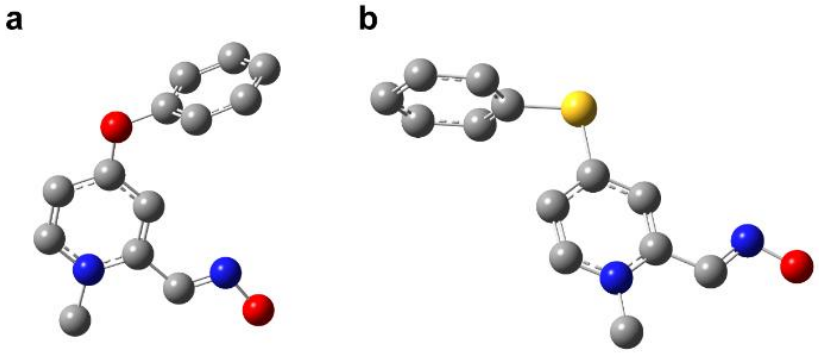

Figure 31. X-ray structures. a) ADG3003. The C–O–C bond angle was found to be 117.1°; Phenyl C–O bond = 1.40 Å; pyridinyl C–O bond = 1.35 Å b) ADG3002. The C–S–C bond angle was found to be 103.8°; Both C-S bonds = 1.77 Å.

2.2.3 Conclusions

The addition of alkyl ethers and sulfides to the 4-position of 2-PAM led to a decrease in enzyme reactivation; alkyl ether and sulfide analogs inhibit AChE. There were marked differences in activity between ethers and sulfides. Of the two, sulfides were more efficient than ethers, especially at lower concentrations. However, the length and branching of the alkyl chain had a minimal effect on reactivation. Phenyl ether **ADG3003** and phenyl sulfide **ADG3002** analogs

exhibited remarkable in vitro activity and were able to reactivate paraoxon- and OPNA-inhibited AChE. Both analogs should be studied further to determine the pharmacokinetic profiles and in vivo activity.

2.3 Structure-activity relationship study of ADG3002 and ADG3003

Inspired by the in vitro reactivation efficiencies of **ADG3002** and **ADG3003**, I began an SAR campaign encompassing various steric and electronic modifications. First, the role of the ether group of **ADG3003** was investigated by replacing it with a hydroxyl group. The hydroxyl group has the potential to function as a hydrogen bond donor and acceptor, while the ether is only a hydrogen bond acceptor. I hypothesized that the electronics of **ADG3002** could be modulated by oxidizing the sulfur atom to the sulfoxide and sulfone. Lastly, substituents were added to each modifiable position of the phenyl ring of **ADG3002** and **ADG3003** to investigate steric and electronic restrictions. For example, fluorine atoms were added because they are frequently incorporated in drug candidates. Fluorine atoms may modulate electron density of aromatic rings and van der Waals interactions and increase lipophilicity and metabolic stability.[115-118] Methyl groups were added, as they are common functional groups in biologically active compounds and are often added to parent structures in effort to improve biological activity and pharmacological properties.[119, 120] Additionally, methoxy groups were incorporated as an electron-rich bioisostere of the methyl group, while minimizing steric hindrance.[121] Larger substituents, such as isopropoxyphenoxy, diphenoxy, and naphthyl, were also included in the campaign to probe the steric constraints of the AChE binding gorge. After completing the synthesis of the analogs, the in

vitro reactivation efficiency of the final compounds was determined using a modified Ellman's assay.

2.3.1 Results

I envisioned that the hydroxyl analog could be synthesized via a Grignard reaction. The starting material for this analog the could be synthesized via the route shown in Scheme 3. The first synthetic step involved *N*-oxidation of commercially available 4-bromo-2-methylpyridine **3-1** following a procedure reported by Limnios and Kokotos[99] to afford *N*-oxide **3-2** in 37% yield. The rearrangement[100] of *N*-oxide **3-2** furnished the corresponding hydroxymethyl pyridine **3-3** in quantitative yield. This alcohol was then oxidized with MnO_2 to form aldehyde **3-4** in 54% yield. Lastly, this aldehyde was protected as a dimethyl acetal to generate **3-5** in 73% yield.

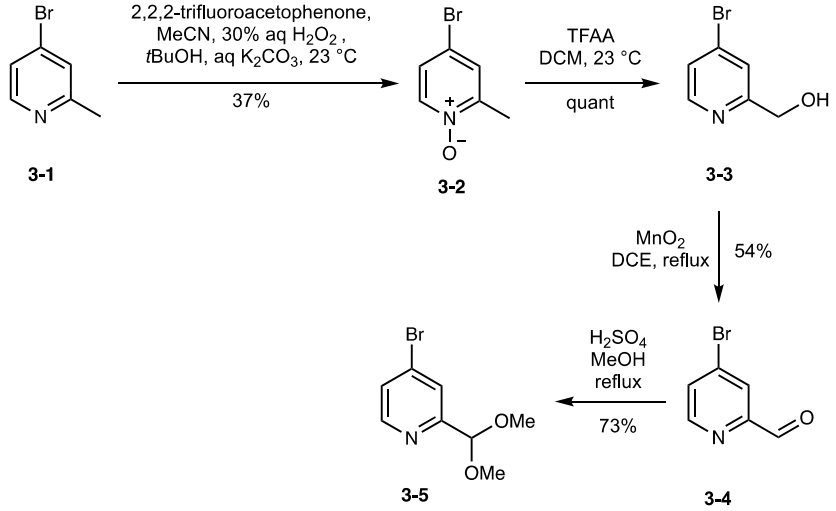

Scheme 3. Synthesis of 3-5.

Initial attempts to transform **3-5** into Grignard reagent **3-6** were unsuccessful (Scheme 4);

a mixture of unreacted started materials was obtained. Magnesium-halogen exchange was pursued as an alternative. Isopropylmagnesium chloride was selected, as it is the typical magnesium reagent of choice for magnesium-halogen exchange.[122] This approach proved to be a viable alternative and **3-7** was successfully formed in 33% yield (Scheme 5). Subsequently, oxime **3-8** was formed via a one-pot procedure for acetal deprotection and condensation with hydroxylamine in 95% yield. The final compound **ADG3230** was synthesized in 44% yield by *N*-methylation with MeI.

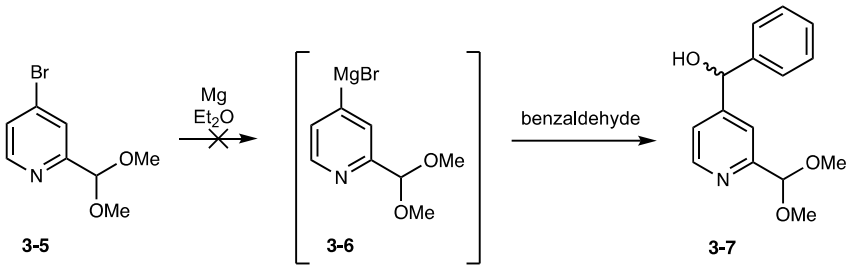

Scheme 4. Failed synthesis of 3-7.

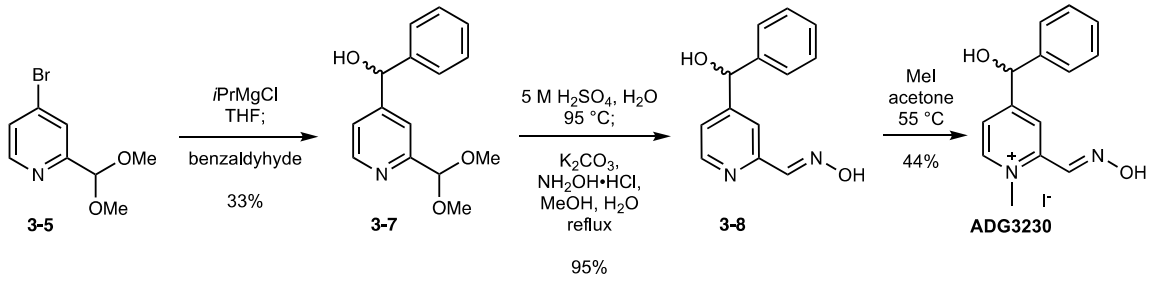

Scheme 5. Synthesis of ADG3230.

The in vitro reactivation efficiency of a racemic mixture of **ADG3230** was determined by the modified Ellman's assay, as previously described. At 18 μM, **ADG3230** was 30% as efficient

as 2-PAM at reactivating paraoxon-inhibited *Ee*AChE after 27 min (Figure 32a). A dose-dependent increase in enzyme reactivation was observed (Figure 32b), but **ADG3230** remined 23–68% less efficient than 2-PAM at all concentrations tested. Enzymatic activity was reduced by 33% when **ADG3230** was incubated with *Ee*AChE in the absence of paraoxon. In the future, synthesis and in vitro evaluation of enantiopure **ADG3230** would reveal whether the data in Figure 32a are an average of an active and inactive enantiomer or if the ether functional group, as in **ADG3003**, is superior to the hydroxyl analog **ADG3230**.

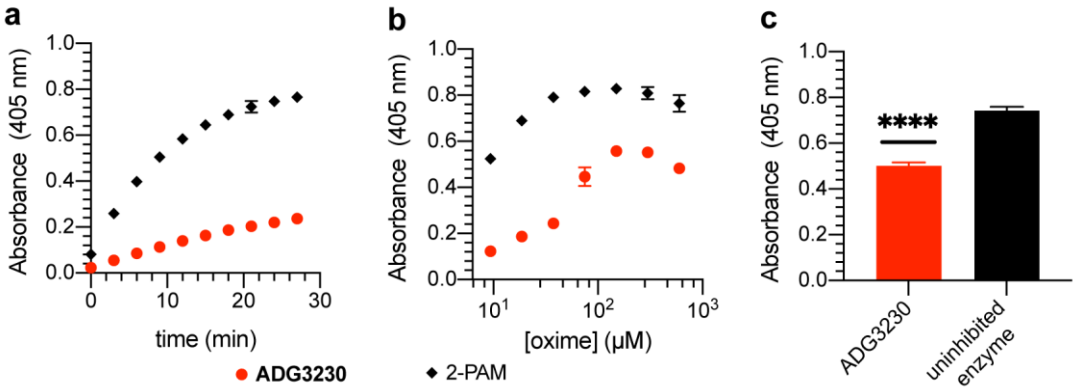

Figure 32. In vitro activity of ADG3230. (a) reactivation of *Ee*AChE inhibited with 2% v/v paraoxon in isopropanol by 18 μM oxime (b) reactivation of *Ee*AChE inhibited with 2% v/v paraoxon in isopropanol dose-response at 18 min (c) inhibition of *Ee*AChE by ADG3230 at 9 min. ****p < 0.0001 as determined by an unpaired, two-tailed t-test. Data are mean ± SD. n = 3.

I envisioned that the sulfoxide and sulfone analogs could be synthesized from sulfide **2-5h (**Scheme 6**)**. Oxidation with *m*CBPA required optimization to avoid the formation of byproducts. Ultimately, dropwise addition of an *m*CBPA solution at 0 °C produced sulfoxide **3-9** as a racemic mixture and sulfone **3-10** in 83 and 67% yields, respectively. A one-pot procedure for acetal

deprotection and condensation with hydroxylamine afforded oximes **3-11** and **3-12** in 74 and 89% yields, respectively. Despite several attempts, the final *N*-methylated analogs **3-13** and **3-14** were not synthesized. This is presumably because the sulfinyl and sulfonyl groups decreases the nucleophilicity of the pyridinyl nitrogen, making it unreactive and resistant to methylation.

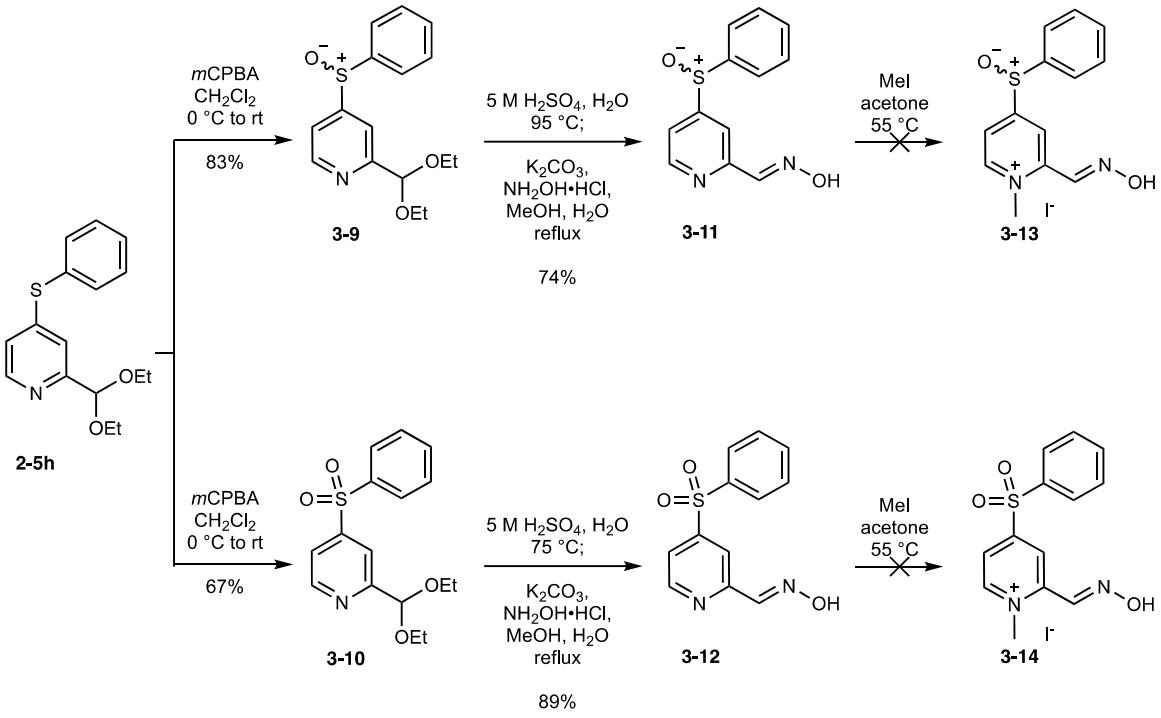

Scheme 6. Failed synthesis of sulfoxide and sulfone analogs.

The series of fluoro, methyl, and methoxyphenyl analogs were synthesized via Scheme 7, Scheme 8, and Scheme 9, respectively. The S_NAr of nitropyridine **2-4** with the corresponding substituted phenol or thiophenol installed the key C–O or C–S bond of **3-15a–f**, **3-16a–f**, and **3-17a–f** in 22–98% yields. Subsequently, oximes **3-18a–f**, **3-19a–f**, and **3-20a–f** were formed via a one-pot procedure for acetal deprotection and condensation with hydroxylamine in 61% to

quantitative yields. The final compounds were synthesized in 32% to quantitative yields by *N*-methylation with MeI.

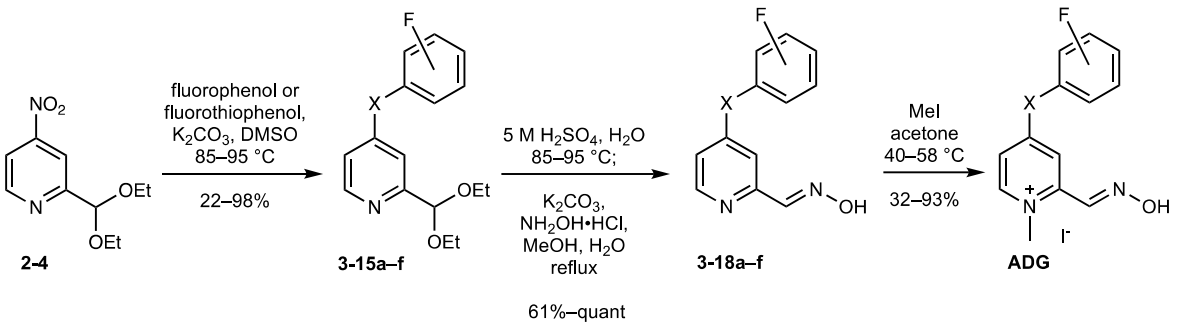

compound	yield	compound	yield	compound	X	R	yield
3-15a	49	**3-18a**	93	**ADG3124**	O	*o*-F	32
3-15b	22	**3-18b**	61	**ADG3123**	O	*m*-F	27
3-15c	56	**3-18c**	97	**ADG3116**	O	*p*-F	66
3-15d	98	**3-18d**	89	**ADG4158**	S	*o*-F	93
3-15e	89	**3-18e**	quant	**ADG4146**	S	*m*-F	57
3-15f	93	**3-18f**	quant	**ADG3193**	S	*p*-F	39

Scheme 7. Synthesis of fluoro-substituted analogs.

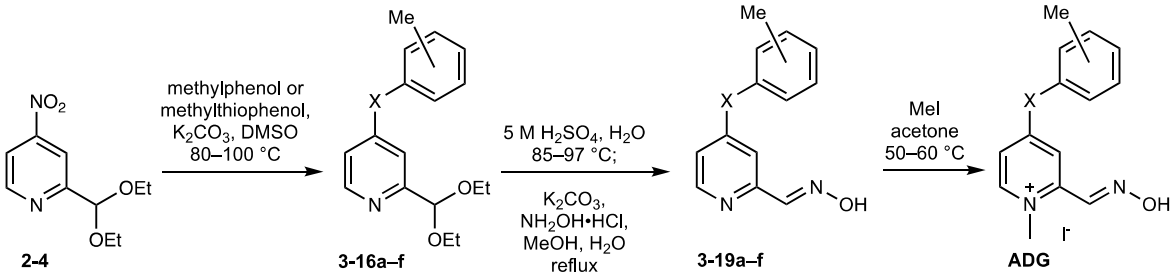

compound	yield	compound	yield	compound	X	R	yield
3-16a	80	**3-19a**	98	**ADG3124**	O	*o*-Me	91
3-16b	66	**3-19b**	quant	**ADG3123**	O	*m*-Me	80
3-16c	85	**3-19c**	75	**ADG3116**	O	*p*-Me	54
3-16d	83	**3-19d**	83	**ADG4158**	S	*o*-Me	98
3-16e	98	**3-19e**	76	**ADG4146**	S	*m*-Me	84
3-16f	98	**3-19f**	52	**ADG3193**	S	*p*-Me	quant

Scheme 8. Synthesis of methyl-substituted analogs.

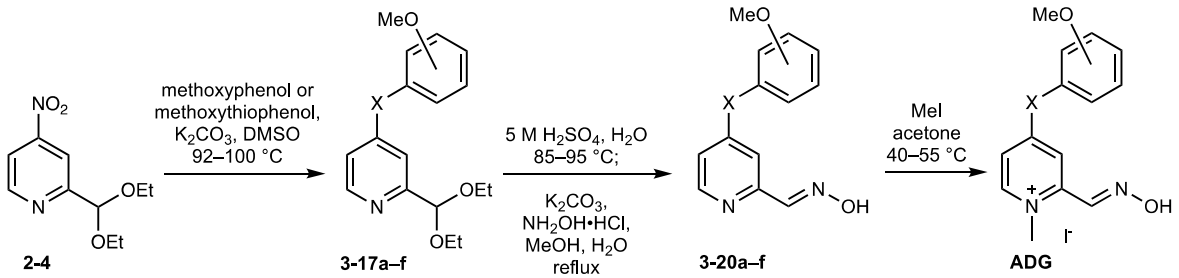

compound	yield	compound	yield	compound	X	compound	yield
3-17a	69	**3-20a**	96	**ADG3124**	O	*o*-OMe	87
3-17b	88	**3-20b**	91	**ADG3123**	O	*m*-OMe	80
3-17c	65	**3-20c**	quant	**ADG3116**	O	*p*-OMe	89
3-17d	95	**3-20d**	91	**ADG4158**	S	*o*-OMe	88
3-17e	98	**3-20e**	69	**ADG4146**	S	*m*-OMe	62
3-17f	76	**3-20f**	87	**ADG3193**	S	*p*-OMe	44

Scheme 9. Synthesis of methoxy-substituted analogs.

Interestingly, inclusion of a fluorine atom at the ortho or meta position of ether analogs significantly reduced reactivation efficiency for paraoxon-inhibited *Ee*AChE (Figure 33a and b). *p*-Fluorophenyl ether **ADG3116** was 66% as efficient as 2-PAM at 18 μM after 27 min (Figure 33a). *o*-Fluorophenyl ether **ADG3124** and *m*-fluorophenyl ether **ADG3123** were ineffective. Moreover, *p*-fluorophenyl ether **ADG3124** remained slightly less efficient than 2-PAM at all concentrations tested (Figure 33b). Increasing the concentration of *m*-fluorophenyl ether **ADG3123** increased AChE reactivation, but this analog was still inferior to 2-PAM; higher concentrations of **ADG3124** did not elicit a response. Upon further examination, I found that *o*-fluorophenyl ether **ADG3124** inhibited AChE enzyme (Figure 34).

In contrast to the ether series, addition of a fluorine atom had no effect on the reactivation efficiency of sulfide analogs; performance of *o*-, *m*-, and *p*-fluorophenyl sulfides **ADG4158**,

ADG4146, and **ADG3193** were identical to 2-PAM at 18 μM (Figure 33c). Enzyme reactivation by these fluorinated sulfides was equivalent to 2-PAM up to approximately 75 μM, above which the enzyme activity slightly decreased (Figure 33d). The decrease in reactivation could be accounted for by enzyme inhibition by the pyridinium oximes (Figure 34). Based on the van der Waals radii of fluorine and hydrogen atoms (1.47 Å and 1.20 Å, respectively), the steric effects should be marginal.[115] The difference in activity from the fluorine-substituted subseries in comparison to parent compounds **ADG3003** and **ADG3002** is likely due to modulation of electronics.

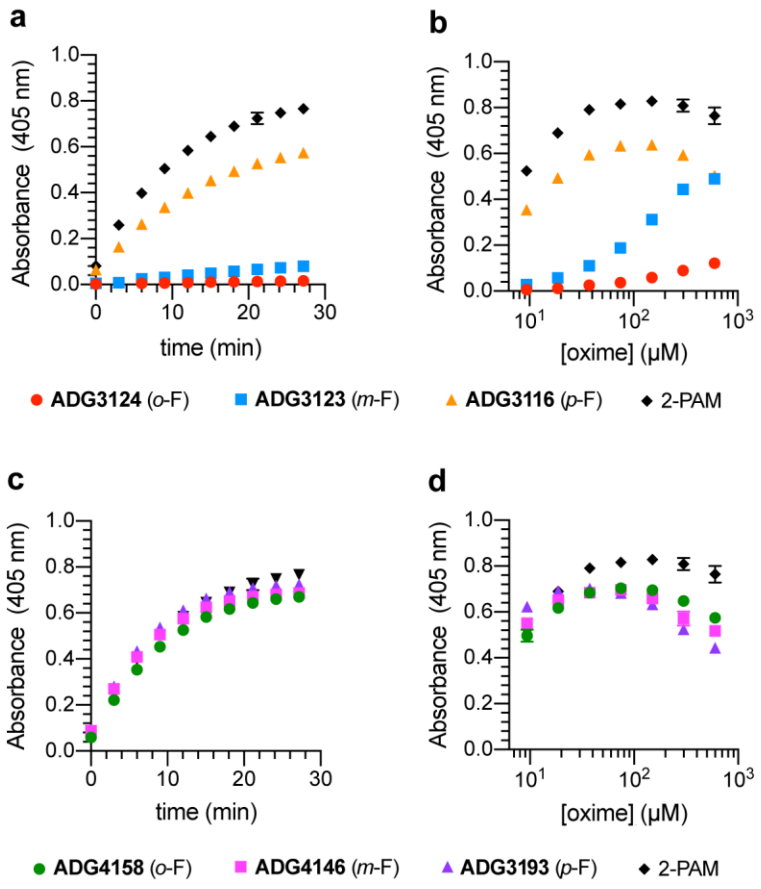

Figure 33. In vitro reactivation of *Ee*AChE inhibited with 2% v/v paraoxon in isopropanol by fluoro-substituted analogs. a) 18 μM phenyl ether analogs. b) dose-response of phenyl ether analogs at 18 min. c) 18 μM phenyl sulfide analogs. d) dose-response of phenyl sulfide analogs at 18 min. Data are mean ± SD. n = 3.

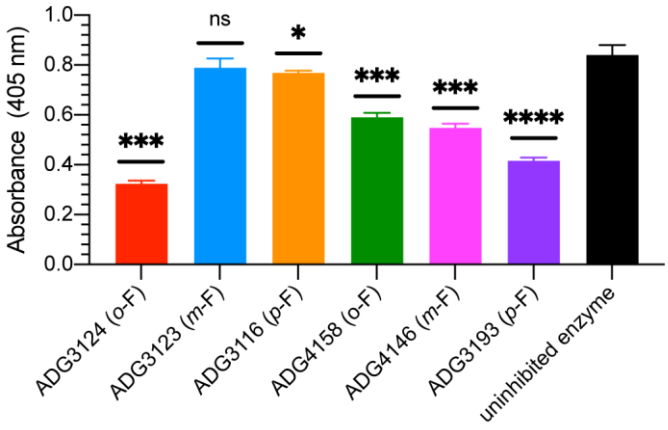

Figure 34. Inhibition of *Ee*AChE by 600 μM fluoro-substituted analogs at 9 min. *p < 0.05; ***p < 0.001; ****p < 0.0001 as determined by an unpaired, two-tailed t-test. Data are mean ± SD. n = 3.

Figure 35 shows the in vitro reactivation of paraoxon-inhibited *Ee*AChE by methyl-substituted phenyl ether and sulfide analogs. Generally, the addition of a methyl group was well tolerated in both ether and sulfide analogs. However, at concentrations greater than 75 μM, there was a decrease in activity amongst the methyl-substituted phenyl sulfides (Figure 35d). The decrease in activity can be attributed to moderate enzyme inhibition by the oximes (Figure 36).

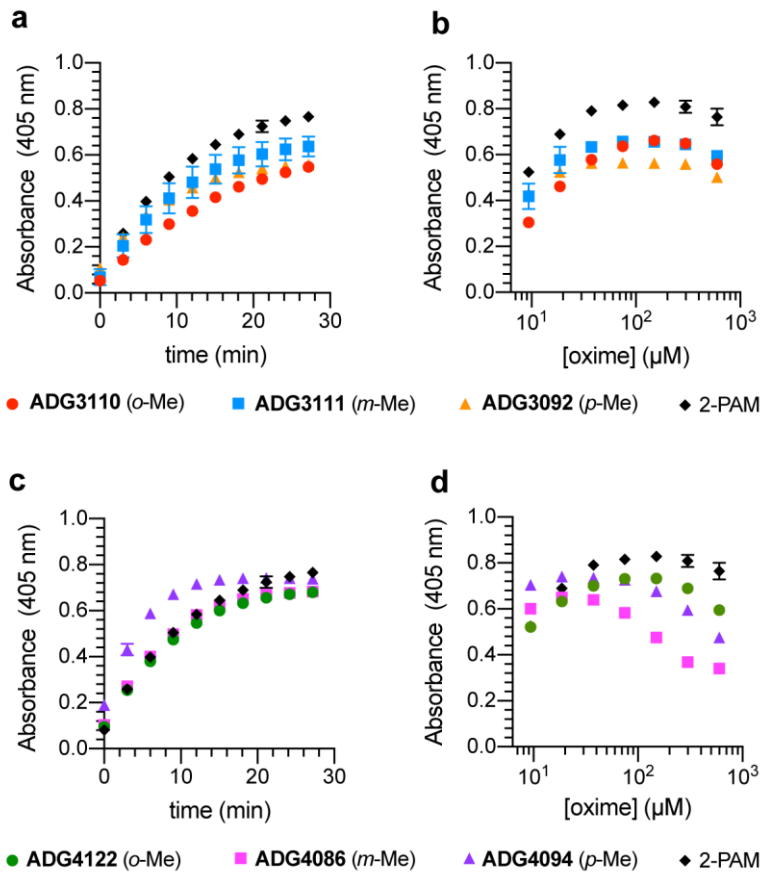

Figure 35. In vitro reactivation of *Ee*AChE inhibited with 2% v/v paraoxon in isopropanol by methyl-substituted analogs. a) 18 μM phenyl ether analogs. b) dose-response of phenyl ether analogs at 18 min. c) 18 μM phenyl sulfide analogs. d) dose-response of phenyl sulfide analogs at 18 min. Data are mean ± SD. n = 3.

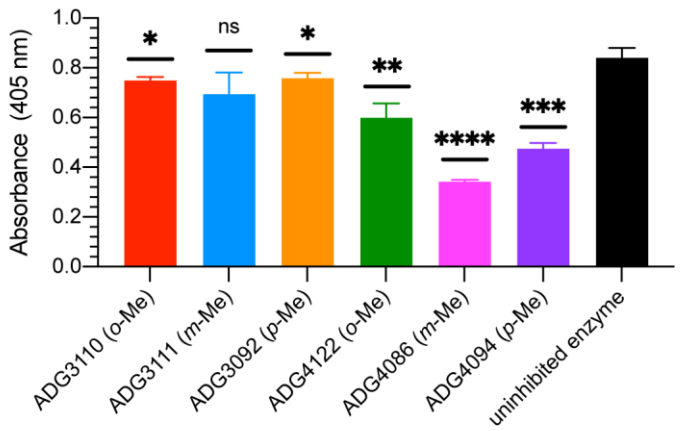

Figure 36. Inhibition of *Ee*AChE by 600 µM methyl-substituted analogs at 9 min. *p < 0.05; **p < 0.01; ***p < 0.001; ****p < 0.0001 as determined by an unpaired, two-tailed t-test. Data are mean ± SD. n =

In contrast to the methyl-substituted phenyl analogs, reactivation efficiency was variably impacted by the addition of a methoxy substituent (Figure 37); phenyl ethers were more sensitive to the substitution. *p*-Methoxyphenyl ether **ADG3121** maintained efficiency and had activity equivalent to 2-PAM at 18 µM (Figure 37a). However, *m*-methoxyphenyl ether **ADG3128** and *o*-methoxyphenyl ether **ADG3120** were only 60% and 25% as efficient as 2-PAM at 18 µM after 27 min, respectively. The dose-response curves revealed similar trends (Figure 37b); **ADG3121** was as effective as 2-PAM at all concentrations tested, while **ADG3128** and **ADG3120** were notably less efficient. Although *o*-methoxyphenyl ether **ADG3120** had inhibitory effect on *Ee*AChE at 600 µM, reducing enzymatic activity by approximately 30% (Figure 38), the low reactivation efficiency at 18 µM suggests that the this analog likely adopts an unfavorable conformation during reactivation.

Incorporation of a methoxy substituent had less of an impact in the sulfide series. At 18 µM, *m*-methoxyphenyl sulfide **ADG4153** and *p*-methoxyphenyl sulfide **ADG3192** exhibited reactivation efficiencies equivalent to 2-PAM. *o*-Methoxyphenyl sulfide **ADG4118** was 57% as

efficient as 2-PAM after 27 min (Figure 37c). At concentrations less than 75 μM, **ADG4153** and **ADG3192** exhibited reactivation efficiencies equivalent to 2-PAM, but enzyme activity decreased in a concentration dependent manner at concentrations greater than 75 μM (Figure 37d). The *o*-methoxyphenyl sulfide **ADG4118** was notably less efficient than 2-PAM at all concentrations tested and also had a slight decrease in reactivation at concentrations greater than 75 μM. The decrease in apparent enzyme activity in the presence of sulfide analogs at concentrations exceeding 75 μM can be attributed to enzyme inhibition by the reactivator (Figure 38). Phenyl ethers are more sensitive to the addition of a methoxy group than phenyl sulfides. It is unclear whether the sensitivity is due to electronics, sterics, or a combination of both factors.

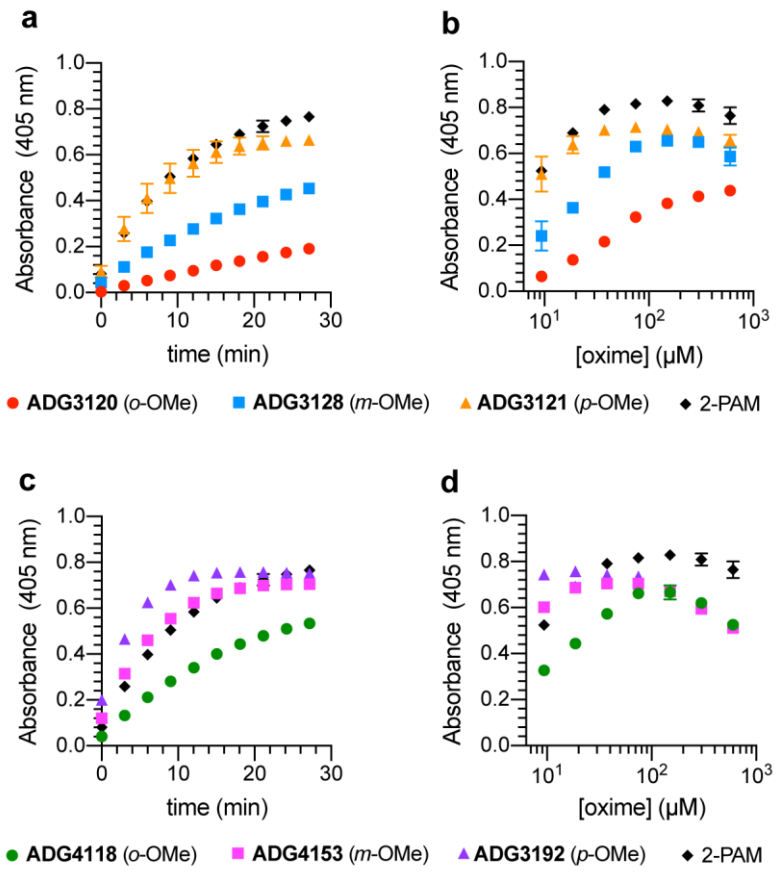

Figure 37. In vitro reactivation of *Ee*AChE inhibited with 2% v/v paraoxon in isopropanol by methoxy-substituted analogs. a) 18 μM phenyl ether analogs. b) dose-response of phenyl ether analogs at 18 min. c) 18 μM phenyl sulfide analogs. d) dose-response of phenyl sulfide analogs at 18 min. Data are mean ± SD. n = 3.

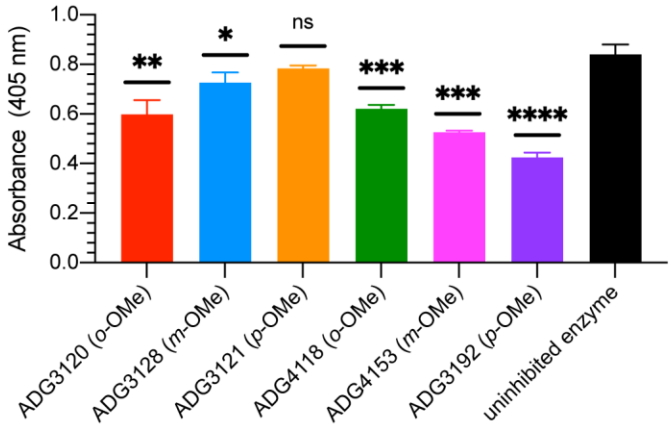

Figure 38. Inhibition of *Ee*AChE by 600 μM methoxy-substituted analogs at 9 min. *p < 0.05; **p < 0.01; ***p < 0.001; ****p < 0.0001 as determined by an unpaired, two-tailed t-test. Data are mean ± SD. n = 3.

Encouraged by the results of methoxy-substituted phenyl ether analogs, larger alkyl and aryl groups were explored in the meta and para positions of the phenyl ring to further probe the steric constraints of the binding gorge. Analogs with an isopropoxyphenoxy substituent could be synthesized via Scheme 10. The synthesis began with the S_NAr of **2-4** with the corresponding diphenol to generate ethers **3-21a** and **3-21b** in 66 and 25% yield, respectively. The etherification of **3-21a** and **3-21b** with 2-iodopropane installed the isopropyl group to yield **3-22a** and **3-22b** in 89 and 83% yield, respectively. Next, oximes **3-23a** and **3-23b** were generated via a one-pot acetal deprotection and condensation with hydroxylamine in 80% to quantitative yield. Lastly, the final analogs **ADG5044** and **ADG5045** were furnished in 72 and 88% yield by *N*-methylation with MeI.

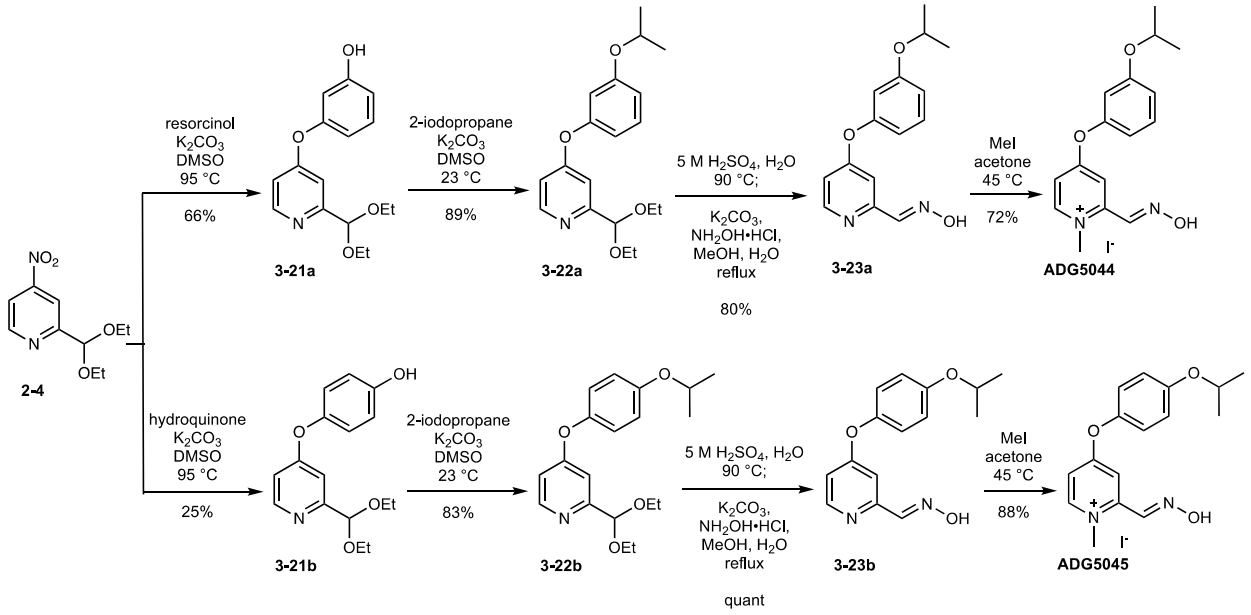

Scheme 10. Synthesis of isopropoxy-substituted analogs.

Similarly, the diphenoxy or naphthyl analogs could be synthesized according to Scheme 11. For both subseries, S_NAr of **2-4** with the corresponding nucleophile forms the key C–O or C–S bonds to afford **3-24a–e** in 82–99% yields. Next, oximes **3-25a–e** were generated in 72–99% yields. Finally, *N*-methylation with MeI produced the desired final compounds in 30% to quantitative yields.

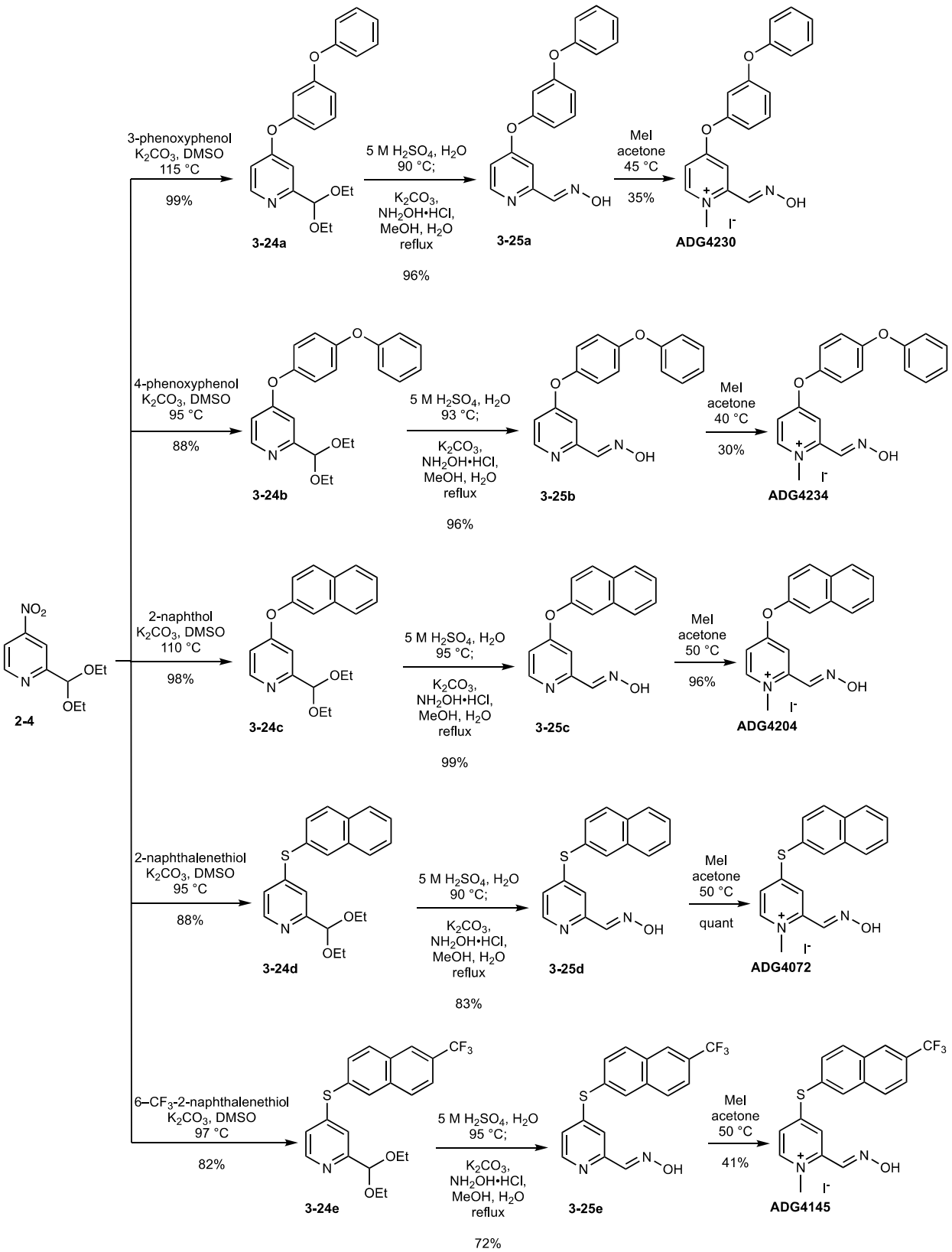

Scheme 11. Synthesis of diphenoxy- and naphthyl-substituted analogs.

Increasing the steric bulk of substituents had varying effects. Reactivation with 18 μM *m*- and *p*-isopropoxyphenyl ethers **ADG5044** and **ADG4045** showed that inclusion of an isopropoxy group decreased activity in comparison to 2-PAM (Figure 39a) and related methoxy-substituted analogs, **ADG3128** and **ADG3121**. This trend was also observed at all concentrations tested (Figure 39b). Further increasing the size of the substituent to a phenoxy had a remarkable impact on reactivation efficacy. *m*-Phenoxy phenyl ether **ADG4230** lacked the ability to reactivate paraoxon-inhibited *Ee*AChE at all concentrations tested (Figure 39c and d). The poor activity cannot be attributed to enzyme inhibition (Figure 40), suggesting that the enzyme binding pocket cannot accommodate the steric bulk of the *m*-phenoxy group. In contrast, *p*-phenoxyphenyl ether **ADG4234** yielded an efficient reactivator at 18 μM (Figure 39c). At concentrations less than 75 μM, this ether exhibited reactivation efficiencies only slightly inferior to 2-PAM, but enzyme activity decreased in a concentration dependent manner at concentrations greater than 75 μM (Figure 39d). The meta position of the phenyl ring was more sensitive to sterics than the para position.

Naphthyl ether **ADG4204** also efficiently reactivated the enzyme at 18 μM (Figure 39c). The naphthyl ether had a similar reactivation profile to *p*-phenoxyphenyl ether **ADG4234** when examining a range of concentrations (Figure 39d). At this time the decrease in enzyme reactivation of **ADG4234** and **ADG4204** at concentrations greater than 75 μM, cannot be explained; neither reactivators have an inhibitory effect on *Ee*AChE (Figure 40). The reactivation profiles of naphthyl sulfide **ADG4072** and its trifluoromethyl variant **ADG4145** showed that they were as efficient as 2-PAM at 18 μM. The dose-response curves reveal negligible differences between these two naphthyl sulfides; both are as effective as 2-PAM at concentration less than 75 μM. As with other sulfide analogs discussed, there was a slight decrease in reactivation when oxime concentrations

exceed 75 μM. In this case, the decrease can be attributed to enzyme inhibition by the reactivator (Figure 40).

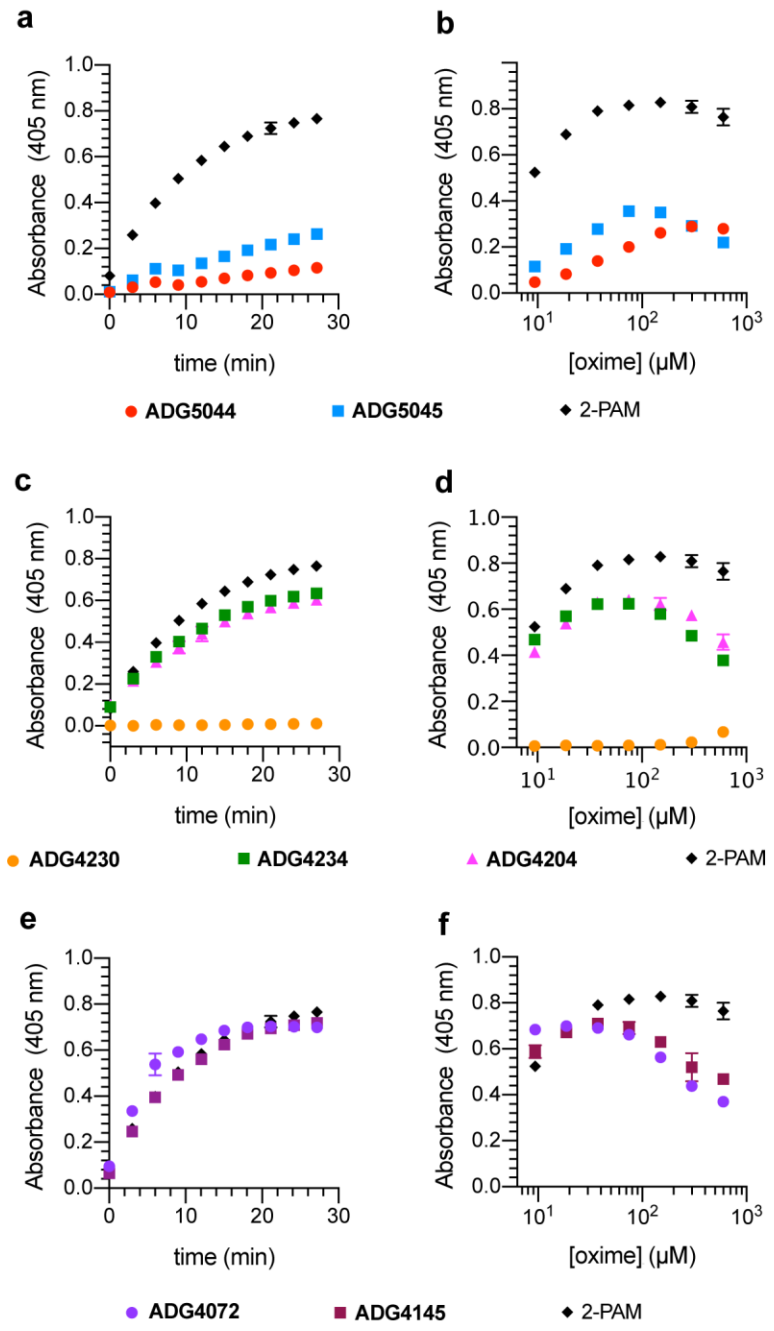

Figure 39. In vitro reactivation of *Ee*AChE inhibited with 2% v/v paraoxon by isopropoxyphenyl ether-, diphenoxy-, and napthyl-substituted analogs. a) 18 μM isopropoxyphenyl ether analogs. b) dose-response of isopropoxyphenyl ether analogs at 18 min. c) 18 μM diphenoxy and naphthyl ether analogs d) dose-response of diphenoxy and naphthyl ether analogs at 18 min. e) 18 μM naphthyl sulfide analogs d) dose-response of naphthyl sulfide analogs at 18 min. Data are mean ± SD. n = 3.

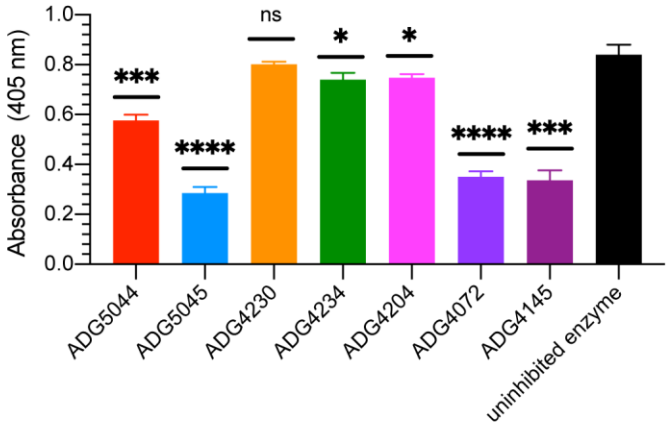

Figure 40. Inhibition of *Ee*AChE by 600 μM isopropoxyphenyl ether-, diphenoxy-, and napthyl-substituted analogs at 9 min. *p < 0.05; ***p < 0.001; ****p < 0.0001 as determined by an unpaired, two-tailed t-test. Data are mean ± SD. n = 3.

The permeability the aryl ether and aryl sulfide analogs involved in this SAR campaign was measured by a parallel artificial membrane permeability assay (PAMPA).[123] This trans-well in vitro assay system determines the passive permeability of small molecules through a lipid-infused artificial membrane. More specifically, the membrane was coated with 4% lecithin in dodecane, then 500 μM solutions of each analog was added to the apical well. After 18 h, the concentration of each reactivator in the basal well was determined by measuring the absorbance at each analogs' λ_{max}. The absorbance was then compared to the absorbance of a 200 μM solutions because that would be the maximum concentration if the apical and basal wells were in equilibrium. Unfortunately, the addition of phenyl ether and phenyl sulfide groups had a negligible effect on the permeability of the novel reactivators presented in this study (Figure 41). These results suggest that the structural modifications made in this study may not be sufficient for improving passive diffusion. However, PAMPA does not consider the possibility of the our compounds being substrates for influx transporters.[124]

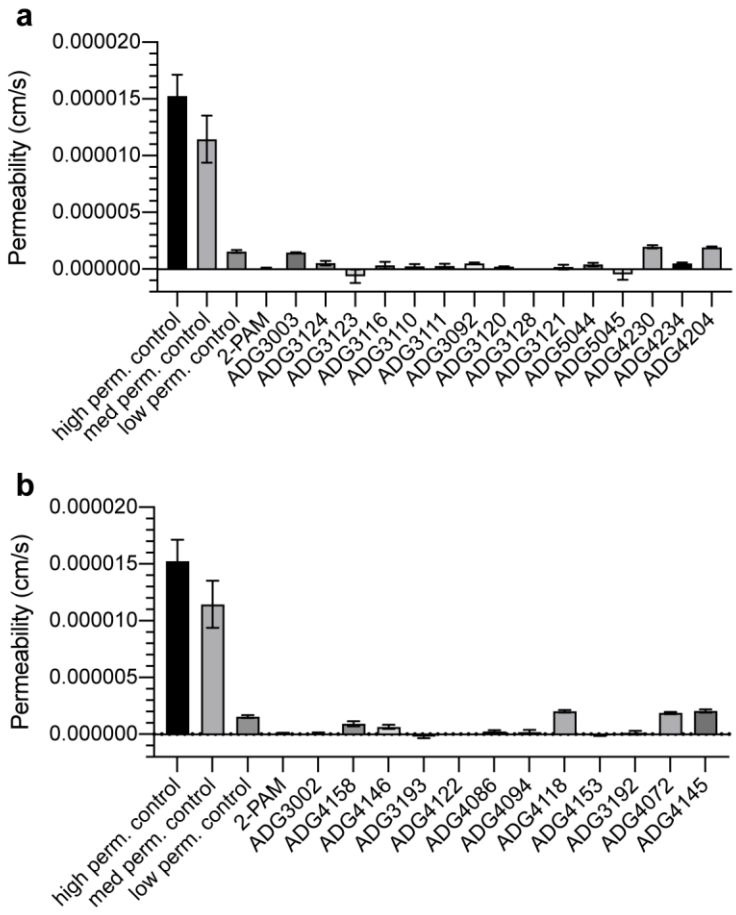

Figure 41. Passive permeability as determined by PAMPA assay. (a) ether analogs. (b) sulfide analogs. Data are mean ± SD. n = 3.

2.3.2 Conclusions

The current work shows that exploration of the 4-position of 2-PAM is a promising approach for the discovery of improved drug candidates. More specifically, incorporation of phenyl ether and sulfides on the core pyridinium scaffold of 2-PAM can enhance the reactivation of paraoxon-inhibited *Ee*AChE. However, the exact contribution of oxygen and sulfur at the

atomic level is unclear at this point. Furthermore, the activity of parent ether and sulfide **ADG3003** and **ADG3002** can be modulated by the addition of fluoro-, methyl-, methoxy-, isopropoxy-, phenoxy-, and naphthyl substituents (summarized in Figure 42). Based on in vitro reactivation alone, it is unlikely that any of the substituted analogs developed and discussed in this section would replace **ADG3003** and **ADG3002** as lead compounds. However, the analogs of this section may serve as viable alternatives if **ADG3003** and **ADG3002** have undesirable pharmacokinetic properties and/or in vivo activity.

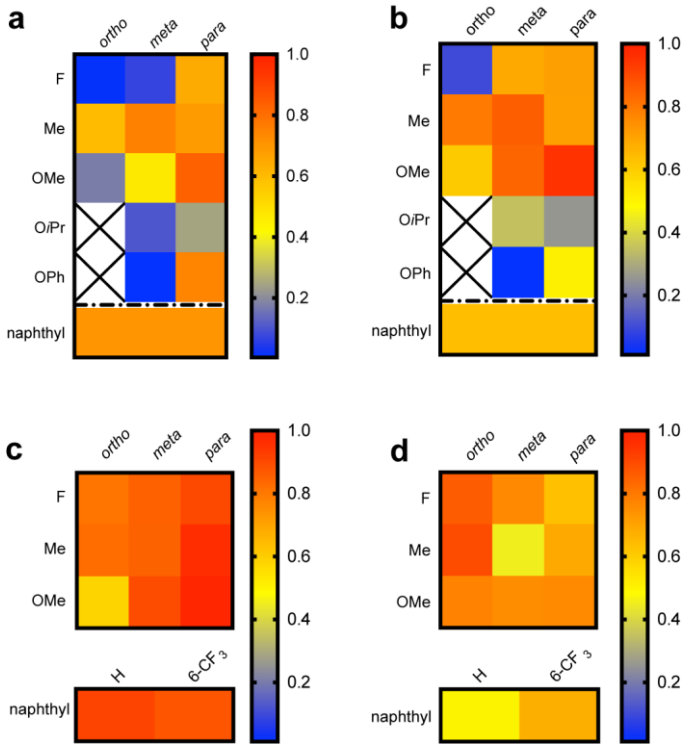

Figure 42. Summary of in vitro reactivation of paraoxon-inhibited *Ee*AChE by aryl ether and aryl sulfide analogs. a) 18 μM aryl ether analogs at 18 min b) 600 μM aryl ether at 18 min c) 18 μM aryl sulfide analogs at 18 min d) 600 μM aryl sulfide at 18 min. The absorbance of each analog at the specificed concentration and time point was used in to generate the above summary. The data was normalized (feature scaling).

2.4 Aryl analogs

Based on the results of the methyl scan series, I designed a series of phenyl analogs with various linkers at the 4-position of 2-PAM. Phenyl substituents were selected in effort to increase hydrophobicity for possibly better BBB permeability and π-π stacking with residues lining the binding gorge of AChE.[4, 15] In this section, ethynyl and ethylene linkers were examined first to determine whether unsaturated or saturated linkers were preferred. Successively, analogs with systematic changes in linker length and atom composition were designed. Because 4-phenoxy-2-PAM (**ADG3003**) was found to be an efficient reactivator of paraoxon- and OPNA-inhibited AChE and tolerant of methyl groups in modifiable positions of the phenyl ring, I fused the phenoxy moiety of **ADG3003** with a phenethyl scaffold to generate a new series of analogs.

2.4.1 Results

Phenylethynyl and phenethyl analogs were synthesized according to Scheme 12. Bromopyridine **3-5** underwent Sonogashira cross-coupling[125] with phenylacetylene to afford **4-1** in 87% yield. The hydrogenation of alkyne **4-1** generated **4-2** in 56% yield. A one-pot acetal deprotection-condensation procedure with **4-1** and **4-2** generated oximes **4-3** and **4-4** in quantitative and 56% yields, respectively. Finally, *N*-methylation of oximes **4-3** and **4-4** with MeI afforded final compounds **ADG2173** and **ADG2180** in 67 and 98% yields, respectively.

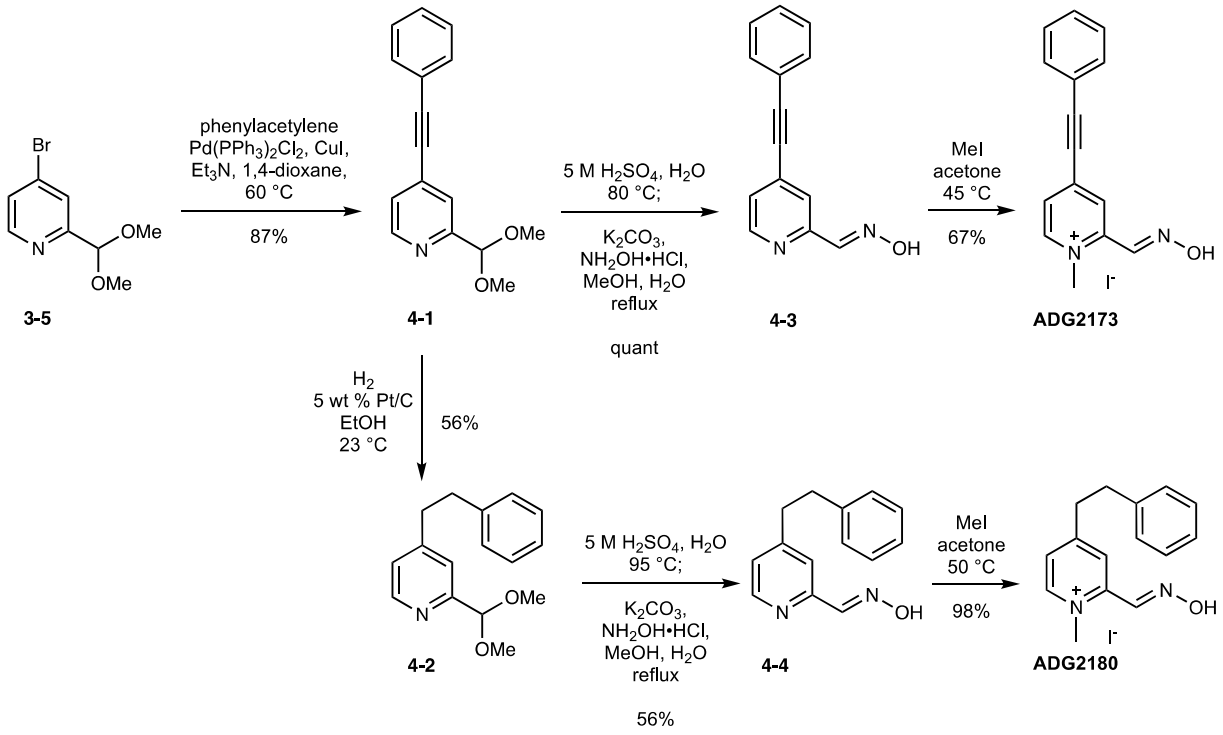

Scheme 12. Synthesis of ADG2173 and ADG2180.

The in vitro reactivation efficiency of 4-phenylethynyl analog **ADG2173** and 4-phenethyl analog **ADG2180** was determined using Ellman's assay as previously described. 4-Phenylethynyl analog **ADG2173** and 4-phenethyl analog **ADG2180** were 46% and 37% as efficient as 2-PAM at 18.8 μM, respectively (Figure 43a). The dose-response curves of **ADG2173** and **ADG2180** revealed that apparent enzyme reactivation is not dose-dependent. 4-Phenylethynyl analog

ADG2173 and 4-phenethyl analog **ADG2180** consistently showed approximately 50 and 25%, respectively, of the activity of 2-PAM at all concentrations tested. (Figure 43b).

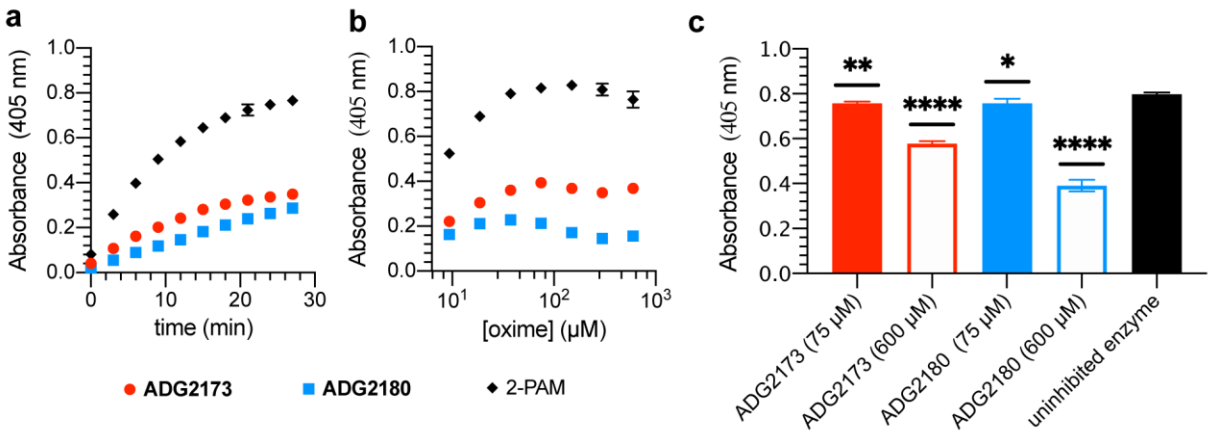

Figure 43. In vitro activity of ADG2173 and ADG2180. (a) reactivation of *Ee*AChE inhibited with 2% v/v paraoxon in isopropanol by 18 μM oxime (b) reactivation of *Ee*AChE inhibited with 2% v/v paraoxon in isopropanol dose-response at 18 min (c) inhibition of *Ee*AChE by ADG2173 and ADG2180 at 9 min. *p < 0.05; **p < 0.01; ***p < 0.001; ****p < 0.0001 as determined by an unpaired, two-tailed t-test. Data are mean ± SD. n = 3.

In effort to understand the reactivation trends, 4-phenylethynyl analog **ADG2173** and 4-phenethyl analog **ADG2180** were incubated with *Ee*AChE to determine whether the oximes could inhibit the enzyme. Figure 43c shows that neither **ADG2173** nor **ADG2180** inhibited *Ee*AChE at 75 μM. However, enzyme activity was reduced by approximately 30% in the presence of 600 μM analog **ADG2173**. Likewise, analog **ADG2180** reduced *Ee*AChE activity by approximately 50%.

Despite the moderate reactivation efficacies, 4-phenylethynyl analog **ADG2173** and 4-phenethyl analog **ADG2180** were tested at USAMRICD to determine the reactivation efficiencies against nerve agents (Figure 44). The multi-agent screening (Figure 44a) revealed that after 53 min, 10 μM doses of **ADG2173** and 2-PAM reactivated 7% of sarin-inhibited *h*AChE, while

ADG2180 reactivated 14%. Against cyclosarin-inhibited *h*AChE, **ADG2173** and **ADG2180** were 2.4- and 2.8-fold more efficient than 2-PAM, respectively. At 10 μM, 2-PAM and **ADG2173** were modest reactivators of VX-inhibited *h*AChE, reactivating 6 and 7%, respectively. However, **ADG2180** reactivated 15% of VX-inhibited *h*AChE at the same dose. **ADG2180** reactivated only 2% of VR-inhibited *h*AChE, while 2-PAM reactivated 6% and **ADG2173** reactivated 11%. The ability of 4-phenethyl analog **ADG2180** to reactivate 7% of tabun-inhibited *h*AChE, especially at a 10 μM dose, is noteworthy. In comparison, 2-PAM and **ADG2173** reactivated ≤1%. None of the oximes were able to reactivate soman-inhibited *h*AChE.

Reactivation using 1000 μM doses (Figure 44b) was also studied. After 53 min, 4-phenethyl analog **ADG2180** was the most efficient reactivator of sarin-inhibited *h*AChE. At the same concentration, unsaturated **ADG2173** was only 63% as effective as 2-PAM. Additionally, 4-phenethyl analog **ADG2180** was also the most efficient reactivator against cyclosarin-inhibited *h*AChE; **ADG2180** was 182% more efficient than 2-PAM. 4-Phenylethynyl analog **ADG2173** was 121% more efficient than 2-PAM. Against VX-inhibited *h*AChE, **ADG2180** was twice as efficient in comparison to 2-PAM, while **ADG2173** was equivalent to 2-PAM. Disappointingly, 4-phenethyl analog **ADG2180** showed poor reactivation of VR-inhibited *h*AChE and was only 16% as efficient as 2-PAM. In contrast, **ADG2173** was equally effective as 2-PAM against VR-inhibited *h*AChE. Remarkably, **ADG2180** moderately reactivated tabun-inhibited *h*AChE, while **ADG2173** and 2-PAM barely reactivated tabun-inhibited *h*AChE. None of the oximes were effective against soman.

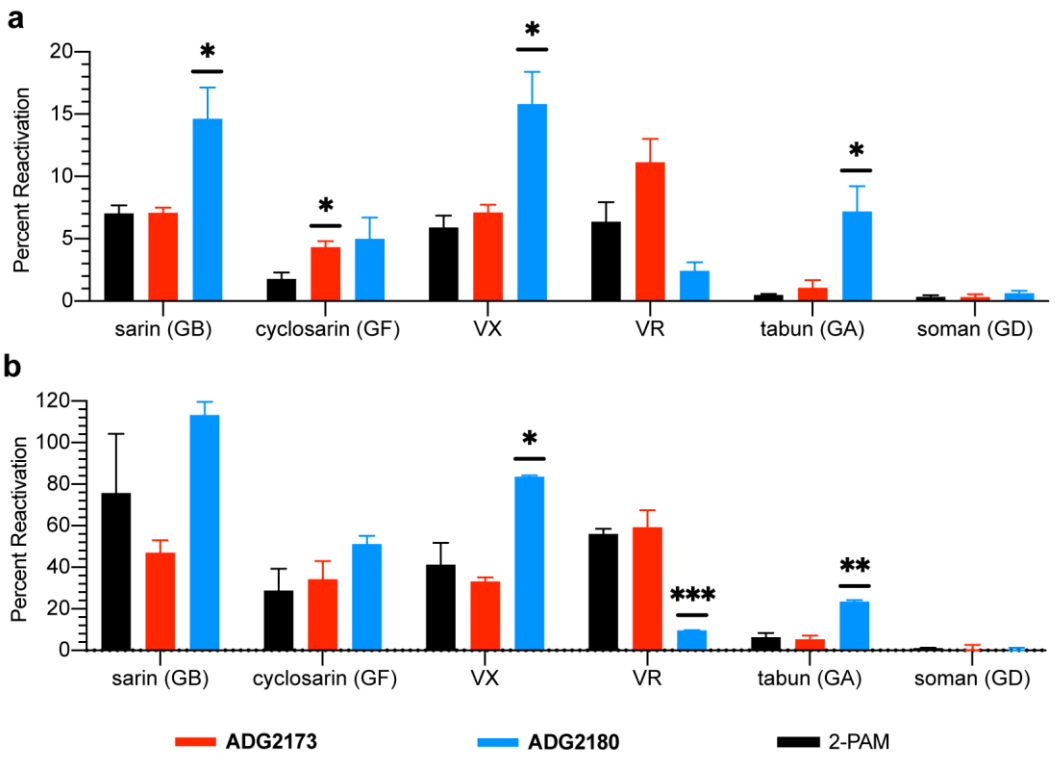

Figure 44. Reactivation of OPNA-inhibited *h*AChE using (a) 10 or (b) 1000 μM 2-PAM, ADG2173, and ADG2180 at 53 min. *p < 0.05; **p < 0.01; ***p < 0.001; as determined by an unpaired, two-tailed t-test. Data are mean ± SD. n = 2.

Although **ADG2173** was the more effective reactivator of paraoxon-inhibited *Ee*AChE, it remained less efficient than 2-PAM. Additionally, performance of **ADG2173** in the multi-agent screen was inadequate to replace 2-PAM. In contrast, 4-phenylethyl analog **ADG2180** elicited limited reactivation of paraoxon-inhibited *Ee*AChE but had exceptional activity in the multi-agent screen and reactivated four of the six nerve agents tested. It is of special note that **ADG2180** has the ability to reactivate tabun-inhibited AChE.

Encouraged by these results, I selected the saturated linker for further investigation and designed additional phenethyl analogs. An analog featuring an amide was proposed, as

cheminformatic analysis of 420,000 bioactive molecules revealed that the amide functional group is the most common, existing in 40% of molecules analyzed.[107] The initial synthetic route for the amido analog began with the reaction of aldehyde **4-5** and phosphonate **4-6** (Scheme 13). Aldehyde **4-5** was transformed into alkyne **4-7** in 81% yield following the Ohira-Bestmann modification[126-128] of Seyferth-Gilbert homologation[129, 130]. However, Sonogashira coupling of alkyne **4-7** and bromopyridine **3-5** was unsuccessful in producing **4-8**; unreacted starting materials were recovered. It is likely that the electron deficiency of alkyne **4-7** prevents formation of the copper acetylide and/or transmetalation. There is literature precedence for the formation of the copper acetylide[131]. However, preparation required stoichiometric CuI and the acetylide was isolated before being subjected to a Castro-Stephens coupling reaction[132] with *p*-iodonitrobenzene. In contrast, the reaction conditions in Scheme 13 used catalytic CuI. Furthermore, *p*-iodonitrobenzene would be more reactive than bromopyridine **3-5** in any type of organometallic coupling reaction.

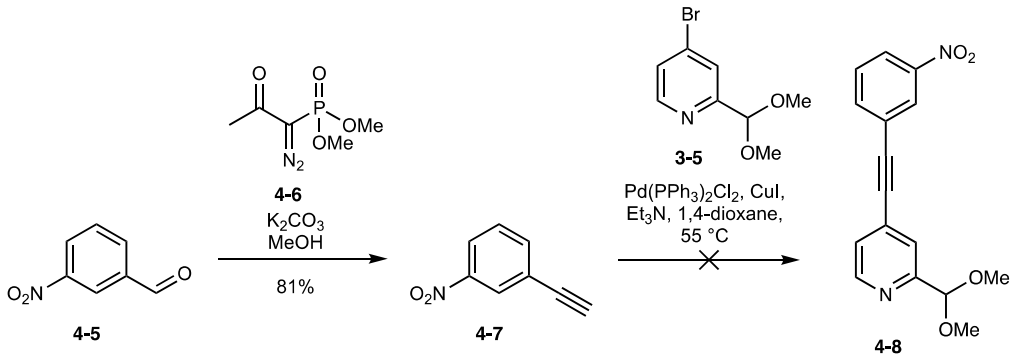

Scheme 13. Failed synthesis of 4-8.

As an alternative, Sonogashira coupling of bromopyridine **3-5** and TMS acetylene yielded alkyne **4-9** in quantitative yield. A literature procedure[133] was adopted for in situ desilylation of **4-**

9 and Sonogashira coupling with nitrobromobenzene **4-10** to furnish **4-8** in 47% yield. Universal reduction of **4-8** produced **4-11** in 93% yield. Amine **4-11** was reacted with propionic anhydride to furnish amide **4-12** in 74% yield. However when **4-12** was subjected to the one-pot acetal deprotection-condensation procedure, a mixture of **4-13** and an unidentifiable byproduct was formed. Attempts to isolate **4-13** were futile. As a result, the amido analog was abandoned.

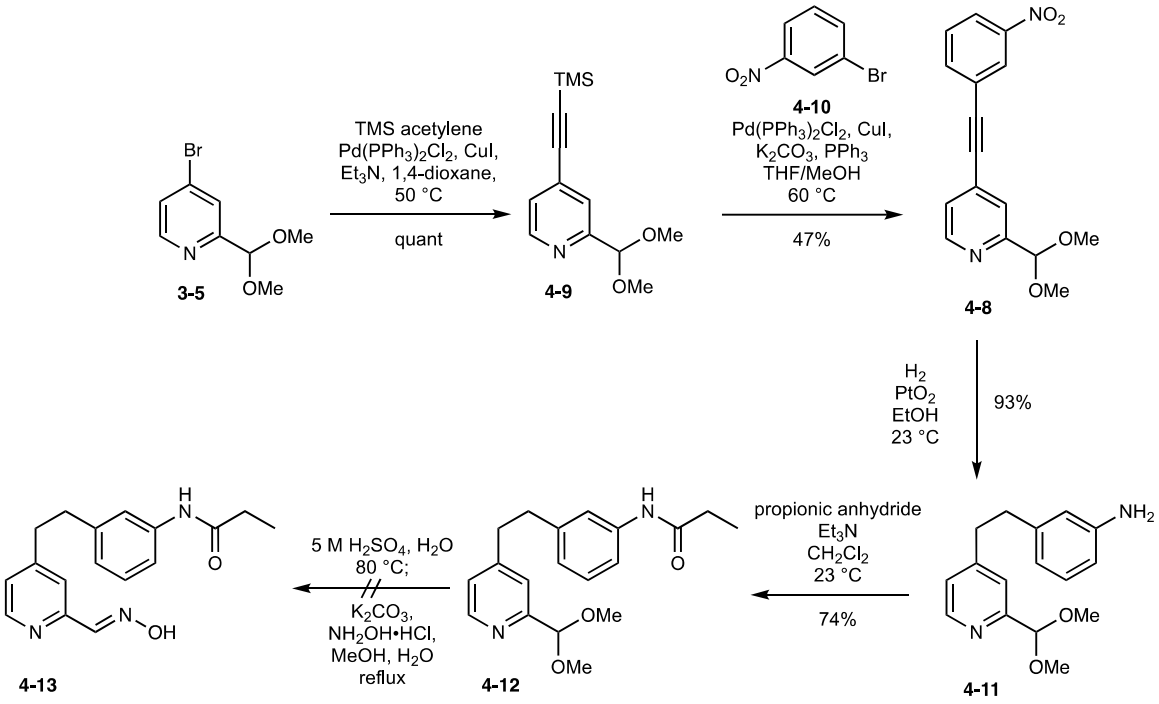

Scheme 14. Synthetic route for amido analog.

Ether substituted-phenethyl analogs were also designed and synthesized. For example, 3-methoxyphenethyl analog **ADG4063** was synthesized according to Scheme 15. Sonogashira cross-coupling of **3-5** with commercially available 3-ethynylanisole afforded the desired coupling product **4-14** excellent yield. Hydrogenation of alkyne **4-14** furnished **4-15** in 62% yield. A one-pot acetal deprotection-condensation procedure generated oxime **4-16** in 74% yield. Finally, *N*-methylation of oxime **4-16** with MeI afforded final product **ADG4063** in 94% yield.

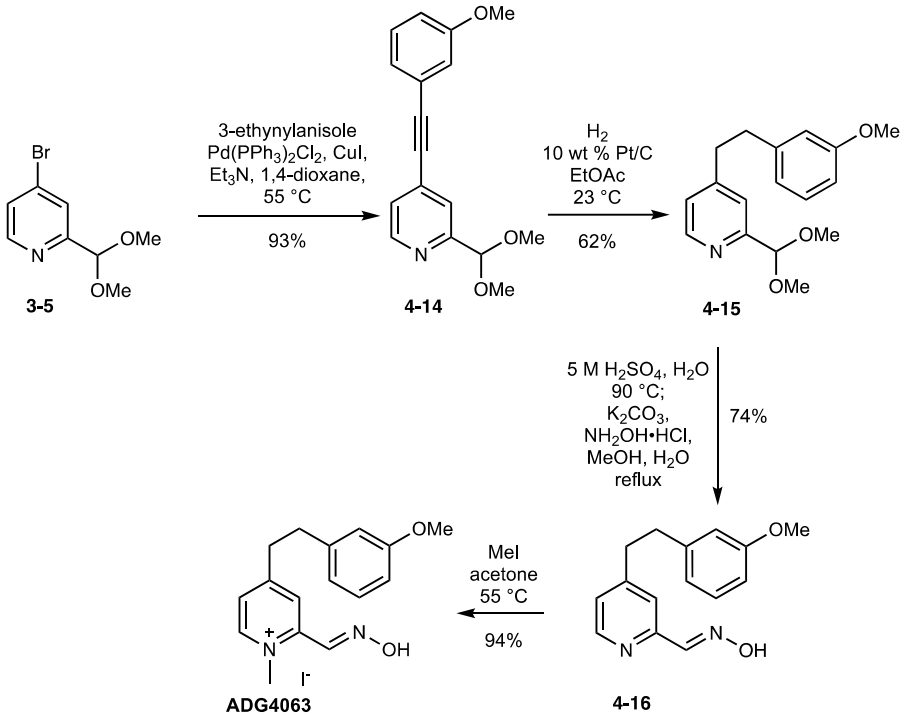

Scheme 15. Synthesis of ADG4063.

To probe steric effects, an isopropoxyphenethyl analog was designed. However, the required alkynyl coupling partner was not commercially available. The initial synthetic route to synthesize the alkynyl coupling partner (Scheme 16) was unsatisfactory. Following a literature procedure [134] for etherification of **4-17** with 2-iodopropane afforded a 3:1 mixture of **4-18** and unreacted **4-17**. The mixture was subjected to reaction with phosphonate **4-6**, which afforded alkyne **4-19** in 45% yield. However, this route was undesirable because etherification did not go to completion despite long reaction times (51 h). Using the mixture of **4-17** and **4-18** for homologation produces a mixture of alkynes, which were troublesome to separate. Homologation was also found to be irreproducible. As a result, an alternate route was pursued. Treatment of bromophenol **4-20** with 2-iodopropane and K_2CO_3 generated ether **4-21** in 69% yield. Subsequent

Sonogashira cross-coupling of **4-21** with trimethylsilylacetylene afforded **4-22** in 91% yield. Finally, desilylation furnished alkyne **4-19** in 81% yield.

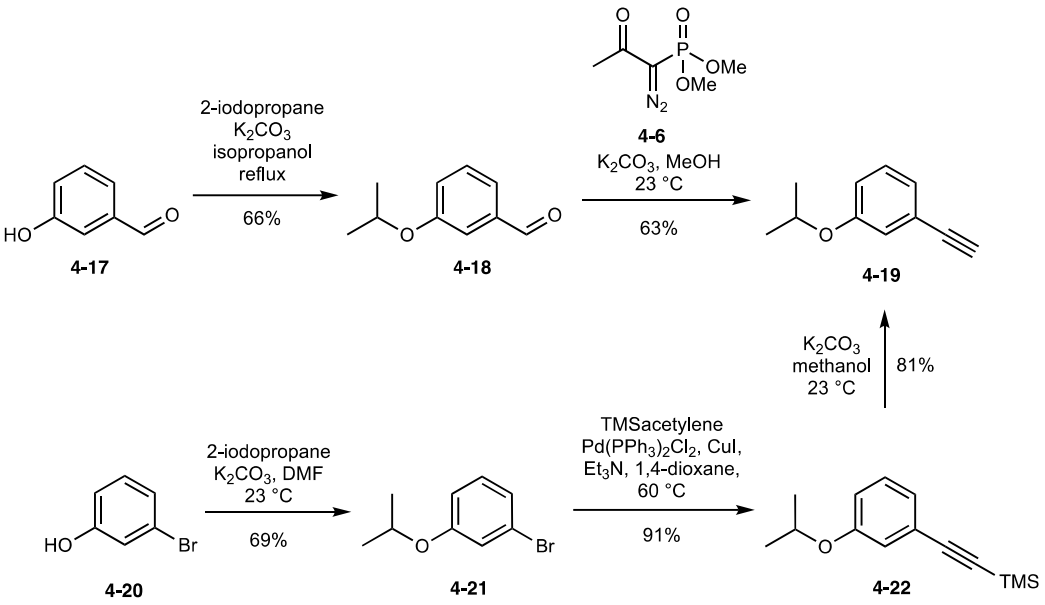

Scheme 16. Synthesis of 4-19.

Prepared alkyne **4-19** was found to undergo Sonogashira cross-coupling with **3-5** to afford the desired coupling product **4-23** in excellent yield. Hydrogenation of alkyne **4-23** furnished **4-24** 80% yield. A one-pot acetal deprotection-condensation procedure generated oxime **4-25** in quantitative yield. Finally, *N*-methylation of oxime **4-25** with MeI afforded final product **ADG4111** in 66% yields.

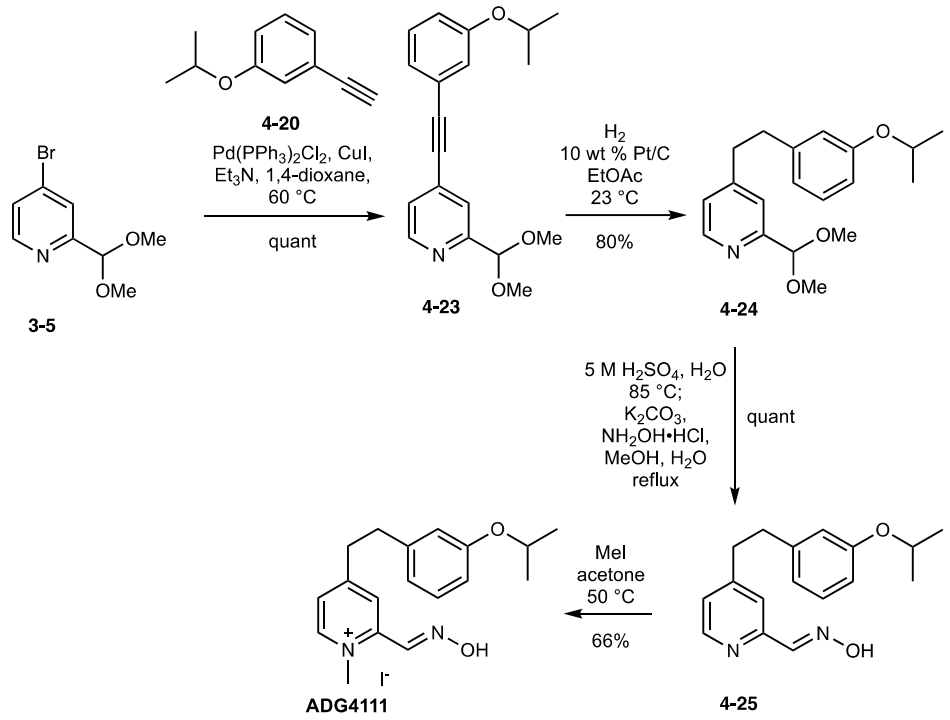

Scheme 17. Synthesis of ADG4111.

The in vitro reactivation efficiency of **ADG4063** and **ADG4111** was determined using the modified Ellman's assay as previously described. At 18.8 μM, the reactivation profiles of **ADG4063** and **ADG4111** were nearly identical to **ADG2180**, the unsubstituted parent compound. Both **ADG4063** and **ADG4111** were approximately 37% as efficient as 2-PAM (Figure 45a). Additionally, **ADG4063** and **ADG4111** were less efficient than 2-PAM at all concentrations tested but had indistinguishable reactivation profiles in comparison to the unsubstituted parent compound, **ADG2180**. The apparent lack of dose-dependent enzyme reactivation was attributed to slight enzyme inhibition by **ADG4063** and **ADG4111** (Figure 46). Unfortunately, at the time of this study, multi-agent screening at USAMRICD has been halted, so the ability of **ADG4063** and **ADG4111** to reactivate OPNA-inhibited *h*AChE remains unknown. However, given that **ADG2180** was only a moderate reactivator of paraoxon-inhibited AChE, but was effective against

OPNA-inhibited AChE, I cannot exclude the possibility of **ADG4063** and **ADG4111** being efficient reactivators of OPNA-inhibited *h*AChE.

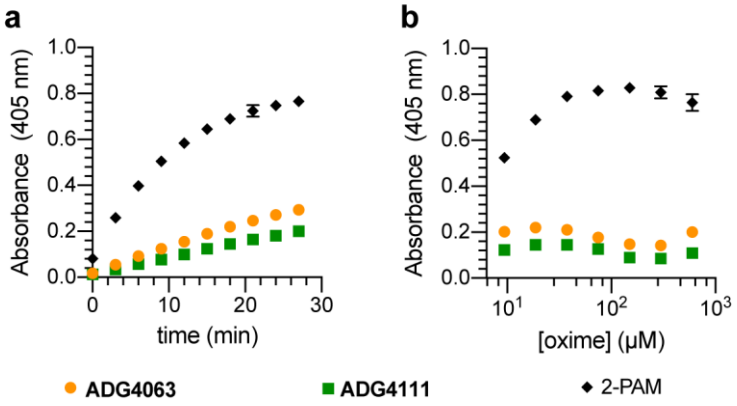

Figure 45. In vitro of *Ee*AChE inhibited with 2% v/v paraoxon in isopropanol by ADG4063 and ADG4111. (a) reactivation of 18 μM oxime.(b) dose-response at 18 min. Data are mean ± SD. n = 3.

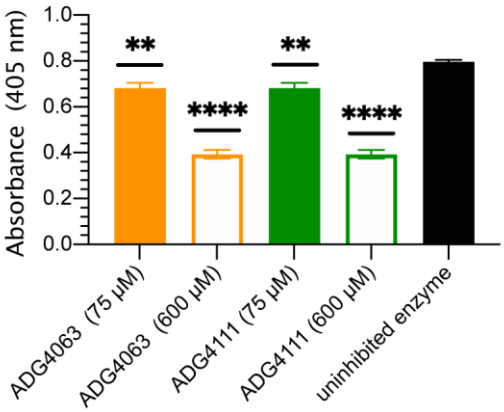

Figure 46. Inhibition of *Ee*AChE by ADG4063 or ADG4111 at 9 min. **p < 0.01; ****p < 0.0001 as determined by an unpaired, two-tailed t-test. Data are mean ± SD. n = 3.

Inspired by the superiority of **ADG2180** over 2-PAM in vitro, I designed a series of analogs with extended alkyl chains and included alkyl ethers to determine the ideal linker length and atom composition. Phenalkyl analogs were synthesized according to

Scheme 18; bromopyridine **3-5** underwent Sonogashira cross-coupling with the corresponding alkyne to afford alkynes **4-26a–c** 30% to quantitative yields. Hydrogenation of alkynes **4-26a–c** generated the corresponding saturated compounds **4-27a–c** in 64–88% yields. A one-pot acetal deprotection-condensation procedure generated oximes **4-28a–c** in 52–96% yields. Finally, *N*-methylation of oximes **4-28a–c** with MeI afforded 2-PAM analogs **ADG4300**, **ADG4244**, and **ADG4282** in 59% to quantitative yields.

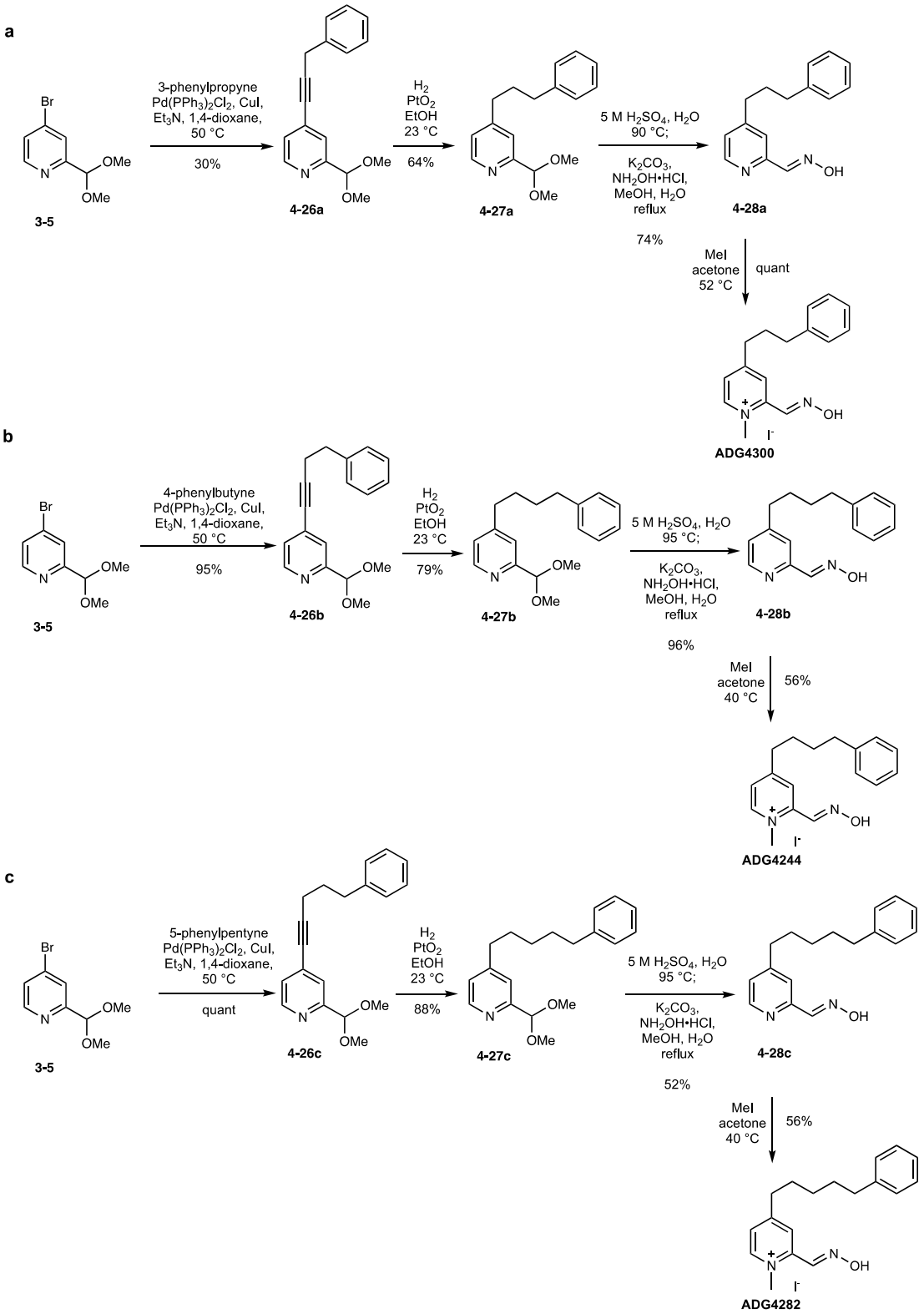

Scheme 18. Synthesis of phenalkyl analogs.

Phenalkyl ether analogs were synthesized according to Scheme 19. Nitropyridine **2-4** underwent nucleophilic aromatic substitution (S_NAr) with the corresponding alcohol to form ethers **4-29a–d** in 70% to quantitative yields. Subsequently, a one-pot procedure for acetal deprotection-condensation with hydroxylamine afforded oximes **4-30a–d** in 56–98% yields. Lastly, *N*-methylation furnished final products in 97% to quantitative yields.

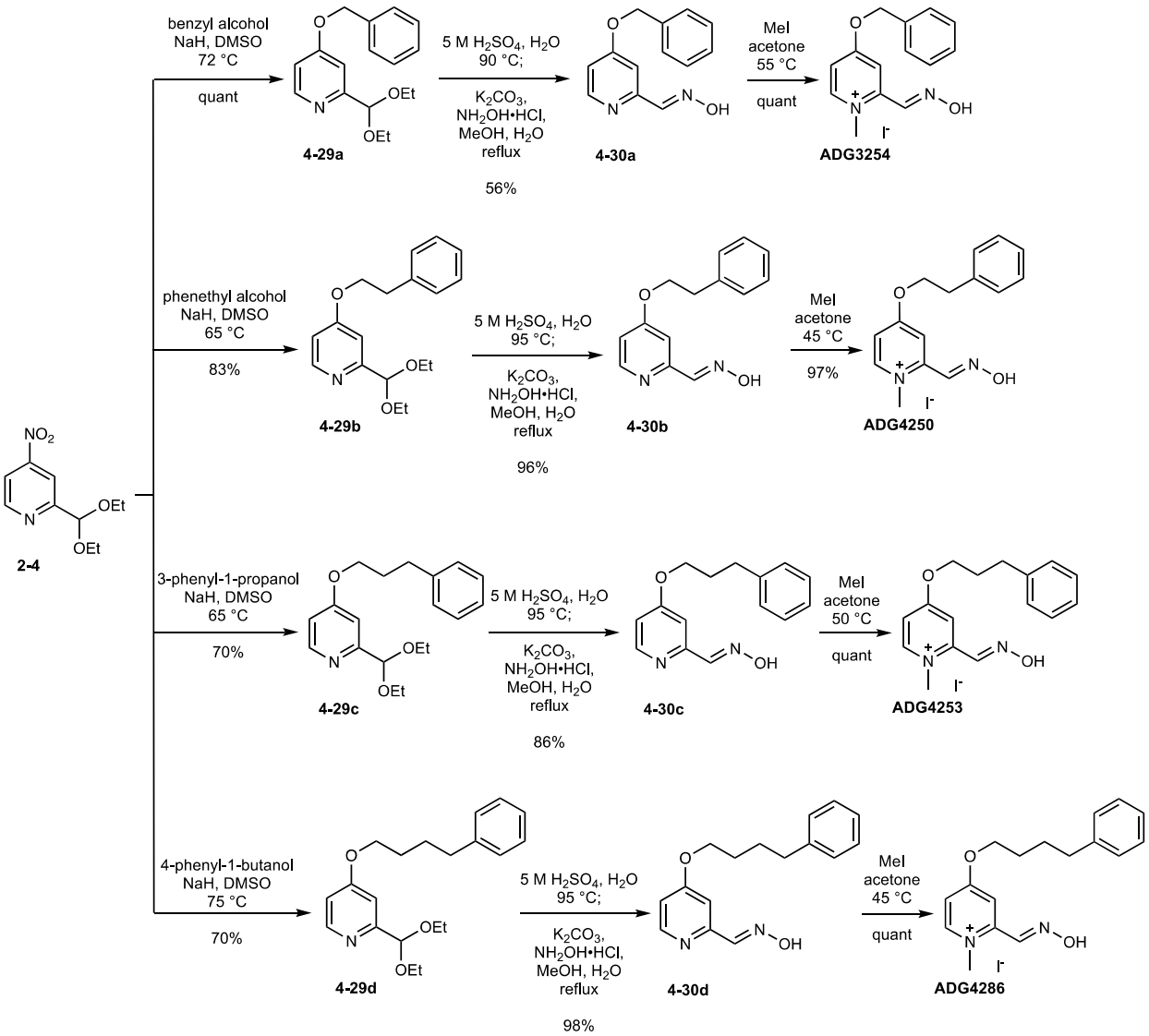

Scheme 19. Synthesis of phenalkyl ether analogs.

The phenalkyl analogs were tested for the ability to reactivate paraoxon-inhibited *Ee*AChE. At 18.8 μM, the reactivation profiles of butyl- and pentyl-linker analogs **ADG4244** and **ADG4282** were identical; both analogs were 65% as efficient as 2-PAM (Figure 47a). Propyl analog **ADG4300** was 45% as efficient as 2-PAM (Figure 47a). When examining the dose-response, butyl- and pentyl-linker analogs **ADG4244** and **ADG4282** exhibited moderate activity at concentrations below 75 μM. Apparent enzyme activity decreased with concentrations exceeding 75 μM, which could be attributed to enzyme inhibition by the oxime (Figure 48). Propyl-linker analog **ADG4300** showed a dose-dependent increase in enzyme activity with concentrations below 75 μM; concentrations greater than 75 μM led to reduced apparent enzyme activity. As with the other phenalkyl analogs, this decrease was due to enzyme inhibition by the oxime (Figure 48). Overall, increasing the length of the alkyl linker provided a slight increase in reactivation efficiency. However, phenalkyl analogs inhibited *Ee*AChE at higher concentrations. Although the phenalkyl series offered limited protection against paraoxon-inhibited *Ee*AChE, further investigation may be warranted given the poor correlation between the activity of **ADG2180** against paraoxon-inhibited *Ee*AChE and OPNA-inhibited *h*AChE.

I also determined the in vitro reactivation of the phenalkyl ether analog series. The phenalkyl ethers elicited partial reactivation at 18.8 μM (Figure 47c). Additionally, enzyme activity increased with an increase in linker length. The dose response of the phenalkyl ether analogs series (Figure 47d) is similar to phenalkyl analogs series; apparent enzyme activity increases with concentrations below 75 μM after which apparent enzyme decreases as a result of inhibition by the oxime (Figure 48). This series also shows a positive correlation between increasing linker-length and apparent enzyme activity.

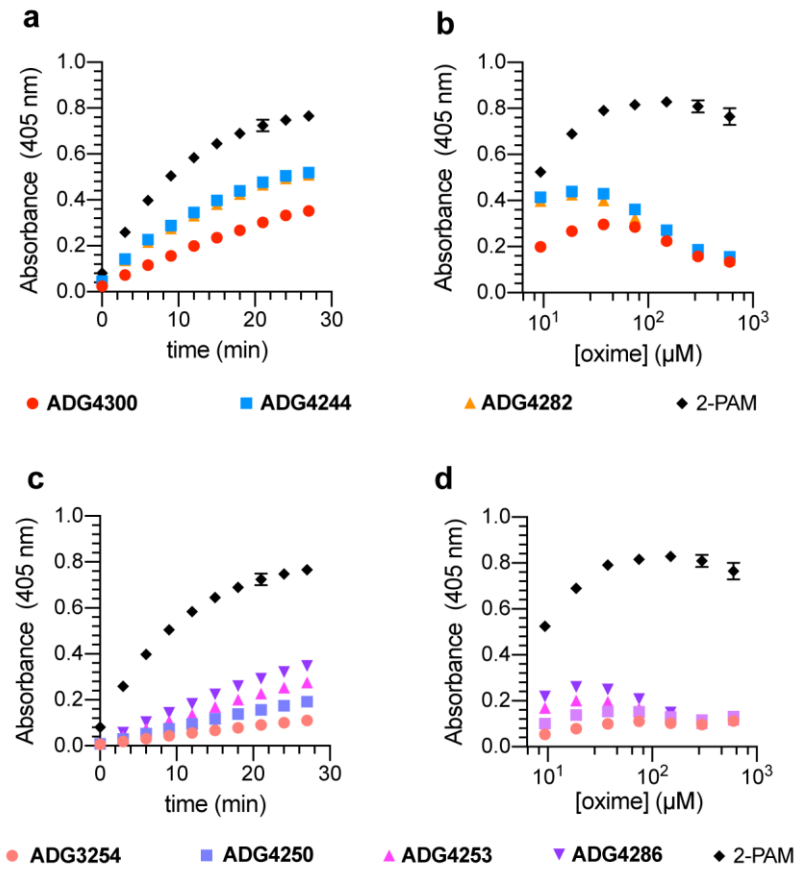

Figure 47. In vitro reactivation of *Ee*AChE inhibited with 2% v/v paraoxon by phenalkyl and phenalkyl ether analogs. (a) reactivation of 18 μM phenalkyl oxime (b) dose-response of phenalkyl oximes at 18 min (c) reactivation of 18 μM phenalkyl ether oxime (d) dose-response of phenalkyl ether oximes at 18 min. Data are mean ± SD. n = 3.

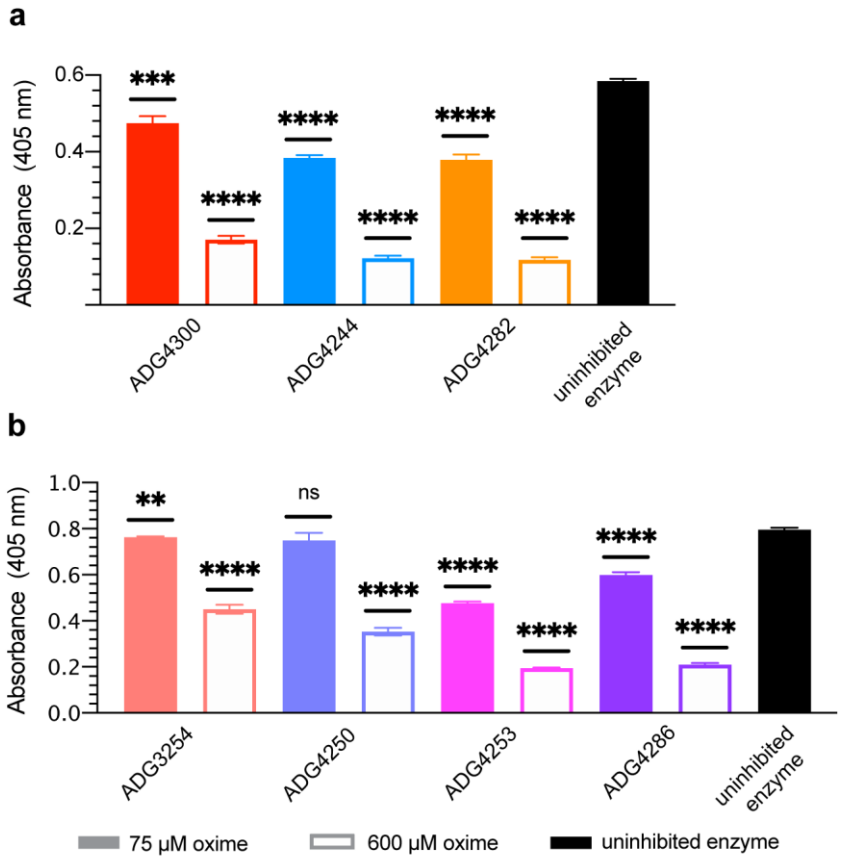

Figure 48. Inhibition of *Ee*AChE by phenalkyl or phenalkyl ether analgos at 9 min. **p < 0.01; ***p < 0.001; ****p < 0.0001 as determined by an unpaired, two-tailed t-test. Data are mean ± SD. n = 3.

As discussed, 4-phenoxy-2-PAM (**ADG3003**) was found to be an exceptional reactivator of paraoxon- and OPNA-inhibited AChE and tolerant of methyl groups in modifiable positions of the phenyl ring. The next series fused the phenyl ether of **ADG3003** with the phenethyl moeity of **ADG2180**. This series was synthesized from nitropyridine **2-4** (Scheme 20). The 2-, 3-, and 4-bromophenols underwent S_NAr with **2-4** to afford **4-31a–c** in 50–99% yields. Sonogashira cross-coupling of these products with phenylacetylene generated alkyne **4-32a–c** products in 83–98% yields. Hydrogenation of alkynes **4-32a–c** afforded the saturated derivatives **4-33a–c** in 84% to quantitative yields. Oximes **4-34a–c** were prepared in 61% to quantitative yields via a one-pot

acetal deprotection and condensation with hydroxylamine. Finally, *N*-methylation of oximes **4-34a–c** with MeI afforded the final products in 50–95% yields.

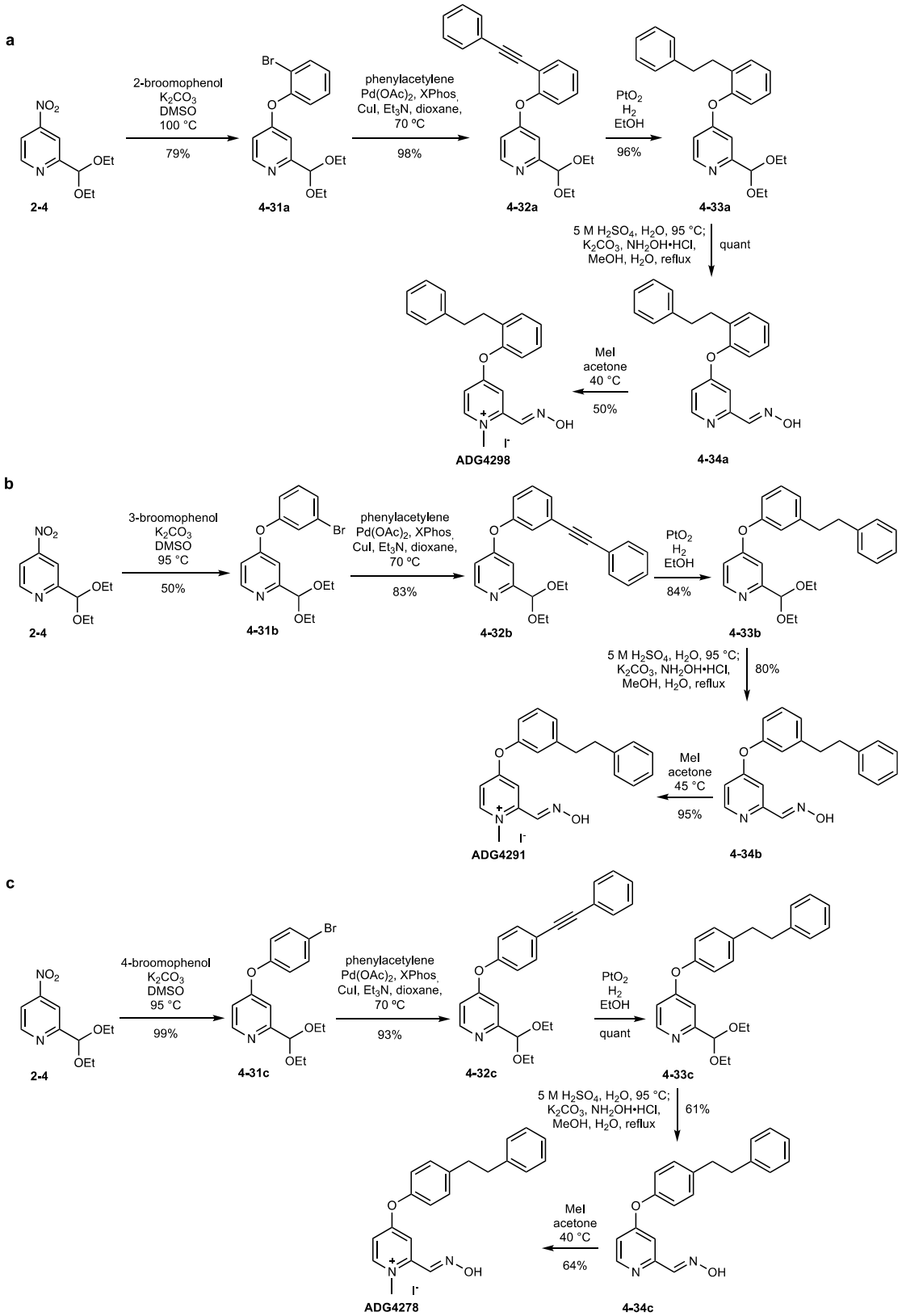

Scheme 20. Synthesis of phenethyl phenoxy analogs.

In vitro testing of the phenethyl phenoxy analogs using paraoxon-inhibited *Ee*AChE was conducted (Figure 49). At 18.8 µM, only *o*-phenethyl phenoxy analog **ADG4298** elicited a response (Figure 49a), although only 46% as effective as 2-PAM at 27 min; **ADG4298** was approximately half as effective as 2-PAM at all concentrations tested (Figure 49b). *m*-Phenethyl phenoxy analog **ADG4291** could not reactivate paraoxon-inhibited *Ee*AChE at any concentration tested (Figure 49b). *p*-Phenethyl phenoxy analog **ADG4278** elicited a partial reactivation at concentrations greater than 150 µM but remained significantly less efficient than 2-PAM. In effort to understand the poor reactivation, I examined whether the phenethyl phenoxy analogs inhibited *Ee*AChE (Figure 50) to find that only *o*-phenethyl phenoxy analog **ADG4298** had a mild inhibitory effect on *Ee*AChE at 600 µM; *m*- and *p*-phenethyl phenoxy analogs did not inhibit *Ee*AChE which suggests that the enzyme cannot accommodate the additional steric bulk at the meta- and para-positions of the phenyl ring.

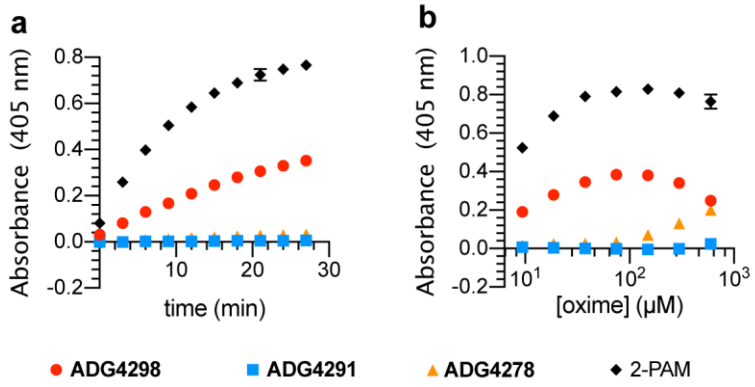

Figure 49. In vitro reactivation of *Ee*AChE inhibited with 2% v/v paraoxon in isopropanol by phenethyl phenoxy analogs. (a) reactivation of 18 µM oxime (b) dose-response at 18 min. Data are mean ± SD. n = 3.

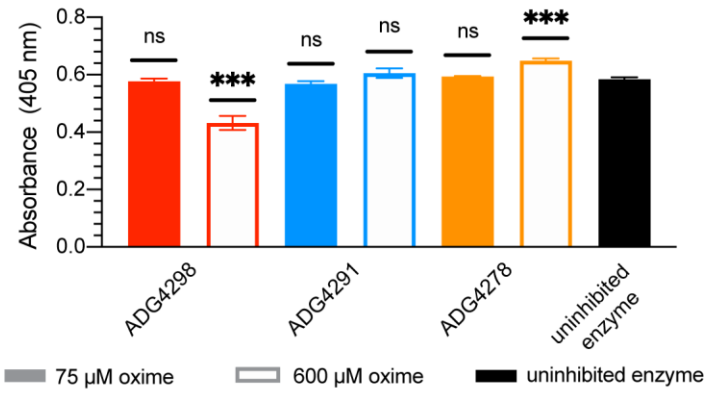

Figure 50. Inhibition of *Ee*AChE by phenethyl phenoxy analogs at 9 min. ***p < 0.001 as determined by an unpaired, two-tailed t-test. Data are mean ± SD. n = 3.

2.4.2 Conclusions

This analog series showed that saturated scaffolds were more efficient at reactivating OPNA-inhibited AChE. Additionally, **ADG2180** was identified as a superior reactivator in comparison to 2-PAM in vitro and has notable activity against tabun-inhibited AChE. The addition of ether substituents to **ADG2180** had a negligible effect on enzyme reactivation. In this section, I also developed a series of phenalkyl and phenalkyl ether analogs, which showed that longer linkers are more effective at reactivating paraoxon-inhibited AChE. Furthermore, analogs with alkyl linkers were generally more efficient than analogs with alkyl ether linkers. Lastly, I examined phenethyl phenoxy analogs, which were generally poor reactivators of paraoxon-inhibited AChE. The poor reactivation is likely due to the size of the analogs; there is not enough space within the enzyme binding pocket to accommodate the phenethyl substituent. Additional studies are needed to determine pharmacokinetic properties of **ADG2180**. The analogs of **ADG2180** presented in this section should be subjected to the multiagent screening at USAMRICD, if available in the future.

3.0 Concluding remarks

This dissertation has focused on the development of new antidotes for OPNA poisoning. The antidotes presented are analogs of 2-PAM, the only antidote approved by the United States Food and Drug Administration for the treatment of OPNA poisoning. Chapter 2.1 involved the methyl scanning of 2-PAM. The in vitro data and molecular modeling revealed that the 4-position of 2-PAM was amenable to substitution. As a result, analogs featuring ethers or sulfides in the 4-position of 2-PAM were investigated in Chapter 0. Through this study, two lead compounds were identified: phenyl ether **ADG3003** and phenyl sulfide **ADG3002**. In Chapter 2.3, analogs of **ADG3003** and **ADG3002** were explored in effort to understand the SAR. This section of work showed that the activity of parent ether and sulfide **ADG3003** and **ADG3002** can be modulated through the addition of fluoro-, methyl-, methoxy-, isopropoxy-, phenoxy-, and naphthyl substituents. Substituents had variable influence on activity. Generally, aryl sulfide analogs were less sensitive to structural modifications. Phenalkyl, phenalkyl ether, and phenethyl phenyl ether analogs were developed in Chapter 2.4. This study revealed that phenethyl analog **ADG2180** was an efficient reactivator of tabun-inhibited *h*AChE. Other analogs from this section were only moderate reactivators of paraoxon-inhibited *Ee*AChE.

In the future, in-depth computational and molecular modeling studies of phenyl ether **ADG3003,** phenyl sulfide **ADG3002**, and related analogs would provide valuable insight into the observed differences in reactivity. For example, electrostatic surface potential maps could explain how significantly the electronics of the phenyl ring is altered by the incorporation of electron withdrawing or donating groups (e.g., fluoro- and methoxy-, respectively). Afterward, the analogs could be modeled using published X-ray structures of AChE. The electrostatic surface potential

maps may aid in predicting the orientation of π-π stacking between the analog and the aromatic residues of the AChE binding gorge. Additionally, pharmacokinetic data for the analogs presented in this dissertation, especially for phenyl ether **ADG3003** and phenyl sulfide **ADG3002,** should be collected before new analog series are designed. Although the PAMPA assay indicated that none of the aryl ether or sulfide analogs were permeable, it is possible that these analogs are substrates for influx transporters. While the throughput remains low, it may be beneficial to explore the in vitro BBB permeability of lead compounds in more recent and advanced models.[135, 136]

Currently, **ADG3002** is being evaluated in vivo. The purpose of this study is to determine the protective and therapeutic indices in mice exposed to paraoxon. Additionally, brain and blood samples are being collected and analyzed to determine the concentration of **ADG3002**. Substituted phenyl sulfide analogs presented herein may be explored as an alternative to **ADG3002** if pharmacokinetic properties are undesirable or if **ADG3002** is ineffective in vivo. As previously mentioned, the analogs discussed in Chapter 2.4 should be revisited if multi-agent screening operations at USMRICD are resumed. Because **ADG2180** was only a moderate reactivator of paraoxon-inhibited *Ee*AChE, testing **ADG2180** in an animal model using paraoxon is nonsensical. However, if the opportunity for in vivo studies using nerve agents arises, phenethyl analog **ADG2180** should be evaluated.

There are several examples presented herein that underscores the importance of the balance of reactivity and binding affinity when designing antidotes for OPNA-poisoning. Based on experimental data, it remains unclear whether analogs that strongly inhibit AChE, *o*-fluorophenyl ether **ADG3124** as just one example, reactivate the enzyme before acting as an inhibitory ligand. Given that there are many regions within the binding gorge or AChE, is also unclear which area(s) inhibitory compounds are binding to. Determining the precise binding interactions between

inhibitory analogs and AChE through X-ray crystallography or 2D NMR studies may provide answers to these intellectual curiosities, however, this information is not requisite for the development of future analogs and/or further investigation of the analogs presented herein.

If a broad spectrum reactivator remain elusive, a cocktail of reactivators may be a viable and reasonable solution. For example, based on in vitro data discussed within this dissertation, if **ADG3002** or **ADG3003** were combined with **ADG2180**, it is possible that an individual would be protected against five of the six tested nerve agents and paraoxon. However, it is unlikely that a reactivator would be able to enter clinical trials if it were not capable of completely replacing 2-PAM. Alternatively, if 2-PAM is ineffective against more modern chemical weapons (i.e., Novichok agents), clinical trials of other possible antidotes may be necessary to ensure protection against all possible threats. The use of mutant *h*AChE as a detoxification and bioscavenging strategy (as reviewed by Kovarik and Hrvat)[137] is also a promising avenue.

Appendix A Supporting information

Appendix A.1 Assay experimental

***General biological procedures*:** Ellman's reagent (5,5'-dithiobis(2-nitrobenzoic acid)) (DTNB) was purchased from Acros Organics and used as received. S-acetylthiocholine iodide (ATCh) was purchased from Alfa Aesar and used as received. Paraoxon and acetylcholinesterase from *Electrophorus electricus* (electric eel) Type VI-S (200-1,000 units/mg protein) (*Ee*AChE) were purchased from Sigma-Aldrich. Absorbance was measured at 405 nm in 3 min intervals in a Modulus II Microplate Multimode Reader. The time point for the absorbance measurement was chosen as the time at which the samples containing 600 μM 2-PAM stopped increasing in absorbance. The background absorbance value was defined as the average of the absorbance values of the samples containing inhibited AChE and no reactivator. The background absorbance was subtracted from all samples. The data were plotted using GraphPad Prism 9 software. Data for each reactivator were plotted with the data for 2-PAM as a reference. The parallel artificial membrane permeability assay (PAMPA) kit was purchased from BioAssays Systems (Cat. No. PAMPA-096). Absorbance values were collected using a Shimadzu UV-1280 UV-Vis spectrophotometer.

Ellman's assay using hAChE: A solution of 1.20 mM reactivator in 100 mM phosphate pH 7.4 buffer (100 μL) was added to the wells of a clear 96-well plate. 100 mM Phosphate pH 7.4 buffer (50 μL) was added to the wells as the diluent, and two-fold serial dilutions of the reactivator were performed; the total volume of reactivator in the wells following the dilution was 50 μL. 1.02 mM DTNB in 100 mM phosphate pH 7.4 buffer (19.5 μL) and 1.36 mM ATCh in 100 mM phosphate

pH 7.4 buffer (19.5 µL) were transferred to the wells with the reactivator solutions.

Separately, 100 U/mL *h*AChE in 20 mM Tris pH 7.4 buffer (10 µL per well) was inhibited with 200 µM paraoxon dissolved in isopropanol (1 µL per well). An additional aliquot of 100 U/mL *h*AChE (40 µL) was mock inhibited with isopropanol (4 µL). After incubating for 10 min at 25 °C, the inhibited enzyme solution (11 µL) was added to the wells containing the reactivator solution. The mock-inhibited (i.e., uninhibited) enzyme (11 µL) was added to wells containing 0 µM reactivator. Absorbance was measured in 3 min intervals in a Modulus II Microplate Multimode Reader (Promega). The time point for the absorbance measurement was chosen as the time at which the samples containing 600 µM 2-PAM stopped increasing in absorbance. The background absorbance value was defined as the average of the absorbance values of the samples containing the inhibited *h*AChE and no reactivator. The background absorbance was subtracted from all samples. The data were plotted using GraphPad Prism 9 software. Data for each reactivator were plotted with the data for 2-PAM as a reference.

Ellman's assay using EeAChE: A solution of 1.20 mM reactivator in 2% v/v DMSO in 100 mM phosphate pH 7.4 buffer (100 µL) was added to the wells of a clear 96-well plate. 2% v/v DMSO in 100 mM Phosphate pH 7.4 buffer (50 µL) was added to the wells as the diluent, and two-fold serial dilutions of the reactivator were performed; the total volume of reactivator in the wells following the dilution was 50 µL. 1.02 mM DTNB in 100 mM phosphate pH 7.4 buffer (19.5 µL) and 1.36 mM ATCh in 100 mM phosphate pH 7.4 buffer (19.5 µL) were transferred to the wells with the reactivator solutions.

Separately, 10 U/mL *Ee*AChE in 20 mM Tris pH 7.4 buffer (10 µL per well) was inhibited with 0.2% v/v paraoxon dissolved in isopropanol (1 µL per well). An additional aliquot of 10 U/mL *Ee*AChE (40 µL) was mock inhibited with isopropanol (4 µL). After incubating for 10 min

at 25 °C, the inhibited enzyme solution (11 µL) was added to the wells containing the reactivator solution. The mock-inhibited (i.e., uninhibited) (11 µL) was added to wells containing 0 µM reactivator. Absorbance was measured in 3 min intervals in a Modulus II Microplate Multimode Reader (Promega). The time point for the absorbance measurement was chosen as the time at which the samples containing 600 µM 2-PAM stopped increasing in absorbance. The background absorbance value was defined as the average of the absorbance values of the samples containing the inhibited *Ee*AChE and no reactivator. The background absorbance was subtracted from all samples. The data were plotted using GraphPad Prism 9 software. Data for each reactivator were plotted with the data for 2-PAM as a reference.

Inhibition of hAChE by the reactivator: A solution of either 0 or 1.2 mM reactivator in 100 mM phosphate pH 7.4 buffer (50 µL) was added to the wells. 0 or 100 U/mL *h*AChE in 20 mM Tris pH 7.4 buffer (10 µL) was added to the reactivators. The solutions were incubated at 24 °C for 10 min. A solution containing 500 µM DTNB and 650 µM ATCh in 100 mM pH 7.4 phosphate buffer (40 µL) was added to the wells, and the absorbance was measured at 405 nm in 3 min intervals in a Modulus II Microplate Multimode Reader. The background absorbance value was defined as the average of the absorbance values of the samples without *h*AChE or reactivator. The background absorbance was subtracted from all samples. The data were plotted using GraphPad Prism 9 software.

Inhibition of EeAChE by the reactivator: A solution of either 0, 150 µM, or 1.2 mM reactivator in 100 mM phosphate pH 7.4 buffer (50 µL) was added to the wells. 0 or 10 U/mL *Ee*AChE in 20 mM Tris pH 7.4 buffer (10 µL) was added to the reactivators. The solutions were incubated at 24 °C for 10 min. A solution containing 500 µM DTNB and 650 µM ATCh in 100 mM pH 7.4 phosphate buffer (40 µL) was added to the wells, and the absorbance was measured at 405

nm in 3 min intervals in a Modulus II Microplate Multimode Reader. The background absorbance value was defined as the average of the absorbance values of the samples without *Ee*AChE or reactivator. The background absorbance was subtracted from all samples. The data were plotted using GraphPad Prism 9 software.

***Multi-agent screening assay*:** Dr. C. Linn Cadieux (USAMRICD) prepared the supplementary information regarding the multi-agent screening assay. This section has been copied from our collaborative manuscript. Aliquots of recombinant *h*AChE at approximately 0.6 mg/mL (Allotropic Tech, PN #AT1002) in 0.1 M phosphate buffer at pH 7.4 with BSA were prepared. The aliquots were incubated with inhibiting agents in at least 100-fold molar excess or buffer for 10 min. The excess inhibitor was removed using size exclusion columns (Princeton Separations, PN# CS-901) to obtain inhibited enzyme and control (uninhibited) enzyme. The resulting enzyme solution (~4 µg/mL, 170 µL) was transferred to 96-well plate.

A second 96-well plate containing 0 mM, 2 mM, 0.2 mM or 0.02 mM reactivator (>170 µL) was prepared. To initiate reactivation, 170 µL of reactivator was simultaneously pipetted via a single 96-well transfer to the enzyme plate (now labeled "Reaction plate") and mixed. At each of nine time points after the reactivation is started, samples from each well of the Reaction plate were diluted by a factor of 50 into a substrate plate with ATCh (0.8 mM) and DTNB (1.6 mM). Optical density at 412 nm was measured every 17 seconds for a total of 5 reads from each well.

Data files from the spectrophotometer were analyzed and the optical density readings and the corresponding times of those readings were used to compute the slope of substrate turnover for the well. The slopes were compared to the associated row-matched control enzyme slope to compute a percentage of reactivation of the inhibited enzyme at the time the reactivation plate was sampled.

Table 4. Example of 96-well plate used in the multi-agent screening assay

		cntrl	inh	inh	inh	inh	inh	inh	inh	inh	inh	inh	buf
[Oxime]		1	2	3	4	5	6	7	8	9	10	11	12
Zero	A	Ez	a1z	a2z	a3z	a4z	a5z	a6z	a7z	a8z	a9z	a10z	z
High	B	Eh	a1h	a2h	a3h	a4h	a5h	a6h	a7h	a8h	a9h	a10h	h
Med	C	Em	a1m	a2m	a3m	a4m	a5m	a6m	a7m	a8m	a9m	a10m	m
Low	D	El	a1l	a2l	a3l	a4l	a5l	a6l	a7l	a8l	a9l	a10l	l
High	E	Eh	a1h	a2h	a3h	a4h	a5h	a6h	a7h	a8h	a9h	a10h	h
Med	F	Em	a1m	a2m	a3m	a4m	a5m	a6m	a7m	a8m	a9m	a10m	m
Low	G	El	a1l	a2l	a3l	a4l	a5l	a6l	a7l	a8l	a9l	a10l	l
Zero	H	Ez	a1z	a2z	a3z	a4z	a5z	a6z	a7z	a8z	a9z	a10z	z

The spontaneous substrate turnover was computed as the average slope of the cells with nothing but substrate.

$$z = (A12 + H12) / 2$$

The reactivator-induced substrate turnover was computed using the cells with have nothing but reactivator.

$$h = (B12 + E12) / 2 – z$$

$$m = (C12 + F12) / 2 – z$$

$$l = (D12 + G12) / 2 – z$$

The control enzyme substrate turnover adjusted for both spontaneous and reactivator induced was computed.

$$eh = (B1 + E1) / 2 – h$$

$$em = (C1 + F1) / 2 – m$$

$$el = (D1 + G1) / 2 – l$$

$$ez = (A1 + H1) / 2 – z$$

The inhibited enzyme substrate turnover was calculated for each inhibitor concentration (agent 4 used as example).

$$a4h = (B5 + E5) / 2 – h$$

$$a4m = (C5 + F5) / 2 – m$$

$$a4l = (D5 + G5) / 2 – l$$

$$a4z = (A5 + H5) / 2 – z$$

Finally, the percent reactivation for an inhibitor was computed (agent 4 used in example) by dividing the inhibited sample slope by the slope of the control enzyme at the sample time.

$$\text{Percent reactivation (high)} = 100 * (a4h / eh)$$

$$\text{Percent reactivation (med)} = 100 * (a4m / em)$$

Percent reactivation (low) = 100 * (a4l / el)

These calculations were completed for each inhibited enzyme/reactivator concentration combination at each time point and the resulting data was analyzed using a nonlinear regression analysis for each reactivator concentration to determine an observed rate of reactivation (k_{obs}) for every sample. These values could be used to generate a calculated percent reactivation for every inhibited enzyme/reactivator combination at any specified time point of interest.

Parallel artificial membrane permeability assay (PAMPA): A 500 µM solution of high, medium, and low permeability controls (Chloramphenicol, Diclofenac, and Theophylline, respectively) in 5% v/v DMSO in PBS (500 µL) was prepared. A solution of 500 µM test compound in 5% v/v DMSO in PBS (500 µL) was prepared. A 200 µM equilibrium standard was prepared by taking an 80 µL aliquot of the 500 µM control or test compound in 5% v/v DMSO in PBS solution and diluting with PBS (120 µL). A blank control was prepared by adding 5 µL DMSO to 245 µL PBS.

300 µL PBS was added to the receiver wells. A 4% lecithin in dodecane solution was prepared by suspending dried lecithin with 750 µL dodecane. The membrane of the donor well was coated with 4% lecithin in dodecane (5 µL). 500 µM Test or control compound in 5% v/v DMSO in PBS (200 µL) was added to the donor wells. The donor plate was placed on top of the receiver plate and was incubated at 24 °C. After 18 h, the donor plate was removed. The absorbance spectrum of the equilibrium standard solution (100 µL) from 200 nm to 500 nm in 10 nm intervals was recorded to determine the peak absorbance (λ_{max}). The absorbance of the receiver well solution (100 µL) at the λ_{max} was recorded. The permeability rate (P_e) was calculated using Equation 1, where $C = 7.72 \times 10^{-16}$ (calculated following Equation 2), OD_A is the absorbance of the acceptor solution, and OD_E is the absorbance of the equilibrium standard. For Equation 2, V_D is the volume

of the donor well (0.2 cm^3) and V_A is the volume of the acceptor well (0.3 cm^3). Area refers to the area of the membrane (0.24 cm^2) and time is reported in seconds.

$$P_e = C \times -\ln\left(1 - \frac{OD_A}{OD_E}\right) \text{ cm/s}$$

Equation 1

$$C = \frac{V_D \times V_A}{(V_D + V_A) \times \text{area} \times \text{time}} \text{ cm/s}$$

Equation 2

Appendix A.2 Computational methods

Dr. James Burnett (University of Pittsburgh) prepared supplementary information regarding computational methods. This section has been copied from our collaborative manuscript.

General computational methods: All molecular modeling was performed on a Linux workstation (Dell T7600) equipped with a three-dimensional (3-D) monitor. Insight II (2005) (Dassault Systèmes BIOVIA, San Diego, CA), Discovery Studio 2018 (Dassault Systèmes BIOVIA, San Diego, CA), and Maestro 2016-1 (Maestro, Schrödinger, LLC, New York, NY) were used to build, energy refine, and inspect models, and for docking studies. The cff91 force field was used during all stages of model energy refinement. The HINT program (eduSoft LC, Richmond, VA) was used to evaluate the quality of the models via the quantitation of intermolecular contacts. The HINT parameter settings used during the studies: steric term = Lennard-Jones 6–12 (for cff91 compatibility); lone pair vector focusing = 10; and distance dependence atom-atom interactions = exp (1/*r*). Figures were generated using Pymol (the PyMOL Molecular Graphics System, Version 2.0 Schrödinger, LLC).

***Electrostatic potential surface maps*:** The Poisson-Boltzmann electrostatic surface map calculator in Maestro (Schrödinger, LLC, New York, NY) was used to generate maps for 2-PAM, 3-Me-2-PAM, 4-Me-2-PAM, 5-Me-2-PAM, and 6-Me-2-PAM (Figure 51). The maps were calculated with the following parameters: all atoms in each molecule included; forcefield: OPLS3;

solute dielectric constant: 1.0, solvent dielectric constant: 80.0; solvent radius: 0.3 Å, temperature: 298.0K; and surface resolution: 0.1.

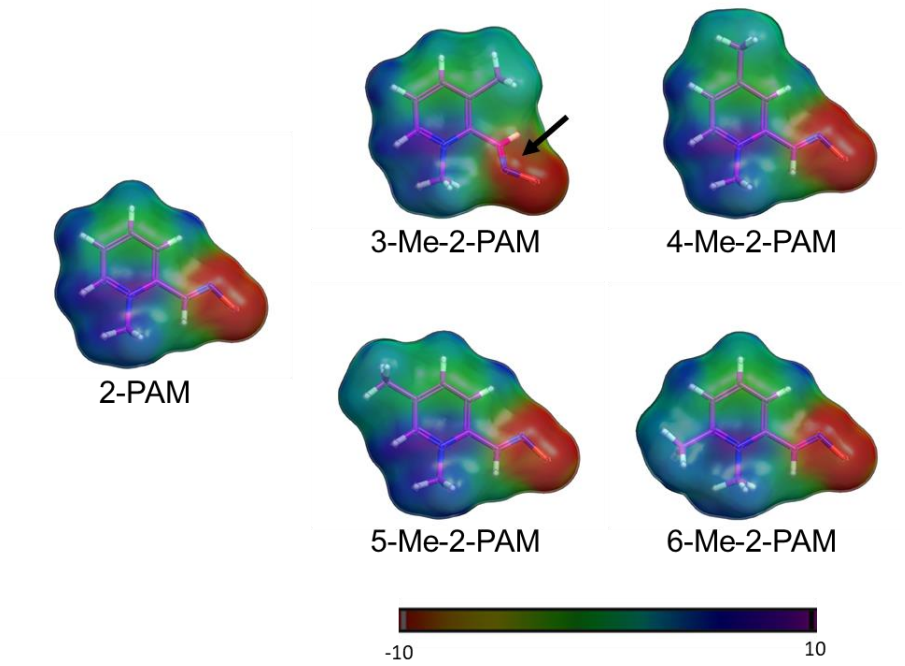

Figure 51. Electrostatic surface potential maps for 2-PAM, 3-Me-2-PAM, 4-Me-2-PAM, 5-Me-2-PAM, and 6-Me-2-PAM. Surface potent color ranges from red, which corresponds to highest electron potential to purple, which corresponds to lowest electron potential. The oxime moiety possesses the highest electron surface potential; the pyridinium nitrogen possesses the lowest electron surface potential. Notably, unlike the other derivatives, the 3-Me-2-PAM oxime group adopts a twist-plane conformation (black arrow).

Protein refinement: The AChE structure co-crystallized with 2-PAM (PDB entry 5HFA, resolution = 2.2 Å)[102] was used for molecular modeling studies to provide biochemically feasible rationales for the assay results. As noted in Section 2.1.3, the 2-PAM in the active site of PDB 5HFA is positioned such that, although engaging in a cation-π interaction with the Trp 86 side chain indole: 1) the oxime moiety points away from the covalently bound paraoxon, with the ligand's oxygen atom located 8.42 Å distance from the phosphorous atom of paraoxon (Figure

52), and 2) methyl substitutions on the pyridinium ring of 2-PAM, as it is located in the X-ray structure (Figure 52b)., did not rationalize the reactivation data (Figure 21) of the methyl scan derivatives. Consequently, 2-PAM was removed from the X-ray structure prior to energy refinement. Using Insight II (2005), a conservative energy minimization strategy was performed on both PDB structures as follows: 1) hydrogens were added, all incorrect bond assignments were corrected, N and C termini were capped, and the distance-dependent dielectric was set to 1.0, 2) hydrogen atoms only were minimized (100 steps steepest descents followed by conjugate gradients until the norm of the gradient was < 0.001 kcal/mol/Å^2), and 3) protein side chains were relaxed using the same protocol (*i.e.*, 100 steps steepest descents followed by conjugate gradients until the norm of the gradient was < 0.001 kcal/mol/Å^2).

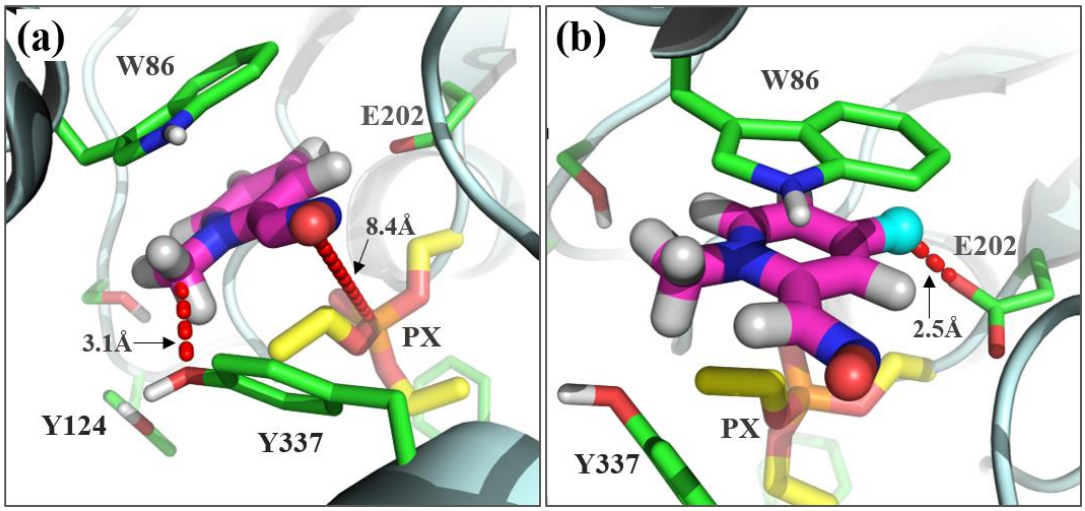

Figure 52. The binding mode of 2-PAM taken directly from PDB entry code 5HFA102 is not biochemically feasible with respect to rationalizing the reactivation of paraoxon deactivated AChE, nor does the position of 2-PAM from the X-ray structure rationalize the observed reactivation of AChE by methyl-scan derivatives. 5HFA is shown in pale cyan cartoon with select residues shown with green carbons. (a) In the X-ray structure of the 2-PAM (magenta carbons) binding mode, the oxime oxygen of the small molecule is oriented away from covalently bound paraoxon (yellow carbons, orange phosphorous), and is 8.4 Å (red dash) away from the

paraoxon phosphorous atom. This distance, and the location of the 2-PAM oxime moiety precludes a rational, structure-based foundation for understanding the reactivation of the enzyme by the small molecule. Moreover, the methyl substituted on the nitrogen atom of the pyridinium ring is located too close to the oxygen atom of the phenol side chain of Tyr 337 (red dash), which would result in a biochemically unacceptable hydrophobic-polar clash. (b) When the 2-PAM (magenta carbons) in the X-ray structure binding mode is substituted with a 4-methyl moiety (cyan carbon, hydrogens not shown for clarity of presentation), a highly unfavorable hydrophobic clash (red dash) is observed with the side chain carboxylate of residue Glu 202. This unfavorable binding is contrary to the biochemical data (Figure 21 and Figure 22) obtained for the reactivation potency of this derivative.

Small molecule docking: 2-PAM and all C-methylated methyl scan analogs described in Section 2.1 were built using Discovery Studio 2016, and energy refined in Insight II (2005) (cff91 forcefield, with the pyridinium nitrogen atom charge set to +1 and the oxime oxygen charge set to -1, distance dialectic = 1.0, and conjugate gradients minimization until the norm of the gradient < 001 kcal/mol/Å^2).

As a starting point for subsequent comparisons with derivatives, 2-PAM was first docked in the AChE binding site of 5HFA using the Insight II (2005) **(**Dassault Systèmes BIOVIA, San Diego, CA**)** graphical user interface with 3-D visualization enabled, thereby allowing for detailed small molecule positional manipulation via dial box control. The covalently bound KTA (i.e., an acetylcholine mimetic) in PDB entry 2HA0[103] was initially used to guide the binding location and orientation of 2-PAM in the AChE binding site (Figure 25a). Specifically, the energy refined structure of 5HFA and the structure of 2HA0 were superimposed in Maestro, and indicated a nearly identical alignment, with an RMSD = 0.482 Å (Figure 53). The protein structures were then imported back into Insight II (2005), and 2-PAM was superimposed on the bound substrate mimetic by aligning its oxygen oxime and pyridinium nitrogen with the KTA carbon atom that is

covalently bound to the Ser-203 side chain oxygen and the ammonium nitrogen, respectively. With 2-PAM positioned in the binding site, the van der Waals bump was set to 0.25 Å, and translational and rotational adjustments, as well as torsional adjustments to protein residue side chains (within acceptable limits defined by rotamer libraries and empirical data) were used to eliminate unacceptable atom-atom overlaps and optimize non-bonded interactions. Subsequently, HINT program (eduSoft, La Jolla, CA) analysis, iterative rounds of additional manual adjustments (translational, rotational, and torsional), conjugate gradients minimizations (2-PAM and surrounding protein residue side chains within a 10 Å radius of the binding site), and additional HINT analysis were used to direct micro-environmental adjustments between enzyme side chain atoms and 2-PAM until an optimized, biochemically feasible binding mode, which also positioned the oxime oxygen 2.3 Å from the paraoxon phosphorous, was achieved. Following, methyl scan analogs were docked in the AChE active site using the same protocol as indicated for 2-PAM (see above).

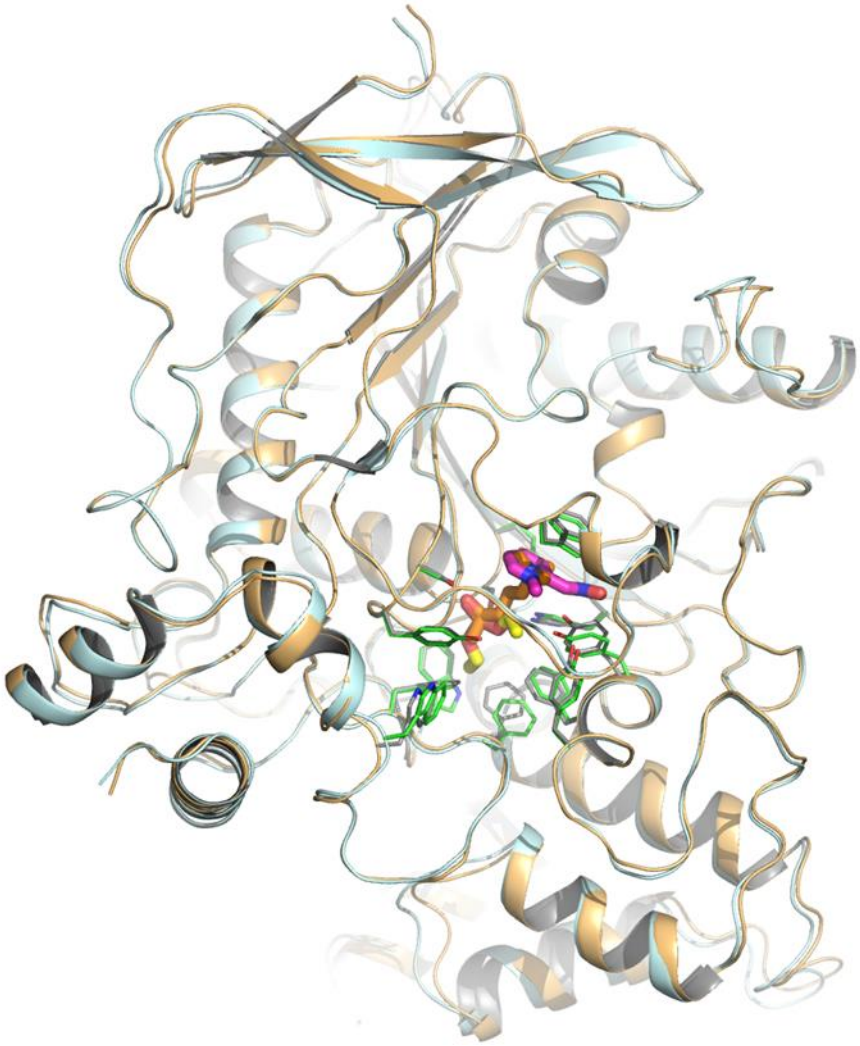

Figure 53. Alignment of the X-ray co-crystal structures PDB entry 2HA0 (mouse AChE (light orange cartoon) with KTA covalently bound to Ser 203) and 5HFA (human AChE (pale cyan cartoon) with bound 2-PAM (magenta carbons), and covalently bound paraoxon (yellow carbons)). The alignment RMSD for the two X-ray structures, including α-helices, sheets, and loops, is 0.482 Å. This image, as with the Figure 54 superimpositions of AChE from different species, shows how analogous AChE structures are across different species. As shown in greater detail in Figure 54 residues surrounding the active sites and gores are equivalent for 2HA0 and 5HFA and are shown with grey and green carbons in 2HA0 and 5HFA, respectively.

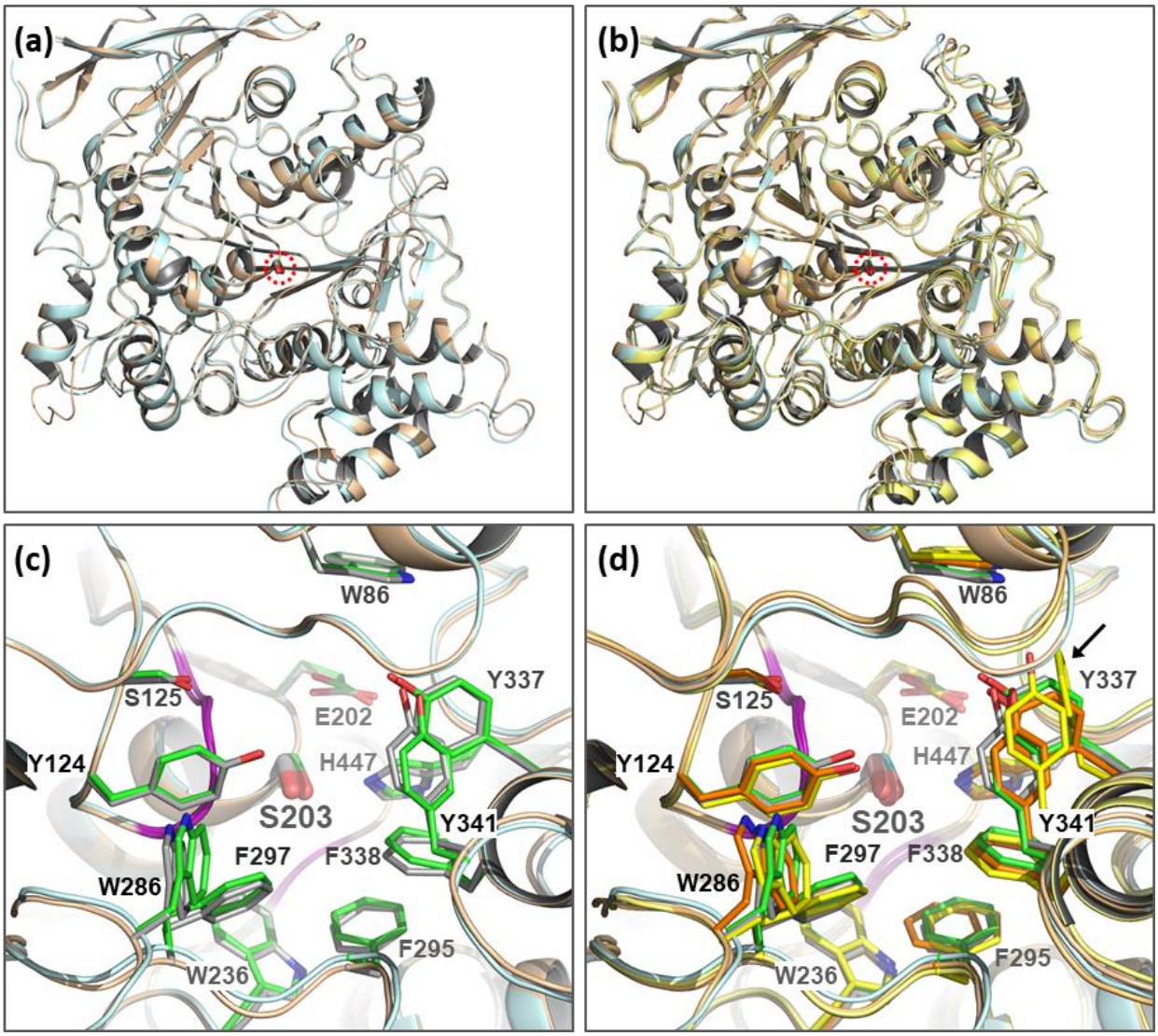

Figure 54. Superimpositions of the highest available resolution apo-state X-ray structures of AChE from phylum *Chordata* species indicate negligible differences in secondary structures, and residue conservation in the active site and gorge - across species. a) the superimposition RMSD of *h*AChE (PDB entry 4EY4[138]; resolution: 2.156 Å; light cyan cartoon) and *Ee*AChE (PDB entry: 1C2O[139]; resolution: 4.2 Å; wheat cartoon) is 0.642 Å. The red dashed circle indicates the location of catalytic Ser 203 in both species (human sequence number). b) superimpose of all X-ray structures of available species from phylum *Chordata*. Human and eel structure descriptions are the same as indicated in panel a. Mouse (*m*AChE) is PDB entry 5DTI[140] (resolution: 2.0 Å; light orange cartoon) and *Torpedo californica* AChE (*Tc*AChE) is PDB entry 1EA5[141] (resolution: 1.8 Å; light yellow cartoon). RMSD values for each non-human species X-ray structure versus the human X-ray structure: 1) human – eel: 0.642 Å, 2) human – *Torpedo*: 1.002 Å, and 3) human – mouse: 0.743

Å. The red dashed circle indicates the location of catalytic Ser-203 in all species (human residue sequence number). c) close-up view of the AChE active sites and gorges from the superimposition of human PDB entry 4EY4 and eel PDB entry 1C2O shown in panel a. Residue side chain carbons are colored green and gray for the human and eel X-ray structures, respectively. The purple cartoon segments in both structures indicate conserved interspecies Gly residues. The image clearly shows both complete residue conservation and identical side chain orientations. d) close up view of the AChE active sites and gorges from the superimposition of human PDB entry 4EY4, eel PDB entry 1C2O, mouse PDB entry 5DTI, and *Torpedo* PDB entry 1EA5 shown in panel b. Residue side chain carbons are colored green, gray, orange, and yellow for human, eel, mouse, and *Torpedo* X-ray structures, respectively. The purple cartoon segments in all structures indicate conserved interspecies Gly residues. As in panel c, the image clearly shows both complete residue and side chain orientation conservation for the human, eel, and mouse X-ray structures. Comparison with the *Torpedo* X-ray structure also indicates near complete residue and side chain orientation conservation, with two exceptions: 1) Tyr 341 (human sequence number) is slightly skewed versus the other three species, and 2) Y337 (human sequence number) is replaced with a Phe residue in *Tc*AChE.

To further elaborate on the HINT (for "Hydropathic INTeractions") program (eduSoft, La Jolla, CA), the software scores a summation of the hydropathic interactions between two interacting species during a binding event.[142-144] In this study, HINT was used to score all intermolecular atom-atom interactions between AChE and either 2-PAM or its methyl scan derivatives. The hydropathic interactions that are scored by the program fall into six categories. Favorable atom-atom contact categories include hydrogen bonds, acid-base, and hydrophobic interactions; unfavorable atom-atom contact categories include acid-acid, base-base, and hydrophobic-polar interactions. In the HINT program, each atom potential type possesses a corresponding hydrophobic atom constant a_i that is derived from the LogP partition coefficient constants calculated by Hansch and Leo.[145] Hence, the derived atom constants implicitly incorporate an estimate of entropy, which is ignored in molecular mechanics models. The

hydropathic interaction value for an atom pair b_{ij} is calculated as a function of the hydrophobic constants for each atom, the distance between the atoms, and the solvent accessible surface areas (SASA) of the two atoms.

$$b_{ij} = s_i a_i s_j a_j R_{ij}$$

The distance function, $R_{ij} = e^{-r}$, has been reported to give a good fit to published Leo polar proximity factors.[138, 139] The SASA for atoms, s_i, is taken from literature values[146] for proteins. The interaction values, b_{ij}, for each interacting atom pair are summed to provide a 'total 'HINT interaction score' for two molecular species during a binding event. The higher and more positive a total HINT interaction score, the more favorable the binding between two species is predicted to be.

Table 5. Final quantitative HINT scores for active compounds 4-Me-2-PAM, 6-Me-2-PAM and 2-PAM

Compound	Total Hint Score*	Hydrogen Bond*	Acid/Base*	Hydrophobic*	Acid/Acid**	Base/Base**	Hydrophobic /Polar**
2-PAM	152.0	21.6	422.2	207.6	79.2	74.7	345.5
4-Me-2-PAM	143.1	21.9	414.2	268.5	55.7	86.4	419.4
6-Me-2-PAM	197.2	22.0	479.4	291.3	54.2	76.1	365.2

*: Favorable interaction

**: Unfavorable interaction

Appendix A.3 Chemistry experimental

General synthetic techniques: All reactions were carried out with solvents and reagents obtained from commercial sources and were used without further purification unless noted. Moisture-sensitive reactions were performed under an inert atmosphere using a nitrogen line with standard Schlenk techniques unless otherwise stated. Unless specifically stated, the temperature of a water bath during the evaporation of organic solvents using a rotary evaporator was 40 ± 5 °C. All syringes in this study were dried in an oven at 80 °C and stored in a desiccator over Drierite©. All reactions were monitored by thin-layer chromatography (TLC) carried out on 0.25-mm Merck silica gel plates (60F-254) using UV light (254 nm) for visualization or with 2.4% phosphomolybdic acid, 1.4% phosphoric acid, and 5% sulfuric acid in water with heat as a developing agent.

Solvents used for NMR spectroscopy were purchased from Cambridge Isotope Laboratories. $CDCl_3$ was stored over anhydrous K_2CO_3. NMR spectra were recorded on a Bruker Advance spectrometer at 300 megahertz (MHz), 400 MHz, or 500 MHz. The chemical shifts are given in parts per million (ppm) on a delta (δ) scale. The solvent peak was used as a reference value, for ^{1}H NMR: $CDCl_3$ = 7.27 ppm, DMSO-d_6 = 2.50 ppm, CD_3OD = 3.31 ppm, acetonde-d_6 = 2.05; for ^{13}C NMR: $CDCl_3$ = 77.00 ppm, DMSO-d_6 = 39.50 ppm, CD_3OD = 49.00 ppm, acetonde-d_6 = 29.84. The following abbreviations are used to indicate the multiplicities: s = singlet; d = doublet; t = triplet; q = quartet; dd = doublet of doublets; dt = doublet of triplets; td = triplet of doublets; quint = quintet; sext = sextet; sept = septet; app = apparent; m = multiplet; br = broad. Melting points were obtained using a DigiMelt MPA160. Infrared (IR) spectra were collected using a Nicolet IR200 FT-IR spectrometer or a Perkin Elmer FT-IR Spectrum Two. Samples for acquiring IR spectra were neat or prepared as a thin film on KBr plate by dissolving the compound

in CH_2Cl_2 and then evaporating the CH_2Cl_2. High-resolution mass spectra were recorded on a VG 7070 spectrometer or Thermo Scientific Q Exactive Orbitrap. Ultraviolet-visible (UV-Vis) spectra were collected using a Shimadzu UV-1280 or HP 8453 UV-Visible spectroscopy system.

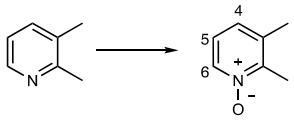

Preparation of 2,3-dimethylpyridine 1-oxide: 2,3-Dimethylpyridine *1*-oxide was synthesized following the literature procedure.[99] A 500-mL pear-shaped flask was charged with 2,3-lutidine (10.7 mL, 100 mmol) at 23 °C under an open atmosphere. Aqueous 0.6 M K_2CO_3 (50 mL), *t*-BuOH (50 mL), MeCN (8.00 mL, 150 mmol), 30% aqueous H_2O_2 (60.0 mL, 500 mmol), and 2,2,2-trifluoroacetophenone (1.4 mL, 10 mmol) were added sequentially in one portion, and the reaction mixture continued to stir at 23 °C under an open atmosphere for 24 h. After this period, H_2O (50 mL) was added, and the resulting reaction mixture was allowed to stir for 6 h at 23 °C under an open atmosphere. The reaction mixture was extracted with CH_2Cl_2 (4 × 50 mL) using a separatory funnel. The combined organic layers were dried over anhydrous Na_2SO_4, filtered, and concentrated *in vacuo*. The crude residue was purified by flash chromatography (60 to 100% EtOAc in hexanes) on silica gel (250 mL) to afford 2,3-dimethylpyridine 1-oxide as a white solid (8.56 g, 70% yield).

2,3-Dimethylpyridine 1-oxide: ^{1}H NMR (300 MHz, 293 K, $CDCl_3$): δ 8.16 (br d, J = 6.0 Hz, 1H, 6-H), 7.06–6.99 (m, 2H, 4-H and 5-H), 2.51 (s, 3H, -CH_3), 2.34 (s, 3H, -CH_3). The ^{1}H NMR spectrum for 2,3-dimethylpyridine 1-oxide was consistent with that in the literature.[147]

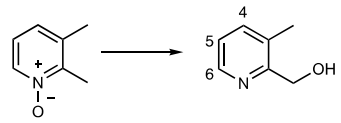

Preparation of (3-methylpyridin-2-yl)methanol: A 250-mL round-bottom flask with 2,3-dimethylpyridine 1-oxide (4.36 g, 35.4 mmol) was evacuated and refilled with nitrogen gas three times and charged with CH_2Cl_2 (60 mL) at 23 °C. TFAA (15.0 mL, 106 mmol) in CH_2Cl_2 (35 mL) was added, and the resulting reaction mixture was stirred at 23 °C for 40 h. After this period, the reaction mixture was cooled to 0 °C. Then, *t*-BuOH (22 mL) and saturated aqueous K_2CO_3 (22 mL) were added to the reaction mixture. The resulting mixture was stirred for 3 h and gradually warmed to 23 °C. The mixture was extracted with CH_2Cl_2 (3 × 70 mL) using a separatory funnel. The combined organic layers were dried over anhydrous Na_2SO_4, filtered, and concentrated *in vacuo*. The resulting crude residue was purified by flash chromatography (50 to 80% EtOAc in hexanes) on silica gel (100 mL) to afford (3-methylpyridin-2-yl)methanol as a dark brown oil (4.18 g, 96% yield).

(3-Methylpyridin-2-yl)methanol: R_f = 0.36 (100% EtOAc); IR (neat): ν_{max} = 3393, 3065, 2983, 1737, 1589, 1452, 1408, 1374, 1243, 1177, 1126, 1055 cm^{-1}; ^1H NMR (300 MHz, 293 K, 1% w/w CD_3OD in $CDCl_3$): δ 8.40 (d, J = 5.0 Hz, 1H, 6-H), 7.46 (d, J = 7.5 Hz, 1H, 4-H), 7.14 (dd, J = 7.5, 5.0 Hz, 1H, 5-H), 4.68 (s, 2H, -CH_2OH), 2.21 (s, 3H, -CH_3); ^{13}C NMR (100 MHz, 293 K, $CDCl_3$): δ 156.0, 145.1, 137.5, 129.5, 122.1, 61.5, 16.4; HRMS (ESI+) calcd for $C_7H_{10}NO$ $[M + H]^+$ = 124.0757, found 124.0776.

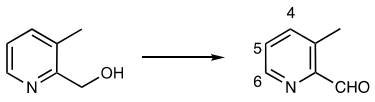

Preparation of 3-methylpicolinaldehyde: A 250-mL pear-shaped flask with a reflux condenser was evacuated and refilled with nitrogen gas three times, and (3-methylpyridin-2-yl)methanol (3.25 g, 26.1 mmol), DCE (113 mL), and MnO_2 (11.38 g, 130.9 mmol) were added consecutively. The mixture was heated to reflux. After 9 h, the reaction mixture was cooled to 23 °C, filtered through Celite®, washed with EtOAc, and concentrated *in vacuo*. The crude residue was purified by flash chromatography (40 to 70% EtOAc in hexanes) on silica gel (100 mL) to afford 3-methylpicolinaldehyde as a yellow oil (1.87 g, 59% yield).

3-Methylpicolinaldehyde: R_f = 0.67 (60% EtOAc in hexanes); IR (neat): ν_{max} = 3385, 3058, 2931, 2826, 1705, 1585, 1569, 1461, 1411, 1383, 1300, 1225, 1205, 1191, 1124, 1078 cm^{-1}; ^1H NMR (300 MHz, 293 K, $CDCl_3$): δ 10.18 (s, 1H, -C*H*O), 8.64 (d, *J* = 4.5 Hz, 1H, 6-H), 7.61 (d, *J* = 7.8 Hz, 1H, 4-H), 7.37 (dd, *J* = 7.6, 4.8 Hz, 1H, 5-H), 2.65 (s, 3H, -CH_3); ^{13}C NMR (100 MHz, 293 K, $CDCl_3$): δ 195.6, 150.2, 147.7, 140.1, 135.9, 126.7, 19.1; HRMS (ESI+) calcd for $C_7H_9N_2O$ $[M + H]^+$ = 122.0600, found 122.0628. All spectroscopic data for 3-methylpicolinaldehyde were consistent with those in the literature.[148]

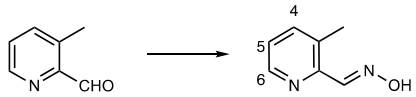

Preparation of (E)-3-methylpicolinaldehyde oxime: A 250-mL pear-shaped flask open to air was charged with 3-methylpicolinaldehyde (1.15 g, 9.53 mmol), MeOH (96 mL), H_2O (15 mL), K_2CO_3 (1.58 g, 11.4 mmol), and NH_2OH•HCl (662 mg, 9.53 mmol). A reflux condenser was attached, and after the reaction mixture was heated to reflux for 4 h, the reaction mixture was cooled to 23 °C. The organic solvent was removed *in vacuo*, and the resulting aqueous layer was extracted with EtOAc (3 × 25 mL) using a separatory funnel. The combined organic layers were

dried over anhydrous Na_2SO_4, filtered, and concentrated *in vacuo* to afford (*E*)-3-methylpicolinaldehyde oxime as a light pink solid (677 mg, 53% yield). This material was used directly without further purification.

(E)-3-Methylpicolinaldehyde oxime: m.p. = 155–157 °C; R_f = 0.42 (60% EtOAc in hexanes); IR (film): ν_{max} = 3423, 1642 cm^{-1}; ^1H NMR (400 MHz, 293 K, DMSO-d_6): δ 11.61 (s, 1H, -CH=NO*H*), 8.46 (d, *J* = 4.8 Hz, 1H, 6-H), 8.24 (s, 1H, -C*H*=NOH), 7.69 (d, *J* = 7.6 Hz, 1H, 4-H), 7.29 (dd, *J* = 7.6, 4.8 Hz, 1H, 5-H), 2.49 (s, 3H, -CH_3); ^{13}C NMR (100 MHz, 293 K, DMSO-d_6): δ 151.1, 150.1, 147.3, 139.4, 132.7, 123.5, 20.6; HRMS (ESI+) calcd for $C_7H_9N_2O$ $[M + H]^+$ = 137.0709, found 137.0709.

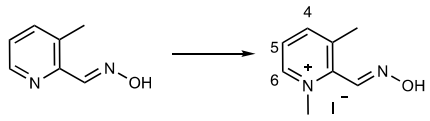

*Preparation of (E)-2-((hydroxyimino)methyl)-1,3-dimethylpyridin-1-ium iodide (**3-Me-2-PAM**):* A 35-mL sealed tube with (*E*)-3-methylpicolinaldehyde oxime (401 mg, 2.94 mmol) was charged with acetone (6 mL), and MeI (1.82 mL, 29.4 mmol). The vessel was sealed and heated to 45 °C (external temperature). After 15 h at the same temperature, the reaction mixture was cooled to 23 °C. A small amount of charcoal was added and the mixture was stirred for 2 h at 23 °C. The mixture was filtered by gravity through filter paper, and the remaining residue was rinsed with MeOH. The filtrate was concentrated *in vacuo* to yield (*E*)-2-[(hydroxyimino)methyl]-1,3-dimethylpyridin-1-ium iodide as a light brown solid (332 mg, 42% yield).

(E)-2-((Hydroxyimino)methyl)-1,3-dimethylpyridin-1-ium iodide: m.p. = 192–193 °C; R_f = 0.18 (4:1:1 *n*-BuOH:H_2O:AcOH); IR (film): ν_{max} = 3444, 1636 cm^{-1}; ^1H NMR (400 MHz, 293 K, DMSO-d_6): δ 12.90 (s, 1H, -CH=NO*H*), 8.97 (d, *J* = 6.2 Hz, 1H, 6-H), 8.58 (s, 1H, -C*H*=NOH),

8.54 (d, J = 8.0 Hz, 1H, 4-H), 8.04 (dd, J = 8.0, 6.2 Hz, 1H, 5-H), 4.33 (s, 3H, -N^+CH_3), 2.57 (s, 3H, -CH_3); ^{13}C NMR (100 MHz, 293 K, DMSO-d_6): δ 147.6, 145.8, 142.4, 138.9, 126.8, 47.8, 20.2; HRMS (ESI+) calcd for $C_8H_{11}N_2O$ $[M]^+$ = 151.0866, found 151.0864.

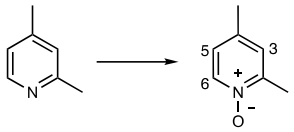

Preparation of 2,4-dimethylpyridine 1-oxide: 2,4-Dimethylpyridine 1-oxide was synthesized following a literature procedure.[99] A 500-mL pear-shaped flask was charged with 2,4-lutidine (4.8 mL, 45 mmol) at 23 °C under an open atmosphere. Aqueous 0.6 M K_2CO_3 (22 mL), *t*-BuOH (22 mL), MeCN (3.5 mL, 67 mmol), 30% aqueous H_2O_2 (27.0 mL, 135 mmol), and 2,2,2-trifluoroacetophenone (620 μL, 4.48 mmol) were added sequentially in one portion, and the reaction mixture continued to stir at 23 °C under an open atmosphere for 27 h. After this period, H_2O (25 mL) was added, and the resulting reaction mixture was allowed to stir for 2 h at 23 °C under an open atmosphere. The reaction mixture was extracted with CH_2Cl_2 (4 × 30 mL) using a separatory funnel. The combined organic layers were dried over anhydrous Na_2SO_4, filtered, and concentrated *in vacuo*. The crude residue was purified by flash chromatography (60 to 100% EtOAc in hexanes) on silica gel (110 mL) to afford 2,4-dimethylpyridine 1-oxide as a yellow oil (3.56 g, 65% yield).

2,4-Dimethylpyridine 1-oxide: ^{1}H NMR (300 MHz, 293 K, $CDCl_3$): δ 8.05 (d, J = 6.6 Hz, 1H, 6-H), 6.97 (s, 1H, 3-H), 6.85 (d, J = 6.6 Hz, 1H, 5-H), 2.38 (s, 3 H, -CH_3), 2.21 (s, 3H, -CH_3). The spectroscopic data for 2,4-dimethylpyridine 1-oxide was consistent with those in the literature.[99]

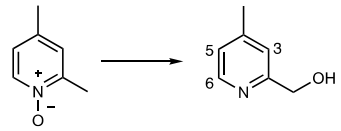

Preparation of (4-methylpyridin-2-yl)methanol: A 250-mL pear-shaped flask with 2,4-dimethylpyridine 1-oxide (1.98 g, 16.1 mmol) was evacuated and refilled with nitrogen gas three times and charged with CH_2Cl_2 (25 mL) at 23 °C. TFAA (6.8 mL, 48 mmol) in CH_2Cl_2 (18 mL) was added, and the resulting reaction mixture was stirred at 23 °C for 48 h. After this period, the reaction mixture was cooled to 0 °C. Then, *t*-BuOH (10 mL) and saturated aqueous K_2CO_3 (10 mL) were added to the reaction mixture. The resulting mixture was stirred for 20 h and gradually warmed to 23 °C. The mixture was extracted with CH_2Cl_2 (3 × 20 mL) using a separatory funnel. The combined organic layers were dried over anhydrous Na_2SO_4, filtered, and concentrated *in vacuo*. The resulting crude residue was purified by flash chromatography (50 to 95% EtOAc in hexanes) on silica gel (60 mL) to afford (4-methylpyridin-2-yl)methanol as a dark brown oil (1.16 g, 51% yield).

(4-Methylpyridin-2-yl)methanol: R_f = 0.27 (100% EtOAc); IR (neat): ν_{max} = 3210, 2923, 1605, 1564, 1448, 1380, 1358, 1266, 1114, 1087, 1004 cm^{-1}; ^1H NMR (400 MHz, 293 K, 1% w/w CD_3OD in $CDCl_3$): δ 8.35 (d, J = 4.8 Hz, 1H, 6-H), 7.11 (s, 1H, 3-H), 7.00 (d, J = 4.8 Hz, 1H, 5-H), 4.70 (s, 2H, -CH_2OH), 2.34 (s, 3H, -CH_3); ^{13}C NMR (100 MHz, 293 K, $CDCl_3$): δ 159.4, 159.4, 148.3, 123.5, 121.7, 64.3, 21.1; HRMS (ESI+) calcd for $C_7H_{10}NO$ $[M + H]^+$ = 124.0757, found 124.0772. The ^1H and ^{13}C NMR spectra for (4-methylpyridin-2-yl)methanol were consistent with those in the literature.[111]

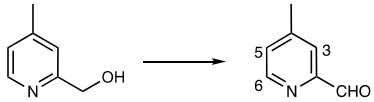

Preparation of 4-methylpicolinaldehyde: A 50-mL pear-shaped flask with a reflux condenser was evacuated and refilled with nitrogen gas three times, and (4-methylpyridin-2-yl)methanol (780 mg, 6.28 mmol), DCE (27 mL), and MnO_2 (2.73 g, 31.4 mmol) were added consecutively. The mixture was heated to reflux. After 13 h, the reaction mixture was cooled to 23 °C, filtered through Celite®, washed with EtOAc, and concentrated *in vacuo*. The crude residue was purified by flash chromatography (40 to 70% EtOAc in hexanes) on silica gel (50 mL) to afford 4-methylpicolinaldehyde as a yellow oil (462 mg, 60% yield).

4-Methylpicolinaldehyde: R_f = 0.57 (60% EtOAc in hexanes); IR (neat): ν_{max} = 3398, 3054, 2926, 2827, 1710, 1603, 1476, 1448, 1381, 1366, 1265, 1246, 1138, 1103, 1088, 1041 cm^{-1}; ^1H NMR (300 MHz, 293 K, $CDCl_3$): δ = 10.06 (s, 1H, C*H*O), 8.63 (d, *J* = 5.0 Hz, 1H, 6-H), 7.78 (s, 1H, 3-H), 7.33 (dd, *J* = 7.6, 5.0 Hz, 1H, 5-H), 2.44 (s, 3H, -CH_3); ^{13}C (100 MHz, 293 K, $CDCl_3$): δ = 193.7, 152.7, 149.9, 148.5, 128.7, 122.5, 21.0; HRMS (ESI+) calcd for $C_7H_9ON_2$ $[M + H]^+$ = 122.0600, found 122.0629.

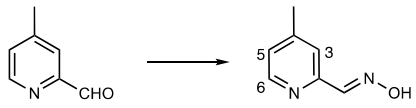

Preparation of (E)-4-methylpicolinaldehyde oxime: A 50-mL pear-shaped flask open to air was charged with 4-methylpicolinaldehyde (312 mg, 2.57 mmol), MeOH (26 mL), H_2O (4 mL), K_2CO_3 (427 mg, 3.08 mmol), and NH_2OH•HCl (179 mg, 2.57 mmol). A reflux condenser was attached, and after the reaction mixture was heated to reflux for 4 h, the reaction mixture was cooled to 23 °C. The organic solvent was removed *in vacuo*, and the resulting aqueous layer was extracted with EtOAc (3 × 30 mL) using a separatory funnel. The combined organic layers were dried over anhydrous Na_2SO_4, filtered, and concentrated *in vacuo* to afford (*E*)-4-

methylpicolinaldehyde oxime as a light brown solid (303 mg, 86% yield). This material was used directly without further purification.

(E)-4-Methylpicolinaldehyde oxime: m.p. = 155–158 °C; R_f = 0.42 (60% EtOAc in hexanes); IR (film): ν_{max} = 3426, 2101, 1631 cm^{-1}; ^1H NMR (400 MHz, 293 K, DMSO-d_6): δ 11.62 (s, 1H, -CH=NO*H*), 8.44 (d, *J* = 4.6 Hz, 1H, 6-H), 8.05 (s, 1H, -C*H*=NOH), 7.63 (s, 1H, 3-H), 7.22 (d, *J* = 4.6 Hz, 1H, 5-H), 2.36 (s, 3H, -CH_3); ^{13}C NMR (100 MHz, 293 K, DMSO-d_6): δ 152.2, 149.4, 149.2, 147.7, 125.1, 120.6, 20.8; HRMS (ESI+) calcd for $C_7H_9N_2O$ $[M + H]^+$ = 137.0709, found 137.0709.

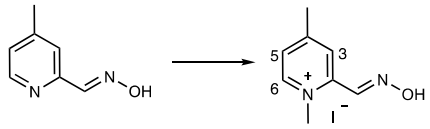

*Preparation of (E)-2-((hydroxyimino)methyl)-1,4-dimethylpyridin-1-ium iodide (**4-Me-2-PAM**):* A 35-mL sealed tube with (*E*)-4-methylpicolinaldehyde oxime (202 mg, 1.48 mmol) was charged with acetone (3 mL), and MeI (978 μL, 14.8 mmol). The vessel was sealed and heated to 45 °C (external temperature). After 20 h at the same temperature, the reaction mixture was cooled to 23 °C. A small amount of charcoal was added and the mixture was stirred for 4 h at 23 °C. The mixture was filtered by gravity through filter paper, and the remaining residue was rinsed with MeOH. The filtrate was concentrated *in vacuo* to yield (*E*)-2-[(hydroxyimino)methyl]-1,4-dimethylpyridin-1-ium iodide as a light brown solid (295 mg, 72% yield).

(E)-2-((Hydroxyimino)methyl)-1,4-dimethylpyridin-1-ium iodide: m.p. = 201–203 °C; R_f = 0.18 (4:1:1 *n*-BuOH:H_2O:AcOH); IR (film): ν_{max} = 3444, 2101, 1640 cm^{-1}; ^1H NMR (400 MHz, 293 K, DMSO-d_6): δ 13.04 (s, 1H, -CH=NO*H*), 8.82 (d, *J* = 6.4 Hz, 1H, 6-H), 8.64 (s, 1H, -C*H*=NOH), 8.21 (s, 1H, 3-H), 7.91 (d, *J* = 6.4 Hz, 1H, 5-H), 4.30 (s, 3H, -N^+CH_3), 2.62 (s, 3H, -

CH_3); ^{13}C NMR (100 MHz, 293 K, DMSO-d_6): δ 158.4, 147.8, 146.0, 142.1, 128.1, 125.4, 45.9, 21.7; HRMS (ESI+) calcd for $C_8H_{11}N_2O$ $[M]^+$ = 151.0866, found 151.0861.

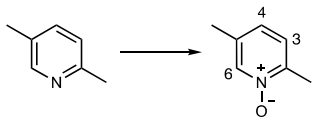

Preparation of 2,5-dimethylpyridine 1-oxide: 2,5-Dimethylpyridine 1-oxide was synthesized following a literature procedure.[99] A 500-mL pear-shaped flask was charged with 2,5-lutidine (10.7 mL, 100 mmol) at 23 °C under an open atmosphere. Aqueous 0.6 M K_2CO_3 (50 mL), *t*-BuOH (50 mL), MeCN (8.00 mL, 150 mmol, 1.5 equiv), 30% aqueous H_2O_2 (60.0 mL, 500 mmol), and 2,2,2-trifluoroacetophenone (1.4 mL, 10 mmol) were added sequentially in one portion, and the reaction mixture continued to stir at 23 °C under an open atmosphere for 24 h. After this period, H_2O (50 mL) was added, and the resulting reaction mixture was allowed to stir for 6 h at 23 °C under an open atmosphere. The reaction mixture was extracted with CH_2Cl_2 (4 × 50 mL) using a separatory funnel. The combined organic layers were dried over anhydrous Na_2SO_4, filtered, and concentrated *in vacuo*. The crude residue was purified by flash chromatography (60 to 100% EtOAc in hexanes) on silica gel (250 mL) to afford 2,5-dimethylpyridine 1-oxide as a white solid (8.47 g, 69% yield).

2,5-Dimethylpyridine 1-oxide: ^{1}H NMR (300 MHz, 293 K, $CDCl_3$): δ = 8.09 (s, 1H, 6-H), 7.09 (d, J = 8.1 Hz, 1H, 4-H), 6.97 (d, J = 8.1 Hz, 1H, 3-H), 2.43 (s, 3 H, -CH_3), 2.23 (s, 3H, -CH_3). The ^{1}H NMR spectra for 2,5-dimethylpyridine 1-oxide was consistent with those in the literature.[147]

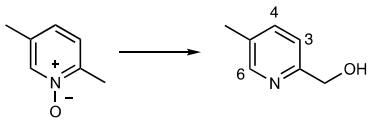

Preparation of (5-methylpyridin-2-yl)methanol: A 250-mL round-bottom flask with 2,5-dimethylpyridine 1-oxide (5.01 g, 40.6 mmol) was evacuated and refilled with nitrogen gas three times and charged with CH_2Cl_2 (75 mL) at 23 °C. TFAA (17.2 mL, 122 mmol) in CH_2Cl_2 (35 mL) was added, and the resulting reaction mixture was stirred at 23 °C for 48 h. After this period, the reaction mixture was cooled to 0 °C. Then, *t*-BuOH (25 mL) and saturated aqueous K_2CO_3 (25 mL) were added to the reaction mixture. The resulting mixture was stirred for 6 h and gradually warmed to 23 °C. The mixture was extracted with CH_2Cl_2 (3 × 40 mL) using a separatory funnel. The combined organic layers were dried over anhydrous Na_2SO_4, filtered, and concentrated *in vacuo*. The resulting crude residue was purified by flash chromatography (50 to 80% EtOAc in hexanes) on silica gel (80 mL) to afford (5-methylpyridin-2-yl)methanol as a dark brown oil (2.60 g, 52% yield).

(5-Methylpyridin-2-yl)methanol: R_f = 0.27 (100% EtOAc); IR (neat): ν_{max} = 3216, 2923, 1681, 1605, 1574, 1491, 1451, 1383, 1200, 1133, 1068 cm^{-1}; ^1H NMR (400 MHz, 293 K, 1% w/w CD_3OD in $CDCl_3$): δ = 8.37 (s, 1H, 6-H), 7.49 (d, J = 8.0 Hz, 1H, 4-H), 7.17 (d, J = 8.0 Hz, 1H, 3-H), 4.72 (s, 2 H, -CH_2OH), 2.33 (s, 3H, -CH_3); ^{13}C (100 MHz, 293 K, $CDCl_3$): δ = 159.2, 148.3, 148.2, 123.5, 121,5, 64.3, 21.2; HRMS (ESI+) calcd for $C_7H_{10}ON$ $[M + H]^+$ = 124.0757, found 124.0772.

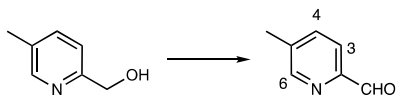

Preparation of 5-methylpicolinaldehyde: A 100-mL pear-shaped flask with a reflux condenser was evacuated and refilled with nitrogen gas three times, and (5-methylpyridin-2-yl)methanol (1.54 g, 12.4 mmol), DCE (54 mL), and MnO_2 (5.39 g, 62.1 mmol) were added consecutively. The mixture was heated to reflux. After 8 h, the reaction mixture was cooled to 23 °C, filtered through Celite®, washed with EtOAc, and concentrated *in vacuo*. The crude residue was purified by flash chromatography (40 to 70% EtOAc in hexanes) on silica gel (60 mL) to afford 5-methylpicolinaldehyde as a yellow oil (1.15 g, 77% yield).

5-Methylpicolinaldehyde: R_f = 0.65 (60% EtOAc in hexanes); IR (neat): ν_{max} = 3398, 3061, 2803, 2709, 2499, 1736, 1587, 1371, 1241, 1045 cm^{-1}; ^1H NMR (300 MHz, 293 K, $CDCl_3$): δ 10.04 (s, 1H, -C*H*O), 8.61 (s, 1H, 6-H), 7.87 (d, *J* = 7.6 Hz, 1H, 4-H), 7.70 (d, *J* = 7.6 Hz, 1H, 3-H), 2.44 (s, 3H, -CH_3); ^{13}C NMR (100 MHz, 293 K, $CDCl_3$): δ 193.6, 151.2, 139.1, 137.7, 121.4, 19.2; HRMS (ESI+) calcd for $C_7H_9N_2O$ $[M + H]^+$ = 122.0600, found 122.0629.

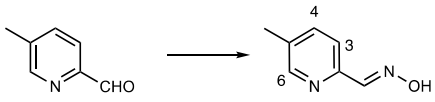

Preparation of (E)-5-methylpicolinaldehyde oxime: A 250-mL pear-shaped flask open to air was charged with 5-methylpicolinaldehyde (756 mg, 6.24 mmol), MeOH (63 mL), H_2O (10 mL), K_2CO_3 (1.03 g, 7.49 mmol), and NH_2OH•HCl (433 mg, 6.24 mmol). A reflux condenser was attached, and after the reaction mixture was heated to reflux for 4 h, the reaction mixture was cooled to 23 °C. The organic solvent was removed *in vacuo*, and the resulting aqueous layer was extracted with EtOAc (3 × 25 mL) using a separatory funnel. The combined organic layers were dried over anhydrous Na_2SO_4, filtered, and concentrated *in vacuo* to afford (*E*)-5-

methylpicolinaldehyde oxime as a white solid (474 mg, 56% yield). This material was used directly without further purification.

(E)-5-Methylpicolinaldehyde oxime: m.p. = 157–158 °C; R_f = 0.45 (60% EtOAc in hexanes); IR (film): ν_{max} = 3436, 2077, 1635 cm^{-1}; ^1H NMR (400 MHz, 293 K, DMSO-d_6): δ 11.55 (s, 1H, -CH=NO*H*), 8.43 (s, 1H, 6-H), 8.05 (s, 1H, -C*H*=NOH), 7.71 (d, J = 8.2 Hz, 1H, 4-H), 7.65 (d, J = 8.2 Hz, 1H, 3-H), 2.33 (s, 3H, -CH_3); ^{13}C NMR (100 MHz, 293 K, DMSO-d_6): δ 150.0, 149.9, 149.3, 137.6, 133.9, 119.7, 18.3; HRMS (ESI+) calcd for $C_7H_9N_2O$ $[M + H]^+$ = 137.0709, found 137.0709.

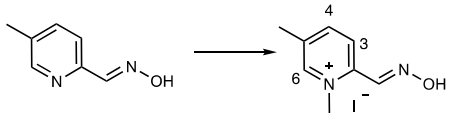

*Preparation of (E)-2-((hydroxyimino)methyl)-1,5-dimethylpyridin-1-ium iodide (**5-Me-2-PAM**):* A 35-mL sealed tube with (*E*)-5-methylpicolinaldehyde oxime (197 mg, 1.45 mmol) was charged with acetone (3 mL), and MeI (897 μL, 14.5 mmol). The vessel was sealed and heated to 45 °C (external temperature). After 15 h at the same temperature, the reaction mixture was cooled to 23 °C. A small amount of charcoal was added and the mixture was stirred for 5 h at 23 °C. The mixture was filtered by gravity through filter paper, and the remaining residue was rinsed with MeOH. The filtrate was concentrated *in vacuo* to yield (*E*)-2-[(hydroxyimino)methyl]-1,5-dimethylpyridin-1-ium iodide as a light brown solid (310 mg, 77% yield).

(E)-2-((Hydroxyimino)methyl)-1,5-dimethylpyridin-1-ium iodide: m.p. = 140–142 °C; R_f = 0.18 (4:1:1 *n*-BuOH:H_2O:AcOH); IR (film): ν_{max} = 3432, 1634 cm^{-1}; ^1H NMR (400 MHz, 293 K, DMSO-d_6): δ 13.01 (s, 1H, -CH=NO*H*), 8.93 (s, 1H, 6-H), 8.67 (s, 1H, -C*H*=NOH), 8.39 (d, J = 8.4 Hz, 1H, 4-H), 8.29 (d, J = 8.4 Hz, 1H, 3-H), 4.34 (s, 3H, -N^+CH_3), 2.49 (s, 3H, -CH_3); ^{13}C

NMR (100 MHz, 293 K, DMSO-d_6): δ 146.4, 145.8, 145.3, 142.0, 138.4, 124.8, 46.5, 18.2; HRMS (ESI+) calcd for $C_8H_{11}N_2O$ $[M]^+$ = 151.0866, found 151.0863.

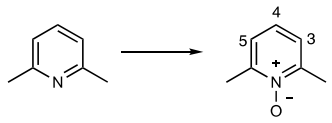

Preparation of 2,6-dimethylpyridine 1-oxide: 2,6-Dimethylpyridine 1-oxide was synthesized following a literature procedure.[99] A 500-mL pear-shaped flask was charged with 2,6-lutidine (10.7 mL, 100 mmol) at 23 °C under an open atmosphere. Aqueous 0.6 M K_2CO_3 (50 mL), *t*-BuOH (50 mL), MeCN (8.00 mL, 150 mmol), 30% aqueous H_2O_2 (60.0 mL, 500 mmol), and 2,2,2-trifluoroacetophenone (1.4 mL, 10 mmol) were added sequentially in one portion, and the reaction mixture continued to stir at 23 °C under an open atmosphere for 28 h. After this period, H_2O (50 mL) was added, and the resulting reaction mixture was allowed to stir for 14 h at 23 °C under an open atmosphere. The reaction mixture was extracted with CH_2Cl_2 (4 × 50 mL) using a separatory funnel. The combined organic layers were dried over anhydrous Na_2SO_4, filtered, and concentrated *in vacuo*. The crude residue was purified by flash chromatography (60 to 100% EtOAc in hexanes) on silica gel (200 mL) to afford 2,6-dimethylpyridine 1-oxide as a white solid (6.66 g, 54% yield).

2,6-Dimethylpyridine 1-oxide: ^{1}H NMR (300 MHz, 293 K, $CDCl_3$): δ 7.15 (d, J = 7.8 Hz, 2H, 3-H and 5-H), 7.10–7.06 (m, 1H, 4-H), 2.54 (s, 6 H, 2 × -CH_3). The spectroscopic data for 2,6-dimethylpyridine 1-oxide were consistent with the literature.[147]

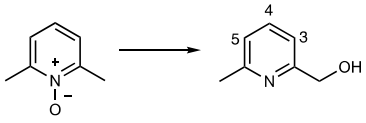

Preparation of (6-methylpyridin-2-yl)methanol: A 250-mL pear-shaped flask with 2,6-dimethylpyridine 1-oxide (2.37 g, 19.3 mmol) was evacuated and refilled with nitrogen gas three times and charged with CH_2Cl_2 (25 mL) at 23 °C. TFAA (8.14 mL, 57.8 mmol) in CH_2Cl_2 (27 mL) was added, and the resulting reaction mixture was stirred at 23 °C for 42 h. After this period, the reaction mixture was cooled to 0 °C. Then, *t*-BuOH (10 mL) and saturated aqueous K_2CO_3 (10 mL) were added to the reaction mixture. The resulting mixture was stirred for 3 h and gradually warmed to 23 °C. The mixture was extracted with CH_2Cl_2 (3 × 50 mL) using a separatory funnel. The combined organic layers were dried over anhydrous Na_2SO_4, filtered, and concentrated *in vacuo*. The resulting crude residue was purified by flash chromatography (50 to 90% EtOAc in hexanes) on silica gel (80 mL) to afford (6-methylpyridin-2-yl)methanol as a dark brown oil (949 mg, 40% yield).

(6-Methylpyridin-2-yl)methanol: R_f = 0.32 (100% EtOAc); IR (neat): ν_{max} = 3256, 2920, 1680, 1598, 1579, 1458, 1206, 1137 cm^{-1}; ^1H NMR (400 MHz, 293 K, 1% w/w CD_3OD in $CDCl_3$): δ 7.56 (app t, J = 7.4 Hz, 1H, 4-H), 7.05 (app t, J = 7.4 Hz, 2H, 3-H and 5-H), 4.71 (s, 2 H, -CH_2OH), 2.54 (s, 3H, -CH_3); ^{13}C NMR (100 MHz, 293 K, $CDCl_3$): δ 158.5, 157.5, 137.1, 122.0, 117.6, 64.1, 24.3; HRMS (ESI+) calcd for $C_7H_{10}NO$ $[M + H]^+$ = 124.0757, found 124.0772.

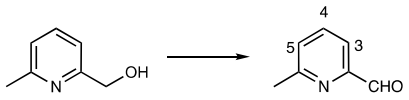

Preparation of 6-methylpicolinaldehyde: A 50-mL pear-shaped flask with a reflux condenser was evacuated and refilled with nitrogen gas three times, and (6-methylpyridin-2-yl)methanol (516 mg, 4.16 mmol), DCE (18 mL), and MnO_2 (1.91 g, 22.0 mmol) were added consecutively. The mixture was heated to reflux. After 22 h, the reaction mixture was cooled to 23 °C, filtered through Celite®, washed with EtOAc, and concentrated *in vacuo*. The crude residue

was purified by flash chromatography (40 to 70% EtOAc in hexanes) on silica gel (10 mL) to afford 6-methylpicolinaldehyde as a yellow oil (213 mg, 42% yield).

6-Methylpicolinaldehyde: R_f = 0.68 (60% EtOAc in hexanes); IR (neat): ν_{max} = 3407, 3064, 2927, 2826, 1712, 1677, 1593, 1461, 1376, 1350,1287, 1254, 1215, 1156, 1087, 1040 cm^{-1}; ^1H NMR (400 MHz, 293 K, DMSO-d_6): δ 9.94 (s, 1H, -C*H*O), 7.93 (app t, *J* = 7.4 Hz, 1H, 4-H), 7.74 (d, *J* = 7.4 Hz, 1H, 3-H), 7.58 (d, *J* = 7.4 Hz, 1H, 5-H), 2.59 (s, 3H, -CH_3); ^{13}C NMR (100 MHz, 293 K, DMSO-d_6): δ 151.1, 150.1, 147.3, 139.4, 132.7, 123.5, 20.6; HRMS (ESI+) calcd for $C_7H_9N_2O$ $[M + H]^+$ = 122.0600, found 122.0627.

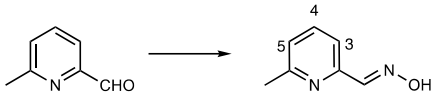

Preparation of (E)-6-methylpicolinaldehyde oxime: A 50-mL pear-shaped flask open to air was charged with 6-methylpicolinaldehyde (309 mg, 2.55 mmol), MeOH (26 mL), H_2O (4 mL), K_2CO_3 (423 mg, 3.05 mmol), and NH_2OH•HCl (177 mg, 2.55 mmol). A reflux condenser was attached, and after the reaction mixture was heated to reflux for 3 h, the reaction mixture was cooled to 23 °C. The organic solvent was removed *in vacuo*, and the resulting aqueous layer was extracted with EtOAc (3 × 20 mL) using a separatory funnel. The combined organic layers were dried over anhydrous Na_2SO_4, filtered, and concentrated *in vacuo* to afford (*E*)-6-methylpicolinaldehyde oxime as an ivory solid (177 mg, 52% yield). This material was used directly without further purification.

(E)-6-Methylpicolinaldehyde oxime: m.p. = 159–161 °C; R_f = 0.53 (60% EtOAc in hexanes); IR (film): ν_{max} = 3423, 2708, 1635, 1591, 1459 cm^{-1}; ^1H NMR (400 MHz, 293 K, DMSO-d_6): δ 11.61 (s, 1H, -CH=NO*H*), 8.04 (s, 1H, -C*H*=NOH), 7.72 (app t, *J* = 8.0 Hz 1H, 4-H), 7.60 (d, *J* = 8.0 Hz, 1H, 3-H), 7.25 (d, *J* = 8.0 Hz, 1H, 5-H), 2.49 (s, 3H, -CH_3); ^{13}C NMR (100

MHz, 293 K, DMSO-d_6): δ 158.1, 151.9, 149.5, 137.3, 123.5, 117.3, 24.3; HRMS (ESI+) calcd for $C_7H_9N_2O$ $[M + H]^+$ = 137.0709, found 137.0709.

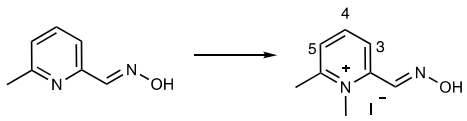

*Preparation of (E)-2-((hydroxyimino)methyl)-1,6-dimethylpyridin-1-ium iodide (**6-Me-2-PAM**):* A 75-mL sealed tube with (*E*)-6-methylpicolinaldehyde oxime (408 mg, 3.00 mmol) was charged with acetone (20 mL), and MeI (1.87 mL, 30.0 mmol). The reaction mixture was stirred at 55 °C for 2 d. After this period, the reaction mixture was transferred to a 50-mL round-bottomed flask, concentrated *in vacuo*, and recrystallized from acetone/EtOAc (1:1) to yield (*E*)-2-[(hydroxyimino)methyl]-1,6-dimethylpyridin-1-ium iodide as a light brown solid (171.2 mg, 21% yield).

(E)-2-((Hydroxyimino)methyl)-1,6-dimethylpyridin-1-ium iodide: m.p. = 140–142 °C; R_f = 0.18 (4:1:1 *n*-BuOH:H_2O:AcOH); IR (film): ν_{max} = 3405, 1653 cm^{-1}; ^1H NMR (400 MHz, 293 K, DMSO-d_6): δ 12.97 (s, 1H, -CH=NO*H*), 8.79 (s, 1H, -C*H*=NOH), 8.41 (app t, J = 8.0 Hz, 1H, 4-H), 8.19 (d, J = 8.0 Hz, 1H, 3-H), 8.02 (d, J = 8.0 Hz, 1H, 5-H), 4.16 (s, 3H, -N^+CH_3), 2.82 (s, 3H, -CH_3); ^{13}C NMR (100 MHz, 293 K, DMSO-d_6): δ 156.9, 148.4, 144.5, 143.0, 129.4, 124.0, 41.6, 21.9; HRMS (ESI+) calcd for $C_8H_{11}N_2O$ $[M]^+$ = 151.0866, found 151.0864.

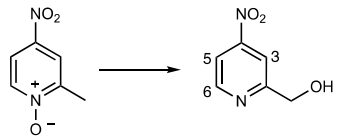

Preparation of (4-nitropyridin-2-yl)methanol: A 500-mL round-bottom flask with 4-nitro-2-picoline 1-oxide (10.09 g, 63.48 mmol) was evacuated and refilled with nitrogen gas three times

and charged with CH_2Cl_2 (120 mL) at 23 °C. TFAA (27.0 mL, 186 mmol) in CH_2Cl_2 (110 mL) was added, and the resulting reaction mixture was stirred at 23 °C for 48 h. After this period, the reaction mixture was cooled to 0 °C. Then, *t*-BuOH (40 mL) and saturated aqueous K_2CO_3 (40 mL) were added to the reaction mixture. The resulting mixture was stirred for 2 h at 0 °C and gradually warmed to 23 °C. The mixture was extracted with CH_2Cl_2 (4 × 125 mL) using a separatory funnel. The combined organic layers were dried over anhydrous Na_2SO_4, filtered, and concentrated in vacuo to afford (4-nitropyridin-2-yl)methanol as a brown solid (8.05 g, 82% yield). This material was used directly without further purification.

(4-Nitropyridin-2-yl)methanol: ^{1}H NMR (300 MHz, 293 K, 1% w/w CD_3OD in $CDCl_3$): δ 8.84 (d, J = 5.4 Hz, 1H, 6-H), 8.09 (d, J = 1.8 Hz, 1H, 3-H), 7.92 (dd, J = 5.4, 1.8 Hz, 1H, 5-H), 4.90 (s, 2H, -CH_2OH). The ^{1}H NMR data for (4-nitropyridin-2-yl)methanol was consistent with the literature.[111]

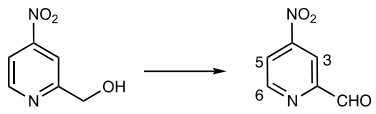

Preparation of 4-nitropicolinaldehyde: A 500-mL pear-shaped flask with a reflux condenser was evacuated and refilled with nitrogen gas three times, and (4-nitropyridin-2-yl)methanol (5.86 g, 37.9 mmol), DCE (155 mL), and MnO_2 (13.21 g, 151.9 mmol) were added consecutively. The mixture was heated to reflux. After 14 h, the reaction mixture was cooled to 23 °C, filtered through Celite®, washed with MeOH, and concentrated *in vacuo*. The crude residue was purified by flash chromatography (10 to 50% EtOAc in hexanes) on silica gel (200 mL) to afford 4-nitropicolinaldehyde as a yellow oil (3.99 g, 69% yield).

4-Nitropicolinaldehyde: ^{1}H NMR (400 MHz, 293 K, $CDCl_3$): δ = 10.19 (s, 1H, C*H*O), 9.12 (d, J = 5.2 Hz, 1H, 6-H), 8.64 (d, J = 2.0 Hz, 1H, 3-H), 8.27 (dd, J = 5.2, 2.0 Hz, 1H, 5-H). The ^{1}H NMR spectrum for (4-nitropyridin-2-yl)methanol was consistent with those in the literature.[111]

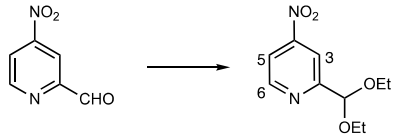

Preparation of 2-(diethoxymethyl)-4-nitropyridine: A 250-mL round-bottomed flask with 4-nitropicolinaldehyde (3.99 g, 26.2 mmol) was charged with ethanol (134 mL), triethylorthoformate (17.5 mL, 105 mmol), and *p*-toluenesulfonic acid monohydrate (748 mg, 3.93 mmol) sequentially. The mixture was heated to reflux for 15 h, after which the reaction mixture was cooled to 23 °C. The reaction mixture was concentrated *in vacuo.* EtOAc (15 mL) was added to the crude residue, followed by saturated aqueous $NaHCO_3$ (15 mL). The layers were separated using a separatory funnel, and the aqueous layer was extracted with EtOAc (2 × 100 mL). The combined organic layers were dried over anhydrous Na_2SO_4, filtered, and concentrated *in vacuo* to afford 2-(diethoxymethyl)-4-nitropyridine as a yellow oil (4.33 g, 91% yield).

2-(Diethoxymethyl)-4-nitropyridine: R_f = 0.71 (60% EtOAc in hexanes); IR (neat): ν_{max} = 2978, 2932, 2882, 1575, 1533, 1266, 1241, 1113, 1055 cm^{-1}; ^{1}H NMR (400 MHz, 293 K, $CDCl_3$): δ 8.88 (d, J = 5.6 Hz, 1H, 6-H), 8.30 (d, J = 2.0 Hz, 1H, 3-H), 7.96 (dd, J = 5.6, 2.0 Hz, 1H, 5-H), 5.57 (s, 1H, -C*H*(OCH_2CH_3)$_2$), 3.74–3.60 (m, 4H, -CH(OCH_2CH_3)$_2$), 1.26 (t, J = 6.8 Hz, 6H, -CH(OCH_2CH_3)$_2$); ^{13}C NMR (100 MHz, 293 K, $CDCl_3$): δ 161.9, 154.4, 151.0, 115.6, 113.9, 101.2, 62.3, 15.0; HRMS (ESI+) calcd for $C_{10}H_{15}N_2O_4$ $[M + H]^+$ = 227.1026, found 227.1025.

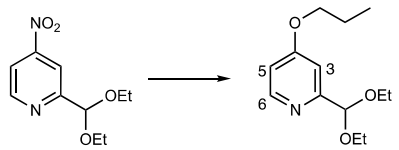

Preparation of 2-(diethoxymethyl)-4-propoxypyridine: A 250-mL pear-shaped flask with a reflux condenser was evacuated and refilled with nitrogen gas three times. 1-Propanol (70 mL) was added, and the flask was cooled with an ice bath. NaH (60% w/w, 397 mg, 9.94 mmol) was added, and the mixture was stirred for 15 min. 2-(Diethoxymethyl)-4-nitropyridine (753 mg, 3.31 mmol) was added, and the resulting mixture was stirred at reflux for 3 h. The reaction mixture was then cooled to 23 °C and concentrated *in vacuo.* EtOAc (10 mL) was added to the crude residue, followed by saturated aqueous NH_4Cl (15 mL). The layers were separated using a separatory funnel, and the aqueous layer was extracted with EtOAc (2 × 20 mL). The combined organic layers were dried over anhydrous Na_2SO_4, filtered, and concentrated *in vacuo.* The crude material was combined with another batch (1.0 mmol scale, with respect to 2-(diethoxymethyl)-4-nitropyridine prepared using the same procedure and purified by flash chromatography (10 to 50% EtOAc in hexanes) on silica gel (40 mL) to afford 2-(diethoxymethyl)-4-propoxypyridine as a yellow oil (823.3 mg, 80% combined yield).

2-(Diethoxymethyl)-4-propoxypyridine: R_f = 0.54 (60% EtOAc in hexanes); IR (neat): ν_{max} = 2973, 2933, 2880, 1596, 1568, 1265, 1242, 1179, 1112, 1057 cm^{-1}; ^1H NMR (400 MHz, 293 K, $CDCl_3$): δ 8.36 (d, J = 5.6 Hz, 1H, 6-H), 7.09 (d, J = 2.4 Hz, 1H, 3-H), 7.96 (dd, J = 5.6, 2.4 Hz, 1H, 5-H), 5.40 (s, 1H, -C*H*$(OCH_2CH_3)_2$), 3.97 (t, J = 7.2 Hz, 2H, -OC*H*$_2CH_2CH_3$), 3.73–3.55 (m, 4H, -CH(OC*H*$_2CH_3)_2$), 1.81 (app sextet, J = 7.2 Hz, 2H, -OCH_2C*H*$_2CH_3$), 1.24 (app t, J = 7.2 Hz, 6H, -CH(OCH_2C*H*$_3)_2$), 1.02 (t, J = 7.2 Hz, 3H, -OCH_2CH_2C*H*$_3$); ^{13}C NMR (100 MHz, 293 K, $CDCl_3$): δ 165.9, 160.0, 150.1, 110.3, 106.9, 102.7, 69.4, 62.3, 22.2, 15.1, 10.4; HRMS (ESI+) calcd for $C_{13}H_{22}NO_3$ $[M + H]^+$ = 240.1594, found 240.1595.

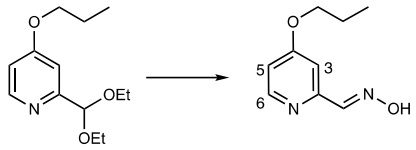

Preparation of (E)-4-propoxypicolinaldehyde oxime: A 50-mL pear-shaped flask, open to air, with 2-(diethoxymethyl)-4-propoxypyridine (455 mg, 1.88 mmol) was charged with H_2O (5 mL) and 5 M H_2SO_4 in H_2O (450 μL, 2.25 mmol). The solution was heated to 85 °C (external temperature). After stirring at the same temperature for 4 h, the reaction mixture was cooled to 23 °C and treated with K_2CO_3 (779 mg, 5.64 mmol) followed by MeOH (20 mL) and NH_2OH•HCl (131 mg, 1.88 mmol) at the same temperature. A reflux condenser was attached, and the reaction was heated to reflux while open to air for 3 h. The reaction mixture was cooled to 23 °C and concentrated *in vacuo.* EtOAc (10 mL) was added to the crude residue, followed by saturated aqueous NH_4Cl (10 mL). The layers were separated using a separatory funnel, and the aqueous layer was extracted with EtOAc (2 × 20 mL). The combined organic layers were dried over anhydrous Na_2SO_4, filtered, and concentrated *in vacuo* to afford (*E*)-4-propoxypicolinaldehyde oxime (335 mg, 98% yield) as a pale pink solid. This material was used directly without further purification.

(E)-4-Propoxypicolinaldehyde oxime: m.p. = 150–152 °C; R_f = 0.56 (100% EtOAc); IR (neat): ν_{max} = 2967, 2880, 2689, 1593, 1562, 1431, 1265, 1248, 1188, 1089, 1065, 1027 cm^{-1}; ^1H NMR (400 MHz, 293 K, DMSO-d_6): δ 11.64 (s, 1H, -CH=NO*H*), 8.37 (d, *J* = 5.6 Hz, 1H, 6-H), 8.03 (s, 1H, -C*H*=NOH), 7.25 (d, *J* = 2.4 Hz, 1H, 3-H), 6.97 (dd, *J* = 5.6, 2.4 Hz, 1H, 5-H), 4.04 (t, *J* = 7.2, 2H, -OC$H_2$$CH_2CH_3$), 1.75 (app sextet, *J* = 6.8, 2H, -$OCH_2CH_2$$CH_3$), 0.98 (t, *J* = 6.8, 3H, -$OCH_2CH_2CH_3$); ^{13}C NMR (100 MHz, 293 K, DMSO-d_6): δ 165.4, 154.2, 151.3, 149.4, 111.6, 105.9, 69.8, 22.3, 10.8; HRMS (ESI+) calcd for $C_9H_{13}N_2O_2$ $[M + H]^+$ = 181.0972, found 181.0968.

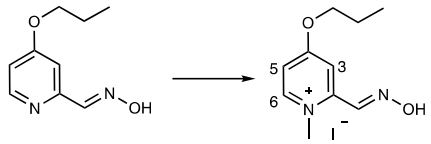

*Preparation of (E)-2-((hydroxyimino)methyl)-1-methyl-4-propoxypyridin-1-ium iodide (**ADG3035**):* A 35-mL sealed tube was charged with (*E*)-4-propoxypicolinaldehyde oxime (152 mg, 0.832 mmol), acetone (4 mL), and MeI (520 μL, 8.32 mmol). The reaction mixture was stirred and heated to 40 °C (external temperature) for 19 h. After this period, the reaction mixture was transferred to a 25-mL round-bottomed flask and concentrated *in vacuo*. The dark brown crude residue was triturated with acetone/EtOAc (1:1) to afford (*E*)-2-((hydroxyimino)methyl)-1-methyl-4-propoxypyridin-1-ium iodide as a yellow solid (147 mg, 55% yield).

(E)-2-((Hydroxyimino)methyl)-1-methyl-4-propoxypyridin-1-ium iodide: m.p. = 163–166 °C; R_f = 0.47 (4:1:1 *n*-BuOH:H_2O:AcOH); IR (neat): ν_{max} = 3079, 2964, 1696, 1592, 1564, 1476, 1332, 1260, 1214, 1069 cm^{-1}; ^1H NMR (400 MHz, 293 K, DMSO-d_6): δ 12.97 (s, 1H, -CH=NO*H*), 8.78 (d, *J* = 7.2 Hz, 1H, 6-H), 8.57 (s, 1H, -C*H*=NOH), 7.67 (d, *J* = 3.2 Hz, 1H, 3-H), 7.61 (d, *J* = 7.2, 3.2 Hz, 1H, 5-H), 4.33 (t, *J* = 6.8 Hz, 2H, -OC*H*$_2$CH$_2$CH$_3$), 4.19 (s, 3H, -N$^+$C*H*$_3$), 1.80 (app sextet, *J* = 6.8 Hz, 2H, -OCH$_2$C*H*$_2$CH$_3$), 0.99 (t, *J* = 6.8 Hz, 3H, -OCH$_2$CH$_2$C*H*$_3$); ^{13}C NMR (100 MHz, 293 K, DMSO-d_6): δ 169.7, 149.0, 148.7, 142.2, 113.6, 110.6, 72.5, 45.1, 21.9, 10.5; HRMS (ESI+) calcd for $C_{10}H_{15}N_2O_2$ $[M]^+$ = 195.1128, found 195.1125.

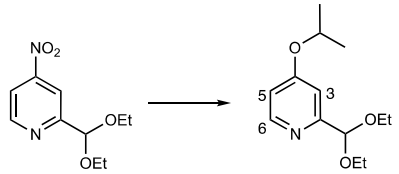

Preparation of 2-(diethoxymethyl)-4-isopropoxypyridine: A 250-mL pear-shaped flask with a reflux condenser was evacuated and refilled with nitrogen gas three times. Isopropanol (80 mL) was added, and the flask was cooled with an ice bath. NaH (60% w/w, 480 mg, 12.0 mmol) was added, and the mixture was stirred for 5 min. 2-(Diethoxymethyl)-4-nitropyridine (761 mg, 3.36 mmol) was added, and the resulting mixture was stirred at reflux for 16 h. The reaction mixture was then cooled to 23 °C and concentrated *in vacuo.* EtOAc (10 mL) was added to the crude residue, followed by saturated aqueous NH_4Cl (20 mL). The layers were separated using a separatory funnel, and the aqueous layer was extracted with EtOAc (2 × 40 mL). The combined organic layers were dried over anhydrous Na_2SO_4, filtered, and concentrated *in vacuo.* The crude material was combined with another batch (1.0 mmol scale, with respect to 2-(diethoxymethyl)-4-nitropyridine prepared using the same procedure) and was purified by flash chromatography (10 to 50% EtOAc in hexanes) on silica gel (50 mL) to afford 2-(diethoxymethyl)-4-isopropoxypyridine as a pale yellow oil (840 mg, 81% combined yield).

2-(Diethoxymethyl)-4-isopropoxypyridine: R_f = 0.61 (60% EtOAc in hexanes); IR (neat): ν_{max} = 2977, 2932, 2880, 1595, 1565, 1266, 1243, 1179, 1139, 1108, 1057 cm^{-1}; ^1H NMR (400 MHz, 293 K, $CDCl_3$): δ 8.35 (d, J = 6.0 Hz, 1H, 6-H), 7.07 (s, 1H, 3-H), 6.69 (d, J = 6.0 Hz, 1H, 5-H), 5.39 (s, 1H, -C*H*$(OCH_2CH_3)_2$), 4.66 (septet, J = 6.0 Hz, 1H, -OC*H*$(CH_3)_2$), 3.73–3.55 (m, 4H, -CH(OC*H*$_2$CH$_3$)$_2$), 1.34 (d, J = 6.0 Hz, 6H, -OCH(C*H*$_3$)$_2$), 1.24 (overlapped t, J = 7.2 Hz, 6H, -CH(OCH$_2$C*H*$_3$)$_2$); ^{13}C NMR (100 MHz, 293 K, $CDCl_3$): δ 164.6, 159.9, 150.0, 117.8, 107.5, 102.5, 69.7, 62.1, 21.5, 15.0; HRMS (ESI+) calcd for $C_{13}H_{22}NO_3$ $[M + H]^+$ = 240.1594, found 240.1594.

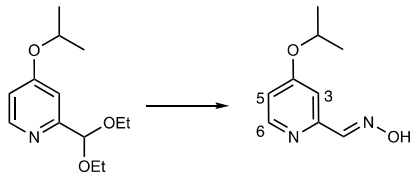

Preparation of (E)-4-isopropoxypicolinaldehyde oxime: A 50-mL pear-shaped flask, open to air, with 2-(diethoxymethyl)-4-isopropoxypyridine (450 mg, 1.88 mmol) was charged with H_2O (5 mL) and 5 M H_2SO_4 in H_2O (450 μL, 2.25 mmol). The solution was heated to 85 °C (external temperature). After stirring at the same temperature for 1 h, the reaction mixture was cooled to 23 °C and treated with K_2CO_3 (780 mg, 5.64 mmol) followed by MeOH (20 mL) and NH_2OH•HCl (131 mg, 1.88 mmol) at the same temperature. A reflux condenser was attached, and the reaction was heated to reflux for 16 h while open to air. The reaction mixture was cooled to 23 °C and concentrated *in vacuo.* EtOAc (10 mL) was added to the crude residue, followed by saturated aqueous NH_4Cl (10 mL). The layers were separated using a separatory funnel, and the aqueous layer was extracted with EtOAc (2 × 20 mL). The combined organic layers were dried over anhydrous Na_2SO_4, filtered, and concentrated *in vacuo.* The crude residue was purified by flash chromatography (10 to 50% EtOAc in hexanes) on silica gel (40 mL) to afford (*E*)-4-isopropoxypicolinaldehyde oxime (135 mg, 40% yield) as a white solid.

(E)-4-Isopropoxypicolinaldehyde oxime: m.p. = 160–163 °C; R_f = 0.44 (60% EtOAc in hexanes); IR (neat): ν_{max} = 2982, 1591, 1560, 1516, 1429, 1244, 1191, 1141, 1108, 1086, 1015 cm^{-1}; ^1H NMR (300 MHz, 293 K, DMSO-d_6): δ 11.63 (s, 1H, -CH=NO*H*), 8.36 (d, *J* = 7.6 Hz, 1H, 6-H), 8.02 (s, 1H, -C*H*=NOH), 7.22 (d, *J* = 3.2 Hz, 1H, 3-H), 6.95 (dd, *J* = 7.6, 3.2 Hz, 1H, 5-H), 4.78 (septet, *J* = 6.3 Hz, 1H, -OC*H*$(CH_3)_2$), 1.30 (d, *J* = 6.0 Hz, 6H, -OCH(C*H*$_3)_2$). ^{13}C NMR (100 MHz, 293 K, DMSO-d_6): δ 164.2, 154.2, 151.3, 149.3, 112.1, 106.5, 70.4, 22.0; HRMS (ESI+) calcd for $C_9H_{13}N_2O_2$ $[M + H]^+$ = 181.0972, found 181.0967.

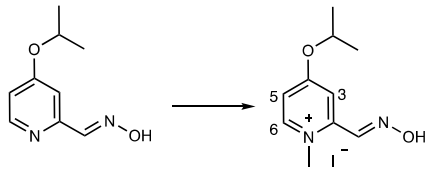

Preparation of (E)-2-((hydroxyimino)methyl)-4-isopropoxy-1-methylpyridin-1-ium ***iodide (ADG2054)****:* A 10-mL sealed tube with (*E*)-4-isopropoxypicolinaldehyde oxime (75 mg, 0.42 mmol) was charged with acetone (2 mL), and MeI (250 μL, 4.16 mmol). The vessel was sealed and heated to 45 °C (external temperature). After 19 h at the same temperature, the reaction mixture was cooled to 23 °C, transferred to a 25-mL round-bottomed flask, and concentrated *in vacuo.* The dark brown crude residue was triturated with acetone/EtOAc (1:1) to afford (*E*)-2-((hydroxyimino)methyl)-1-methyl-4-isopropoxypyridin-1-ium iodide as a yellow solid (99 mg, 73% yield).

(*E)-4-Isopropoxy-2-[(hydroxyimino)methyl]-1-methylpyridin-1-ium iodide:* m.p. = 150–153 °C; R_f = 0.42 (4:1:1 *n*-BuOH:H_2O:AcOH); IR (neat): ν_{max} = 3182, 3078, 2978, 1634, 1590, 1562, 1461, 1336, 1271, 1207, 1100 cm^{-1}; ^1H NMR (400 MHz, 293 K, DMSO-d_6): δ 12.96 (s, 1H, -CH=NO*H*), 8.75 (d, *J* = 7.2 Hz, 1H, 6-H), 8.56 (s, 1H, -C*H*=NOH), 7.65 (d, *J* = 2.8 Hz, 1H, 3-H), 7.61 (dd, *J* = 7.2, 2.8 Hz, 1H, 5-H), 5.09 (septet, *J* = 6.0 Hz, 1H, -OC*H*$(CH_3)_2$), 4.16 (s, 3H, -N^+CH_3), 1.36 (d, *J* = 6.0 Hz, 6H, -OCH$(CH_3)_2$). ^{13}C NMR (100 MHz, 293 K, DMSO-d_6): δ 168.7, 148.9, 148.8, 142.3, 113.8, 111.3, 74.4, 45.0, 21.7; HRMS (ESI+) calcd for $C_{10}H_{15}N_2O_2$ $[M]^+$ = 195.1128, found 195.1126.

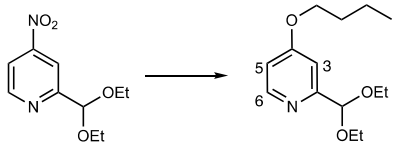

Preparation of 2-(diethoxymethyl)-4-butoxypyridine: A 100-mL pear-shaped flask with a reflux condenser was evacuated and refilled with nitrogen gas three times. 1-Butanol (50 mL) was added, and the flask was cooled with an ice bath. NaH (60% w/w, 288 mg, 7.20 mmol) was added, and the mixture was stirred for 5 min. 2-(Diethoxymethyl)-4-nitropyridine (544 mg, 2.40 mmol) was added, and the resulting mixture was stirred at reflux for 16 h. The reaction mixture was then cooled to 23 °C and concentrated *in vacuo*. EtOAc (10 mL) was added to the crude residue, followed by saturated aqueous NH_4Cl (20 mL). The layers were separated using a separatory funnel, and the aqueous layer was extracted with EtOAc (2 × 30 mL). The combined organic layers were dried over anhydrous Na_2SO_4, filtered, and concentrated *in vacuo*. The crude residue was purified by flash chromatography (10 to 50% EtOAc in hexanes) on silica gel (50 mL) to afford 2-(diethoxymethyl)-4-butoxypyridine as a yellow oil (468 mg, 77% yield).

2-(Diethoxymethyl)-4-butoxypyridine: R_f = 0.50 (60% EtOAc in hexanes); IR (neat): ν_{max} = 2972, 2933, 2875, 1595, 1568, 1266, 1243, 1178, 1113, 1058 cm^{-1}; ^1H NMR (400 MHz, 293 K, $CDCl_3$): δ 8.37 (d, J = 5.6 Hz, 1H, 6-H), 7.10 (d, J = 2.4 Hz, 1H, 3-H), 6.74 (dd, J = 5.6, 2.4 Hz, 1H, 5-H), 5.41 (s, 1H, -C*H*(OCH_2CH_3)$_2$), 4.03 (t, J = 6.4 Hz, 2H, -OC*H*$_2$$CH_2CH_2CH_3$), 3.75–3.57 (m, 4H, -CH(OC*H*$_2$$CH_3$)$_2$), 1.77 (app quintet, J = 6.4 Hz, 2H, -OCH_2C*H*$_2$$CH_2CH_3$), 1.54–1.41 (m, 2H, -$OCH_2CH_2$C*H*$_2$$CH_3$), 1.25 (d, J = 6.0 Hz, 6H, -CH(OCH_2C*H*$_3$)$_2$), 0.98 (t, J = 7.6 Hz, 3H, -$OCH_2CH_2CH_2$C*H*$_3$); ^{13}C NMR (100 MHz, 293 K, $CDCl_3$): δ 165.9, 160.0, 150.0, 110.3, 106.9, 102.6, 67.6, 62.3, 30.9, 19.1, 15.1, 13.7; HRMS (ESI+) calcd for $C_{14}H_{24}NO_3$ $[M + H]^+$ = 254.1751, found 254.1751.

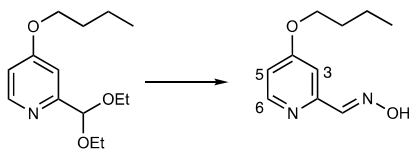

Preparation of (E)-4-butoxypicolinaldehyde oxime: A 25-mL pear-shaped flask, open to air, with 2-(diethoxymethyl)-4-butoxypyridine (156 mg, 0.590 mmol) was charged with H_2O (2 mL) and 5 M H_2SO_4 in H_2O (140 μL, 0.710 mmol). The solution was heated to 85 °C (external temperature). After stirring at the same temperature for 4 h, the reaction mixture was cooled to 23 °C and treated with K_2CO_3 (245 mg, 1.76 mmol) followed by MeOH (8 mL) and NH_2OH•HCl (41 mg, 0.59 mmol) at the same temperature. A reflux condenser was attached, and the reaction was heated to reflux for 3 h while open to air. The reaction mixture was cooled to 23 °C and concentrated *in vacuo*. EtOAc (10 mL) was added to the crude residue, followed by saturated aqueous NH_4Cl (10 mL). The layers were separated using a separatory funnel, and the aqueous layer was extracted with EtOAc (2 × 10 mL). The combined organic layers were dried over anhydrous Na_2SO_4, filtered, and concentrated *in vacuo* to afford (*E*)-4-butoxypicolinaldehyde oxime (113 mg, 98% yield) as a white solid. This material was used directly without further purification.

(E)-4-Butoxypicolinaldehyde oxime: m.p. = 140–143 °C; R_f = 0.31 (60% EtOAc in hexanes); IR (neat): ν_{max} = 2959, 2873, 1593, 1562, 1429, 1249, 1187, 1088, 1067, 1036 cm^{-1}; ^1H NMR (400 MHz, 293 K, DMSO-d_6): δ 11.63 (s, 1H, -CH=NO*H*), 8.36 (d, *J* = 5.6 Hz, 1H, 6-H), 8.02 (s, 1H, -C*H*=NOH), 7.25 (d, *J* = 2.4 Hz, 1H, 3-H), 6.80 (dd, *J* = 5.6, 2.4 Hz, 1H, 5-H), 4.09 (t, *J* = 6.4 Hz, 2H, -OC*H*$_2$CH$_2$CH$_2$CH$_3$), 1.80 (app quintet, *J* = 6.4 Hz, 2H, -OCH$_2$C*H*$_2$CH$_2$CH$_3$), 1.43 (app sextet, *J* = 7.2 Hz, 2H, -OCH$_2$CH$_2$C*H*$_2$CH$_3$), 0.93 (t, *J* = 7.2 Hz, 3H, -OCH$_2$CH$_2$CH$_2$C*H*$_3$); ^{13}C NMR (100 MHz, 293 K, DMSO-d_6): δ 164.8, 153.6, 150.7, 148.78, 111.0, 105.3, 67.4, 30.3, 18.6, 13.6; HRMS (ESI+) calcd for $C_{10}H_{15}N_2O_2$ $[M + H]^+$ = 195.1128, found 195.1126.

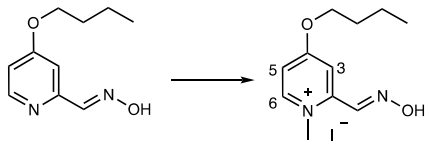

*Preparation of (E)-2-((hydroxyimino)methyl)-1-methyl-4-butoxypyridin-1-ium iodide (**ADG2058**):* A 35-mL sealed tube with (*E*)-4-butoxypicolinaldehyde oxime (102 mg, 0.510 mmol) was charged with acetone (2 mL), and MeI (318 μL, 5.14 mmol). The vessel was sealed and heated to 45 °C (external temperature). After 19 h at the same temperature, the reaction mixture was cooled to 23 °C, transferred to a 25-mL round-bottomed flask, and concentrated *in vacuo*. The dark brown crude residue was triturated with acetone/EtOAc (1:1) to afford (*E*)-2-((hydroxyimino)methyl)-1-methyl-4-butoxypyridin-1-ium iodide as a yellow solid (119 mg, 69% yield).

(E)-2-((Hydroxyimino)methyl)-1-methyl-4-butoxypyridin-1-ium iodide: m.p. = 118–121 °C; R_f = 0.47 (4:1:1 *n*-BuOH:H_2O:AcOH); IR (neat): ν_{max} = 3060, 2956, 2871. 1598, 1567, 1466, 1329, 1261, 1215, 1078 cm^{-1}; ^1H NMR (400 MHz, 293 K, DMSO-d_6): δ 12.96 (s, 1H, -CH=NO*H*), 8.76 (d, *J* = 7.6 Hz, 1H, 6-H), 8.56 (s, 1H, -C*H*=NOH), 7.67 (d, *J* = 2.8 Hz, 1H, 3-H), 7.60 (dd, *J* = 7.6, 2.8 Hz, 1H, 5-H), 4.35 (t, *J* = 6.4 Hz, 2H, -OC*H*$_2$CH$_2$CH$_2$CH$_3$), 4.17 (s, 3H, -N$^+$C*H*$_3$), 1.75 (app quintet, *J* = 7.6 Hz, 2H, -OCH$_2$C*H*$_2$CH$_2$CH$_3$), 1.43 (app sextet, *J* = 7.6 Hz, 2H, -OCH$_2$CH$_2$C*H*$_2$CH$_3$), 0.93 (t, *J* = 7.3 Hz, 3H, -OCH$_2$CH$_2$CH$_2$C*H*$_3$); ^{13}C NMR (100 MHz, 293 K, DMSO-d_6): δ 169.6, 148.9, 148.6, 142.2, 113.6, 110.6, 70.8, 45.0, 30.4, 18.8, 14.0; HRMS (ESI+) calcd for $C_{11}H_{17}N_2O_2$ $[M]^+$ = 209.1284, found 209.1282.

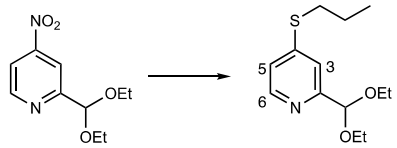

Preparation of 2-(diethoxymethyl)-4-(propylthio)pyridine: A 75-mL sealed tube was charged with dimethyl sulfoxide (2 mL), K_2CO_3 (830 mg, 6.00 mmol), and *n*-propanethiol (540 μL, 6.00 mmol). The mixture was stirred at room temperature for 20 min. 2-(Diethoxymethyl)-4-nitropyridine (453 mg, 2.00 mmol) was added, and the vessel was sealed and heated to 95 °C (external temperature) for 16 h. The reaction mixture was then cooled to 23 °C and neutralized with saturated aqueous NH_4Cl (20 mL). The resulting solution was extracted with EtOAc (3 × 15 mL). The combined organic layers were dried over anhydrous Na_2SO_4, filtered, and concentrated *in vacuo*. The crude material was purified by flash chromatography (0 to 60% EtOAc in hexanes) on silica gel (40 mL) to afford 2-(diethoxymethyl)-4-propylthiopyridine as a pale yellow oil (460 mg, 90% yield).

2-(Diethoxymethyl)-4-(propylthio)pyridine: R_f = 0.60 (60% EtOAc in hexanes); IR (neat): ν_{max} = 2972, 2874, 1577, 1542, 1264, 1231, 1112, 1091, 1056 cm^{-1}; ^1H NMR (400 MHz, 293 K, $CDCl_3$): δ 8.35 (d, J = 5.2 Hz, 1H, 6-H), 7.41 (app s, 1H, 3-H), 7.04 (dd, J = 5.2, 1.2 Hz, 1H, 5-H), 5.41 (s, 1H, -C*H*(OCH_2CH_3)$_2$), 3.75–3.57 (m, 4H, -CH(OC*H*$_2$$CH_3$)$_2$), 2.97 (t, J = 7.4 Hz, 2H, -SC*H*$_2$$CH_2CH_3$), 1.75 (app sextet, t, J = 7.4 Hz, 2H, -SCH_2C*H*$_2$$CH_3$), 1.26 (t, J = 7.2 Hz, 6H, -CH(OCH_2C*H*$_3$)$_2$), 1.07 (t, J = 7.4 Hz, 3H, -SCH_2CH_2C*H*$_3$); ^{13}C NMR (100 MHz, 293 K, $CDCl_3$): δ 157.8, 150.4, 148.2, 120.2, 117.5, 102.5, 62.2, 32.5, 21.8, 15.1, 13.4; HRMS (ESI+) calcd for $C_{13}H_{22}NO_2S$ $[M + H]^+$ = 256.1366, found 256.1367.

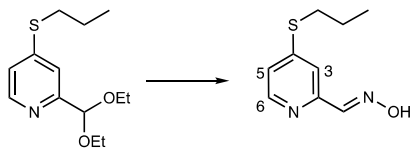

Preparation of (E)-4-(propylthio)picolinaldehyde oxime: A 25-mL pear-shaped flask, open to air, with 2-(diethoxymethyl)-4-propylthiopyridine **(**237 mg, 0.920 mmol) was charged with H_2O

(4 mL) and 5 M H_2SO_4 in H_2O (280 μL, 1.40 mmol). The solution was heated to 92 °C (external temperature). After stirring at the same temperature for 3 h, the reaction mixture was cooled to 23 °C and treated with K_2CO_3 (509 mg, 3.68 mmol) followed by MeOH (14 mL) and NH_2OH•HCl (64 mg, 0.92 mmol) at the same temperature. A reflux condenser was attached, and the reaction was heated to reflux for 2 h while open to air. The reaction mixture was cooled to 23 °C and concentrated *in vacuo.* EtOAc (8 mL) was added to the crude residue, followed by saturated aqueous NH_4Cl (10 mL). The layers were separated using a separatory funnel, and the aqueous layer was extracted with EtOAc (2 × 15 mL). The combined organic layers were dried over anhydrous Na_2SO_4, filtered, and concentrated *in vacuo* to afford (*E*)-4-(propylthio)picolinaldehyde oxime (180 mg, quantitative yield) as a pale pink solid. This material was used directly without further purification.

(E)-4-(Propylthio)picolinaldehyde oxime: m.p. = 145–147 °C; R_f = 0.43 (60% EtOAc in hexanes); IR (neat): ν_{max} = 2971, 2871, 2710, 1579, 1575, 1464, 1404, 1322, 1231, 1113 cm^{-1}; ^1H NMR (400 MHz, 293 K, DMSO-d_6): δ 11.71 (s, 1H, -CH=NO*H*), 8.36 (d, *J* = 5.6 Hz, 1H, 6-H), 8.02 (s, 1H, -C*H*=NOH), 7.56 (d, *J* = 1.6 Hz, 1H, 3-H), 7.26 (dd, *J* = 5.6, 1.6 Hz, 1H, 5-H), 3.05 (t, *J* = 7.2 Hz, 2H, -SC*H*$_2$CH$_2$CH$_3$), 1.66 (app sextet, *J* = 7.2 Hz, 2H, -SCH$_2$C*H*$_2$CH$_3$), 1.00 (t, *J* = 7.2 Hz, 3H, -SCH$_2$CH$_2$C*H*$_3$); ^{13}C NMR (100 MHz, 293 K, DMSO-d_6): δ 152.3, 149.8, 149.5, 149.0, 121.1, 116.3, 32.0, 22.0, 13.7; HRMS (ESI+) calcd for $C_9H_{13}N_2OS$ $[M + H]^+$ = 197.0743, found 197.0740.

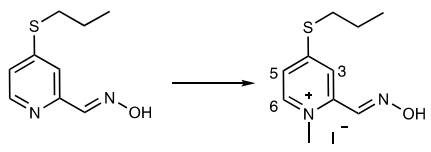

*Preparation of (E)-2-((hydroxyimino)methyl)-1-methyl-4-(propylthio)pyridin-1-ium iodide (**ADG2293**):* A 35-mL sealed tube with (*E*)-4-(propylthio)picolinaldehyde oxime (150 mg, 0.770 mmol) was charged with acetone (2 mL), and MeI (473 μL, 7.70 mmol). The vessel was sealed and heated to 40 °C (external temperature). After 17 h at the same temperature, the reaction mixture was cooled to 23 °C, transferred to a 25-mL round-bottomed flask, concentrated *in vacuo*, and recrystallized from EtOH to afford (*E*)-2-((hydroxyimino)methyl)-1-methyl-4-(propylthio)pyridin-1-ium iodide as a yellow solid (66 mg, 25% yield).

(E)-2-((Hydroxyimino)methyl)-1-methyl-4-(propylthio)pyridin-1-ium iodide: m.p. = 166–168 °C; R_f = 0.08 (10% MeOH in CH_2Cl_2); IR (neat): ν_{max} = 3108, 2971, 1582, 1554, 1492, 1315, 1238, 1081 cm^{-1}; ^1H NMR (400 MHz, 293 K, DMSO-d_6): δ 13.04 (s, 1H, -CH=NO*H*), 8.65 (d, *J* = 6.8 Hz, 1H, 6-H), 8.59 (s, 1H, -C*H*=NOH), 8.02 (d, *J* = 2.4 Hz, 1H, 3-H), 7.90 (dd, *J* = 6.8, 2.4 Hz, 1H, 5-H), 4.19 (s, 3H, -N^+CH_3), 3.27 (t, *J* = 7.2 Hz, 2H, -S$CH_2CH_2CH_3$), 1.71 (app sextet, t, *J* = 7.42 Hz, 2H, -$SCH_2CH_2CH_3$), 1.03 (t, *J* = 7.2 Hz, 3H, -$SCH_2CH_2CH_3$); ^{13}C NMR (100 MHz, 293 K, DMSO-d_6): δ 161.8, 145.6, 145.0, 142.1, 122.5, 120.0, 45.4. 32.7, 21.5, 13.5; HRMS (ESI+) calcd for $C_{10}H_{15}N_2OS$ $[M]^+$ = 211.0899, found 211.0898.

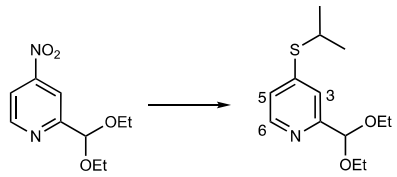

Preparation of 2-(diethoxymethyl)-4-(isopropylthio)pyridine: A 75-mL sealed tube was charged with dimethyl sulfoxide (4 mL), K_2CO_3 (1.66 g, 12.0 mmol) and isopropylthiol (1.12 mL, 12.0 mmol). The mixture was stirred at room temperature for 20 min. 2-(Diethoxymethyl)-4-nitropyridine (905 mg, 4.00 mmol) was added, and the vessel was sealed and heated to 85 °C

(external temperature) for 17 h. The reaction mixture was then cooled to 23 °C and neutralized with saturated aqueous NH_4Cl (20 mL). The resulting solution was extracted with EtOAc (3 × 15 mL). The combined organic layers were dried over anhydrous Na_2SO_4, filtered, and concentrated *in vacuo*. The crude material was combined with another batch (1.0 mmol scale, with respect to 2-(diethoxymethyl)-4-nitropyridine prepared using the same procedure and purified by flash chromatography (0 to 40% EtOAc in hexanes) on silica gel (100 mL) to afford 2-(diethoxymethyl)-4-isopropylthiopyridine as a pale yellow oil (1.25 g, 98% combined yield).

2-(Diethoxymethyl)-4-(isopropylthio)pyridine: R_f = 0.45 (60% EtOAc in hexanes); IR (neat): ν_{max} = 2974, 2929, 2870, 1577, 1541, 1274, 1238, 1156, 1113, 1092, 1053 cm^{-1}; ^1H NMR (400 MHz, 293 K, $CDCl_3$): δ 8.37 (d, J = 5.2 Hz, 1H, 6-H), 7.43 (d, J = 1.4 Hz, 1H, 3-H), 7.07 (dd, J = 5.2, 1.4 Hz, 1H, 5-H), 5.41 (s, 1H, -C*H*(OCH_2CH_3)$_2$), 3.75–3.57 (m, 5H, -CH(OCH_2CH_3)$_2$ and -SC*H*(CH_3)$_2$), 1.39 (d, J = 6.8 Hz, 6H, -SCH(CH_3)$_2$), 1.25 (overlapped t, J = 6.0 Hz, 6H, -CH(OCH_2CH_3)$_2$); ^{13}C NMR (100 MHz, 293 K, $CDCl_3$): δ 158.0, 149.7, 148.4, 121.2, 118.7, 102.5, 62.2, 35.0, 22.7, 15.1; HRMS (ESI+) calcd for $C_{13}H_{22}NO_2S$ $[M + H]^+$ = 256.1366, found 256.1367.

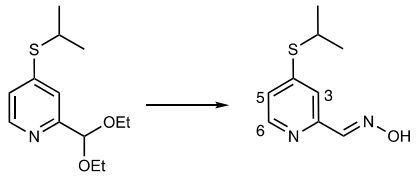

Preparation of (E)-4-(isopropylthio)picolinaldehyde oxime: A 100-mL pear-shaped flask, open to air, with 2-(diethoxymethyl)-4-isopropylthiopyridine (650 mg, 2.54 mmol) was charged with H_2O (7 mL) and 5 M H_2SO_4 in H_2O (610 μL, 3.05 mmol). The solution was heated to 88 °C (external temperature). After stirring at the same temperature for 6 h, the reaction mixture was cooled to 23 °C and treated with K_2CO_3 (1.40 g, 10.2 mmol) followed by MeOH (27 mL) and NH_2OH•HCl (177 mg, 2.54 mmol) at the same temperature. A reflux condenser was attached, and

the reaction was heated to reflux for 4 h while open to air. The reaction mixture was cooled to 23 °C and concentrated *in vacuo.* EtOAc (10 mL) was added to the crude residue, followed by saturated aqueous NH_4Cl (10 mL). The layers were separated using a separatory funnel, and the aqueous layer was extracted with EtOAc (2 × 15 mL). The combined organic layers were dried over anhydrous Na_2SO_4, filtered, and concentrated *in vacuo* to afford (*E*)-4-isopropylthiopicolinaldehyde oxime (449 mg, 90% yield) as a light peach solid. This material was used directly without further purification.

(E)-4-(Isopropylthio)picolinaldehyde oxime: m.p. = 164–168 °C; R_f = 0.46 (60% EtOAc in hexanes); IR (neat): ν_{max} = 2964, 2866, 2724, 1580, 1539, 1406, 1280, 1241, 1223, 1157, 1112, 1102, 1052 cm^{-1}; ^1H NMR (300 MHz, 293 K, DMSO-d_6): δ 11.71 (s, 1H, -CH=NO*H*), 8.38 (d, *J* = 5.4 Hz, 1H, 6-H), 8.02 (s, 1H, -C*H*=NOH), 7.57 (d, *J* = 1.5 Hz, 1H, 3-H), 7.26 (dd, *J* = 5.4, 1.5 Hz, 1H, 5-H), 3.77 (septet, *J* = 6.6 Hz, 1H, -SC*H*$(CH_3)_2$), 1.33 (d, *J* = 6.6 Hz, 6H, -SCH(C*H*$_3)_2$); ^{13}C NMR (100 MHz, 293 K, DMSO-d_6): δ 152.5, 149.7, 149.2, 149.0, 122.0, 117.2, 34.9, 23.0; HRMS (ESI+) calcd for $C_9H_{13}N_2OS$ $[M + H]^+$ = 197.0743, found 197.0741.

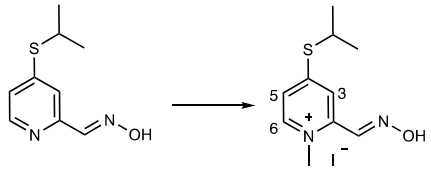

*Preparation of (E)-2-((hydroxyimino)methyl)-4-(isopropylthio)-1-methylpyridin-1-ium iodide (**ADG3060**):* A 35-mL sealed tube with (*E*)-4-isopropylthiopicolinaldehyde oxime (200 mg, 1.02 mmol) was charged with acetone (2 mL), and MeI (630 μL, 10.2 mmol). The vessel was sealed and heated to 55 °C (external temperature). After 19 h at the same temperature, the reaction mixture was cooled to 23 °C, transferred to a 25-mL round-bottomed flask, concentrated *in vacuo*,

and recrystallized from acetone/EtOAc (1:1) to afford (*E*)-2-((hydroxyimino)methyl)-1-methyl-4-(isopropylthio)pyridin-1-ium iodide as a yellow solid (344 mg, quantitative yield).

(E)-2-((Hydroxyimino)methyl)-4-(isopropylthio)-1-methylpyridin-1-ium iodide: m.p. = 163–166 °C; R_f = 0.11 (100% EtOAc); IR (neat): ν_{max} = 3139, 2964, 1582, 1549, 1498, 1312, 1230, 1088 cm^{-1}; ^1H NMR (300 MHz, 293 K, DMSO-d_6): δ 13.04 (s, 1H, -CH=NO*H*), 8.66 (d, *J* = 6.9 Hz, 1H, 6-H), 8.59 (s, 1H, -C*H*=NOH), 8.01 (d, *J* = 2.1 Hz, 1H, 3-H), 7.90 (dd, *J* = 6.9, 2.4 Hz, 1H, 5-H), 4.19 (s, 3H, -N^+CH_3), 4.03 (sept, *J* = 6.9 Hz, 1H, -SC*H*$(CH_3)_2$), 1.40 (d, *J* = 6.9 Hz, 6H, -SCH(CH_3)$_2$; ^{13}C NMR (100 MHz, 293 K, DMSO-d_6): δ 161.0, 145.8, 145.2, 142.1, 122.8, 120.3, 45.4, 36.1, 22.4; HRMS (ESI+) calcd for $C_{10}H_{15}N_2OS$ $[M]^+$ = 211.0899, found 211.0898.

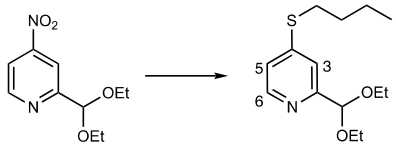

Preparation of 2-(diethoxymethyl)-4-butylthiopyridine: A 25-mL sealed tube was charged with dimethyl sulfoxide (3 mL), K_2CO_3 (1.24 g, 9.00 mmol) and *n*-butylthiol (920 μL, 9.00 mmol). The mixture was stirred at room temperature for 15 min. 2-(Diethoxymethyl)-4-nitropyridine (320 mg, 1.41 mmol) was added, and the vessel was sealed and heated to 95 °C (external temperature) for 16 h. The reaction mixture was then cooled to 23 °C and neutralized with saturated aqueous NH_4Cl (10 mL). The resulting solution was extracted with EtOAc (3 × 20 mL). The combined organic layers were dried over anhydrous Na_2SO_4, filtered, and concentrated *in vacuo*. The crude material was combined with another batch (1.0 mmol scale, with respect to 2-(diethoxymethyl)-4-nitropyridine prepared using the same procedure and purified by flash chromatography (0 to 50% EtOAc in hexanes) on silica gel (50 mL) to afford 2-(diethoxymethyl)-4-butylthiopyridine as a pale yellow oil (477 mg, 74% combined yield).

2-(Diethoxymethyl)-4-butylthiopyridine: R_f = 0.59 (60% EtOAc in hexanes); IR (neat): ν_{max} = 2972, 2930, 2874, 1578, 1542, 1272, 1225, 1114, 1092, 1057 cm^{-1}; ^1H NMR (400 MHz, 293 K, $CDCl_3$): δ 8.35 (d, *J* = 5.6 Hz, 1H, 6-H), 7.41 (d, *J* = 1.2 Hz, 1H, 3-H), 7.06 (dd, *J* = 5.6, 2.0 Hz, 1H, 5-H), 5.41 (s, 1H, -C*H*(OCH_2CH_3)$_2$), 3.75–3.57 (m, 4H, -CH(OCH_2CH_3)$_2$), 2.99 (t, *J* = 7.2 Hz, 2H, -S$CH_2CH_2CH_2CH_3$), 1.70 (app quintet, *J* = 7.2 Hz, 2H, -$SCH_2CH_2CH_2CH_3$), 1.49 (app sextet, *J* = 7.2 Hz, 2H, -$SCH_2CH_2CH_2CH_3$), 1.26 (t, *J* = 7.2 Hz, 6H, -CH(OCH_2CH_3)$_2$), 0.96 (t, *J* = 7.2 Hz, 3H, -$SCH_2CH_2CH_2CH_3$); ^{13}C NMR (100 MHz, 293 K, $CDCl_3$): δ 157.8, 150.2, 148.2, 120.2, 117.5, 102.5, 62.2, 30.4, 30.2, 21.9, 15.1, 13.5; HRMS (ESI+) calcd for $C_{14}H_{24}NO_2S$ [M + H]$^+$ = 270.1522, found 270.1526.

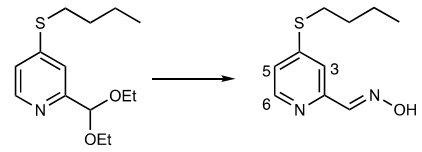

Preparation of (E)-4-(butylthio)picolinaldehyde oxime: A 50-mL pear-shaped flask, open to air, with 2-(diethoxymethyl)-4-butylthiopyridine (300 mg, 1.11 mmol) was charged with H_2O (4 mL) and 5 M H_2SO_4 in H_2O (270 μL, 1.33 mmol). The solution was heated to 92 °C (external temperature). After stirring at the same temperature for 3 h, the reaction mixture was cooled to 23 °C and treated with K_2CO_3 (614 mg, 4.44 mmol) followed by MeOH (14 mL) and NH_2OH•HCl (77 mg, 1.1 mmol) at the same temperature. A reflux condenser was attached, and the reaction was heated to reflux for 2 h while open to air. The reaction mixture was cooled to 23 °C and concentrated *in vacuo.* EtOAc (10 mL) was added to the crude residue, followed by saturated aqueous NH_4Cl (10 mL). The layers were separated using a separatory funnel, and the aqueous layer was extracted with EtOAc (2 × 10 mL). The combined organic layers were dried over anhydrous Na_2SO_4, filtered, and concentrated *in vacuo* to afford (*E*)-4-butylthiopicolinaldehyde

oxime (216 mg, 93% yield) as a light pink solid. This material was used directly without further purification.

(E)-4-(Butylthio)picolinaldehyde oxime: m.p. = 125–128 °C; R_f = 0.48 (60% EtOAc in hexanes); IR (neat): ν_{max} = 2953, 2869, 2714, 1634, 1579, 1535, 1436, 1230, 1112, 1097 cm^{-1}; ^1H NMR (400 MHz, 293 K, DMSO-d_6): δ 11.71 (s, 1H, -CH=NO*H*), 8.36 (d, *J* = 5.2 Hz, 1H, 6-H), 8.02 (s, 1H, -C*H*=NOH), 7.56 (d, *J* = 1.6 Hz, 1H, 3-H), 7.26 (dd, *J* = 5.2, 1.6 Hz, 1H, 5-H), 3.07 (t, *J* = 7.2 Hz, 2H, -SC*H*$_2$CH$_2$CH$_2$CH$_3$), 1.62 (app quint, *J* = 7.2 Hz, 2H, -SCH$_2$C*H*$_2$CH$_2$CH$_3$),1.43 (app sextet, *J* = 7.2 Hz, 2H, -SCH$_2$CH$_2$C*H*$_2$CH$_3$) 0.97 (t, *J* = 7.2 Hz, 3H, -SCH$_2$CH$_2$CH$_2$C*H*$_3$); ^{13}C NMR (100 MHz, 293 K, DMSO-d_6): δ 152.3, 149.8, 149.5, 149.0, 121.1, 116.2, 30.5, 29.7, 21.8, 13.9; HRMS (ESI+) calcd for $C_{10}H_{15}N_2OS$ $[M + H]^+$ = 211.0899, found 211.0896.

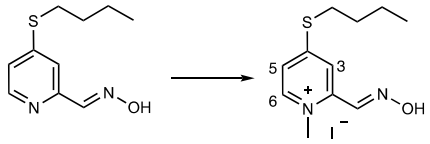

*Preparation of (E)-4-(butylthio)-2-((hydroxyimino)methyl)-1-methylpyridin-1-ium iodide (**ADG2294**):* A 35-mL sealed tube with (*E*)-4-butylthiopicolinaldehyde oxime (150 mg, 0.710 mmol) was charged with acetone (2 mL), and MeI (440 μL, 7.14 mmol). The vessel was sealed and heated to 55 °C (external temperature). After 18 h at the same temperature, the reaction mixture was cooled to 23 °C, transferred to a 25-mL round-bottomed flask, and concentrated *in vacuo*, and recrystallized from acetone/EtOAc (1:1) to afford (*E*)-2-((hydroxyimino)methyl)-1-methyl-4-(butylthio)pyridin-1-ium iodide as a yellow solid (206 mg, 82% yield).

(E)-2-((Hydroxyimino)methyl)-4-(butylthio)-1-methylpyridin-1-ium iodide: m.p. = 150–153 °C; R_f = 0.11 (100% EtOAc); IR (neat): ν_{max} = 3069, 2960, 1549, 1500, 1316, 1222, 1088 cm^{-1}; ^1H NMR (400 MHz, 293 K, DMSO-d_6): δ 13.04 (s, 1H, -CH=NO*H*), 8.64 (d, *J* = 7.2 Hz, 1H, 6-

H), 8.58 (s, 1H, -C*H*=NOH), 8.02 (d, *J* = 2.4 Hz, 1H, 3-H), 7.89 (dd, *J* = 7.2, 2.4 Hz, 1H, 5-H), 4.19 (s, 3H, -N^+CH_3), 3.28 (t, *J* = 7.2 Hz, 2H, -$SCH_2CH_2CH_2CH_3$), 1.66 (app quint, *J* = 7.2 Hz, 2H, -$SCH_2CH_2CH_2CH_3$), 1.45 (app sextet, *J* = 7.2 Hz, 2H, -$SCH_2CH_2CH_2CH_3$) 0.92 (t, *J* = 7.2 Hz, 3H, -$SCH_2CH_2CH_2CH_3$); ^{13}C NMR (100 MHz, 293 K, DMSO-d_6): δ 161.7, 145.6, 145.0, 142.1, 122.5, 119.9, 45.4, 30.5, 29.9, 21.7, 13.9; HRMS (ESI+) calcd for $C_{11}H_{17}N_2OS$ $[M]^+$ = 225.1056, found 225.1055.

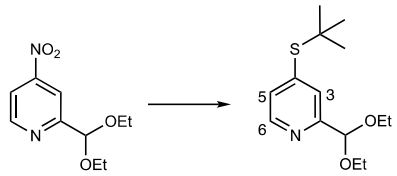

Preparation of 2-(diethoxymethyl)-4-tert-butylthiopyridine: A 35-mL sealed tube was charged with dimethyl sulfoxide (2 mL), K_2CO_3 (830 g, 6.00 mmol) and *tert*-butylthiol (570 μL, 6.00 mmol). The mixture was stirred at room temperature for 5 min. 2-(Diethoxymethyl)-4-nitropyridine (452 mg, 2.00 mmol) was added, and the vessel was sealed and heated to 90 °C (external temperature) for 8 h. The reaction mixture was then cooled to 23 °C and neutralized with saturated aqueous NH_4Cl (10 mL). The resulting solution was extracted with EtOAc (3 × 20 mL). The combined organic layers were dried over anhydrous Na_2SO_4, filtered, and concentrated *in vacuo.* The crude material was purified by flash chromatography (0 to 50% EtOAc in hexanes) on silica gel (20 mL) to afford 2-(diethoxymethyl)-4-*tert*-butylthiopyridine as a yellow oil (351 mg, 65% yield).

2-(Diethoxymethyl)-4-tert-butylthiopyridine: R_f = 0.45 (60% EtOAc in hexanes); IR (neat): ν_{max} = 2974, 1576, 1541, 1458, 1267, 1161, 1114, 1057 cm^{-1}; ^{1}H NMR (400 MHz, 293 K, $CDCl_3$): δ 8.50 (d, *J* = 5.2 Hz, 1H, 6-H), 7.69 (d, *J* = 1.4 Hz,), 7.33 (dd, *J* = 5.2, 1.4 Hz, 1H, 5-H), 5.48 (s,

1H, -C*H*(OCH_2CH_3)$_2$), 3.74–3.58 (m, 4H, -CH(OC*H*$_2$CH$_3$)$_2$), 1.39 (s, 9H, -SC(C*H*$_3$)$_3$), 1.26 (t, J = 7.2 Hz, 6H, -CH(OCH_2CH_3)$_2$); ^{13}C NMR (100 MHz, 293 K, $CDCl_3$): δ 158.0, 148.5, 145.1, 128.8, 126.6, 102.1, 61.9, 46.8, 31.0 15.0; HRMS (ESI+) calcd for $C_{14}H_{24}NO_2S$ $[M + H]^+$ = 270.1522, found 270.1529.

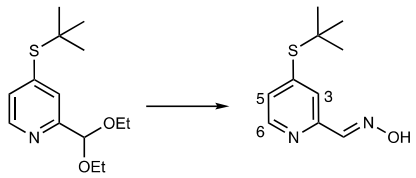

Preparation of (E)-4-(tert-butylthio)picolinaldehyde oxime: A 10-mL pear-shaped flask, open to air, with 2-(diethoxymethyl)-4-*tert*-butylthiopyridine (105 mg, 0.370 mmol) was charged with H_2O (1 mL) and 5 M H_2SO_4 in H_2O (90 μL, 0.44 mmol). The solution was heated to 90 °C (external temperature). After stirring at the same temperature for 3 h, the reaction mixture was cooled to 23 °C and treated with K_2CO_3 (205 mg, 1.48 mmol) followed by MeOH (5 mL) and NH_2OH•HCl (26 mg, 0.37 mmol) at the same temperature. A reflux condenser was attached, and the reaction was heated to reflux for 1.5 h while open to air. The reaction mixture was cooled to 23 °C and concentrated *in vacuo.* EtOAc (10 mL) was added to the crude residue, followed by saturated aqueous NH_4Cl (15 mL). The layers were separated using a separatory funnel, and the aqueous layer was extracted with EtOAc (2 × 10 mL). The combined organic layers were dried over anhydrous Na_2SO_4, filtered, and concentrated *in vacuo* to afford (*E*)-4-*tert*-butylthiopicolinaldehyde oxime (78 mg, quantitative yield) as a peach-colored solid. This material was used directly without further purification.

(E)-4-tert-Butylthiopicolinaldehyde oxime: m.p. = 130–132 °C; R_f = 0.59 (100% EtOAc); IR (neat): ν_{max} = 3157, 3057, 2967, 2864, 2740, 1578, 1539, 1456, 1225, 1158, 1114, 1094 cm^{-1};

^{1}H NMR (400 MHz, 293 K, DMSO-d_6): δ 11.80 (s, 1H, -CH=NO*H*), 8.51 (d, *J* = 5.2 Hz, 1H, 6-H), 8.09 (s, 1H, -C*H*=NOH), 7.78 (d, *J* = 1.6 Hz, 1H, 3-H), 7.43 (dd, *J* = 5.2, 1.6 Hz, 1H, 5-H), 1.37 (s, 9H, -SC(CH_3)$_3$); ^{13}C NMR (100 MHz, 293 K, DMSO-d_6): δ 152.7, 149.9, 148.9, 145.0, 128.8, 124.4, 47.5, 31.2; HRMS (ESI+) calcd for $C_{10}H_{15}N_2OS$ $[M + H]^+$ =211.0899, found 211.0897.

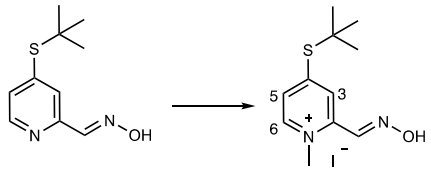

*Preparation of (E)-4-(tert-butylthio)-2-((hydroxyimino)methyl)-1-methylpyridin-1-ium iodide (**ADG3001**):* A 35-mL sealed tube with (*E*)-4-*tert*-butylthiopicolinaldehyde oxime (150 mg, 0.710 mmol) was charged with acetone (2 mL), and MeI (430 μL, 7.10 mmol). The vessel was sealed and heated to 45 °C (external temperature). After 13 h at the same temperature, the reaction mixture was cooled to 23 °C, transferred to a 25-mL round-bottomed flask, concentrated *in vacuo*, and recrystallized from EtOH to afford (*E*)-2-((hydroxyimino)methyl)-1-methyl-4-(*tert*-butylthio)pyridin-1-ium iodide as a yellow solid (43.3 mg, 17% yield).

(E)-4-(tert-Butylthio)-2-((hydroxyimino)methyl)-1-methylpyridin-1-ium iodide: m.p. = 171–175 °C; R_f = 0.08 (10% MeOH in CH_2Cl_2); IR (neat): ν_{max} = 3086, 2966, 1547, 1495, 1303, 1238, 1084 cm^{-1}; ^{1}H NMR (400 MHz, 293 K, DMSO-d_6): δ 13.09 (s, 1H, -CH=NO*H*), 8.65–8.62 (m, 2H, 6-H and -C*H*=NOH), 8.08 (app s, 1H, 3-H), 7.98 (app d, *J* = 4.8 Hz, 1H, 5-H), 4.21 (s, 3H, -N$^+$CH_3), 1.59 (s, 9H, -SC(CH_3)$_3$; ^{13}C NMR (100 MHz, 293 K, DMSO-d_6): δ 160.0, 145.9, 145.3, 142.1, 124.7, 121.7, 49.8, 45.5, 30.4; HRMS (ESI+) calcd for $C_{11}H_{17}N_2OS$ $[M]^+$ = 225.1056, found 225.1055.

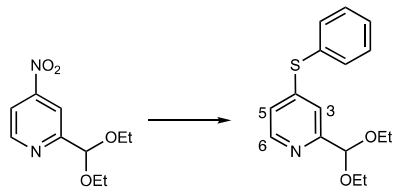

Preparation of 2-(diethoxymethyl)-4-(phenylthio)pyridine: A 35-mL sealed tube was charged with dimethyl sulfoxide (3 mL), K_2CO_3 (1.24 g, 9.00 mmol), and thiophenol (930 μL, 9.00 mmol). The mixture was stirred at room temperature for 10 min. 2-(Diethoxymethyl)-4-nitropyridine (680 mg, 3.00 mmol) was added, and the vessel was sealed and heated to 95 °C (external temperature) for 17 h. The reaction mixture was then cooled to 23 °C and neutralized with saturated aqueous NH_4Cl (10 mL). The resulting solution was extracted with EtOAc (3 × 20 mL). The combined organic layers were dried over anhydrous Na_2SO_4, filtered, and concentrated *in vacuo*. The crude material was combined with another batch (1.0 mmol scale, with respect to 2-(diethoxymethyl)-4-nitropyridine prepared using the same procedure and purified by flash chromatography (0 to 50% EtOAc in hexanes) on silica gel (200 mL) to afford 2-(diethoxymethyl)-4-(phenylthio)pyridine as a colorless oil (850 mg, 73% combined yield).

2-(Diethoxymethyl)-4-(phenylthio)pyridine: R_f = 0.55 (60% EtOAc in hexanes); IR (neat): ν_{max} = 3052, 2975, 2877, 1575, 1544, 1273, 1231, 1112, 1087, 1056 cm^{-1}; ^1H NMR (400 MHz, 293 K, $CDCl_3$): δ 8.32 (d, J = 5.2 Hz, 1H, 6-H), 7.56–7.54 (m, 2H, -*Ph*), 7.45–7.44 (m, 3H, -*Ph*), 7.32 (d, J = 1.6 Hz, 1H, 3-H), 6.82 (dd, J = 5.2, 1.6 Hz, 1H, 5-H), 5.38 (s, 1H, -C*H*$(OCH_2CH_3)_2$), 3.71–3.53 (m, 4H, -CH(OC*H*$_2$$CH_3)_2$), 1.22 (t, J = 7.2 Hz, 6H, -CH$(OCH_2$C*H*$_3)_2$); ^{13}C NMR (100 MHz, 293 K, $CDCl_3$): δ 157.8, 151.0, 148.6, 134.9, 129.7, 129.4, 129.3, 120.1, 117.9, 102.1, 62.0. 14.9; HRMS (ESI+) calcd for $C_{16}H_{20}NO_2S$ $[M + H]^+$ = 290.1209, found 290.1222.

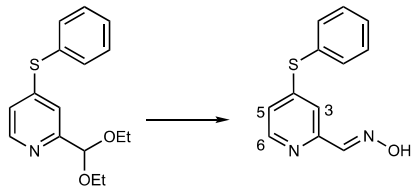

Preparation of (E)-4-(phenylthio)picolinaldehyde oxime: A 100-mL pear-shaped flask, open to air, with 2-(diethoxymethyl)-4-(phenylthio)pyridine (645 mg, 2.23 mmol) was charged with H_2O (7 mL) and 5 M H_2SO_4 in H_2O (530 μL, 2.67 mmol). The solution was heated to 95 °C (external temperature). After stirring at the same temperature for 4 h, the reaction mixture was cooled to 23 °C and treated with K_2CO_3 (1.23 g, 8.92 mmol) followed by MeOH (27 mL) and NH_2OH•HCl (155 mg, 2.23 mmol) at the same temperature. A reflux condenser was attached, and the reaction was heated to reflux while open to air. After 2 h, the reaction mixture was cooled to 23 °C and concentrated *in vacuo.* EtOAc (10 mL) was added to the crude residue, followed by saturated aqueous NH_4Cl (10 mL). The layers were separated using a separatory funnel and the aqueous layer was extracted with EtOAc (2 × 15 mL). The combined organic layers were dried over anhydrous Na_2SO_4, filtered, and concentrated *in vacuo*. The crude material was purified by flash chromatography (10 to 50% EtOAc in hexanes) on silica gel (25 mL) to afford (*E*)- 4-(phenylthio)picolinaldehyde oxime (441 mg, 86% yield) as a pale pink solid.

(E)-4-(Phenylthio)picolinaldehyde oxime: m.p. = 172–175 °C; R_f = 0.38 (60% EtOAc in hexanes); IR (neat): ν_{max} = 2982, 2715, 1575, 1537, 1325, 1230, 1116, 1025 cm^{-1}; ^1H NMR (400 MHz, 293 K, DMSO-d_6): δ 11.71 (s, 1H, -CH=NO*H*), 8.37 (d, *J* = 5.2 Hz, 1H, 6-H), 7.96 (s, 1H, -C*H*=NOH), 7.64–7.62 (m, 2H, -*Ph*), 7.58–7.55 (m, 3H, -*Ph*), 7.28 (d, *J* = 1.6 Hz, 1H, 3-H), 7.11 (dd, *J* = 5.2, 1.6 Hz, 1H, 5-H); ^{13}C NMR (100 MHz, 293 K, DMSO-d_6): δ 152.7, 150.4, 149.7, 148.8, 135.5, 130.8, 130.6, 128.6, 121.0, 115.7; HRMS (ESI+) calcd for $C_{12}H_{11}N_2OS$ $[M + H]^+$ = 231.0587, found 231.0589.

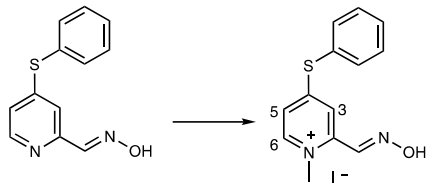

*Preparation of (E)-2-((hydroxyimino)methyl)-1-methyl-4-(phenylthio)pyridin-1-ium iodide (**ADG3002**):* A 35-mL sealed tube with (*E*)-4-(phenylthio)picolinaldehyde oxime (230 mg, 1.00 mmol) was charged with acetone (2 mL), and MeI (610 μL, 10.0 mmol). The vessel was sealed and heated to 55 °C (external temperature). After 18 h at the same temperature, the reaction mixture was cooled to 23 °C, transferred to a 25-mL round-bottomed flask, concentrated *in vacuo*, and recrystallized from acetone/EtOAc (1:1) to afford (*E*)-2-((hydroxyimino)methyl)-1-methyl-4-(phenylthio)pyridin-1-ium iodide as a yellow solid (299 mg, 80% yield).

(E)-2-(Hydroxyimino)methyl)-1-methyl-4-(phenylthio)pyridin-1-ium iodide: m.p. = 175–177 °C; R_f = 0.10 (100% EtOAc); IR (neat): ν_{max} = 3067, 2961, 1548, 1495, 1301, 1235, 1081 cm^{-1}; ^1H NMR (400 MHz, 293 K, DMSO-d_6): δ 13.02 (s, 1H, -CH=NO*H*), 8.63 (d, *J* = 6.8 Hz, 1H, 6-H), 8.54 (s, 1H, -C*H*=NOH), 7.72–7.62 (m, 7H, 3-H, 5-H, -*Ph*), 4.17 (s, 3H, $-N^+CH_3$); ^{13}C NMR (100 MHz, 293 K, DMSO-d_6): δ 161.8, 146.6, 145.5, 141.8, 135.9, 132.1, 131.5, 126.1, 122.4, 118.5, 45.4; HRMS (ESI+) calcd for $C_{13}H_{13}N_2OS$ $[M]^+$ = 245.0743, found 245.0733.

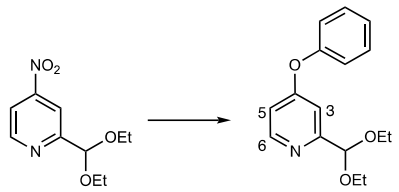

Preparation of 2-(diethoxymethyl)-4-phenoxypyridine: A 35-mL sealed tube was charged with dimethyl sulfoxide (3 mL), K_2CO_3 (1.24 g, 9.00 mmol), and phenol (847 mg, 9.00 mmol).

The mixture was stirred at room temperature for 30 min. 2-(Diethoxymethyl)-4-nitropyridine (680 mg, 3.00 mmol) was added, and the vessel was sealed and heated to 85 °C (external temperature) for 6 h. The reaction mixture was then cooled to 23 °C and neutralized with saturated aqueous NH_4Cl (20 mL). The resulting solution was extracted with EtOAc (3 × 20 mL). The combined organic layers were dried over anhydrous Na_2SO_4, filtered, and concentrated *in vacuo.* The crude material was combined with another batch (1.0 mmol scale, with respect to 2-(diethoxymethyl)-4-nitropyridine prepared using the same procedure and purified by flash chromatography (0 to 40% EtOAc in hexanes) on silica gel (200 mL) to afford 2-(diethoxymethyl)-4-phenoxypyridine as an orange oil (991 mg, 91% yield).

2-(Diethoxymethyl)-4-phenoxypyridine: R_f = 0.55 (60% EtOAc in hexanes); IR (neat): ν_{max} = 2976, 2880, 1582, 1287, 1257, 1209, 1152, 1109, 1057 cm^{-1}; ^1H NMR (400 MHz, 293 K, $CDCl_3$): δ 8.43 (d, *J* = 5.6 Hz, 1H, 6-H), 7.42 (t, *J* = 7.6 Hz, 2H, -*Ph*), 7.27–7.22 (m, 1H, - *Ph*), 7.17 (d, *J* = 2.0 Hz, 1H, 3-H), 7.09 (d, *J* = 7.6 Hz, 2H, -*Ph*), 6.75 (dd, *J* = 5.6, 2.0 Hz, 1H, 5-H), 5.42 (s, 1H, -C*H*(OCH_2CH_3)$_2$), 3.74–3.56 (m, 4H, -CH(OC*H*$_2$$CH_3$)$_2$), 1.24 (t, *J* = 7.2 Hz, 6H, -CH(OCH_2C*H*$_3$)$_2$); ^{13}C NMR (100 MHz, 293 K, $CDCl_3$): δ 165.5, 160.4, 153.9, 150.5, 130.0, 125.2, 120.3, 62.2, 15.0; HRMS (ESI+) calcd for $C_{16}H_{20}NO_3$ $[M + H]^+$ = 274.1438, found 274.1446.

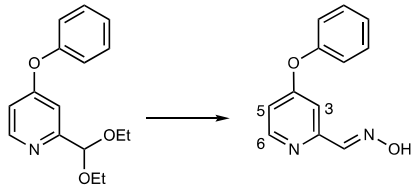

Preparation of (E)-4-phenoxypicolinaldehyde oxime: A 100-mL pear-shaped flask, open to air, with 2-(diethoxymethyl)-4-phenoxypyridine (683 mg, 2.50 mmol) was charged with H_2O (7 mL) and 5 M H_2SO_4 in H_2O (600 μL, 2.75 mmol). The solution was heated to 94 °C (external

temperature). After stirring at the same temperature for 6 h, the reaction mixture was cooled to 23 °C and treated with K_2CO_3 (1.38 g, 10.0 mmol) followed by MeOH (27 mL) and NH_2OH•HCl (174 mg, 2.50 mmol) at the same temperature. A reflux condenser was attached, and the reaction was heated to reflux while open to air. After 2 h, the reaction mixture was cooled to 23 °C and concentrated *in vacuo*. EtOAc (10 mL) was added to the crude residue, followed by saturated aqueous NH_4Cl (10 mL). The layers were separated using a separatory funnel, and the aqueous layer was extracted with EtOAc (2 × 10 mL). The combined organic layers were dried over anhydrous Na_2SO_4, filtered, and concentrated *in vacuo*. The crude residue was purified by flash chromatography (10 to 50% EtOAc in hexanes) on silica gel (20 mL) to afford to afford (*E*)-4-phenoxypicolinaldehyde oxime (505 mg, 94% yield) as a white solid.

(E)-4-Phenoxypicolinaldehyde oxime: m.p. = 133–135 °C; R_f = 0.44 (60% EtOAc in hexanes); IR (neat): ν_{max} = 2982, 1564, 1489, 1406, 1316, 1271, 1200 cm^{-1}; ^1H NMR (400 MHz, 293 K, DMSO-d_6): δ 11.70 (s, 1H, -CH=NO*H*), 8.46 (d, *J* = 5.6 Hz, 1H, 6-H), 8.02 (s, 1H, -C*H*=NOH), 7.51 (t, *J* = 8.0 Hz, 1H, -*Ph*), 7.33 (t, *J* = 8.0 Hz, 1H, -*Ph*), 7.22 (d, *J* = 8.0 Hz, 1H, -*Ph*), 7.13 (d, *J* = 2.4 Hz, 1H, 3-H), 6.99 (dd, *J* = 5.6, 2.4 Hz, 1H, 5-H); ^{13}C NMR (100 MHz, 293 K, DMSO-d_6): δ 164.6, 154.2, 153.3, 151.3, 148.4, 130.5, 125.8, 121.0, 112.6, 106.2; HRMS (ESI+) calcd for $C_{12}H_{11}N_2O_2$ $[M + H]^+$ = 215.0815, found 215.0817.

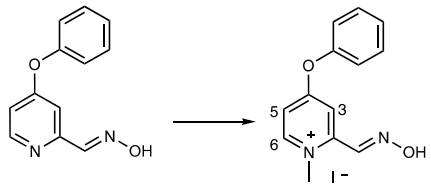

*Preparation of (E)-2-((hydroxyimino)methyl)-1-methyl-4-phenoxypyridin-1-ium iodide (**ADG3003**):* A 35-mL sealed tube with (*E*)-4-phenoxypicolinaldehyde oxime (102 mg, 0.510

mmol) was charged with acetone (2 mL), and MeI (318 μL, 5.14 mmol). The vessel was sealed and heated to 45 °C (external temperature). After 19 h at the same temperature, the reaction mixture was cooled to 23 °C, transferred to a 25-mL round-bottomed flask, and concentrated *in vacuo*. The dark brown crude residue was triturated with acetone/EtOAc (1:1) to afford (*E*)-2-((hydroxyimino)methyl)-1-methyl-4-phenoxypyridin-1-ium iodide as a yellow solid (119 mg, 66% yield).

(E)-2-((Hydroxyimino)methyl)-1-methyl-4-phenoxypyridin-1-ium iodide: m.p. = 147–150 °C; R_f = 0.10 (100% EtOAc); IR (neat): ν_{max} = 3052, 2164, 1584, 1485, 1301, 1261, 1072 cm^{-1}; ^1H NMR (300 MHz, 293 K, DMSO-d_6): δ 13.05 (s, 1H, -CH=NO*H*), 8.83 (d, *J* = 7.2 Hz, 1H, 6-H), 8.59 (s, 1H, -C*H*=NOH), 7.63–7.58 (m, 3H, -*Ar*), 7.52–7.43 (m, 3H, -*Ar*), 7.35 (d, *J* = 7.8 Hz, 2H, -*Ph*), 4.23 (s, 3H, -N^+CH_3); ^{13}C NMR (100 MHz, 293 K, DMSO-d_6): δ 169.0, 152.4, 150.0, 149.2, 141.8, 131.5, 127.9, 121.4, 115.1, 110.2, 45.2; HRMS (ESI+) calcd for $C_{13}H_{13}N_2O_2$ $[M]^+$ = 229.0971, found 229.0970.

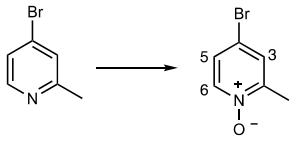

Preparation of 4-bromo-2-methylpyridine 1-oxide: 4-Bromo-2-methylpyridine 1-oxide was prepared according to a procedure found in the literature.[99] A 1-L round-bottomed flask was charged with 4-bromo-2-methylpyridine (31.0 g, 180 mmol) at 0 °C under an open atmosphere. Aqueous 0.6 M K_2CO_3 (90 mL), *t*-BuOH (90 mL), MeCN (14.0 mL, 270 mmol), 30% aqueous H_2O_2 (108 mL, 900 mmol), and 2,2,2-trifluoroacetophenone (2.5 mL, 18 mmol) were added sequentially in one portion. The reaction mixture was stirred under open atmosphere for 22 h and was allowed to warm to 23 °C. After this period, brine (100 mL) was added, and reaction mixture

was extracted with CH_2Cl_2 (6 × 100 mL) using a separatory funnel. The combined organic layers were dried over anhydrous Na_2SO_4, filtered, and concentrated *in vacuo*. The crude residue was purified by flash chromatography (60 to 100% EtOAc in hexanes) on silica gel (200 mL) to afford 4-bromo-2-methylpyridine 1-oxide (12.43 g, 37% yield) as a pale yellow oil .

4-Bromo-2-methylpyridine 1-oxide: ^{1}H NMR (300 MHz, 293 K, $CDCl_3$) δ 8.14 (d, *J* = 6.9 Hz, 1H, 6-H), 7.43 (d, *J* = 2.4 Hz, 1H, 3-H), 7.29 (dd, *J* = 6.9, 2.4 Hz, 1H, 5-H), 2.50 (s, 3H). The ^{1}H NMR data for 4-bromo-2-methylpyridine 1-oxide was consistent with those in the literature.[149]

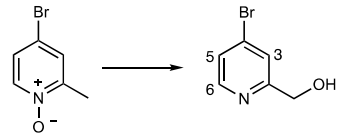

Preparation of (4-bromopyridin-2-yl)methanol: A 1-L round-bottomed flask with 4-bromo-2-methylpyridine 1-oxide (19.7 g, 104 mmol) was evacuated and refilled with nitrogen gas three times and charged with CH_2Cl_2 (140 mL) at 0 °C. TFAA (44.0 mL, 313 mmol) in CH_2Cl_2 (140 mL) was added. The reaction mixture was allowed to warm to 23 °C and was stirred for 42 h. After this period, the reaction mixture was cooled to 0 °C. Then, *t*-BuOH (60 mL) and saturated aqueous K_2CO_3 (60 mL) were added to the reaction mixture. The resulting mixture was stirred for 24 h and gradually warmed to 23 °C. The mixture was extracted with CH_2Cl_2 (4 × 125 mL) using a separatory funnel. The combined organic layers were dried over anhydrous Na_2SO_4, filtered, and concentrated *in vacuo* to afford (4-bromopyridin-2-yl)methanol (20.4 g, quantitative yield) as an amber oil. This material was used directly without further purification.

(4-Bromopyridin-2-yl)methanol: ^{1}H NMR (300 MHz, 293 K, 1% w/w CD_3OD in $CDCl_3$) δ 8.31 (d, *J* = 5.4 Hz, 1H, 6-H), 7.57 (d, *J* = 1.5 Hz, 1H, 3-H), 7.37 (dd, *J* = 5.4 1.5 Hz, 1H, 5-H),

4.73 (s, 2H, -C*H*$_2$OH). The ^{1}H NMR data for (4-bromopyridin-2-yl)methanol was consistent with those in the literature.[150]

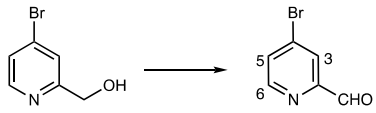

Preparation of 4-bromopicolinaldehyde: A 1-L round bottomed flask with a reflux condenser was evacuated and refilled with nitrogen gas three times, and (4-bromopyridin-2-yl)methanol (20.4 g, 108 mmol), DCE (450 mL), and MnO_2 (42.3 g, 487 mmol) were added consecutively. The mixture was heated to reflux. After 17 h, the reaction mixture was cooled to 23 °C, filtered through Celite®, washed with EtOAc, and concentrated *in vacuo*. The crude residue was purified by flash chromatography (20 to 40% EtOAc in hexanes) on silica gel (300 mL) to afford **4-bromopicolinaldehyde** (10.9 g, 54% yield) as a red solid.

4-Bromopicolinaldehyde: ^{1}H NMR (400 MHz, 293 K, $CDCl_3$): δ = 10.03 (s, 1H, C*H*O), 8.60 (d, *J* = 5.2 Hz, 1H, 6-H), 8.10 (d, *J* = 1.2 Hz, 1H, 3-H), 7.69 (dd, *J* = 5.2, 1.2 Hz, 1H, 5-H). The ^{1}H NMR data for **4-bromopicolinaldehyde** was consistent with those in the literature.[151]

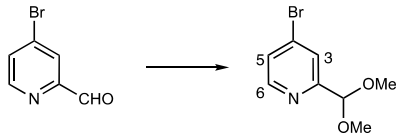

Preparation of 4-bromo-2-(dimethoxymethyl)pyridine: A 250-mL round-bottom flask with 4-bromopicolinaldehyde (10.9 g, 58.1 mmol) was charged with MeOH (80 mL) and 7.0 M H_2SO_4 in MeOH (9.13 mL, 63.9 mmol). A reflux condenser was attached, and the solution was heated to reflux open to air. After 5 h, the reaction mixture was cooled to 23 °C and quenched with saturated aqueous $NaHCO_3$ (75 mL). The organic solvent was removed *in vacuo*, and the aqueous layer was

extracted with CH_2Cl_2 (2 × 75 mL) using a separatory funnel. The combined organic layers were dried over anhydrous Na_2SO_4, filtered, and concentrated *in vacuo*. The crude residue was purified by flash chromatography (20 to 50% EtOAc in hexanes) on silica gel (400 mL) to afford 4-bromo-2-(dimethoxymethyl)pyridine (9.77 g, 73% yield) as an amber oil.

4-Bromo-2-(dimethoxymethyl)pyridine: ^{1}H NMR (400 MHz, 293 K, $CDCl_3$) δ 8.44 (d, *J* = 5.2 Hz, 1H, 6-H), 7.74 (d, *J* = 2.0 Hz, 1H, 3-H), 7.42 (dd, *J* = 5.2, 2.0 Hz, 1H, 5-H), 5.36 (s, 1H, -C*H*$(OCH_3)_2$), 3.41 (s, 6H, -CH(OC*H*$_3)_2$). The ^{1}H NMR data for 4-bromo-2-(dimethoxymethyl)pyridine was consistent with those in the literature.[152]

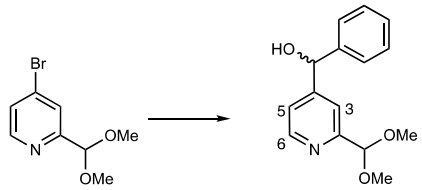

Preparation of (2-(dimethoxymethyl)pyridin-4-yl)(phenyl)methanol: A 100-mL flame-dried, round-bottom flask with 4-bromo-2-(dimethoxymethyl)pyridine (1.62 g, 7.00 mmol) was evacuated and refilled with nitrogen gas three times and charged with THF (30 mL) and isopropylmagnesium chloride (2.0 M in THF, 3.5 mL). After stirring for 8 h, benzaldehyde (0.71 mL, 7.0 mmol) was added to the reaction mixture. The crude material was purified by flash chromatography (50 to 100% EtOAc in hexanes) on silica gel (90 mL) to afford (2-(dimethoxymethyl)pyridin-4-yl)(phenyl)methanol (596 mg, 33% yield) as a light orange solid.

2-(Diethoxymethyl)-4-(phenylsulfonyl)pyridine: m.p. = 87–90 °C; R_f = 0.15 (60% EtOAc in hexanes); IR (neat): ν_{max} = 3167, 2942, 2834, 1736, 1607, 1456, 1368, 1250, 1149, 1114, 1026, 983 cm^{-1}; ^{1}H NMR (300 MHz, 293 K, DMSO-d_6): δ 8.45 (d, *J* = 4.8 Hz, 1H, 6-H), 7.51 (s, 1H, 3-H), 7.39–7.30 (m, 5H, -*Ar*), 7.64 (t, *J* = 6.9 Hz, 1H, -*Ph*), 6.15 (d, *J* = 3.9 Hz, 1H, -CHO*H*), 5.75

(d, J = 3.9 Hz, 1H, -C*H*OH), 5.25 (s, 1H, -C*H*(OCH_3)$_2$), 3.28 (s, 6H, -C*H*(OCH_3)$_2$); ^{13}C NMR (75 MHz, 293 K, DMSO-d_6): δ 157.45, 155.3, 149.1, 144.8, 128.8, 127.8, 126.9, 121.6, 118.4, 104.6, 73.6, 54.0, 53.9; HRMS (ESI+) calcd for $C_{15}H_{18}NO_3$ $[M + H]^+$ = 260.1281, found 260.1285.

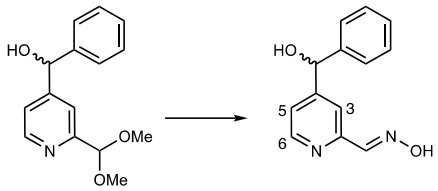

Preparation of (E)-4-(hydroxy(phenyl)methyl)picolinaldehyde oxime: A 50-mL pear-shaped flask, open to air, with (2-(dimethoxymethyl)pyridin-4-yl)(phenyl)methanol (478 mg, 1.84 mmol) was charged with H_2O (4 mL) and 5 M H_2SO_4 in H_2O (440 μL, 2.21 mmol). The solution was heated to 95 °C (external temperature). After stirring at the same temperature for 4 h, the reaction mixture was cooled to 23 °C and treated with K_2CO_3 (1.01 g, 7.36 mmol) followed by MeOH (10 mL) and NH_2OH•HCl (127 mg, 1.84 mmol) at the same temperature. A reflux condenser was attached, and the reaction was heated to reflux while open to air. After 5 h, the reaction mixture was cooled to 23 °C and concentrated *in vacuo.* EtOAc (20 mL) was added to the crude residue, followed by saturated aqueous NH_4Cl (25 mL). The layers were separated using a separatory funnel and the aqueous layer was extracted with EtOAc (2 × 20 mL). The combined organic layers were dried over anhydrous Na_2SO_4, filtered, and concentrated *in vacuo* to afford (*E*)-4-(hydroxy(phenyl)methyl)picolinaldehyde oxime (396 mg, 95% yield) as a pale yellow solid.

(E)-4-(Phenylsulfonyl)picolinaldehyde oxime: m.p. = 157–160 °C; R_f = 0.46 (100% EtOAc); IR (neat): ν_{max} = 3409, 2972, 2873, 2563, 1771, 1599, 1561, 1523, 1492, 1451, 1422, 1336, 1248, 1177, 1049, 963 cm^{-1}; ^{1}H NMR (400 MHz, 293 K, DMSO-d_6): δ 11.62 (s, 1H, -CH=NO*H*), 8.47 (d, J = 4.8 Hz, 1H, 6-H), 8.03 (s, 1H, -C*H*=NOH), 7.78 (br s, 1H, 3-H), 7.40–

7.22 (m, 6H, -*Ar*), 6.18 (d, *J* = 3.6 Hz, 1H, CHO*H*), 5.74 (d, *J* = 3.6 Hz, 1H, C*H*OH); ^{13}C NMR (100 MHz, 293 K, DMSO-d_6): δ 155.2, 152.5, 149.7, 149.4, 144.7, 128.8, 127.8, 126.9, 121.9, 117.3, 73.4; HRMS (ESI+) calcd for $C_{13}H_{13}N_2O_2$ $[M + H]^+$ = 229.0972, found 229.0973.

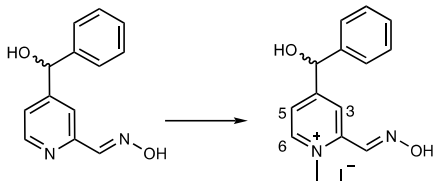

*Preparation of (E)-4-(hydroxy(phenyl)methyl)-2-((hydroxyimino)methyl)-1-methylpyridin-1-ium iodide (**ADG3230**):* A 35-mL sealed tube with (E)-4-(hydroxy(phenyl)methyl)picolinaldehyde oxime (29 mg, 0.13 mmol) was charged with acetone (2 mL), and MeI (80 μL, 1.3 mmol). The vessel was sealed and heated to 55 °C (external temperature). After 19.5 h at the same temperature, the reaction mixture was cooled to 23 °C, transferred to a 25-mL round-bottomed flask, and concentrated *in vacuo*. The crude residue was dry-loaded and purified by flash chromatography (10 to 50% MeOH in CH_2Cl_2) on silica gel (10 mL) to afford (*E*)-4-(hydroxy(phenyl)methyl)-2-((hydroxyimino)methyl)-1-methylpyridin-1-ium iodide as a brown solid (23 mg, 44% yield).

(E)-4-(hydroxy(phenyl)methyl)-2-((hydroxyimino)methyl)-1-methylpyridin-1-ium iodide: m.p. = 73–75 °C; R_f = 0.08 (100% EtOAc); IR (neat): ν_{max} = 3149, 2981, 1699, 1637, 1595, 1570, 1509, 1491, 1449, 1299, 1180, 1049, 1001 cm^{-1}; ^{1}H NMR (500 MHz, 293 K, DMSO-d_6): δ 13.07 (s, 1H, -CH=NO*H*), 8.85 (d, *J* = 6.5 Hz, 1H, 6-H), 8.63 (s, 1H, -C*H*=NOH), 8.33 (d, *J* = 2.0 Hz, 1H, 3-H), 8.02 (dd, *J* = 6.5, 2.0 Hz, 1H, 5-H), 7.45 (d, *J* = 7.0 Hz, 2H, -*Ph*), 7.37 (app t, *J* = 7.0 Hz, 2H, -*Ph*), 7.29 (app t, *J* = 7.0 Hz, 1H, -*Ph*), 6.69 (d, *J* = 4.0 Hz, 1H, CHO*H*), 6.05 (d, *J* = 4.0 Hz, 1H, C*H*OH), 4.27 (s, 3H, -N$^+$C*H*$_3$); ^{13}C NMR (100 MHz, 293 K, DMSO-d_6): δ 163.5, 147.7,

146.9, 143.0, 142.2, 129.2, 128.5, 127.2, 124.3, 121.3, 72.8, 46.0; HRMS (ESI+) calcd for $C_{14}H_{15}N_2O_2$ $[M]^+$ = 243.1128, found 243.1129.

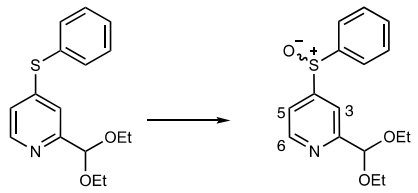

Preparation of 2-(diethoxymethyl)-4-(phenylsulfinyl)pyridine: A 500-mL round-bottom flask with an attached addition funnel was charged with 2-(diethoxymethyl)-4-(phenylthio)pyridine (1.30 g, 4.50 mmol) and CH_2Cl_2 (100 mL). The flask was cooled with an ice bath. A solution of *m*CPBA (1.15 g, 4.50 mmol) in CH_2Cl_2 (75 mL) was added to the reaction mixture via addition funnel over 50 min. The reaction mixture was gradually warmed to 23 °C. After stirring for 24 h, K_2CO_3 (623 mg, 4.50 mmol) and H_2O (100 mL) were added to the reaction mixture. The resulting solution was extracted with CH_2Cl_2 (2 × 75 mL). The combined organic layers were dried over anhydrous Na_2SO_4, filtered, and concentrated *in vacuo.* The crude material was purified by flash chromatography (20 to 70% EtOAc in hexanes) on silica gel (100 mL) to afford 2-(diethoxymethyl)-4-(phenylsulfinyl)pyridine as a white solid (1.14 g, 83% yield).

2-(Diethoxymethyl)-4-(phenylsulfinyl)pyridine: m.p. = 59–61 °C; R_f = 0.32 (60% EtOAc in hexanes); IR (neat): ν_{max} = 3042, 2972, 2928, 2879, 1577, 1446, 1344, 1283, 1234, 1109, 1091, 1063, 1048, 1012, 977 cm^{-1}; ^1H NMR (300 MHz, 293 K, $CDCl_3$): δ 8.32 (d, J = 5.1 Hz, 1H, 6-H), 7.78 (d, J = 0.9 Hz, 1H, 3-H), 7.79–7.64 (m, 2H, -*Ph*), 7.52–7.46 (m, 4H, -*Ph*), 5.46 (s, 1H, -C*H*$(OCH_2CH_3)_2$), 3.71–3.48 (m, 4H, -CH(OC*H*$_2CH_3)_2$), 1.25–1.16 (m, 6H, -CH$(OCH_2CH_3)_2$); ^{13}C NMR (75 MHz, 293 K, $CDCl_3$): δ 159.4, 156.5, 149.7, 144.2, 131.8, 129.6, 124.8, 117.7, 115.9, 101.7, 62.2, 15.1; HRMS (ESI+) calcd for $C_{16}H_{20}NO_3S$ $[M + H]^+$ = 306.1158, found 306.1155.

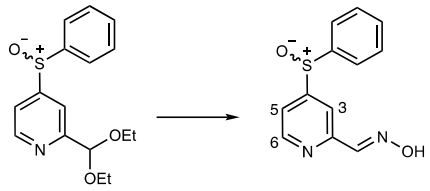

Preparation of (E)-4-(phenylsulfinyl)picolinaldehyde oxime: A 100-mL pear-shaped flask, open to air, with 2-(diethoxymethyl)-4-(phenylsulfinyl)pyridine (641 mg, 2.10 mmol) was charged with H_2O (10 mL) and 5 M H_2SO_4 in H_2O (460 μL, 2.31 mmol). The solution was heated to 95 °C (external temperature). After stirring at the same temperature for 4.5 h, the reaction mixture was cooled to 23 °C and treated with K_2CO_3 (1.16 g, 8.40 mmol) followed by MeOH (25 mL) and NH_2OH•HCl (146 mg, 2.10 mmol) at the same temperature. A reflux condenser was attached, and the reaction was heated to reflux while open to air. After 3 h, the reaction mixture was cooled to 23 °C and concentrated *in vacuo.* EtOAc (20 mL) was added to the crude residue, followed by saturated aqueous NH_4Cl (30 mL). The layers were separated using a separatory funnel and the aqueous layer was extracted with EtOAc (2 × 10 mL). The combined organic layers were dried over anhydrous Na_2SO_4, filtered, and concentrated *in vacuo* to afford (*E*)-4-(phenylsulfinyl)picolinaldehyde oxime (385 mg, 74% yield) as an ivory solid.

(E)-4-(Phenylsulfinyl)picolinaldehyde oxime: m.p. = 140–142 °C; R_f = 0.30 (60% EtOAc in hexanes); IR (neat): ν_{max} = 3159, 3056, 2981, 2855, 2746, 1576, 1550, 1507, 1473, 1442, 1392, 1319, 1272, 1240, 1223, 1156, 1094, 1074, 1055, 996 cm^{-1}; ^1H NMR (400 MHz, 293 K, DMSO-d_6): δ 11.92 (s, 1H, -CH=NO*H*), 8.68 (d, *J* = 5.2 Hz, 1H, 6-H), 8.01 (s, 1H, -C*H*=NOH), 8.68 (d, *J* = 1.2 Hz, 1H, 3-H), 7.82–7.80 (m, 2H, -*Ph*), 7.68 (dd, *J* = 5.2, 1.2 Hz, 1H, 5-H), 7.58–7.56 (m, 3H, -*Ph*); ^{13}C NMR (75 MHz, 293 K, DMSO-d_6): δ 157.1, 153.6, 150.8, 148.6, 144.9, 132.4, 130.3, 124.9, 118.7, 113.9; HRMS (ESI+) calcd for $C_{12}H_{11}N_2O_2S$ $[M + H]^+$ = 247.0535, found 247.0538.

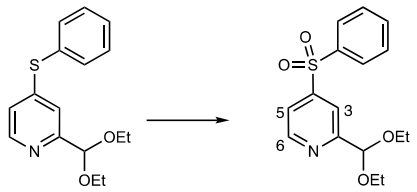

Preparation of 2-(diethoxymethyl)-4-(phenylsulfonyl)pyridine: A 500-mL round-bottom flask with an attached addition funnel was charged with 2-(diethoxymethyl)-4-(phenylthio)pyridine (1.30 g, 4.50 mmol) and CH_2Cl_2 (100 mL). The flask was cooled with an ice bath. A solution of *m*CPBA (2.30 g, 9.00 mmol) in CH_2Cl_2 (150 mL) was added to the reaction mixture via addition funnel over 1.5 h. The reaction mixture was gradually warmed to 23 °C. After stirring for 17.5 h, K_2CO_3 (1.24 mg, 9.00 mmol) and H_2O (100 mL) were added to the reaction mixture. The resulting solution was extracted with CH_2Cl_2 (2 × 75 mL). The combined organic layers were dried over anhydrous Na_2SO_4, filtered, and concentrated *in vacuo*. The crude material was purified by flash chromatography (20 to 60% EtOAc in hexanes) on silica gel (125 mL) to afford 2-(diethoxymethyl)-4-(phenylsulfonyl)pyridine as a white solid (970 mg, 67% yield).

2-(Diethoxymethyl)-4-(phenylsulfonyl)pyridine: m.p. = 52–54 °C; R_f = 0.65 (100% EtOAc); IR (neat): ν_{max} = 3076, 2982, 2913, 2882, 1582, 1476, 1445, 1392, 1368, 1341, 1324, 1305, 1289, 1269, 1223, 1150, 1115, 1101, 1089, 1048, 1005 cm^{-1}; ^1H NMR (400 MHz, 293 K, $CDCl_3$): δ 8.32 (d, J = 4.8 Hz, 1H, 6-H), 8.07 (d, J = 1.2 Hz, 1H, 3-H), 7.99–7.97 (m, 2H, -*Ph*), 7.71 (dd, J = 4.8, 1.2 Hz, 1H, 5-H), 7.64 (t, J = 7.6 Hz, 1H, -*Ph*), 7.55 (t, J = 7.6 Hz, 2H, -*Ph*), 5.50 (s, 1H, -C*H*$(OCH_2CH_3)_2$), 3.73–3.58 (m, 4H, -CH(OC*H*$_2CH_3)_2$), 1.25 (t, J = 7.2 Hz 6H, -CH$(OCH_2CH_3)_2$); ^{13}C NMR (100 MHz, 293 K, $CDCl_3$): δ 160.6, 150.5, 150.3, 139.7, 134.0, 129.5, 128.1, 120.2, 118.2, 101.6, 62.5, 15.1; HRMS (ESI+) calcd for $C_{16}H_{20}NO_4S$ $[M + H]^+$ = 322.1108, found 322.1120.

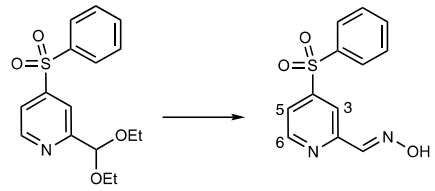

Preparation of (E)-4-(phenylsulfonyl)picolinaldehyde oxime: A 100-mL pear-shaped flask, open to air, with 2-(diethoxymethyl)-4-(phenylsulfonyl)pyridine (430 mg, 1.33 mmol) was charged with H_2O (6 mL) and 5 M H_2SO_4 in H_2O (290 μL, 1.47 mmol). The solution was heated to 75 °C (external temperature). After stirring at the same temperature for 23 h, the reaction mixture was cooled to 23 °C and treated with K_2CO_3 (735 mg, 5.32 mmol) followed by MeOH (16 mL) and NH_2OH•HCl (92 mg, 1.3 mmol) at the same temperature. A reflux condenser was attached, and the reaction was heated to reflux while open to air. After 3.5 h, the reaction mixture was cooled to 23 °C and concentrated *in vacuo.* EtOAc (25 mL) was added to the crude residue, followed by saturated aqueous NH_4Cl (25 mL). The layers were separated using a separatory funnel and the aqueous layer was extracted with EtOAc (2 × 20 mL). The combined organic layers were dried over anhydrous Na_2SO_4, filtered, and concentrated *in vacuo* to afford (*E*)-4-(phenylsulfonyl)picolinaldehyde oxime (234 mg, 89% yield) as a yellow solid.

(E)-4-(Phenylsulfonyl)picolinaldehyde oxime: m.p. = 184–185 °C; R_f = 0.50 (60% EtOAc in hexanes); IR (neat): ν_{max} = 3170, 3080, 3009, 2980, 2883, 2804, 2771, 1734, 1581, 1552, 1498, 1463, 1446, 1394, 1327, 1275, 1233, 1180, 1153, 1099, 1023, 985 cm^{-1}; ^1H NMR (400 MHz, 293 K, DMSO-d_6): δ 12.06 (s, 1H, -CH=NO*H*), 8.68 (d, *J* = 5.2 Hz, 1H, 6-H), 8.17 (s, 1H, -C*H*=NOH), 8.11 (br s, 1H, 3-H), 8.04 (d, *J* = 7.6 Hz, 2H, -*Ph*), 7.89 (dd, *J* = 5.2, 1.6 Hz, 1H, 5-H), 7.78 (d, *J* = 7.2 Hz, 1H, -*Ph*), 7.68 (t, *J* = 7.6 Hz, 2H, -*Ph*); ^{13}C NMR (100 MHz, 293 K, DMSO-d_6): δ 154.5,

152.0, 150.2, 148.2, 139.3, 135.2, 130.5, 128.4, 120.6, 116.4; HRMS (ESI+) calcd for $C_{12}H_{11}N_2O_3S$ $[M + H]^+$ = 263.0485, found 263.0489.

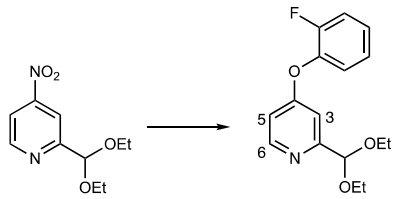

Preparation of 2-(diethoxymethyl)-4-(2-fluorophenoxy)pyridine: A 75-mL sealed tube was charged with dimethyl sulfoxide (6 mL), K_2CO_3 (1.32 g, 9.00 mmol), and 2-fluorophenol (810 μL, 9.00 mmol). The mixture was stirred at room temperature for 5 min. 2-(Diethoxymethyl)-4-nitropyridine (680 mg, 3.00 mmol) was added, the vessel was sealed and heated to 95 °C (external temperature) for 5 h. The reaction mixture was cooled to 23 °C and acidified with saturated aqueous NH_4Cl (30 mL). The resulting solution was extracted with EtOAc (3 × 15 mL). The combined organic layers were dried over anhydrous Na_2SO_4, filtered, and concentrated *in vacuo.* The crude material was purified by flash chromatography (0 to 50% EtOAc in hexanes) on silica gel (85 mL) to afford 2-(diethoxymethyl)-4-(2-fluorophenoxy)pyridine as a yellow oil (425 mg, 49% yield).

2-(Diethoxymethyl)-4-(2-fluorophenoxy)pyridine: R_f = 0.51 (60% EtOAc in hexanes); IR (neat): ν_{max} = 2979, 2884, 1587, 1573, 1289, 1263, 1194, 1158, 1104, 1057, 1027 cm^{-1}; ^1H NMR (400 MHz, 293 K, $CDCl_3$): δ 8.45 (d, J = 5.6 Hz, 1H, 6-H), 7.25–7.16 (m, 5H, -*Ar*), 6.75 (dd, J = 5.6, 2.8 Hz, 1H, 5-H), 5.43 (s, 1H, -C*H*$(OCH_2CH_3)_2$), 3.74–3.56 (m, 4H, -CH(OC*H*$_2CH_3)_2$) 1.23 (t, J = 7.2 Hz, 6H, -CH$(OCH_2CH_3)_2$); ^{13}C NMR (100 MHz, 293 K, $CDCl_3$): δ 164.8, 160.5, 154.4 (d, J = 248 Hz), 150.5, 140.7 (d, J = 12 Hz), 126.6 (d, J = 7 Hz), 124.9 (d, J = 4 Hz), 123.3, 117.2

(d, J = 18 Hz), 110.6, 108.4, 102.2, 62.2, 14.9; HRMS (ESI+) calcd for $C_{16}H_{19}FNO_3$ $[M + H]^+$ = 292.1343, found 292.1343.

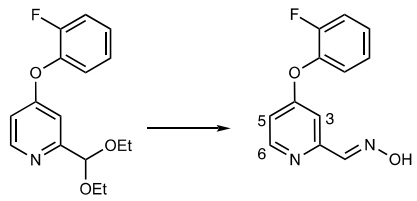

Preparation of (E)-4-(2-fluorophenoxy)picolinaldehyde oxime: A 50-mL pear-shaped flask open to air with 2-(diethoxymethyl)-4-(2-fluorophenoxy)pyridine (230 mg, 0.790 mmol) was charged with H_2O (3 mL) and 5 M H_2SO_4 in H_2O (170 μL, 0.860 mmol). The solution was heated to 85 °C (external temperature). After stirring at the same temperature for 3 h, the reaction mixture was cooled to 23 °C and treated with K_2CO_3 (442 mg, 3.16 mmol) followed by MeOH (11 mL) and NH_2OH•HCl (57 mg, 0.82 mmol) at the same temperature. A reflux condenser was attached, and the reaction was heated to reflux while open to air. After 2 h, the reaction mixture was cooled to 23 °C and concentrated *in vacuo.* EtOAc (10 mL) was added to the crude residue, followed by saturated aqueous NH_4Cl (20 mL). The layers were separated using a separatory funnel and the aqueous layer was extracted with EtOAc (2 × 10 mL). The combined organic layers were dried over anhydrous Na_2SO_4, filtered, and concentrated *in vacuo* to afford (*E*)-4-(2-fluorophenoxy)picolinaldehyde oxime (170 mg, 93% yield) as a white solid. This material was used directly without further purification.

(E)-4-(2-Fluorophenoxy)picolinaldehyde oxime: m.p. = 131–135 °C; R_f = 0.36 (60% EtOAc in hexanes); IR (neat): ν_{max} = 2982, 1588, 1423, 1298, 1260, 1191, 1102 cm^{-1}; ^1H NMR (400 MHz, 293 K, DMSO-d_6): δ 11.73 (s, 1H, -CH=NO*H*), 8.48 (d, J = 5.6 Hz, 1H, 6-H), 8.03 (s, 1H, -C*H*=NOH), 7.51–7.31 (m, 4H, -*Ph*), 7.13 (d, J = 2.4 Hz, 1H, 3-H), 7.02 (dd, J = 5.6, 2.4 Hz,

1H, 5-H); ^{13}C NMR (100 MHz, 293 K, DMSO-d_6): δ 164.6, 154.9, 154.4 (d, J = 246 Hz), 151.9, 148.8, 140.4 (d, J = 12 Hz), 128.2 (d, J = 7 Hz), 126.5 (d, J = 4 Hz), 124.4, 118.0 (d, J = 18 Hz), 112.3, 105.8; HRMS (ESI+) calcd for $C_{12}H_{10}FN_2O_2$ $[M + H]^+$ = 233.0721, found 233.0721.

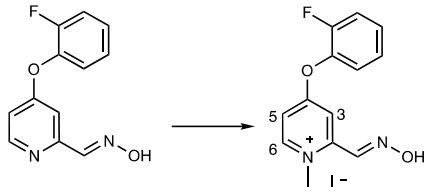

*Preparation of (E)-2-((hydroxyimino)methyl)-1-methyl-4-(2-fluorophenoxy)pyridin-1-ium iodide (**ADG3124**):* A 35-mL sealed tube with (*E*)-4-(2-fluorophenoxy)picolinaldehyde oxime (70 mg, 0.30 mmol) was charged with acetone (1 mL) and MeI (180 μL, 3.00 mmol). The vessel was sealed and heated to 58 °C (external temperature). After 17 h at the same temperature, the reaction mixture was cooled to 23 °C, transferred to a 25-mL round-bottomed flask, concentrated *in vacuo*, and recrystallized from acetone/EtOAc (1:1) to afford (*E*)-2-((hydroxyimino)methyl)-1-methyl-4-(2-fluorophenoxy)pyridin-1-ium iodide as a yellow solid (35 mg, 32% yield).

(E)-2-((Hydroxyimino)methyl)-1-methyl-4-(2-fluorophenoxy)pyridin-1-ium iodide: m.p. = 160–162 °C; R_f = 0.11 (10% MeOH in CH_2Cl_2); IR (neat): ν_{max} = 3035, 2962, 1644, 1587, 1514, 1481, 1445, 1333, 1315, 1306, 1262, 1202, 1158, 1145, 1111, 1071, 1009 cm^{-1}; ^{1}H NMR (300 MHz, 293 K, CD_3OD): δ 8.72 (d, J = 7.2 Hz, 1H, 6-H), 8.57 (s, 1H, -C*H*=NOH), 7.75 (d, J = 3.0 Hz, 1H, 3-H), 7.52–7.36 (m, 5H, 5-H and -*Ph*), 4.28 (s, 3H, -N$^+$C*H*$_3$); ^{13}C NMR (100 MHz, 293 K, CD_3OD): δ 170.2, 155.1 (d, J = 248 Hz), 151.9, 150.1, 141.7, 140.5 (d, J = 12 Hz), 130.4 (d, J = 7 Hz), 127.3 (d, J = 5 Hz), 124.5, 118.9 (d, J = 17 Hz), 114.9, 111.9, 45.9; HRMS (ESI+) calcd for $C_{12}H_{10}N_2O_2F$ $[M]^+$ = 247.0877, found 247.0875.

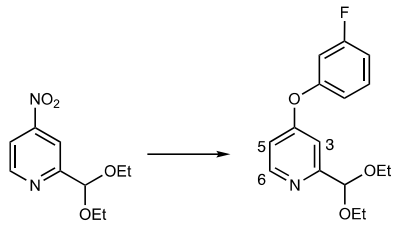

Preparation of 2-(diethoxymethyl)-4-(3-fluorophenoxy)pyridine: A 75-mL sealed tube was charged with dimethyl sulfoxide (6 mL), K_2CO_3 (1.26 g, 9.00 mmol), and 3-fluorophenol (810 μL, 9.00 mmol). The mixture was stirred at room temperature for 30 min. 2-(Diethoxymethyl)-4-nitropyridine (680 mg, 3.00 mmol) was added, the vessel was sealed and heated to 90 °C (external temperature) for 5 h. The reaction mixture was cooled to 23 °C and acidified with saturated aqueous NH_4Cl (25 mL). The resulting solution was layers was extracted with EtOAc (3 × 20 mL). The combined organic layers were dried over anhydrous Na_2SO_4, filtered, and concentrated *in vacuo.* The crude material was purified by flash chromatography (0 to 50% EtOAc in hexanes) on silica gel (100 mL) to afford 2-(diethoxymethyl)-4-(3-fluorophenoxy)pyridine as a brown oil (194 mg, 22% yield).

2-(Diethoxymethyl)-4-(3-fluorophenoxy)pyridine: R_f = 0.50 (60% EtOAc in hexanes); IR (neat): ν_{max} = 2978, 2883, 1585, 1576, 1287, 1264, 1169, 1117, 1057 cm^{-1}; ^1H NMR (400 MHz, 293 K, $CDCl_3$): δ 8.47 (d, J = 5.6 Hz, 1H, 6-H), 7.37 (app q, J = 8.0 Hz, 1H, -*Ph*), 7.19 (d, J = 2.4 Hz, 1H, 3-H), 6.95 (dt, J = 8.4, 2.4 Hz, 1H, -*Ph*), 6.89 (dd, J = 8.4, 2.4 Hz, 1H, -*Ph*), 6.84–6.80 (m, 2H, -*Ar*), 5.43 (s, 1H, -C*H*(OCH_2CH_3)$_2$), 3.75–3.57 (m, 4H, -CH(OC*H*$_2$$CH_3$)$_2$) 1.24 (t, J = 7.2 Hz, 6H, -CH(OCH_2C*H*$_3$)$_2$); ^{13}C NMR (100 MHz, 293 K, $CDCl_3$): δ 164.8, 163.3 (d, J = 247 Hz), 160.8, 155.2 (d, J = 10 Hz), 150.7, 130.8 (d, J = 10 Hz), 116.1 (d, J = 4 Hz), 112.2 (d, J = 21 Hz), 111.9, 109.6, 108.3 (d, J = 24 Hz), 102.3, 62.3, 15.0; HRMS (ESI+) calcd for $C_{16}H_{19}FNO_3$ [M + H]$^+$ = 292.1343, found 292.1343.

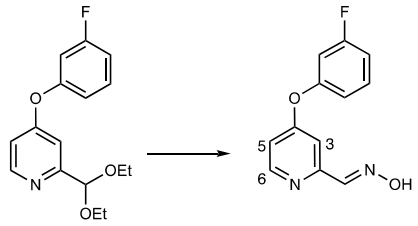

Preparation of (E)-4-(3-fluorophenoxy)picolinaldehyde oxime: A 25-mL pear-shaped flask open to air with 2-(diethoxymethyl)-4-(3-fluorophenoxy)pyridine (132 mg, 0.450 mmol) was charged with H_2O (2 mL) and 5 M H_2SO_4 in H_2O (100 μL, 0.490 mmol). The solution was heated to 85 °C (external temperature). After stirring at the same temperature for 3 h, the reaction mixture was cooled to 23 °C and treated with K_2CO_3 (262 mg, 1.89 mmol) followed by MeOH (7 mL) and NH_2OH•HCl (36 mg, 0.45 mmol) at the same temperature. A reflux condenser was attached, and the reaction was heated to reflux while open to air. After 2 h, the reaction mixture was cooled to 23 °C and concentrated *in vacuo.* EtOAc (10 mL) was added to the crude residue, followed by saturated aqueous NH_4Cl (15 mL). The layers were separated using a separatory funnel and the aqueous layer was extracted with EtOAc (2 × 10 mL). The combined organic layers were dried over anhydrous Na_2SO_4, filtered, and concentrated *in vacuo* to afford (*E*)-4-(3-fluorophenoxy)picolinaldehyde oxime (64 mg, 61% yield) as a pale peach solid. This material was used directly without further purification.

(E)-4-(3-Fluoro)picolinaldehyde oxime: m.p. = 123–126 °C; R_f = 0.42 (60% EtOAc in hexanes); IR (neat): ν_{max} = 2982, 1587, 1482, 1299, 1247, 1174, 1113 cm^{-1}; ^1H NMR (400 MHz, 293 K, DMSO-d_6): δ 11.73 (s, 1H, -CH=NO*H*), 8.49 (d, *J* = 5.6 Hz, 1H, 6-H), 8.04 (s, 1H, -C*H*=NOH), 7.58–7.52 (m, 1H, -*Ph*), 7.24–7.16 (m, 3H, -*Ar*), 7.09 (dd, *J* = 8.0, 2.0 Hz, 1H, -*Ph*), 7.03 (dd, *J* = 5.6, 2.4 Hz, 1H, 5-H); ^{13}C NMR (100 MHz, 293 K, DMSO-d_6): δ 164.5, 163.2 (d, *J* = 239 Hz), 155.0 (d, *J* = 11 Hz), 154.7, 151.9, 148.7, 132.2 (d, *J* = 10 Hz), 117.4 (d, *J* = 3 Hz),

113.2, 113.1 (d, J = 18 Hz), 109.2 (d, J = 24 Hz), 107.1; HRMS (ESI+) calcd for $C_{12}H_{10}FN_2O_2$ [M + H]$^+$ = 233.0721, found 233.0723.

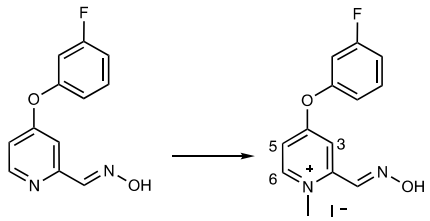

*Preparation of (E)-2-((hydroxyimino)methyl)-1-methyl-4-(3-fluorophenoxy)pyridin-1-ium iodide (**ADG3123**):* A 35-mL sealed tube with (*E*)-4-(3-fluorophenoxy)picolinaldehyde oxime (208 mg, 0.890 mmol) was charged with acetone (2 mL) and MeI (650 μL, 8.90 mmol). The vessel was sealed and heated to 40 °C (external temperature). After 21.5 h at the same temperature, the reaction mixture was cooled to 23 °C, transferred to a 25-mL round-bottomed flask, concentrated *in vacuo*, and recrystallized from acetone/EtOAc (1:1) to afford (*E*)-2-((hydroxyimino)methyl)-1-methyl-4-(3-fluorophenoxy)pyridin-1-ium iodide as a tan solid (91 mg, 27% yield).

(E)-2-((Hydroxyimino)methyl)-1-methyl-4-(3-fluorophenoxy)pyridin-1-ium iodide: m.p. = 160–162 °C; R_f = 0.11 (10% MeOH in CH_2Cl_2); IR (film): ν_{max} = 3052, 2963, 1644, 1600, 1587, 1574, 1514, 1481, 1464, 1445, 1333, 1315, 1306, 1262, 1253, 1202, 1158, 1145, 1111, 1071 cm^{-1}; ^{1}H NMR (400 MHz, 293 K, DMSO-d_6): δ 13.10 (s, 1H, -CH=NO*H*), 8.86 (d, J = 7.2 Hz, 1H, 6-H), 8.61 (s, 1H, -C*H*=NOH), 7.69–7.64 (m, 2H, -*Ph*), 7.60 (d, J = 2.8 Hz, 1H, 3-H), 7.40 (dt, J = 9.6, 2.0 Hz, 1H, -*Ph*), 7.40 (td, J = 8.4, 2.0 Hz, 1H, -*Ph*), 7.23 (dd, J = 8.4, 2.8 Hz, 1H, 5-H), 4.25 (s, 3H, -N$^+$C*H*$_3$); ^{13}C NMR (100 MHz, 293 K, DMSO-d_6): δ 168.6, 163.4 (d, J = 246 Hz), 153.4 (d, J = 11 Hz), 150.1, 149.5, 141.9, 133.0 (d, J = 10 Hz), 117.8 (d, J = 3 Hz), 115.2, 114.9 (d, J = 21 Hz), 110.8, 109.8 (d, J = 25 Hz), 45.4; HRMS (ESI+) calcd for $C_{13}H_{12}FN_2O_2$ [M]$^+$ = 247.0877, found 247.0880.

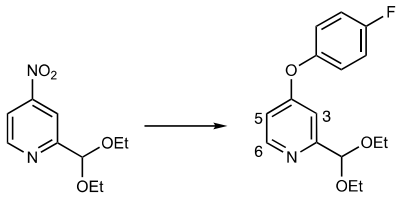

Preparation of 2-(diethoxymethyl)-4-(4-fluorophenoxy)pyridine: A 75-mL sealed tube was charged with dimethyl sulfoxide (6 mL), K_2CO_3 (1.27 g, 9.00 mmol), and 4-fluorophenol (1.06 g, 9.00 mmol). The mixture was stirred at room temperature for 30 min. 2-(Diethoxymethyl)-4-nitropyridine (682 mg, 3.00 mmol) was added, the vessel was sealed and heated to 85 °C (external temperature) for 17 h. The reaction mixture was cooled to 23 °C and acidified with saturated aqueous NH_4Cl (20 mL). The resulting solution was layers was extracted with EtOAc (3 × 20 mL). The combined organic layers were dried over anhydrous Na_2SO_4, filtered, and concentrated *in vacuo.* The crude material was purified by flash chromatography (0 to 50% EtOAc in hexanes) on silica gel (100 mL) to afford 2-(diethoxymethyl)-4-(4-fluorophenoxy)pyridine as a pale yellow oil (490 mg, 56% yield).

2-(Diethoxymethyl)-4-(4-fluorophenoxy)pyridine: R_f = 0.54 (60% EtOAc in hexanes); IR (neat): ν_{max} = 2977, 2880, 1603, 1587, 1572, 1290, 1260, 1236, 1196, 1156, 1110, 1089, 1056 cm^{-1}; ^1H NMR (300 MHz, 293 K, $CDCl_3$): δ 8.43 (d, J = 5.7 Hz, 1H, 6-H), 7.14–7.04 (m, 5H, -*Ar*), 6.73 (dd, J = 5.7, 2.4 Hz, 1H, 5-H), 5.41 (s, 1H, -C*H*$(OCH_2CH_3)_2$), 3.76–3.55 (m, 4H, -CH(OC*H*$_2$CH$_3$)$_2$), 1.24 (t, J = 6.9 Hz, 6H, -CH(OCH$_2$C*H*$_3$)$_2$); ^{13}C NMR (100 MHz, 293 K, $CDCl_3$): δ 165.6, 160.7, 159.9 (d, J = 243 Hz), 150.6, 149.8 (d, J = 27 Hz), 122.3 (d, J = 8 Hz), 116.8 (d, J = 24 Hz), 111.4, 109.1, 102.4, 62.4, 15.1; HRMS (ESI+) calcd for $C_{16}H_{19}FNO_3$ $[M + H]^+$ = 292.1343, found 292.1348.

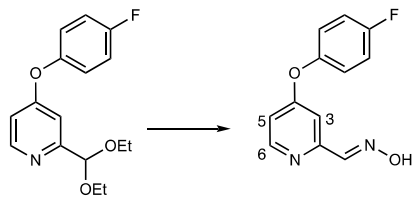

Preparation of (E)-4-(4-fluorophenoxy)picolinaldehyde oxime: A 50-mL pear-shaped flask open to air with 2-(diethoxymethyl)-4-(4-fluorophenoxy)pyridine (279 mg, 0.960 mmol) was charged with H_2O (4 mL) and 5 M H_2SO_4 in H_2O (290 μL, 1.44 mmol). The solution was heated to 93 °C (external temperature). After stirring at the same temperature for 3 h, the reaction mixture was cooled to 23 °C and treated with K_2CO_3 (546 mg, 3.84 mmol) followed by MeOH (14 mL) and NH_2OH•HCl (67 mg, 0.96 mmol) at the same temperature. A reflux condenser was attached, and the reaction was heated to reflux while open to air. After 3 h, the reaction mixture was cooled to 23 °C and concentrated *in vacuo.* EtOAc (10 mL) was added to the crude residue, followed by saturated aqueous NH_4Cl (30 mL). The layers were separated using a separatory funnel and the aqueous layer was extracted with EtOAc (2 × 15 mL). The combined organic layers were dried over anhydrous Na_2SO_4, filtered, and concentrated *in vacuo* to afford (*E*)-(4-fluorophenoxy)picolinaldehyde oxime (216 mg, 97% yield) as a white solid. This material was used directly without further purification.

(E)-4-(4-Fluorophenoxy)picolinaldehyde oxime: m.p. = 170–172 °C; R_f = 0.53 (60% EtOAc in hexanes); IR (neat): ν_{max} = 2982, 1587, 1564, 1430, 1261, 1247, 1196, 1092 cm^{-1}; ^1H NMR (400 MHz, 293 K, DMSO-d_6): δ 11.70 (s, 1H, -CH=NO*H*), 8.46 (d, *J* = 5.6 Hz, 1H, 6-H), 8.02 (s, 1H, -C*H*=NOH), 7.38–7.28 (m, 4H, -*Ph*), 7.13 (d, *J* = 2.8 Hz, 1H, 3-H), 6.98 (dd, *J* = 5.6, 2.8 Hz, 1H, 5-H); ^{13}C NMR (100 MHz, 293 K, DMSO-d_6): δ 165.2, 159.9 (d, *J* = 240 Hz), 154.7, 151.8, 149.9 (d, *J* = 3 Hz), 148.8, 123.5 (d, *J* = 9 Hz), 117.6 (d, *J* = 23 Hz), 112.9, 106.6; HRMS (ESI+) calcd for $C_{12}H_{10}FN_2O_2$ $[M + H]^+$ = 233.0721, found 233.0717.

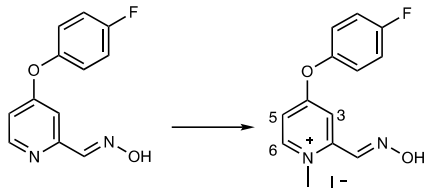

*Preparation of (E)-2-((hydroxyimino)methyl)-1-methyl-4-(4-fluorophenoxy)pyridin-1-ium iodide (**ADG3116**):* A 35-mL sealed tube with (*E*)-4-(4-fluorophenoxy)picolinaldehyde oxime (102 mg, 0.440 mmol) was charged with acetone (1 mL) and MeI (270 μL, 4.39 mmol). The vessel was sealed and heated to 55 °C (external temperature). After 13 h at the same temperature, the reaction mixture was cooled to 23 °C, transferred to a 25-mL round-bottomed flask, concentrated *in vacuo*, and recrystallized from acetone/EtOAc (1:1) to afford (*E*)-2-((hydroxyimino)methyl)-1-methyl-4-(4-fluorophenoxy)pyridin-1-ium iodide as a yellow solid (109 mg, 66% yield).

(E)-2-((Hydroxyimino)methyl)-1-methyl-4-(4-fluorophenoxy)pyridin-1-ium iodide: m.p. = 160–162 °C; R_f = 0.10 (10% MeOH in CH_2Cl_2); IR (neat): ν_{max} = 3037, 2982, 1642, 1575, 1311, 1230, 1094, 1065 cm^{-1}; ^1H NMR (400 MHz, 293 K, DMSO-d_6): δ 13.07 (s, 1H, -CH=NO*H*), 8.83 (d, *J* = 7.2 Hz, 1H, 6-H), 8.60 (s, 1H, -C*H*=NOH), 7.60 (dd, *J* = 7.2, 3.2 Hz, 1H, 5-H), 7.54 (d, *J* = 3.2 Hz, 1H, 3-H), 7.48–7.41 (m, 4H, -*Ph*), 4.24 (s, 3H, $-N^+CH_3$); ^{13}C NMR (100 MHz, 293 K, DMSO-d_6): δ 169.0, 160.7 (d, *J* = 243 Hz), 149.9, 149.3, 148.5 (d, *J* = 3 Hz), 141.9, 123.5 (d, *J* = 9 Hz), 118.1 (d, *J* = 23 Hz), 114.8, 110.4, 45.2; HRMS (ESI+) calcd for $C_{13}H_{12}FN_2O$ $[M]^+$ = 247.0877, found 247.0879.

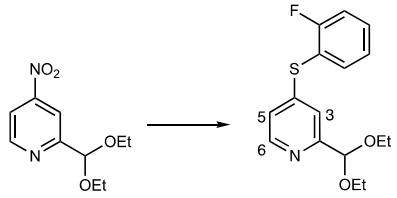

Preparation of 2-(diethoxymethyl)-4-((2-fluorophenyl)thio)pyridine: A 75-mL sealed tube was charged with dimethyl sulfoxide (4 mL), K_2CO_3 (1.66 g, 12.0 mmol), and 2-fluorobenzenethiol (1.28 mL, 12.0 mmol). The mixture was stirred at room temperature for 5 min. 2-(Diethoxymethyl)-4-nitropyridine (909 mg, 4.00 mmol) was added, the vessel was sealed and heated to 95 °C for 19 h. The reaction mixture was cooled to 23 °C and neutralized with saturated aqueous NH_4Cl (20 mL). The resulting solution was extracted with EtOAc (3 × 20 mL). The combined organic layers were dried over anhydrous Na_2SO_4, filtered, and concentrated *in vacuo*. The crude material was purified by flash chromatography (0 to 40% EtOAc in hexanes) on silica gel (100 mL) to afford 2-(diethoxymethyl)-4-((2-fluorophenyl)thio)pyridine as a pale yellow oil (1.20 g, 98% yield).

2-(Diethoxymethyl)-4-((2-fluorophenyl)thio)pyridine: R_f = 0.53 (60% EtOAc in hexanes); IR (neat): ν_{max} = 2975, 2878, 1575, 1545, 1473, 1444, 1393, 1369, 1333, 1262, 1226, 1112, 1092, 1057 cm^{-1}; ^1H NMR (300 MHz, 293 K, DMSO-d_6): δ 8.35 (d, J = 5.1 Hz, 1H, 6-H), 7.73–7.63 (m, 2H, -*Ph*), 7.50–7.36 (m, 2H, -*Ph*), 7.07 (d, J = 1.8 Hz, 1H, 3-H), 7.02 (dd, J = 5.1, 1.8 Hz, 1H, 5-H), 5.30 (s, 1H, -C*H*$(OCH_2CH_3)_2$), 3.61–3.40 (m, 4H, -CH$(OCH_2CH_3)_2$), 1.07 (t, J = 6.9 Hz, 6H, -CH$(OCH_2CH_3)_2$); ^{13}C NMR (100 MHz, 293 K, DMSO-d_6): δ 162.5 (d, J = 246 Hz), 158.7, 149.3, 148.4, 137.8, 133.7 (d, J = 8 Hz), 126.5 (d, J = 3 Hz), 120.4, 117.2 (d, J = 22 Hz), 117.0, 115.7 (d, J = 18 Hz), 102.2, 62.2, 15.4; HRMS (ESI+) calcd for $C_{16}H_{19}FNO_2S$ $[M + H]^+$ = 308.1115, found 308.1111.

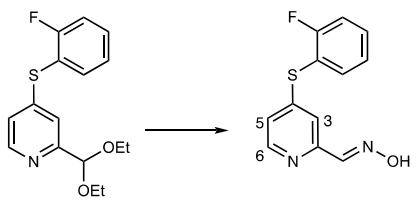

Preparation of (E)-4-((2-fluorophenyl)thio)picolinaldehyde oxime: A 50-mL pear-shaped flask open to air with 2-(diethoxymethyl)-4-((2-fluorophenyl)thio)pyridine (471 mg, 1.53 mmol) was charged with H_2O (5 mL) and 5 M H_2SO_4 in H_2O (340 μL, 1.68 mmol). The solution was heated to 95 °C. After stirring at the same temperature for 3 h, the reaction mixture was cooled to 23 °C and treated with K_2CO_3 (846 mg, 6.12 mmol) followed by MeOH (20 mL) and NH_2OH•HCl (106 mg, 1.53 mmol) at the same temperature. A reflux condenser was attached, and the reaction was heated to reflux while open to air. After 2.7 h, the reaction mixture was cooled to 23 °C and concentrated *in vacuo*. EtOAc (10 mL) was added to the crude residue, followed by saturated aqueous NH_4Cl (20 mL). The layers were separated using a separatory funnel and the aqueous layer was extracted with EtOAc (2 × 10 mL). The combined organic layers were dried over anhydrous Na_2SO_4, filtered, and concentrated *in vacuo* to afford (*E*)-4-((2-fluorophenyl)thio)picolinaldehyde oxime (340 mg, 89% yield) as a light pink solid. This material was used directly without further purification.

(E)-4-((2-Fluorophenyl)thio)picolinaldehyde oxime: m.p. = 182–184 °C; R_f = 0.36 (60% EtOAc in hexanes); IR (neat): ν_{max} = 3065, 2993, 2861, 2730, 1736, 1576, 1539, 1512, 1472, 1444, 1398, 1331, 1261, 1244, 1228, 1115, 1095, 1070, 1030 cm^{-1}; ^1H NMR (400 MHz, 293 K, DMSO-d_6): δ 11.73 (s, 1H, -CH=NO*H*), 8.40 (d, *J* = 5.6 Hz, 1H, 6-H), 7.94 (s, 1H, -C*H*=NOH), 7.76–7.65 (m, 2H, -*Ph*), 7.51–7.47 (m, 1H, -*Ph*), 7.39 (td, *J* = 7.6, 1.2 Hz, 1H, -*Ph*), 7.26 (d, *J* = 2.0 Hz, 1H, 3-H), 7.14 (dd, *J* = 5.2, 2.0 Hz, 1H, 5-H); ^{13}C NMR (100 MHz, 293 K, DMSO-d_6): δ 162.1 (d, *J* = 246 Hz), 152.4, 149.4, 148.2 (d, *J* = 19 Hz), 137.5, 133.5 (d, *J* = 8 Hz), 126.2 (d, *J* = 4 Hz), 120.5, 116.8 (d, *J* = 4 Hz), 115.0 (d, *J* = 18 Hz), 114.9; HRMS (ESI+) calcd for $C_{12}H_{10}FN_2O_2S$ $[M + H]^+$ =249.0492, found 249.0494.

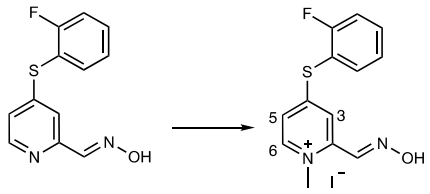

*Preparation of (E)-4-((2-fluorophenyl)thio)-2-((hydroxyimino)methyl)-1-methylpyridin-1-ium iodide (**ADG4158**):* A 35-mL sealed tube with (*E*)-4-((2-fluorophenyl)thio)picolinaldehyde oxime (109 mg, 0.430 mmol) was charged with acetone (2 mL) and MeI (270 μL, 4.30 mmol). The vessel was sealed and heated to 50 °C. After 20 h at the same temperature, the reaction mixture was cooled to 23 °C, transferred to a 25-mL round-bottomed flask, concentrated *in vacuo* to afford (*E*)-4-((2-fluorophenyl)thio)-2-((hydroxyimino)methyl)-1-methylpyridin-1-ium iodide as an orange solid (156 mg, 93% yield).

(E)-4-((2-Fluorophenyl)thio)-2-((hydroxyimino)methyl)-1-methylpyridin-1-ium iodide: m.p. = 178–180 °C; R_f = 0.11 (10% MeOH in CH_2Cl_2); IR (neat): ν_{max} = 2970, 1629, 1471, 1304, 1263, 1226, 1124, 1090, 1016 cm^{-1}; ^1H NMR (300 MHz, 293 K, DMSO-d_6): δ 13.06 (s, 1H, -CH=NO*H*), 8.66 (d, *J* = 6.6 Hz, 1H, 6-H), 8.56 (s, 1H, -C*H*=NOH), 7.84–7.73 (m, 3H, -*Ar*), 7.69 (d, *J* = 2.4 Hz, 1H, -*Ph*), 7.59 (t, *J* = 8.7 Hz, 1H, -*Ph*), 7.48 (td, *J* = 7.8, 1.2 Hz, 1H, -*Ph*), 4.19 (s, 3H, -N^+CH_3); ^{13}C NMR (100 MHz, 293 K, DMSO-d_6): δ 162.4 (d, *J* = 247 Hz), 159.7, 146.8, 145.8, 141.9, 138.0, 135.4 (d, *J* = 8 Hz), 127.2 (d, *J* = 3 Hz), 122.4, 118.7, 117.8 (d, *J* = 22 Hz), 113.2 (d, *J* = 18 Hz), 45.6; HRMS (ESI+) calcd for $C_{13}H_{12}FN_2OS$ $[M]^+$ = 263.0649, found 263.0652.

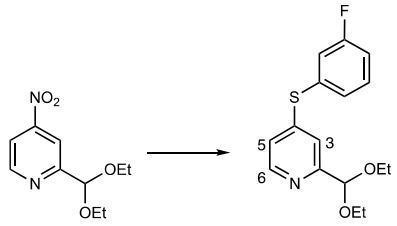

Preparation of 2-(diethoxymethyl)-4-((3-fluorophenyl)thio)pyridine: A 75-mL sealed tube was charged with dimethyl sulfoxide (4 mL), K_2CO_3 (1.66 g, 12.0 mmol), and 3-fluorobenzenethiol (1.01 mL, 12.0 mmol). The mixture was stirred at room temperature for 5 min. 2-(Diethoxymethyl)-4-nitropyridine (905 mg, 4.00 mmol) was added, the vessel was sealed and heated to 95 °C for 16 h. The reaction mixture was cooled to 23 °C and neutralized with saturated aqueous NH_4Cl (20 mL). The resulting solution was extracted with EtOAc (3 × 20 mL). The combined organic layers were dried over anhydrous Na_2SO_4, filtered, and concentrated *in vacuo*. The crude material was purified by flash chromatography (0 to 40% EtOAc in hexanes) on silica gel (100 mL) to afford 2-(diethoxymethyl)-4-((3-fluorophenyl)thio)pyridine as an amber oil (1.10 g, 89% yield).

2-(Diethoxymethyl)-4-((3-fluorophenyl)thio)pyridine: R_f = 0.58 (60% EtOAc in hexanes); IR (neat): ν_{max} = 2975, 2878, 1597, 1575, 1544, 1474, 1422, 1392, 1369, 1344, 1264, 1219, 1113, 1089, 1059, 1002 cm^{-1}; ^1H NMR (400 MHz, 293 K, DMSO-d_6): δ 8.36 (d, J = 5.2 Hz, 1H, 6-H), 7.62–7.56 (m, 1H, -*Ph*), 7.50–7.47 (m, 1H, -*Ph*), 7.44–7.38 (m, 2H, -*Ph*), 7.13 (d, J = 1.8 Hz, 1H, 3-H), 7.07 (dd, J = 5.2, 1.8 Hz, 1H, 5-H), 5.31 (s, 1H, -C*H*(OCH_2CH_3)$_2$), 3.60–3.43 (m, 4H, -CH(OCH_2CH_3)$_2$), 1.08 (t, J = 6.8 Hz, 6H, -CH(OCH_2CH_3)$_2$); ^{13}C NMR (100 MHz, 293 K, DMSO-d_6): δ 162.9 (d, J = 246 Hz), 158.8, 149.5, 149.1, 132.4 (d, J = 8 Hz), 131.6 (d, J = 8 Hz), 131.1 (d, J = 3 Hz), 121.5 (d, J = 22 Hz), 121.3, 117.9, 117.4 (d, J = 21 Hz), 102.2, 62.2, 15.5; HRMS (ESI+) calcd for $C_{16}H_{19}FNO_2S$ $[M + H]^+$ = 308.1115, found 308.1106.

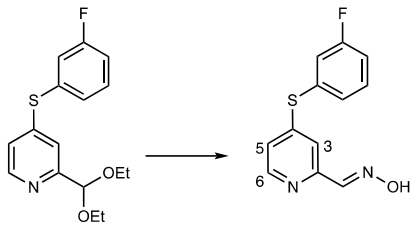

Preparation of (E)-4-((3-fluorophenyl)thio)picolinaldehyde oxime: A 100-mL pear-shaped flask open to air with 2-(diethoxymethyl)-4-((3-fluorophenyl)thio)pyridine (500 mg, 1.62 mmol) was charged with H_2O (4 mL) and 5 M H_2SO_4 in H_2O (350 μL, 1.79 mmol). The solution was heated to 85 °C. After stirring at the same temperature for 2.8 h, the reaction mixture was cooled to 23 °C and treated with K_2CO_3 (896 mg, 6.48 mmol) followed by MeOH (20 mL) and NH_2OH•HCl (113 mg, 1.62 mmol) at the same temperature. A reflux condenser was attached, and the reaction was heated to reflux while open to air. After 3.8 h, the reaction mixture was cooled to 23 °C and concentrated *in vacuo*. EtOAc (15 mL) was added to the crude residue, followed by saturated aqueous NH_4Cl (20 mL). The layers were separated using a separatory funnel and the aqueous layer was extracted with EtOAc (2 × 10 mL). The combined organic layers were dried over anhydrous Na_2SO_4, filtered, and concentrated *in vacuo* to afford (*E*)-4-((3-fluorophenyl)thio)picolinaldehyde oxime (398 mg, quantitative yield) as a white solid. This material was used directly without further purification.

(E)-4-((3-Fluorophenyl)thio)picolinaldehyde oxime: m.p. = 169–171 °C; R_f = 0.40 (60% EtOAc in hexanes); IR (neat): ν_{max} = 3060, 2978, 2860, 2727, 1574, 1538, 1510, 1467, 1419, 1399, 1330, 1296, 1262, 1243, 1232, 1218, 1154, 1117 cm^{-1}; ^1H NMR (400 MHz, 293 K, DMSO-d_6): δ 11.74 (s, 1H, -CH=NO*H*), 8.41 (d, *J* = 5.2 Hz, 1H, 6-H), 7.99 (s, 1H, -C*H*=NOH), 7.62–7.53 (m, 2H, -*Ph*), 7.47–7.39 (m, 2H, -*Ph*), 7.33 (d, *J* = 1.6 Hz, 1H, 3-H), 7.16 (dd, *J* = 5.2, 1.6 Hz, 1H, 5-H); ^{13}C NMR (100 MHz, 293 K, DMSO-d_6): δ 162.9 (d, *J* = 246 Hz), 152.9, 149.9, 149.4, 148.8, 132.5 (d, *J* = 8 Hz), 131.4 (d, *J* = 3 Hz), 131.2 (d, *J* = 8 Hz), 121.8 (d, *J* = 22 Hz), 121.5, 117.4 (d, *J* = 21 Hz), 116.3; HRMS (ESI+) calcd for $C_{12}H_{10}FN_2OS$ $[M + H]^+$ = 249.0492, found 249.0496.

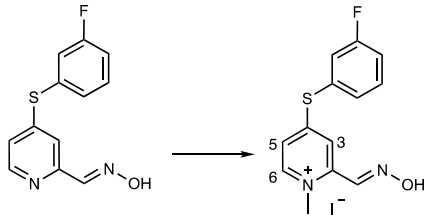

*Preparation of (E)-4-((3-fluorophenyl)thio)-2-((hydroxyimino)methyl)-1-methylpyridin-1-ium iodide (**ADG4146**):* A 35-mL sealed tube with (*E*)-4-((3-fluorophenyl)thio)picolinaldehyde oxime (183 mg, 0.740 mmol) was charged with acetone (2 mL) and MeI (450 μL, 7.40 mmol). The vessel was sealed and heated to 50 °C. After 15 h at the same temperature, the reaction mixture was cooled to 23 °C, transferred to a 25-mL round-bottomed flask, concentrated *in vacuo*, and recrystallized from acetone/EtOAc (1:1) to yield (*E*)-4-((3-fluorophenyl)thio)-2-((hydroxyimino)methyl)-1-methylpyridin-1-ium iodide as a light brown solid (166 mg, 57% yield).

(E)-4-((3-Fluorophenyl)thio)-2-((hydroxyimino)methyl)-1-methylpyridin-1-ium iodide: m.p. = 169–171 °C; R_f = 0.15 (10% MeOH in CH_2Cl_2); IR (neat): ν_{max} = 3056, 2980, 1627, 1579, 1553, 1472, 1437, 1422, 1320, 1303, 1237, 1213, 1082, 1067, 1016 cm^{-1}; ^1H NMR (400 MHz, 293 K, DMSO-d_6): δ 13.07 (s, 1H, -CH=NO*H*), 8.66 (d, *J* = 6.8 Hz, 1H, 6-H), 8.57 (s, 1H, -C*H*=NOH), 7.76–7.68 (m, 4H, -*Ar*), 7.61–7.57 (m, 2H, -*Ar*), 4.21 (s, 3H, -N^+CH_3); ^{13}C NMR (100 MHz, 293 K, DMSO-d_6): δ 163.1 (d, *J* = 243 Hz), 160.9, 146.6, 145.6, 141.8, 133.3 (d, *J* = 9 Hz), 132.1 (d, *J* = 3 Hz), 128.3, 128.2, 122.6, 122.6 (d, *J* = 23 Hz), 119.3 (d, *J* = 20 Hz), 119.0, 45.5; HRMS (ESI+) calcd for $C_{13}H_{12}FN_2OS$ $[M]^+$ = 263.0648, found 263.0650.

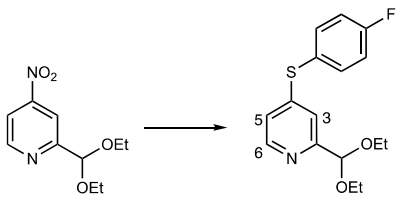

Preparation of 2-(diethoxymethyl)-4-((4-fluorophenyl)thio)pyridine: A 35-mL sealed tube was charged with dimethyl sulfoxide (1 mL), K_2CO_3 (414 g, 3.00 mmol), and 4-fluorothiophenol (320 μL, 3.00 mmol). The mixture was stirred at room temperature for 10 min. 2-(Diethoxymethyl)-4-nitropyridine (226 mg, 1.00 mmol) was added, the vessel was sealed and heated to 95 °C for 16 h. The reaction mixture was cooled to 23 °C and neutralized with saturated aqueous NH_4Cl (10 mL). The resulting solution was extracted with EtOAc (3 × 10 mL). The combined organic layers were dried over anhydrous Na_2SO_4, filtered, and concentrated *in vacuo.* The crude material was purified by flash chromatography (0 to 40% EtOAc in hexanes) on silica gel (20 mL) to afford 2-(diethoxymethyl)-4-((4-fluorophenyl)thio)pyridine as a yellow oil (296 mg, 93% yield).

2-(Diethoxymethyl)-4-((4-fluorophenyl)thio)pyridine: R_f = 0.53 (60% EtOAc in hexanes); IR (neat): ν_{max} = 2975, 2879, 1577, 1487, 1393, 1340, 1274, 1226, 1156, 1112, 1060 cm^{-1}; ^1H NMR (300 MHz, 293 K, DMSO-d_6): δ 8.31 (d, J = 5.2 Hz, 1H, 6-H), 7.68–7.64 (m, 2H, -*Ph*), 7.41–7.37 (m, 2H, -*Ph*), 7.04 (d, J = 1.6 Hz, 1H, 3-H), 6.96 (dd, J = 5.2, 1.6 Hz, 1H, 5-H), 5.27 (s, 1H, -C*H*(OCH_2CH_3)$_2$), 3.58–3.40 (m, 4H, -CH(OCH_2CH_3)$_2$), 1.06 (t, J = 7.2 Hz, 6H, -CH(OCH_2CH_3)$_2$); ^{13}C NMR (100 MHz, 293 K, DMSO-d_6): δ 163.5 (J = 247 Hz), 158.6, 150.3, 149.2, 138.1 (d, J = 8.0 Hz), 136.0, 120.3, 117.8 (d, J = 23 Hz), 117.1, 102.2, 62.1, 15.4; HRMS (ESI+) calcd for $C_{16}H_{19}FNO_2S$ $[M + H]^+$ = 308.1115, found 308.1131.

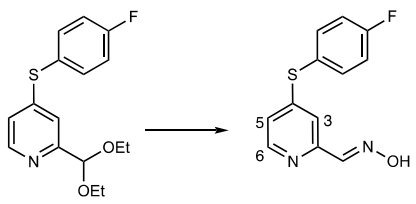

Preparation of (E)-4-((4-fluorophenyl)thio)picolinaldehyde oxime: A 100-mL pear-shaped flask open to air with 2-(diethoxymethyl)-4-((4-fluorophenyl)thio)pyridine (123 mg, 0.400 mmol) was charged with H_2O (2 mL) and 5 M H_2SO_4 in H_2O (80 μL, 0.44 mmol). The solution was heated to 95 °C. After stirring at the same temperature for 2 h, the reaction mixture was cooled to 23 °C and treated with K_2CO_3 (221 mg, 1.60 mmol) followed by MeOH (8 mL) and NH_2OH•HCl (28 mg, 0.40 mmol) at the same temperature. A reflux condenser was attached, and the reaction was heated to reflux while open to air. After 3 h, the reaction mixture was cooled to 23 °C and concentrated *in vacuo*. EtOAc (10 mL) was added to the crude residue, followed by saturated aqueous NH_4Cl (20 mL). The layers were separated using a separatory funnel and the aqueous layer was extracted with EtOAc (2 × 10 mL). The combined organic layers were dried over anhydrous Na_2SO_4, filtered, and concentrated *in vacuo* to afford (*E*)-4-((4-fluorophenyl)thio)picolinaldehyde oxime (99 mg, quantitative yield) as a white solid. This material was used directly without further purification.

(E)-4-((4-Fluorophenyl)thio)picolinaldehyde oxime: m.p. = 194–198 °C; R_f = 0.46 (60% EtOAc in hexanes); IR (neat): ν_{max} = 2979, 2885, 2736, 1574, 1487, 1395, 1329, 1220, 1155, 1112 cm^{-1}; ^1H NMR (300 MHz, 293 K, DMSO-d_6): δ 11.71 (s, 1H, -CH=NO*H*), 8.38 (d, *J* = 5.1 Hz, 1H, 6-H), 7.98 (s, 1H, -C*H*=NOH), 7.74–7.69 (m, 2H, -*Ph*), 7.45–7.40 (m, 2H, -*Ph*), 7.26 (d, *J* = 1.2 Hz, 1H, 3-H), 7.10 (dd, *J* = 5.1, 1.2 Hz, 1H, 5-H); ^{13}C NMR (125 MHz, 293 K, DMSO-d_6): 163.7 (d, *J* = 247 Hz), 152.8, 150.5, 149.7, 148.8, 138.4 (d, *J* = 9 Hz), 124.3, 120.9, 118.0 (d, *J* = 22 Hz), 115.6; HRMS (ESI+) calcd for $C_{12}H_{10}FN_2OS$ $[M + H]^+$ = 249.0492, found 249.0517.

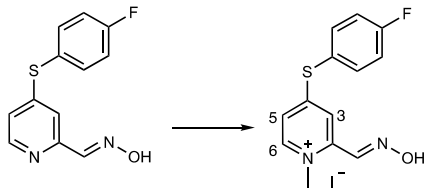

*Preparation of (E)-4-((4-fluorophenyl)thio)-2-((hydroxyimino)methyl)-1-methylpyridin-1-ium iodide (**ADG3193**):* A 35-mL sealed tube with (*E*)-4-((4-fluorophenyl)thio)picolinaldehyde oxime (248 mg, 1.00 mmol) was charged with acetone (2 mL) and MeI (620 μL, 10.0 mmol). The vessel was sealed and heated to 50 °C. After 17 h at the same temperature, the reaction mixture was cooled to 23 °C, transferred to a 25-mL round-bottomed flask, concentrated *in vacuo*, and recrystallized from acetone/EtOAc (1:1) to afford (*E*)-4-((4-fluorophenyl)thio)-2-((hydroxyimino)methyl)-1-methylpyridin-1-ium iodide as an orange solid (152 mg, 39% yield).

(E)-4-((4-Fluorophenyl)thio)-2-((hydroxyimino)methyl)-1-methylpyridin-1-ium iodide: m.p. = 166–168 °C; R_f = 0.41 (10% MeOH in CH_2Cl_2); IR (neat): ν_{max} = 2977, 1624, 1584, 1487, 1429, 1395, 1300, 1222, 1158, 1081, 1011 cm^{-1}; ^1H NMR (400 MHz, 293 K, CD_3OD): δ 8.54–8.51 (m, 2H, 6-H and -C*H*=NOH), 7.80–7.75 (m, 3H, -*Ar*), 7.50 (d, *J* = 6.8, 2.4 Hz, 1H, 5-H), 7.50 (app t, *J* = 8.8 Hz, 2H, -*Ph*), 4.26 (s, 3H, $-N^+CH_3$); ^{13}C NMR (100 MHz, 293 K, CD_3OD): δ 166.0 (d, *J* = 250 Hz), 164.5, 147.8, 146.0, 141.5, 139.4 (d, *J* = 9 Hz), 122.9, 122.7, 120.5, 119.2 (d, *J* = 22 Hz), 46.1; HRMS (ESI+) calcd for $C_{13}H_{12}FN_2OS$ $[M]^+$ = 263.0649, found 263.0672.

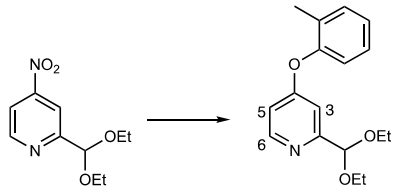

Preparation of 2-(diethoxymethyl)-4-(o-tolyloxy)pyridine: A 75-mL sealed tube was charged with dimethyl sulfoxide (6 mL), K_2CO_3 (1.29 g, 9.00 mmol), and *o*-cresol (920 μL, 9.00

mmol). The mixture was stirred at room temperature for 5 min. 2-(Diethoxymethyl)-4-nitropyridine (679 mg, 3.00 mmol) was added, the vessel was sealed and heated to 80 °C (external temperature) for 5 h. The reaction mixture was cooled to 23 °C and acidified with saturated aqueous NH_4Cl (20 mL). The resulting solution was layers was extracted with EtOAc (3 × 10 mL). The combined organic layers were dried over anhydrous Na_2SO_4, filtered, and concentrated *in vacuo.* The crude material was purified by flash chromatography (0 to 40% EtOAc in hexanes) on silica gel (70 mL) to afford 2-(diethoxymethyl)-4-(*o*-tolyloxy)pyridine as a pale yellow oil (459 mg, 80% yield).

2-(Diethoxymethyl)-4-(o-tolyloxy)pyridine: R_f = 0.44 (60% EtOAc in hexanes); IR (neat): ν_{max} = 2977, 2883, 1595, 1570, 1289, 1257, 1226, 1184, 1157, 1110, 1057 cm^{-1}; ^1H NMR (300 MHz, 293 K, $CDCl_3$): δ 8.39 (d, J = 5.7 Hz, 1H, 6-H), 7.28–7.13 (m, 3H, -*Ph*), 7.10 (d, J = 2.7 Hz, 1H, 3-H), 6.99 (dd, J = 7.8, 1.2 Hz, 1H, -*Ph*), 6.64 (dd, J = 5.7, 2.7 Hz, 1H, 5-H), 5.41 (s, 1H, -C*H*$(OCH_2CH_3)_2$), 3.75–3.54 (m, 4H, -CH$(OCH_2CH_3)_2$), 2.15 (s, 3H, -CH_3), 1.23 (t, J = 6.9 Hz, 6H, -CH$(OCH_2CH_3)_2$); ^{13}C NMR (100 MHz, 293 K, $CDCl_3$): δ 165.3, 160.3, 151.7, 150.4, 131.6, 130.4, 127.4, 125.6, 121.0, 110.6, 108.6, 102.2, 62.1, 15.8, 14.9; HRMS (ESI+) calcd for $C_{17}H_{22}NO_3$ $[M + H]^+$ = 288.1594, found 288.1600.

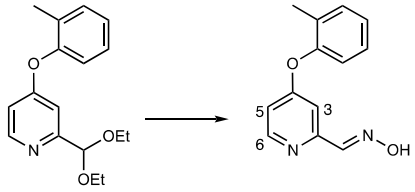

Preparation of (E)-4-(o-tolyloxy)picolinaldehyde oxime: A 50-mL pear-shaped flask open to air with 2-(diethoxymethyl)-4-(*o*-tolyloxy)pyridine (252 mg, 0.870 mmol) was charged with H_2O (4 mL) and 5 M H_2SO_4 in H_2O (260 μL, 1.31 mmol). The solution was heated to 97 °C

(external temperature). After stirring at the same temperature for 3 h, the reaction mixture was cooled to 23 °C and treated with K_2CO_3 (481 mg, 3.48 mmol) followed by MeOH (14 mL) and NH_2OH•HCl (60 mg, 0.87 mmol) at the same temperature. A reflux condenser was attached, and the reaction was heated to reflux while open to air. After 2.5 h, the reaction mixture was cooled to 23 °C and concentrated *in vacuo.* EtOAc (10 mL) was added to the crude residue, followed by saturated aqueous NH_4Cl (30 mL). The layers were separated using a separatory funnel and the aqueous layer was extracted with EtOAc (2 × 30 mL). The combined organic layers were dried over anhydrous Na_2SO_4, filtered, and concentrated *in vacuo* to afford (*E*)-4-(*o*-tolyloxy)picolinaldehyde oxime (195 mg, 98% yield) as a tan solid. This material was used directly without further purification.

(E)-4-(o-Tolyloxy)picolinaldehyde oxime: m.p. = 148–151 °C; R_f = 0.54 (100% EtOAc in hexanes); IR (neat): ν_{max} = 2982, 1561, 1427, 1243, 1230, 1184, 1112 cm^{-1}; ^1H NMR (400 MHz, 293 K, DMSO-d_6): δ 11.67 (s, 1H, -CH=NO*H*), 8.44 (d, *J* = 6.0 Hz, 1H, 6-H), 8.00 (s, 1H, -C*H*=NOH), 7.39 (app d, *J* = 7.6 Hz, 1H, -*Ph*), 7.32 (app t, *J* = 6.4 Hz, 1H, -*Ph*), 7.25 (app t, *J* = 6.4 Hz, 1H, -*Ph*), 7.14 (app d, *J* = 7.6 Hz, 1H, -*Ph*), 7.02 (d, *J* = 2.4 Hz, 1H, 3-H), 6.94 (dd, *J* = 6.0, 2.4 Hz, 1H, 5-H), 2.10 (s, 3H, -CH_3); ^{13}C NMR (100 MHz, 293 K, DMSO-d_6): δ 164.8, 154.7, 151.8, 151.7, 148.8, 132.4, 130.6, 128.5, 126.7, 122.0, 112.5, 105.9, 16.0; HRMS (ESI+) calcd for $C_{13}H_{13}N_2O_2$ $[M + H]^+$ = 229.0971, found 229.0971.

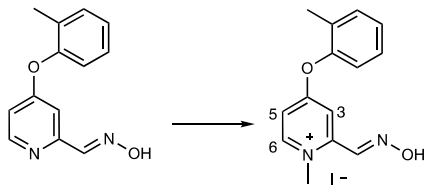

*Preparation of (E)-2-((hydroxyimino)methyl)-1-methyl-4-(o-tolyloxy)pyridin-1-ium iodide (**ADG3110**):* A 35-mL sealed tube with (*E*)-4-(*o*-tolyloxy)picolinaldehyde oxime (96 mg, 0.42 mmol) was charged with acetone (1 mL) and MeI (260 μL, 4.20 mmol). The vessel was sealed and heated to 58 °C (external temperature). After 14.5 h at the same temperature, the reaction mixture was cooled to 23 °C, transferred to a 25-mL round-bottomed flask, concentrated *in vacuo* and recrystallized from acetone/EtOAc (1:1) to afford (*E*)-2-((hydroxyimino)methyl)-1-methyl-4-(*o*-tolyloxy)pyridin-1-ium iodide as a yellow solid (141 mg, 91% yield).

(E)-2-((Hydroxyimino)methyl)-1-methyl-4-(o-tolyloxy)pyridin-1-ium iodide: m.p. = 140–143 °C; R_f = 0.10 (10% MeOH in CH_2Cl_2); IR (neat): ν_{max} = 2966, 1643, 1569, 1487, 1306, 1222, 1104 cm^{-1}; ^1H NMR (400 MHz, 293 K, DMSO-d_6): δ 13.05 (s, 1H, -CH=NO*H*), 8.82 (d, *J* = 7.2 Hz, 1H, 6-H), 8.59 (s, 1H, -C*H*=NOH), 7.57 (dd, *J* = 7.2, 2.8 Hz, 1H, 5-H), 7.48 (app d, *J* = 6.8 Hz, 1H, -*Ph*), 7.43–7.35 (m, 3H, -*Ar*), 7.27 (app d, *J* = 8.0 Hz, 1H, -*Ar*), 4.22 (s, 3H, -N^+CH_3), 2.13 (s, 3H, -CH_3); ^{13}C NMR (100 MHz, 293 K, DMSO-d_6): δ 168.6, 150.7, 150.2, 149.4, 141.9, 132.9, 130.2, 129.0, 128.1, 121.7, 114.7, 109.7, 45.2, 15.8; HRMS (ESI+) calcd for $C_{14}H_{15}N_2O_2$ $[M]^+$ = 243.1128, found 243.1130.

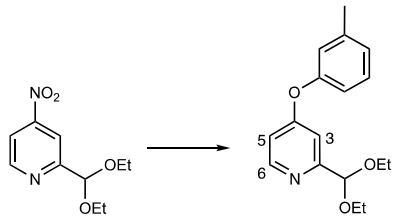

Preparation of 2-(diethoxymethyl)-4-(m-tolyloxy)pyridine: A 75-mL sealed tube was charged with dimethyl sulfoxide (6 mL), K_2CO_3 (1.22 g, 9.00 mmol), and *m*-cresol (950 μL, 9.00 mmol). The mixture was stirred at room temperature for 5 min. 2-(Diethoxymethyl)-4-nitropyridine (680 mg, 3.00 mmol) was added, the vessel was sealed and heated to 100 °C (external

temperature) for 5 h. The reaction mixture was cooled to 23 °C and acidified with saturated aqueous NH_4Cl (20 mL). The resulting solution was layers was extracted with EtOAc (3 × 20 mL). The combined organic layers were dried over anhydrous Na_2SO_4, filtered, and concentrated *in vacuo.* The crude material was purified by flash chromatography (0 to 40% EtOAc in hexanes) on silica gel (75 mL) to afford 2-(diethoxymethyl)-4-(*m*-tolyloxy)pyridine as a yellow oil (569 mg, 66% yield).

2-(Diethoxymethyl)-4-(m-tolyloxy)pyridine: R_f = 0.54 (60% EtOAc in hexanes); IR (neat): ν_{max} = 2976, 2880, 1597, 1569, 1538, 1288, 1257, 1171, 1136, 1110, 1083, 1057 cm^{-1}; ^1H NMR (300 MHz, 293 K, $CDCl_3$): δ 8.39 (d, J = 7.6 Hz, 1H, 6-H), 7.29–7.24 (m, 1H, -*Ph*), 7.15 (d, J = 3.2 Hz, 1H, 3-H), 7.02 (d, J = 7.5 Hz, 1H, -*Ph*), 6.88–6.85 (m, 1H, -*Ph*), 6.72 (dd, J = 7.6, 3.2 Hz, 1H, 5-H), 5.40 (s, 1H, -C*H*(OCH_2CH_3)$_2$), 3.74–3.52 (m, 4H, -CH(OC*H*$_2$$CH_3$)$_2$), 2.34 (s, 3H, -C*H*$_3$), 1.21 (t, J = 9.2 Hz, 6H, -CH(OCH_2C*H*$_3$)$_2$); ^{13}C NMR (100 MHz, 293 K, $CDCl_3$): δ 165.6, 160.4, 153.9, 150.5, 140.3, 129.7, 126.0, 121.2, 117.6, 111.6, 109.4, 102.4, 62.25, 21.2, 15.0; HRMS (ESI+) calcd for $C_{17}H_{22}NO_3$ $[M + H]^+$ = 288.1594, found 288.1602.

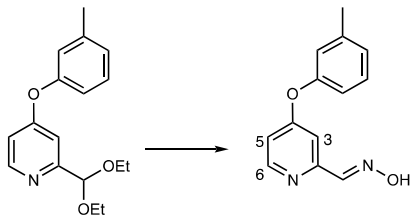

Preparation of (E)-4-(m-tolyloxy)picolinaldehyde oxime: A 50-mL pear-shaped flask open to air with 2-(diethoxymethyl)-4-(*m*-tolyloxy)pyridine (276 mg, 0.960 mmol) was charged with H_2O (4 mL) and 5 M H_2SO_4 in H_2O (290 μL, 1.44 mmol). The solution was heated to 97 °C (external temperature). After stirring at the same temperature for 3 h, the reaction mixture was cooled to 23 °C and treated with K_2CO_3 (531 mg, 3.84 mmol) followed by MeOH (14 mL) and

NH_2OH•HCl (67 mg, 0.96 mmol) at the same temperature. A reflux condenser was attached, and the reaction was heated to reflux while open to air. After 2.5 h, the reaction mixture was cooled to 23 °C and concentrated *in vacuo.* EtOAc (10 mL) was added to the crude residue, followed by saturated aqueous NH_4Cl (30 mL). The layers were separated using a separatory funnel and the aqueous layer was extracted with EtOAc (2 × 30 mL). The combined organic layers were dried over anhydrous Na_2SO_4, filtered, and concentrated *in vacuo* to afford (*E*)-4-(*m*-tolyloxy)picolinaldehyde oxime (219 mg, quantitative yield) as a tan solid. This material was used directly without further purification.

(E)-4-(m-Tolyloxy)picolinaldehyde oxime: m.p. = 116–118 °C; R_f = 0.65 (100% EtOAc); IR (neat): ν_{max} = 2982, 2854, 2762, 1597, 1564, 1456, 1292, 1268, 1241, 1163, 1087, 1010 cm^{-1}; ^1H NMR (400 MHz, 293 K, DMSO-d_6): δ 11.68 (s, 1H, -CH=NO*H*), 8.44 (d, *J* = 6.0 Hz, 1H, 6-H), 8.01 (s, 1H, -C*H*=NOH), 7.37 (app t, *J* = 7.6, 1H, -*Ph*), 7.14–7.12 (m, 2H, -*Ar*), 7.03–6.96 (m, 3H, -*Ar*), 2.33 (s, 3H, -CH_3); ^{13}C NMR (100 MHz, 293 K, DMSO-d_6): δ 165.1, 154.6, 153.8, 151.7, 148.9, 140.9, 130.6, 126.9, 121.8, 118.4, 113.1, 106.8, 21.3; HRMS (ESI+) calcd for $C_{13}H_{13}N_2O_2$ $[M + H]^+$ = 229.0972, found 229.0972.

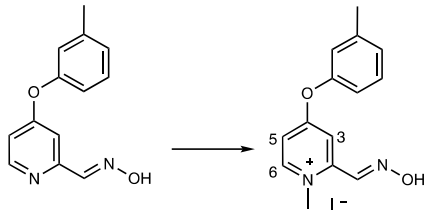

*Preparation of (E)-2-((hydroxyimino)methyl)-1-methyl-4-(m-tolyloxy)pyridin-1-ium iodide (**ADG3111**):* A 35-mL sealed tube with (*E*)-4-(*m*-tolyloxy)picolinaldehyde oxime (106 mg, 0.460 mmol) was charged with acetone (1 mL) and MeI (290 μL, 4.65 mmol). The vessel was sealed and heated to 58 °C (external temperature). After 14.5 h at the same temperature, the

reaction mixture was cooled to 23 °C, transferred to a 25-mL round-bottomed flask, concentrated *in vacuo*, and recrystallized from acetone/EtOAc (1:1) to afford (*E*)-2-((hydroxyimino)methyl)-1-methyl-4-(*m*-tolyloxy)pyridin-1-ium iodide as a yellow solid (136 mg, 80% yield).

(E)-2-((Hydroxyimino)methyl)-1-methyl-4-(m-tolyloxy)pyridin-1-ium iodide: m.p. = 165–167 °C; R_f = 0.10 (10% MeOH in CH_2Cl_2); IR (neat): ν_{max} = 2977, 1640, 1573, 1457, 1304, 1260, 1239, 1146, 1004 cm^{-1}; ^1H NMR (400 MHz, 293 K, DMSO-d_6): δ 13.05 (s, 1H, -CH=NO*H*), 8.82 (d, *J* = 7.2 Hz, 1H, 6-H), 8.59 (s, 1H, -C*H*=NOH), 7.60 (dd, *J* = 7.2, 2.8 Hz, 1H, 5-H), 7.51–7.46 (m, 2H, -*Ar*), 7.27 (d, *J* = 7.6 Hz, 1H, -*Ar*), 7.16–7.12 (m, 2H, -*Ar*), 4.22 (s, 3H, -N^+CH_3), 2.37 (s, 3H, -CH_3); ^{13}C NMR (100 MHz, 293 K, DMSO-d_6): δ 169.0, 152.4, 149.9, 149.2, 141.8, 141.5, 131.1, 128.4, 121.6, 118.2, 115.0, 110.2, 45.1, 21.2; HRMS (ESI+) calcd for $C_{14}H_{15}N_2O_2$ $[M]^+$ = 243.1128, found 243.1132.

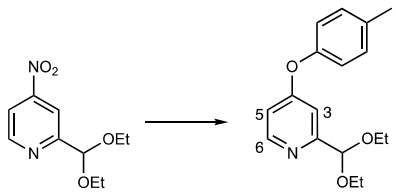

Preparation of 2-(diethoxymethyl)-4-(p-tolyloxy)pyridine: A 35-mL sealed tube was charged with dimethyl sulfoxide (3 mL), K_2CO_3 (1.04 g, 7.50 mmol), and *p*-cresol (811 mg, 7.50 mmol). The mixture was stirred at room temperature for 5 min. 2-(Diethoxymethyl)-4-nitropyridine (566 mg, 2.50 mmol) was added, the vessel was sealed and heated to 85 °C (external temperature) for 6 h. The reaction mixture was cooled to 23 °C and acidified with saturated aqueous NH_4Cl (30 mL). The resulting solution was layers was extracted with EtOAc (3 × 40 mL). The combined organic layers were dried over anhydrous Na_2SO_4, filtered, and concentrated *in vacuo.* The crude material was combined with another batch (1.0 mmol scale, with respect to 2-

(diethoxymethyl)-4-nitropyridine) prepared using the same procedure and purified by flash chromatography (0 to 50% EtOAc in hexanes) on silica gel (150 mL) to afford 2-(diethoxymethyl)-4-(*p*-tolyloxy)pyridine as a pale yellow oil (852 mg, 85% yield).

2-(Diethoxymethyl)-4-(p-tolyloxy)pyridine: R_f = 0.50 (60% EtOAc in hexanes); IR (neat): ν_{max} = 2974, 2922, 1587, 1504, 1474, 1421, 1344, 1291, 1258, 1212, 1156, 1108, 1060 cm^{-1}; ^1H NMR (400 MHz, 293 K, $CDCl_3$): δ 8.38 (d, J = 5.6 Hz, 1H, 6-H), 7.18 (d, J = 8.0 Hz, 2H, -*Ph*), 7.13 (d, J = 2.4 Hz, 1H, 3-H), 6.95 (d, J = 8.0 Hz, 2H, -*Ph*), 7.71 (dd, J = 5.6, 2.4 Hz, 1H, 5-H), 5.39 (s, 1H, -C*H*(OCH_2CH_3)$_2$), 3.72–3.54 (m, 4H, -CH(OCH_2CH_3)$_2$), 2.35 (s, 3H, -CH_3), 1.22 (t, J = 7.2 Hz, 6H, -CH(OCH_2CH_3)$_2$); ^{13}C NMR (100 MHz, 293 K, $CDCl_3$): δ 165.7, 160.3, 151.5, 150.4, 134.9, 130.5, 120.5, 111.3, 109.1, 102.3, 62.2, 20.6, 15.0; HRMS (ESI+) calcd for $C_{17}H_{22}NO_3$ $[M + H]^+$ = 288.1594, found 288.1597.

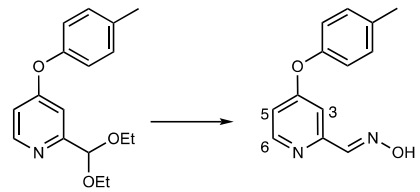

Preparation of (E)-4-(p-tolyloxy)picolinaldehyde oxime: A 25-mL pear-shaped flask open to air with 2-(diethoxymethyl)-4-(*p*-tolyloxy)pyridine (575 mg, 2.00 mmol) was charged with H_2O (7 mL) and 5 M H_2SO_4 in H_2O (480 μL, 2.40 mmol). The solution was heated to 85 °C (external temperature). After stirring at the same temperature for 4 h, the reaction mixture was cooled to 23 °C and treated with K_2CO_3 (1.11 g, 8.00 mmol) followed by MeOH (25 mL) and NH_2OH•HCl (139 mg, 2.00 mmol) at the same temperature. A reflux condenser was attached, and the reaction was heated to reflux while open to air. After 3 h, the reaction mixture was cooled to 23 °C and concentrated *in vacuo.* EtOAc (15 mL) was added to the crude residue, followed by saturated

aqueous NH_4Cl (20 mL). The layers were separated using a separatory funnel and the aqueous layer was extracted with EtOAc (2 × 25 mL). The combined organic layers were dried over anhydrous Na_2SO_4, filtered, and concentrated *in vacuo*. The crude residue was purified by flash chromatography (10 to 50% EtOAc in hexanes) on silica gel (20 mL) to afford to afford (*E*)-4-(*p*-tolyloxy)picolinaldehyde oxime (344 mg, 75% yield) as a light pink solid.

(E)-4-(p-Tolyloxy)picolinaldehyde oxime: m.p. = 163–167 °C; R_f = 0.42 (60% EtOAc in hexanes); IR (neat): ν_{max} = 2982, 2889, 1587, 1562, 1430, 1260, 1246, 1216, 1205, 1173 cm^{-1}; ^1H NMR (400 MHz, 293 K, DMSO-d_6): δ 11.68 (s, 1H, -CH=NO*H*), 8.44 (d, *J* = 6.0 Hz, 1H, 6-H), 8.00 (s, 1H, -C*H*=NOH), 7.29 (d, *J* = 8.4 Hz, 2H, -*Ph*), 7.11–7.09 (m, 3H, -*Ar*), 6.97 (dd, *J* = 6.0, 2.4 Hz, 1H, 5-H), 2.34 (s, 3H, -CH_3); ^{13}C NMR (100 MHz, 293 K, DMSO-d_6): δ 165.4, 154.6, 151.7, 151.5, 148.9, 135.6, 131.4, 121.3, 113.0, 106.5, 20.9; HRMS (ESI+) calcd for $C_{13}H_{13}N_2O_2$ $[M + H]^+$ = 229.0971, found 229.0972.

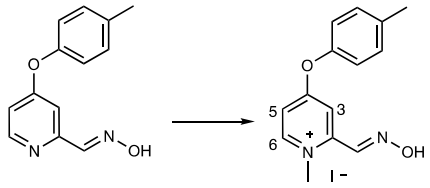

*Preparation of (E)-2-((hydroxyimino)methyl)-1-methyl-4-(p-tolyloxy)pyridin-1-ium iodide (**ADG3092**):* A 35-mL sealed tube with (*E*)-4-(*p*-tolyloxy)picolinaldehyde oxime (175 mg, 0.760 mmol) was charged with acetone (750 μL) and MeI (470 μL, 7.60 mmol). The vessel was sealed and heated to 60 °C (external temperature). After 17 h at the same temperature, the reaction mixture was cooled to 23 °C, transferred to a 25-mL round-bottomed flask, concentrated *in vacuo*, and recrystallized from EtOAc/acetone (1:1) to afford (*E*)-2-((hydroxyimino)methyl)-1-methyl-4-(*p*-tolyloxy)pyridin-1-ium iodide as a yellow solid (153 mg, 54% yield).

(E)-2-((Hydroxyimino)methyl)-1-methyl-4-(p-tolyloxy)pyridin-1-ium iodide: m.p. = 160–163 °C; R_f = 0.10 (10% MeOH in CH_2Cl_2); IR (neat): ν_{max} = 2982, 1642, 1567, 1462, 1312, 1217, 1101 cm^{-1}; ^1H NMR (400 MHz, 293 K, DMSO-d_6): δ 13.05 (s, 1H, -CH=NO*H*), 8.81 (d, *J* = 7.2 Hz, 1H, 6-H), 8.59 (s, 1H, -C*H*=NOH), 7.59 (dd, *J* = 7.2, 3.2 Hz, 1H, 5-H), 7.49 (d, *J* = 3.2 Hz, 1H, 3-H), 7.39 (d, *J* = 8.0 Hz, 2H, -*Ph*), 7.22 (d, *J* = 8.0 Hz, 2H, -*Ph*), 4.22 (s, 3H, -N^+CH_3), 2.37 (s, 3H, -CH_3); ^{13}C NMR (100 MHz, 293 K, DMSO-d_6): δ 169.2, 150.3, 150.0, 149.2, 141.9, 137.3, 131.8, 121.1, 115.0, 110.1, 45.2, 20.9; HRMS (ESI+) calcd for $C_{14}H_{15}N_2O_2$ $[M]^+$ = 243.1128, found 243.1127.

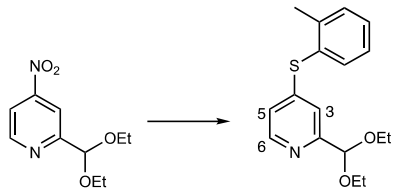

Preparation of 2-(diethoxymethyl)-4-(o-tolylthio)pyridine: A 75-mL sealed tube was charged with dimethyl sulfoxide (4 mL), K_2CO_3 (1.68 g, 12.0 mmol), and *o*-thiocresol (1.42 mL, 12.0 mmol). The mixture was stirred at room temperature for 10 min. 2-(Diethoxymethyl)-4-nitropyridine (912 mg, 4.00 mmol) was added, the vessel was sealed and heated to 95 °C for 16 h. The reaction mixture was cooled to 23 °C and neutralized with saturated aqueous NH_4Cl (20 mL). The resulting solution was extracted with EtOAc (3 × 15 mL). The combined organic layers were dried over anhydrous Na_2SO_4, filtered, and concentrated *in vacuo.* The crude material was purified by flash chromatography (0 to 40% EtOAc in hexanes) on silica gel (90 mL) to afford 2-(diethoxymethyl)-4-(*o*-tolylthio)pyridine as a pale yellow oil (1.01 g, 83% yield).

2-(Diethoxymethyl)-4-(o-tolylthio)pyridine: R_f = 0.45 (60% EtOAc in hexanes); IR (neat): ν_{max} = 2974, 2876, 1575, 1542, 1470, 1455, 1392, 1368, 1342, 1273, 1222, 1112, 1090, 1059 cm^-

[1]; ^{1}H NMR (400 MHz, 293 K, DMSO-d_6): δ 8.31 (d, J = 5.6 Hz, 1H, 6-H), 7.58 (d, J = 7.6 Hz, 1H, -*Ph*), 7.50–7.48 (m, 2H, -*Ph*), 7.39–7.34 (m, 1H, -*Ph*), 6.97 (d, J = 1.6 Hz, 1H, 3-H), 6.90 (dd, J = 5.6, 1.6 Hz, 1H, 5-H), 5.27 (s, 1H, -C*H*(OCH_2CH_3)$_2$), 3.59–3.40 (m, 4H, -CH(OCH_2CH_3)$_2$), 2.30 (s, 3H, -CH_3), 1.06 (t, J = 7.2 Hz, 6H, -CH(OCH_2CH_3)$_2$); ^{13}C NMR (100 MHz, 293 K, DMSO-d_6): δ 158.6, 149.7, 149.2, 142.7, 136.9, 131.8, 131.2, 128.2, 127.9, 120.2, 116.8, 102.3, 62.2, 20.6, 15.5; HRMS (ESI+) calcd for $C_{17}H_{22}NO_2S$ $[M + H]^+$ = 304.1366 found 304.1370.

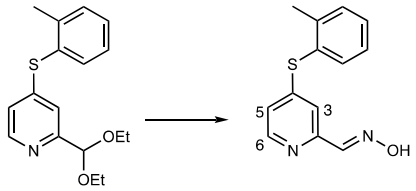

Preparation of (E)-4-(o-tolylthio)picolinaldehyde oxime: A 100-mL pear-shaped flask open to air with 2-(diethoxymethyl)-4-(*o*-tolylthio)pyridine (556 mg, 1.74 mmol) was charged with H_2O (8 mL) and 5 M H_2SO_4 in H_2O (380 μL, 1.91 mmol). The solution was heated to 95 °C. After stirring at the same temperature for 2.7 h, the reaction mixture was cooled to 23 °C and treated with K_2CO_3 (962 mg, 6.96 mmol) followed by MeOH (20 mL) and NH_2OH•HCl (121 mg, 1.74 mmol) at the same temperature. A reflux condenser was attached, and the reaction was heated to reflux while open to air. After 3 h, the reaction mixture was cooled to 23 °C and concentrated *in vacuo*. EtOAc (10 mL) was added to the crude residue, followed by saturated aqueous NH_4Cl (20 mL). The layers were separated using a separatory funnel and the aqueous layer was extracted with EtOAc (2 × 15 mL). The combined organic layers were dried over anhydrous Na_2SO_4, filtered, and concentrated *in vacuo* to afford (*E*)-4-(*o*-tolylthio)picolinaldehyde oxime (354 mg, 83% yield) as a white solid. This material was used directly without further purification.

(E)-4-(o-Tolylthio)picolinaldehyde oxime: m.p. = 181–184 °C; R_f = 0.40 (60% EtOAc in hexanes); IR (neat): ν_{max} = 3166, 3056, 2978, 2868, 2744, 1575, 1536, 1470, 1398, 1331 cm^{-1}; ^1H NMR (400 MHz, 293 K, DMSO-d_6): δ 11.69 (s, 1H, -CH=NO*H*), 8.36 (d, *J* = 5.6 Hz, 1H, 6-H), 7.95 (s, 1H, -C*H*=NOH), 7.60 (d, *J* = 7.6 Hz, 1H, -*Ar*), 7.50–8.49 (m, 2H, -*Ph*), 7.38–7.34 (m, 1H, -*Ar*), 7.16 (d, *J* = 1.6 Hz, 1H, 3-H), 7.16 (dd, *J* = 5.2, 1.6 Hz, 1H, 5-H); ^{13}C NMR (100 MHz, 293 K, DMSO-d_6): δ 152.7, 149.8, 149.6, 148.8, 142.8, 137.1, 131.9, 131.4, 128.2, 127.6, 120.8, 115.1, 20.6; HRMS (ESI+) calcd for $C_{13}H_{13}N_2OS$ $[M + H]^+$ = 245.0743, found 245.0747.

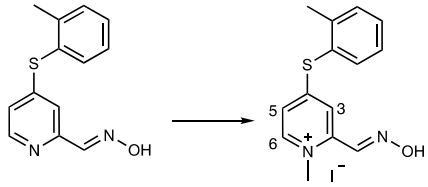

*Preparation of (E)-2-((hydroxyimino)methyl)-1-methyl-4-(o-tolylthio)pyridin-1-ium iodide (**ADG4122**):* A 35-mL sealed tube with (*E*)-4-(*o*-tolylthio)picolinaldehyde oxime (122 mg, 0.490 mmol) was charged with acetone (2 mL) and MeI (310 μL, 4.90 mmol). The vessel was sealed and heated to 50 °C. After 24 h at the same temperature, the reaction mixture was cooled to 23 °C, transferred to a 25-mL round-bottomed flask, concentrated *in vacuo* to afford (*E*)-2-((hydroxyimino)methyl)-1-methyl-4-(*o*-tolylthio)pyridin-1-ium iodide as an orange solid (186 mg, 98% yield).

(E)-2-((Hydroxyimino)methyl)-1-methyl-4-(o-tolylthio)pyridin-1-ium iodide: m.p. = 173–175 °C; R_f = 0.11 (10% MeOH in CH_2Cl_2); IR (neat): ν_{max} = 2959, 1624, 1579, 1551, 1494, 1415, 1306, 1230, 1186, 1086 cm^{-1}; ^1H NMR (400 MHz, 293 K, DMSO-d_6): δ 13.01 (s, 1H, -CH=NO*H*), 8.63 (d, *J* = 6.8 Hz, 1H, 6-H), 8.54 (s, 1H, -C*H*=NOH), 7.68–7.57 (m, 4H, -*Ar*), 7.51 (d, *J* = 2.4 Hz, 1H, 3-H), 7.47–7.43 (m, 1H, -*Ph*), 4.17 (s, 3H, -N^+CH_3), 2.35 (s, 3H, -CH_3); ^{13}C NMR (100

MHz, 293 K, DMSO-d_6): δ 161.0, 146.6, 145.5, 143.1, 141.9, 137.1, 132.6, 132.4, 128.8, 125.44, 122.3, 118.2, 45.4, 20.5; HRMS (ESI+) calcd for $C_{12}H_{10}N_2OS$ $[M]^+$ = 259.0899, found 259.0901.

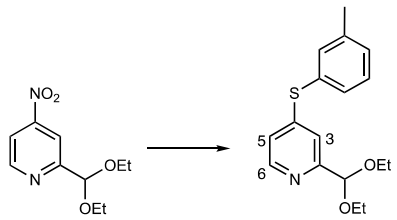

Preparation of 2-(diethoxymethyl)-4-(m-tolylthio)pyridine: A 75-mL sealed tube was charged with dimethyl sulfoxide (4 mL), K_2CO_3 (1.66 g, 12.0 mmol), and 3-methylbenzenethiol (1.93 g, 12.0 mmol). The mixture was stirred at room temperature for 10 min. 2-(Diethoxymethyl)-4-nitropyridine (905 mg, 4.00 mmol) was added, the vessel was sealed and heated to 90 °C for 16 h. The reaction mixture was cooled to 23 °C and neutralized with saturated aqueous NH_4Cl (20 mL). The resulting solution was extracted with EtOAc (3 × 10 mL). The combined organic layers were dried over anhydrous Na_2SO_4, filtered, and concentrated *in vacuo.* The crude material was purified by flash chromatography (0 to 50% EtOAc in hexanes) on silica gel (100 mL) to afford 2-(diethoxymethyl)-4-(*m*-tolylthio)pyridine as an amber oil (1.18 g, 98% yield).

2-(Diethoxymethyl)-4-(m-tolylthio)pyridine: R_f = 0.68 (60% EtOAc in hexanes); IR (neat): ν_{max} = 2974, 2877, 1574, 1543, 1475, 1392, 1369, 1343, 1272, 1223, 1113, 1059 cm^{-1}; ^1H NMR (400 MHz, 293 K, $CDCl_3$): δ 8.30 (d, J = 5.2 Hz, 1H, 6-H), 7.36–7.29 (m, 4H, -*Ar*), 7.25–7.23 (m, 1H, -*Ar*), 6.81 (dd, J = 5.2, 2.0 Hz, 1H, 5-H), 5.37 (s, 1H, -C*H*$(OCH_2CH_3)_2$), 3.70–3.52 (m, 4H, -CH$(OCH_2CH_3)_2$), 2.36 (s, 3H, -C*H*$_3$), 1.21 (t, J = 7.2 Hz, 6H, -CH$(OCH_2CH_3)_2$); ^{13}C NMR (100 MHz, 293 K, $CDCl_3$): δ 157.8, 151.3, 148.7, 139.7, 135.5, 132.0, 130.3, 129.6, 129.0, 120.2, 118.0, 102.3, 62.2, 21.1, 15.0; HRMS (ESI+) calcd for $C_{17}H_{22}NO_2S$ $[M + H]^+$ = 304.1365, found 304.1360.

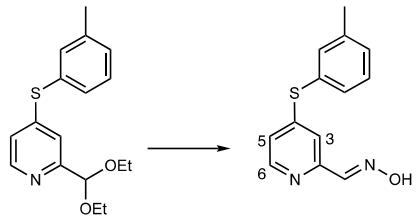

Preparation of (E)-4-(m-tolylthio)picolinaldehyde oxime: A 100-mL pear-shaped flask open to air with 2-(diethoxymethyl)-4-(*m*-tolylthio)pyridine (581 mg, 1.92 mmol) was charged with H_2O (5 mL) and 5 M H_2SO_4 in H_2O (420 μL, 2.10 mmol). The solution was heated to 90 °C. After stirring at the same temperature for 2.8 h, the reaction mixture was cooled to 23 °C and treated with K_2CO_3 (1.06 g, 7.68 mmol) followed by MeOH (20 mL) and NH_2OH•HCl (133 mg, 1.92 mmol) at the same temperature. A reflux condenser was attached, and the reaction was heated to reflux while open to air. After 2 h, the reaction mixture was cooled to 23 °C and concentrated *in vacuo.* EtOAc (10 mL) was added to the crude residue, followed by saturated aqueous NH_4Cl (20 mL). The layers were separated using a separatory funnel and the aqueous layer was extracted with EtOAc (2 × 10 mL). The combined organic layers were dried over anhydrous Na_2SO_4, filtered, and concentrated *in vacuo* to afford (*E*)-4-(*m*-tolylthio)picolinaldehyde oxime (358 mg, 76% yield) as a light tan solid. This material was used directly without further purification.

(E)-4-(m-Tolylthio)picolinaldehyde oxime: m.p. = 157–160 °C; R_f = 0.32 (60% EtOAc in hexanes); IR (neat): ν_{max} = 2847, 2718, 1574, 1533, 1501, 1398, 1310, 1225 cm^{-1}; ^1H NMR (300 MHz, 293 K, DMSO-d_6): δ 11.69 (s, 1H, -CH=NO*H*), 8.36 (d, *J* = 5.4 Hz, 1H, 6-H), 7.96 (s, 1H, -C*H*=NOH), 7.45–7.36 (m, 4H, -*Ph*), 7.30 (d, *J* = 1.5 Hz, 1H, 3-H), 7.16 (dd, *J* = 5.4, 1.5 Hz, 1H, 5-H), 2.36 (s, 3H, -CH_3); ^{13}C NMR (100 MHz, 293 K, DMSO-d_6): δ 152.2, 150.1, 149.2, 148.4, 139.9, 135.4, 132.2, 130.9, 130.1, 127.9, 120.5, 115.3, 20.7; HRMS (ESI+) calcd for $C_{13}H_{13}N_2OS$ $[M + H]^+$ =245.0743, found 245.0744.

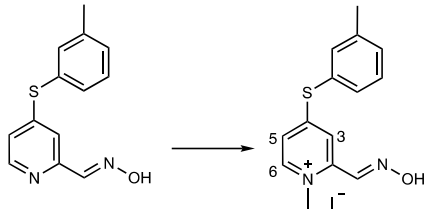

*Preparation of (E)-2-((hydroxyimino)methyl)-1-methyl-4-(m-tolylthio)pyridin-1-ium iodide (**ADG4086**):* A 35-mL sealed tube with (*E*)-4-(*m*-tolylthio)picolinaldehyde oxime (107 mg, 0.430 mmol) was charged with acetone (2 mL) and MeI (270 μL, 4.30 mmol). The vessel was sealed and heated to 55 °C. After 18.4 h at the same temperature, the reaction mixture was cooled to 23 °C, transferred to a 25-mL round-bottomed flask, concentrated *in vacuo* to afford (*E*)-2-((hydroxyimino)methyl)-1-methyl-4-(*m*-tolylthio)pyridin-1-ium iodide as an orange solid (140 mg, 84% yield).

(E)-2-((Hydroxyimino)methyl)-1-methyl-4-(m-tolylthio)pyridin-1-ium iodide: m.p. = 175–178 °C; R_f = 0.11 (10% MeOH in CH_2Cl_2); IR (neat): ν_{max} = 3034, 2989, 2861, 1626, 1598, 1573, 1552, 1491, 1471, 1450, 1428, 1319, 1301, 1230, 1194, 1085, 1076 cm^{-1}; ^1H NMR (300 MHz, 293 K, DMSO-d_6): δ 13.02 (s, 1H, -CH=NO*H*), 8.62 (d, *J* = 6.6 Hz, 1H, 6-H), 8.55 (s, 1H, -C*H*=NOH), 7.69–7.66 (m, 2H, -*Ar*), 7.55–7.51 (m, 4H, -*Ar*), 4.13 (s, 3H, -N^+CH_3), 2.38 (s, 3H, -CH_3); ^{13}C NMR (100 MHz, 293 K, DMSO-d_6): δ 161.9, 146.5, 145.5, 141.9, 141.2, 136.0, 132.8, 132.7, 131.2, 125.8, 122.3, 118.6, 45.4, 21.2; HRMS (ESI+) calcd for $C_{14}H_{15}N_2OS$ $[M]^+$ = 259.0899, found 259.0897.

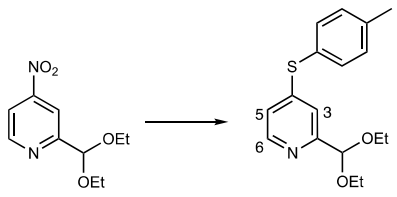

Preparation of 2-(diethoxymethyl)-4-(p-tolylthio)pyridine: A 75-mL sealed tube was charged with dimethyl sulfoxide (4 mL), K_2CO_3 (1.69 g, 12.0 mmol), and *p*-methylbenzenethiol (1.49 g, 12.0 mmol). The mixture was stirred at room temperature for 12 min. 2-(Diethoxymethyl)-4-nitropyridine (905 mg, 4.00 mmol) was added, the vessel was sealed and heated to 85 °C for 17 h. The reaction mixture was cooled to 23 °C and neutralized with saturated aqueous NH_4Cl (20 mL). The resulting solution was extracted with EtOAc (3 × 20 mL). The combined organic layers were dried over anhydrous Na_2SO_4, filtered, and concentrated *in vacuo.* The crude material was purified by flash chromatography (10 to 50% EtOAc in hexanes) on silica gel (150 mL) to afford 2-(diethoxymethyl)-4-(*p*-tolylthio)pyridine as a pale yellow oil (1.19 g, 98% yield).

2-(Diethoxymethyl)-4-(p-tolylthio)pyridine: R_f = 0.55 (60% EtOAc in hexanes); IR (neat): ν_{max} = 2974, 2876, 1575, 1543, 1493, 1444, 1392, 1369, 1343, 1302, 1272, 1224, 1112, 1088, 1058, 1018 cm^{-1}; ^1H NMR (400 MHz, 293 K, DMSO-d_6): δ 8.30 (d, J = 5.2 Hz, 1H, 6-H), 7.47 (d, J = 8.0 Hz, 2H, -*Ph*), 7.35 (d, J = 8.0 Hz, 2H, -*Ph*), 7.06 (d, J = 2.0 Hz, 2H, 3-H), 6.79 (dd, J = 5.2, 2.0 Hz, 1H, 5-H), 5.27 (s, 1H, -C*H*$(OCH_2CH_3)_2$), 3.59–3.41 (m, 4H, -CH(OC*H*$_2CH_3)_2$), 2.38 (s, 3H, -C*H*$_3$), 1.07 (t, J = 7.2 Hz, 6H, -CH$(OCH_2CH_3)_2$); ^{13}C NMR (100 MHz, 293 K, DMSO-d_6): δ 158.1, 150.4, 148.7, 140.0, 135.1, 130.9, 124.8, 119.8, 116.6, 101.9, 61.7, 20.8, 14.9; HRMS (ESI+) calcd for $C_{17}H_{22}NO_2S$ $[M + H]^+$ = 304.1366, found 304.1364.

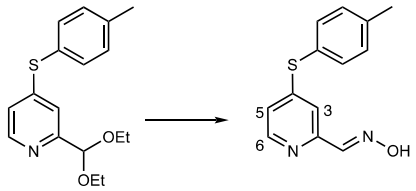

Preparation of (E)-4-(p-tolylthio)picolinaldehyde oxime: A 100-mL pear-shaped flask open to air with 2-(diethoxymethyl)-4-(*p*-tolylthio)pyridine (592 mg, 1.95 mmol) was charged

with H_2O (5 mL) and 5 M H_2SO_4 in H_2O (430 μL, 2.14 mmol). The solution was heated to 85 °C. After stirring at the same temperature for 2.4 h, the reaction mixture was cooled to 23 °C and treated with K_2CO_3 (1.07 g, 7.80 mmol) followed by MeOH (20 mL) and NH_2OH•HCl (136 mg, 1.95 mmol) at the same temperature. A reflux condenser was attached, and the reaction was heated to reflux while open to air. After 4 h, the reaction mixture was cooled to 23 °C and concentrated *in vacuo*. EtOAc (20 mL) was added to the crude residue, followed by saturated aqueous NH_4Cl (30 mL). The layers were separated using a separatory funnel and the aqueous layer was extracted with EtOAc (2 × 20 mL). The combined organic layers were dried over anhydrous Na_2SO_4, filtered, and concentrated *in vacuo* to afford (*E*)-4-(*p*-tolylthio)picolinaldehyde oxime (247 mg, 52% yield) as a light tan solid. This material was used directly without further purification.

(E)-4-(p-Tolylthio)picolinaldehyde oxime: m.p. = 189–192 °C; R_f = 0.40 (60% EtOAc in hexanes); IR (neat): ν_{max} = 2974, 2869, 2756, 1572, 1534, 1488, 1397, 1316, 1103 cm^{-1}; ^1H NMR (300 MHz, 293 K, DMSO-d_6): δ 11.67 (s, 1H, -CH=NO*H*), 8.35 (d, *J* = 5.4 Hz, 1H, 6-H), 7.96 (s, 1H, -C*H*=NOH), 7.51 (d, *J* = 7.8 Hz, 2H, -*Ph*), 7.51 (d, *J* = 7.8 Hz, 2H, -*Ph*), 7.28 (d, *J* = 1.8 Hz, 1H, 3-H), 7.06 (dd, *J* = 5.4, 1.8 Hz, 1H, 5-H), 2.39 (s, 3H, -CH_3); ^{13}C NMR (100 MHz, 293 K, DMSO-d_6): δ 152.3, 150.5, 149.2, 148.5, 140.2, 135.3, 131.0 124.5, 120.4, 115.0, 20.9; HRMS (ESI+) calcd for $C_{13}H_{13}N_2OS$ $[M + H]^+$ = 245.0743, found 245.0741.

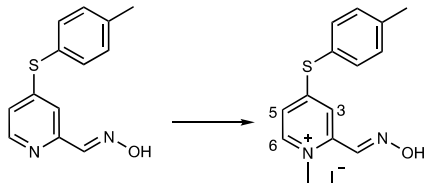

*Preparation of (E)-2-((hydroxyimino)methyl)-1-methyl-4-(p-tolylthio)pyridin-1-ium iodide (**ADG4094**):* A 35-mL sealed tube with (*E*)-4-(*p*-tolylthio)picolinaldehyde oxime (125 mg,

0.510 mmol) was charged with acetone (2 mL) and MeI (320 μL, 5.10 mmol). The vessel was sealed and heated to 55 °C. After 16 h at the same temperature, the reaction mixture was cooled to 23 °C, transferred to a 25-mL round-bottomed flask, concentrated *in vacuo* to afford (*E*)-2-((hydroxyimino)methyl)-1-methyl-4-(*p*-tolylthio)pyridin-1-ium iodide as an orange solid (205 mg, quantitative yield).

(E)-2-((Hydroxyimino)methyl)-1-methyl-4-(p-tolylthio)pyridin-1-ium iodide: m.p. = 167–169 °C; R_f = 0.11 (10% MeOH in CH_2Cl_2); IR (neat): ν_{max} = 2985, 1630, 1588, 1556, 1489, 1430, 1318, 1230, 1187, 1082, 1016 cm^{-1}; ^1H NMR (400 MHz, 293 K, CD_3OD): δ 8.49 (s, 1H, -C*H*=NOH), 8.44 (d, *J* = 6.8 Hz, 1H, 6-H), 7.80 (d, *J* = 2.0 Hz, 1H, 3-H), 7.56 (d, *J* = 8.0 Hz, 2H, -*Ph*), 7.47–7.45 (m, 3H, 5-H and -*Ph*), 4.21 (s, 3H, $-N^+CH_3$), 2.45 (s, 3H, $-CH_3$); ^{13}C NMR (100 MHz, 293 K, CD_3OD): δ 165.4, 147.8, 145.8, 143.7, 141.5, 136.6, 132.8, 123.6, 122.7, 120.4, 45.7, 21.4; HRMS (ESI+) calcd for $C_{14}H_{15}N_2OS$ $[M]^+$ = 259.0899, found 259.0901.

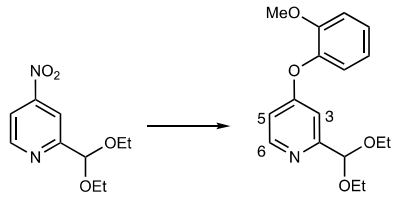

Preparation of 2-(diethoxymethyl)-4-(2-methoxyphenoxy)pyridine: A 75-mL sealed tube was charged with dimethyl sulfoxide (6 mL), K_2CO_3 (1.31 g, 9.00 mmol), and 2-methoxyphenol (990 μL, 9.00 mmol). The mixture was stirred at room temperature for 5 min. 2-(Diethoxymethyl)-4-nitropyridine (681 mg, 3.00 mmol) was added, the vessel was sealed and heated to 92 °C (external temperature) for 4 h. The reaction mixture was cooled to 23 °C and acidified with saturated aqueous NH_4Cl (30 mL). The resulting solution was extracted with EtOAc (3 × 30 mL). The combined organic layers were dried over anhydrous Na_2SO_4, filtered, and concentrated *in*

vacuo. The crude material was purified by flash chromatography (10 to 50% EtOAc in hexanes) on silica gel (150 mL) to afford 2-(diethoxymethyl)-4-(2-methoxyphenoxy)pyridine as a red oil (633 mg, 69% yield).

2-(Diethoxymethyl)-4-(2-methoxyphenoxy)pyridine: R_f = 0.50 (60% EtOAc in hexanes); IR (neat): ν_{max} = 2975, 1595, 1571, 1261, 1205, 1178, 1158, 1111, 1057, 1042 cm^{-1}; ^1H NMR (400 MHz, 293 K, $CDCl_3$): δ 8.40 (d, J = 6.0 Hz, 1H, 6-H), 7.27–7.22 (m, 1H, -*Ph*), 7.12–7.08 (m, 2H, -*Ar*), 7.02–6.97 (m, 1H, -*Ph*), 6.69 (dd, J = 6.0, 2.8 Hz, 1H, 5-H), 5.41 (s, 1H, -C*H*(OCH_2CH_3)$_2$), 3.77 (s, 3H, -OC*H*$_3$), 3.73–3.55 (m, 4H, -CH(OC*H*$_2$$CH_3$)$_2$), 1.23 (t, J = 7.2 Hz, 6H, -CH(OCH_2C*H*$_3$)$_2$); ^{13}C NMR (100 MHz, 293 K, $CDCl_3$): δ 165.4, 159.9, 151.4, 150.1, 141.8, 126.5, 122.4, 121.1, 112.7, 110.5, 108.3, 102.2, 62.0, 55.4, 14.9; HRMS (ESI+) calcd for $C_{17}H_{22}NO_4$ [M + H]$^+$ = 304.1543, found 304.1544.

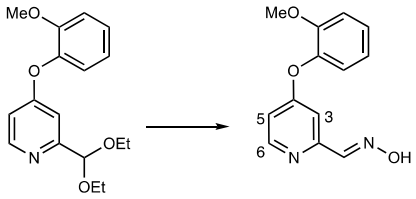

Preparation of (E)-4-(2-methoxyphenoxy)picolinaldehyde oxime: A 50-mL pear-shaped flask open to air with 2-(diethoxymethyl)-4-(2-methoxyphenoxy)pyridine (290 mg, 0.950 mmol) was charged with H_2O (4 mL) and 5 M H_2SO_4 in H_2O (290 μL, 1.05 mmol). The solution was heated to 95 °C (external temperature). After stirring at the same temperature for 3 h, the reaction mixture was cooled to 23 °C and treated with K_2CO_3 (525 mg, 3.79 mmol) followed by MeOH (14 mL) and NH_2OH•HCl (67 mg, 0.95 mmol) at the same temperature. A reflux condenser was attached, and the reaction was heated to reflux while open to air. After 4 h, the reaction mixture was cooled to 23 °C and concentrated *in vacuo*. EtOAc (10 mL) was added to the crude residue,

followed by saturated aqueous NH_4Cl (35 mL). The layers were separated using a separatory funnel and the aqueous layer was extracted with EtOAc (2 × 20 mL). The combined organic layers were dried over anhydrous Na_2SO_4, filtered, and concentrated *in vacuo* to afford (*E*)-4-(2-methoxyphenoxy)picolinaldehyde oxime (223 mg, 96% yield) as a pale peach solid. This material was used directly without further purification.

(E)-4-(2-Methoxyphenoxy)picolinaldehyde oxime: m.p. = 170–172 °C; R_f = 0.46 (60% EtOAc in hexanes); IR (neat): ν_{max} = 2971, 1599, 1580, 1439, 1279, 1249, 1177, 1044, 1029 cm^{-1}; ^1H NMR (400 MHz, 293 K, DMSO-d_6): δ 11.66 (s, 1H, -CH=NO*H*), 8.41 (d, *J* = 5.6 Hz, 1H, 6-H), 7.99 (s, 1H, -C*H*=NOH), 7.35–7.30 (m, 1H, -*Ph*), 7.25–7.21 (m, 2H, -*Ph*), 7.07–7.02 (m, 2H, -*Ar*), 6.90 (dd, *J* = 5.6, 2.4 Hz, 1H, 5-H), 3.72 (s, 3H, -OC*H*$_3$); ^{13}C NMR (100 MHz, 293 K, DMSO-d_6): δ 165.1, 154.4, 151.8, 151.5, 148.9, 141.4, 127.8, 123.2, 121.8, 114.1 112.1, 105.6, 56.2; HRMS (ESI+) calcd for $C_{13}H_{13}N_2O_3$ [M + H] = 245.0921, found 245.0923.

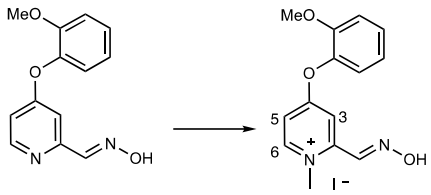

*Preparation of (E)-2-((hydroxyimino)methyl)-1-methyl-4-(2-methoxyphenoxy)pyridin-1-ium iodide (**ADG3120**):* A 35-mL sealed tube with (*E*)-4-(2-methoxyphenoxy)picolinaldehyde oxime (108 mg, 0.440 mmol) was charged with acetone (1 mL) and MeI (270 μL, 4.40 mmol). The vessel was sealed and heated to 55 °C (external temperature). After 17 h at the same temperature, the reaction mixture was cooled to 23 °C, transferred to a 25-mL round-bottomed flask, concentrated *in vacuo*, and recrystallized from acetone/EtOAc (1:1) to yield (*E*)-2-

((hydroxyimino)methyl)-1-methyl-4-(2-methoxyphenoxy)pyridin-1-ium iodide as a light yellow solid (149 mg, 87% yield).

(E)-2-((Hydroxyimino)methyl)-1-methyl-4-(2-methoxyphenoxy)pyridin-1-ium iodide: m.p. = 180–182 °C; R_f = 0.11 (10% MeOH in CH_2Cl_2); IR (neat): ν_{max} = 3122, 2982, 1578, 1497, 1462, 1419, 1337, 1297, 1270, 1171, 1104, 1006 cm^{-1}; ^1H NMR (300 MHz, 293 K, DMSO-d_6): δ 13.01 (s, 1H, -CH=NO*H*), 8.79 (d, *J* = 7.2 Hz, 1H, 6-H), 8.56 (s, 1H, -C*H*=NOH), 7.54 (dd, *J* = 7.2, 3.3 Hz, 1H, 5-H), 7.45–7.40 (m, 2H, -*Ph*), 7.36–7.31 (m, 2H, -*Ar*), 7.14–7.09 (m, 1H, -*Ph*), 4.20 (s, 3H, -N^+CH_3), 3.75 (s, 3H, -O*C*H_3); ^{13}C NMR (100 MHz, 293 K, DMSO-d_6): δ 168.8, 150.9, 149.9, 149.2, 141.9, 140.2, 129.1, 122.8, 122.2, 114.5, 114.4, 109.6, 56.5, 45.2; HRMS (ESI+) calcd for $C_{14}H_{15}N_2O_3$ $[M]^+$ = 259.1077, found 259.1083.

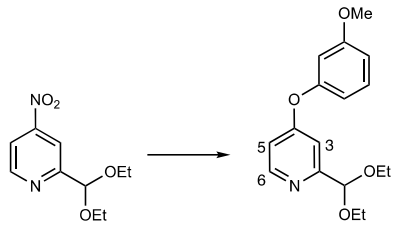

Preparation of 2-(diethoxymethyl)-4-(3-methoxyphenoxy)pyridine: A 75-mL sealed tube was charged with dimethyl sulfoxide (6 mL), K_2CO_3 (1.23 g, 9.00 mmol), and 3-methoxyphenol (980 μL, 9.00 mmol). The mixture was stirred at room temperature for 5 min. 2-(Diethoxymethyl)-4-nitropyridine (680 mg, 3.00 mmol) was added, the vessel was sealed and heated to 100 °C (external temperature) for 6 h. The reaction mixture was cooled to 23 °C and acidified with saturated aqueous NH_4Cl (20 mL). The resulting solution was extracted with EtOAc (3 × 15 mL). The combined organic layers were dried over anhydrous Na_2SO_4, filtered, and concentrated *in vacuo.* The crude material was purified by flash chromatography (0 to 50% EtOAc in hexanes) on silica gel (80 mL) to afford 2-(diethoxymethyl)-4-(3-methoxyphenoxy)pyridine as a yellow oil (812 mg, 88% yield).

2-(Diethoxymethyl)-4-(3-methoxyphenoxy)pyridine: R_f = 0.61 (60% EtOAc in hexanes); IR (neat): ν_{max} = 2975, 1583, 1346, 1284, 1264, 1192, 1170, 1132, 1110, 1057 cm^{-1}; ^1H NMR (400 MHz, 293 K, $CDCl_3$): δ 8.43 (d, J = 5.6 Hz, 1H, 6-H), 7.31 (app t, J = 8.0 Hz, 1H, -*Ar*), 7.19 (d, J = 2.4 Hz, 1H, 3-H), 6.80–6.76 (m, 2H, -*Ar*), 6.69–6.63 (m, 2H, -*Ph*), 5.42 (s, 1H, -C*H*(OCH_2CH_3)$_2$), 3.80 (s, 3H, -OC*H*$_3$), 3.76–3.56 (m, 4H, -CH(OC*H*$_2$CH$_3$)$_2$) 1.24 (t, J = 7.2 Hz, 6H, -CH(OCH_2CH_3)$_2$); ^{13}C NMR (100 MHz, 293 K, $CDCl_3$): δ 165.2, 161.0, 160.4, 155.0, 150.4, 130.4, 112.6, 111.6, 110.9, 109.4, 106.5, 102.3, 62.2. 55.2, 15.0; HRMS (ESI+) calcd for $C_{17}H_{22}NO_4$ $[M + H]^+$ = 304.1543, found 304.1548.

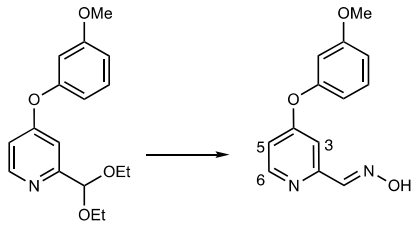

Preparation of (E)-4-(3-methoxyphenoxy)picolinaldehyde oxime: A 50-mL pear-shaped flask open to air with 2-(diethoxymethyl)-4-(3-methoxyphenoxy)pyridine (260 mg, 0.850 mmol) was charged with H_2O (4 mL) and 5 M H_2SO_4 in H_2O (190 μL, 0.950 mmol). The solution was heated to 85 °C (external temperature). After stirring at the same temperature for 3 h, the reaction mixture was cooled to 23 °C and treated with K_2CO_3 (475 mg, 3.44 mmol) followed by MeOH (14 mL) and NH_2OH•HCl (69 mg, 0.99 mmol) at the same temperature. A reflux condenser was attached, and the reaction was heated to reflux while open to air. After 2 h, the reaction mixture was cooled to 23 °C and concentrated *in vacuo.* EtOAc (10 mL) was added to the crude residue, followed by saturated aqueous NH_4Cl (10 mL). The layers were separated using a separatory funnel and the aqueous layer was extracted with EtOAc (2 × 10 mL). The combined organic layers were dried over anhydrous Na_2SO_4, filtered, and concentrated *in vacuo* to afford (*E*)-4-(3-

methoxyphenoxy)picolinaldehyde oxime (190 mg, 91% yield) as a pale green solid. This material was used directly without further purification.

(E)-4-(3-Methoxyphenoxy)picolinaldehyde oxime: m.p. = 144–147 °C; R_f = 0.36 (60% EtOAc in hexanes); IR (neat): ν_{max} = 2982, 1582, 1487, 1283, 1246, 1194, 1173, 1132, 1039 cm^{-1}; ^1H NMR (400 MHz, 293 K, DMSO-d_6): δ 11.70 (s, 1H, -CH=NO*H*), 8.46 (d, *J* = 5.6 Hz, 1H, 6-H), 8.02 (s, 1H, -C*H*=NOH), 7.41 (app t, *J* = 8.0, 1H, -*Ph*), 7.16 (d, *J* = 2.4 Hz, 1H, 3-H), 7.00 (dd, *J* = 5.6, 2.4 Hz, 1H, 5-H), 6.90 (dd, *J* = 8.4, 2.0 Hz, 1H, -*Ph*), 6.90 (dd, *J* = 8.4, 2.0 Hz, 1H, -*Ph*), 6.81 (app t, *J* = 2.0, 1H, -*Ph*), 6.76 (dd, *J* = 8.0, 2.0 Hz, 1H, -*Ph*), 3.77 (s, 3H, -OCH_3); ^{13}C NMR (100 MHz, 293 K, DMSO-d_6): δ 164.9, 161.4, 154.8, 154.6, 151.7, 148.8, 131.4, 113.2, 113.0, 112.0, 107.3, 106.8, 55.9; HRMS (ESI+) calcd for $C_{13}H_{13}N_2O_3$ $[M + H]^+$ = 245.0921, found 245.0925.

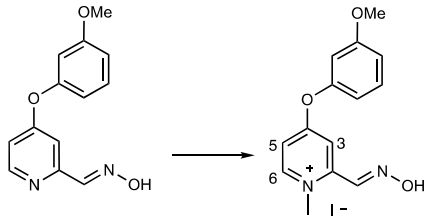

*Preparation of (E)-2-((hydroxyimino)methyl)-1-methyl-4-(3-methoxyphenoxy)pyridin-1-ium iodide (**ADG3128**):* A 35-mL sealed tube with (*E*)-4-(3-methoxyphenoxy)picolinaldehyde oxime (196 mg, 0.800 mmol) was charged with acetone (2 mL) and MeI (490 μL, 8.00 mmol). The vessel was sealed and heated to 40 °C (external temperature). After 18 h at the same temperature, the reaction mixture was cooled to 23 °C, transferred to a 25-mL round-bottomed flask, and concentrated *in vacuo*. The crude residue was dry-loaded and purified by flash chromatography (5 to 40% MeOH in CH_2Cl_2) on silica gel (10 mL) to afford (*E*)-2-

((hydroxyimino)methyl)-1-methyl-4-(3-methoxyphenoxy)pyridin-1-ium iodide as a light brown solid (247 mg, 80% yield).

(E)-2-((Hydroxyimino)methyl)-1-methyl-4-(3-methoxyphenoxy)pyridin-1-ium iodide: m.p. = 67–70 °C; R_f = 0.11 (10% MeOH in CH_2Cl_2); IR (neat): ν_{max} = 3107, 1639, 1605, 1583, 1514, 1486, 1460, 1448, 1333, 1298, 1284, 1259, 1202, 1142, 1123, 1074, 1031 cm^{-1}; ^1H NMR (400 MHz, 293 K, DMSO-d_6): δ 13.07 (s, 1H, -CH=NO*H*), 8.83 (d, *J* = 6.8 Hz, 1H, 6-H), 8.60 (s, 1H, -C*H*=NOH), 7.61 (dd, *J* = 6.8, 2.4 Hz, 1H, 5-H), 7.54 (d, *J* = 3.2 Hz, 1H, -*Ph*), 7.50 (t, *J* = 8.0 Hz, 1H, -*Ph*), 7.02 (dd, *J* = 8.0, 2.0 Hz, 1H, -*Ph*), 6.96 (d, *J* = 2.4 Hz, 1H, 3-H), 6.89 (dd, *J* = 8.0, 2.0 Hz, 1H, -*Ph*), 4.23 (s, 3H, -N^+CH_3), 3.79 (s, 3H, -OCH_3); ^{13}C NMR (100 MHz, 293 K, DMSO-d_6): δ 168.9, 161.6, 153.4, 149.9, 149.3, 141.9, 132.0, 115.1, 113.6, 113.1, 110.4, 107.3, 56.1, 45.2; HRMS (ESI+) calcd for $C_{14}H_{15}N_2O_3$ $[M]^+$ = 259.1077, found 259.1084.

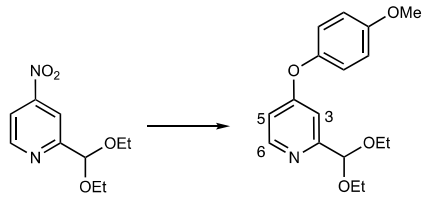

Preparation of 2-(diethoxymethyl)-4-(4-methoxyphenoxy)pyridine: A 75-mL sealed tube was charged with dimethyl sulfoxide (6 mL), K_2CO_3 (1.26 g, 9.00 mmol), and 4-methoxyphenol (1.34 g, 9.00 mmol). The mixture was stirred at room temperature for 30 min. 2-(Diethoxymethyl)-4-nitropyridine (689 mg, 3.00 mmol) was added, the vessel was sealed and heated to 95 °C (external temperature) for 17 h. The reaction mixture was cooled to 23 °C and acidified with saturated aqueous NH_4Cl (20 mL). The resulting solution was layers was extracted with EtOAc (3 × 15 mL). The combined organic layers were dried over anhydrous Na_2SO_4, filtered, and concentrated *in vacuo*. The crude material was purified by flash chromatography (0 to 50% EtOAc

in hexanes) on silica gel (80 mL) to afford 2-(diethoxymethyl)-4-(4-methoxyphenoxy)pyridine as a pale yellow oil (587 mg, 65% yield).

2-(Diethoxymethyl)-4-(4-methoxyphenoxy)pyridine: R_f = 0.53 (60% EtOAc in hexanes); IR (neat): ν_{max} = 2975, 2880, 1609, 1589, 1570, 1288, 1244, 1180, 1109, 1082 cm^{-1}; ^1H NMR (400 MHz, 293 K, $CDCl_3$): δ 8.40 (d, J = 6.0 Hz, 1H, 6-H), 7.13 (d, J = 2.4 Hz, 1H, 3-H), 7.03–7.00 (m, 2H, -*Ph*), 6.95–6.92 (m, 2H, -*Ar*), 6.70 (dd, J = 6.0, 2.4 Hz, 1H, 5-H), 5.41 (s, 1H, -C*H*$(OCH_2CH_3)_2$), 3.83 (s, 3H, -OC*H*$_3$), 3.74–3.55 (m, 4H, -CH(OC*H*$_2$CH$_3$)$_2$), 1.24 (t, J = 6.8 Hz, 6H, -CH(OCH$_2$C*H*$_3$)$_2$); ^{13}C NMR (100 MHz, 293 K, $CDCl_3$): δ 166.1, 160.3, 156.9, 150.3, 147.1, 121.8, 115.0, 111.0, 108.8, 62.2, 55.4, 15.0; HRMS (ESI+) calcd for $C_{17}H_{22}NO_4$ $[M + H]^+$ = 304.1543, found 304.1545.

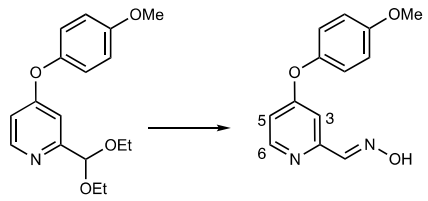

Preparation of (E)-4-(4-methoxyphenoxy)picolinaldehyde oxime: A 50-mL pear-shaped flask open to air with 2-(diethoxymethyl)-4-(4-methoxyphenoxy)pyridine (298 mg, 0.980 mmol) was charged with H_2O (4 mL) and 5 M H_2SO_4 in H_2O (290 μL, 1.47 mmol). The solution was heated to 95 °C (external temperature). After stirring at the same temperature for 3 h, the reaction mixture was cooled to 23 °C and treated with K_2CO_3 (548 mg, 3.92 mmol) followed by MeOH (14 mL) and NH_2OH•HCl (68 mg, 0.98 mmol) at the same temperature. A reflux condenser was attached, and the reaction was heated to reflux while open to air. After 3.5 h, the reaction mixture was cooled to 23 °C and concentrated *in vacuo*. EtOAc (10 mL) was added to the crude residue, followed by saturated aqueous NH_4Cl (35 mL). The layers were separated using a separatory

funnel and the aqueous layer was extracted with EtOAc (2 × 20 mL). The combined organic layers were dried over anhydrous Na_2SO_4, filtered, and concentrated *in vacuo* to afford (*E*)-4-(4-methoxyphenoxy)picolinaldehyde oxime (240 mg, quantitative yield) as a white solid. This material was used directly without further purification.

(E)-4-(4-Methoxyphenoxy)picolinaldehyde oxime: m.p. = 147–150 °C; R_f = 0.34 (60% EtOAc in hexanes); IR (neat): ν_{max} = 2982, 2692, 1589, 1560, 1432, 1294, 1265, 1244, 1181, 1102, 1035, 1007 cm^{-1}; ^1H NMR (400 MHz, 293 K, DMSO-d_6): δ 11.67 (s, 1H, -CH=NO*H*), 8.43 (d, *J* = 6.0 Hz, 1H, 6-H), 8.01 (s, 1H, -C*H*=NOH), 7.17–7.14 (m, 2H, -*Ph*), 7.10 (d, *J* = 2.4 Hz, 1H, 3-H), 7.06–7.03 (m, 2H, -*Ph*), 6.95 (dd, *J* = 6.0, 2.4 Hz, 1H, 5-H), 3.79 (s, 3H, -OCH_3); ^{13}C NMR (100 MHz, 293 K, DMSO-d_6): δ 165.7, 157.4, 154.6, 151.6, 148.9, 146.9, 122.7, 115.9, 112.7, 106.3, 56.0; HRMS (ESI+) calcd for $C_{13}H_{13}N_2O_3$ $[M + H]^+$ = 245.0920, found 245.0923.

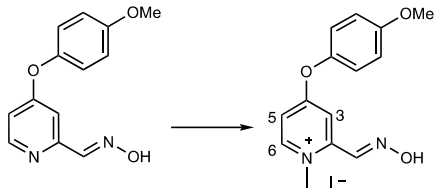

*Preparation of (E)-2-((hydroxyimino)methyl)-1-methyl-4-(4-methoxyphenoxy)pyridin-1-ium iodide (**ADG3121**):* A 35-mL sealed tube with (*E*)-4-(4-methoxyphenoxy)picolinaldehyde oxime (116 mg, 0.470 mmol) was charged with acetone (1 mL) and MeI (290 μL, 4.70 mmol). The vessel was sealed and heated to 55 °C (external temperature). After 17 h at the same temperature, the reaction mixture was cooled to 23 °C, transferred to a 25-mL round-bottomed flask, concentrated *in vacuo*, and recrystallized from acetone/EtOAc (1:1) to afford (*E*)-2-((hydroxyimino)methyl)-1-methyl-4-(4-methoxyphenoxy)pyridin-1-ium iodide as a tan solid (161 mg, 89% yield).

(E)-2-((Hydroxyimino)methyl)-1-methyl-4-(4-methoxyphenoxy)pyridin-1-ium iodide: m.p. = 160–162 °C; R_f = 0.10 (10% MeOH in CH_2Cl_2); IR (neat): ν_{max} = 2982, 1633, 1597, 1498, 1451, 1339, 1297, 1248, 1182, 1136, 1103, 1002 cm^{-1}; ^1H NMR (400 MHz, 293 K, DMSO-d_6): δ 13.05 (s, 1H, -CH=NO*H*), 8.81 (d, *J* = 7.2 Hz, 1H, 6-H), 8.59 (s, 1H, -C*H*=NOH), 7.58 (dd, *J* = 7.2, 3.2 Hz, 1H, 5-H), 7.50 (d, *J* = 3.2 Hz, 1H, 3-H), 7.27 (br d, *J* = 8.8 Hz, 2H, -*Ph*), 7.12 (br d, *J* = 8.8 Hz, 2H, -*Ph*), 4.22 (s, 3H, -N^+CH_3), 3.81 (s, 3H, -O*C*H_3); ^{13}C NMR (100 MHz, 293 K, DMSO-d_6): δ 169.6, 158.3, 149.9, 149.2, 145.8, 141.9, 122.5, 116.3, 114.9, 110.1, 56.1, 45.2; HRMS (ESI+) calcd for $C_{14}H_{15}N_2O_3$ $[M]^+$ = 259.1077, found 259.1085.

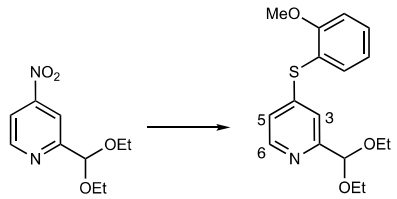

Preparation of 2-(diethoxymethyl)-4-((2-methoxyphenyl)thio)pyridine: A 75-mL sealed tube was charged with dimethyl sulfoxide (4 mL), K_2CO_3 (1.65 g, 12.0 mmol), and 2-methoxybenzenethiol (1.46 g, 12.0 mmol). The mixture was stirred at room temperature for 30 min. 2-(Diethoxymethyl)-4-nitropyridine (905 mg, 4.00 mmol) was added, the vessel was sealed and heated to 95 °C for 18 h. The reaction mixture was cooled to 23 °C and neutralized with saturated aqueous NH_4Cl (20 mL). The resulting solution was extracted with EtOAc (3 × 15 mL). The combined organic layers were dried over anhydrous Na_2SO_4, filtered, and concentrated *in vacuo.* The crude material was purified by flash chromatography (15 to 50% EtOAc in hexanes) on silica gel (100 mL) to afford 2-(diethoxymethyl)-4-((2-methoxyphenyl)thio)pyridine as an amber oil (1.21 g, 95% yield).

2-(Diethoxymethyl)-4-((2-methoxyphenyl)thio)pyridine: R_f = 0.40 (60% EtOAc in hexanes); IR (neat): ν_{max} = 2973, 1575, 1542, 1476, 1446, 1432, 1392, 1368, 1343, 1294, 1275, 1248, 1179, 1162, 1112, 1090, 1059 cm^{-1}; ^1H NMR (400 MHz, 293 K, DMSO-d_6): δ 8.28 (d, J = 5.2 Hz, 1H, 6-H), 7.59–7.53 (m, 2H, -*Ph*), 7.22 (dd, J = 8.2, 0.8 Hz, 1H, -*Ph*), 7.07 (td, J = 8.2, 0.8 Hz, 1H, -*Ph*), 6.97 (d, J = 1.6 Hz, 1H, 3-H), 6.93 (dd, J = 5.2, 1.6 Hz, 1H, 5-H), 5.26 (s, 1H, -C*H*(OCH_2CH_3)$_2$), 3.75 (s, 3H, -OC*H*$_3$), 3.58–3.40 (m, 4H, -CH(OC*H*$_2$CH$_3$)$_2$), 1.07 (t, J = 6.8 Hz, 6H, -CH(OCH_2C*H*$_3$)$_2$); ^{13}C NMR (100 MHz, 293 K, DMSO-d_6): δ 159.5, 157.8, 149.1, 148.4, 136.7, 132.5, 121.6, 119.8, 116.4, 115.5, 112.4, 101.9, 61.7, 55.9, 15.0; HRMS (ESI+) calcd for $C_{17}H_{22}NO_3S$ $[M + H]^+$ = 320.1315, found 320.1315.

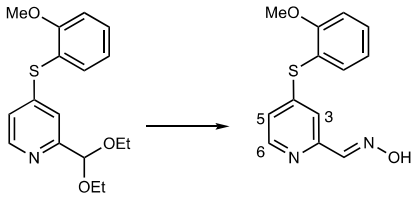

Preparation of (*E*)*-4-((2-methoxyphenyl)thio)picolinaldehyde oxime:* A 100-mL pear-shaped flask open to air with 2-(diethoxymethyl)-4-((2-methoxyphenyl)thio)pyridine (628 mg, 1.97 mmol) was charged with H_2O (5 mL) and 5 M H_2SO_4 in H_2O (430 μL, 2.16 mmol). The solution was heated to 85 °C. After stirring at the same temperature for 2.5 h, the reaction mixture was cooled to 23 °C and treated with K_2CO_3 (1.09 g, 7.88 mmol) followed by MeOH (25 mL) and NH_2OH•HCl (137 mg, 1.97 mmol) at the same temperature. A reflux condenser was attached, and the reaction was heated to reflux while open to air. After 5.8 h, the reaction mixture was cooled to 23 °C and concentrated *in vacuo.* EtOAc (20 mL) was added to the crude residue, followed by saturated aqueous NH_4Cl (30 mL). The layers were separated using a separatory funnel and the aqueous layer was extracted with EtOAc (2 × 15 mL). The combined organic layers were dried

over anhydrous Na_2SO_4, filtered, and concentrated *in vacuo* to afford (*E*)-4-((2-methoxyphenyl)thio)picolinaldehyde oxime (237 mg, 91% yield) as a light tan solid. This material was used directly without further purification.

(E)-4-((2-Methoxyphenyl)thio)picolinaldehyde oxime: m.p. = 193–196 °C; R_f = 0.22 (60% EtOAc in hexanes); IR (neat): ν_{max} = 2927, 2860, 2753, 1575, 1536, 1475, 1463, 1430, 1275, 1249, 1229, 1023 cm^{-1}; ^1H NMR (300 MHz, 293 K, DMSO-d_6): δ 11.66 (s, 1H, -CH=NO*H*), 8.33 (d, *J* = 5.4 Hz, 1H, 6-H), 7.96 (s, 1H, -C*H*=NOH), 7.60–7.55 (m, 2H, -*Ar*), 7.25–7.21 (m, 2H, -*Ar*), 7.12–7.02 (m, 2H, -*Ar*), 3.77 (s, 3H, -OCH_3); ^{13}C NMR (100 MHz, 293 K, DMSO-d_6): δ 160.1, 152.4, 149.8, 149.4, 148.9, 137.4, 133.1, 122.1, 120.7, 115.6, 115.3, 113.0, 56.4; HRMS (ESI+) calcd for $C_{13}H_{13}N_2O_2S$ $[M + H]^+$ = 261.0692, found 261.0694.

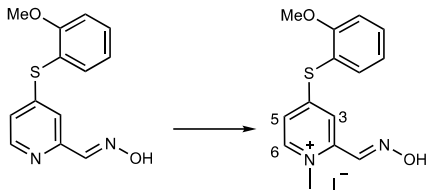

*Preparation of (E)-2-((hydroxyimino)methyl)-4-((2-methoxyphenyl)thio)-1-methylpyridin-1-ium iodide (**ADG4118**):* A 35-mL sealed tube with (*E*)-4-((2-methoxyphenyl)thio)picolinaldehyde oxime (54 mg, 0.21 mmol) was charged with acetone (1 mL) and MeI (130 μL, 2.10 mmol). The vessel was sealed and heated to 50 °C. After 20 h at the same temperature, the reaction mixture was cooled to 23 °C, transferred to a 25-mL round-bottomed flask, concentrated *in vacuo* to afford (*E*)-2-((hydroxyimino)methyl)-4-((2-methoxyphenyl)thio)-1-methylpyridin-1-ium iodide as a yellow orange solid (66 mg, 88% yield).

(E)-2-((Hydroxyimino)methyl)-4-((2-methoxyphenyl)thio)-1-methylpyridin-1-ium iodide: m.p. = 178–180 °C; R_f = 0.10 (100% EtOAc); IR (neat): ν_{max} = 3129, 1625, 1581, 1552, 1472,

1433, 1275, 1238, 1183, 1081, 1002 cm^{-1}; ^1H NMR (400 MHz, 293 K, DMSO-d_6): δ 12.99 (s, 1H, -CH=NO*H*), 8.59 (d, *J* = 6.8 Hz, 1H, 6-H), 8.53 (s, 1H, -C*H*=NOH), 7.72–7.59 (m, 4H, -*Ar*), 7.33 (d, *J* = 8.0 Hz, 1H, -*Ar*), 7.17 (t, *J* = 7.2 Hz, 1H, -*Ar*), 4.16 (s, 3H, $-N^+CH_3$), 3.80 (s, 3H, -OCH_3); ^{13}C NMR (100 MHz, 293 K, DMSO-d_6): δ 161.0, 159.9, 146.3, 145.3, 141.9, 137.4, 134.6, 122.6, 122.2, 118.4, 113.6, 113.1, 56.8, 45.4; HRMS (ESI+) calcd for $C_{14}H_{15}N_2O_2S$ $[M]^+$ = 275.0849, found 275.0853.

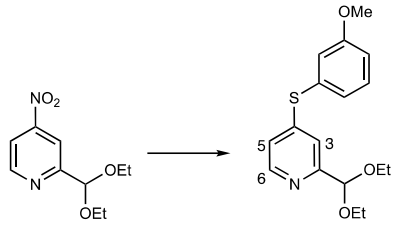

Preparation of 2-(diethoxymethyl)-4-((3-methoxyphenyl)thio)pyridine: A 75-mL sealed tube was charged with dimethyl sulfoxide (4 mL), K_2CO_3 (1.66 g, 12.0 mmol), and 3-methoxybenzenethiol (1.74 mL, 12.0 mmol). The mixture was stirred at room temperature for 15 min. 2-(Diethoxymethyl)-4-nitropyridine (905 mg, 4.00 mmol) was added, the vessel was sealed and heated to 95 °C for 14 h. The reaction mixture was cooled to 23 °C and neutralized with saturated aqueous NH_4Cl (20 mL). The resulting solution was extracted with EtOAc (3 × 20 mL). The combined organic layers were dried over anhydrous Na_2SO_4, filtered, and concentrated *in vacuo.* The crude material was purified by flash chromatography (0 to 40% EtOAc in hexanes) on silica gel (100 mL) to afford 2-(diethoxymethyl)-4-((3-methoxyphenyl)thio)pyridine as an amber oil (1.26 g, 98% yield).

2-(Diethoxymethyl)-4-((3-methoxyphenyl)thio)pyridine: R_f = 0.55 (60% EtOAc in hexanes); IR (neat): ν_{max} = 2978, 1589, 1573, 1479, 1343, 1283, 1246, 1231, 1159, 1111, 1091, 1056, 1038 cm^{-1}; ^1H NMR (400 MHz, 293 K, $CDCl_3$): δ 8.33 (d, *J* = 5.2 Hz, 1H, 6-H), 7.35 (app

t, *J* = 7.6 Hz, 2H, 3-H and -*Ph*), 7.13 (d, *J* = 7.6 Hz, 1H, -*Ph*), 7.07 (t, *J* = 2.4 Hz, 1H, -*Ph*), 6.99 (dd, *J* = 7.6, 2.4 Hz, 1H, -*Ph*), 6.85 (dd, *J* = 5.2, 2.4 Hz, 1H, 5-H), 5.39 (s, 1H, -C*H*(OCH_2CH_3)$_2$), 3.81 (s, 3H, -OCH_3), 3.74–3.53 (m, 4H, -CH(OC$H_2$$CH_3$)$_2$), 1.22 (t, *J* = 7.2 Hz, 6H, -CH(OCH_2CH_3)$_2$); ^{13}C NMR (100 MHz, 293 K, $CDCl_3$): δ 160.3, 157.9, 150.9, 148.7, 130.6, 130.4, 127.0, 120.4, 119.7, 118.2, 115.7, 102.3, 62.2, 55.3, 15.0; HRMS (ESI+) calcd for $C_{17}H_{22}NO_3S$ $[M + H]^+$ = 320.1315, found 320.1315.

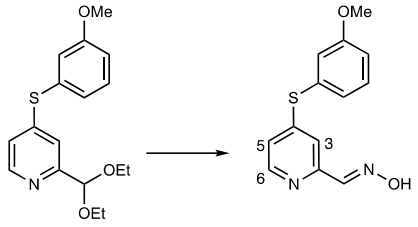

Preparation of (E)-4-((3-methoxyphenyl)thio)picolinaldehyde oxime: A 100-mL pear-shaped flask open to air with 2-(diethoxymethyl)-4-((3-methoxyphenyl)thio)pyridine (481 mg, 1.50 mmol) was charged with H_2O (5 mL) and 5 M H_2SO_4 in H_2O (330 μL, 1.65 mmol). The solution was heated to 95 °C. After stirring at the same temperature for 3 h, the reaction mixture was cooled to 23 °C and treated with K_2CO_3 (829 mg, 6.00 mmol) followed by MeOH (20 mL) and NH_2OH•HCl (104 mg, 1.50 mmol) at the same temperature. A reflux condenser was attached, and the reaction was heated to reflux while open to air. After 3.5 h, the reaction mixture was cooled to 23 °C and concentrated *in vacuo.* EtOAc (20 mL) was added to the crude residue, followed by saturated aqueous NH_4Cl (20 mL). The layers were separated using a separatory funnel and the aqueous layer was extracted with EtOAc (2 × 10 mL). The combined organic layers were dried over anhydrous Na_2SO_4, filtered, and concentrated *in vacuo* to afford (*E*)-4-((3-methoxyphenyl)thio)picolinaldehyde oxime (271 mg, 69% yield) as an off white solid. This material was used directly without further purification.

(E)-4-((3-Methoxyphenyl)thio)picolinaldehyde oxime: m.p. = 190–193 °C; R_f = 0.36 (60% EtOAc in hexanes); IR (neat): ν_{max} = 2980, 2834, 2698, 1590, 1571, 1534, 1500, 1479, 1462, 1440, 1413, 1401, 1309, 1281, 1245, 1231, 1156, 1117, 1036 cm^{-1}; ^1H NMR (400 MHz, 293 K, DMSO-d_6): δ 11.71 (s, 1H, -CH=NO*H*), 8.37 (d, *J* = 5.2 Hz, 1H, 6-H), 7.97 (s, 1H, -C*H*=NOH), 7.46 (t, *J* = 8.4 Hz, 1H, -*Ph*), 7.13 (d, *J* = 1.6 Hz, 1H, 3-H), 7.19–7.14 (m, 4H, -*Ar*), 3.78 (s, 3H, -OCH_3); ^{13}C NMR (100 MHz, 293 K, DMSO-d_6): δ 160.7, 152.7, 150.2, 149.7, 148.9, 131.7, 129.7, 127.5, 121.2, 120.3, 116.7, 115.9, 55.9; HRMS (ESI+) calcd for $C_{13}H_{13}N_2O_2S$ $[M + H]^+$ = 261.0692, found 261.0689.

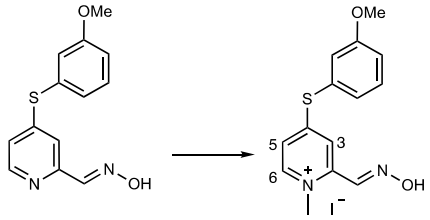

*Preparation of (E)-2-((hydroxyimino)methyl)-4-((3-methoxyphenyl)thio)-1-methylpyridin-1-ium iodide (**ADG4153**):* A 25-mL sealed tube with (*E*)-4-((3-methoxyphenyl)thio)picolinaldehyde oxime (64 mg, 0.24 mmol) was charged with acetone (2 mL) and MeI (150 μL, 2.40 mmol). The vessel was sealed and heated to 45 °C. After 20 h at the same temperature, the reaction mixture was cooled to 23 °C, transferred to a 25-mL round-bottomed flask, and concentrated *in vacuo*. The crude residue was dry-loaded and purified by flash chromatography (5 to 40% MeOH in CH_2Cl_2) on silica gel (10 mL) to afford (*E*)-2-((hydroxyimino)methyl)-4-((3-methoxyphenyl)thio)-1-methylpyridin-1-ium iodide as a yellow solid (60 mg, 62% yield).

(E)-2-((Hydroxyimino)methyl)-4-((3-methoxyphenyl)thio)-1-methylpyridin-1-ium iodide: m.p. = 170–173 °C; R_f = 0.10 (10% MeOH in CH_2Cl_2); IR (neat): ν_{max} = 2980, 1628, 1584, 1553,

1492, 1474, 1424, 1318, 1306, 1286, 1235, 1188, 1086, 1036, 1013 cm^{-1}; ^1H NMR (400 MHz, 293 K, CD_3OD): δ 8.50 (s, 1H, -C*H*=NOH), 8.44 (d, *J* = 7.2 Hz, 1H, 6-H), 7.85 (d, *J* = 2.0 Hz, 1H, 3-H), 7.54 (t, *J* = 8.0 Hz, 1H, -*Ph*), 7.48 (dd, *J* = 7.2, 2.0 Hz, 1H, 5-H), 7.26–7.21 (m, 3H, -*Ph*), 4.21 (s, 3H, -N^+CH_3), 3.85 (s, 3H, -O*C*H_3); ^{13}C NMR (100 MHz, 293 K, CD_3OD): δ 164.9, 162.7, 147.8, 145.9, 141.5, 132.9, 128.4, 128.0, 122.8, 121.4, 120.5, 118.6, 56.2, 45.8; HRMS (ESI+) calcd for $C_{14}H_{15}N_2O_2S$ $[M]^+$ =275.0848, found 275.0836.

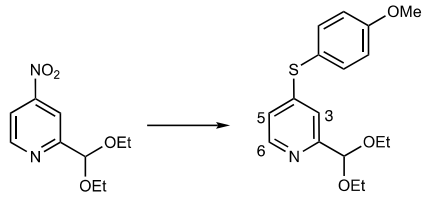

Preparation of 2-(diethoxymethyl)-4-((4-methoxyphenyl)thio)pyridine: A 75-mL sealed tube was charged with dimethyl sulfoxide (4 mL), K_2CO_3 (1.65 g, 12.0 mmol), and 4-methoxythiophenol (1.48 mL, 12.0 mmol). The mixture was stirred at room temperature for 5 min. 2-(Diethoxymethyl)-4-nitropyridine (909 mg, 4.00 mmol) was added, the vessel was sealed and heated to 93 °C for 6 h. The reaction mixture was cooled to 23 °C and neutralized with saturated aqueous NH_4Cl (25 mL). The resulting solution was extracted with EtOAc (3 × 25 mL). The combined organic layers were dried over anhydrous Na_2SO_4, filtered, and concentrated *in vacuo.* The crude material was purified by flash chromatography (0 to 40% EtOAc in hexanes) on silica gel (170 mL) to afford 2-(diethoxymethyl)-4-((4-methoxyphenyl)thio)pyridine as a pale yellow oil (973 mg, 76% yield).

2-(Diethoxymethyl)-4-((4-methoxyphenyl)thio)pyridine: R_f = 0.41 (60% EtOAc in hexanes); IR (neat): ν_{max} = 2974, 2884, 1577, 1492, 1461, 1393, 1340, 1290, 1248, 1174, 1109, 1059, 1030 cm^{-1}; ^1H NMR (400 MHz, 293 K, DMSO-d_6): δ 8.29 (d, *J* = 5.2 Hz, 1H, 6-H), 7.54

(dd, *J* = 8.8, 3.2 Hz, 2H, -*Ph*), 7.12 (dd, *J* = 8.8, 3.2 Hz, 2H, -*Ph*), 7.03 (d, *J* = 1.6 Hz, 1H, 3-H), 6.91 (dd, *J* = 5.2, 1.6 Hz, 1H, 5-H), 5.27 (s, 1H, -C*H*(OCH_2CH_3)$_2$), 3.83 (s, 3H, -OC*H*$_3$) 3.60–3.41 (m, 4H, -CH(OC*H*$_2$CH$_3$)$_2$), 1.08 (t, *J* = 7.2 Hz, 6H, -CH(OCH_2CH_3)$_2$); ^{13}C NMR (100 MHz, 293 K, DMSO-d_6): δ 161.3, 158.5, 151.7, 149.1, 137.7, 119.9, 118.8, 116.7, 116.3, 102.4, 62.2, 55.9, 15.5; HRMS (ESI+) calcd for $C_{17}H_{22}NO_3S$ $[M + H]^+$ = 320.1315, found 320.1314.

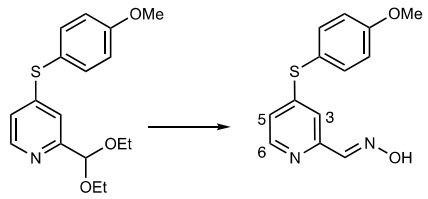

Preparation of (E)-4-((4-methoxyphenyl)thio)picolinaldehyde oxime: A 50-mL pear-shaped flask open to air with 2-(diethoxymethyl)-4-((4-methoxyphenyl)thio)pyridine (212 mg, 0.660 mmol) was charged with H_2O (2 mL) and 5 M H_2SO_4 in H_2O (150 μL, 0.730 mmol). The solution was heated to 95 °C. After stirring at the same temperature for 2.5 h, the reaction mixture was cooled to 23 °C and treated with K_2CO_3 (365 mg, 2.64 mmol) followed by MeOH (10 mL) and NH_2OH•HCl (46 mg, 0.66 mmol) at the same temperature. A reflux condenser was attached, and the reaction was heated to reflux while open to air. After 2.5 h, the reaction mixture was cooled to 23 °C and concentrated *in vacuo.* EtOAc (10 mL) was added to the crude residue, followed by saturated aqueous NH_4Cl (20 mL). The layers were separated using a separatory funnel and the aqueous layer was extracted with EtOAc (2 × 10 mL). The combined organic layers were dried over anhydrous Na_2SO_4, filtered, and concentrated *in vacuo* to afford (*E*)-4-((4-methoxyphenyl)thio)picolinaldehyde oxime (150 mg, 87% yield) as a light tan solid. This material was used directly without further purification.

(E)-4-((4-Methoxyphenyl)thio)picolinaldehyde oxime: m.p. = 203–206 °C; R_f = 0.36 (60% EtOAc in hexanes); IR (neat): ν_{max} = 2975, 2747, 1576, 1491, 1456, 1395, 1290, 1246, 1175, 1105, 1028 cm^{-1}; ^1H NMR (300 MHz, 293 K, DMSO-d_6): δ 11.69 (s, 1H, -CH=NO*H*), 8.35 (d, *J* = 5.1 Hz, 1H, 6-H), 7.96 (s, 1H, -C*H*=NOH), 8.57 (d, *J* = 8.7 Hz, 2H, -*Ph*), 7.24 (d, *J* = 1.5 Hz, 1H, 3-H), 7.12 (d, *J* = 8.7 Hz, 2H, -*Ph*), 7.06 (dd, *J* = 5.1, 1.5 Hz, 1H, 5-H), 3.84 (s, 3H, -OCH_3); ^{13}C NMR (100 MHz, 293 K, DMSO-d_6): δ 161.3, 152.7, 151.7, 149.5, 148.9, 137.8, 120.5, 118.5, 116.4, 115.2, 55.9; HRMS (ESI+) calcd for $C_{13}H_{13}N_2O_2S$ $[M + H]^+$ = 261.0692, found 261.0715.

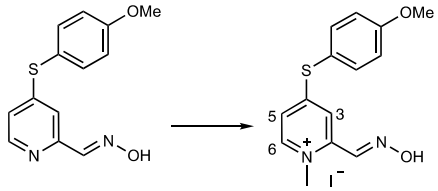

*Preparation of (E)-2-((hydroxyimino)methyl)-4-((4-methoxyphenyl)thio)-1-methylpyridin-1-ium iodide (**ADG3192**):* A 35-mL sealed tube with (*E*)-4-((4-methoxyphenyl)thio)picolinaldehyde oxime (149 mg, 0.570 mmol) was charged with acetone (2 mL) and MeI (350 μL, 5.57 mmol). The vessel was sealed and heated to 47 °C. After 15 h at the same temperature, the reaction mixture was cooled to 23 °C, transferred to a 25-mL round-bottomed flask, concentrated *in vacuo* to afford (*E*)-2-((hydroxyimino)methyl)-4-((4-methoxyphenyl)thio)-1-methylpyridin-1-ium iodide as an orange solid (101 mg, 44% yield).

(E)-2-((Hydroxyimino)methyl)-4-((4-methoxyphenyl)thio)-1-methylpyridin-1-ium iodide: m.p. = 190–193 °C; R_f = 0.15 (100% EtOAc); IR (neat): ν_{max} = 2979, 1623, 1590, 1489, 1430, 1296, 1249, 1170, 1078, 1026 cm^{-1}; ^1H NMR (500 MHz, 293 K, CD_3OD): δ 8.49 (s, 1H, -C*H*=NOH), 8.42 (d, *J* = 7.0 Hz, 1H, 6-H), 7.78 (d, *J* = 2.0 Hz, 1H, 3-H), 7.59 (d, *J* = 8.5 Hz, 2H, -*Ph*), 7.46 (dd, *J* = 7.0, 2.0 Hz, 1H, 5-H), 7.17 (d, *J* = 8.5 Hz, 2H, -*Ph*), 4.20 (s, 3H, -N^+CH_3), 3.89

(s, 3H, -OC*H*$_3$); ^{13}C NMR (125 MHz, 293 K, CD_3OD): δ 165.9, 163.7, 147.6, 145.7, 141.4, 138.4, 122.6, 120.2, 117.5, 117.1, 56.1, 45.8; HRMS (ESI+) calcd for $C_{14}H_{15}N_2O_2S$ $[M]^+$ = 275.0849, found 275.0836.

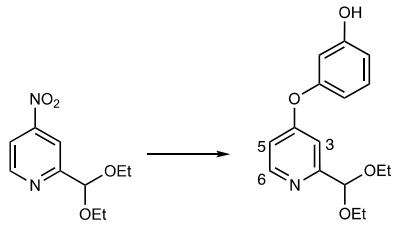

Preparation of 3-((2-(diethoxymethyl)pyridin-4-yl)oxy)phenol: A 25-mL round-bottomed flask was charged with dimethyl sulfoxide (4 mL), K_2CO_3 (1.66 g, 12.0 mmol), and resorcinol (1.32 g, 12.0 mmol). The mixture was stirred at room temperature for 10 min. 2-(Diethoxymethyl)-4-nitropyridine (904 mg, 4.00 mmol) was added, the vessel was sealed and heated to 95 °C (external temperature) for 16 h. The reaction mixture was cooled to 23 °C and acidified with saturated aqueous NH_4Cl (30 mL). The resulting solution was extracted with EtOAc (3 × 25 mL). The combined organic layers were dried over anhydrous Na_2SO_4, filtered, and concentrated *in vacuo.* The crude material was purified by flash chromatography (30 to 50% EtOAc in hexanes) on silica gel (50 mL) to afford 3-((2-(diethoxymethyl)pyridin-4-yl)oxy)phenol as a yellow oil (625 mg, 66% yield).

3-((2-(Diethoxymethyl)pyridin-4-yl)oxy)phenol: R_f = 0.24 (60% EtOAc in hexanes); IR (neat): ν_{max} = 2981, 2872, 1586, 1478, 1427, 1349, 1293, 1173, 1128, 1056, 1000 cm^{-1}; ^{1}H NMR (300 MHz, 293 K, DMSO-d_6): δ 9.83 (s, 1H, -O*H*), 8.41 (d, *J* = 5.4 Hz, 1H, 6-H), 7.27 (t, *J* = 8.1 Hz, 1H, -*Ph*), 6.95–6.89 (m, 2H, -*Ar*), 6.73–6.69 (m, 1H, -*Ar*), 6.60–6.56 (m, 1H, -*Ar*), 7.27 (t, *J* = 2.1 Hz, 1H, -*Ph*), 5.34 (s, 1H, -C*H*$(OCH_2CH_3)_2$), 3.65–3.46 (m, 4H, -CH$(OCH_2CH_3)_2$), 1.11 (t, *J* = 6.9 Hz, 6H, -CH$(OCH_2CH_3)_2$); ^{13}C NMR (100 MHz, 293 K, DMSO-d_6): δ 165.1, 160.8, 159.6,

155.0, 151.1, 131.3, 113.2, 112.4, 111.3, 108.7, 108.0, 102.3, 62.2, 15.5; HRMS (ESI+) calcd for $C_{16}H_{20}NO_4$ $[M + H]^+$ = 290.1386, found 290.1372.

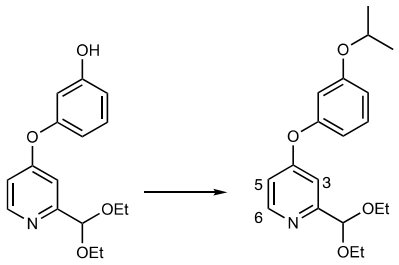

Preparation of 2-(diethoxymethyl)-4-(3-isopropoxyphenoxy)pyridine: A 25-mL round-bottomed flask was charged with dimethyl sulfoxide (3 mL), K_2CO_3 (464 mg, 3.36 mmol), 3-((2-(diethoxymethyl)pyridin-4-yl)oxy)phenol (488 mg, 1.68 mmol), and 2-iodopropane (0.84 mL, 8.4 mmol). After stirring at the same temperature for 48 h, 2-iodopropane (0.84 mL, 8.4 mmol) was added to the reaction mixture. After stirring at the same temperature for 16 h, the reaction mixture was acidified with saturated aqueous NH_4Cl (20 mL). The resulting solution was extracted with EtOAc (3 × 10 mL). The combined organic layers were dried over anhydrous Na_2SO_4, filtered, and concentrated *in vacuo.* The crude material was purified by flash chromatography (40 to 70% EtOAc in hexanes) on silica gel (30 mL) to afford 2-(diethoxymethyl)-4-(3-isopropoxyphenoxy)pyridine as a yellow oil (468 mg, 89% yield).

2-(Diethoxymethyl)-4-(3-isopropoxyphenoxy)pyridine: R_f = 0.46 (60% EtOAc in hexanes); IR (neat): ν_{max} = 2981, 2876, 1581, 1482, 1421, 1371, 1346, 1285, 1261, 1174, 1127, 1111, 1059, 1003 cm^{-1}; ^1H NMR (300 MHz, 293 K, DMSO-d_6): δ 8.42 (d, J = 5.4 Hz, 1H, 6-H), 7.37 (t, J = 8.1 Hz, 1H, -*Ph*), 6.96–6.84 (m, 3H, -*Ar*), 6.76–6.69 (m, 2H, -*Ar*), 5.34 (s, 1H, -C*H*$(OCH_2CH_3)_2$), 4.63 (sept, J = 6.0, 1H, -OC*H*$(CH_3)_2$), 3.65–3.45 (m, 4H, -CH(OC*H*$_2$CH$_3$)$_2$), 1.25 (d, J = 6.0, 6H, -OCH(C*H*$_3$)$_2$), 1.10 (t, J = 7.2 Hz, 6H, -CH(OCH$_2$C*H*$_3$)$_2$); ^{13}C NMR (100 MHz, 293 K, DMSO-

d_6): δ 165.1, 160.8, 159.5, 155.0, 151.1, 131.4, 113.6, 112.8, 112.3, 108.5, 108.4, 102.3, 70.0, 62.2, 22.1, 15.5; HRMS (ESI+) calcd for $C_{19}H_{26}NO_4$ $[M + H]^+$ = 332.1856, found 332.1840.

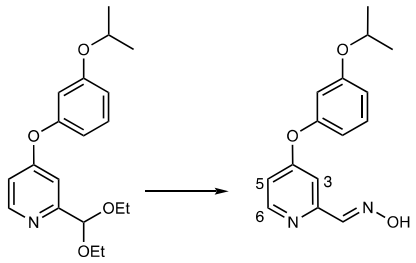

Preparation of (E)-4-(3-isopropoxyphenoxy)picolinaldehyde oxime: A 50-mL pear-shaped flask open to air with 2-(diethoxymethyl)-4-(3-isopropoxyphenoxy)pyridine (327 mg, 0.980 mmol) was charged with H_2O (4 mL) and 5 M H_2SO_4 in H_2O (220 μL, 1.08 mmol). The solution was heated to 90 °C (external temperature). After stirring at the same temperature for 2.5 h, the reaction mixture was cooled to 23 °C and treated with K_2CO_3 (541 mg, 3.92 mmol) followed by MeOH (16 mL) and NH_2OH•HCl (68 mg, 0.98 mmol) at the same temperature. A reflux condenser was attached, and the reaction was heated to reflux while open to air. After 3 h, the reaction mixture was cooled to 23 °C and concentrated *in vacuo.* EtOAc (10 mL) was added to the crude residue, followed by saturated aqueous NH_4Cl (15 mL). The layers were separated using a separatory funnel and the aqueous layer was extracted with EtOAc (2 × 10 mL). The combined organic layers were dried over anhydrous Na_2SO_4, filtered, and concentrated *in vacuo* to afford (*E*)-4-(3-isopropoxyphenoxy)picolinaldehyde oxime (213 mg, 80% yield) as a light tan solid. This material was used directly without further purification.

(E)-4-(3-Isopropoxyphenoxy)picolinaldehyde oxime: m.p. = 133–136 °C; R_f = 0.38 (60% EtOAc in hexanes); IR (neat): ν_{max} = 2981, 1564, 1476, 1320, 1296, 1258, 1246, 1183, 1128, 1111 cm^{-1}; ^1H NMR (300 MHz, 293 K, DMSO-d_6): δ 11.69 (s, 1H, -CH=NO*H*), 8.46 (d, J = 5.7 Hz,

1H, 6-H), 8.03 (s, 1H, -C*H*=NOH), 7.37 (t, *J* = 8.4 Hz, 1H, -*Ph*), 7.17 (d, *J* = 2.7 Hz, 1H, 3-H), 7.00 (dd, *J* = 5.7, 2.7 Hz, 1H, 5-H), 6.86 (dd, *J* = 8.1, 1.8 Hz, 1H, -*Ph*), 6.79–6.72 (m, 2H, -*Ph*), 4.66 (sept, *J* = 6.0, 1H, -OC*H*(CH_3)$_2$), 1.26 (d, *J* = 6.0, 6H, -OCH(CH_3)$_2$); ^{13}C NMR (100 MHz, 293 K, DMSO-d_6): δ 165.0, 159.6, 154.9, 154.7, 151.7, 148.9, 131.4, 113.6, 113.0, 112.9, 108.6, 106.9, 70.0, 22.1; HRMS (ESI+) calcd for $C_{15}H_{17}N_2O_3$ $[M + H]^+$ = 273.1233, found 273.1222.

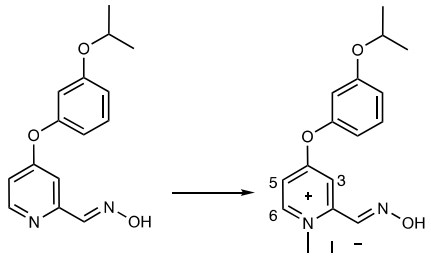

*Preparation of (E)-2-((hydroxyimino)methyl)-1-methyl-4-(3-isopropoxyphenoxy)pyridin-1-ium iodide (**ADG5044**):* A 35-mL sealed tube with (*E*)-4-(3-isopropoxyphenoxy)picolinaldehyde oxime (96 mg, 0.35 mmol) was charged with acetone (2 mL) and MeI (220 μL, 3.50 mmol). The vessel was sealed and heated to 45 °C (external temperature). After 14 h at the same temperature, the reaction mixture was cooled to 23 °C, transferred to a 25-mL round-bottomed flask and concentrated *in vacuo.* The crude residue was dry-loaded and purified by flash chromatography (5 to 40% MeOH in CH_2Cl_2) on silica gel (10 mL) to afford (*E*)-2-((hydroxyimino)methyl)-1-methyl-4-(3-isopropoxyphenoxy)pyridin-1-ium iodide as an orange solid (104 mg, 72% yield).

(E)-2-((Hydroxyimino)methyl)-1-methyl-4-(3-isopropoxyphenoxy)pyridin-1-ium iodide: m.p. = 124–126 °C; R_f = 0.10 (100% EtOAc); IR (neat): ν_{max} = 3158, 2977, 1640, 1608, 1596, 1574, 1512, 1482, 1460, 1418, 1382, 1336, 1295, 1257, 1196, 1178, 1160, 1144, 1135, 1106, 1075 cm^{-1}; ^{1}H NMR (300 MHz, 293 K, CD_3OD): δ 8.67 (d, *J* = 7.2 Hz, 1H, 6-H), 8.55 (s, 1H, -

C*H*=NOH), 7.70 (d, *J* = 2.7 Hz, 1H, 3-H), 7.48–7.38 (m, 2H, -*Ph*), 6.97 (dd, *J* = 8.4, 1.8 Hz, 1H, -*Ar*), 6.85–6.79 (m, 2H, -*Ar*), 4.65 (sept, *J* = 6.3, 1H, -OC*H*$(CH_3)_2$), 4.27 (s, 3H, -N^+CH_3), 1.26 (d, *J* = 6.0, 6H, -OCH(CH_3)$_2$); ^{13}C NMR (100 MHz, 293 K, CD_3OD): δ 171.0, 161.4, 154.7, 151.5, 149, 141.8, 132.5, 115.9, 115.4, 113.3, 112.3, 109.4, 71.5, 45.8, 22.1; HRMS (ESI+) calcd for $C_{16}H_{19}N_2O_3$ $[M]^+$ = 287.1390, found 287.1376.

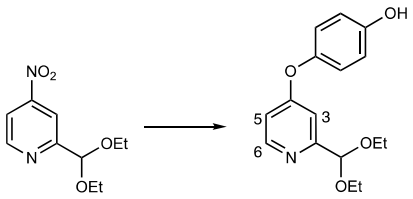

Preparation of 4-((2-(diethoxymethyl)pyridin-4-yl)oxy)phenol: A 25-mL round-bottomed flask was charged with dimethyl sulfoxide (5 mL), K_2CO_3 (1.66 g, 12.0 mmol), and hydroquinone (1.32 g, 12.0 mmol). The mixture was stirred at room temperature for 10 min. 2-(Diethoxymethyl)-4-nitropyridine (904 mg, 4.00 mmol) was added, the vessel was sealed and heated to 95 °C (external temperature) for 16 h. The reaction mixture was cooled to 23 °C and acidified with saturated aqueous NH_4Cl (40 mL). The resulting solution was extracted with EtOAc (4 × 20 mL). The combined organic layers were dried over anhydrous Na_2SO_4, filtered, and concentrated *in vacuo.* The crude material was purified by flash chromatography (30 to 60% EtOAc in hexanes) on silica gel (50 mL) to afford 4-((2-(diethoxymethyl)pyridin-4-yl)oxy)phenol as a pale yellow oil (289 mg, 25% yield).

4-((2-(Diethoxymethyl)pyridin-4-yl)oxy)phenol: R_f = 0.19 (60% EtOAc in hexanes); IR (neat): ν_{max} = 2981, 2884, 1594, 1505, 1478, 1430, 1350, 1298, 1239, 1199, 1110, 1092, 1055, 1005 cm^{-1}; ^{1}H NMR (300 MHz, 293 K, 1% CD_3OD in $CDCl_3$): δ 8.39 (d, *J* = 5.7 Hz, 1H, 6-H), 7.16 (d, *J* = 2.4 Hz, 1H, 3-H), 6.96–6.86 (m, 4H, -*Ph*), 6.74 (dd, *J* = 5.7, 2.4 Hz, 1H, 5-H), 5.44 (s,

1H, -C*H*(OCH_2CH_3)$_2$), 3.75–3.54 (m, 4H, -CH(OC*H*$_2$$CH_3$)$_2$), 1.22 (t, *J* = 7.2 Hz, 6H, -CH(OCH_2C*H*$_3$)$_2$); ^{13}C NMR (100 MHz, 293 K, $CDCl_3$): δ 166.7, 160.2, 153.9, 150.1, 149.6, 146.8, 122.1, 116.8, 116.2, 111.4, 109.1, 102.2, 62.6, 15.1; HRMS (ESI+) calcd for $C_{16}H_{20}NO_4$ $[M + H]^+$ = 290.1387, found 290.1374.

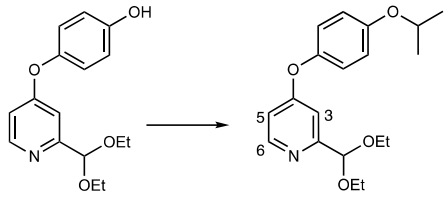

Preparation of 2-(diethoxymethyl)-4-(4-isopropoxyphenoxy)pyridine: A 25-mL round-bottomed flask was charged with dimethyl sulfoxide (2 mL), K_2CO_3 (138 mg, 1.00 mmol), 4-((2-(diethoxymethyl)pyridin-4-yl)oxy)phenol (289 mg, 1.00 mmol), and 2-iodopropane (0.50 mL, 1.0 mmol). After stirring at the same temperature for 48 h, 2-iodopropane (0.50 mL, 5.0 mmol) was added to the reaction mixture. After stirring at the same temperature for 24 h, 2-iodopropane (0.50 mL, 5.0 mmol) was added to the reaction mixture. After stirring at the same temperature for 18 h, the reaction mixture was acidified with saturated aqueous NH_4Cl (20 mL). The resulting solution was extracted with EtOAc (3 × 10 mL). The combined organic layers were dried over anhydrous Na_2SO_4, filtered, and concentrated *in vacuo.* The crude material was purified by flash chromatography (40 to 70% EtOAc in hexanes) on silica gel (30 mL) to afford 2-(diethoxymethyl)-4-(4-isopropoxyphenoxy)pyridine as an amber oil (275 mg, 83% yield).

2-(Diethoxymethyl)-4-(4-isopropoxyphenoxy)pyridine: R_f = 0.38 (60% EtOAc in hexanes); IR (neat): ν_{max} = 2981, 2884, 1588, 1499, 1475, 1422, 1288, 1242, 1202, 1111, 1055, 1016 cm^{-1}; ^{1}H NMR (400 MHz, 293 K, DMSO-d_6): δ 8.39 (d, *J* = 5.6 Hz, 1H, 6-H), 7.13–7.09 (m, 2H, -*Ph*), 7.03–7.00 (m, 2H, -*Ph*), 6.88 (d, *J* = 2.4 Hz, 1H, 3-H), 6.85 (dd, *J* = 5.6, 2.4 Hz, 1H, 5-H), 5.32 (s,

1H, -C*H*(OCH_2CH_3)$_2$), 4.62 (sept, *J* = 6.0, 1H, -OC*H*(CH_3)$_2$), 3.63–3.46 (m, 4H, -CH(OCH_2CH_3)$_2$), 1.28 (d, *J* = 6.0, 6H, -OCH(CH_3)$_2$), 1.11 (t, *J* = 6.8 Hz, 6H, -CH(OCH_2CH_3)$_2$); ^{13}C NMR (100 MHz, 293 K, DMSO-d_6): 165.9, 160.7, 155.4, 150.9, 146.8, 122.5, 117.5, 111.7, 108.1, 102.3, 70.1, 62.2, 22.2, 15.5; HRMS (ESI+) calcd for $C_{19}H_{26}NO_4$ $[M + H]^+$ = 332.1856, found 332.1840.

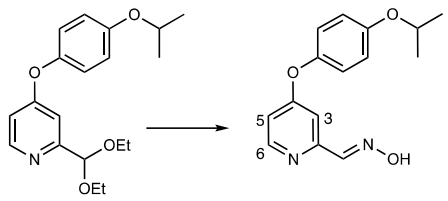

Preparation of (E)-4-(4-isopropoxyphenoxy)picolinaldehyde oxime: A 25-mL pear-shaped flask open to air with 2-(diethoxymethyl)-4-(4-isopropoxyphenoxy)pyridine (128 mg, 0.380 mmol) was charged with H_2O (2 mL) and 5 M H_2SO_4 in H_2O (80 μL, 0.43 mmol). The solution was heated to 90 °C (external temperature). After stirring at the same temperature for 2.5 h, the reaction mixture was cooled to 23 °C and treated with K_2CO_3 (210 mg, 1.52 mmol) followed by MeOH (8 mL) and NH_2OH•HCl (26 mg, 0.38 mmol) at the same temperature. A reflux condenser was attached, and the reaction was heated to reflux while open to air. After 3 h, the reaction mixture was cooled to 23 °C and concentrated *in vacuo.* EtOAc (10 mL) was added to the crude residue, followed by saturated aqueous NH_4Cl (20 mL). The layers were separated using a separatory funnel and the aqueous layer was extracted with EtOAc (2 × 10 mL). The combined organic layers were dried over anhydrous Na_2SO_4, filtered, and concentrated *in vacuo* to afford (*E*)-4-(4-isopropoxyphenoxy)picolinaldehyde oxime (104 mg, quantitative yield) as a light tan solid. This material was used directly without further purification.

(E)-4-(4-Isopropoxyphenoxy)picolinaldehyde oxime: m.p. = 150–153 °C; R_f = 0.35 (60% EtOAc in hexanes); IR (neat): ν_{max} = 2977, 1583, 1499, 1491, 1471, 1321, 1240, 1197, 1115, 1101 cm^{-1}; ^1H NMR (400 MHz, 293 K, DMSO-d_6): δ 11.67 (s, 1H, -CH=NO*H*), 8.44 (d, *J* = 5.6 Hz, 1H, 6-H), 8.01 (s, 1H, -C*H*=NOH), 7.14–7.09 (m, 3H, -*Ar*), 7.07–7.00 (m, 2H, -*Ar*), 6.98 (dd, *J* = 5.6, 2.4 Hz, 1H, -*Ar*), 4.62 (sept, *J* = 5.6, 1H, -OC*H*$(CH_3)_2$), 1.29 (d, *J* = 5.6, 6H, -OCH(C*H*$_3)_2$); ^{13}C NMR (100 MHz, 293 K, DMSO-d_6): δ 165.7, 155.5, 154.5, 151.6, 148.9, 146.6, 122.6, 117.4, 112.6, 106.3, 70.1, 22.2; HRMS (ESI+) calcd for $C_{15}H_{17}N_2O_3$ $[M + H]^+$ = 273.1233, found 273.1220.

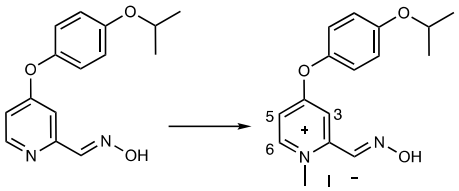

*Preparation of (E)-2-((hydroxyimino)methyl)-1-methyl-4-(3-isopropoxyphenoxy)pyridin-1-ium iodide (**ADG5045**):* A 35-mL sealed tube with (*E*)-4-(4-isopropoxyphenoxy)picolinaldehyde oxime (76 mg, 0.35 mmol) was charged with acetone (2 mL) and MeI (170 μL, 2.70 mmol). The vessel was sealed and heated to 45 °C (external temperature). After 14 h at the same temperature, the reaction mixture was cooled to 23 °C, transferred to a 25-mL round-bottomed flask and concentrated *in vacuo.* The crude residue was dry-loaded and purified by flash chromatography (5 to 40% MeOH in CH_2Cl_2) on silica gel (10 mL) to afford (*E*)-2-((hydroxyimino)methyl)-1-methyl-4-(4-isopropoxyphenoxy)pyridin-1-ium iodide as an orange solid (98 mg, 88% yield).

(E)-2-((Hydroxyimino)methyl)-1-methyl-4-(4-isopropoxyphenoxy)pyridin-1-ium iodide: m.p. = 75–77 °C; R_f = 0.10 (100% EtOAc); IR (neat): ν_{max} = 2979, 1638, 1593, 1571, 1495, 1459,

1383, 1333, 1295, 1244, 1204, 1183, 1134, 1114, 1004 cm^{-1}; ^1H NMR (400 MHz, 293 K, CD_3OD): δ 8.64 (d, *J* = 7.2 Hz, 1H, 6-H), 8.54 (s, 1H, -C*H*=NOH), 7.68 (d, *J* = 2.8 Hz, 1H, 3-H), 7.36 (dd, *J* = 7.2, 2.8 Hz, 1H, 5-H), 7.18–7.15 (m, 2H, -*Ph*), 7.09–7.04 (m, 2H, -*Ph*), 4.64 (sept, *J* = 6.0, 1H, -OC*H*$(CH_3)_2$), 4.25 (s, 3H, -N^+CH_3), 1.34 (d, *J* = 6.0, 6H, -OCH(C$H_3)_2$); ^{13}C NMR (100 MHz, 293 K, CD_3OD): δ 171.4, 158.1, 151.2, 149.7, 146.7, 141.8, 122.9, 118.6, 115.2, 112.2, 71.6, 45.9, 22.2; HRMS (ESI+) calcd for $C_{16}H_{19}N_2O_3$ $[M]^+$ = 287.1390, found 287.1377.

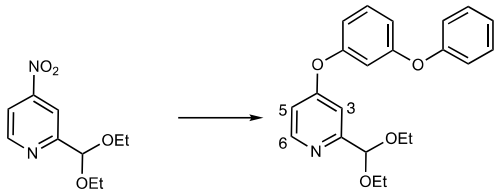

Preparation of 2-(diethoxymethyl)-4-(3-phenoxyphenoxy)pyridine: A 10-mL round-bottomed flask was charged with dimethyl sulfoxide (3 mL), K_2CO_3 (830 g, 6.00 mmol), and 3-phenoxyphenol (970 μL, 6.00 mmol). The mixture was stirred at room temperature for 10 min. 2-(Diethoxymethyl)-4-nitropyridine (453 mg, 2.00 mmol) was added, the vessel was sealed and heated to 115 °C (external temperature) for 7.7 h. The reaction mixture was cooled to 23 °C and acidified with saturated aqueous NH_4Cl (20 mL). The resulting solution was layers was extracted with EtOAc (3 × 10 mL). The combined organic layers were dried over anhydrous Na_2SO_4, filtered, and concentrated *in vacuo.* The crude material was purified by flash chromatography (0 to 40% EtOAc in hexanes) on silica gel (40 mL) to afford 2-(diethoxymethyl)-4-(3-phenoxyphenoxy)pyridine as an amber oil (726 mg, 99% yield).

2-(Diethoxymethyl)-4-(3-phenoxyphenoxy)pyridine: R_f = 0.61 (60% EtOAc in hexanes); IR (neat): ν_{max} = 2797, 2883, 1640, 1582, 1514, 1476, 1444, 1418, 1370, 1334, 1290, 1252, 1207, 1166, 1138, 1117, 1058, 1021 cm^{-1}; ^1H NMR (400 MHz, 293 K, $CDCl_3$): δ 8.43 (d, *J* = 5.6 Hz,

1H, 6-H), 7.37–7.21 (m, 3H, -*Ar*), 7.17 (d, *J* = 2.4 Hz, 1H, 3-H), 7.13 (t, *J* = 7.2 Hz, 1H, -*Ar*), 7.05–7.02 (m, 2H, -*Ar*), 6.86 (dd, *J* = 8.4, 2.4 Hz, 1H, -*Ar*), 6.81–6.76 (m, 2H, -*Ar*), 7.13 (t, *J* = 2.4 Hz, 1H, -*Ar*), 5.41 (s, 1H, -C*H*(OCH_2CH_3)$_2$), 3.73–3.54 (m, 4H, -CH(OC*H*$_2$$CH_3$)$_2$), 1.23 (t, *J* = 7.0 Hz, 6H, -CH(OCH_2C*H*$_3$)$_2$); ^{13}C NMR (100 MHz, 293 K, $CDCl_3$): δ 165.1, 160.5, 159.0, 156.2, 155.1, 150.6, 130.8, 129.8, 123.9, 119.3, 115.1, 114.9, 111.7, 110.9, 109.5, 102.3, 62.3, 15.07; HRMS (ESI+) calcd for $C_{22}H_{24}NO_4$ $[M + H]^+$ = 366.1699, found 366.1714.

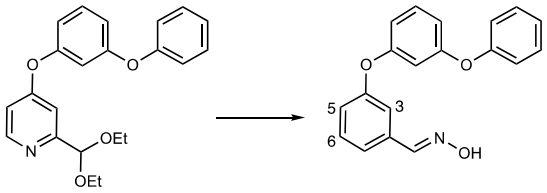

Preparation of (E)-4-(3-phenoxyphenoxy)picolinaldehyde oxime: A 50-mL pear-shaped flask open to air with 2-(diethoxymethyl)-4-(3-phenoxyphenoxy)pyridine (396 mg, 1.08 mmol) was charged with H_2O (4 mL) and 5 M H_2SO_4 in H_2O (240 μL, 1.19 mmol). The solution was heated to 90 °C (external temperature). After stirring at the same temperature for 3 h, the reaction mixture was cooled to 23 °C and treated with K_2CO_3 (597 mg, 4.32 mmol) followed by MeOH (14 mL) and NH_2OH•HCl (75 mg, 1.1 mmol) at the same temperature. A reflux condenser was attached, and the reaction was heated to reflux while open to air. After 3.5 h, the reaction mixture was cooled to 23 °C and concentrated *in vacuo.* EtOAc (10 mL) was added to the crude residue, followed by saturated aqueous NH_4Cl (20 mL). The layers were separated using a separatory funnel and the aqueous layer was extracted with EtOAc (2 × 10 mL). The combined organic layers were dried over anhydrous Na_2SO_4, filtered, and concentrated *in vacuo* to afford *(E)*-4-(3-phenoxyphenoxy)picolinaldehyde oxime (361 mg, 96% yield) as a light tan solid. This material was used directly without further purification.

(E)-4-(3-Phenoxyphenoxy)picolinaldehyde oxime: m.p. = 122–124 °C; R_f = 0.55 (60% EtOAc in hexanes); IR (neat): ν_{max} = 3069, 2855, 1579, 1563, 1475, 1443, 1420, 1403, 1308, 1289, 1258, 1244, 1207, 1168, 1120, 1070 cm^{-1}; ^1H NMR (300 MHz, 293 K, DMSO-d_6): δ 11.73 (s, 1H, -CH=NO*H*), 8.47 (d, *J* = 5.6 Hz, 1H, 6-H), 8.03 (s, 1H, -C*H*=NOH), 7.53–7.39 (m, 4H, -*Ar*), 7.21–7.15 (m, 2H, -*Ar*), 7.10–7.07 (m, 2H, -*Ar*), 7.02–6.91 (m, 4H, -*Ar*), 6.84 (t, *J* = 2.1 Hz, 1H, -*Ar*); ^{13}C NMR (100 MHz, 293 K, DMSO-d_6): δ 164.7, 158.9, 156.4, 155.1, 154.7, 151.9, 148.9, 132.1, 130.7, 124.6, 119.6, 115.9, 115.8, 113.2, 111.5, 107.1; HRMS (ESI+) calcd for $C_{18}H_{15}N_2O_3$ $[M + H]^+$ = 307.1077, found 307.1088.

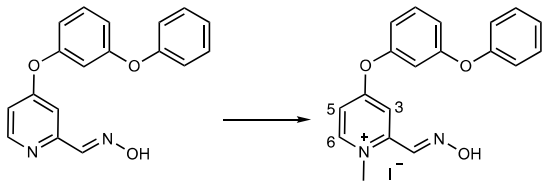

*Preparation of (E)-2-((hydroxyimino)methyl)-1-methyl-4-(3-phenoxyphenoxy)pyridin-1-ium iodide (**ADG4230**):* A 35-mL sealed tube with *(E)*-4-(3-phenoxyphenoxy)picolinaldehyde oxime (307 mg, 1.00 mmol) was charged with acetone (3 mL) and MeI (620 μL, 10.0 mmol). The vessel was sealed and heated to 45 °C (external temperature). After 19 h at the same temperature, the reaction mixture was cooled to 23 °C, transferred to a 25-mL round-bottomed flask, concentrated *in vacuo*, and recrystallized from acetone/EtOAc (1:1) to afford (*E*)-2-((hydroxyimino)methyl)-1-methyl-4-(3-phenoxyphenoxy)pyridin-1-ium iodide as an orange solid (158 mg, 35% yield).

(E)-2-((Hydroxyimino)methyl)-1-methyl-4-(3-phenoxyphenoxy)pyridin-1-ium iodide: m.p. = 62–64 °C; R_f = 0.11 (10% MeOH in CH_2Cl_2); IR (neat): ν_{max} = 3048, 2981, 1640, 1538, 1514, 1476, 1459, 1332, 1302, 1251, 1203, 1160, 1139, 1113, 1071 cm^{-1}; ^1H NMR (400 MHz, 293 K,

CD_3OD): δ 8.71 (d, J = 7.2 Hz, 1H, 6-H), 8.55 (s, 1H, -C*H*=NOH), 7.71 (d, J = 2.8 Hz, 1H, 3-H), 7.54 (t, J = 8.0 Hz, 1H, -*Ph*), 7.43–7.38 (m, 3H, -*Ph*), 7.18 (t, J = 8.0 Hz, 1H, -*Ph*), 7.09–7.02 (m, 4H, -*Ph*), 6.88 (app s, 1H, -*Ph*), 4.24 (s, 3H, -N^+CH_3); ^{13}C NMR (100 MHz, 293 K, CD_3OD): δ 170.6, 161.0, 157.3, 154.5, 151.4, 149.9, 141.8, 133.0, 131.2, 125.5, 120.6, 117.9, 116.1, 115.4, 112.3, 111.8, 46.0; HRMS (ESI+) calcd for $C_{19}H_{17}N_2O_3$ $[M]^+$ = 321.1233, found 321.1221.

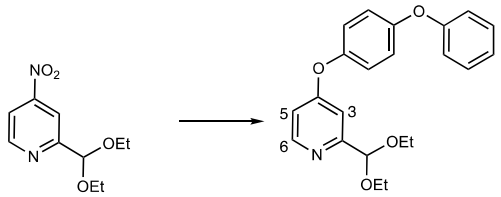

Preparation of 2-(diethoxymethyl)-4-(4-phenoxyphenoxy)pyridine: A 10-mL round-bottomed flask was charged with dimethyl sulfoxide (3 mL), K_2CO_3 (839 mg, 6.00 mmol), and 4-phenoxyphenol (1.12 g, 6.00 mmol). The mixture was stirred at room temperature for 5 min. 2-(Diethoxymethyl)-4-nitropyridine (453 mg, 2.00 mmol) was added, the vessel was sealed and heated to 95 °C (external temperature) for 6 h. The reaction mixture was cooled to 23 °C and acidified with saturated aqueous NH_4Cl (20 mL). The resulting solution was extracted with EtOAc (3 × 10 mL). The combined organic layers were dried over anhydrous Na_2SO_4, filtered, and concentrated *in vacuo*. The crude material was purified by flash chromatography (0 to 40% EtOAc in hexanes) on silica gel (30 mL) to afford 2-(diethoxymethyl)-4-(4-phenoxyphenoxy)pyridine as a yellow oil (644 mg, 88% yield).

2-(Diethoxymethyl)-4-(4-phenoxyphenoxy)pyridine: R_f = 0.57 (60% EtOAc in hexanes); IR (neat): ν_{max} = 2975, 2879, 1589, 1497, 1423, 1369, 1346, 1334, 1289, 1239, 1204, 1192, 1160, 1109, 1084, 1056 cm^{-1}; ^{1}H NMR (300 MHz, 293 K, $CDCl_3$): δ 8.43 (d, J = 5.7 Hz, 1H, 6-H), 7.36 (t, J = 7.5, 2H, -*Ar*), 7.17 (d, J = 2.1 Hz, 1H, 3-H), 7.13 (t, J = 7.5, 1H, -*Ar*), 7.06–7.03 (m, 6H, -

Ar), 6.77 (dd, *J* = 5.7, 2.1 Hz, 1H, 5-H), 5.42 (s, 1H, -C*H*(OCH_2CH_3)$_2$), 3.77–3.55 (m, 4H, -CH(OC*H*$_2$CH$_3$)$_2$), 1.24 (t, *J* = 6.9 Hz, 6H, -CH(OCH$_2$C*H*$_3$)$_2$); ^{13}C NMR (100 MHz, 293 K, $CDCl_3$): δ 165.5, 160.2, 156.8, 154.2, 150.3, 148.9, 129.5, 123.1, 121.8, 119.9, 118.4, 111.1, 108.8, 102.1, 102.1, 62.0, 14.8; HRMS (ESI+) calcd for $C_{22}H_{24}NO_4$ $[M + H]^+$ = 366.1699, found 366.1713.

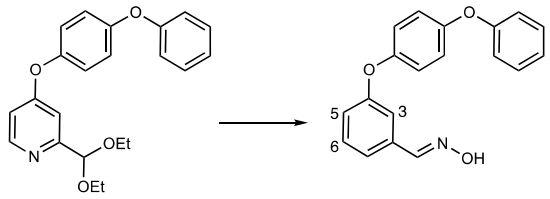

Preparation of (E)-4-(4-phenoxyphenoxy)picolinaldehyde oxime: A 25-mL pear-shaped flask open to air with 2-(diethoxymethyl)-4-(4-phenoxyphenoxy)pyridine (300 mg, 0.820 mmol) was charged with H_2O (3 mL) and 5 M H_2SO_4 in H_2O (180 μL, 0.900 mmol). The solution was heated to 93 °C (external temperature). After stirring at the same temperature for 2.5 h, the reaction mixture was cooled to 23 °C and treated with K_2CO_3 (453 mg, 3.28 mmol) followed by MeOH (10 mL) and NH_2OH•HCl (57 mg, 0.82 mmol) at the same temperature. A reflux condenser was attached, and the reaction was heated to reflux while open to air. After 3.6 h, the reaction mixture was cooled to 23 °C and concentrated *in vacuo.* EtOAc (10 mL) was added to the crude residue, followed by saturated aqueous NH_4Cl (20 mL). The layers were separated using a separatory funnel and the aqueous layer was extracted with EtOAc (2 × 10 mL). The combined organic layers were dried over anhydrous Na_2SO_4, filtered, and concentrated *in vacuo* to afford *(E)*-4-(4-phenoxyphenoxy)picolinaldehyde oxime (241 mg, 96% yield) as a light tan solid. This material was used directly without further purification.

(E)-4-(4-Phenoxyphenoxy)picolinaldehyde oxime: m.p. = 157–160 °C; R_f = 0.57 (60% EtOAc in hexanes); IR (neat): ν_{max} = 3177, 3064, 3005, 2869, 2799, 1586, 1496, 1462, 1318, 1296,

1253, 1204, 1190, 1164, 1098, 1023, 1003 cm^{-1}; ^1H NMR (500 MHz, 293 K, DMSO-d_6): δ 11.70 (s, 1H, -CH=NO*H*), 8.46 (d, *J* = 5.5 Hz, 1H, 6-H), 8.03 (s, 1H, -C*H*=NOH), 7.44–7.40 (m, 2H, -*Ar*), 7.26–7.24 (m, 2H, -*Ar*), 7.19–7.15 (m, 2H, -*Ar*), 7.13–7.11 (m, 2H, -*Ar*), 7.07–7.06 (m, 2H, -*Ar*), 6.98 (dd, *J* = 5.5, 2.5 Hz, 1H, 5-H); ^{13}C NMR (100 MHz, 293 K, DMSO-d_6): δ 165.2, 157.0, 154.7, 154.6, 151.7, 149.2, 148.8, 130.6, 124.1, 123.0, 120.7, 119.1, 112.7, 106.7; HRMS (ESI+) calcd for $C_{18}H_{15}N_2O_3$ $[M + H]^+$ = 307.1077, found 307.1062.

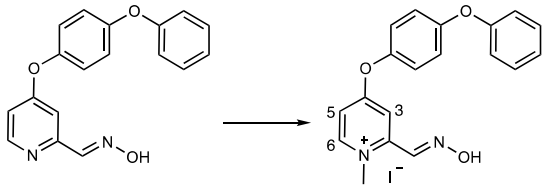

*Preparation of (E)-2-((hydroxyimino)methyl)-1-methyl-4-(4-phenoxyphenoxy)pyridin-1-ium iodide (**ADG4234**):* A 35-mL sealed tube with *(E)*-4-(4-phenoxyphenoxy)picolinaldehyde oxime (115 mg, 0.380 mmol) was charged with acetone (1 mL) and MeI (230 μL, 3.80 mmol). The vessel was sealed and heated to 40 °C (external temperature). After 17.5 h at the same temperature, the reaction mixture was cooled to 23 °C, transferred to a 25-mL round-bottomed flask, concentrated *in vacuo,* and recrystallized from acetone/EtOAc (1:1) to afford (*E*)-2-((hydroxyimino)methyl)-1-methyl-4-(4-phenoxyphenoxy)pyridin-1-ium iodide as a yellow solid (133 mg, 30% yield).

(E)-2-((Hydroxyimino)methyl)-1-methyl-4-(4-phenoxyphenoxy)pyridin-1-ium iodide: m.p. = 182–184 °C; R_f = 0.11 (10% MeOH in CH_2Cl_2); IR (neat): ν_{max} = 3063, 2980, 2884, 1639, 1596, 1586, 1570, 1514, 1487, 1460, 1421, 1407, 1323, 1303, 1261, 1239, 1204, 1171, 1134, 1114, 1089, 1008 cm^{-1}; ^1H NMR (400 MHz, 293 K, DMSO-d_6): δ 13.08 (s, 1H, -CH=NO*H*), 8.83 (d, *J* = 7.2 Hz, 1H, 6-H), 8.61 (s, 1H, -C*H*=NOH), 7.62–7.60 (m, 2H, -*Ar*), 7.47–7.43 (m, 2H, -*Ar*), 7.38–7.36

(m, 2H, -*Ar*), 7.22–7.19 (m, 3H, -*Ar*), 7.12–7.09 (m, 2H, -*Ar*), 4.24 (s, 3H, -$N^+C\mathit{H}_3$); ^{13}C NMR (100 MHz, 293 K, DMSO-d_6): δ 169.2, 156.7, 155.8, 149.9, 149.4, 147.8, 142.0, 130.7, 130.6, 124.5, 123.2, 121.0, 120.8, 119.4, 119.2, 114.8, 110.6, 45.3; HRMS (ESI+) calcd for $C_{19}H_{17}N_2O_3$ $[M]^+$ = 321.1233, found 321.1247.

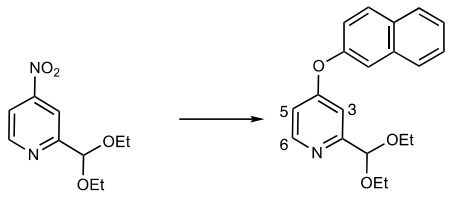

Preparation of 2-(diethoxymethyl)-4-(naphthalen-2-yloxy)pyridine: A 25-mL round-bottomed flask was charged with dimethyl sulfoxide (4 mL), K_2CO_3 (1.65 g, 12.0 mmol), and 2-naphthol (1.73 g, 12.0 mmol). The mixture was stirred at room temperature for 5 min. 2-(Diethoxymethyl)-4-nitropyridine (905 mg, 4.00 mmol) was added, the vessel was sealed and heated to 110 °C (external temperature) for 4.5 h. The reaction mixture was cooled to 23 °C and acidified with saturated aqueous NH_4Cl (25 mL). The resulting solution was extracted with EtOAc (3 × 10 mL). The combined organic layers were dried over anhydrous Na_2SO_4, filtered, and concentrated *in vacuo*. The crude material was purified by flash chromatography (0 to 50% EtOAc in hexanes) on silica gel (75 mL) to afford 2-(diethoxymethyl)-4-(naphthalen-2-yloxy)pyridine as a dark red oil (1.27 g, 98% yield).

2-(Diethoxymethyl)-4-(naphthalen-2-yloxy)pyridine: R_f = 0.53 (60% EtOAc in hexanes); IR (neat): ν_{max} = 2977, 2883, 1588, 1572, 1509, 1463, 1421, 1368, 1346, 1288, 1256, 1243, 1211, 1172, 1148, 1136, 1109, 1082, 1056 cm^{-1}; ^{1}H NMR (300 MHz, 293 K, DMSO-d_6): δ 8.44 (d, J = 4.8 Hz, 1H, 6-H), 8.06 (d, J = 8.7 Hz, 1H, -*Ar*), 8.00 (dd, J = 6.9, 2.1 Hz, 1H, -*Ar*), 7.93 (dd, J = 8.7, 2.1 Hz, 1H, -*Ar*), 7.72 (d, J = 2.1 Hz, 1H, 3-H), 7.59–7.51 (m, 2H, -*Ar*), 7.37 (dd, J = 8.7, 2.4

Hz, 1H, -*Ar*), 6.99–6.95 (m, 2H, -*Ar*), 5.35 (s, 1H, -C*H*(OCH_2CH_3)$_2$), 3.64–3.45 (m, 4H, -CH(OC*H*$_2$CH$_3$)$_2$), 1.08 (t, *J* = 7.2 Hz, 6H, -CH(OCH_2CH_3)$_2$); ^{13}C NMR (100 MHz, 293 K, DMSO-d_6): δ 165.2, 161.0, 151.7, 151.2, 134.3, 131.3, 131.1, 128.3, 127.9, 127.4, 126.3, 120.9, 117.6, 112.5, 108.9, 102.3, 62.2, 15.5; HRMS (ESI+) calcd for $C_{20}H_{22}NO_3$ $[M + H]^+$ = 324.1594, found 324.1591.

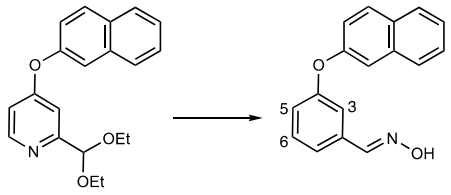

Preparation of (E)-4-(naphthalen-2-yloxy)picolinaldehyde oxime: A 100-mL round-bottomed flask open to air with 2-(diethoxymethyl)-4-(naphthalen-2-yloxy)pyridine (646 mg, 2.00 mmol) was charged with H_2O (7 mL) and 5 M H_2SO_4 in H_2O (440 μL, 2.20 mmol). The solution was heated to 95 °C (external temperature). After stirring at the same temperature for 2.5 h, the reaction mixture was cooled to 23 °C and treated with K_2CO_3 (1.11 g, 8.00 mmol) followed by MeOH (25 mL) and NH_2OH•HCl (139 mg, 2.00 mmol) at the same temperature. A reflux condenser was attached, and the reaction was heated to reflux while open to air. After 2.3 h, the reaction mixture was cooled to 23 °C and concentrated *in vacuo.* EtOAc (10 mL) was added to the crude residue, followed by saturated aqueous NH_4Cl (25 mL). The layers were separated using a separatory funnel and the aqueous layer was extracted with EtOAc (2 × 8 mL). The combined organic layers were dried over anhydrous Na_2SO_4, filtered, and concentrated *in vacuo* to afford (*E*)-4-(naphthalen-2-yloxy)picolinaldehyde oxime (527 mg, 99% yield) as a brown solid. This material was used directly without further purification.

(E)-4-(Naphthalen-2-yloxy)picolinaldehyde oxime: m.p. = 150–153 °C; R_f = 0.43 (60% EtOAc in hexanes); IR (neat): ν_{max} = 2867, 2729, 1591, 1579, 1562, 1509, 1461, 1427, 1325, 1292, 1260, 1241, 1208, 1176, 1146, 1137, 1117 cm^{-1}; ^1H NMR (300 MHz, 293 K, DMSO-d_6): δ 11.65 (s, 1H, -CH=NO*H*), 8.49 (d, *J* = 5.7 Hz, 1H, 6-H), 8.09–7.92 (m, 4H, -CH=NO*H* and -*Ar*), 7.76 (d, *J* = 2.4 Hz, 1H, 3-H), 7.60–7.51 (m, 2H, -*Ar*), 7.40 (dd, *J* = 9.0, 2.4 Hz, 1H, -*Ar*), 7.20 (d, *J* = 2.4 Hz, 1H, -*Ar*), 7.06 (dd, *J* = 5.7, 2.4 Hz, 1H, 5-H); ^{13}C NMR (100 MHz, 293 K, DMSO-d_6): δ 165.3, 154.9, 152.0, 151.6, 149.0, 134.5, 131.5, 131.3, 128.4, 128.1, 127.6, 126.6, 121.3, 118.1, 113.4, 107.2; HRMS (ESI+) calcd for $C_{16}H_{13}N_2O_2$ $[M + H]^+$ = 265.0971 found 265.0984.

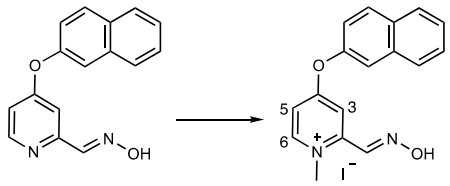

*Preparation of (E)-2-((hydroxyimino)methyl)-1-methyl-4-(naphthalen-2-yloxy)pyridin-1-ium iodide (**ADG4204**):* A 35-mL sealed tube with (*E*)-4-(naphthalen-2-yloxy)picolinaldehyde oxime (264 mg, 1.00 mmol) was charged with acetone (3 mL) and MeI (620 μL, 10.0 mmol). The vessel was sealed and heated to 50 °C (external temperature). After 18 h at the same temperature, the reaction mixture was cooled to 23 °C, transferred to a 25-mL round-bottomed flask, and concentrated *in vacuo,* to afford (*E*)-2-((hydroxyimino)methyl)-1-methyl-4-(naphthalen-2-yloxy)pyridin-1-ium iodide as a yellow solid (392 mg, 96% yield).

(E)-2-((Hydroxyimino)methyl)-1-methyl-4-(naphthalen-2-yloxy)pyridin-1-ium iodide: m.p. = 175–178 °C; R_f = 0.11 (10% MeOH in CH_2Cl_2); IR (neat): ν_{max} = 3108, 3014, 1640, 1624, 1591, 1567, 1504, 1458, 1438, 1417, 1353, 1326, 1294, 1258, 1240, 1213, 1179, 1150, 1112 cm^{-1}; ^1H NMR (300 MHz, 293 K, DMSO-d_6): δ 12.99 (s, 1H, -CH=NO*H*), 8.85 (d, *J* = 7.2 Hz, 1H, 6-

H), 8.60 (s, 1H, -C*H*=NOH), 8.18 (d, *J* = 9.0 Hz, 1H, -*Ar*), 8.09–7.94 (m, 2H, -*Ar*), 7.93 (d, *J* = 2.4 Hz, 1H, -*Ar*), 7.71–7.59 (m, 4H, -*Ar*), 7.49 (dd, *J* = 9.0, 2.4 Hz, 1H, -*Ar*), 4.24 (s, 3H, -N^+C*H*$_3$); ^{13}C NMR (100 MHz, 293 K, DMSO-d_6): δ 169.1, 150.0, 149.4, 141.9, 134.2, 132.0, 131.9, 128.5, 128.3, 127.9, 127.2, 120.4, 118.7, 115.2, 110.6, 45.3; HRMS (ESI+) calcd for $C_{17}H_{15}N_2O_2$ $[M]^+$ = 279.1128, found 279.1141.

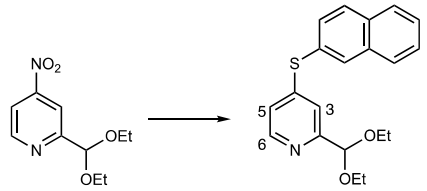

Preparation of 2-(diethoxymethyl)-4-(naphthalen-2-ylthio)pyridine: A 75-mL sealed tube was charged with dimethyl sulfoxide (4 mL), K_2CO_3 (1.66 g, 12.0 mmol), and 2-naphthalenethiol (1.93 g, 12.0 mmol). The mixture was stirred at room temperature for 20 min. 2-(Diethoxymethyl)-4-nitropyridine (905 mg, 4.00 mmol) was added, the vessel was sealed and heated to 95 °C for 16 h. The reaction mixture was cooled to 23 °C and neutralized with saturated aqueous NH_4Cl (20 mL). The resulting solution was extracted with EtOAc (3 × 20 mL). The combined organic layers were dried over anhydrous Na_2SO_4, filtered, and concentrated *in vacuo*. The crude material was purified by flash chromatography (0 to 50% EtOAc in hexanes) on silica gel (200 mL) to afford 2-(diethoxymethyl)-4-(naphthalen-2-ylthio)pyridine as an amber oil (1.20 g, 88% yield).

2-(Diethoxymethyl)-4-(naphthalen-2-ylthio)pyridine: R_f = 0.51 (60% EtOAc in hexanes); IR (neat): ν_{max} = 3053, 2974, 2877, 1574, 1543, 1499, 1455, 1391, 1368, 1342, 1269, 1234, 1112, 1091, 1059 cm^{-1}; ^{1}H NMR (300 MHz, 293 K, $CDCl_3$): δ 8.30 (d, *J* = 5.1 Hz, 1H, 6-H), 8.09 (s, 1H, -*Ar*), 7.89–7.81 (m, 3H, -*Ar*), 7.58–7.49 (m, 3H, -*Ar*), 7.36 (d, *J* = 1.8 Hz, 1H, 3-H), 6.84 (dd, *J* = 5.1, 1.8 Hz, 1H, 5-H), 5.37 (s, 1H, -C*H*(OCH_2CH_3)$_2$), 3.70–3.50 (m, 4H, -CH(OCH_2CH_3)$_2$),

1.18 (t, J = 7.2 Hz, 6H, -CH(OCH_2CH_3)$_2$); ^{13}C NMR (100 MHz, 293 K, $CDCl_3$): δ 158.0, 150.9, 148.8, 134.8, 133.8, 133.2, 130.9, 129.5, 127.8, 127.7, 127.3, 126.8, 126.7, 120.4, 118.3, 102.3, 62.2, 15.0; HRMS (ESI+) calcd for $C_{20}H_{22}N_2O_2S$ [M + H]$^+$ = 340.1366, found 340.1360.

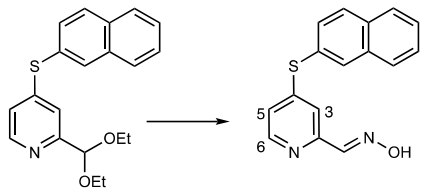

Preparation of (E)-4-(naphthalen-2-ylthio)picolinaldehyde oxime: A 100-mL pear-shaped flask open to air with 2-(diethoxymethyl)-4-(naphthalen-2-ylthio)pyridine (692 mg, 2.03 mmol) was charged with H_2O (7 mL) and 5 M H_2SO_4 in H_2O (450 μL, 2.23 mmol). The solution was heated to 90 °C. After stirring at the same temperature for 2.5 h, the reaction mixture was cooled to 23 °C and treated with K_2CO_3 (1.12 g, 8.12 mmol) followed by MeOH (22 mL) and NH_2OH•HCl (142 mg, 2.03 mmol) at the same temperature. A reflux condenser was attached, and the reaction was heated to reflux while open to air. After 2.8 h, the reaction mixture was cooled to 23 °C and concentrated *in vacuo.* EtOAc (10 mL) was added to the crude residue, followed by saturated aqueous NH_4Cl (20 mL). The layers were separated using a separatory funnel and the aqueous layer was extracted with EtOAc (2 × 10 mL). The combined organic layers were dried over anhydrous Na_2SO_4, filtered, and concentrated *in vacuo* to afford (*E*)-4-(naphthalen-2-ylthio)picolinaldehyde oxime (470 mg, 83% yield) as a light tan solid. This material was used directly without further purification.

(E)-4-(Naphthalen-2-ylthio)picolinaldehyde oxime: m.p. = 173–176 °C; R_f = 0.32 (60% EtOAc in hexanes); IR (neat): ν_{max} = 2979, 2881, 2742, 1572, 1537, 1399, 1325 cm^{-1}; ^{1}H NMR (400 MHz, 293 K, DMSO-d_6): δ 11.61 (s, 1H, -CH=NO*H*), 8.37 (d, J = 5.2 Hz, 1H, 6-H), 8.31 (d,

J = 5.6 Hz, 1H, -*Ar*), 8.08–8.01 (m, 3H, -*Ar*), 7.58–7.49 (m, 3H, -*Ar*), 7.94 (s, 1H, -C*H*=NOH), 7.66–7.59 (m, 3H, -*Ar*), 7.30 (d, *J* = 1.2 Hz, 1H, 3-H), 7.16 (dd, *J* = 5.6, 1.2 Hz, 1H, 5-H); ^{13}C NMR (100 MHz, 293 K, DMSO-d_6): δ 152.8, 150.3, 149.8, 148.8, 135.5, 134.0, 133.5, 131.5, 130.4, 128.5, 128.3, 128.2, 127.6, 126.0, 121.3, 115.9; HRMS (ESI+) calcd for $C_{16}H_{13}N_2OS$ [M + H]$^+$ = 281.0743, found 281.0739.

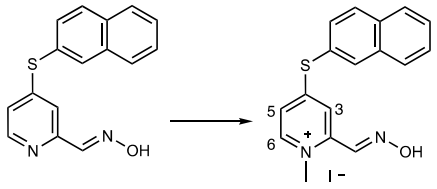

*Preparation of (E)-2-((hydroxyimino)methyl)-1-methyl-4-(naphthalen-2-ylthio)pyridin-1-ium iodide (**ADG4072**):* A 35-mL sealed tube with (*E*)-4-(naphthalen-2-ylthio)picolinaldehyde oxime (157 mg, 0.550 mmol) was charged with acetone (2 mL) and MeI (350 μL, 5.50 mmol). The vessel was sealed and heated to 50 °C. After 24 h at the same temperature, the reaction mixture was cooled to 23 °C, transferred to a 25-mL round-bottomed flask, concentrated *in vacuo* to afford (*E*)-2-((hydroxyimino)methyl)-1-methyl-4-(naphthalen-2-ylthio)pyridin-1-ium iodide as an orange solid (252 mg, quantitative yield).

(E)-2-((Hydroxyimino)methyl)-1-methyl-4-(naphthalen-2-ylthio)pyridin-1-ium iodide: m.p. = 113–115 °C; R_f = 0.11 (100% EtOAc); IR (neat): ν_{max} = 2979, 1623, 1585, 1551, 1495, 1427, 1296, 1233, 1086, 1000, 940 cm^{-1}; ^{1}H NMR (400 MHz, 293 K, DMSO-d_6): δ 12.92 (s, 1H, -CH=NO*H*), 8.62 (d, *J* = 6.8 Hz, 1H, 6-H), 8.53 (s, 1H, -C*H*=NOH), 8.18 (d, *J* = 8.4 Hz, 1H, -*Ar*), 8.08 (app t, *J* = 8.4 Hz, 2H, -*Ar*), 7.75–7.65 (m, 5H, -*Ar*), 4.17 (s, 3H, -N$^+$C*H*$_3$); ^{13}C NMR (100 MHz, 293 K, DMSO-d_6): δ 161.7, 146.5, 145.5, 141.8, 136.5, 134.0, 134.0, 131.2, 131.0, 128.9,

128.7, 128.5, 128.0, 123.4, 122.6, 118.8, 45.4; HRMS (ESI+) calcd for $C_{17}H_{15}N_2O_2S$ $[M]^+$ = 295.0899, found 295.0903.

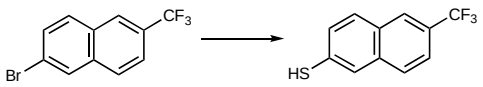

Preparation of 6-(trifluoromethyl)naphthalene-2-thiol: 6-(Trifluoromethyl)naphthalene-2-thiol was prepared according to a procedure found in the literature.[153] A 75-mL sealed tube was charged with 2-bromo-6-(trifluoromethyl)naphthalene (830 mg, 3.00 mmol), $CuSO_4•5H_2O$ (38 mg, 0.15 mmol), and KOH (842 mg, 15.0 mmol) and flushed with argon gas. The mixture was dissolved in dimethyl sulfoxide (7 mL) and H_2O (700 μL). 1,2-Ethanedithiol (300 μL, 3.60 mmol) was added, the vessel was sealed and heated to 110 °C (external temperature) for 16 h. The reaction mixture was cooled to 23 °C and diluted with 1.0 M HCl (120 mL). The resulting solution was extracted with EtOAc (3 × 30 mL). The combined organic layers were dried over anhydrous Na_2SO_4, filtered, and concentrated *in vacuo.* The crude material was purified by flash chromatography (0 to 20% EtOAc in hexanes) on silica gel (75 mL) to afford 6-(trifluoromethyl)naphthalene-2-thiol as a pale yellow solid (700 mg, quantitative yield).

6-(Trifluoromethyl)naphthalene-2-thiol: R_f = 0.65 (60% EtOAc in hexanes); ^{1}H NMR (400 MHz, 293 K, $CDCl_3$): δ 8.07 (s, 1H), 7.81–7.78 (m, 3H), 7.62 (dd, J = 8.4, 1.6 Hz, 1H), 7.42 (dd, J = 8.4, 1.6 Hz, 1H), 3.68 (s, 1H); HRMS (ESI−) calcd for $C_{11}H_6F_3S$ $[M - H]^-$ = 227.0137, found 227.0145.

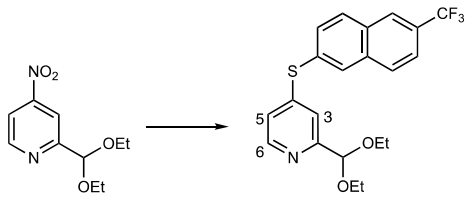

Preparation of 2-(diethoxymethyl)-4-((6-(trifluoromethyl)naphthalen-2-yl)thio)pyridine: A 35-mL sealed tube was charged with dimethyl sulfoxide (3 mL), K_2CO_3 (1.24 g, 9.00 mmol), and 6-(trifluoromethyl)naphthalene-2-thiol (700 mg, 3.00 mmol). The mixture was stirred at room temperature for 10 min. 2-(Diethoxymethyl)-4-nitropyridine (588 mg, 2.60 mmol) was added, the vessel was sealed and heated to 97 °C for 16 h. The reaction mixture was cooled to 23 °C and neutralized with saturated aqueous NH_4Cl (20 mL). The resulting solution was extracted with EtOAc (3 × 20 mL). The combined organic layers were dried over anhydrous Na_2SO_4, filtered, and concentrated *in vacuo.* The crude material was purified by flash chromatography (0 to 40% EtOAc in hexanes) on silica gel (30 mL) to afford 2-(diethoxymethyl)-4-((6-(trifluoromethyl)naphthalen-2-yl)thio)pyridine as an amber oil (872 mg, 82% yield).

2-(Diethoxymethyl)-4-((6-(trifluoromethyl)naphthalen-2-yl)thio)pyridine: R_f = 0.55 (60% EtOAc in hexanes); IR (neat): ν_{max} = 2976, 2887, 1575, 1539, 1468, 1388, 1367, 1335, 1313, 1271, 1236, 1184, 1164, 1153, 1117, 1061, 1010 cm^{-1}; ^1H NMR (300 MHz, 293 K, $CDCl_3$): δ 8.36 (d, J = 5.4 Hz, 1H, 6-H), 8.18 (s, 1H, -*Ar*), 8.13 (s, 1H, -*Ar*), 7.96 (d, J = 9.0 Hz, 1H, -*Ar*), 7.71 (dd, J = 8.7, 1.5 Hz, 1H, -*Ar*), 7.61 (dd, J = 8.7, 1.5 Hz, 1H, -*Ar*), 7.40 (d, J = 1.8 Hz, 1H, 3-H), 6.90 (dd, J = 5.4, 1.8 Hz, 1H, 5-H), 5.39 (s, 1H, -C*H*$(OCH_2CH_3)_2$), 3.73–3.52 (m, 4H, -CH(OC*H*$_2CH_3)_2$), 1.18 (t, J = 7.2 Hz, 6H, -CH$(OCH_2CH_3)_2$); ^{13}C NMR (100 MHz, 293 K, $CDCl_3$): δ 158.4, 149.7, 148.9, 134.9, 133.8, 131.9, 131.8, 130.4, 130.3, 128.8, 125.5 (q, J = 4.0 Hz), 125.5 (q, J = 270.0 Hz), 122.5 (q, J = 3.0 Hz), 121.0, 118.9, 102.3, 62.4, 15.1; HRMS (ESI+) calcd for $C_{21}H_{21}F_3NO_2S$ $[M + H]^+$ = 408.1239, found 408.1226.

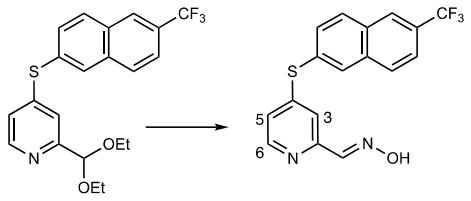

Preparation of (E)-4-((6-(trifluoromethyl)naphthalen-2-yl)thio)picolinaldehyde oxime: A 100-mL pear-shaped flask open to air with 2-(diethoxymethyl)-4-((6-(trifluoromethyl)naphthalen-2-yl)thio)pyridine (872 mg, 2.14 mmol) was charged with H_2O (6 mL) and 5 M H_2SO_4 in H_2O (470 μL, 2.35 mmol). The solution was heated to 95 °C. After stirring at the same temperature for 2 h, the reaction mixture was cooled to 23 °C and treated with K_2CO_3 (1.12 g, 8.56 mmol) followed by MeOH (26 mL) and NH_2OH•HCl (148 mg, 2.14 mmol) at the same temperature. A reflux condenser was attached, and the reaction was heated to reflux while open to air. After 3 h, the reaction mixture was cooled to 23 °C and concentrated *in vacuo.* EtOAc (20 mL) was added to the crude residue, followed by saturated aqueous NH_4Cl (20 mL). The layers were separated using a separatory funnel and the aqueous layer was extracted with EtOAc (2 × 20 mL). The combined organic layers were dried over anhydrous Na_2SO_4, filtered, and concentrated *in vacuo* to afford (*E*)-4-((6-(trifluoromethyl)naphthalen-2-yl)thio)picolinaldehyde oxime (535 mg, 72% yield) as an orange solid. This material was used directly without further purification.

(E)-4-((6-(Trifluoromethyl)naphthalen-2-yl)thio)picolinaldehyde oxime: m.p. = 183–186 °C; R_f = 0.35 (60% EtOAc in hexanes); IR (neat): ν_{max} = 2917, 2857, 2763, 1575, 1536, 1467, 1400, 1365, 1335, 1314, 1272, 1235, 1183, 1163, 1149, 1116, 1063 cm^{-1}; ^1H NMR (400 MHz, 293 K, CD_3OD): δ 8.35–8.29 (m, 3H, -*Ar*), 8.17–8.12 (m, 2H, -*Ar*), 7.97 (s, 1H, -C*H*=NOH), 7.77 (dd, *J* = 8.8, 1.6 Hz, 1H, -*Ar*), 7.70 (dd, *J* = 8.8, 1.6 Hz, 1H, -*Ar*), 7.50 (d, *J* = 1.6 Hz, 1H, 3-H), 7.11 (dd, *J* = 5.6, 1.6 Hz, 1H, 5-H); ^{13}C NMR (125 MHz, 293 K, DMSO-d_6): δ 152.9, 149.9, 149.3,

148.7, 135.2, 134.7, 132.6, 132.2, 131.4, 130.0, 129.8, 128.1, 127.8, 126.3 (q, J = 5.0 Hz), 124.7 (q, J = 270.0 Hz), 122.7 (q, J = 2.5 Hz), 121.7, 116.6; HRMS (ESI+) calcd for $C_{17}H_{12}F_3N_2OS$ [M + H]$^+$ = 349.0616, found 349.0615.

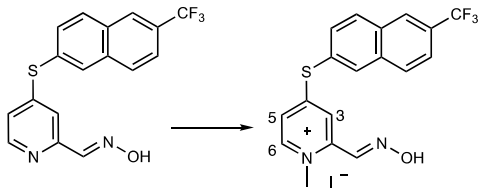

*Preparation of (E)-2-((hydroxyimino)methyl)-1-methyl-4-((6-(trifluoromethyl)naphthalen-2-yl)thio)pyridin-1-ium iodide (**ADG4145**):* A 35-mL sealed tube with (*E*)-4-((6-(trifluoromethyl)naphthalen-2-yl)thio)picolinaldehyde oxime (200 mg, 0.570 mmol) was charged with acetone (2 mL) and MeI (350 μL, 5.70 mmol). The vessel was sealed and heated to 50 °C. After 5.5 h at the same temperature, the reaction mixture was cooled to 23 °C, transferred to a 25-mL round-bottomed flask, and concentrated *in vacuo*. The crude residue was dry-loaded and purified by flash chromatography (5 to 40% MeOH in CH_2Cl_2) on silica gel (10 mL) to afford (*E*)-2-((hydroxyimino)methyl)-1-methyl-4-((6-(trifluoromethyl)naphthalen-2-yl)thio)pyridin-1-ium iodide as an orange solid (115 mg, 41% yield).

(E)-2-((Hydroxyimino)methyl)-1-methyl-4-((6-(trifluoromethyl)naphthalen-2-yl)thio)pyridin-1-ium iodide: m.p. = 188–190 °C; R_f = 0.10 (100% EtOAc); IR (neat): ν_{max} = 3017, 2857, 1626, 1594, 1553, 1496, 1468, 1429, 1335, 1313, 1273, 1236, 1185, 1165, 1153, 1117, 1088, 1063 cm^{-1}; ^{1}H NMR (400 MHz, 293 K, CD_3OD): δ 8.48–8.43 (m, 4H, -C*H*=NOH and -*Ar*), 8.30 (d, J = 8.8 Hz, 1H, -*Ar*), 8.21 (d, J = 8.8 Hz, 1H, -*Ar*), 7.87–7.89 (m, 3H, -*Ar*), 7.57 (d, J = 7.8, 2.4 Hz, 1H, 5-H), 4.22 (s, 3H, -N$^+$C*H*$_3$); ^{13}C NMR (100 MHz, 293 K, CD_3OD): δ 163.8, 148.0, 146.1,

141.4, 137.3, 136.5, 134.4, 133.2, 132.9, 131.7 (q, J = 267.0 Hz), 130.9, 127.6, 126.8, 123.8, 123.3, 120.7, 46.0; HRMS (ESI+) calcd for $C_{18}H_{14}F_3N_2OS$ $[M]^+$ = 363.0773, found 363.0756.

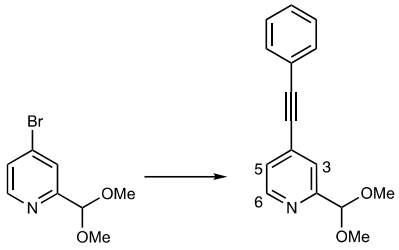

Preparation of 2-(dimethoxymethyl)-4-(phenylethynyl)pyridine: A 500-mL round-bottom flask with 4-bromo-2-(dimethoxymethyl)pyridine (5.00 g, 21.5 mmol) was purged with nitrogen gas three times, treated with $Pd(PPh_3)_2Cl_2$ (754 mg, 1.08 mmol) and CuI (205 mg, 1.08 mmol), and then purged again with nitrogen gas three times. The mixture was dissolved in anhydrous 1,4-dioxane (16 mL), Et_3N (12.0 mL, 86.0 mmol), and phenylacetylene (3.54 mL, 32.3 mmol) at 23 °C. The resulting solution was heated to 60 °C (external temperature) and stirred. After 19 h, the reaction mixture was cooled to 23 °C, concentrated *in vacuo*, and purified by flash chromatography (0 to 50% EtOAc in hexanes) on silica gel (250 mL) to afford 2-(dimethoxymethyl)-4-(phenylethynyl)pyridine (4.76 g, 87% yield) as a dark brown oil.

2-(Dimethoxymethyl)-4-(phenylethynyl)pyridine: R_f = 0.19 (30% EtOAc in hexanes); IR (neat): ν_{max} = 2981, 1737, 1599, 1591, 1539, 1492, 1442, 1403, 1366, 1239, 1211, 1192, 1132, 1111, 1091, 1057, 1026 cm^{-1}; ^1H NMR (400 MHz, 293 K, DMSO-d_6): δ 8.61 (d, J = 4.8 Hz, 1H, 6-H), 7.63 (m, 2H, -*Ph*), 7.56 (br s, 1H, 3-H), 7.51 (dd, J = 4.8, 1.2 Hz, 1H, 5-H), 7.47 (m, 3H, -*Ph*), 5.33 (s, 1H, -C*H*$(OCH_3)_2$), 3.32 (s, 6H, -CH$(OCH_3)_2$); ^{13}C NMR (100 MHz, 293 K, DMSO-d_6): 158.0, 149.8, 132.2, 131.2, 130.2, 129.3, 125.5, 122.8, 121.6, 103.8, 94.1, 87.1, 53.9; HRMS (ESI+) calcd for $C_{16}H_{16}NO_2$ $[M + H]^+$ = 254.1176, found 254.1176.

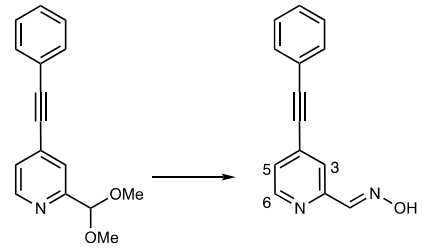

Preparation of (E)-4-(phenylethynyl)picolinaldehyde oxime: A 50-mL pear-shaped flask open to air with 2-(dimethoxymethyl)-4-(phenylethynyl)pyridine (384 mg, 1.50 mmol) was charged with H_2O (7 mL) and 5 M H_2SO_4 in H_2O (330 μL, 1.65 mmol). The solution was heated to 80 °C (external temperature). After stirring at the same temperature for 3 h, the reaction mixture was cooled to 23 °C and treated with K_2CO_3 (829 mg, 6.00 mmol) followed by MeOH (18 mL) and NH_2OH•HCl (104 mg, 1.50 mmol) at the same temperature. A reflux condenser was attached, and the reaction was heated to reflux while open to air. After 3.5 h, the reaction mixture was cooled to 23 °C and concentrated *in vacuo.* EtOAc (10 mL) was added to the crude residue, followed by saturated aqueous NH_4Cl (30 mL). The layers were separated using a separatory funnel and the aqueous layer was extracted with EtOAc (2 × 20 mL). The combined organic layers were dried over anhydrous Na_2SO_4, filtered, and concentrated *in vacuo* to afford (*E*)-4-(phenylethynyl)picolinaldehyde oxime (369 mg, quantitative yield) as a light brown solid. This material was used directly without further purification.

(E)-4-(Phenylethynyl)picolinaldehyde oxime: m.p. = 146–148 °C; R_f = 0.60 (100% EtOAc); IR (neat): ν_{max} = 3055, 2980, 2883, 2761, 2218, 1592, 1542, 1534, 1507, 1490, 1441, 1408, 1329, 1310, 1103, 1071 cm^{-1}; ^1H NMR (400 MHz, 293 K, DMSO-d_6): δ 11.82 (s, 1H, -CH=NO*H*), 8.62 (d, *J* = 4.8 Hz, 1H, 6-H), 8.09 (s, 1H, -C*H*=NOH), 7.84 (s, 1H, 3-H), 7.65–7.63 (m, 2H, -*Ph*), 7.52–7.44 (m, 4H, 5-H and -*Ph*); ^{13}C NMR (75 MHz, 293 K, DMSO-d_6): δ 153.0,

150.4, 148.8, 132.3, 132.0, 131.2, 130.3, 129.4, 125.7, 121.7, 121.6, 94.3, 86.9; HRMS (ESI+) calcd for $C_{14}H_{11}N_2O$ $[M + H]^+$ = 223.0866, found 223.0894.

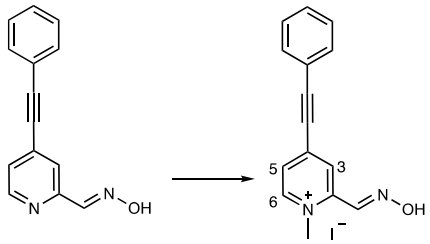

*Preparation of (E)-2-((hydroxyimino)methyl)-1-methyl-4-(phenylethynyl)pyridin-1-ium iodide (**ADG2173**):* A 10-mL sealed tube with (*E*)-4-(phenylethynyl)picolinaldehyde oxime (50 mg, 0.21 mmol) was charged with acetone (700 μL) and MeI (130 μL, 2.11 mmol). The vessel was sealed and heated to 45 °C (external temperature). After 17 h at the same temperature, the reaction mixture was cooled to 23 °C, transferred to a 10-mL round-bottomed flask, and concentrated *in vacuo* to yield (*E*)-2-((hydroxyimino)methyl)-1-methyl-4-(phenylethynyl)pyridin-1-ium iodide as a black solid (52 mg, 67% yield).

(E)-2-((Hydroxyimino)methyl)-1-methyl-4-(phenylethynyl)pyridin-1-ium iodide: m.p. = 178–180 °C; R_f = 0.55 (4:1:1 *n*-BuOH:H_2O:AcOH); IR (neat): ν_{max} = 3052, 2981, 2214, 1637, 1590, 1556, 1436, 1332, 1310, 1293, 1272, 1007 cm^{-1}; ^1H NMR (300 MHz, 293 K, DMSO-d_6): δ 13.21 (s, 1H, -CH=NO*H*), 8.98 (d, *J* = 6.4 Hz, 1H, 6-H), 8.67 (s, 1H, -C*H*=NOH), 8.40 (d, *J* = 2.0 Hz, 1H, 3-H), 8.18 (dd, *J* = 6.4, 2.0 Hz, 1H, 5-H), 7.75–7.73 (m, 2H, -*Ph*), 7.65–7.47 (m, 3H, -*Ph*), 4.33 (s, 3H, $-N^+CH_3$); ^{13}C NMR (75 MHz, 293 K, DMSO-d_6): δ 148.0, 147.1, 142.1, 138.6, 132.9, 131.7, 129.6, 129.4, 128.5, 126.7, 120.4, 102.3, 85.8, 46.6; HRMS (ESI+) calcd for $C_{15}H_{14}N_2O$ $[M]^+$ = 238.1101, found 238.1069.

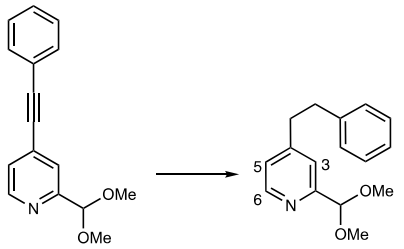

Preparation of 2-(dimethoxymethyl)-4-phenethylpyridine: A 250-mL round-bottom flask was charged with 2-(dimethoxymethyl)-4-(phenylethynyl)pyridine (1.27 g, 5.01 mmol), EtOH (84 mL), 5 wt % Pt/C (195 mg, 50.0 μmol) at 23 °C. The resulting suspension was purged with hydrogen gas three times and stirred vigorously at the same temperature for 17 h. The suspension was filtered by gravity through filter paper, and the resulting filtrate was concentrated *in vacuo* to yield 2-(dimethoxymethyl)-4-phenethylpyridine as a brown oil (720 mg, 56% yield). This material was used directly without further purification.

2-(Dimethoxymethyl)-4-phenethylpyridine: R_f = 0.18 (30% EtOAc in hexanes); IR (neat): ν_{max} = 2981, 2932, 2829, 1736, 1603, 1561, 1496, 1453, 1416, 1363, 1241, 1209, 1191, 1161, 1112, 1097, 1054 cm^{-1}; ^1H NMR (400 MHz, 293 K, DMSO-d_6): δ 8.41 (d, J = 4.8 Hz, 1H, 6-H), 7.32 (br s, 1H, 3-H), 7.27–7.14 (m, 6H, 5-H and-*Ph*), 5.24 (s, 1H, -C*H*$(OCH_3)_2$), 3.25 (s, 6H, -CH$(OCH_3)_2$), 2.95–2.87 (m, 4H, -CH_2CH_2Ph); ^{13}C NMR (75 MHz, 293 K, $CDCl_3$): δ 156.9, 151.1. 148.8, 140.4, 128.2, 128.1, 125.9, 123.5, 121.1, 103.8, 53.4, 36.9, 36.3; HRMS (ESI+) calcd for $C_{16}H_{15}NO_2$ $[M + H]^+$ = 258.1489, found 258.1509.

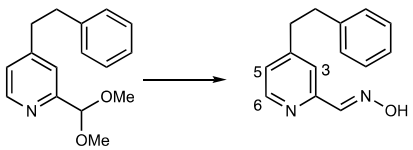

Preparation of (E)-4-phenethylpicolinaldehyde oxime: A 25-mL pear-shaped flask open to air with 2-(dimethoxymethyl)-4-phenethylpyridine (193 mg, 0.770 mmol) was charged with H_2O

(4 mL) and 5 M H_2SO_4 in H_2O (170 μL, 0.850 mmol). The solution was heated to 95 °C (external temperature). After stirring at the same temperature for 4 h, the reaction mixture was cooled to 23 °C and treated with K_2CO_3 (426 mg, 3.08 mmol) followed by MeOH (6 mL) and NH_2OH•HCl (54 mg, 0.77 mmol) at the same temperature. A reflux condenser was attached, and the reaction was heated to reflux while open to air. After 3 h, the reaction mixture was cooled to 23 °C and concentrated *in vacuo.* EtOAc (10 mL) was added to the crude residue, followed by saturated aqueous NH_4Cl (15 mL). The layers were separated using a separatory funnel and the aqueous layer was extracted with EtOAc (2 × 10 mL). The combined organic layers were dried over anhydrous Na_2SO_4, filtered, and concentrated *in vacuo* to afford (*E*)-4-phenethylpicolinaldehyde oxime (157 mg, 56% yield) as a light brown solid. This material was used directly without further purification.

(E)-4-Phenethylpicolinaldehyde oxime: m.p. = 192–195 °C; R_f = 0.20 (30% EtOAc in hexanes); IR (neat): ν_{max} = 2981, 2852, 2715, 1601, 1556, 1519, 1500, 1454, 1418, 1364, 1341, 1108 cm^{-1}; ^1H NMR (500 MHz, 293 K, DMSO-d_6): δ 11.59 (s, 1H, -CH=NO*H*), 8.43 (d, *J* = 5.0 Hz, 1H, 6-H), 8.03 (s, 1H, -C*H*=NOH), 7.63 (s, 1H, 3-H), 7.28–7.16 (m, 6H, 5-H and -*Ph*), 2.96–2.89 (m, 4H, -CH_2CH_2Ph); ^{13}C NMR (75 MHz, 293 K, DMSO-d_6): δ 152.4, 151.4, 149.7, 149.5, 141.3, 128.9, 128.7, 126.5, 124.7, 120.1, 36.5, 36.0; HRMS (ESI+) calcd for $C_{14}H_{15}N_2O$ $[M + H]^+$ = 227.1179, found 227.1206.

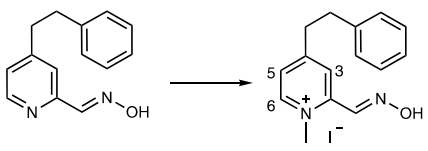

*Preparation of (E)-2-((hydroxyimino)methyl)-1-methyl-4-phenethylpyridin-1-ium iodide (**ADG2180**):* A 10-mL sealed tube with (*E*)-4-phenethylpicolinaldehyde oxime (78 mg, 0.34

mmol) was charged with acetone (1 mL) and MeI (213 μL, 3.44 mmol). The vessel was sealed and heated to 50 °C (external temperature). After 15 h at the same temperature, the reaction mixture was cooled to 23 °C, transferred to a 10-mL round-bottomed flask, and concentrated *in vacuo* to yield (*E*)-2-((hydroxyimino)methyl)-1-methyl-4-phenethylpyridin-1-ium iodide as a brown solid (125 mg, 98% yield).

(E)-2-((Hydroxyimino)methyl)-1-methyl-4-phenethylpyridin-1-ium iodide: m.p. = 160–163 °C; R_f = 0.61 (4:1:1 *n*-BuOH:H_2O:AcOH); IR (neat): ν_{max} = 3097, 2971, 1569, 1443, 1425, 1403, 1306, 1005 cm^{-1}; ^1H NMR (400 MHz, 293 K, DMSO-d_6): δ 13.03 (s, 1H, -CH=NO*H*), 8.84 (d, *J* = 6.8 Hz 1H, 6-H), 8.62 (s, 1H, -C*H*=NOH), 8.21 (d, *J* = 1.6 Hz, 1H, 3-H), 7.95 (dd, *J* = 6.8, 1.6 Hz, 1H, 5-H), 7.31–7.17 (m, 5H, -*Ph*), 4.29 (s, 3H, -N^+CH_3), 3.22 (t, *J* = 7.2, 2H, -CH_2CH_2Ph), 2.99 (t, *J* = 7.2, 2H, -CH_2CH_2Ph); ^{13}C NMR (75 MHz, 293 K, DMSO-d_6): δ 161.2, 147.0, 146.3, 142.1, 140.4, 128.9, 128.8, 127.4, 126.7, 124.9, 45.9, 36.4, 35.1; HRMS (ESI+) calcd for $C_{15}H_{17}N_2O$ $[M]^+$ = 241.1335, found 241.1361.

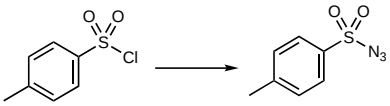

Preparation of 4-methylbenzenesulfonyl azide: A 500-mL round-bottom flask was charged with *p*-toluenesulfonyl chloride (95.6 g, 0.500 mol) and acetone (100 ml). The vessel was cooled to 0°C. A solution of sodium azide (35.7 g, 0.550 mol) in H_2O (100 mL) was added. The reaction mixture was stirred under open atmosphere and was allowed to warm to 23 °C. After 7 h, the reaction mixture was extracted with EtOAc (2 × 250 mL). The combined organic layers were dried over anhydrous Na_2SO_4, filtered, and concentrated *in vacuo* to 4-methylbenzenesulfonyl azide

(99.6 g, quantitative yield) as a colorless liquid. This material was used directly without further purification.

4-Methylbenzenesulfonyl azide: ^{1}H NMR (400 MHz, 293 K, $CDCl_3$): δ 7.85 (d, J = 8.0 Hz, 2H), 7.41 (d, J = 8.0 Hz, 2H), 2.49 (s, 3H, -CH_3). The ^{1}H NMR data for dimethyl (1-diazo-2-oxopropyl)phosphonate was consistent with those in the literature.[154]

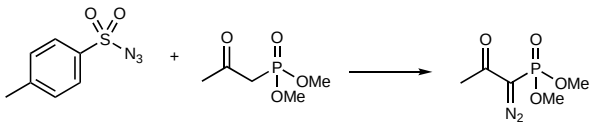

Preparation of dimethyl (1-diazo-2-oxopropyl)phosphonate: A 250-mL flame-dried, round-bottom flask with was charged with NaH (60% w/w, 1.14 g, 28.4 mmol), then evacuated and refilled with nitrogen gas three times. THF (30 mL) was added and the vessel was cooled to 0°C. A solution of dimethyl (2-oxopropyl)phosphonate (3.73 mL, 27.0 mmol) in THF (10 mL) was added in two portions, followed by THF (20 mL). A solution of 4-methylbenzenesulfonyl azide (5.32 g, 27.0 mmol) in THF (20 mL) was added to the reaction mixture. After 1 h, the reaction mixture was concentrated *in vacuo.* EtOAc (50 mL) was added to the crude residue, followed by saturated aqueous NH_4Cl (20 mL). The layers were separated using a separatory funnel and the aqueous layer was extracted with EtOAc (50 mL). The combined organic layers were dried over anhydrous Na_2SO_4, filtered, and concentrated *in vacuo*. The crude residue was purified by flash chromatography (50 to 80% EtOAc in hexanes) on silica gel (300 mL) to afford dimethyl (1-diazo-2-oxopropyl)phosphonate (3.52 g, 68% yield) as a pale yellow liquid.

Dimethyl (1-diazo-2-oxopropyl)phosphonate: ^{1}H NMR (300 MHz, 293 K, $CDCl_3$): δ 3.88 (s, 3H), 3.84 (s, 3H), 2.28 (s, 3H). The ^{1}H NMR data for dimethyl (1-diazo-2-oxopropyl)phosphonate was consistent with those in the literature.[154]

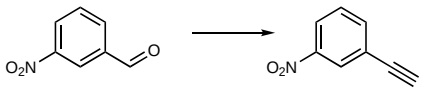

Preparation of 1-ethynyl-3-nitrobenzene: A 50-mL flame-dried, round-bottom flask with was charged with dimethyl (1-diazo-2-oxopropyl)phosphonate (1.44 g, 7.50 mmol), then evacuated and refilled with nitrogen gas three times. 3-Nitrobenzaldehyde (755mg, 5.00 mmol) and MeOH (20 mL) were added. The vessel was cooled to 0°C. K_2CO_3 (1.38 g, 10.0 mmol) was added and reaction mixture was stirred at the same temperature. After 30 min, the ice bath was removed and the reaction mixture was allowed to warm to 23 °C. After 1.5 h, the reaction mixture was concentrated *in vacuo*. EtOAc (15 mL) was added to the crude residue, followed by saturated aqueous NH_4Cl (20 mL). The layers were separated using a separatory funnel and the aqueous layer was extracted with EtOAc (2 × 15 mL). The combined organic layers were dried over anhydrous Na_2SO_4, filtered, and concentrated *in vacuo*. The crude residue was purified by flash chromatography (10 to 20% EtOAc in hexanes) on silica gel (10 mL) to afford 1-ethynyl-3-nitrobenzene (594 mg, 81% yield) as a pale yellow oil.

1-Ethynyl-3-nitrobenzene: ^{1}H NMR (300 MHz, 293 K, $CDCl_3$): δ 8.32 (br s, 1H), 8.21 (ddd, J = 8.4, 0.9, 0.9 Hz, 1H), 7.79 (dt, J = 7.5, 0.9 Hz, 1H), 7.50 (t, J = 8.4 Hz, 1H), 3.21 (s, 1H). The ^{1}H NMR data for 1-ethynyl-3-nitrobenzene was consistent with those in the literature.[155]

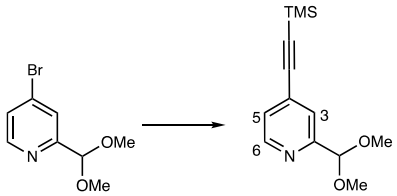

Preparation of 2-(dimethoxymethyl)-4-((trimethylsilyl)ethynyl)pyridine: A 75-mL sealed tube was charged with 4-bromo-2-(dimethoxymethyl)pyridine (2.32 g, 10.0 mmol) was flush with

argon gas, treated with $Pd(PPh_3)_2Cl_2$ (351 mg, 0.500 mmol) and CuI (95 mg, 0.50 mmol), and then flushed again with argon gas. The mixture was dissolved in anhydrous 1,4-dioxane (10 mL), Et_3N (5.54 mL, 40.0 mmol), and trimethylsilylacetylene (1.86 mL, 15.0 mmol) at 23 °C. The resulting solution was heated to 50 °C (external temperature) and stirred. After 20.5 h, the reaction mixture was cooled to 23 °C. The crude residue was dry-loaded and purified by flash chromatography (0 to 40% EtOAc in hexanes) on silica gel (250 mL). The semi-pure material was stirred with CH_2Cl_2 and Amberlite™ IRC-748 resin to remove residual copper. After 1 h, the mixture was filtered by gravity through a cotton plug and concentrated *in vacuo* to afford 2-(dimethoxymethyl)-4-((trimethylsilyl)ethynyl)pyridine (2.58 g, quantitative yield) as an amber oil.

2-(Dimethoxymethyl)-4-((trimethylsilyl)ethynyl)pyridine: R_f = 0.49 (60% EtOAc in hexanes); IR (neat): ν_{max} = 2981, 2830, 2164, 1595, 1543, 1471, 1401, 1361, 1282, 1250, 1191, 1163, 1111, 1096, 1060 cm^{-1}; ^1H NMR (400 MHz, 293 K, DMSO-d_6): δ 8.35 (d, J = 5.2 Hz, 1H, 6-H), 7.43 (br s, 1H, 3-H), 7.40 (d, J = 5.2, 1.6 Hz, 1H, 5-H), 5.30 (s, 1H, -C*H*$(OCH_3)_2$), 3.29 (s, 6H, -CH(OC*H*$_3)_2$), 0.25 (s, 9H, -Si(C*H*$_3)_3$; ^{13}C NMR (100 MHz, 293 K, DMSO-d_6): δ 157.4, 149.3, 130.4, 125.1, 122.6, 103.1, 102.0, 99.7, 53.3; HRMS (ESI+) calcd for $C_{13}H_{20}NO_2Si$ [M + H] = 250.1258, found 250.1254.

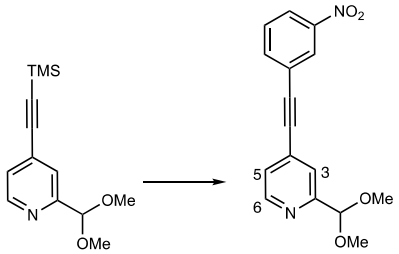

Preparation of 2-(dimethoxymethyl)-4-((3-nitrophenyl)ethynyl)pyridine: 2-(Dimethoxymethyl)-4-((3-nitrophenyl)ethynyl)pyridine was synthesized following the literature

procedure.[133] A 50-mL round-bottom flask with was charged with 3-nitrobromobenzene (809 mg, 4.00 mmol), $Pd(PPh_3)_2Cl_2$ (140 mg, 0.200 mmol), CuI (38 mg, 0.20 mmol), and K_2CO_3 (1.66 g, 12.0 mmol), and then evacuated and refilled with nitrogen gas three times. THF (6 mL) was added and the mixture was stirred. A solution of 2-(dimethoxymethyl)-4-((trimethylsilyl)ethynyl)pyridine (1.50 g, 6.00 mmol) in THF (4 mL)/MeOH (5 mL) was added over 30 min. The resulting solution was heated to 57 °C (external temperature) and stirred. After 17 h, the reaction mixture was cooled to 23 °C and concentrated *in vacuo*. H_2O (20 mL) was added to the crude residue, followed by CH_2Cl_2 (15 mL). The layers were separated using a separatory funnel and the aqueous layer was extracted with CH_2Cl_2 (2 × 15 mL). The crude residue was purified by flash chromatography (15 to 50% EtOAc in hexanes) on silica gel (100 mL). The semi-pure material was stirred with CH_2Cl_2 and Amberlite™ IRC-748 resin to remove residual copper. After 1 h, the mixture was filtered by gravity through a cotton plug and concentrated *in vacuo* to afford 2-(dimethoxymethyl)-4-((3-nitrophenyl)ethynyl)pyridine (835 mg, 47% yield) as a brown solid.

2-(Dimethoxymethyl)-4-((3-nitrophenyl)ethynyl)pyridine: m.p. = 90–92 °C; R_f = 0.33 (60% EtOAc in hexanes); IR (neat): ν_{max} = 2964, 2917, 2219, 1596, 1530, 1349, 1197, 1113, 1047 cm^{-1}; ^1H NMR (300 MHz, 293 K, $CDCl_3$): δ 8.64 (d, *J* = 5.1 Hz, 1H, 6-H), 8.39 (t, *J* = 1.8 Hz, 1H, -*Ph*), 8.39 (ddd, *J* = 8.4, 2.4, 1.2 Hz, 1H, -*Ph*), 7.83 (dt, *J* = 7.8, 1.2 Hz, 1H, -*Ph*), 7.69 (br s, 1H, 3-H), 7.57 (app t, *J* = 8.1, 1H, -*Ph*), 7.36 (dd, *J* = 5.1,1.5 Hz, 1H, 5-H), 5.40 (s, 1H, -C*H*$(OCH_3)_2$), 3.43 (s, 6H, -CH(OC*H*$_3)_2$); ^{13}C NMR (100 MHz, 293 K, $CDCl_3$): δ 157.7, 149.5, 148.2, 137.5, 131.0, 129.7, 126.8, 125.2, 123.9, 123.8, 123.5, 103.4, 91.0, 89.0, 53.7; HRMS (ESI+) calcd for $C_{16}H_{15}N_2O_4$ [M + H] = 299.1026, found 299.1030.

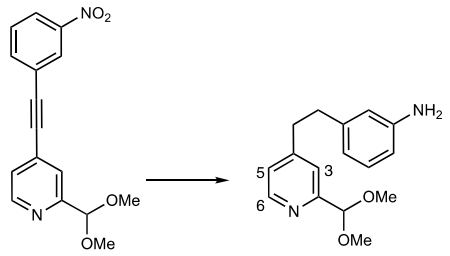

Preparation of 3-(2-(2-(dimethoxymethyl)pyridin-4-yl)ethyl)aniline: A 100-mL round-bottom flask was charged with 2-(dimethoxymethyl)-4-((3-nitrophenyl)ethynyl)pyridine (834 mg, 2.79 mmol), EtOH (27 mL), PtO_2 (32 mg, 0.14 mmol) at 23 °C. The resulting suspension was purged with hydrogen gas three times and stirred vigorously at the same temperature for 5 d. EtOH (10 mL) and PtO_2 (19 mg, 0.080 mmol) at 23 °C were added. The resulting suspension was purged with hydrogen gas three times and stirred vigorously at the same temperature for 24 h. The suspension was filtered by gravity through filter paper, and the resulting filtrate was concentrated *in vacuo* to yield 3-(2-(2-(dimethoxymethyl)pyridin-4-yl)ethyl)aniline (710 mg, 93% yield) as a dark brown oil.

3-(2-(2-(Dimethoxymethyl)pyridin-4-yl)ethyl)aniline: R_f = 0.13 (60% EtOAc in hexanes); IR (neat): ν_{max} = 3354, 3220, 2981, 2830, 1708, 1602, 1561, 1493, 1460, 1417, 1363, 1296, 1191, 1163, 1113, 1096, 1055, 983 cm^{-1}; ^1H NMR (300 MHz, 293 K, $CDCl_3$): δ 8.56 (d, J = 5.1 Hz, 1H, 6-H), 7.37 (br s, 1H, 3-H), 7.07–7.02 (m, 2H, -*Ar*), 6.56–6.48 (m, 3H, -*Ar*), 5.35 (s, 1H, -C*H*$(OCH_3)_2$), 3.39 (s, 6H, -CH(OC*H*$_3)_2$), 2.94–2.79 (m, 4H, -C*H*$_2$C*H*$_2$Ph); ^{13}C NMR (100 MHz, 293 K, $CDCl_3$): δ 156.9, 151.6, 148.9, 146.5, 141.9, 129.3, 123.7, 121.2, 118.6, 115.1, 113.0, 103.9, 53.7, 37.0, 36.5; HRMS (ESI+) calcd for $C_{16}H_{21}N_2O_2$ [M + H] = 273.1597, found 273.1596.

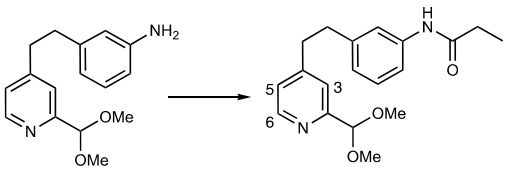

Preparation of N-(3-(2-(2-(dimethoxymethyl)pyridin-4-yl)ethyl)phenyl)propionamide: A 50-mL round-bottom flask was charged with 3-(2-(2-(dimethoxymethyl)pyridin-4-yl)ethyl)aniline (658 mg, 2.42 mmol), then evacuated and refilled with nitrogen gas three times. CH_2Cl_2 (15 mL), propionic anhydride (0.34 mL, 2.7 mmol), and Et_3N (0.37 mL, 2.7 mmol). The reaction mixture was stirred at 23 °C. After 1 h, saturated aqueous $NaHCO_3$ (15 mL) was added to the reaction mixture. The layers were separated using a separatory funnel and the aqueous layer was extracted with CH_2Cl_2 (2 × 15 mL). The crude residue was purified by flash chromatography (70 to 100% EtOAc in hexanes) on silica gel (40 mL) to afford *N*-(3-(2-(2-(dimethoxymethyl)pyridin-4-yl)ethyl)phenyl)propionamide (585 mg, 74% yield) as an amber oil.

N-(3-(2-(2-(dimethoxymethyl)pyridin-4-yl)ethyl)phenyl)propionamide: R_f = 0.25 (100% EtOAc); IR (neat): ν_{max} = 3299, 2981, 2830, 1665, 1605, 1549, 1488, 1439, 1362, 1304, 1265, 1193, 1163, 1114, 1098, 1058, 984 cm^{-1}; ^1H NMR (400 MHz, 293 K, DMSO-d_6): δ 9.76 (s, 1H, NH), 8.41 (d, J = 2.8 Hz, 1H, 6-H), 7.45 (br s, 1H, 3-H), 7.38 (d, J = 8.0 Hz, 1H, -*Ph*), 7.30 (br s, 1H, -*Ph*), 7.23 (dd, J = 5.2, 1.2 Hz, 1H, 5-H), 7.16 (d, J = 7.6 Hz, 1H, -*Ph*), 6.87 (d, J = 7.6 Hz, 1H, -*Ph*), 5.23 (s, 1H, -C*H*$(OCH_3)_2$), 3.25 (s, 6H, -CH$(OCH_3)_2$), 2.93–2.82 (m, 4H, -CH_2CH_2Ph), 2.28 (q, J = 7.6 Hz, 2H, -C$H_2$$CH_3$), 1.06 (t, J = 7.6 Hz, 3H, -CH_2CH_3); ^{13}C NMR (100 MHz, 293 K, DMSO-d_6): δ 172.3, 157.3, 151.3, 149.0, 141.7, 139.8, 128.9, 124.3, 123.5, 121.4, 119.5, 117.3, 104.4, 53.7, 36.6, 36.4, 29.9, 10.2; HRMS (ESI+) calcd for $C_{19}H_{25}N_2O_3$ [M + H] = 329.1865, found 329.1858.

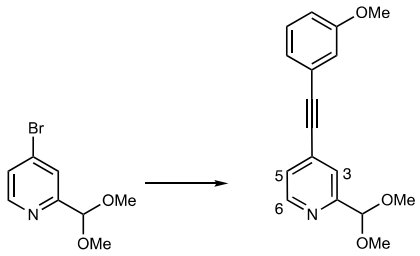

Preparation of 2-(dimethoxymethyl)-4-((3-methoxyphenyl)ethynyl)pyridine: A 25-mL round-bottom flask with 4-bromo-2-(dimethoxymethyl)pyridine (764 mg, 3.29 mmol) was purged with nitrogen gas three times, treated with $Pd(PPh_3)_2Cl_2$ (123 mg, 0.180 mmol) and CuI (33 mg, 0.18 mmol), and then purged again with nitrogen gas three times. The mixture was dissolved in anhydrous 1,4-dioxane (4 mL), Et_3N (1.82 mL, 13.1 mmol), and 3-ethynylanisole (630 μL, 4.97 mmol) at 23 °C. The resulting solution was heated to 55 °C (external temperature) and stirred. After 17 h, the reaction mixture was cooled to 23 °C. The crude residue was dry-loaded and purified by flash chromatography (0 to 50% EtOAc in hexanes) on silica gel (90 mL). The semi-pure material was stirred with H_2O (25 mL) and Diaion® CR20 resin to remove residual copper. After 1.7 h, the mixture was filtered by gravity through a cotton plug. EtOAc (30 mL) was added to the aqueous solution. The layers were separated using a separatory funnel and the aqueous layer was extracted with EtOAc (10 mL). The combined organic layers were dried over anhydrous Na_2SO_4, filtered, and concentrated *in vacuo* to afford 2-(dimethoxymethyl)-4-((3-methoxyphenyl)ethynyl)pyridine (868 mg, 93% yield) as a dark brown oil.

2-(Dimethoxymethyl)-4-((3-methoxyphenyl)ethynyl)pyridine: R_f = 0.45 (60% EtOAc in hexanes); IR (neat): ν_{max} = 2936, 2831, 2211, 1596, 1574, 1541, 1489, 1463, 1421, 1361, 1323, 1283, 1243, 1194, 1178, 1159, 1110, 1095, 1047 cm^{-1}; ^1H NMR (400 MHz, 293 K, DMSO-d_6): δ 8.61 (d, J = 4.8 Hz, 1H, 6-H), 7.57 (s, 1H, -*Ph*), 7.51 (dd, J = 4.8, 1.6 Hz, 1H, 5-H), 7.47 (t, J = 8.0 Hz, 1H, -*Ph*), 7.21–7.19 (m, 2H, -*Ar*), 7.07–7.04 (m, 1H, -*Ph*), 5.33 (s, 1H, -C*H*$(OCH_3)_2$), 3.79

(s, 3H, -OCH_3), 3.31 (s, 6H, -CH(OCH_3)$_2$); ^{13}C NMR (100 MHz, 293 K, DMSO-d_6): δ 159.6, 157.9, 149.8, 131.1, 130.5, 125.5, 124.6, 122.8, 122.6, 116.9, 116.8, 103.8, 94.1, 84.9, 55.7, 53.9; HRMS (ESI+) calcd for $C_{17}H_{18}NO_3$ $[M + H]^+$ = 284.1281, found 284.1280.

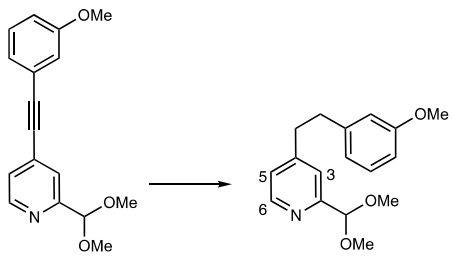

Preparation of 2-(dimethoxymethyl)-4-(3-methoxyphenethyl)pyridine: A 100-mL round-bottom flask was charged with 2-(dimethoxymethyl)-4-((3-methoxyphenyl)ethynyl)pyridine (474 mg, 1.67 mmol), EtOAc (20 mL), 10 wt % Pt/C (180 mg, 0.170 mmol) at 23 °C. The resulting suspension was purged with hydrogen gas three times and stirred vigorously at the same temperature for 7 h. The suspension was filtered by gravity through filter paper. The resulting filtrate was concentrated *in vacuo* and purified by flash chromatography (50 to 80% EtOAc in hexanes) on silica gel (35 mL) to yield 2-(dimethoxymethyl)-4-(3-methoxyphenethyl)pyridine as an amber oil (297 mg, 62% yield).

2-(Dimethoxymethyl)-4-(3-methoxyphenethyl)pyridine: R_f = 0.23 (60% EtOAc in hexanes); IR (neat): ν_{max} = 2984, 2831, 1592, 1562, 1465, 1455, 1426, 1327, 1300, 1262, 1247, 1183, 1162, 1112, 1092, 1051, 1012 cm^{-1}; ^{1}H NMR (400 MHz, 293 K, acetone-d_6): δ 8.41 (d, J = 4.8 Hz, 1H, 6-H), 7.32 (br s, 1H, 3-H), 7.20–7.15 (m, 2H, *Ph*), 6.82–6.79 (m, 2H, *Ph*), 6.76–6.73 (m, 1H, 5-H), 5.24 (s, 1H, -C*H*(OCH$_3$)$_2$), 3.75 (s, 3H, -OCH_3), 3.31 (s, 6H, -CH(OCH_3)$_2$), 3.00–2.90 (m, 4H, -CH_2CH_2Ph); ^{13}C NMR (100 MHz, 293 K, acetone-d_6): δ 160.8, 158.5, 151.8, 149.5, 143.5, 133.9,

130.6, 130.1, 124.5, 121.9, 121.6, 115.0, 112.3, 105.6, 55.3, 53.9, 53.8, 37.6, 37.3; HRMS (ESI+) calcd for $C_{17}H_{22}NO_3$ $[M + H]^+$ = 288.1594, found 288.1592.

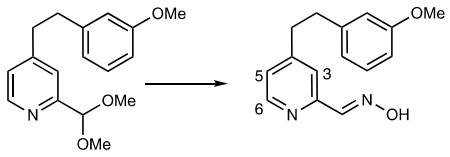

Preparation of (E)-4-(3-methoxyphenethyl)picolinaldehyde oxime: A 25-mL pear-shaped flask open to air with 2-(dimethoxymethyl)-4-(3-methoxyphenethyl)pyridine (179 mg, 0.620 mmol) was charged with H_2O (2 mL) and 5 M H_2SO_4 in H_2O (130 μL, 0.680 mmol). The solution was heated to 90 °C (external temperature). After stirring at the same temperature for 2.8 h, the reaction mixture was cooled to 23 °C and treated with K_2CO_3 (343 mg, 2.48 mmol) followed by MeOH (7 mL) and NH_2OH•HCl (43 mg, 0.62 mmol) at the same temperature. A reflux condenser was attached, and the reaction was heated to reflux while open to air. After 2.5 h, the reaction mixture was cooled to 23 °C and concentrated *in vacuo.* EtOAc (15 mL) was added to the crude residue, followed by saturated aqueous NH_4Cl (20 mL). The layers were separated using a separatory funnel and the aqueous layer was extracted with EtOAc (2 × 10 mL). The combined organic layers were dried over anhydrous Na_2SO_4, filtered, and concentrated *in vacuo* to afford (*E*)-4-(3-methoxyphenethyl)picolinaldehyde oxime (117 mg, 74% yield) as a white solid. This material was used directly without further purification.

(E)-4-(3-Methoxyphenethyl)picolinaldehyde oxime: m.p. = 147–150 °C; R_f = 0.50 (60% EtOAc in hexanes); IR (neat): ν_{max} = 2980, 2889, 2836, 2729, 1602, 1583, 1556, 1516, 1491, 1454, 1436, 1417, 1320, 1264, 1150, 1049 cm^{-1}; ^1H NMR (400 MHz, 293 K, CD_3OD): δ 8.35 (d, J = 5.2 Hz, 1H, 6-H), 8.06 (s, 1H, -C*H*=NOH), 7.68 (s, 1H, -*Ar*), 7.22–7.14 (m, 2H, -*Ar*), 6.75–6.72 (m, 3H, -*Ar*), 3.74 (s, 3H, -OCH_3), 3.00–2.90 (m, 4H, -CH_2CH_2Ph); ^{13}C NMR (100 MHz, 293 K,

CD_3OD): δ 161.2, 153.8, 153.2, 149.7, 149.4, 143.5, 130.4, 125.7, 122.0, 121.8, 115.1, 112.6, 55.5, 37.9, 37.4; HRMS (ESI+) calcd for $C_{15}H_{17}N_2O_2$ [M + H] = 257.1285, found 257.1272.

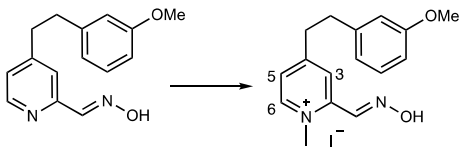

*Preparation of (E)-2-((hydroxyimino)methyl)-4-(3-methoxyphenethyl)-1-methylpyridin-1-ium iodide (**ADG4063**):* A 35-mL sealed tube with (*E*)-4-(3-methoxyphenethyl)picolinaldehyde oxime (88 mg, 0.34 mmol) was charged with acetone (2 mL) and MeI (210 μL, 3.40 mmol). The vessel was sealed and heated to 55 °C (external temperature). After 20.5 h at the same temperature, the reaction mixture was cooled to 23 °C, transferred to a 10-mL round-bottomed flask and concentrated *in vacuo* to yield (*E*)-2-((hydroxyimino)methyl)-4-(3-methoxyphenethyl)-1-methylpyridin-1-ium iodide as an orange solid (127 mg, 94% yield).

(E)-2-((Hydroxyimino)methyl)-4-(3-methoxyphenethyl)-1-methylpyridin-1-ium iodide: m.p. = 169–172 °C; R_f = 0.08 (5% MeOH in CH_2Cl_2); IR (neat): ν_{max} = 3151, 2998, 1635, 1604, 1574, 1484, 1446, 1292, 1259, 1143, 1048 cm^{-1}; ^1H NMR (300 MHz, 293 K, DMSO-d_6): δ 13.01 (s, 1H, -CH=NO*H*), 8.83 (d, *J* = 6.3 Hz, 1H, 6-H), 8.62 (s, 1H, -C*H*=NOH), 8.22 (d, *J* = 1.8 Hz, 1H, 3-H), 7.54 (dd, *J* = 6.3, 1.8 Hz, 1H, 5-H), 7.19 (t, *J* = 8.1 Hz, 1H, -*Ph*), 6.86–6.75 (m, 3H, -*Ph*), 4.29 (s, 3H, -N^+CH_3), 3.73 (s, 3H, -OCH_3), 3.22 (t, *J* = 7.2 Hz, 2H, -CH_2CH_2Ph), 2.96 (t, *J* = 7.2 Hz, 2H, -CH_2CH_2Ph); ^{13}C NMR (100 MHz, 293 K, DMSO-d_6): δ 161.2, 159.8, 147.0, 146.5, 146.3, 142.2, 142.0, 129.9, 127.4, 124.9, 121.1, 114.6, 112.1, 55.4, 45.9, 36.3, 35.1; HRMS (ESI+) calcd for $C_{16}H_{19}N_2O_2$ $[M]^+$ = 271.1441, found 271.1449.

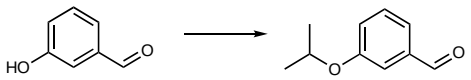

Preparation of 3-isopropoxybenzaldehyde: 3-Isopropoxybenzaldehyde was synthesized following the literature procedure.[134] A 100-mL round-bottomed flask was charged with 3-hydroxybenzaldehyde (5.60 g, 45.9 mmol), K_2CO_3 (20.00 g, 145.0 mmol), and isopropanol (50 mL). A reflux condenser was attached, and the reaction was heated to reflux. After 2 d, the reaction mixture was cooled to 23 °C and concentrated *in vacuo.* EtOAc (40 mL) was added to the crude residue, followed by saturated aqueous NH_4Cl (40 mL). The layers were separated using a separatory funnel and the aqueous layer was extracted with EtOAc (2 × 40 mL). The combined organic layers were dried over anhydrous Na_2SO_4, filtered, and concentrated *in vacuo* to afford an inseparable mixture (3:1) of and 3-isopropoxybenzaldehyde (5.74 g, 76% yield) and 3-hydroxybenzaldehyde as a pale yellow oil. This material was used directly without further purification.

3-Isopropoxybenzaldehyde: ^{1}H NMR (400 MHz, 293 K, $CDCl_3$): δ 9.96 (s, 1H, -C*H*O), 7.45–7.38 (m, 3H), 7.19–7.13 (m, 1H), 4.63 (sept, J = 6.0 Hz, 1H, -OC*H*$(CH_3)_2$), 1.36 (d, J = 6.0, 6H, -OCH(C*H*$_3)_2$). The ^{1}H NMR data for 3-isopropoxybenzaldehyde was consistent with those in the literature. [134, 155 143,125 143,125156]

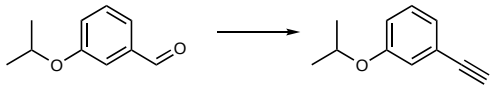

Preparation of 1-ethynyl-3-isopropoxybenzene: A 50-mL flame-dried, round-bottom flask with was charged with dimethyl (1-diazo-2-oxopropyl)phosphonate (1.00 g, 5.20 mmol), then evacuated and refilled with nitrogen gas three times. MeOH (15 mL) was added and the vessel was cooled to 0°C. 3-Isopropoxybenzaldehyde (500 mg, 3.47 mmol) in MeOH (5 mL) was added,

followed by K_2CO_3 (959 mg, 6.94 mmol). The reaction mixture was stirred at the same temperature. After 1 h, the ice bath was removed and the reaction mixture was allowed to warm to 23 °C. After 18.5 h, the reaction mixture was concentrated *in vacuo.* EtOAc (15 mL) was added to the crude residue, followed by saturated aqueous NH_4Cl (25 mL). The layers were separated using a separatory funnel and the aqueous layer was extracted with EtOAc (2 × 10 mL). The combined organic layers were dried over anhydrous Na_2SO_4, filtered, and concentrated *in vacuo*. The crude residue was purified by flash chromatography (0 to 30% EtOAc in hexanes) on silica gel (30 mL) to afford 1-ethynyl-3-isopropoxybenzene (249 mg, 45% yield) as a pale yellow oil.

1-Ethynyl-3-isopropoxybenzene: ^{1}H NMR (300 MHz, 293 K, $CDCl_3$): δ 7.20 (t, J = 7.8 Hz, 1H), 7.07–7.00 (m, 2H), 6.89 (ddd, J = 7.8, 2.4, 0.9 Hz, 1H), 4.54 (sept, J = 6.0, 1H, -OC*H*$(CH_3)_2$), 3.04 (s, 1H, -C*H*), 1.33 (d, J = 6.0, 6H, -OCH(C*H*$_3)_2$). The ^{1}H NMR data for 1-ethynyl-3-isopropoxybenzene was consistent with those in the literature.[157]

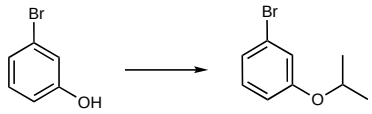

Preparation of 1-bromo-3-isopropoxybenzene: A 25-mL round-bottomed flask was charged with dimethylformamide (5 mL), K_2CO_3 (941 mg, 6.81 mmol), 3-bromophenol (1.07 g, 6.19 mmol), and 2-iodopropane (3.10 mL, 30.9 mmol). The reaction mixture was stirred at 23 °C. After 40 h, the reaction mixture was extracted with EtOAc (2 × 40 mL). The combined organic layers were washed with H_2O (3 × 30 mL), dried over anhydrous Na_2SO_4, filtered, and concentrated *in vacuo* to afford 1-bromo-3-isopropoxybenzene as a pale yellow oil (929 mg, 69% yield).

1-Bromo-3-isopropoxybenzene: ^{1}H NMR (300 MHz, 293 K, $CDCl_3$): δ 7.09 (t, J = 8.2 Hz, 1H), 7.04–7.00 (m, 2H), 6.78 (ddd, J = 8.0, 2.3, 1.1 Hz, 1H), 4.50 (sept, J = 6.3, 1H, -OC*H*$(CH_3)_2$), 1.31 (d, J = 6.3, 6H, -OCH(C*H*$_3)_2$). The ^{1}H NMR data for 1-bromo-3-isopropoxybenzene was consistent with those in the literature.[158]

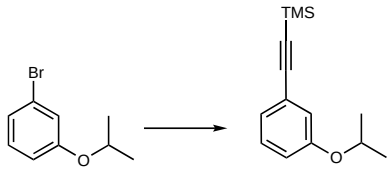

Preparation of ((3-isopropoxyphenyl)ethynyl)trimethylsilane: A 75-mL sealed tube with 1-bromo-3-isopropoxybenzene (1.53 g, 7.00 mmol) was flushed with argon gas, treated with $Pd(PPh_3)_2Cl_2$ (246 mg, 0.350 mmol) and CuI (67 mg, 0.35 mmol), and then flushed again with argon gas. The mixture was dissolved in anhydrous 1,4-dioxane (7 mL), Et_3N (3.90 mL, 28.0 mmol), and trimethylsilylacetylene (1.50 mL, 10.5 mmol) at 23 °C. The resulting solution was heated to 55 °C (external temperature) and stirred. After 21 h, the reaction mixture was cooled to 23 °C. The crude residue was dry-loaded and purified by flash chromatography (0 to 20% EtOAc in hexanes) on silica gel (50 mL). The semi-pure material was stirred with H_2O (20 mL) and Diaion® CR20 resin to remove residual copper. After 1 h, the mixture was filtered by gravity through a cotton plug. EtOAc (10 mL) was added to the aqueous solution. The layers were separated using a separatory funnel and the aqueous layer was extracted with EtOAc (10 mL). The combined organic layers were dried over anhydrous Na_2SO_4, filtered, and concentrated *in vacuo* to afford ((3-isopropoxyphenyl)ethynyl)trimethylsilane (1.47 g, 91% yield) as an amber oil.

((3-Isopropoxyphenyl)ethynyl)trimethylsilane: ^{1}H NMR (400 MHz, 293 K, $CDCl_3$): δ 7.19 (t, J = 7.6 Hz, 1H), 7.04 (dt, J = 7.6, 1.2 Hz, 1H), 6.99 (t, J = 1.2 Hz, 1H), 6.86 (ddd, J = 7.6, 2.4,

0.8 Hz, 1H), 4.54 (sept, J = 6.0, 1H, -OC*H*(CH_3)$_2$), 1.33 (d, J = 6.0, 6H, -OCH(C*H*$_3$)$_2$), 0.26 (s, 9H, -Si(C*H*$_3$)$_3$.

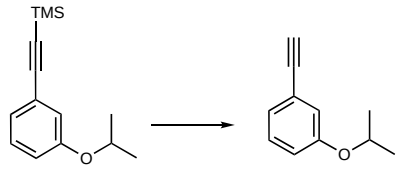

Preparation of 1-ethynyl-3-isopropoxybenzene: A 50-mL round-bottomed flask was charged with ((3-isopropoxyphenyl)ethynyl)trimethylsilane (702 mg, 3.02 mmol), K_2CO_3 (626 mg, 4.53 mmol), and MeOH (20 mL). The mixture was stirred at 23 °C. After 1.7 h, the reaction mixture was cooled concentrated *in vacuo.* EtOAc (10 mL) was added to the crude residue, followed by saturated aqueous NH_4Cl (20 mL). The layers were separated using a separatory funnel and the aqueous layer was extracted with EtOAc (15 mL). The combined organic layers were dried over anhydrous Na_2SO_4, filtered, and concentrated *in vacuo* to afford 1-ethynyl-3-isopropoxybenzene (394 mg, 81% yield) as a colorless oil. This material was used directly without further purification.

1-Ethynyl-3-isopropoxybenzene: ^{1}H NMR (300 MHz, 293 K, $CDCl_3$): δ 7.21 (t, J = 7.8 Hz, 1H), 7.06 (d, J = 7.8, 1H), 7.01 (t, J = 2.1 Hz, 1H), 6.89 (ddd, J = 7.8, 2.4, 0.9 Hz, 1H), 4.54 (sept, J = 6.0, 1H, -OC*H*(CH_3)$_2$), 3.05 (s, 1H, -C*H*), 1.33 (d, J = 6.0, 6H, -OCH(C*H*$_3$)$_2$). The ^{1}H NMR data for 1-ethynyl-3-isopropoxybenzene was consistent with those in the literature.[157]

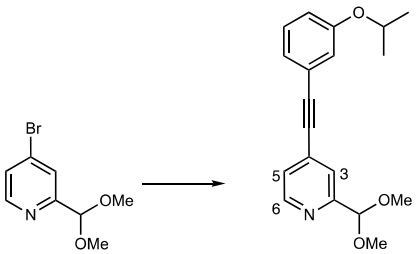

Preparation of 2-(dimethoxymethyl)-4-((3-isopropoxyphenyl)ethynyl)pyridine: A 10-mL round-bottom flask with 4-bromo-2-(dimethoxymethyl)pyridine (336 mg, 1.44 mmol) was purged with nitrogen gas three times, treated with $Pd(PPh_3)_2Cl_2$ (51 mg, 0.72 mmol) and CuI (7 mg, 0.4 mmol), and then purged again with nitrogen gas three times. The mixture was dissolved in anhydrous 1,4-dioxane (2 mL), Et_3N (630 μL, 4.89 mmol), and 1-ethynyl-3-isopropoxybenzene (394 mg, 2.46 mmol) at 23 °C. The resulting solution was heated to 55 °C (external temperature) and stirred. After 17 h, the reaction mixture was cooled to 23 °C. The crude residue was dry-loaded and purified by flash chromatography (0 to 40% EtOAc in hexanes) on silica gel (40 mL). The semi-pure material was stirred with H_2O (15 mL) and Diaion® CR20 resin to remove residual copper. After 1 h, the mixture was filtered by gravity through a cotton plug. EtOAc (10 mL) was added to the aqueous solution. The layers were separated using a separatory funnel and the aqueous layer was extracted with EtOAc (10 mL). The combined organic layers were dried over anhydrous Na_2SO_4, filtered, and concentrated *in vacuo* to afford 2-(dimethoxymethyl)-4-((3-isopropoxyphenyl)ethynyl)pyridine (483 mg, quantitative yield) as an amber brown oil.

2-(Dimethoxymethyl)-4-((3-isopropoxyphenyl)ethynyl)pyridine: R_f = 0.44 (60% EtOAc in hexanes); IR (neat): ν_{max} = 2978, 2932, 2831, 2215, 1597, 1572, 1487, 1466, 1452, 1426, 1383, 1361, 1321, 1281, 1240, 1190, 1159, 1111, 1096, 1058 cm^{-1}; ^1H NMR (400 MHz, 293 K, acetone-d_6): δ 8.59 (d, J = 4.8 Hz, 1H, 6-H), 7.60 (br s, 1H, 3-H), 7.44 (dd, J = 4.8, 1.6 Hz, 1H, 5-H), 7.34 (t, J = 8.0 Hz, 1H, -*Ph*), 7.17–7.15 (m, 2H, -*Ph*), 7.02 (ddd, J = 8.0, 2.4, 0.8 Hz, 1H, -*Ph*), 5.31 (s, 1H, -C*H*$(OCH_3)_2$), 4.69 (sept, J = 6.0, 1H, -OC*H*$(CH_3)_2$), 3.38 (s, 6H, -CH(OC*H*$_3)_2$), 1.31 (d, J = 6.0, 6H, -OCH(C*H*$_3)_2$); ^{13}C NMR (100 MHz, 293 K, acetone-d_6): δ 158.3, 158.0, 149.2, 131.3, 129.9, 124.9, 123.9, 123.0, 122.6, 118.5, 117.6, 104.1, 93.4, 86.2, 69.7, 53.0, 21.3; HRMS (ESI+) calcd for $C_{19}H_{22}NO_3$ $[M + H]^+$ = 312.1594, found 312.1585.

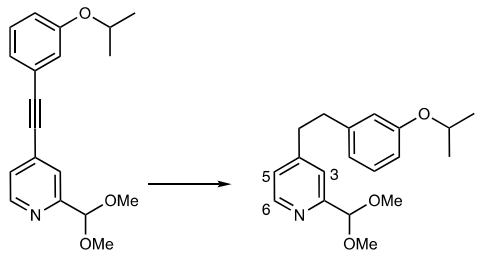

Preparation of 2-(dimethoxymethyl)-4-(3-isopropoxyphenethyl)pyridine: A 100-mL round-bottom flask was charged with 2-(dimethoxymethyl)-4-((3-isopropoxyphenyl)ethynyl)pyridine (315 g, 1.01 mmol), EtOAc (20 mL), 10 wt % Pt/C (108 mg, 0.100 mmol) at 23 °C. The resulting suspension was purged with hydrogen gas three times and stirred vigorously at the same temperature for 18 h. The suspension was filtered by gravity through filter paper, and the resulting filtrate was concentrated *in vacuo* to yield 2-(dimethoxymethyl)-4-(3-isopropoxyphenethyl)pyridine as an amber oil (252 mg, 80% yield). This material was used directly without further purification.

2-(Dimethoxymethyl)-4-(3-isopropoxyphenethyl)pyridine: R_f = 0.32 (60% EtOAc in hexanes); IR (neat): ν_{max} = 2978, 2932, 2831, 2215, 1602, 1581, 1561, 1486, 1443, 1416, 1383, 1364, 1256, 1183, 1156, 1137, 1113, 1098, 1056 cm^{-1}; ^1H NMR (400 MHz, 293 K, $CDCl_3$): δ 8.49 (d, J = 5.2 Hz, 1H, 6-H), 7.37 (br s, 1H, 3-H), 7.17 (app t, J = 8.0 Hz, 1H, -*Ph*), 7.05 (dd, J = 5.2, 1.6 Hz, 1H, 5-H), 6.74–6.68 (m, 3H, -*Ph*), 5.35 (s, 1H, -C*H*$(OCH_3)_2$), 4.51 (sept, J = 6.0, 1H, -OC*H*$(CH_3)_2$), 3.40 (s, 6H, -CH(OC*H*$_3)_2$), 2.97–6.87 (m, 4H, -C*H*$_2$C*H*$_2$Ph), 1.31 (d, J = 6.0, 6H, -OCH(C*H*$_3)_2$); ^{13}C NMR (100 MHz, 293 K, $CDCl_3$): δ 158.0, 157.1, 151.4, 149.1, 142.3, 129.4, 123.8, 121.3, 120.6, 116.3, 113.4, 104.1, 69.7, 53.7, 37.1, 36.6, 22.1; HRMS (ESI+) calcd for $C_{19}H_{26}NO_3$ $[M + H]^+$ = 316.1907, found 316.1907.

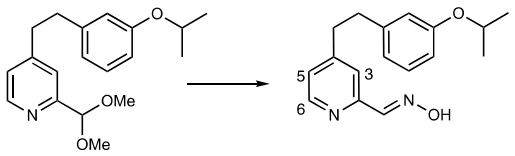

Preparation of (E)-4-(3-isopropoxyphenethyl)picolinaldehyde oxime: A 25-mL pear-shaped flask open to air with 2-(dimethoxymethyl)-4-(3-isopropoxyphenethyl)pyridine (153 mg, 0.490 mmol) was charged with H_2O (2 mL) and 5 M H_2SO_4 in H_2O (110 μL, 0.530 mmol). The solution was heated to 85 °C (external temperature). After stirring at the same temperature for 5 h, the reaction mixture was cooled to 23 °C and treated with K_2CO_3 (270 mg, 1.96 mmol) followed by MeOH (6 mL) and NH_2OH•HCl (34 mg, 0.49 mmol) at the same temperature. A reflux condenser was attached, and the reaction was heated to reflux while open to air. After 2.5 h, the reaction mixture was cooled to 23 °C and concentrated *in vacuo.* EtOAc (10 mL) was added to the crude residue, followed by saturated aqueous NH_4Cl (15 mL). The layers were separated using a separatory funnel and the aqueous layer was extracted with EtOAc (2 × 10 mL). The combined organic layers were dried over anhydrous Na_2SO_4, filtered, and concentrated *in vacuo* to afford (*E*)-4-(3-isopropoxyphenethyl)picolinaldehyde oxime (144 mg, quantitative yield) as a light tan solid. This material was used directly without further purification.

(E)-4-(3-Isopropoxyphenethyl)picolinaldehyde oxime: m.p. = 153–155 °C; R_f = 0.50 (60% EtOAc in hexanes); IR (neat): ν_{max} = 2973, 1602, 1579, 1486, 1453, 1384, 1261, 1110 cm^{-1}; ^1H NMR (400 MHz, 293 K, DMSO-d_6): δ 11.63 (s, 1H, -CH=NO*H*), 8.44 (d, *J* = 5.2 Hz, 1H, 6-H), 8.03 (s, 1H, -C*H*=NOH), 7.63 (s, 1H, -*Ar*), 6.90 (dd, *J* = 5.2, 1.2 Hz, 1H, -*Ar*), 7.15 (t, *J* = 8.0 Hz, 1H, -*Ar*), 6.77–6.75 (m, 2H, -*Ph*), 6.70 (d, *J* = 8.0 Hz, 1H, -*Ar*), 4.55 (sept, *J* = 6.0, 1H, -OC*H*$(CH_3)_2$), 2.94–2.84 (m, 4H, -CH_2CH_2Ph), 1.22 (d, *J* = 6.0, 6H, -OCH(CH_3)$_2$); ^{13}C NMR (100 MHz, 293 K, DMSO-d_6): δ 157.9, 152.5, 151.4, 149.6, 149.4, 142.9, 129.8, 124.6, 120.9, 120.1, 116.3, 113.7, 69.3, 36.4, 36.0, 22.3; HRMS (ESI+) calcd for $C_{17}H_{21}N_2O_2$ [M + H] = 285.1597,

found 285.1599.

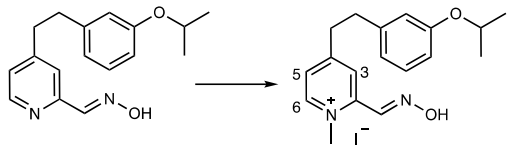

*Preparation of (E)-2-((hydroxyimino)methyl)-4-(3-isopropoxyphenethyl)-1-methylpyridin-1-ium iodide (**ADG4111**):* A 35-mL sealed tube with (*E*)-4-(3-isopropoxyphenethyl)picolinaldehyde oxime (77 mg, 0.27 mmol) was charged with acetone (1 mL) and MeI (170 μL, 2.70 mmol). The vessel was sealed and heated to 50 °C (external temperature). After 21 h at the same temperature, the reaction mixture was cooled to 23 °C, transferred to a 25-mL round-bottomed flask and concentrated *in vacuo* to yield (*E*)-2-((hydroxyimino)methyl)-4-(3-isopropoxyphenethyl)-1-methylpyridin-1-ium iodide as a light yellow solid (76 mg, 66% yield).

(E)-2-((Hydroxyimino)methyl)-4-(3-isopropoxyphenethyl)-1-methylpyridin-1-ium iodide: m.p. = 156–159 °C; R_f = 0.08 (5% MeOH in CH_2Cl_2); IR (neat): ν_{max} = 3081, 2967, 1589, 1446, 1320, 1254, 1237, 1187, 1154, 1110 cm^{-1}; ^1H NMR (400 MHz, 293 K, CD_3OD): δ 8.67 (d, J = 6.4 Hz, 1H, 6-H), 8.58 (s, 1H, -C*H*=NOH), 8.20 (d, J = 2.0, 1H, 3-H), 7.79 (dd, J = 6.4, 2.0 Hz, 1H, 5-H), 7.15 (t, J = 8.0, 1H, -*Ar*), 6.77–6.72 (m, 3H, -*Ar*), 4.55 (sept, J = 6.0, 1H, -OC*H*$(CH_3)_2$), 4.33 (s, 3H, -N^+C*H*$_3$), 3.25 (t, J = 7.6, 1H, -C*H*$_2$CH$_2$Ph), 3.03 (t, J = 7.6, 1H, -CH$_2$C*H*$_2$Ph), 1.27 (d, J = 6.0, 6H, -OCH(C*H*$_3$)$_2$); ^{13}C NMR (100 MHz, 293 K, CD_3OD): δ 163.1, 159.4, 148.7, 146.8, 142.3, 141.9, 130.6, 128.3, 126.6, 121.8, 117.4, 114.9, 70.8, 46.4, 37.9, 36.3, 22.3; HRMS (ESI+) calcd for $C_{18}H_{23}N_2O_2$ $[M]^+$ = 299.1754, found 299.1704.

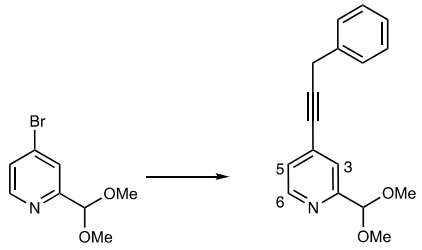

Preparation of 2-(dimethoxymethyl)-4-(3-phenylprop-1-yn-1-yl)pyridine: A 50-mL 3-neck round-bottom flask affixed with a septum, reflux condenser, and a nitrogen inlet was charged with 4-bromo-2-(dimethoxymethyl)pyridine (1.39 g, 6.00 mmol), $Pd(PPh_3)_2Cl_2$ (211 mg, 0.300 mmol), and CuI (57 mg, 0.30 mmol). The flask was evacuated and refilled with nitrogen gas three times. The mixture was dissolved in anhydrous 1,4-dioxane (6 mL) and Et_3N (2.50 mL, 18.0 mmol). 3-Phenylpropyne (1.12 mL, 9.00 mmol) was added over 4 h at 50 °C. After 5 h, the reaction mixture was cooled to 23 °C. The crude residue was dry-loaded and purified by flash chromatography (10 to 50% EtOAc in hexanes) on silica gel (100 mL). The semi-pure material was stirred with CH_2Cl_2 and Amberlite™ IRC-748 resin to remove residual copper. After 1 h, the mixture was filtered by gravity through a cotton plug and concentrated *in vacuo* to afford an inseparable mixture (2:1) of 4-bromo-2-(dimethoxymethyl)pyridine and 2-(dimethoxymethyl)-4-(3-phenylprop-1-yn-1-yl)pyridine (482 mg, 30% yield) as a dark brown oil. This material was used directly without further purification due to instability.

2-(Dimethoxymethyl)-4-(3-phenylprop-1-yn-1-yl)pyridine: R_f = 0.40 (60% EtOAc in hexanes); IR (neat): ν_{max} = 2932, 2829, 2235, 1596, 1568, 1554, 1495, 1435, 1387, 1357, 1212, 1191, 1113, 1095, 1060 cm^{-1}; ^1H NMR (400 MHz, 293 K, acetone-d_6): δ 8.53 (d, J = 5.2 Hz, 1H, 6-H), 7.51 (br s, 1H, 3-H), 7.46–7.44 (m, 3H, -*Ar*), 7.39–7.35 (m, 4H, -*Ar*), 5.28 (s, 1H, -C*H*$(OCH_3)_2$), 3.94 (s, 2H, -C*H*$_2$Ph), 3.35 (s, 6H, -CH(OC*H*$_3$)$_2$); ^{13}C NMR (100 MHz, 293 K, acetone-d_6): δ 158.9, 149.9, 137.1, 132.8, 129.5, 128.8, 127.6, 126.0, 123.6, 104.9, 93.9, 80.8, 53.9, 25.8; HRMS (ESI+) calcd for $C_{17}H_{18}NO_2$ $[M + H]^+$ = 268.1332, found 268.1319.

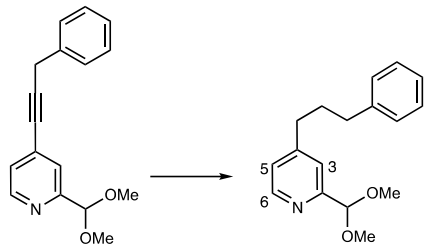

Preparation of 2-(dimethoxymethyl)-4-(3-phenylpropyl)pyridine: A 50-mL round-bottom flask was charged with 2-(dimethoxymethyl)-4-(3-phenylprop-1-yn-1-yl)pyridine (393 mg, 1.05 mmol), EtOH (15 mL), PtO_2 (31 mg, 0.14 mmol) at 23 °C. The resulting suspension was purged with hydrogen gas three times and stirred vigorously at the same temperature for 3.5 h. The suspension was filtered by gravity through filter paper, and the resulting filtrate was concentrated *in vacuo*. The crude residue was purified by flash chromatography (40 to 60% EtOAc in hexanes) on silica gel (25 mL) to yield 2-(dimethoxymethyl)-4-(3-phenylpropyl)pyridine as an orange oil (175 mg, 64% yield).

2-(Dimethoxymethyl)-4-(3-phenylpropyl)pyridine: R_f = 0.38 (60% EtOAc in hexanes); IR (neat): ν_{max} = 2930, 2858, 2829, 1603, 1559, 1495, 1452, 1418, 1362, 1191, 1161, 1112, 1098, 1057 cm^{-1}; ^1H NMR (400 MHz, 293 K, DMSO-d_6): δ 8.42 (d, J = 5.2 Hz, 1H, 6-H), 7.31–7.26 (m, 3H, -*Ar*), 7.23–7.15 (m, 4H, -*Ar*), 5.24 (s, 1H, -C*H*$(OCH_3)_2$), 3.28 (s, 6H, -CH$(OCH_3)_2$), 2.66–2.57 (m, 4H, -C*H*$_2$CH$_2$C*H*$_2$Ph), 1.92–1.84 (m, 2H, -CH$_2$C*H*$_2$CH$_2$Ph); ^{13}C NMR (100 MHz, 293 K, DMSO-d_6): δ 157.4, 151.9, 149.1, 142.0, 128.8, 128.7, 126.2, 124.2, 121.1, 104.4, 53.8, 35.1, 34.4, 32.0; HRMS (ESI+) calcd for $C_{17}H_{22}NO_2$ $[M + H]^+$ = 272.1645, found 272.1653.

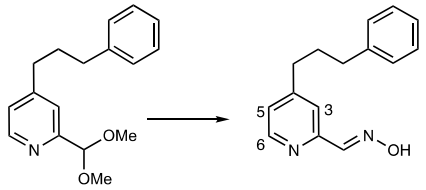

Preparation of (*E*)*-4-(3-phenylpropyl)picolinaldehyde oxime:* A 50-mL pear-shaped flask open to air with 2-(dimethoxymethyl)-4-(3-phenylpropyl)pyridine (151 mg, 0.550 mmol) was charged with H_2O (4 mL) and 5 M H_2SO_4 in H_2O (120 μL, 0.610 mmol). The solution was heated to 90 °C (external temperature). After stirring at the same temperature for 2.5 h, the reaction mixture was cooled to 23 °C and treated with K_2CO_3 (304 mg, 2.20 mmol) followed by MeOH (12 mL) and NH_2OH•HCl (38 mg, 0.55 mmol) at the same temperature. A reflux condenser was attached, and the reaction was heated to reflux while open to air. After 3 h, the reaction mixture was cooled to 23 °C and concentrated *in vacuo.* EtOAc (10 mL) was added to the crude residue, followed by saturated aqueous NH_4Cl (25 mL). The layers were separated using a separatory funnel and the aqueous layer was extracted with EtOAc (2 × 8 mL). The combined organic layers were dried over anhydrous Na_2SO_4, filtered, and concentrated *in vacuo* to afford (*E*)-4-(3-phenylpropyl)picolinaldehyde oxime (98 mg, 74% yield) as a brown solid. This material was used directly without further purification.

(E)-4-(3-Phenylpropyl)picolinaldehyde oxime: m.p. = 99–102 °C; R_f = 0.42 (60% EtOAc in hexanes); IR (neat): ν_{max} = 2980, 2925, 2859, 2738, 1601, 1555, 1495, 1453, 1420, 1320, 992 cm^{-1}; ^1H NMR (500 MHz, 293 K, DMSO-d_6): δ 11.59 (s, 1H, -CH=NO*H*), 8.45 (d, J = 5.0 Hz, 1H, 6-H), 8.04 (s, 1H, -C*H*=NOH), 7.61 (br s, 1H, 3-H), 7.29–7.17 (m, 6H, -*Ar*), 2.66–2.59 (m, 4H, -CH_2CH_2CH_2Ph), 1.90 (app quint, J = 7.5 Hz, 2H, -CH_2CH_2CH_2Ph); ^{13}C NMR (125 MHz, 293 K, DMSO-d_6): δ 152.4, 151.9, 149.7, 149.4, 142.0, 128.7, 128.7, 126.2, 124.5, 120.0, 35.0, 34.3, 31.8; HRMS (ESI+) calcd for $C_{15}H_{17}N_2O$ [M + H] = 241.1335, found 241.1326.

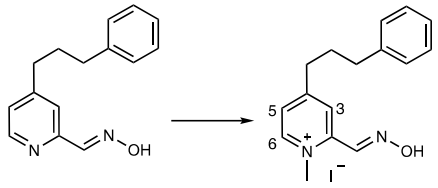

*Preparation of (E)-2-((hydroxyimino)methyl)-1-methyl-4-(3-phenylpropyl)pyridin-1-ium (**ADG4300**):* A 35-mL sealed tube with (*E*)-4-(3-phenylpropyl)picolinaldehyde oxime (32 mg, 0.13 mmol) was charged with acetone (1 mL) and MeI (82 μL, 1.3 mmol). The vessel was sealed and heated to 52 °C (external temperature). After 13 h at the same temperature, the reaction mixture was cooled to 23 °C, transferred to a 25-mL round-bottomed flask, and concentrated *in vacuo* to yield *(E)*-2-((hydroxyimino)methyl)-1-methyl-4-(3-phenylpropyl)pyridin-1-ium iodide as a brown solid (50 mg, quantitative yield).

(E)-2-((Hydroxyimino)methyl)-1-methyl-4-(3-phenylpropyl)pyridin-1-ium iodide: m.p. = 68–70 °C; R_f = 0.10 (10% MeOH in CH_2Cl_2); IR (neat): ν_{max} = 3056, 2926, 2855, 1738, 1636, 1597, 1569, 1511, 1494, 1450, 1301, 1185, 1132, 1079, 999 cm^{-1}; ^1H NMR (400 MHz, 293 K, CD_3OD): δ 8.68 (d, J = 6.0 Hz, 1H, 6-H), 8.60 (s, 1H, -C*H*=NOH), 8.22 (br s, 1H, 3-H), 7.82 (d, J = 6.0 Hz, 1H, 5-H), 7.29–7.15 (m, 5H, -*Ar*), 4.34 (s, 3H, -N^+CH_3), 2.95 (t, J = 7.6 Hz, 2H, -$CH_2CH_2CH_2Ph$), 2.73 (t, J = 7.6 Hz, 2H, -$CH_2CH_2CH_2Ph$), 1.90 (app quint, J = 7.6 Hz, 2H, -$CH_2CH_2CH_2Ph$); ^{13}C NMR (100 MHz, 293 K, CD_3OD): δ 163.9, 148.6, 146.9, 142.5, 142.0, 129.6, 129.5, 128.2, 127.1, 126.5, 46.7, 36.1, 36.1, 32.4; HRMS (ESI+) calcd for $C_{16}H_{19}N_2O$ $[M]^+$ = 255.1492, found 255.1479.

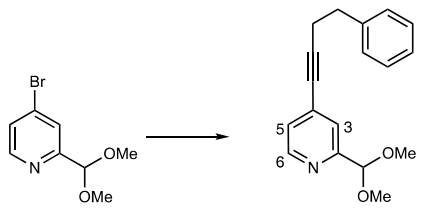

Preparation of 2-(dimethoxymethyl)-4-(4-phenylbut-1-yn-1-yl)pyridine: A 75-mL sealed tube with 4-bromo-2-(dimethoxymethyl)pyridine (1.16 g, 5.00 mmol) was treated with $Pd(PPh_3)_2Cl_2$ (175 mg, 0.250 mmol) and CuI (48 mg, 0.25 mmol) and flushed with argon gas. The mixture was dissolved in anhydrous 1,4-dioxane (5 mL), Et_3N (2.10 mL, 15.0 mmol), and 4-phenyl-1-butyne (1.05 mL, 7.50 mmol) at 23 °C. The resulting solution was heated to 50 °C (external temperature) and stirred. After 14 h, the reaction mixture was cooled to 23 °C. The crude residue was dry-loaded and purified by flash chromatography (10 to 60% EtOAc in hexanes) on silica gel (75 mL). The semi-pure material was stirred with CH_2Cl_2 and Amberlite™ IRC-748 resin to remove residual copper. After 1 h, the mixture was filtered by gravity through a cotton plug and concentrated *in vacuo* to afford 2-(dimethoxymethyl)-4-(4-phenylbut-1-yn-1-yl)pyridine (1.33 g, 95% yield) as a dark brown oil.

2-(Dimethoxymethyl)-4-(4-phenylbut-1-yn-1-yl)pyridine: R_f = 0.50 (60% EtOAc in hexanes); IR (neat): ν_{max} = 2927, 2830, 2234, 1596, 1453, 1360, 1191, 1111, 1095, 1057 cm^{-1}; ^1H NMR (300 MHz, 293 K, acetone-d_6): δ 8.49 (d, J = 5.1 Hz, 1H, 6-H), 7.42 (app s, 1H, 3-H), 7.33–7.21 (m, 6H, -*Ar*), 5.25 (s, 1H, -C*H*$(OCH_3)_2$), 3.34 (s, 6H, -CH$(OCH_3)_2$), 2.93 (t, J = 7.3 Hz, 2H, -CH_2CH_2Ph), 2.76 (t, J = 7.3 Hz, 2H, -CH_2CH_2Ph); ^{13}C NMR (100 MHz, 293 K, acetone-d_6): δ 158.9, 149.8, 141.4, 133.0, 129.4, 129.1, 127.1, 125.9, 123.6, 105.0, 95.7, 79.8, 53.9, 35.2, 22.0; HRMS (ESI+) calcd for $C_{18}H_{20}NO_2$ $[M + H]^+$ = 282.1488, found 282.1477.

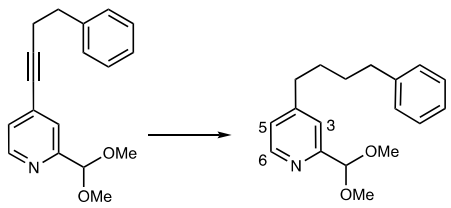

Preparation of 2-(dimethoxymethyl)-4-(4-phenylbutyl)pyridine: A 250-mL round-bottom flask was charged with 2-(dimethoxymethyl)-4-(4-phenylbut-1-yn-1-yl)pyridine (1.00 g, 3.55 mmol), EtOH (70 mL), PtO_2 (40 mg, 0.18 mmol) at 23 °C. The resulting suspension was purged with hydrogen gas three times and stirred vigorously at the same temperature for 26 h. The suspension was filtered by gravity through filter paper, and the resulting filtrate was concentrated *in vacuo* to yield 2-(dimethoxymethyl)-4-(4-phenylbutyl)pyridine as an amber oil (800 mg, 79% yield). This material was used directly without further purification.

2-(Dimethoxymethyl)-4-(4-phenylbutyl)pyridine: R_f = 0.54 (60% EtOAc in hexanes); IR (neat): ν_{max} = 2932, 1603, 1496, 1453, 1362, 1209, 1190, 1161, 1113, 1098, 1057 cm^{-1}; ^1H NMR (400 MHz, 293 K, DMSO-d_6): δ 8.40 (d, J = 4.8 Hz, 1H, 6-H), 7.28–7.24 (m, 3H, -*Ar*), 7.20–7.14 (m, 4H, -*Ar*), 5.24 (s, 1H, -C*H*$(OCH_3)_2$), 3.28 (s, 6H, -CH$(OCH_3)_2$), 2.66–2.57 (m, 4H, -CH_2CH_2CH_2CH_2Ph), 1.60–1.55 (m, 4H, -CH_2CH_2CH_2CH_2Ph); ^{13}C NMR (100 MHz, 293 K, DMSO-d_6): δ 157.4, 152.1, 149.0, 142.5, 128.8, 128.7, 126.1, 124.2, 121.1, 104.5, 53.8, 35.2, 34.6, 30.9, 29.9; HRMS (ESI+) calcd for $C_{18}H_{24}NO_2$ [M + H] = 286.1801, found 286.1792.

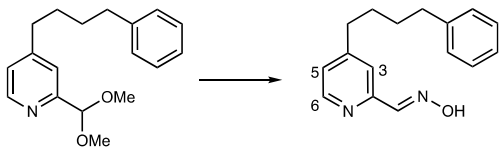

Preparation of (E)-4-(4-phenylbutyl)picolinaldehyde oxime: A 100-mL pear-shaped flask open to air with 2-(dimethoxymethyl)-4-(4-phenylbutyl)pyridine (459 mg, 1.61 mmol) was charged with H_2O (6 mL) and 5 M H_2SO_4 in H_2O (350 μL, 1.77 mmol). The solution was heated

to 95 °C (external temperature). After stirring at the same temperature for 3 h, the reaction mixture was cooled to 23 °C and treated with K_2CO_3 (890 mg, 6.44 mmol) followed by MeOH (20 mL) and NH_2OH•HCl (112 mg, 1.61 mmol) at the same temperature. A reflux condenser was attached, and the reaction was heated to reflux while open to air. After 2.8 h, the reaction mixture was cooled to 23 °C and concentrated *in vacuo.* EtOAc (10 mL) was added to the crude residue, followed by saturated aqueous NH_4Cl (25 mL). The layers were separated using a separatory funnel and the aqueous layer was extracted with EtOAc (2 × 10 mL). The combined organic layers were dried over anhydrous Na_2SO_4, filtered, and concentrated *in vacuo* to afford (*E*)-4-(4-phenylbutyl)picolinaldehyde oxime (391 mg, 96% yield) as a yellow solid. This material was used directly without further purification.

(E)-4-(4-Phenylbutyl)picolinaldehyde oxime: m.p. = 139–142 °C; R_f = 0.39 (60% EtOAc in hexanes); IR (neat): ν_{max} = 2992, 2919, 2856, 2753, 1601, 1556, 1514, 1495, 1453, 1420, 1321, 989, cm^{-1}; ^1H NMR (400 MHz, 293 K, DMSO-d_6): δ 11.60 (s, 1H, -CH=NO*H*), 8.44 (d, *J* = 5.2 Hz, 1H, 6-H), 8.04 (s, 1H, -C*H*=NOH), 7.60 (br s, 1H, 3-H), 7.29–7.25 (m, 2H, -*Ar*), 7.21–7.15 (m, 4H, -*Ar*), 2.68–2.59 (m, 4H, -CH_2CH_2CH_2CH_2Ph), 1.60–1.58 (m, 4H, -CH_2CH_2CH_2CH_2Ph); ^{13}C NMR (100 MHz, 293 K, DMSO-d_6): δ 152.4, 152.1, 149.7, 149.4, 142.4, 128.7, 126.1, 124.5, 119.9, 35.2, 34.4, 30.9, 29.8; HRMS (ESI+) calcd for $C_{16}H_{19}N_2O$ [M + H] = 255.1492, found 255.1479.

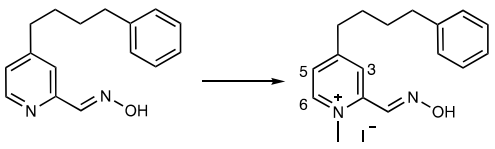

*Preparation of (E)-2-((hydroxyimino)methyl)-1-methyl-4-(4-phenylbutyl)pyridin-1-ium iodide (**ADG4244**):* A 35-mL sealed tube with (*E*)-4-(4-phenylbutyl)picolinaldehyde oxime (202

mg, 0.790 mmol) was charged with acetone (2 mL) and MeI (490 μL, 7.90 mmol). The vessel was sealed and heated to 40 °C (external temperature). After 14.5 h at the same temperature, the reaction mixture was cooled to 23 °C, transferred to a 25-mL round-bottomed flask, concentrated *in vacuo*, and recrystallized from acetone/EtOAc (1:1) to yield (*E*)-2-((hydroxyimino)methyl)-1-methyl-4-(4-phenylbutyl)pyridin-1-ium iodide as a light yellow solid (184 mg, 59% yield).

(E)-2-((Hydroxyimino)methyl)-1-methyl-4-(4-phenylbutyl)pyridin-1-ium iodide: m.p. = 125–129 °C; R_f = 0.10 (5% MeOH in CH_2Cl_2); IR (neat): ν_{max} = 3119, 2981, 1638, 1591, 1568, 1512, 1494, 1449, 1427, 1417, 1326, 1306, 1187, 1132, 1009 cm^{-1}; ^1H NMR (300 MHz, 293 K, DMSO-d_6): δ 13.02 (s, 1H, -CH=NO*H*), 8.83 (d, *J* = 6.3 Hz, 1H, 6-H), 8.63 (s, 1H, -C*H*=NOH), 8.18 (d, *J* = 1.8 Hz, 1H, 3-H), 7.92 (dd, *J* = 6.3, 1.8 Hz, 1H, 5-H), 7.30–7.15 (m, 5H, -*Ar*), 4.29 (s, 3H, -N^+CH_3), 2.93 (t, *J* = 6.6 Hz, 2H, -$CH_2CH_2CH_2CH_2Ph$), 2.62 (t, *J* = 7.5 Hz, 2H, -$CH_2CH_2CH_2CH_2Ph$), 1.73–1.55 (m, 4H, -$CH_2CH_2CH_2CH_2Ph$); ^{13}C NMR (100 MHz, 293 K, DMSO-d_6): δ 162.1, 147.0, 146.3, 142.3, 142.2, 128.7, 127.3, 126.2, 124.7, 45.9, 35.1, 34.6, 30.6, 29.2; HRMS (ESI+) calcd for $C_{17}H_{21}N_2O$ $[M]^+$ = 269.1648, found 269.1657.

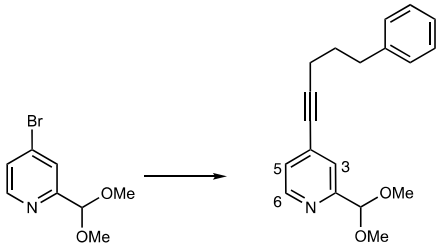

Preparation of 2-(dimethoxymethyl)-4-(5-phenylpent-1-yn-1-yl)pyridine: A 75-mL sealed tube with 4-bromo-2-(dimethoxymethyl)pyridine (1.40 g, 6.00 mmol) was treated with $Pd(PPh_3)_2Cl_2$ (211 mg, 0.300 mmol) and CuI (57 mg, 0.30 mmol) and flushed with argon gas. The mixture was dissolved in anhydrous 1,4-dioxane (6 mL), Et_3N (2.5 mL, 18 mmol), and 5-phenyl-

1-pentyne (1.37 mL, 9.00 mmol) at 23 °C. The resulting solution was heated to 50 °C (external temperature) and stirred. After 18 h, the reaction mixture was cooled to 23 °C. The crude residue was dry-loaded and purified by flash chromatography (10 to 40% EtOAc in hexanes) on silica gel (75 mL). The semi-pure material was stirred with CH_2Cl_2 and Amberlite™ IRC-748 resin to remove residual copper. After 1 h, the mixture was filtered by gravity through a cotton plug and concentrated *in vacuo* to afford 2-(dimethoxymethyl)-4-(5-phenylpent-1-yn-1-yl)pyridine (1.81 g, quantitative yield) as a dark brown oil.

2-(Dimethoxymethyl)-4-(5-phenylpent-1-yn-1-yl)pyridine: R_f = 0.55 (60% EtOAc in hexanes); IR (neat): ν_{max} = 2934, 2829, 2234, 1596, 1541, 1495, 1453, 1404, 1360, 1209, 1191, 1179, 1111, 1095, 1058 cm^{-1}; ^1H NMR (400 MHz, 293 K, acetone-d_6): δ 8.55 (d, J = 5.2 Hz, 1H, 6-H), 7.51 (app s, 1H, 3-H), 7.36–7.29 (m, 5H, 5-H and -*Ph*), 7.25–7.21 (m, 1H, -*Ph*), 5.31 (s, 1H, -C*H*$(OCH_3)_2$), 3.38 (s, 6H, -CH$(OCH_3)_2$), 2.84 (t, J = 7.2 Hz, 2H, -$CH_2CH_2CH_2$Ph), 2.52 (t, J = 7.2 Hz, 2H, -$CH_2CH_2CH_2$Ph), 1.97 (app quint, J = 7.2 Hz, 2H, -$CH_2CH_2CH_2$Ph); ^{13}C NMR (100 MHz, 293 K acetone-d_6): δ 158.9, 149.8, 142.3, 133.1, 129.3, 129.2, 126.7, 126.0, 123.6, 105.0, 95.9, 79.6, 53.8, 35.3, 30.8, 19.1; HRMS (ESI+) calcd for $C_{19}H_{22}NO_2$ $[M + H]^+$ = 296.1645, found 296.1637.

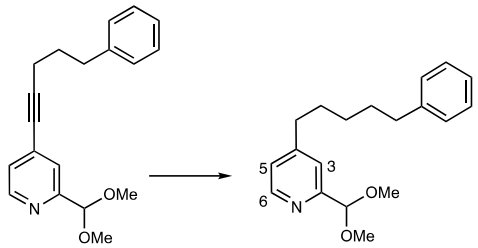

Preparation of 2-(dimethoxymethyl)-4-(5-phenylpentyl)pyridine: A 250-mL round-bottom flask was charged with 2-(dimethoxymethyl)-4-(5-phenylpent-1-yn-1-yl)pyridine (1.30 g, 4.37 mmol), EtOH (80 mL), PtO_2 (50 mg, 0.22 mmol) at 23 °C. The resulting suspension was purged

with hydrogen gas three times and stirred vigorously at the same temperature for 24 h. The suspension was filtered by gravity through filter paper, and the resulting filtrate was concentrated *in vacuo* to yield 2-(dimethoxymethyl)-4-(5-phenylpentyl)pyridine as a dark brown oil (1.15 g, 88% yield). This material was used directly without further purification.

2-(Dimethoxymethyl)-4-(5-phenylpentyl)pyridine: R_f = 0.50 (60% EtOAc in hexanes); IR (neat): ν_{max} = 2930, 2856, 1603, 1560, 1495, 1452, 1416, 1362, 1191, 1161, 1113, 1098, 1070 cm^{-1}; ^1H NMR (300 MHz, 293 K, acetone-d_6): δ 8.40 (d, J = 4.8 Hz, 1H, 6-H), 7.37 (app s, 1H, 3-H), 7.28–7.13 (m, 6H, 5-H and -*Ph*), 5.24 (s, 1H, -C*H*$(OCH_3)_2$), 3.34 (s, 6H, -CH$(OCH_3)_2$), 2.63 (app quint, J = 7.8 Hz, 4H, -C*H*$_2$CH$_2$CH$_2$CH$_2$C*H*$_2$Ph), 1.67 (app sext, J = 6.6 Hz, 4H, -CH$_2$C*H*$_2$CH$_2$C*H*$_2$CH$_2$Ph), 1.39 (app quint, J = 8.1 Hz, 2H, -CH$_2$CH$_2$C*H*$_2$CH$_2$CH$_2$Ph); ^{13}C NMR (100 MHz, 293 K, acetone-d_6): δ 157.5, 151.8, 148.5, 142.4, 128.1, 125.4, 123.4, 120.7, 104.7, 52.9, 35.4, 34.7, 31.0, 30.1; HRMS (ESI+) calcd for $C_{19}H_{26}NO_2$ $[M + H]^+$ = 300.1958, found 300.1946.

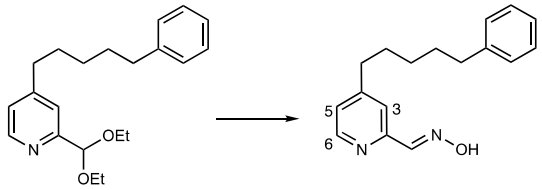

Preparation of (E)-4-(5-phenylpentyl)picolinaldehyde oxime: A 50-mL pear-shaped flask open to air with 2-(dimethoxymethyl)-4-(5-phenylpentyl)pyridine (499 mg, 1.66 mmol) was charged with H_2O (8 mL) and 5 M H_2SO_4 in H_2O (370 μL, 1.83 mmol). The solution was heated to 95 °C (external temperature). After stirring at the same temperature for 3 h, the reaction mixture was cooled to 23 °C and treated with K_2CO_3 (918 mg, 6.64 mmol) followed by MeOH (18 mL) and NH_2OH•HCl (115 mg, 1.66 mmol) at the same temperature. A reflux condenser was attached,

and the reaction was heated to reflux while open to air. After 3 h, the reaction mixture was cooled to 23 °C and concentrated *in vacuo.* EtOAc (15 mL) was added to the crude residue, followed by saturated aqueous NH_4Cl (30 mL). The layers were separated using a separatory funnel and the aqueous layer was extracted with EtOAc (2 × 10 mL). The combined organic layers were dried over anhydrous Na_2SO_4, filtered, and concentrated *in vacuo* to afford (*E*)-4-(5-phenylpentyl)picolinaldehyde oxime (231 mg, 52% yield) as a light brown solid. This material was used directly without further purification.

(E)-4-(5-Phenylpentyl)picolinaldehyde oxime: m.p. = 97–99 °C; R_f = 0.31 (60% EtOAc in hexanes); IR (neat): ν_{max} = 2996, 2926, 2855, 2772, 1602, 1555, 1489, 1451, 1419, 1319, 988 cm^{-1}; ^1H NMR (400 MHz, 293 K, CD_3OD): δ 8.37 (d, *J* = 5.2 Hz, 1H, 6-H), 8.07 (s, 1H, -C*H*=NOH), 7.69 (br s, 1H, 3-H), 7.25–7.21 (m, 3H, -*Ar*), 7.15–7.11 (m, 3H, -*Ar*), 2.67 (t, *J* = 7.6 Hz, 2H, -C*H*$_2$CH$_2$CH$_2$CH$_2$CH$_2$Ph), 2.61 (t, *J* = 7.2 Hz, 2H, -CH$_2$CH$_2$CH$_2$CH$_2$C*H*$_2$Ph), 1.73–1.64 (m, 4H, -CH$_2$C*H*$_2$CH$_2$C*H*$_2$CH$_2$Ph), 1.37 (app quint, *J* = 8.0 Hz, 2H, -CH$_2$CH$_2$C*H*$_2$CH$_2$CH$_2$Ph); ^{13}C NMR (100 MHz, 293 K, CD_3OD): δ 154.7, 153.2, 149.7, 149.4, 143.6, 129.3, 129.2, 126.6, 125.5, 121.8, 36.6, 35.9, 32.3, 31.1, 29.6; HRMS (ESI+) calcd for $C_{17}H_{21}N_2O$ [M + H] = 269.1648, found 269.1644.

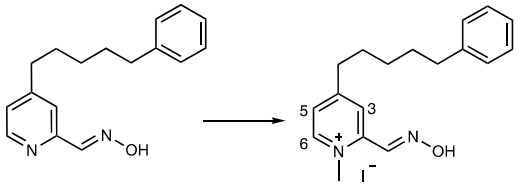

*Preparation of (E)-2-((hydroxyimino)methyl)-1-methyl-4-(5-phenylpentyl)pyridin-1-ium iodide (**ADG4282**):* A 35-mL sealed tube with (*E*)-4-(5-phenylpentyl)picolinaldehyde oxime (100 mg, 0.370 mmol) was charged with acetone (1 mL) and MeI (230 μL, 3.70 mmol). The vessel was

sealed and heated to 45 °C (external temperature). After 15 h at the same temperature, the reaction mixture was cooled to 23 °C, transferred to a 25-mL round-bottomed flask and concentrated *in vacuo*. The crude residue was dry-loaded and purified by flash chromatography (5 to 40% MeOH in CH_2Cl_2) on silica gel (10 mL) to yield (*E*)-2-((hydroxyimino)methyl)-1-methyl-4-(5-phenylpentyl)pyridin-1-ium iodide as a brown solid (121 mg, 80% yield).

(E)-2-((Hydroxyimino)methyl)-1-methyl-4-(5-phenylpentyl)pyridin-1-ium iodide: m.p. = 110–112 °C; R_f = 0.76 (50% MeOH in CH_2Cl_2); IR (neat): ν_{max} = 3075, 2966, 2931, 2855, 1637, 1591, 1569, 1514, 1491, 1450, 1422, 1299, 1263, 1184, 1006 cm^{-1}; ^1H NMR (300 MHz, 293 K, CD_3OD): δ 8.67 (d, *J* = 6.6 Hz, 1H, 6-H), 8.61 (s, 1H, -C*H*=NOH), 8.23 (d, *J* = 1.5 Hz, 1H, 3-H), 7.82 (dd, *J* = 6.6, 1.5 Hz, 1H, 5-H), 7.27–7.12 (m, 5H, -*Ar*), 4.34 (s, 3H, $-N^+CH_3$), 2.92 (t, *J* = 7.6 Hz, 2H, -C*H*$_2$CH$_2$CH$_2$CH$_2$CH$_2$Ph), 2.63 (t, *J* = 7.5 Hz, 2H, -CH$_2$CH$_2$CH$_2$CH$_2$C*H*$_2$Ph), 1.83–1.64 (m, 4H, -CH$_2$C*H*$_2$CH$_2$C*H*$_2$CH$_2$Ph), 1.37 (app quint, *J* = 8.1 Hz, 2H, -CH$_2$CH$_2$C*H*$_2$CH$_2$CH$_2$Ph); ^{13}C NMR (125 MHz, 293 K, CD_3OD): δ 164.1, 148.5, 147.0, 143.5, 142.1, 129.4, 129.2, 128.2, 126.6, 126.4, 46.8, 36.5, 36.4, 32.1, 30.4, 29.5; HRMS (ESI+) calcd for $C_{18}H_{23}N_2O$ $[M]^+$ = 283.1805, found 283.1791.

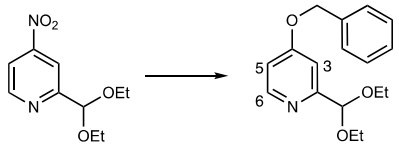

Preparation of 4-(benzyloxy)-2-(diethoxymethyl)pyridine: A 50-mL pear-shaped flask with a reflux condenser was charged with NaH (60% w/w, 480 mg, 12.0 mmol), then evacuated and refilled with nitrogen gas three times. Benzyl alcohol (930 μL, 9.00 mmol) and dimethyl sulfoxide (15 mL) were added, and the mixture was stirred at 23 °C. After 30 min, 2-(diethoxymethyl)-4-nitropyridine (677 mg, 3.00 mmol) was added, and the resulting mixture was stirred and heated to

72 °C. After 9 h, the reaction mixture was cooled to 23 °C and acidified with saturated aqueous NH_4Cl (20 mL). The resulting solution was extracted with EtOAc (3 × 20 mL). The combined organic layers were dried over anhydrous Na_2SO_4, filtered, and concentrated *in vacuo*. The crude material was combined with another batch (1.0 mmol scale, with respect to 2-(diethoxymethyl)-4-nitropyridine prepared using the same procedure and was purified by flash chromatography (10 to 60% EtOAc in hexanes) on silica gel (125 mL) to afford 4-(benzyloxy)-2-(diethoxymethyl)pyridine as a yellow oil (1.15 g, quantitative yield).

4-(Benzyloxy)-2-(diethoxymethyl)pyridine: R_f = 0.48 (60% EtOAc in hexanes); IR (neat): ν_{max} = 2975, 1594, 1568, 1497, 1481, 1454, 1432, 1421, 1369, 1346, 1300, 1266, 1242, 1175, 1111, 1082, 1056, 1023 cm^{-1}; ^1H NMR (400 MHz, 293 K, $CDCl_3$): δ 8.40 (d, J = 5.6 Hz, 1H, 6-H), 7.43–7.33 (m, 5H, -*Ph*), 7.21 (d, J = 2.8 Hz, 1H, 3-H), 6.82 (dd, J = 5.6, 2.8 Hz, 1H, 5-H), 5.42 (s, 1H, -C*H*(OCH_2CH_3)$_2$), 5.12 (s, 2H, -OC*H*$_2$Ph), 3.74–3.55 (m, 4H, -CH(OC*H*$_2$$CH_3$)$_2$), 1.23 (t, J = 7.2 Hz, 6H, -CH(OCH_2C*H*$_3$)$_2$); ^{13}C NMR (100 MHz, 293 K, $CDCl_3$): δ 165.5, 160.1, 150.2, 135.6, 128.7, 128.3, 127.6, 110.6, 107.2, 102.6, 69.8, 62.3, 15.2; HRMS (ESI+) calcd for $C_{17}H_{22}NO_3$ $[M + H]^+$ = 288.1594, found 288.1596.

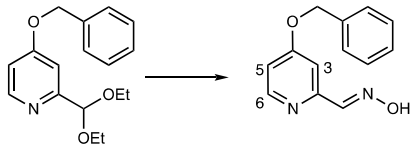

Preparation of (E)-4-(benzyloxy)picolinaldehyde oxime: A 50-mL pear-shaped flask open to air with 4-(benzyloxy)-2-(diethoxymethyl)pyridine (782 mg, 2.72 mmol) was charged with H_2O (12 mL) and 5 M H_2SO_4 in H_2O (560 μL, 2.99 mmol). The solution was heated to 90 °C (external temperature). After stirring at the same temperature for 3.7 h, the reaction mixture was cooled to 23 °C and treated with K_2CO_3 (1.50 g, 10.9 mmol) followed by MeOH (10 mL) and NH_2OH•HCl

(189 mg, 2.72 mmol) at the same temperature. A reflux condenser was attached, and the reaction was heated to reflux while open to air. After 2.7 h, the reaction mixture was cooled to 23 °C and concentrated *in vacuo.* EtOAc (20 mL) was added to the crude residue, followed by saturated aqueous NH_4Cl (20 mL). The layers were separated using a separatory funnel and the aqueous layer was extracted with EtOAc (2 × 25 mL). The combined organic layers were dried over anhydrous Na_2SO_4, filtered, and concentrated *in vacuo* to afford (*E*)-4-(benzyloxy)picolinaldehyde oxime (349 mg, 56% yield) as a light pink solid. This material was used directly without further purification.

(E)-4-(Benzyloxy)picolinaldehyde oxime: m.p. = 198–201 °C; R_f = 0.19 (60% EtOAc in hexanes); IR (neat): ν_{max} = 2979, 2877, 2699, 1591, 1563, 1519, 1497, 1465, 1455, 1425, 1379, 1327, 1300, 1263, 1246, 1181, 1090, 1012 cm^{-1}; ^1H NMR (300 MHz, 293 K, DMSO-d_6): δ 11.65 (s, 1H, -CH=NO*H*), 8.39 (d, *J* = 5.7 Hz, 1H, 6-H), 8.02 (s, 1H, -C*H*=NOH), 7.48–7.34 (m, 6H, 3-H and -*Ph*), 7.05 (dd, *J* = 5.7, 2.7 Hz, 1H, 5-H), 5.24 (s, 2H, -OCH_2Ph); ^{13}C NMR (100 MHz, 293 K, DMSO-d_6): δ 165.0, 154.2, 151.2, 149.3, 136.5, 129.0, 128.6, 128.3, 111.8, 106.1, 69.7; HRMS (ESI+) calcd for $C_{13}H_{13}N_2O_2$ [M + H] = 229.0972, found 229.0968.

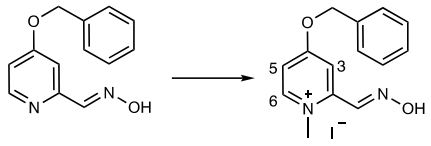

*Preparation of (E)-4-(benzyloxy)-2-((hydroxyimino)methyl)-1-methylpyridin-1-ium iodide (**ADG3254**):* A 35-mL sealed tube with (*E*)-4-(benzyloxy)picolinaldehyde oxime (166 mg, 0.720 mmol) was charged with acetone (2.5 mL) and MeI (450 μL, 7.20 mmol). The vessel was sealed and heated to 55 °C (external temperature). After 17 h at the same temperature, the reaction mixture was cooled to 23 °C, transferred to a 25-mL round-bottomed flask and concentrated *in vacuo* to

yield (*E*)-4-(benzyloxy)-2-((hydroxyimino)methyl)-1-methylpyridin-1-ium iodide as an orange solid (266 mg, quantitative yield).

(E)-4-(Benzyloxy)-2-((hydroxyimino)methyl)-1-methylpyridin-1-ium iodide: m.p. = 143–146 °C; R_f = 0.10 (5% MeOH in CH_2Cl_2); IR (neat): ν_{max} = 3086, 3055, 2981, 1643, 1596, 1567, 1518, 1497, 1444, 1434, 1392, 1323, 1300, 1260, 1218, 1185, 1145, 1112, 1074, 1020 cm^{-1}; ^1H NMR (400 MHz, 293 K, DMSO-d_6): δ 12.99 (s, 1H, -CH=NO*H*), 8.79 (d, *J* = 7.2 Hz, 1H, 6-H), 8.57 (s, 1H, -C*H*=NOH), 7.78 (d, *J* = 3.2 Hz, 1H, 3-H), 7.68 (dd, *J* = 7.2, 3.2 Hz, 1H, 5-H), 7.52–7.49 (m, 2H, -*Ph*), 7.46–7.38 (m, 3H, -*Ph*), 5.51 (s, 2H, -OC*H*$_2$Ph), 4.19 (s, 3H, -N^+C*H*$_3$); ^{13}C NMR (125 MHz, 293 K, DMSO-d_6): δ 169.3, 149.1, 148.7, 142.2, 134.9, 129.3, 129.2, 128.8, 113.9, 110.8, 72.3, 45.1; HRMS (ESI+) calcd for $C_{14}H_{15}N_2O_2$ $[M]^+$ = 243.1128 found 243.1135.

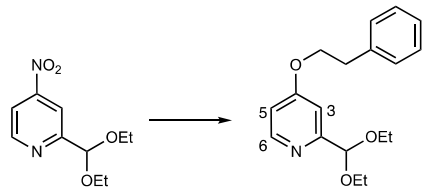

Preparation of 2-(diethoxymethyl)-4-phenethoxypyridine: A 50-mL pear-shaped flask with a reflux condenser was charged with NaH (60% w/w, 360 mg, 9.00 mmol), then evacuated and refilled with nitrogen gas three times. Phenethyl alcohol (1.08 mL, 9.00 mmol) and THF (15 mL) were added, and the mixture was stirred at 23 °C. After 5 min, 2-(diethoxymethyl)-4-nitropyridine (678 mg, 3.00 mmol) was added, and the resulting mixture was stirred and heated to 65 °C (external temperature). After 18 h, the reaction mixture was cooled to 23 °C and acidified with saturated aqueous NH_4Cl (20 mL). The resulting solution was extracted with EtOAc (3 × 10 mL). The combined organic layers were dried over anhydrous Na_2SO_4, filtered, and concentrated *in vacuo.* The crude material was combined with another batch (1.0 mmol scale, with respect to 2-

(diethoxymethyl)-4-nitropyridine) prepared using the same procedure and was purified by flash chromatography (10 to 60% EtOAc in hexanes) on silica gel (75 mL) to afford 2-(diethoxymethyl)-4-phenethoxypyridine as a pale yellow oil (1.00 g, 83% yield).

2-(Diethoxymethyl)-4-phenethoxypyridine: R_f = 0.50 (60% EtOAc in hexanes); IR (neat): ν_{max} = 2974, 1594, 1567, 1470, 1454, 1433, 1369, 1346, 1303, 1265, 1243, 1176, 1110, 1086, 1056, 1026 cm^{-1}; ^1H NMR (300 MHz, 293 K, DMSO-d_6): δ 8.32 (d, J = 5.1 Hz, 1H, 6-H), 7.33–7.28 (m, 4H, -*Ar*), 7.27–7.20 (m, 1H, -*Ph*), 6.95–6.92 (m, 2H, -*Ar*), 5.32 (s, 1H, -C*H*$(OCH_2CH_3)_2$), 4.28 (t, J = 6.6 Hz, 2H, -OC*H*$_2$CH$_2$Ph), 3.64–3.46 (m, 4H, -CH(OC*H*$_2$CH$_3$)$_2$), 3.04 (t, J = 6.6 Hz, 2H, -OCH$_2$C*H*$_2$Ph), 1.12 (t, J = 7.2 Hz, 6H, -CH(OCH$_2$C*H*$_3$)$_2$); ^{13}C NMR (100 MHz, 293 K, DMSO-d_6): δ 165.6, 160.4, 150.8, 138.7, 129.6, 129.1, 127.1, 110.7, 107.7, 102.6, 69.0, 62.4, 35.3, 15.8; HRMS (ESI+) calcd for $C_{18}H_{24}NO_3$ $[M + H]^+$ = 302.1751, found 302.1762.

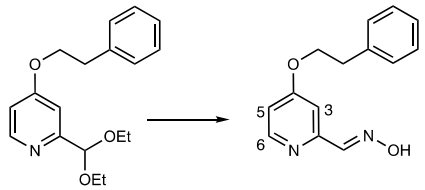

Preparation of (E)-4-phenethoxypicolinaldehyde oxime: A 50-mL pear-shaped flask open to air with 2-(diethoxymethyl)-4-phenethoxypyridine (474 mg, 1.57 mmol) was charged with H_2O (6 mL) and 5 M H_2SO_4 in H_2O (340 μL, 1.73 mmol). The solution was heated to 95 °C (external temperature). After stirring at the same temperature for 2.5 h, the reaction mixture was cooled to 23 °C and treated with K_2CO_3 (868 mg, 6.28 mmol) followed by MeOH (20 mL) and NH_2OH•HCl (109 mg, 1.57 mmol) at the same temperature. A reflux condenser was attached, and the reaction was heated to reflux while open to air. After 3 h, the reaction mixture was cooled to 23 °C and concentrated *in vacuo.* EtOAc (10 mL) was added to the crude residue, followed by saturated

aqueous NH_4Cl (15 mL). The layers were separated using a separatory funnel and the aqueous layer was extracted with EtOAc (2 × 10 mL). The combined organic layers were dried over anhydrous Na_2SO_4, filtered, and concentrated *in vacuo* to afford (*E*)-4-phenethoxypicolinaldehyde oxime (365 mg, 96% yield) as a light tan solid. This material was used directly without further purification.

(E)-4-Phenethoxypicolinaldehyde oxime: m.p. = 127–130 °C; R_f = 0.18 (60% EtOAc in hexanes); IR (neat): ν_{max} = 2981, 2872, 2729, 1732, 1591, 1561, 1517, 1494, 1454, 1430, 1388, 1329, 1249, 1185, 1089, 1053, 1018 cm^{-1}; ^1H NMR (300 MHz, 293 K, DMSO-d_6): δ 11.63 (s, 1H, -CH=NO*H*), 8.37 (d, *J* = 5.7 Hz, 1H, 6-H), 8.02 (s, 1H, -C*H*=NOH), 7.34–7.23 (m, 6H, -*Ar*), 6.98 (dd, *J* = 5.7, 2.4 Hz, 1H, 5-H), 4.33 (t, *J* = 6.6 Hz, 2H, -OC$H_2$$CH_2$Ph), 3.06 (t, *J* = 6.6 Hz, 2H, -$OCH_2C$$H_2$Ph); ^{13}C NMR (100 MHz, 293 K, DMSO-d_6): δ 165.0, 154.1, 151.2, 149.3, 138.4, 129.4, 128.8, 126.8, 111.4, 106.0, 68.7, 34.9; HRMS (ESI+) calcd for $C_{14}H_{15}N_2O_2$ [M + H] = 243.1128, found 243.1129.

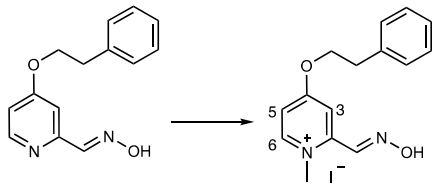

*Preparation of (E)-2-((hydroxyimino)methyl)-1-methyl-4-phenethoxypyridin-1-ium iodide (**ADG4250**):* A 35-mL sealed tube with (*E*)-4-phenethoxypicolinaldehyde oxime (172 mg, 0.770 mmol) was charged with acetone (2 mL) and MeI (670 μL, 7.70 mmol). The vessel was sealed and heated to 45 °C (external temperature). After 14 h at the same temperature, the reaction mixture was cooled to 23 °C, transferred to a 25-mL round-bottomed flask and concentrated *in vacuo* to

yield (*E*)-2-((hydroxyimino)methyl)-1-methyl-4-phenethoxypyridin-1-ium iodide as a light yellow solid (265 mg, 97% yield).

(E)-2-((Hydroxyimino)methyl)-1-methyl-4-phenethoxypyridin-1-ium iodide: m.p. = 186–188 °C; R_f = 0.10 (5% MeOH in CH_2Cl_2); IR (neat): ν_{max} = 3092, 3017, 2969, 1642, 1591, 1566, 1523, 1499, 1468, 1453, 1430, 1404, 1334, 1325, 1302, 1267, 1146, 1025, 1012 cm^{-1}; ^1H NMR (400 MHz, 293 K, DMSO-d_6): δ 12.98 (s, 1H, -CH=NO*H*), 8.78 (d, *J* = 7.2 Hz, 1H, 6-H), 8.56 (s, 1H, -C*H*=NOH), 7.69 (d, *J* = 2.8 Hz, 1H, 3-H), 7.54 (dd, *J* = 7.2, 2.8 Hz, 1H, 5-H), 7.36–7.23 (m, 5H, -*Ph*), 4.61 (t, *J* = 6.8 Hz, 2H, -OC*H*$_2$CH$_2$Ph), 4.18 (s, 3H, -N$^+$C*H*$_3$), 3.13 (t, *J* = 6.8 Hz, 2H, -OCH$_2$C*H*$_2$Ph); ^{13}C NMR (125 MHz, 293 K, DMSO-d_6): δ 169.4, 148.9, 148.7, 142.2, 137.6, 129.4, 128.8, 127.0, 113.5, 110.8, 71.3, 45.0, 34.5; HRMS (ESI+) calcd for $C_{15}H_{17}N_2O_2$ $[M]^+$ = 257.1285, found 257.1293.

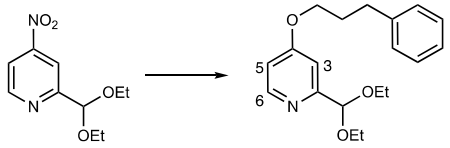

Preparation of 2-(diethoxymethyl)-4-(3-phenylpropoxy)pyridine: A 50-mL pear-shaped flask with a reflux condenser was charged with NaH (60% w/w, 360 mg, 9.00 mmol), then evacuated and refilled with nitrogen gas three times. 3-Phenyl-1-propanol (1.23 mL, 9.00 mmol) and THF (15 mL) were added, and the mixture was stirred at 23 °C. After 5 min, 2-(diethoxymethyl)-4-nitropyridine (678 mg, 3.00 mmol) was added, and the resulting mixture was stirred and heated to 65 °C (external temperature). After 18 h, the reaction mixture was cooled to 23 °C and acidified with saturated aqueous NH_4Cl (20 mL). The resulting solution was extracted with EtOAc (3 × 10 mL). The combined organic layers were dried over anhydrous Na_2SO_4, filtered, and concentrated *in vacuo*. The crude material was purified by flash chromatography (20

to 60% EtOAc in hexanes) on silica gel (75 mL) to afford 2-(diethoxymethyl)-4-(3-phenylpropoxy)pyridine as a pale yellow oil (450 mg, 70% yield).

2-(Diethoxymethyl)-4-(3-phenylpropoxy)pyridine: R_f = 0.46 (60% EtOAc in hexanes); IR (neat): ν_{max} = 2974, 1594, 1567, 1468, 1454, 1433, 1369, 1345, 1302, 1265, 1242, 1176, 1111, 1089, 1056, 1029 cm^{-1}; ^1H NMR (300 MHz, 293 K, DMSO-d_6): δ 8.32 (d, J = 5.7 Hz, 1H, 6-H), 7.32–7.16 (m, 5H, -*Ph*), 6.96 (d, J = 2.4 Hz, 1H, 3-H), 6.91 (dd, J = 5.7, 2.4 Hz, 1H, 5-H), 5.32 (s, 1H, -C*H*($OCH_2CH_3)_2$), 4.05 (t, J = 6.3 Hz, 2H, -OC*H*$_2CH_2CH_2Ph$), 3.65–3.46 (m, 4H, -CH(OC*H*$_2CH_3)_2$), 2.74 (t, J = 7.3 Hz, 2H, -$OCH_2CH_2CH_2$Ph), 2.02 (app quint, J = 6.3 Hz, 2H, -$OCH_2CH_2CH_2$Ph), 1.13 (t, J = 7.2 Hz, 6H, -CH($OCH_2CH_3)_2$); ^{13}C NMR (100 MHz, 293 K, DMSO-d_6): δ 165.5, 160.2, 150.6, 141.7, 128.8, 128.8, 126.4, 110.5, 107.3, 102.5, 67.4, 62.1, 31.8, 30.5, 15.6; HRMS (ESI+) calcd for $C_{19}H_{26}NO_3$ $[M + H]^+$ = 316.1907, found 316.1910.

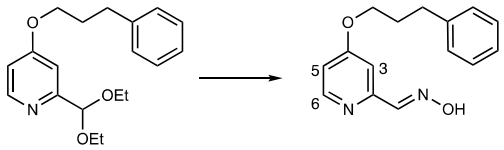

Preparation of (E)-4-(3-phenylpropoxy)picolinaldehyde oxime: A 50-mL pear-shaped flask open to air with 2-(diethoxymethyl)-4-(3-phenylpropoxy)pyridine (295 mg, 0.930 mmol) was charged with H_2O (4 mL) and 5 M H_2SO_4 in H_2O (210 μL, 1.03 mmol). The solution was heated to 95 °C (external temperature). After stirring at the same temperature for 3 h, the reaction mixture was cooled to 23 °C and treated with K_2CO_3 (514 mg, 3.72 mmol) followed by MeOH (10 mL) and NH_2OH•HCl (65 mg, 0.93 mmol) at the same temperature. A reflux condenser was attached, and the reaction was heated to reflux while open to air. After 3 h, the reaction mixture was cooled to 23 °C and concentrated *in vacuo.* EtOAc (10 mL) was added to the crude residue, followed by saturated aqueous NH_4Cl (20 mL). The layers were separated using a separatory

funnel and the aqueous layer was extracted with EtOAc (2 × 10 mL). The combined organic layers were dried over anhydrous Na_2SO_4, filtered, and concentrated *in vacuo* to afford (*E*)-4-(3-phenylpropoxy)picolinaldehyde oxime (215 mg, 86% yield) as a white solid. This material was used directly without further purification.

(E)-4-(3-Phenylpropoxy)picolinaldehyde oxime: m.p. = 145–147 °C; R_f = 0.23 (60% EtOAc in hexanes); IR (neat): ν_{max} = 2985, 2884, 1592, 1556, 1330, 1310, 1039,1031 cm^{-1}; ^1H NMR (300 MHz, 293 K, DMSO-d_6): δ 11.62 (s, 1H, -CH=NO*H*), 8.36 (d, *J* = 5.7 Hz, 1H, 6-H), 8.02 (s, 1H, -C*H*=NOH), 7.32–7.16 (m, 6H, 3-H and-*Ph*), 6.96 (dd, *J* = 5.7, 2.4 Hz, 1H, 5-H), 4.08 (t, *J* = 6.3 Hz, 2H, -OC*H*$_2$CH$_2$CH$_2$Ph), 2.74 (t, *J* = 7.5 Hz, 2H, -OCH$_2$CH$_2$C*H*$_2$Ph), 2.02 (app quint, *J* = 6.3 Hz, 2H, -OCH$_2$C*H*$_2$CH$_2$Ph); ^{13}C NMR (100 MHz, 293 K, DMSO-d_6): δ 165.3, 154.2, 151.2, 149.3, 141.7, 128.9, 128.8, 126.4, 111.5, 105.9, 67.5, 31.8, 30.5; HRMS (ESI+) calcd for $C_{15}H_{17}N_2O_2$ [M + H] = 257.1284, found 257.1283.

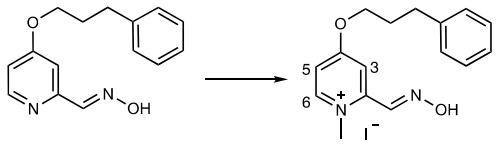

*Preparation of (E)-2-((hydroxyimino)methyl)-1-methyl-4-(3-phenylpropoxy)pyridin-1-ium iodide (**ADG4253**):* A 35-mL sealed tube with (*E*)-4-(3-phenylpropoxy)picolinaldehyde oxime (122 mg, 0.450 mmol) was charged with acetone (1 mL) and MeI (280 μL, 4.50 mmol). The vessel was sealed and heated to 40 °C (external temperature). After 14 h at the same temperature, the reaction mixture was cooled to 23 °C, transferred to a 25-mL round-bottomed flask and was concentrated *in vacuo* to yield (*E*)-2-((hydroxyimino)methyl)-1-methyl-4-(3-phenylpropoxy)pyridin-1-ium iodide as a peach solid (189 mg, quantitative yield).

(E)-2-((Hydroxyimino)methyl)-1-methyl-4-(3-phenylpropoxy)pyridin-1-ium iodide: m.p. = 155–158 °C; R_f = 0.10 (5% MeOH in CH_2Cl_2); IR (neat): ν_{max} = 3039, 2988, 1646, 1595, 1568, 1521, 1497, 1460, 1451, 1401, 1334, 1322, 1305, 1263, 1146, 1021 cm^{-1}; ^1H NMR (400 MHz, 293 K, DMSO-d_6): δ 12.97 (s, 1H, -CH=NO*H*), 8.77 (d, *J* = 7.2 Hz, 1H, 6-H), 8.57 (s, 1H, -C*H*=NOH), 7.67 (d, *J* = 3.2 Hz, 1H, 3-H), 7.60 (dd, *J* = 7.2, 3.2 Hz, 1H, 5-H), 7.31–7.27 (m, 2H, -*Ph*), 7.24–7.17 (m, 3H, -*Ph*), 4.35 (t, *J* = 6.4 Hz, 2H, -OC*H*$_2$CH$_2$CH$_2$Ph), 4.18 (s, 3H, -N$^+$C*H*$_3$), 2.75 (t, *J* = 7.2 Hz, 2H, -OCH$_2$CH$_2$C*H*$_2$Ph), 2.13–2.06 (m, 2H, -OCH$_2$C*H*$_2$CH$_2$Ph); ^{13}C NMR (100 MHz, 293 K, DMSO-d_6): δ 169.2, 148.5, 148.3, 141.8, 140.9, 128.5, 128.4, 126.0, 113.1, 110.3, 69.9, 44.6, 31.1, 29.6; HRMS (ESI+) calcd for $C_{16}H_{19}N_2O_2$ $[M]^+$ = 271.1441, found 271.1449.

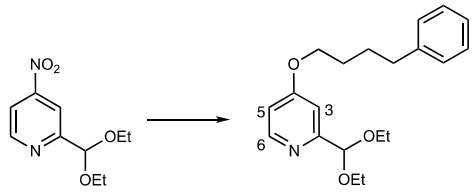

Preparation of 2-(diethoxymethyl)-4-(4-phenylbutoxy)pyridine: A 50-mL pear-shaped flask with a reflux condenser was charged with NaH (60% w/w, 480 mg, 12.0 mmol), then evacuated and refilled with nitrogen gas three times. 4-Phenyl-1-butanol (1.84 mL, 12.0 mmol) and THF (15 mL) were added, and the mixture was stirred at 23 °C. After 10 min, 2-(diethoxymethyl)-4-nitropyridine (905 mg, 4.00 mmol) was added, and the resulting mixture was stirred and heated to 75 °C (external temperature). After 6.5 h, the reaction mixture was cooled to 23 °C and acidified with saturated aqueous NH_4Cl (15 mL). The resulting solution was extracted with EtOAc (3 × 10 mL). The combined organic layers were dried over anhydrous Na_2SO_4, filtered, and concentrated *in vacuo.* The crude material was purified by flash chromatography (10

to 50% EtOAc in hexanes) on silica gel (75 mL) 2-(diethoxymethyl)-4-(4-phenylbutoxy)pyridine as an orange oil (920 mg, 70% yield).

2-(Diethoxymethyl)-4-(4-phenylbutoxy)pyridine: R_f = 0.28 (60% EtOAc in hexanes); IR (neat): ν_{max} = 2979, 2882, 1593, 1566, 1454, 1432, 1390, 1369, 1332, 1303, 1265, 1246, 1178, 1056, 1021 cm^{-1}; ^1H NMR (400 MHz, 293 K, DMSO-d_6): δ 8.31 (d, J = 5.6 Hz, 1H, 6-H), 7.29–7.26 (m, 2H, -*Ph*), 7.22–7.15 (m, 3H, -*Ph*), 6.95 (d, J = 2.4 Hz, 1H, 3-H), 6.90 (dd, J = 5.6, 2.4 Hz, 1H, 5-H), 5.31 (s, 1H, -C*H*($OCH_2CH_3)_2$), 4.07 (t, J = 5.6 Hz, 2H, -O*C*$H_2CH_2CH_2CH_2$Ph), 3.63–3.48 (m, 4H, -CH(O*C*$H_2CH_3)_2$), 2.63 (t, J = 6.8 Hz, 2H, -$OCH_2CH_2CH_2$*C*H_2Ph), 1.73–1.71 (m, 4H, -OCH_2*C*H_2*C*H_2CH_2Ph), 1.12 (t, J = 7.2 Hz, 6H, -CH(OCH_2*C*$H_3)_2$); ^{13}C NMR (100 MHz, 293 K, DMSO-d_6): δ 165.5, 160.2, 150.5, 142.3, 128.7, 128.7, 126.1, 110.4, 107.3, 102.5, 67.9, 62.0, 35.2, 28.4, 27.7, 15.6; HRMS (ESI+) calcd for $C_{20}H_{27}NO_3Na$ $[M + Na]^+$ = 352.1883, found 352.1900.

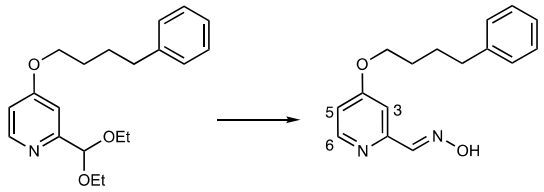

Preparation of (E)-4-(4-phenylbutoxy)picolinaldehyde oxime: A 50-mL pear-shaped flask open to air with 2-(diethoxymethyl)-4-(4-phenylbutoxy)pyridine (459 mg, 1.39 mmol) was charged with H_2O (6 mL) and 5 M H_2SO_4 in H_2O (310 μL, 1.53 mmol). The solution was heated to 95 °C (external temperature). After stirring at the same temperature for 3.5 h, the reaction mixture was cooled to 23 °C and treated with K_2CO_3 (768 mg, 5.56 mmol) followed by MeOH (10 mL) and NH_2OH•HCl (97 mg, 1.4 mmol) at the same temperature. A reflux condenser was attached, and the reaction was heated to reflux while open to air. After 2.5 h, the reaction mixture

was cooled to 23 °C and concentrated *in vacuo*. EtOAc (10 mL) was added to the crude residue, followed by saturated aqueous NH_4Cl (15 mL). The layers were separated using a separatory funnel and the aqueous layer was extracted with EtOAc (2 × 10 mL). The combined organic layers were dried over anhydrous Na_2SO_4, filtered, and concentrated *in vacuo* to afford (*E*)-4-(4-phenylbutoxy)picolinaldehyde oxime (367 mg, 98% yield) as a pale peach solid. This material was used directly without further purification.

(E)-4-(4-Phenylbutoxy)picolinaldehyde oxime: m.p. = 123–125 °C; R_f = 0.33 (60% EtOAc in hexanes); IR (neat): ν_{max} = 2980, 2730, 1592, 1562, 1519, 1493, 1462, 1429, 1395, 1328, 1304, 1249, 1189, 1089, 1074, 1062, 1042 cm^{-1}; ^1H NMR (400 MHz, 293 K, DMSO-d_6): δ 11.62 (s, 1H, -CH=NO*H*), 8.35 (d, *J* = 6.0 Hz, 1H, 6-H), 8.01 (s, 1H, -C*H*=NOH), 7.29–7.15 (m, 6H, 3-H and -*Ph*), 6.94 (dd, *J* = 6.0, 2.8 Hz, 1H, 5-H), 4.10 (t, *J* = 5.6 Hz, 2H, -OC$H_2$$CH_2CH_2CH_2$Ph), 2.64 (t, *J* = 7.2 Hz, 2H, -$OCH_2CH_2CH_2CH_2$Ph), 1.73–1.70 (m, 4H, -$OCH_2CH_2CH_2CH_2$Ph); ^{13}C NMR (100 MHz, 293 K, DMSO-d_6): δ 165.3, 154.2, 151.1, 149.3, 142.4, 128.8, 128.7, 126.2, 111.5, 105.8, 68.0, 35.2, 28.3, 27.7; HRMS (ESI+) calcd for $C_{16}H_{19}N_2O_2$ [M + H] = 271.144, found 271.1437.

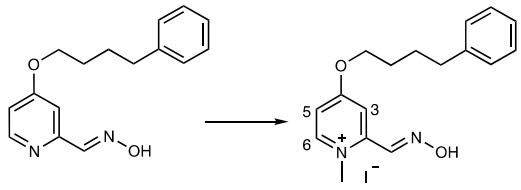

*Preparation of (E)-2-((hydroxyimino)methyl)-1-methyl-4-(4-phenylbutoxy)pyridin-1-ium iodide (**ADG4286**):* A 35-mL sealed tube with (*E*)-4-(4-phenylbutoxy)picolinaldehyde oxime (150 mg, 0.550 mmol) was charged with acetone (2 mL) and MeI (340 μL, 5.50 mmol). The vessel was sealed and heated to 45 °C (external temperature). After 17 h at the same temperature, the reaction mixture was cooled to 23 °C, transferred to a 25-mL round-bottomed flask and concentrated *in*

vacuo to yield (*E*)-2-((hydroxyimino)methyl)-1-methyl-4-(4-phenylbutoxy)pyridin-1-ium iodide as an orange yellow solid (231 mg, quantitative yield).

(E)-2-((Hydroxyimino)methyl)-1-methyl-4-(4-phenylbutoxy)pyridin-1-ium iodide: m.p. = 154–155 °C; R_f = 0.10 (5% MeOH in CH_2Cl_2); IR (neat): ν_{max} = 2971, 1644, 1592, 1567, 1524, 1495, 1468, 1453, 1434, 1330, 1304, 1266, 1146, 1019 cm^{-1}; ^1H NMR (400 MHz, 293 K, DMSO-d_6): δ 12.97 (s, 1H, -CH=NO*H*), 8.77 (d, *J* = 7.2 Hz, 1H, 6-H), 8.56 (s, 1H, -C*H*=NOH), 7.66 (d, *J* = 2.8 Hz, 1H, 3-H), 7.59 (dd, *J* = 7.2, 2.8 Hz, 1H, 5-H), 7.30–7.27 (m, 2H, -*Ar*), 7.22–7.16 (m, 3H, -*Ar*), 4.38 (t, *J* = 6.0, 2H, -OC*H*$_2$CH$_2$CH$_2$CH$_2$Ph), 4.18 (s, 3H, -N$^+$C*H*$_3$), 2.65 (t, *J* = 7.6, 2H, -OCH$_2$CH$_2$CH$_2$C*H*$_2$Ph), 1.81–1.70 (m, 4H, -OCH$_2$C*H*$_2$C*H*$_2$CH$_2$Ph); ^{13}C NMR (100 MHz, 293 K, DMSO-d_6): δ 169.1, 148.4, 148.1, 141.7, 128.3, 125.8, 113.1, 110.1, 70.4, 44.5, 34.5, 27.4, 26.9; HRMS (ESI+) calcd for $C_{17}H_{21}N_2O_2$ $[M]^+$ = 285.1598, found 285.1602.

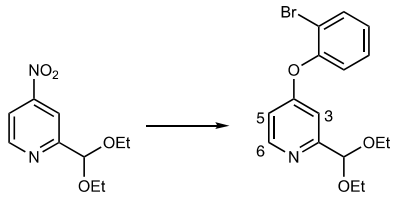

Preparation of 4-(2-bromophenoxy)-2-(diethoxymethyl)pyridine: A 25-mL round bottom flask was charged with dimethyl sulfoxide (4 mL), K_2CO_3 (1.65 g, 12.0 mmol) and 2-bromophenol (1.39 mL, 12.0 mmol). The mixture was stirred at room temperature for 5 min. 2-(Diethoxymethyl)-4-nitropyridine (905 mg, 4.00 mmol) was added. A reflux condenser was attached, and the vessel was heated to 100 °C (external temperature) for 13.5 h. The reaction mixture was cooled to 23 °C and acidified with saturated aqueous NH_4Cl (25 mL). The resulting solution was extracted with EtOAc (3 × 15 mL). The combined organic layers were dried over anhydrous Na_2SO_4, filtered, and concentrated *in vacuo.* The crude material was purified by flash

chromatography (0 to 40% EtOAc in hexanes) on silica gel (100 mL) to afford 4-(2-bromophenoxy)-2-(diethoxymethyl)pyridine as a dark brown oil (1.11 mg, 79% yield).

4-(2-Bromophenoxy)-2-(diethoxymethyl)pyridine: R_f = 0.45 (60% EtOAc in hexanes); IR (neat): ν_{max} = 2974, 2880, 1595, 1569, 1468, 1442, 1422, 1369, 1346, 1287, 1261, 1221, 1157, 1109, 1057, 1047, 1029 cm^{-1}; ^1H NMR (400 MHz, 293 K, DMSO-d_6): δ 8.43 (d, J = 7.6 Hz, 1H, 6-H), 7.82 (dd, J = 8.0, 1.2 Hz, 1H, -*Ph*), 7.52 (td, J = 8.0, 1.6 Hz, 1H, -*Ph*), 7.82 (dd, J = 8.0, 1.6 Hz, 1H, -*Ph*), 7.31 (td, J = 8.0, 1.6 Hz, 1H, -*Ph*), 6.87–6.84 (m, 2H, -*Ar*), 5.35 (s, 1H, -C*H*(OCH_2CH_3)$_2$), 3.63–3.46 (m, 4H, -CH(OC*H*$_2$CH$_3$)$_2$), 1.10 (t, J = 6.8 Hz, 6H, -CH(OCH_2CH_3)$_2$); ^{13}C NMR (100 MHz, 293 K, DMSO-d_6): δ164.4, 160.9, 151.1, 150.4, 134.5, 130.3, 128.2, 123.8, 115.9, 111.4, 108.0, 102.2, 62.2, 15.5; HRMS (ESI+) calcd for $C_{16}H_{19}BrNO_3$ $[M + H]^+$ = 352.0543, found 352.0544.

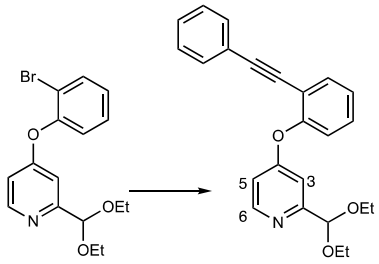

Preparation of 2-(diethoxymethyl)-4-(2-(phenylethynyl)phenoxy)pyridine: A 25-mL sealed tube with 4-(2-bromophenoxy)-2-(diethoxymethyl)pyridine (456 mg, 1.30 mmol) was treated with $Pd(OAc)_2$ (14 mg, 0.060 mmol), XPhos (57 mg, 0.12 mmol), and CuI (11 mg, 0.060 mmol) and flushed with argon gas. The mixture was dissolved in anhydrous 1,4-dioxane (1.0 mL), Et_3N (540 μL, 3.90 mmol), and phenylacetylene (220 μL, 1.90 mmol) at 23 °C. The resulting solution was heated to 70 °C (external temperature) and stirred. After 15 h, the reaction mixture was cooled to 23 °C. The crude residue was dry-loaded and purified by flash chromatography (10 to 40% EtOAc

in hexanes) on silica gel (75 mL). The semi-pure material was stirred with CH_2Cl_2 and Amberlite™ IRC-748 resin to remove residual copper. After 1 h, the mixture was filtered by gravity through a cotton plug and concentrated *in vacuo* to afford 2-(diethoxymethyl)-4-(2-(phenylethynyl)phenoxy)pyridine (475 mg, 98% yield) as a dark brown oil.

2-(Diethoxymethyl)-4-(2-(phenylethynyl)phenoxy)pyridine: R_f = 0.40 (60% EtOAc in hexanes); IR (neat): ν_{max} = 2974, 2882, 1590, 1566, 1495, 1475, 1445, 1422, 1369, 1345, 1288, 1263, 1211, 1157, 1109, 1097, 1059 cm^{-1}; ^1H NMR (300 MHz, 293 K, DMSO-d_6): δ 8.43 (d, J = 5.7 Hz, 1H, 6-H), 7.71 (dd, J = 7.5, 1.2 Hz, 1H, -*Ph*), 7.58 (td, J = 7.5, 1.2 Hz, 1H, -*Ph*), 7.43–7.29 (m, 5H, -*Ar*), 7.15 (dd, J = 7.8, 1.5 Hz, 2H, -*Ph*), 6.93–6.91 (m, 2H, -*Ph*), 5.33 (s, 1H, -C*H*(OCH_2CH_3)$_2$), 3.58–3.39 (m, 4H, -CH(OC*H*$_2$$CH_3$)$_2$), 1.04 (t, J = 6.9 Hz, 6H, -CH(OCH_2C*H*$_3$)$_2$); ^{13}C NMR (100 MHz, 293 K, DMSO-d_6): δ 164.9, 160.8, 153.9, 151.1, 133.9, 131.5, 131.4, 129.5, 129.1, 128.4, 126.9, 122.8, 122.1, 116.7, 111.7, 108.1, 102.2, 95.5, 84.7, 62.0, 15.48; HRMS (ESI+) calcd for $C_{24}H_{24}NO_3$ $[M + H]^+$ = 374.1751, found 374.1744.

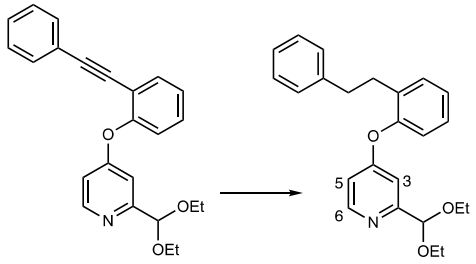

Preparation of 2-(diethoxymethyl)-4-(2-phenethylphenoxy)pyridine: A 50-mL round-bottom flask was charged with 2-(diethoxymethyl)-4-(2-(phenylethynyl)phenoxy)pyridine (332 mg, 0.890 mmol), EtOH (15 mL), PtO_2 (9 mg, 0.04 mmol) at 23 °C. The resulting suspension was purged with hydrogen gas three times and stirred vigorously at the same temperature for 19 h. The suspension was filtered by gravity through filter paper, and the resulting filtrate was concentrated

in vacuo to yield 2-(diethoxymethyl)-4-(2-phenethylphenoxy)pyridine as a dark brown oil (321 mg, 96% yield). This material was used directly without further purification.

2-(Diethoxymethyl)-4-(2-phenethylphenoxy)pyridine: R_f = 0.55 (60% EtOAc in hexanes); IR (neat): ν_{max} = 2978, 1594, 1569, 1487, 1474, 1452, 1422, 1369, 1345, 1289, 1258, 1221, 1181, 1156, 1109, 1099, 1058 cm^{-1}; ^1H NMR (400 MHz, 293 K, DMSO-d_6): δ 8.40 (d, J = 5.6 Hz, 1H, 6-H), 7.41–7.30 (m, 2H, -*Ph*), 7.27–7.09 (m, 5H, -*Ar*), 7.06–7.04 (m, 2H, -*Ph*), 6.90 (d, J = 2.8 Hz, 1H, -*Ph*), 8.40 (dd, J = 5.6, 2.8 Hz, 1H, 5-H), 5.33 (s, 1H, -C*H*($OCH_2CH_3)_2$), 3.59–3.44 (m, 4H, -CH($OCH_2CH_3)_2$), 2.78–2.69 (m, 4H, -CH_2CH_2Ph), 1.08 (t, J = 7.2 Hz, 6H, -CH($OCH_2CH_3)_2$); ^{13}C NMR (100 MHz, 293 K, DMSO-d_6): δ 165.4, 160.9, 151.6, 151.1, 141.5, 134.1, 131.7, 128.7, 128.6, 126.5, 126.4, 121.9, 111.6, 108.0, 102.4, 62.2, 36.1, 31.9, 15.5; HRMS (ESI+) calcd for $C_{24}H_{28}NO_3$ $[M + H]^+$ = 378.2063, found 378.2060.

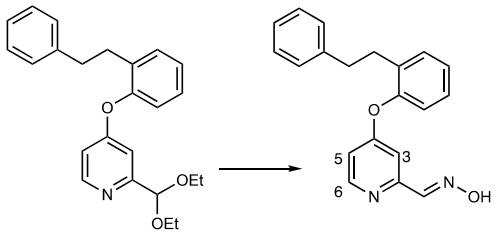

Preparation of (E)-4-(2-phenethylphenoxy)picolinaldehyde oxime: A 50-mL pear-shaped flask open to air with 2-(diethoxymethyl)-4-(2-phenethylphenoxy)pyridine (171 mg, 0.450 mmol) was charged with H_2O (3 mL) and 5 M H_2SO_4 in H_2O (100 μL, 0.490 mmol). The solution was heated to 95 °C (external temperature). After stirring at the same temperature for 2.5 h, the reaction mixture was cooled to 23 °C and treated with K_2CO_3 (249 mg, 1.80 mmol) followed by MeOH (10 mL) and NH_2OH•HCl (31 mg, 0.45 mmol) at the same temperature. A reflux condenser was attached, and the reaction was heated to reflux while open to air. After 3 h, the reaction mixture was cooled to 23 °C and concentrated *in vacuo*. EtOAc (10 mL) was added to the crude residue,

followed by saturated aqueous NH_4Cl (15 mL). The layers were separated using a separatory funnel and the aqueous layer was extracted with EtOAc (2 × 10 mL). The combined organic layers were dried over anhydrous Na_2SO_4, filtered, and concentrated *in vacuo* to afford (*E*)-4-(2-phenethylphenoxy)picolinaldehyde oxime (145 mg, quantitative yield) as a brown solid. This material was used directly without further purification.

(E)-4-(2-Phenethylphenoxy)picolinaldehyde oxime: m.p. = 109–111 °C; R_f = 0.32 (60% EtOAc in hexanes); IR (neat): ν_{max} = 2871, 2746, 1596, 1575, 1561, 1487, 1451, 1425, 1321, 1291, 1244, 1225, 1181, 1000 cm^{-1}; ^1H NMR (500 MHz, 293 K, DMSO-d_6): δ 11.70 (s, 1H, -CH=NO*H*), 8.46 (d, *J* = 6.0 Hz, 1H, 6-H), 8.01 (s, 1H, -C*H*=NOH), 7.42 (dd, *J* = 7.5, 1.5 Hz, 1H, -*Ph*), 7.34 (td, *J* = 8.0, 2.0 Hz, 1H, -*Ph*), 7.26 (td, *J* = 7.4, 1.0 Hz, 1H, -*Ph*), 7.23–7.19 (m, 2H, -*Ar*), 7.16–7.13 (m, 2H, -*Ar*), 7.07–7.06 (m, 3H, -*Ar*), 6.97 (dd, *J* = 6.0, 2.5 Hz, 1H, 5-H), 2.80–2.73 (m, 4H, -CH_2CH_2Ph); ^{13}C NMR (125 MHz, 293 K, DMSO-d_6): δ 165.1, 154.7, 151.8, 151.5, 148.8, 141.5, 134.1, 131.7, 128.8, 128.7, 128.6, 126.6, 126.4, 122.1, 112.6, 106.0, 36.1, 31.8; HRMS (ESI+) calcd for $C_{20}H_{19}N_2O_2$ [M + H] =319.1441, found 319.1449.

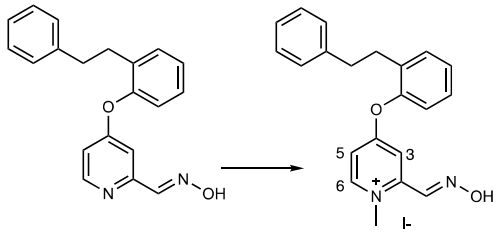

*Preparation of (E)-2-((hydroxyimino)methyl)-1-methyl-4-(2-phenethylphenoxy)pyridin-1-ium iodide (**ADG4298**):* A 35-mL sealed tube with (*E*)-4-(2-phenethylphenoxy)picolinaldehyde oxime (145 mg, 0.460 mmol) was charged with acetone (2 mL) and MeI (280 μL, 4.60 mmol). The vessel was sealed and heated to 40 °C (external temperature). After 15.5 h at the same temperature, the reaction mixture was cooled to 23 °C, transferred to a 25-mL round-bottomed

flask and concentrated *in vacuo* to yield (*E*)-2-((hydroxyimino)methyl)-1-methyl-4-(2-phenethylphenoxy)pyridin-1-ium iodide as a light tan solid (105 mg, 50% yield).

(E)-2-((Hydroxyimino)methyl)-1-methyl-4-(2-phenethylphenoxy)pyridin-1-ium iodide: m.p. = 165–167 °C; R_f = 0.76 (10% MeOH in CH_2Cl_2); IR (neat): ν_{max} = 3174, 3009, 1642, 1568, 1519, 1488, 1463, 1445, 1330, 1293, 1259, 1217, 1170, 1149, 1140, 993 cm^{-1}; ^1H NMR (400 MHz, 293 K, DMSO-d_6): δ 13.06 (s, 1H, -CH=NO*H*), 8.82 (d, *J* = 7.2 Hz, 1H, 6-H), 8.59 (s, 1H, -C*H*=NOH), 7.59–7.52 (m, 2H, -*Ar*), 7.45–7.37 (m, 3H, -*Ar*), 7.27–7.08 (m, 6H, -*Ar*), 4.22 (s, 3H, -N^+CH_3), 2.81 (app s, 4H, -CH_2CH_2Ph); ^{13}C NMR (125 MHz, 293 K, DMSO-d_6): δ 168.8, 150.4, 150.0, 149.2, 141.8, 141.2, 133.7, 132.2, 129.1, 128.8, 128.6, 128.0, 126.4, 121.6, 114.7, 109.5, 45.1, 36.0, 31.4; HRMS (ESI+) calcd for $C_{21}H_{21}N_2O_2$ $[M]^+$ = 333.1597, found 333.1606.

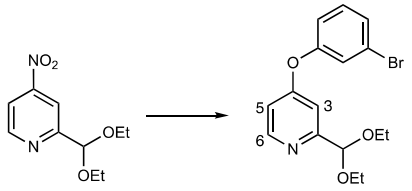

Preparation of 4-(3-bromophenoxy)-2-(diethoxymethyl)pyridine: A 25-mL round bottom flask was charged with dimethyl sulfoxide (4 mL), K_2CO_3 (1.65 g, 12.0 mmol) and 3-bromophenol (1.27 mL, 12.0 mmol). The mixture was stirred at room temperature for 10 min. 2-(Diethoxymethyl)-4-nitropyridine (905 mg, 4.00 mmol) was added. A reflux condenser was attached, and the vessel was heated to 95 °C (external temperature) for 5.5 h. The reaction mixture was cooled to 23 °C and acidified with saturated aqueous NH_4Cl (20 mL). The resulting solution was extracted with EtOAc (3 × 10 mL). The combined organic layers were dried over anhydrous Na_2SO_4, filtered, and concentrated *in vacuo.* The crude material was purified by flash

chromatography (0 to 40% EtOAc in hexanes) on silica gel (75 mL) to afford 4-(3-bromophenoxy)-2-(diethoxymethyl)pyridine as an amber oil (706 mg, 50% yield).

4-(3-Bromophenoxy)-2-(diethoxymethyl)pyridine: R_f = 0.50 (60% EtOAc in hexanes); IR (neat): ν_{max} = 2975, 1598, 1574, 1536, 1467, 1422, 1369, 1346, 1286, 1264, 1208, 1154, 1110, 1085, 1059 cm^{-1}; ^1H NMR (400 MHz, 293 K, DMSO-d_6): δ 8.46 (d, J = 5.6 Hz, 1H, 6-H), 7.54–7.51 (m, 1H, -*Ph*), 7.48–7.44 (m, 2H, -*Ph*), 7.23 (ddd, J = 8.0, 2.4, 0.8 Hz, 1H, -*Ph*), 6.97 (d, J = 2.8 Hz, 1H, 3-H), 6.94 (dd, J = 5.6, 2.8 Hz, 1H, 5-H), 5.36 (s, 1H, -C*H*$(OCH_2CH_3)_2$), 3.65–3.48 (m, 4H, -CH(OC*H*$_2$CH$_3$)$_2$), 1.12 (t, J = 6.8 Hz, 6H, -CH(OCH$_2$C*H*$_3$)$_2$); ^{13}C NMR (100 MHz, 293 K, DMSO-d_6): δ 164.7, 161.0, 155.0, 151.3, 132.6, 129.0, 124.2, 122.9, 120.3, 112.5, 109.0, 102.2, 62.2, 15.5; HRMS (ESI+) calcd for $C_{16}H_{19}NO_3Br$ $[M + H]^+$ = 352.0542, found 352.0534.

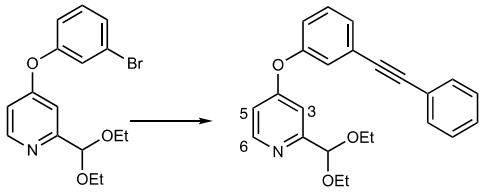

Preparation of 2-(diethoxymethyl)-4-(3-(phenylethynyl)phenoxy)pyridine: A 35-mL sealed tube with 4-(3-bromophenoxy)-2-(diethoxymethyl)pyridine (300 mg, 0.860 mmol) was treated with $Pd(OAc)_2$ (8 mg, 0.04 mmol), XPhos (38 mg, 0.80 mmol), and CuI (8 mg, 0.04 mmol) and flushed with argon gas. The mixture was dissolved in anhydrous 1,4-dioxane (1.0 mL), Et_3N (480 μL, 3.40 mmol), and phenylacetylene (141 μL, 1.30 mmol) at 23 °C. The resulting solution was heated to 70 °C (external temperature) and stirred. After 14 h, the reaction mixture was cooled to 23 °C. The crude residue was dry-loaded and purified by flash chromatography (10 to 40% EtOAc in hexanes) on silica gel (50 mL). The semi-pure material was stirred with CH_2Cl_2 and Amberlite™ IRC-748 resin to remove residual copper. After 1.5 h, the mixture was filtered by gravity through

a cotton plug and concentrated *in vacuo* to afford 2-(diethoxymethyl)-4-(2-(phenylethynyl)phenoxy)pyridine (298 mg, 83% yield) as a dark brown oil.

2-(Diethoxymethyl)-4-(3-(phenylethynyl)phenoxy)pyridine: R_f = 0.41 (60% EtOAc in hexanes); IR (neat): ν_{max} = 2974, 2880, 1591, 1566, 1493, 1475, 1442, 1422, 1369, 1346, 1287, 1259, 1204, 1158, 1110, 1059 cm^{-1}; ^1H NMR (400 MHz, 293 K, DMSO-d_6): δ 8.45 (d, J = 5.6 Hz, 1H, 6-H), 7.57–7.48 (m, 4H, -*Ar*), 7.44–7.42 (m, 3H, -*Ar*), 7.38 (br s, 1H, -*Ar*), 7.27–7.25 (m, 1H, -*Ar*), 6.98–6.93 (m, 2H, -*Ar*), 5.35 (s, 1H, -C*H*(OCH_2CH_3)$_2$), 3.64–3.47 (m, 4H, -CH(OC*H*$_2$$CH_3$)$_2$), 1.11 (t, J = 7.2 Hz, 6H, -CH(OCH_2CH_3)$_2$); ^{13}C NMR (100 MHz, 293 K, DMSO-d_6: δ 164.9, 161.0, 154.2, 151.3, 131.9, 131.4, 129.5, 129.2, 129.0, 124.8, 123.7, 122.3, 121.9, 112.5, 108.9, 102.3, 90.8, 88.6, 62.3, 15.5; HRMS (ESI+) calcd for $C_{24}H_{24}NO_3$ $[M + H]^+$ = 374.1751, found 374.1747.

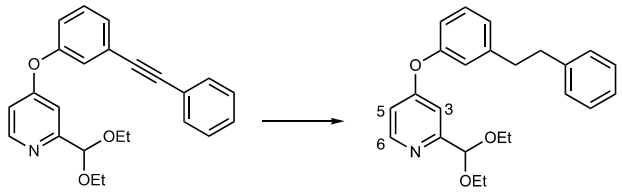

Preparation of 2-(diethoxymethyl)-4-(3-phenethylphenoxy)pyridine: A 50-mL round-bottom flask was charged with 2-(diethoxymethyl)-4-(2-(phenylethynyl)phenoxy)pyridine (318 mg, 0.850 mmol), EtOH (15 mL), PtO_2 (9 mg, 0.04 mmol) at 23 °C. The resulting suspension was purged with hydrogen gas three times and stirred vigorously at the same temperature for 24 h. The suspension was filtered by gravity through filter paper, and the resulting filtrate was concentrated *in vacuo* to yield 2-(diethoxymethyl)-4-(3-phenethylphenoxy)pyridine as a dark brown oil (269 mg, 84% yield). This material was used directly without further purification.

2-(Diethoxymethyl)-4-(3-phenethylphenoxy)pyridine: R_f = 0.45 (60% EtOAc in hexanes); IR (neat): ν_{max} = 2974, 2927, 2880, 1596, 1579, 1483, 1443, 1422, 1369, 1345, 1288, 1258, 1240,

1169, 1135, 1110, 1059 cm^{-1}; ^1H NMR (300 MHz, 293 K, DMSO-d_6): δ 8.41 (d, J = 5.7 Hz, 1H, 6-H), 7.38 (t, J = 7.8 Hz, 1H, -*Ph*), 7.29–7.14 (m, 6H, -*Ar*), 7.29–7.14 (m, 6H, -*Ar*), 7.02–6.97 (m, 2H, -*Ar*), 6.94 (d, J = 2.4 Hz, 1H, 3-H), 6.80 (d, J = 5.7, 2.4 Hz, 1H, 5-H), 5.35 (s, 4H, -C*H*(OCH_2CH_3)$_2$), 3.65–3.46 (m, 4H, -CH(OC*H*$_2$$CH_3$)$_2$), 2.90 (app s, 4H, -C*H*$_2$C*H*$_2$Ph), 1.08 (t, J = 7.2 Hz, 6H, -CH(OCH_2CH_3)$_2$); ^{13}C NMR (100 MHz, 293 K, DMSO-d_6): δ 165.3, 160.8, 153.8, 151.0, 144.8, 141.6, 130.6, 128.8, 128.6, 126.3, 126.2, 121.2, 118.6, 112.1, 108.6, 102.3, 62.1, 37.3, 37.1, 15.5; HRMS (ESI+) calcd for $C_{24}H_{28}NO_3$ $[M + H]^+$ = 378.2064, found 378.2047.

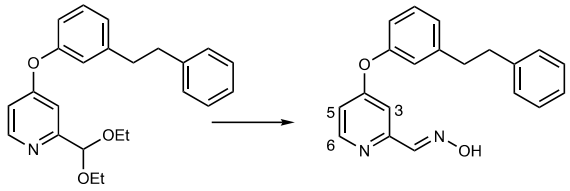

Preparation of (E)-4-(3-phenethylphenoxy)picolinaldehyde oxime: A 50-mL pear-shaped flask open to air with 2-(diethoxymethyl)-4-(3-phenethylphenoxy)pyridine (146 mg, 0.380 mmol) was charged with H_2O (3 mL) and 5 M H_2SO_4 in H_2O (80 μL, 0.42 mmol). The solution was heated to 95 °C (external temperature). After stirring at the same temperature for 3.5 h, the reaction mixture was cooled to 23 °C and treated with K_2CO_3 (210 mg, 1.52 mmol) followed by MeOH (10 mL) and NH_2OH•HCl (27 mg, 0.38 mmol) at the same temperature. A reflux condenser was attached, and the reaction was heated to reflux while open to air. After 2.5 h, the reaction mixture was cooled to 23 °C and concentrated *in vacuo.* EtOAc (10 mL) was added to the crude residue, followed by saturated aqueous NH_4Cl (25 mL). The layers were separated using a separatory funnel and the aqueous layer was extracted with EtOAc (2 × 10 mL). The combined organic layers were dried over anhydrous Na_2SO_4, filtered, and concentrated *in vacuo* to afford (*E*)-4-(3-phenethylphenoxy)picolinaldehyde oxime (97 mg, 80% yield) as a dark brown oil. This material

was used directly without further purification.

(E)-4-(3-Phenethylphenoxy)picolinaldehyde oxime: R_f = 0.46 (60% EtOAc in hexanes); IR (neat): ν_{max} = 2980, 2745, 1596, 1578, 1561, 1514, 1483, 1444, 1427, 1330, 1290, 1258, 1241, 1175, 1136, 1071 cm^{-1}; ^1H NMR (400 MHz, 293 K, DMSO-d_6): δ 11.70 (s, 1H, -CH=NO*H*), 8.43 (d, *J* = 5.6 Hz, 1H, 6-H), 8.02 (s, 1H, -C*H*=NOH), 7.39 (t, *J* = 7.6 Hz, 1H, -*Ph*), 7.27–7.13 (m, 7H, -*Ar*), 7.03–7.00 (m, 2H, -*Ar*), 6.88 (dd, *J* = 5.6, 2.4 Hz, 1H, 5-H), 2.93–2.87 (m, 4H, -CH_2CH_2Ph); ^{13}C NMR (100 MHz, 293 K, DMSO-d_6): δ 165.1, 154.7, 153.7, 151.7, 148.9, 144.9, 141.7, 130.7, 128.9, 128.7, 126.5, 126.3, 121.5, 118.9, 112.9, 106.9, 37.2; HRMS (ESI+) calcd for $C_{20}H_{19}N_2O_2$ [M + H] = 319.1441, found 319.1426.

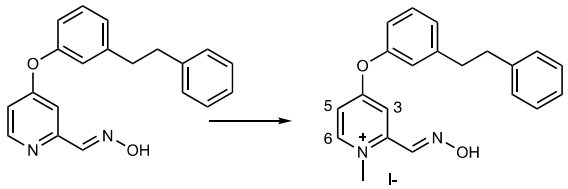

*Preparation of (E)-2-((hydroxyimino)methyl)-1-methyl-4-(3-phenethylphenoxy)pyridin-1-ium iodide (**ADG4291**):* A 35-mL sealed tube with (*E*)-4-(3-phenethylphenoxy)picolinaldehyde oxime (97 mg, 0.30 mmol) was charged with acetone (1 mL) and MeI (190 μL, 3.00 mmol). The vessel was sealed and heated to 45 °C (external temperature). After 19.5 h at the same temperature, the reaction mixture was cooled to 23 °C, transferred to a 25-mL round-bottomed flask and concentrated *in vacuo*. The crude residue was dry-loaded and purified by flash chromatography (5 to 40% MeOH in CH_2Cl_2) on silica gel (10 mL) to yield (*E*)-2-((hydroxyimino)methyl)-1-methyl-4-(3-phenethylphenoxy)pyridin-1-ium iodide as a light yellow oil (132 mg, 95% yield).

(E)-2-((Hydroxyimino)methyl)-1-methyl-4-(3-phenethylphenoxy)pyridin-1-ium iodide: R_f = 0.23 (50% MeOH in CH_2Cl_2); IR (neat): ν_{max} = 2997, 2853, 1638, 1607, 1574, 1513, 1484, 1452,

1332, 1298, 1260, 1232, 1184, 1144, 1020 cm^{-1}; ^1H NMR (300 MHz, 293 K, DMSO-d_6): δ 13.06 (s, 1H, -CH=NO*H*), 8.82 (d, *J* = 8.8 Hz, 1H, 6-H), 8.60 (s, 1H, -C*H*=NOH), 7.54–7.46 (m, 3H, -*Ar*), 7.32–7.13 (m, 8H, -*Ar*), 4.24 (s, 3H, -N^+CH_3), 2.98–2.86 (m, 4H, -CH_2CH_2Ph); ^{13}C NMR (100 MHz, 293 K, CD_3OD): δ 171.0, 153.5, 151.4, 149.8, 146.7, 142.3, 141.8, 131.8, 129.6, 129.3, 128.9, 127.0, 122.1, 119.2, 115.2, 112.4, 45.8, 38.5, 38.5; HRMS (ESI+) calcd for $C_{21}H_{21}N_2O_2$ $[M]^+$ = 333.1598, found 333.1595.

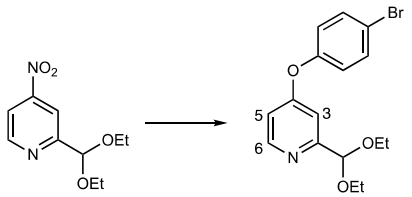

Preparation of 4-(4-bromophenoxy)-2-(diethoxymethyl)pyridine: A 25-mL sealed tube was charged with dimethyl sulfoxide (3 mL), K_2CO_3 (829 mg, 6.00 mmol) and 4-bromophenol (1.03 g, 6.00 mmol). The mixture was stirred at room temperature for 5 min. 2-(diethoxymethyl)-4-nitropyridine (452 mg, 2.00 mmol) was added, a reflux condenser was attached, and the vessel was heated to 95 °C (external temperature) for 5.5 h. The reaction mixture was cooled to 23 °C and acidified with saturated aqueous NH_4Cl (15 mL). The resulting solution was extracted with EtOAc (3 × 10 mL). The combined organic layers were dried over anhydrous Na_2SO_4, filtered, and concentrated *in vacuo.* The crude material was purified by flash chromatography (0 to 50% EtOAc in hexanes) on silica gel (20 mL) to afford 4-(4-bromophenoxy)-2-(diethoxymethyl)pyridine as a yellow oil (695 mg, 99% yield).

4-(4-Bromophenoxy)-2-(diethoxymethyl)pyridine: R_f = 0.63 (60% EtOAc in hexanes); IR (neat): ν_{max} = 2974, 2881, 1597, 1570, 1481, 1420, 1399, 1369, 1346, 1287, 1257, 1212, 1165, 1151, 1109, 1062, 1010 cm^{-1}; ^1H NMR (400 MHz, 293 K, DMSO-d_6): δ 8.44 (d, *J* = 6.0 Hz, 1H,

6-H), 7.68 (app dt, J = 8.8, 3.6 Hz, 2H, -*Ph*), 7.18 (app dt, J = 8.8, 3.6 Hz, 2H, -*Ph*), 6.96 (d, J = 2.4 Hz, 1H, 3-H), 6.69 (dd, J = 5.6, 2.4 Hz, 1H, 5-H), 5.35 (s, 1H, -C*H*(OCH_2CH_3)$_2$), 3.64–3.48 (m, 4H, -CH(OCH_2CH_3)$_2$), 1.11 (t, J = 7.2 Hz, 6H, -CH(OCH_2CH_3)$_2$); ^{13}C NMR (100 MHz, 293 K, DMSO-d_6): δ 164.7, 161.0, 153.4, 151.2, 133.7, 123.4, 118.0, 112.3, 108.8, 102.2, 62.2, 15.5; HRMS (ESI+) calcd for $C_{16}H_{19}NO_3Br$ $[M + H]^+$ = 352.0542, found 352.0535.

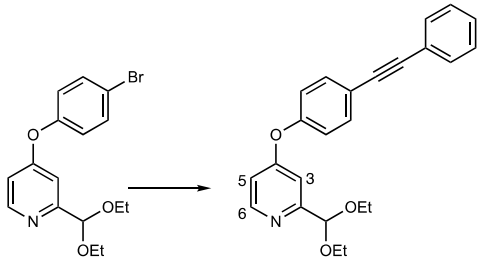

Preparation of 2-(diethoxymethyl)-4-(4-(phenylethynyl)phenoxy)pyridine: A 25-mL sealed tube with 4-(4-bromophenoxy)-2-(diethoxymethyl)pyridine (566 mg, 1.61 mmol) was treated with $Pd(OAc)_2$ (18 mg, 0.080 mmol), XPhos (75 mg, 0.16 mmol), and CuI (15 mg, 0.080 mmol) and flushed with argon gas. The mixture was dissolved in anhydrous 1,4-dioxane (2.0 mL), Et_3N (670 μL, 4.83 mmol), and phenylacetylene (270 μL, 2.40 mmol) at 23 °C. The resulting solution was heated to 70 °C (external temperature) and stirred. After 16.5 h, the reaction mixture was cooled to 23 °C. The crude residue was dry-loaded and purified by flash chromatography (10 to 50% EtOAc in hexanes) on silica gel (75 mL). The semi-pure material was stirred with CH_2Cl_2 and Amberlite™ IRC-748 resin to remove residual copper. After 1 h, the mixture was filtered by gravity through a cotton plug and concentrated *in vacuo* to afford 2-(diethoxymethyl)-4-(4-(phenylethynyl)phenoxy)pyridine (558 g, 93% yield) as a dark brown oil.

2-(Diethoxymethyl)-4-(4-(phenylethynyl)phenoxy)pyridine: R_f = 0.53 (60% EtOAc in hexanes); IR (neat): ν_{max} = 2975, 2872, 1606, 1568, 1504, 1471, 1442, 1420, 1368, 1357, 1332,

1286, 1262, 1238, 1216, 1168, 1153, 1132, 1111, 1084, 1048, 1032, 1010 cm^{-1}; ^1H NMR (400 MHz, 293 K, $CDCl_3$): δ 8.49 (d, J = 6.0 Hz, 1H, 6-H), 7.62–7.54 (m, 4H, -*Ar*), 7.39–7.37 (m, 3H, -*Ar*), 7.22 (d, J = 2.4 Hz, 1H, 3-H), 7.11–7.09 (m, 2H, -*Ar*), 6.82 (dd, J = 6.0, 2.4 Hz, 1H, 5-H), 5.45 (s, 1H, -C*H*$(OCH_3)_2$), 3.77–3.59 (m, 4H, -CH$(OCH_2CH_3)_2$), 1.26 (t, J = 7.2 Hz, 6H, -CH$(OCH_2CH_3)_2$); ^{13}C NMR (100 MHz, 293 K, $CDCl_3$): δ 165.0, 160.7, 154.0, 150.7, 133.5, 131.5, 128.3, 123.0, 120.5, 120.3, 111.9, 109.7, 102.3, 89.5, 88.3, 62.3, 15.1; HRMS (ESI+) calcd for $C_{24}H_{24}NO_3$ $[M + H]^+$ = 374.1751, found 374.1739.

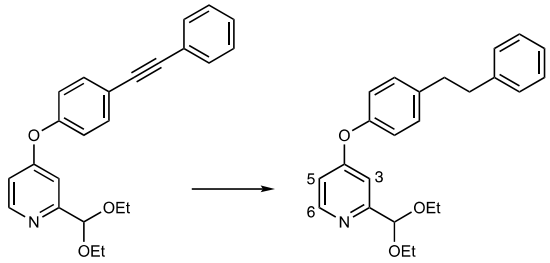

Preparation of 2-(diethoxymethyl)-4-(4-phenethylphenoxy)pyridine: A 50-mL round-bottom flask was charged with 2-(diethoxymethyl)-4-(4-(phenylethynyl)phenoxy)pyridine (426 mg, 1.14 mmol), EtOH (20 mL), PtO_2 (13 mg, 0.060 mmol) at 23 °C. The resulting suspension was purged with hydrogen gas three times and stirred vigorously at the same temperature for 6.5 h. The suspension was filtered by gravity through filter paper, and the resulting filtrate was concentrated *in vacuo* to yield 2-(diethoxymethyl)-4-(4-phenethylphenoxy)pyridine as a dark brown oil (435 mg, quantitative yield). This material was used directly without further purification.

2-(Diethoxymethyl)-4-(4-phenethylphenoxy)pyridine: R_f = 0.53 (60% EtOAc in hexanes); IR (neat): ν_{max} = 2975, 2928, 1586, 1570, 1504, 1474, 1453, 1422, 1369, 1345, 1288, 1257, 1213, 1168, 1152, 1110, 1059, 1016 cm^{-1}; ^1H NMR (300 MHz, 293 K, DMSO-d_6): δ 8.40 (d, J = 5.7 Hz, 1H, 6-H), 7.34–7.15 (m, 7H, -*Ph*), 7.09–7.07 (m, 2H, -*Ph*), 6.90 (d, J = 2.4 Hz, 1H, 3-H), 6.87 (dd,

J = 5.7, 2.4 Hz, 1H, 5-H), 5.33 (s, 1H, -C*H*(OCH_3)$_2$), 3.64–3.44 (m, 4H, -CH(OC*H*$_2$$CH_3$)$_2$), 2.91 (app s, 4H, -C*H*$_2$C*H*$_2$Ph), 1.23 (t, J = 6.9 Hz, 6H, -CH(OCH_2C*H*$_3$)$_2$); ^{13}C NMR (100 MHz, 293 K, DMSO-d_6): δ 165.5, 160.9, 151.9, 151.0, 141.7, 139.4, 130.8, 128.9, 128.7, 126.3, 121.1, 112.1, 108.4, 102.4, 62.2, 37.5, 36.9, 15.5; HRMS (ESI+) calcd for $C_{24}H_{28}NO_3$ $[M + H]^+$ = 378.2064, found 378.2062.

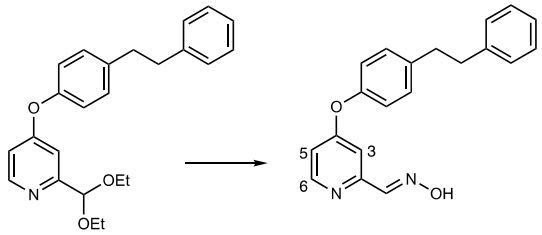

Preparation of (E)-4-(4-phenethylphenoxy)picolinaldehyde oxime: A 50-mL pear-shaped flask open to air with 2-(diethoxymethyl)-4-(4-phenethylphenoxy)pyridine (232 mg, 0.610 mmol) was charged with H_2O (3 mL) and 5 M H_2SO_4 in H_2O (130 μL, 0.680 mmol). The solution was heated to 95 °C (external temperature). After stirring at the same temperature for 3 h, the reaction mixture was cooled to 23 °C and treated with K_2CO_3 (337 mg, 2.44 mmol) followed by MeOH (10 mL) and NH_2OH•HCl (42 mg, 0.61 mmol) at the same temperature. A reflux condenser was attached, and the reaction was heated to reflux while open to air. After 4 h, the reaction mixture was cooled to 23 °C and concentrated *in vacuo.* EtOAc (10 mL) was added to the crude residue, followed by saturated aqueous NH_4Cl (20 mL). The layers were separated using a separatory funnel and the aqueous layer was extracted with EtOAc (2 × 10 mL). The combined organic layers were dried over anhydrous Na_2SO_4, filtered, and concentrated *in vacuo* to afford (*E*)-4-(4-phenethylphenoxy)picolinaldehyde oxime (118 mg, 61% yield) as an orange solid. This material was used directly without further purification.

(E)-4-(4-Phenethylphenoxy)picolinaldehyde oxime: m.p. = 142–144 °C; R_f = 0.49 (60%

EtOAc in hexanes); IR (neat): ν_{max} = 2985, 1586, 1561, 1504, 1428, 1323, 1293, 1256, 1243, 1219, 1174 cm^{-1}; ^1H NMR (400 MHz, 293 K, DMSO-d_6): δ 11.68 (s, 1H, -CH=NO*H*), 8.45 (d, *J* = 5.6 Hz, 1H, 6-H), 8.01 (s, 1H, -C*H*=NOH), 7.35–7.33 (m, 2H, -*Ph*), 7.32–7.23 (m, 4H, -*Ar*), 7.21–7.16 (m, 1H, -*Ph*), 7.13–7.10 (m, 3H, -*Ar*), 6.95 (dd, *J* = 5.6, 2.8 Hz, 1H, 5-H), 2.91 (s, 4H, -CH_2CH_2Ph); ^{13}C NMR (75 MHz, 293 K, DMSO-d_6): δ 165.3, 154.6, 151.8, 151.7, 148.9, 141.8, 139.6, 130.8, 128.9, 128.7, 126.3, 121.2, 112.9, 106.6, 37.5, 36.9; HRMS (ESI+) calcd for $C_{20}H_{19}N_2O_2$ [M + H] = 319.1441, found 319.1441.

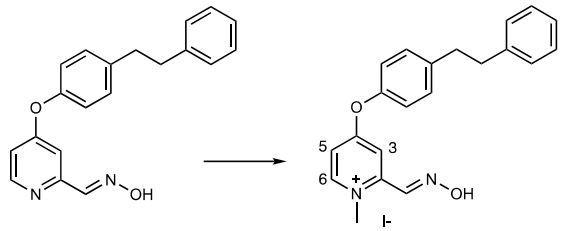

*Preparation of (E)-2-((hydroxyimino)methyl)-1-methyl-4-(4-phenethylphenoxy)pyridin-1-ium iodide (**ADG4278**):* A 35-mL sealed tube with (*E*)-4-(4-phenethylphenoxy)picolinaldehyde oxime (73 mg, 0.23 mmol) was charged with acetone (1 mL) and MeI (140 μL, 2.28 mmol). The vessel was sealed and heated to 40 °C (external temperature). After 16 h at the same temperature, the reaction mixture was cooled to 23 °C, transferred to a 25-mL round-bottomed flask and concentrated *in vacuo* to yield (*E*)-2-((hydroxyimino)methyl)-1-methyl-4-(4-phenethylphenoxy)pyridin-1-ium iodide as a yellow solid (68 mg, 64% yield).

(E)-2-((Hydroxyimino)methyl)-1-methyl-4-(4-phenethylphenoxy)pyridin-1-ium iodide: m.p. = 182–184 °C; R_f = 0.68 (50% MeOH in CH_2Cl_2); IR (neat): ν_{max} = 3068, 1642, 1582, 1567, 1499, 1460, 1415, 1327, 1299, 1262, 1213, 1182, 1160, 1011 cm^{-1}; ^1H NMR (400 MHz, 293 K, CD_3OD): δ 8.66 (d, *J* = 5.2 Hz, 1H, 6-H), 8.54 (s, 1H, -C*H*=NOH), 7.66 (d, *J* = 7.2, 2.4 Hz, 1H, 3-H), 7.36–7.34 (m, 3H, -*Ar*), 7.26–7.23 (m, 2H, -*Ar*), 7.18–7.14 (m, 5H, -*Ar*), 4.25 (s, 3H, -

N^+CH_3), 2.99–2.94 (m, 4H, -CH_2CH_2Ph); ^{13}C NMR (100 MHz, 293 K, CD_3OD): δ 171.2, 151.8, 151.4, 149.7, 142.7, 142.5, 141.8, 132.1, 129.6, 129.3, 127.0, 121.6, 115.3, 112.2, 45.7, 38.8, 38.3; HRMS (ESI+) calcd for $C_{21}H_{21}N_2O_2$ $[M]^+$ = 333.1597, found 333.1582.

Appendix A.4 NMR spectra

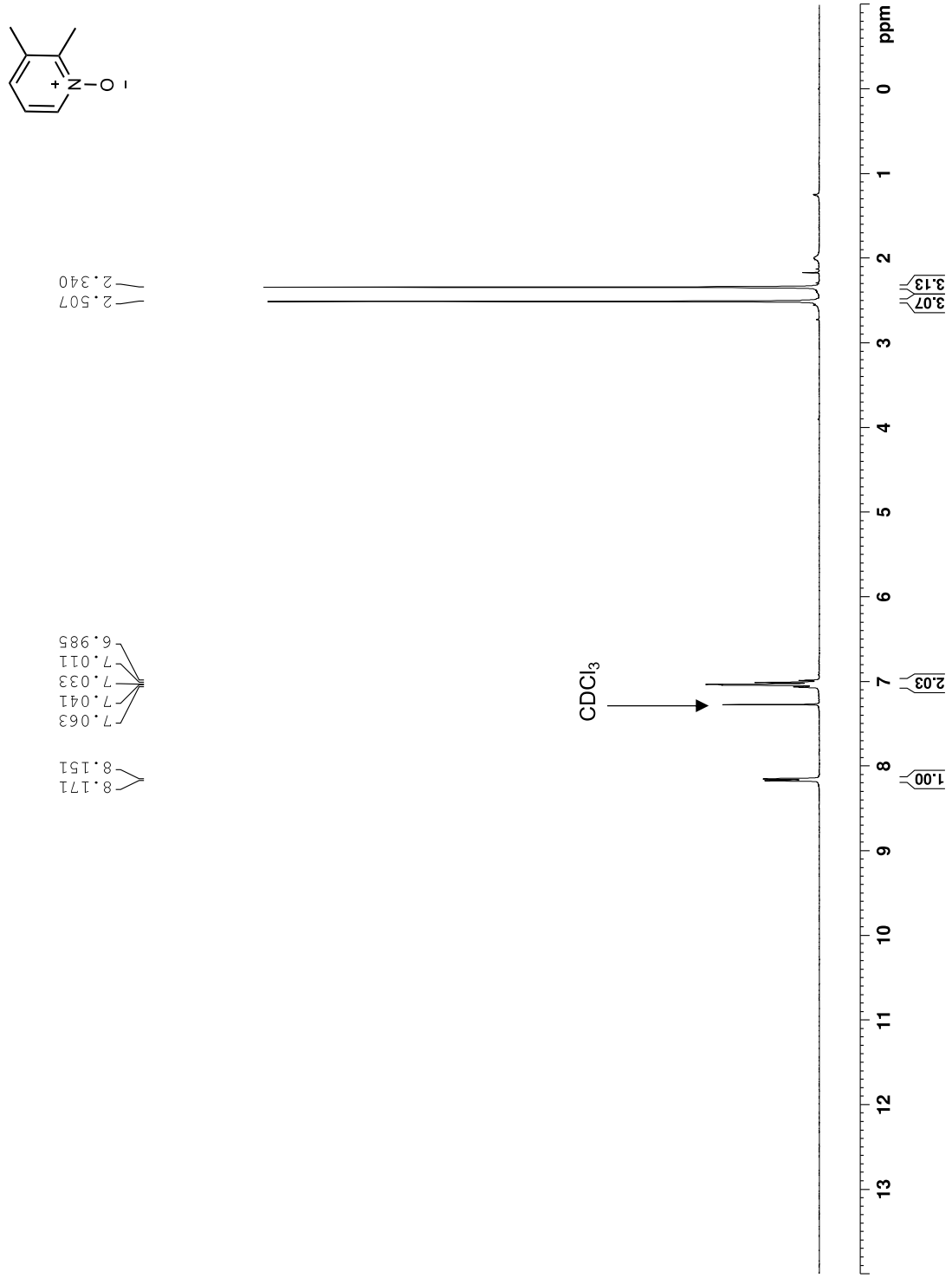

Spectrum 1. ^{1}H NMR of 2,3-dimethylpyridine 1-oxide (300 MHz, 293 K, $CDCl_3$).

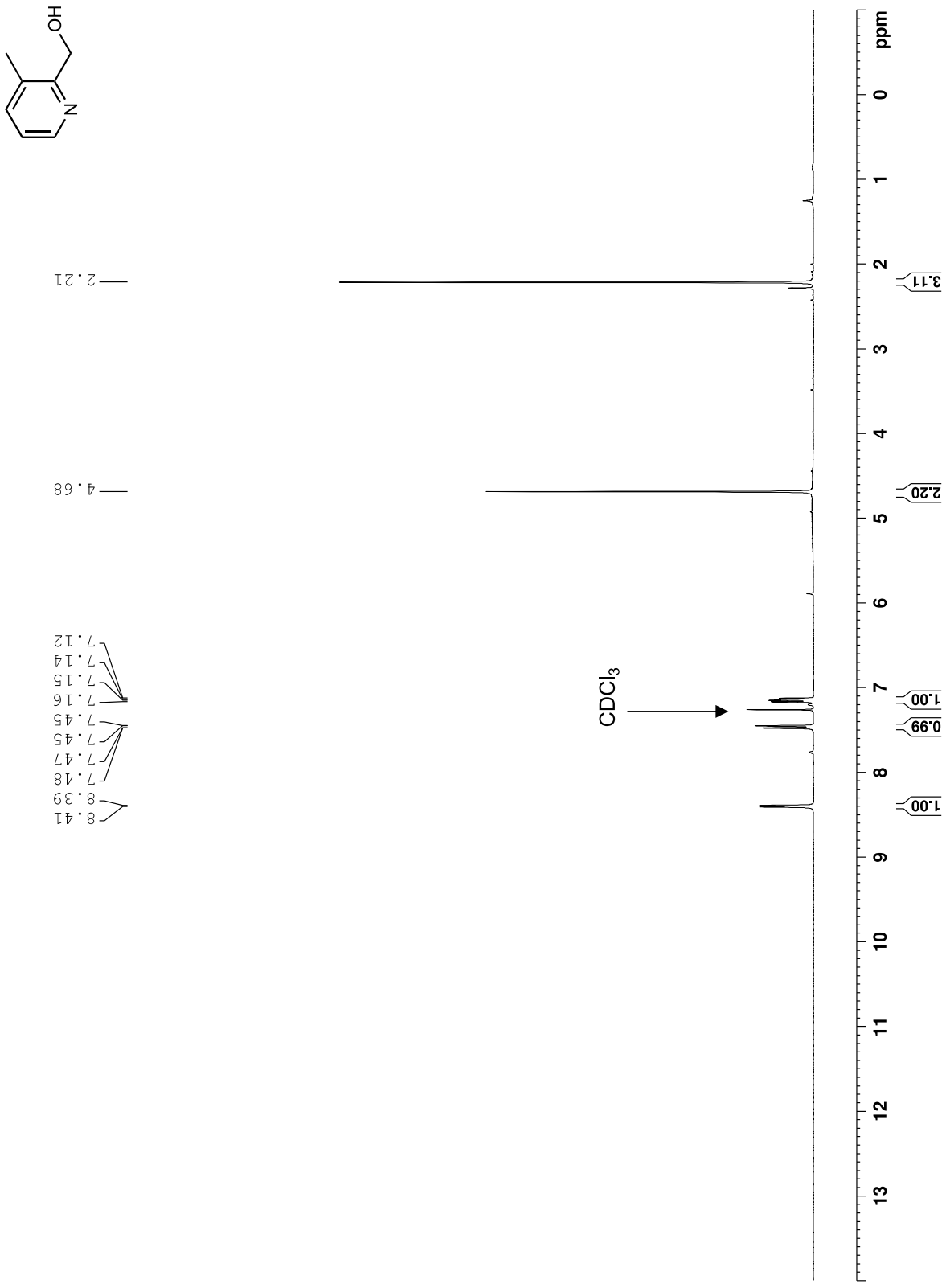

Spectrum 2. ^{1}H NMR of (3-methylpyridin-2-yl)methanol (300 MHz, 293 K, 1% w/w CD_3OD in $CDCl_3$).

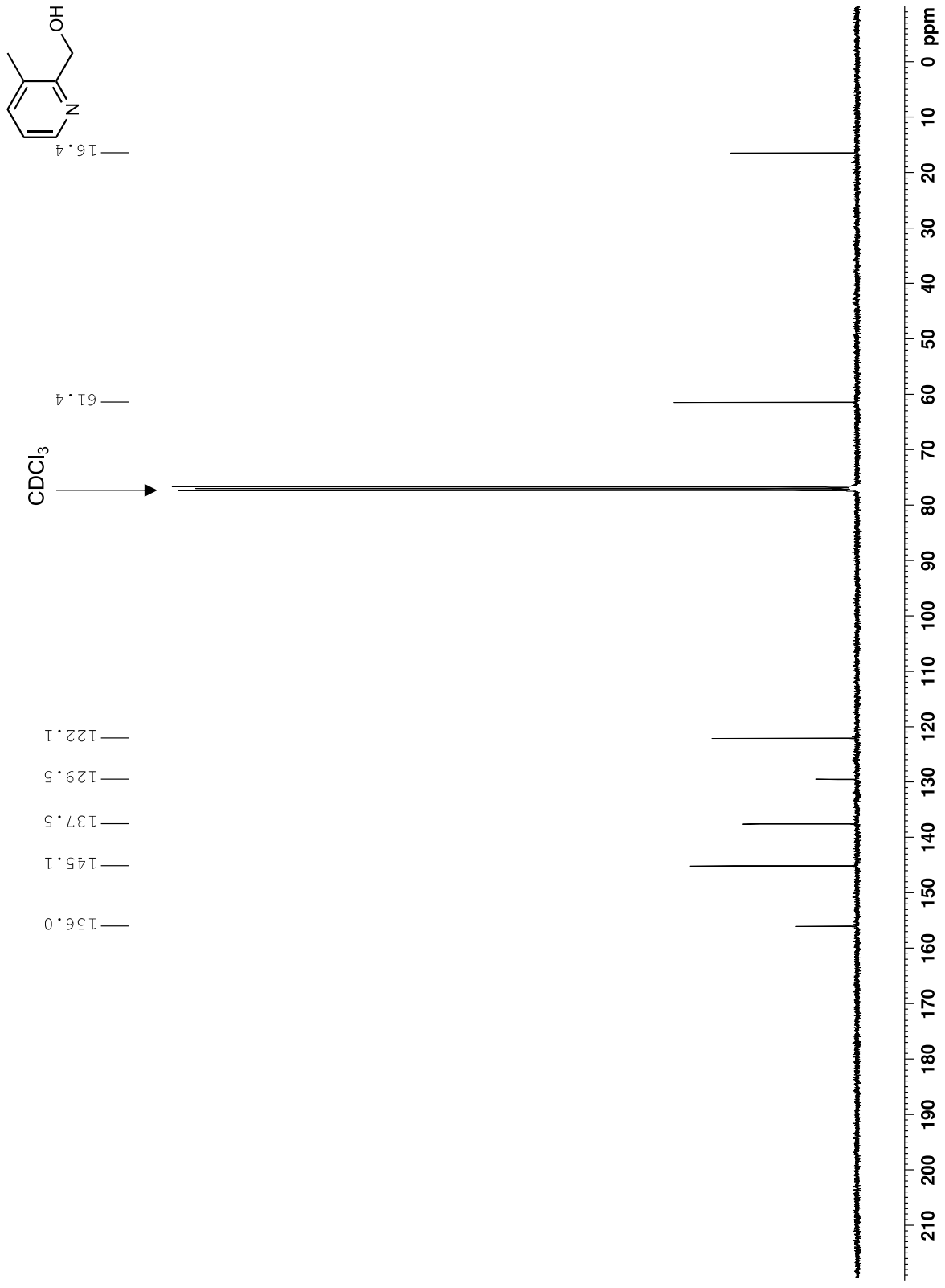

Spectrum 3. ^{13}C NMR of (3-methylpyridin-2-yl)methanol (100 MHz, 293 K, $CDCl_3$).

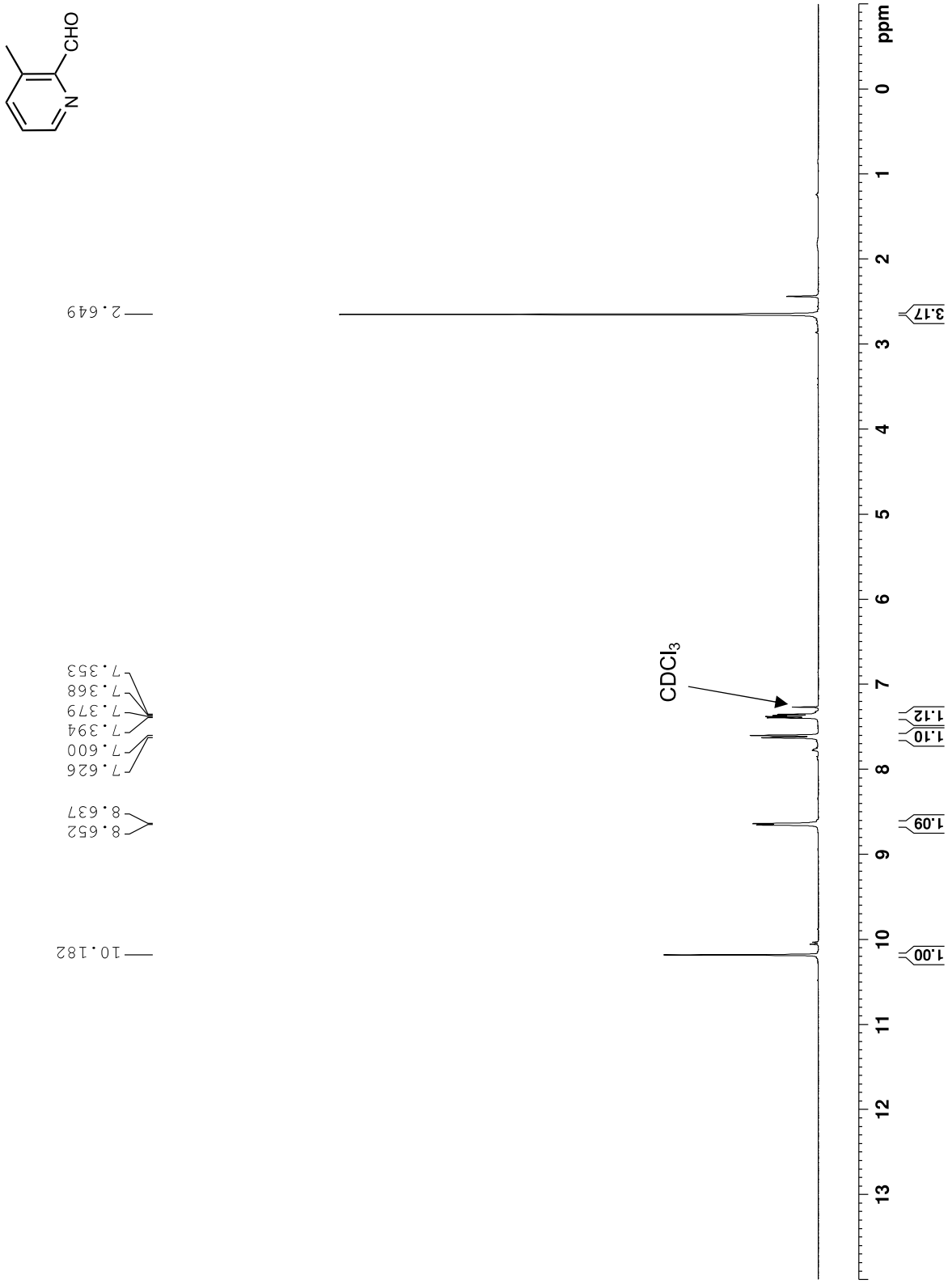

Spectrum 4. ^{1}H NMR of 3-methylpicolinaldehyde (300 MHz, 293 K, $CDCl_3$).

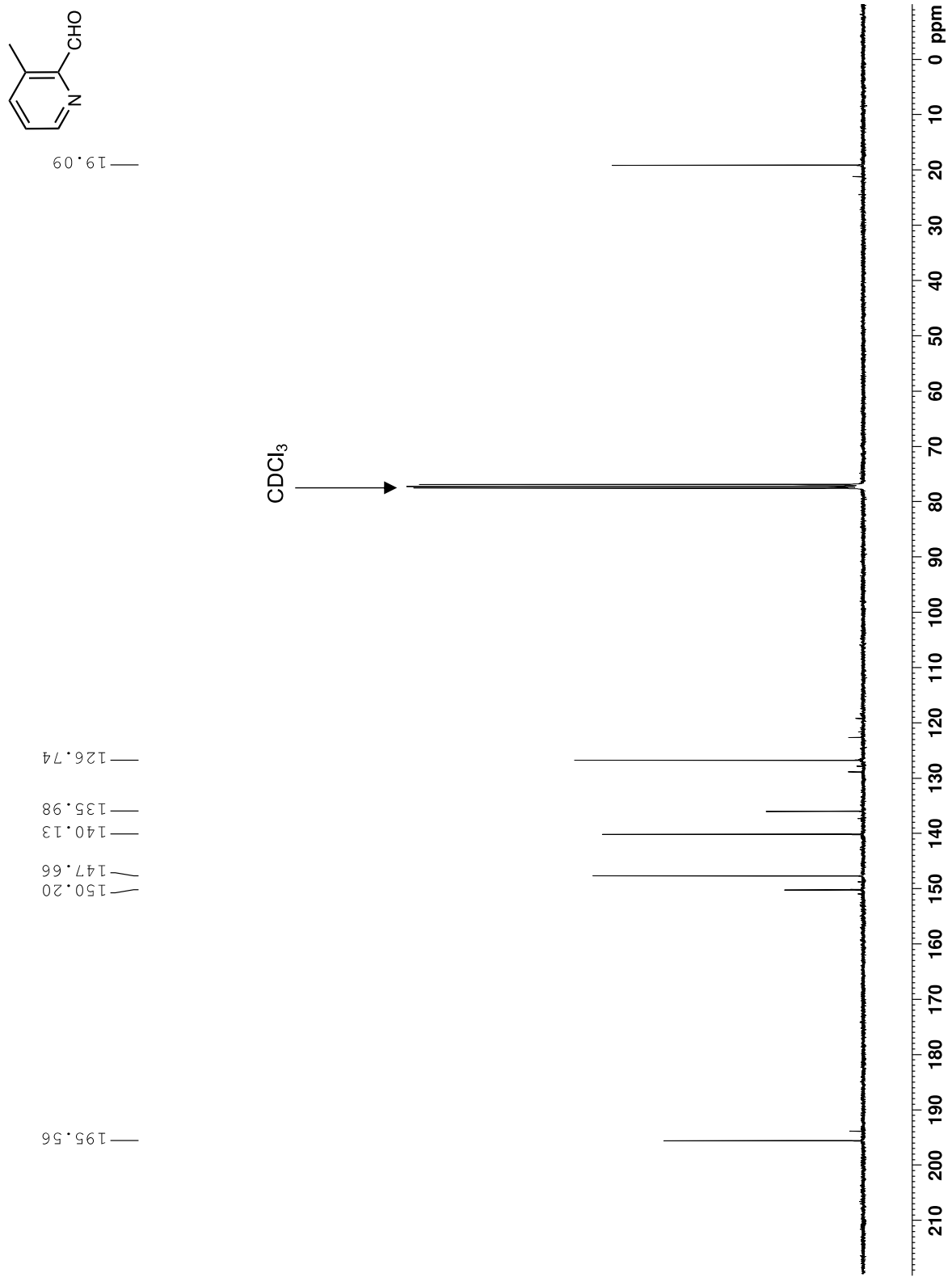

Spectrum 5. ^{13}C NMR of 3-methylpicolinaldehyde (100 MHz, 293 K, $CDCl_3$).

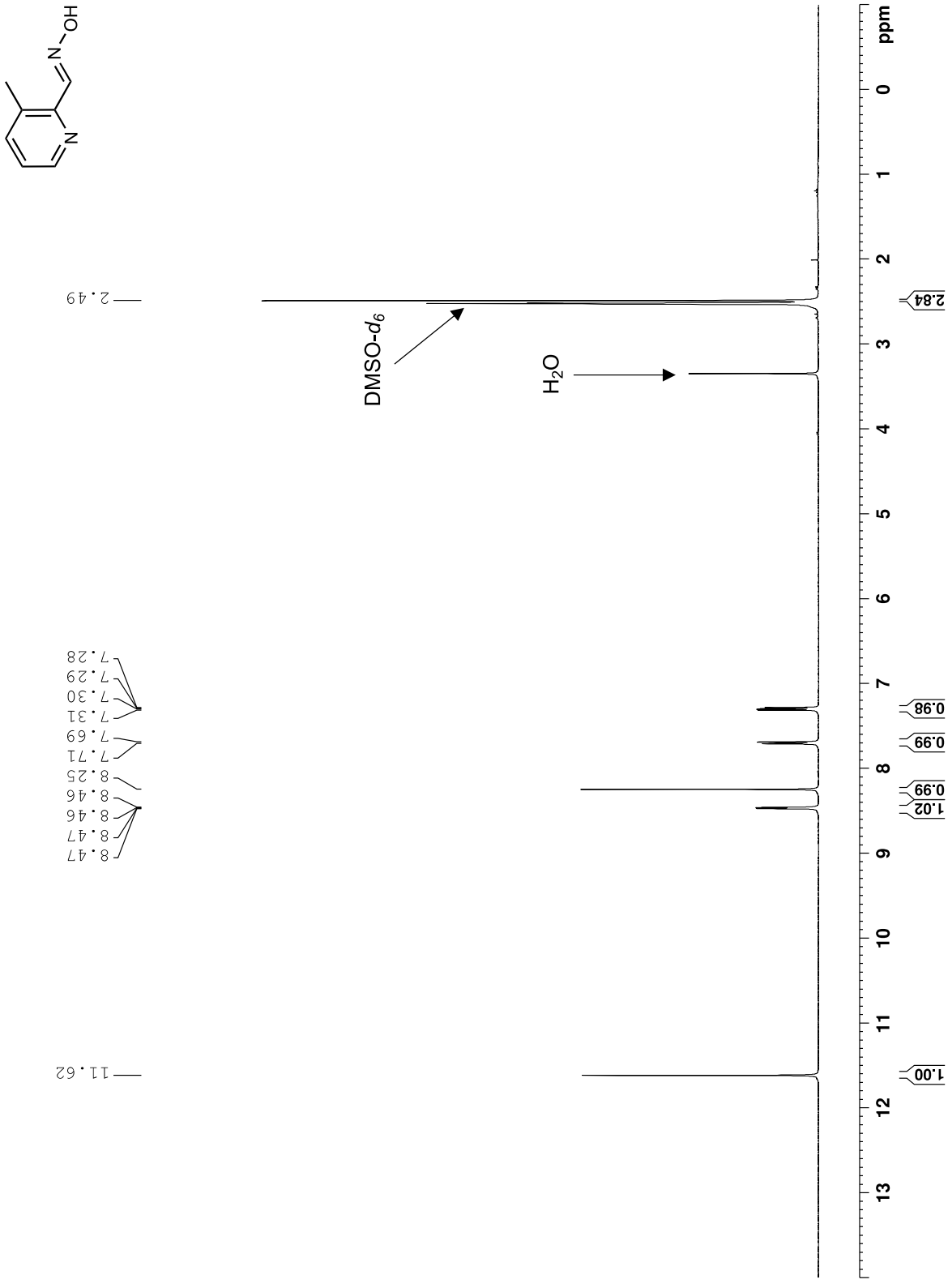

Spectrum 6. ^{1}H NMR of (*E*)-3-methylpicolinaldehyde oxime (400 MHz, 293 K, DMSO-d_6).

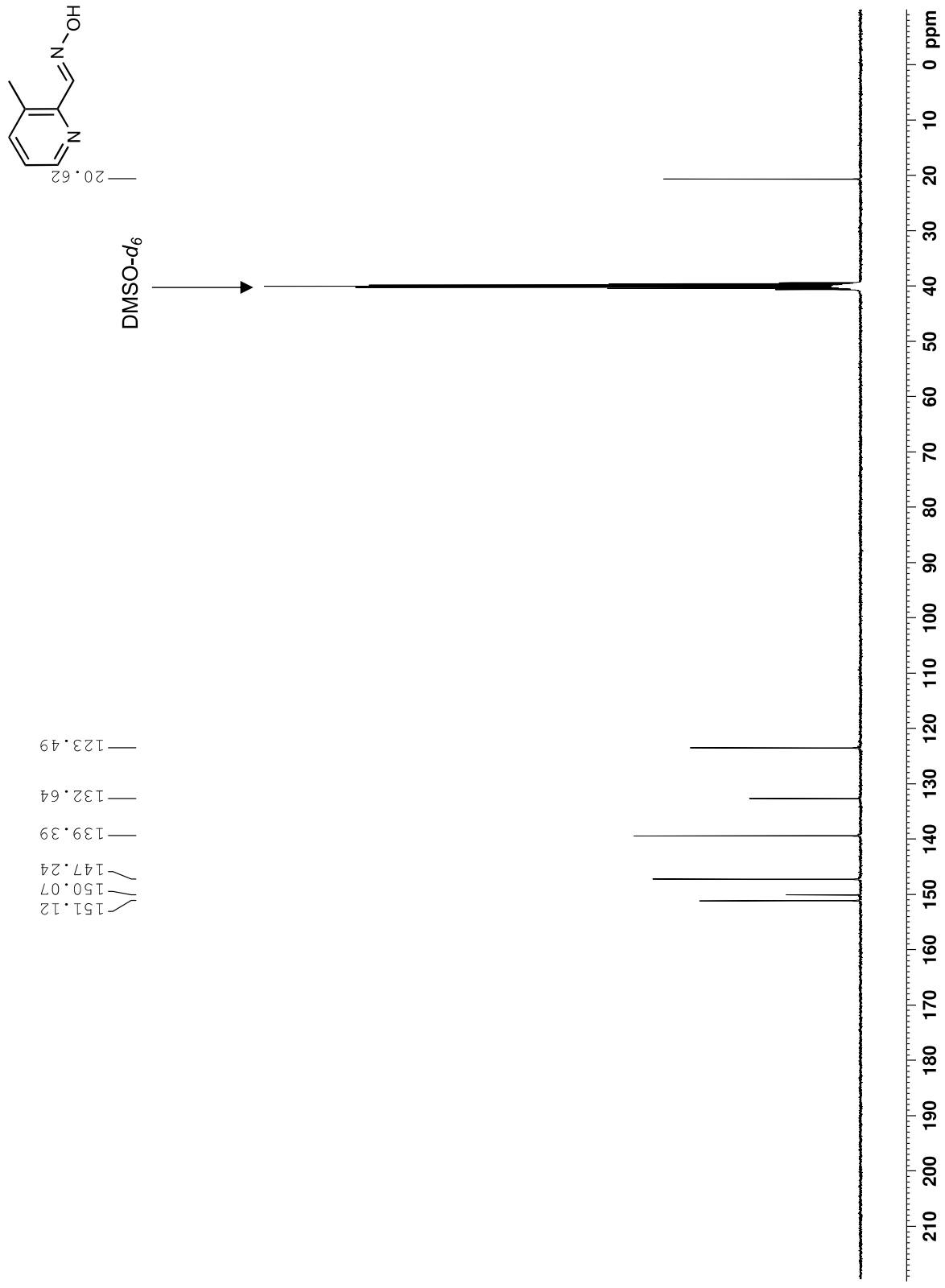

Spectrum 7. ^{13}C NMR of (*E*)-3-methylpicolinaldehyde oxime (100 MHz, 293 K, DMSO-d_6).

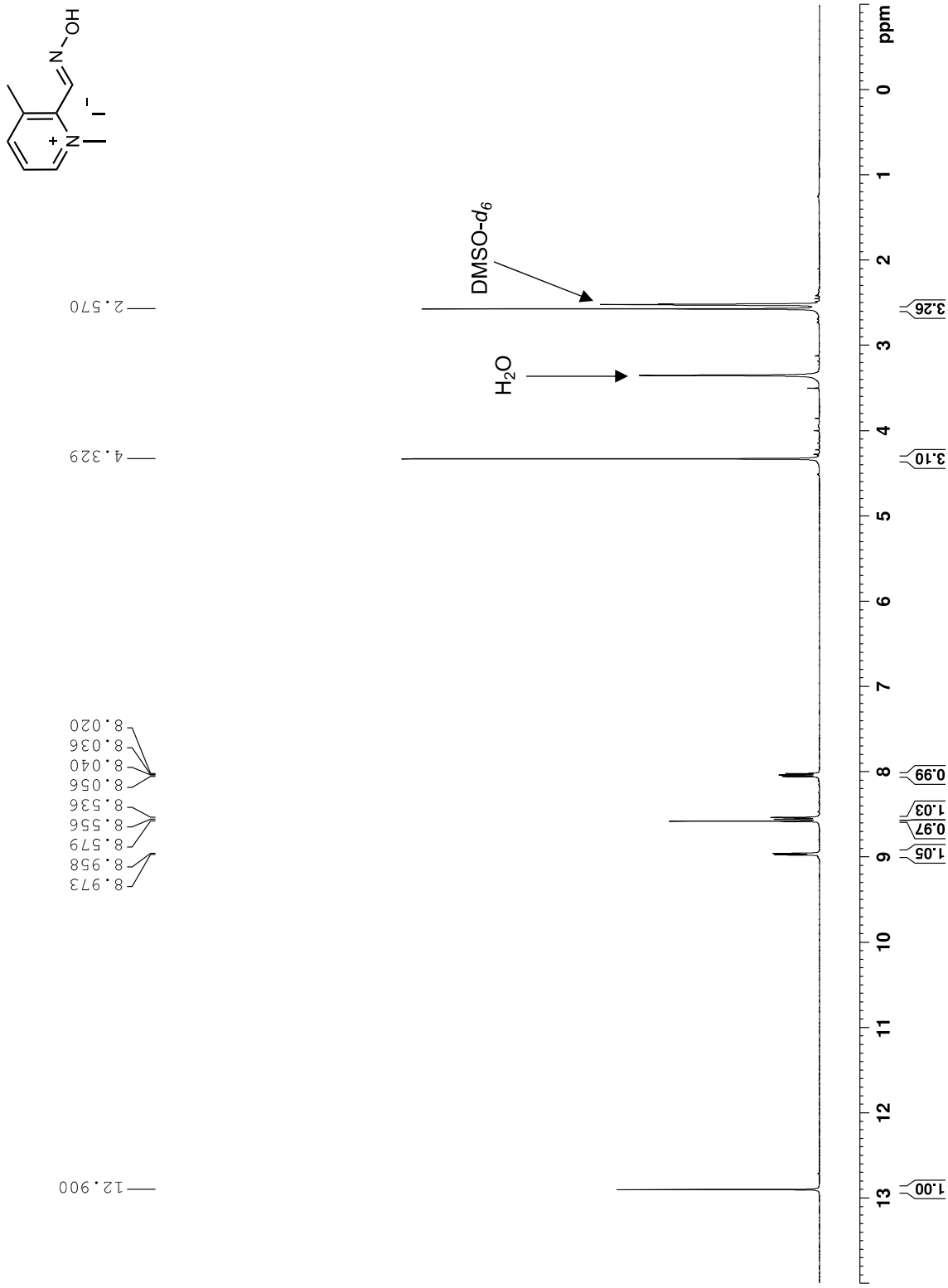

Spectrum 8. ^{1}H NMR of (*E*)-2-[(hydroxyimino)methyl]-1,3-dimethylpyridin-1-ium iodide (**3-Me-2-PAM**) (400 MHz, 293 K, DMSO-d_6).

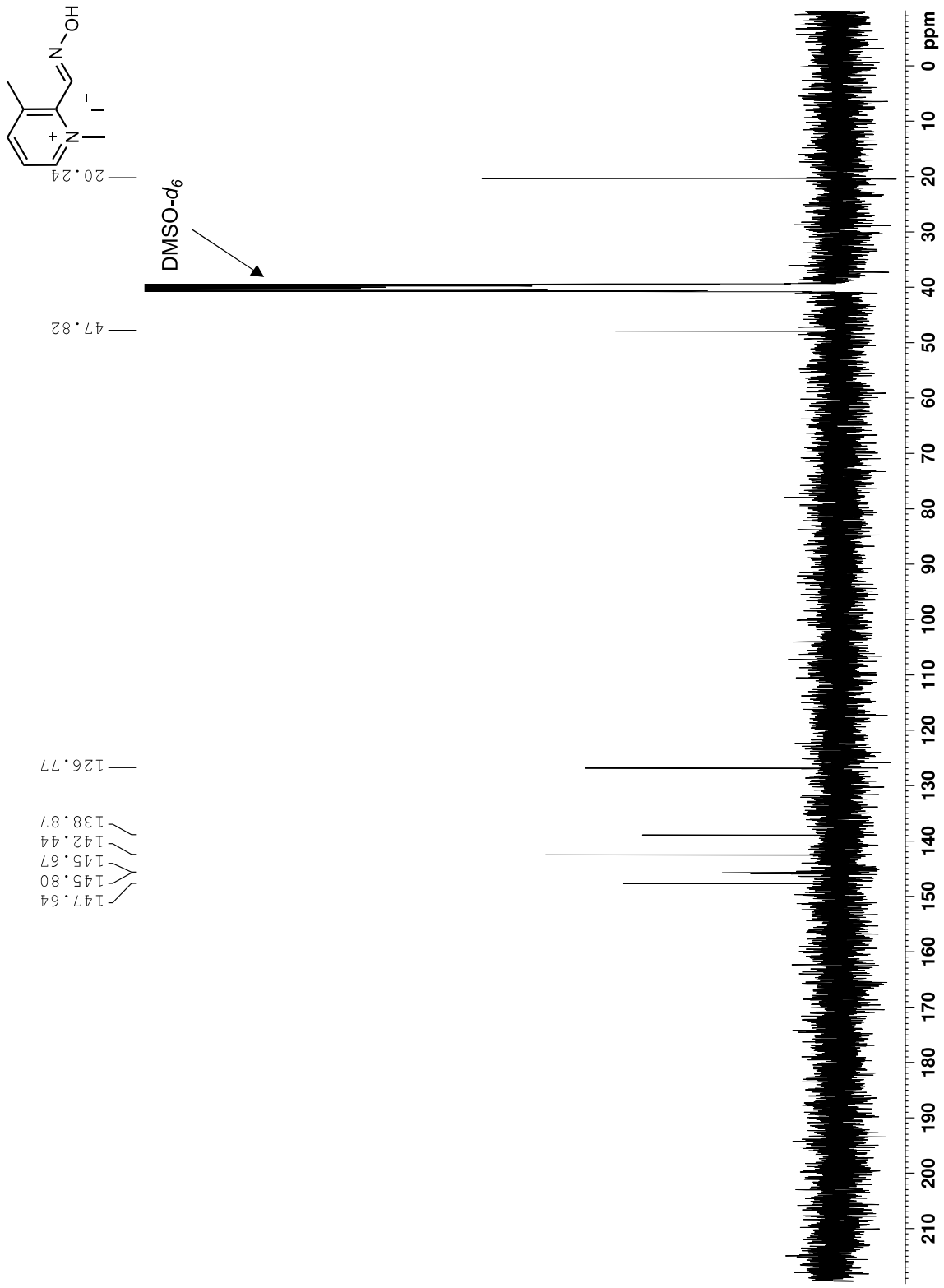

Spectrum 9. ^{13}C NMR of (*E*)-2-[(hydroxyimino)methyl]-1,3-dimethylpyridin-1-ium iodide (**3-Me-2-PAM**) (100 MHz, 293 K, DMSO-d_6).

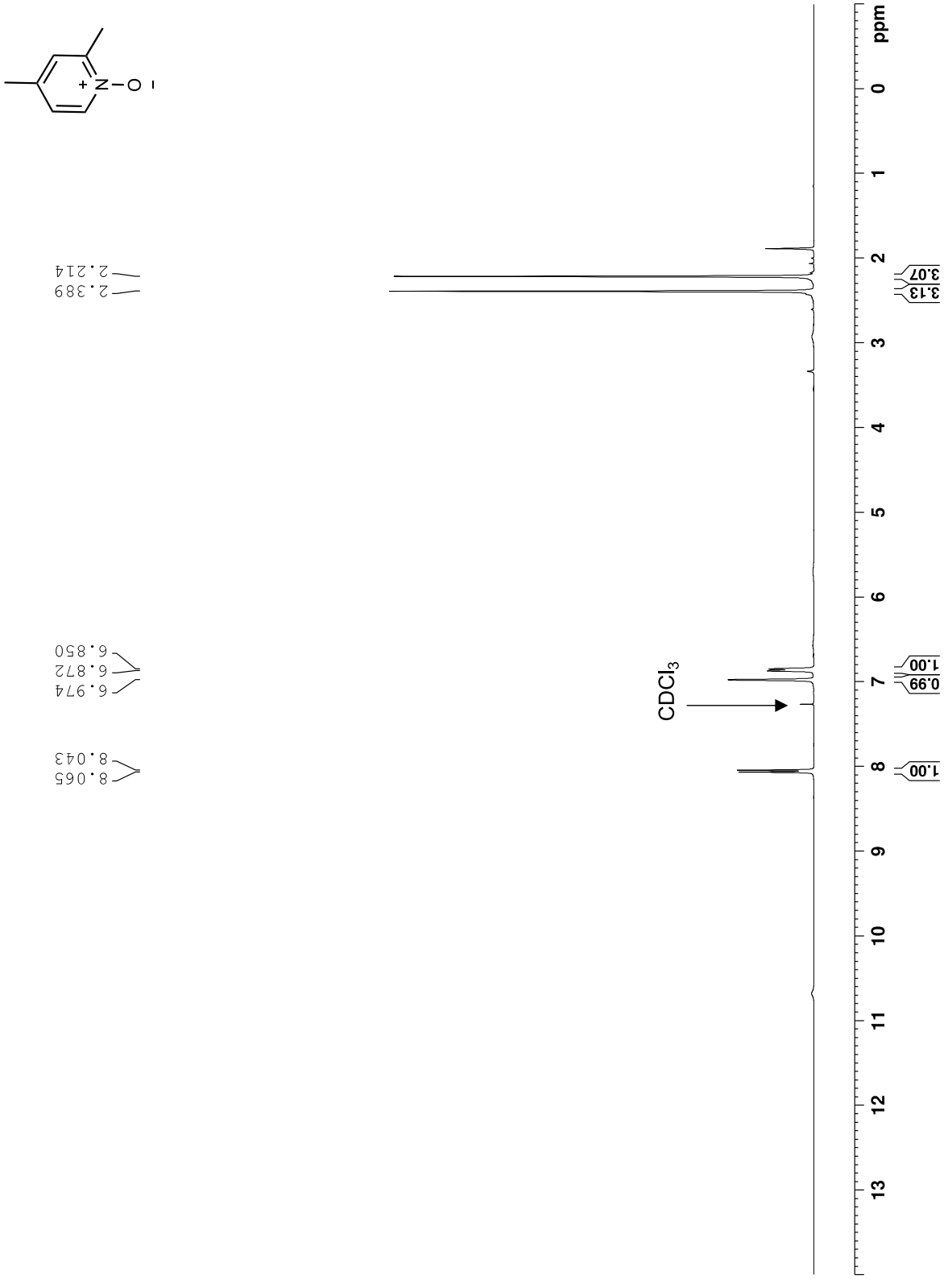

Spectrum 10. ^{1}H NMR of 2,4-dimethylpyridine 1-oxide (300 MHz, 293 K, $CDCl_3$).

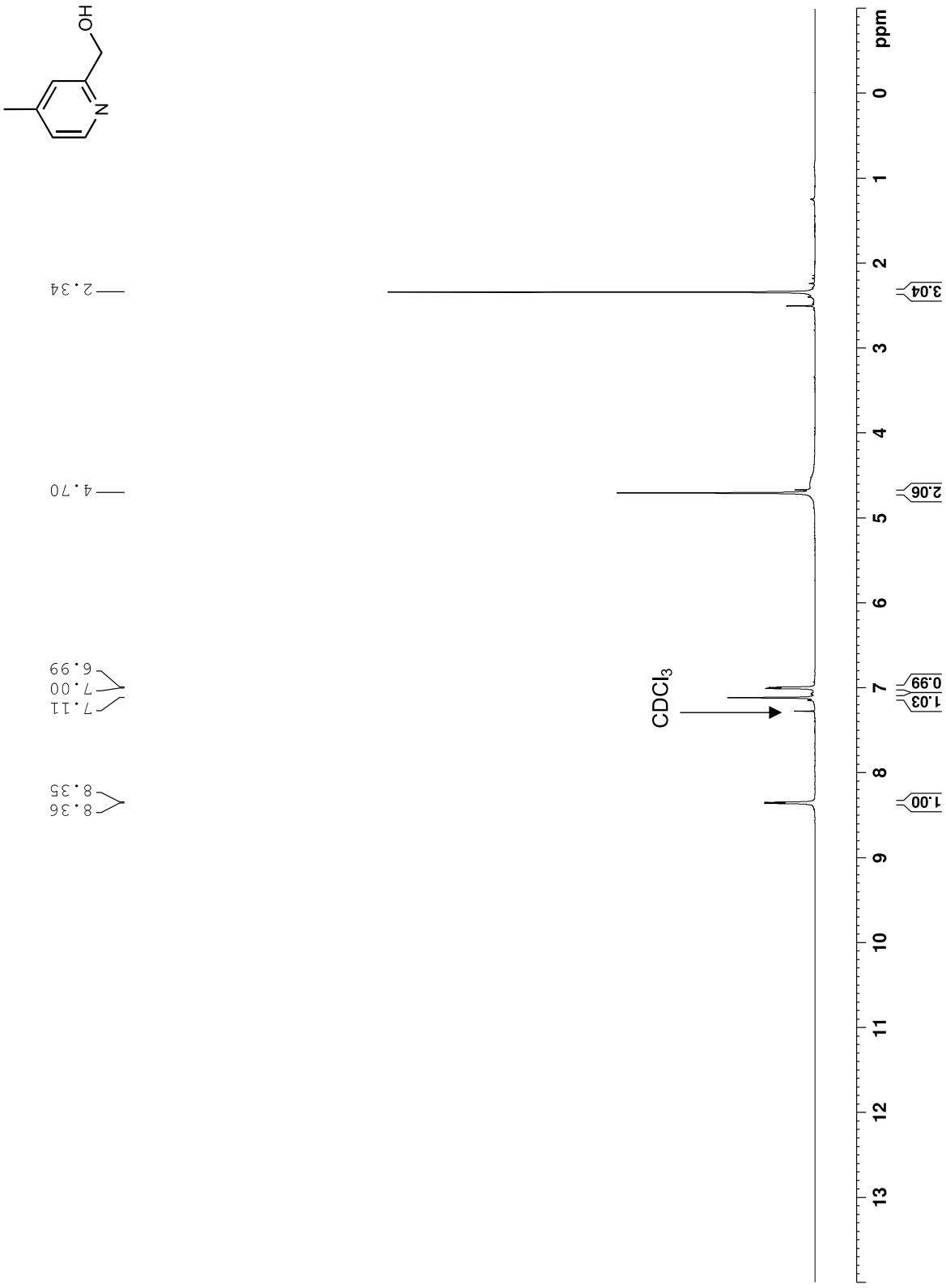

Spectrum 11. ^{1}H NMR of (4-methylpyridin-2-yl)methanol (400 MHz, 293 K, 1% w/w CD_3OD in $CDCl_3$).

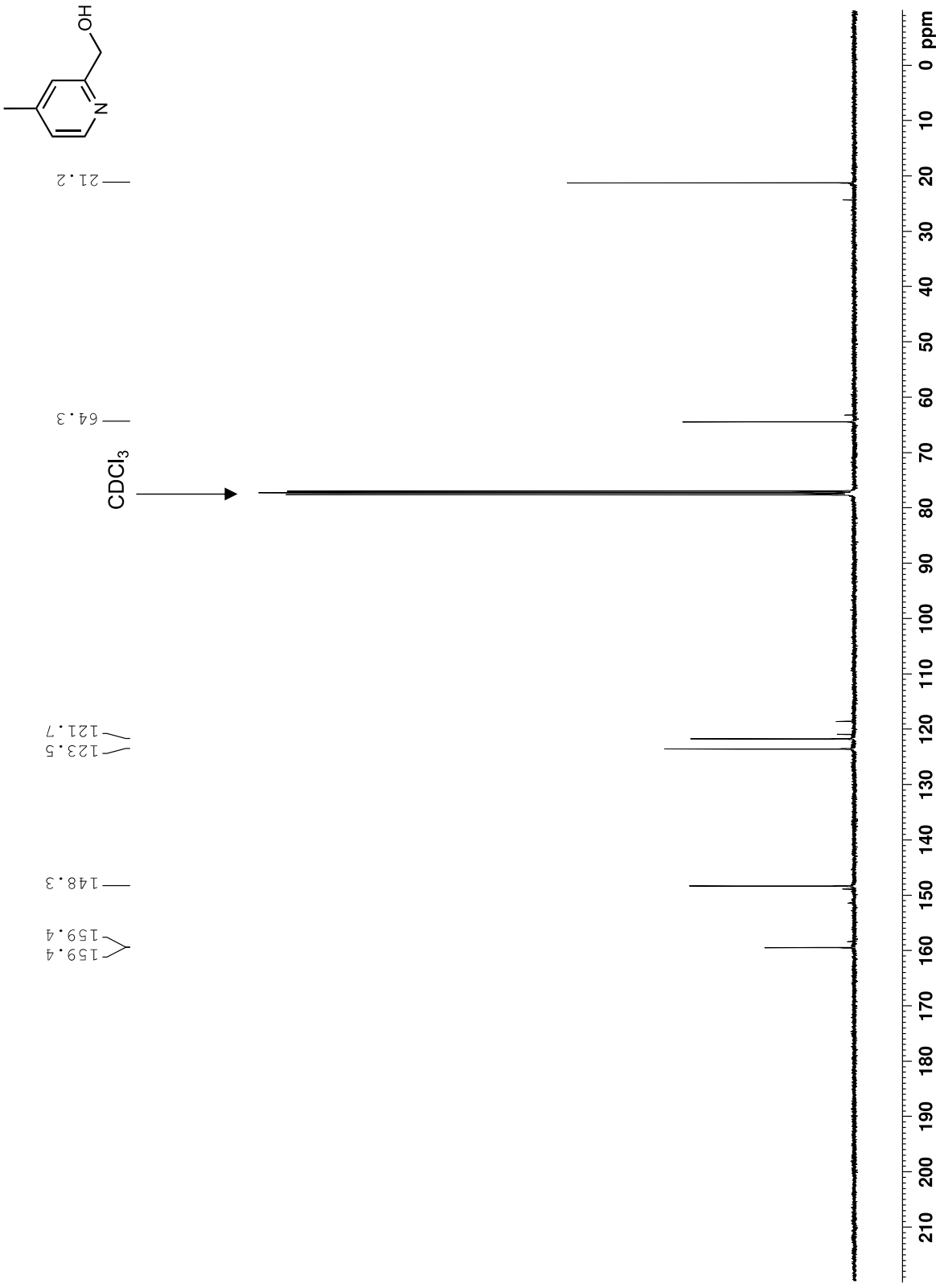

Spectrum 12. ^{13}C NMR of (4-methylpyridin-2-yl)methanol (100 MHz, 293 K, $CDCl_3$).

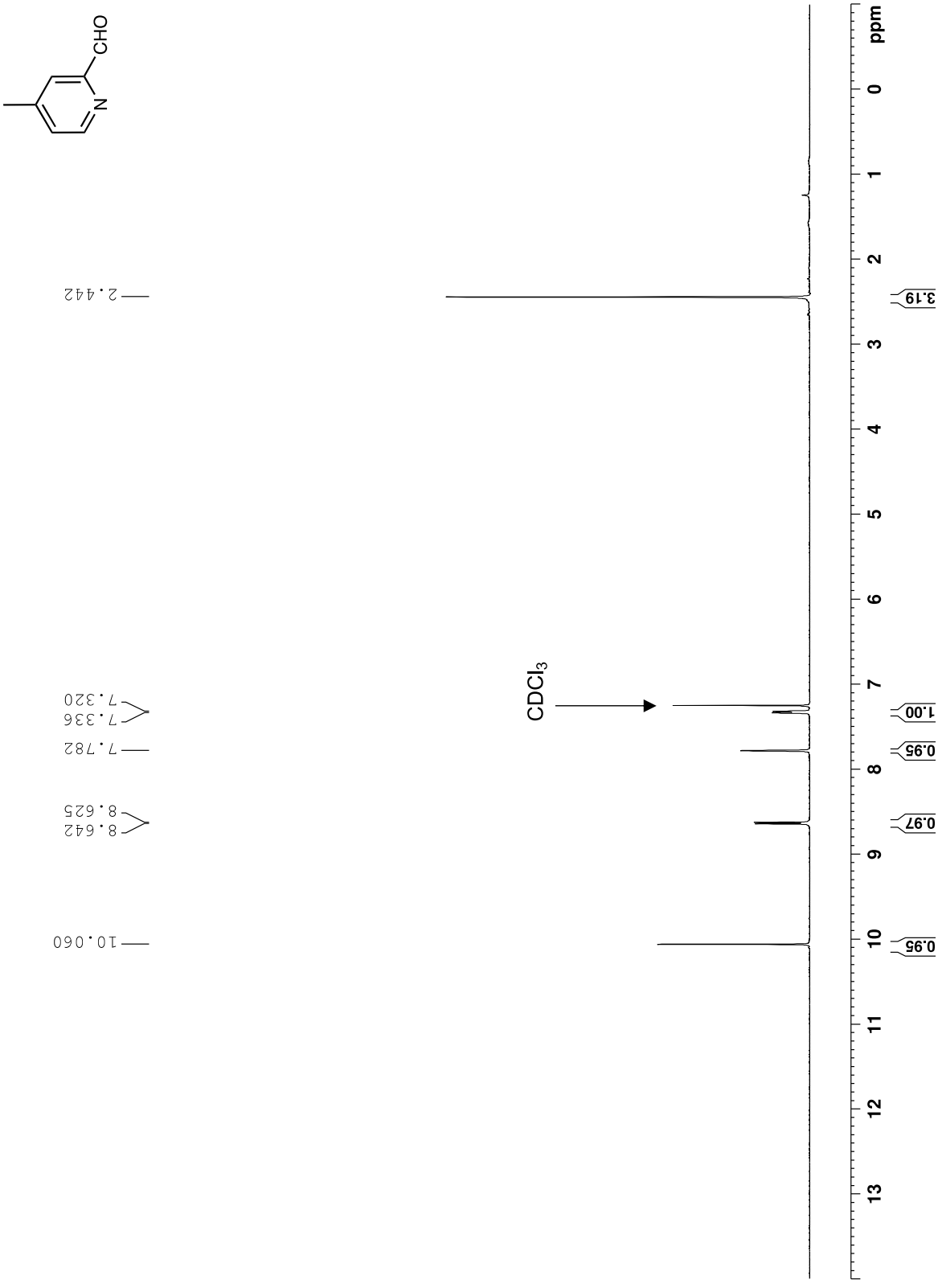

Spectrum 13. ^{1}H NMR of 4-methylpicolinaldehyde (300 MHz, 293 K, $CDCl_3$).

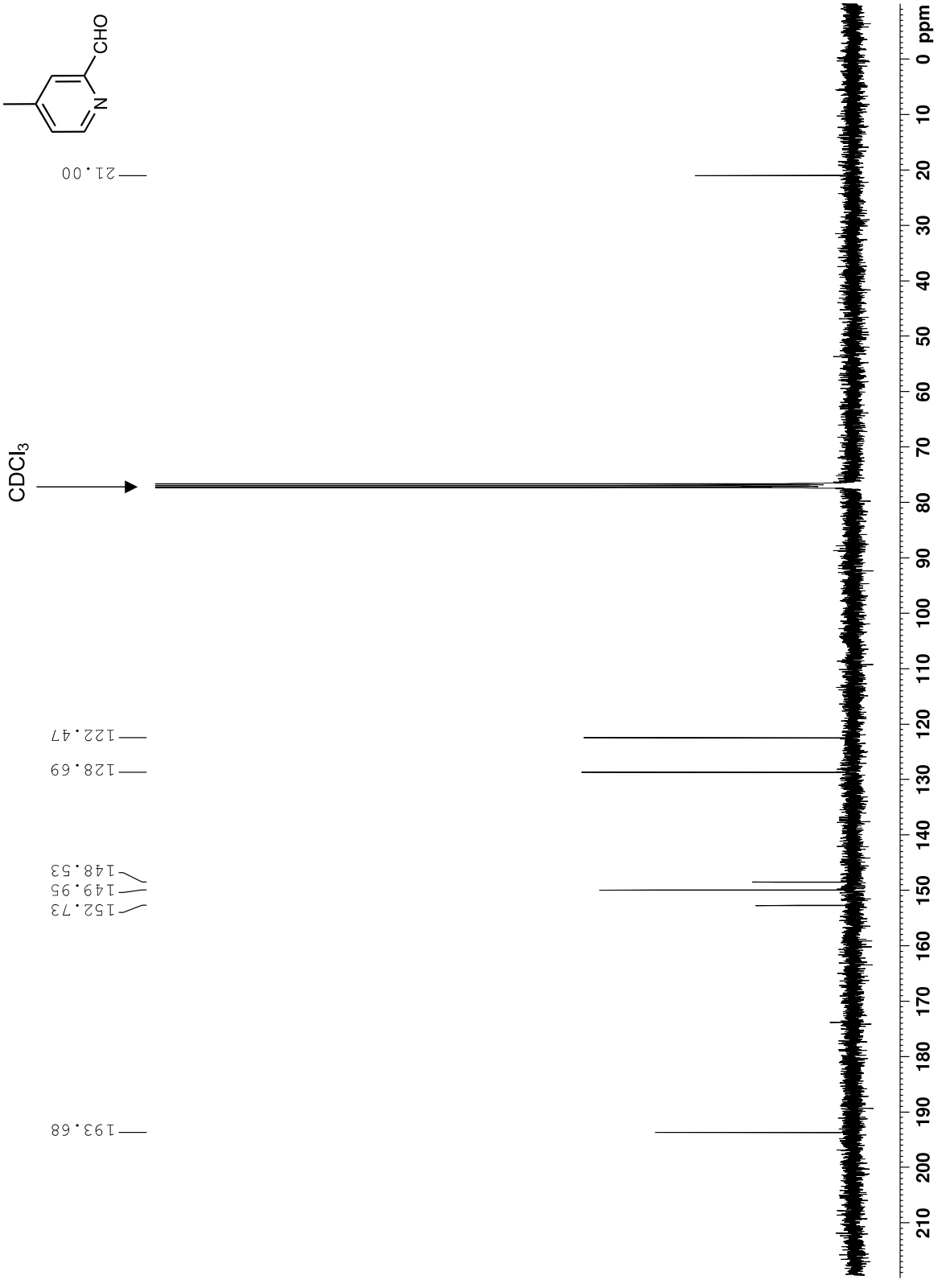

Spectrum 14. ^{13}C NMR of 4-methylpicolinaldehyde (100 MHz, 293 K, $CDCl_3$).

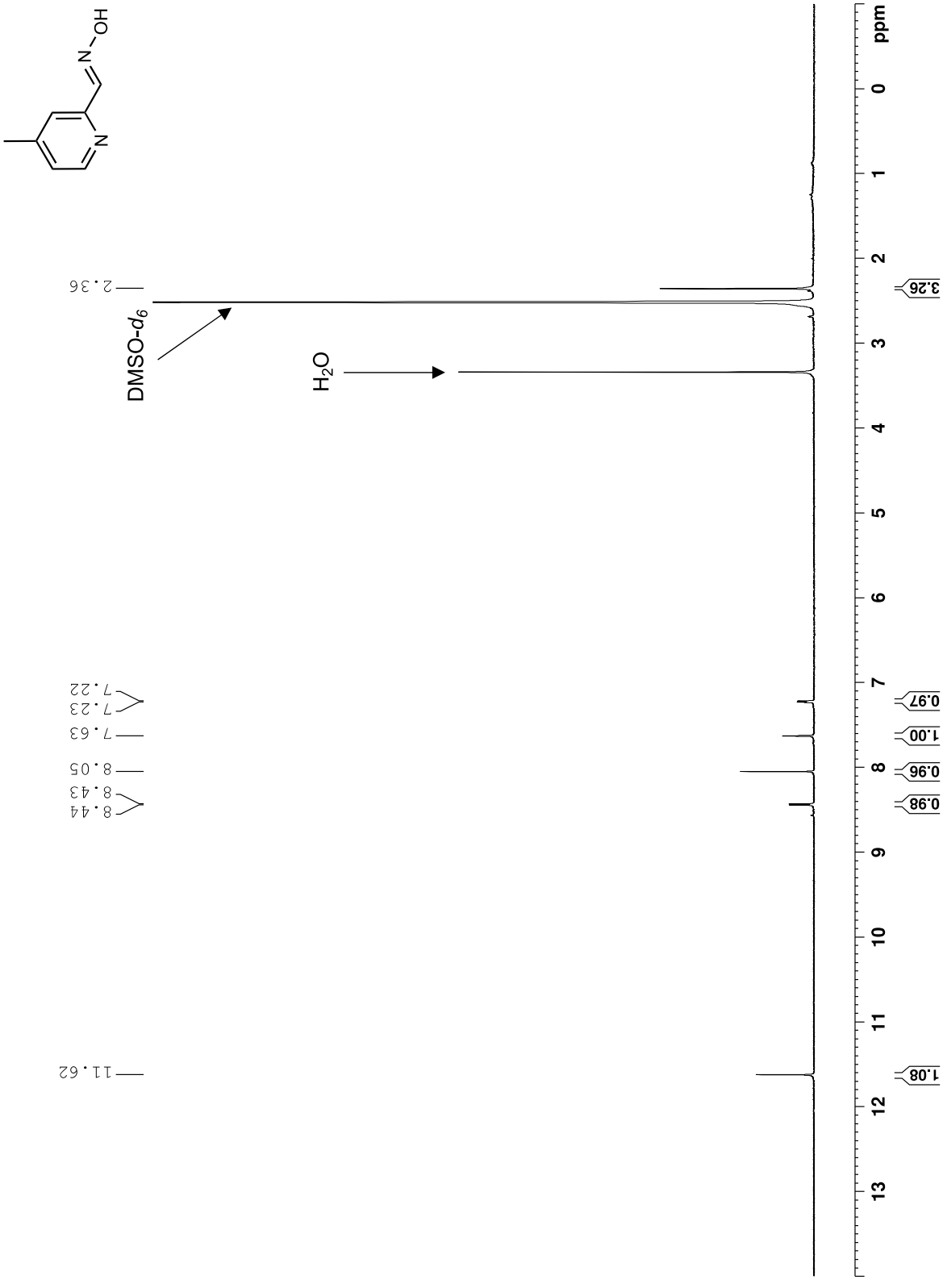

Spectrum 15. ^{1}H NMR of (*E*)-4-methylpicolinaldehyde oxime (400 MHz, 293 K, DMSO-d_6).

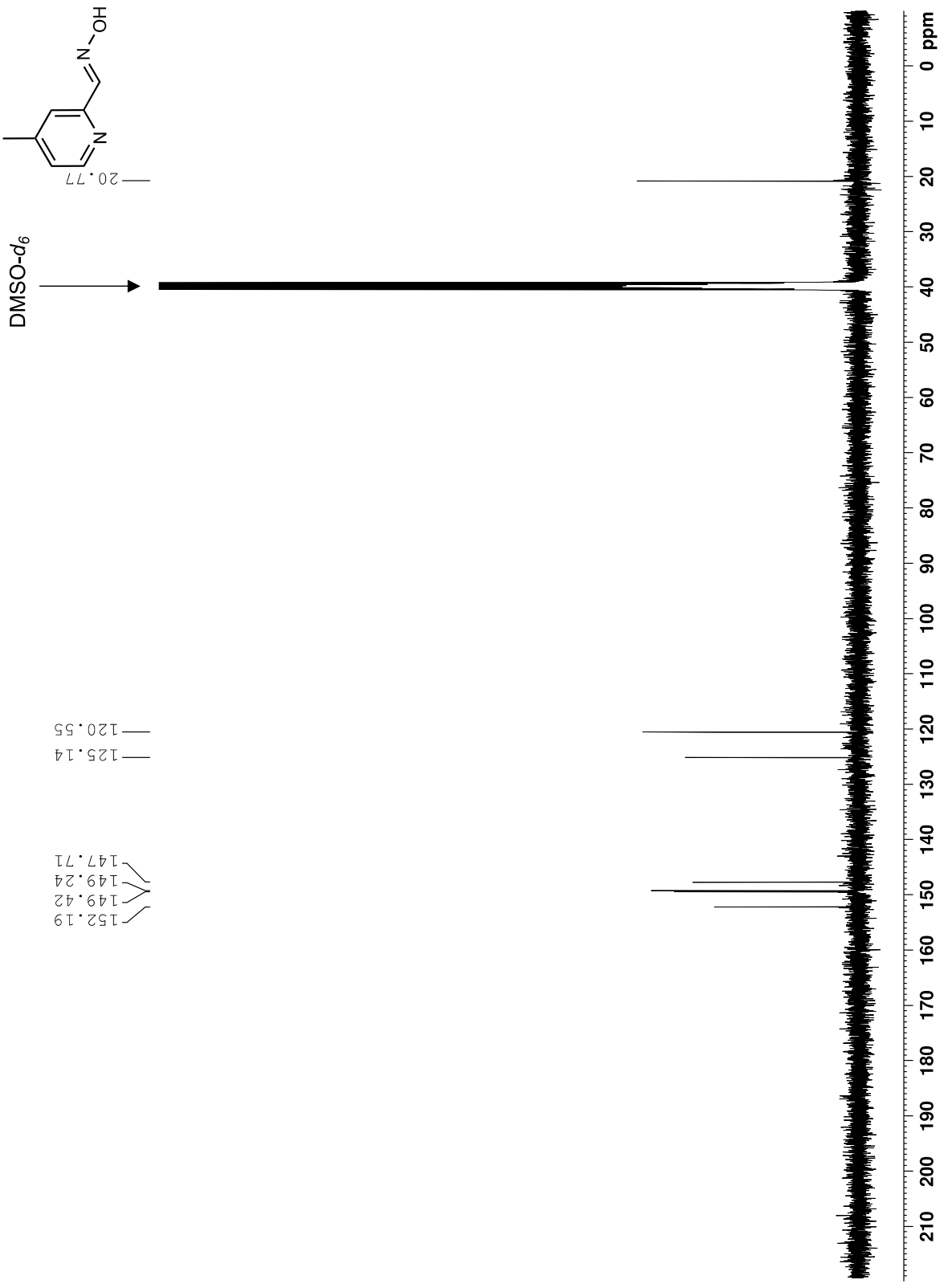

Spectrum 16. ^{13}C NMR of (*E*)-4-methylpicolinaldehyde oxime (100 MHz, 293 K, DMSO-d_6).

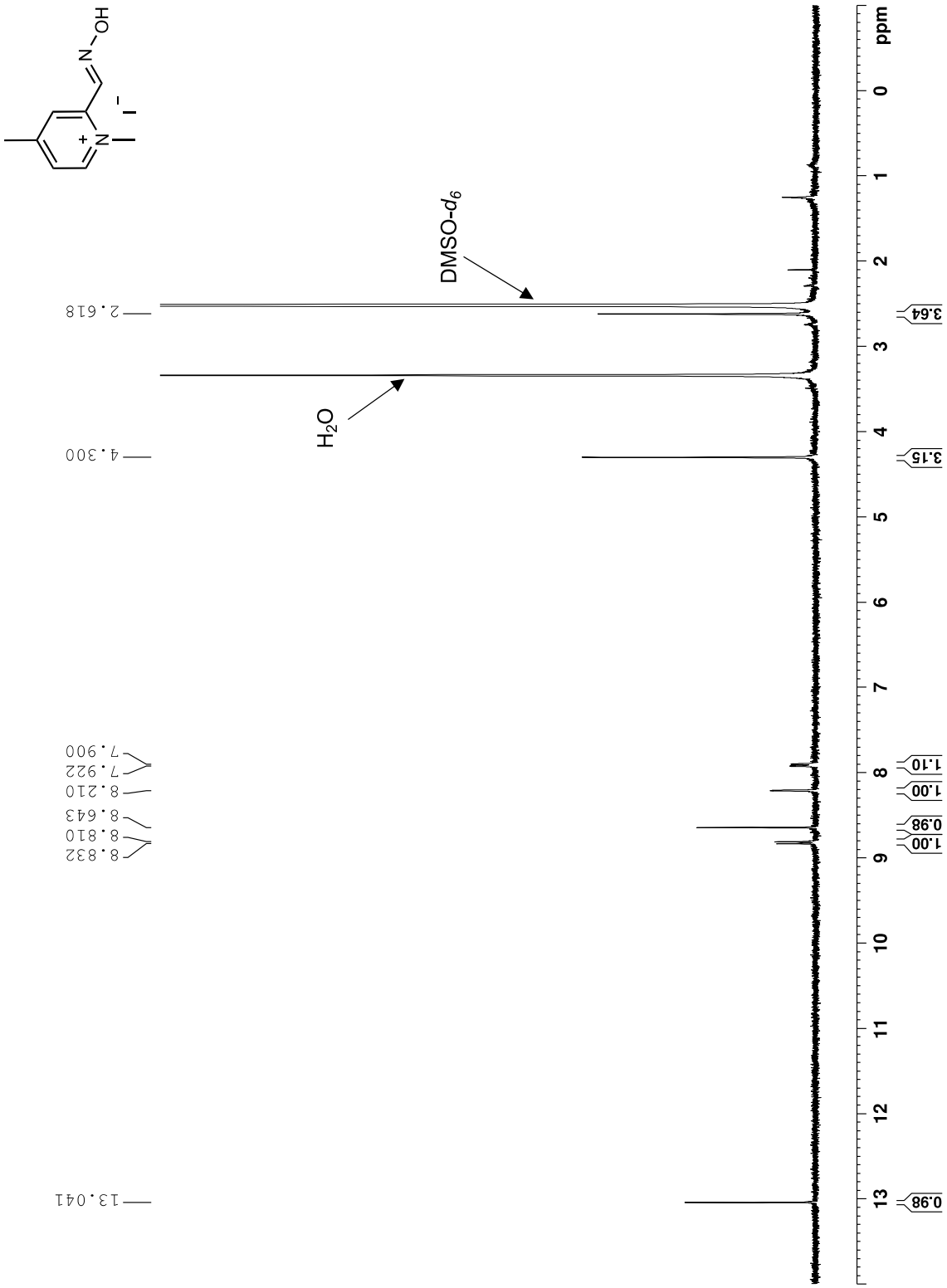

Spectrum 17. ^{1}H NMR of (*E*)-2-[(hydroxyimino)methyl]-1,4-dimethylpyridin-1-ium iodide (**4-Me-2-PAM**) (400 MHz, 293 K, DMSO-d_6).

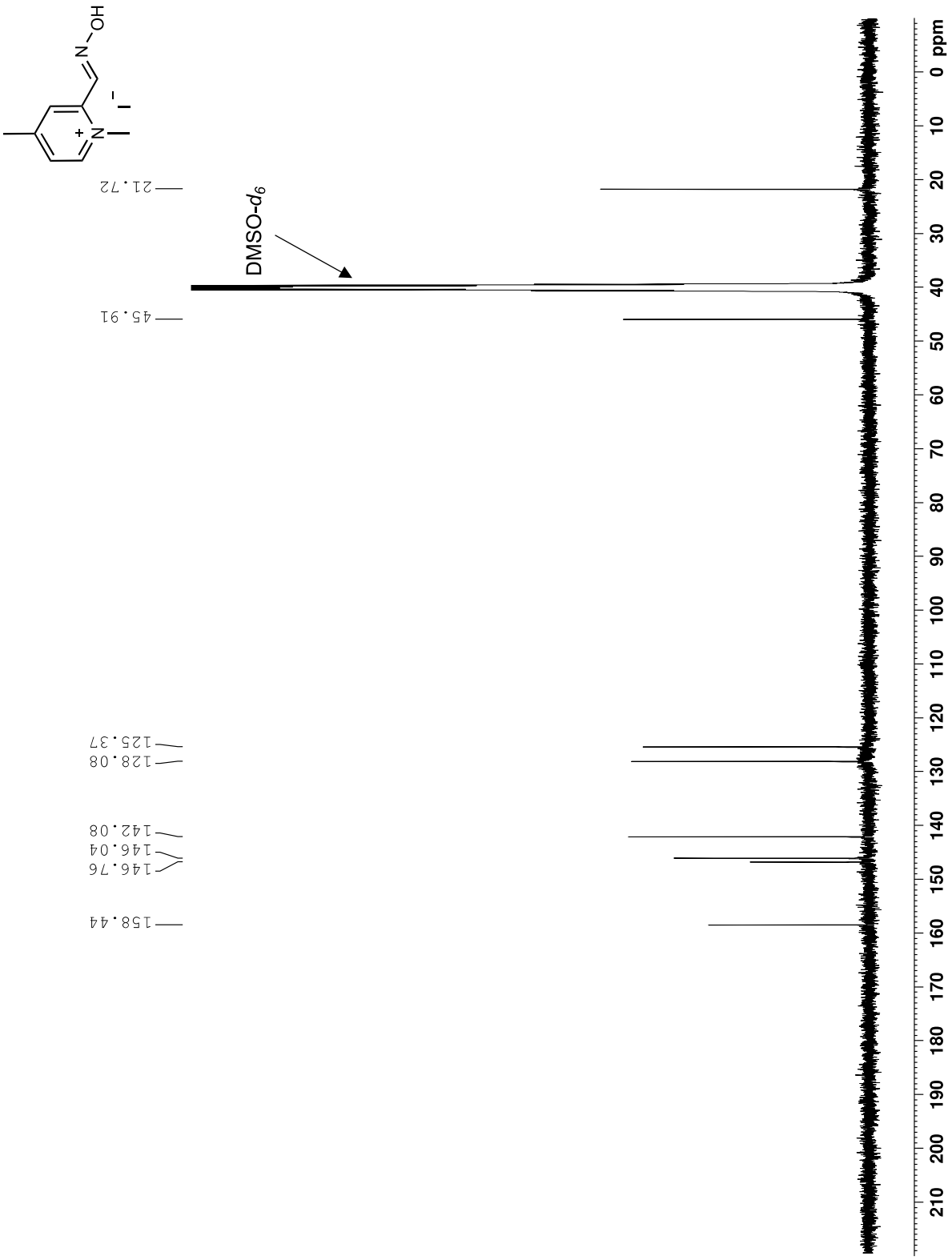

Spectrum 18. ^{13}C NMR of (*E*)-2-[(hydroxyimino)methyl]-1,4-dimethylpyridin-1-ium iodide (**4-Me-2-PAM**) (100 MHz, 293 K, DMSO-d_6).

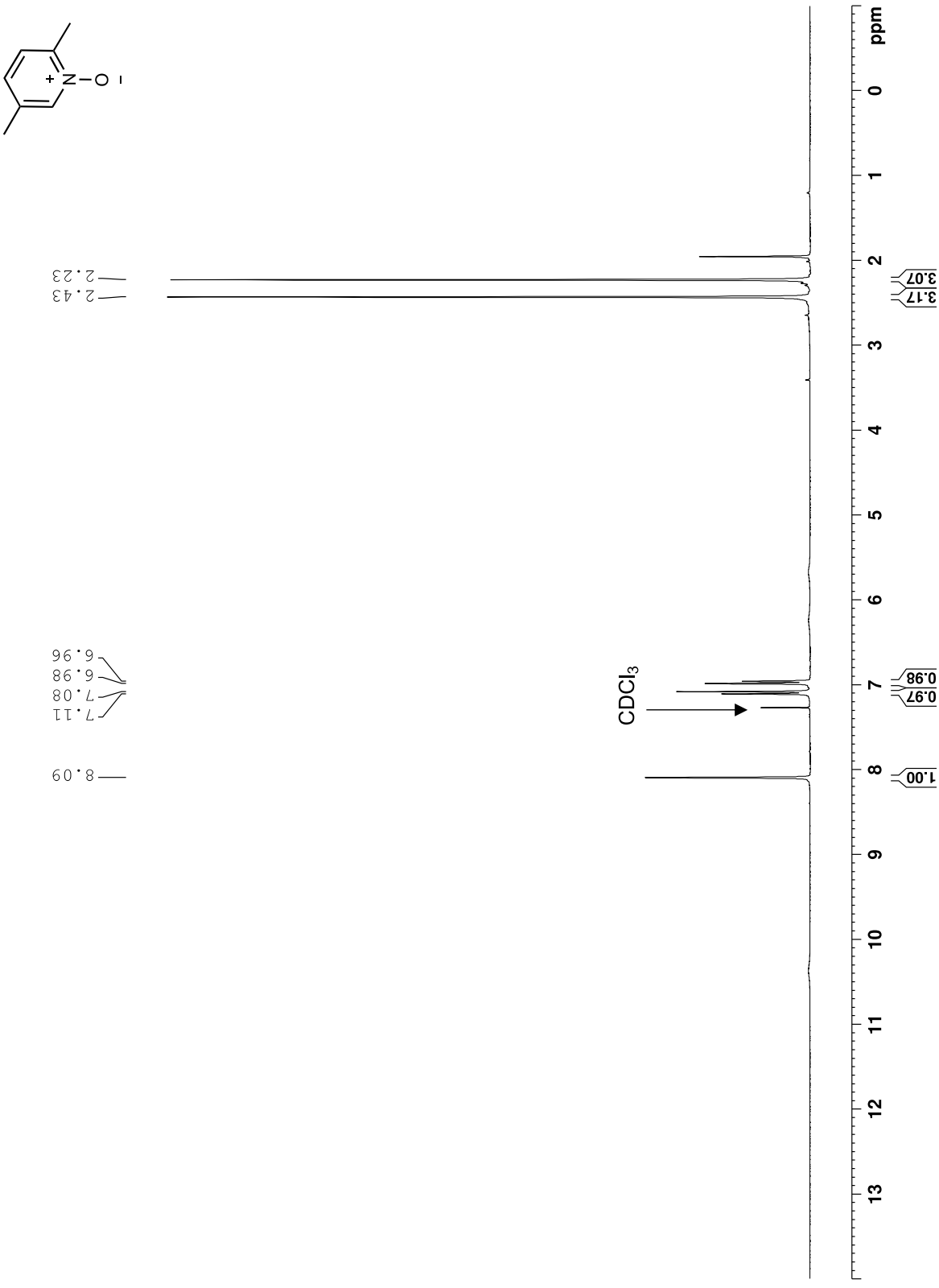

Spectrum 19. ^{1}H NMR of 2,5-dimethylpyridine 1-oxide (300 MHz, 293 K, $CDCl_3$).

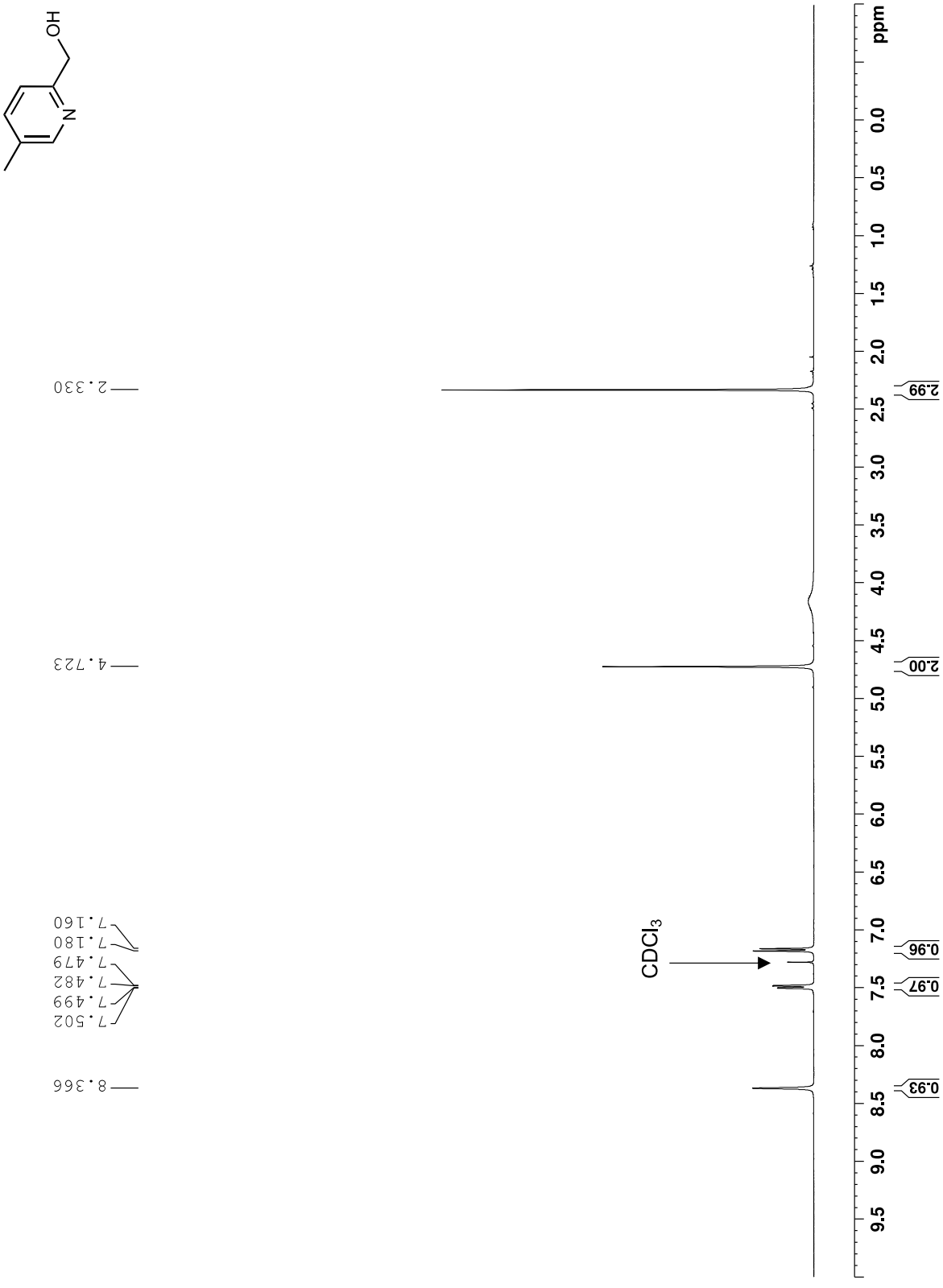

Spectrum 20. ^{1}H NMR of (5-methylpyridin-2-yl)methanol (400 MHz, 293 K, 1% w/w CD_3OD in $CDCl_3$).

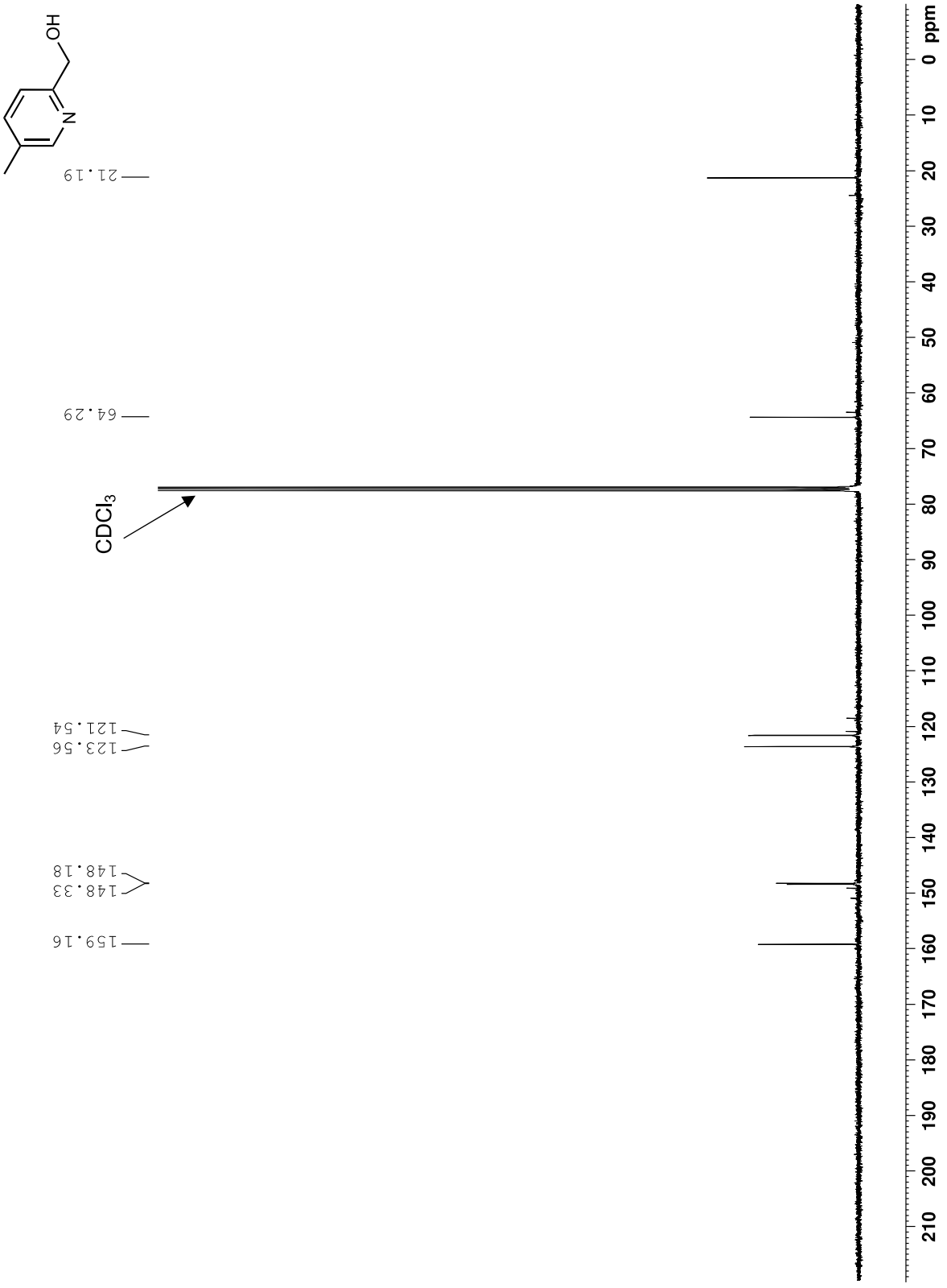

Spectrum 21. ^{13}C NMR of (5-methylpyridin-2-yl)methanol (100 MHz, 293 K, $CDCl_3$).

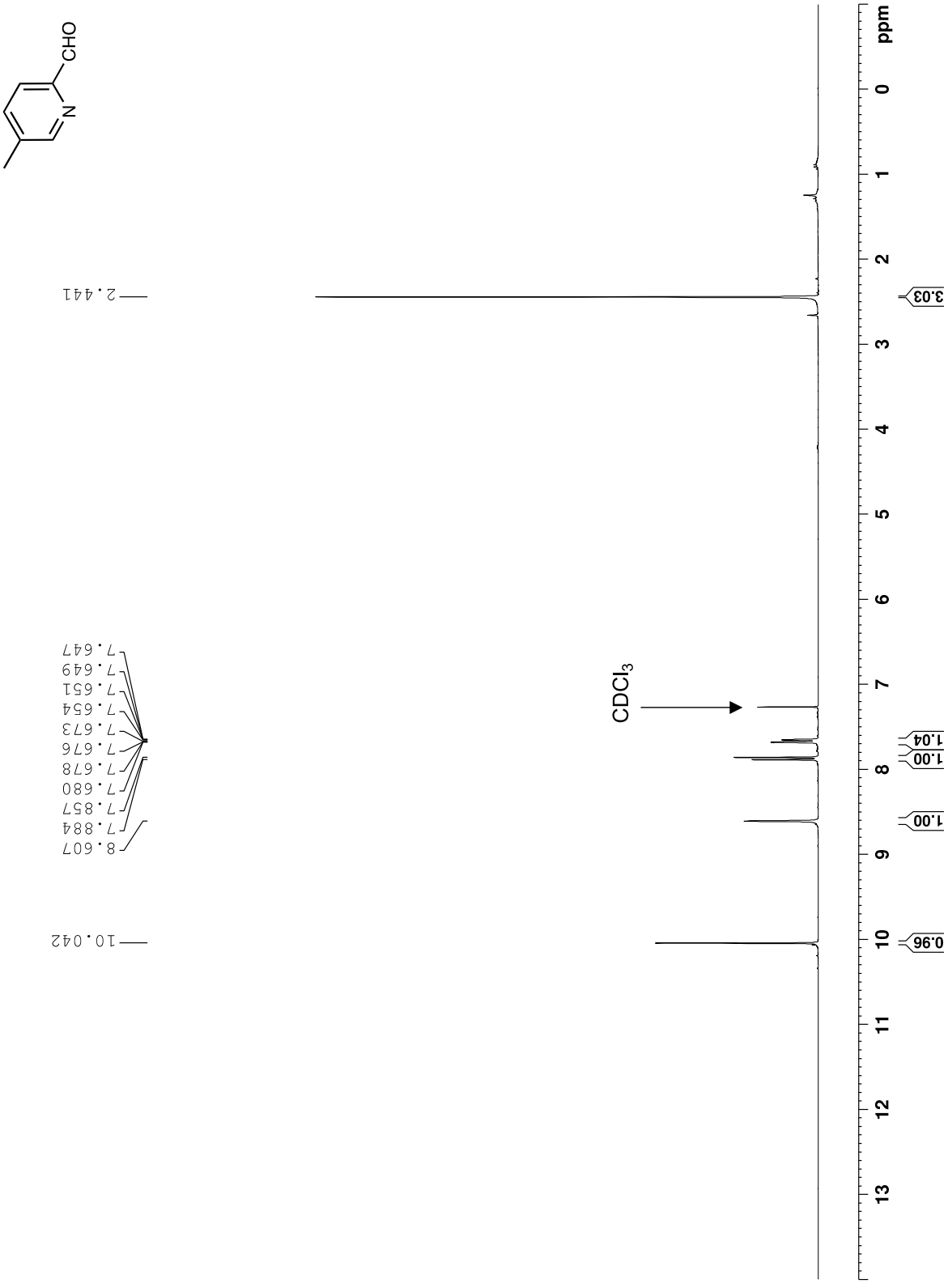

Spectrum 22. ^{1}H NMR of 5-methylpicolinaldehyde (300 MHz, 293 K, $CDCl_3$).

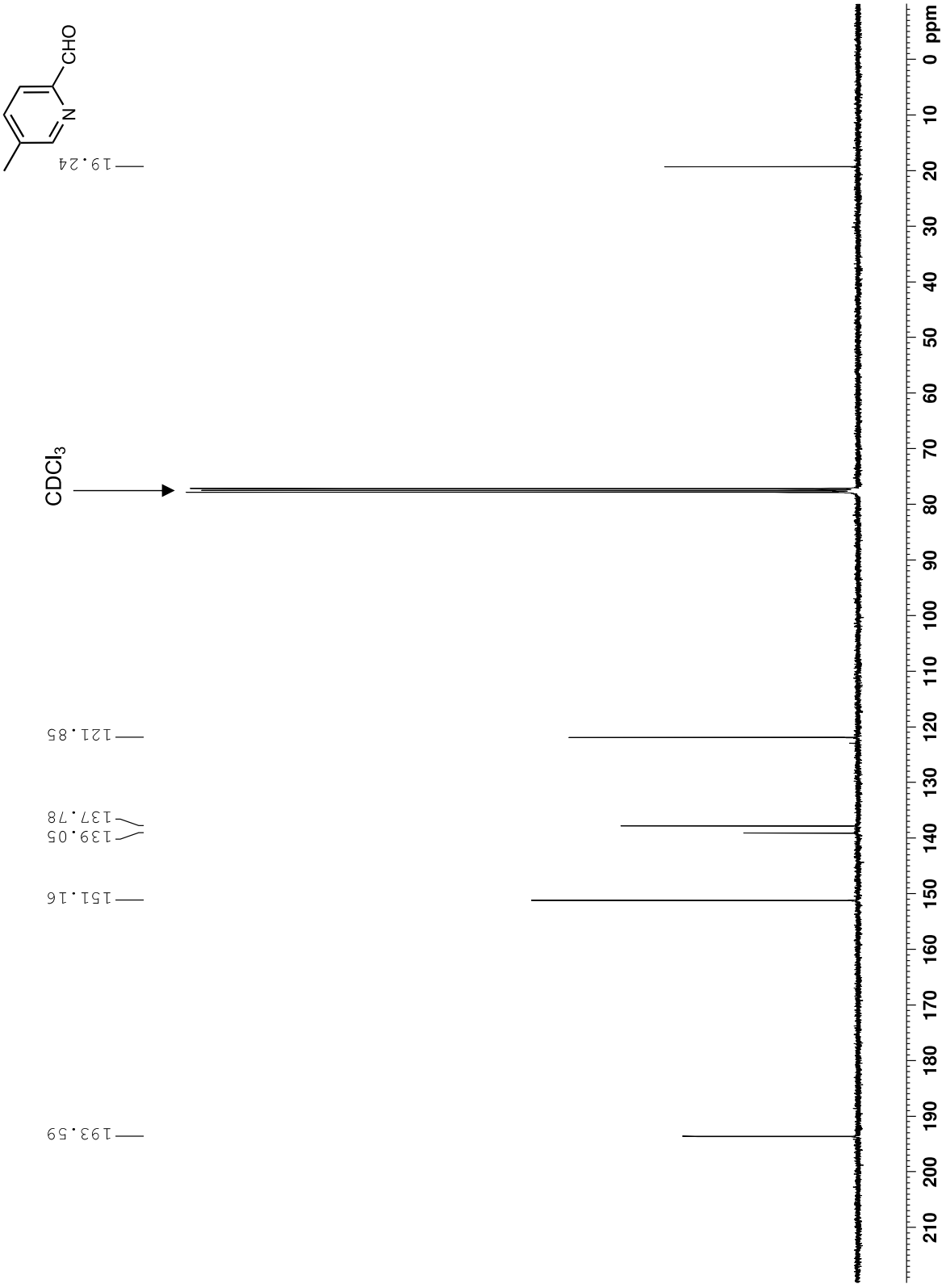

Spectrum 23. ^{13}C NMR of 5-methylpicolinaldehyde (100 MHz, 293 K, $CDCl_3$).

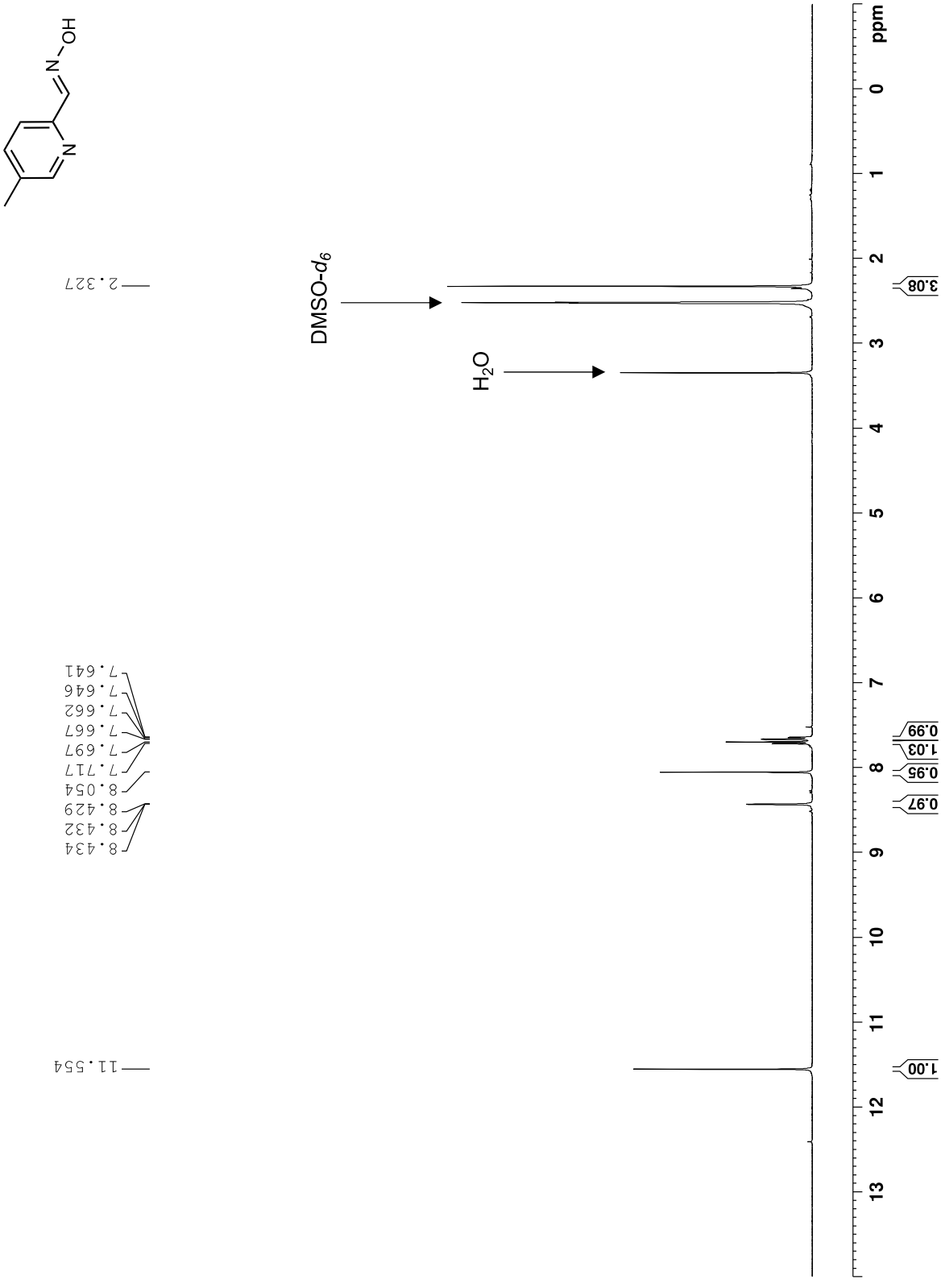

Spectrum 24. ^{1}H NMR of (*E*)-5-methylpicolinaldehyde oxime (400 MHz, 293 K, DMSO-d_6).

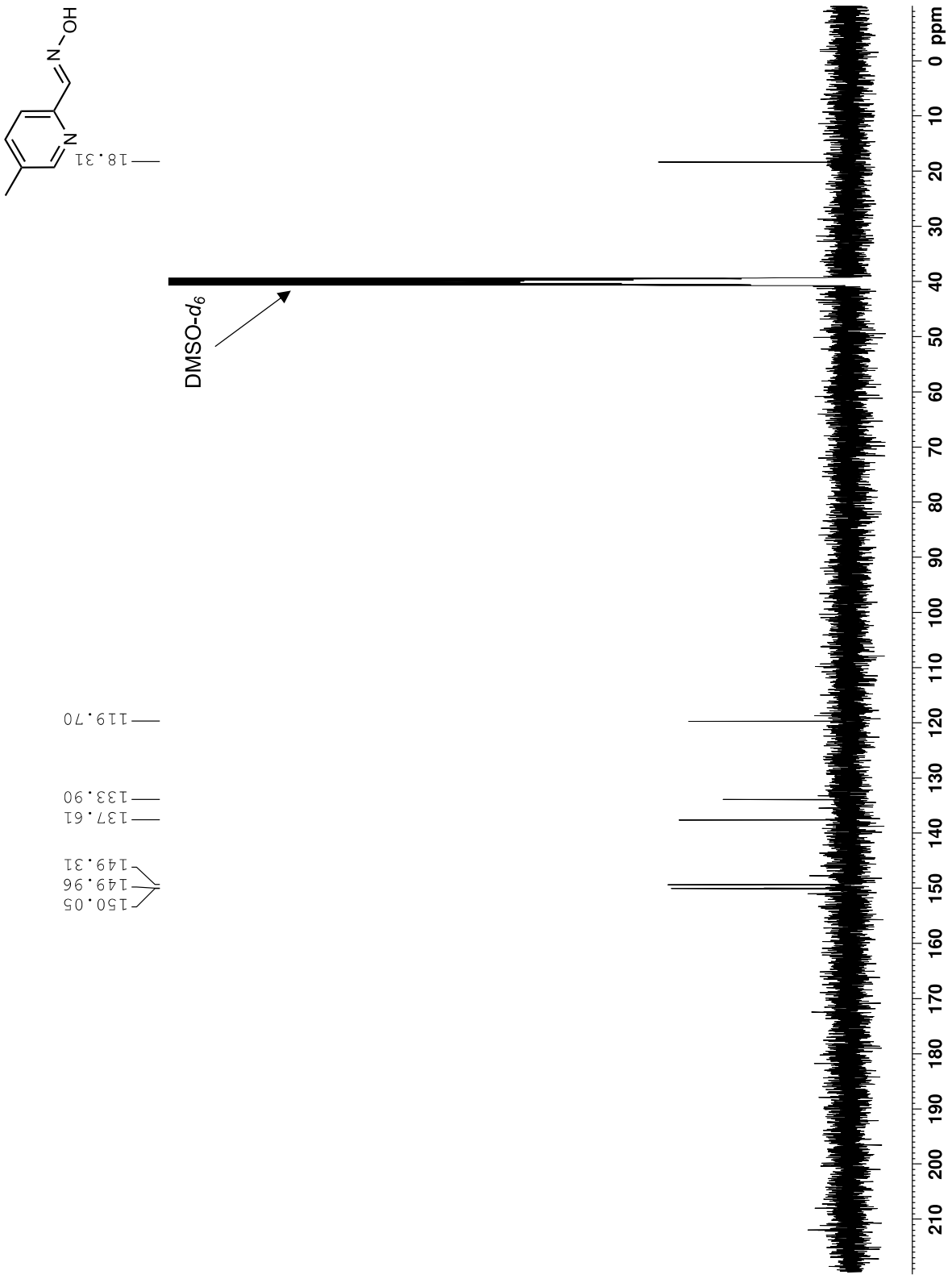

Spectrum 25. ^{13}C NMR of (*E*)-5-methylpicolinaldehyde oxime (100 MHz, 293 K, DMSO-d_6).

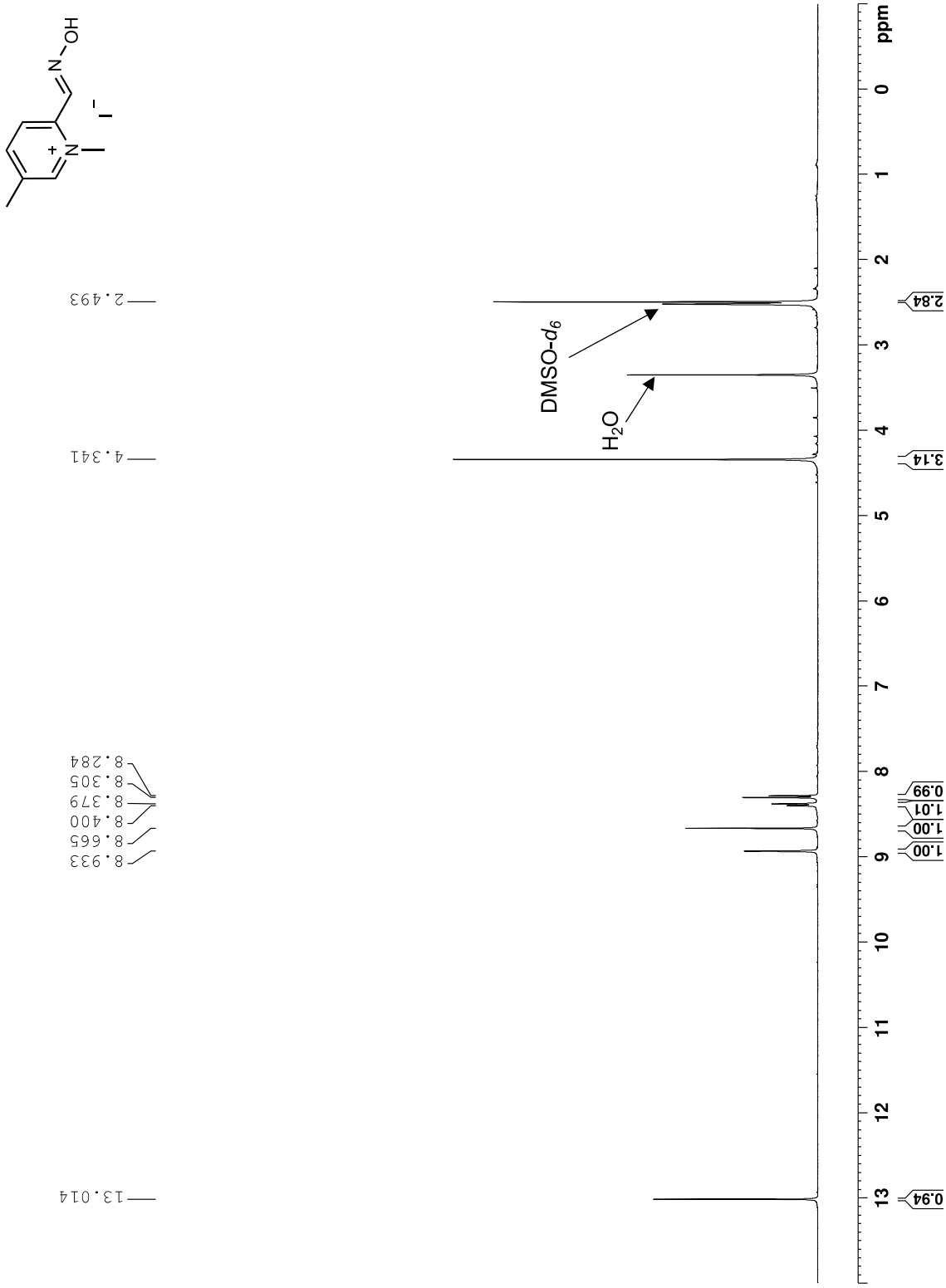

Spectrum 26. ^{1}H NMR of (*E*)-2-[(hydroxyimino)methyl]-1,5-dimethylpyridin-1-ium iodide (**5-Me-2-PAM**) (400 MHz, 293 K, DMSO-d_6).

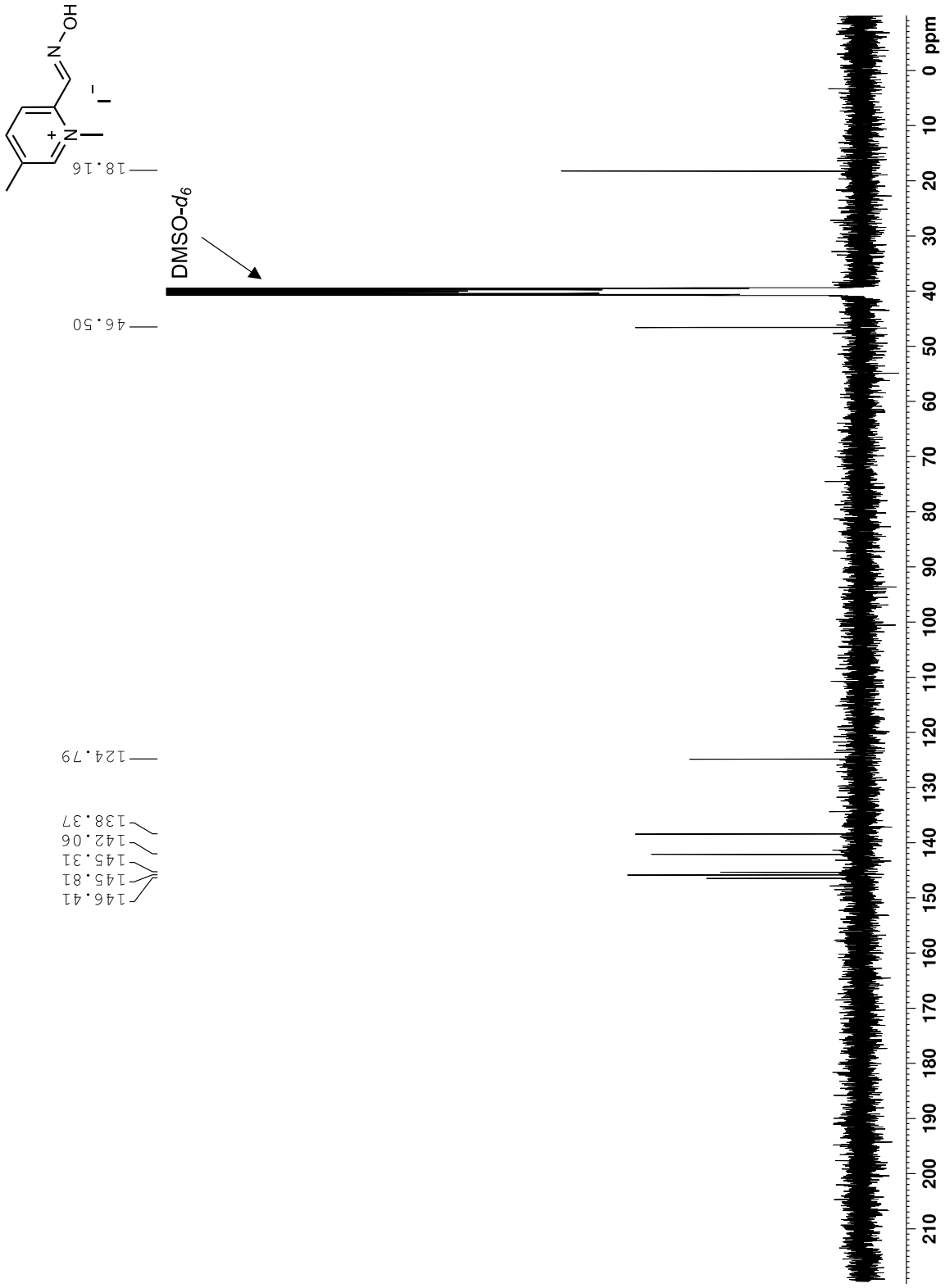

Spectrum 27. ^{13}C NMR of (*E*)-2-[(hydroxyimino)methyl]-1,5-dimethylpyridin-1-ium iodide (**5-Me-2-PAM**) (100 MHz, 293 K, DMSO-d_6).

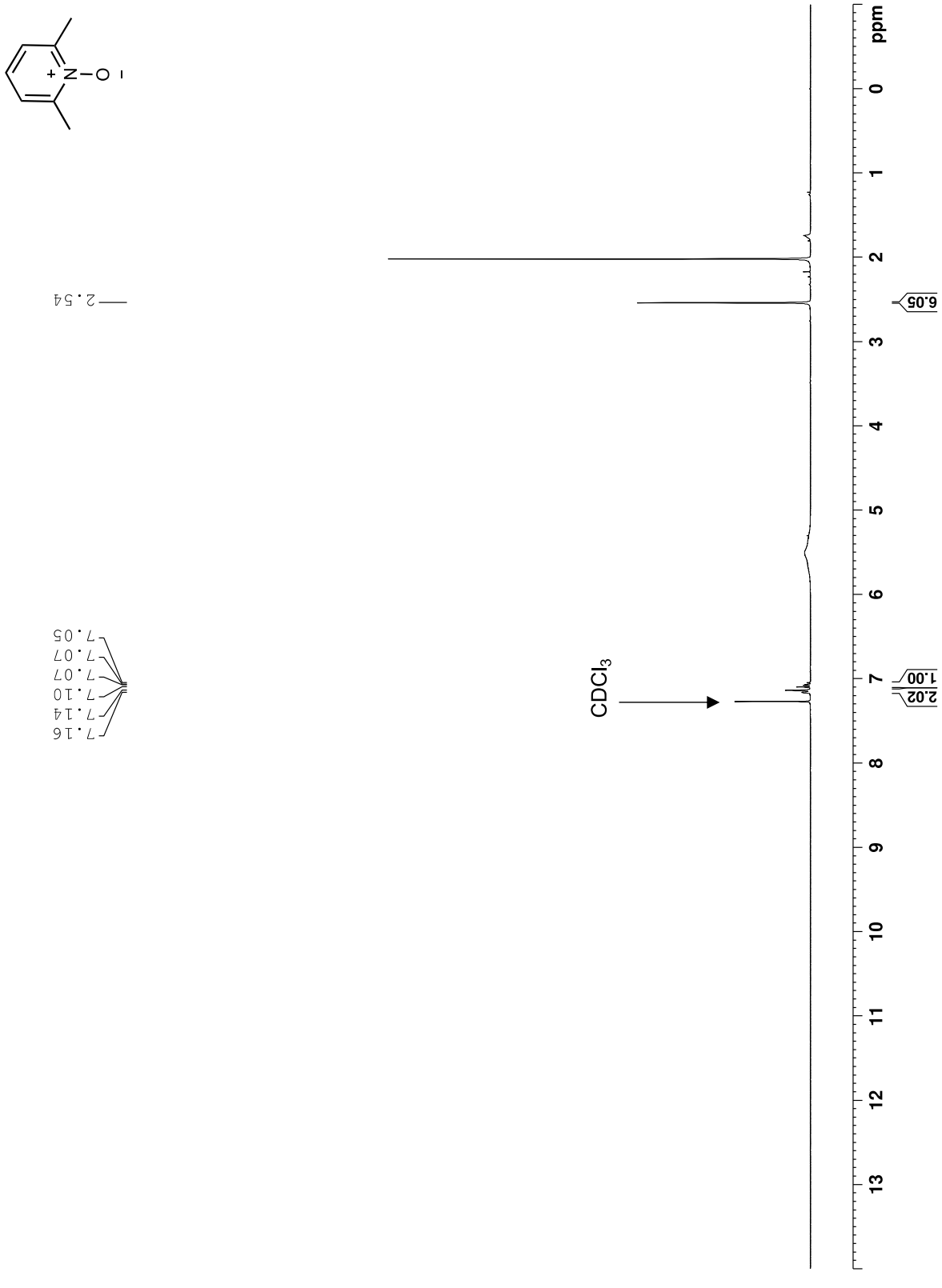

Spectrum 28. ^{1}H NMR of 2,6-dimethylpyridine 1-oxide (300 MHz, 293 K, $CDCl_3$).

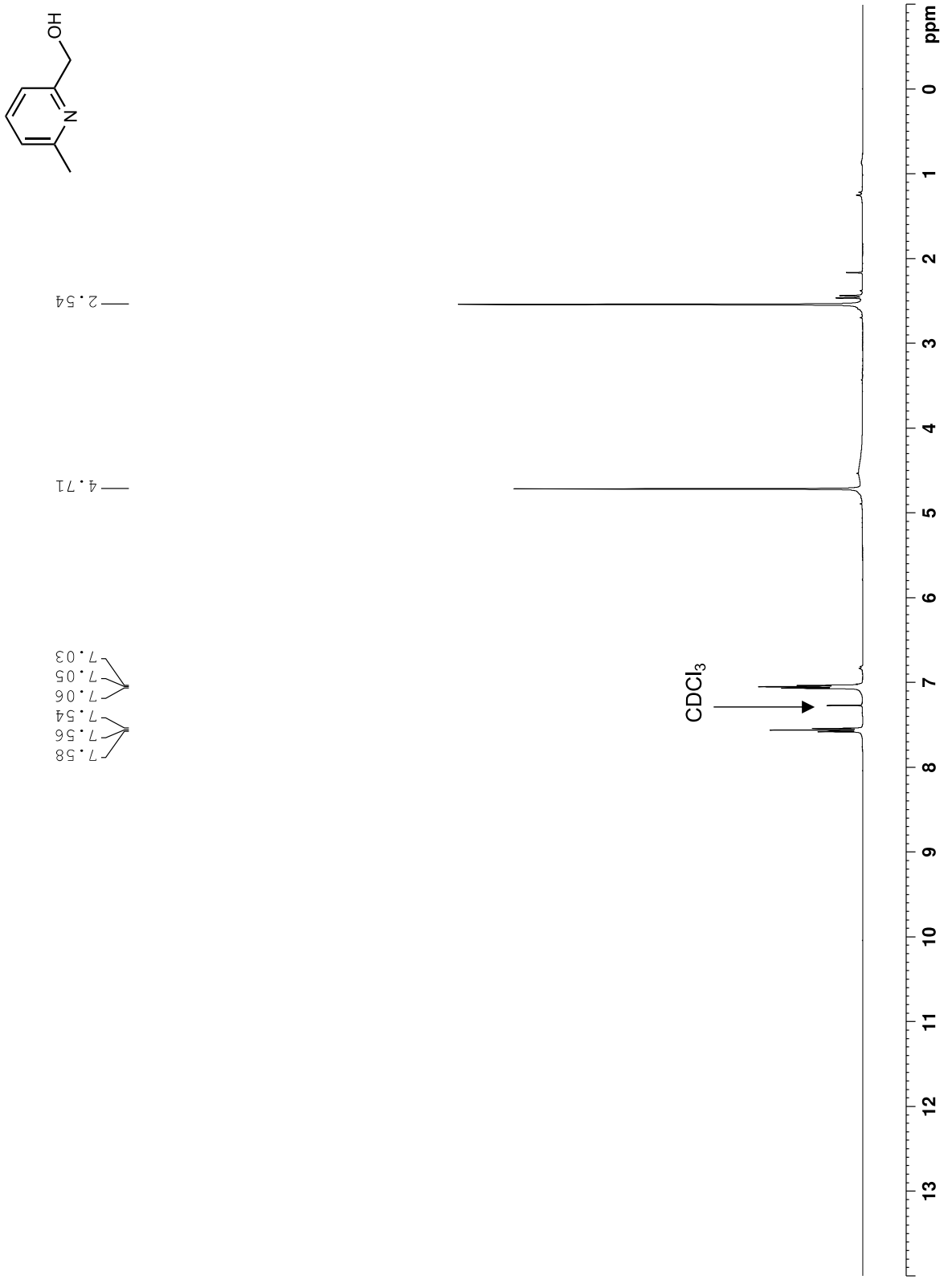

Spectrum 29. ^{1}H NMR of (6-methylpyridin-2-yl)methanol (400 MHz, 293 K, 1% w/w CD_3OD in $CDCl_3$).

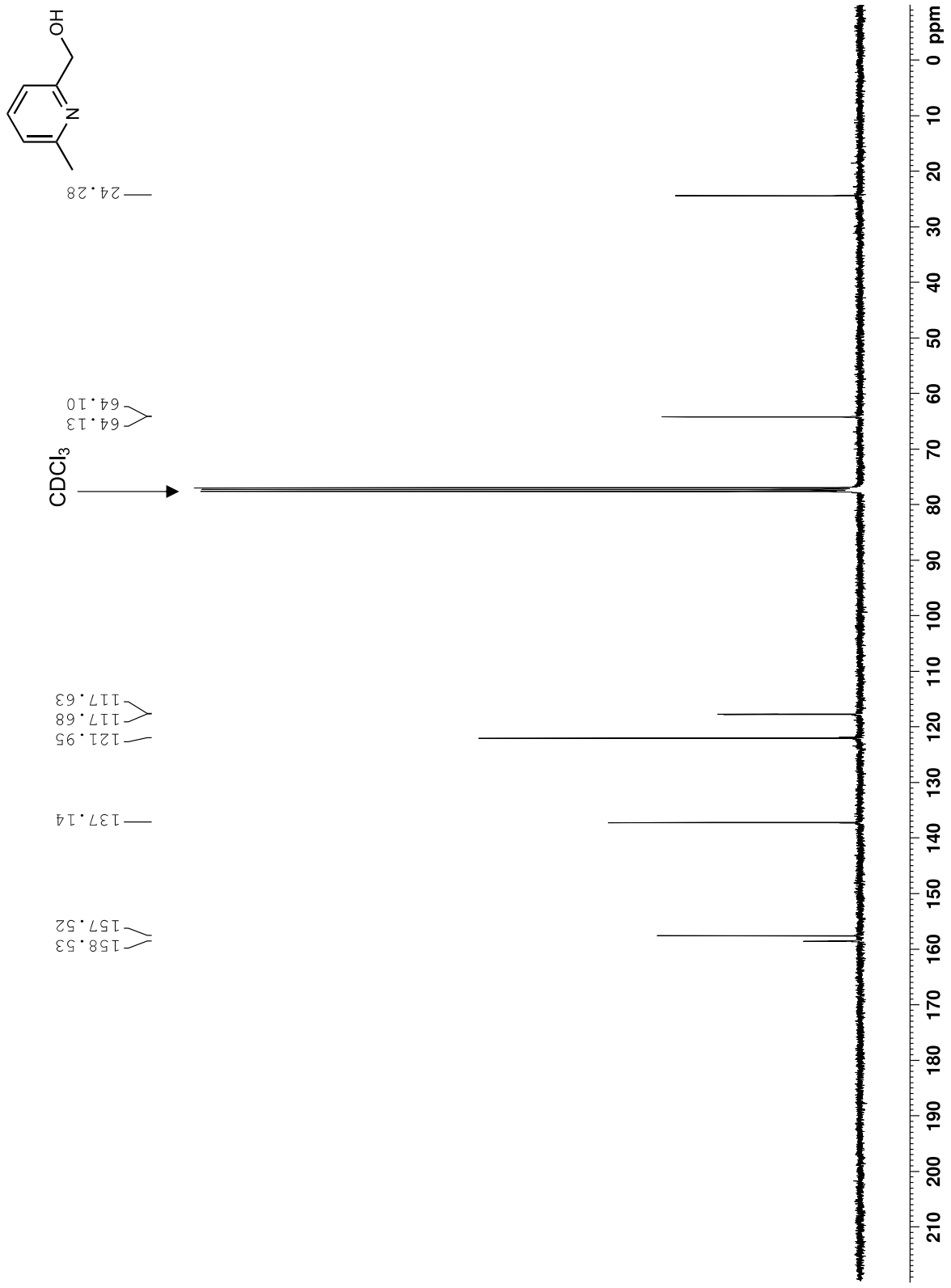

Spectrum 30. ^{13}C NMR of (6-methylpyridin-2-yl)methanol (100 MHz, 293 K, $CDCl_3$).

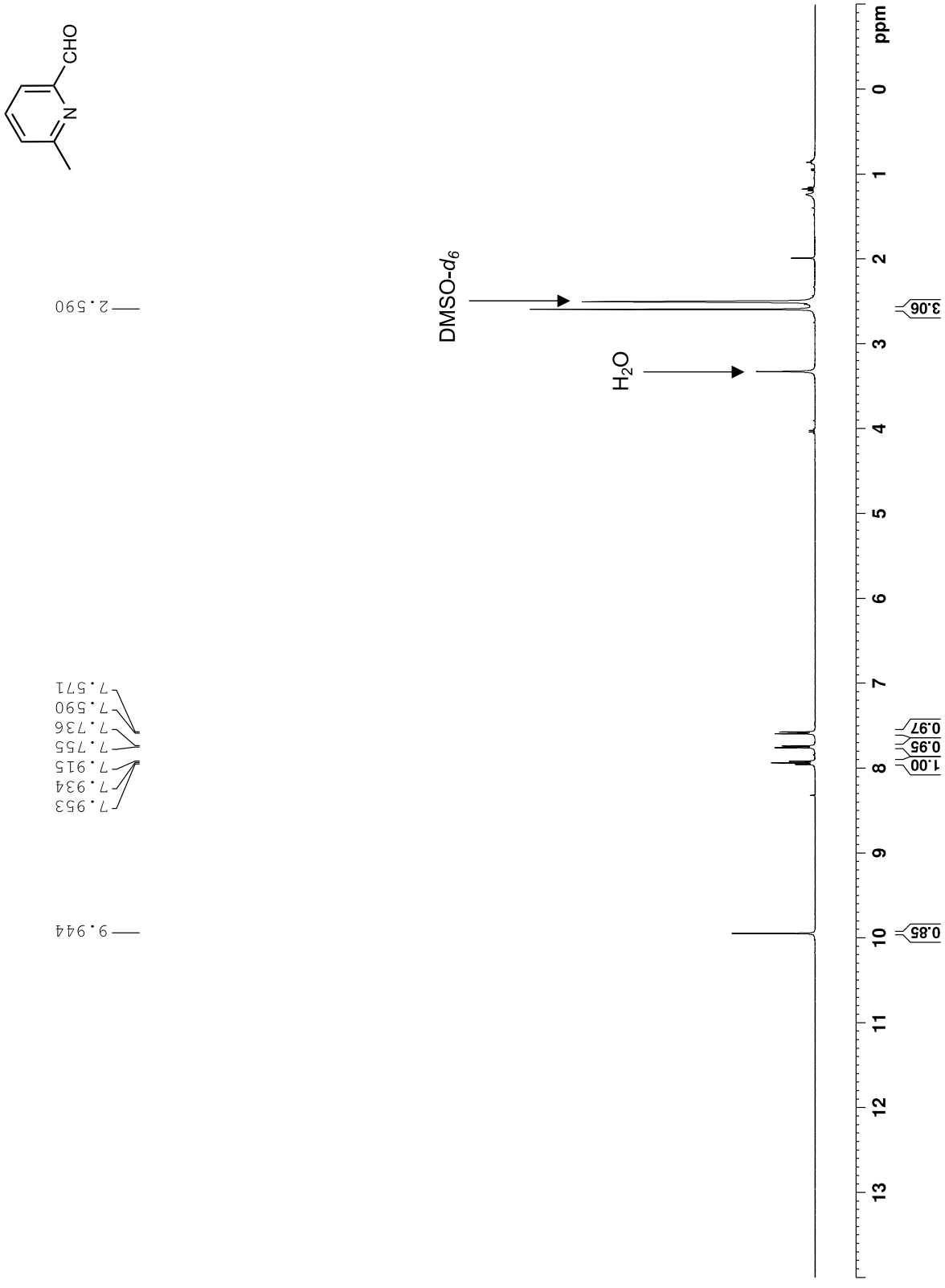

Spectrum 31. ^{1}H NMR of 6-methylpicolinaldehyde (400 MHz, 293 K, DMSO-d_6).

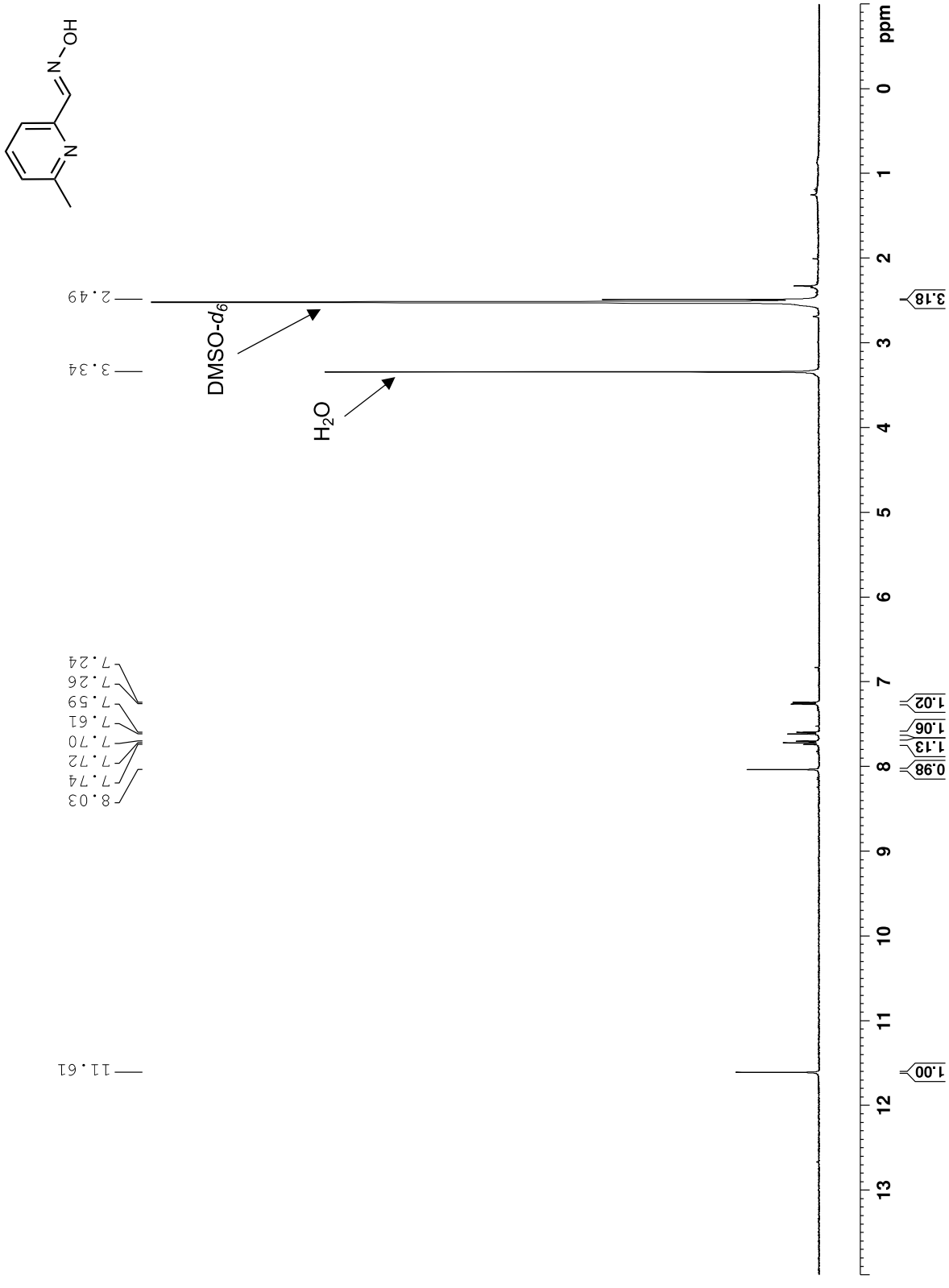

Spectrum 32. ^{1}H NMR of (*E*)-6-methylpicolinaldehyde oxime (400 MHz, 293 K, DMSO-d_6).

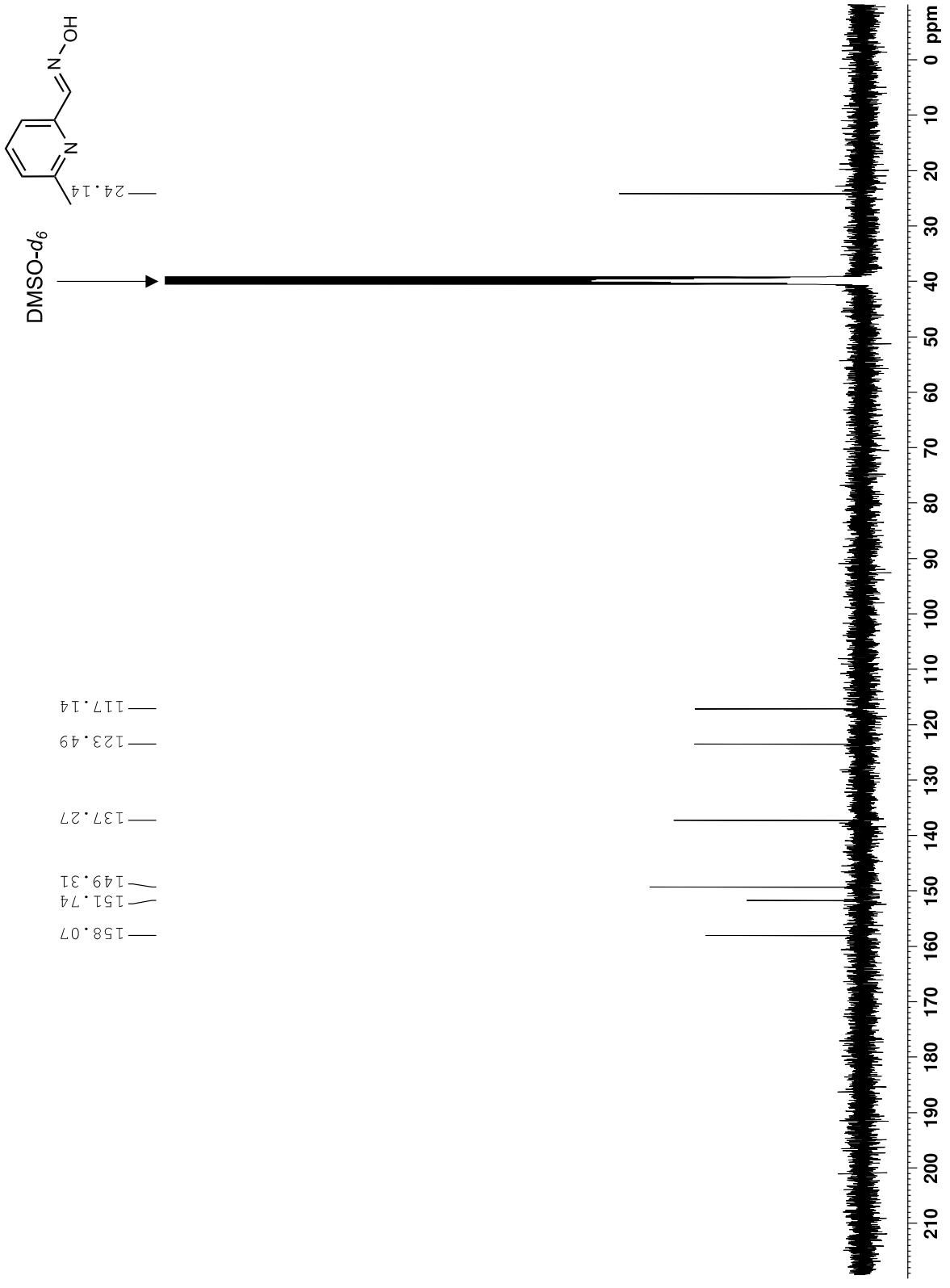

Spectrum 33. ^{13}C NMR of (*E*)-6-methylpicolinaldehyde oxime (100 MHz, 293 K, DMSO-d_6).

DMSO-d_6
12.969
8.789
8.424
8.404
8.384
8.189
8.169
8.030
8.011
4.161
2.824
97.94
99.80
100.00
99.59
110.25
303.78
306.32
ppm
0
1
2
3
4
5
6
7
8
9
10
11
12
13
HO
N
I

Spectrum 34. ^{1}H NMR of (*E*)-2-[(hydroxyimino)methyl]-1,6-dimethylpyridin-1-ium iodide (**6-Me-2-PAM**) (400 MHz, 293 K, DMSO-d_6).

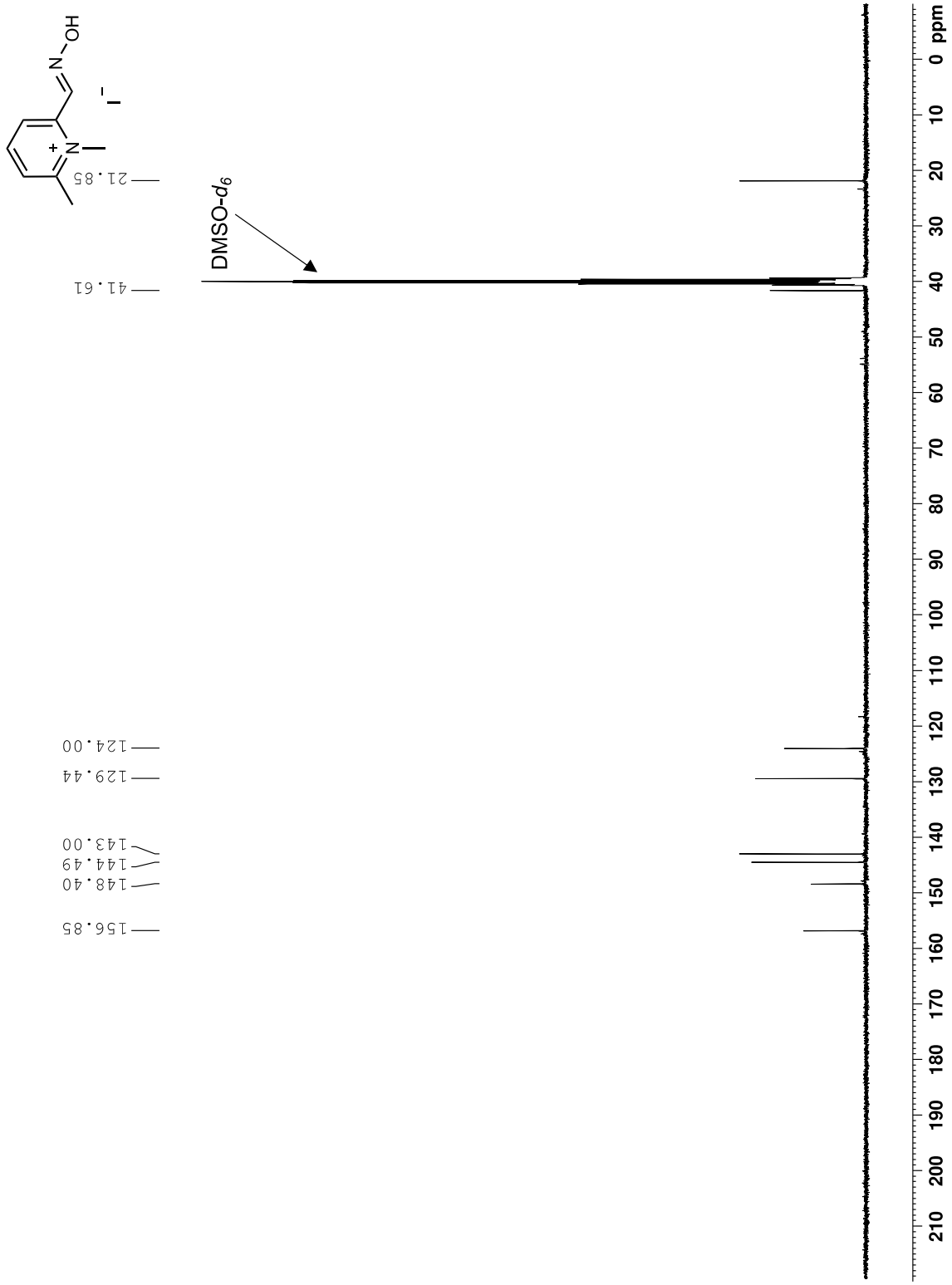

Spectrum 35. ^{13}C NMR of (*E*)-2-[(hydroxyimino)methyl]-1,6-dimethylpyridin-1-ium iodide (**6-Me-2-PAM**) (100 MHz, 293 K, DMSO-d_6).

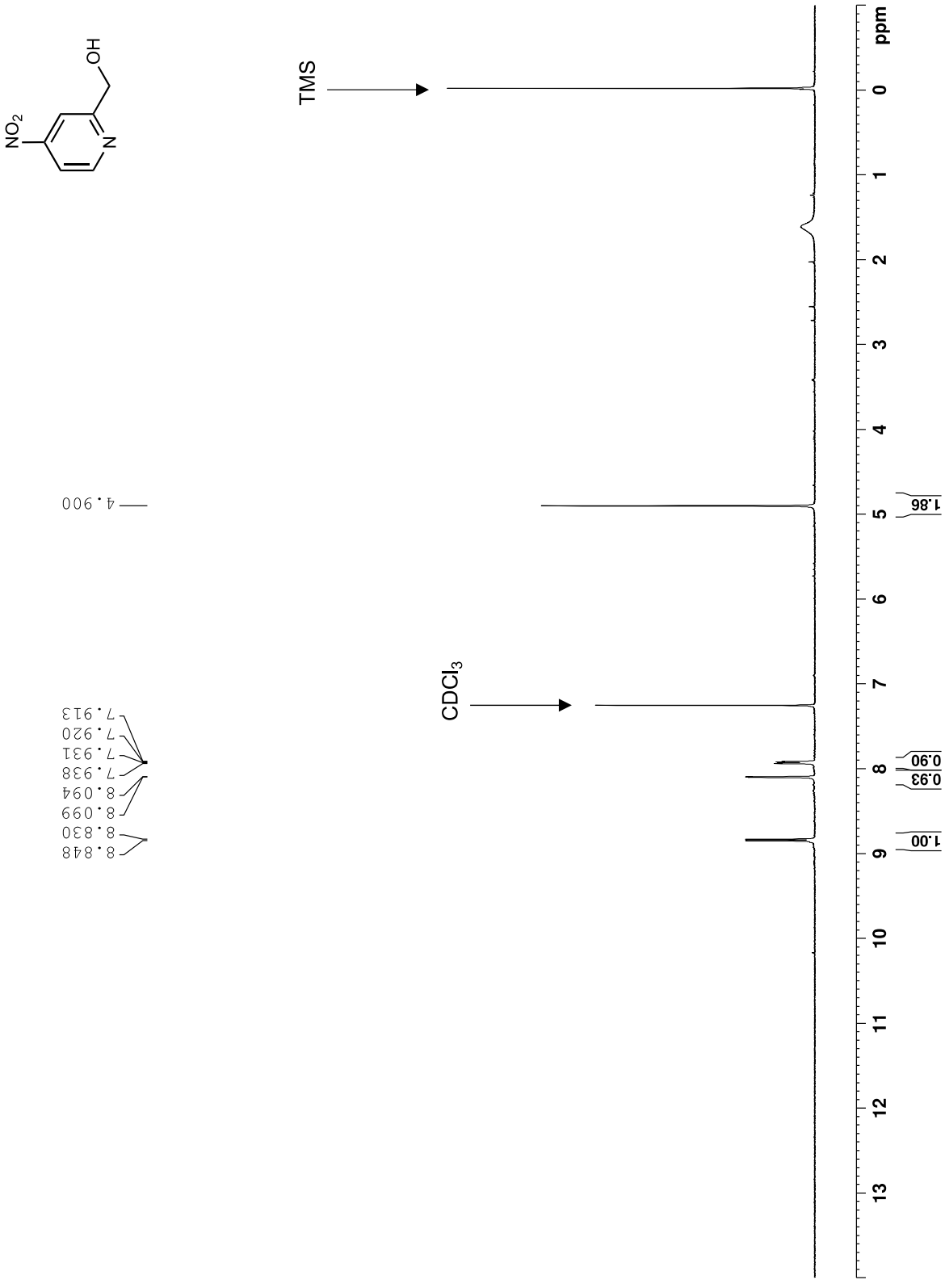

Spectrum 36. ^{1}H NMR of (4-nitropyridin-2-yl)methanol (300 MHz, 293 K, 1% w/w CD_3OD in $CDCl_3$).

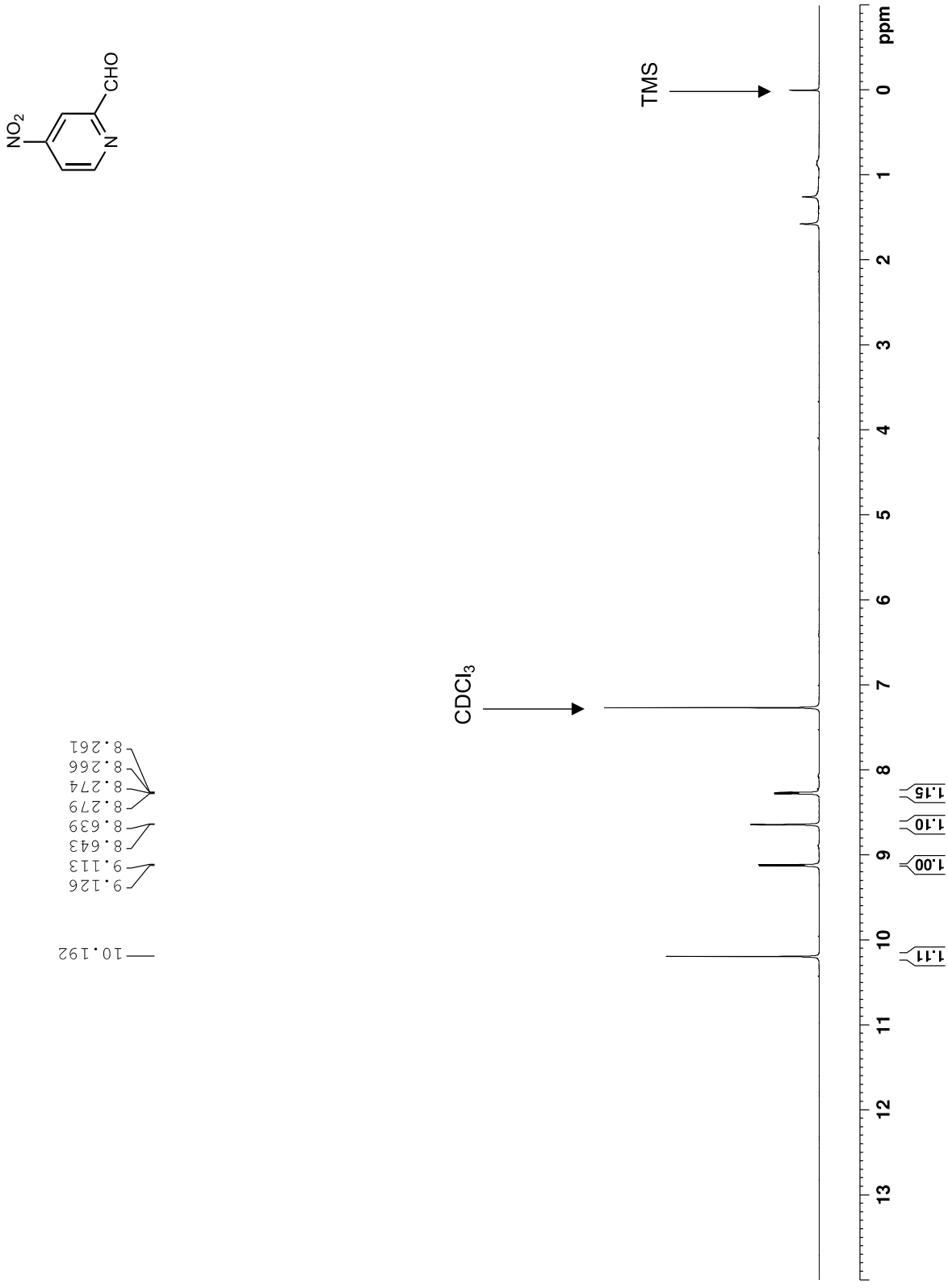

Spectrum 37. ^{1}H NMR of 4-nitropicolinaldehyde (400 MHz, 293 K, $CDCl_3$).

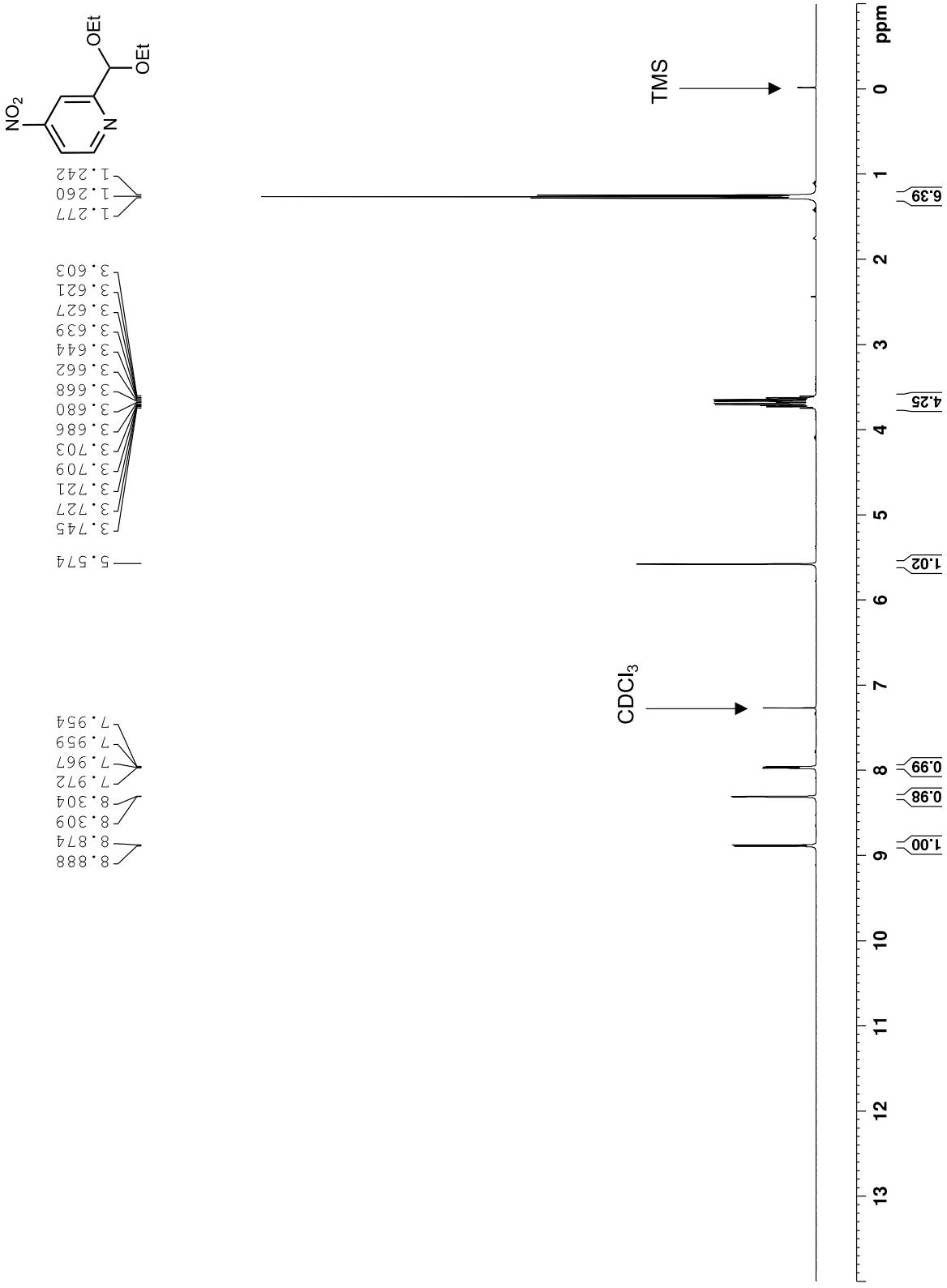

Spectrum 38. ^{1}H NMR of 2-(diethoxymethyl)-4-nitropyridine (400 MHz, 293 K, $CDCl_3$).

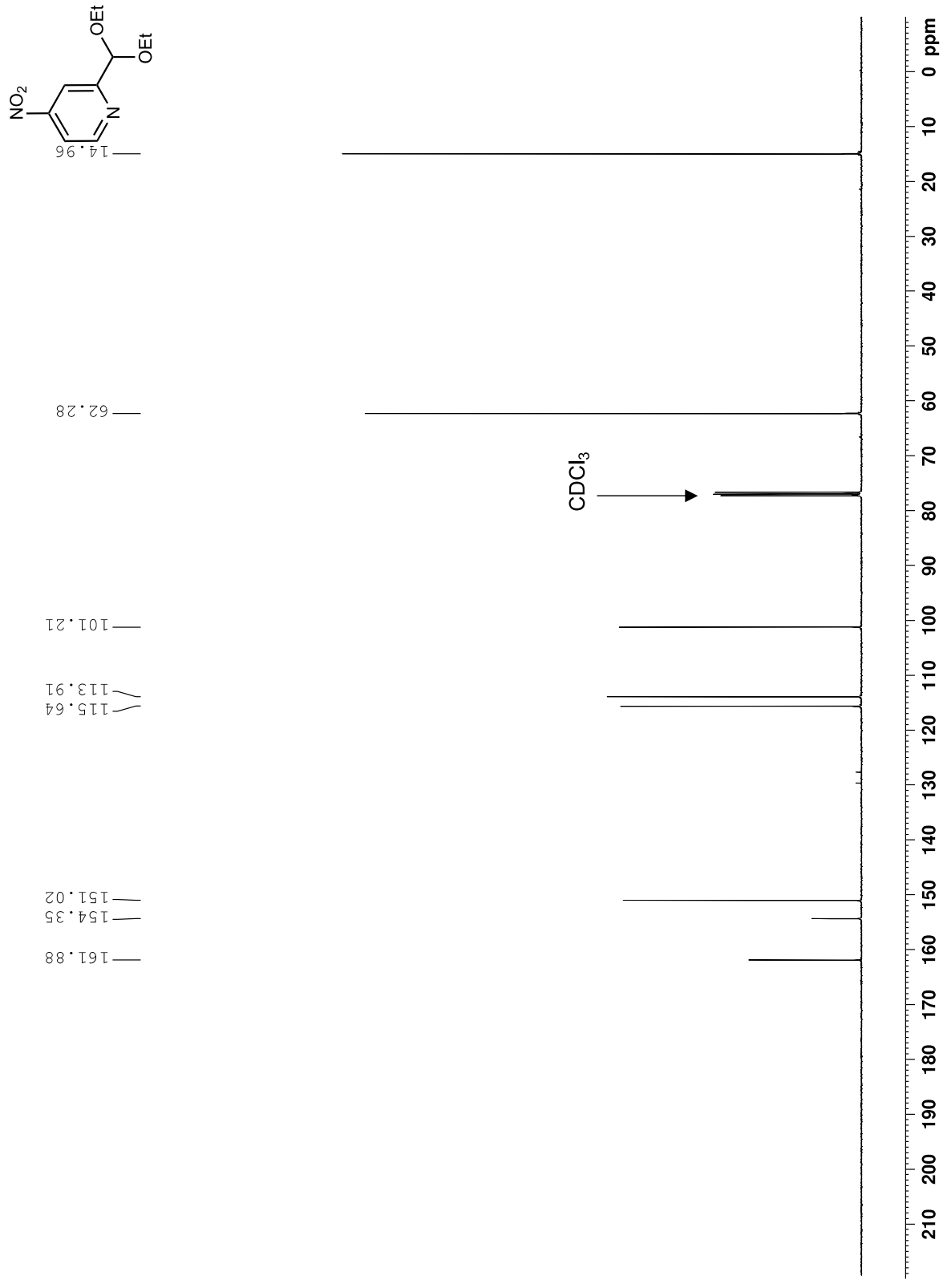

Spectrum 39. ^{13}C NMR of 2-(diethoxymethyl)-4-nitropyridine (100 MHz, 293 K, $CDCl_3$).

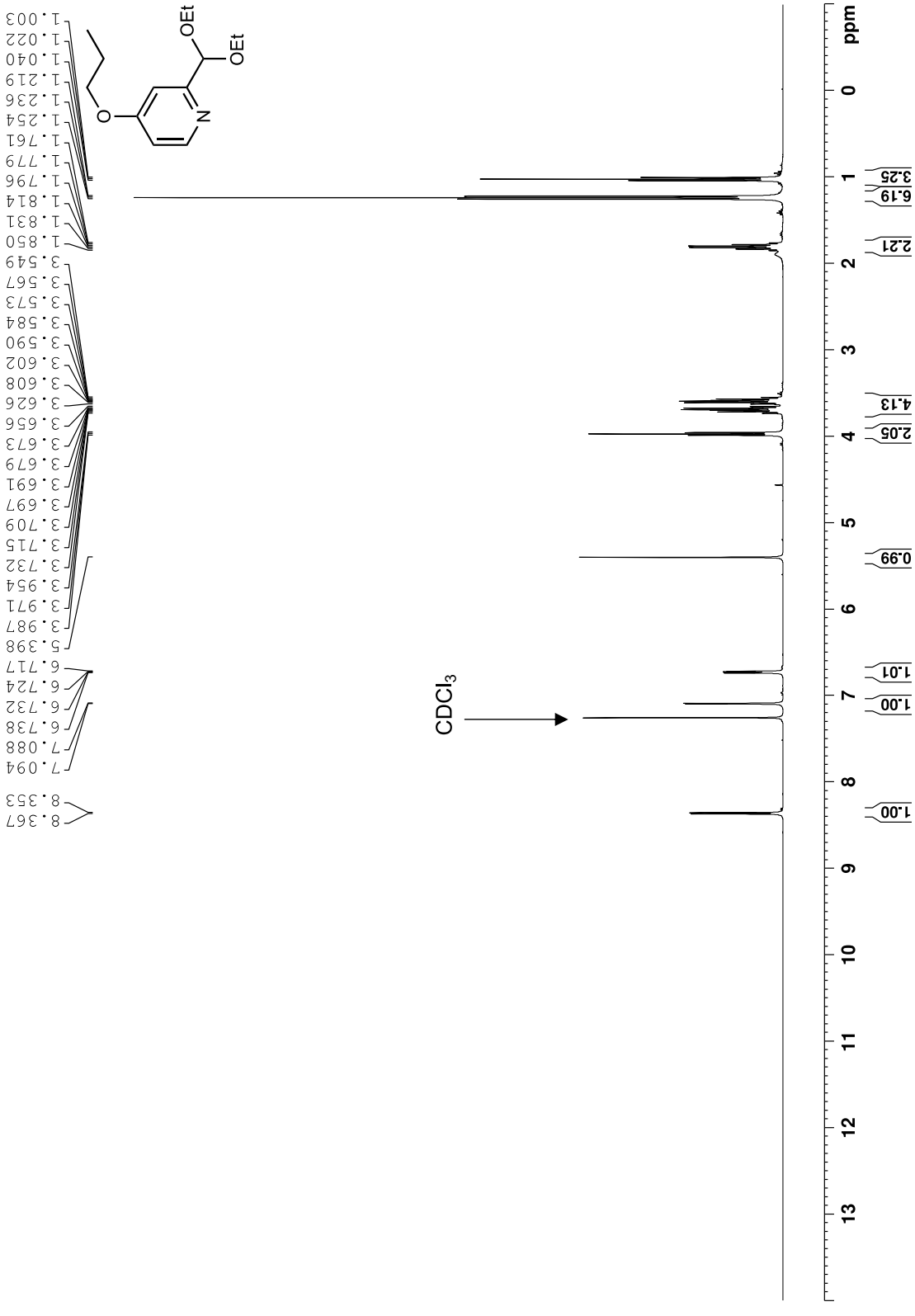

Spectrum 40. ^{1}H NMR of 2-(diethoxymethyl)-4-propoxypyridine (400 MHz, 293 K, $CDCl_3$).

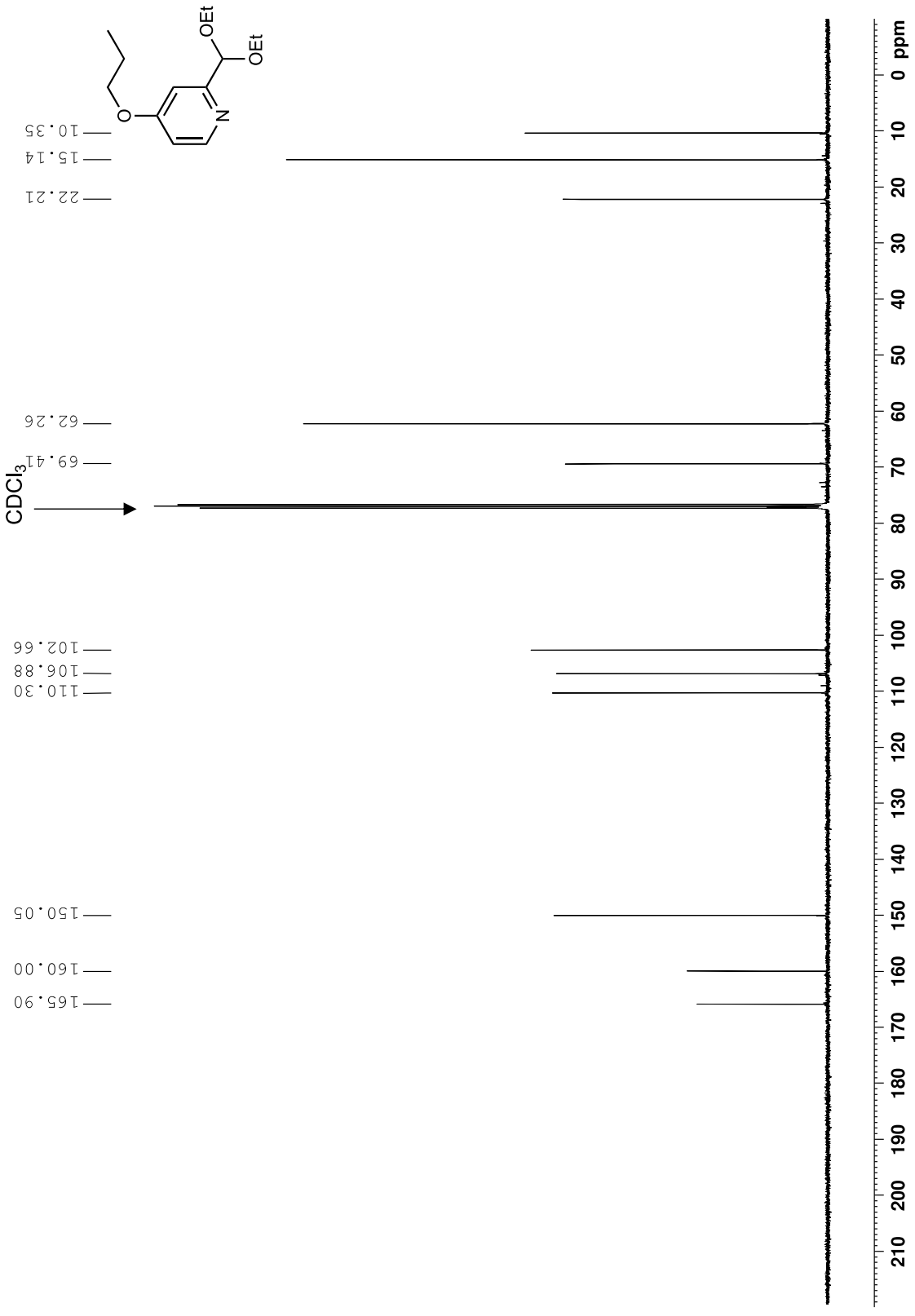

Spectrum 41. ^{13}C NMR of 2-(diethoxymethyl)-4-propoxypyridine (100 MHz, 293 K, $CDCl_3$).

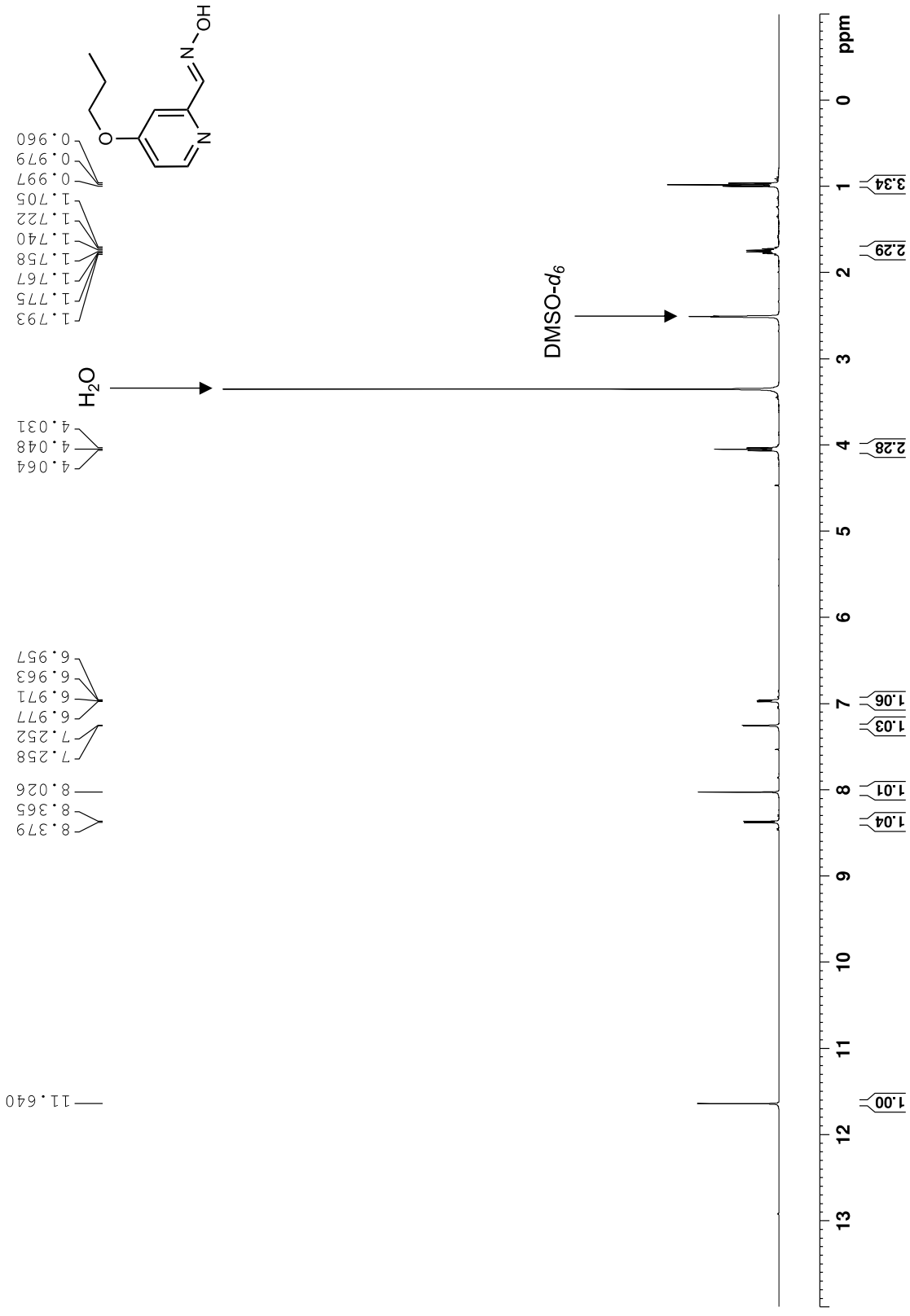

Spectrum 42. ^{1}H NMR of (*E*)-4-propoxypicolinaldehyde oxime (400 MHz, 293 K, DMSO-d_6).

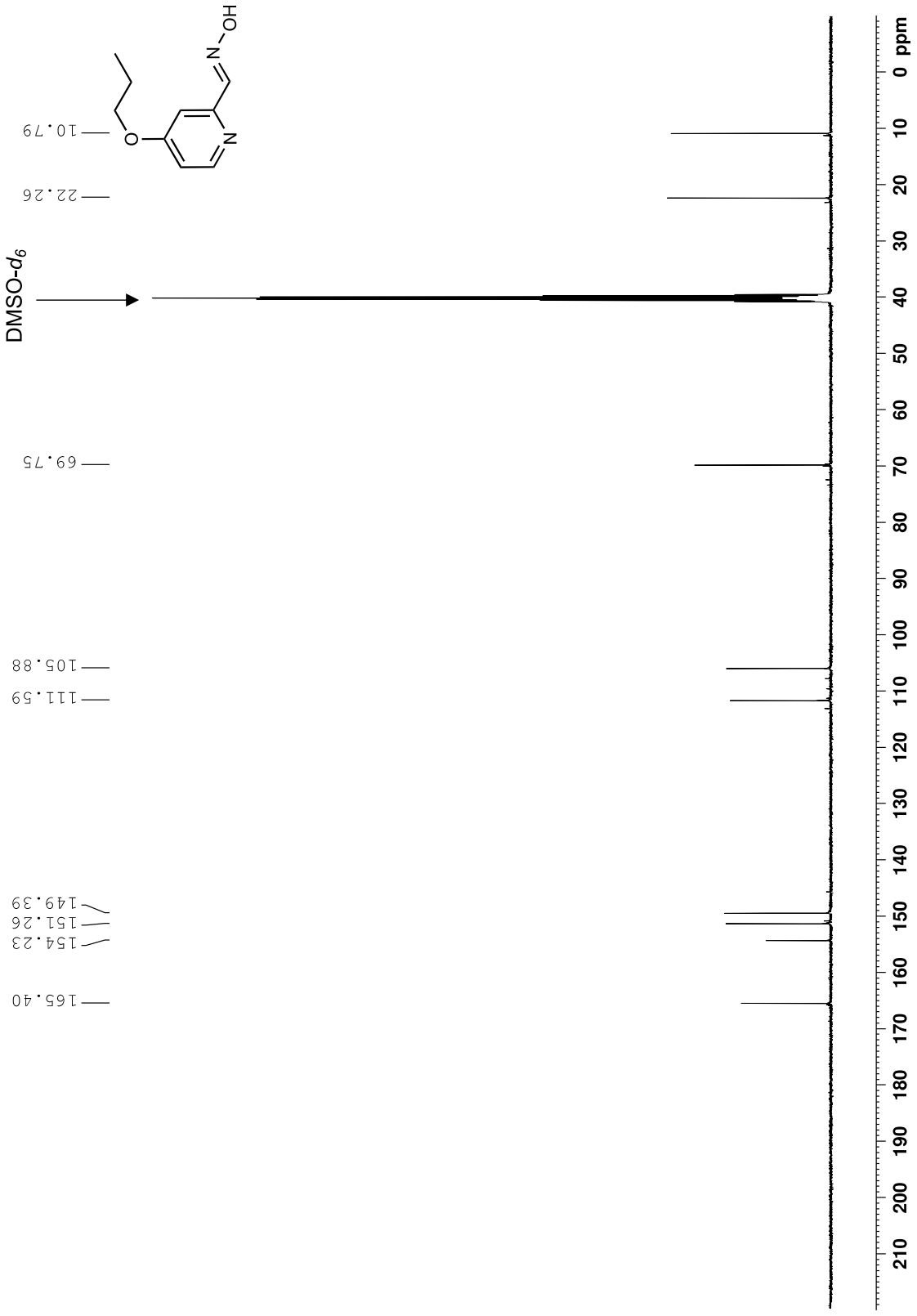

Spectrum 43. ^{13}C NMR of (*E*)-4-propoxypicolinaldehyde oxime (100 MHz, 293 K, DMSO-d_6).

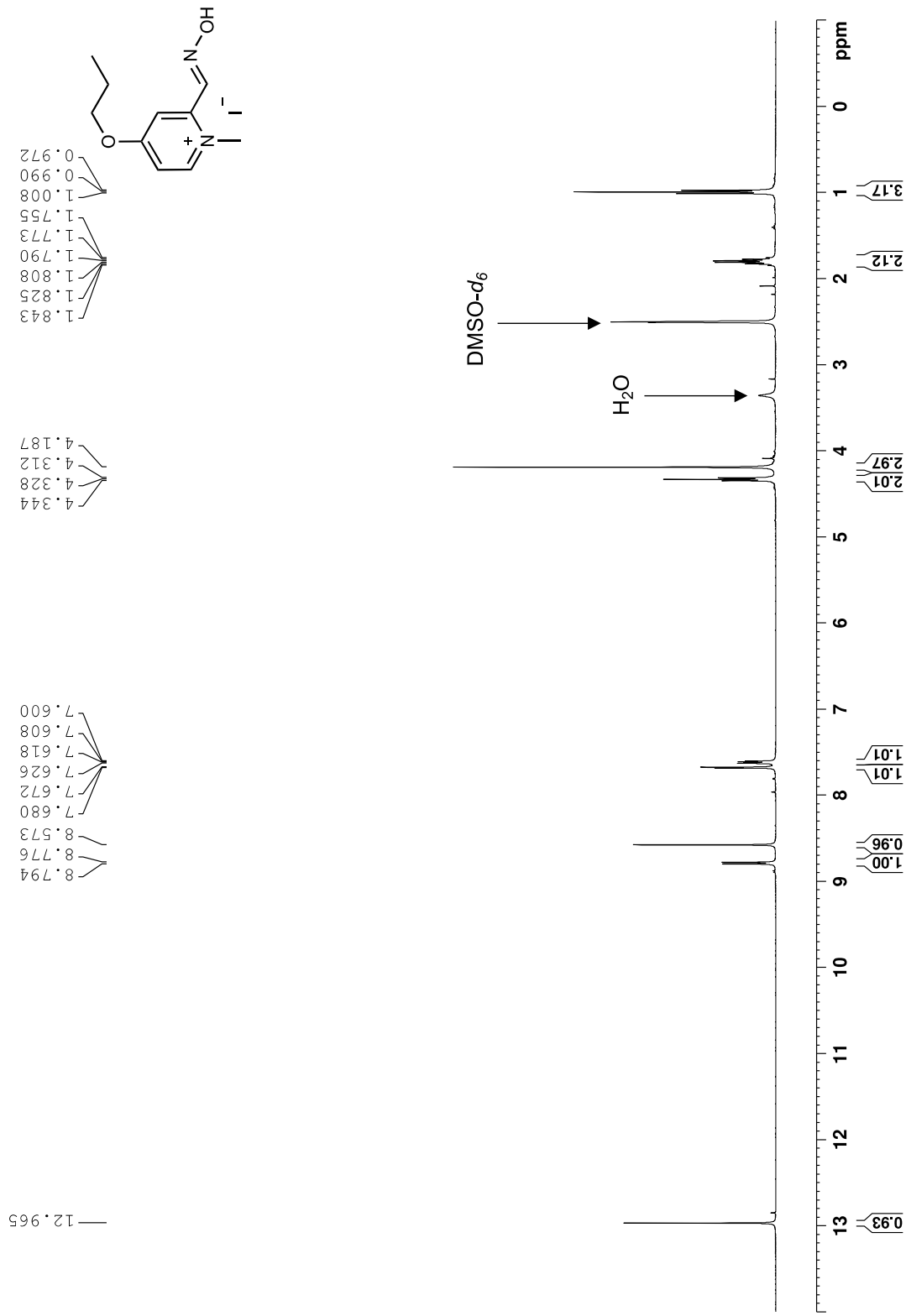

Spectrum 44. ^{1}H NMR of (*E*)-2-((hydroxyimino)methyl)-1-methyl-4-propoxypyridin-1-ium (**ADG3035)** (400 MHz, 293 K, DMSO-d_6).

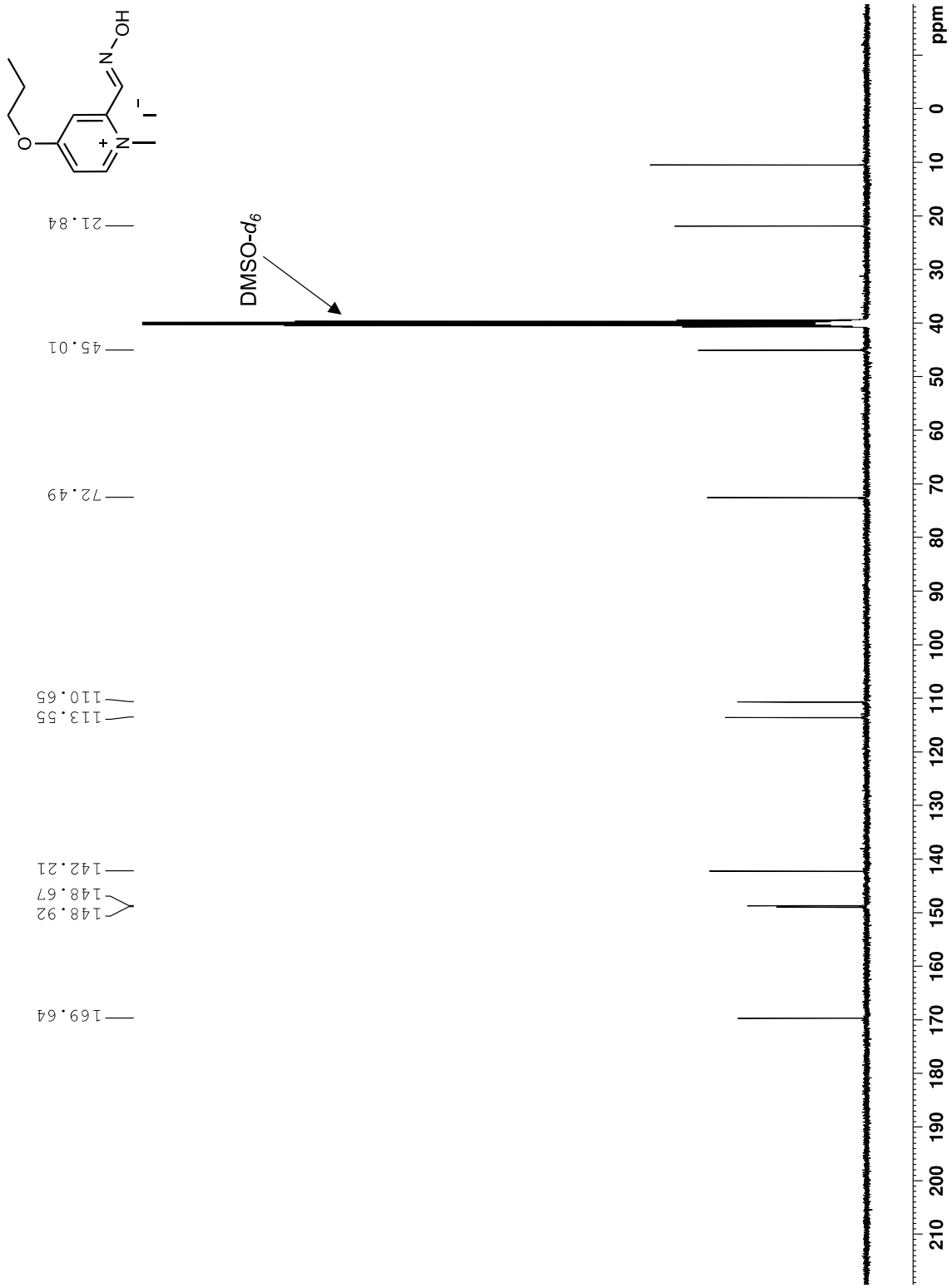

Spectrum 45. ^{13}C NMR of (*E*)-2-((hydroxyimino)methyl)-1-methyl-4-propoxypyridin-1-ium (**ADG3035)** (100 MHz, 293 K, DMSO-d_6).

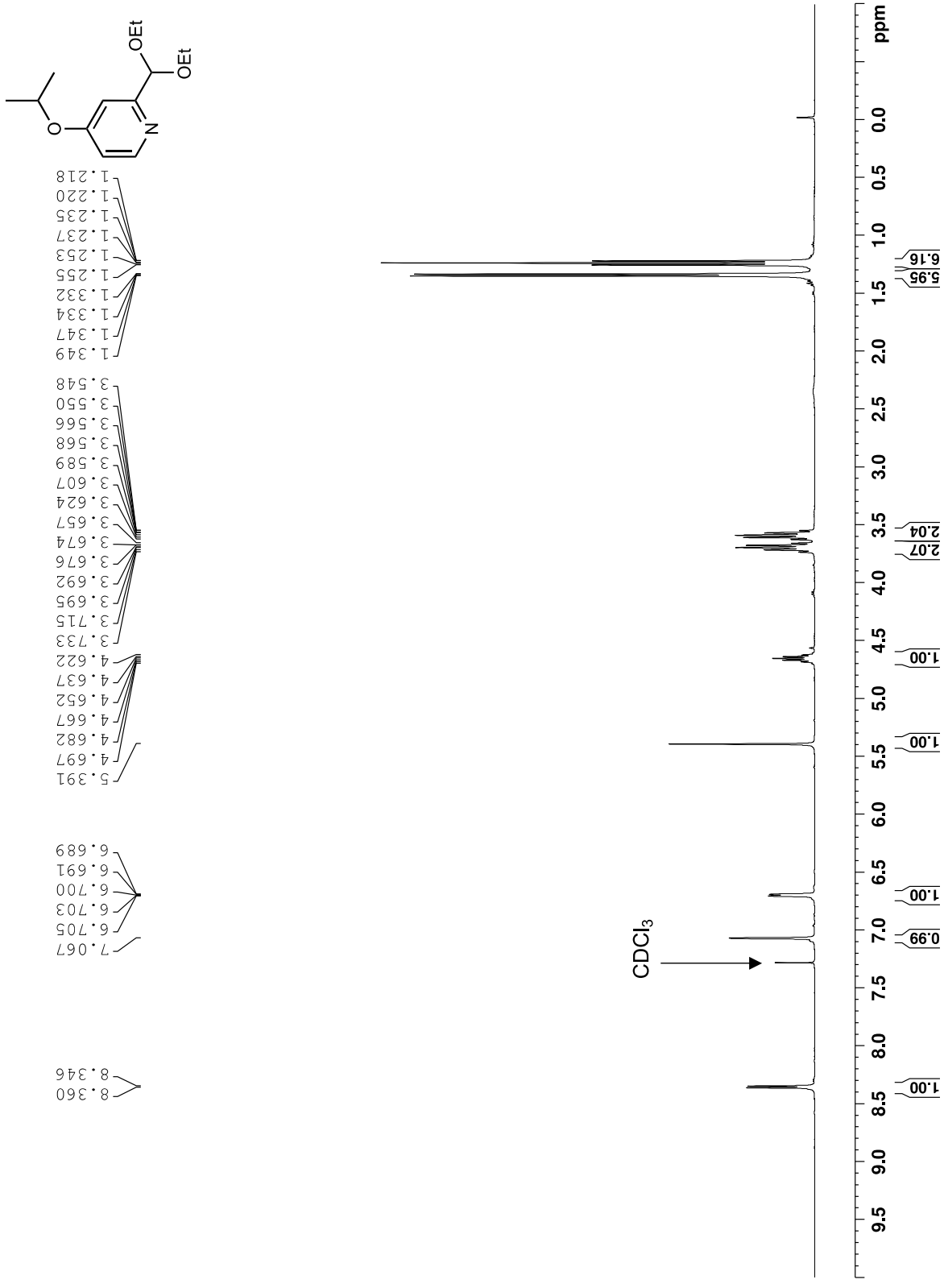

Spectrum 46. ^{1}H NMR of 2-(diethoxymethyl)-4-propoxypyridine (400 MHz, 293 K, $CDCl_3$).

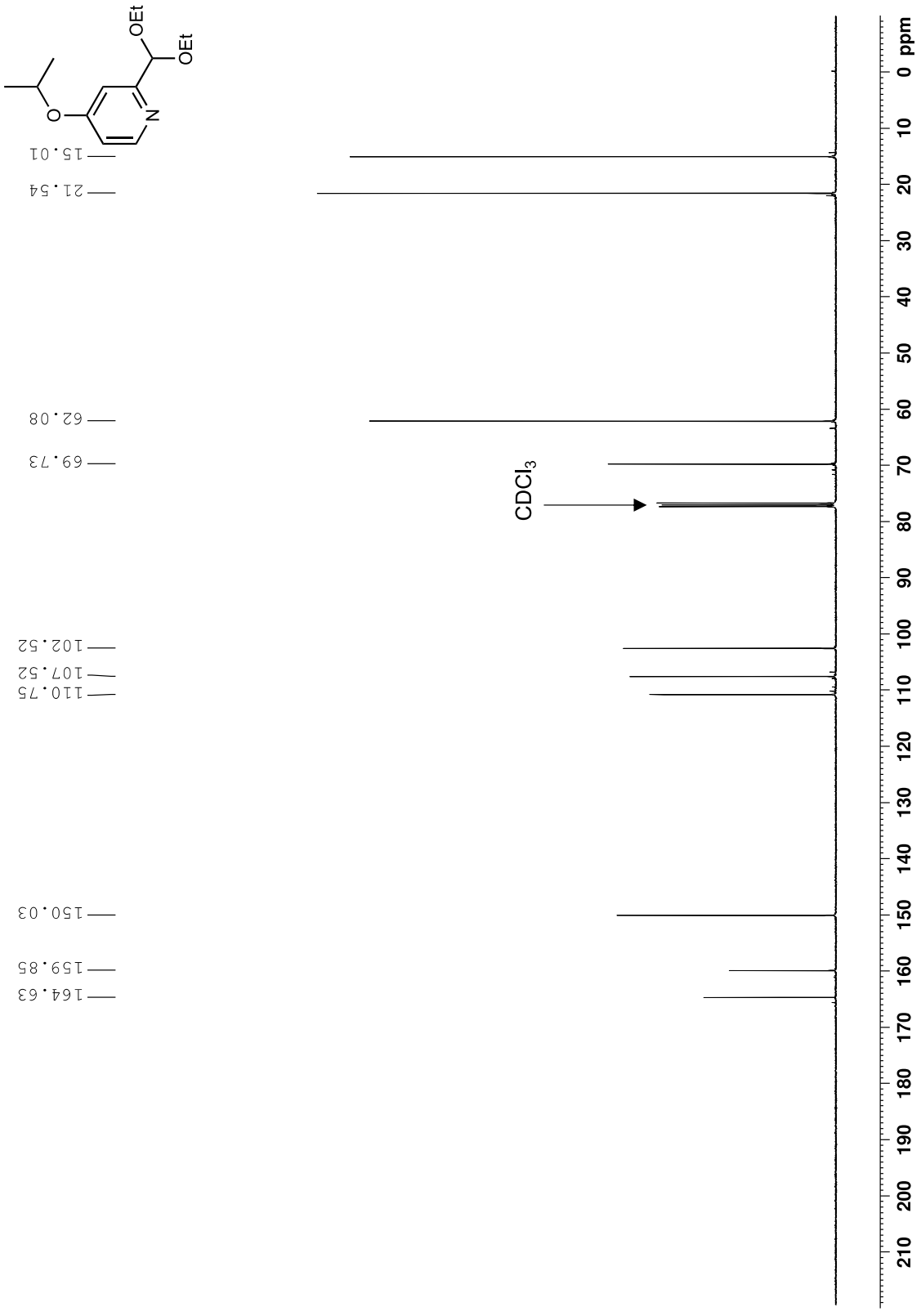

Spectrum 47. ^{13}C NMR of 2-(diethoxymethyl)-4-propoxypyridine (100 MHz, 293 K, $CDCl_3$).

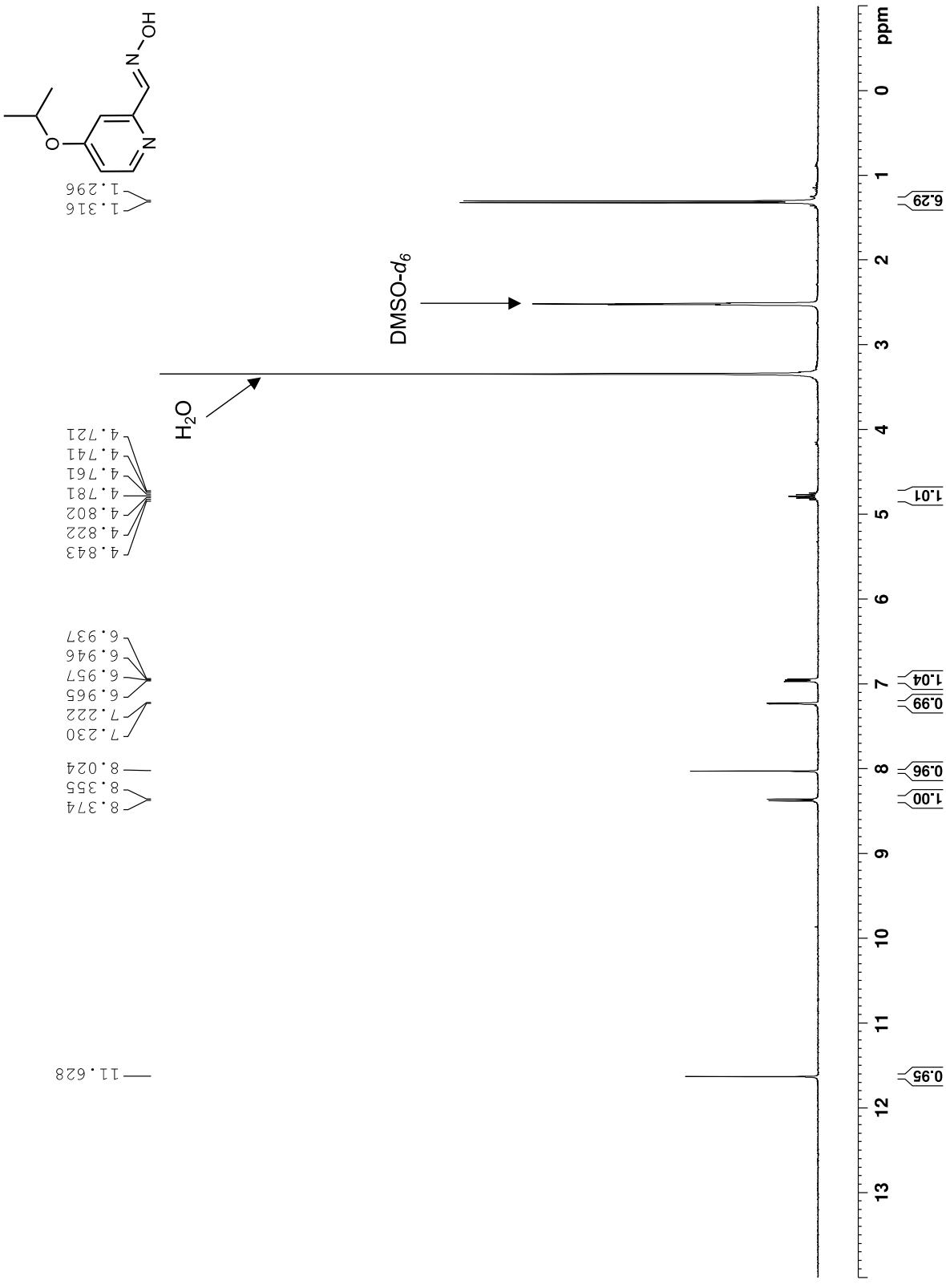

Spectrum 48. ^{1}H NMR of (*E*)-4-isopropoxypicolinaldehyde oxime (300 MHz, 293 K, DMSO-d_6).

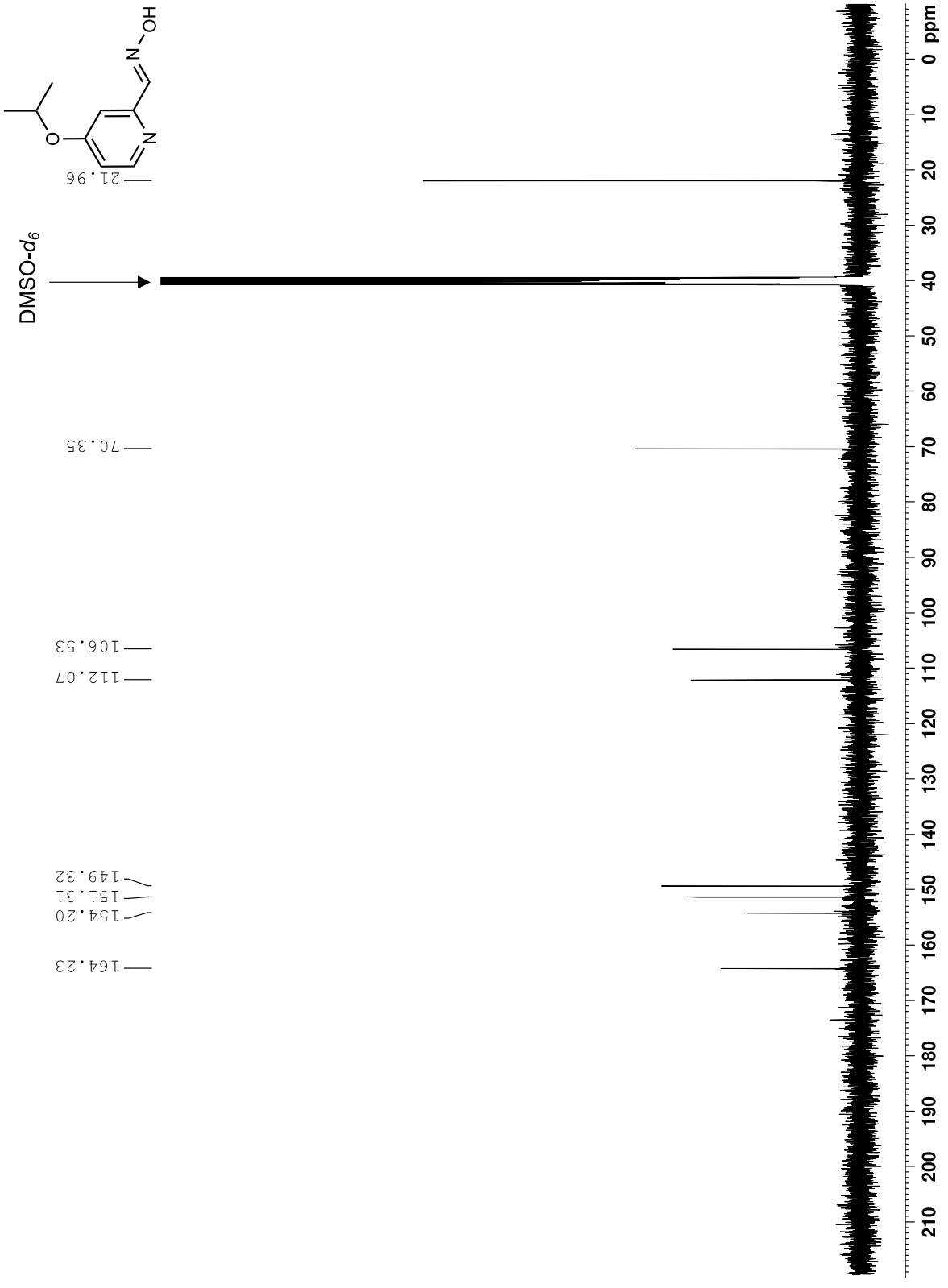

Spectrum 49. ^{13}C NMR of (*E*)-4-isopropoxypicolinaldehyde oxime (100 MHz, 293 K, DMSO-d_6).

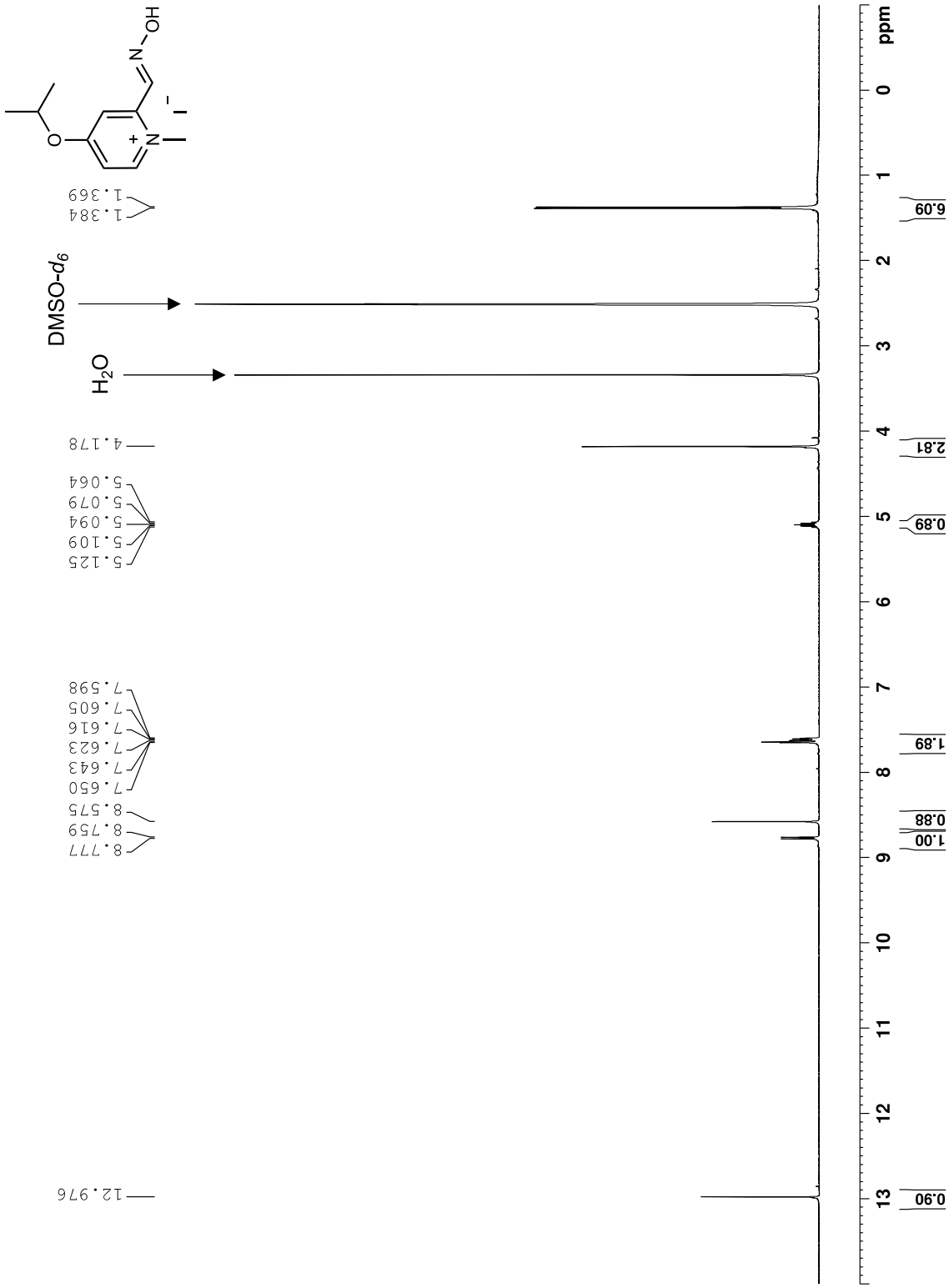

Spectrum 50. ^{1}H NMR of (*E*)-2-((hydroxyimino)methyl)-1-methyl-4-isopropoxypyridin-1-ium iodide (**ADG2054)** (400 MHz, 293 K, DMSO-d_6).

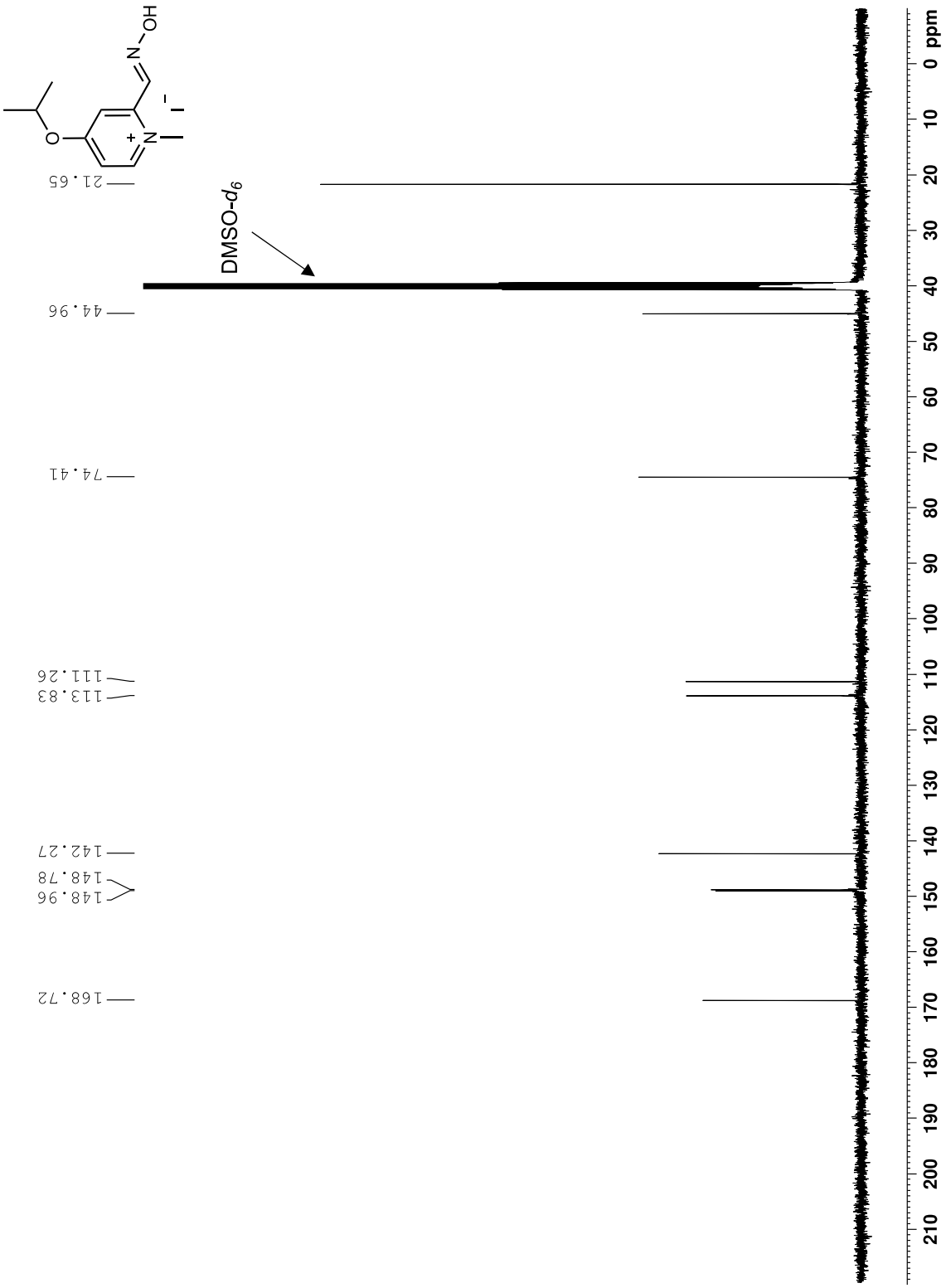

Spectrum 51. ^{13}C NMR of (*E*)-2-((hydroxyimino)methyl)-1-methyl-4-isopropoxypyridin-1-ium iodide (**ADG2054)** (100 MHz, 293 K, DMSO-d_6).

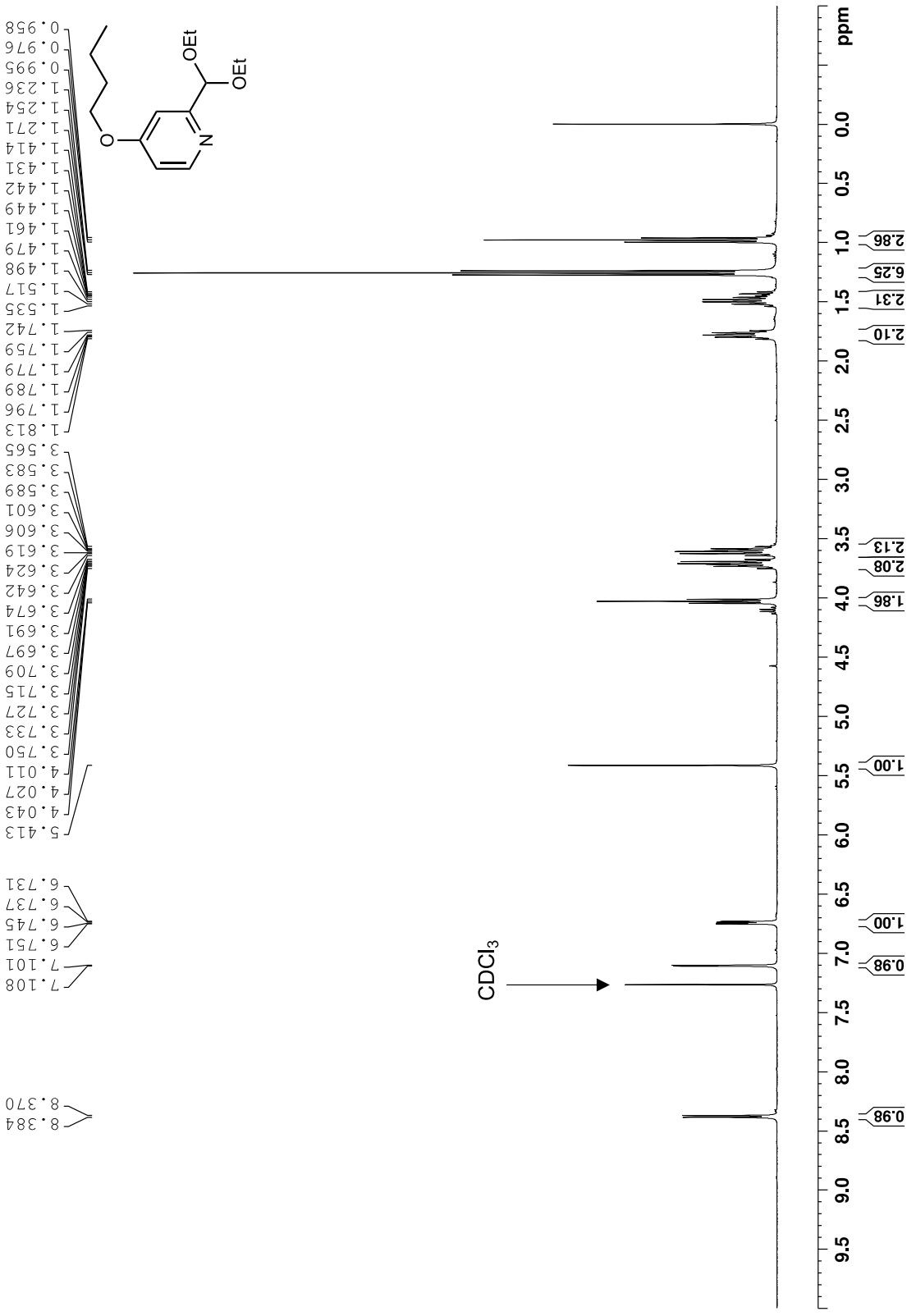

Spectrum 52. ^{1}H NMR of 2-(diethoxymethyl)-4-butoxypyridine (400 MHz, 293 K, $CDCl_3$).

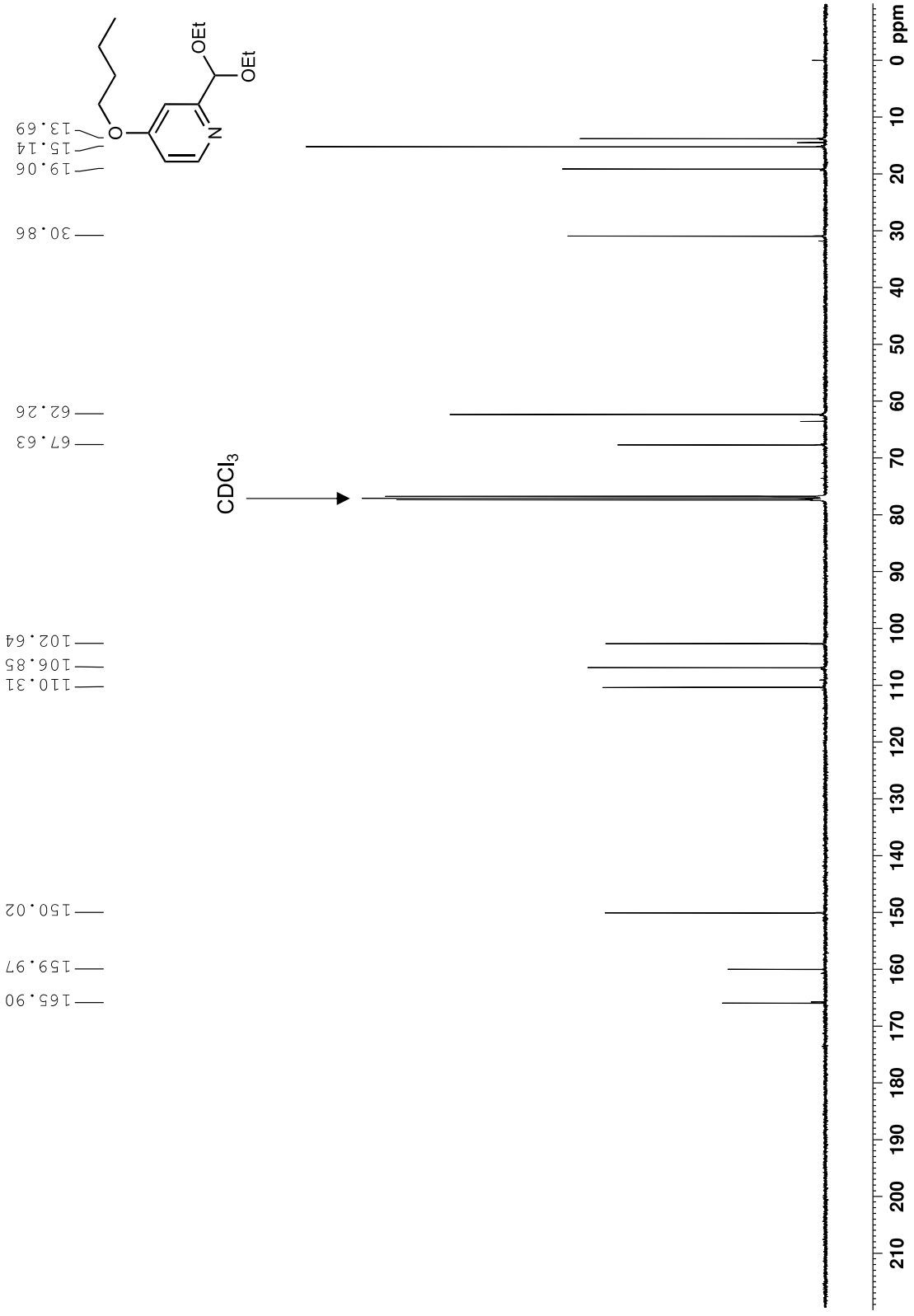

Spectrum 53. ^{13}C NMR of 2-(diethoxymethyl)-4-butoxypyridine (100 MHz, 293 K, $CDCl_3$).

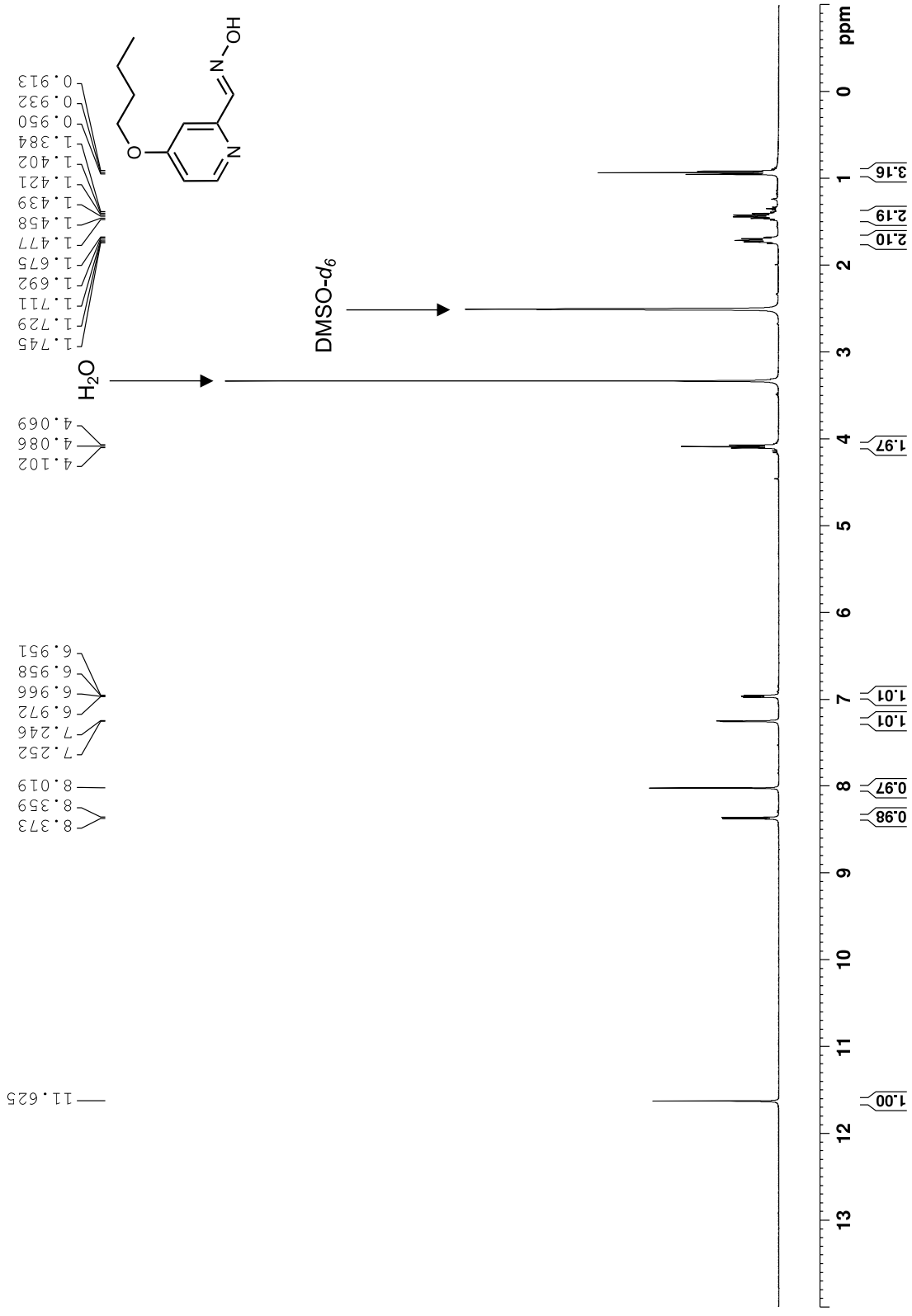

Spectrum 54. [1]H NMR of (*E*)-4-butoxypicolinaldehyde oxime (400 MHz, 293 K, DMSO-d_6).

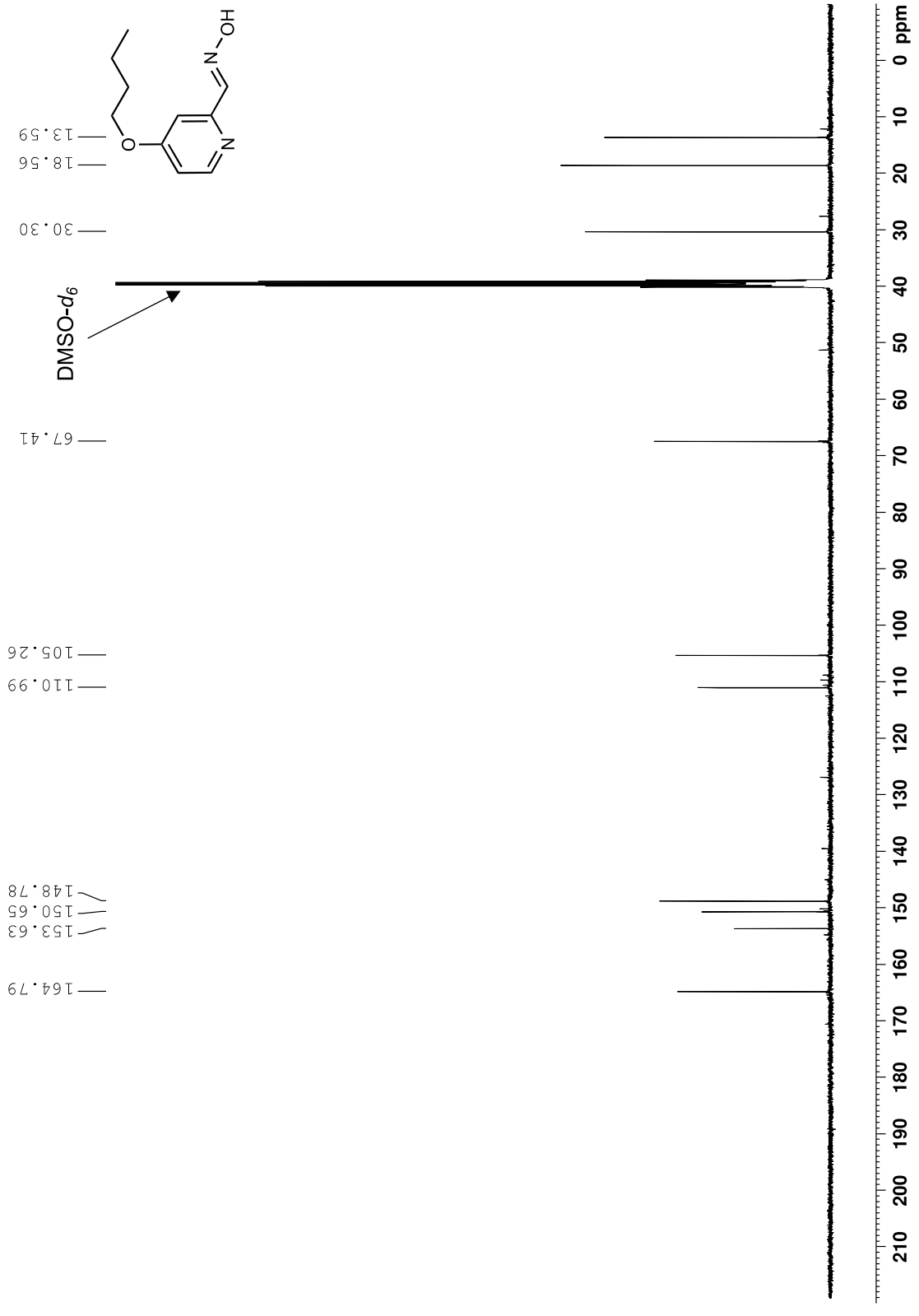

Spectrum 55. ^{13}C NMR of (*E*)-4-butoxypicolinaldehyde oxime (100 MHz, 293 K, DMSO-d_6).

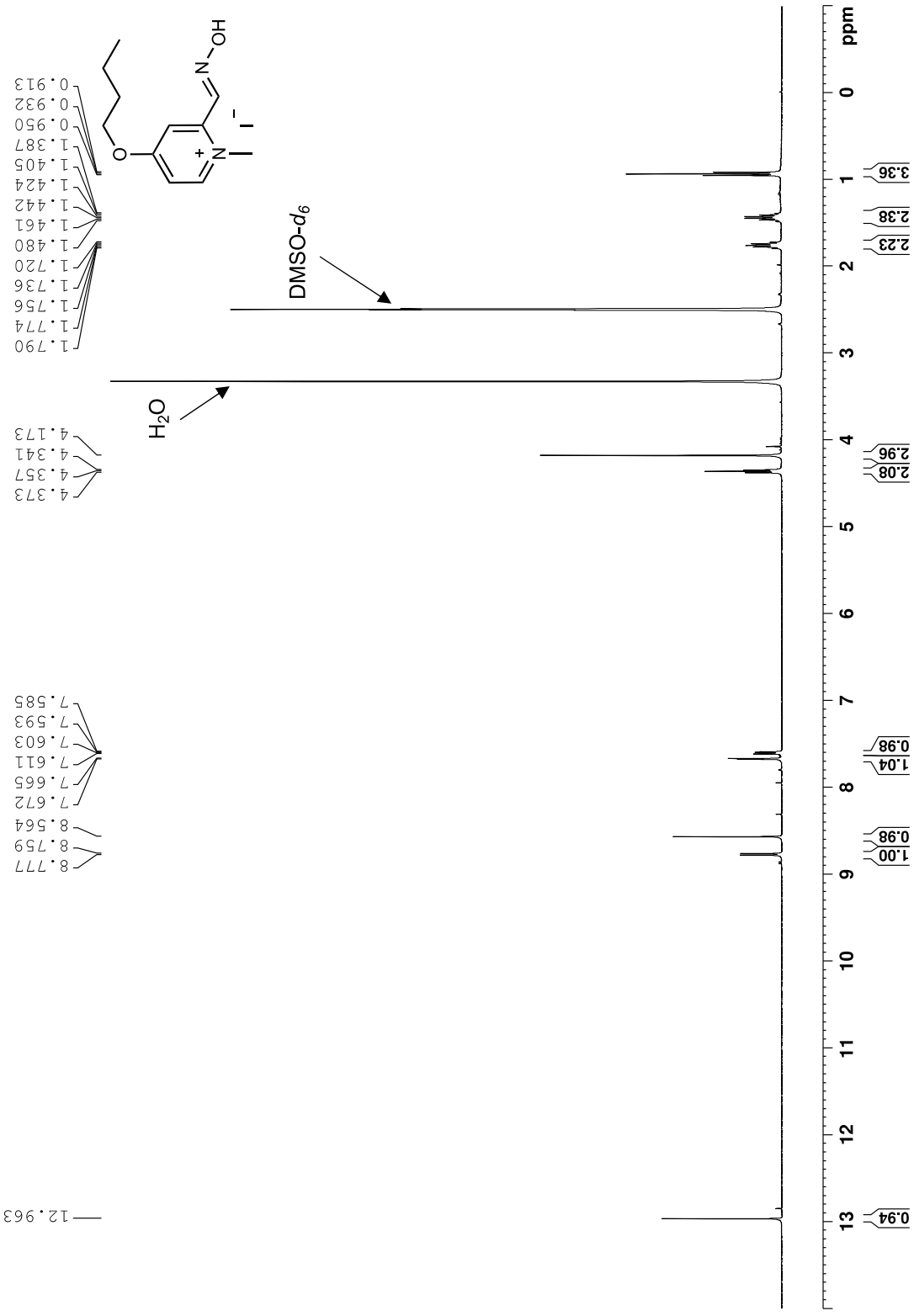

Spectrum 56. ^{1}H NMR of (*E*)-2-((hydroxyimino)methyl)-1-methyl-4-butoxypyridin-1-ium iodide (**ADG2058)** (400 MHz, 293 K, DMSO-d_6).

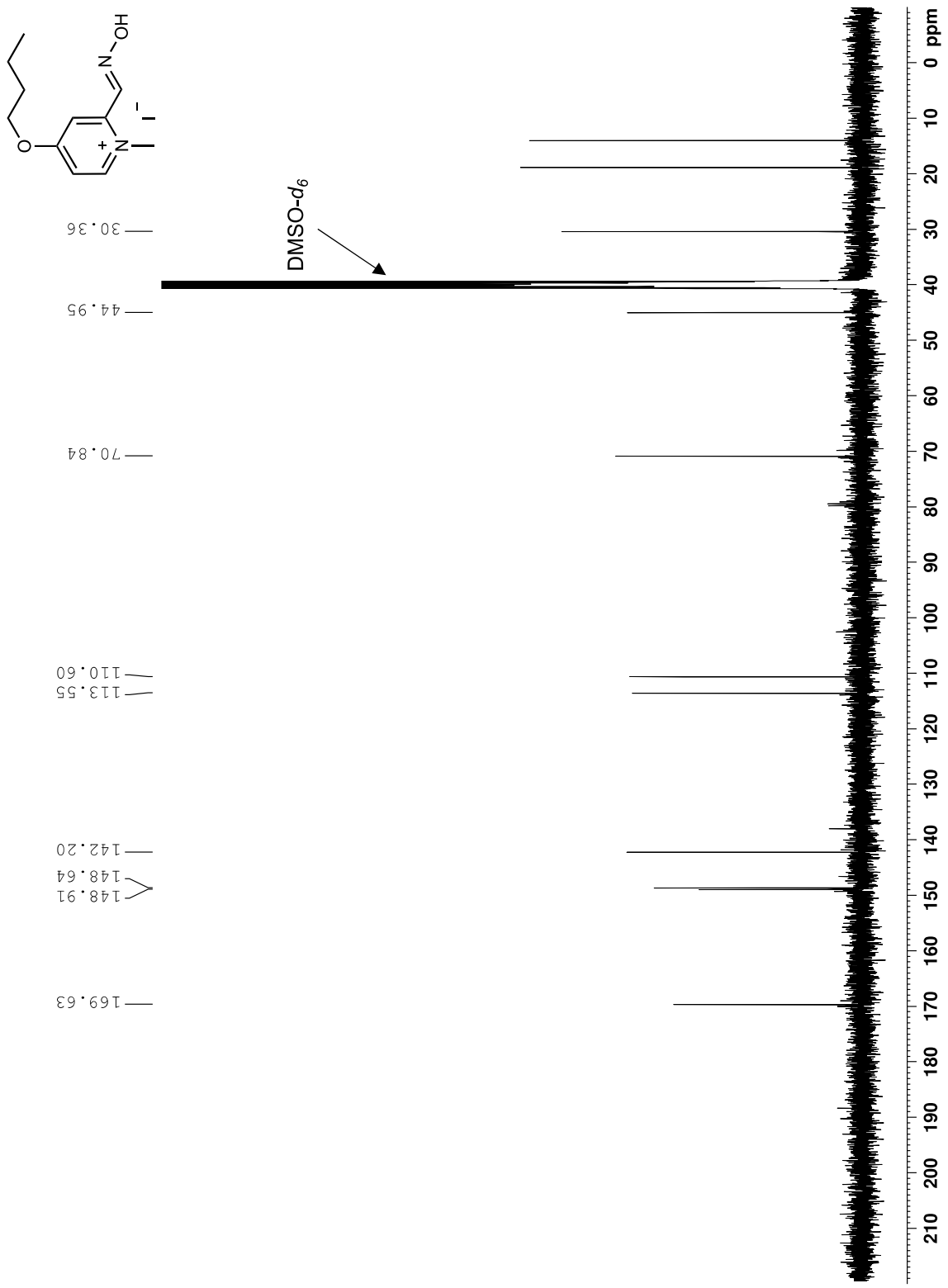

Spectrum 57. ^{13}C NMR of (*E*)-2-((hydroxyimino)methyl)-1-methyl-4-butoxypyridin-1-ium iodide (**ADG2058)** (100 MHz, 293 K, DMSO-d_6).

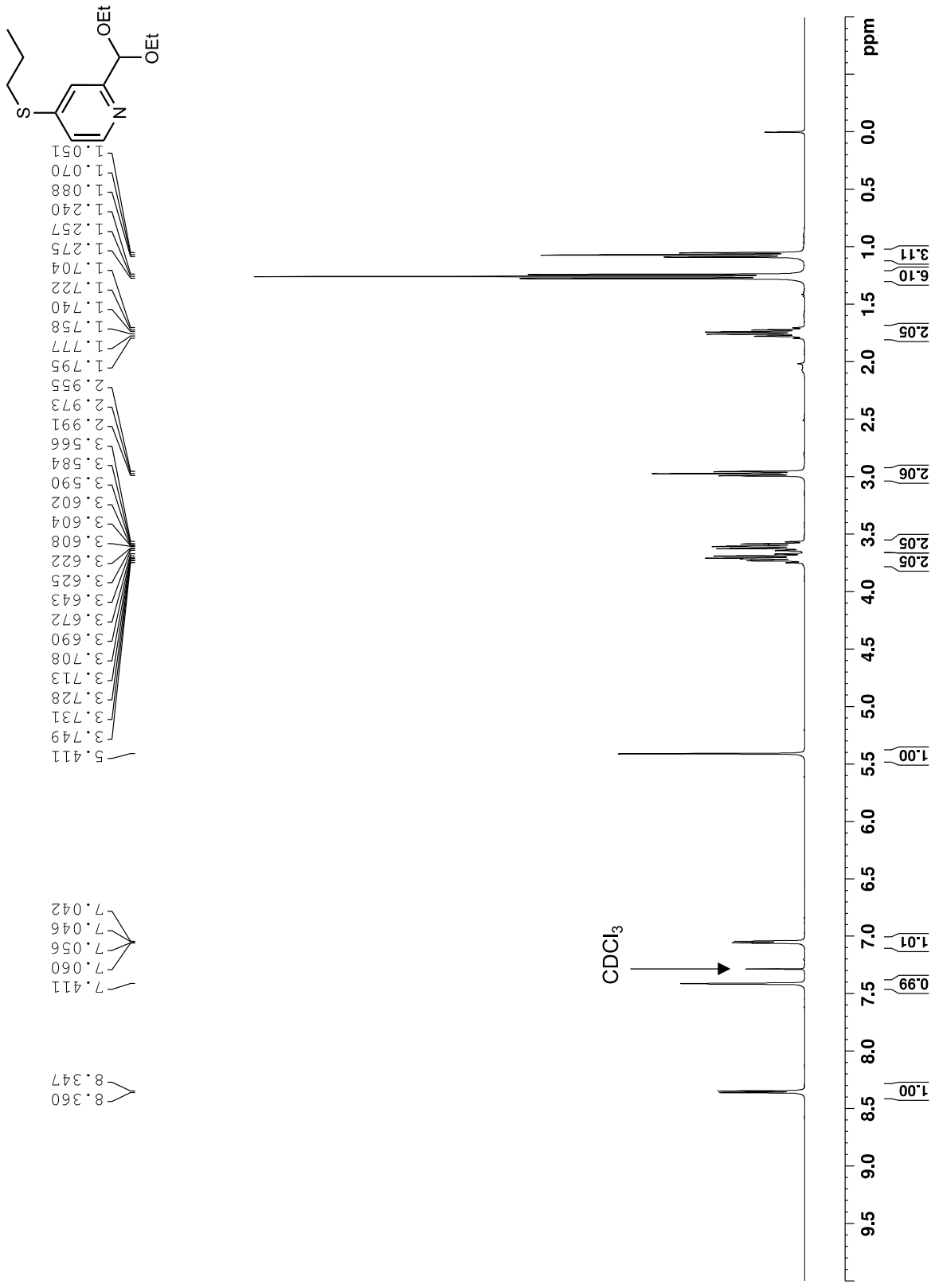

Spectrum 58. ^{1}H NMR of 2-(diethoxymethyl)-4-propylthiopyridine (400 MHz, 293 K, $CDCl_3$).

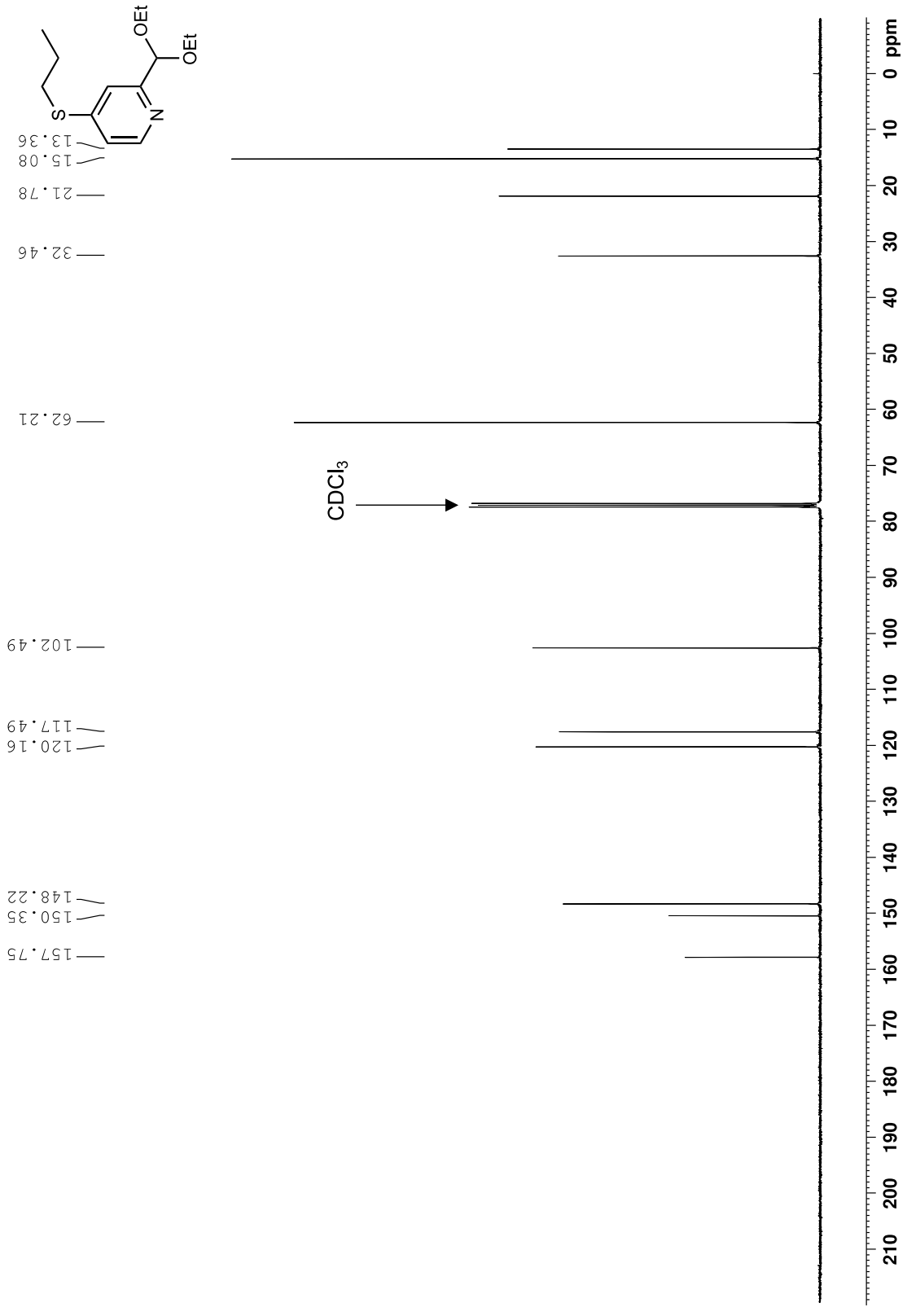

Spectrum 59. ^{13}C NMR of 2-(diethoxymethyl)-4-propylthiopyridine (100 MHz, 293 K, $CDCl_3$).

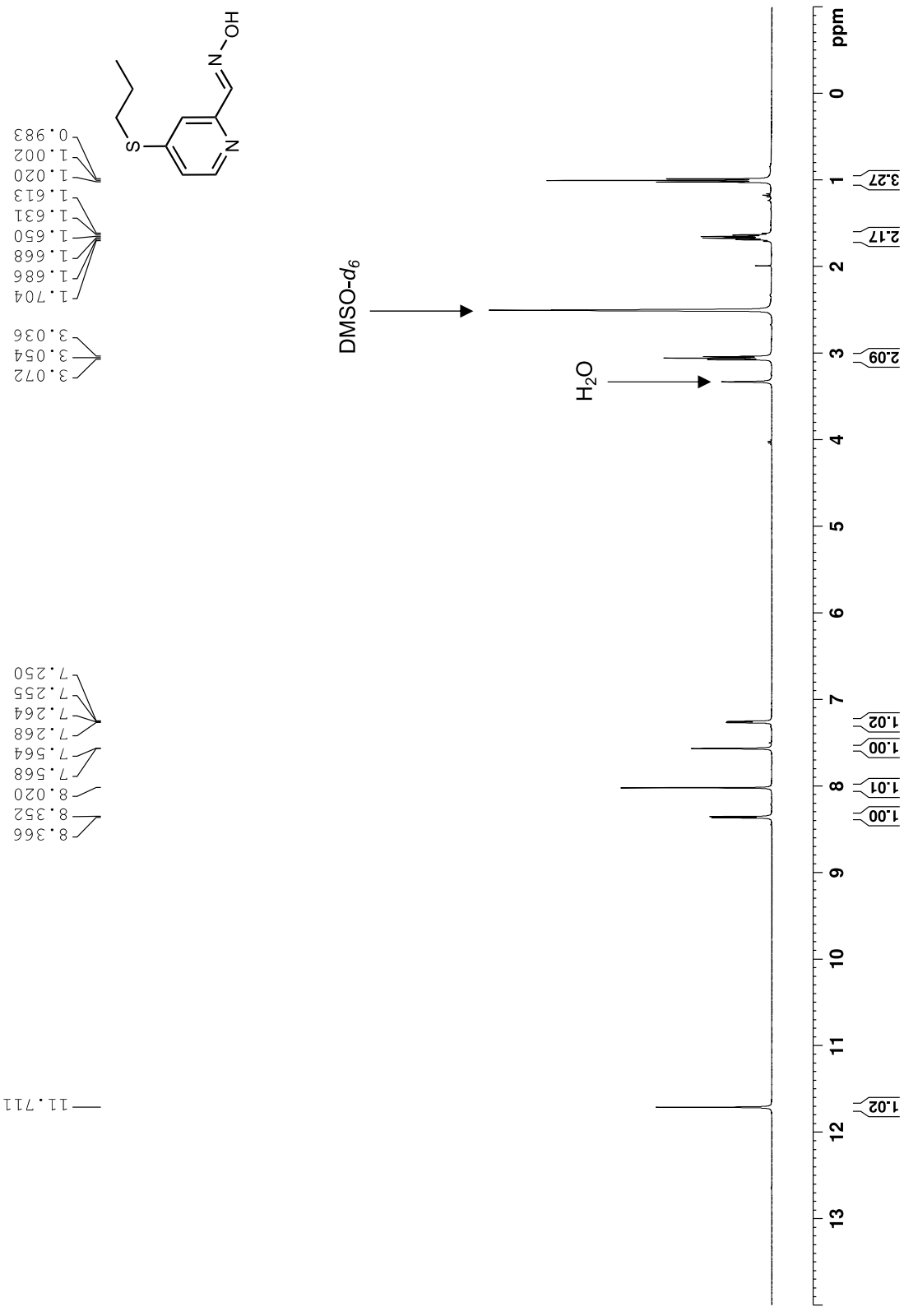

Spectrum 60. ^{1}H NMR of (*E*)-4-(propylthio)picolinaldehyde oxime (400 MHz, 293 K, DMSO-d_6).

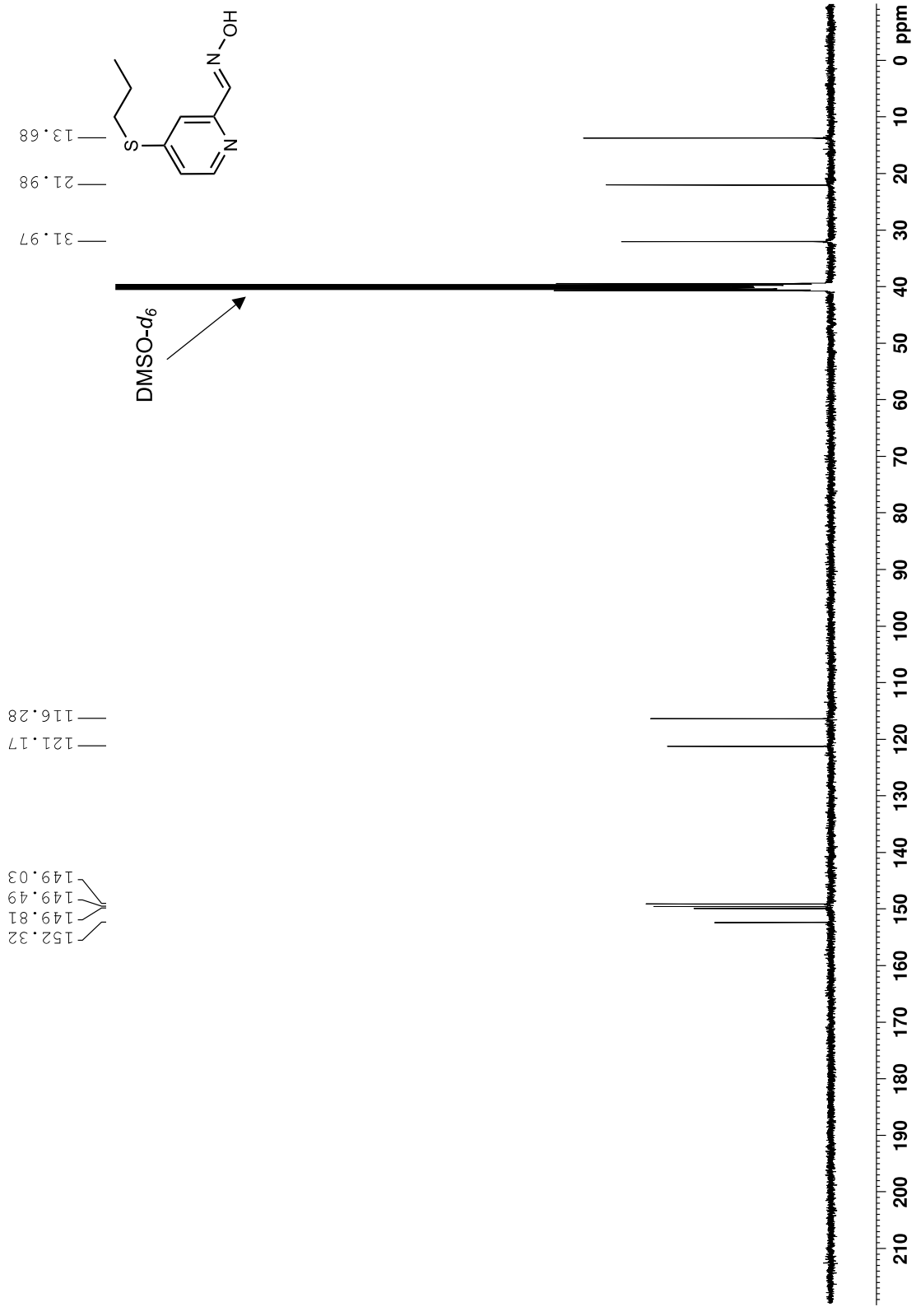

Spectrum 61. ^{13}C NMR of (*E*)-4-(propylthio)picolinaldehyde oxime (100 MHz, 293 K, DMSO-d_6).

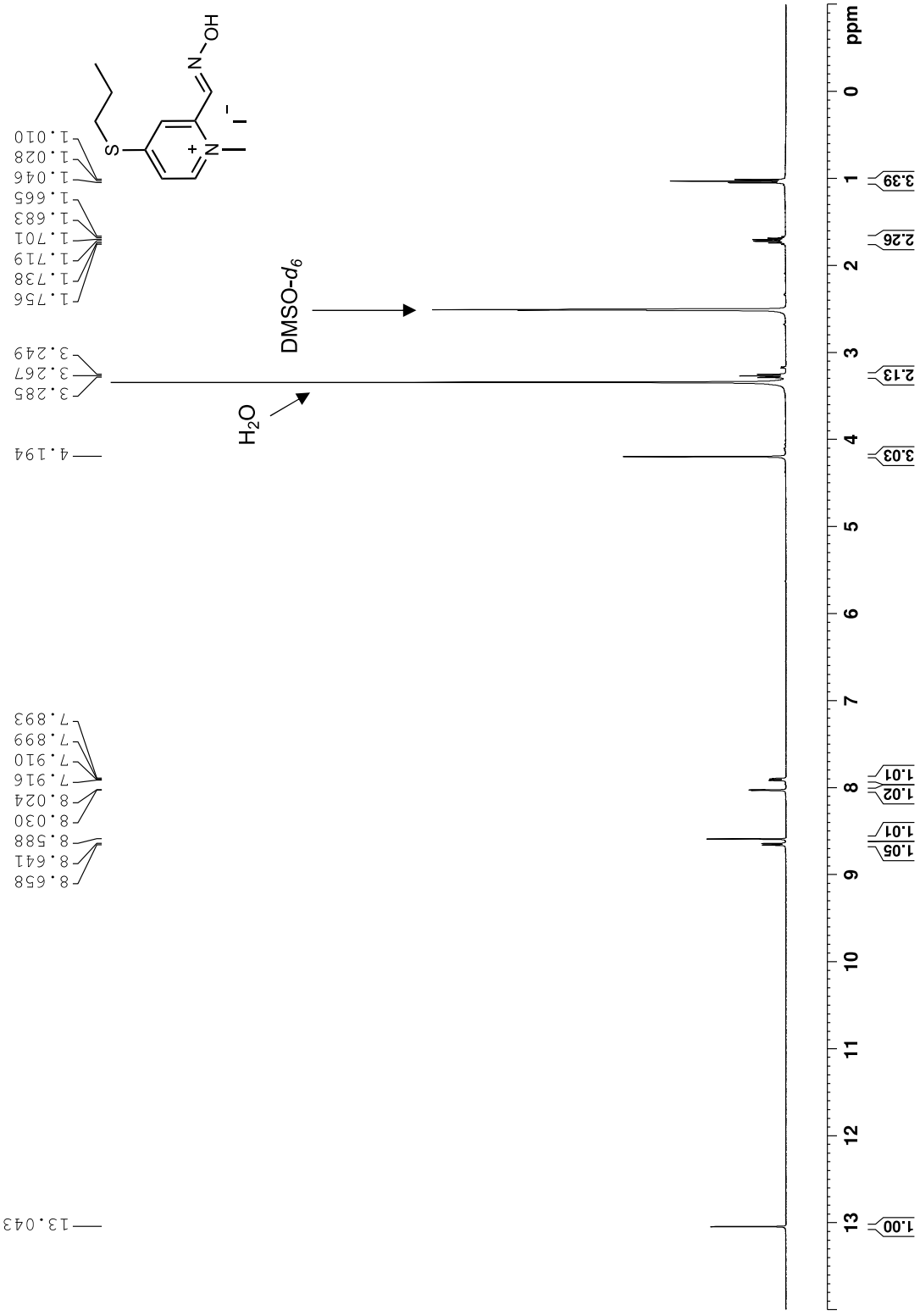

Spectrum 62. ^{1}H NMR of (*E*)-2-((hydroxyimino)methyl)-1-methyl-4-(propylthio)pyridin-1-ium iodide (**ADG2293**) (400 MHz, 293 K, DMSO-d_6).

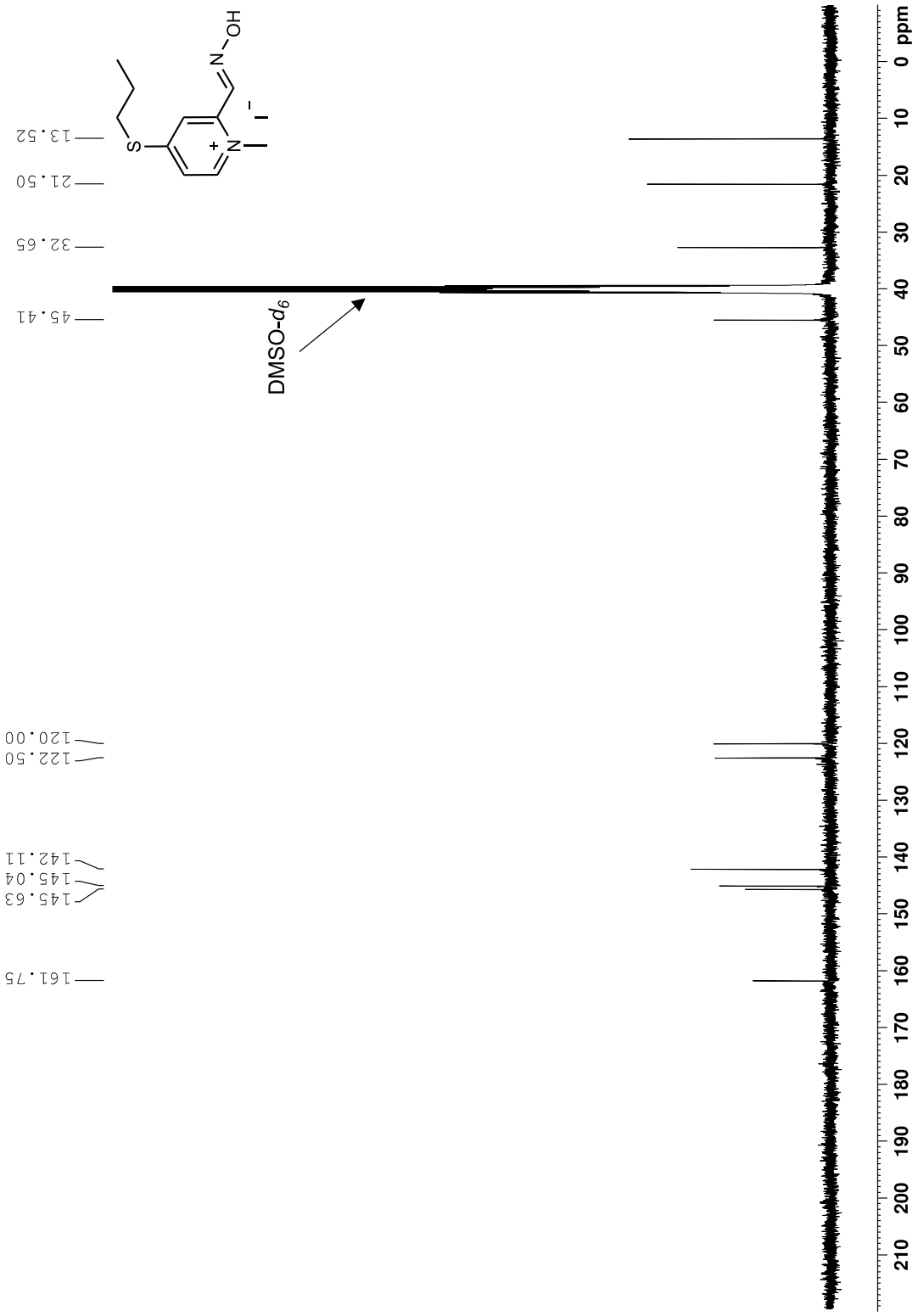

Spectrum 63. ^{13}C NMR of (*E*)-2-((hydroxyimino)methyl)-1-methyl-4-(propylthio)pyridin-1-ium iodide (**ADG2293)**

(100 MHz, 293 K, DMSO-d_6).

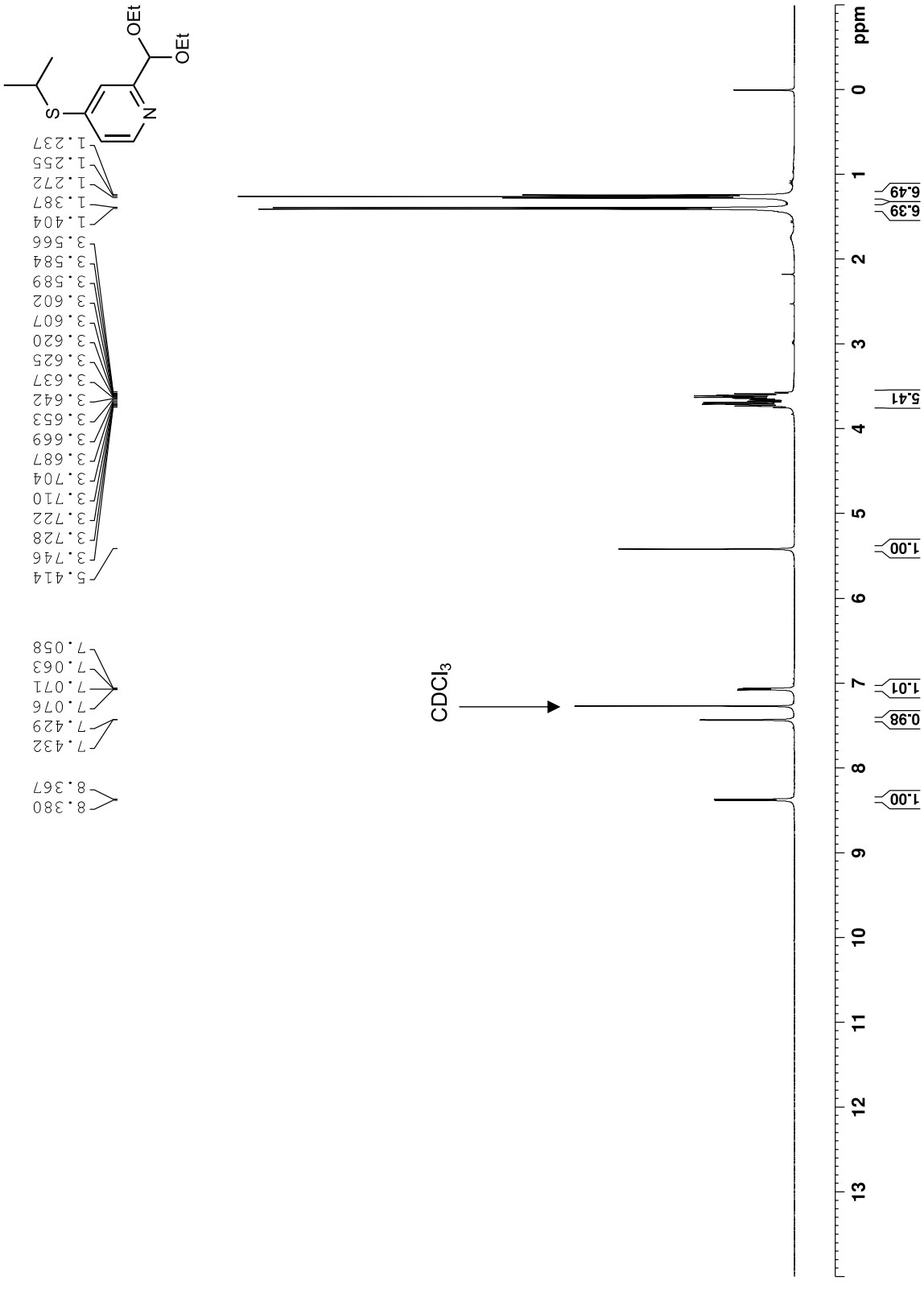

Spectrum 64. ^{1}H NMR of 2-(diethoxymethyl)-4-isopropylthiopyridine (400 MHz, 293 K, $CDCl_3$).

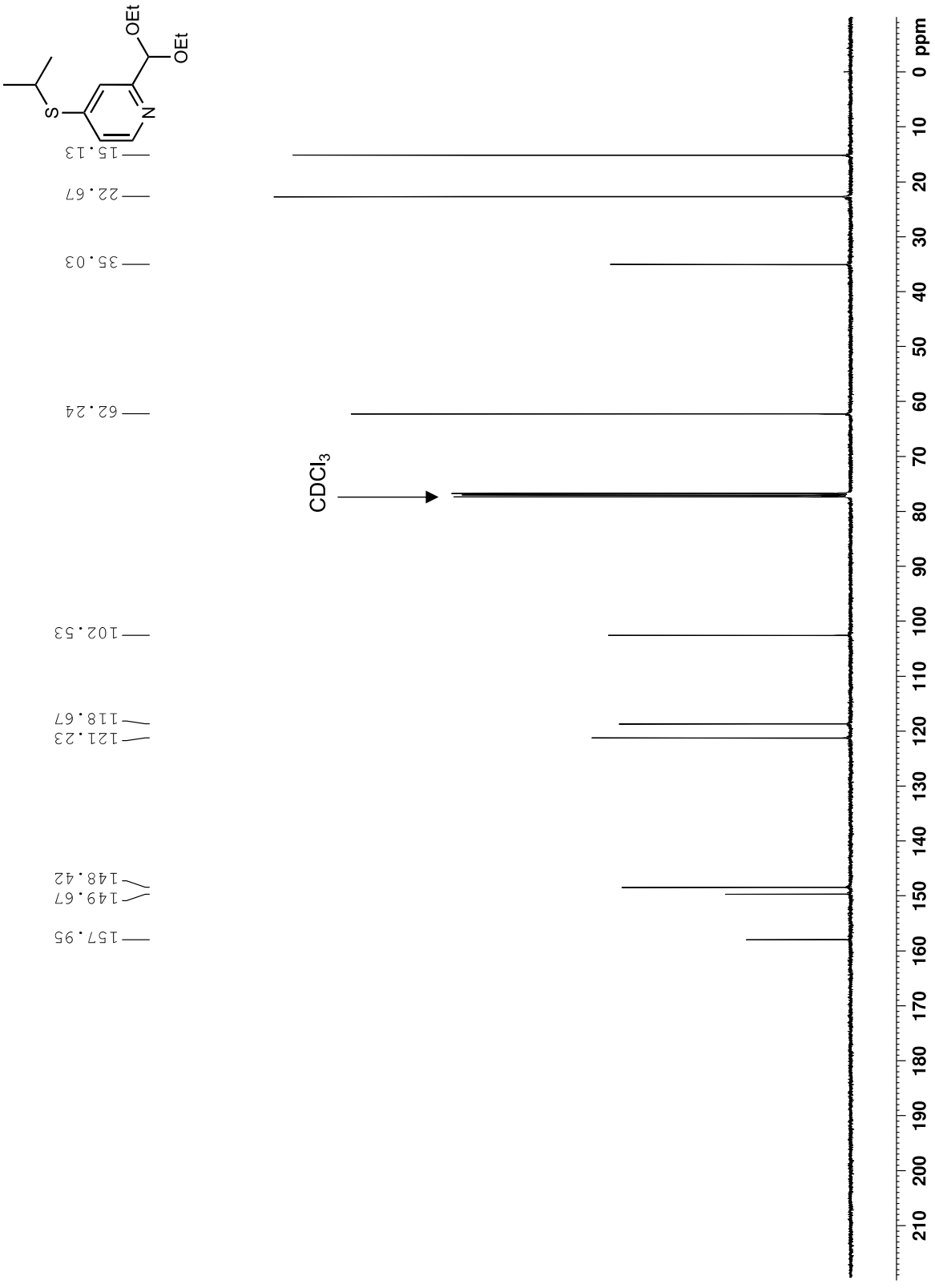

Spectrum 65. ^{13}C NMR of 2-(diethoxymethyl)-4-isopropylthiopyridine (100 MHz, 293 K, $CDCl_3$).

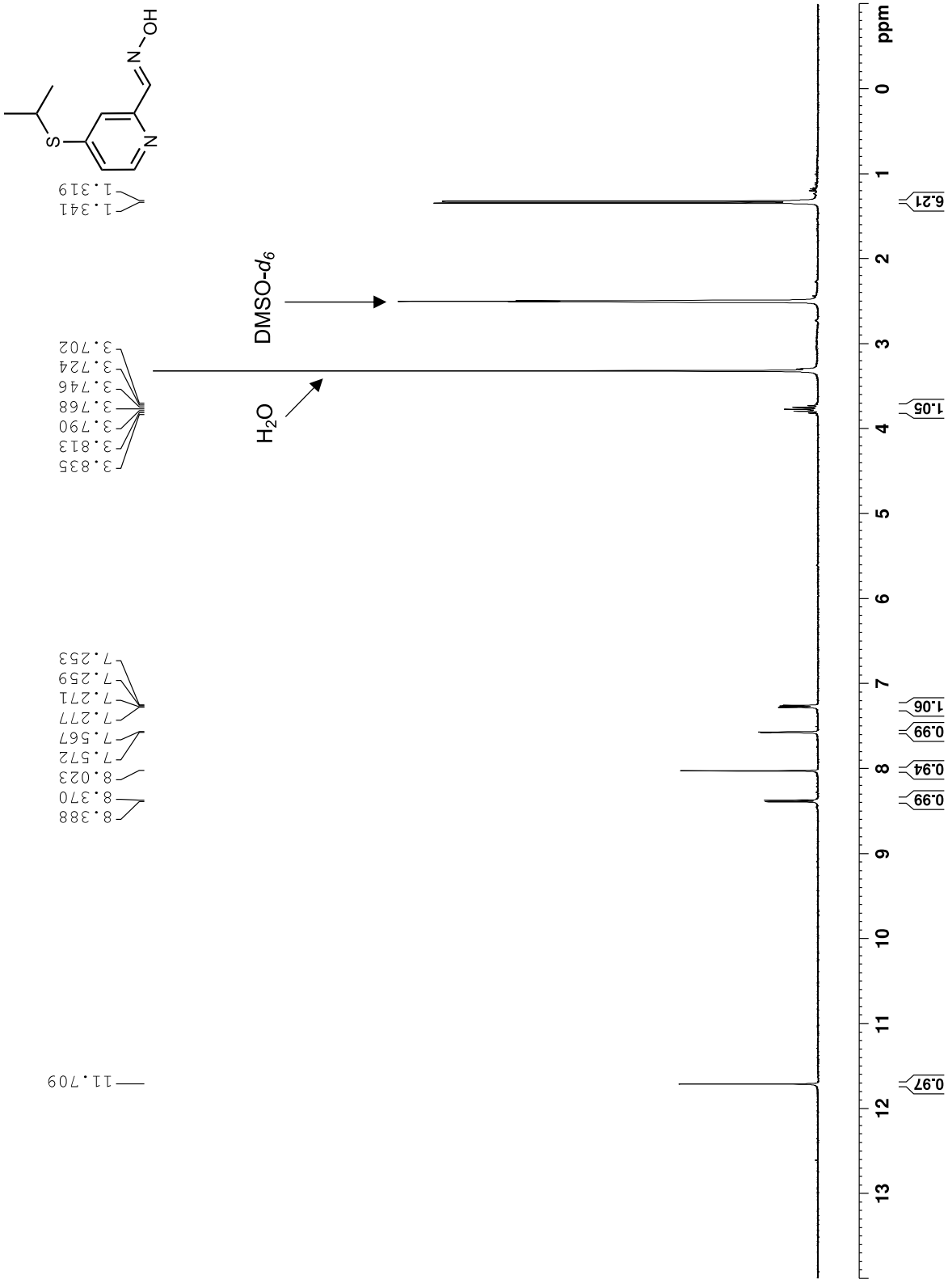

Spectrum 66. ^{1}H NMR of (*E*)-4-isopropylthiopicolinaldehyde oxime (300 MHz, 293 K, DMSO-d_6).

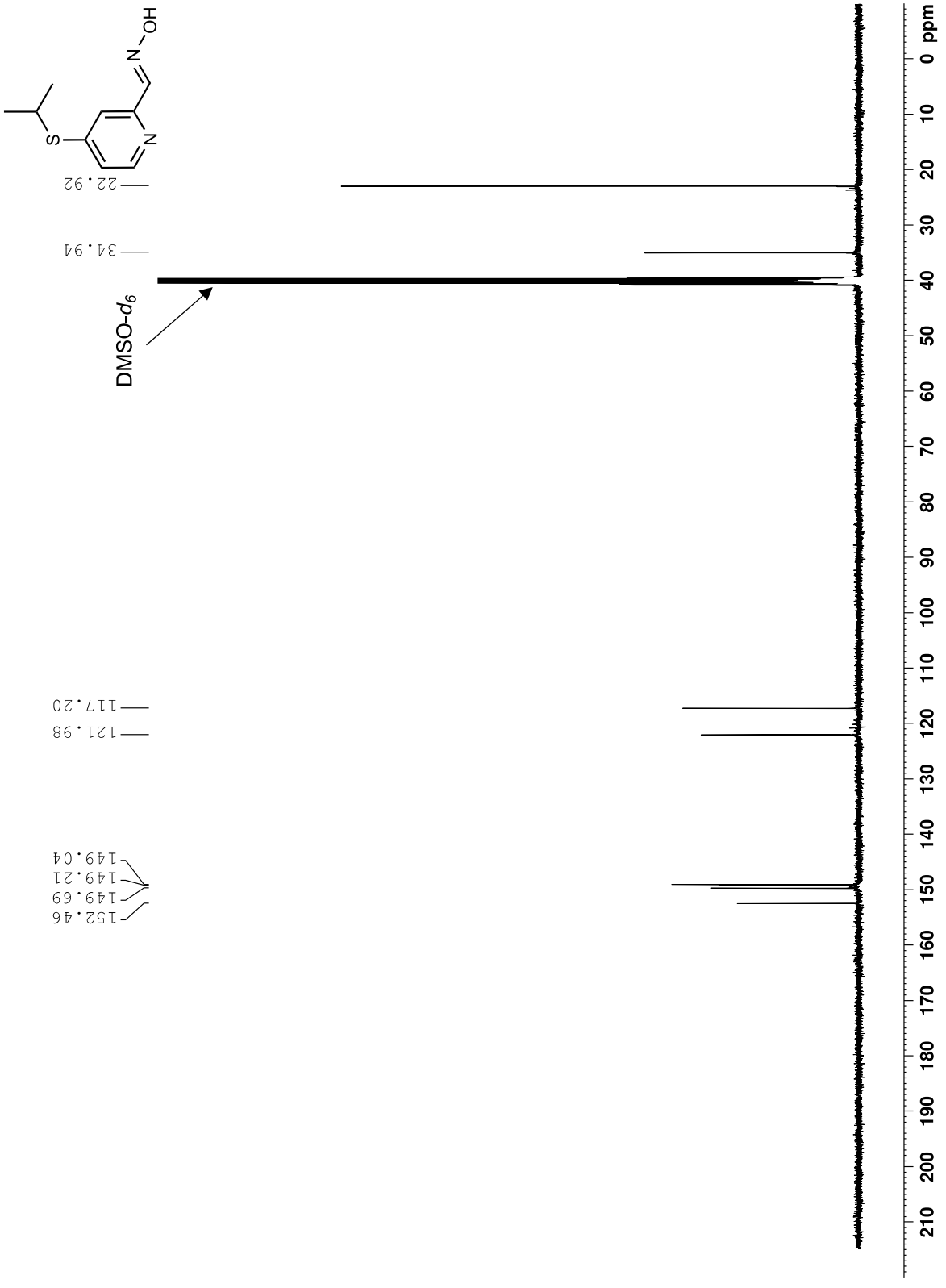

Spectrum 67. ^{13}C NMR of (*E*)-4-isopropylthiopicolinaldehyde oxime (100 MHz, 293 K, DMSO-d_6).

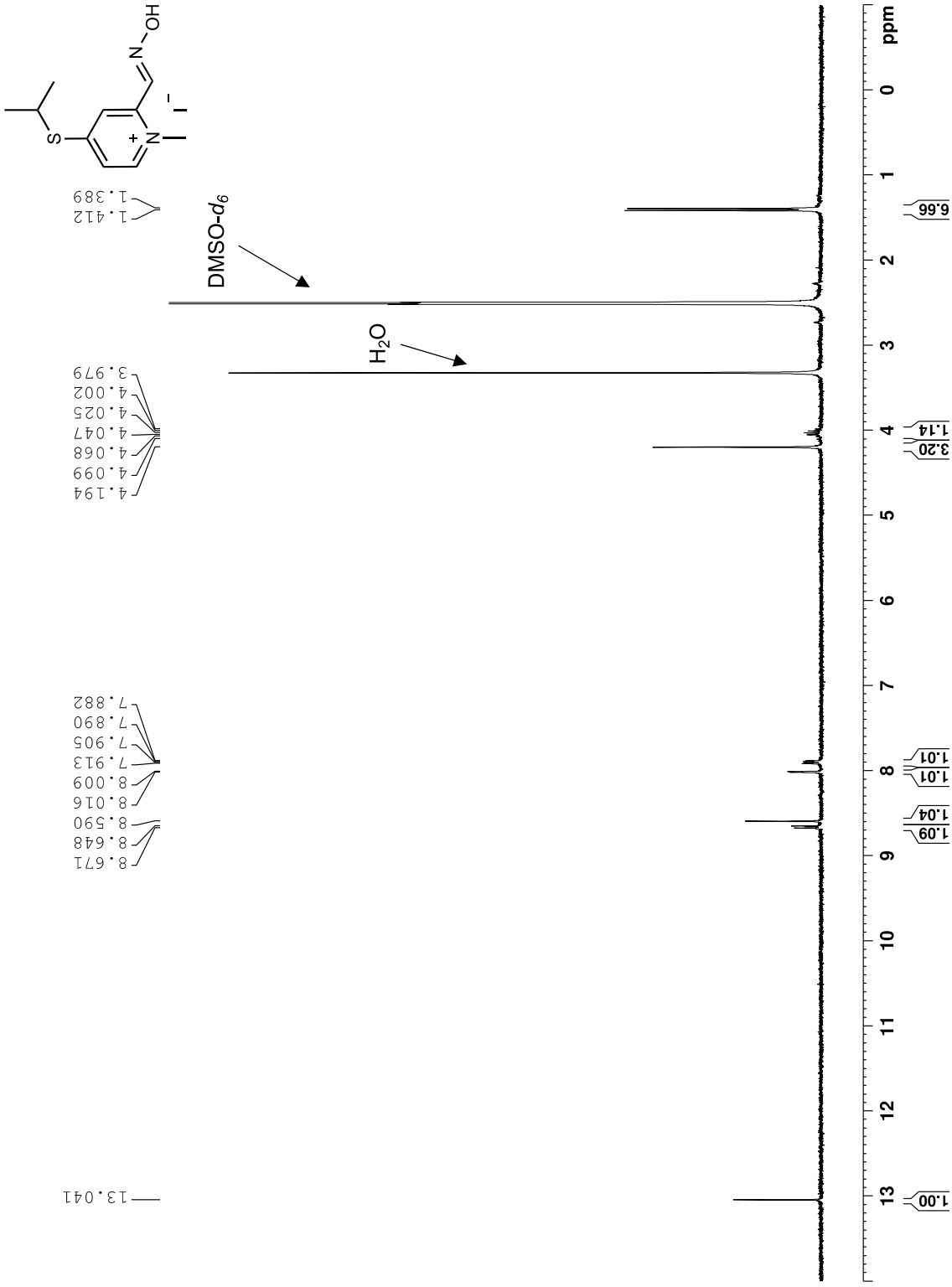

Spectrum 68. ^{1}H NMR of (*E*)-2-((hydroxyimino)methyl)-1-methyl-4-(isopropylthio)pyridin-1-ium iodide (**ADG3060)** (300 MHz, 293 K, DMSO-d_6).

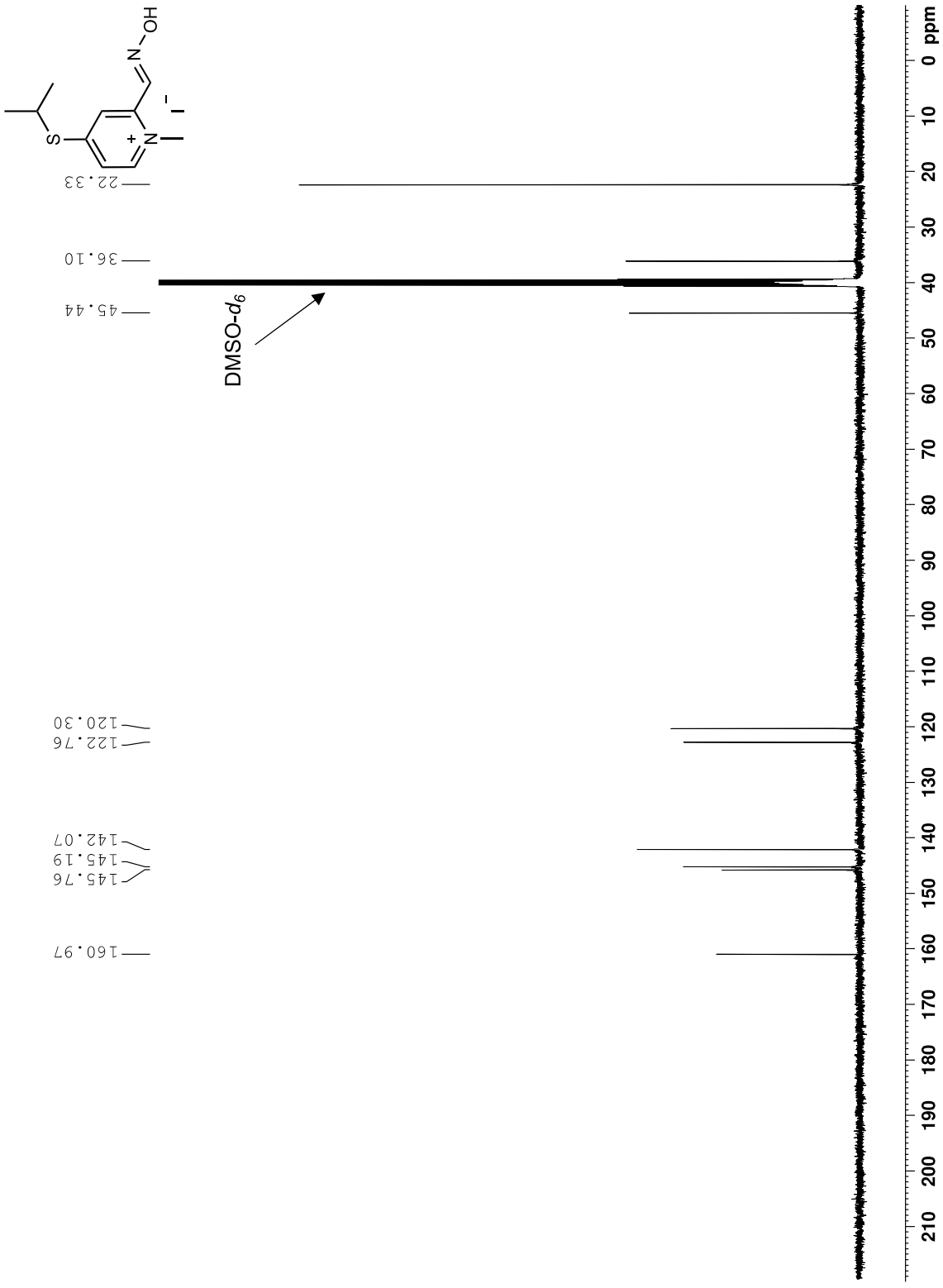

Spectrum 69. ^{13}C NMR of (*E*)-2-((hydroxyimino)methyl)-1-methyl-4-(isopropylthio)pyridin-1-ium iodide (**ADG3060)** (100 MHz, 293 K, DMSO-d_6).

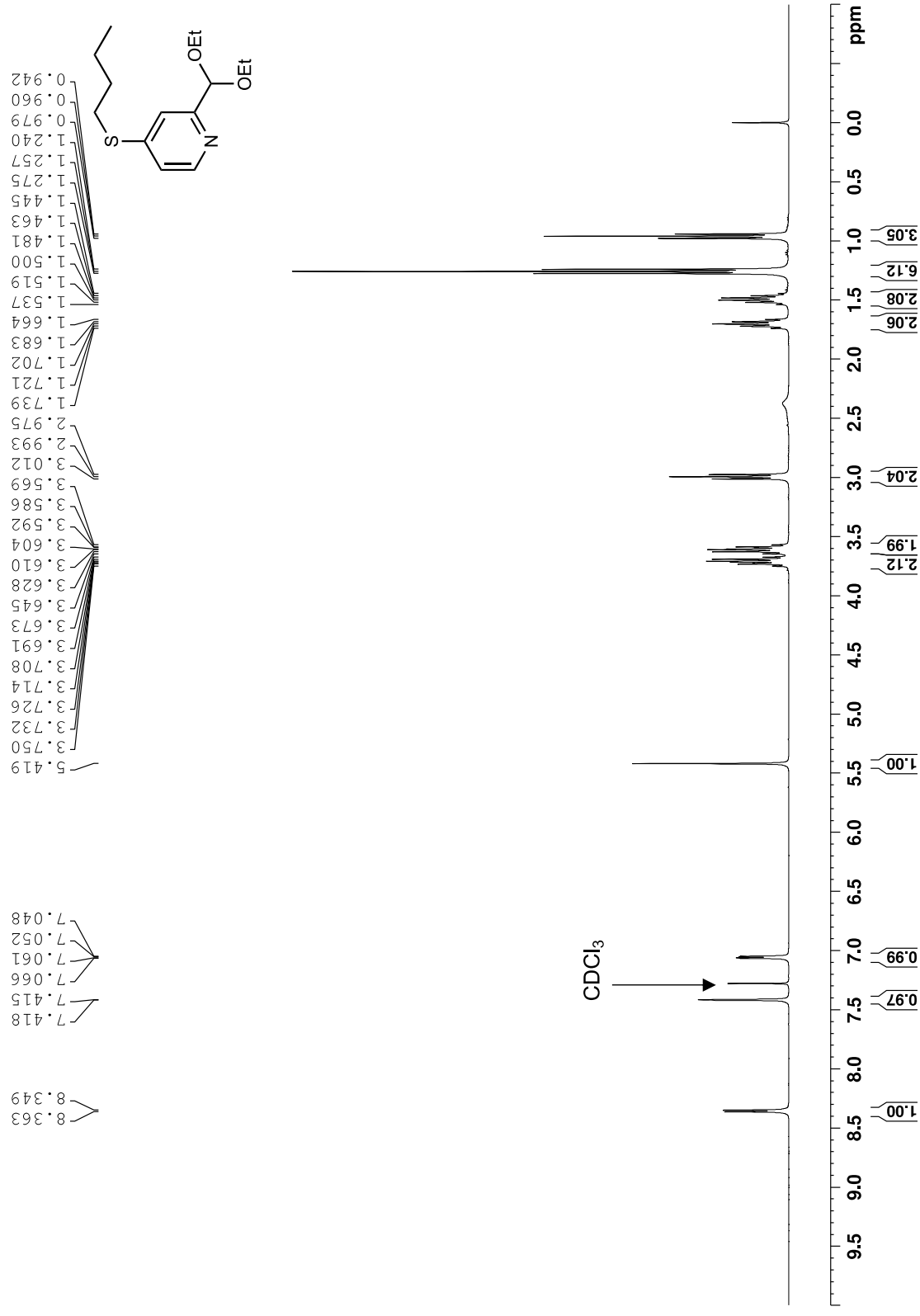

Spectrum 70. ^{1}H NMR of 2-(diethoxymethyl)-4-butylthiopyridine (400 MHz, 293 K, $CDCl_3$).

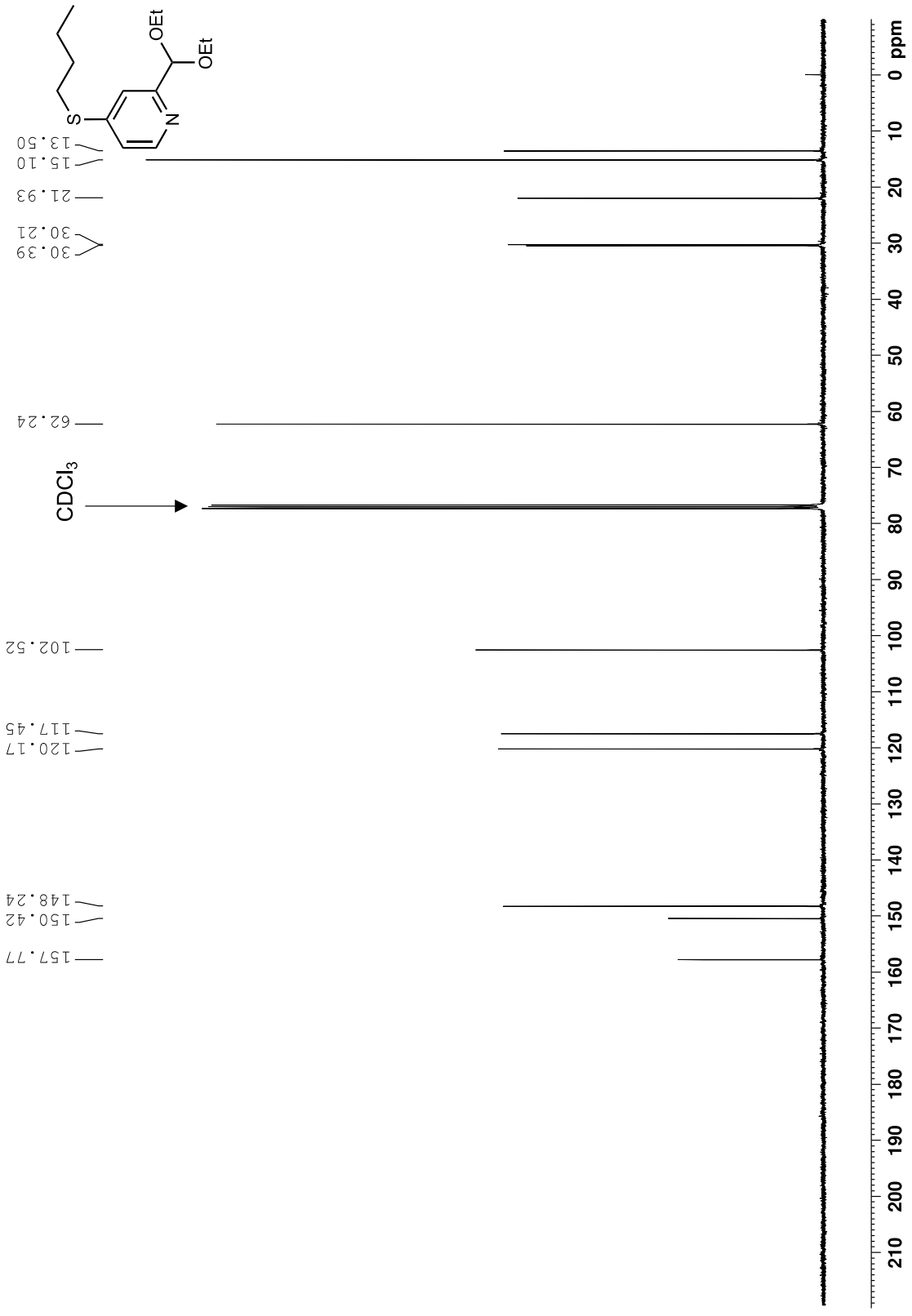

Spectrum 71. ^{13}C NMR of 2-(diethoxymethyl)-4-butylthiopyridine (100 MHz, 293 K, $CDCl_3$).

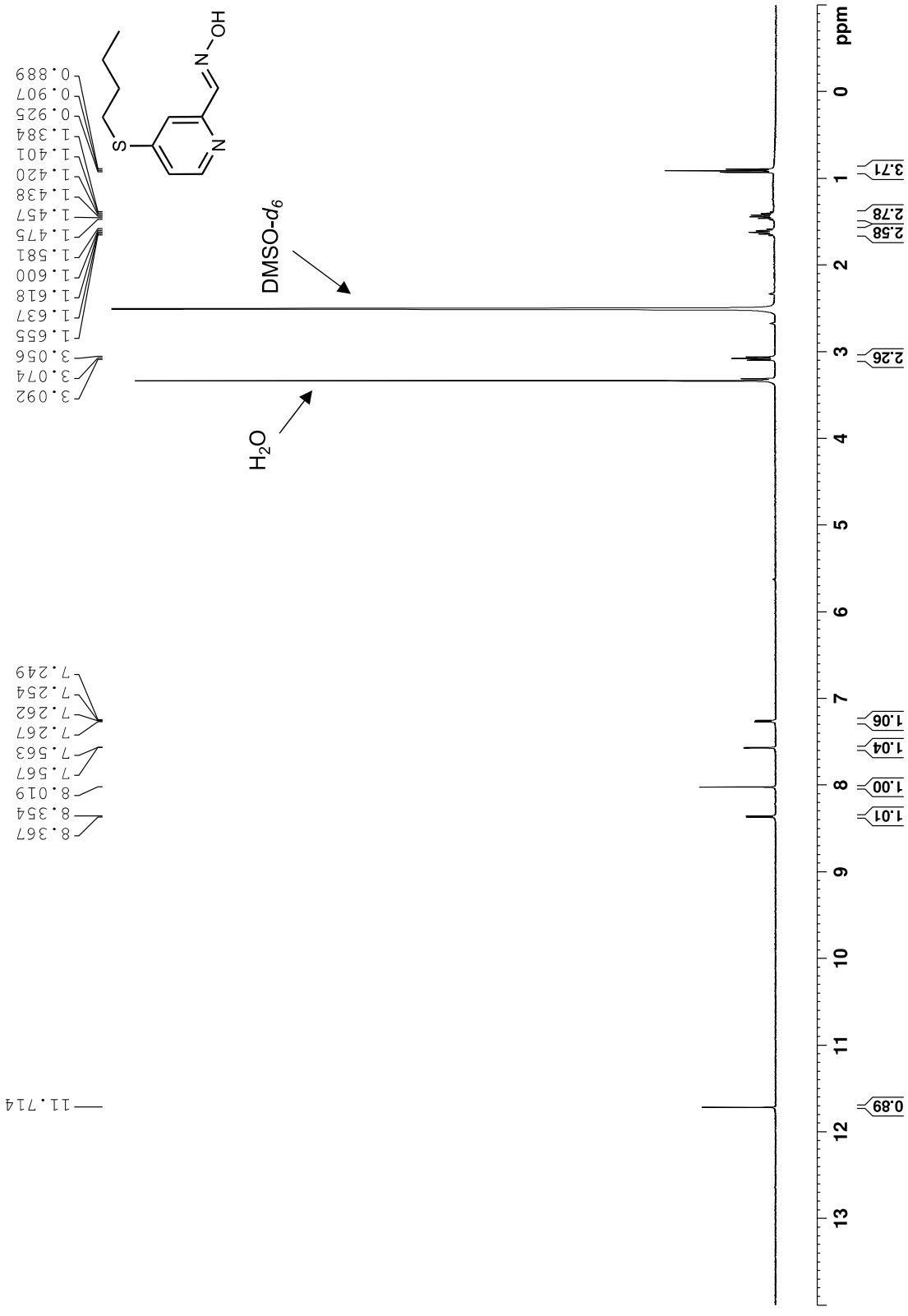

Spectrum 72. ^{1}H NMR of (*E*)-4-butylthiopicolinaldehyde oxime (400 MHz, 293 K, DMSO-d_6).

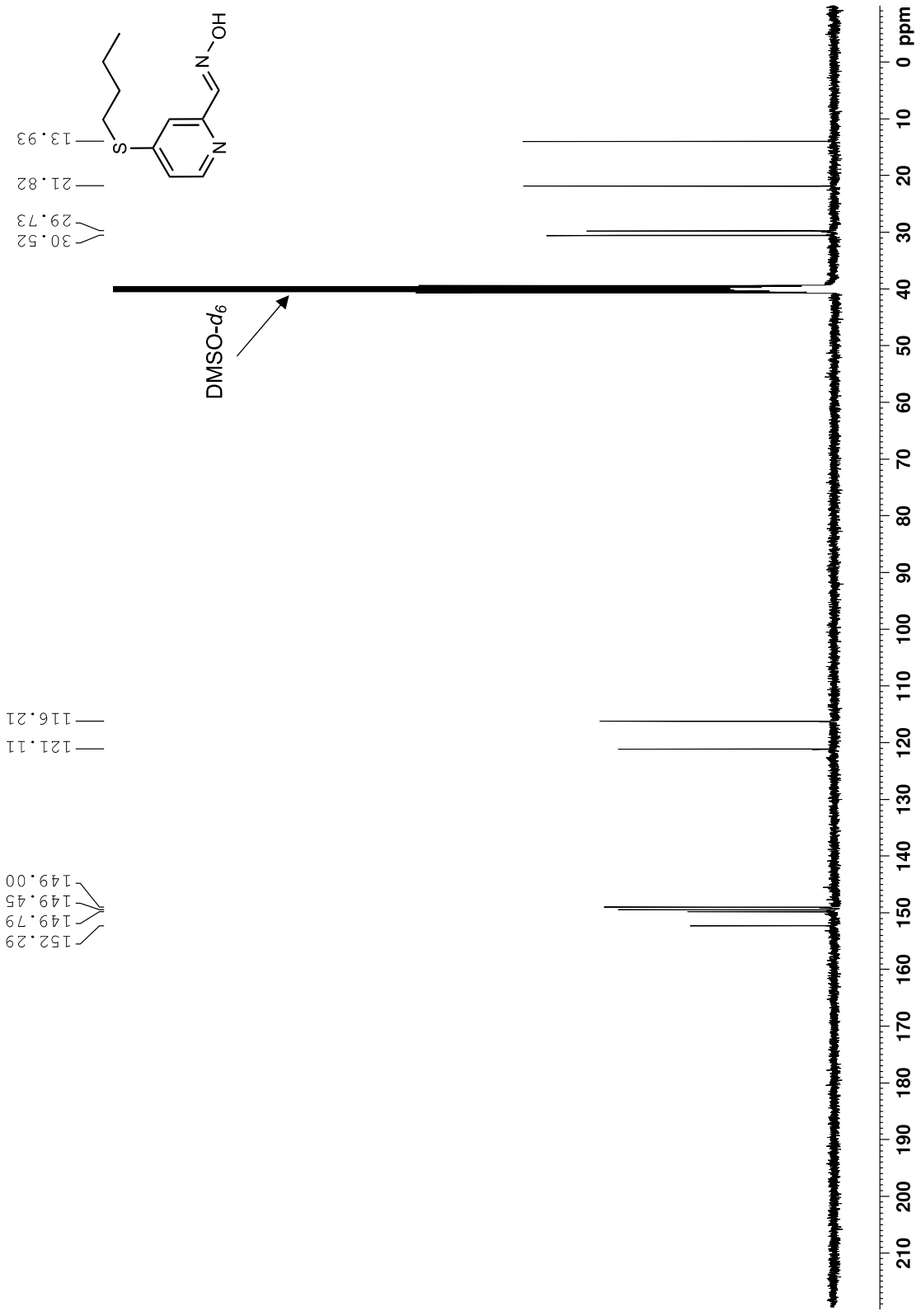

Spectrum 73. ^{13}C NMR of (*E*)-4-butylthiopicolinaldehyde oxime (100 MHz, 293 K, DMSO-d_6).

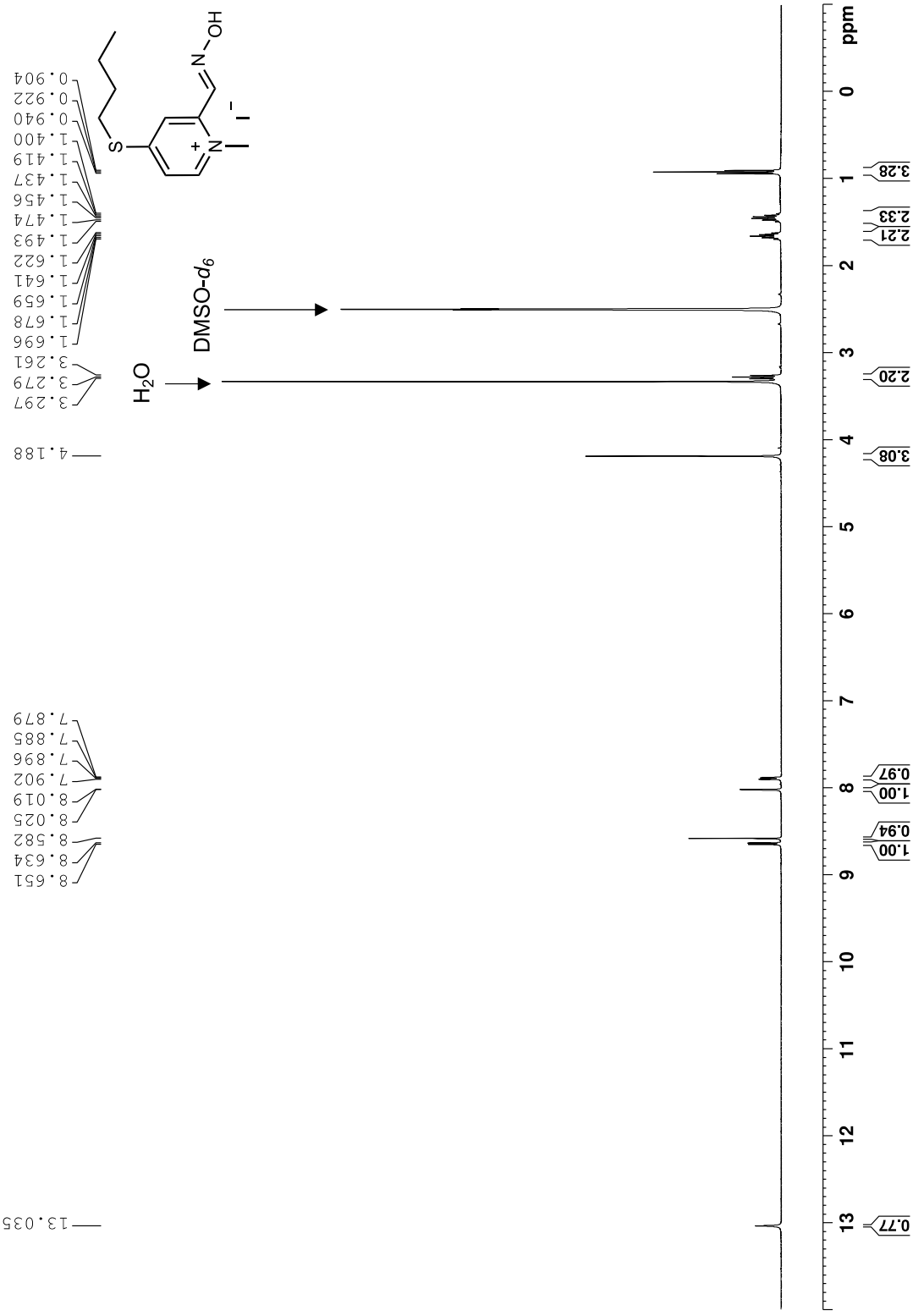

Spectrum 74. ^{1}H NMR of (*E*)-2-((hydroxyimino)methyl)-1-methyl-4-(butylthio)pyridin-1-ium iodide (**ADG2294)** (400 MHz, 293 K, DMSO-d_6).

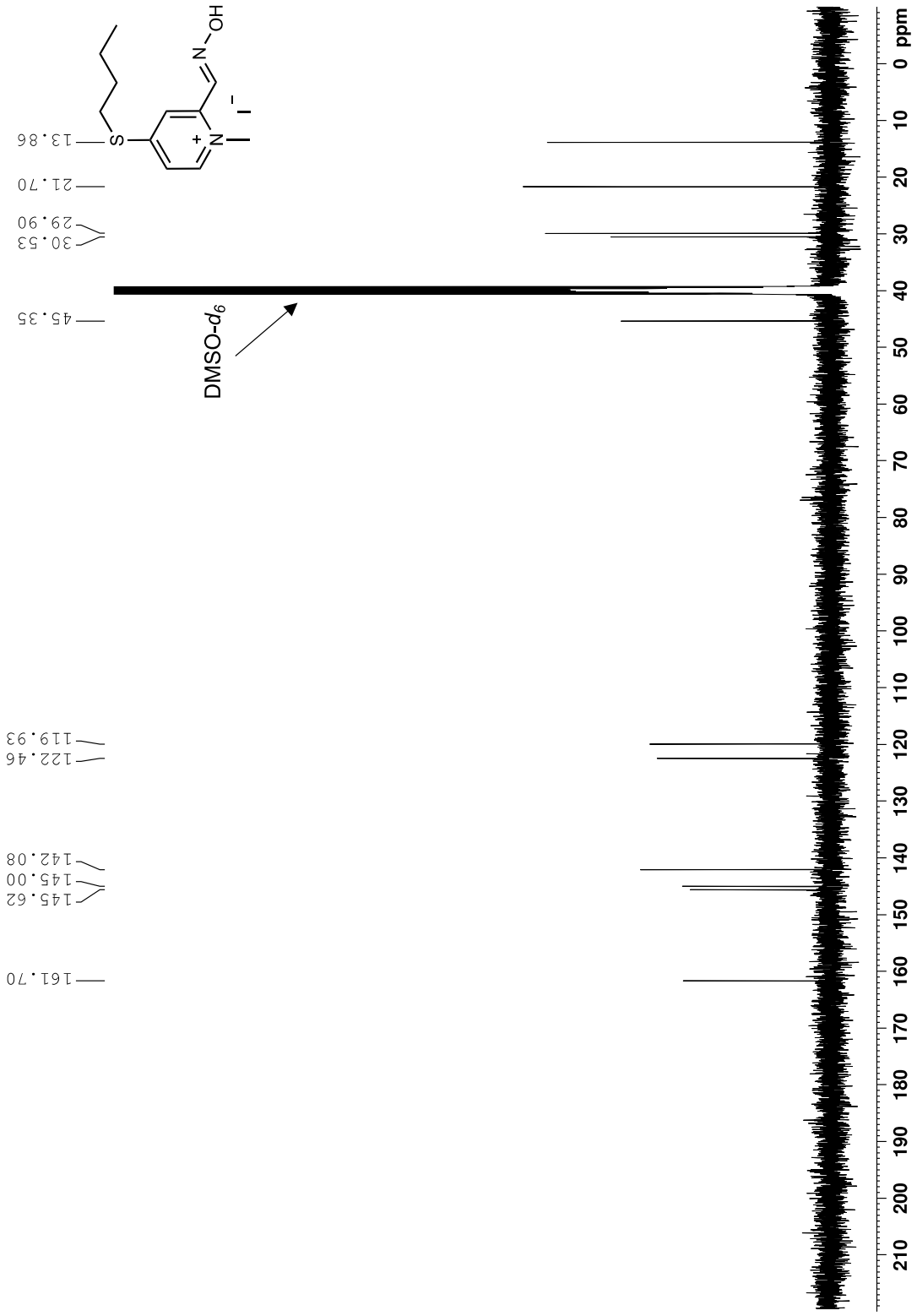

Spectrum 75. ^{13}C NMR of (*E*)-2-((hydroxyimino)methyl)-1-methyl-4-(butylthio)pyridin-1-ium iodide (**ADG2294)** (100 MHz, 293 K, DMSO-d_6).

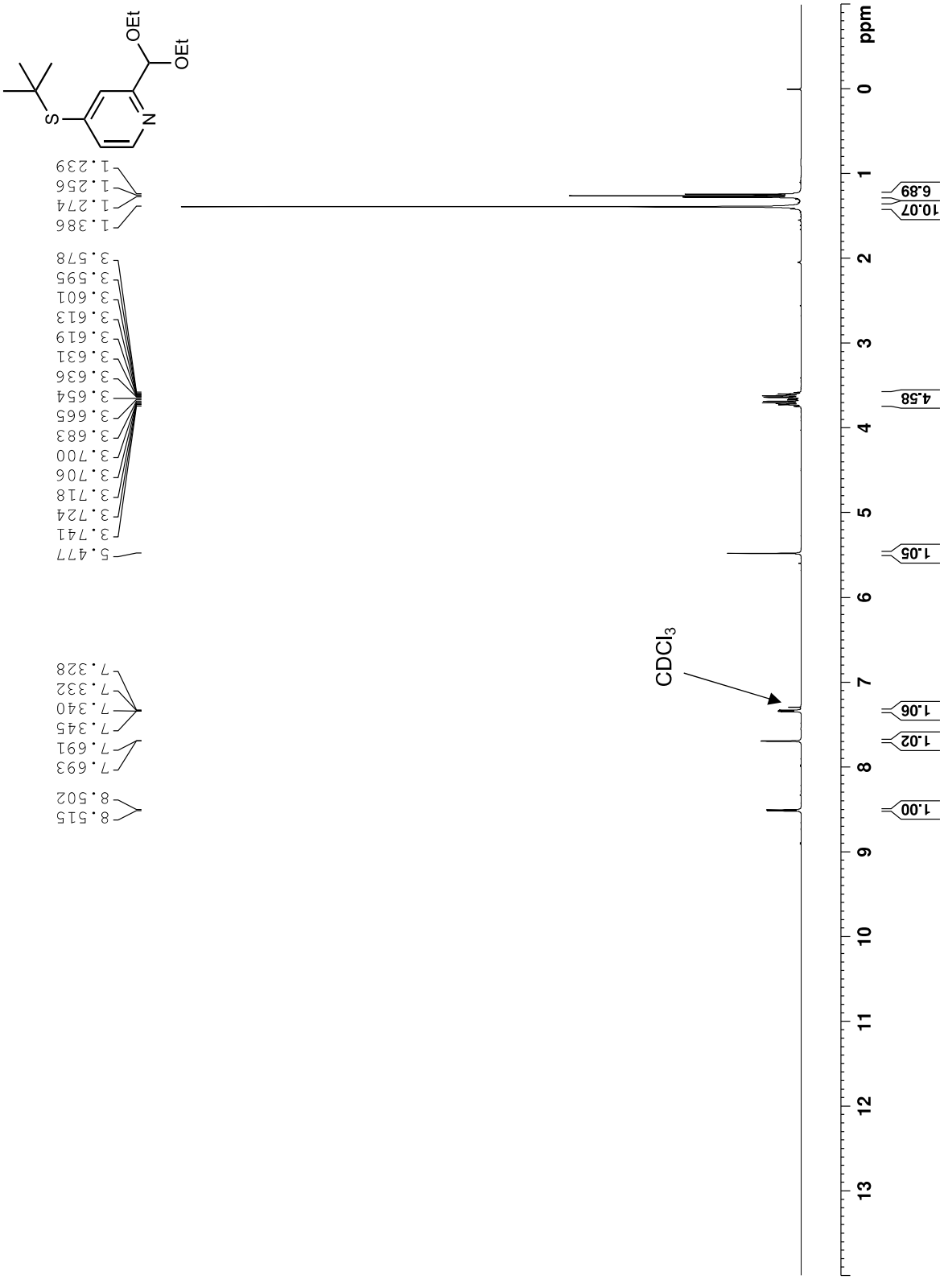

Spectrum 76. ^{1}H NMR of 2-(diethoxymethyl)-4-*tert*-butylthiopyridine (400 MHz, 293 K, $CDCl_3$).

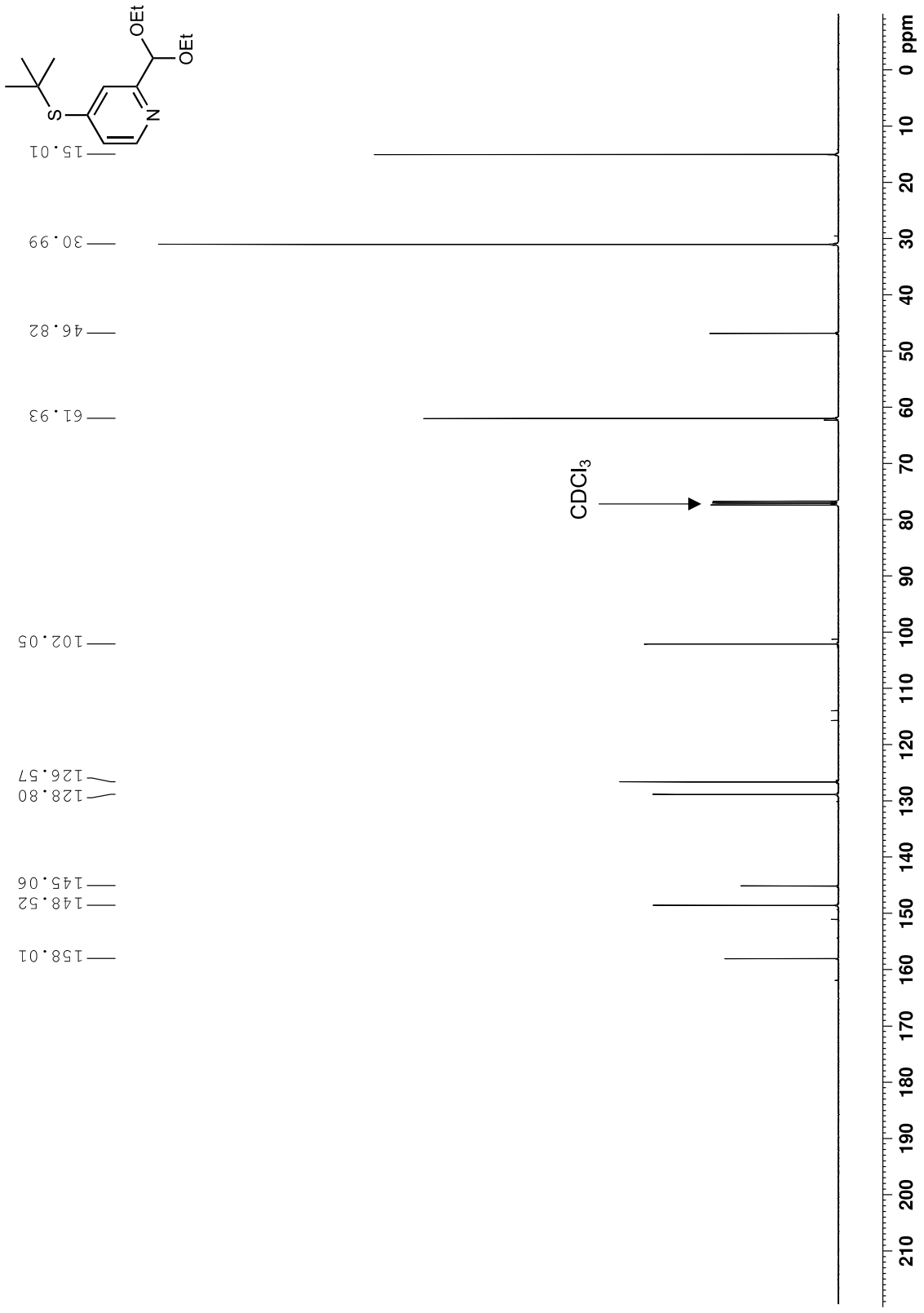

Spectrum 77. ^{13}C NMR of 2-(diethoxymethyl)-4-*tert*-butylthiopyridine (100 MHz, 293 K, $CDCl_3$).

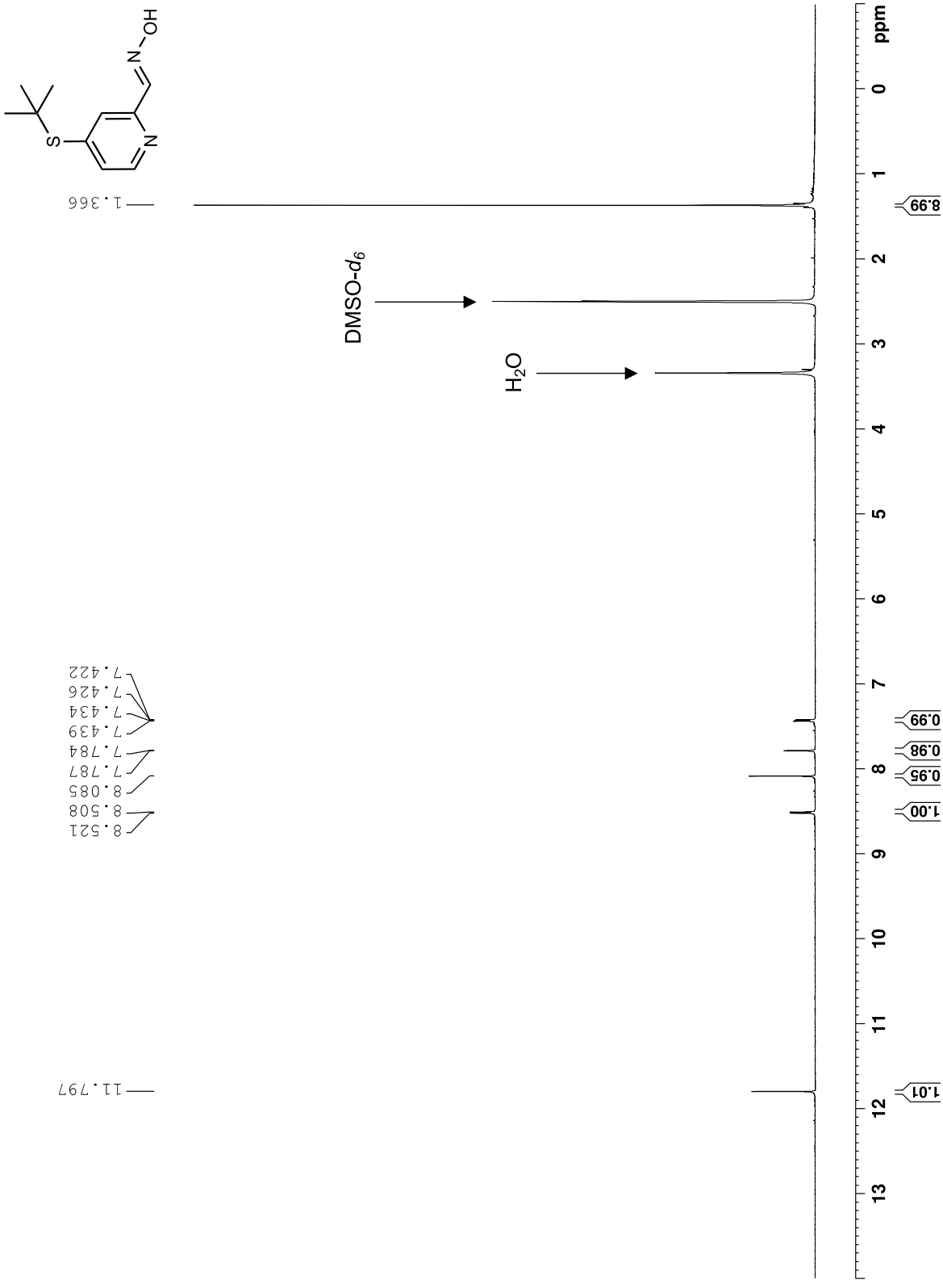

Spectrum 78. [1]H NMR of (*E*)-4-*tert*-butylthiopicolinaldehyde oxime (400 MHz, 293 K, DMSO-d_6).

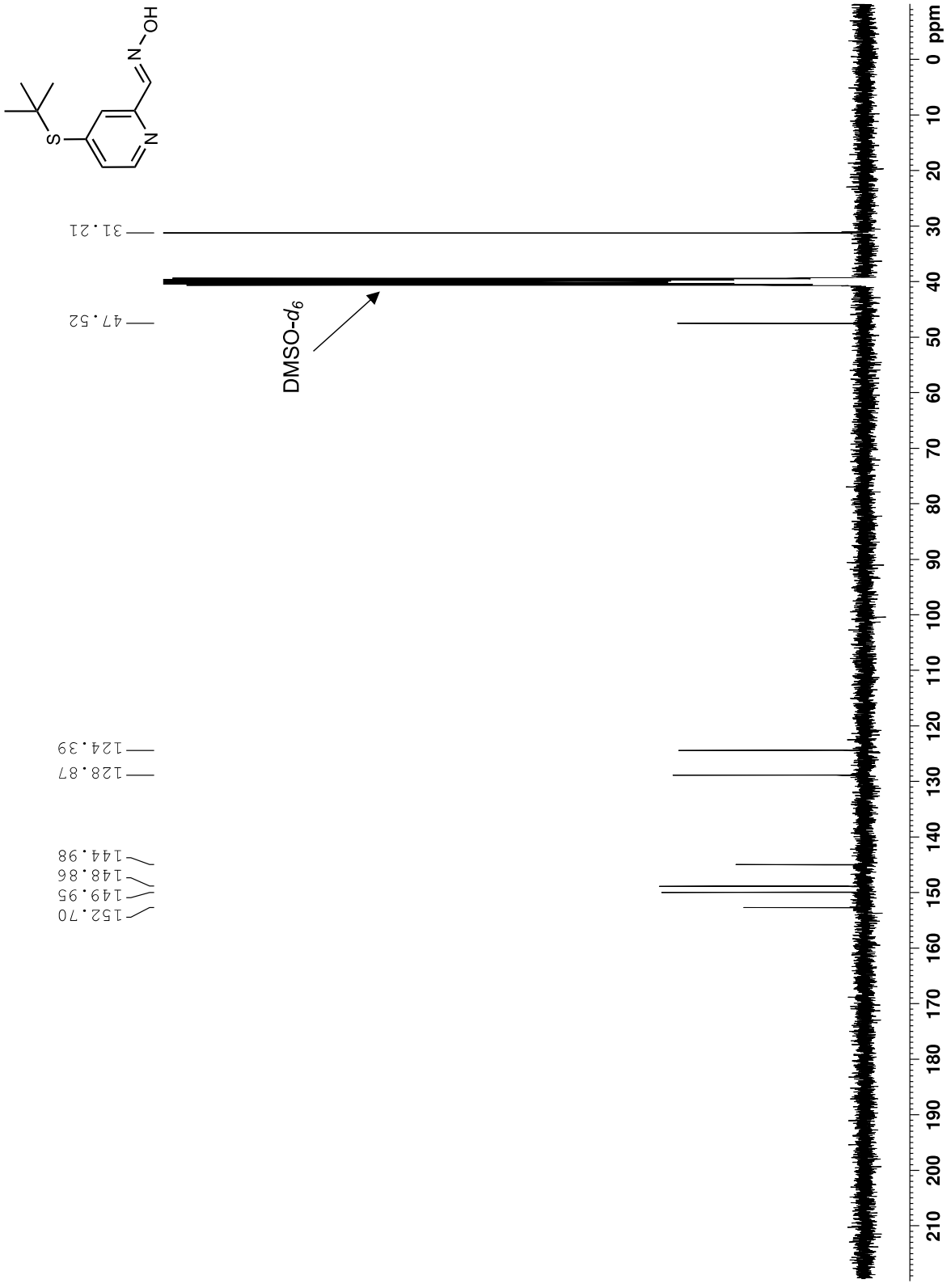

Spectrum 79. ^{13}C NMR of (*E*)-4-*tert*-butylthiopicolinaldehyde oxime (100 MHz, 293 K, DMSO-d_6).

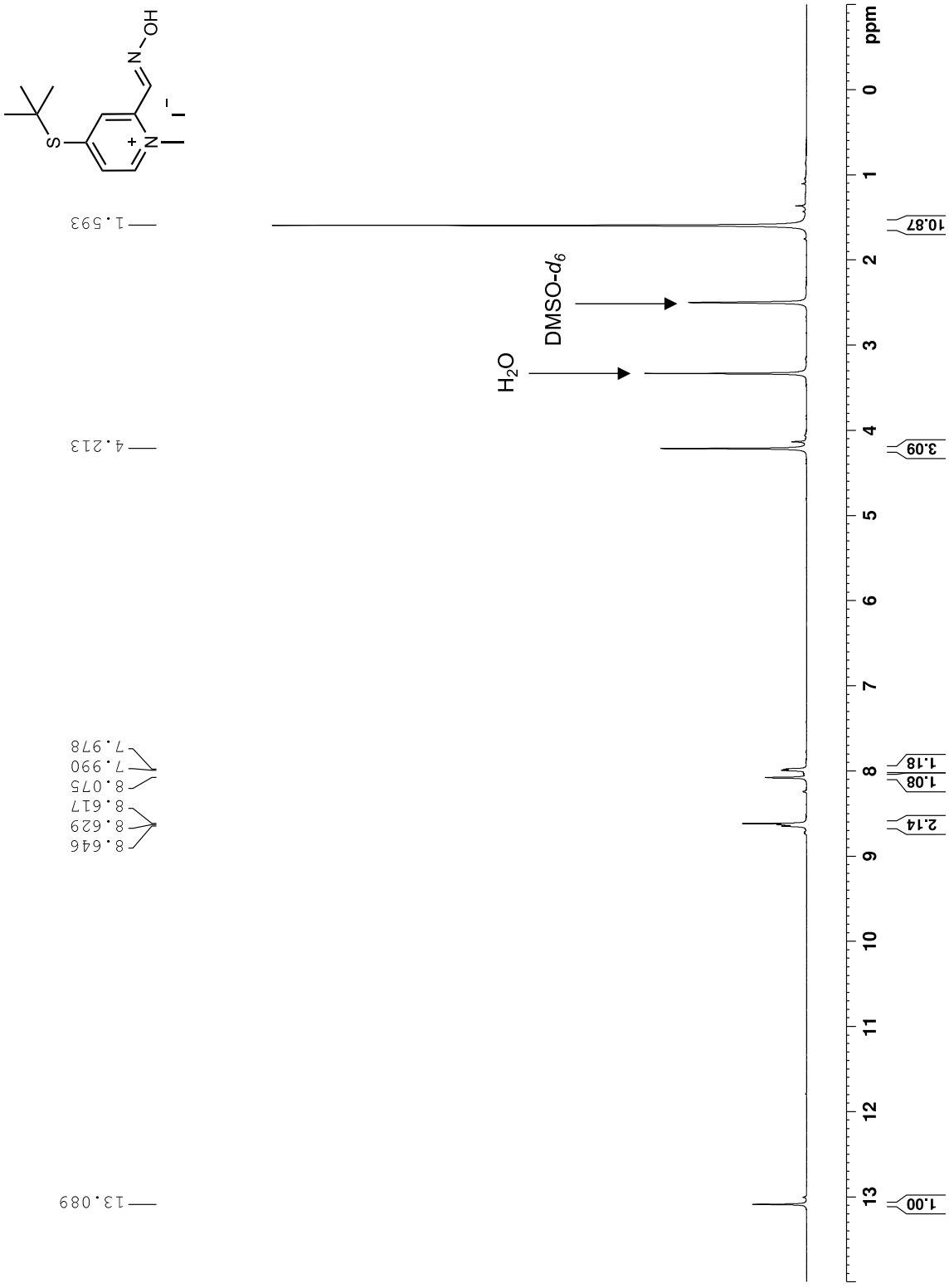

Spectrum 80. ^{1}H NMR of (*E*)-2-((hydroxyimino)methyl)-1-methyl-4-(*tert*-butylthio)pyridin-1-ium iodide (**ADG3001)** (400 MHz, 293 K, DMSO-d_6).

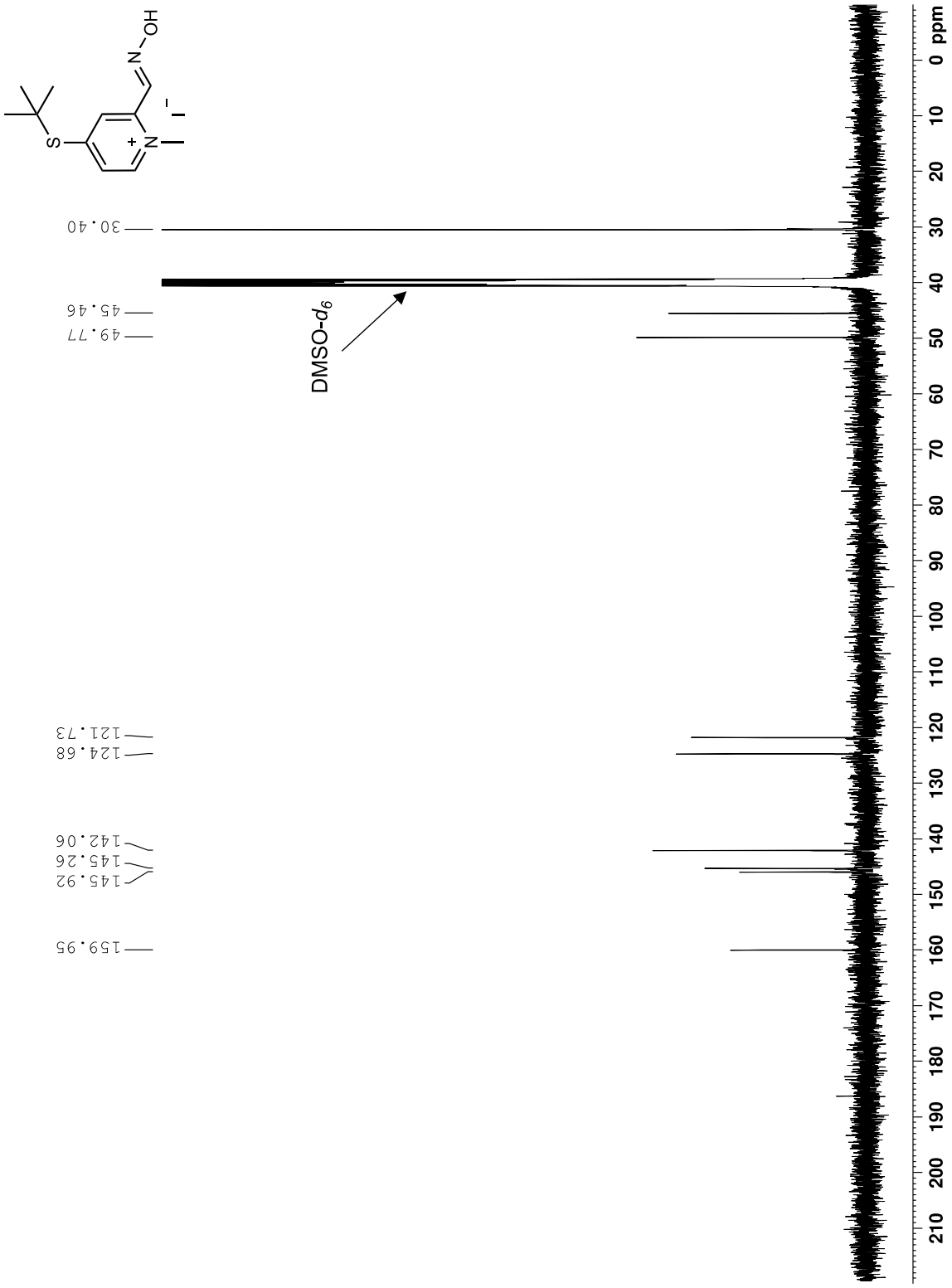

Spectrum 81. ^{13}C NMR of (*E*)-2-((hydroxyimino)methyl)-1-methyl-4-(*tert*-butylthio)pyridin-1-ium iodide (**ADG3001)** (100 MHz, 293 K, DMSO-d_6).

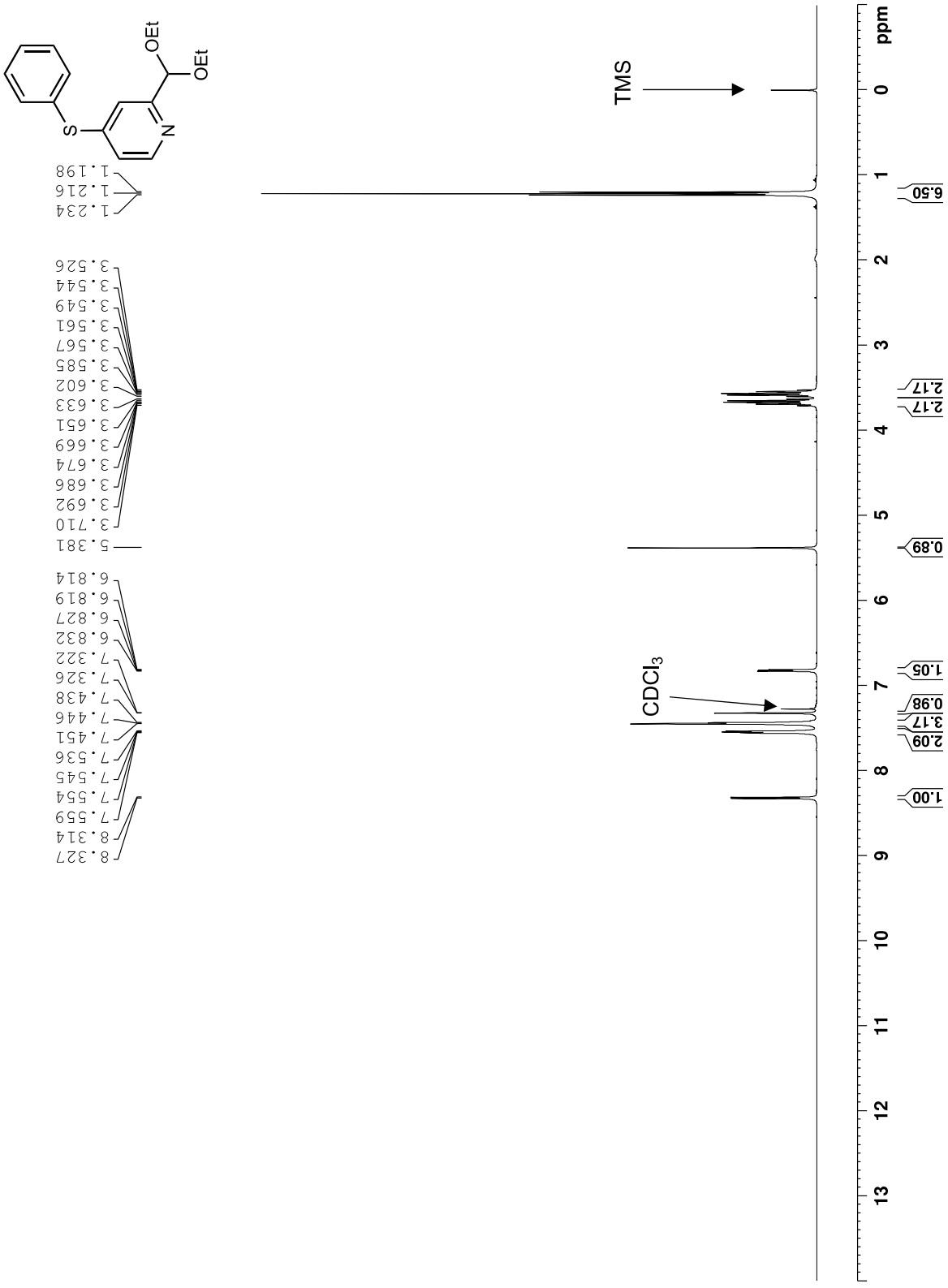

Spectrum 82. ^{1}H NMR of 2-(diethoxymethyl)-4-(phenylthio)pyridine (400 MHz, 293 K, $CDCl_3$).

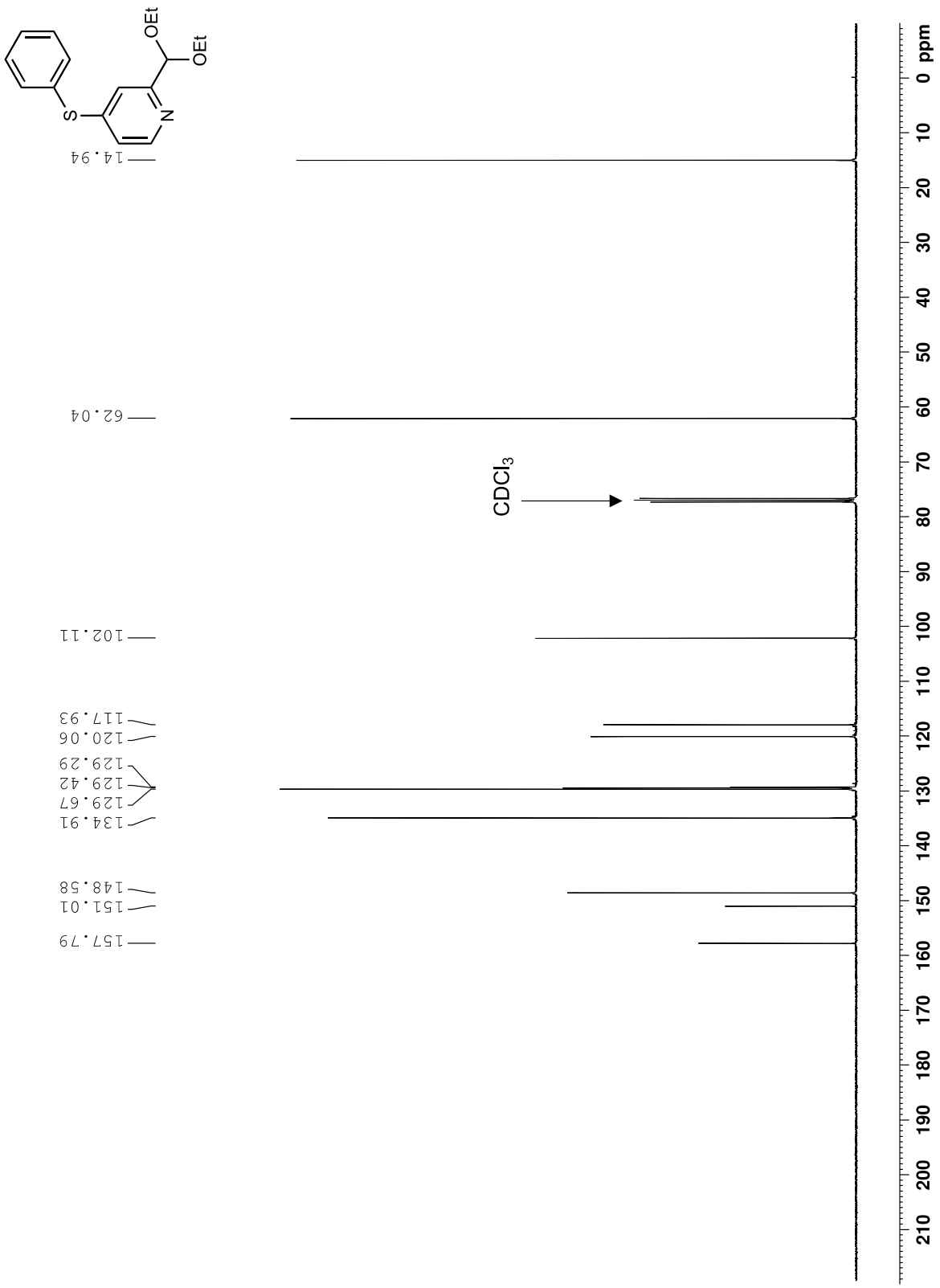

Spectrum 83. ^{13}C NMR of 2-(diethoxymethyl)-4-(phenylthio)pyridine (100 MHz, 293 K, $CDCl_3$).

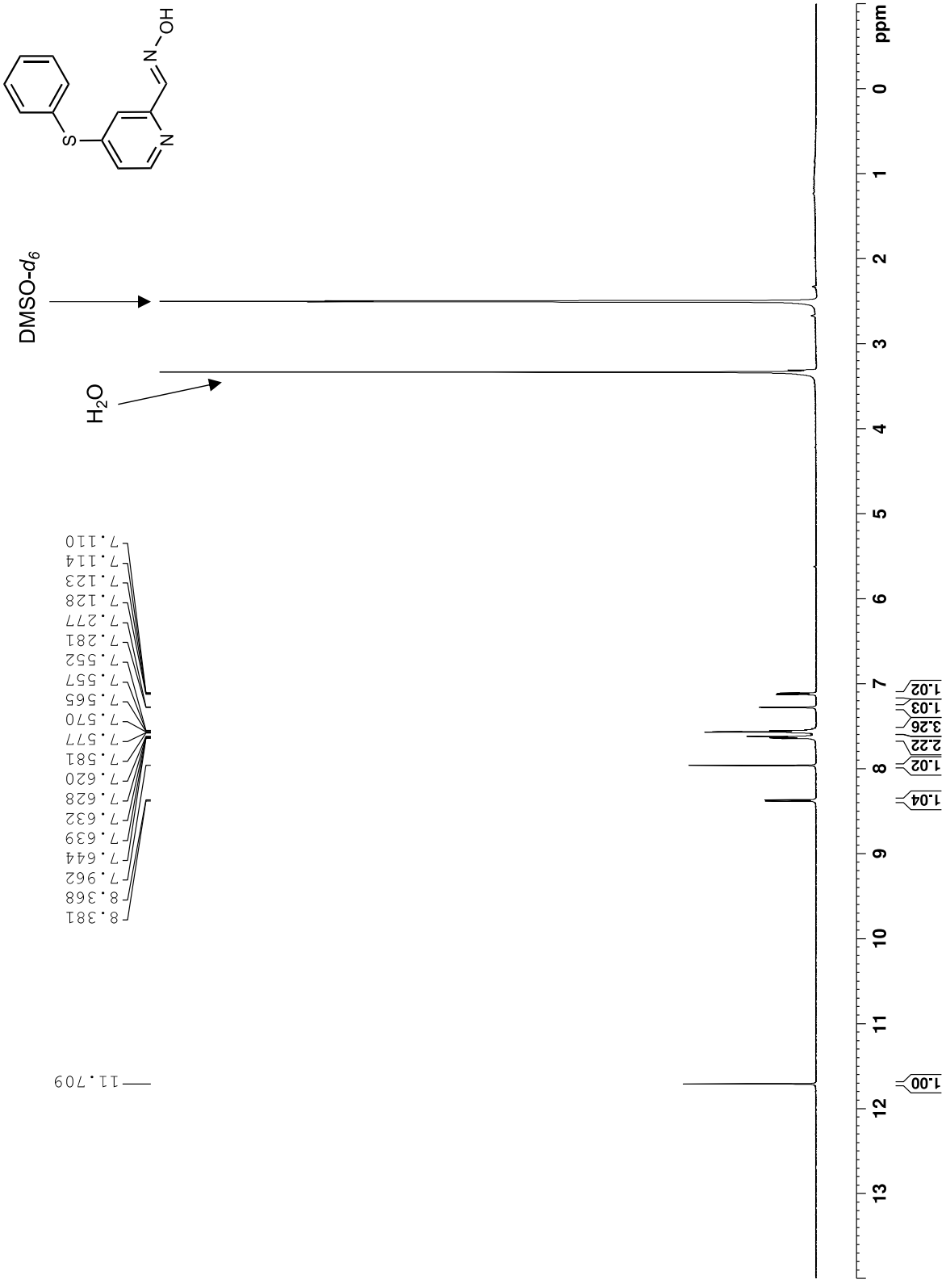

Spectrum 84. ^{1}H NMR of *(E)*-4-(phenylthio)picolinaldehyde oxime (400 MHz, 293 K, DMSO-d_6).

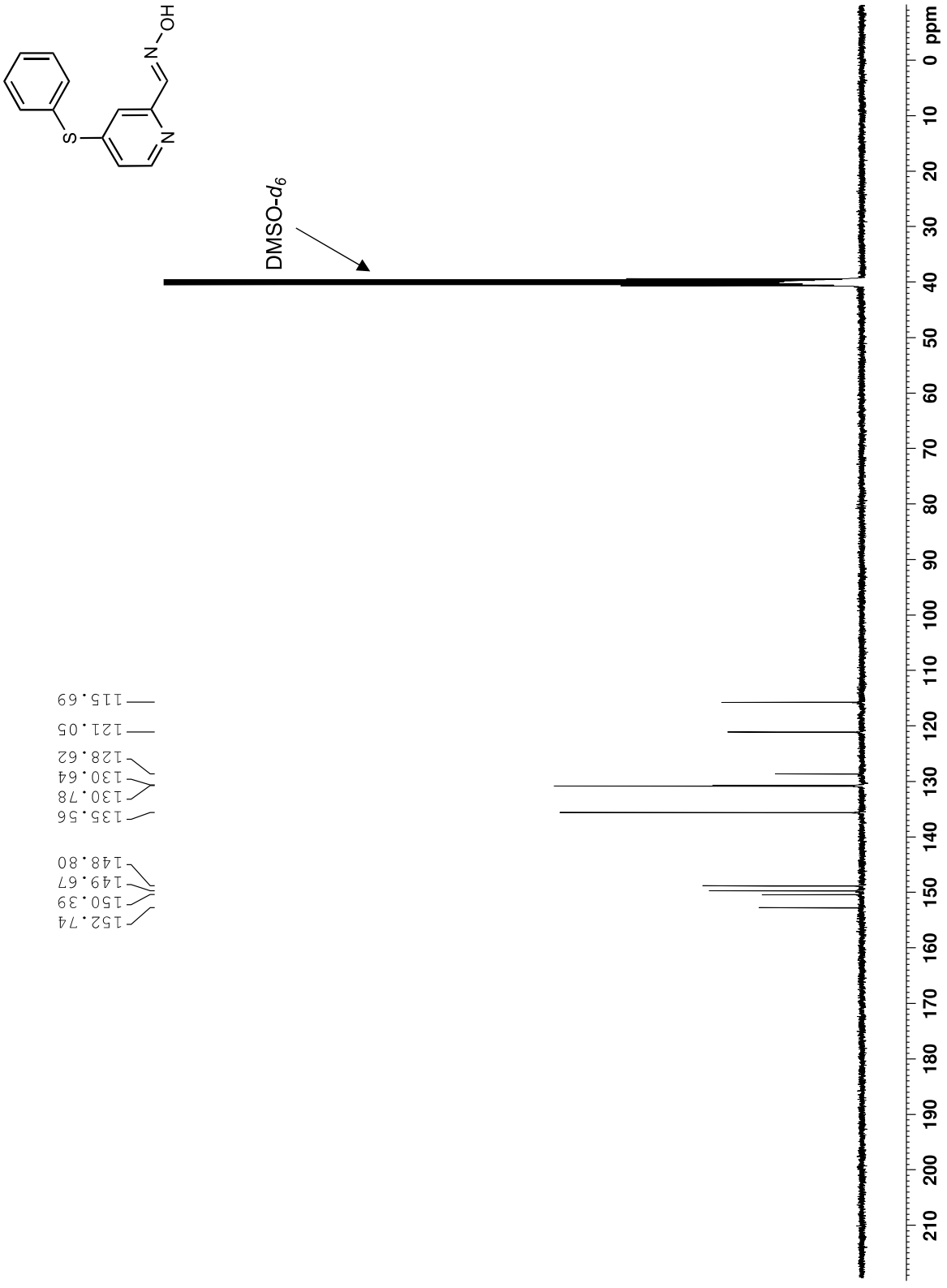

Spectrum 85. ^{13}C NMR of *(E)*-4-(phenylthio)picolinaldehyde oxime (100 MHz, 293 K, DMSO-d_6).

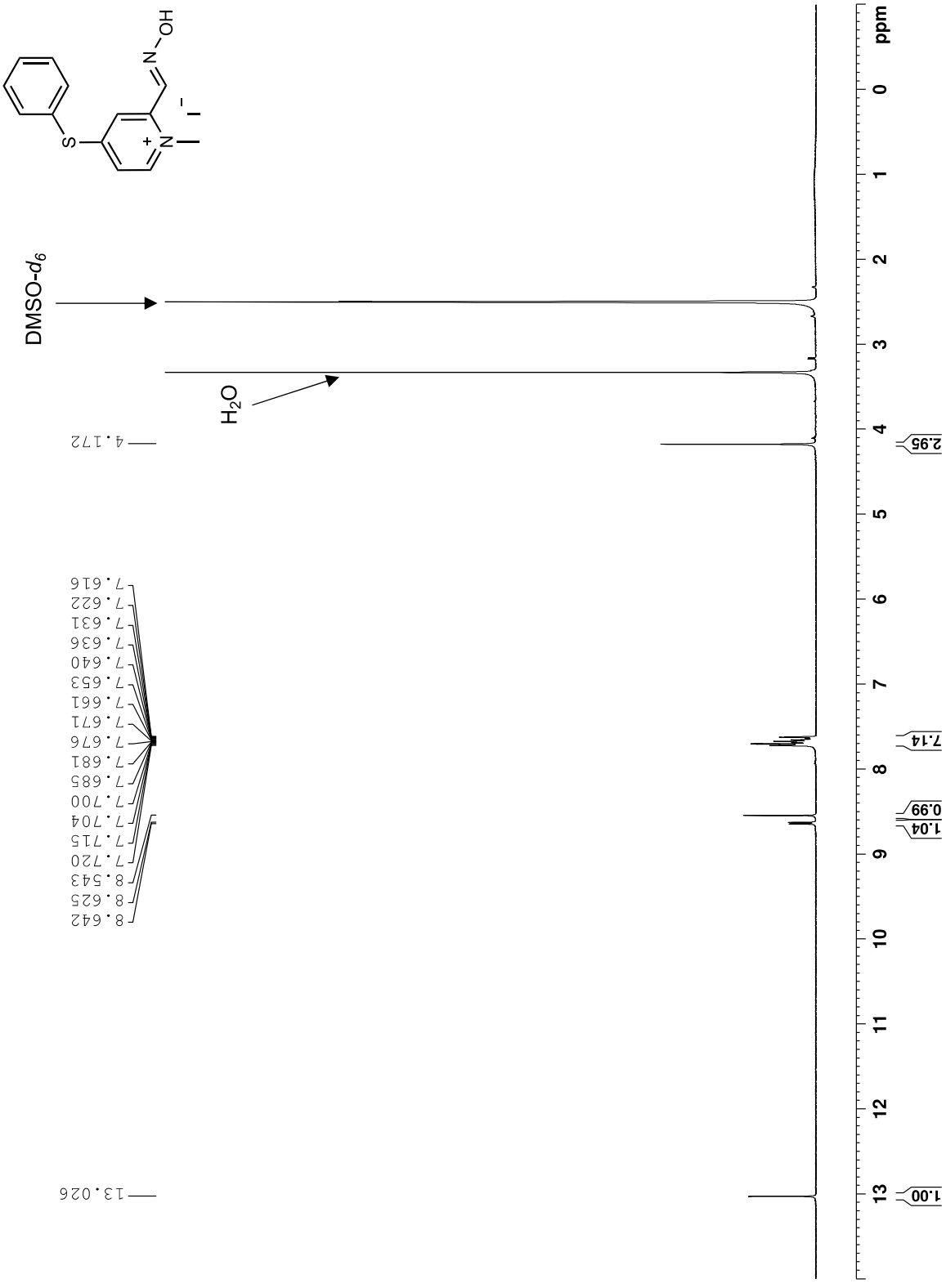

Spectrum 86. ^{1}H NMR of *(E)*-2-((hydroxyiminoye)methyl)-1-methyl-4-(phenylthio)pyridin-1-ium iodide (**ADG3002**) (400 MHz, 293 K, DMSO-d_6).

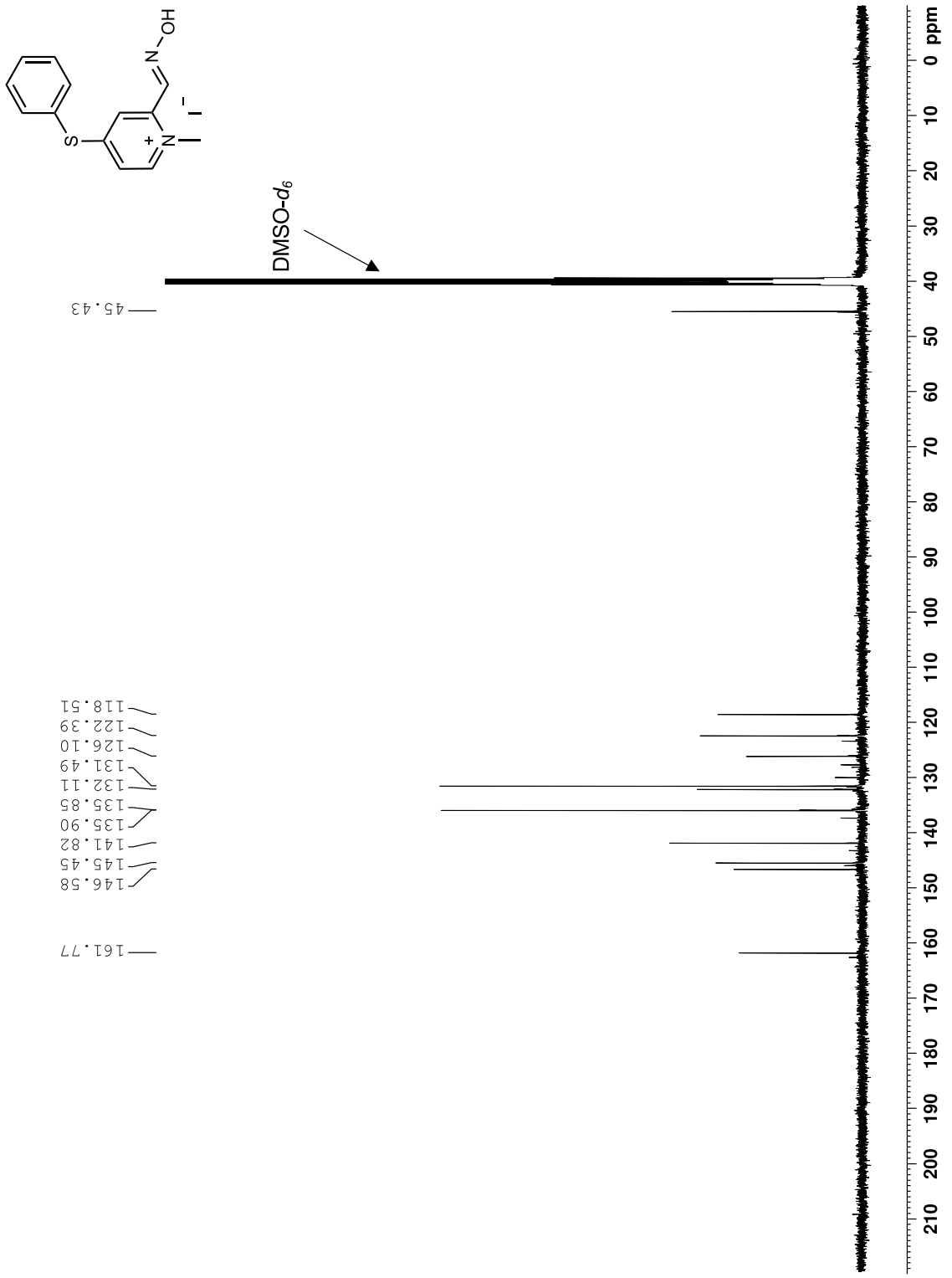

Spectrum 87. ^{13}C NMR of *(E)*-2-((hydroxyimino)methyl)-1-methyl-4-(phenylthio)pyridin-1-ium iodide (**ADG3002**) (100 MHz, 293 K, DMSO-d_6).

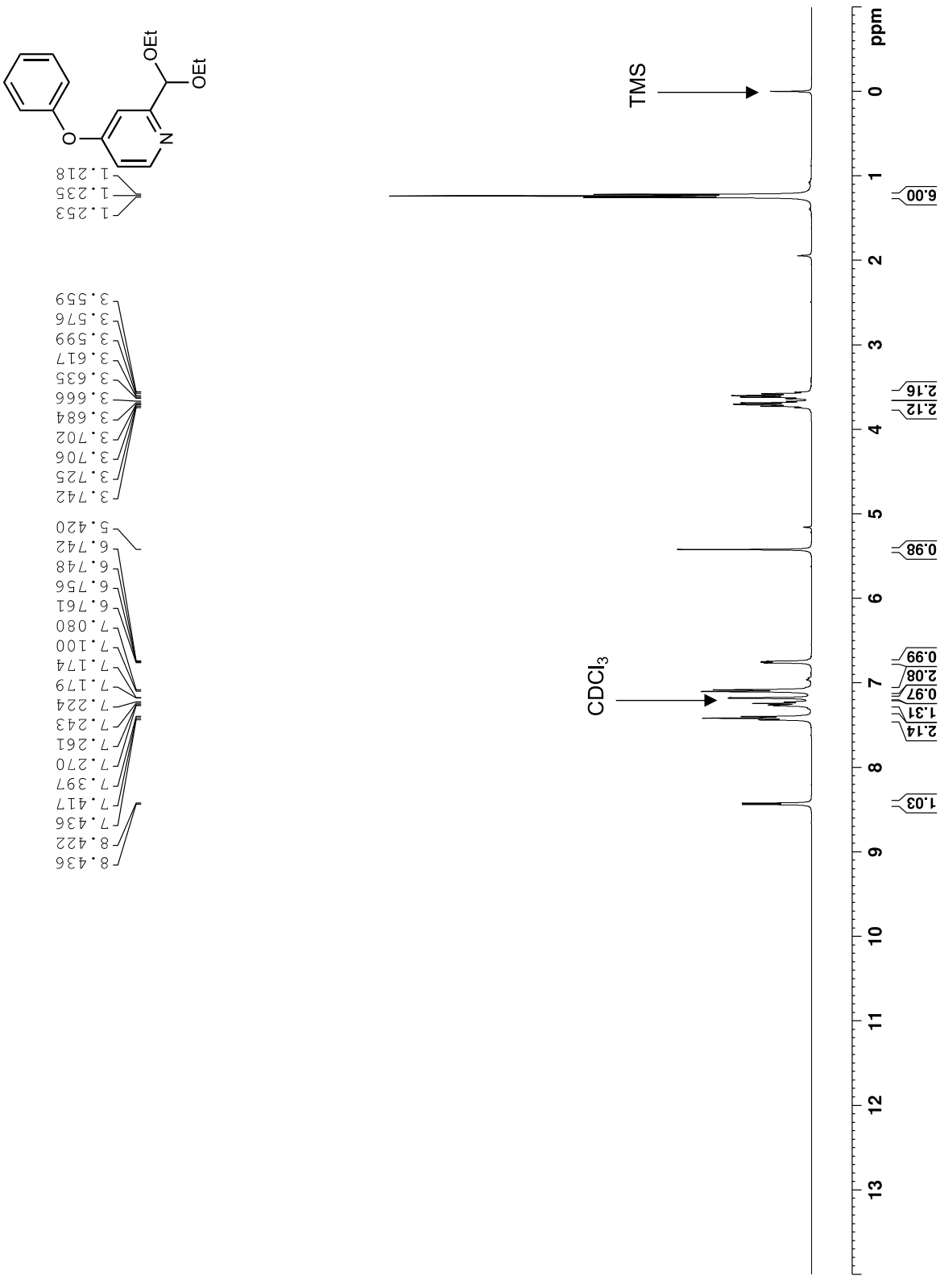

Spectrum 88. ^{1}H NMR of 2-(diethoxymethyl)-4-phenoxypyridine (400 MHz, 293 K, $CDCl_3$).

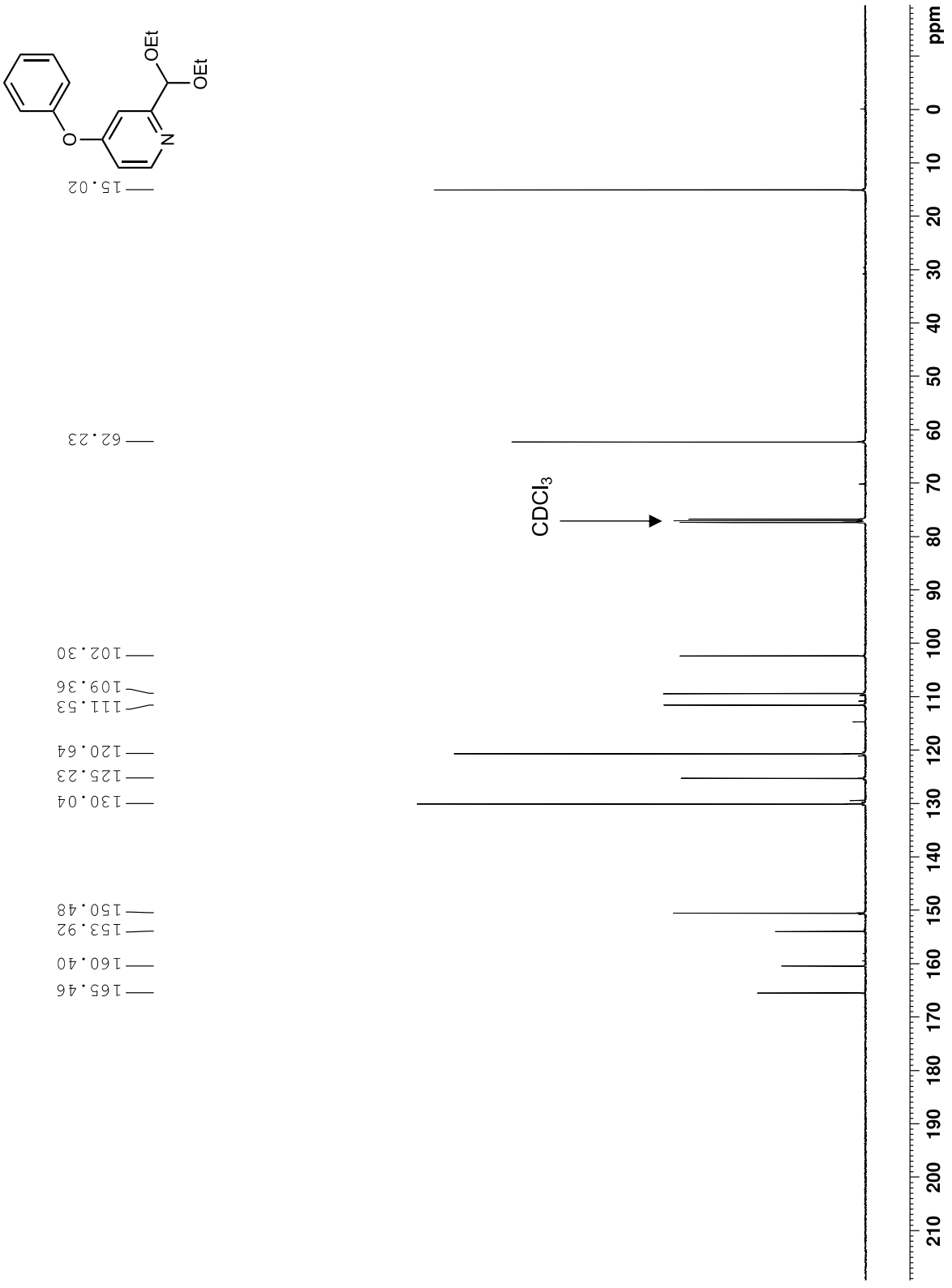

Spectrum 89. ^{13}C NMR of 2-(diethoxymethyl)-4-phenoxypyridine (100 MHz, 293 K, $CDCl_3$).

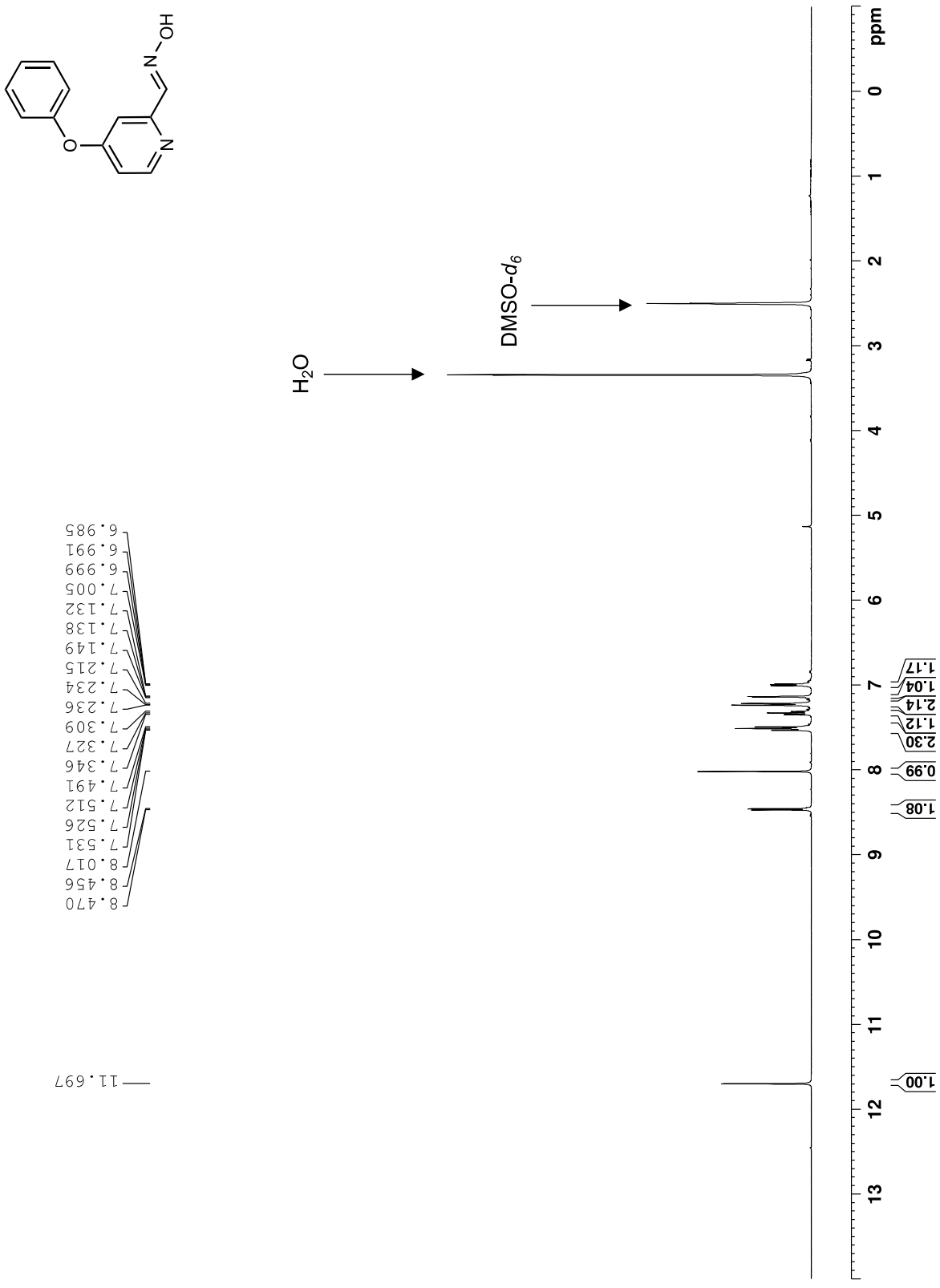

Spectrum 90. ^{1}H NMR of *(E)*-4-phenoxypicolinaldehyde oxime (400 MHz, 293 K, DMSO-d_6).

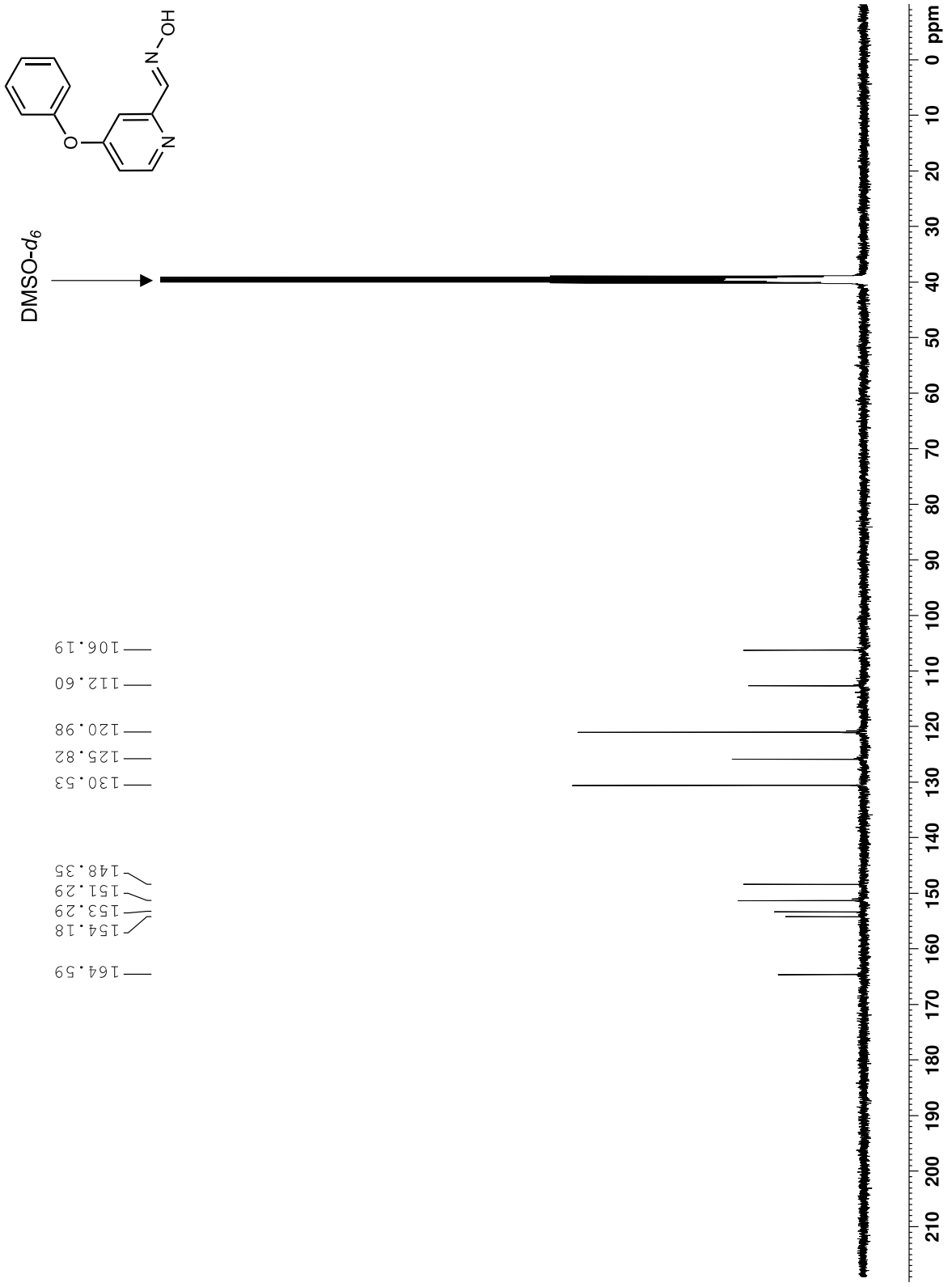

Spectrum 91. ^{13}C NMR of *(E)*-4-phenoxypicolinaldehyde oxime (100 MHz, 293 K, DMSO-d_6).

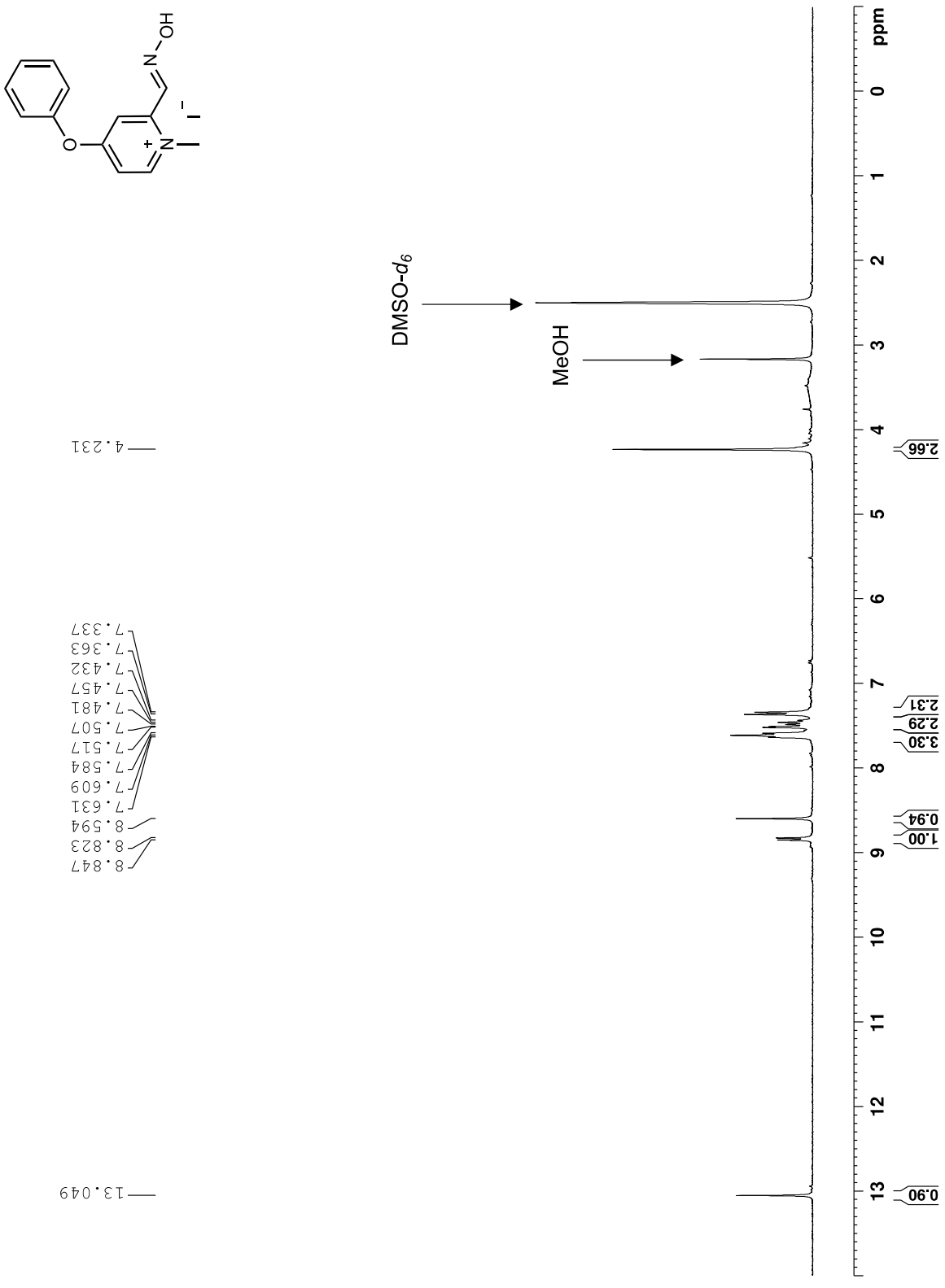

Spectrum 92. ^{1}H NMR of *(E)*-2-((hydroxyimino)methyl)-1-methyl-4-phenoxypyridin-1-ium iodide (**ADG3003**) (300 MHz, 293 K, DMSO-d_6).

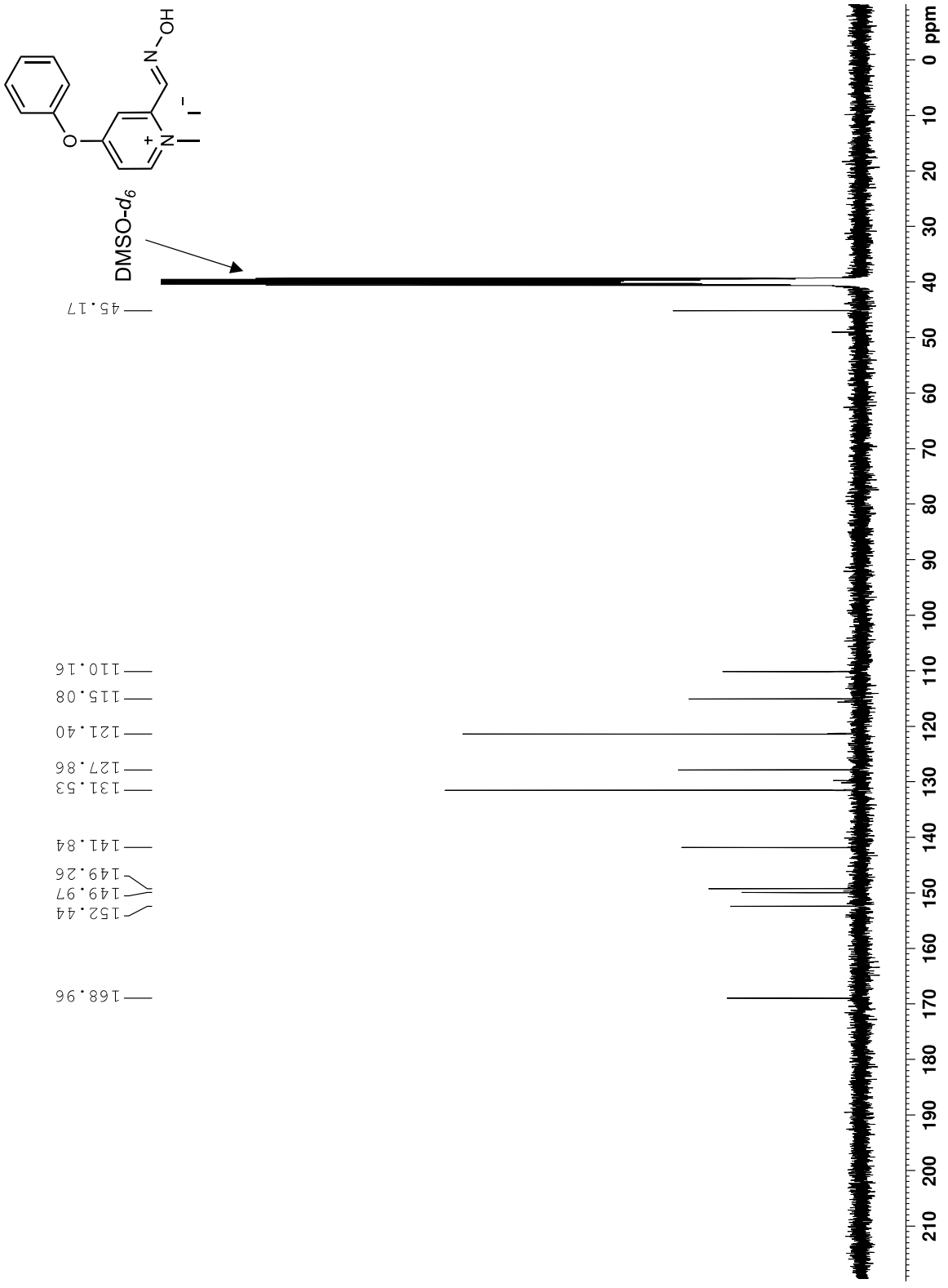

Spectrum 93. ^{13}C NMR of *(E)*-2-((hydroxyimino)methyl)-1-methyl-4-phenoxypyridin-1-ium iodide (**ADG3003**) (100 MHz, 293 K, DMSO-d_6).

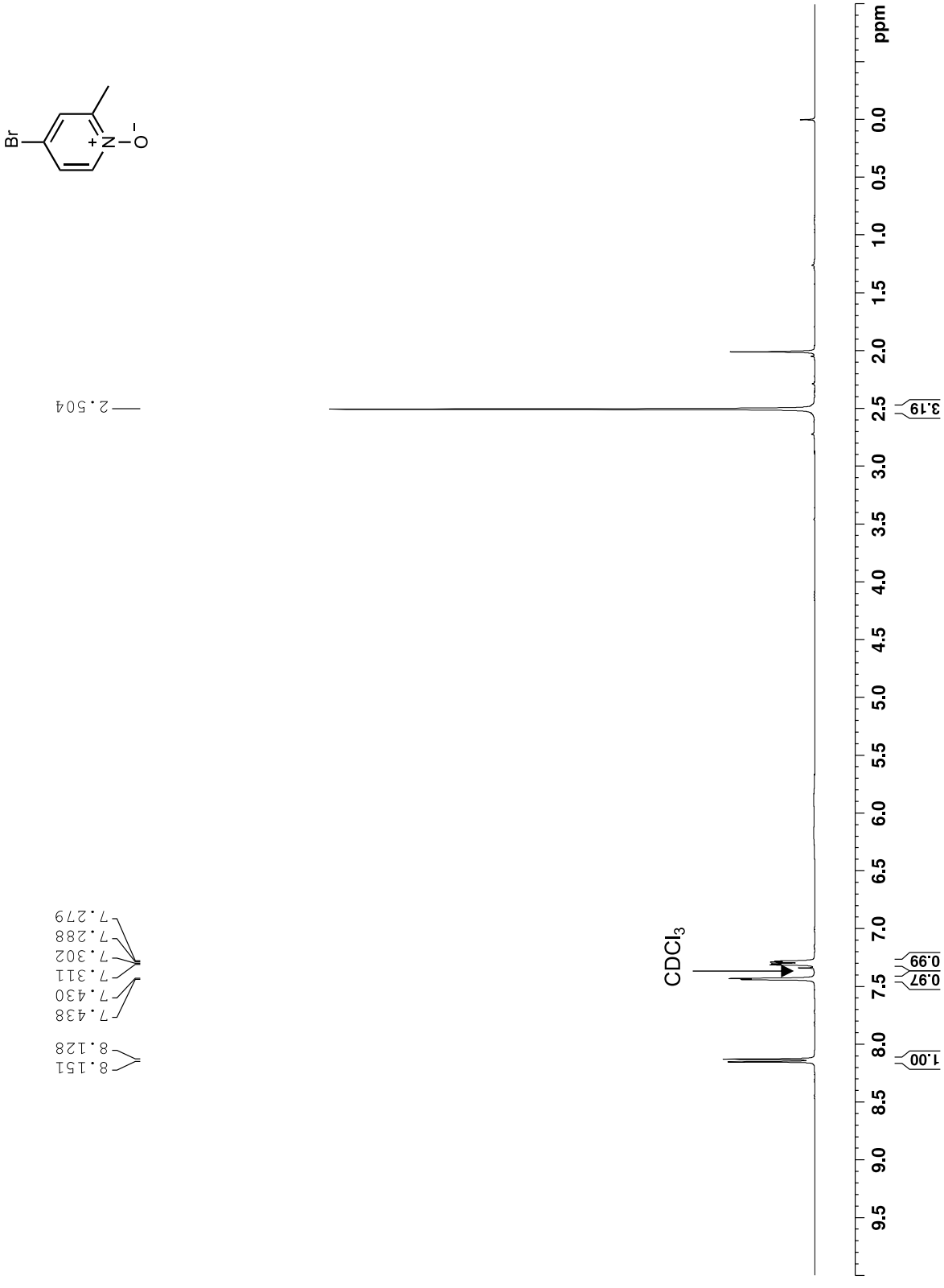

Spectrum 94. ^{1}H NMR for 4-bromo-2-methylpyridine 1-oxide (300 MHz, 293 K, $CDCl_3$).

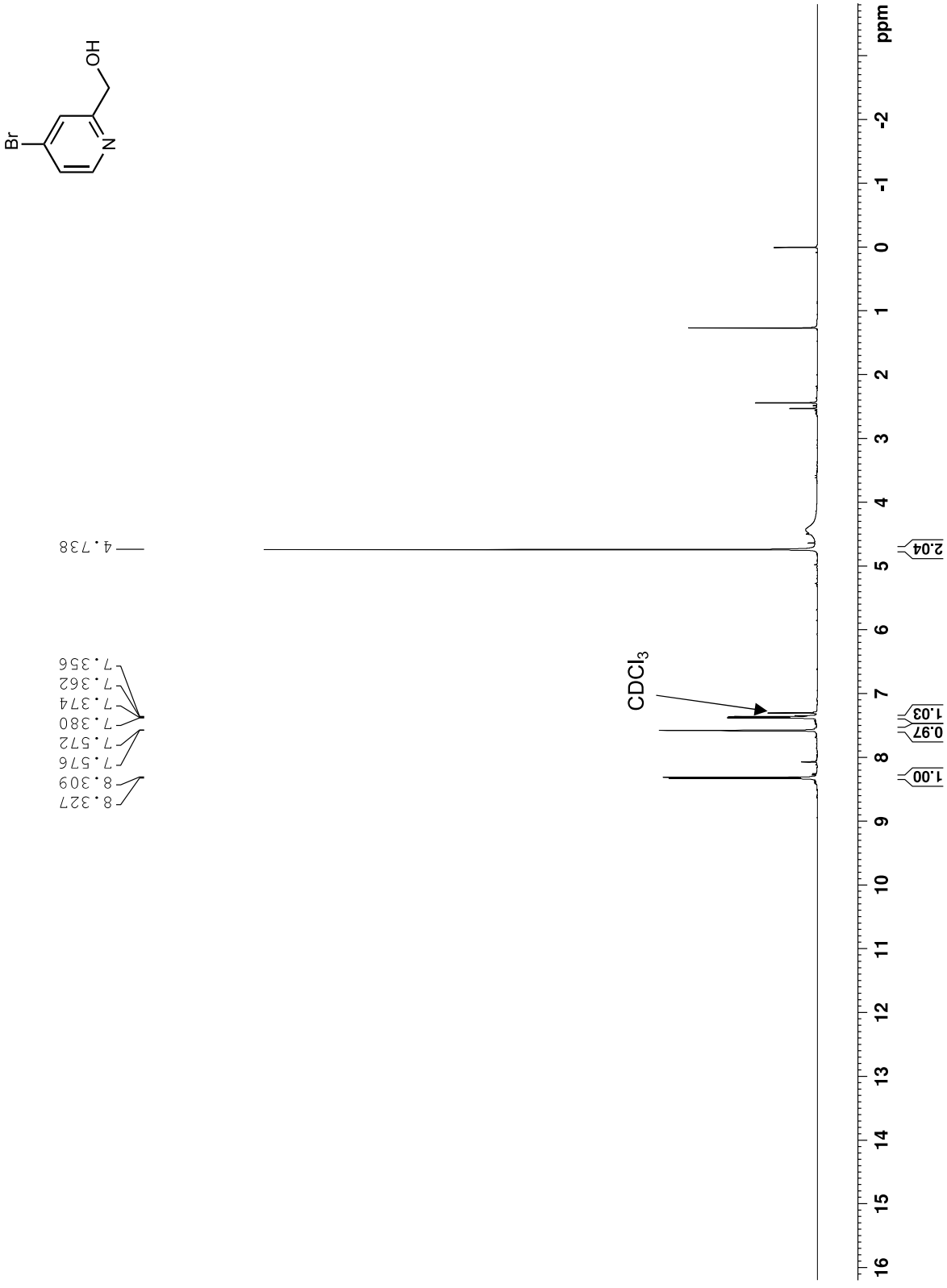

Spectrum 95. ^{1}H NMR for (4-bromopyridin-2-yl)methanol (300 MHz, 293 K, 1% w/w CD_3OD in $CDCl_3$).

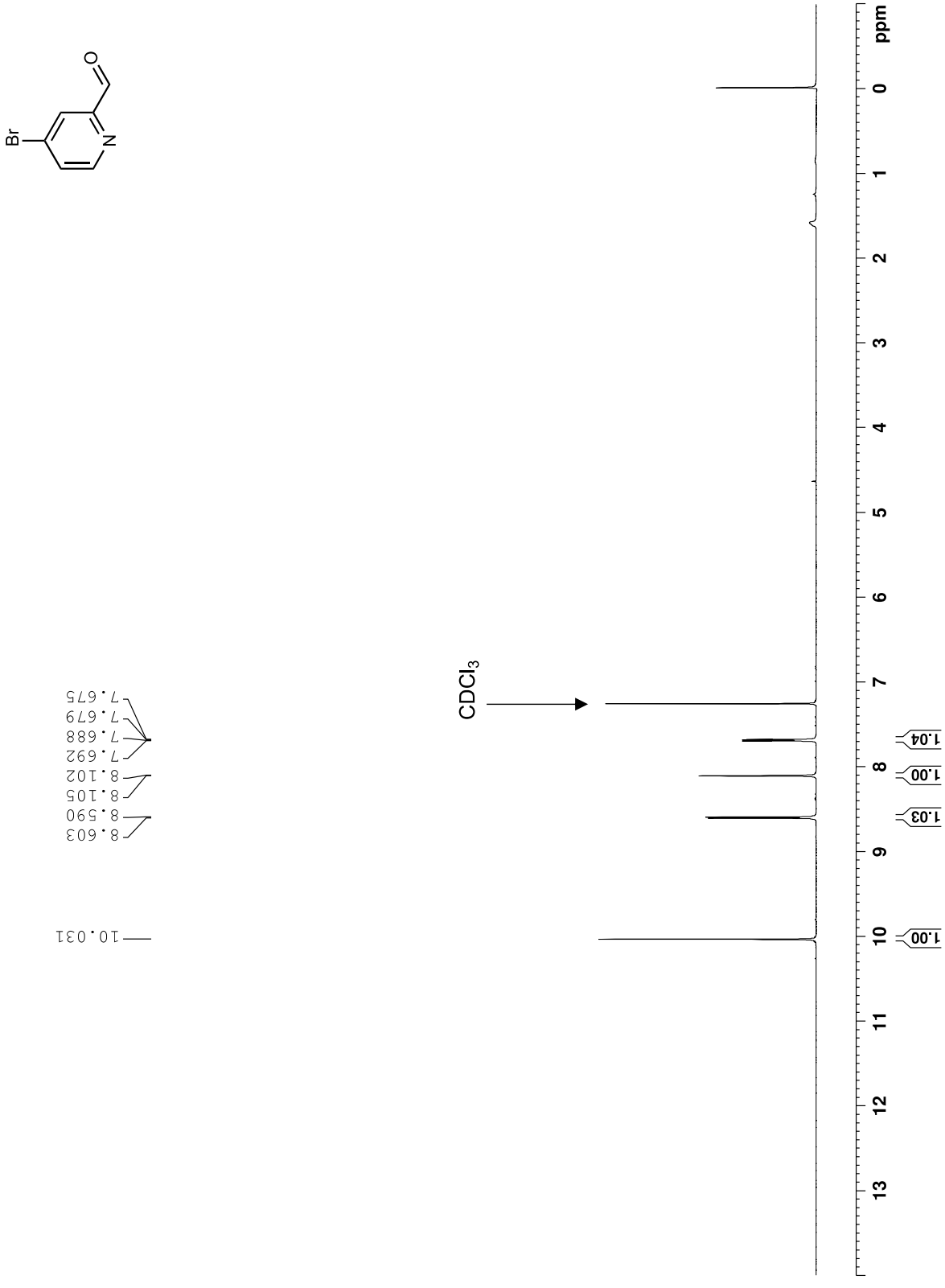

Spectrum 96. ^{1}H NMR for 4-bromopicolinaldehyde (400 MHz, 293 K, $CDCl_3$).

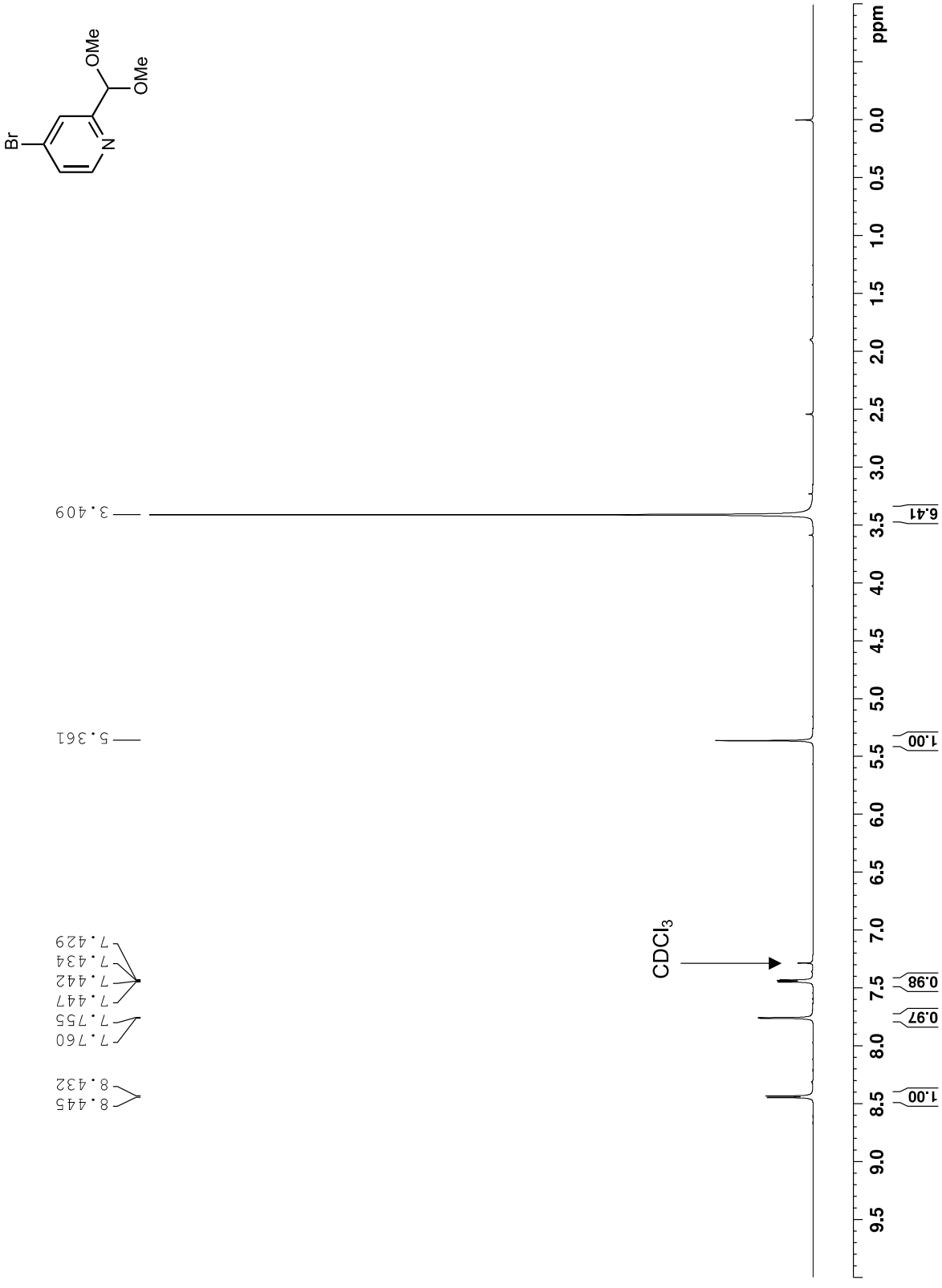

Spectrum 97. ^{1}H NMR for 4-bromo-2-(dimethoxymethyl)pyridine (400 MHz, 293 K, $CDCl_3$).

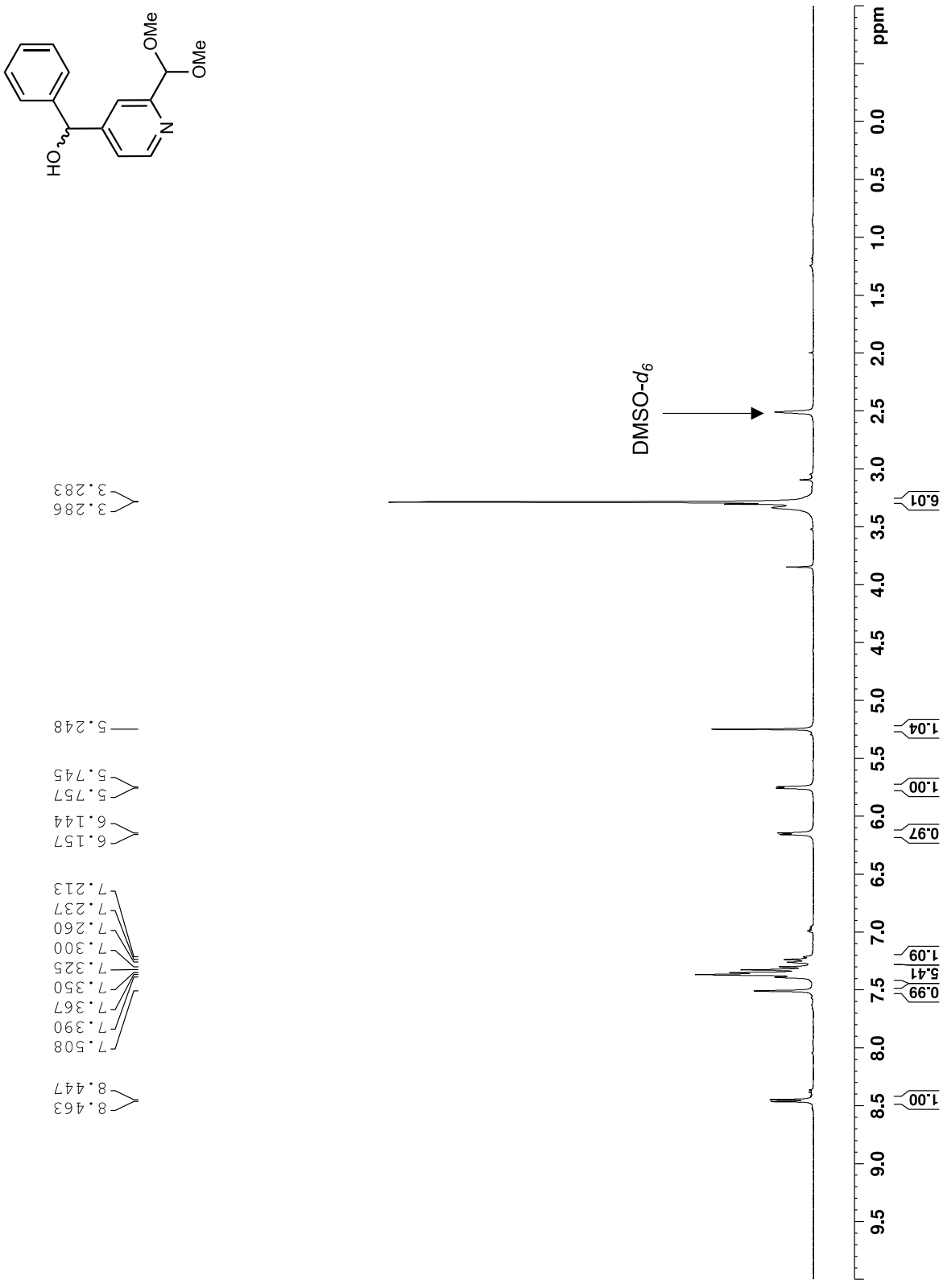

Spectrum 98. ^{1}H NMR of (2-(dimethoxymethyl)pyridin-4-yl)(phenyl)methanol (300 MHz, 293 K, DMSO-d_6).

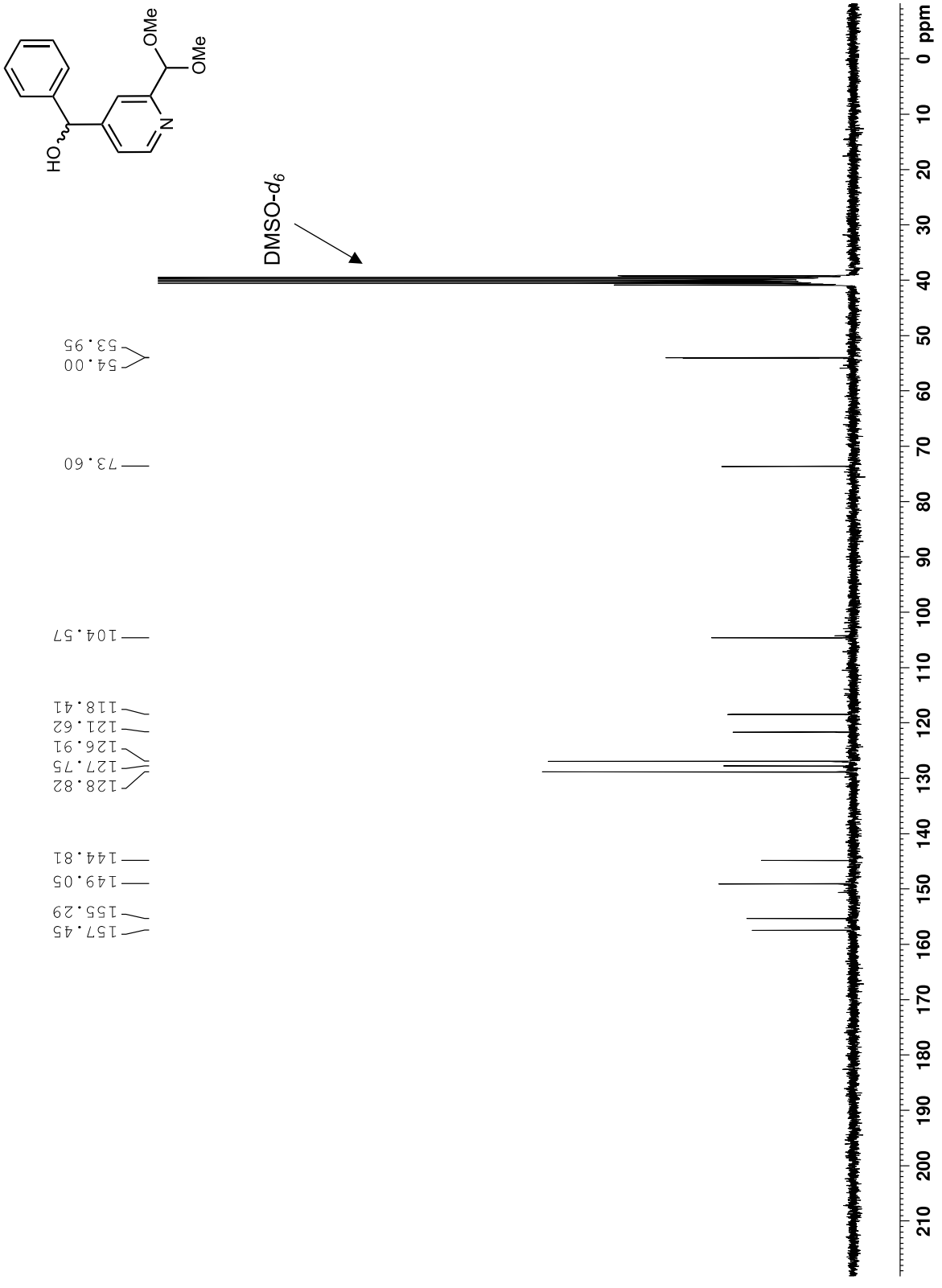

Spectrum 99. ^{13}C NMR of (2-(dimethoxymethyl)pyridin-4-yl)(phenyl)methanol (75 MHz, 293 K, DMSO-d_6).

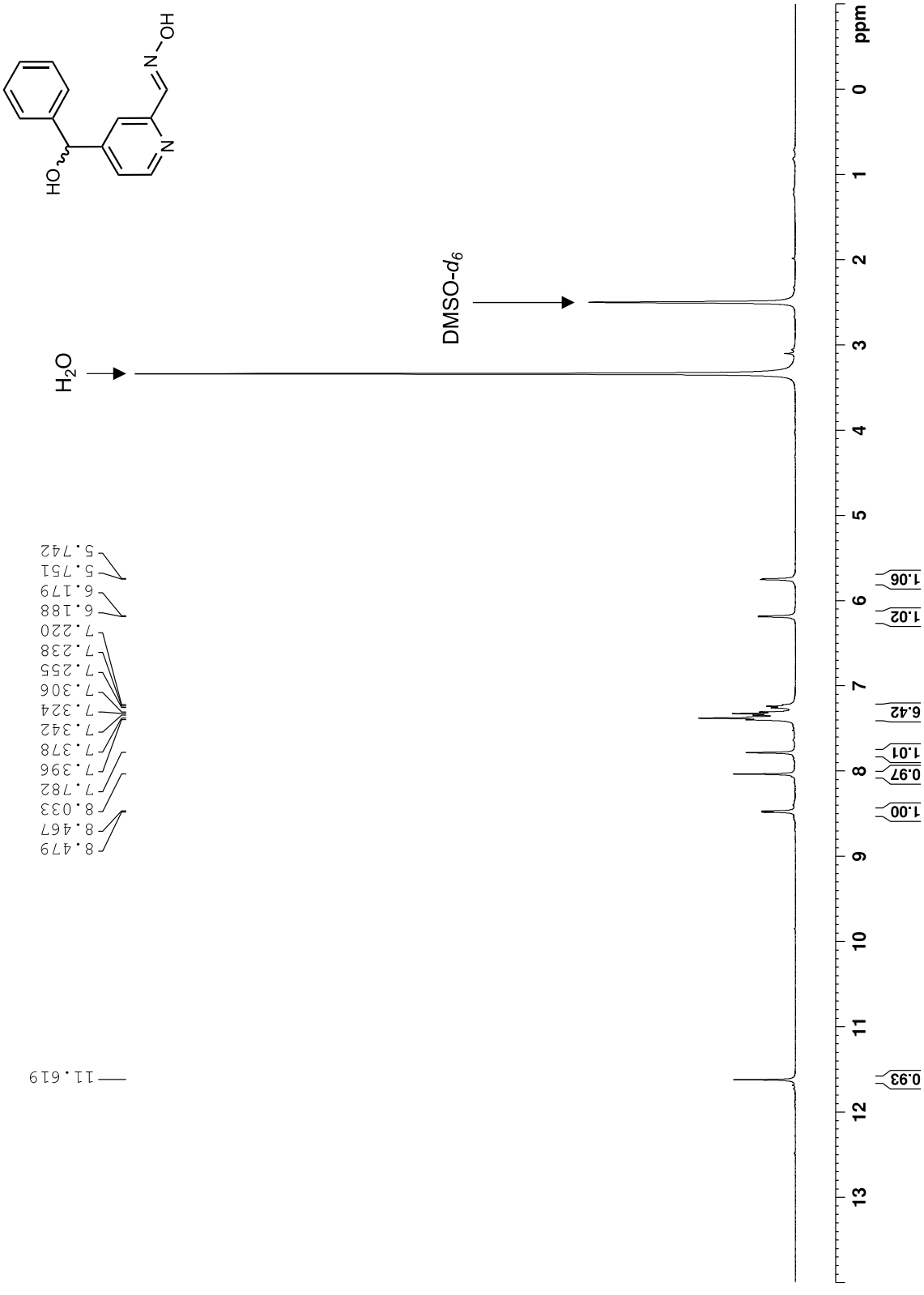

Spectrum 100. ^{1}H NMR of (*E*)-4-(hydroxy(phenyl)methyl)picolinaldehyde oxime (400 MHz, 293 K, DMSO-d_6).

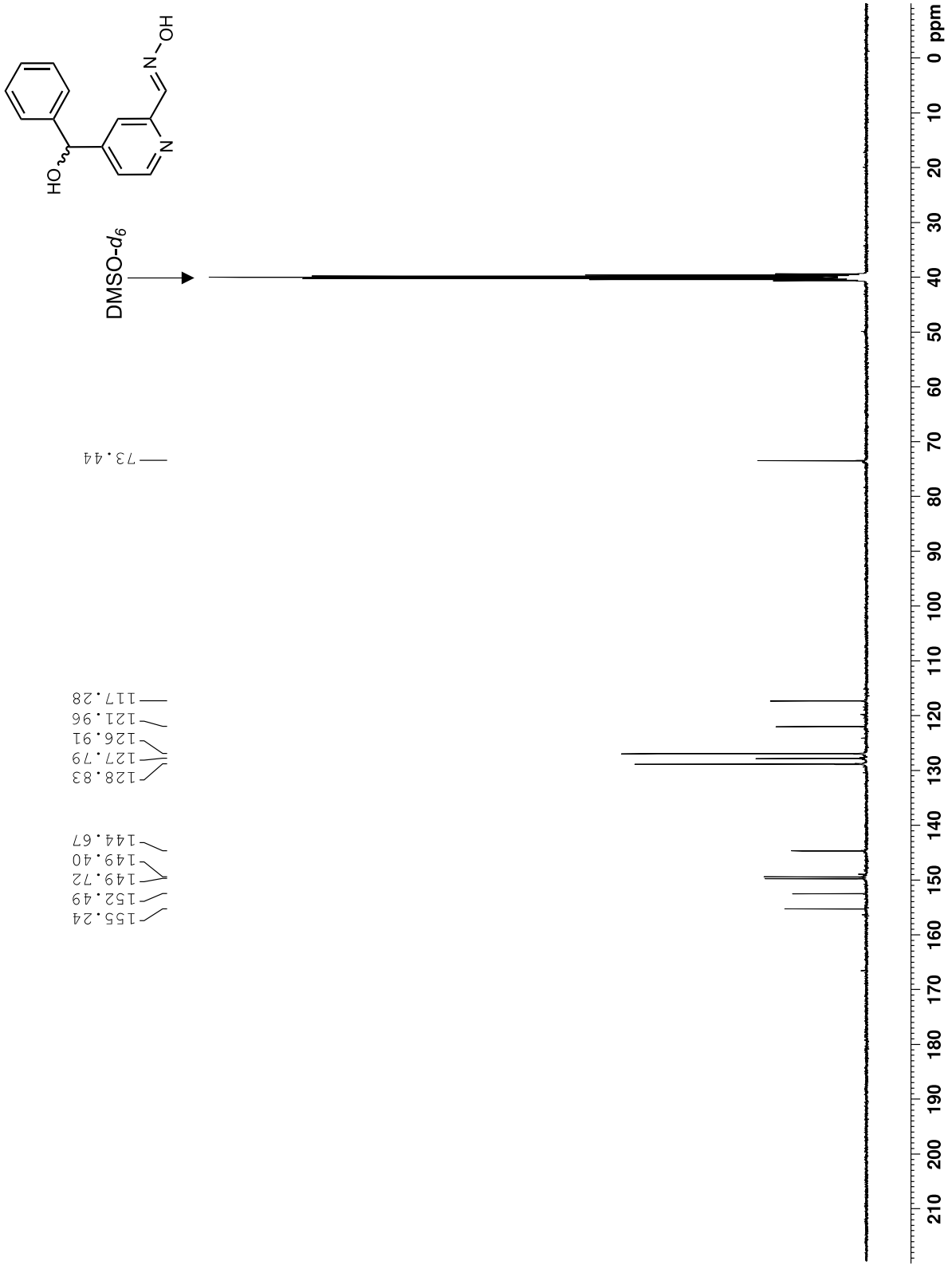

Spectrum 101. ^{13}C NMR of (*E*)-4-(hydroxy(phenyl)methyl)picolinaldehyde oxime (100 MHz, 293 K, DMSO-d_6).

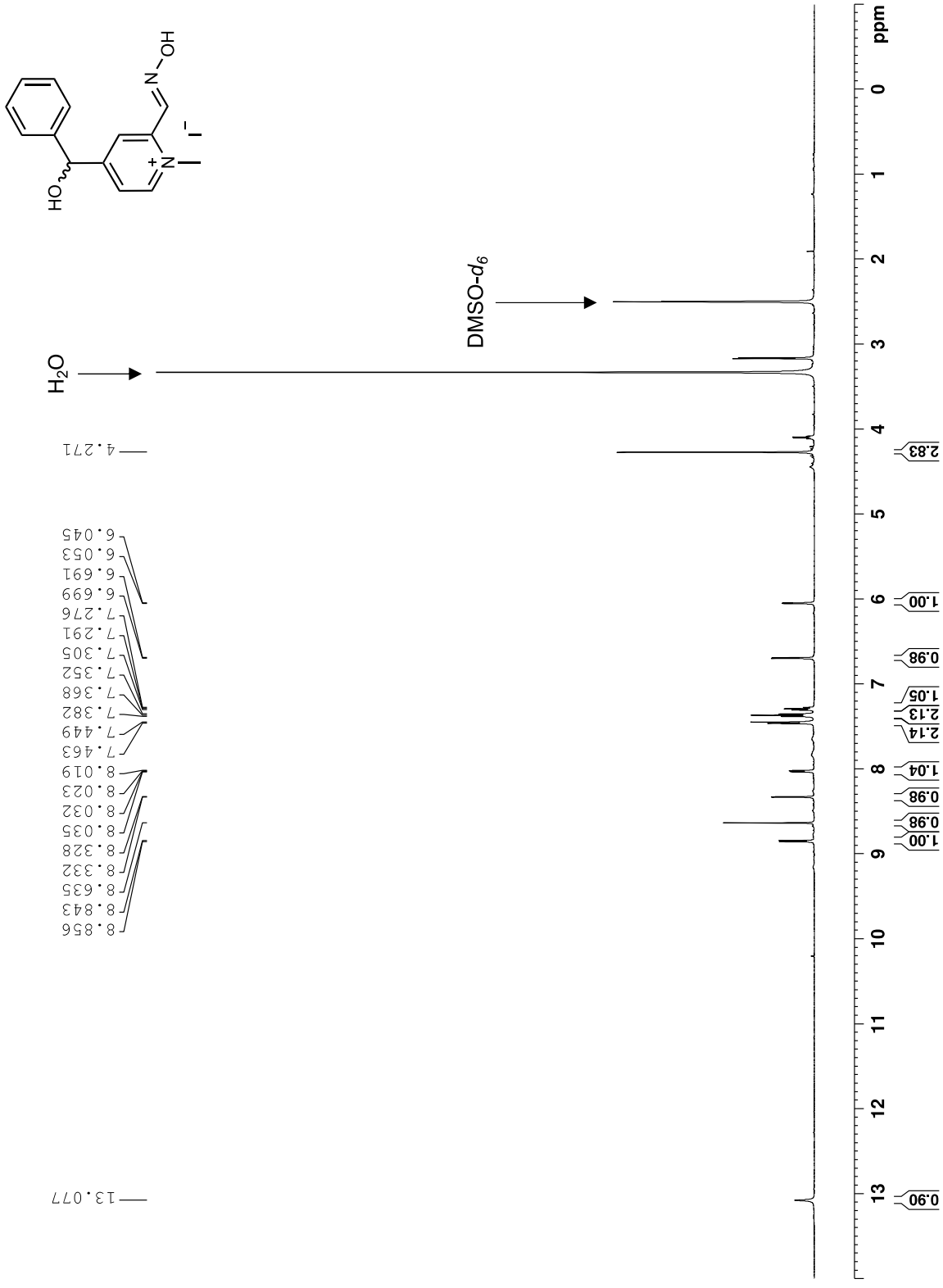

Spectrum 102. [1]H NMR of (*E*)-4-(hydroxy(phenyl)methyl)-2-((hydroxyimino)methyl)-1-methylpyridin-1-ium iodide (**ADG3230)** (500 MHz, 293 K, DMSO-d_6).

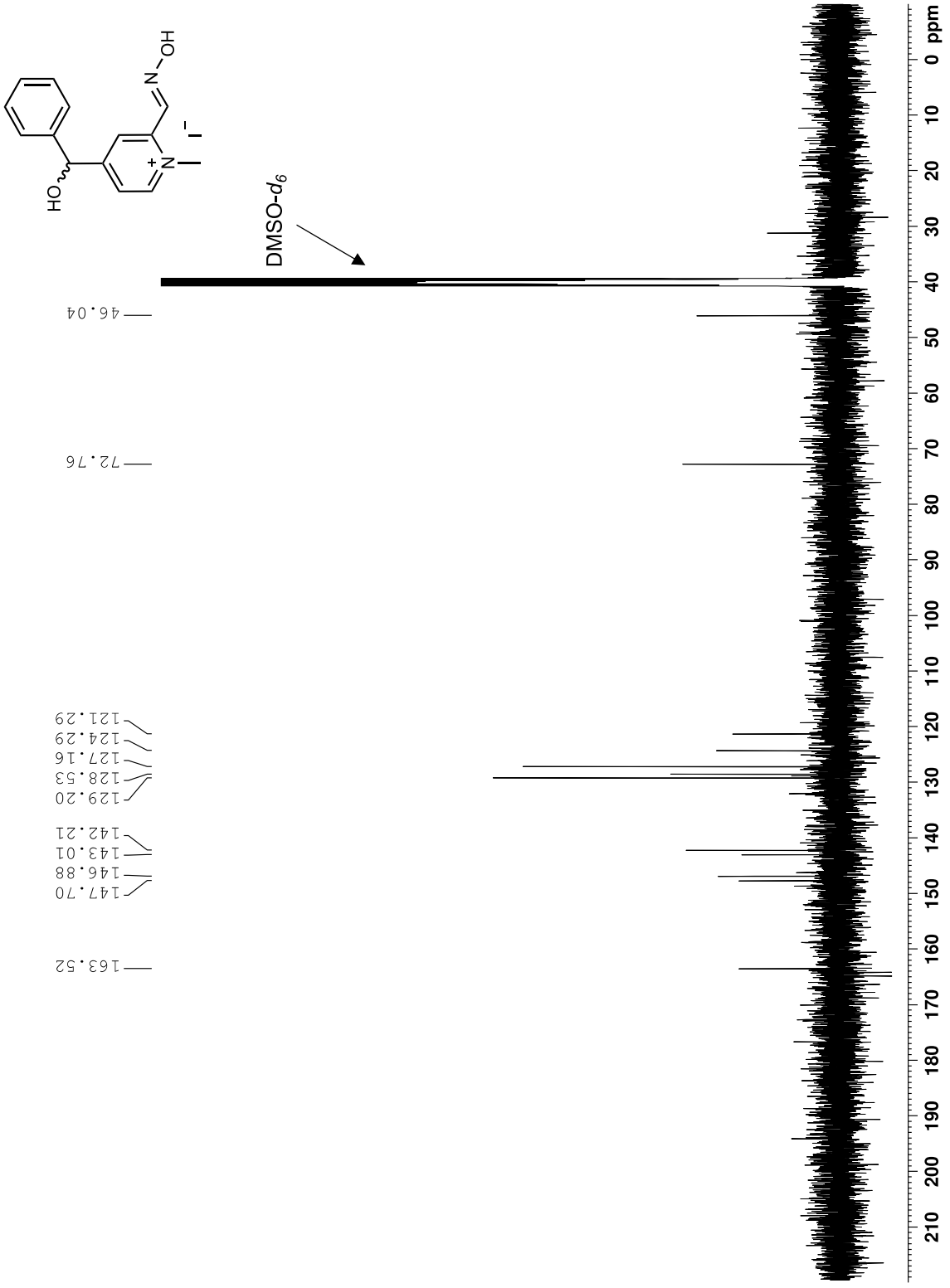

Spectrum 103. ^{13}C NMR of (*E*)-4-(hydroxy(phenyl)methyl)-2-((hydroxyimino)methyl)-1-methylpyridin-1-ium iodide (**ADG3230)** (100 MHz, 293 K, DMSO-d_6).

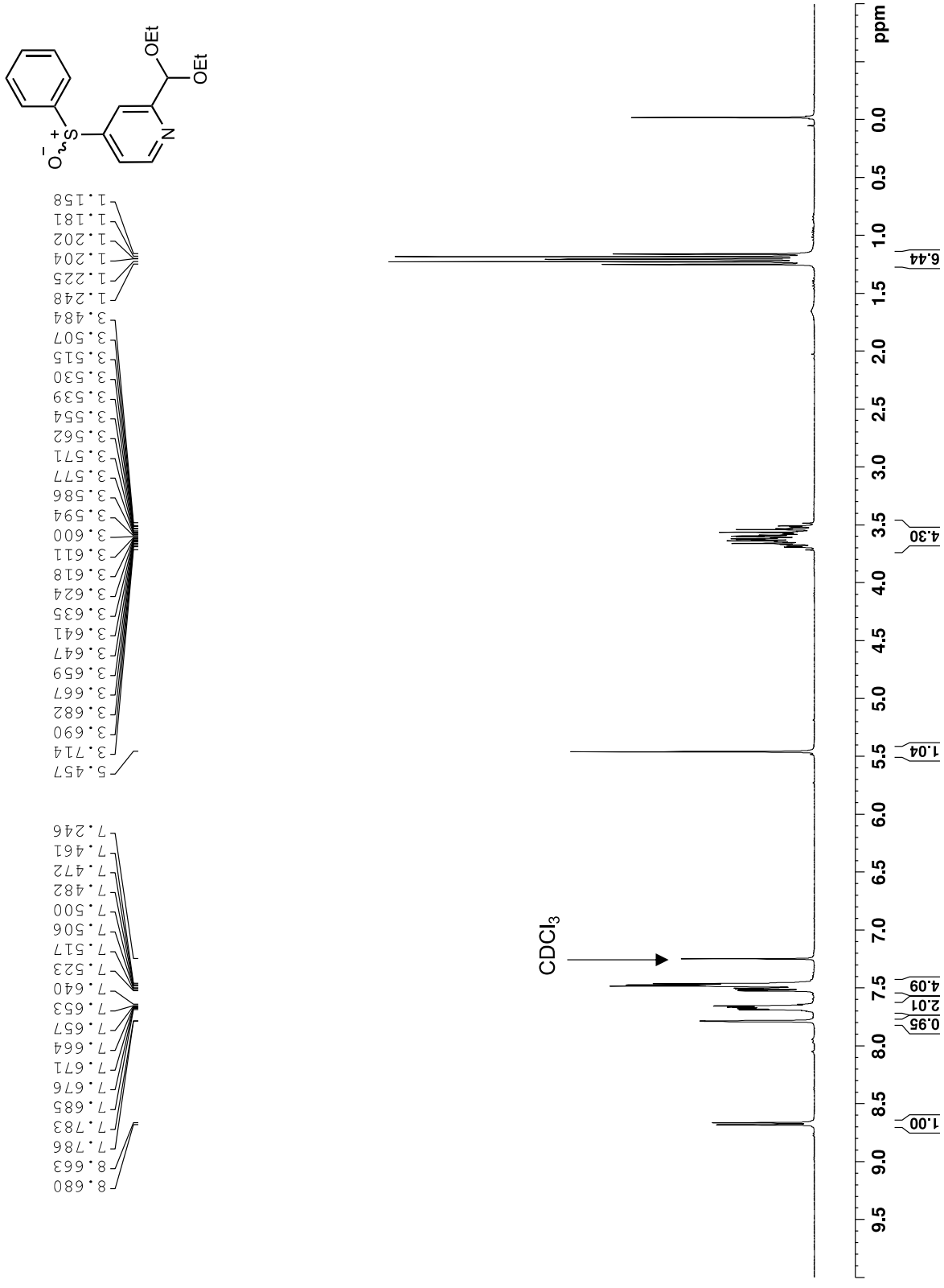

Spectrum 104. ^{1}H NMR of 2-(diethoxymethyl)-4-(phenylsulfinyl)pyridine (300 MHz, 293 K, $CDCl_3$).

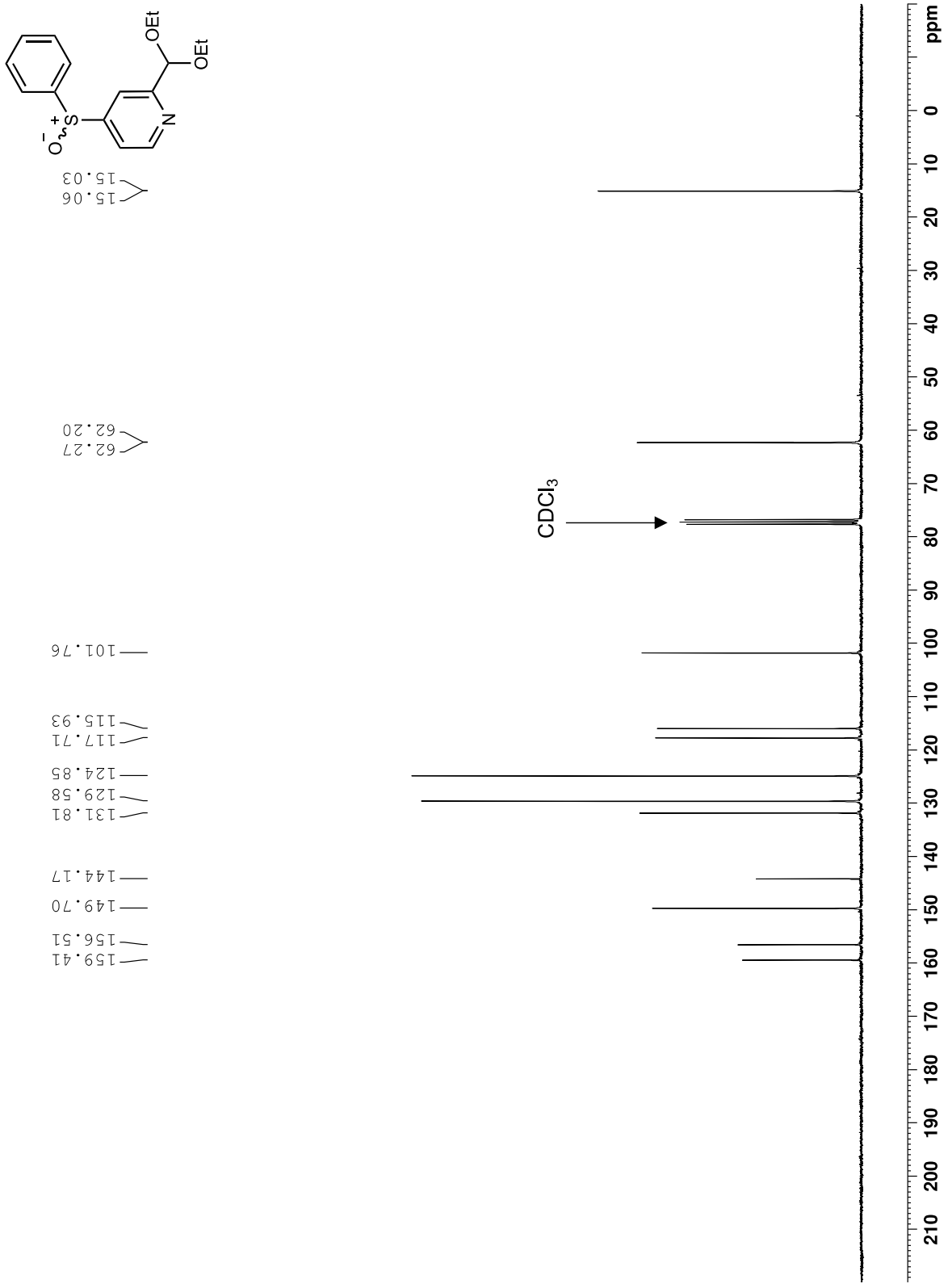

Spectrum 105. ^{13}C NMR of 2-(diethoxymethyl)-4-(phenylsulfinyl)pyridine (75 MHz, 293 K, $CDCl_3$).

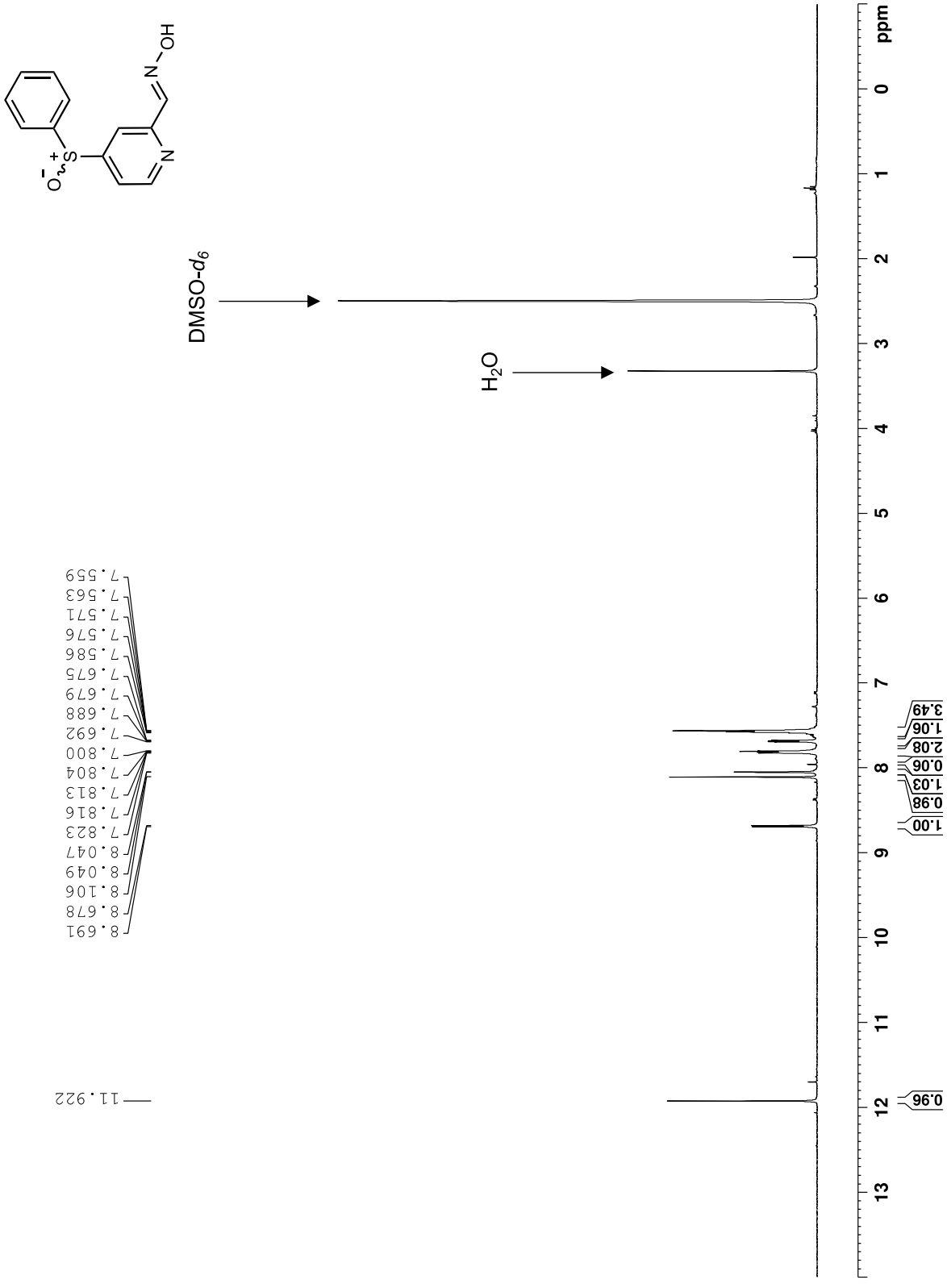

Spectrum 106. ^{1}H NMR of (*E*)-4-(phenylsulfinyl)picolinaldehyde oxime (400 MHz, 293 K, DMSO-d_6).

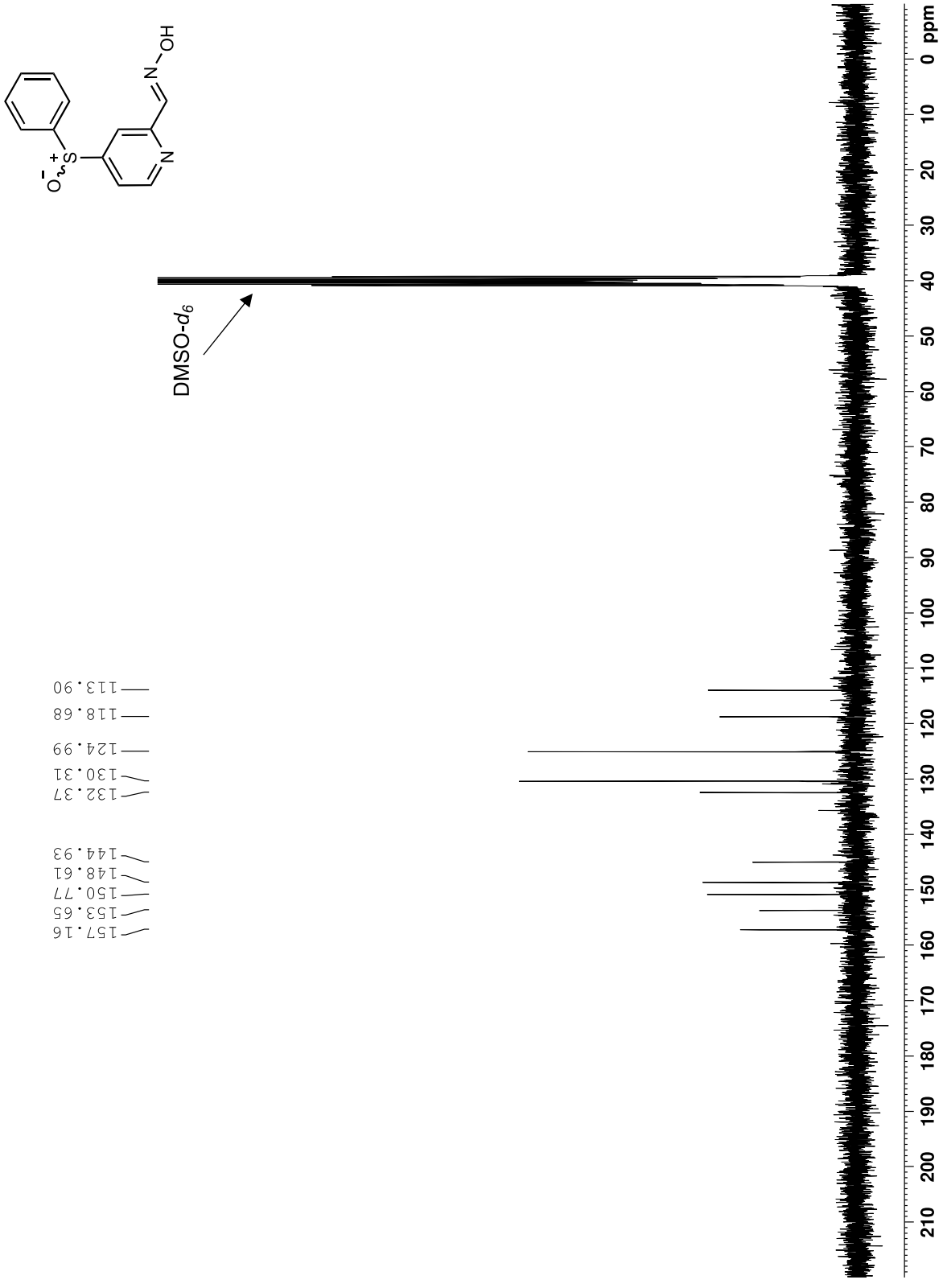

Spectrum 107. ^{13}C NMR of (*E*)-4-(phenylsulfinyl)picolinaldehyde oxime (75 MHz, 293 K, DMSO-d_6).

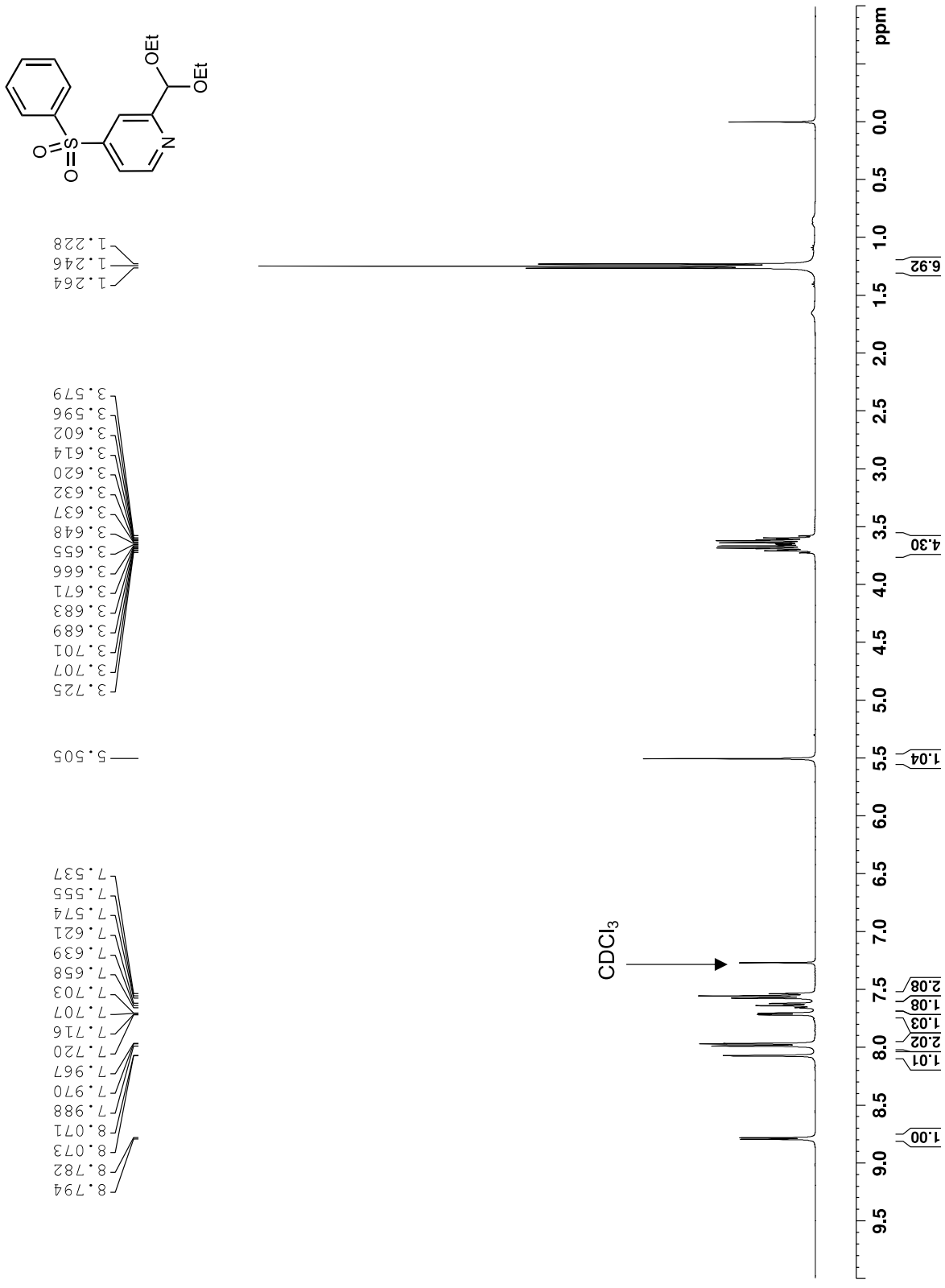

Spectrum 108. ^{1}H NMR of 2-(diethoxymethyl)-4-(phenylsulfonyl)pyridine (400 MHz, 293 K, $CDCl_3$).

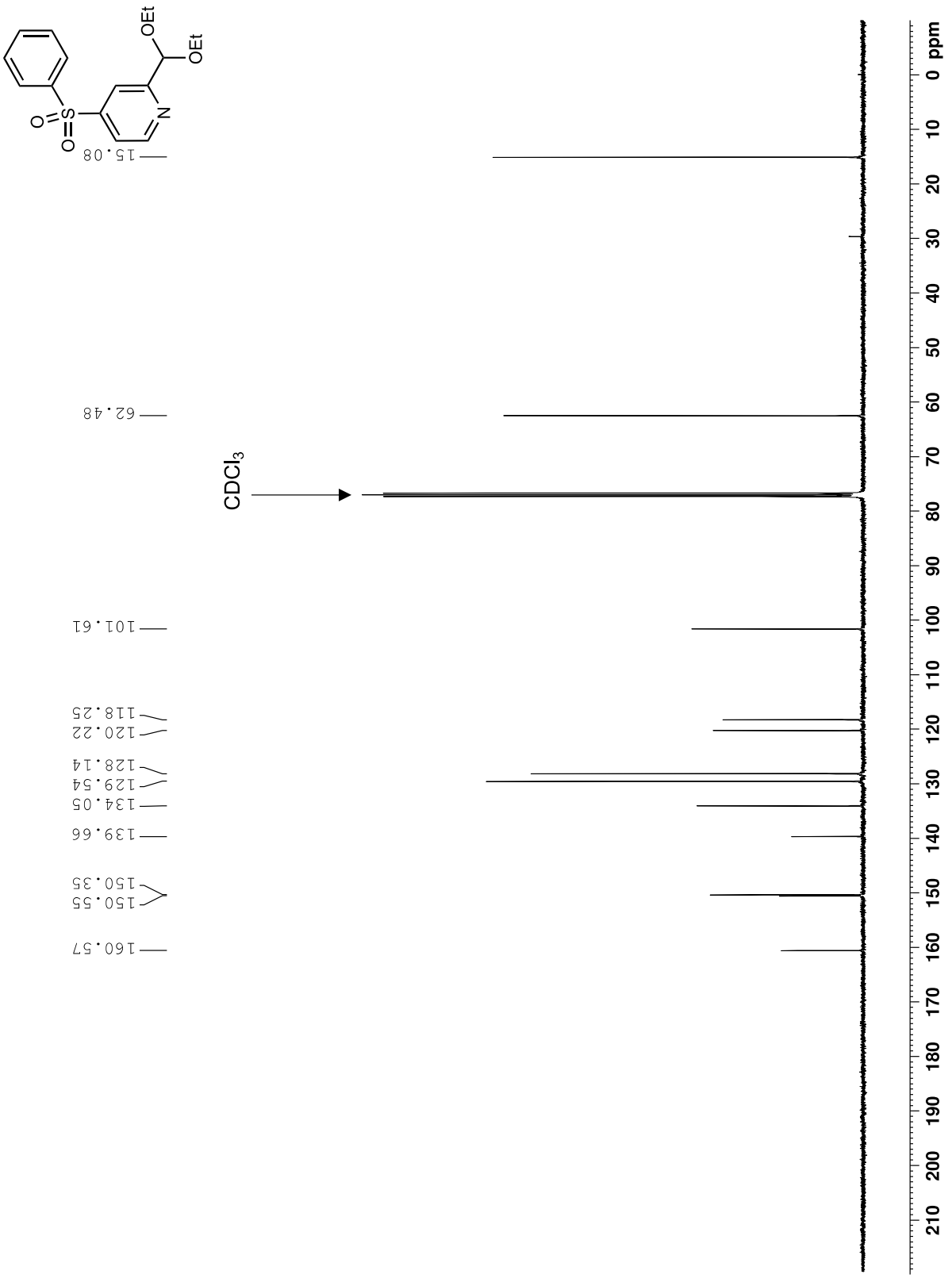

Spectrum 109. ^{13}C NMR of 2-(diethoxymethyl)-4-(phenylsulfonyl)pyridine (100 MHz, 293 K, $CDCl_3$).

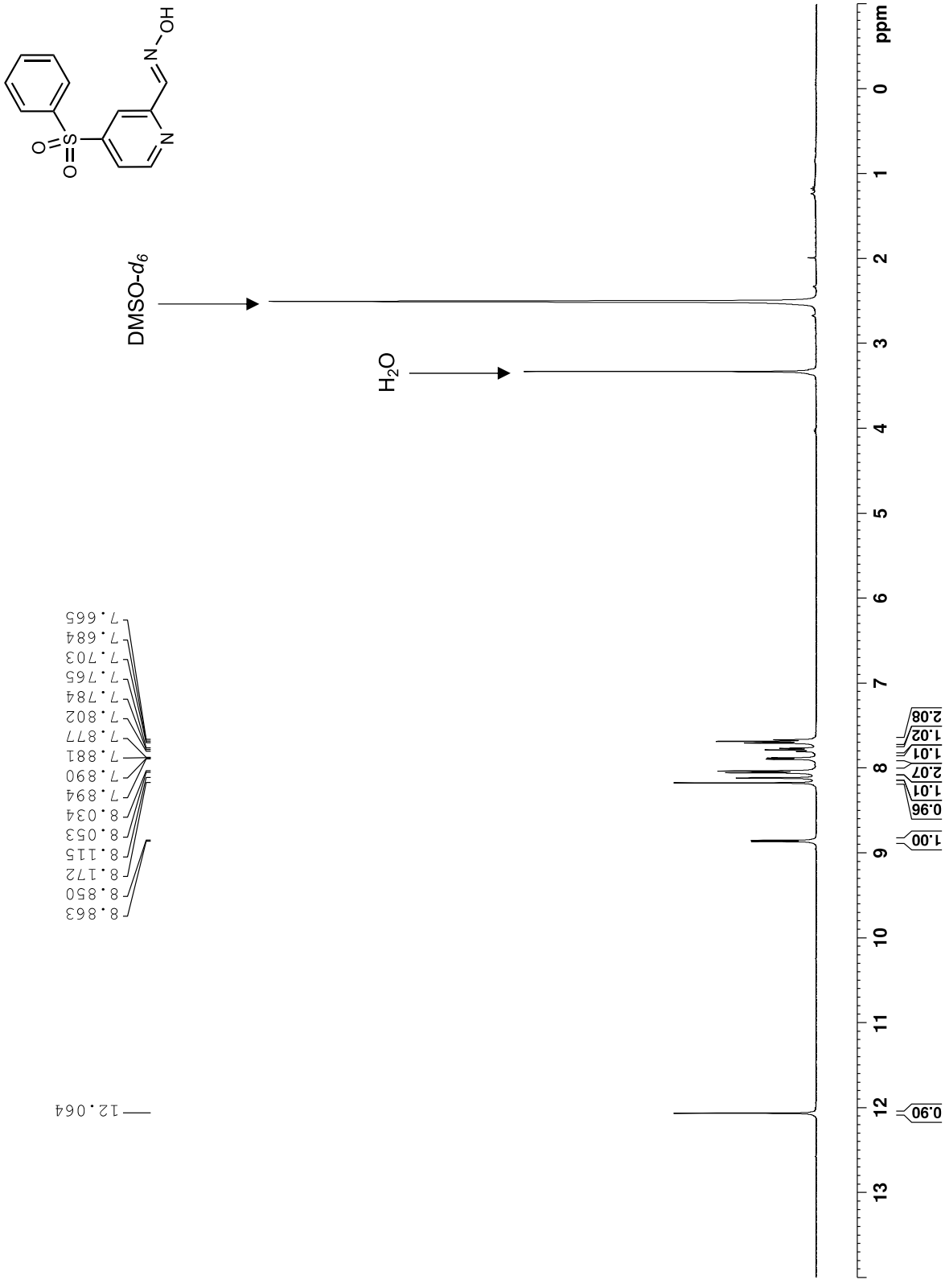

Spectrum 110. ^{1}H NMR of (*E*)-4-(phenylsulfonyl)picolinaldehyde oxime (400 MHz, 293 K, DMSO-d_6).

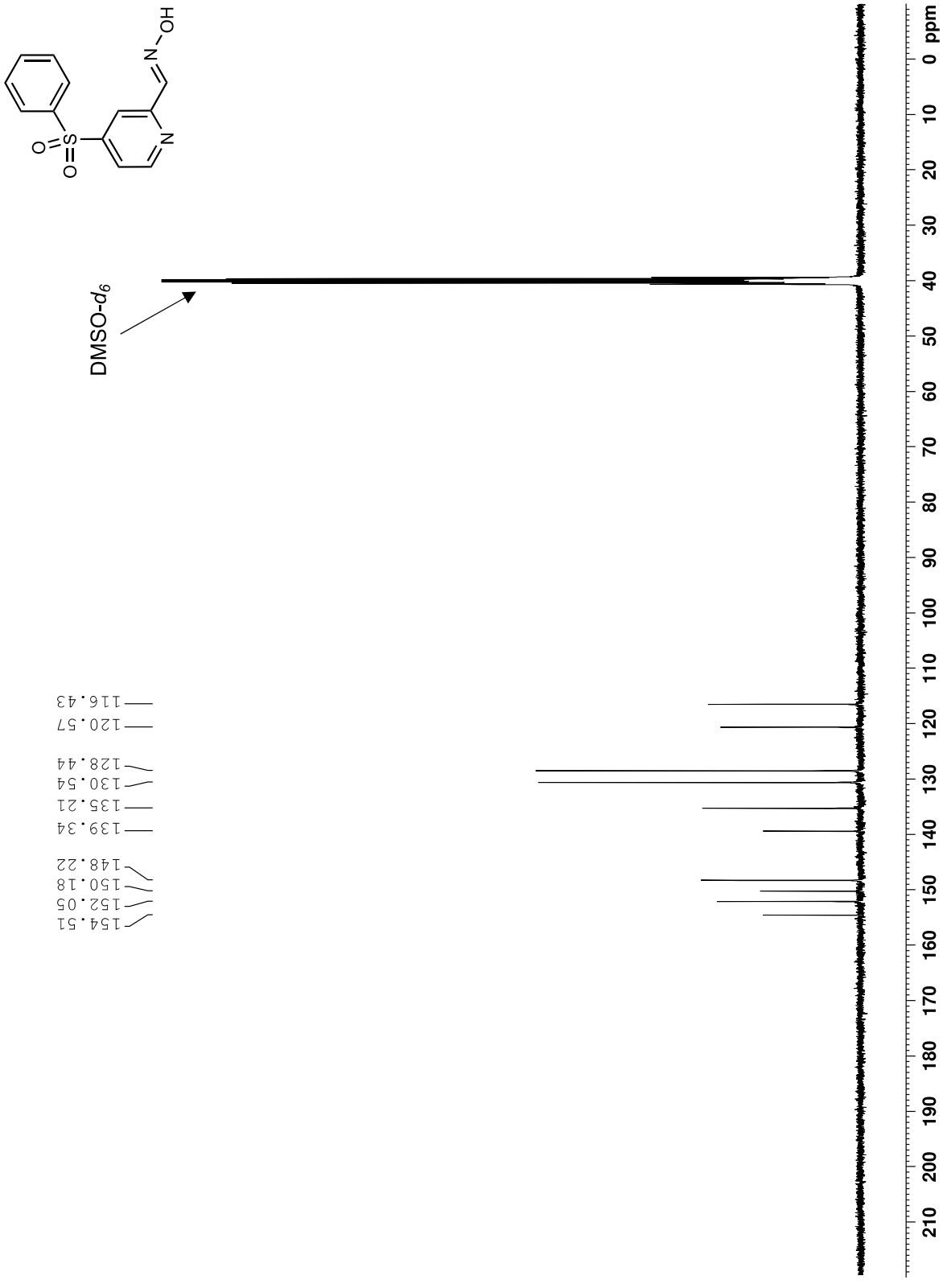

Spectrum 111. ^{13}C NMR of (*E*)-4-(phenylsulfonyl)picolinaldehyde oxime (100 MHz, 293 K, DMSO-d_6).

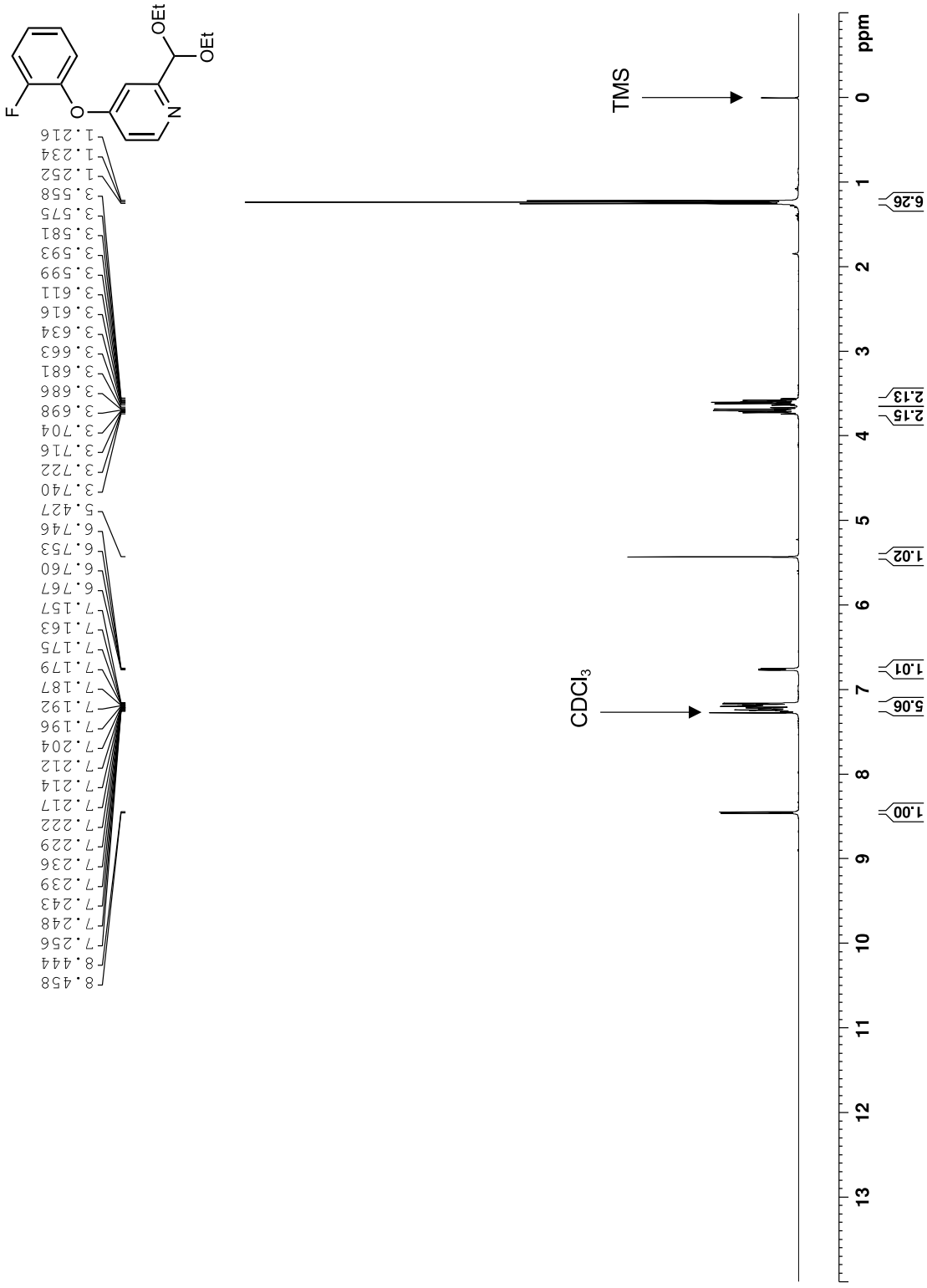

Spectrum 112. ^{1}H NMR of 2-(diethoxymethyl)-4-(2-fluorophenoxy)pyridine (400 MHz, 293 K, $CDCl_3$).

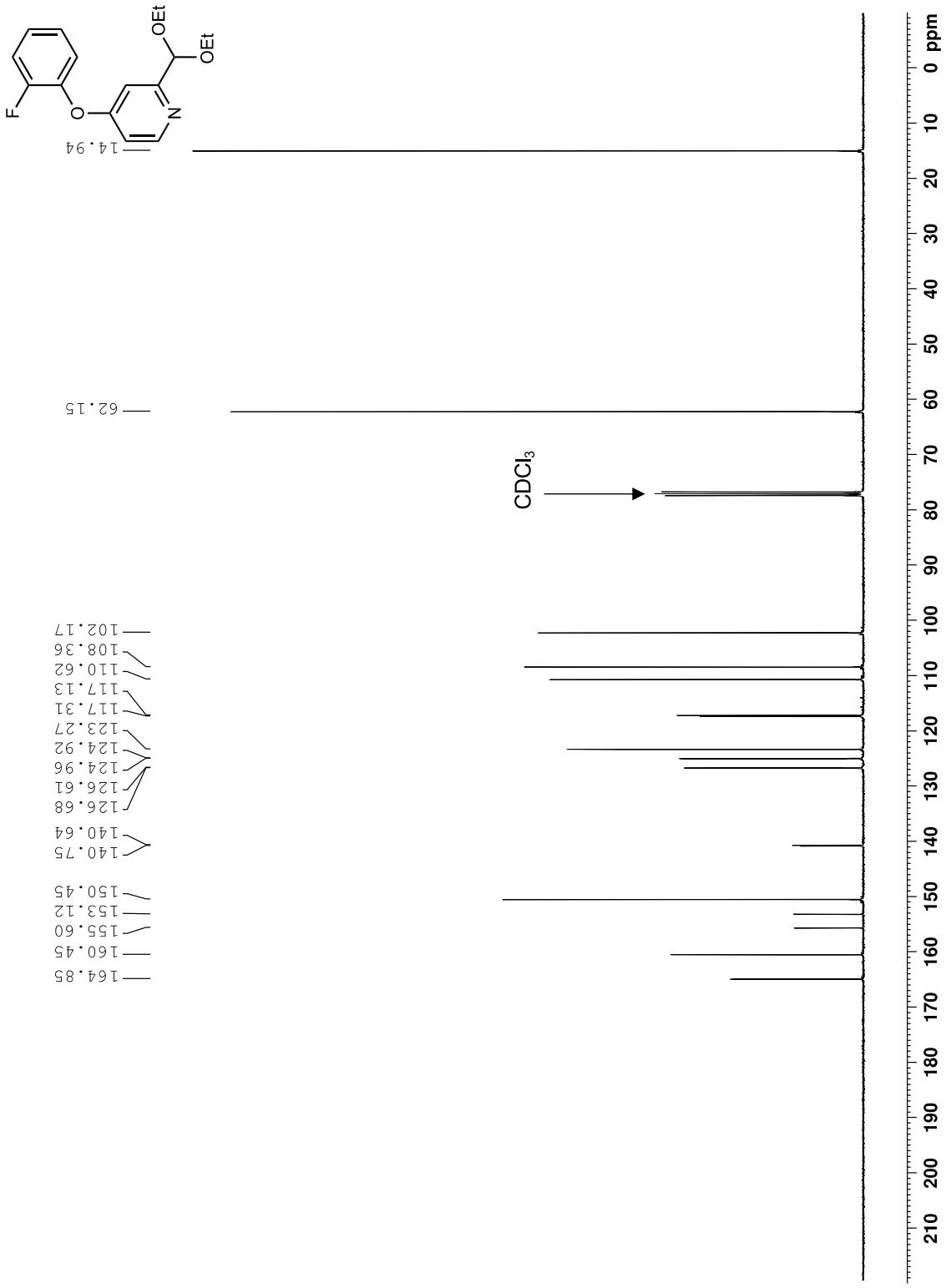

Spectrum 113. ^{13}C NMR of 2-(diethoxymethyl)-4-(2-fluorophenoxy)pyridine (100 MHz, 293 K, $CDCl_3$).

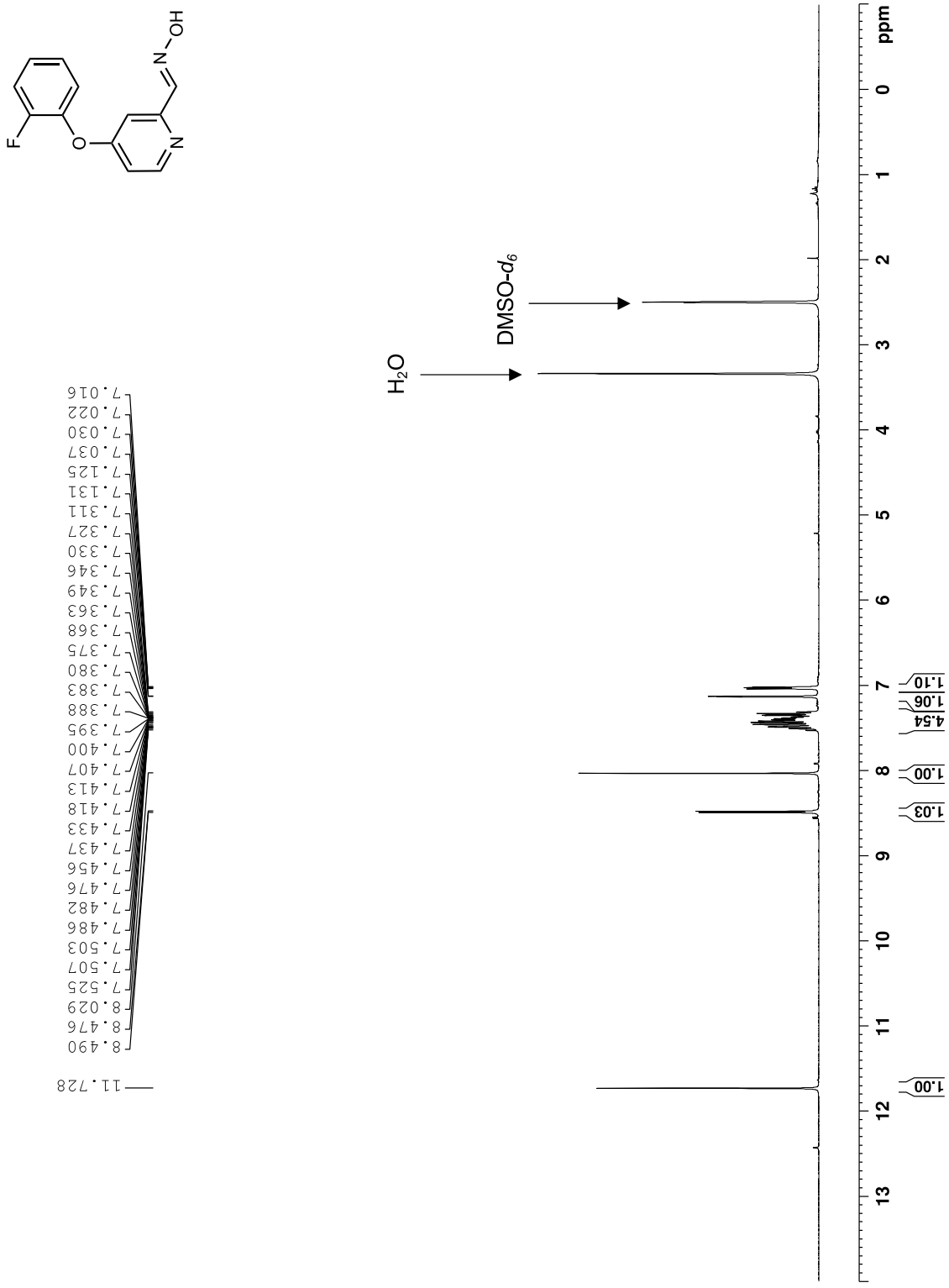

Spectrum 114. ^{1}H NMR of *(E)*-4-(2-fluorophenoxy)picolinaldehyde oxime (400 MHz, 293 K, DMSO-d_6).

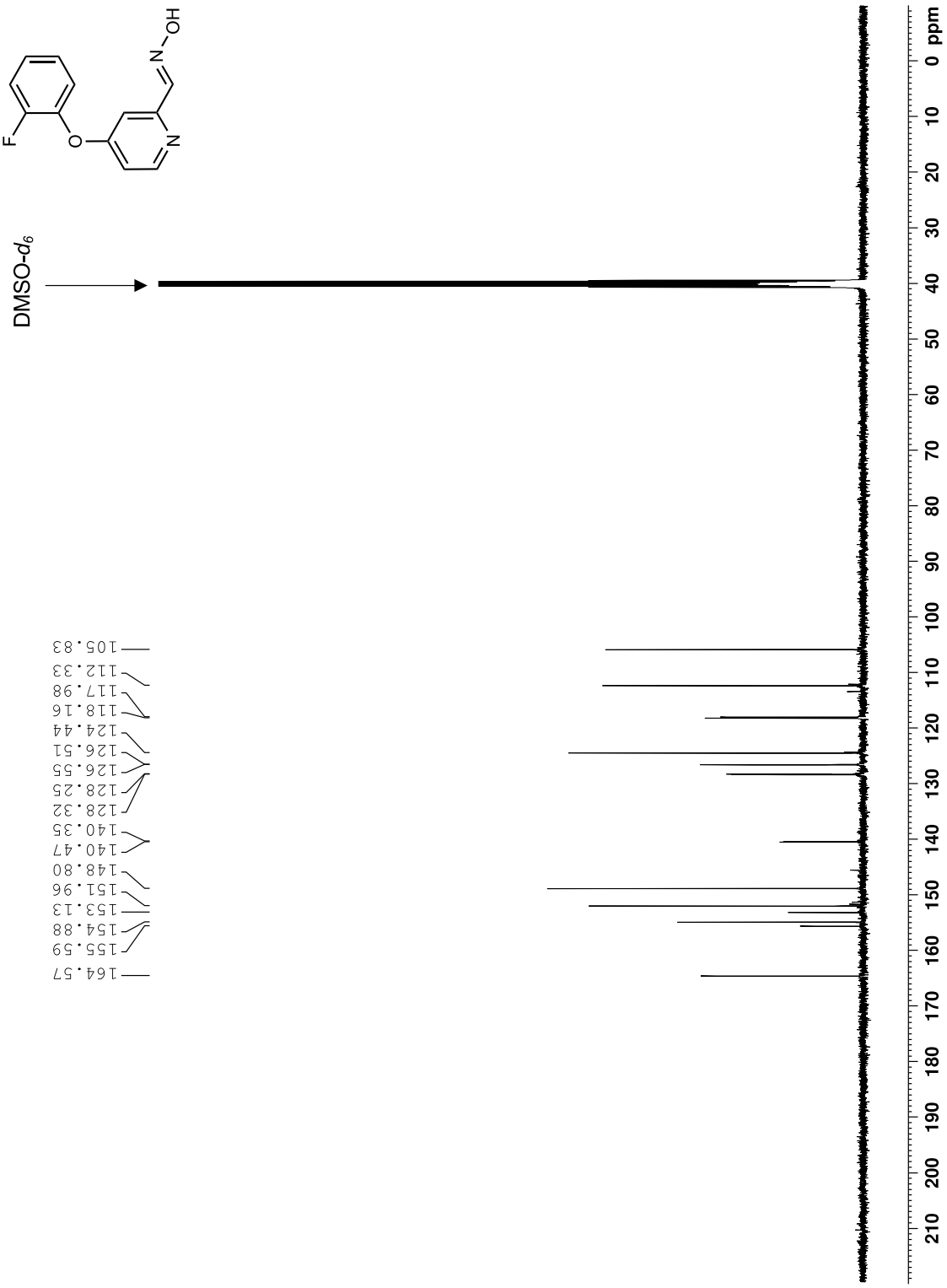

Spectrum 115. ^{13}C NMR of *(E)*-4-(2-fluorophenoxy)picolinaldehyde oxime (100 MHz, 293 K, DMSO-d_6).

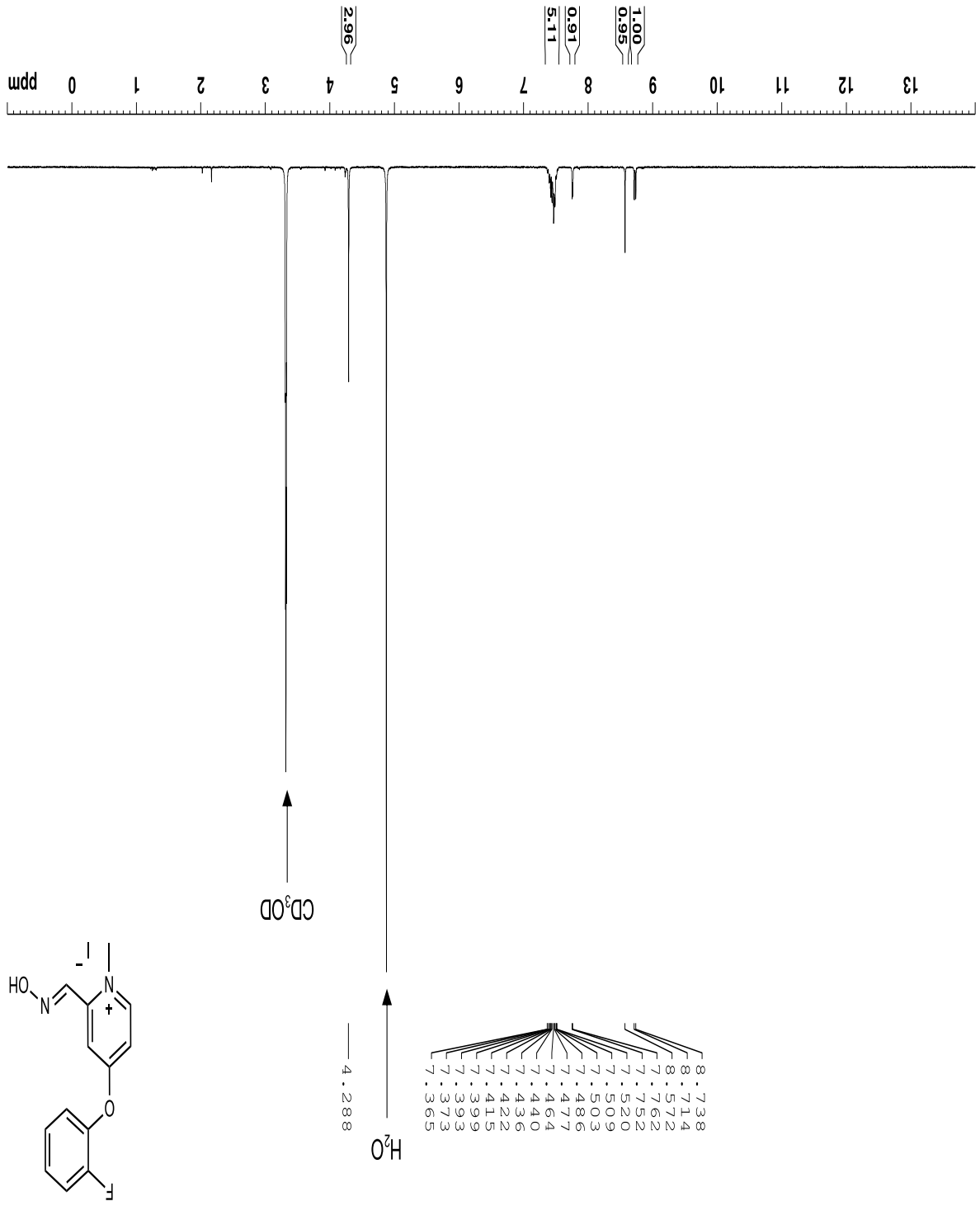

Spectrum 116. ^{1}H NMR of *(E)*-2-((hydroxyimino)methyl)-1-methyl-4-(2-fluorophenoxy)pyridin-1-ium iodide (**ADG3124**) (300 MHz, 293 K, CD_3OD).

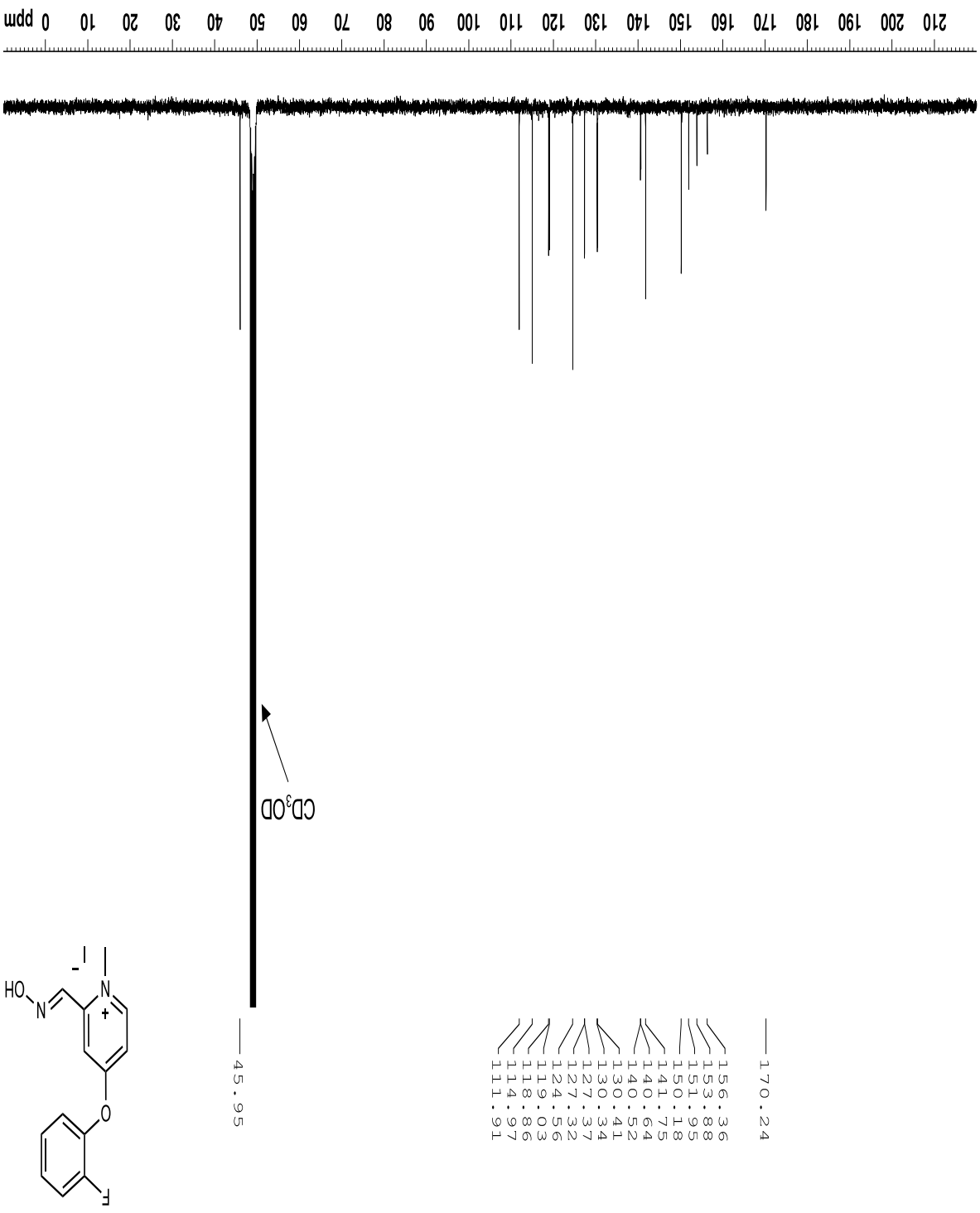

Spectrum 117. ^{13}C NMR of *(E)*-2-((hydroxyimino)methyl)-1-methyl-4-(2-fluorophenoxy)pyridin-1-ium iodide (**ADG3124**) (100 MHz, 293 K, CD_3OD).

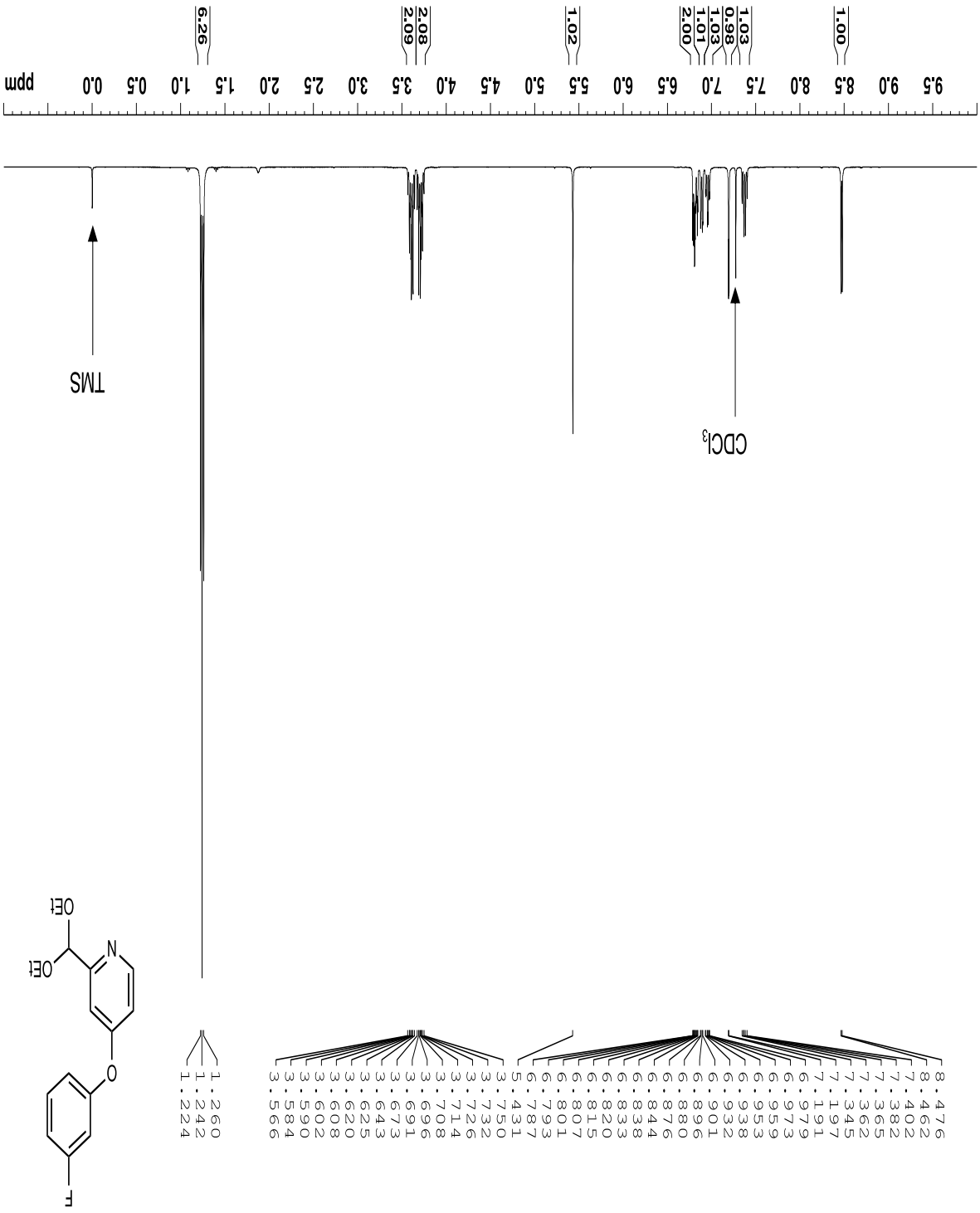

Spectrum 118. ^{1}H NMR of 2-(diethoxymethyl)-4-(3-fluorophenoxy)pyridine (400 MHz, 293 K, $CDCl_3$).

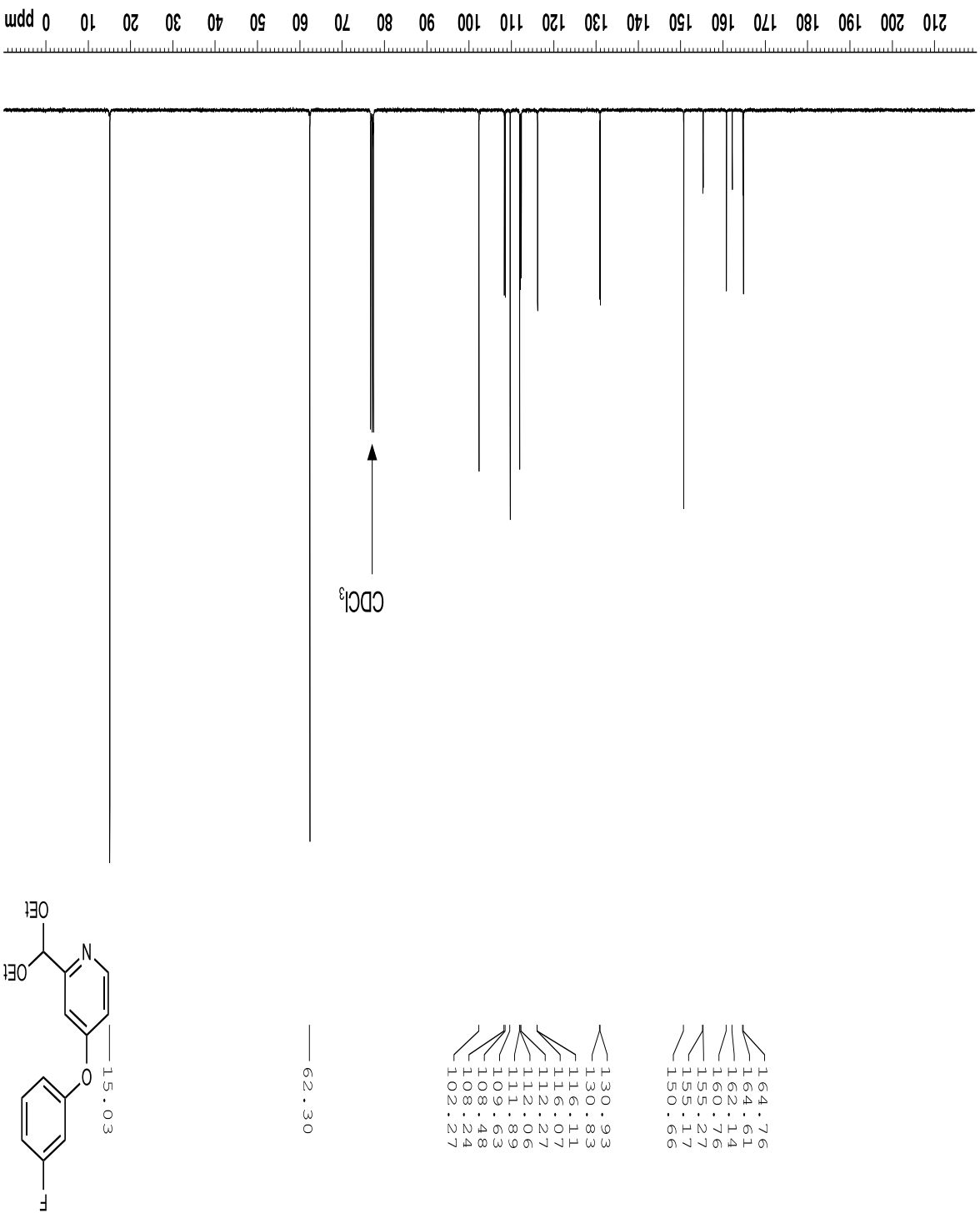

Spectrum 119. ^{13}C NMR of 2-(diethoxymethyl)-4-(3-fluorophenoxy)pyridine (100 MHz, 293 K, $CDCl_3$).

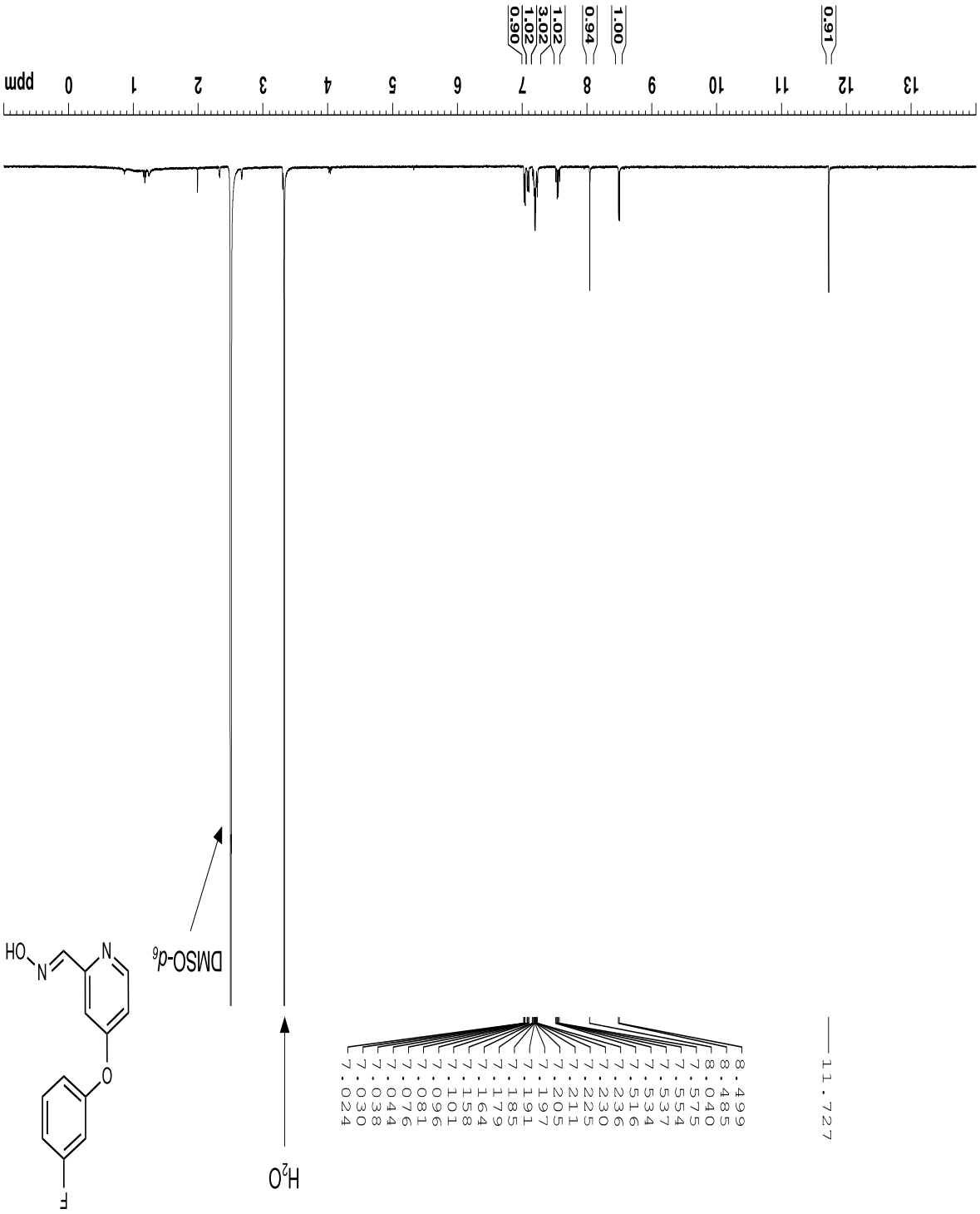

Spectrum 120. ^{1}H NMR of *(E)*-4-(3-fluorophenoxy)picolinaldehyde oxime (400 MHz, 293 K, DMSO-d_6).

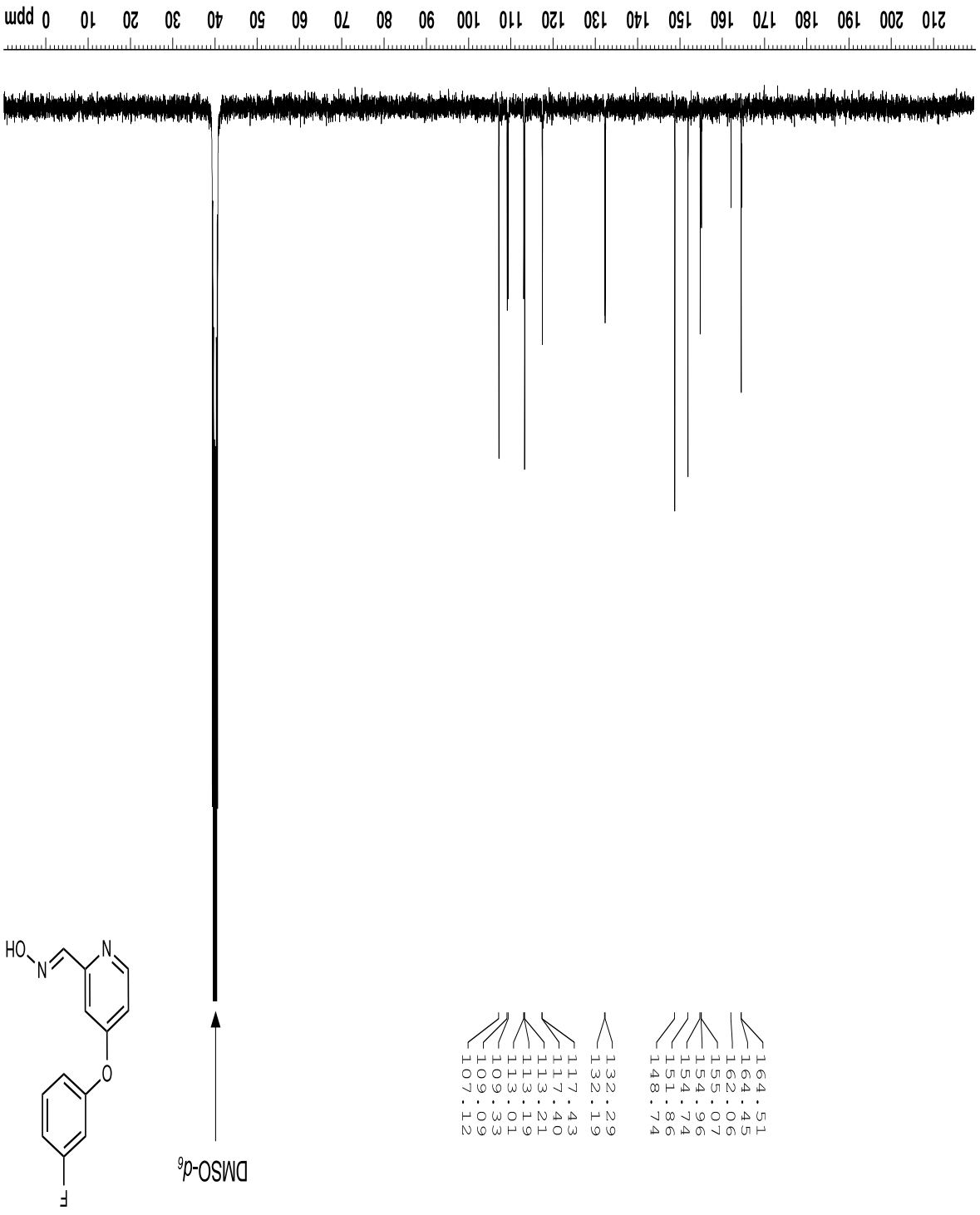

Spectrum 121. ^{13}C NMR of *(E)*-4-(3-fluorophenoxy)picolinaldehyde oxime (100 MHz, 293 K, DMSO-d_6).

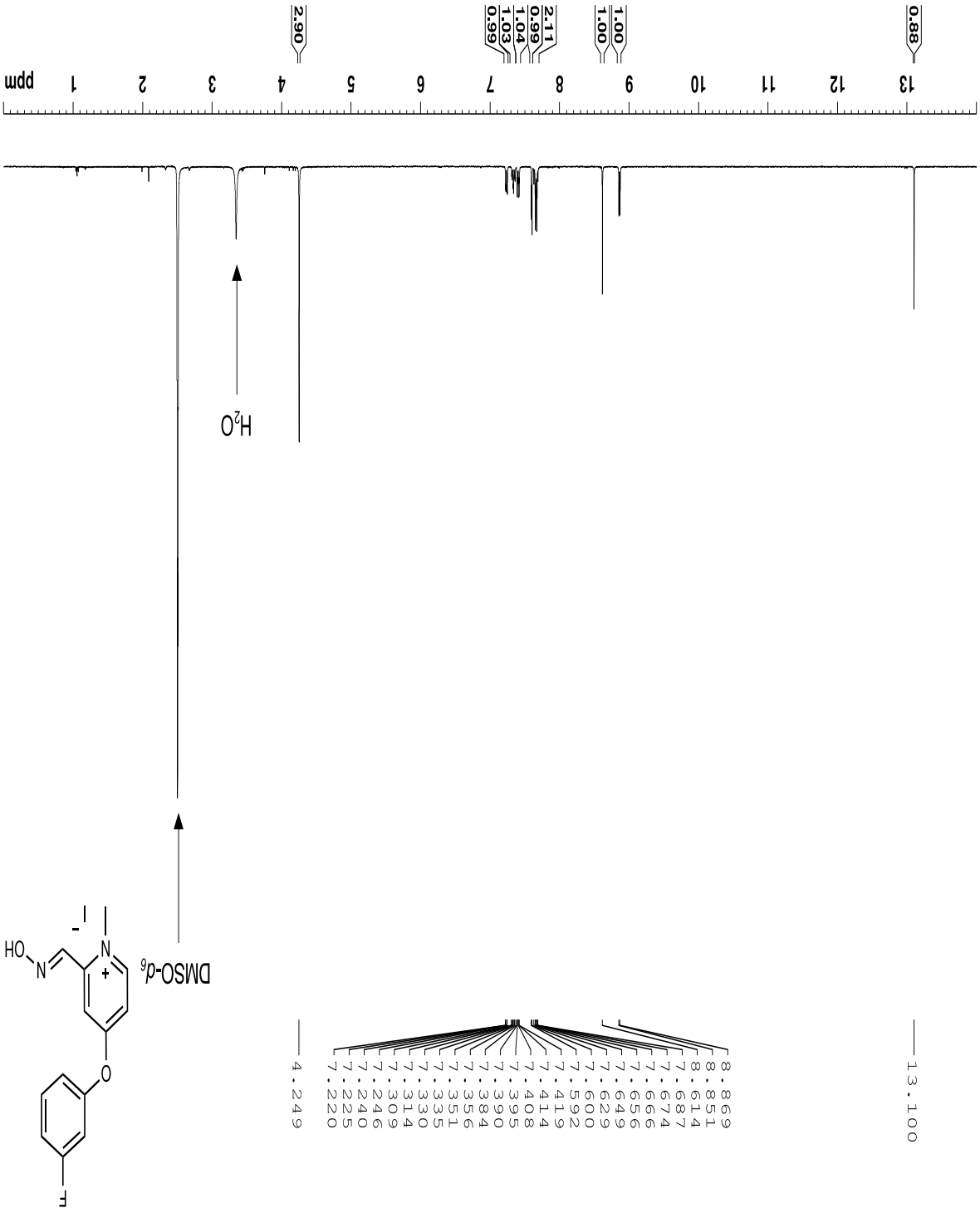

Spectrum 122. ^{1}H NMR of *(E)*-2-((hydroxyimino)methyl)-1-methyl-4-(3-fluorophenoxy)pyridin-1-ium iodide (**ADG3123**) (400 MHz, 293 K, DMSO-d_6).

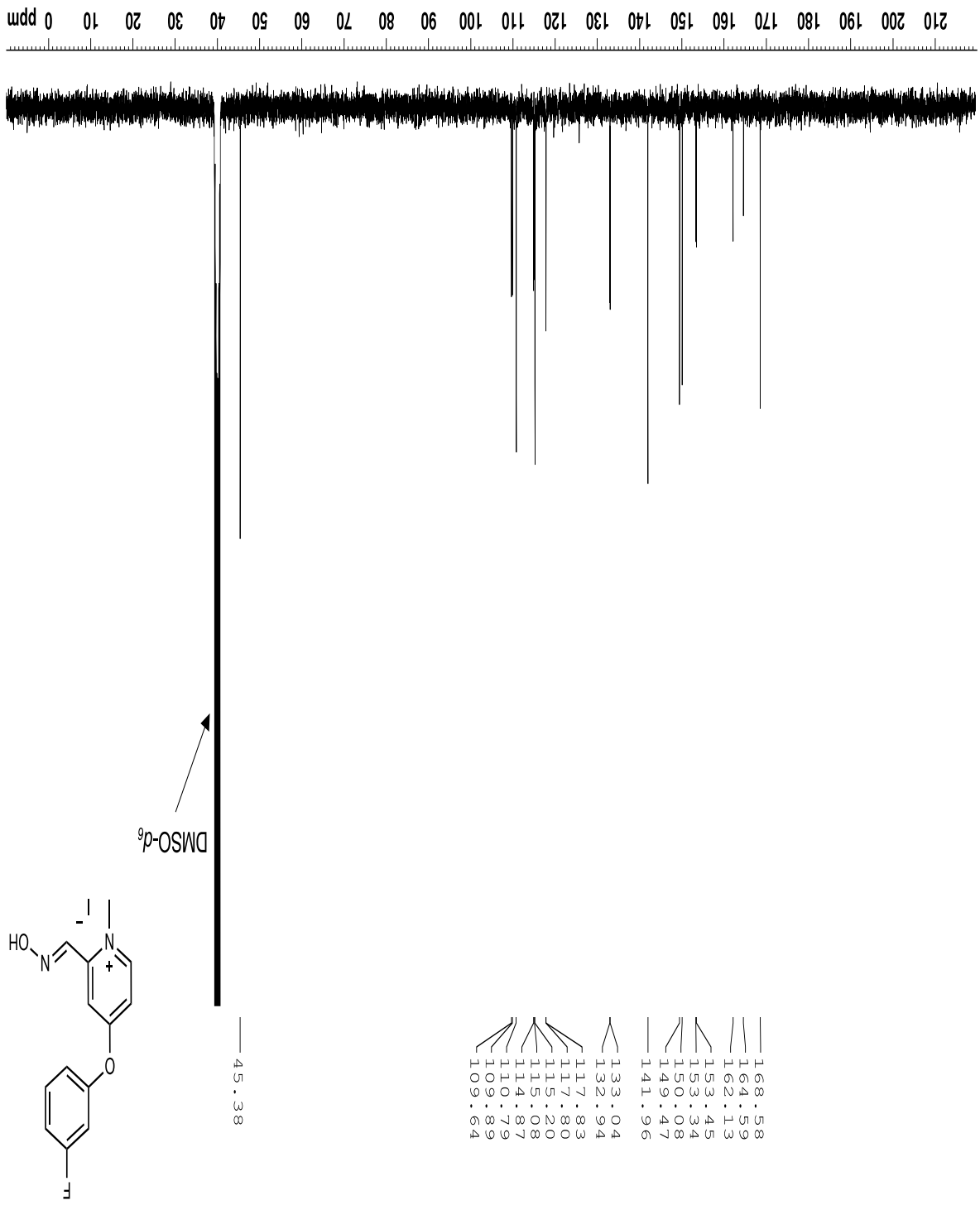

Spectrum 123. ^{13}C NMR of *(E)*-2-((hydroxyimino)methyl)-1-methyl-4-(3-fluorophenoxy)pyridin-1-ium iodide (**ADG3123**) (100 MHz, 293 K, DMSO-d_6).

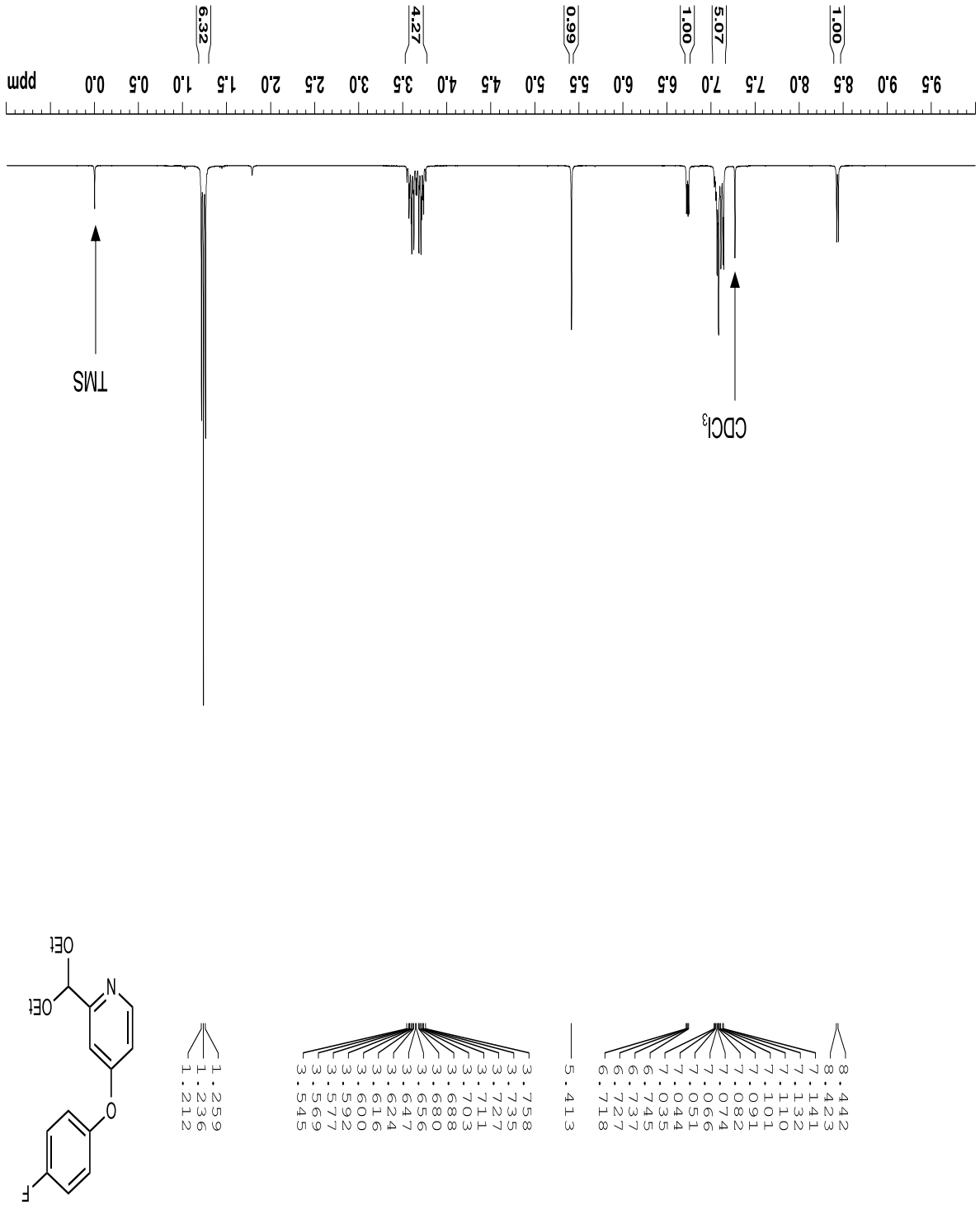

Spectrum 124. ^{1}H NMR of 2-(diethoxymethyl)-4-(4-fluorophenoxy)pyridine (300 MHz, 293 K, $CDCl_3$).

Spectrum 125. ^{13}C NMR of 2-(diethoxymethyl)-4-(4-fluorophenoxy)pyridine (100 MHz, 293 K, $CDCl_3$).

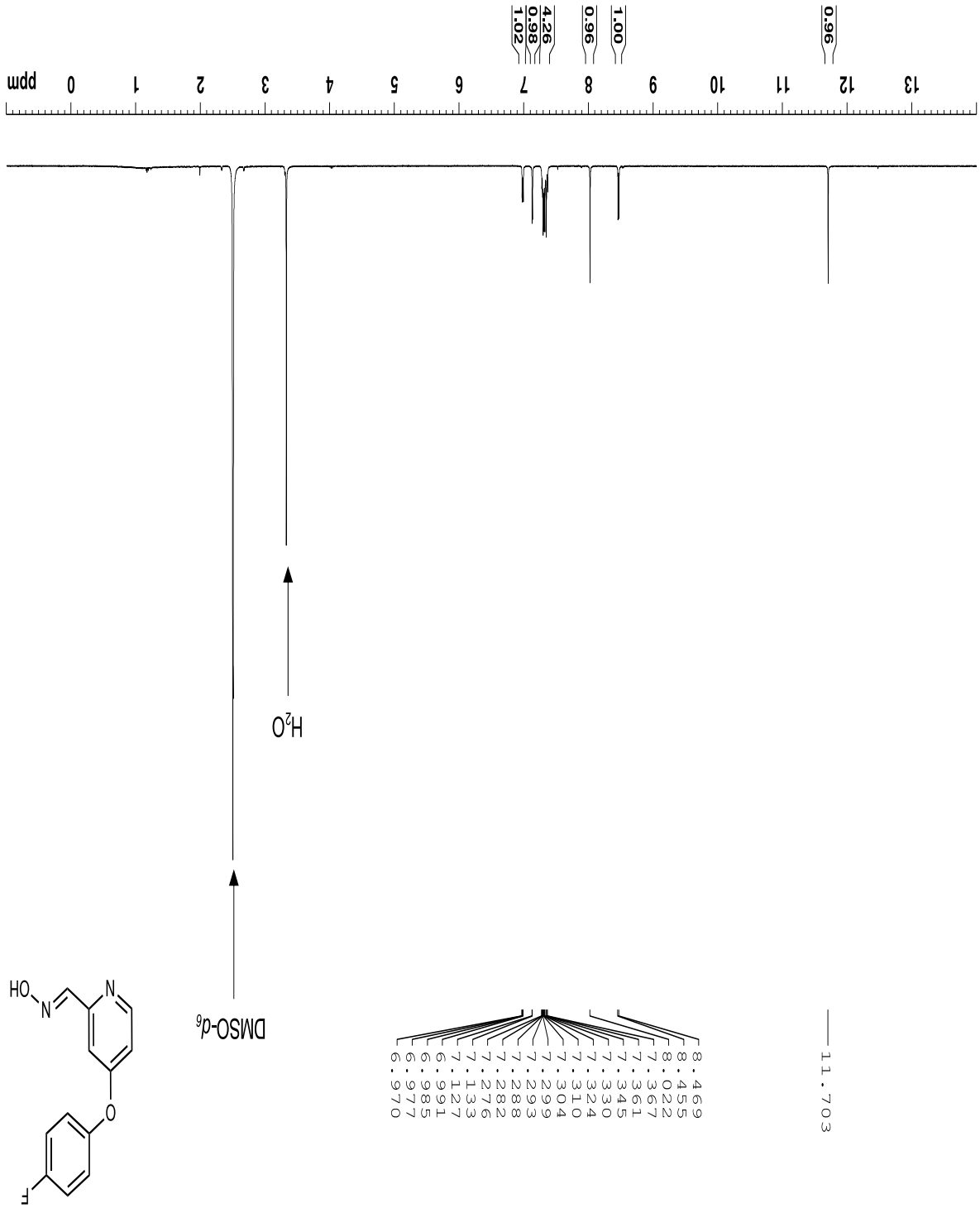

Spectrum 126. ^{1}H NMR of *(E)*-4-(4-fluorophenoxy)picolinaldehyde oxime (400 MHz, 293 K, DMSO-d_6).

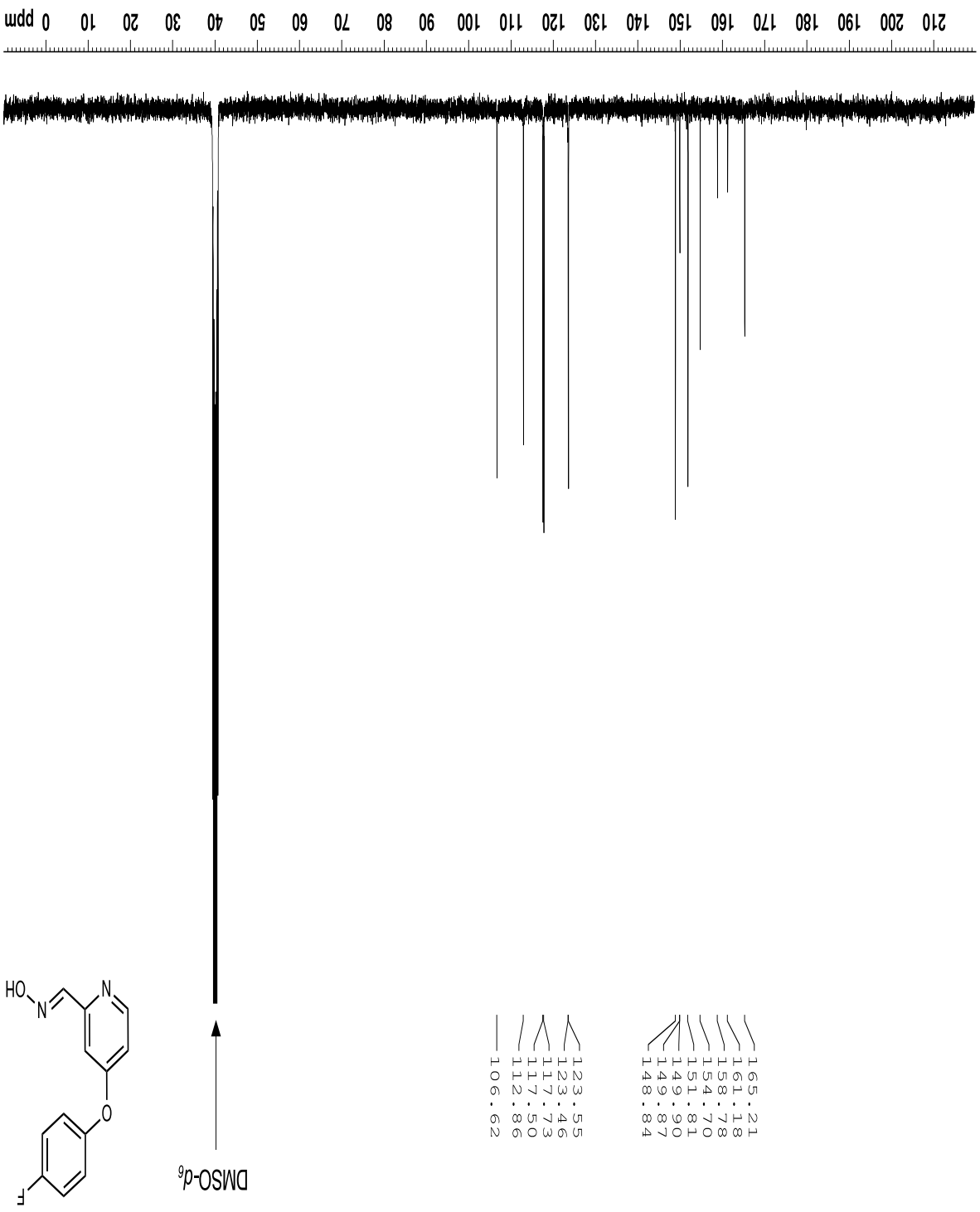

Spectrum 127. ^{13}C NMR of *(E)*-4-(4-fluorophenoxy)picolinaldehyde oxime (100 MHz, 293 K, DMSO-d_6).

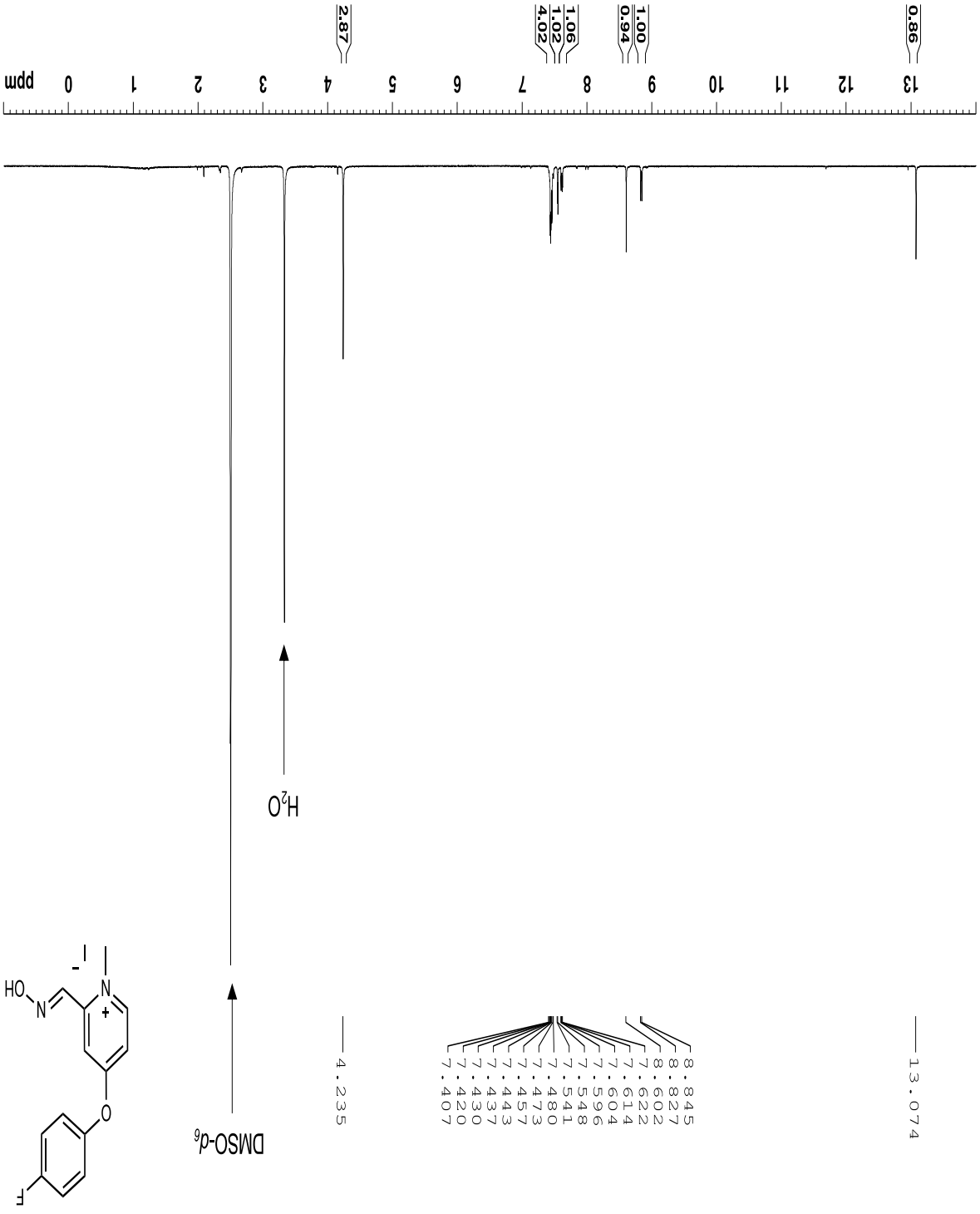

Spectrum 128. ^{1}H NMR of *(E)*-2-((hydroxyimino)methyl)-1-methyl-4-(4-fluorophenoxy)pyridin-1-ium iodide (**ADG3116**) (400 MHz, 293 K, DMSO-d_6).

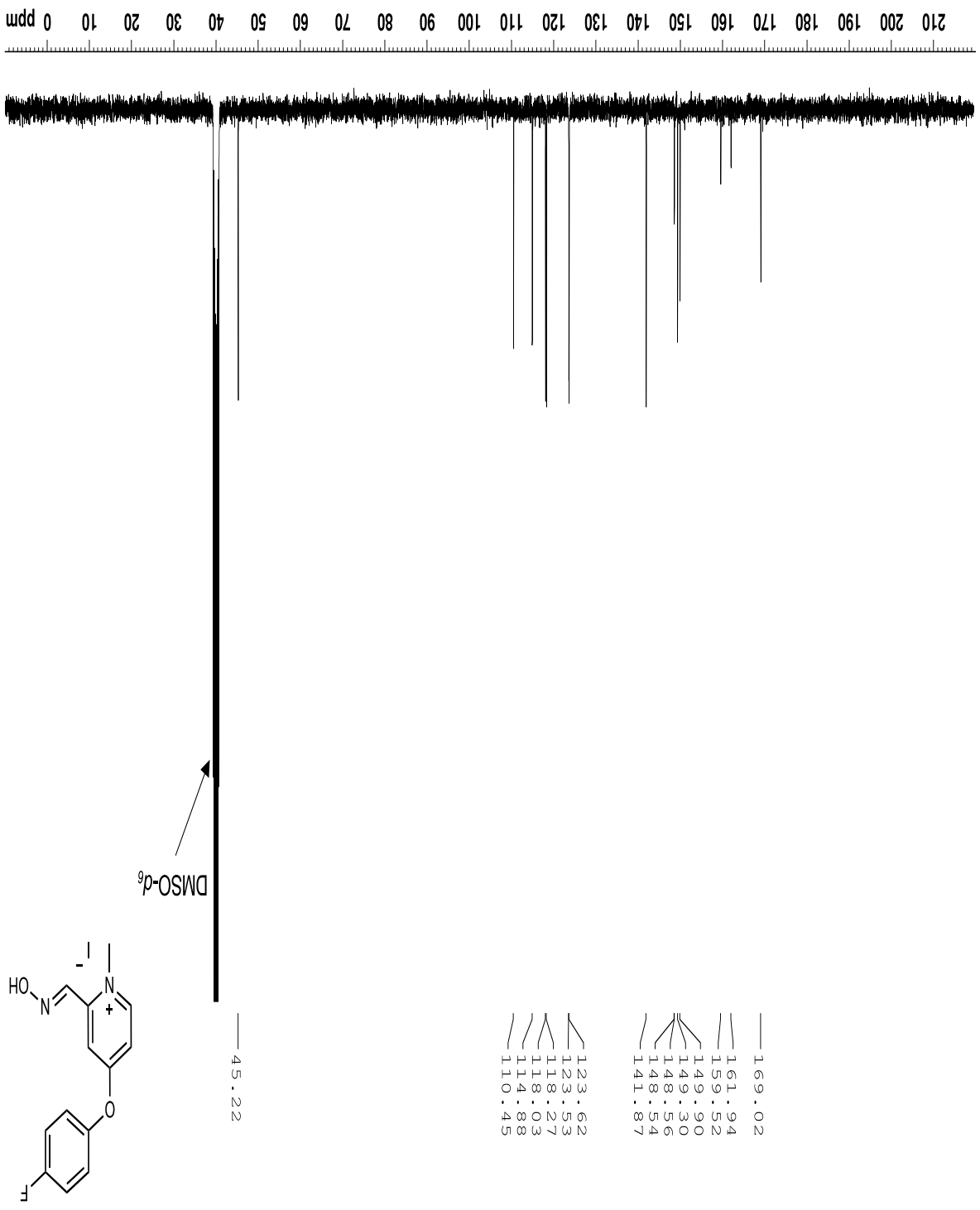

Spectrum 129. ^{13}C NMR of *(E)*-2-((hydroxyimino)methyl)-1-methyl-4-(4-fluorophenoxy)pyridin-1-ium iodide (**ADG3116**) (100 MHz, 293 K, DMSO-d_6).

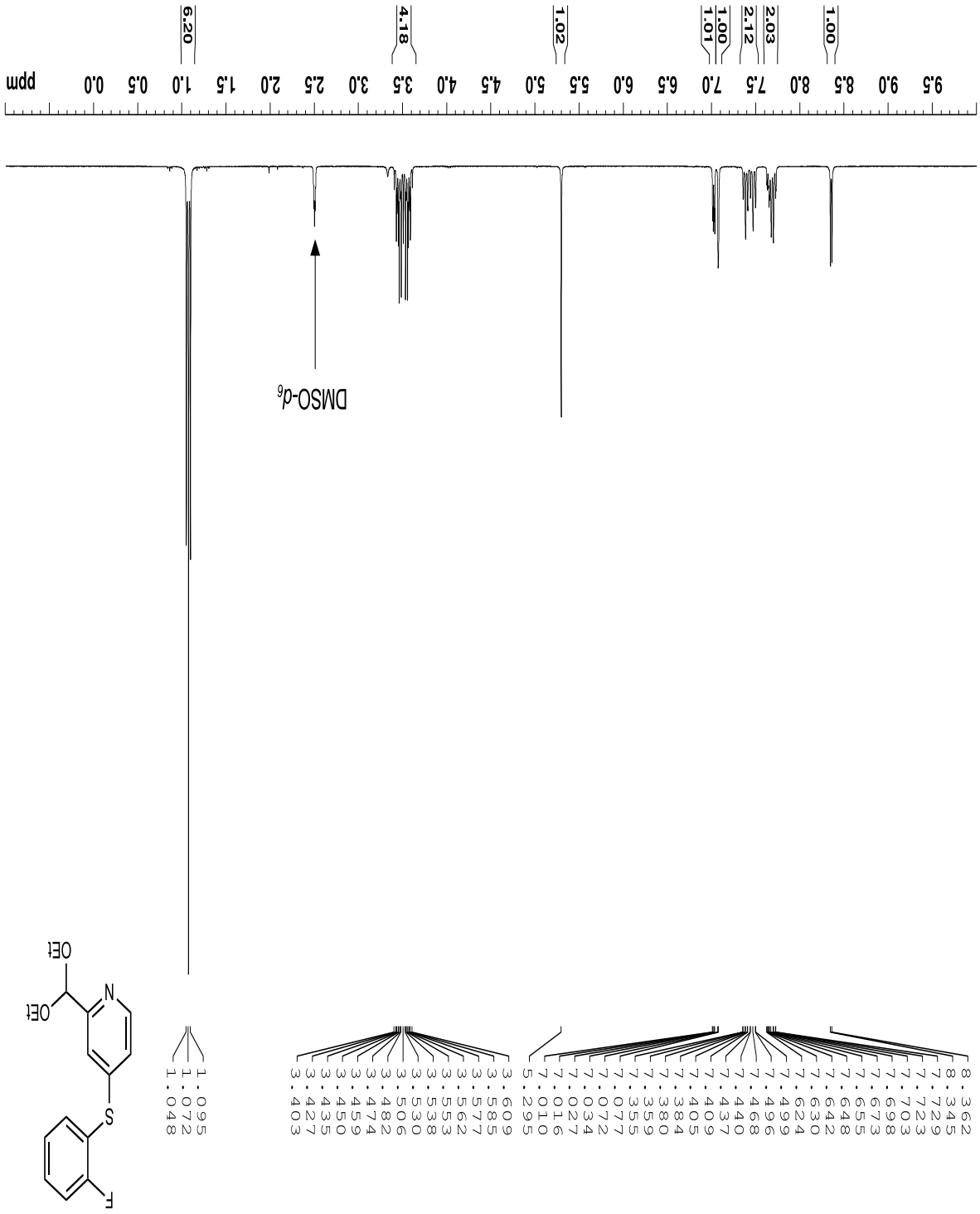

Spectrum 130. ^{1}H NMR of 2-(diethoxymethyl)-4-((2-fluorophenyl)thio)pyridine (300 MHz, 293 K, DMSO-d_6).

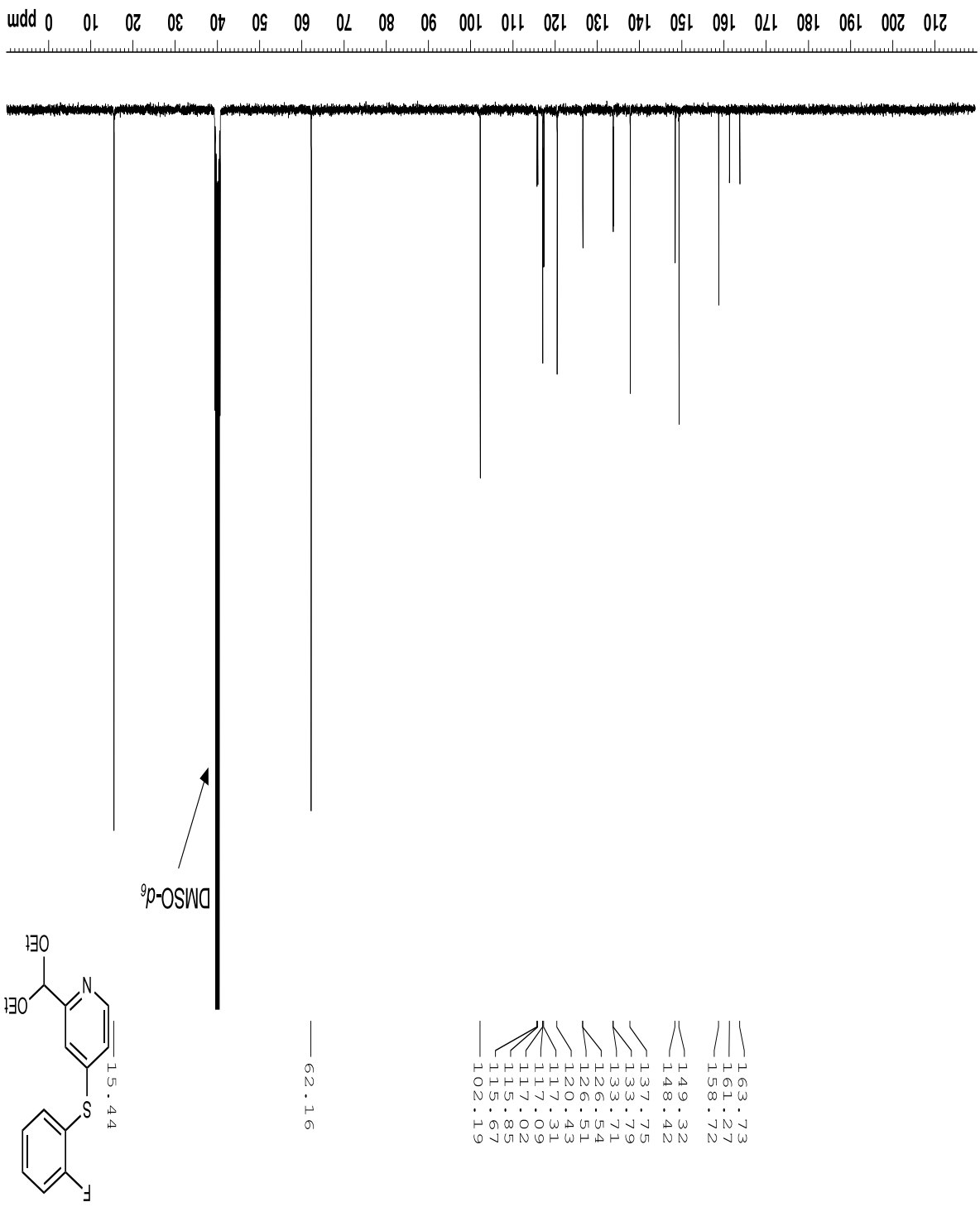

Spectrum 131. ^{13}C NMR of 2-(diethoxymethyl)-4-(4-fluorophenoxy)pyridine (100 MHz, 293 K, DMSO-d_6).

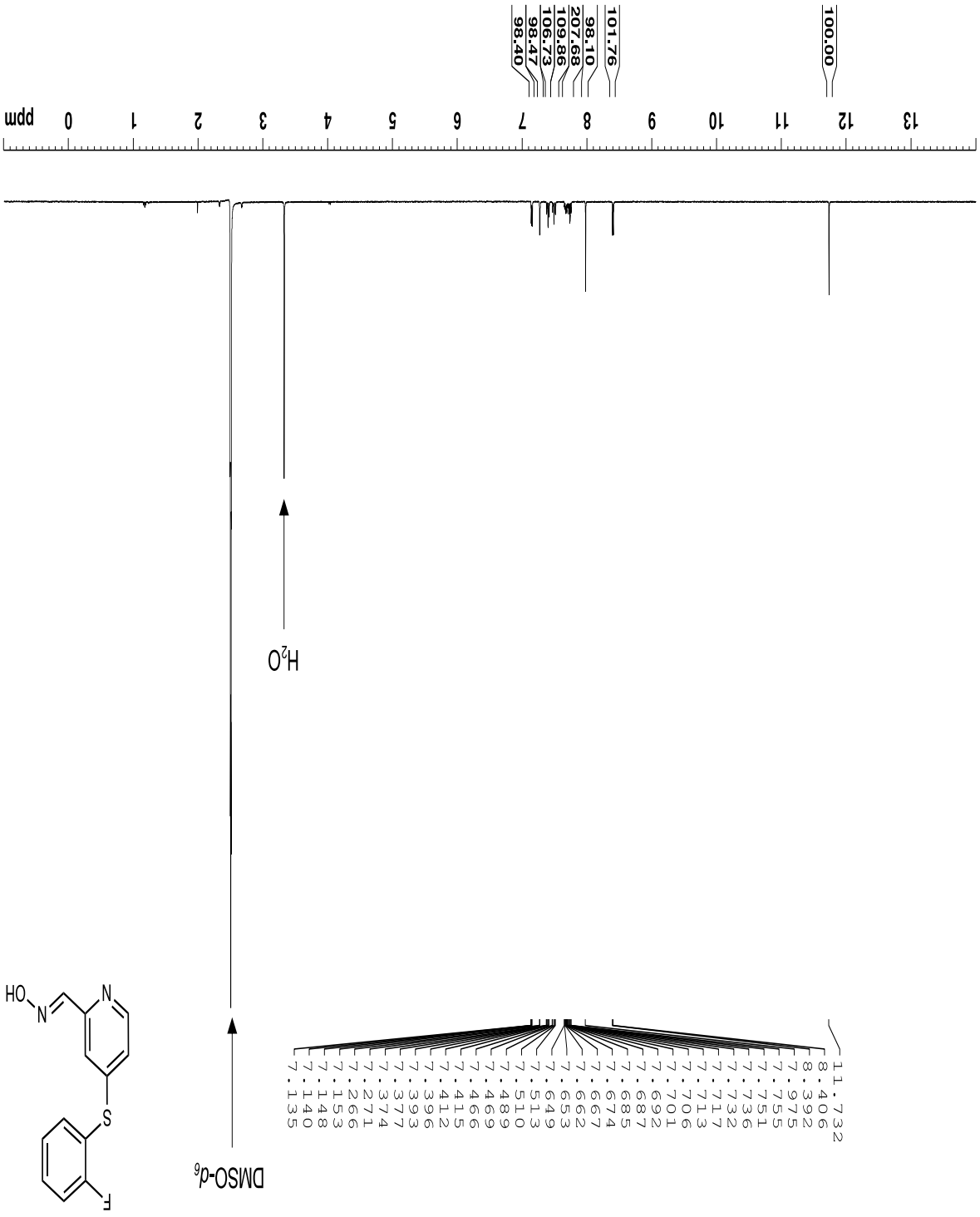

Spectrum 132. ^{1}H NMR of *(E)*-4-((2-fluorophenyl)thio)picolinaldehyde oxime (400 MHz, 293 K, DMSO-d_6).

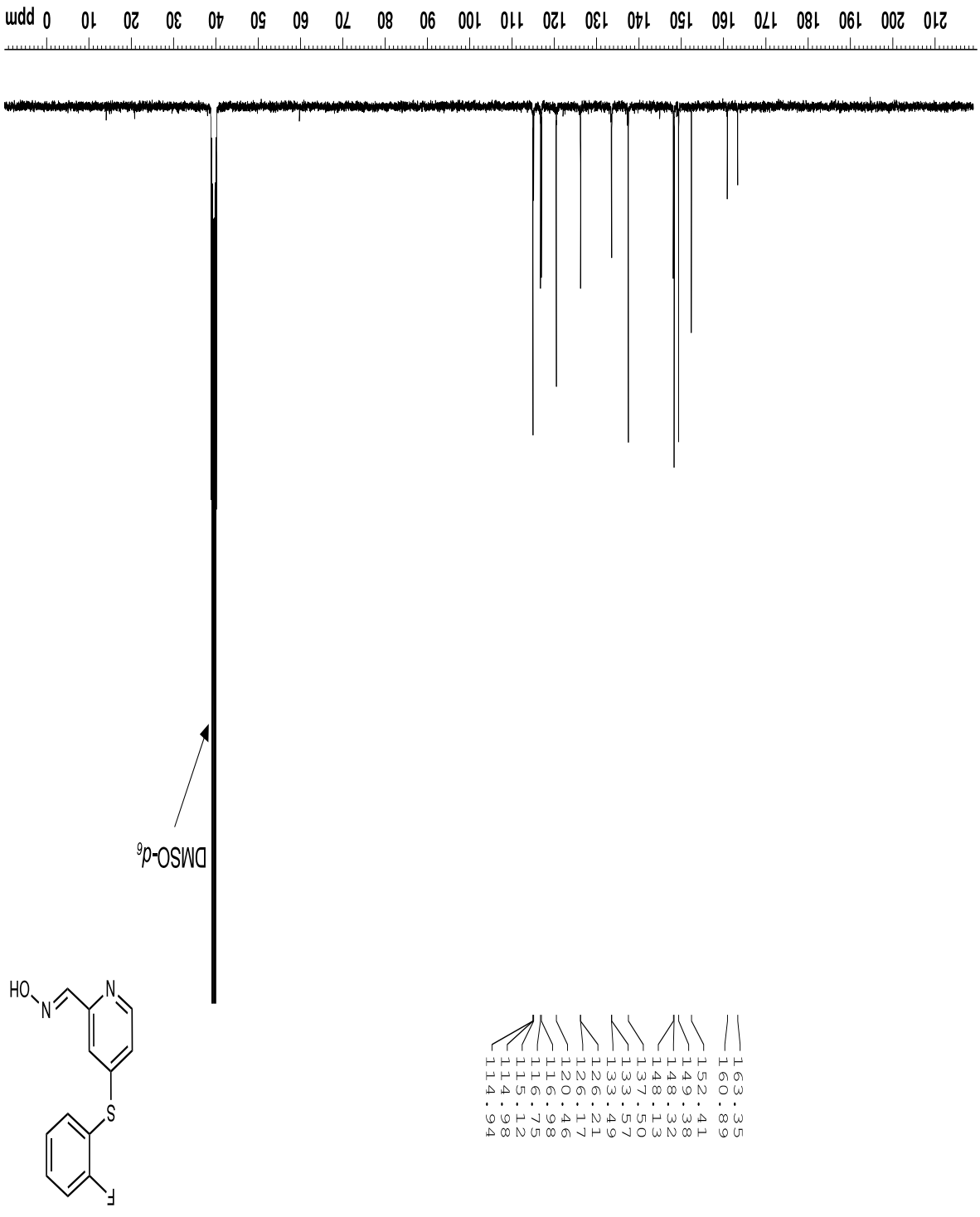

Spectrum 133. ^{13}C NMR of *(E)*-4-((2-fluorophenyl)thio)picolinaldehyde oxime (100 MHz, 293 K, DMSO-d_6).

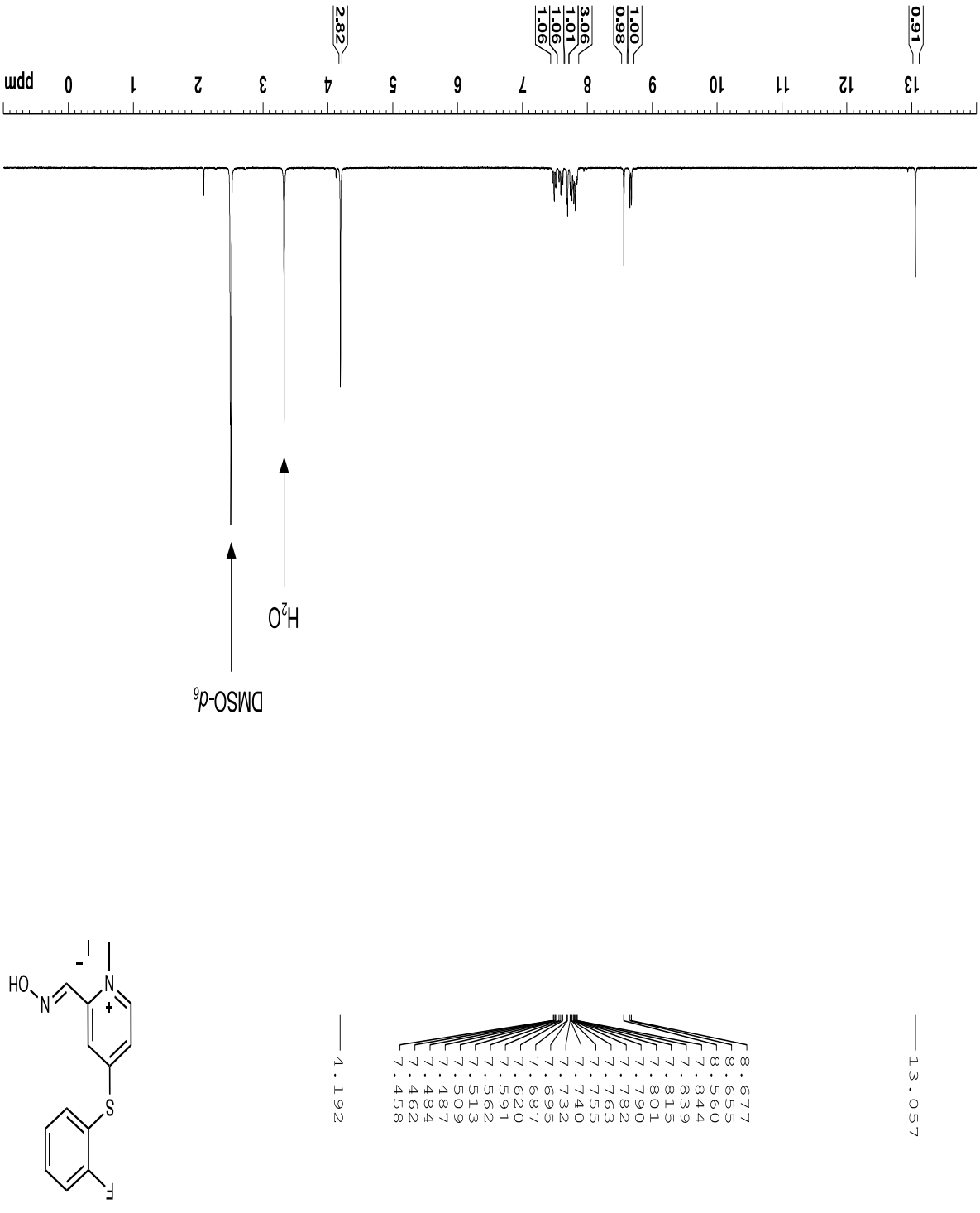

Spectrum 134. ^{1}H NMR of *(E)*-4-((2-fluorophenyl)thio)-2-((hydroxyimino)methyl)-1-methylpyridin-1-ium iodide (**ADG4158**) (300 MHz, 293 K, DMSO-d_6).

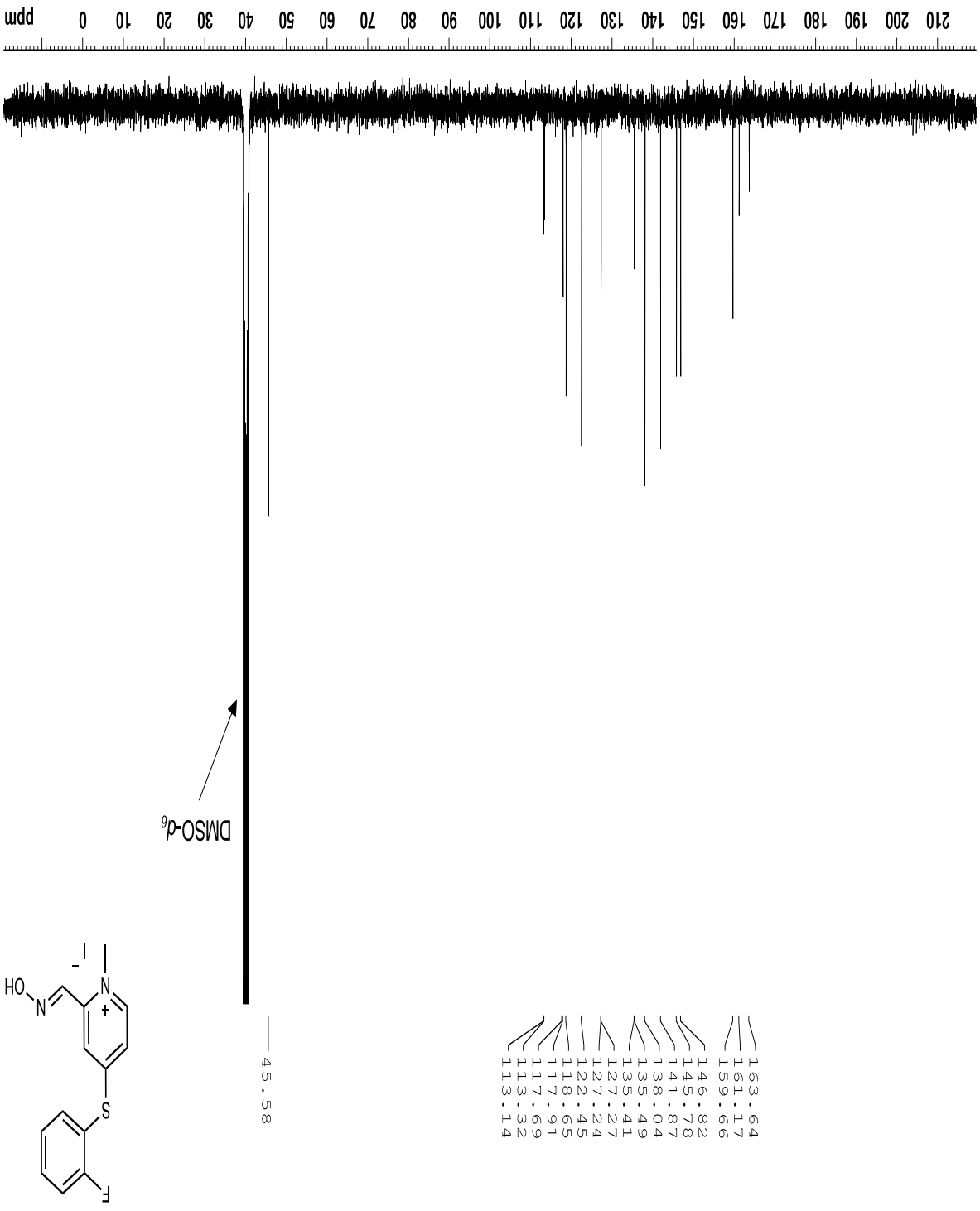

Spectrum 135. ^{13}C NMR of *(E)*-4-((2-fluorophenyl)thio)-2-((hydroxyimino)methyl)-1-methylpyridin-1-ium iodide (**ADG4158**) (100 MHz, 293 K, DMSO-d_6).

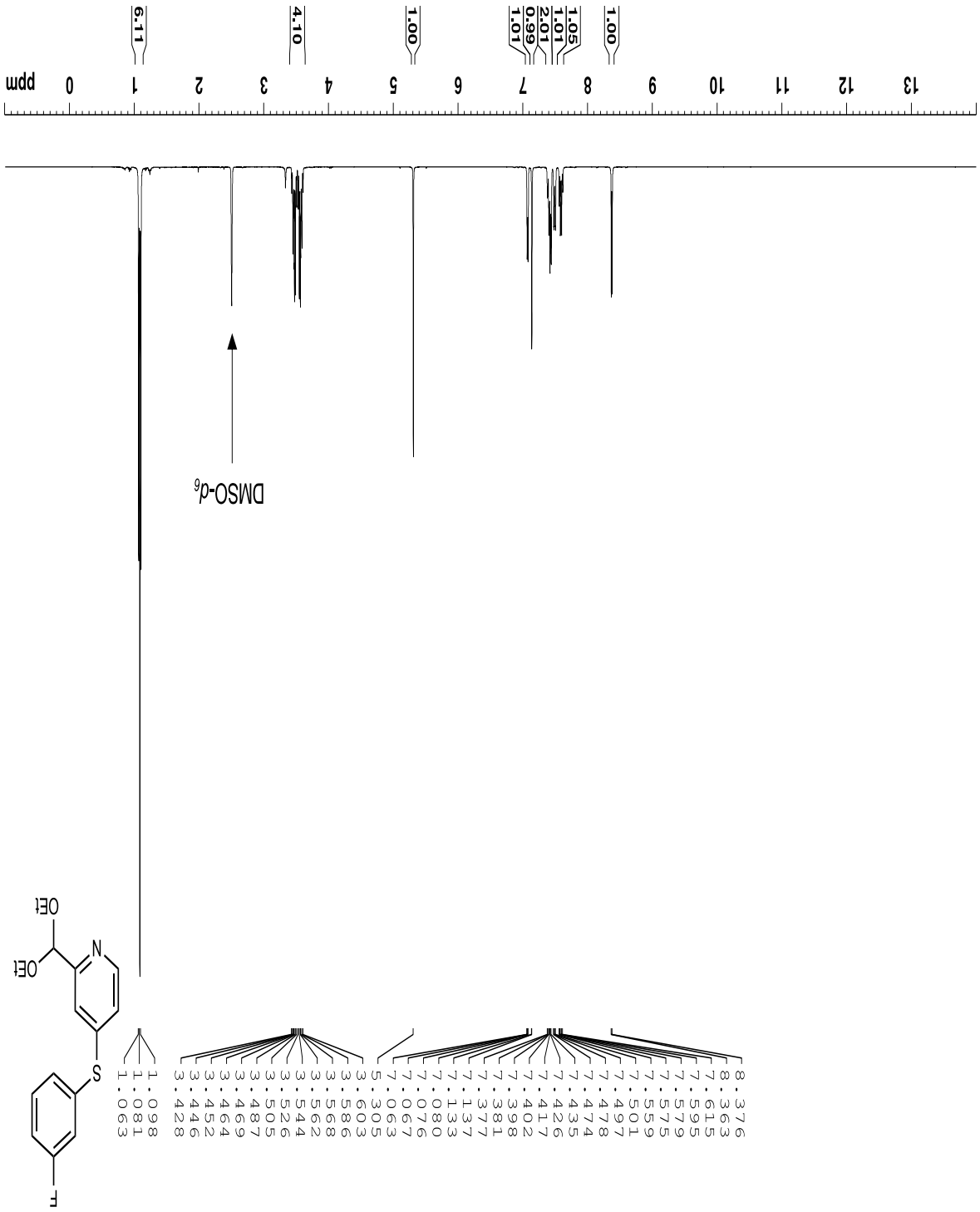

Spectrum 136. ^{1}H NMR of 2-(diethoxymethyl)-4-((3-fluorophenyl)thio)pyridine (400 MHz, 293 K, DMSO-d_6).

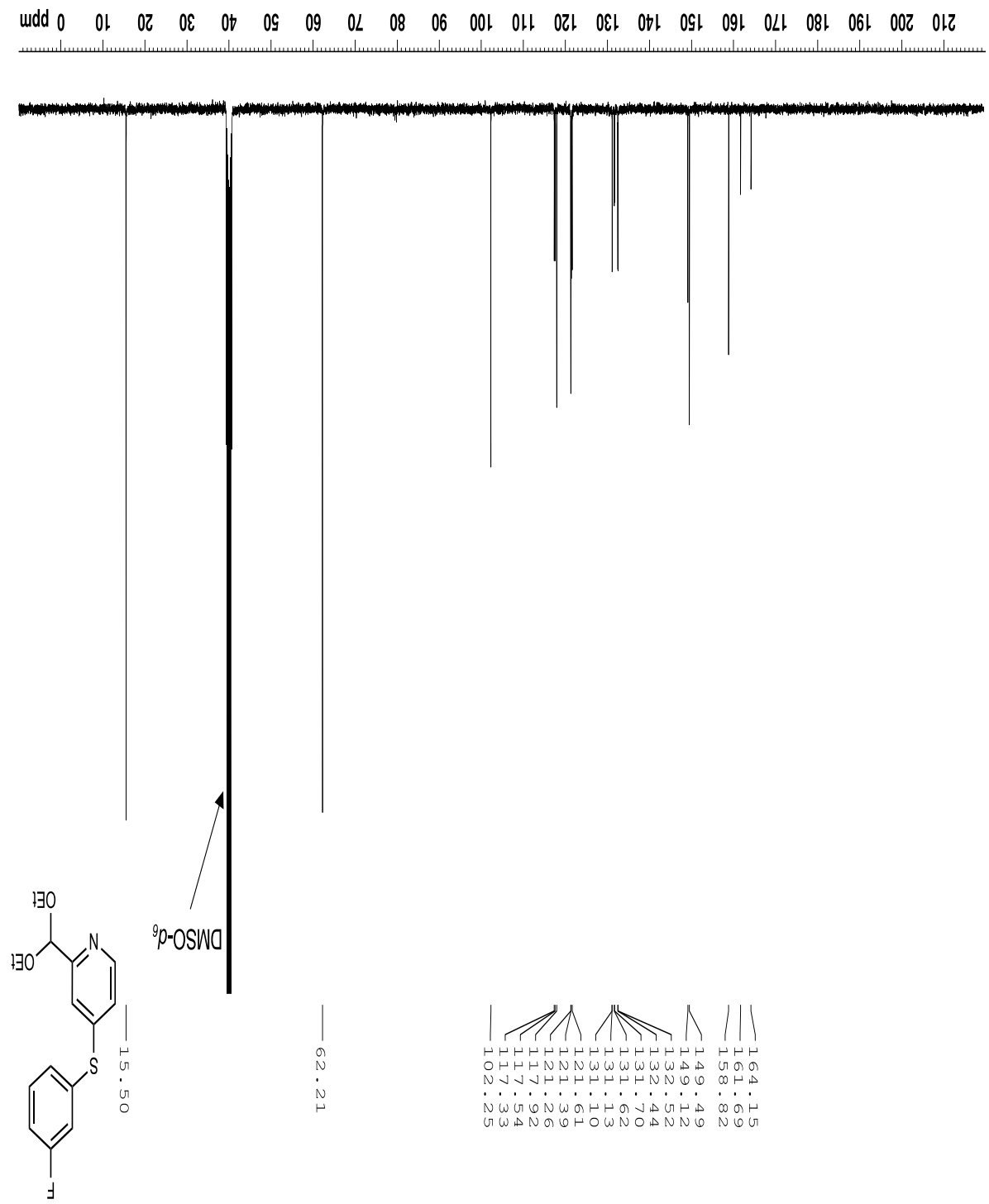

Spectrum 137. ^{13}C NMR of 2-(diethoxymethyl)-4-((3-fluorophenyl)thio)pyridine (100 MHz, 293 K, DMSO-d_6).

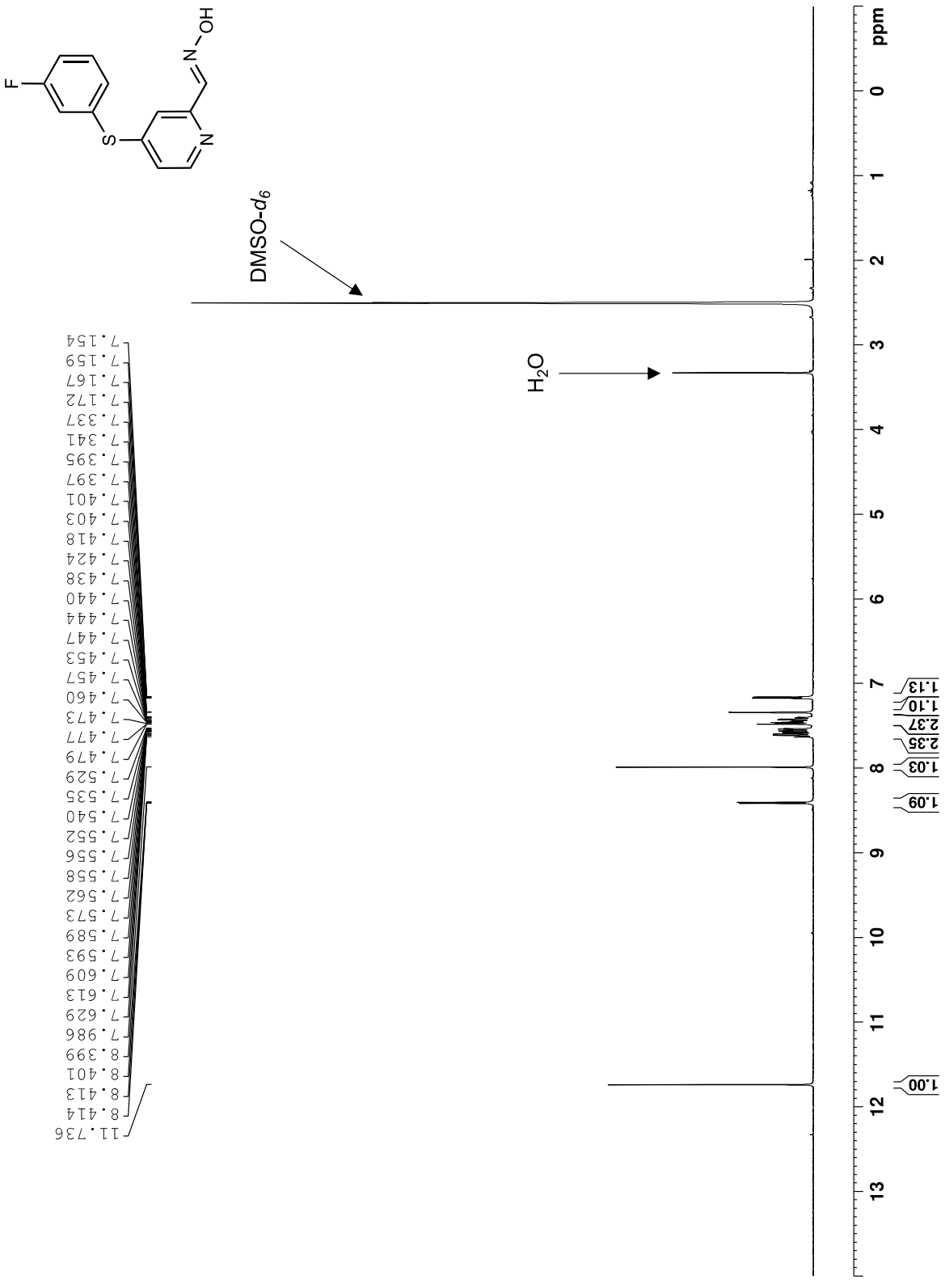

Spectrum 138. ^{1}H NMR of 2-(diethoxymethyl)-4-((3-fluorophenyl)thio)pyridine (400 MHz, 293 K, DMSO-d_6).

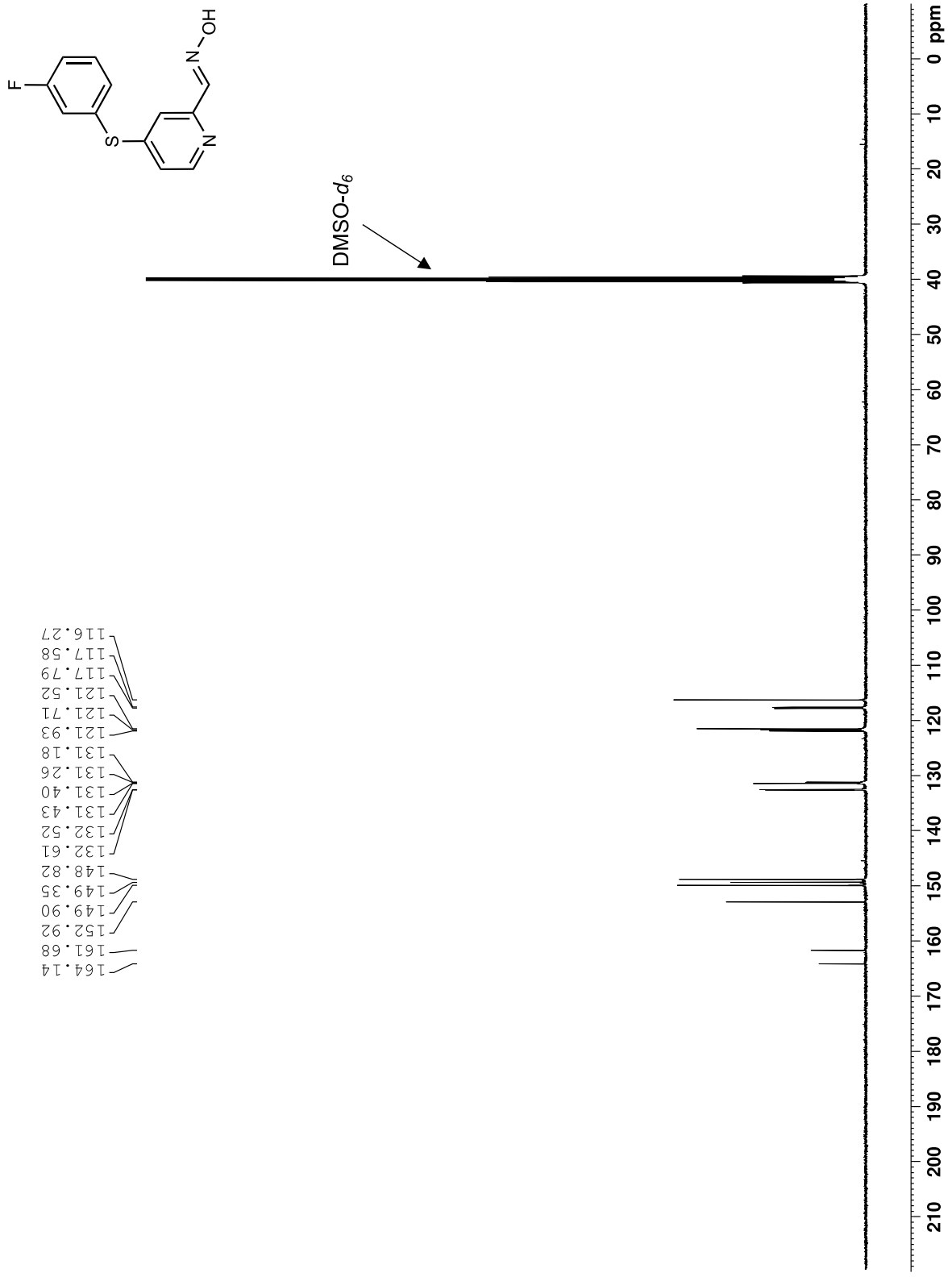

Spectrum 139. ^{13}C NMR of 2-(diethoxymethyl)-4-((3-fluorophenyl)thio)pyridine (100 MHz, 293 K, DMSO-d_6).

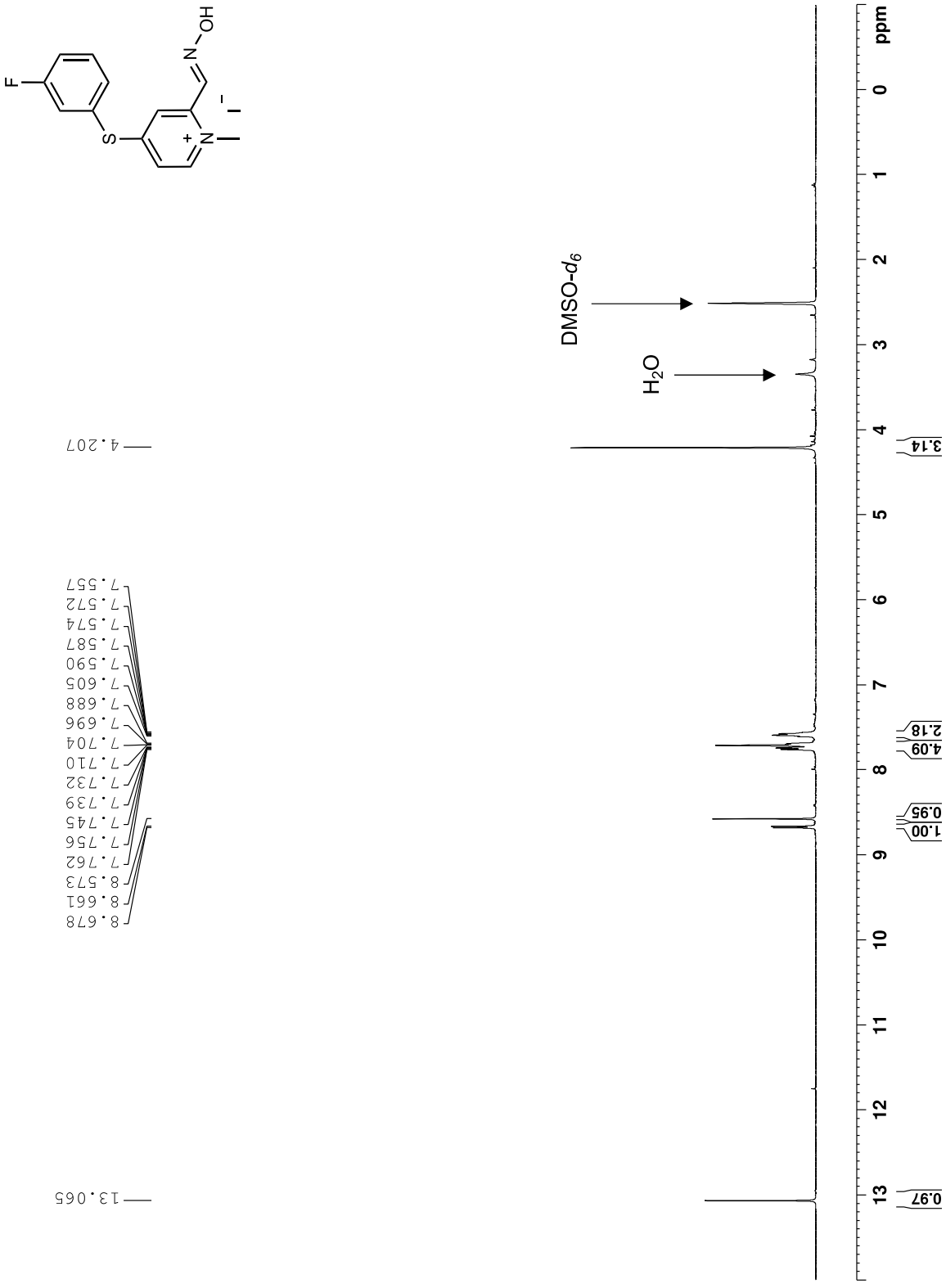

Spectrum 140. ^{1}H NMR of *(E)*-4-((3-fluorophenyl)thio)-2-((hydroxyimino)methyl)-1-methylpyridin-1-ium iodide (**ADG4146**) (400 MHz, 293 K, DMSO-d_6).

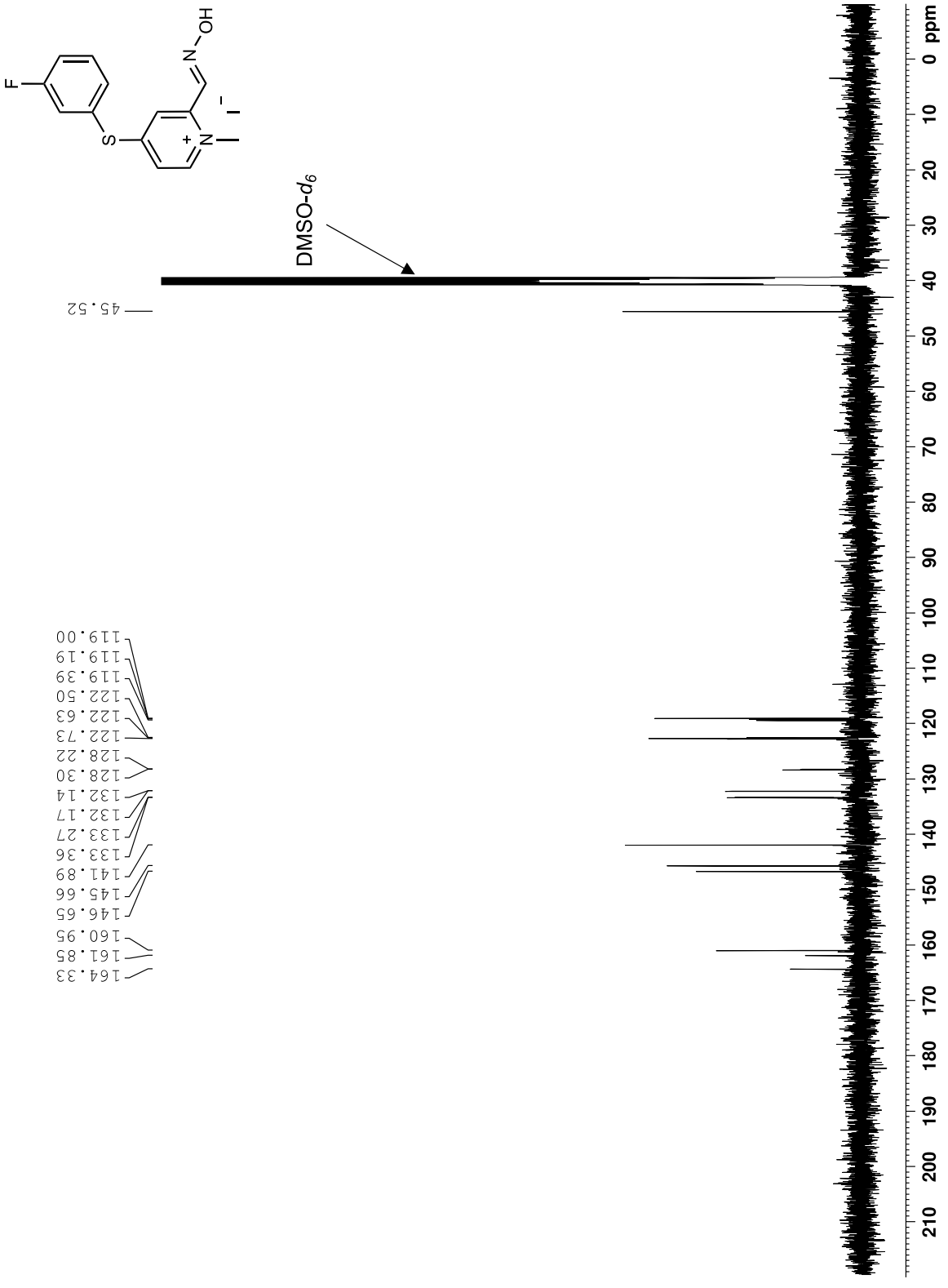

Spectrum 141. ^{13}C NMR of *(E)*-4-((3-fluorophenyl)thio)-2-((hydroxyimino)methyl)-1-methylpyridin-1-ium iodide (**ADG4146**) (100 MHz, 293 K, DMSO-d_6).

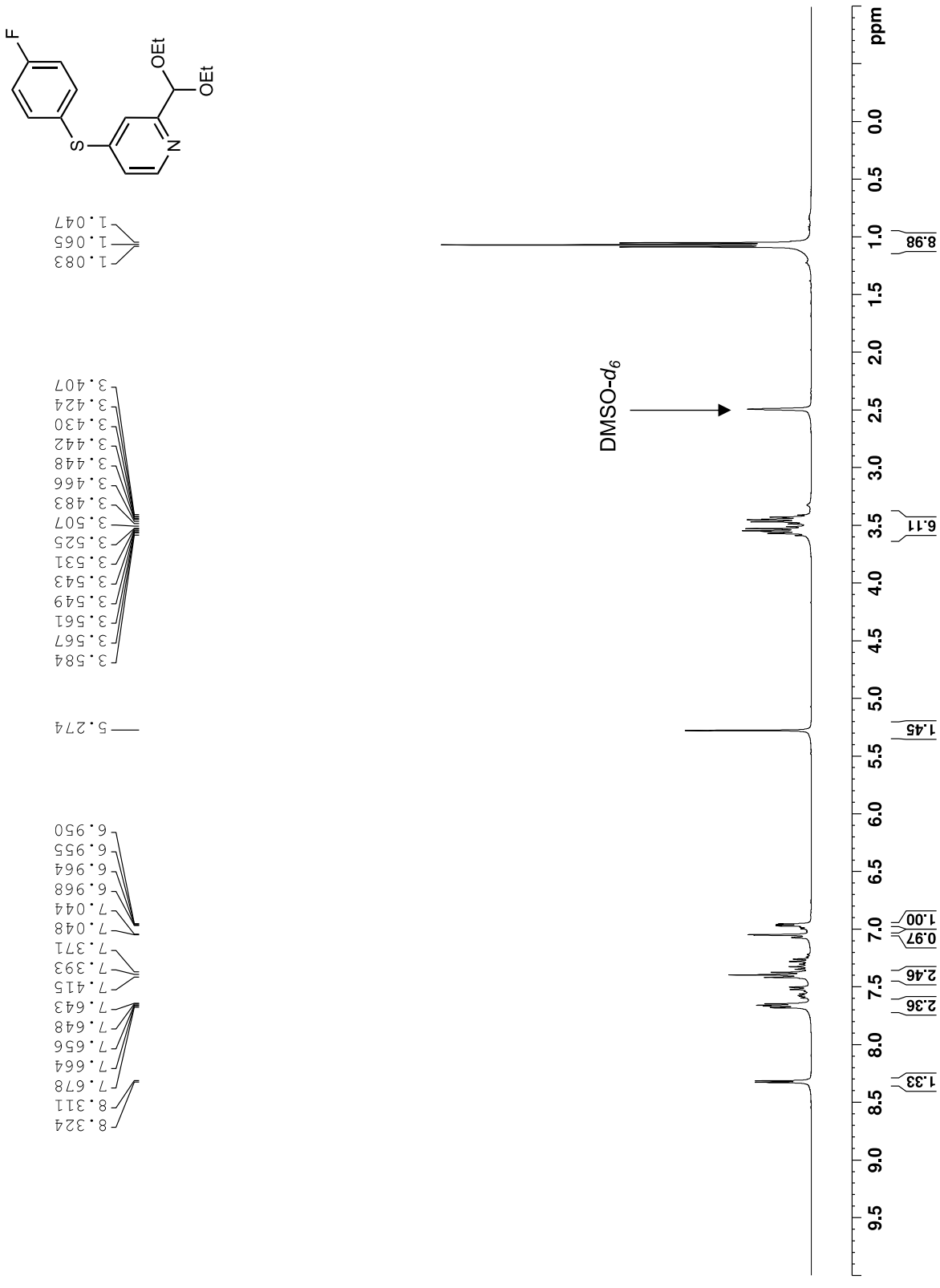

Spectrum 142. ^{1}H NMR of 2-(diethoxymethyl)-4-((4-fluorophenyl)thio)pyridine (300 MHz, 293 K, DMSO-d_6).

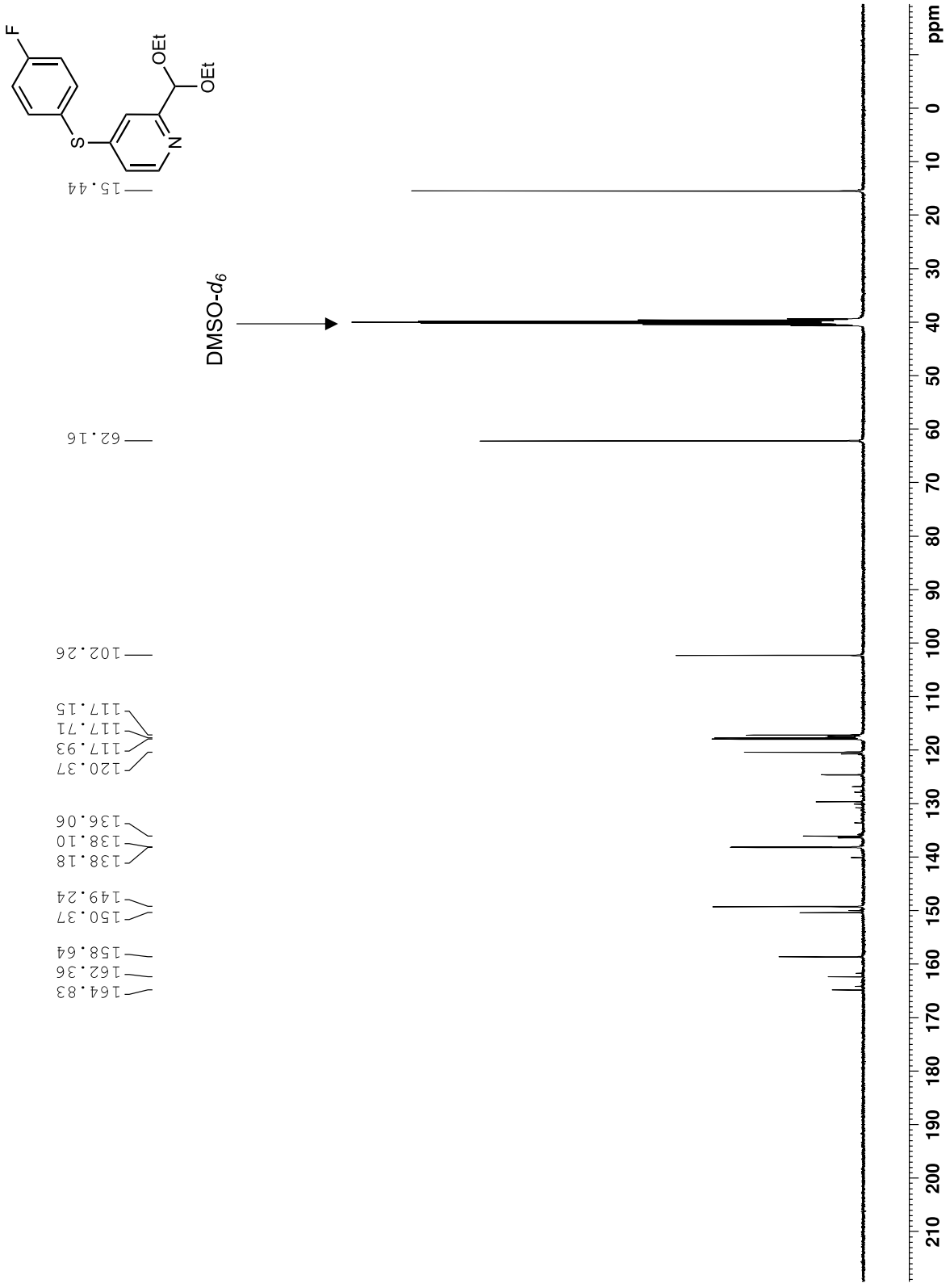

Spectrum 143. ^{13}C NMR of 2-(diethoxymethyl)-4-((4-fluorophenyl)thio)pyridine (100 MHz, 293 K, DMSO-d_6).

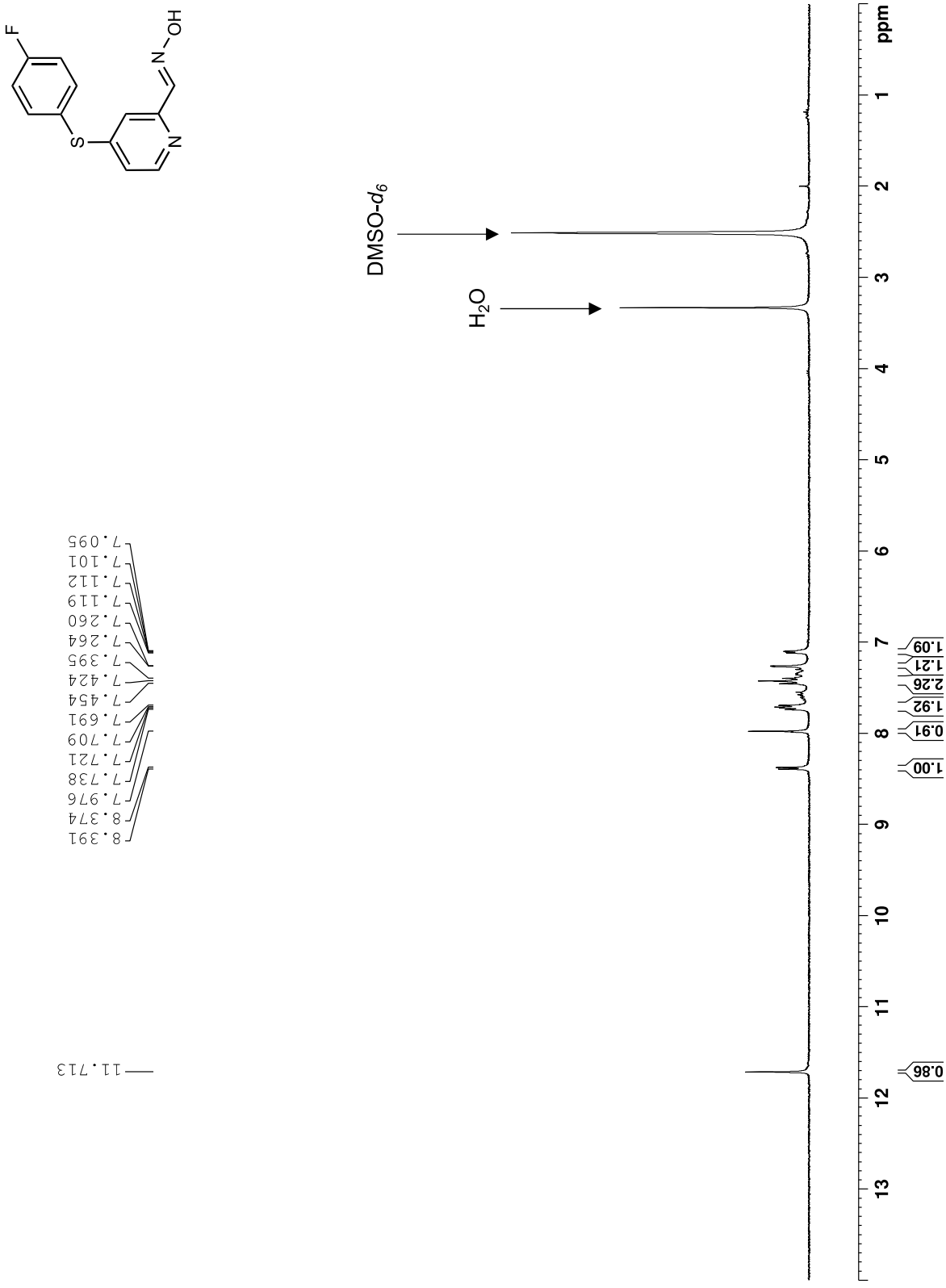

Spectrum 144. ^{1}H NMR of *(E)*-4-((4-fluorophenyl)thio)picolinaldehyde oxime (300 MHz, 293 K, DMSO-d_6).

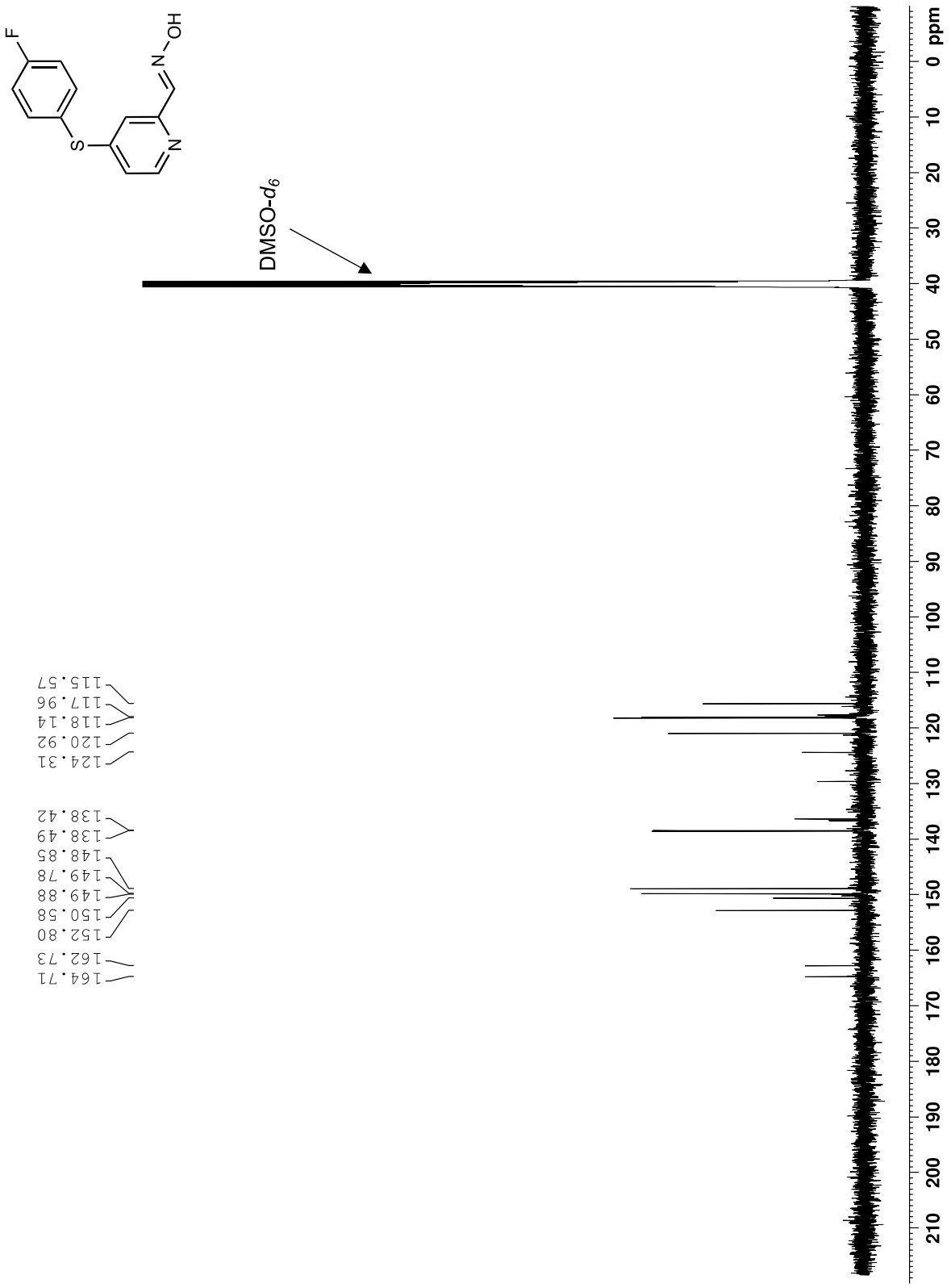

Spectrum 145. ^{13}C NMR of *(E)*-4-((4-fluorophenyl)thio)picolinaldehyde oxime (125 MHz, 293 K, DMSO-d_6).

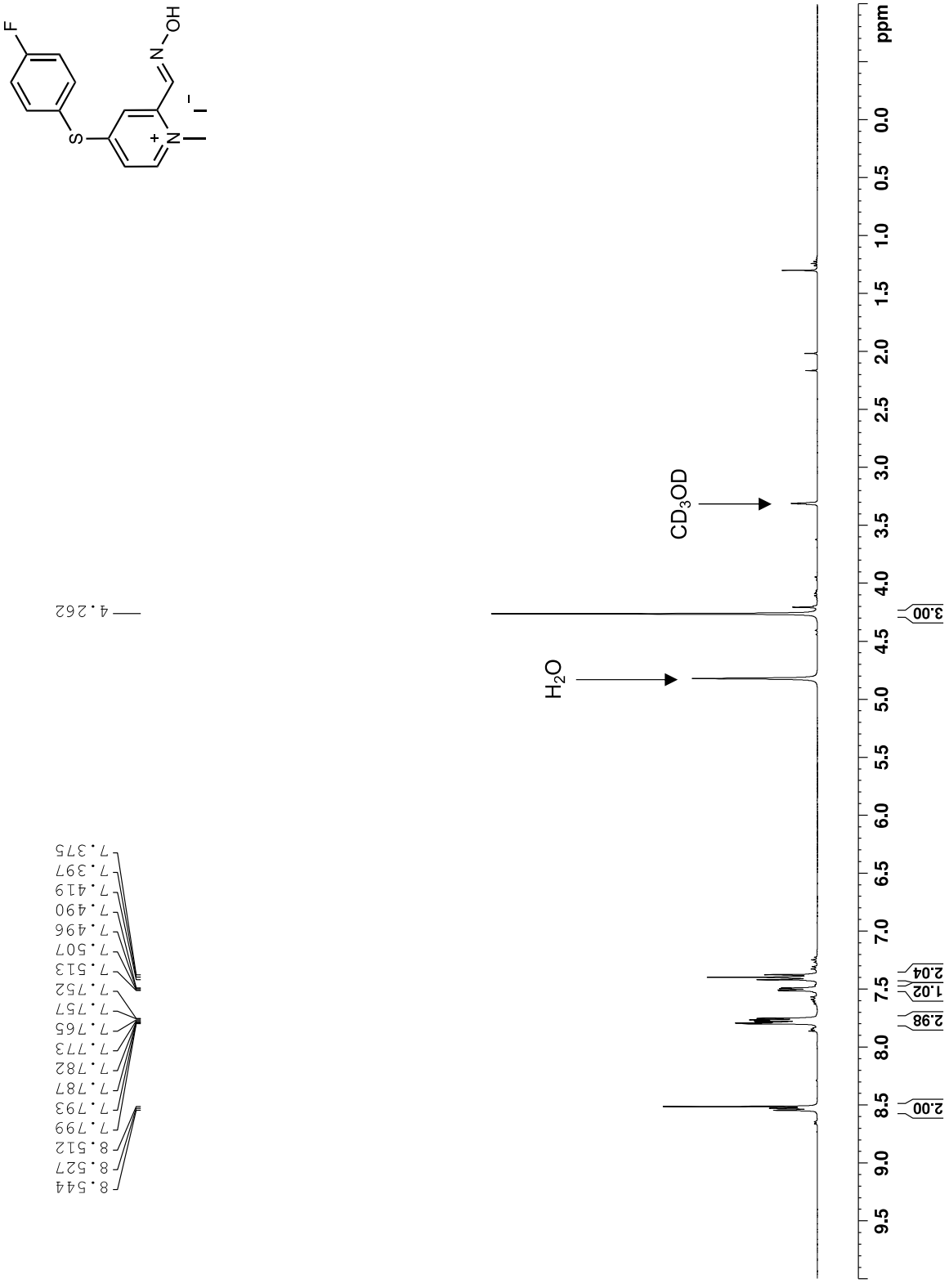

Spectrum 146. ^{1}H NMR of *(E)*-4-((4-fluorophenyl)thio)-2-((hydroxyimino)methyl)-1-methylpyridin-1-ium iodide (**ADG3193**) (400 MHz, 293 K, CD_3OD).

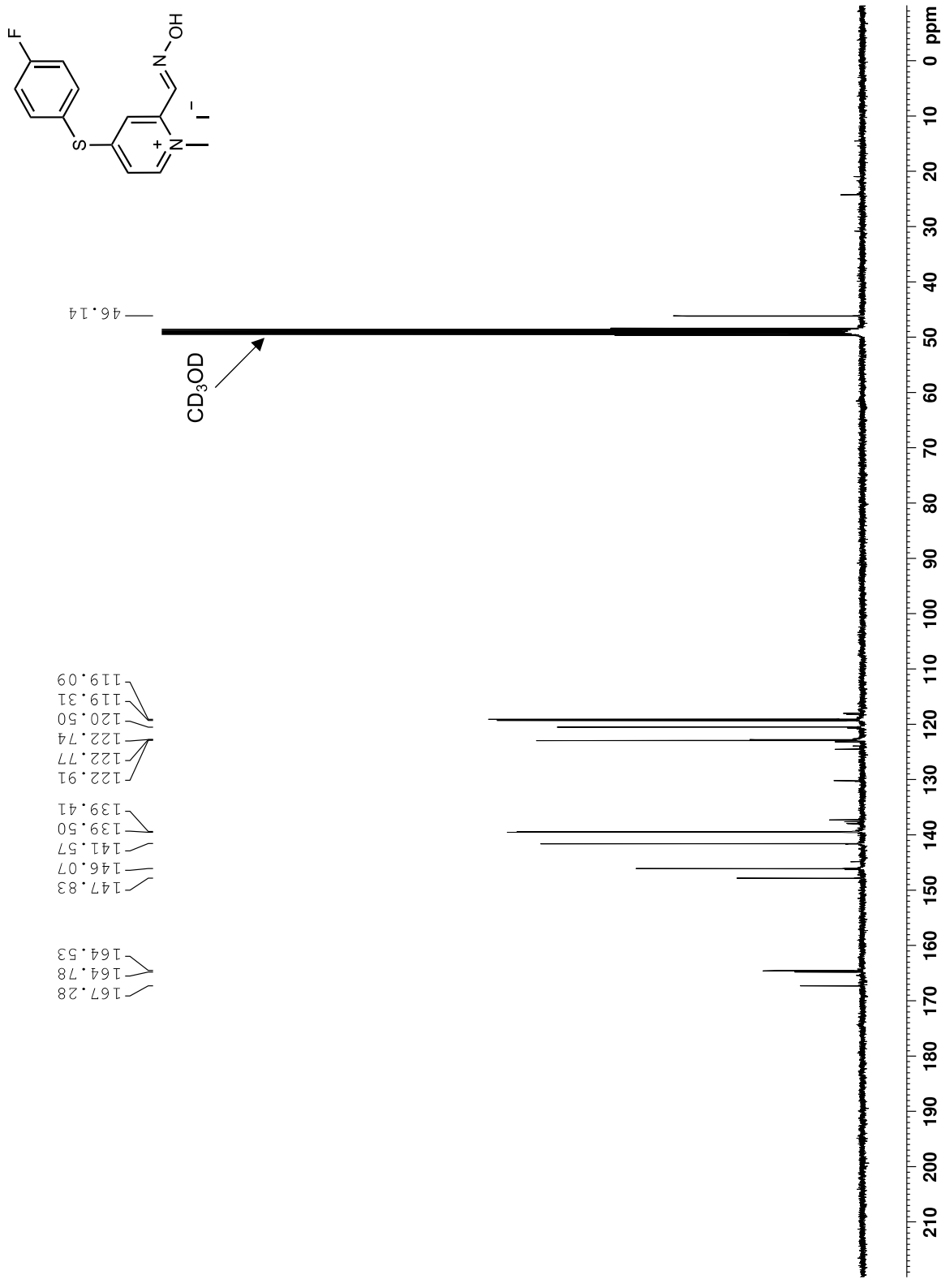

Spectrum 147. ^{13}C NMR of *(E)*-4-((4-fluorophenyl)thio)-2-((hydroxyimino)methyl)-1-methylpyridin-1-ium iodide (**ADG3193**) (100 MHz, 293 K, CD_3OD).

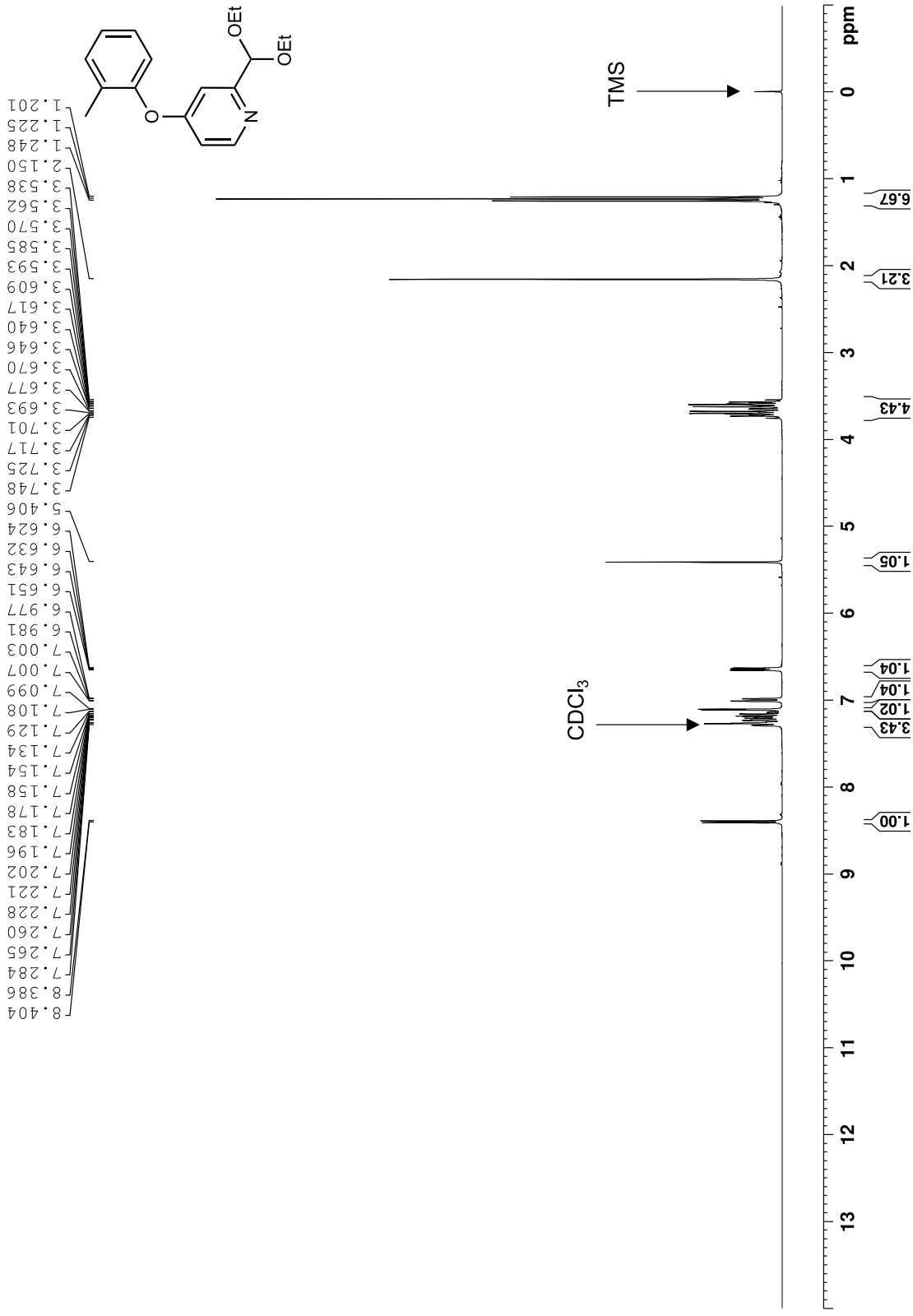

Spectrum 148. ^{1}H NMR of 2-(diethoxymethyl)-4-(*o*-tolyloxy)pyridine (300 MHz, 293 K, $CDCl_3$).

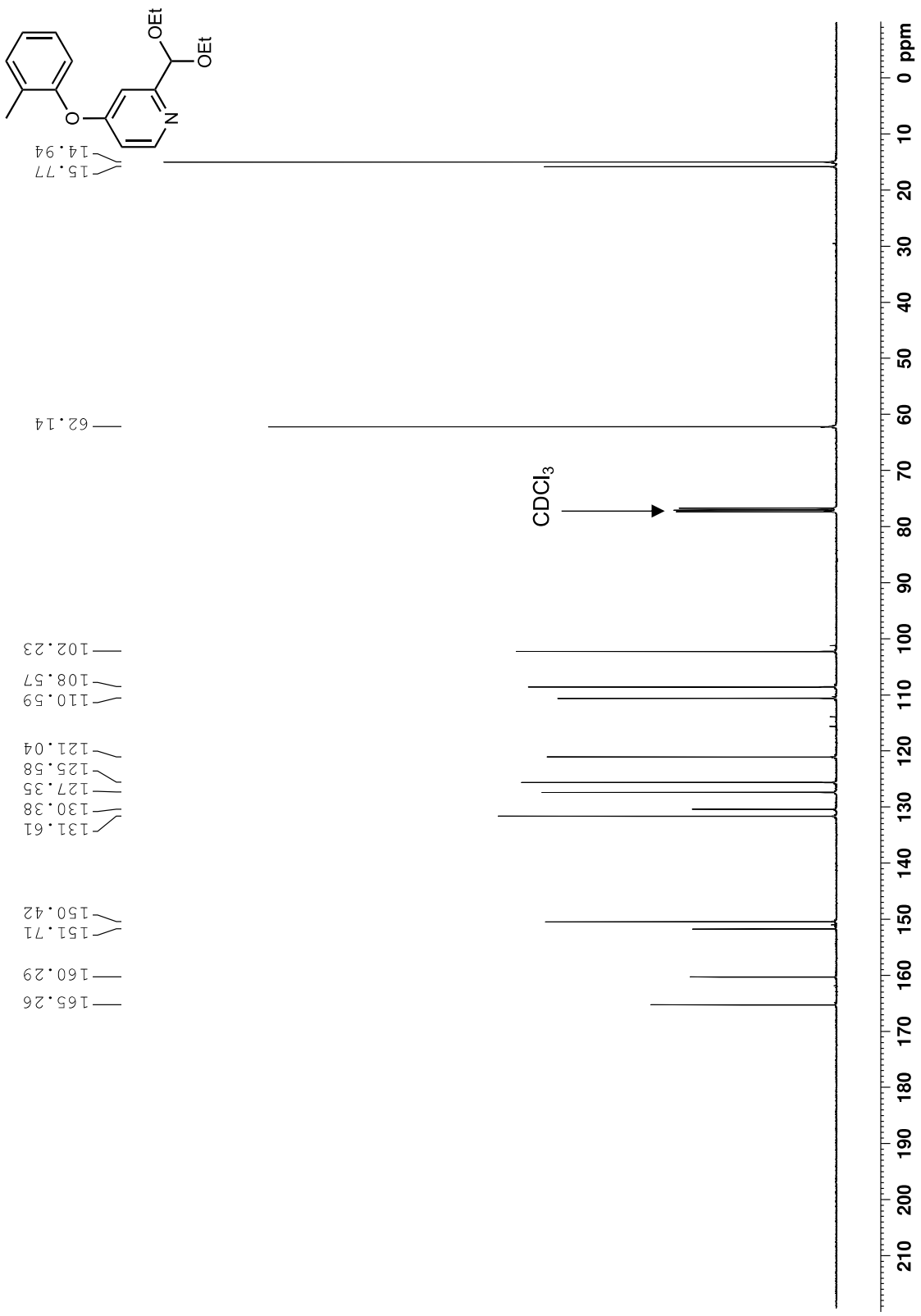

Spectrum 149. ^{13}C NMR of 2-(diethoxymethyl)-4-(*o*-tolyloxy)pyridine (100 MHz, 293 K, $CDCl_3$).

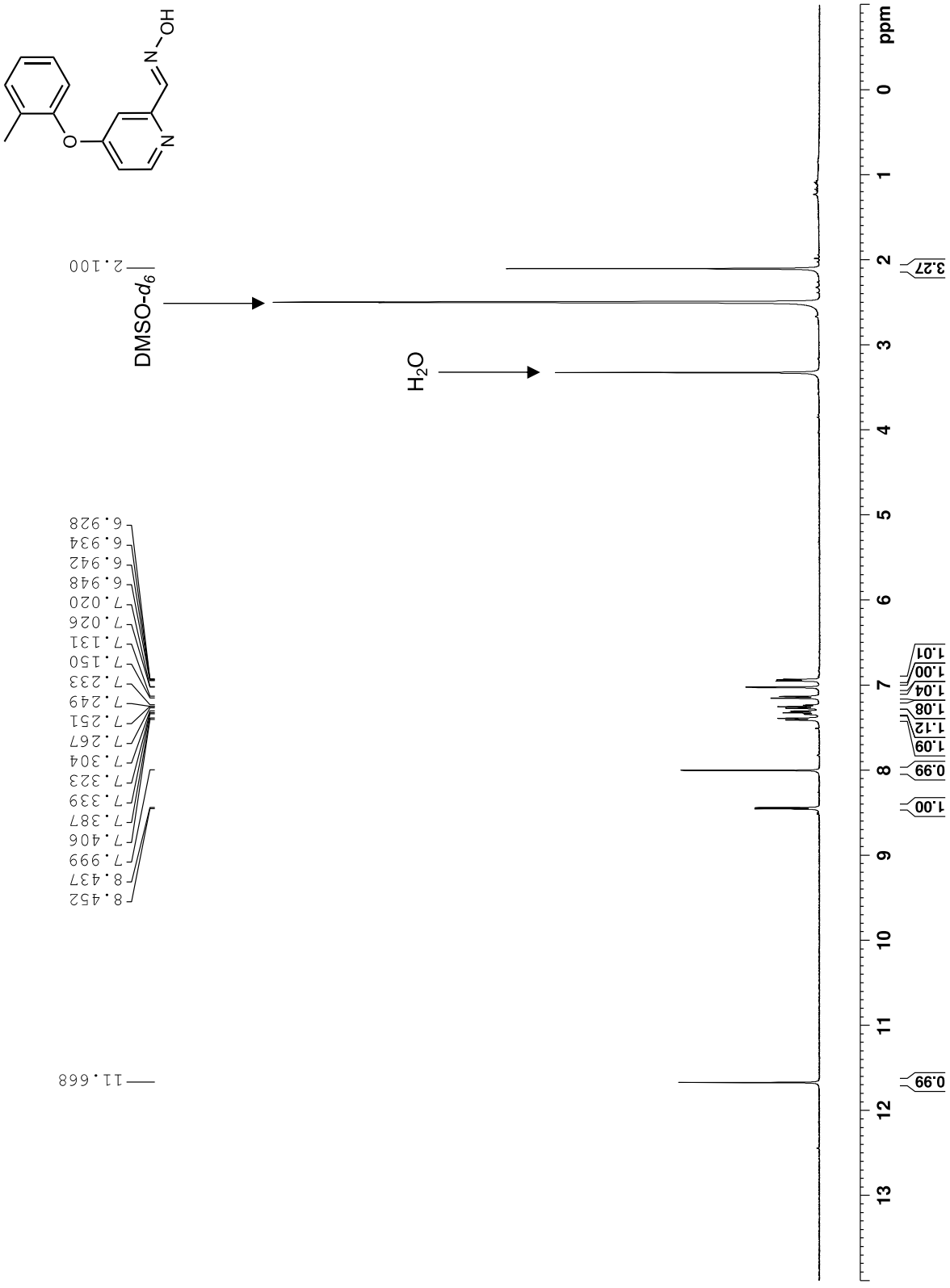

Spectrum 150. ^{1}H NMR of *(E)*-4-(*o*-tolyloxy)picolinaldehyde oxime (400 MHz, 293 K, DMSO-d_6).

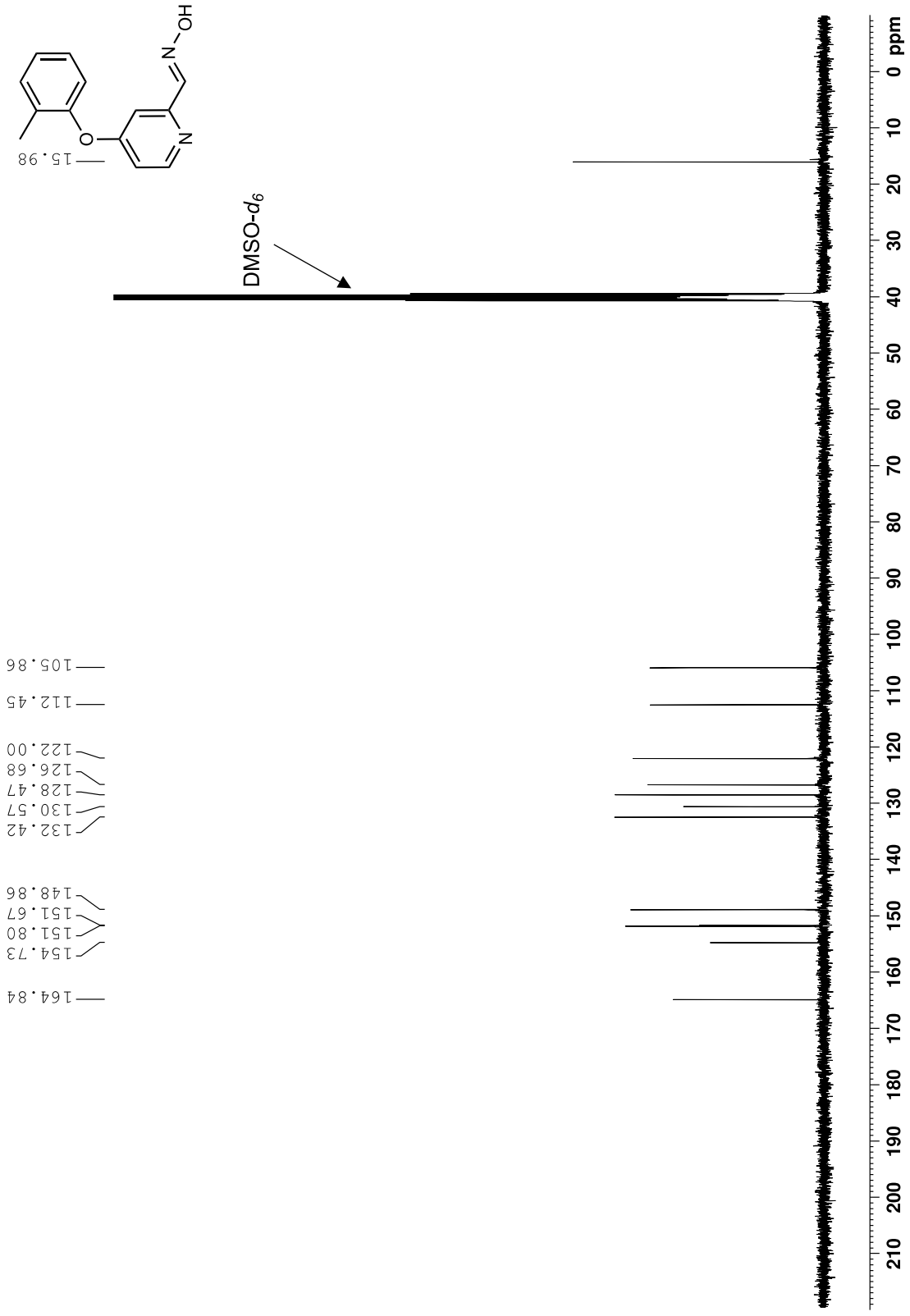

Spectrum 151. ^{13}C NMR of *(E)*-4-(*o*-tolyloxy)picolinaldehyde oxime (100 MHz, 293 K, DMSO-d_6).

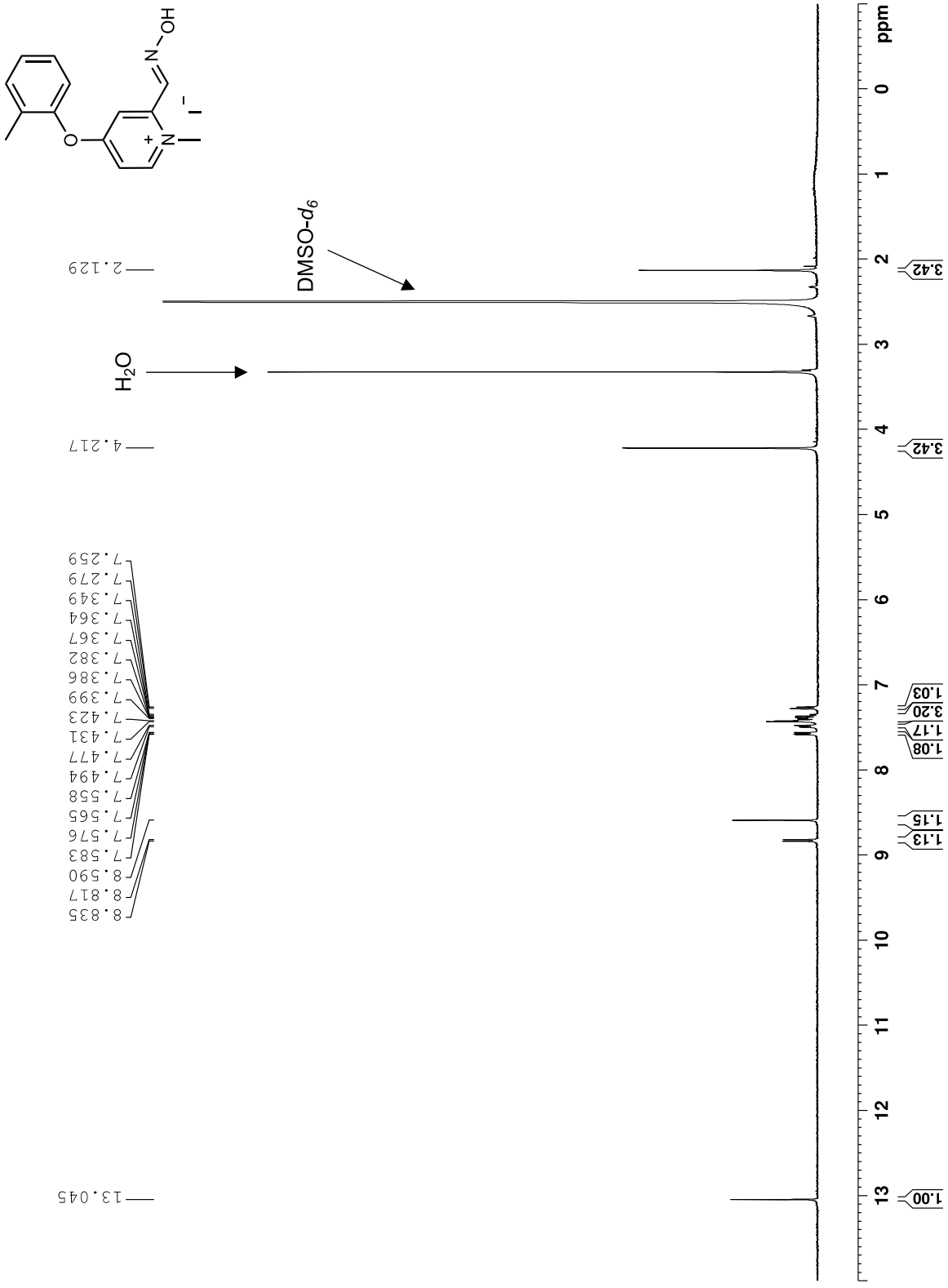

Spectrum 152. ^{1}H NMR of *(E)*-2-((hydroxyimino)methyl)-1-methyl-4-(*o*-tolyloxy)pyridin-1-ium iodide (**ADG3110**) (400 MHz, 293 K, DMSO-d_6).

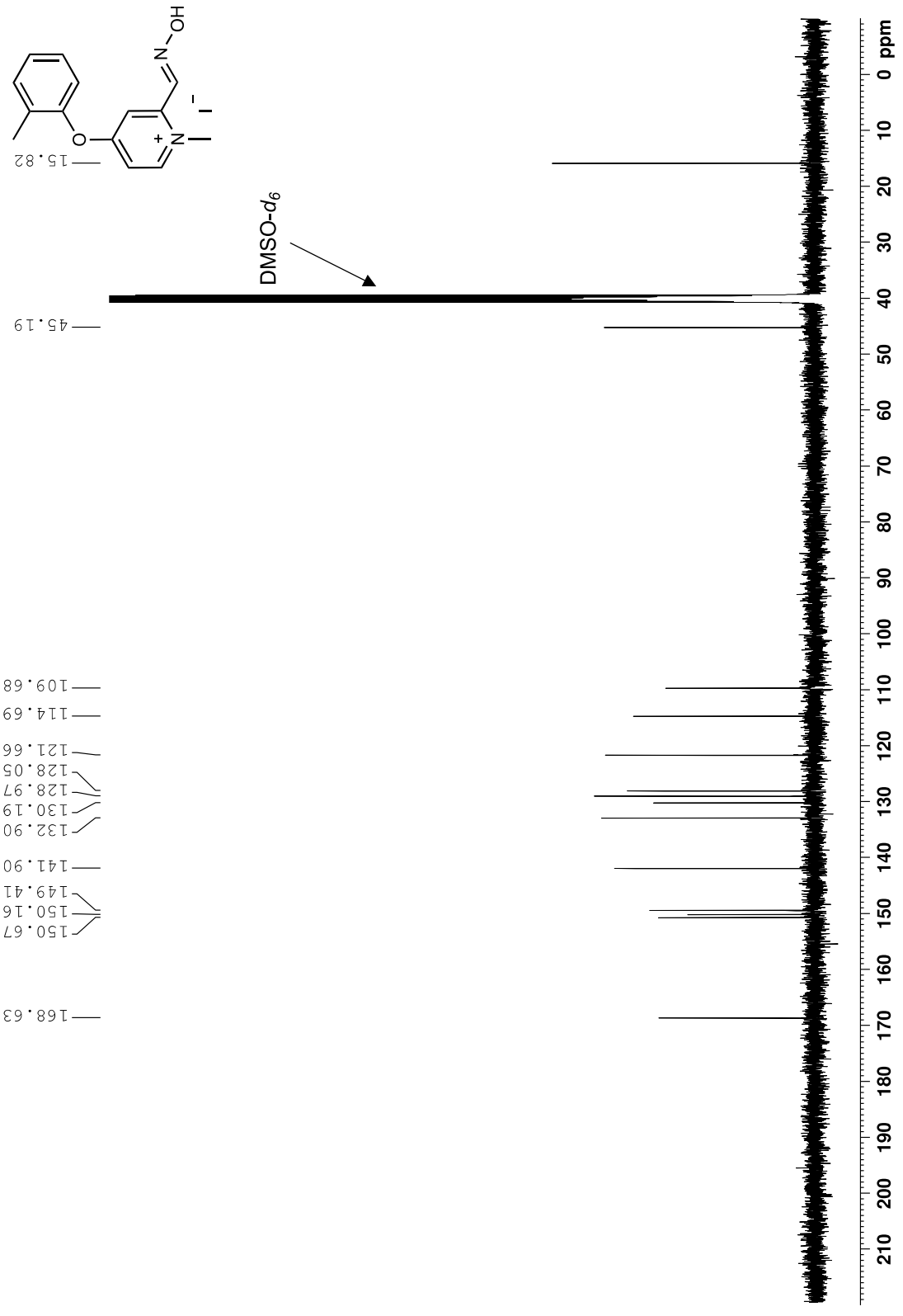

Spectrum 153. ^{13}C NMR of *(E)*-2-((hydroxyimino)methyl)-1-methyl-4-(*o*-tolyloxy)pyridin-1-ium iodide (**ADG3110**) (100 MHz, 293 K, DMSO-d_6).

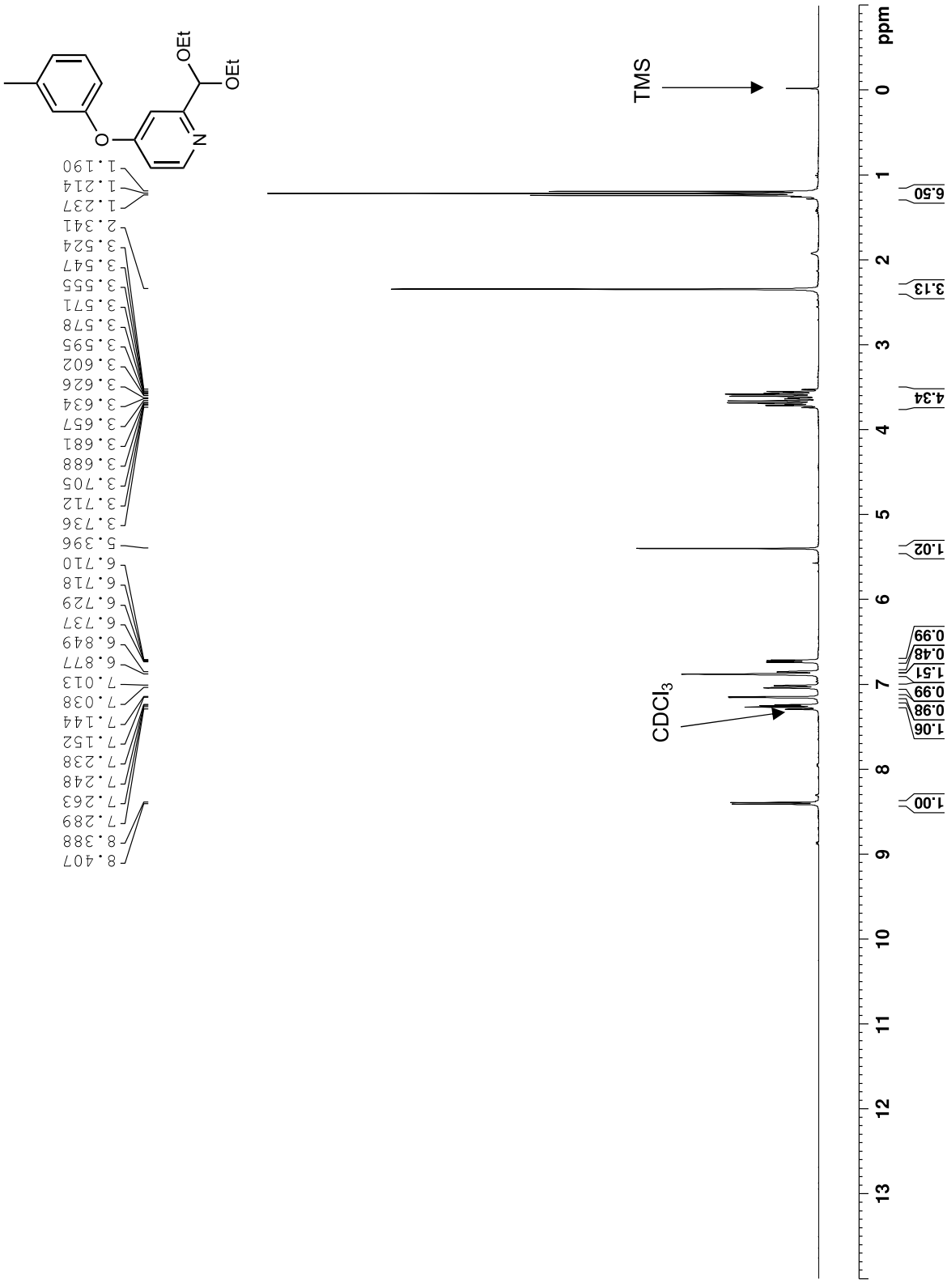

Spectrum 154. ^{1}H NMR of 2-(diethoxymethyl)-4-(*m*-tolyloxy)pyridine (300 MHz, 293 K, $CDCl_3$).

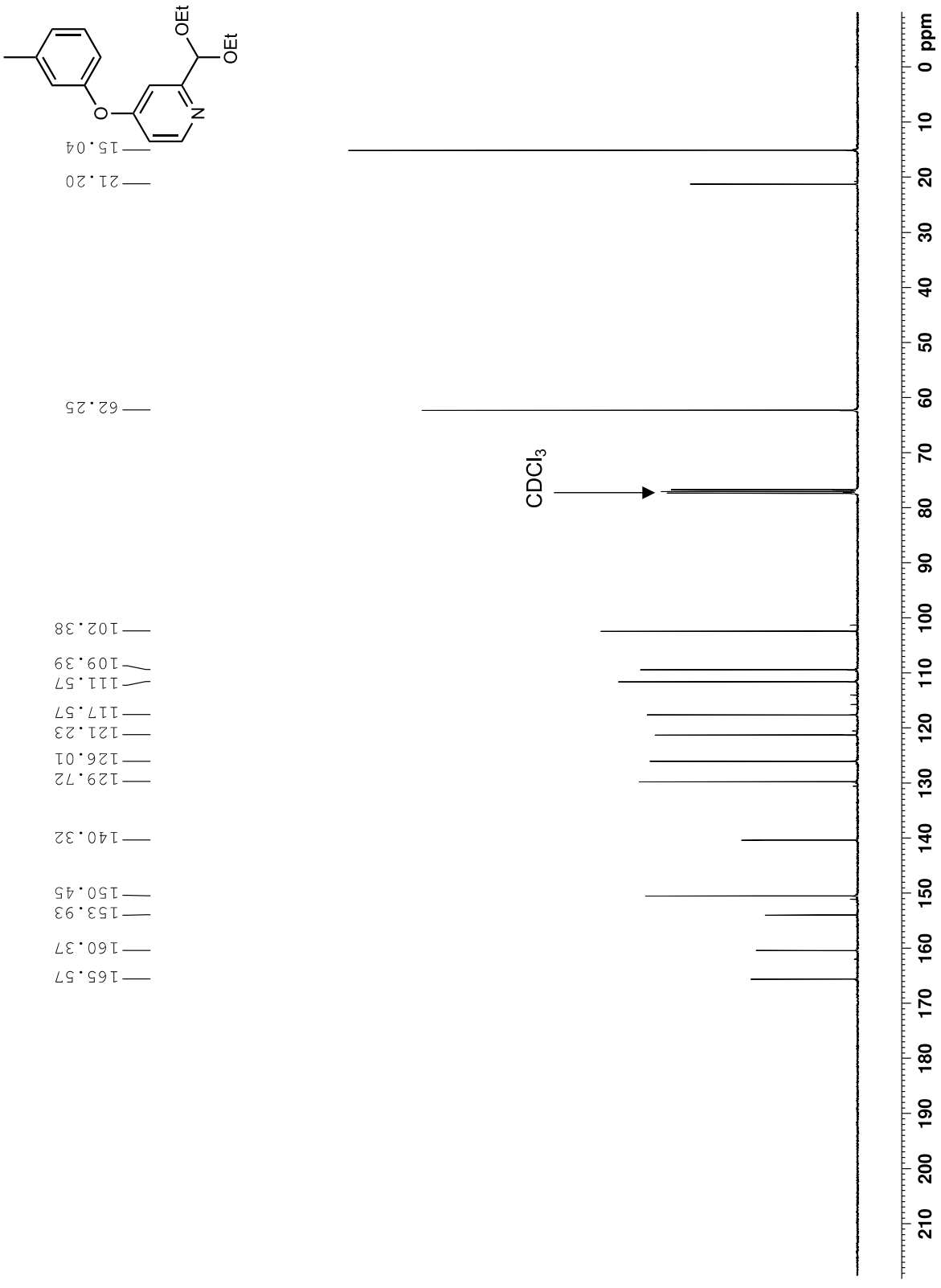

Spectrum 155. ^{13}C NMR of 2-(diethoxymethyl)-4-(*m*-tolyloxy)pyridine (100 MHz, 293 K, $CDCl_3$).

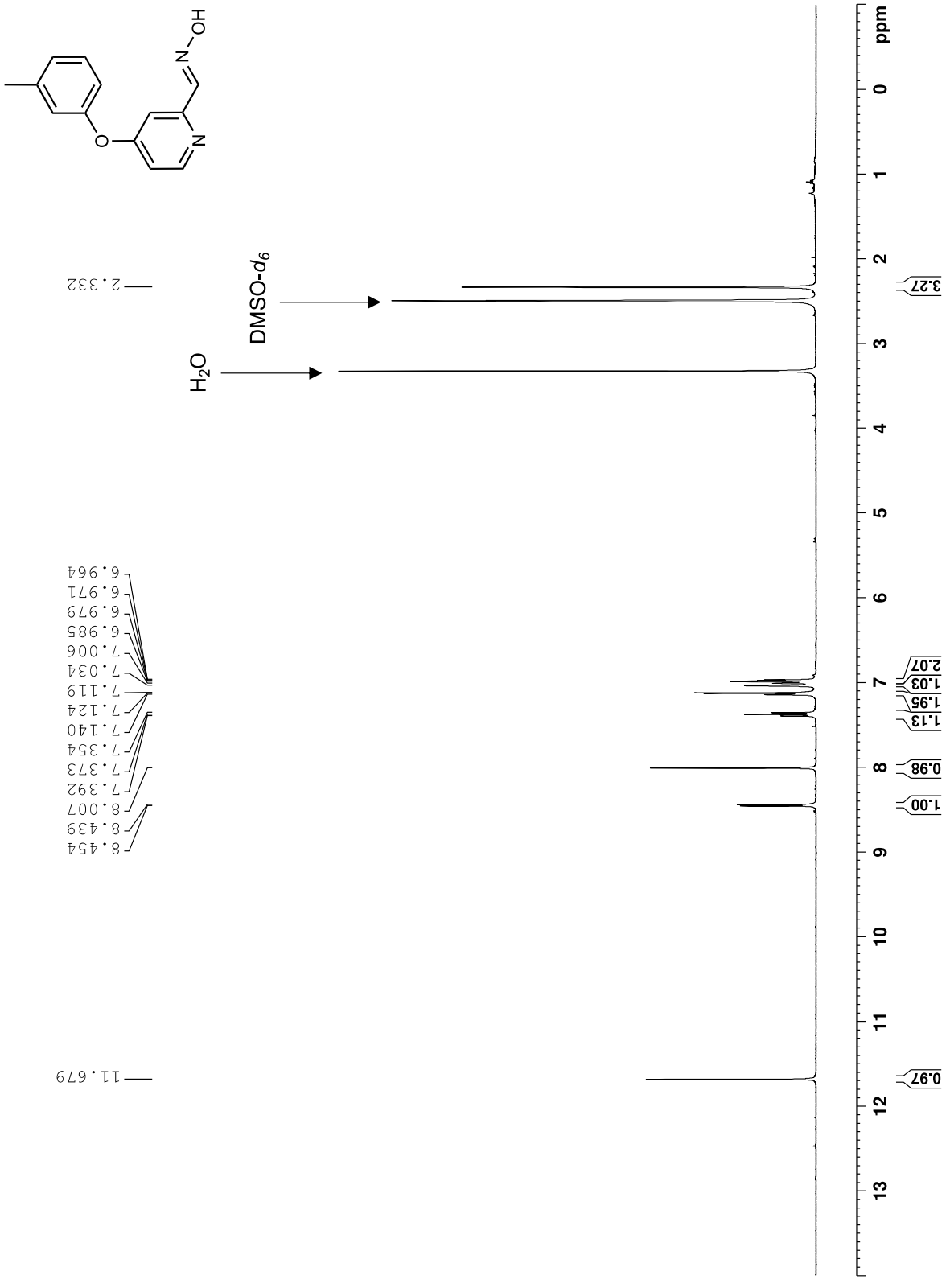

Spectrum 156. ^{1}H NMR of *(E)*-4-(*m*-tolyloxy)picolinaldehyde oxime (400 MHz, 293 K, DMSO-d_6).

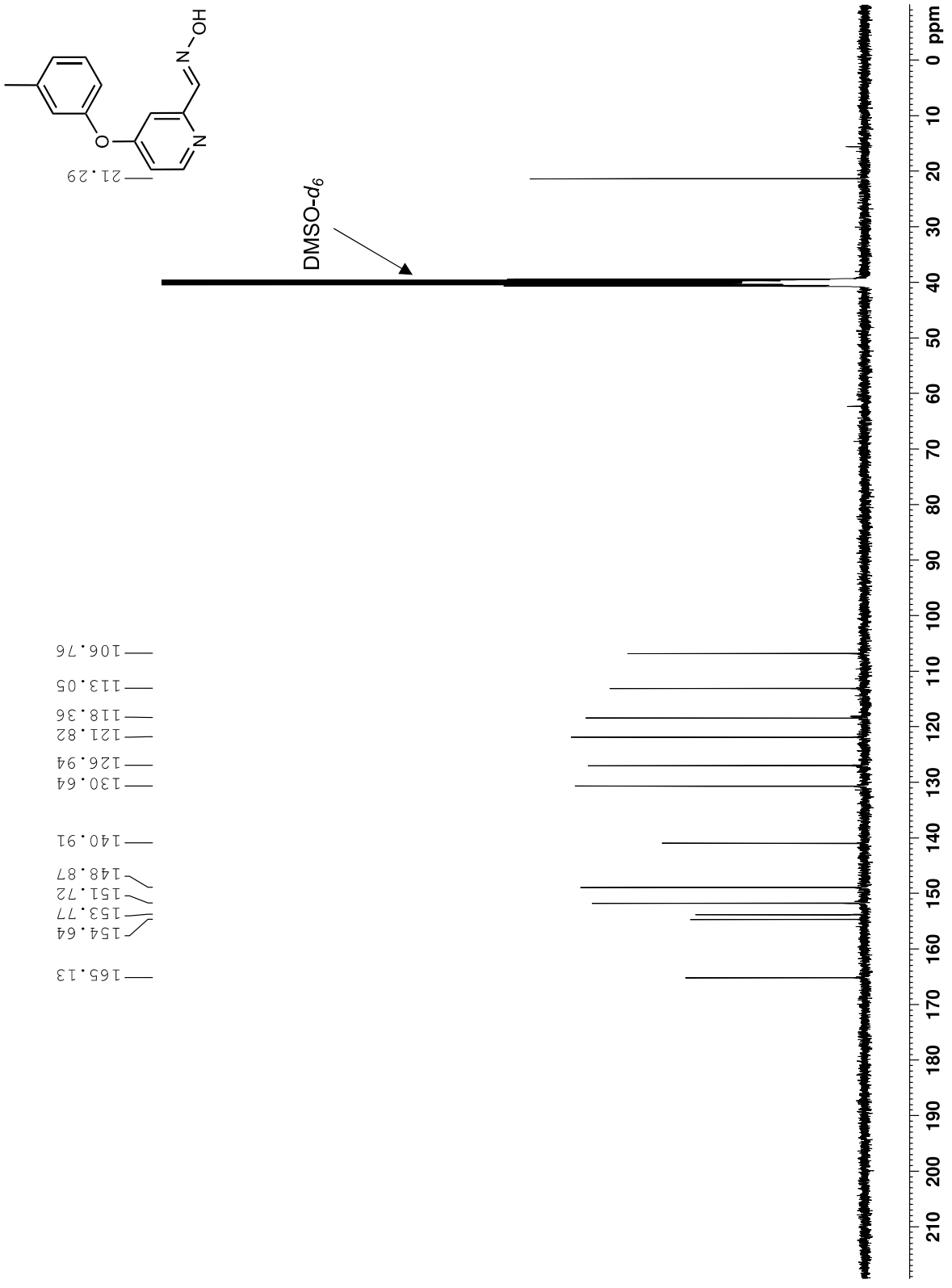

Spectrum 157. ^{13}C NMR of *(E)*-4-(*m*-tolyloxy)picolinaldehyde oxime (100 MHz, 293 K, DMSO-d_6).

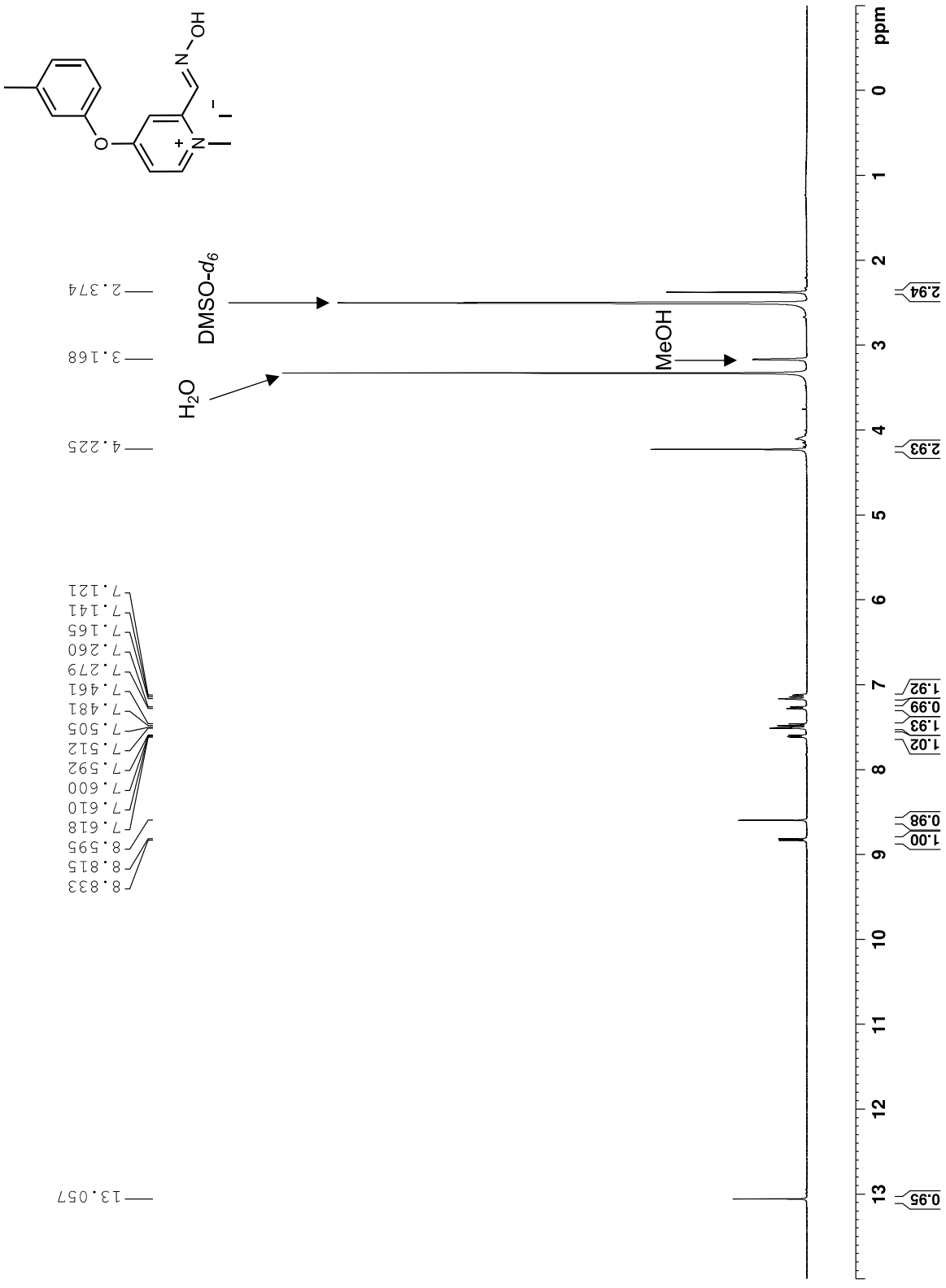

Spectrum 158. ^{1}H NMR of *(E)*-2-((hydroxyimino)methyl)-1-methyl-4-(*m*-tolyloxy)pyridin-1-ium iodide (**ADG3111**) (400 MHz, 293 K, DMSO-d_6).

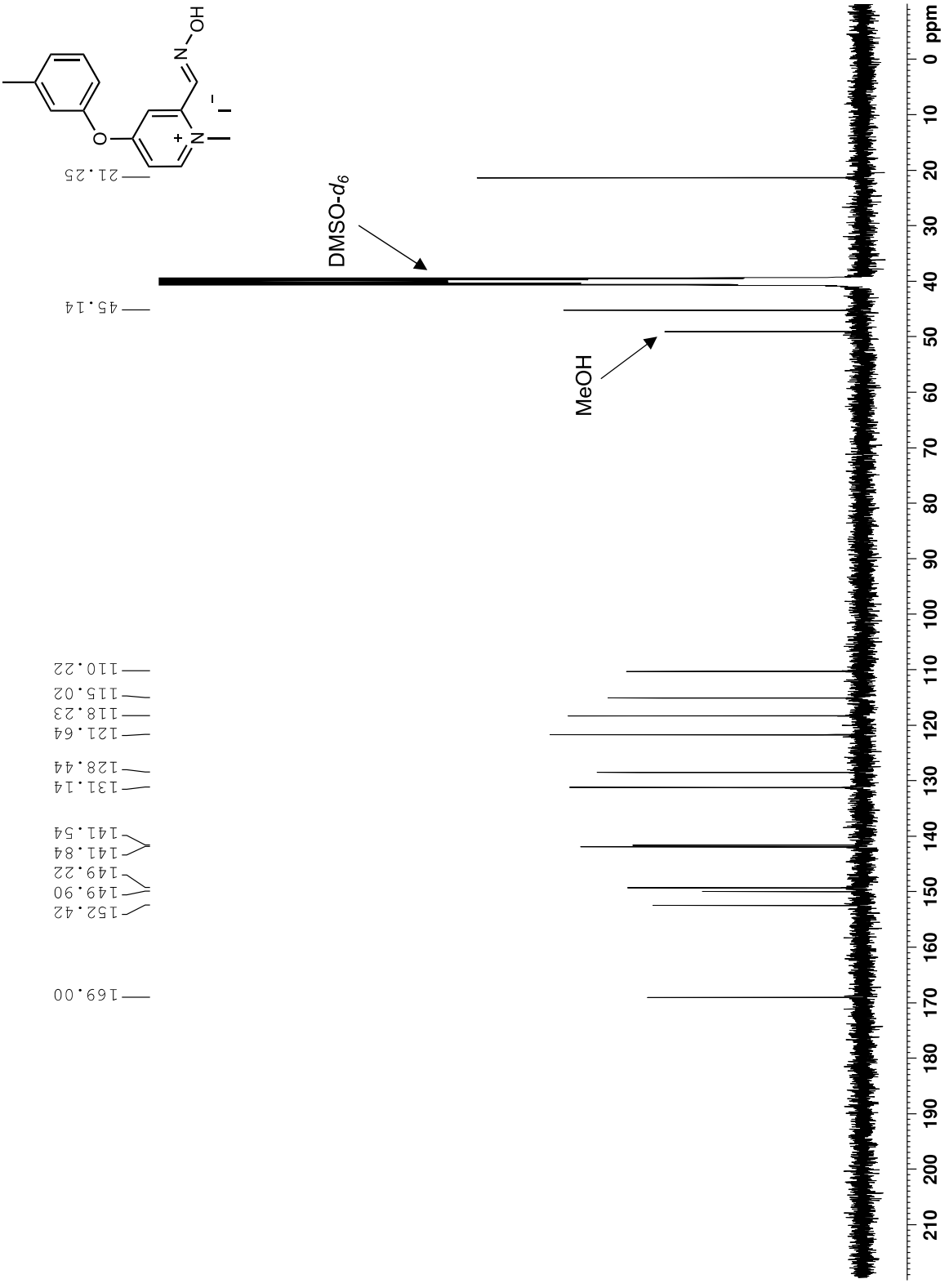

Spectrum 159. ^{13}C NMR of *(E)*-2-((hydroxyimino)methyl)-1-methyl-4-(*m*-tolyloxy)pyridin-1-ium iodide (**ADG3111**) (100 MHz, 293 K, DMSO-d_6).

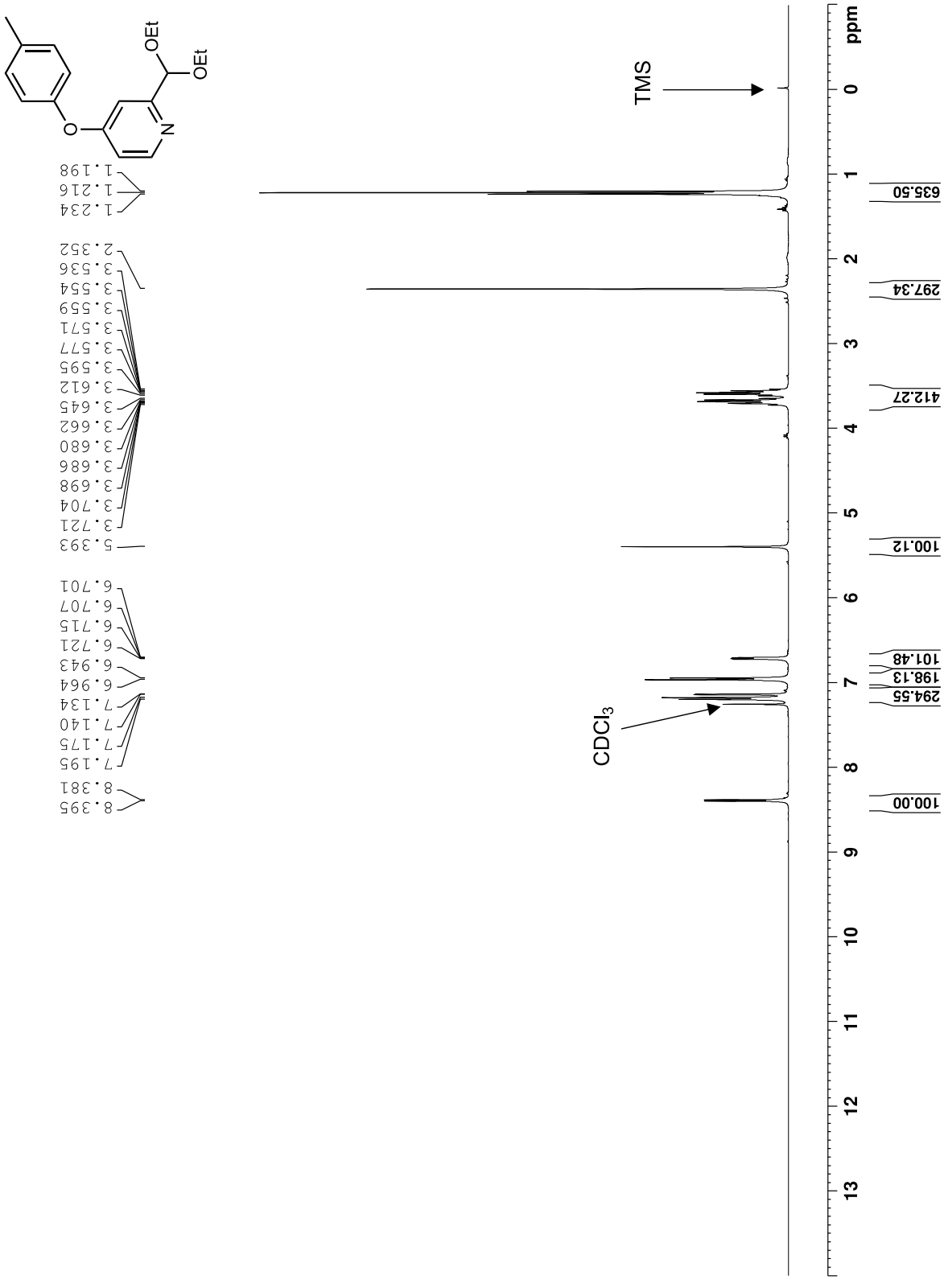

Spectrum 160. ^{1}H NMR of 2-(diethoxymethyl)-4-(*p*-tolyloxy)pyridine (400 MHz, 293 K, $CDCl_3$).

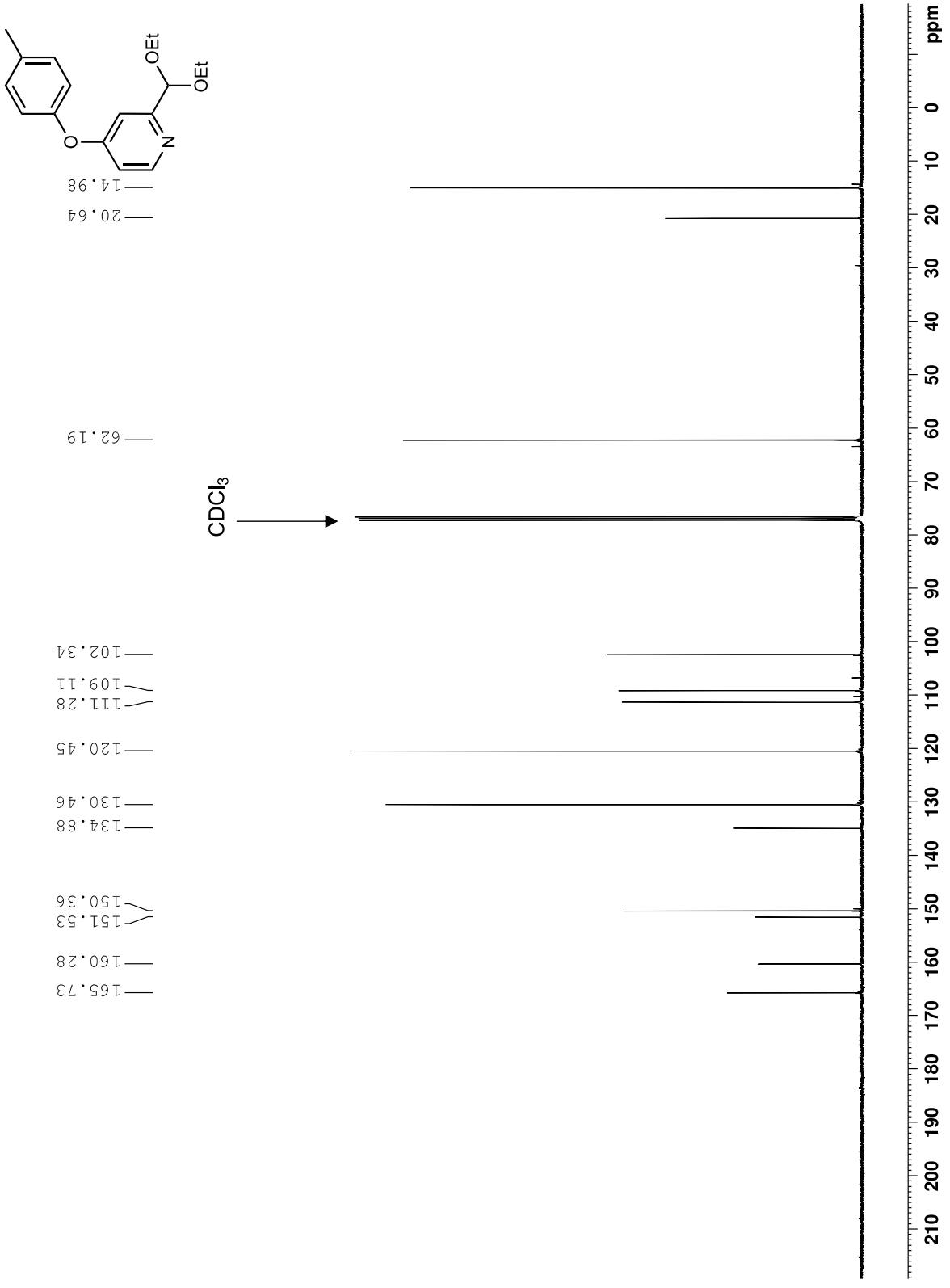

Spectrum 161. ^{13}C NMR of 2-(diethoxymethyl)-4-(*p*-tolyloxy)pyridine (100 MHz, 293 K, $CDCl_3$).

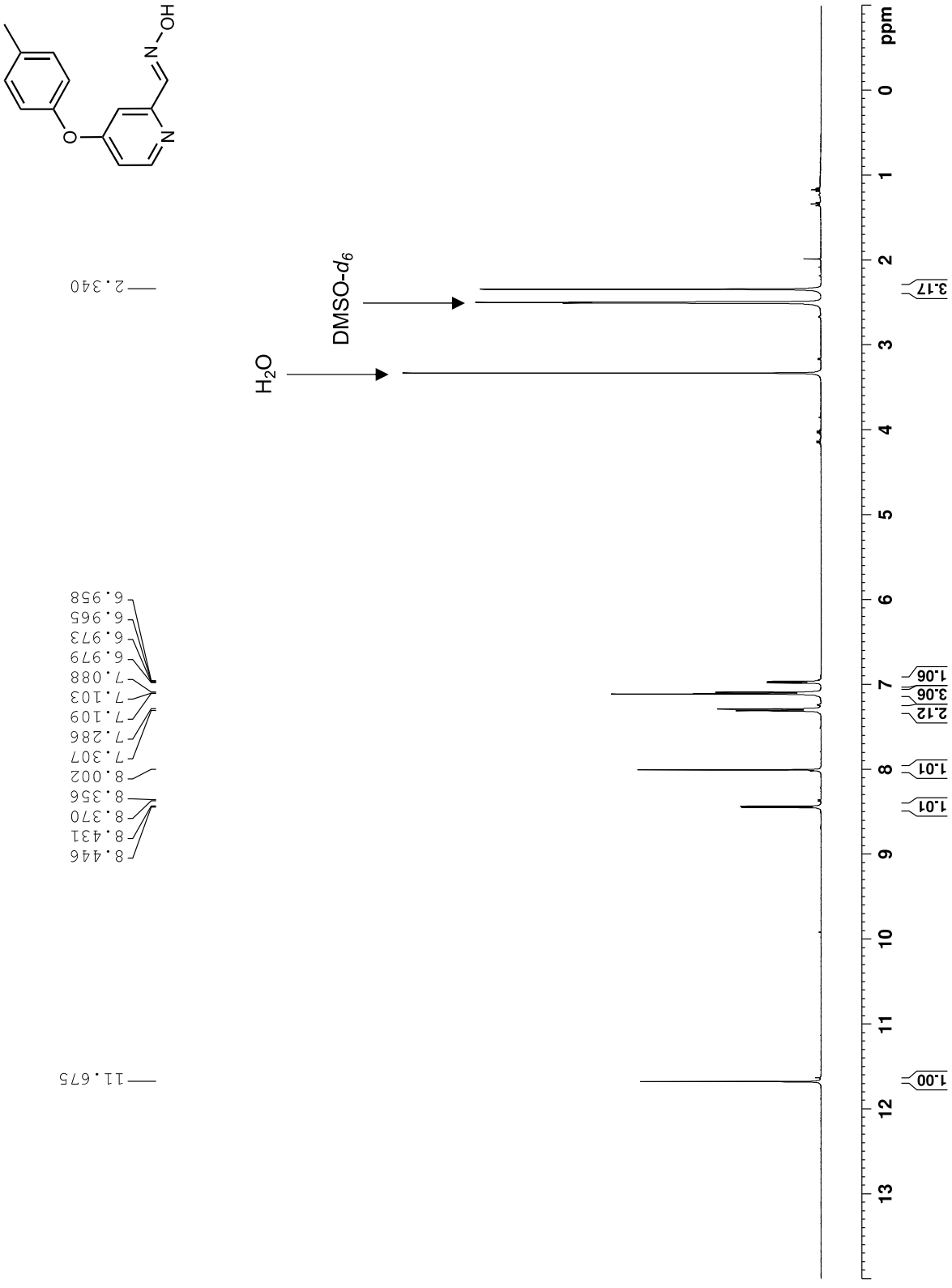

Spectrum 162. ^{1}H NMR of *(E)*-4-(*p*-tolyloxy)picolinaldehyde oxime (400 MHz, 293 K, DMSO-d_6).

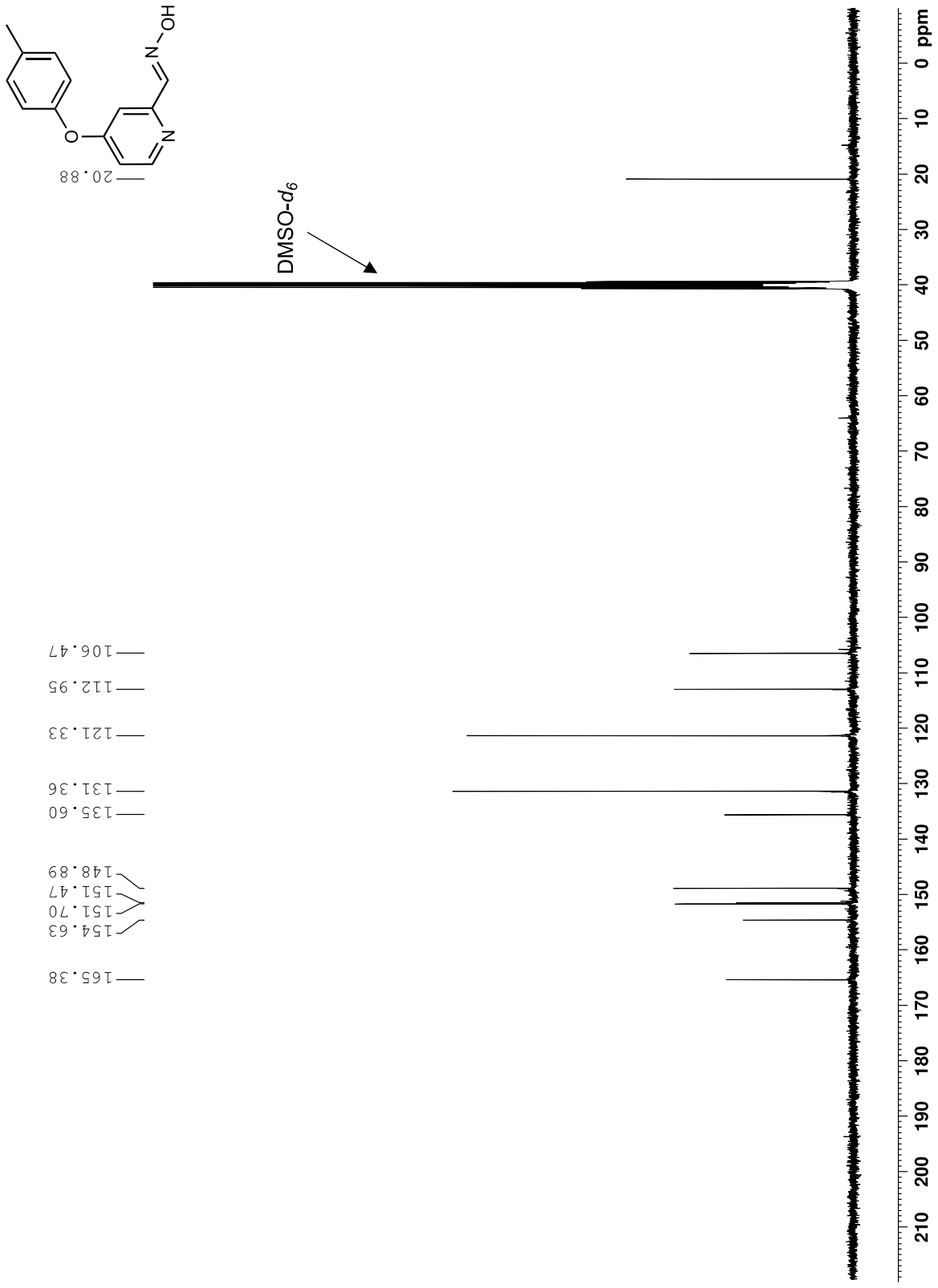

Spectrum 163. ^{13}C NMR of *(E)*-4-(*p*-tolyloxy)picolinaldehyde oxime (100 MHz, 293 K, DMSO-d_6).

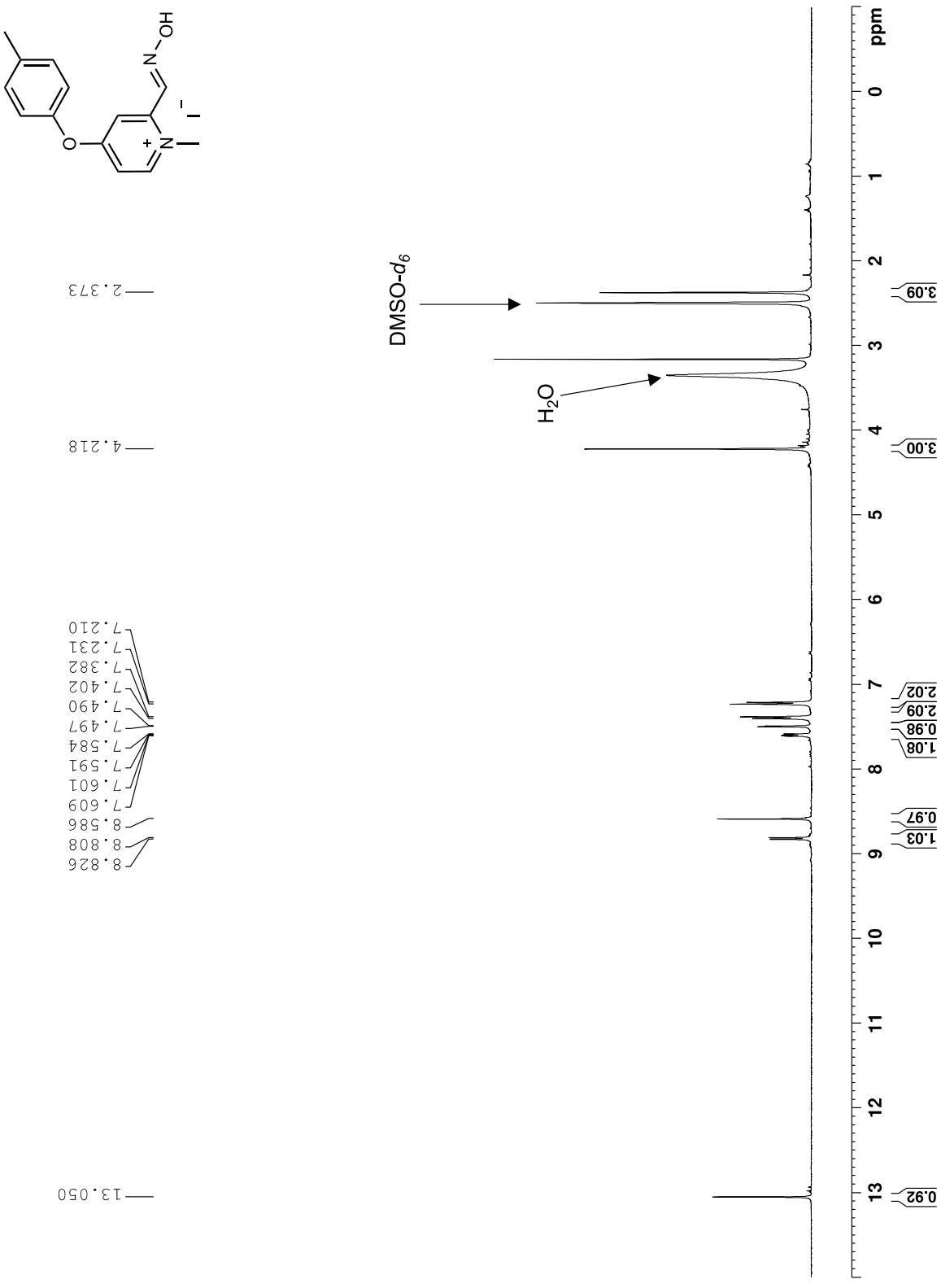

Spectrum 164. ^{1}H NMR of *(E)*-2-((hydroxyimino)methyl)-1-methyl-4-(*p*-tolyloxy)pyridin-1-ium iodide (**ADG3092**) (400 MHz, 293 K, DMSO-d_6).

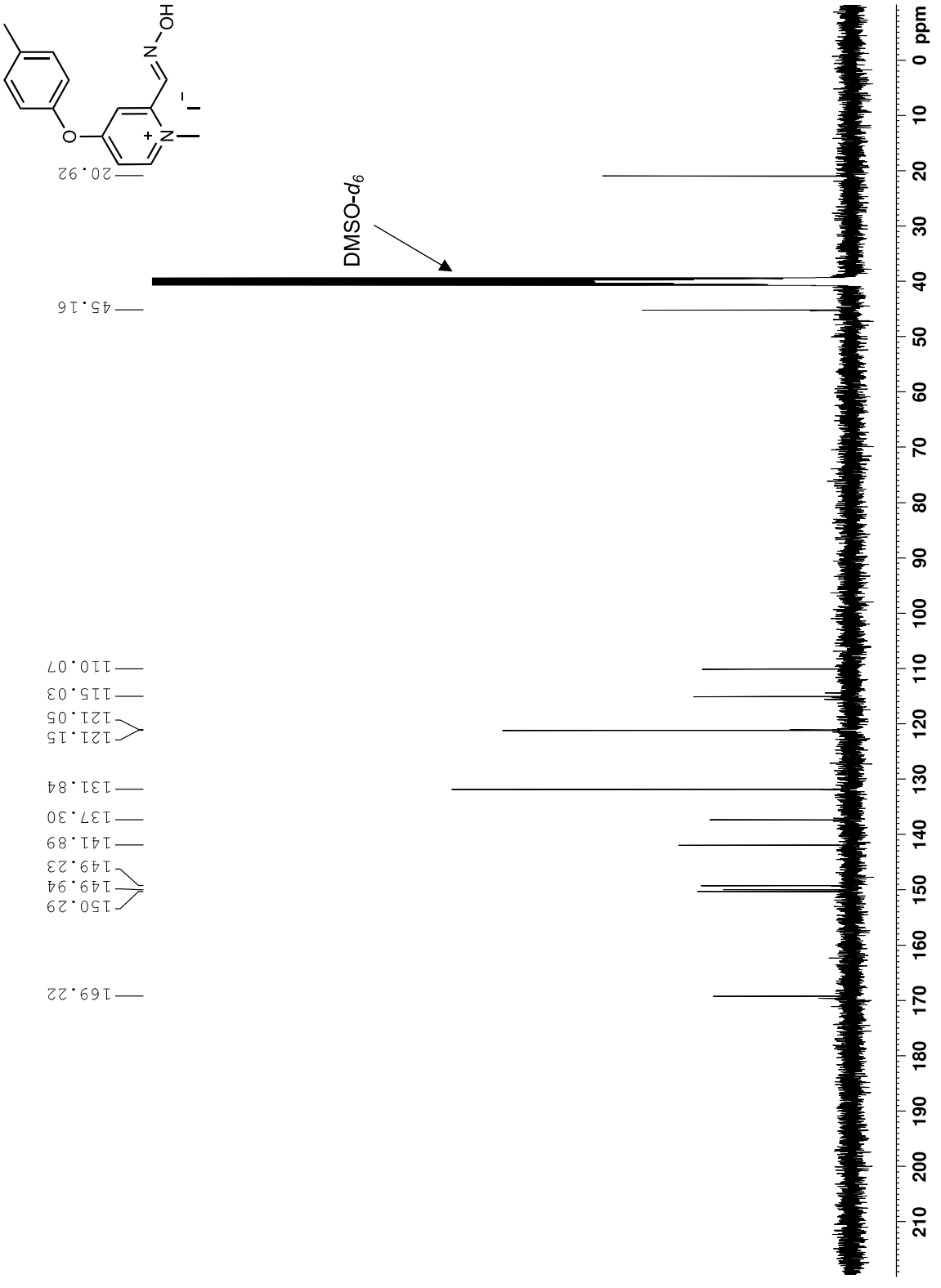

Spectrum 165. ^{13}C NMR of *(E)*-2-((hydroxyimino)methyl)-1-methyl-4-(*p*-tolyloxy)pyridin-1-ium iodide (**ADG3092**) (100 MHz, 293 K, DMSO-d_6).

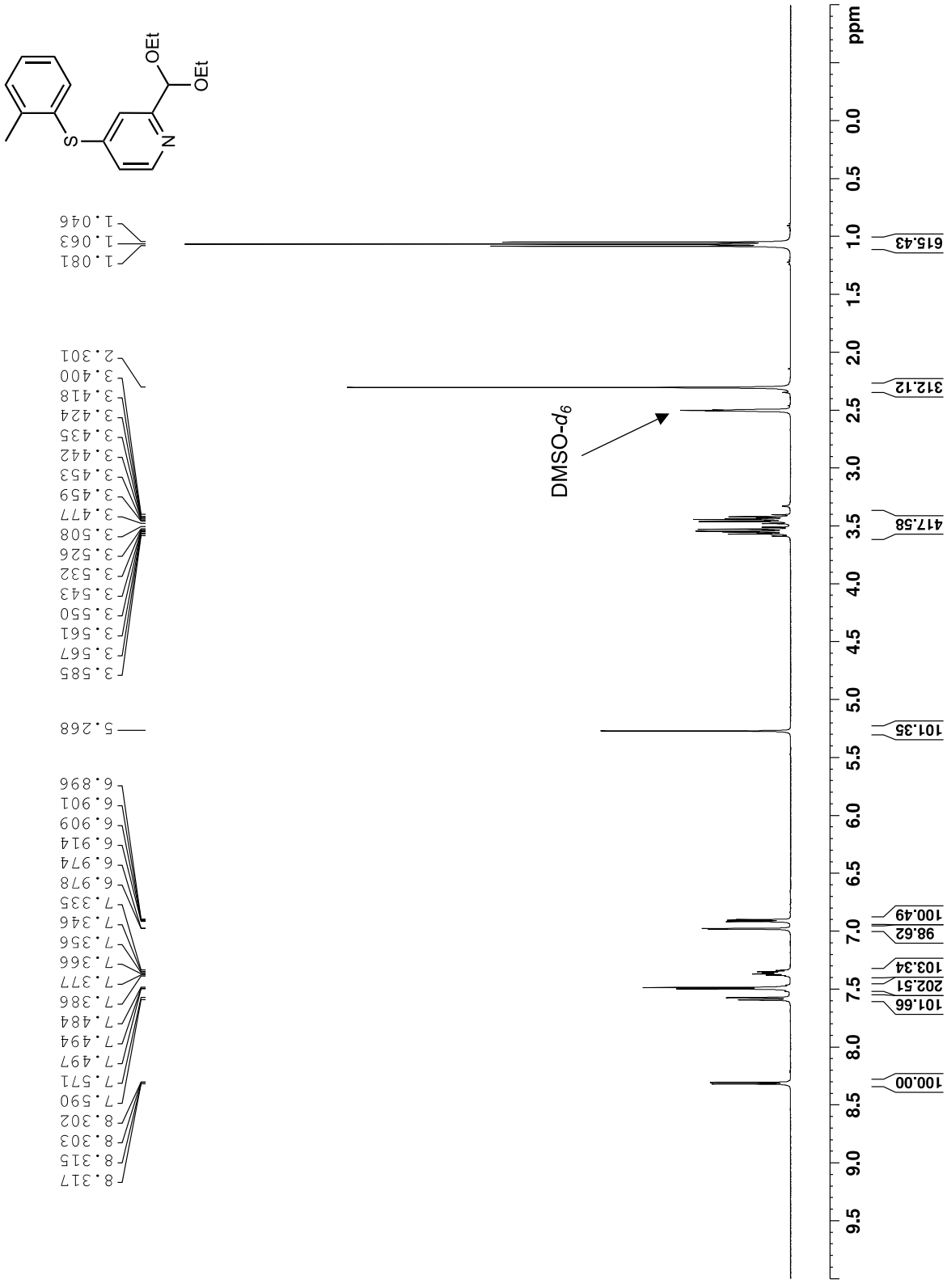

Spectrum 166. ^{1}H NMR of 2-(diethoxymethyl)-4-(*o*-tolylthio)pyridine (400 MHz, 293 K, DMSO-d_6).

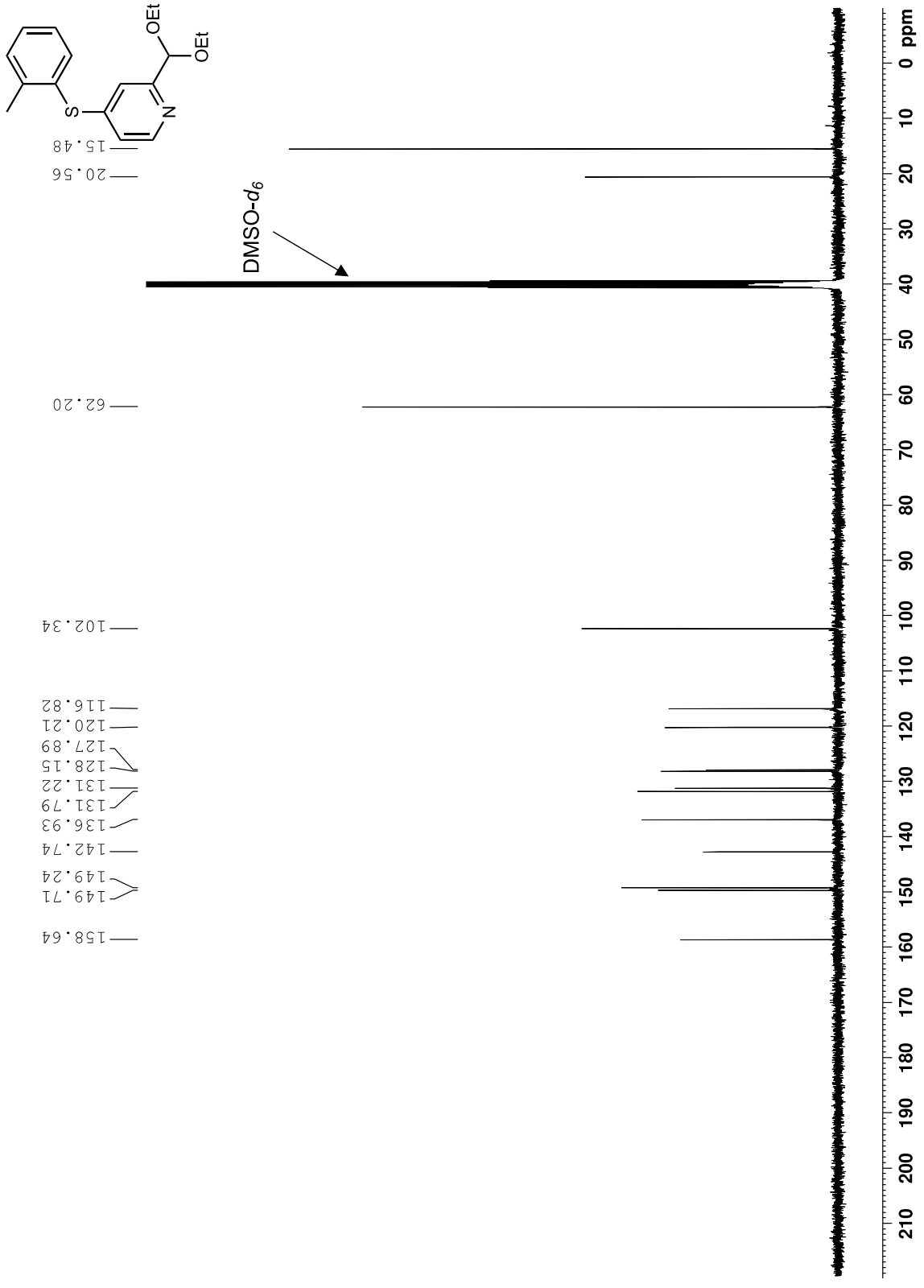

Spectrum 167. ^{13}C NMR of 2-(diethoxymethyl)-4-(*o*-tolylthio)pyridine (100 MHz, 293 K, DMSO-d_6).

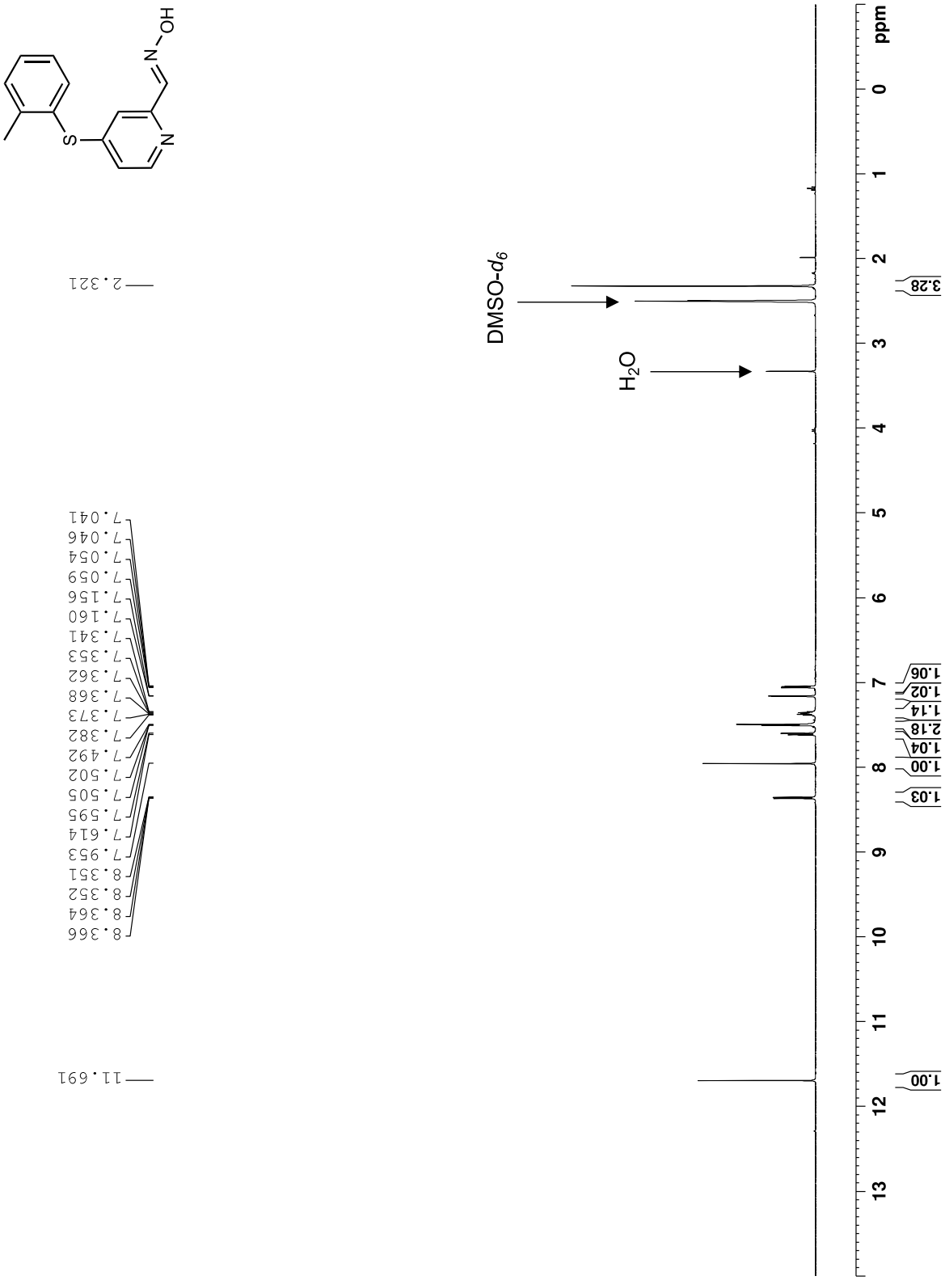

Spectrum 168. ^{1}H NMR of *(E)*-4-(*o*-tolylthio)picolinaldehyde oxime (400 MHz, 293 K, DMSO-d_6).

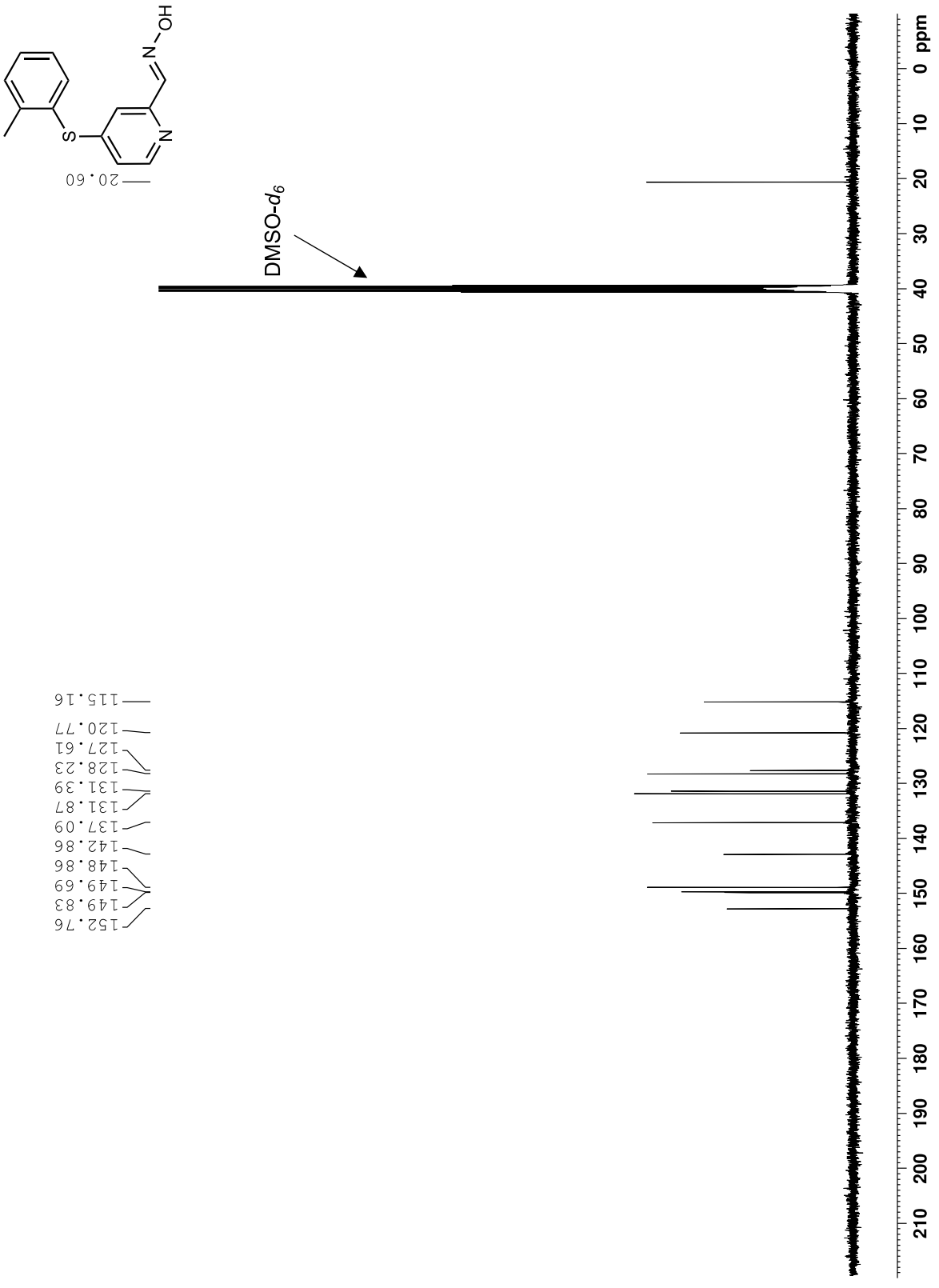

Spectrum 169. ^{13}C NMR of *(E)*-4-(*o*-tolylthio)picolinaldehyde oxime (100 MHz, 293 K, DMSO-d_6).

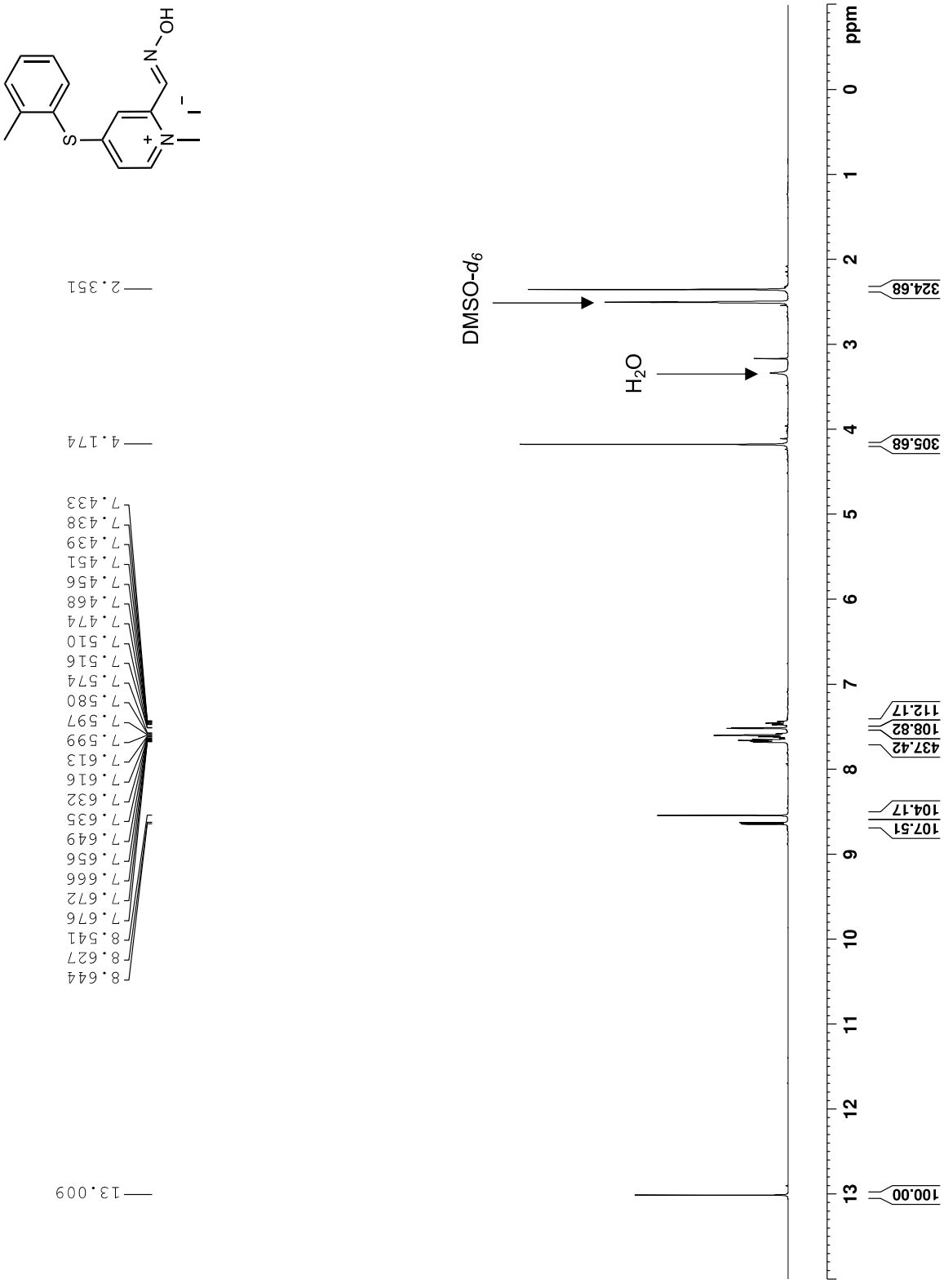

Spectrum 170. ^{1}H NMR of *(E)*-2-((hydroxyimino)methyl)-1-methyl-4-(*o*-tolylthio)pyridin-1-ium iodide (**ADG4122**) (400 MHz, 293 K, DMSO-d_6).

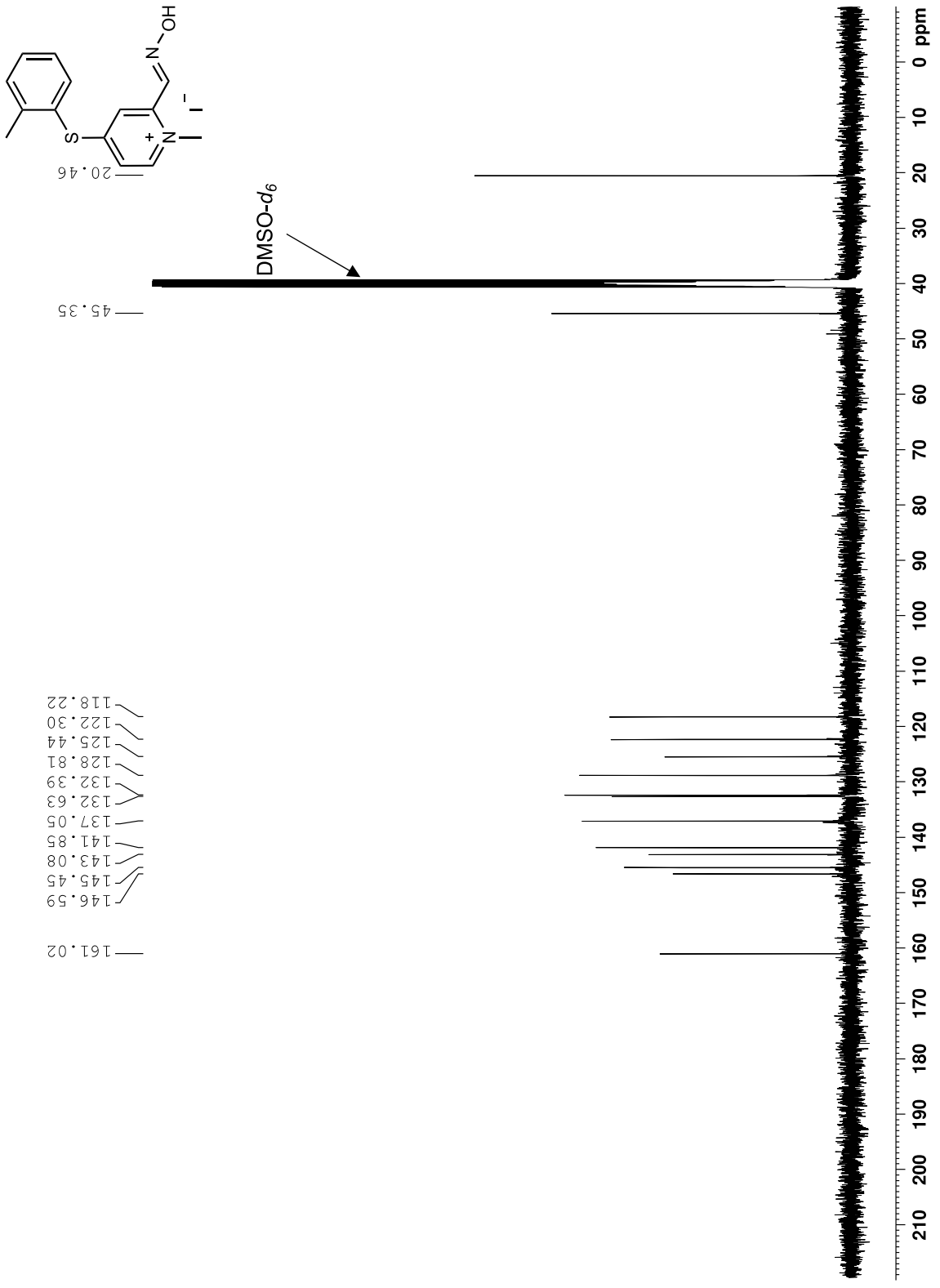

Spectrum 171. ^{13}C NMR of *(E)*-2-((hydroxyimino)methyl)-1-methyl-4-(*o*-tolylthio)pyridin-1-ium iodide (**ADG4122**) (100 MHz, 293 K, DMSO-d_6).

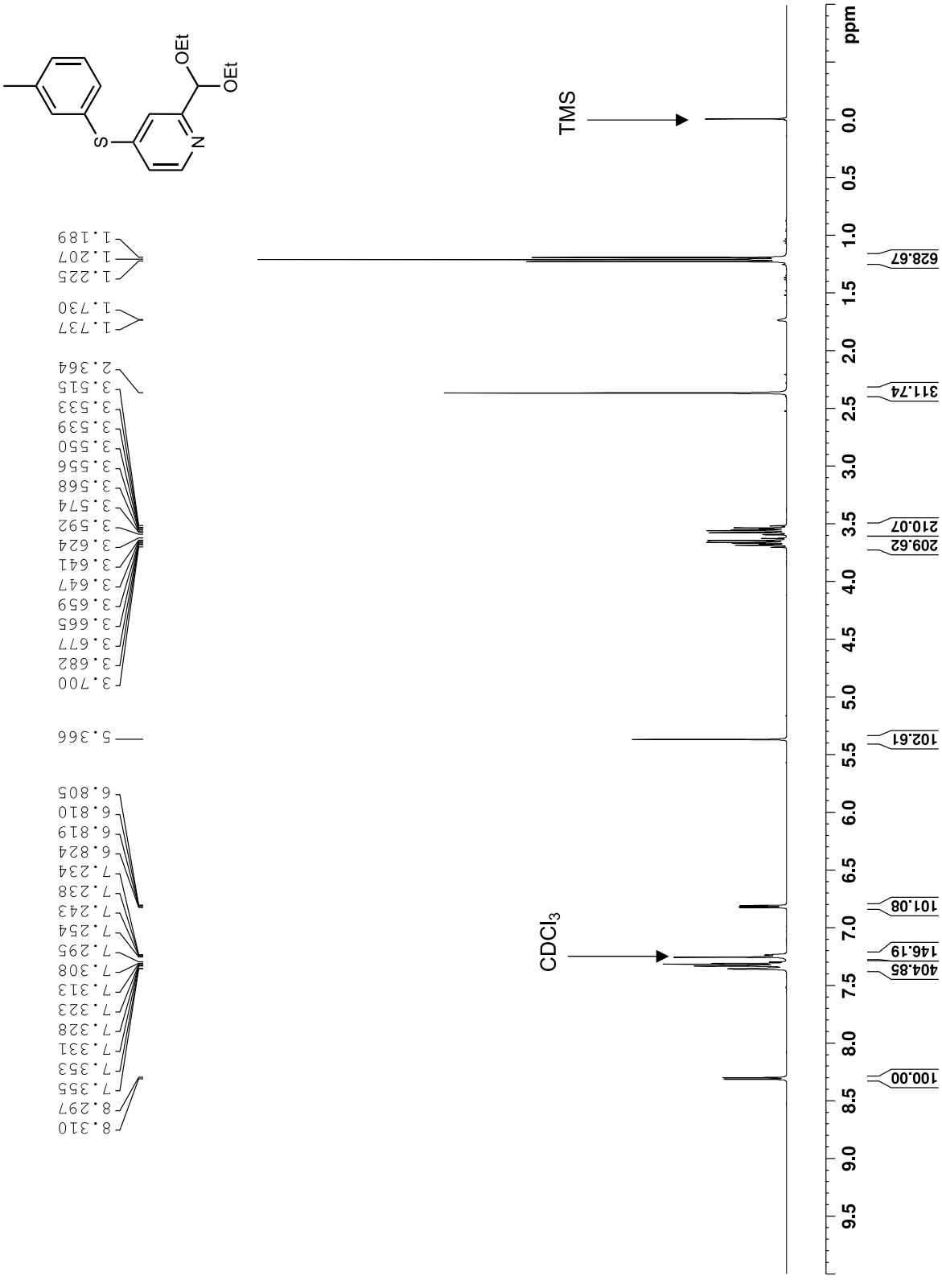

Spectrum 172. ^{1}H NMR of 2-(diethoxymethyl)-4-(*m*-tolylthio)pyridine (400 MHz, 293 K, $CDCl_3$).

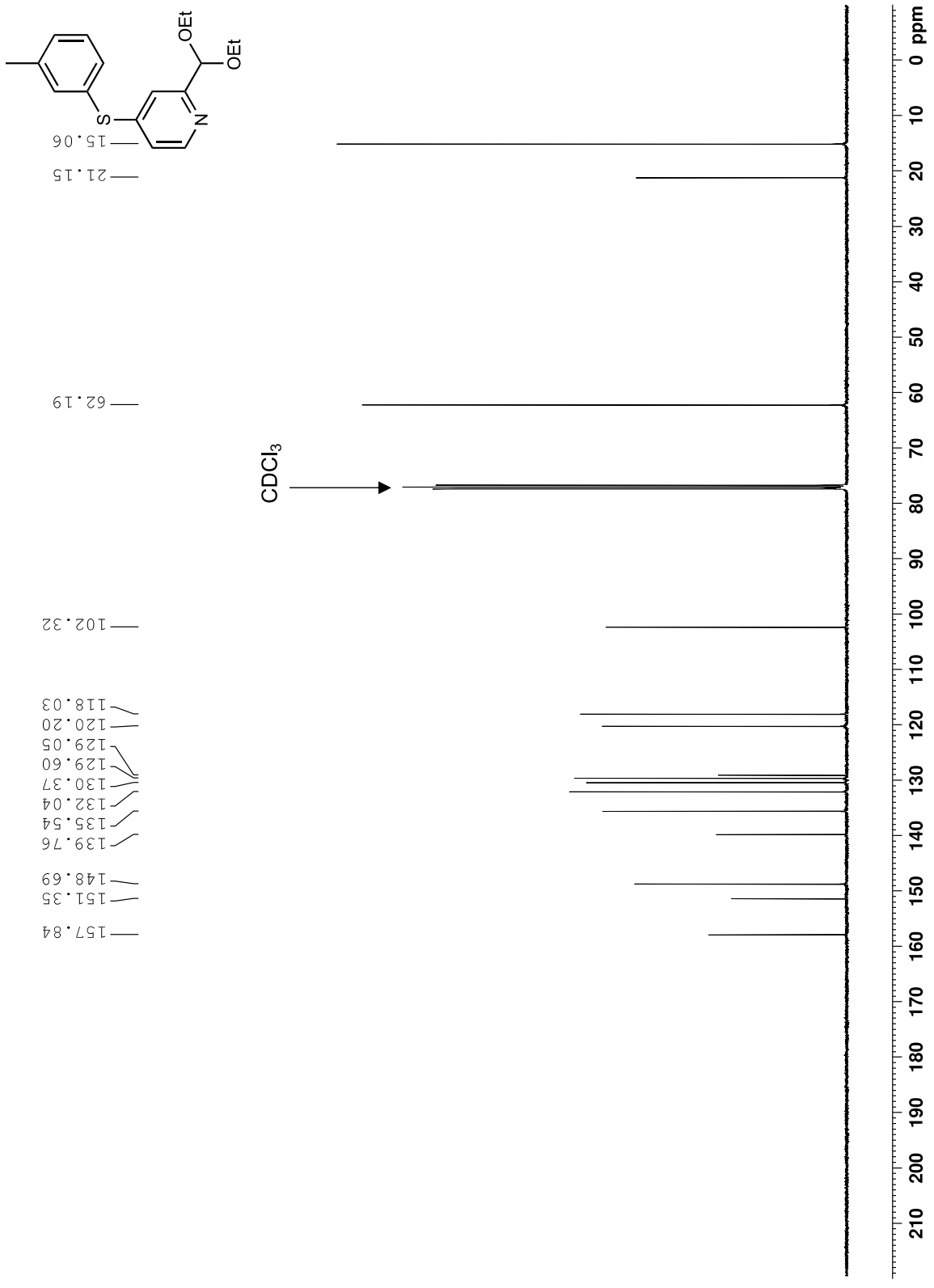

Spectrum 173. ^{13}C NMR of 2-(diethoxymethyl)-4-(*m*-tolylthio)pyridine (100 MHz, 293 K, $CDCl_3$).

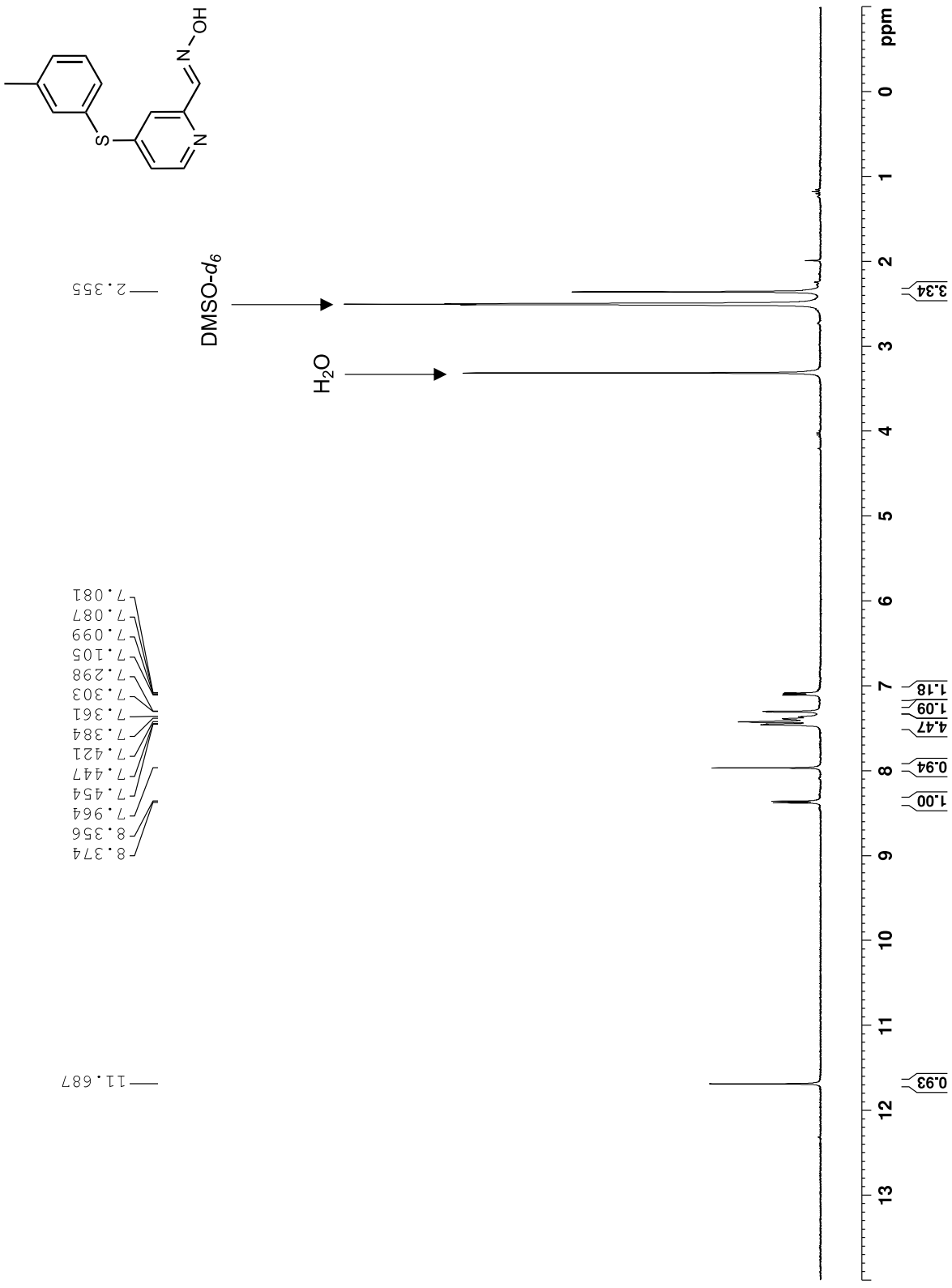

Spectrum 174. ^{1}H NMR of *(E)*-4-(*m*-tolylthio)picolinaldehyde oxime (300 MHz, 293 K, DMSO-d_6).

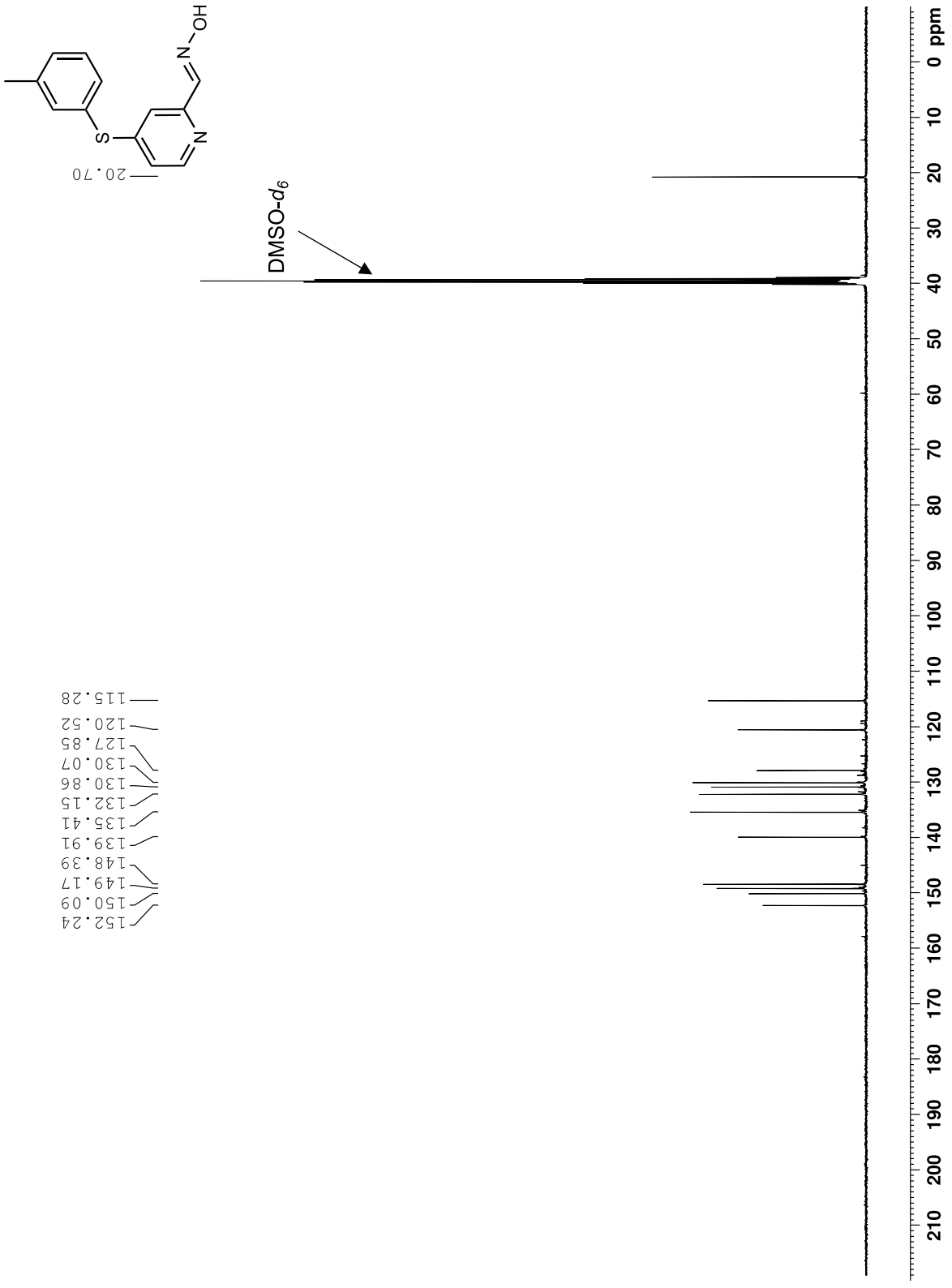

Spectrum 175. ^{13}C NMR of *(E)*-4-(*m*-tolylthio)picolinaldehyde oxime (100 MHz, 293 K, DMSO-d_6).

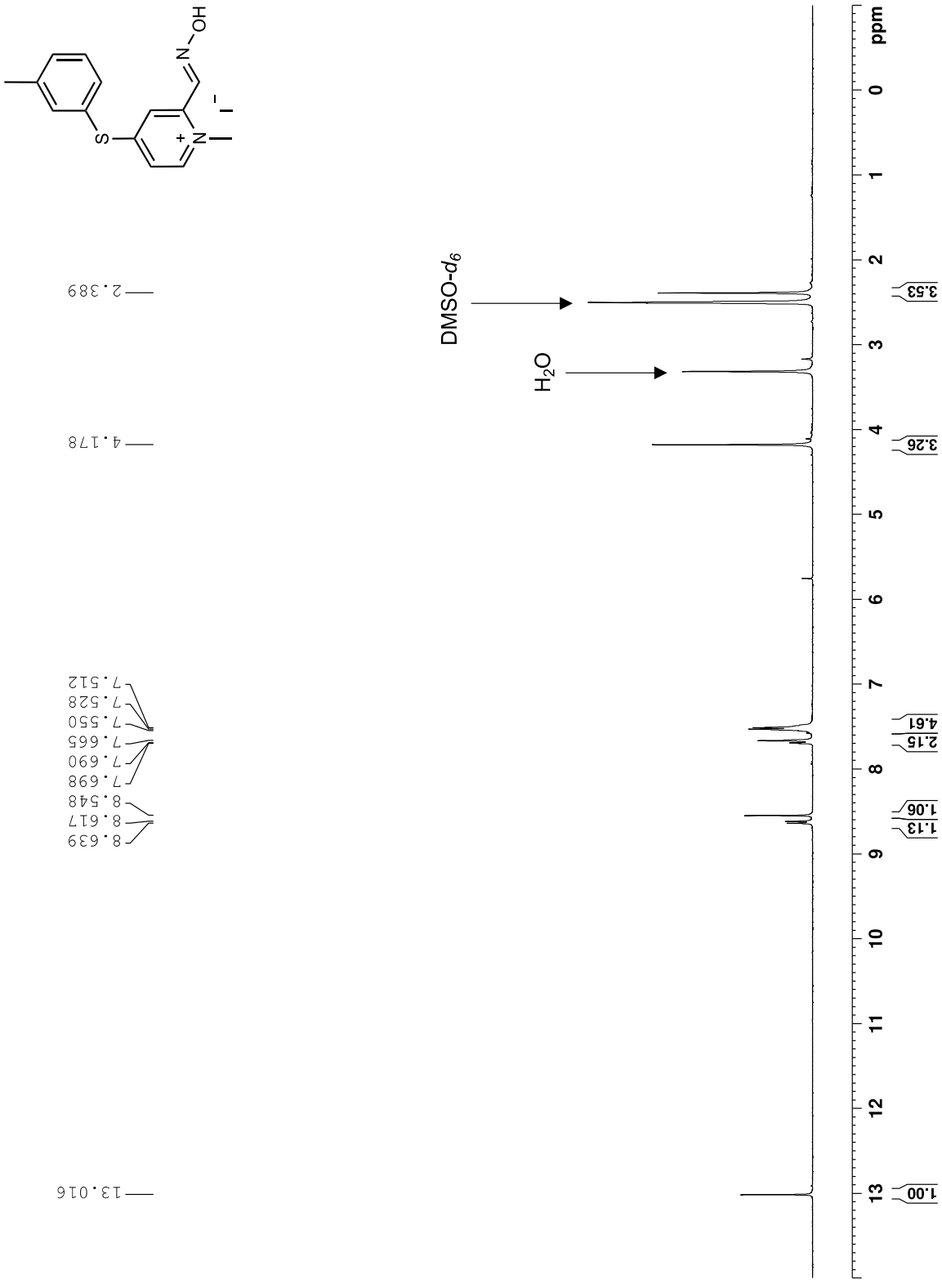

Spectrum 176. ^{1}H NMR of *(E)*-2-((hydroxyimino)methyl)-1-methyl-4-(*m*-tolylthio)pyridin-1-ium iodide (**ADG4086**) (300 MHz, 293 K, DMSO-d_6).

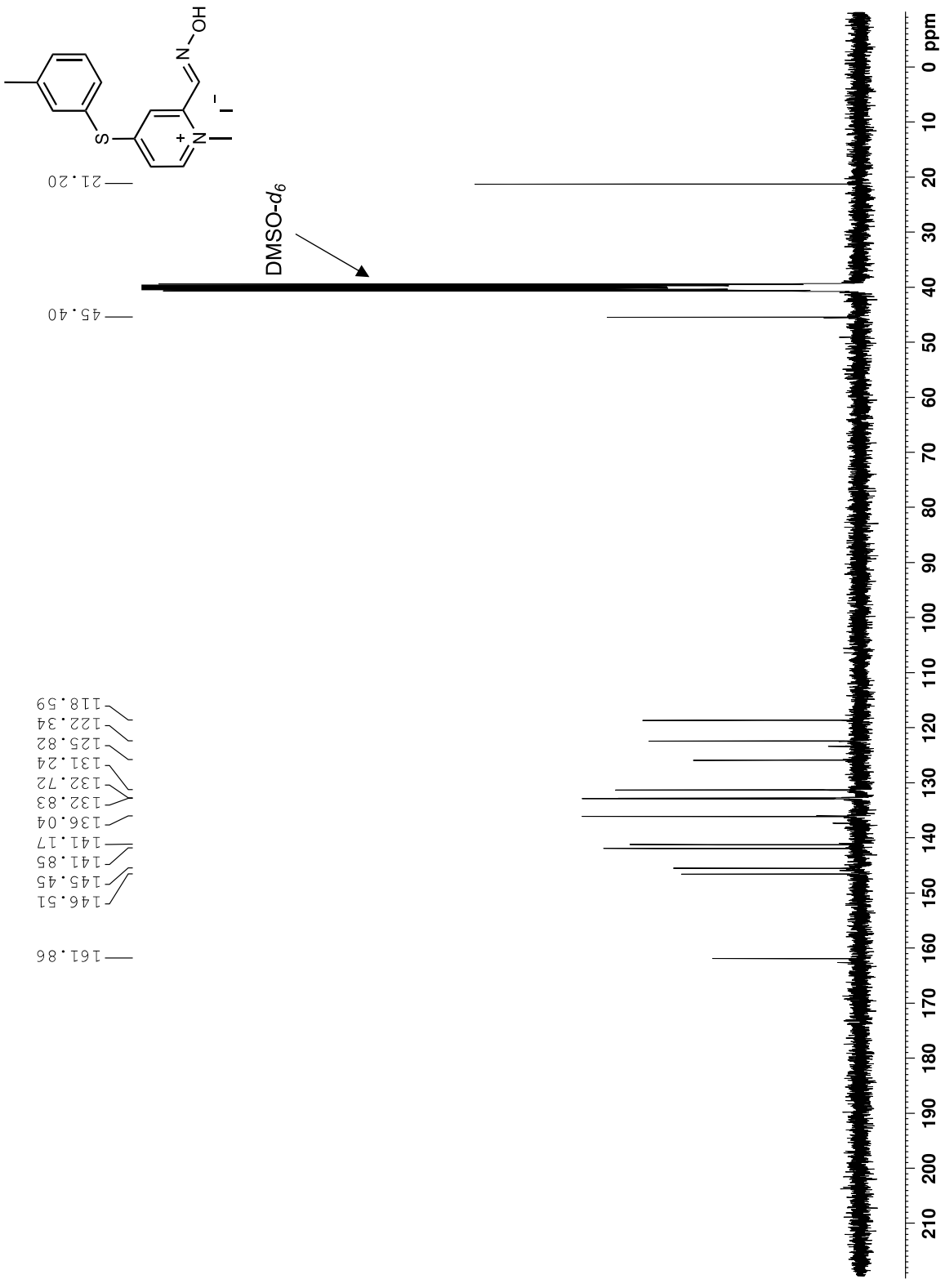

Spectrum 177. ^{13}C NMR of *(E)*-2-((hydroxyimino)methyl)-1-methyl-4-(*m*-tolylthio)pyridin-1-ium iodide (**ADG4086**) (100 MHz, 293 K, DMSO-d_6).

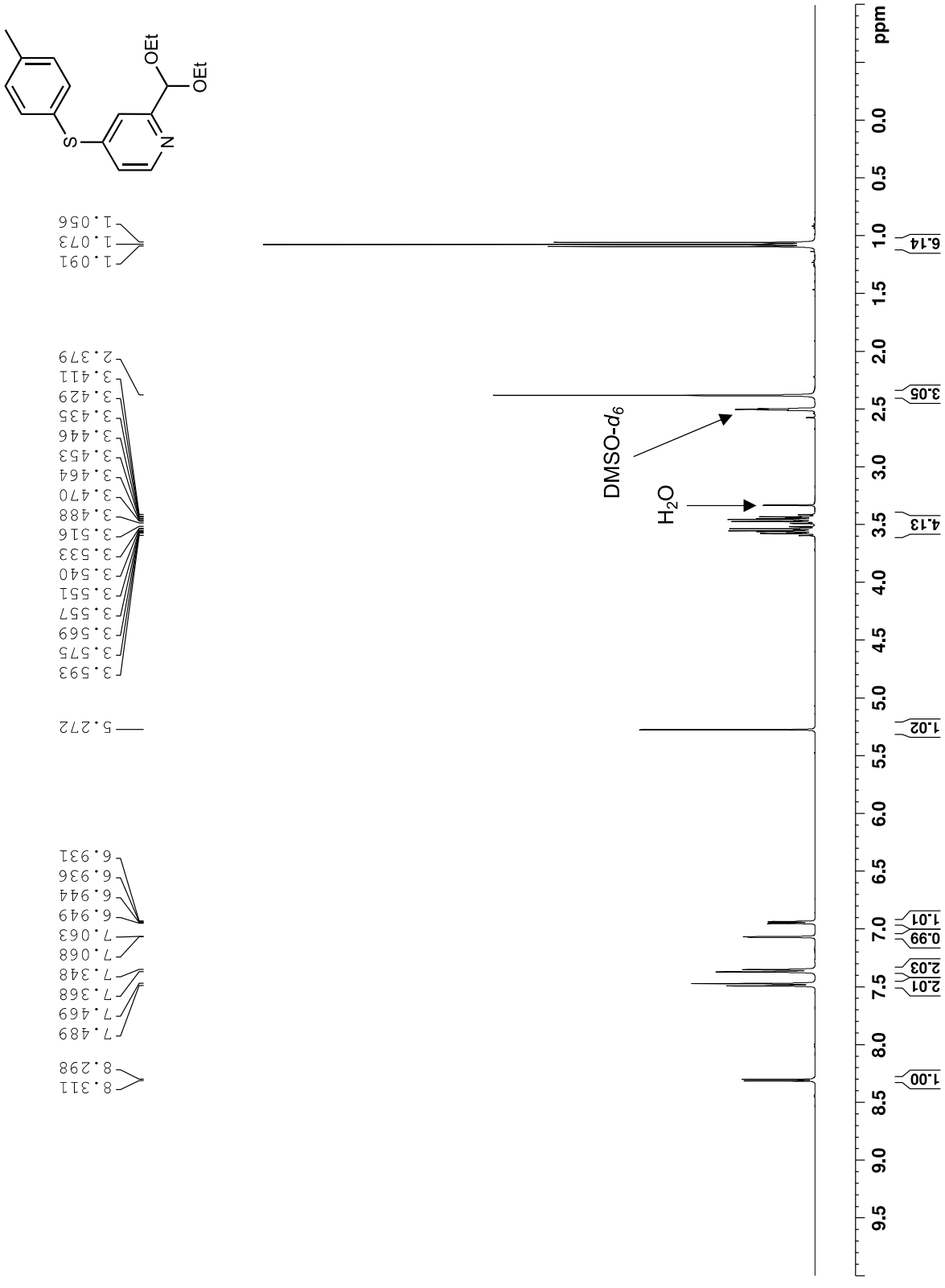

Spectrum 178. ^{1}H NMR of 2-(diethoxymethyl)-4-(*p*-tolylthio)pyridine (400 MHz, 293 K, DMSO-d_6).

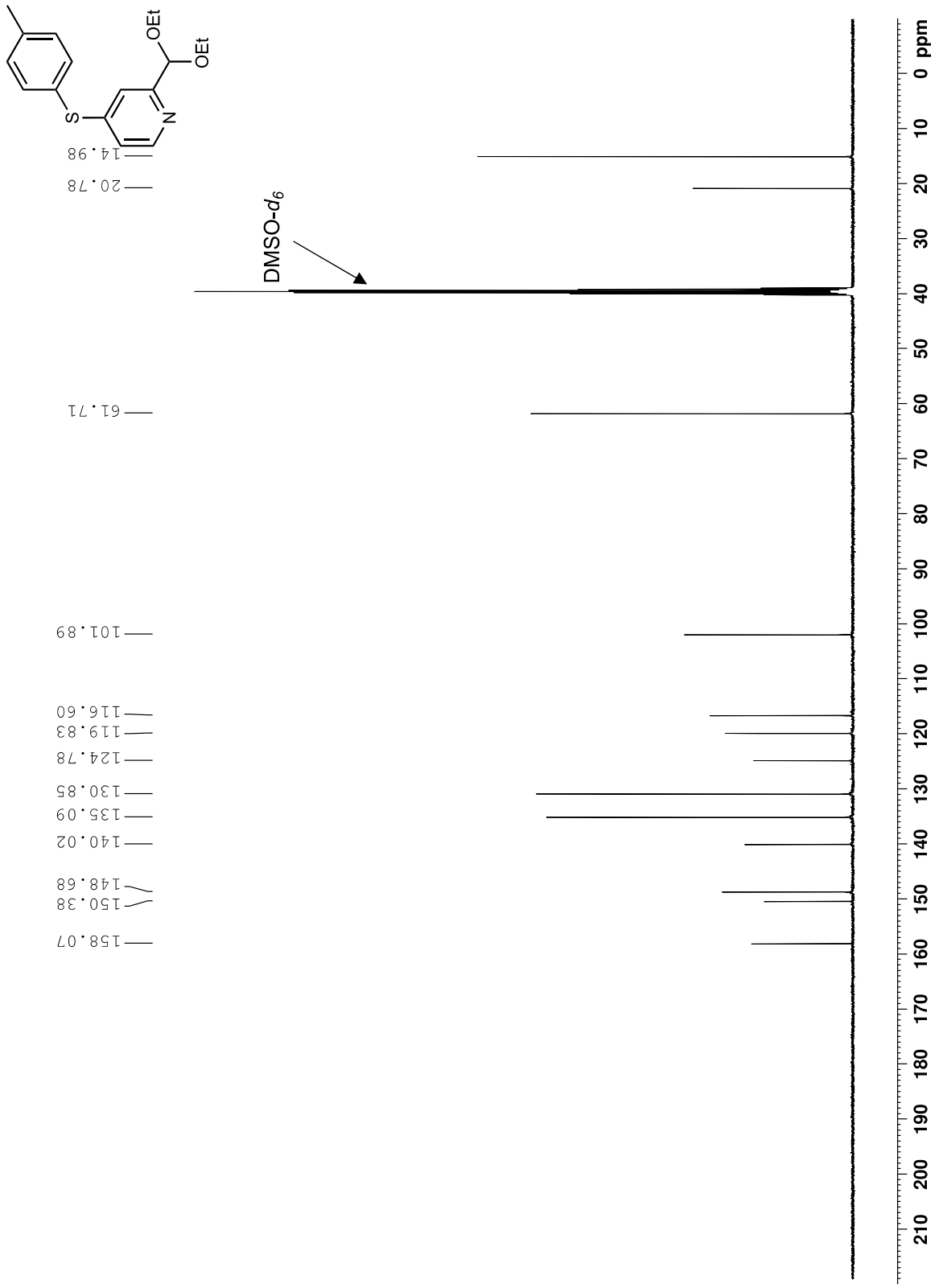

Spectrum 179. ^{13}C NMR of 2-(diethoxymethyl)-4-(*p*-tolylthio)pyridine (100 MHz, 293 K, DMSO-d_6).

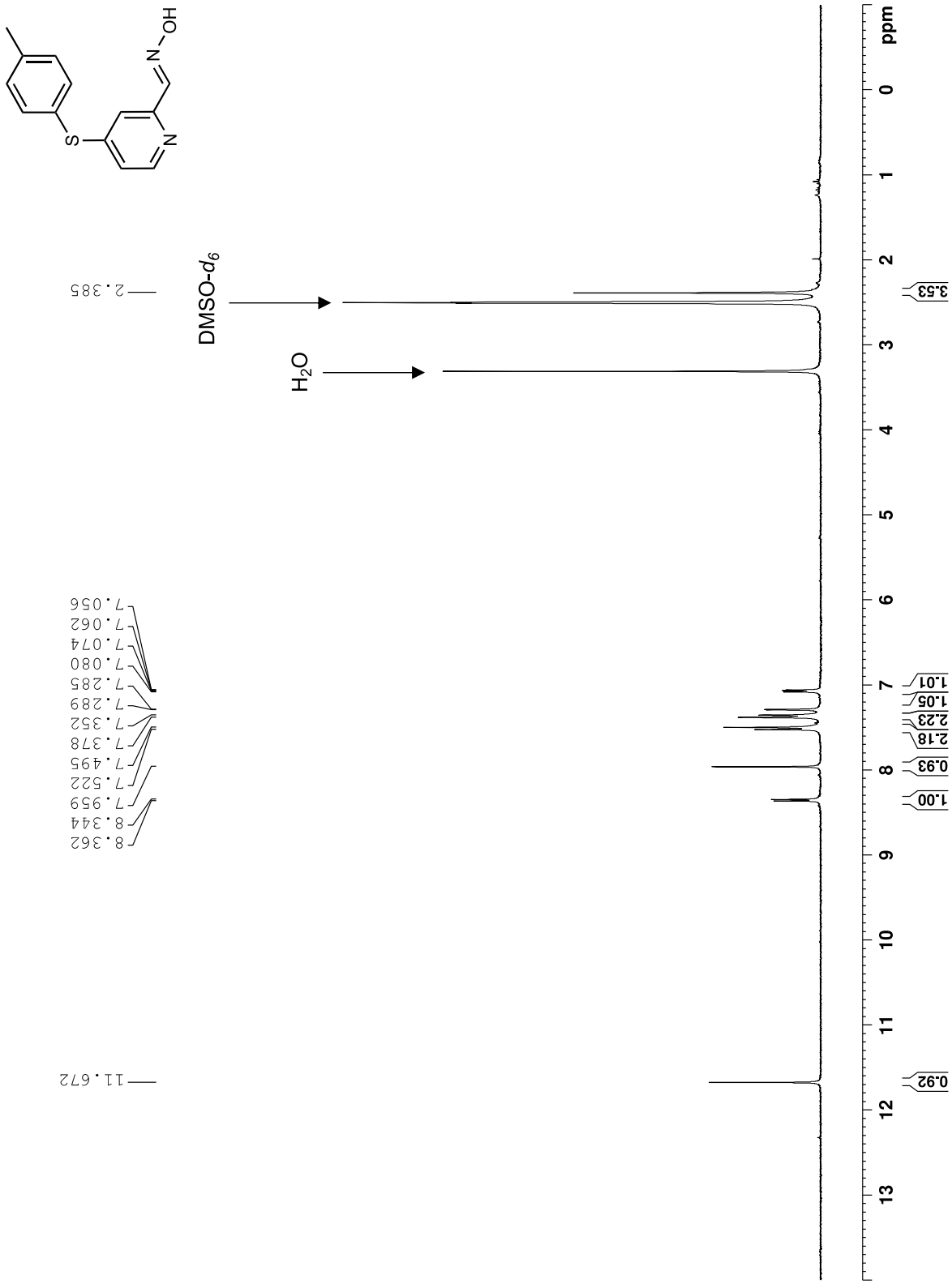

Spectrum 180. ^{1}H NMR of *(E)*-4-(*p*-tolylthio)picolinaldehyde oxime (300 MHz, 293 K, DMSO-d_6).

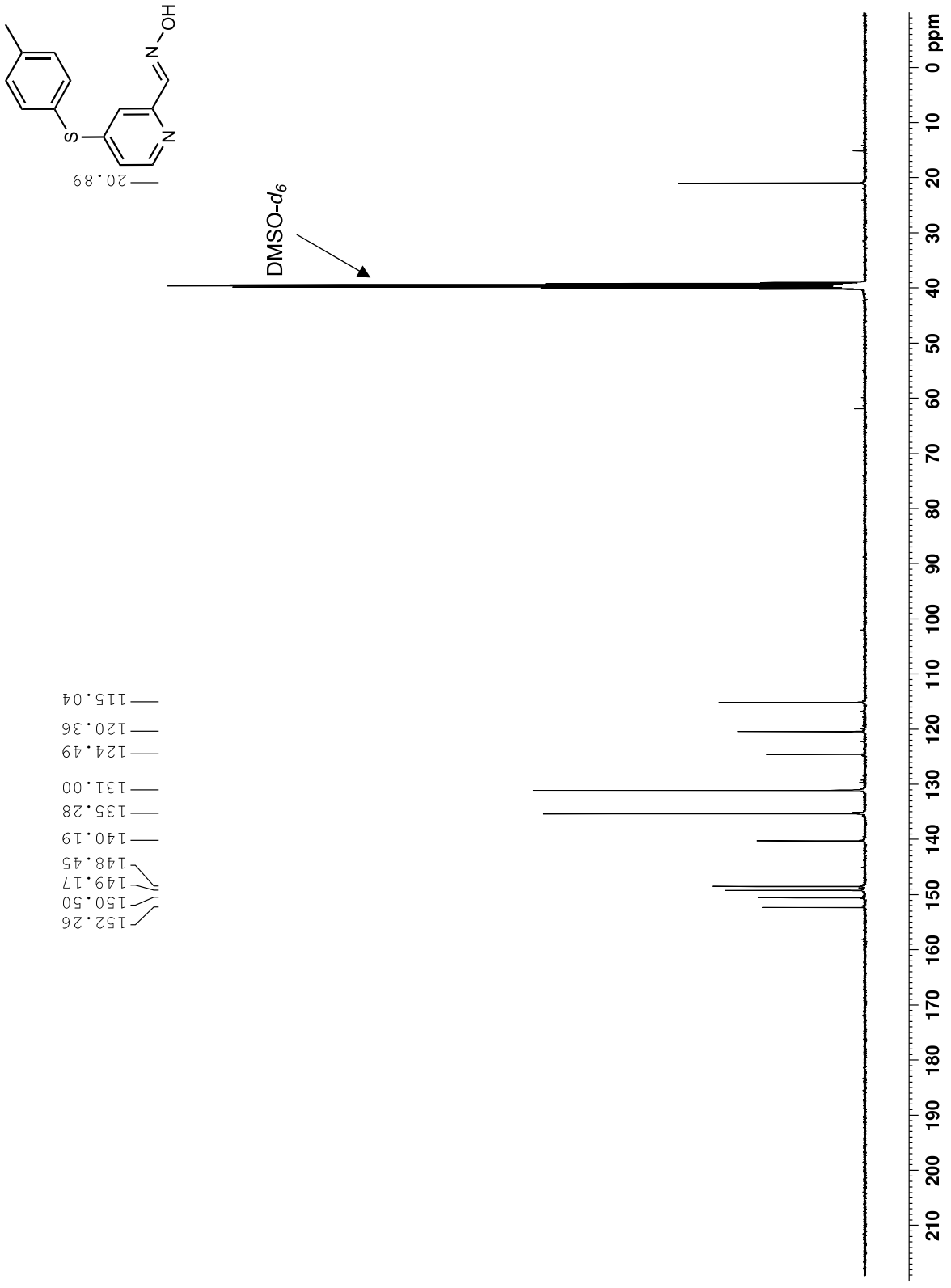

Spectrum 181. ^{13}C NMR of *(E)*-4-(*p*-tolylthio)picolinaldehyde oxime (100 MHz, 293 K, DMSO-d_6).

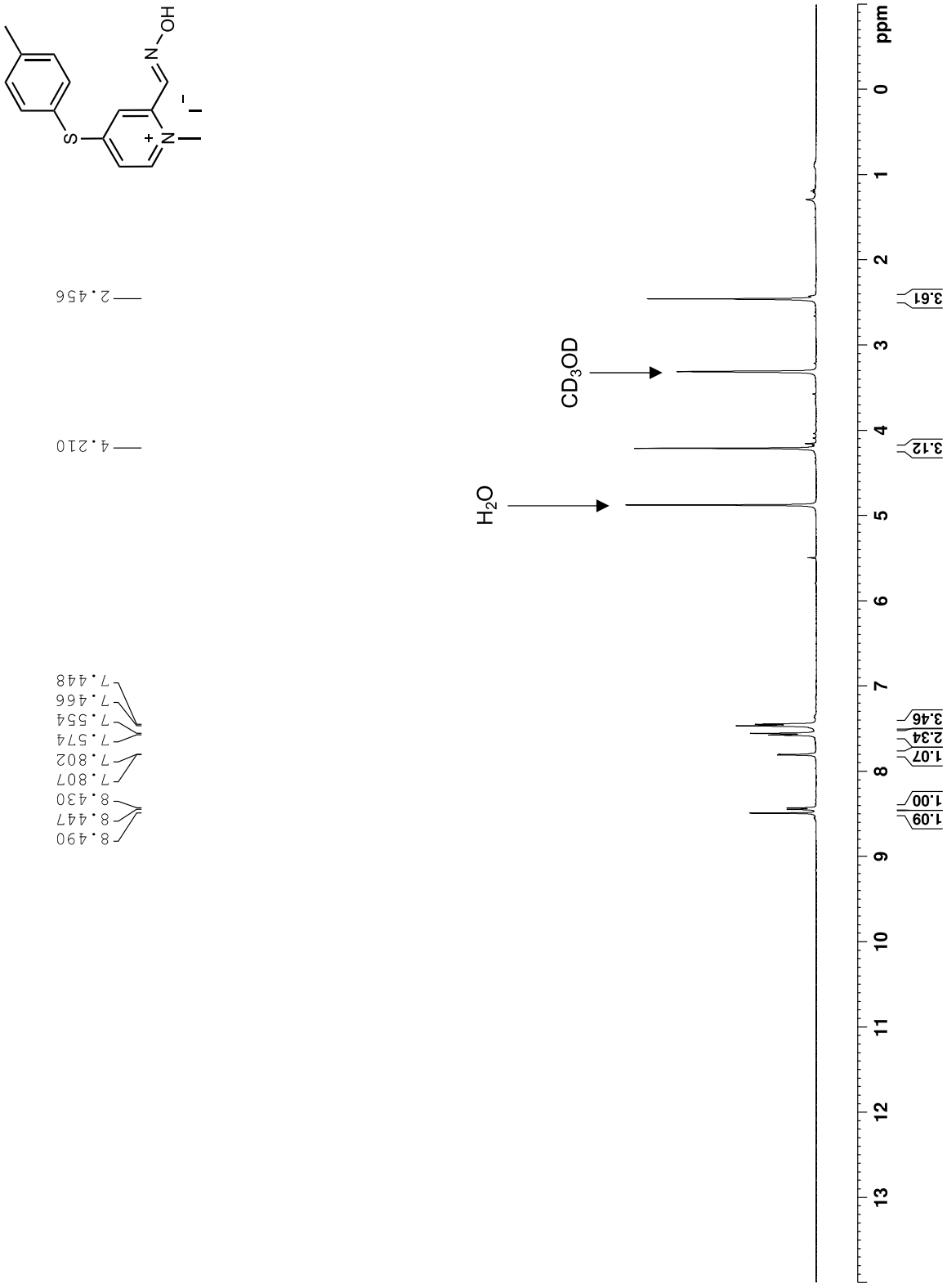

Spectrum 182. ^{1}H NMR of *(E)*-2-((hydroxyimino)methyl)-1-methyl-4-(*p*-tolylthio)pyridin-1-ium iodide (**ADG4094**) (400 MHz, 293 K, CD_3OD).

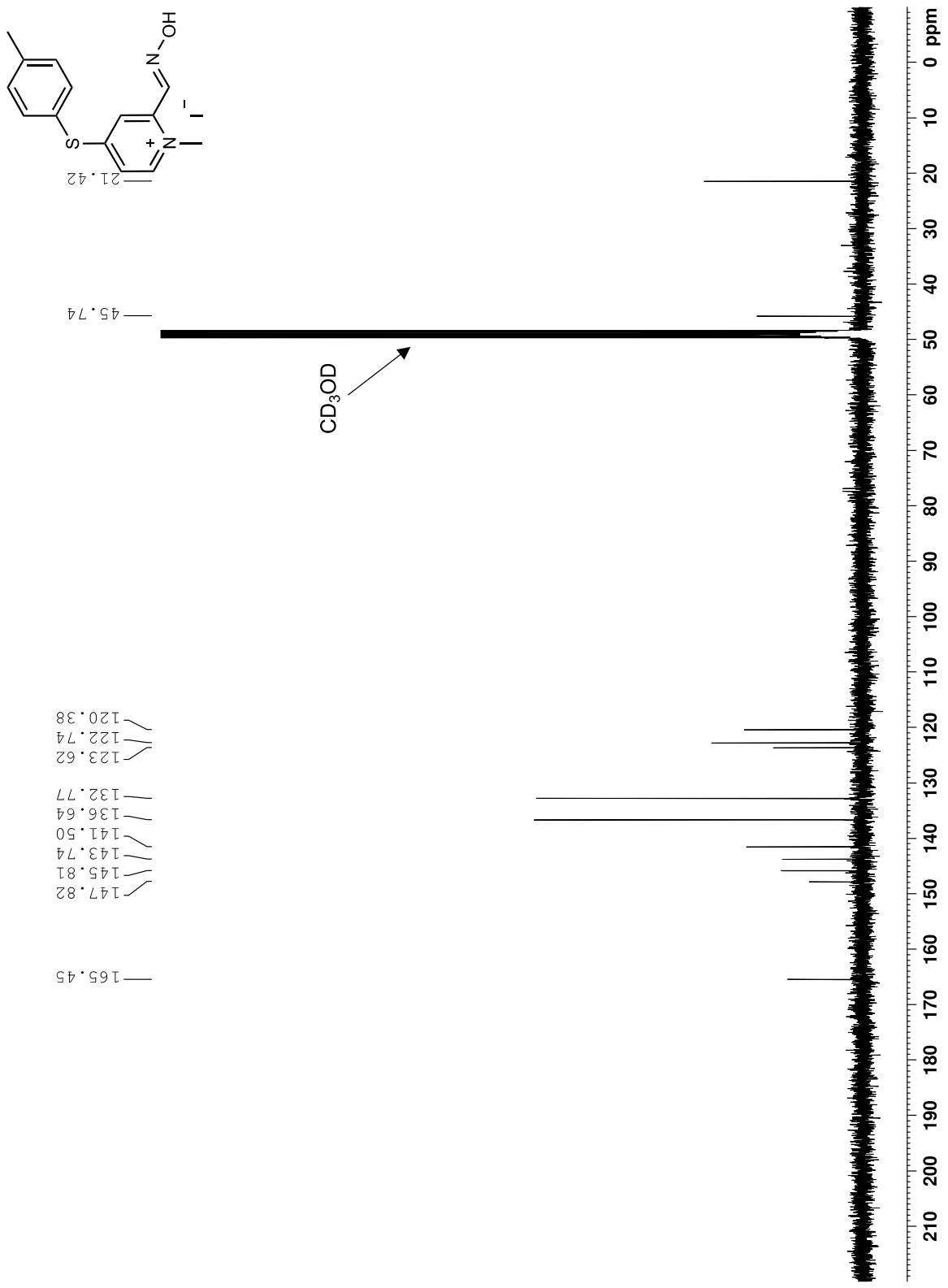

Spectrum 183. ^{13}C NMR of *(E)*-2-((hydroxyimino)methyl)-1-methyl-4-(*p*-tolylthio)pyridin-1-ium iodide (**ADG4094**) (100 MHz, 293 K, CD_3OD).

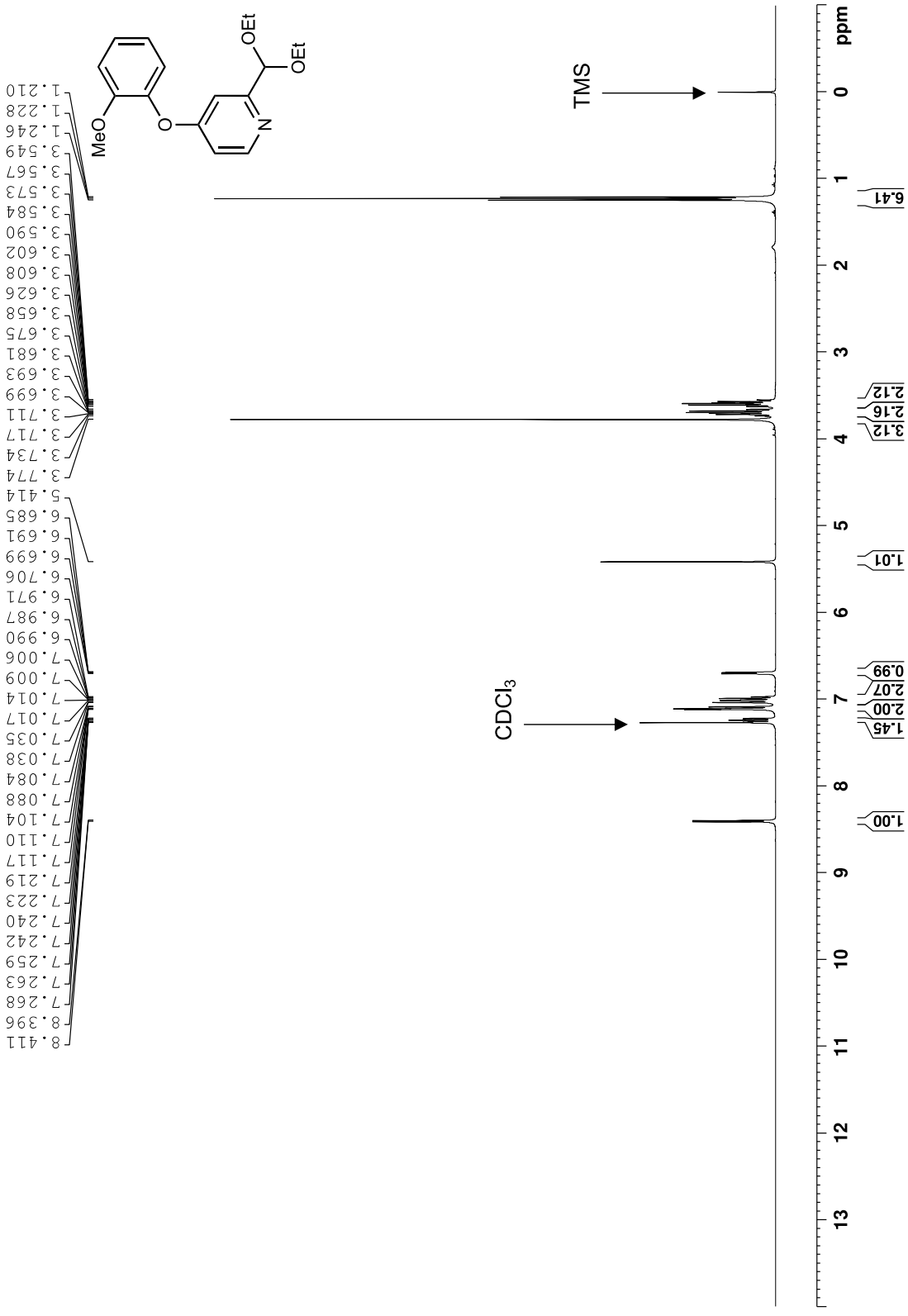

Spectrum 184. ^{1}H NMR of 2-(diethoxymethyl)-4-(2-methoxyphenoxy)pyridine. (400 MHz, 293 K, $CDCl_3$).

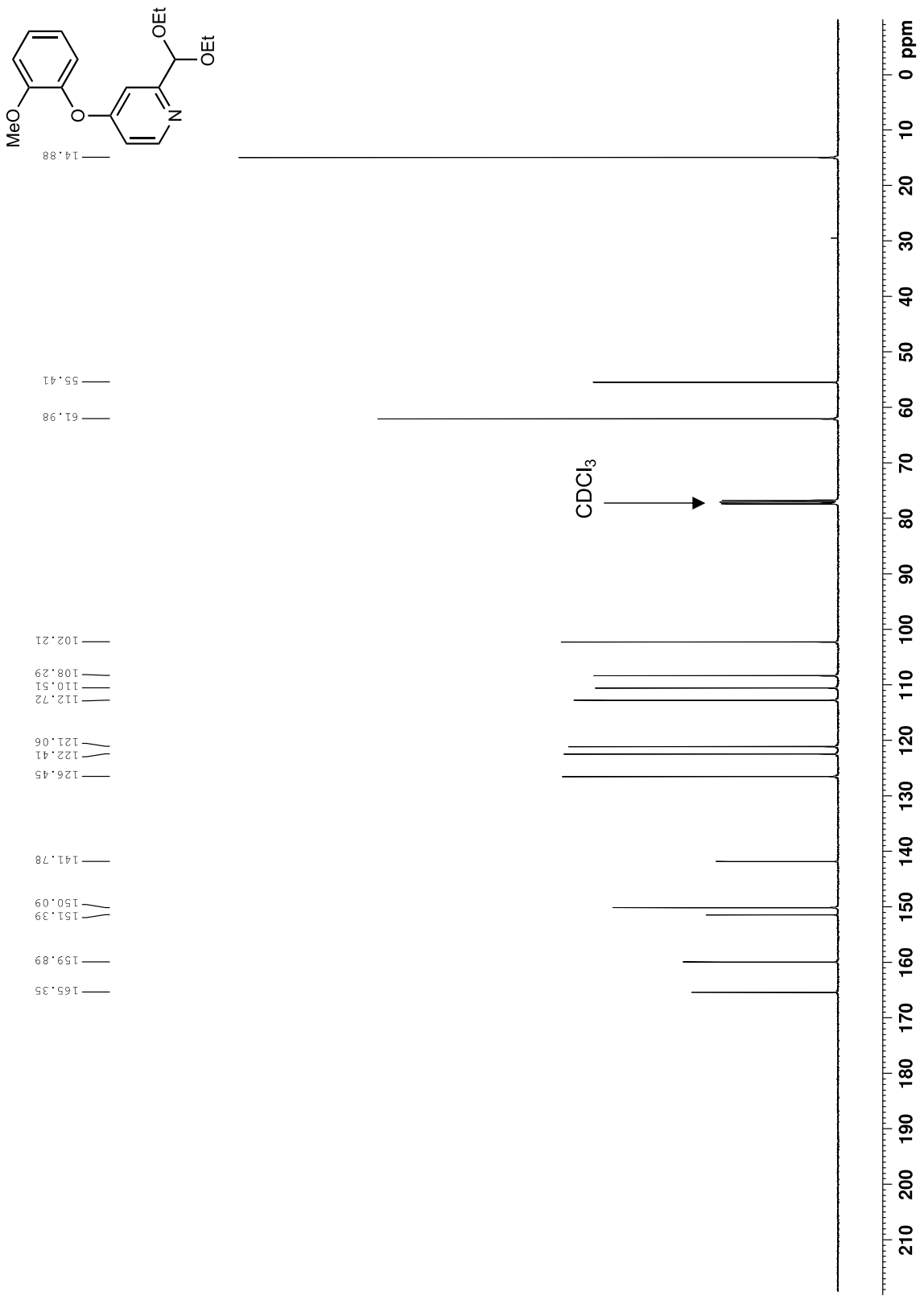

Spectrum 185. ^{13}C NMR of 2-(diethoxymethyl)-4-(2-methoxyphenoxy)pyridine (100 MHz, 293 K, $CDCl_3$).

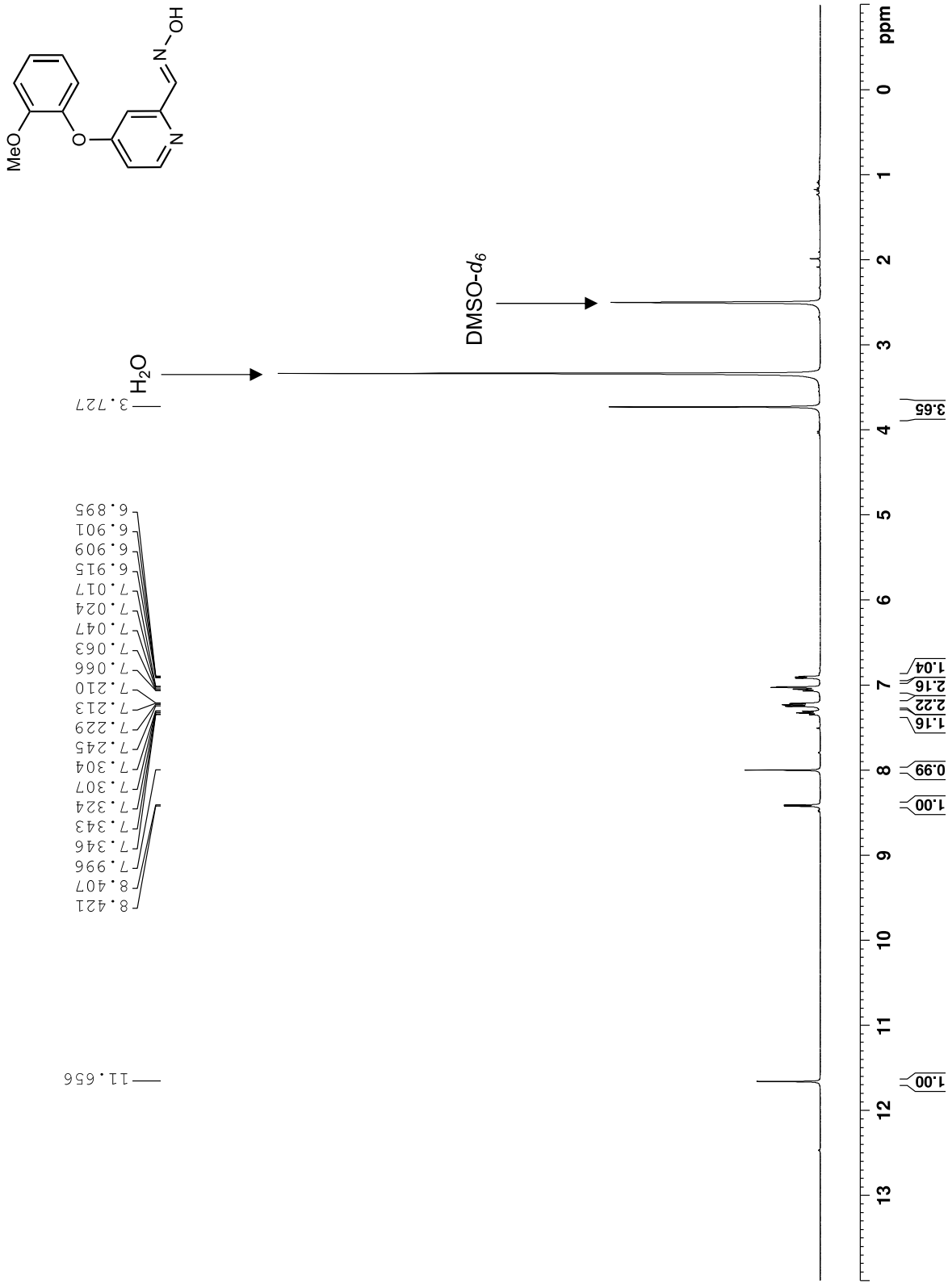

Spectrum 186. ^{1}H NMR of *(E)*-4-(2-methoxyphenoxy)picolinaldehyde oxime (400 MHz, 293 K, DMSO-d_6).

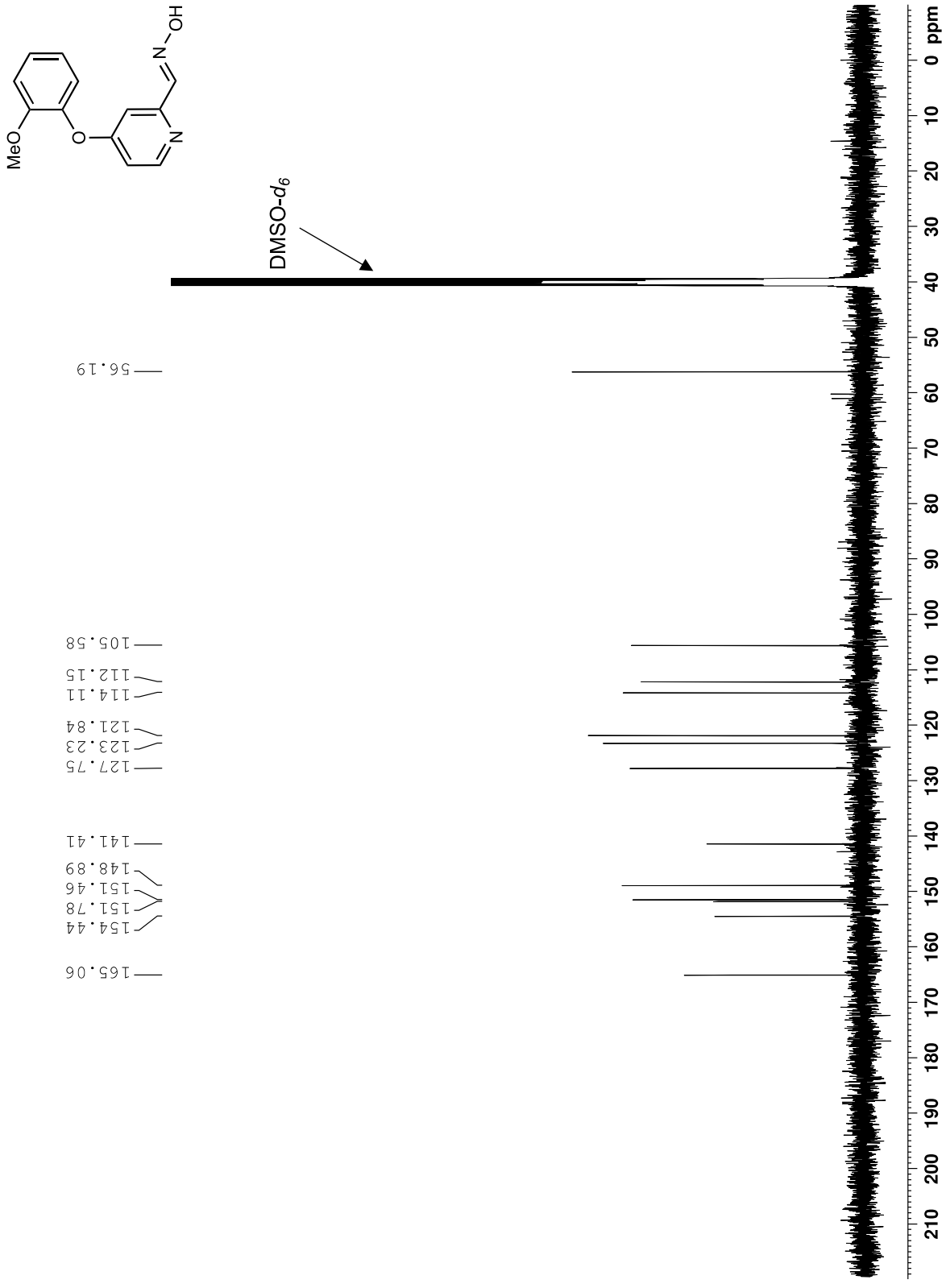

Spectrum 187. ^{13}C NMR of *(E)*-4-(2-methoxyphenoxy)picolinaldehyde oxime (100 MHz, 293 K, DMSO-d_6).

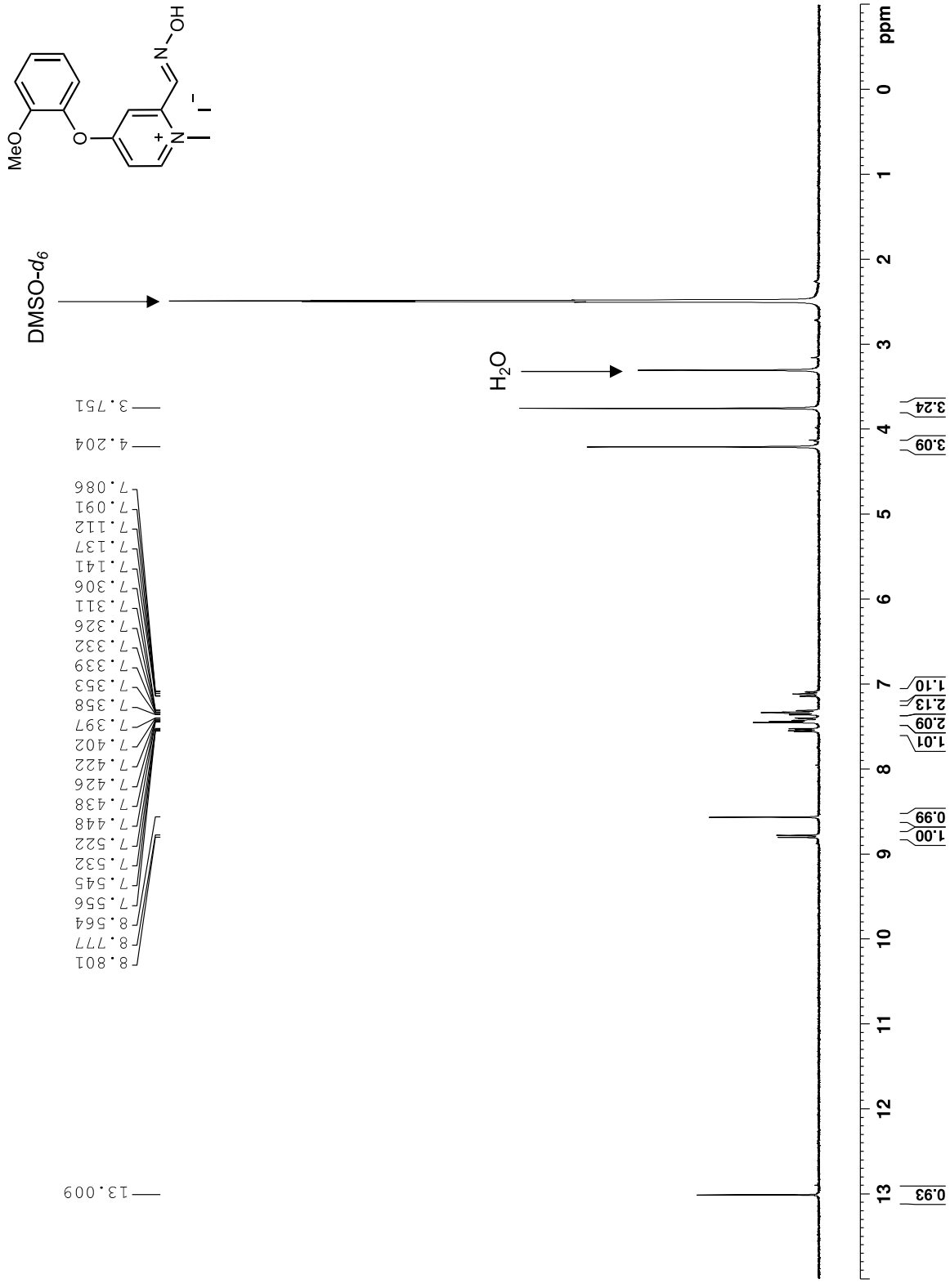

Spectrum 188. ^{1}H NMR of *(E)*-2-((hydroxyimino)methyl)-1-methyl-4-(2-methoxyphenoxy)pyridin-1-ium iodide (**ADG3120**) (300 MHz, 293 K, DMSO-d_6).

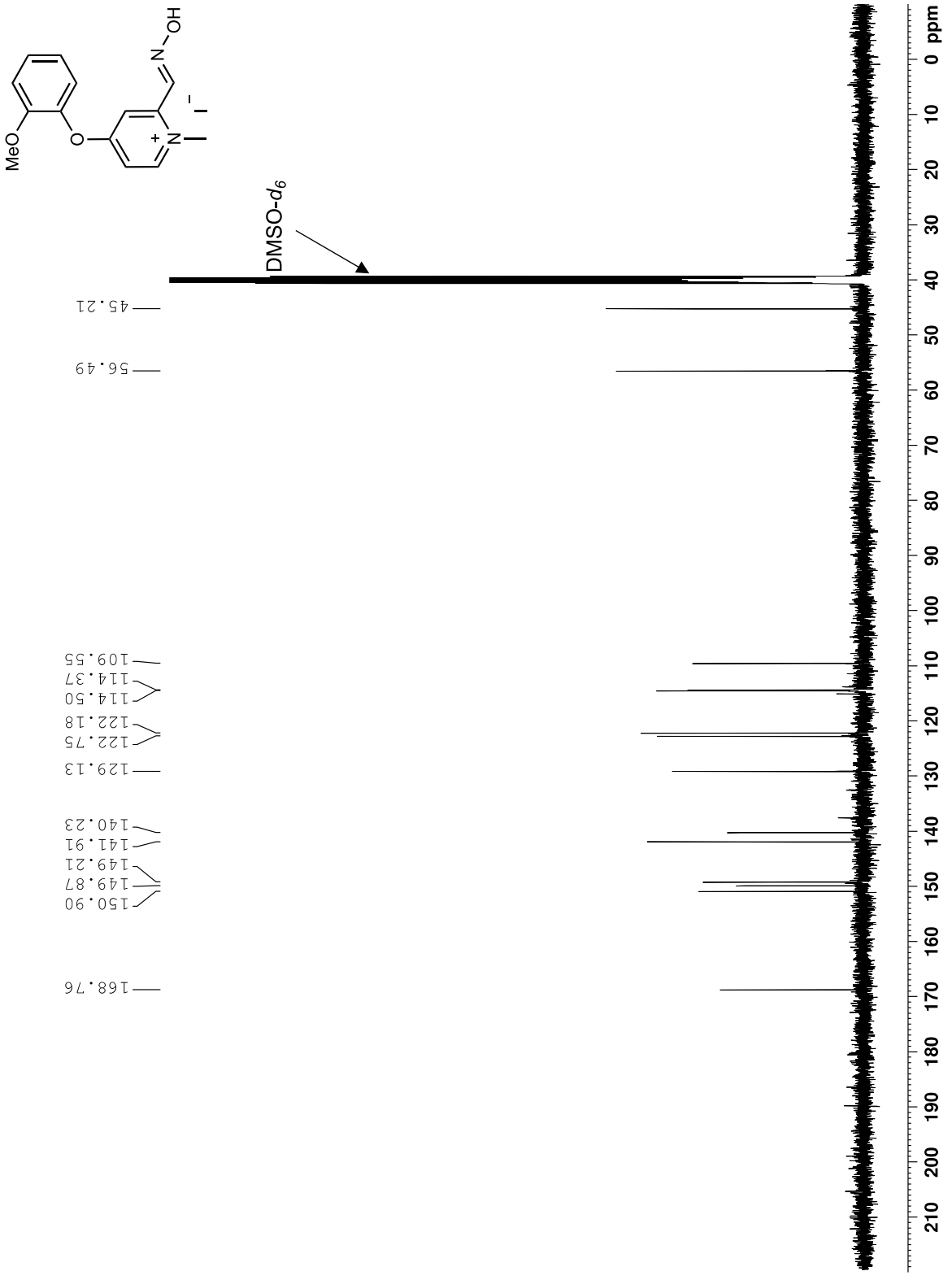

Spectrum 189. ^{13}C NMR of *(E)*-2-((hydroxyimino)methyl)-1-methyl-4-(2-methoxyphenoxy)pyridin-1-ium iodide (**ADG3120**) (100 MHz, 293 K, DMSO-d_6).

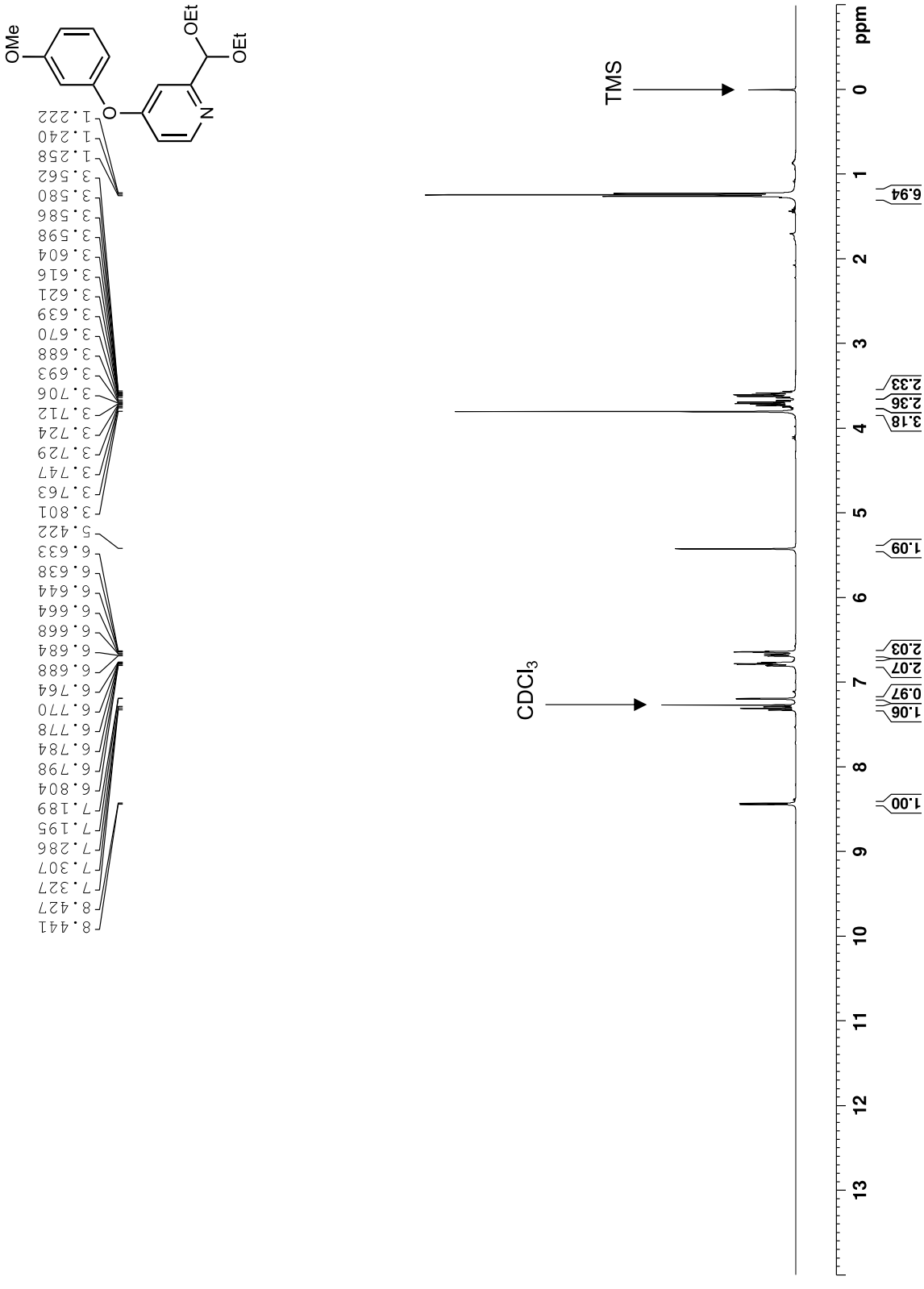

Spectrum 190. ^{1}H NMR of 2-(diethoxymethyl)-4-(3-methoxyphenoxy)pyridine (400 MHz, 293 K, $CDCl_3$).

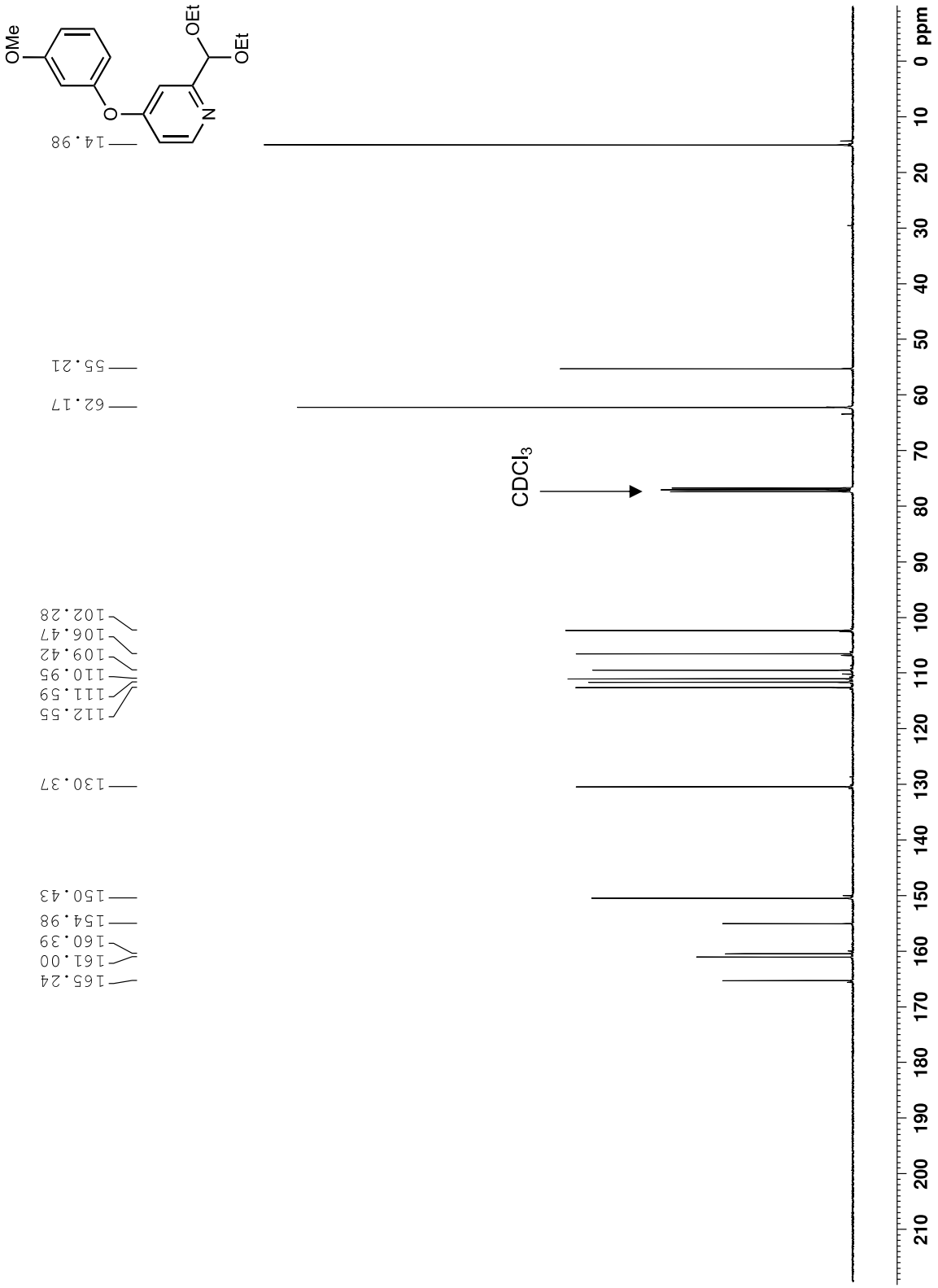

Spectrum 191. ^{13}C NMR of 2-(diethoxymethyl)-4-(3-methoxyphenoxy)pyridine (100 MHz, 293 K, $CDCl_3$).

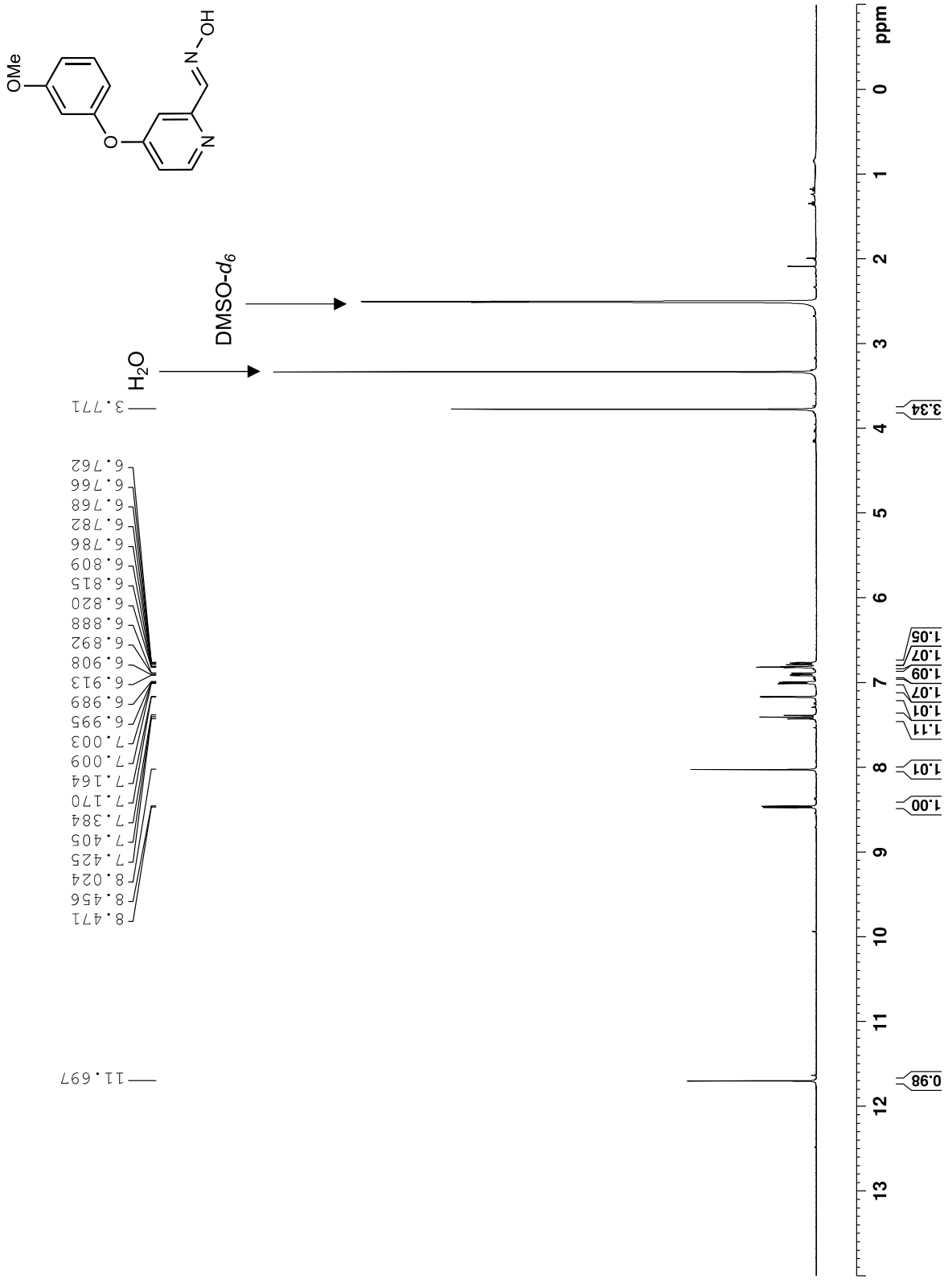

Spectrum 192. ^{1}H NMR of *(E)*-4-(3-methoxyphenoxy)picolinaldehyde oxime (400 MHz, 293 K, DMSO-d_6).

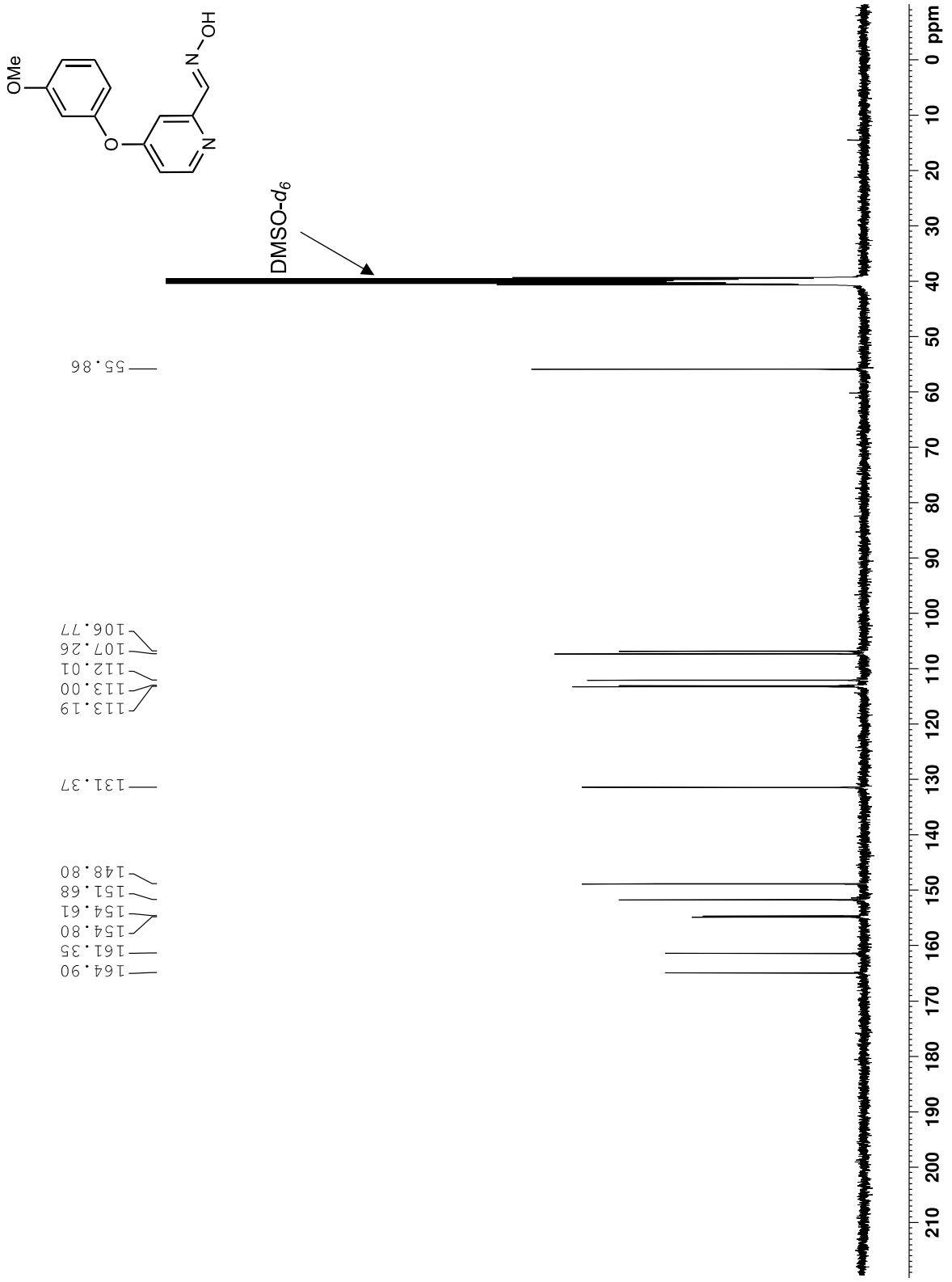

Spectrum 193. ^{13}C NMR of *(E)*-4-(3-methoxyphenoxy)picolinaldehyde oxime (100 MHz, 293 K, DMSO-d_6).

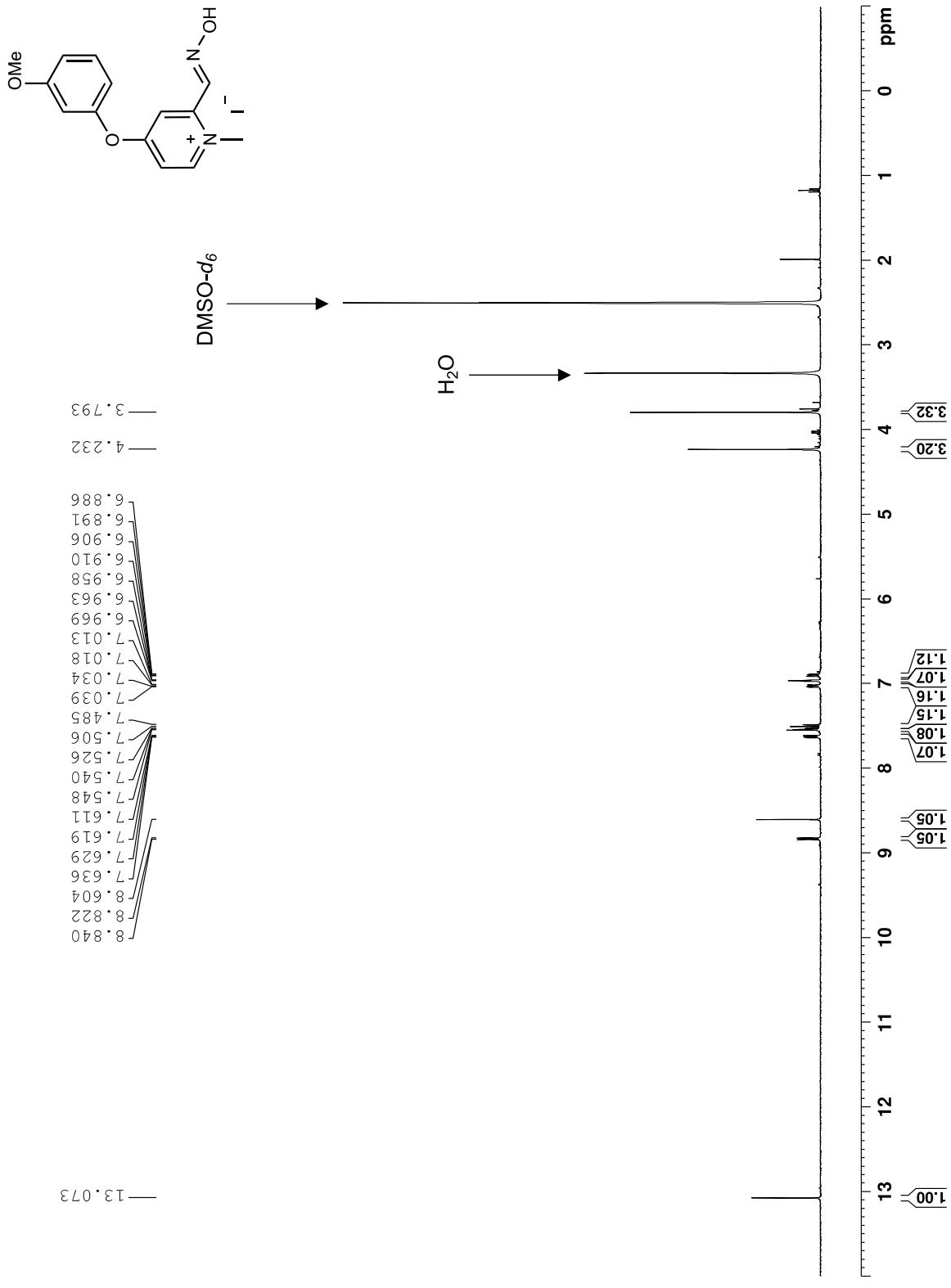

Spectrum 194. ^{1}H NMR of *(E)*-2-((hydroxyimino)methyl)-1-methyl-4-(3-methoxyphenoxy)pyridin-1-ium iodide (**ADG3128**) (400 MHz, 293 K, DMSO-d_6).

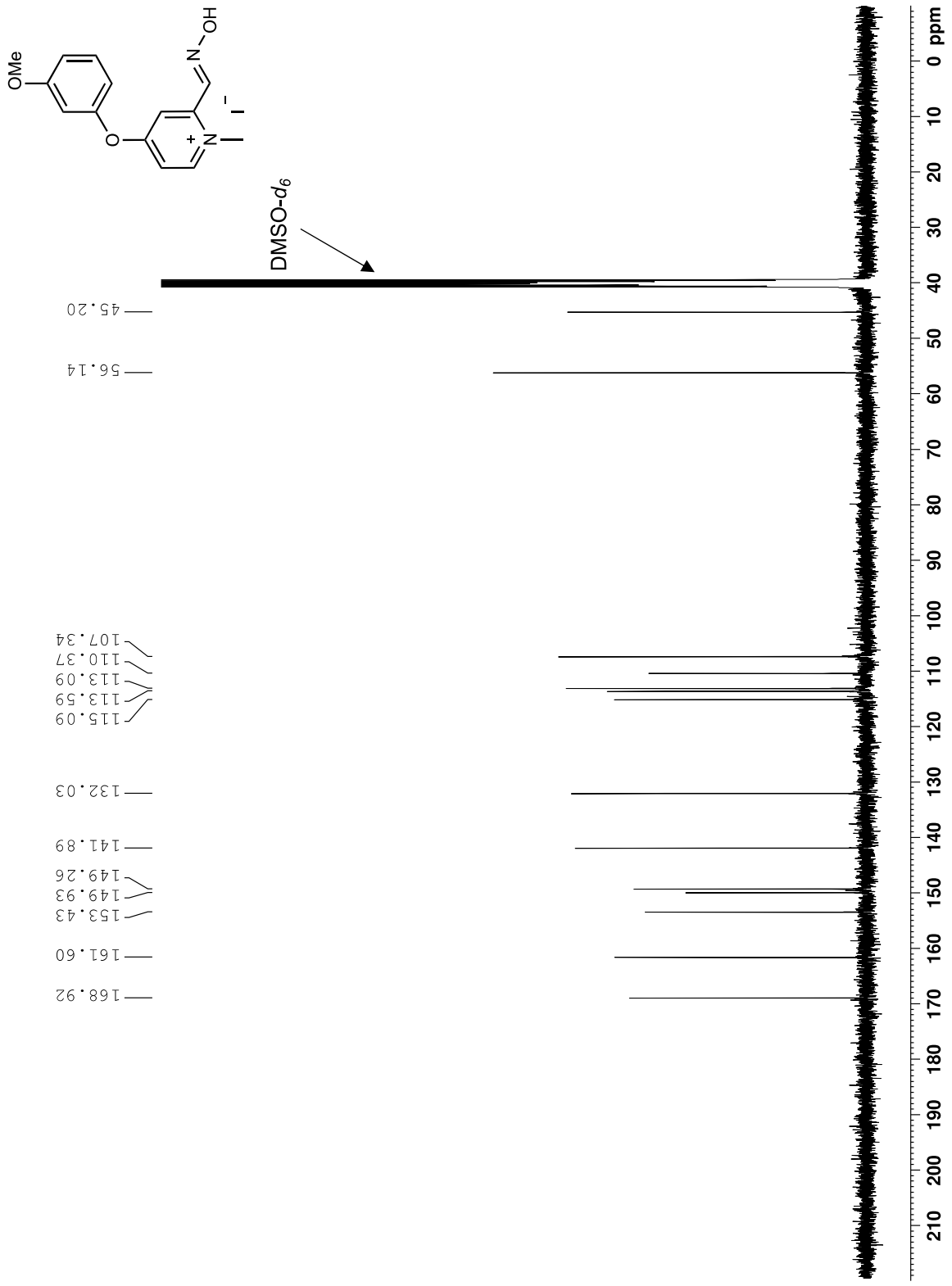

Spectrum 195. ^{13}C NMR of *(E)*-2-((hydroxyimino)methyl)-1-methyl-4-(3-methoxyphenoxy)pyridin-1-ium iodide (**ADG3128**) (100 MHz, 293 K, DMSO-d_6).

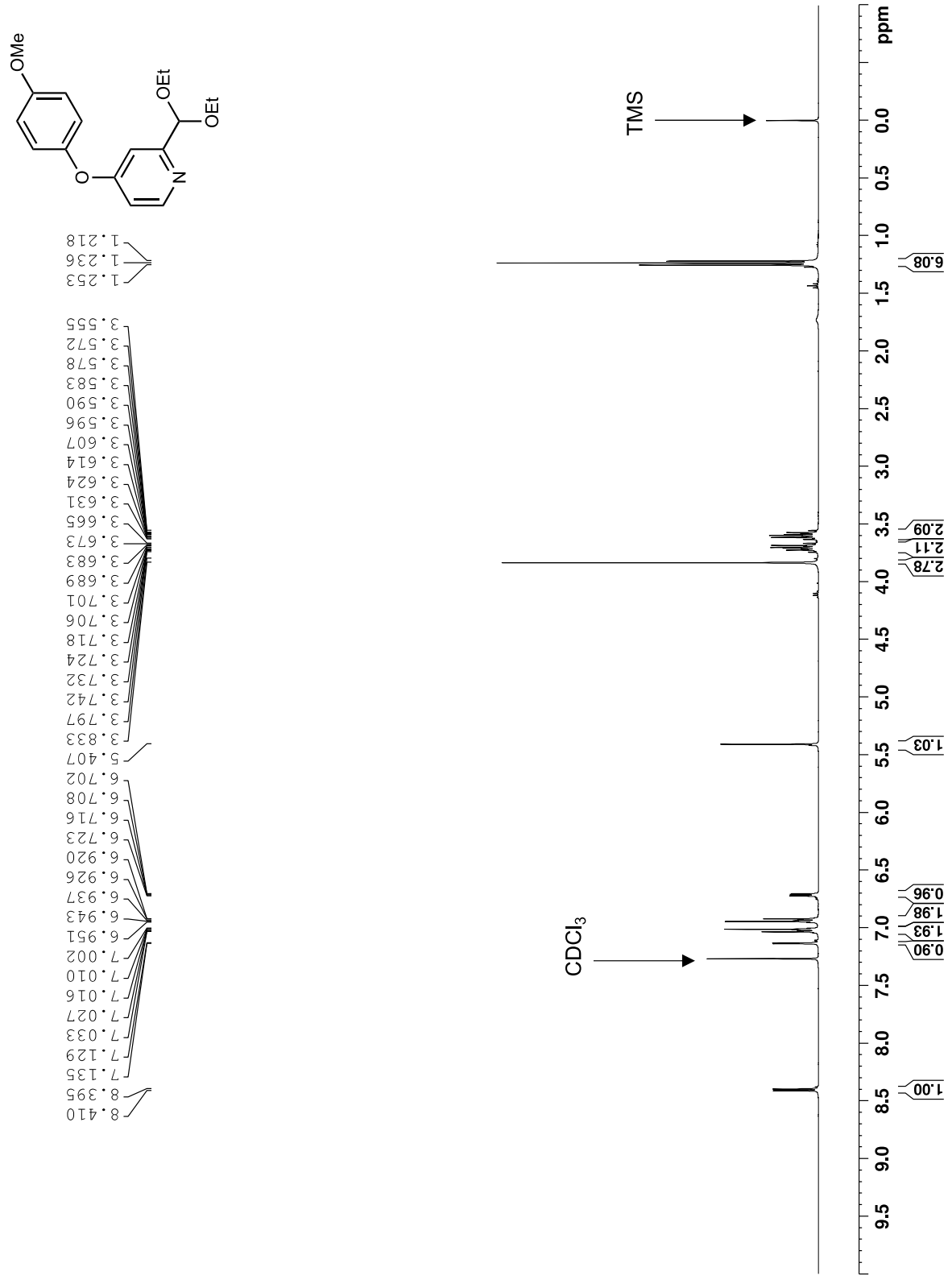

Spectrum 196. ^{1}H NMR of 2-(diethoxymethyl)-4-(4-methoxyphenoxy)pyridine (400 MHz, 293 K, $CDCl_3$).

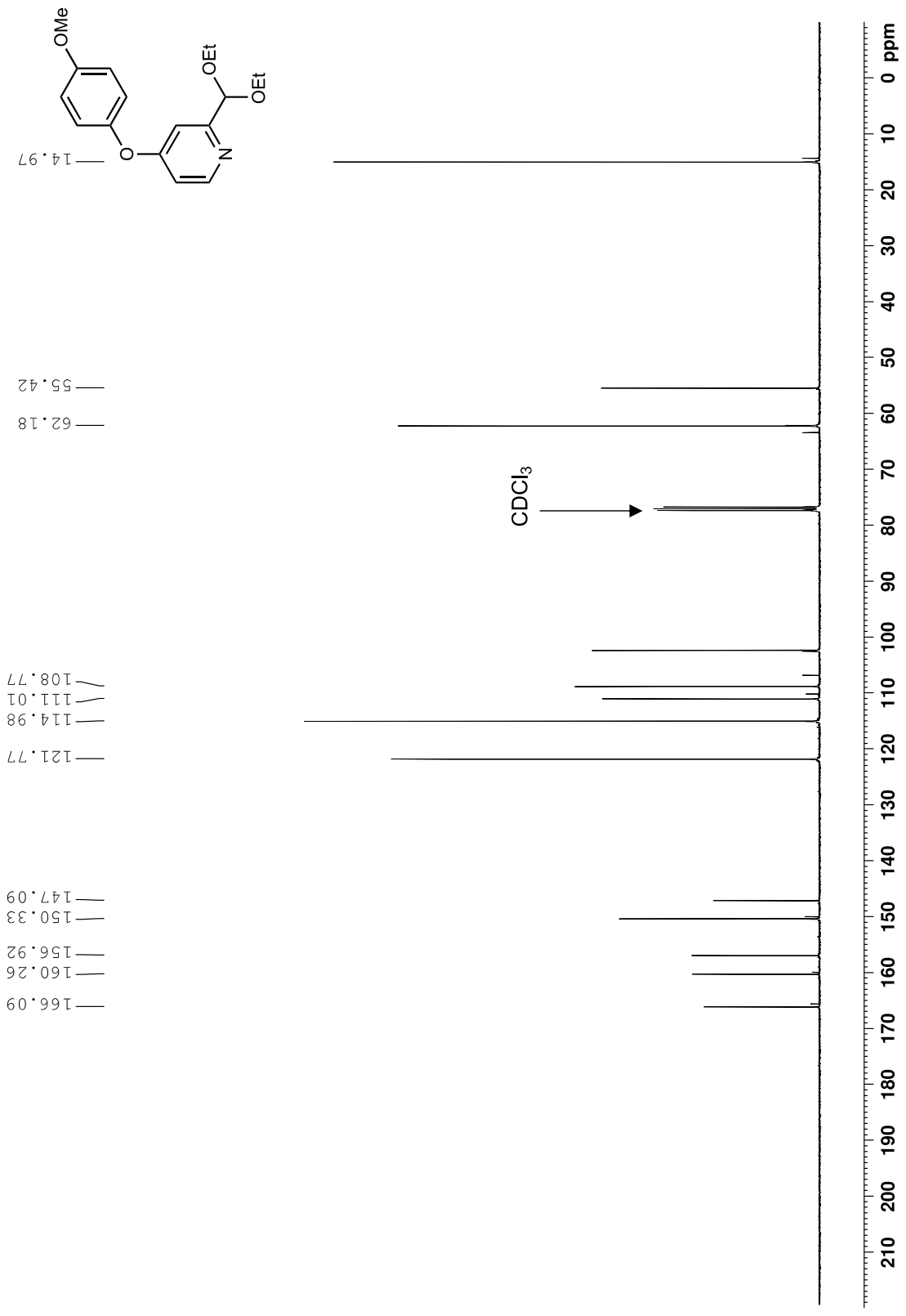

Spectrum 197. ^{13}C NMR of 2-(diethoxymethyl)-4-(4-methoxyphenoxy)pyridine (100 MHz, 293 K, $CDCl_3$).

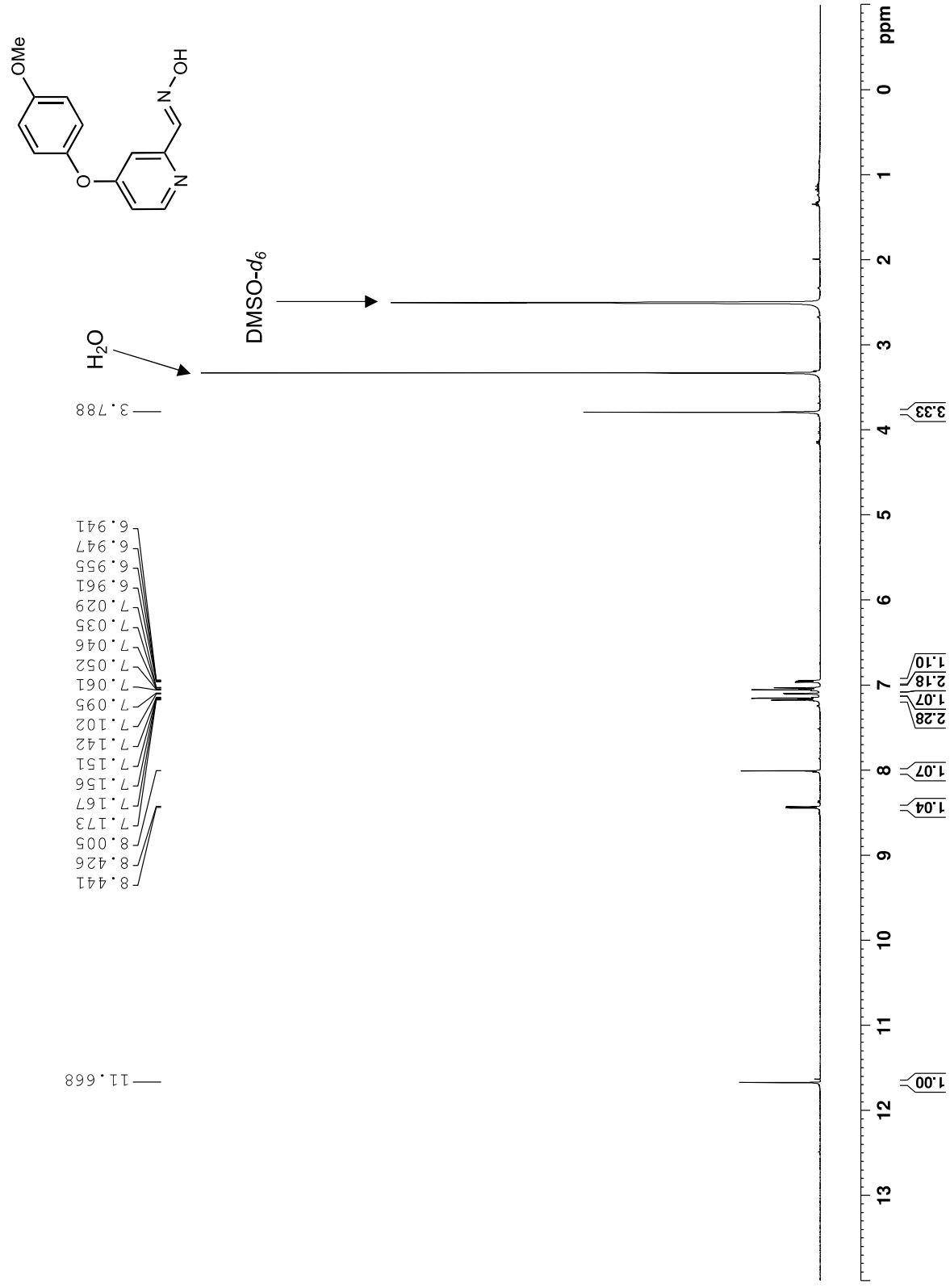

Spectrum 198. ^{1}H NMR of *(E)*-4-(4-methoxyphenoxy)picolinaldehyde oxime (400 MHz, 293 K, DMSO-d_6).

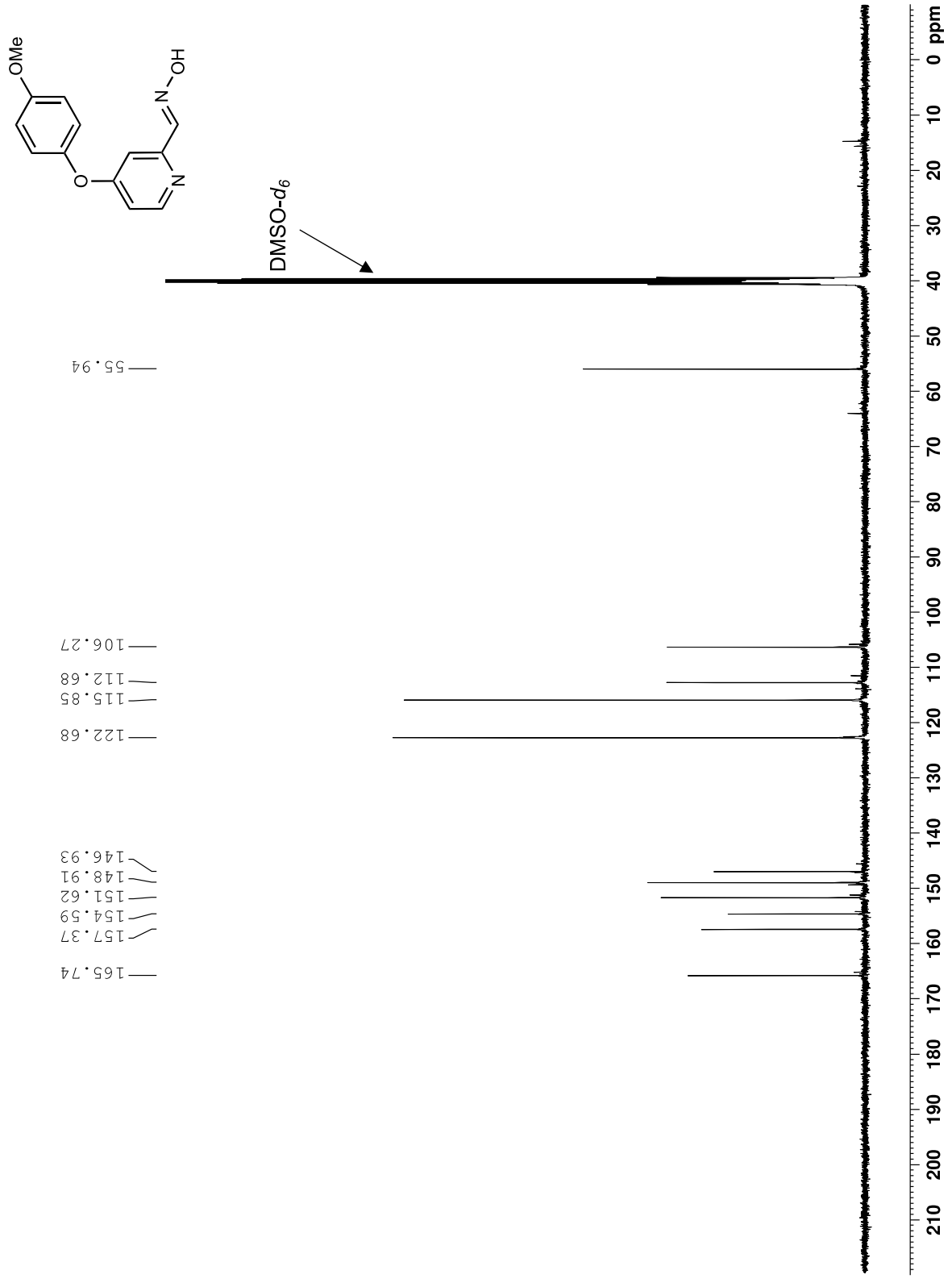

Spectrum 199. ^{13}C NMR of *(E)*-4-(4-methoxyphenoxy)picolinaldehyde oxime (100 MHz, 293 K, DMSO-d_6).

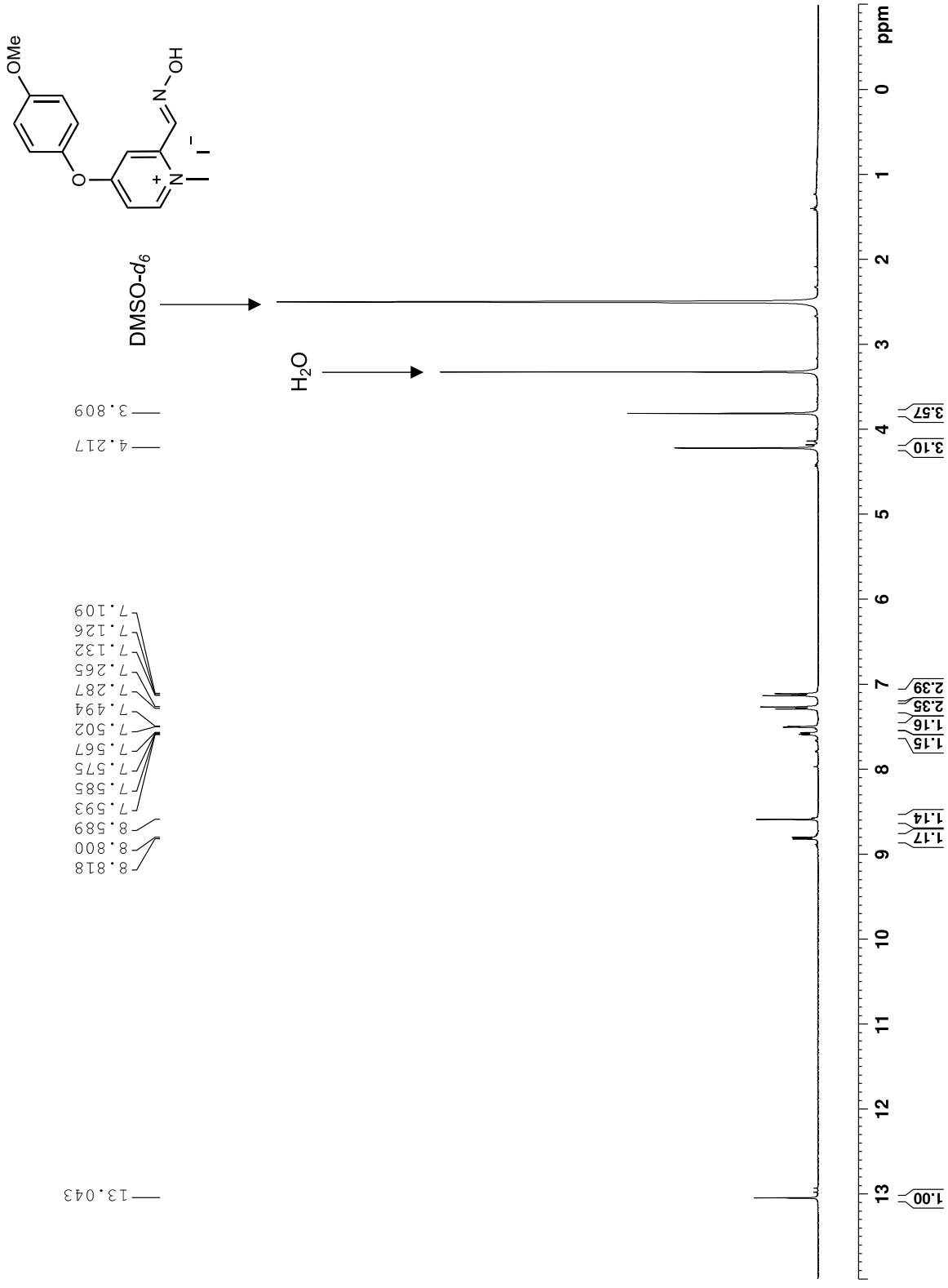

Spectrum 200. [1]H NMR of *(E)*-2-((hydroxyimino)methyl)-1-methyl-4-(4-methoxyphenoxy)pyridin-1-ium iodide (**ADG3121**) (400 MHz, 293 K, DMSO-d_6).

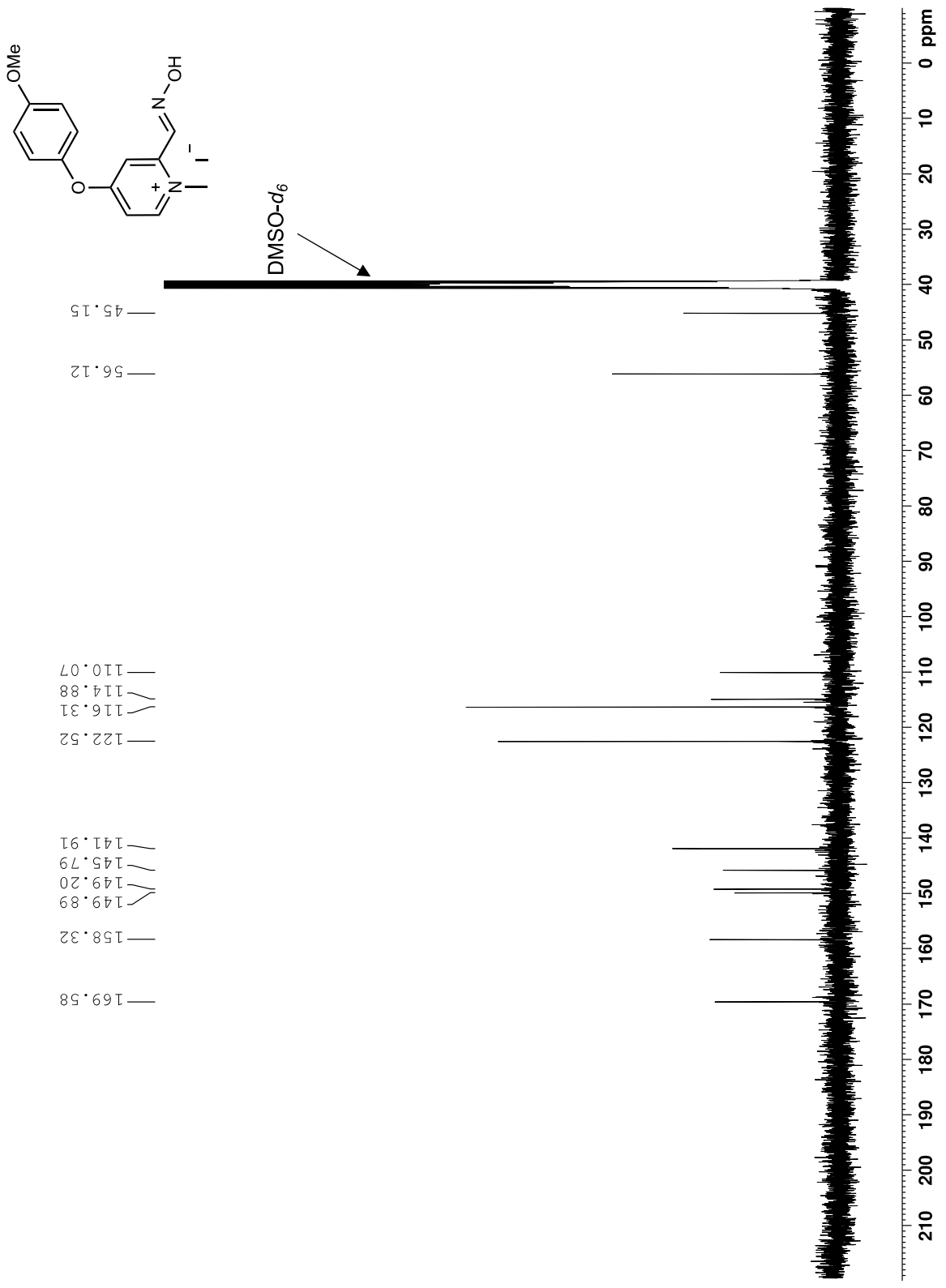

Spectrum 201. ^{13}C NMR of *(E)*-2-((hydroxyimino)methyl)-1-methyl-4-(4-methoxyphenoxy)pyridin-1-ium iodide (**ADG3121**) (100 MHz, 293 K, DMSO-d_6).

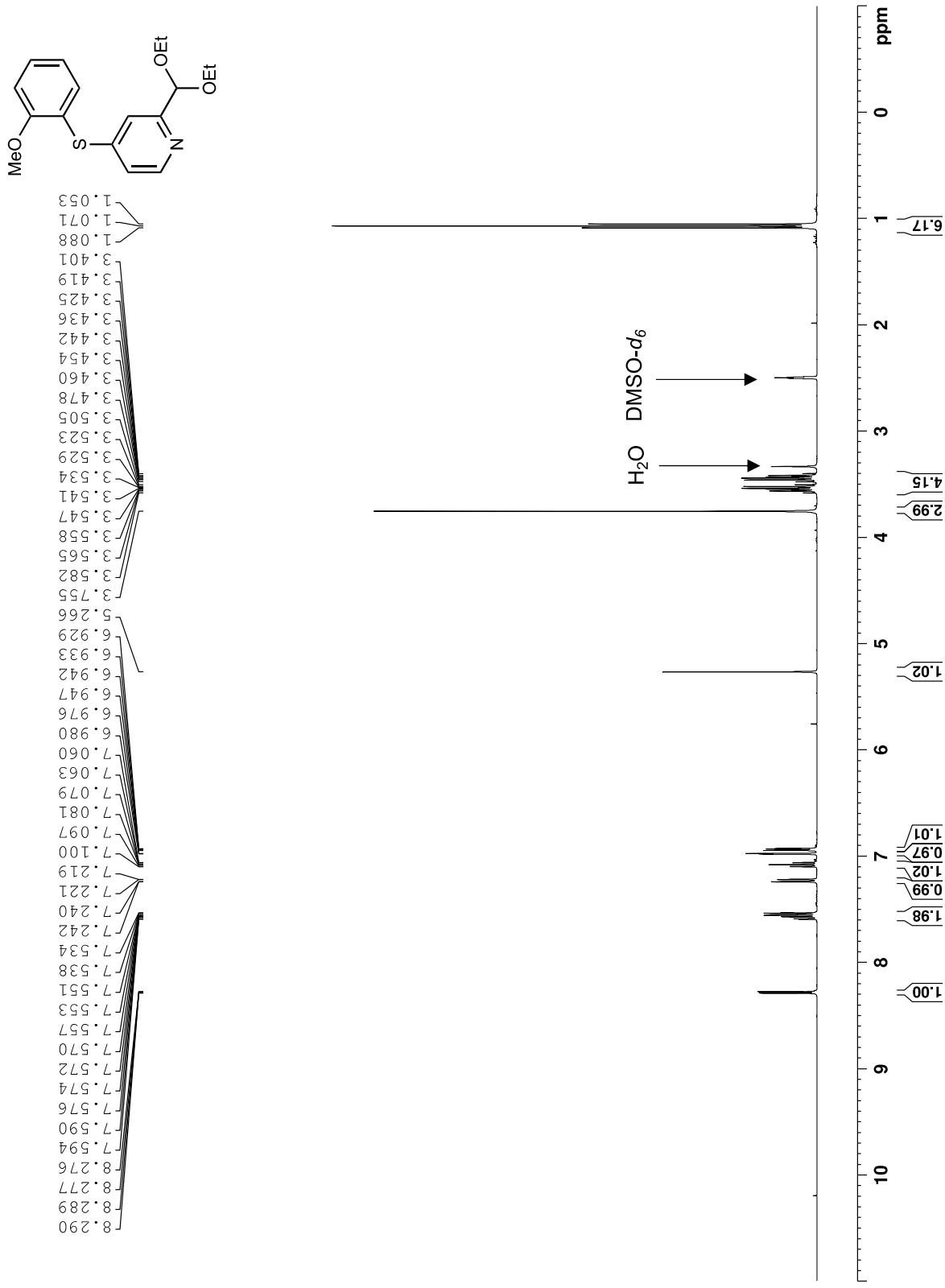

Spectrum 202. ^{1}H NMR of 2-(diethoxymethyl)-4-((2-methoxyphenyl)thio)pyridine (400 MHz, 293 K, DMSO-d_6).

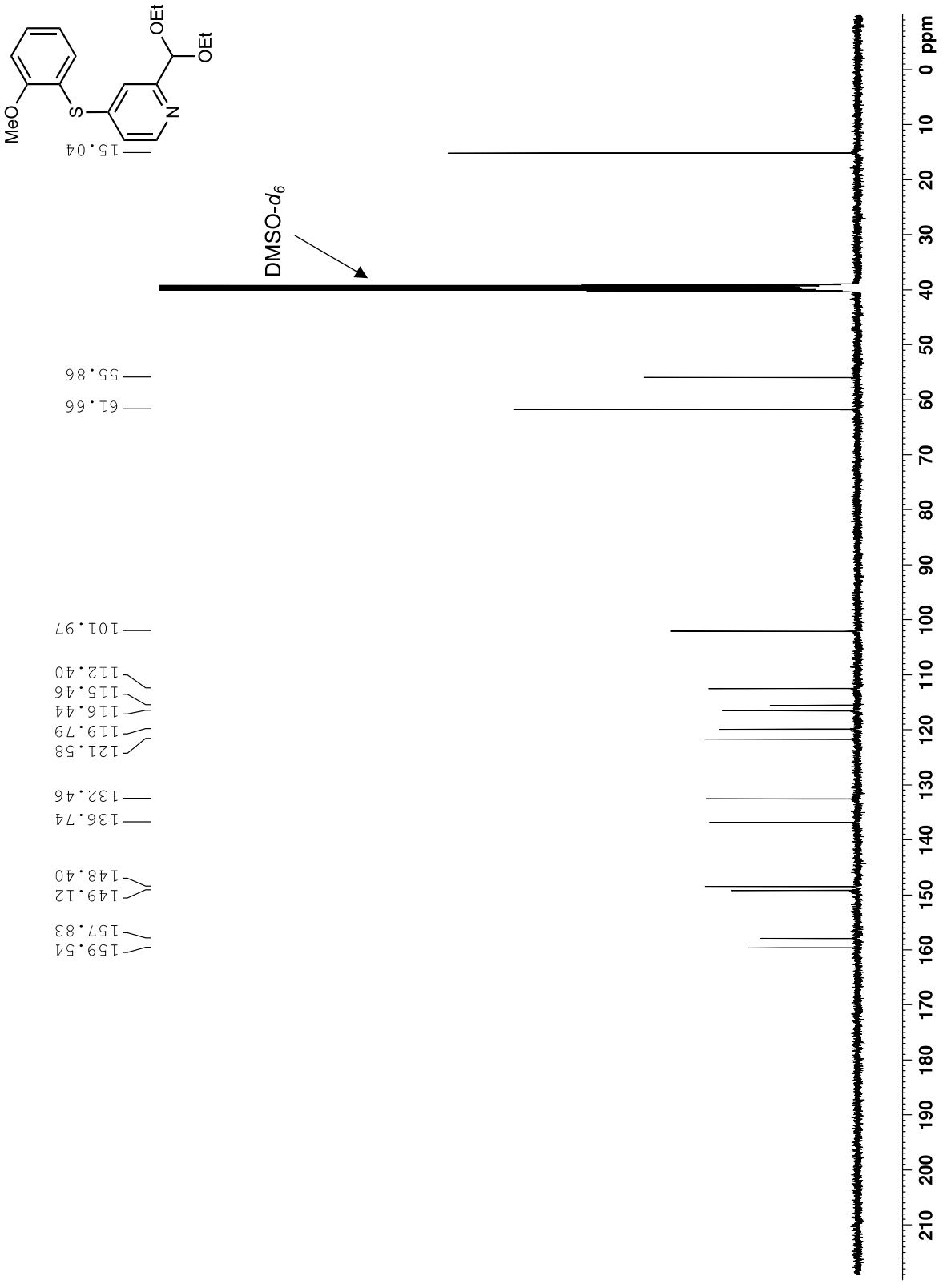

Spectrum 203. ^{13}C NMR of 2-(diethoxymethyl)-4-((2-methoxyphenyl)thio)pyridine (100 MHz, 293 K, DMSO-d_6).

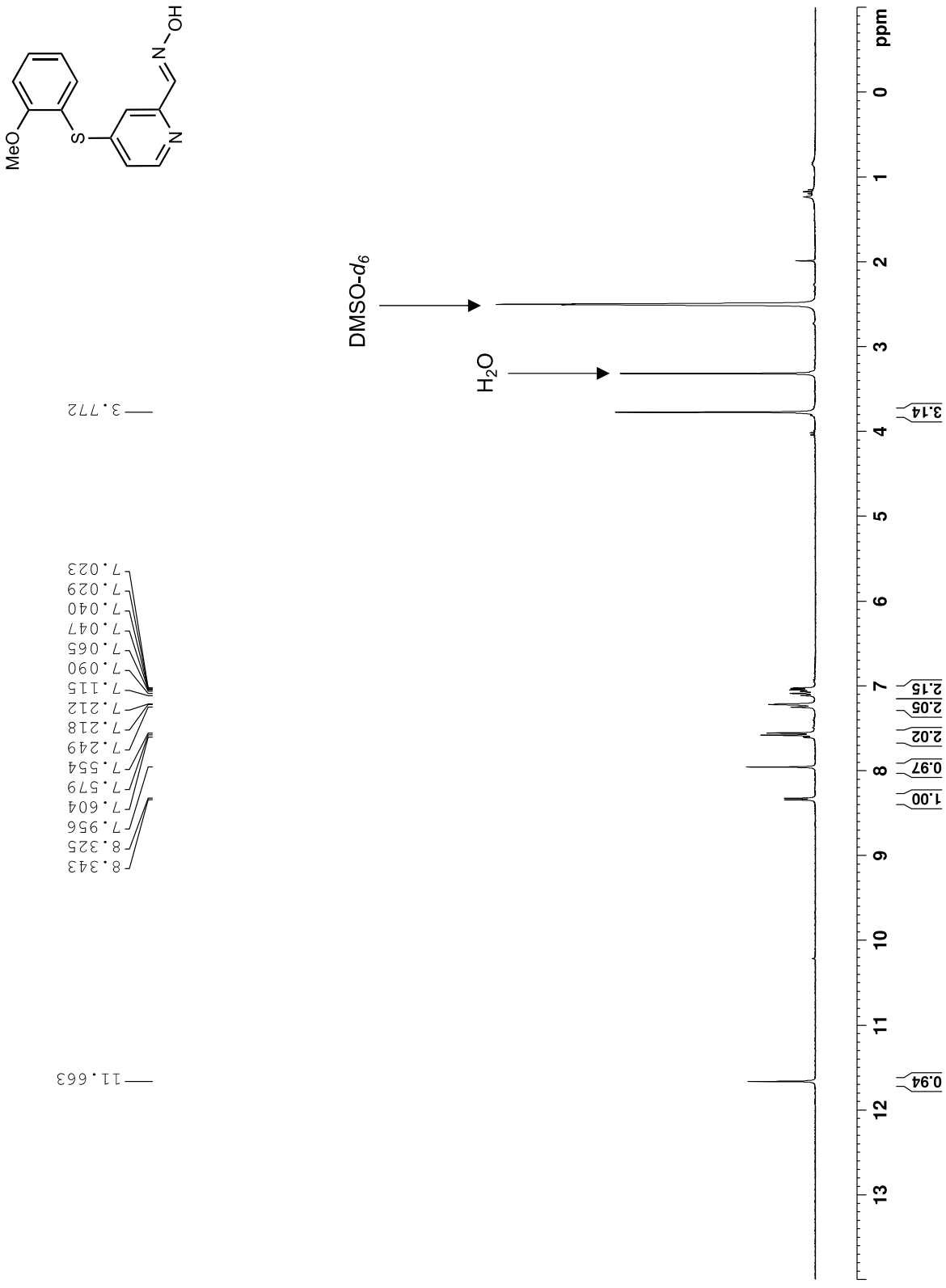

Spectrum 204. ^{1}H NMR of (*E*)-4-((2-methoxyphenyl)thio)picolinaldehyde oxime (300 MHz, 293 K, DMSO-d_6).

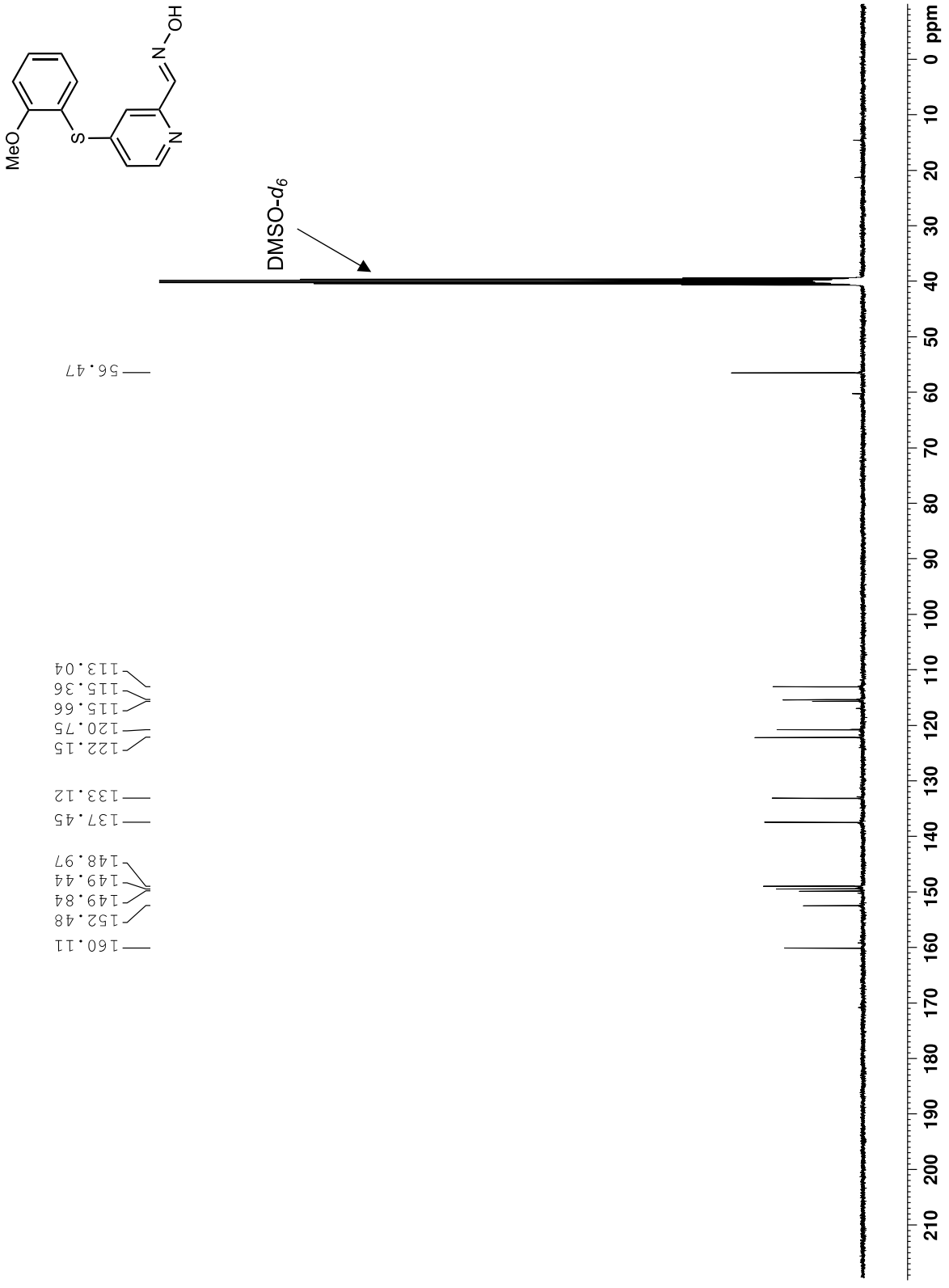

Spectrum 205. ^{13}C NMR of (*E)*-4-((2-methoxyphenyl)thio)picolinaldehyde oxime (100 MHz, 293 K, DMSO-d_6).

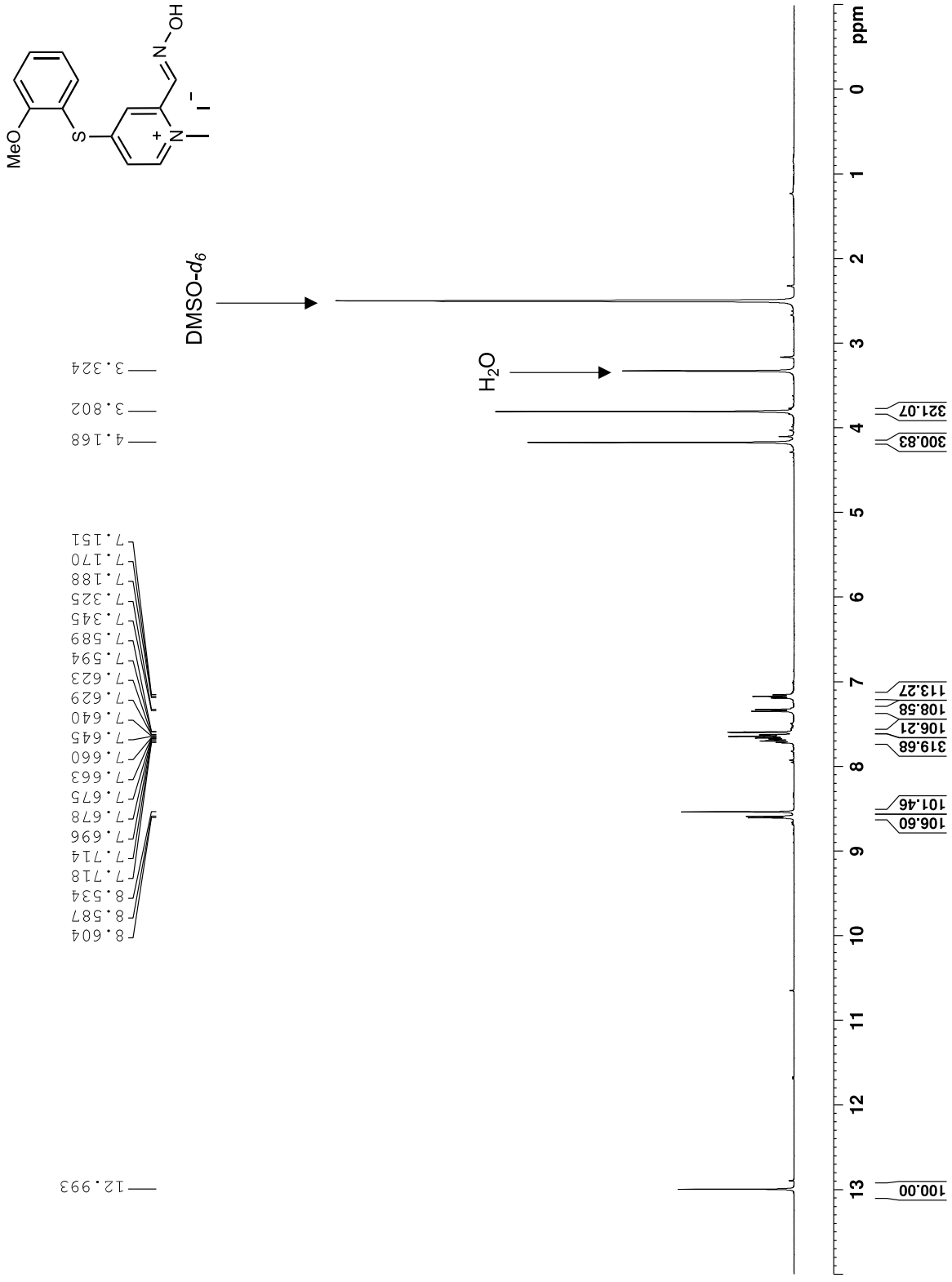

Spectrum 206. ^{1}H NMR of *(E)*-2-((hydroxyimino)methyl)-4-((2-methoxyphenyl)thio)-1-methylpyridin-1-ium iodide (**ADG4118**) (400 MHz, 293 K, DMSO-d_6).

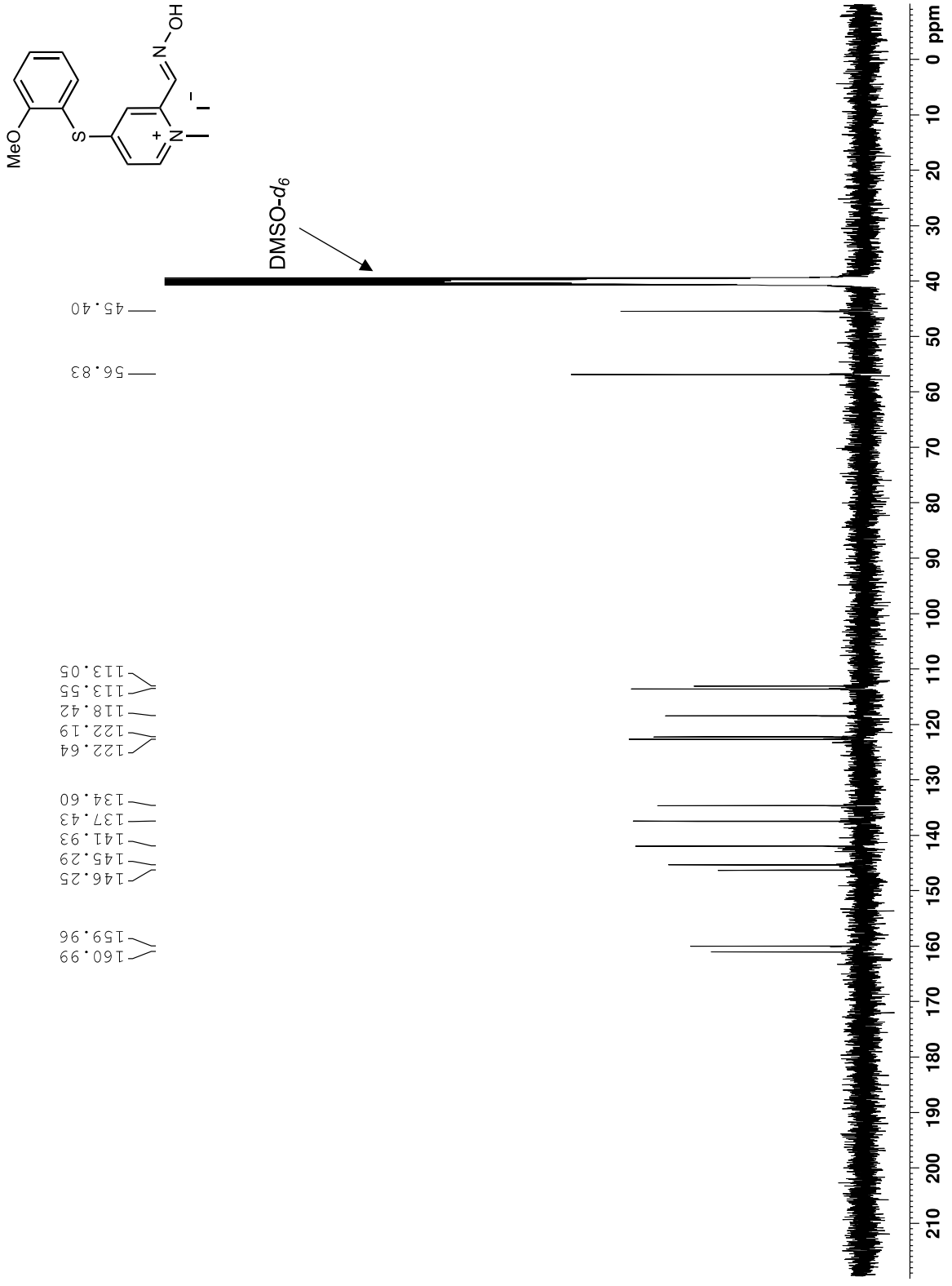

Spectrum 207. ^{13}C NMR of *(E)*-2-((hydroxyimino)methyl)-4-((2-methoxyphenyl)thio)-1-methylpyridin-1-ium iodide (**ADG4118**) (100 MHz, 293 K, DMSO-d_6).

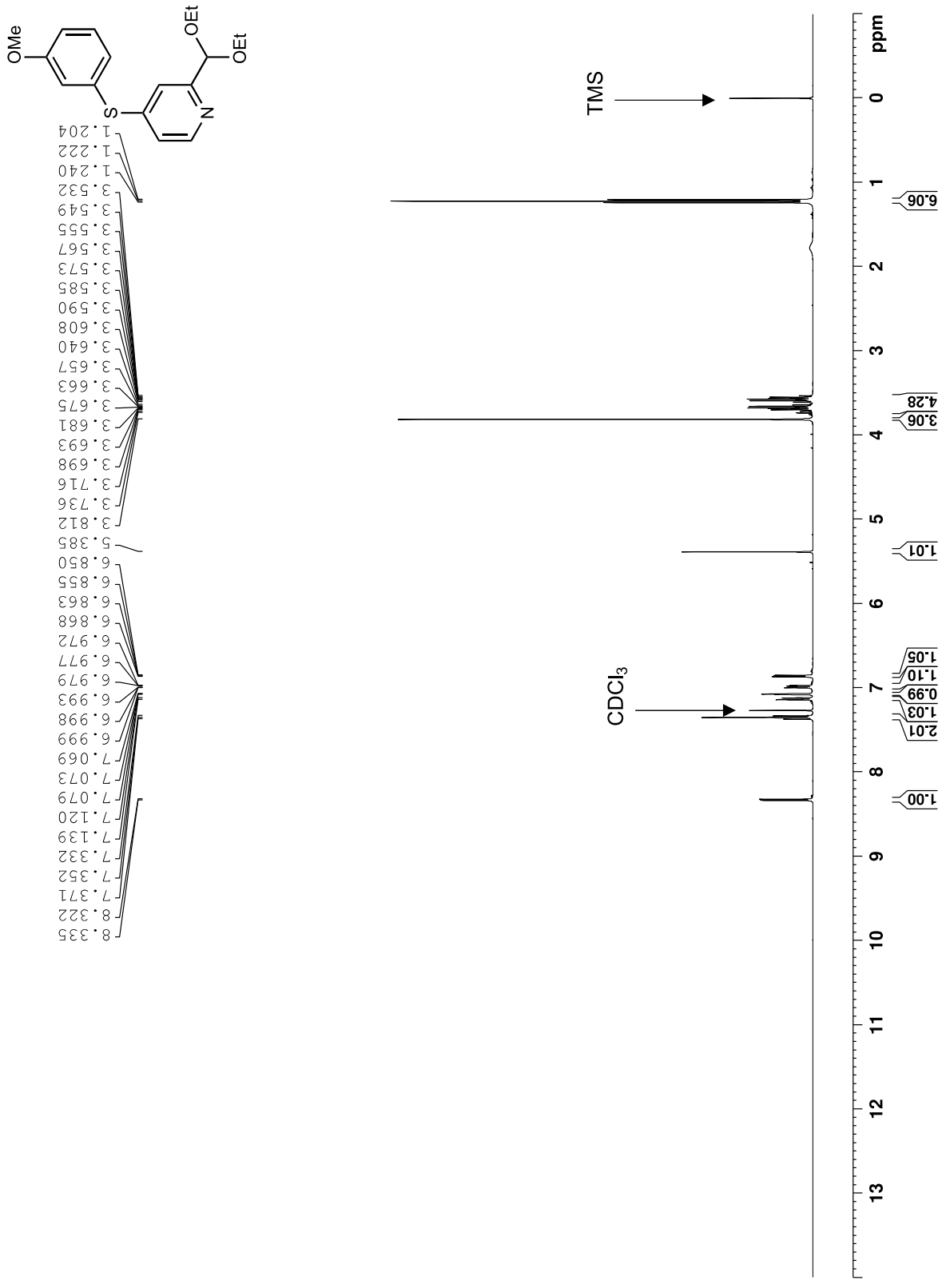

Spectrum 208. ^{1}H NMR of 2-(diethoxymethyl)-4-((3-methoxyphenyl)thio)pyridine (400 MHz, 293 K, $CDCl_3$).

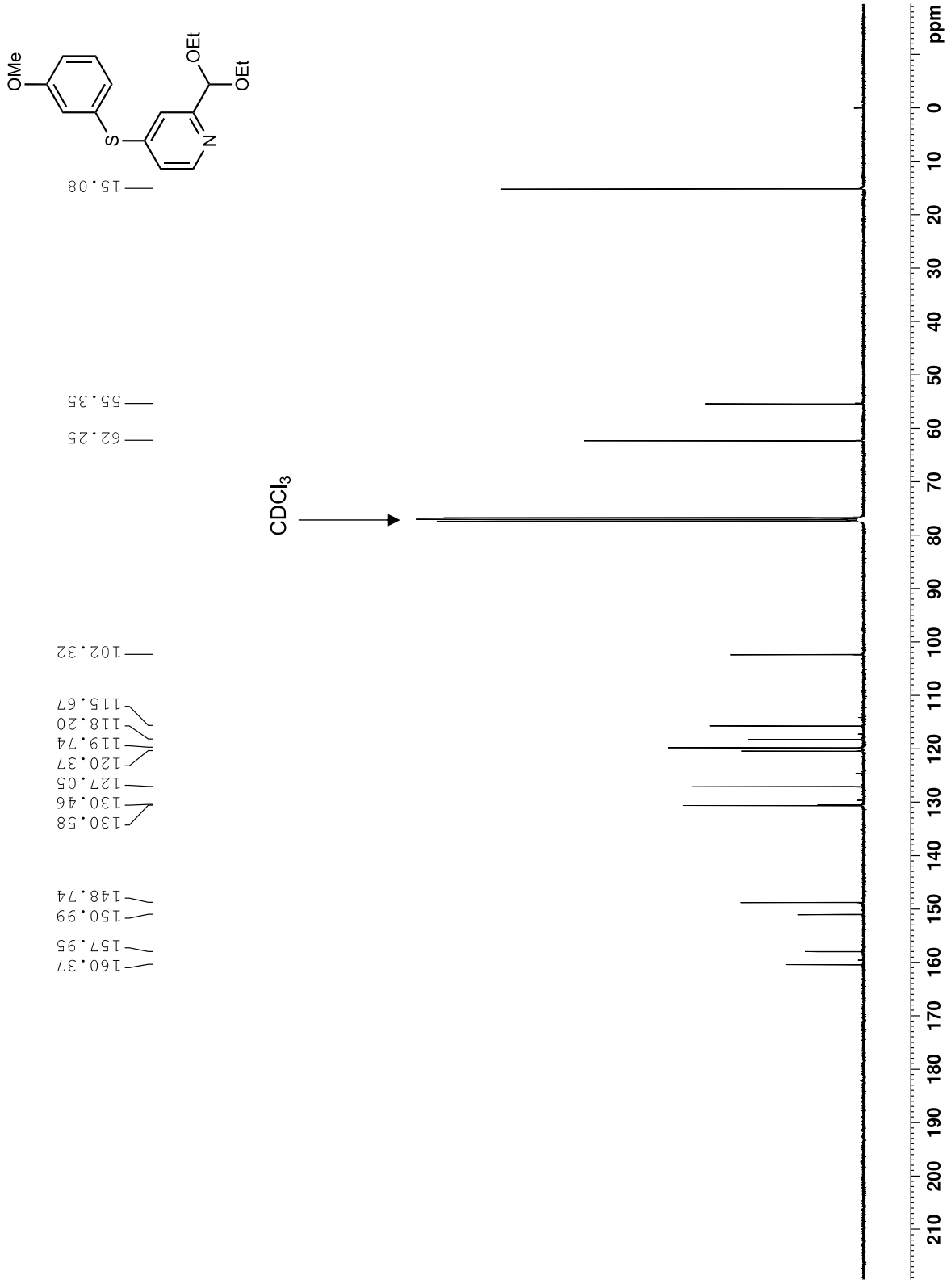

Spectrum 209. ^{13}C NMR of 2-(diethoxymethyl)-4-((3-methoxyphenyl)thio)pyridine (100 MHz, 293 K, $CDCl_3$).

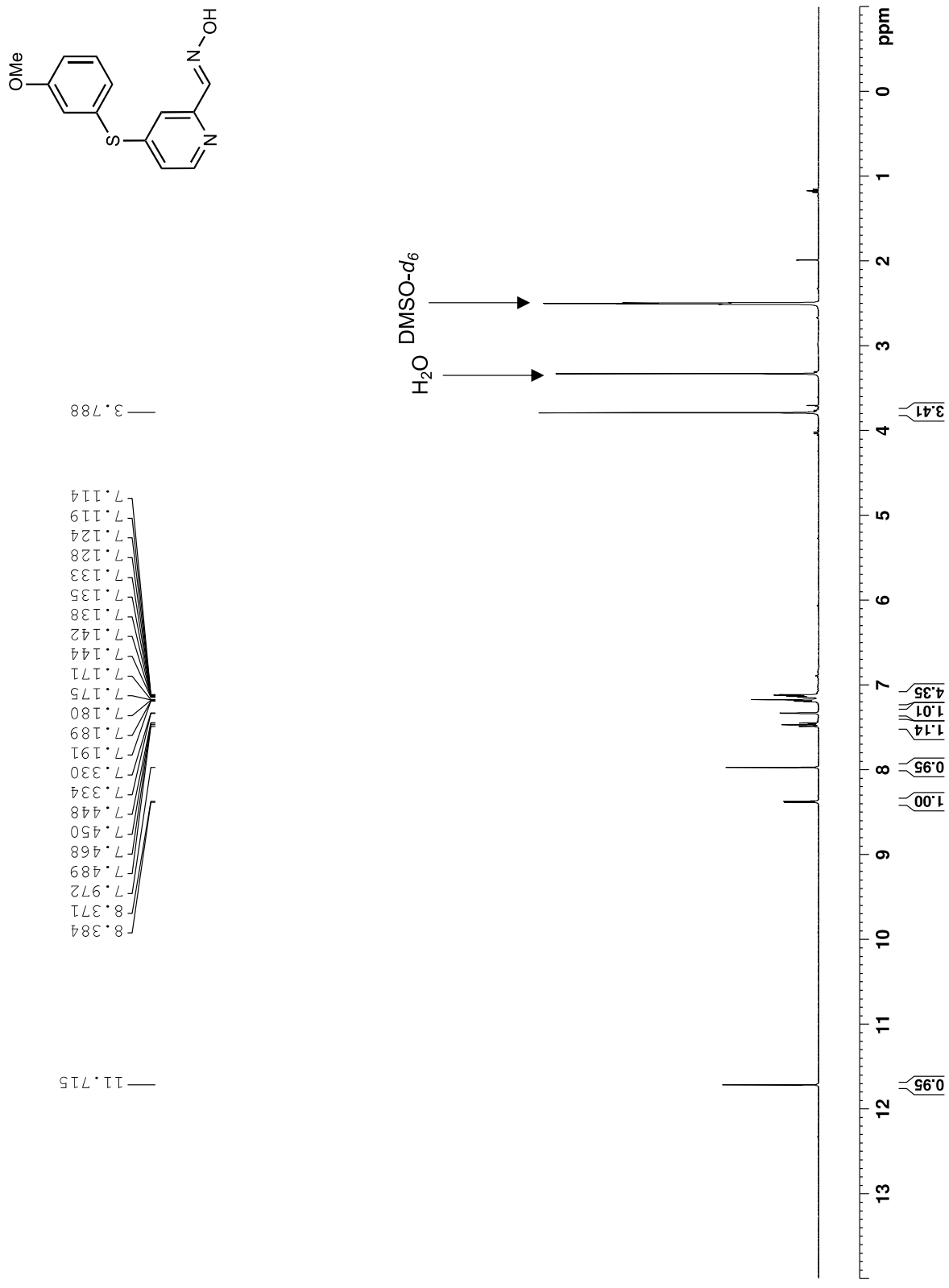

Spectrum 210. ^{1}H NMR of *(E)*-4-((3-methoxyphenyl)thio)picolinaldehyde oxime (400 MHz, 293 K, DMSO-d_6).

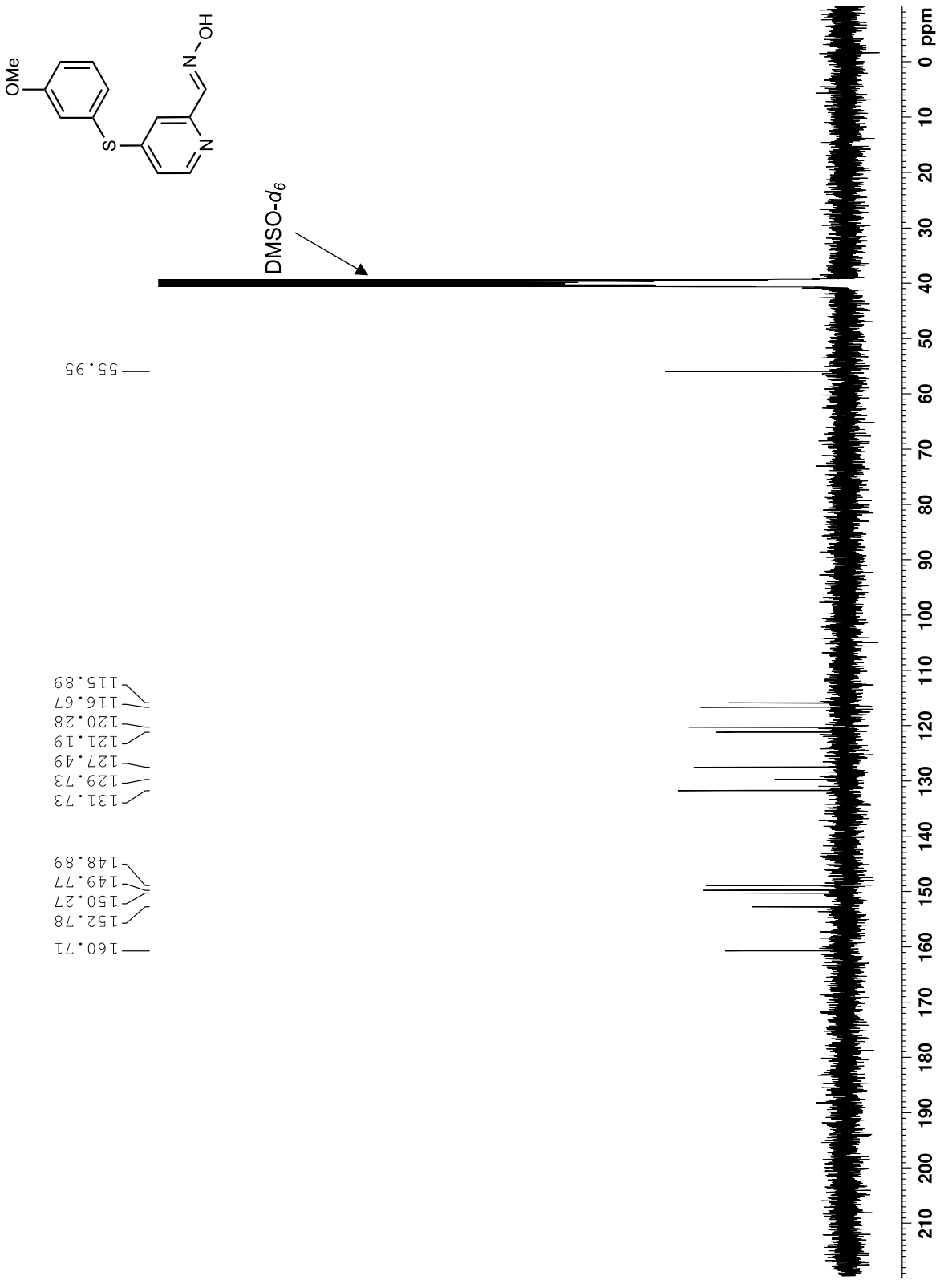

Spectrum 211. ^{13}C NMR of *(E)*-4-((3-methoxyphenyl)thio)picolinaldehyde oxime (100 MHz, 293 K, DMSO-d_6).

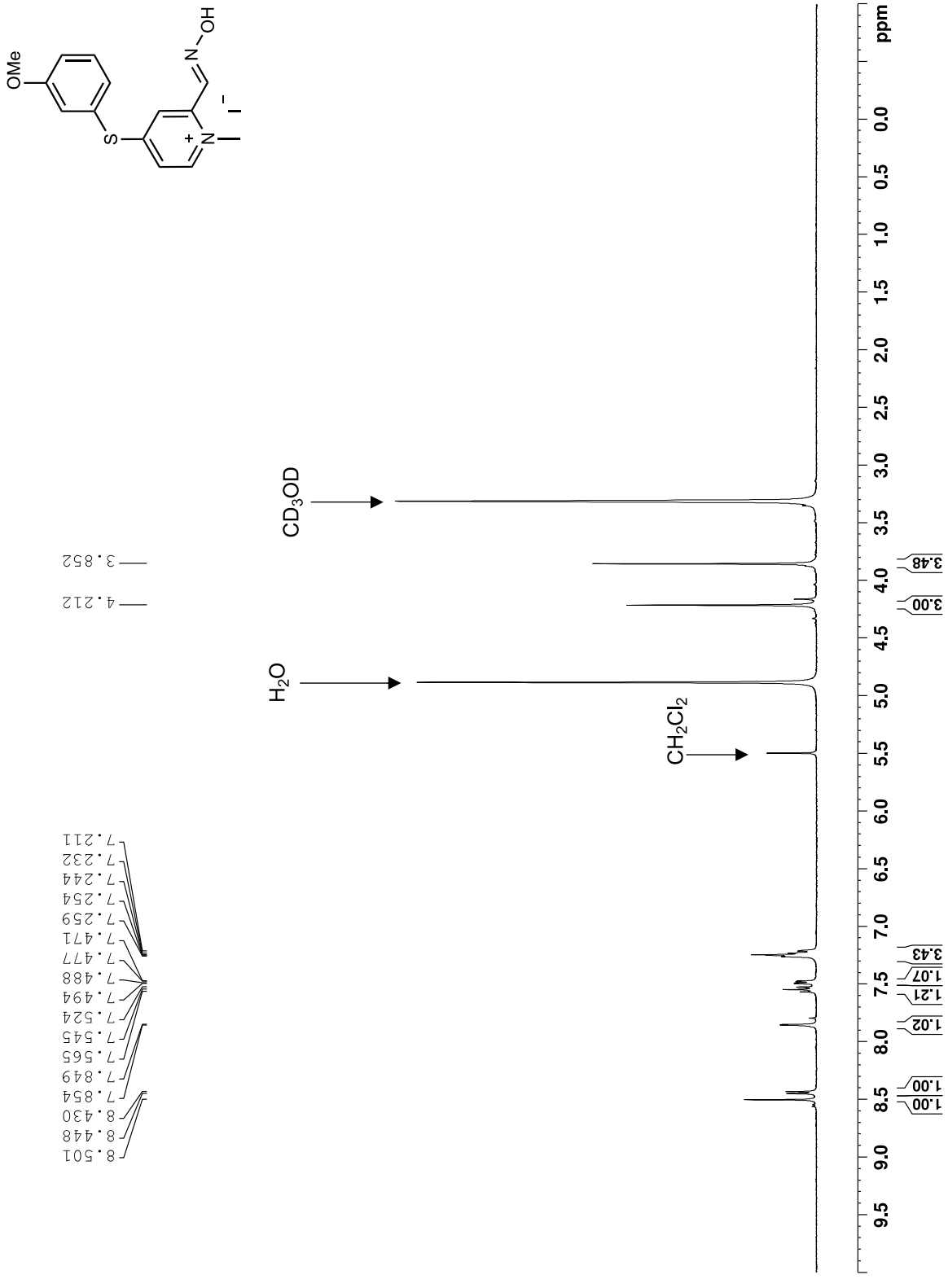

Spectrum 212. ^{1}H NMR of (*E*)-2-((hydroxyimino)methyl)-4-((3-methoxyphenyl)thio)-1-methylpyridin-1-ium iodide (**ADG4153**) (400 MHz, 293 K, CD_3OD).

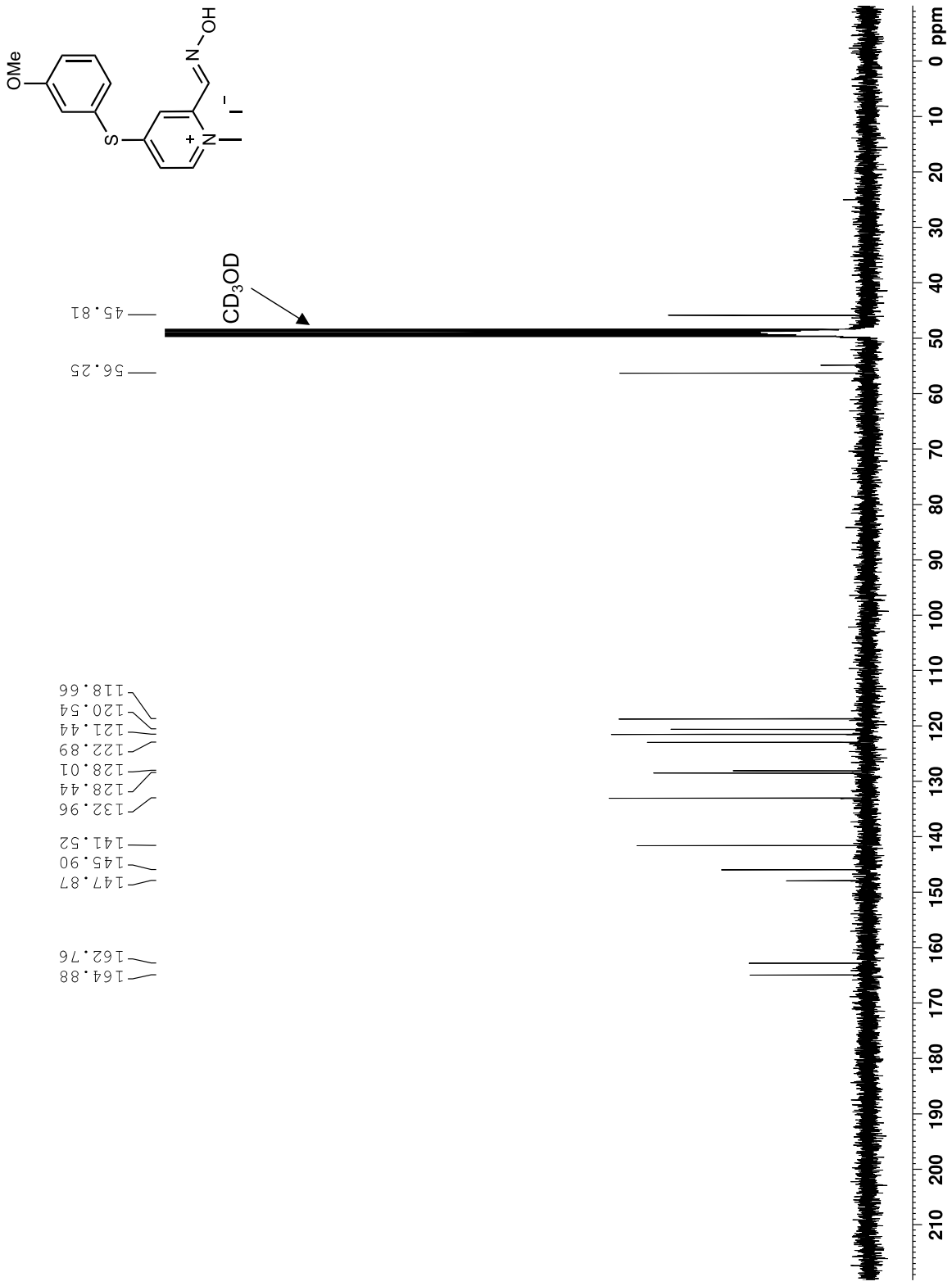

Spectrum 213. ^{13}C NMR of (*E*)-2-((hydroxyimino)methyl)-4-((3-methoxyphenyl)thio)-1-methylpyridin-1-ium iodide (**ADG4153**) (100 MHz, 293 K, CD_3OD).

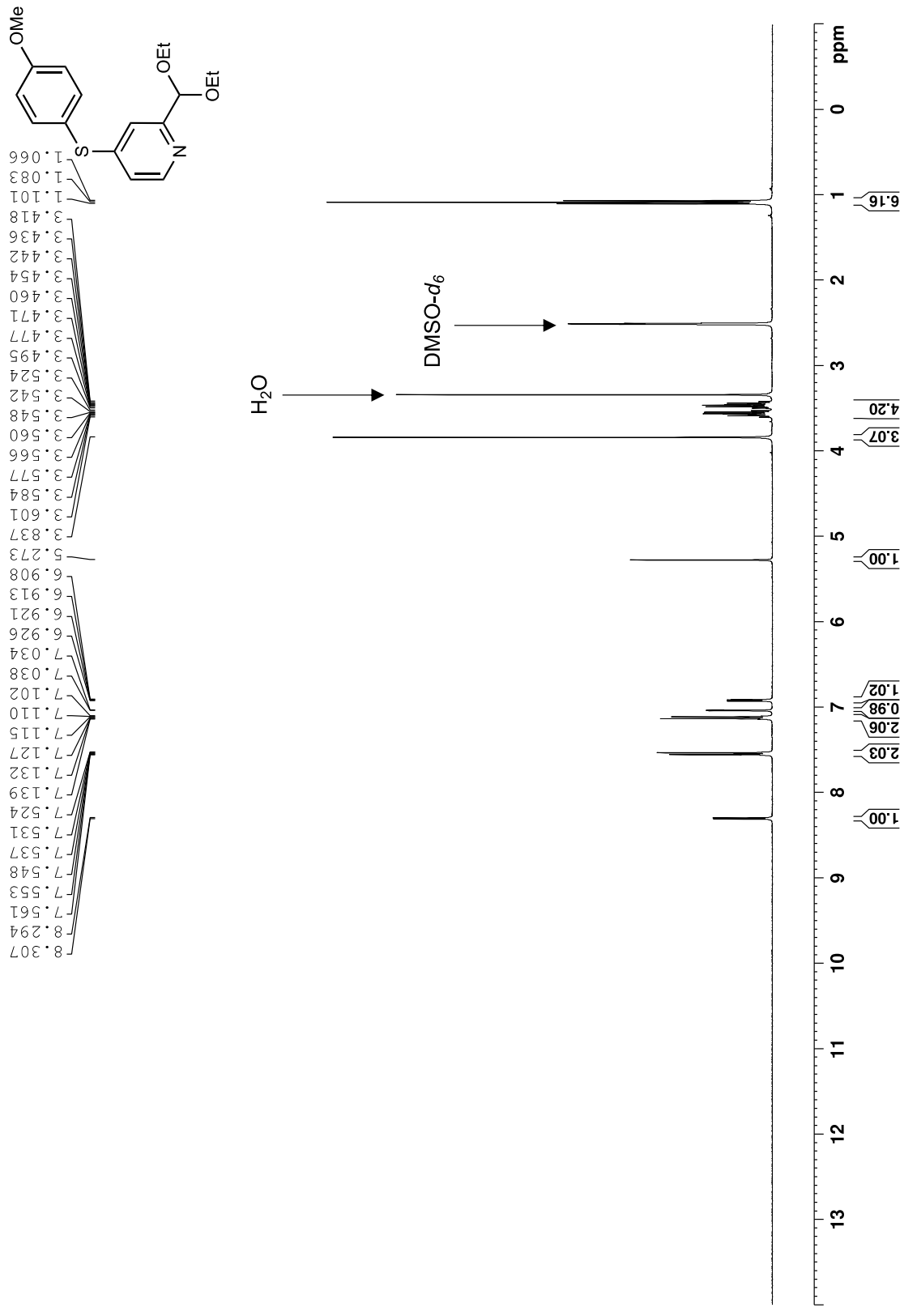

Spectrum 214. ^{1}H NMR of 2-(diethoxymethyl)-4-((4-methoxyphenyl)thio)pyridine (400 MHz, 293 K, DMSO-d_6).

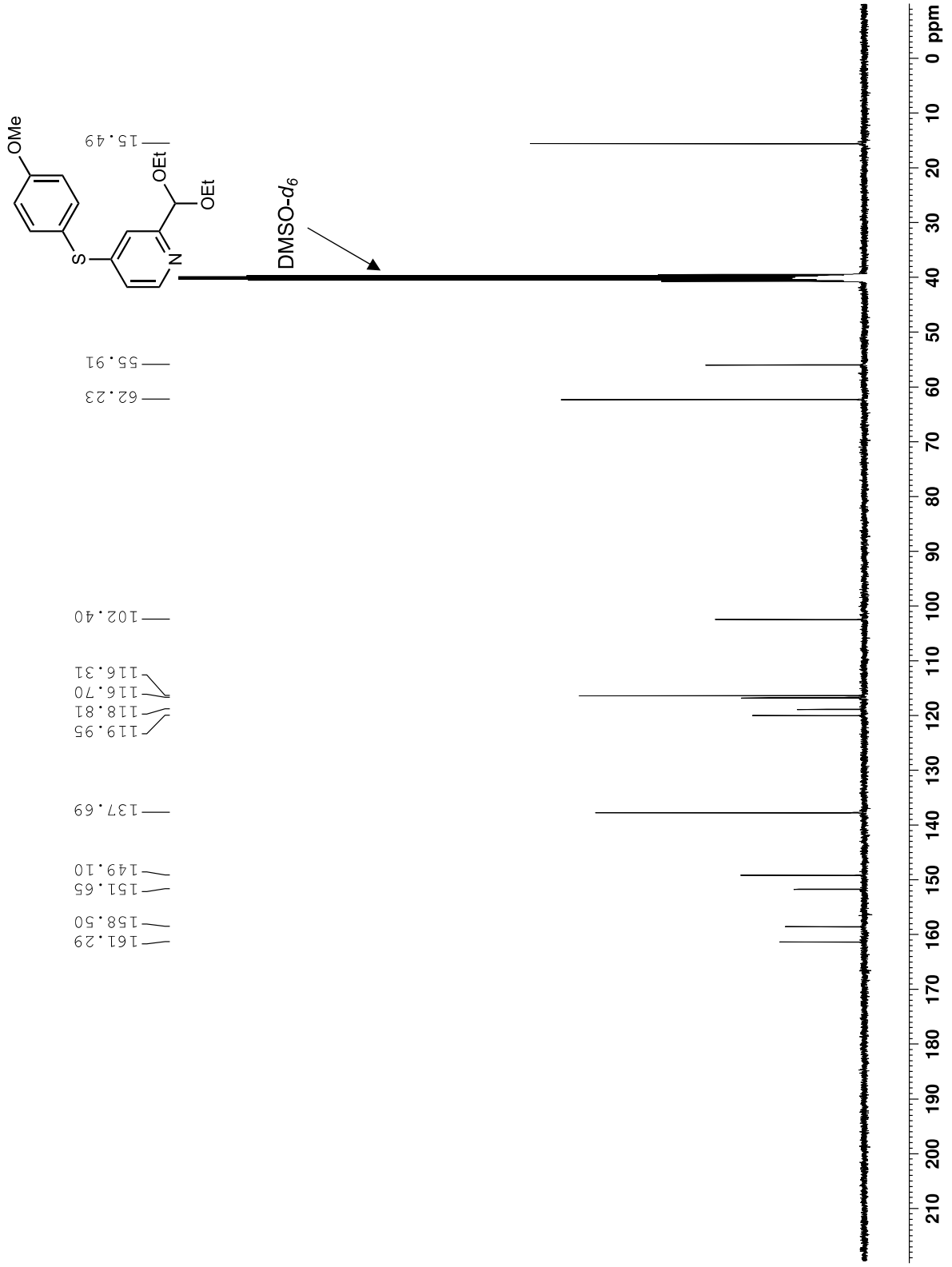

Spectrum 215. ^{13}C NMR of 2-(diethoxymethyl)-4-((4-methoxyphenyl)thio)pyridine (100 MHz, 293 K, DMSO-d_6).

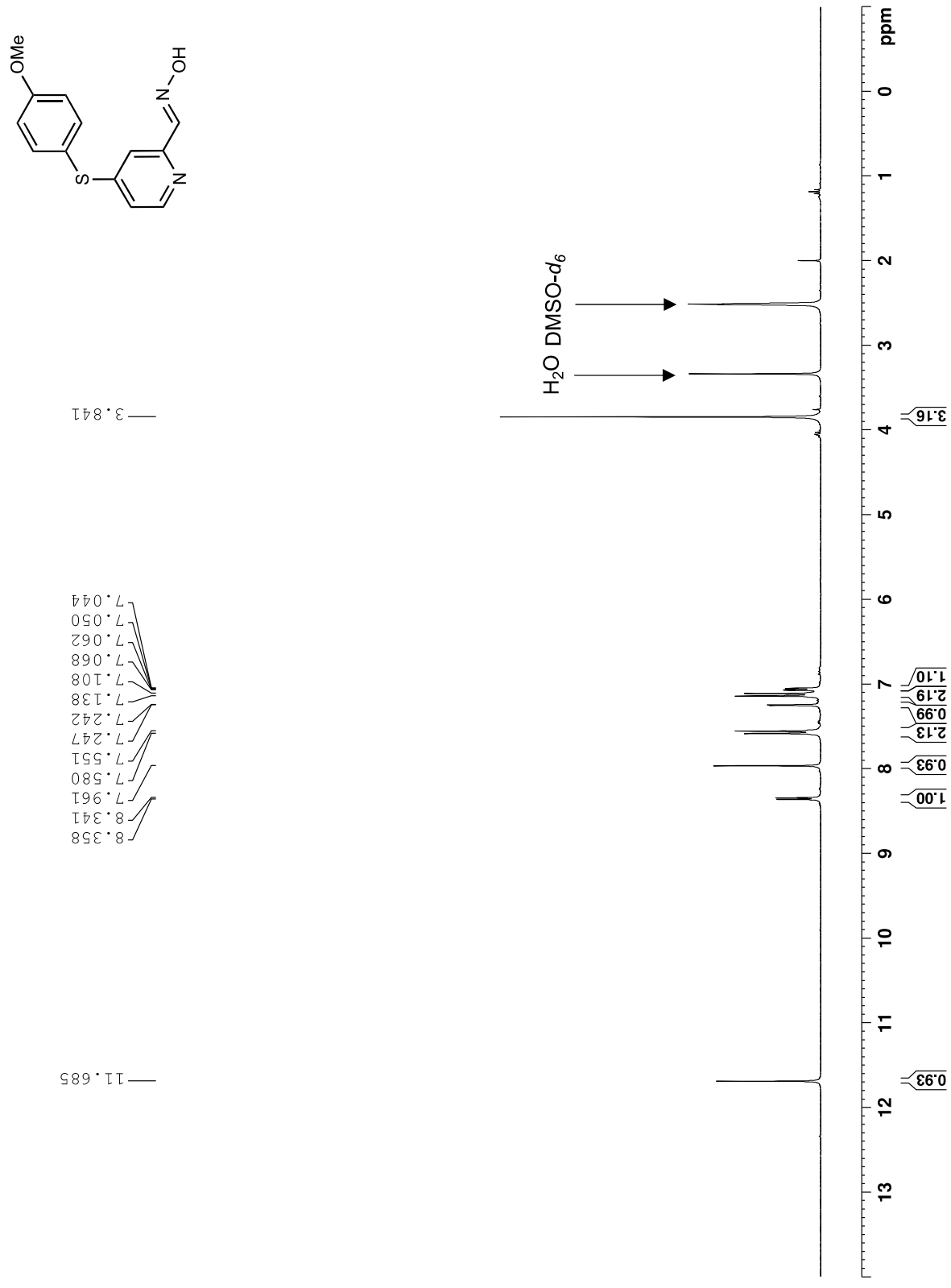

Spectrum 216. ^{1}H NMR of *(E)*-4-((4-methoxyphenyl)thio)picolinaldehyde oxime (300 MHz, 293 K, DMSO-d_6).

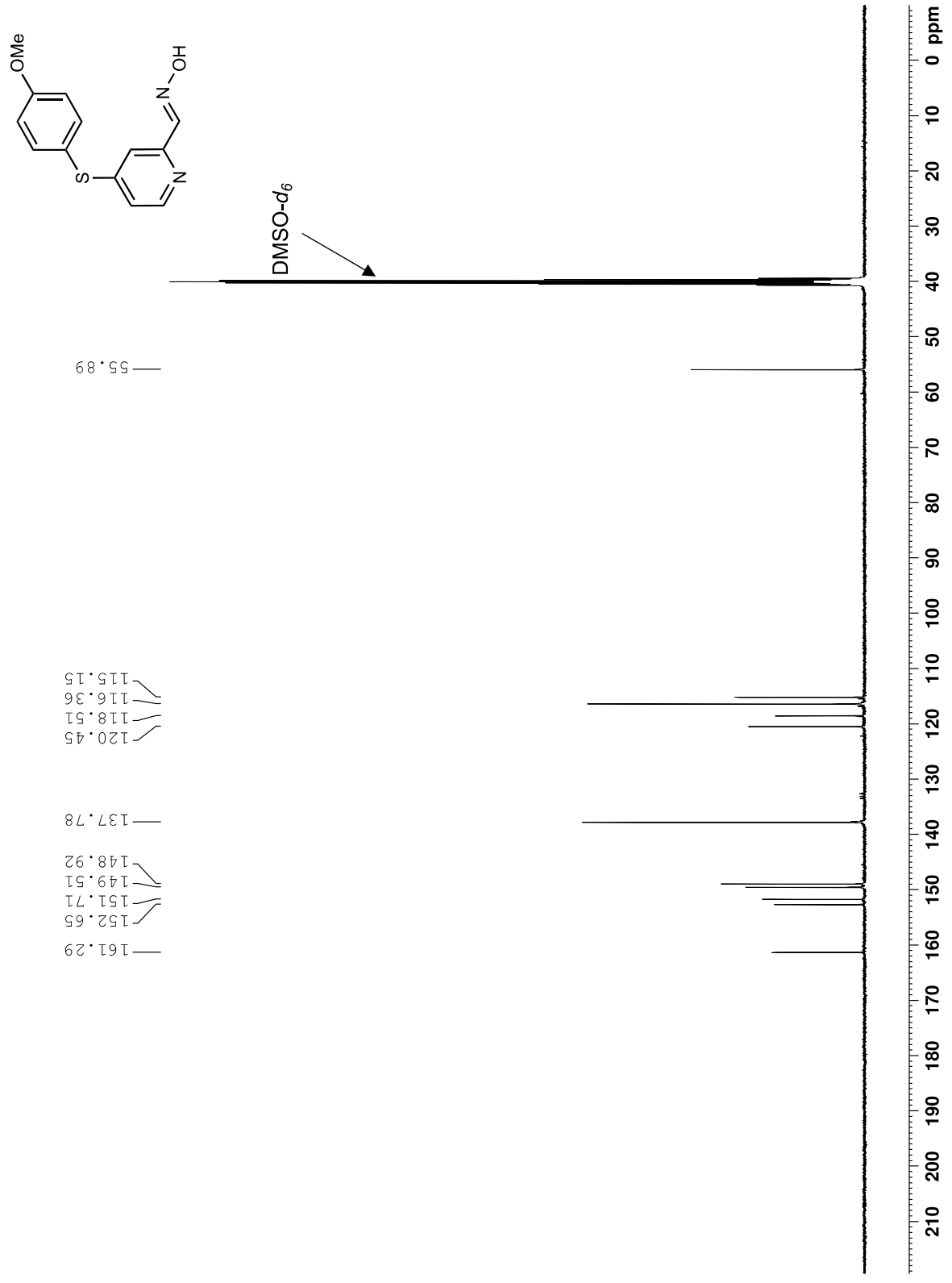

Spectrum 217. ^{13}C NMR of *(E)*-4-((4-methoxyphenyl)thio)picolinaldehyde oxime (100 MHz, 293 K, DMSO-d_6).

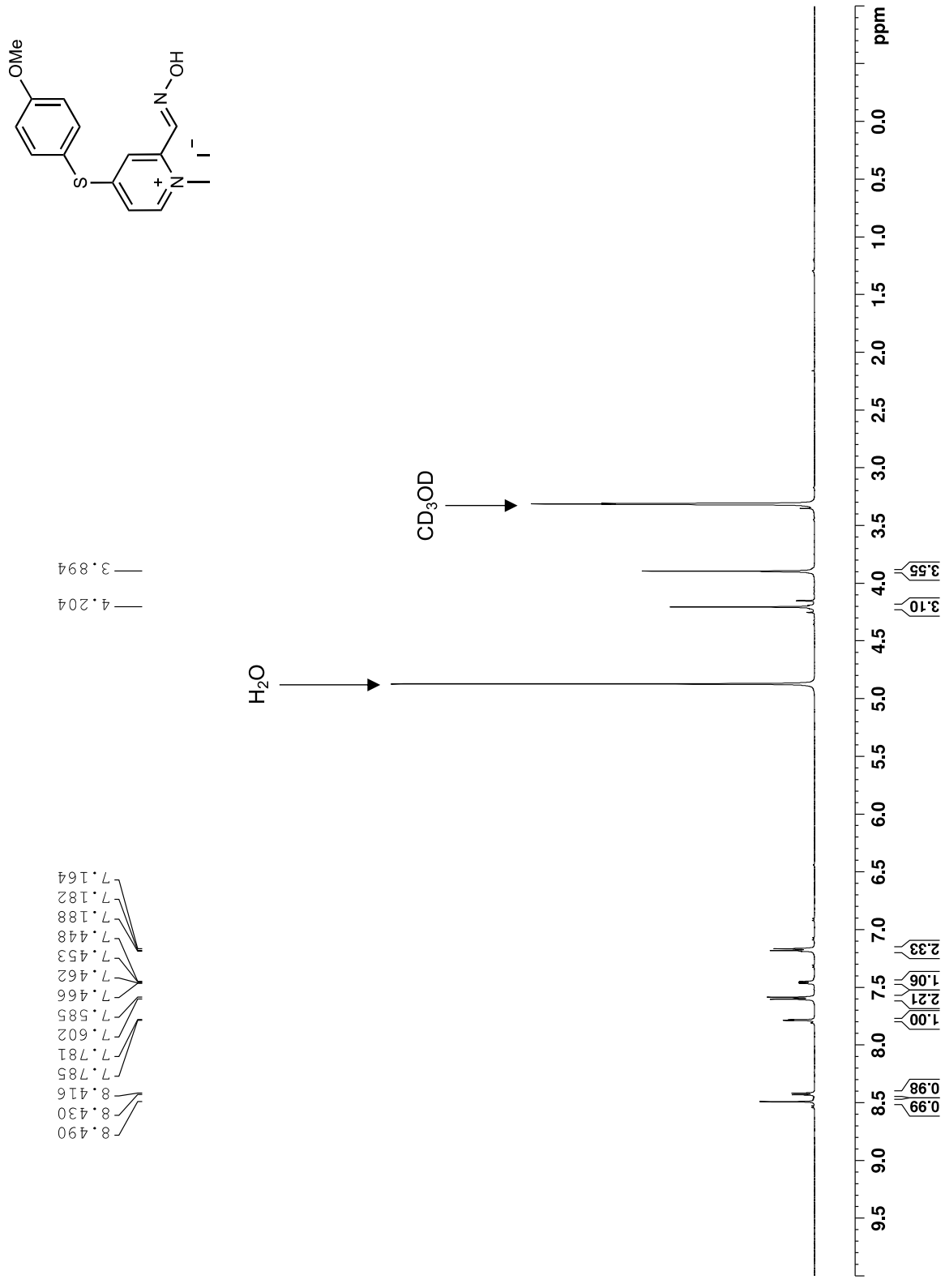

Spectrum 218. ^{1}H NMR of (*E*)-2-((hydroxyimino)methyl)-4-((4-methoxyphenyl)thio)-1-methylpyridin-1-ium iodide (**ADG3192**) (500 MHz, 293 K, CD_3OD).

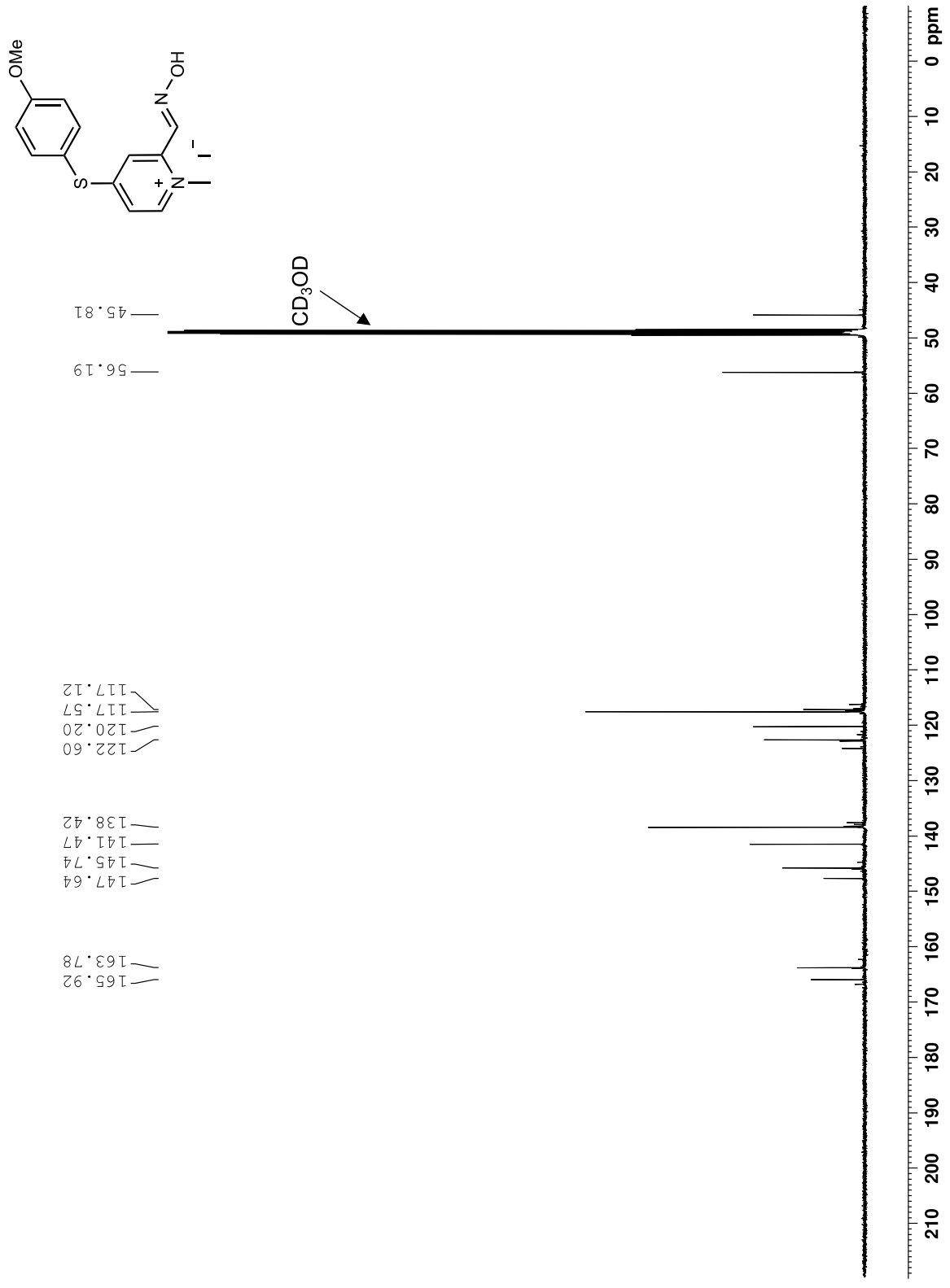

Spectrum 219. ^{13}C NMR of (*E*)-2-((hydroxyimino)methyl)-4-((4-methoxyphenyl)thio)-1-methylpyridin-1-ium iodide (**ADG3192**) (125 MHz, 293 K, CD_3OD).

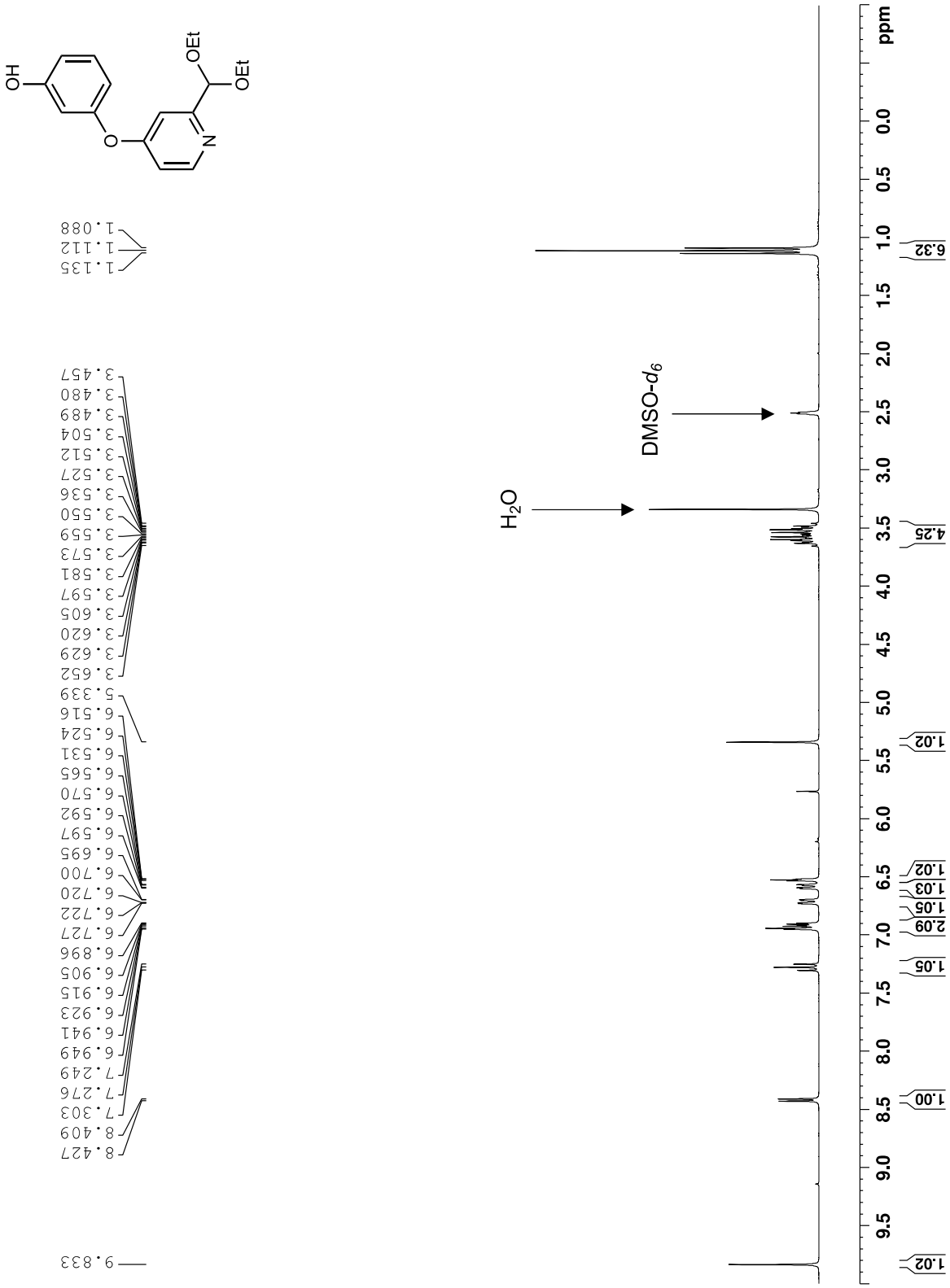

Spectrum 220. ^{1}H NMR of 3-((2-(diethoxymethyl)pyridin-4-yl)oxy)phenol (300 MHz, 293 K, DMSO-d_6).

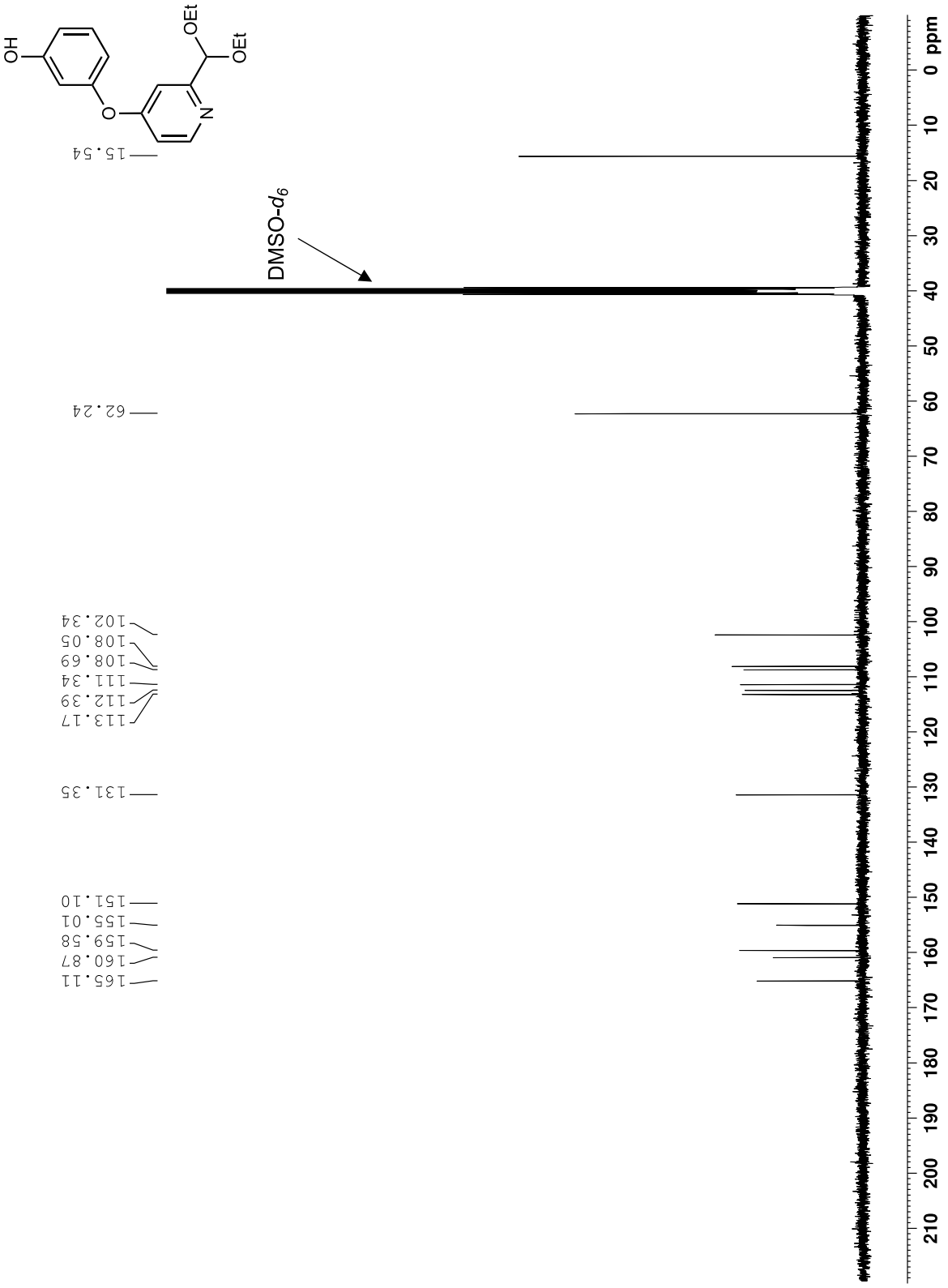

Spectrum 221. ^{13}C NMR of 3-((2-(diethoxymethyl)pyridin-4-yl)oxy)phenol (100 MHz, 293 K, DMSO-d_6).

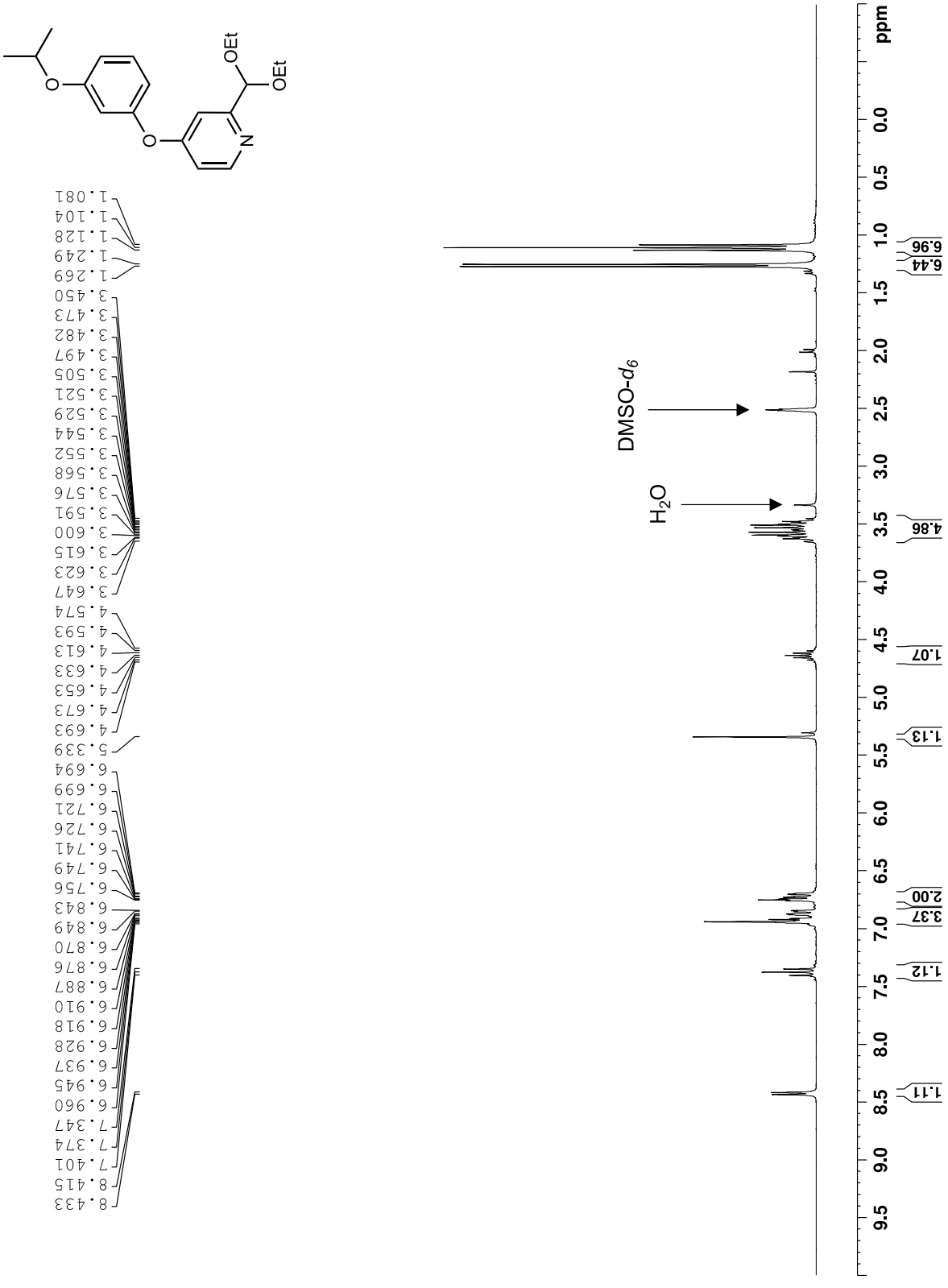

Spectrum 222. ^{1}H NMR of 2-(diethoxymethyl)-4-(3-isopropoxyphenoxy)pyridine (300 MHz, 293 K, DMSO-d_6).

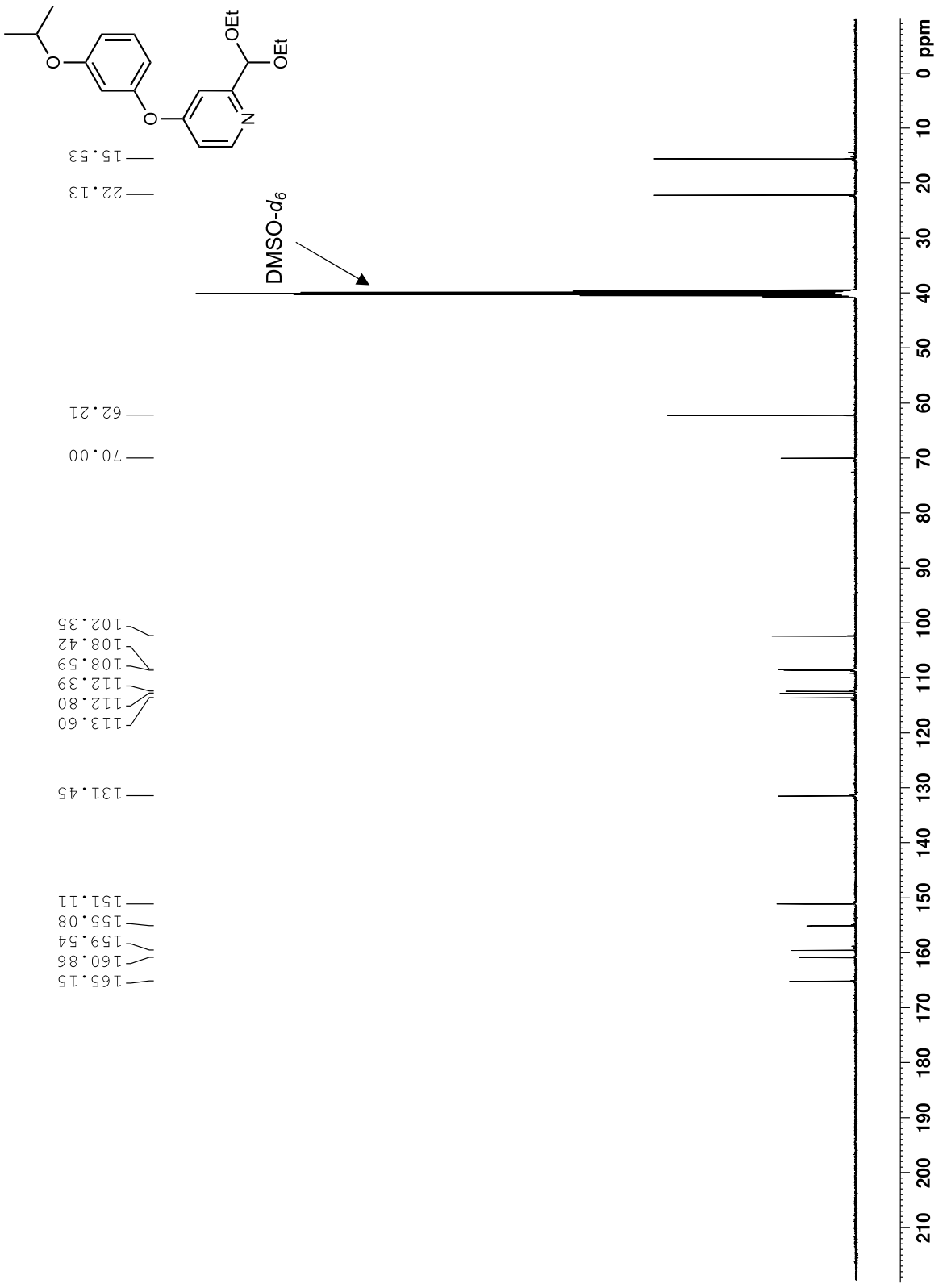

Spectrum 223. ^{13}C NMR of 2-(diethoxymethyl)-4-(3-isopropoxyphenoxy)pyridine (100 MHz, 293 K, DMSO-d_6).

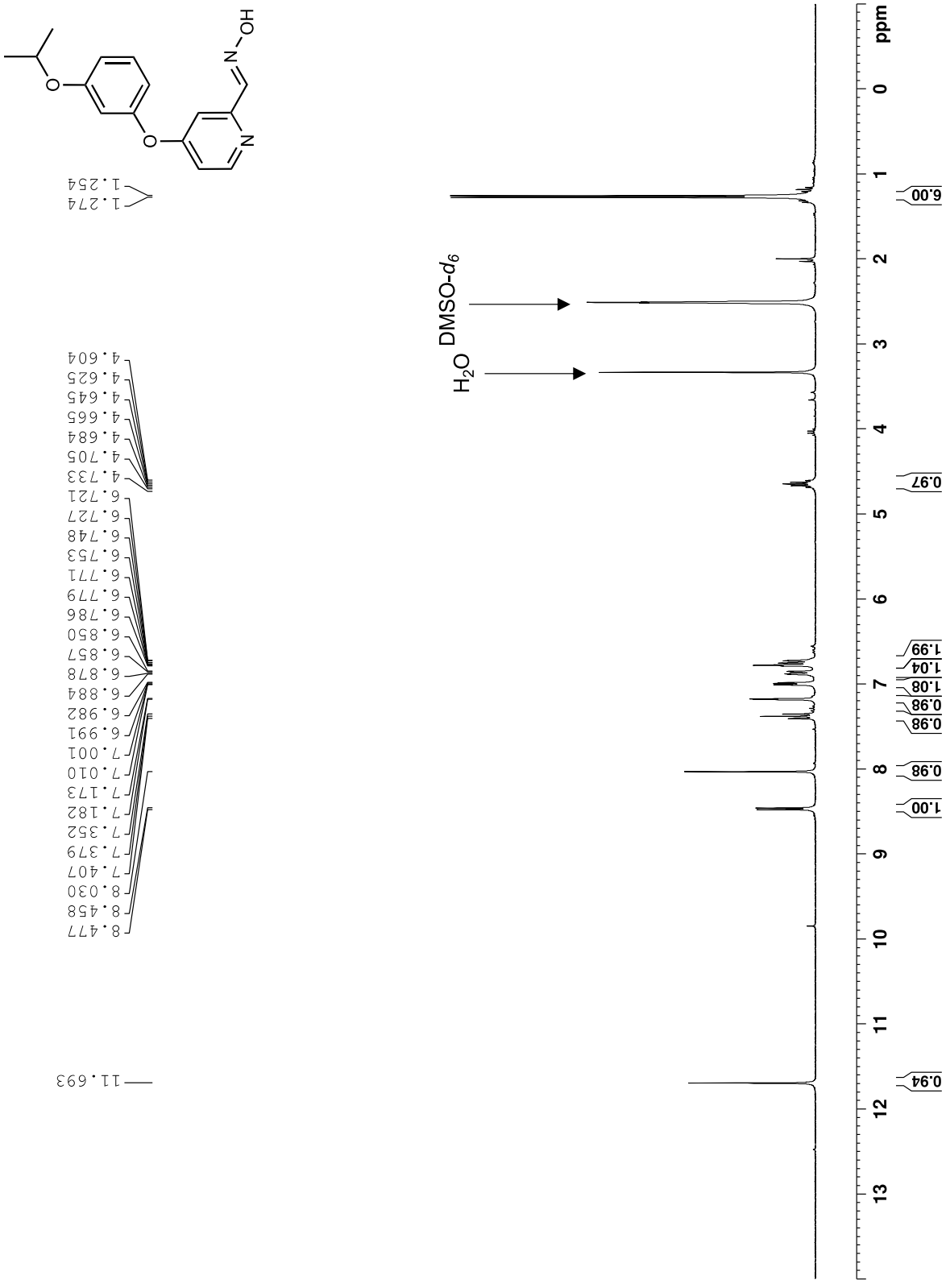

Spectrum 224. ^{1}H NMR of (*E*)-4-(3-isopropoxyphenoxy)picolinaldehyde oxime (300 MHz, 293 K, DMSO-d_6).

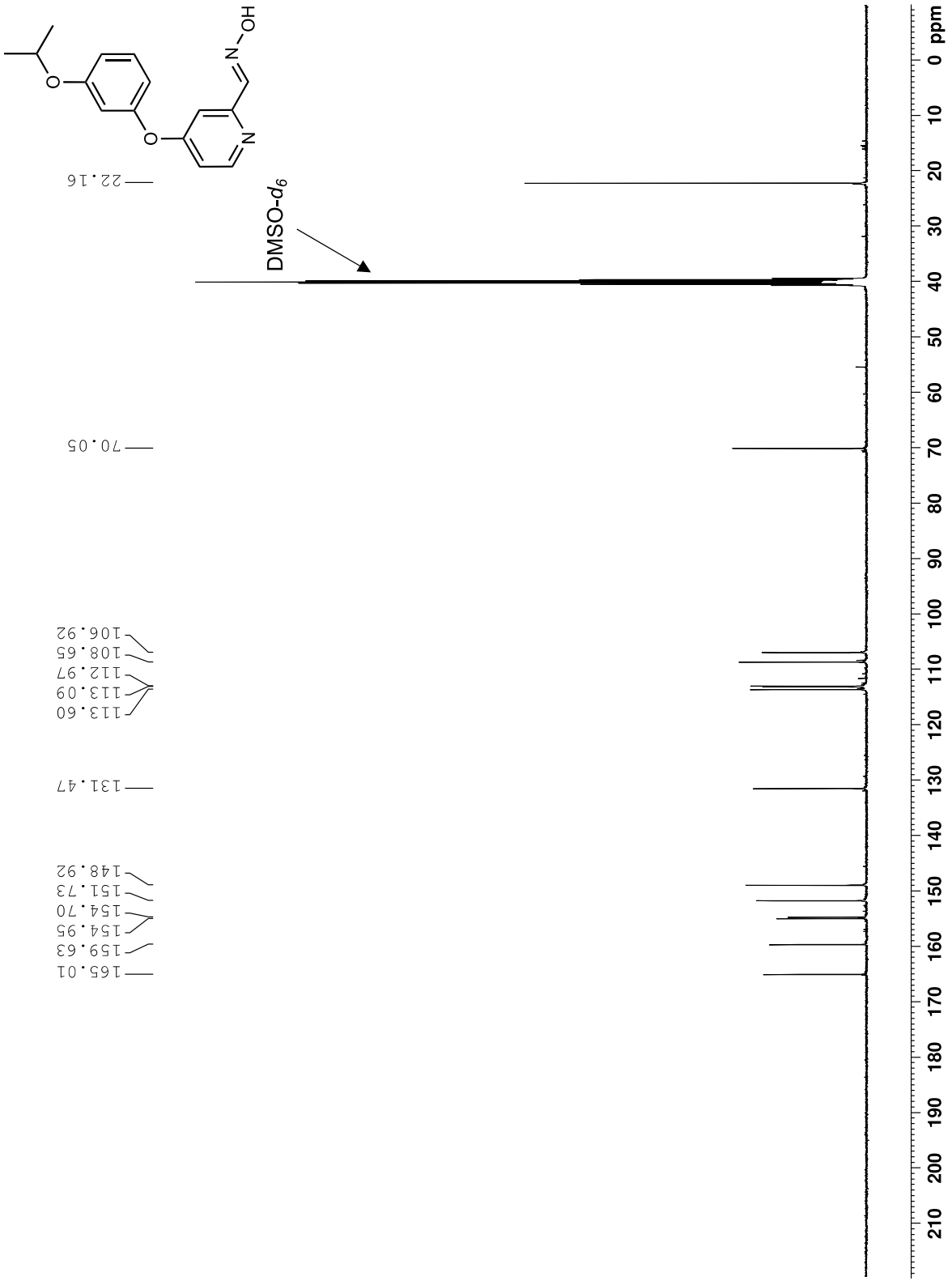

Spectrum 225. ^{13}C NMR of (*E*)-4-(3-isopropoxyphenoxy)picolinaldehyde oxime (100 MHz, 293 K, DMSO-d_6).

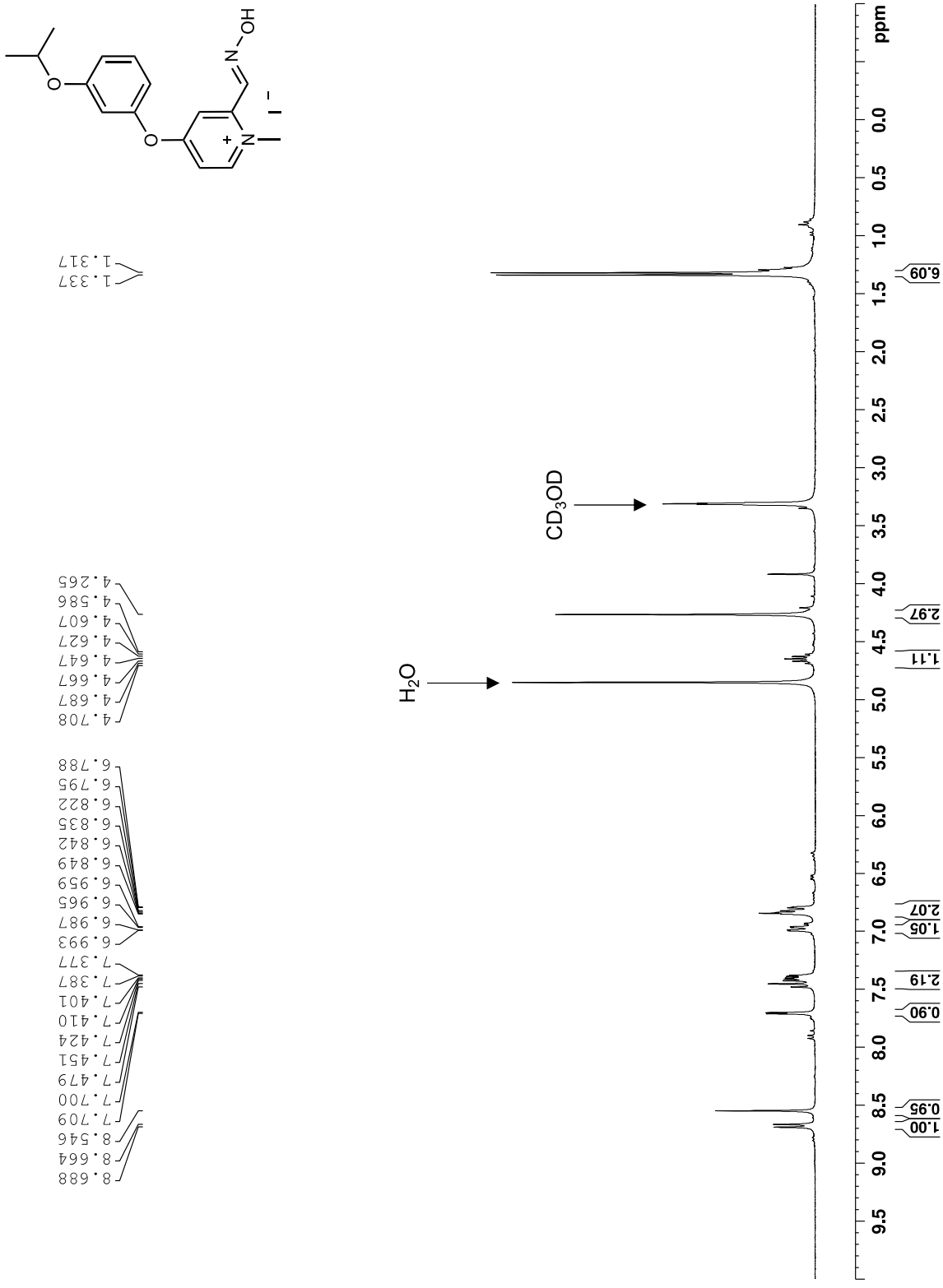

Spectrum 226. ^{1}H NMR of *(E)*-2-((hydroxyimino)methyl)-1-methyl-4-(3-isopropoxyphenoxy)pyridin-1-ium iodide (ADG5044) (300 MHz, 293 K, CD_3OD).

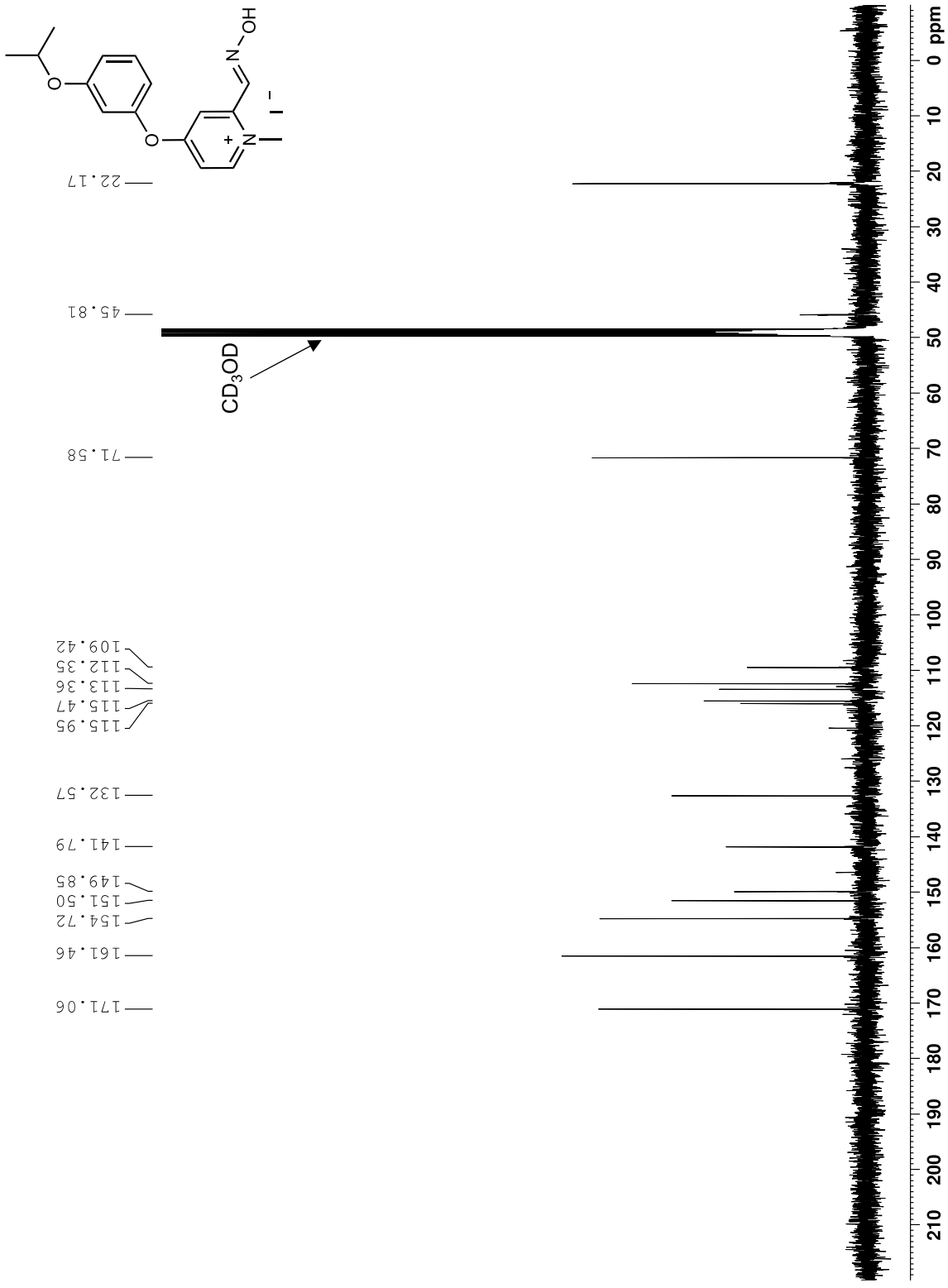

Spectrum 227. ^{13}C NMR of *(E)*-2-((hydroxyimino)methyl)-1-methyl-4-(3-isopropoxyphenoxy)pyridin-1-ium iodide (ADG5044) (100 MHz, 293 K, CD_3OD).

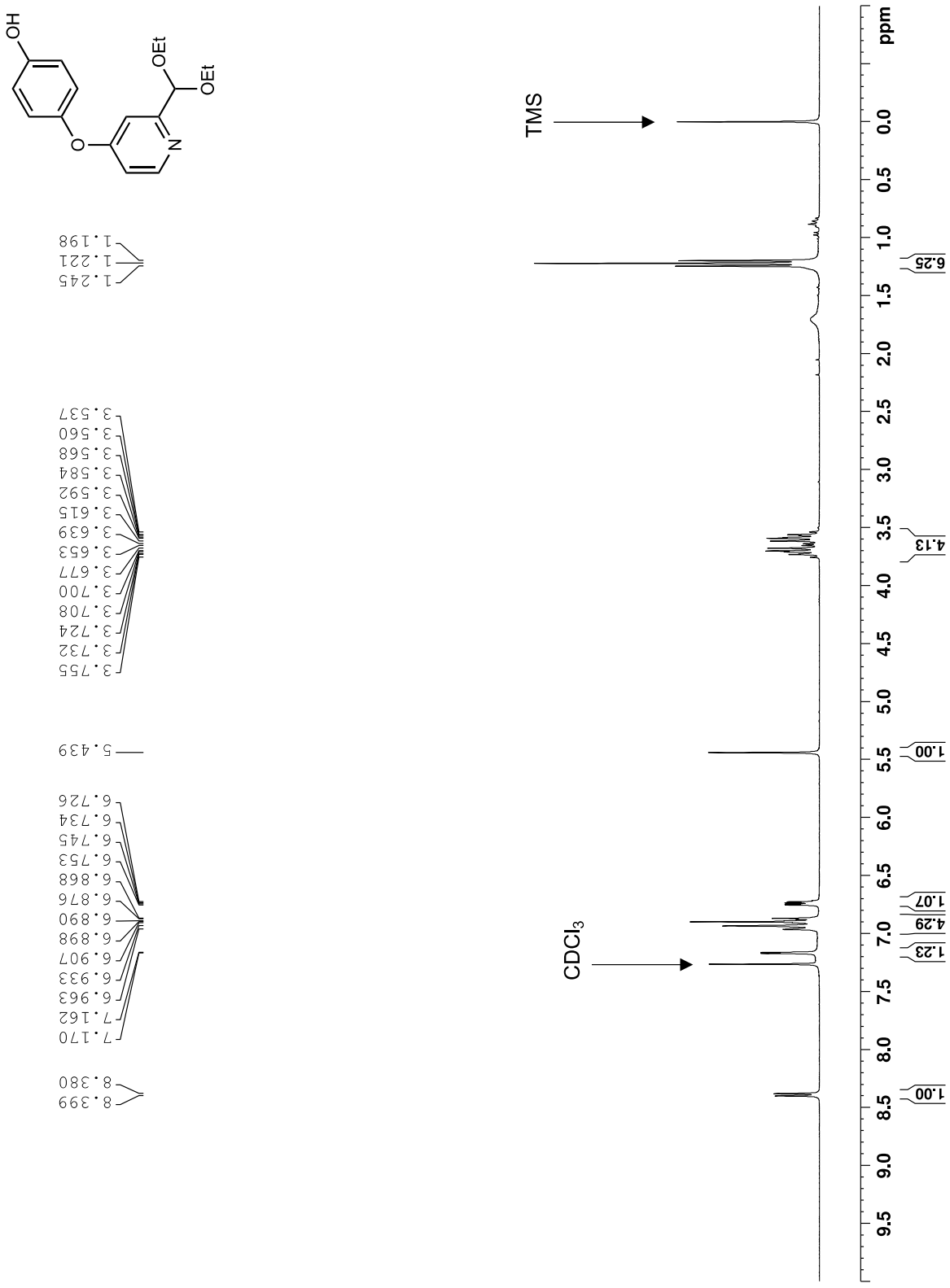

Spectrum 228. ^{1}H NMR of 4-((2-(diethoxymethyl)pyridin-4-yl)oxy)phenol (300 MHz, 293 K, 1% w/w CD_3OD in $CDCl_3$).

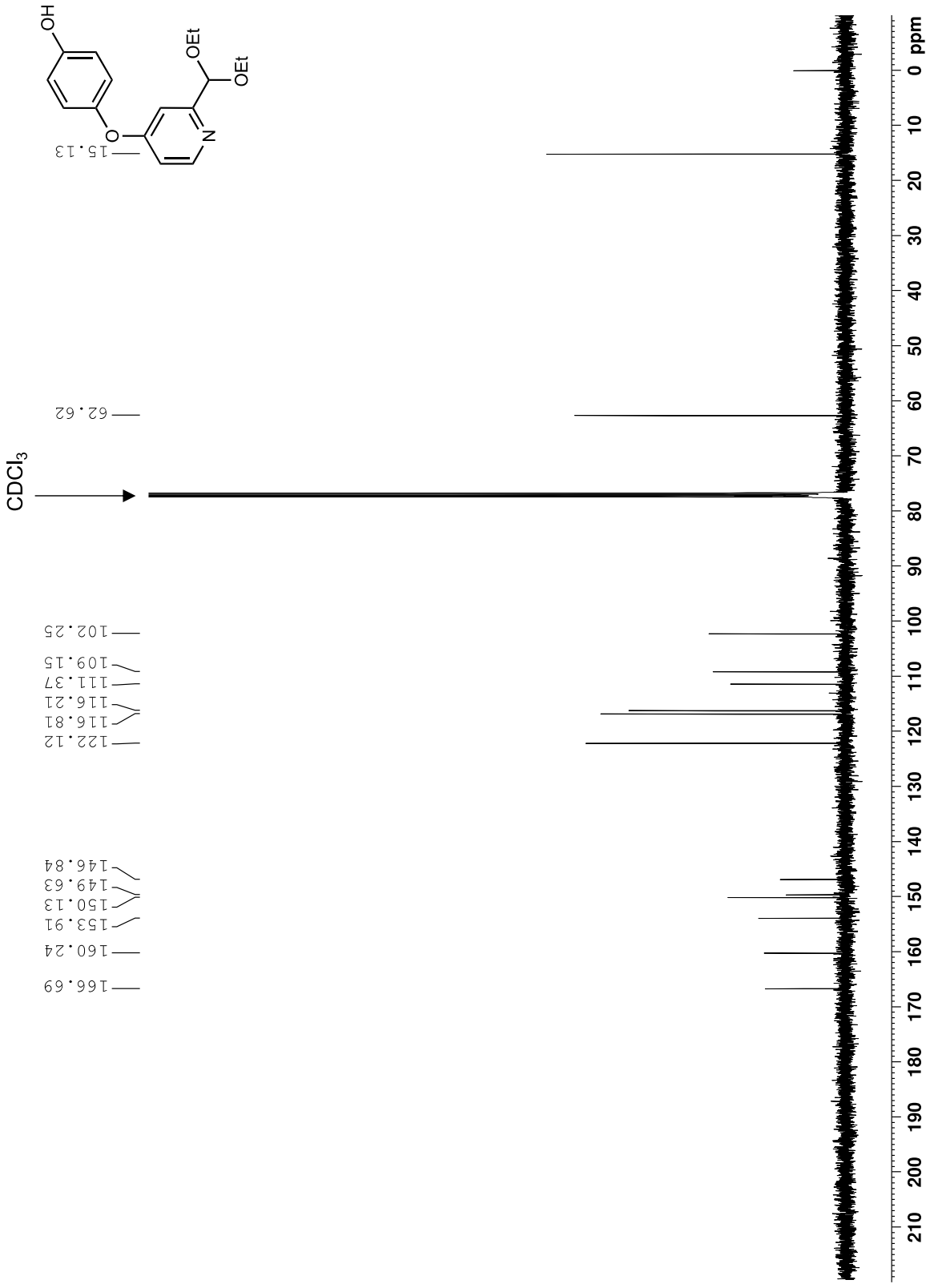

Spectrum 229. ^{13}C NMR of 4-((2-(diethoxymethyl)pyridin-4-yl)oxy)phenol (100 MHz, 293 K, $CDCl_3$).

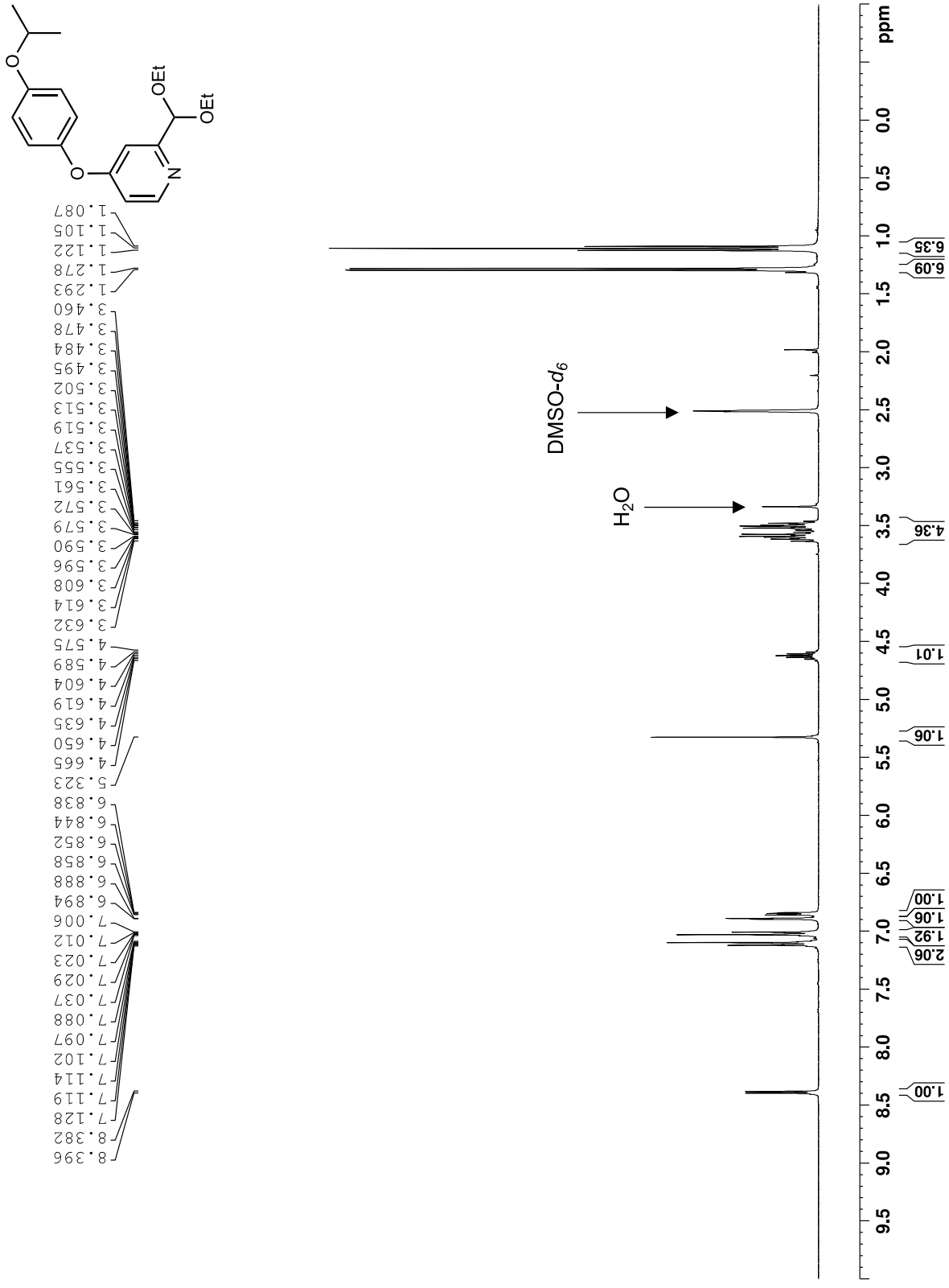

Spectrum 230. [1]H NMR of 2-(diethoxymethyl)-4-(4-isopropoxyphenoxy)pyridine (400 MHz, 293 K, DMSO-d_6).

Spectrum 231. ^{13}C NMR of 2-(diethoxymethyl)-4-(4-isopropoxyphenoxy)pyridine (100 MHz, 293 K, DMSO-d_6).

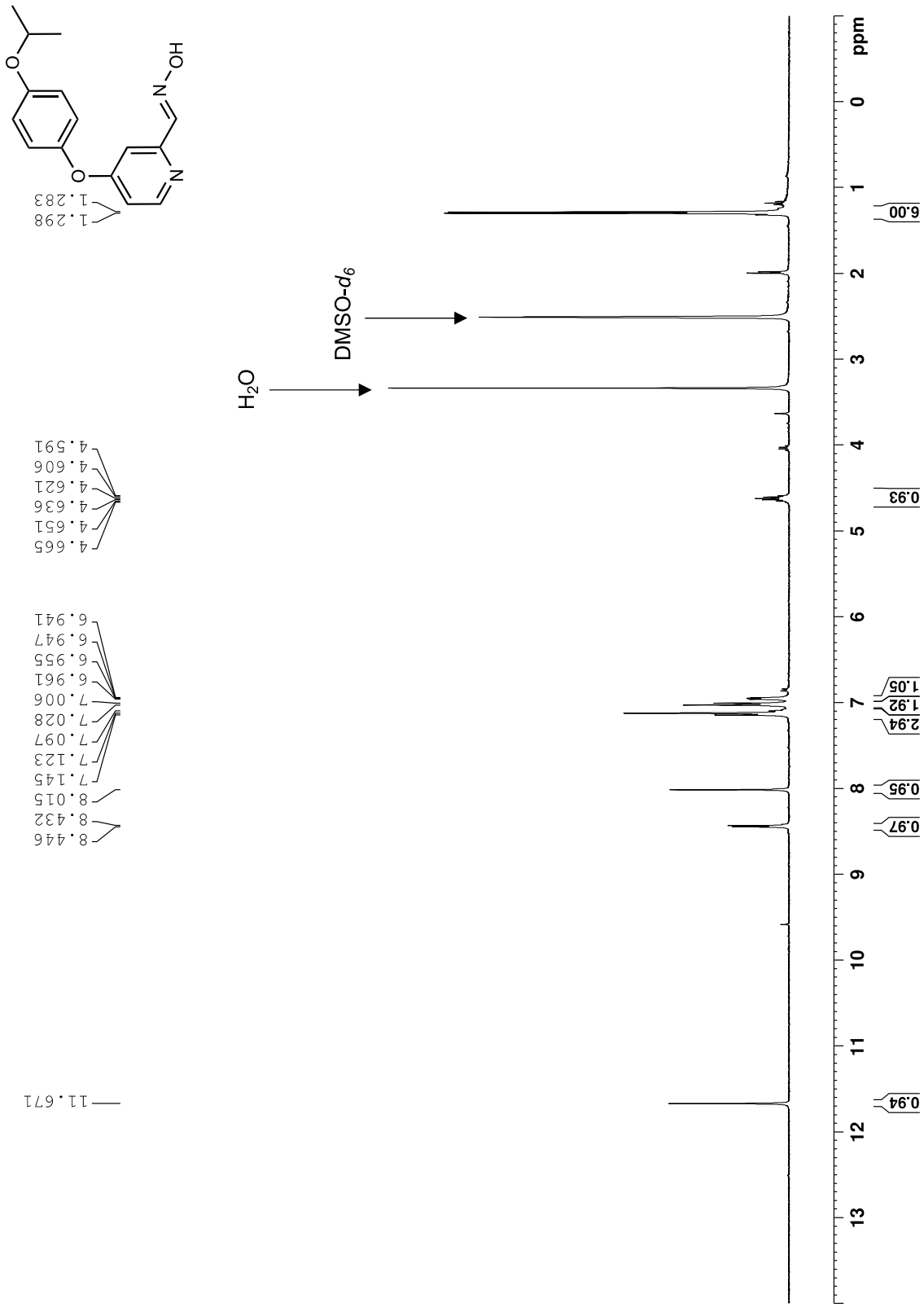

Spectrum 232. ^{1}H NMR of (*E*)-4-(4-isopropoxyphenoxy)picolinaldehyde oxime (400 MHz, 293 K, DMSO-d_6).

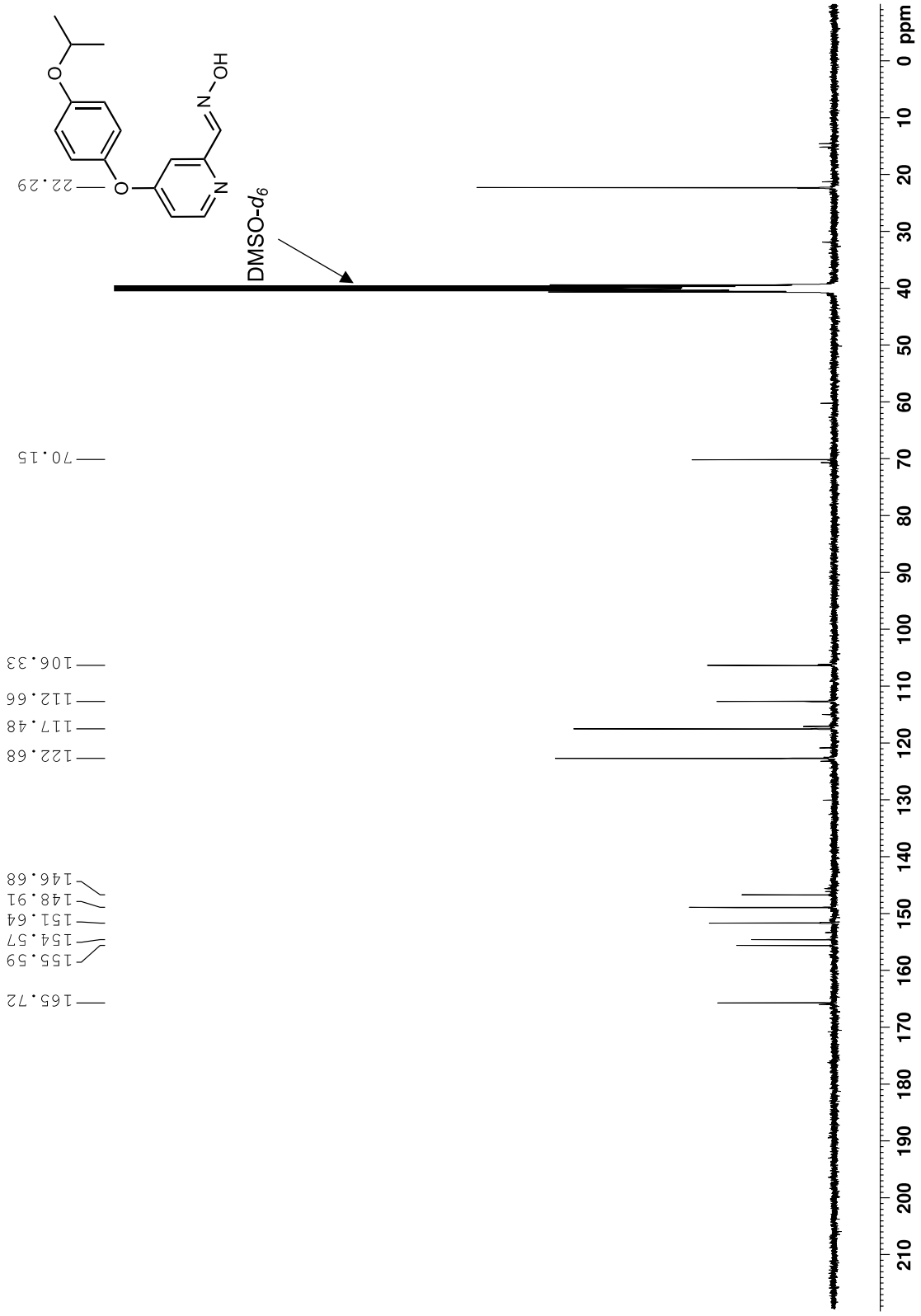

Spectrum 233. ^{13}C NMR of (*E*)-4-(4-isopropoxyphenoxy)picolinaldehyde oxime (100 MHz, 293 K, DMSO-d_6).

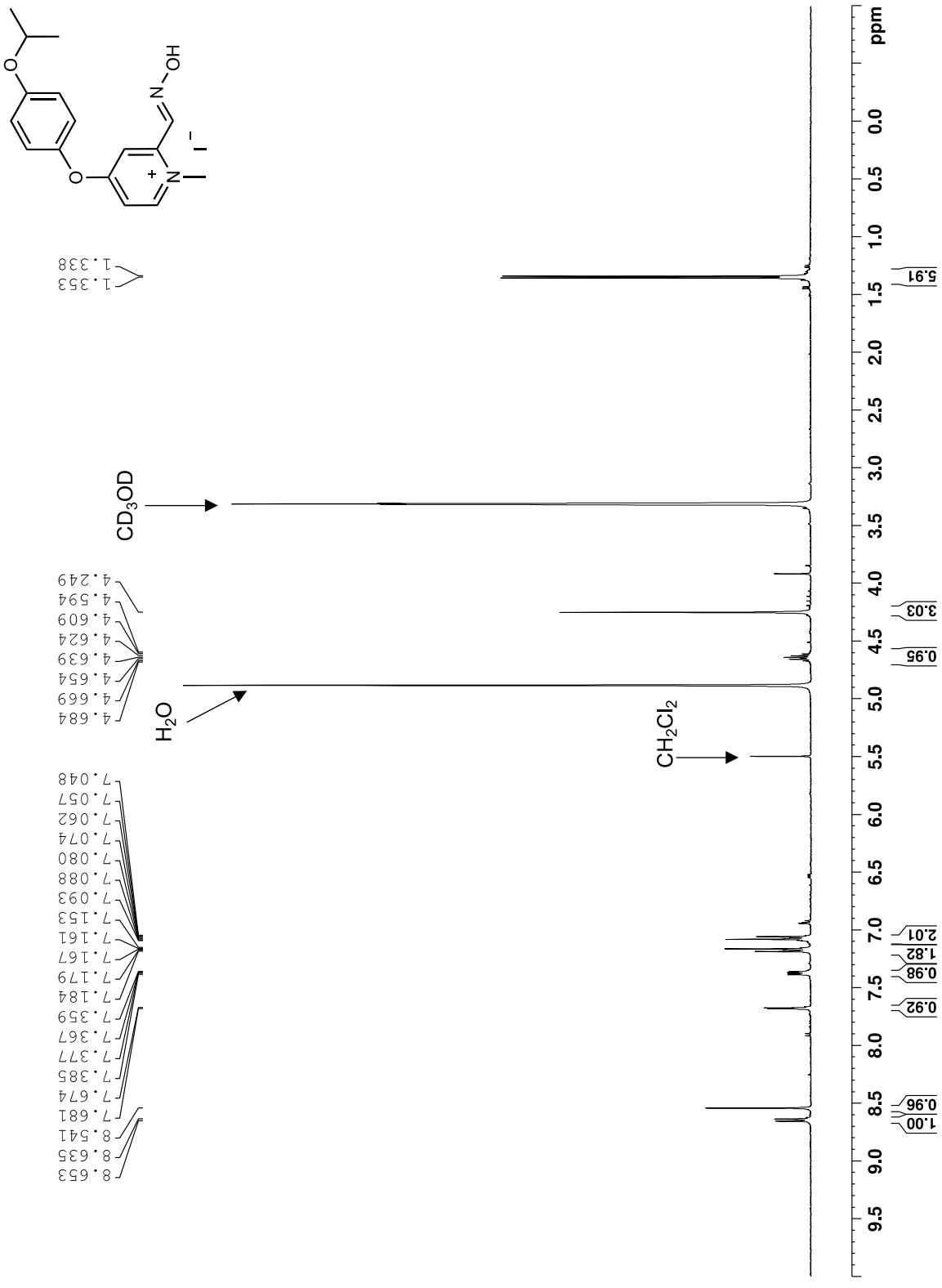

Spectrum 234. ^{1}H NMR of *(E)*-2-((hydroxyimino)methyl)-1-methyl-4-(3-isopropoxyphenoxy)pyridin-1-ium iodide (**ADG5045**) (400 MHz, 293 K, CD_3OD).

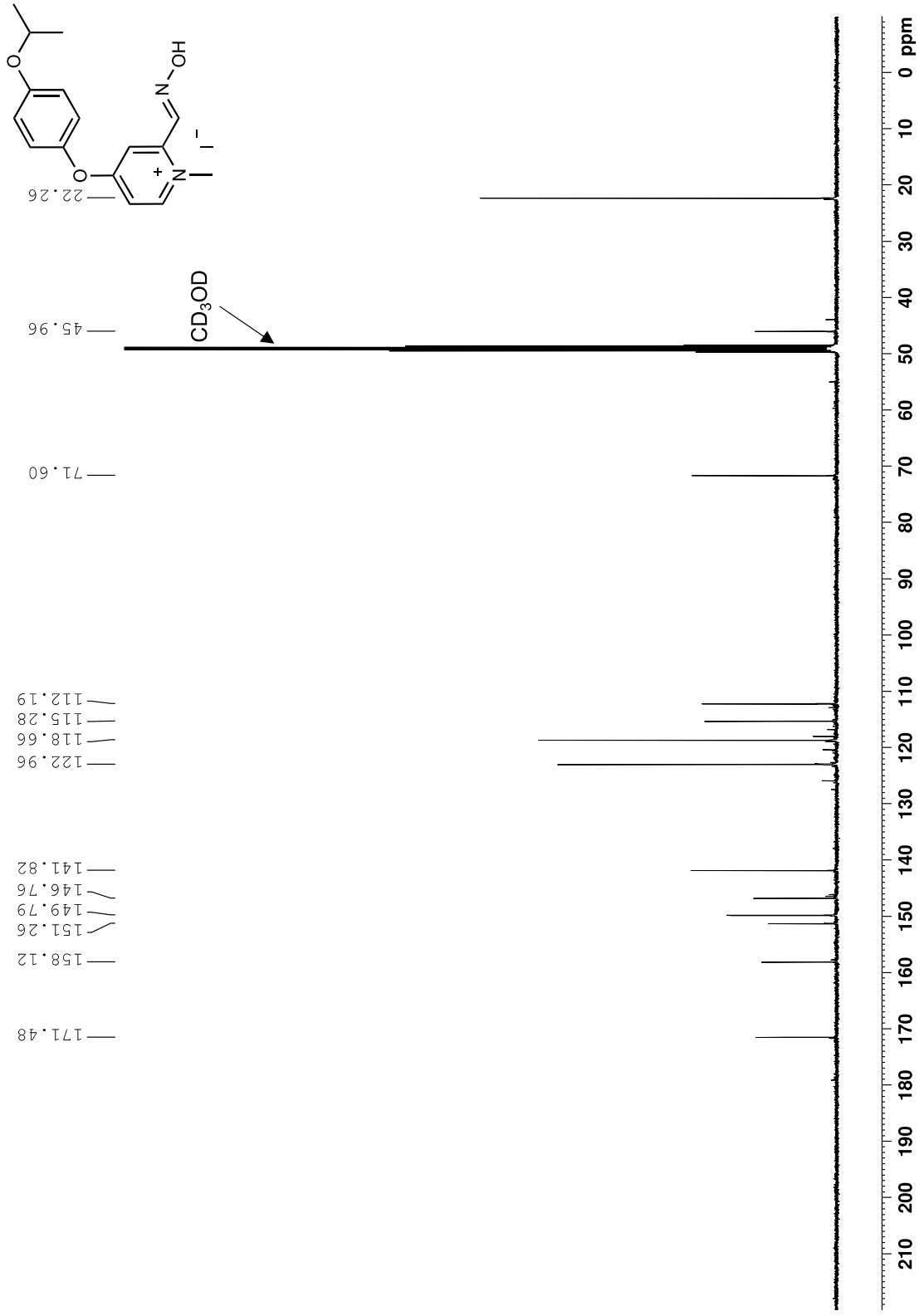

Spectrum 235. ^{13}C NMR of 2-((hydroxyimino)methyl)-1-methyl-4-(3-isopropoxyphenoxy)pyridin-1-ium iodide (**ADG5045**) (100 MHz, 293 K, CD_3OD).

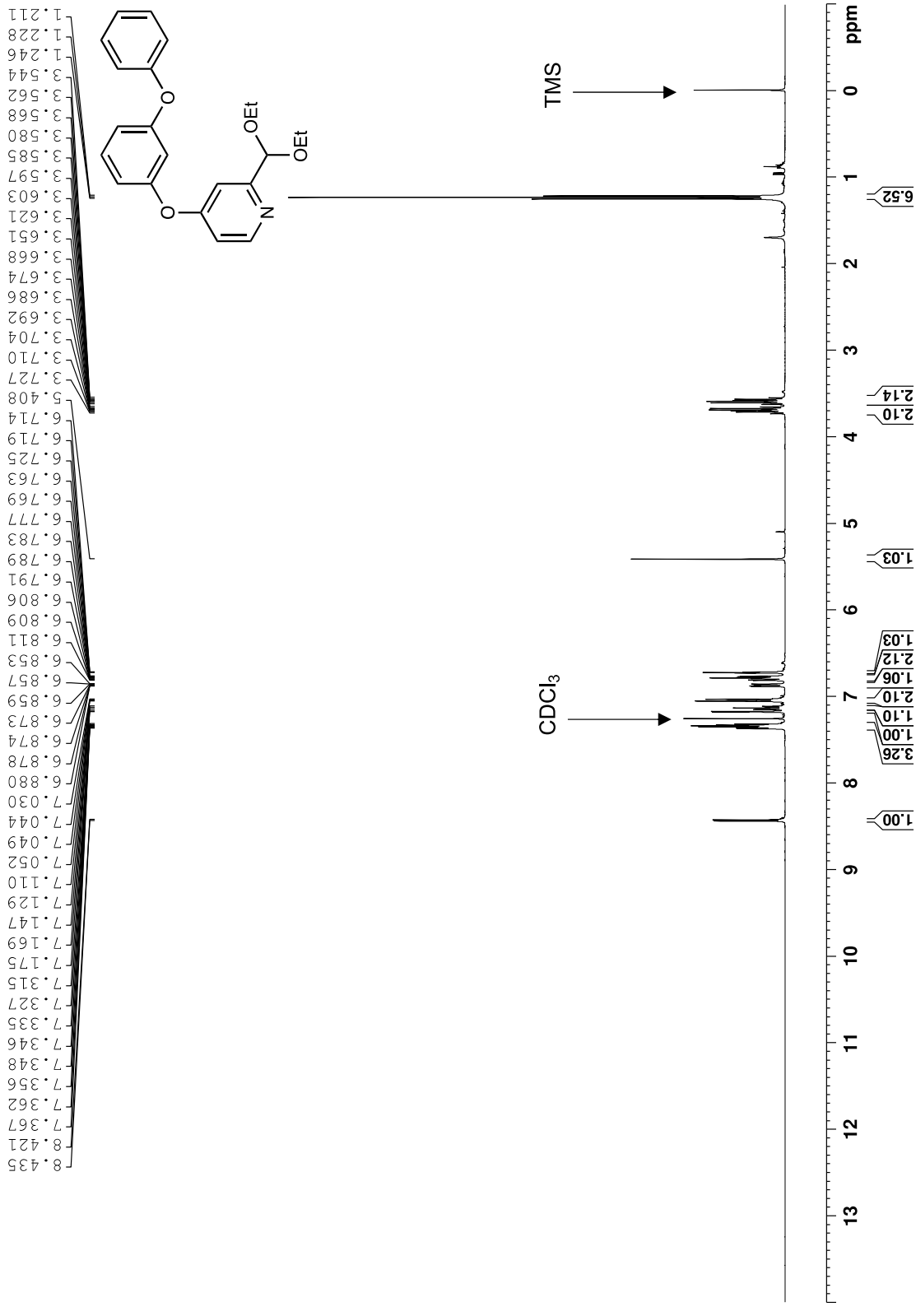

Spectrum 236. ^{1}H NMR of 2-(diethoxymethyl)-4-(3-phenoxyphenoxy)pyridine (400 MHz, 293 K, $CDCl_3$).

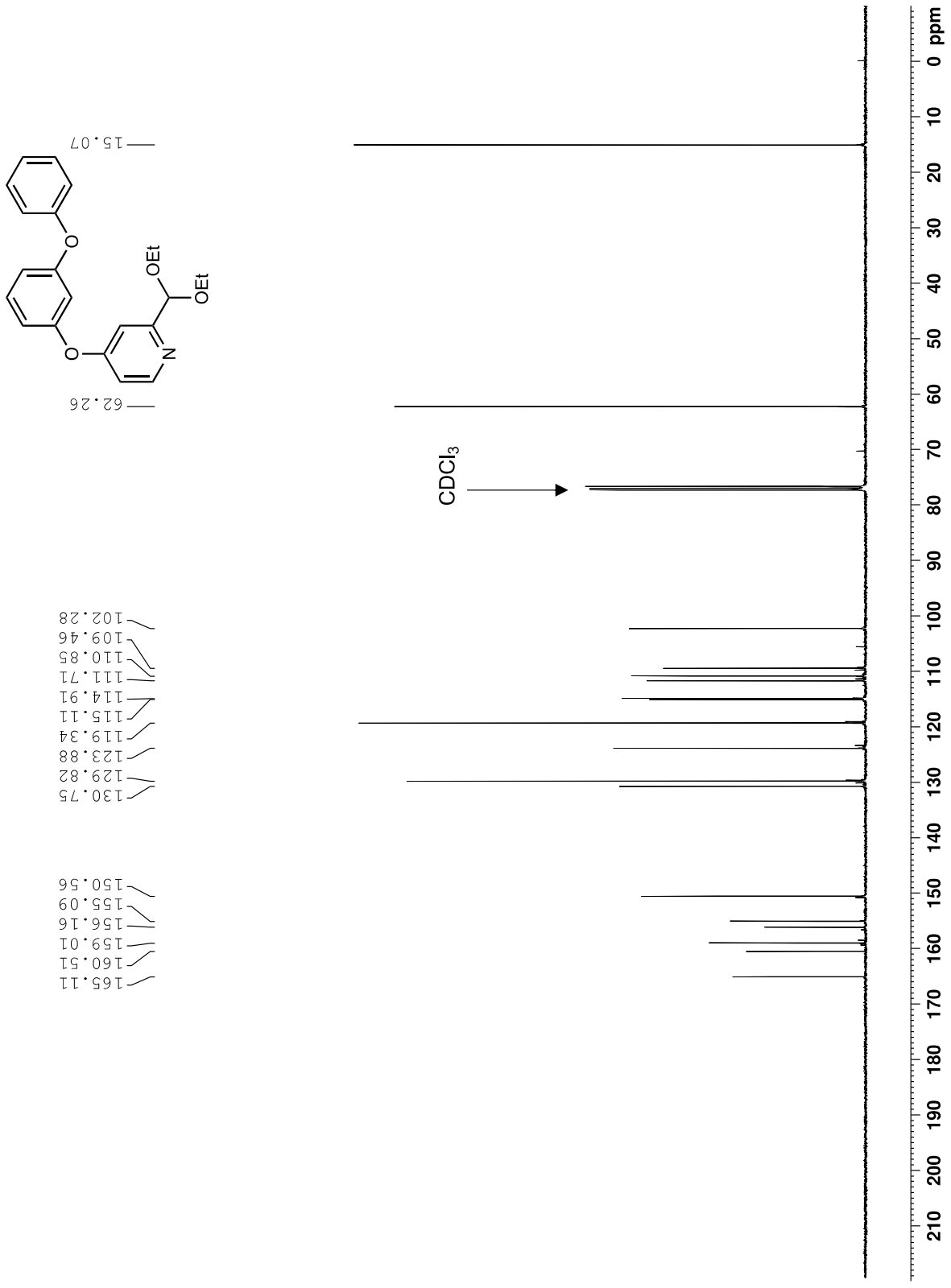

Spectrum 237. ^{13}C NMR of 2-(diethoxymethyl)-4-(3-phenoxyphenoxy)pyridine (100 MHz, 293 K, $CDCl_3$).

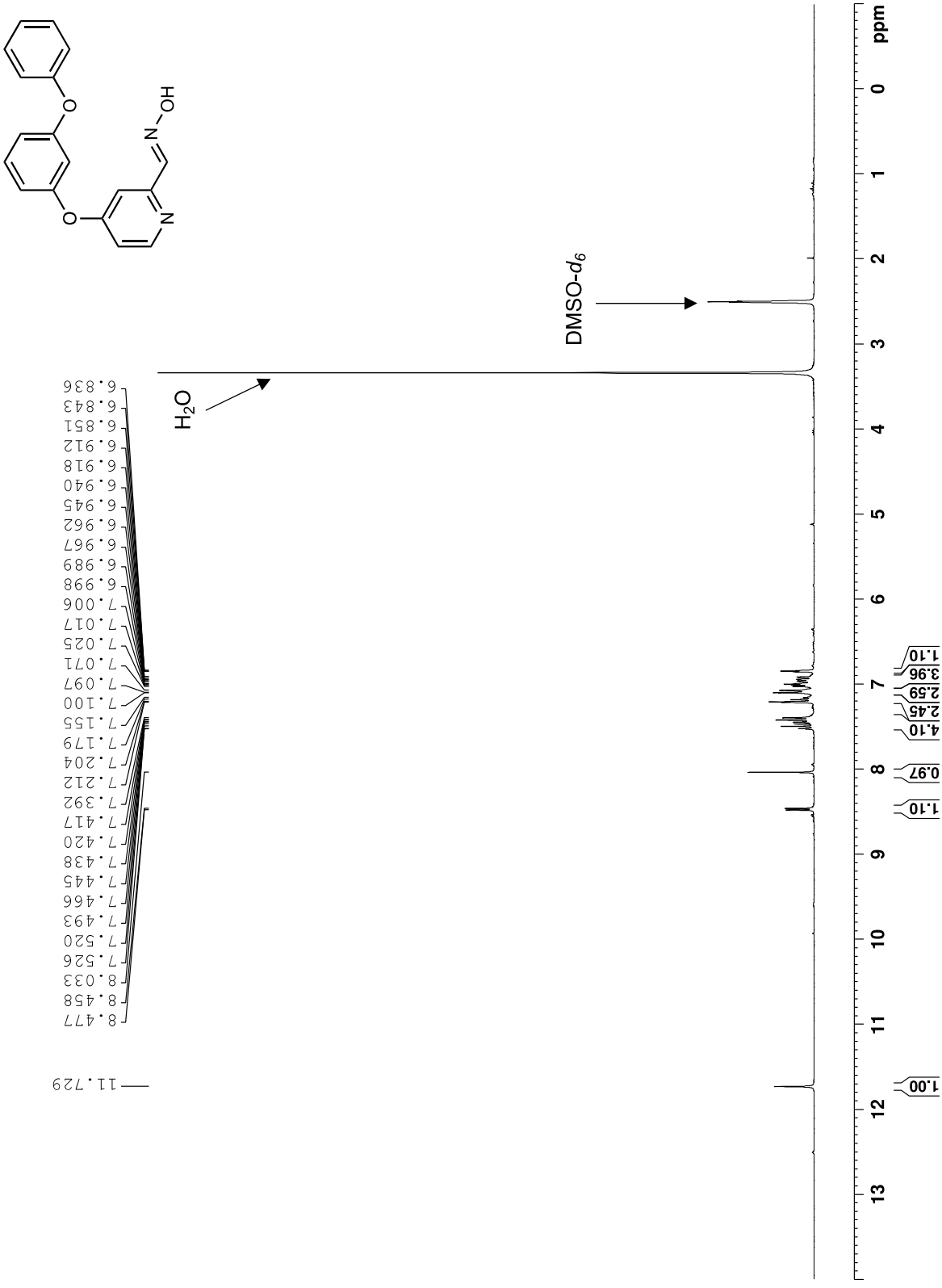

Spectrum 238. ^{1}H NMR of *(E)*-4-(3-phenoxyphenoxy)picolinaldehyde oxime (300 MHz, 293 K, DMSO-d_6).

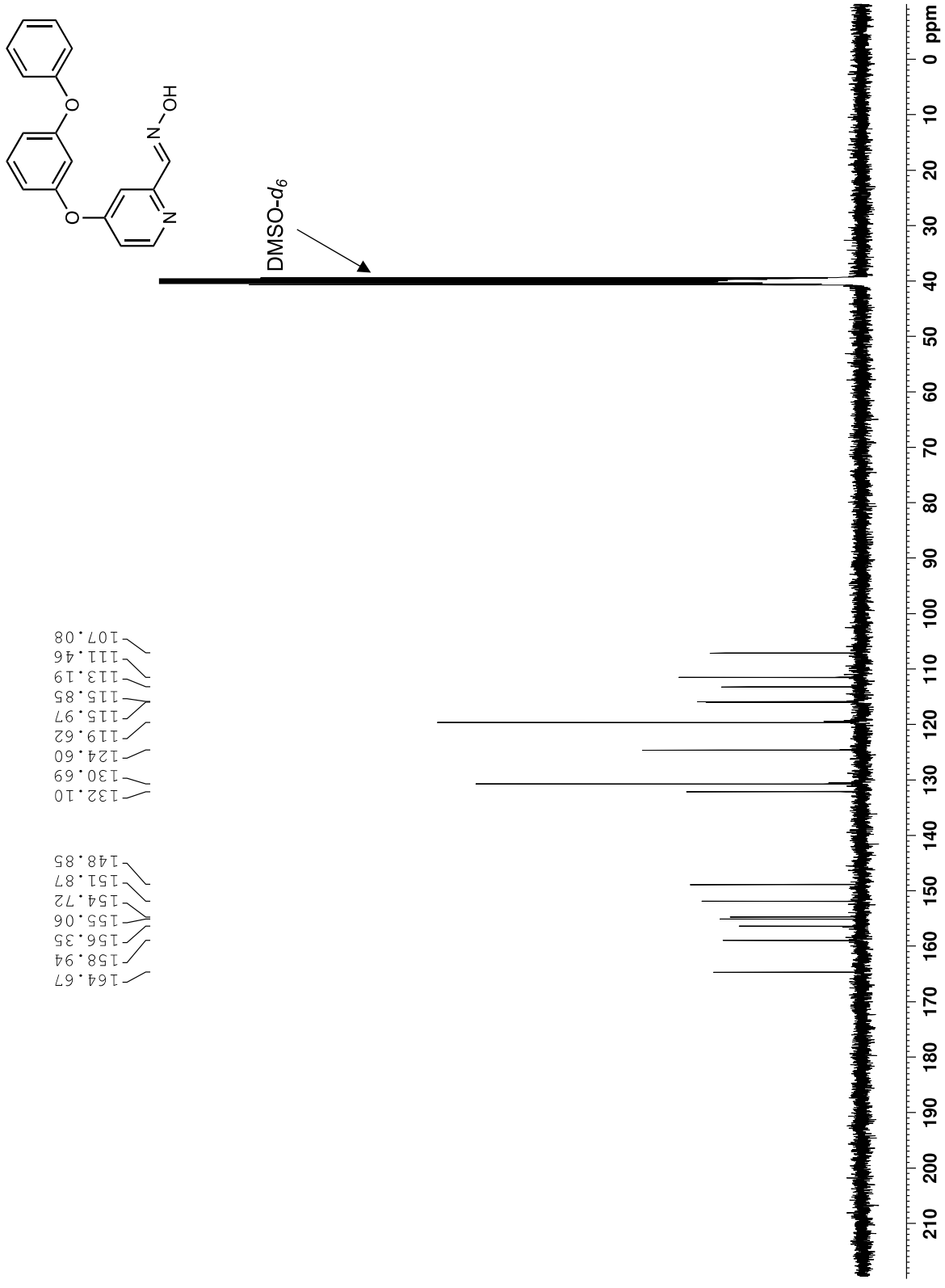

Spectrum 239. ^{13}C NMR of *(E)*-4-(3-phenoxyphenoxy)picolinaldehyde oxime (100 MHz, 293 K, DMSO-d_6).

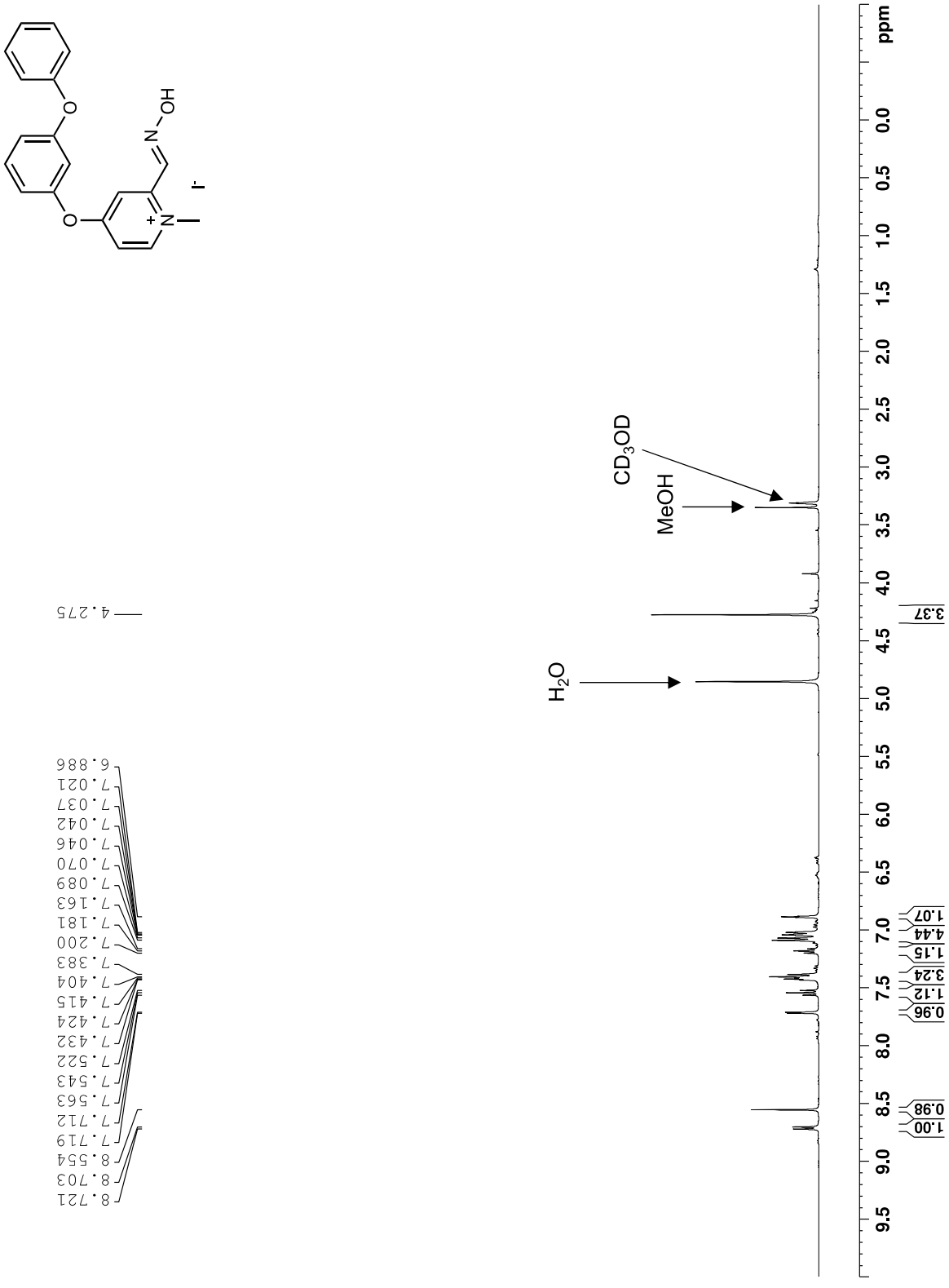

Spectrum 240. ^{1}H NMR of *(E)*-2-((hydroxyimino)methyl)-1-methyl-4-(3-phenoxyphenoxy)pyridin-1-ium iodide (**ADG4230**) (400 MHz, 293 K, CD_3OD).

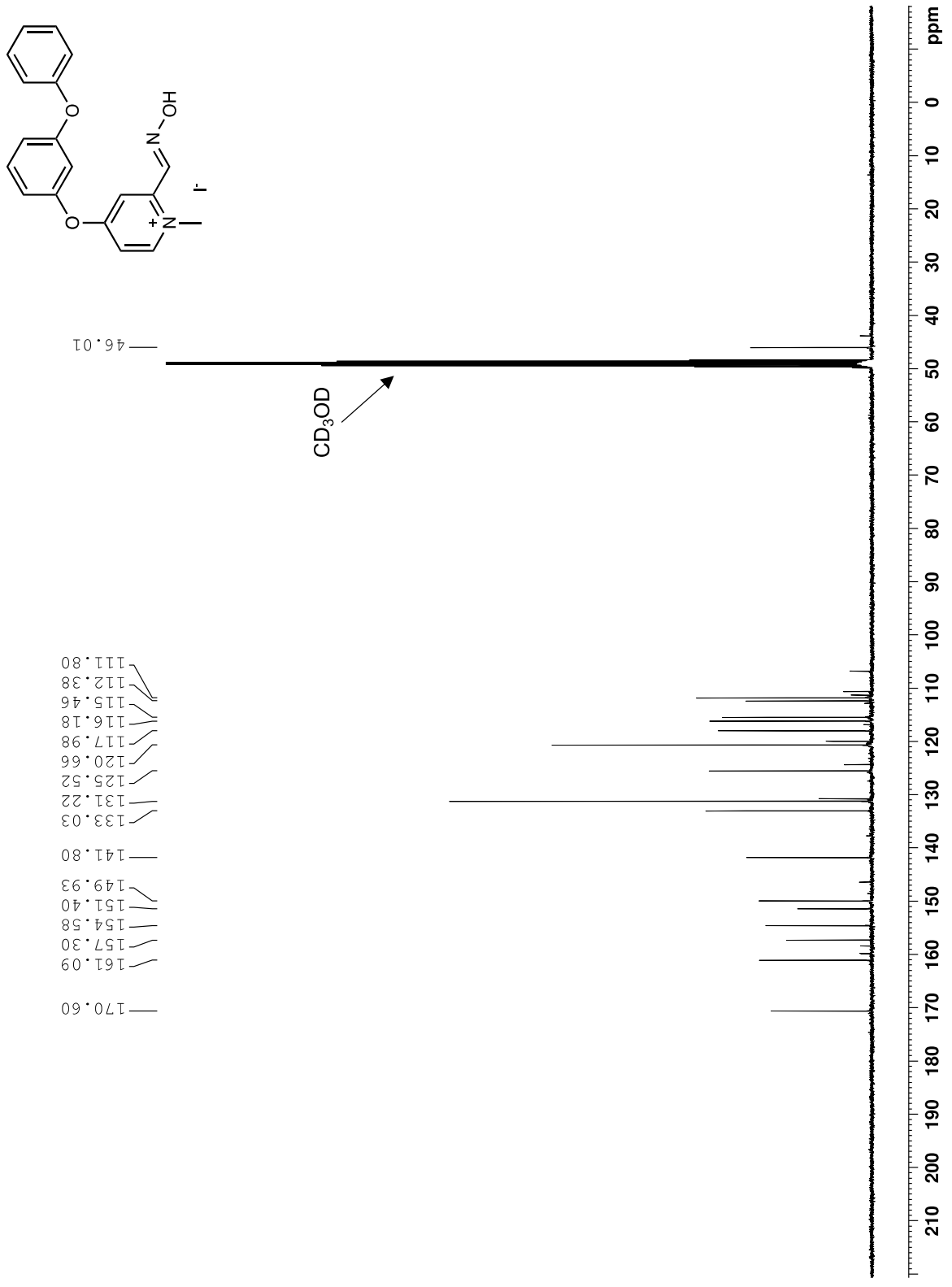

Spectrum 241. ^{13}C NMR of *(E)*-2-((hydroxyimino)methyl)-1-methyl-4-(3-phenoxyphenoxy)pyridin-1-ium iodide (**ADG4230**) (100 MHz, 293 K, CD_3OD).

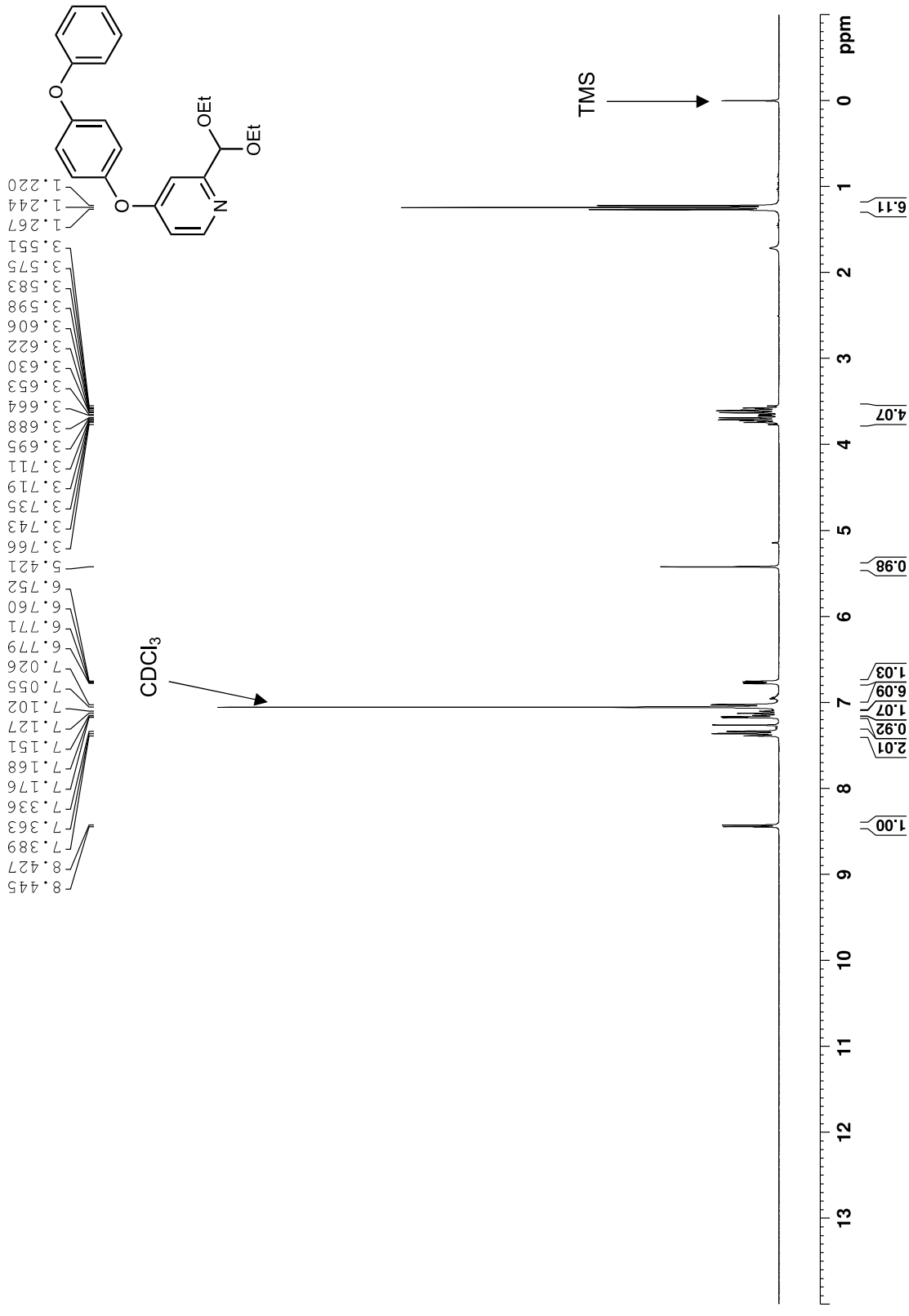

Spectrum 242. ^{1}H NMR of 2-(diethoxymethyl)-4-(4-phenoxyphenoxy)pyridine (300 MHz, 293 K, $CDCl_3$).

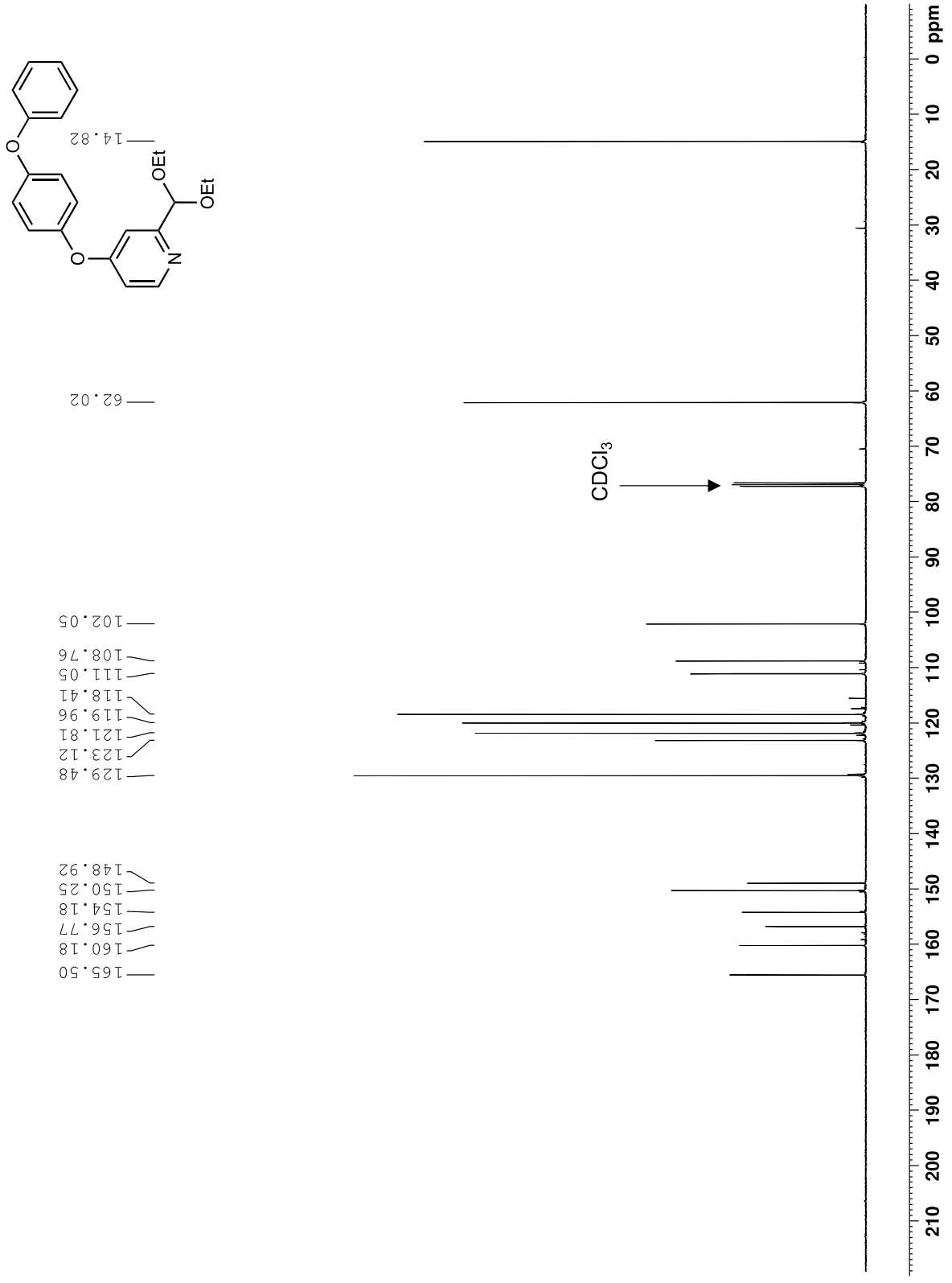

Spectrum 243. ^{13}C NMR of 2-(diethoxymethyl)-4-(4-phenoxyphenoxy)pyridine (100 MHz, 293 K, $CDCl_3$).

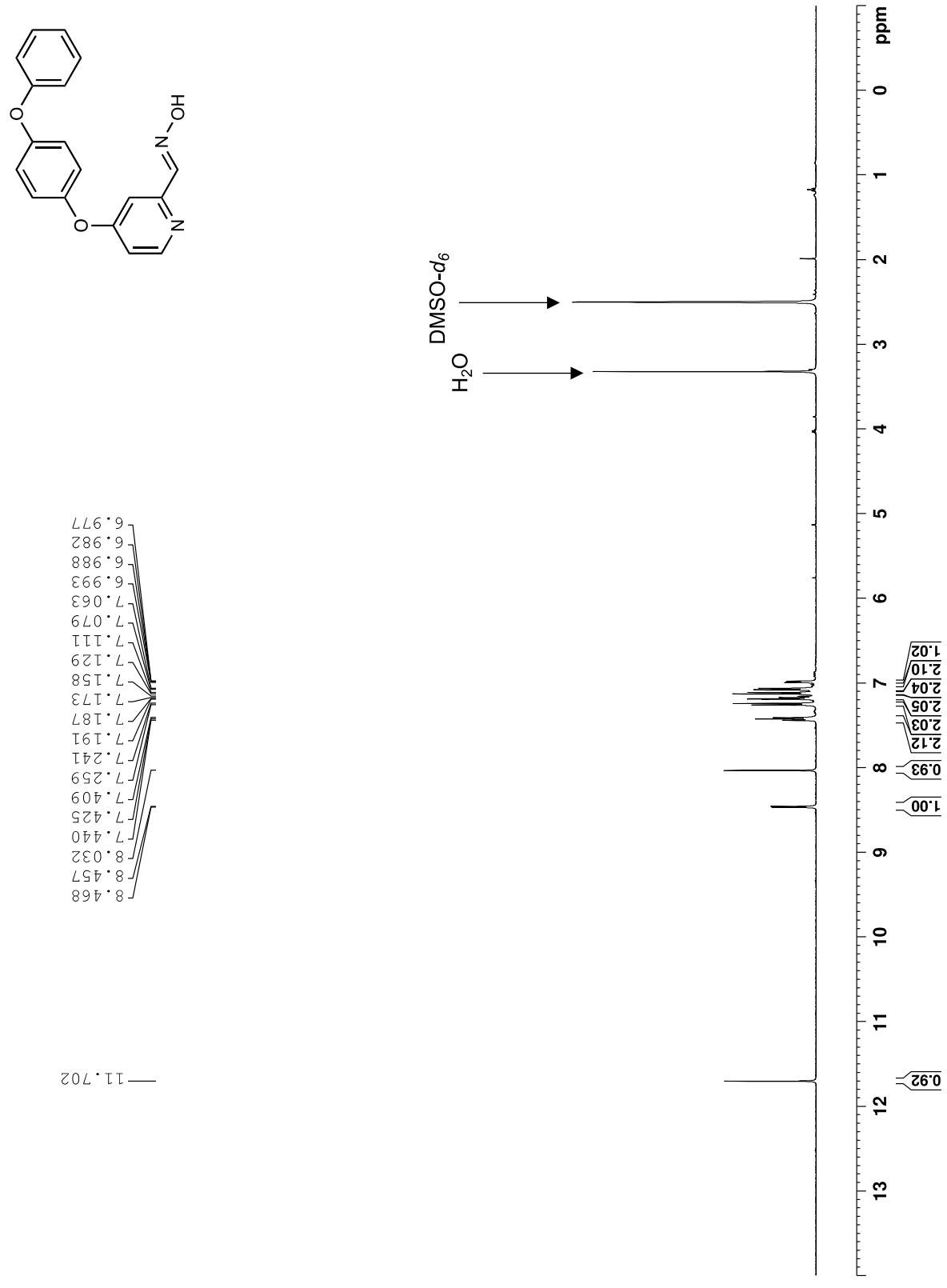

Spectrum 244. ^{1}H NMR of *(E)*-4-(4-phenoxyphenoxy)picolinaldehyde oxime (500 MHz, 293 K, DMSO-d_6).

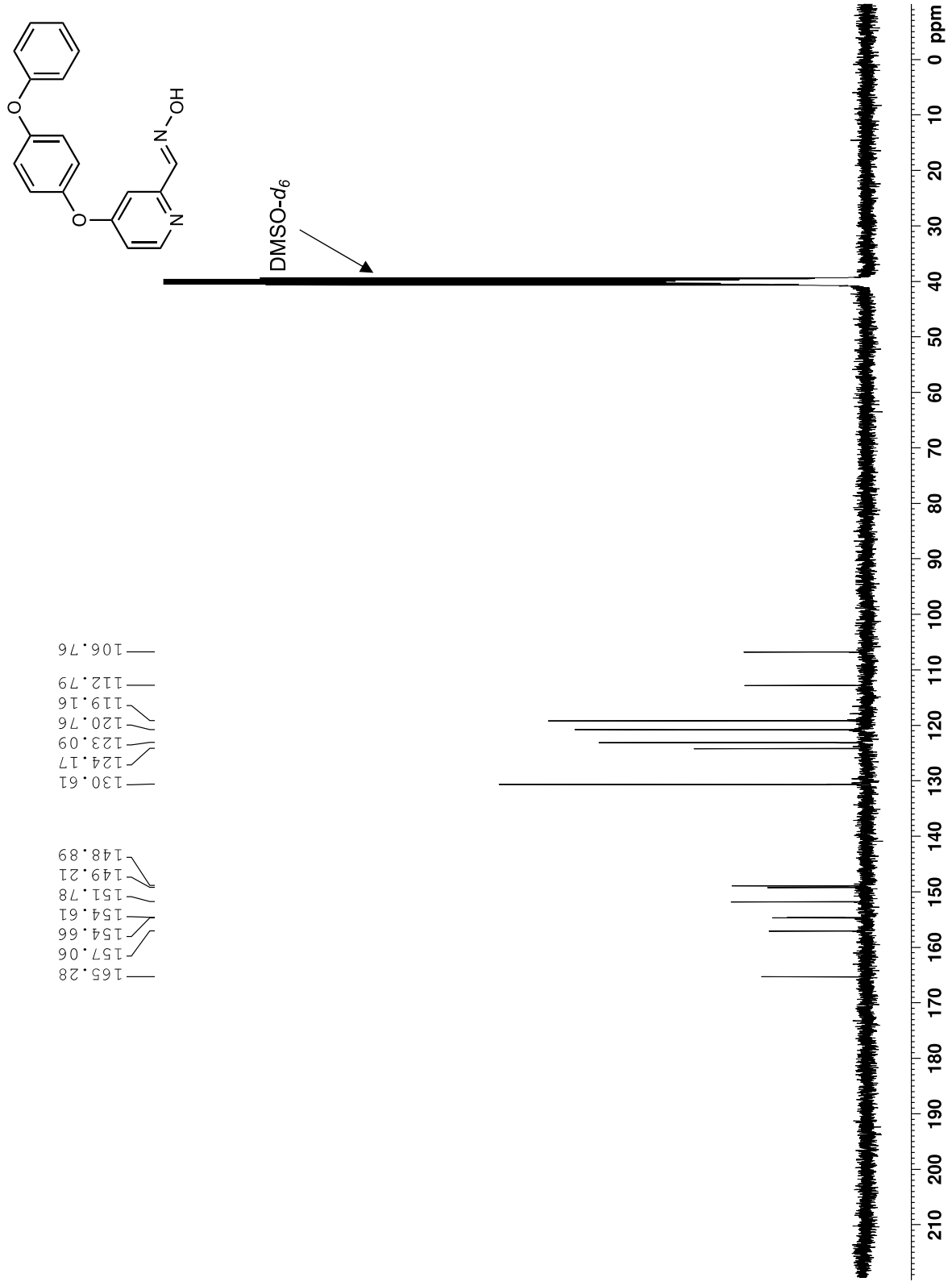

Spectrum 245. ^{13}C NMR of *(E)*-4-(4-phenoxyphenoxy)picolinaldehyde oxime (100 MHz, 293 K, DMSO-d_6).

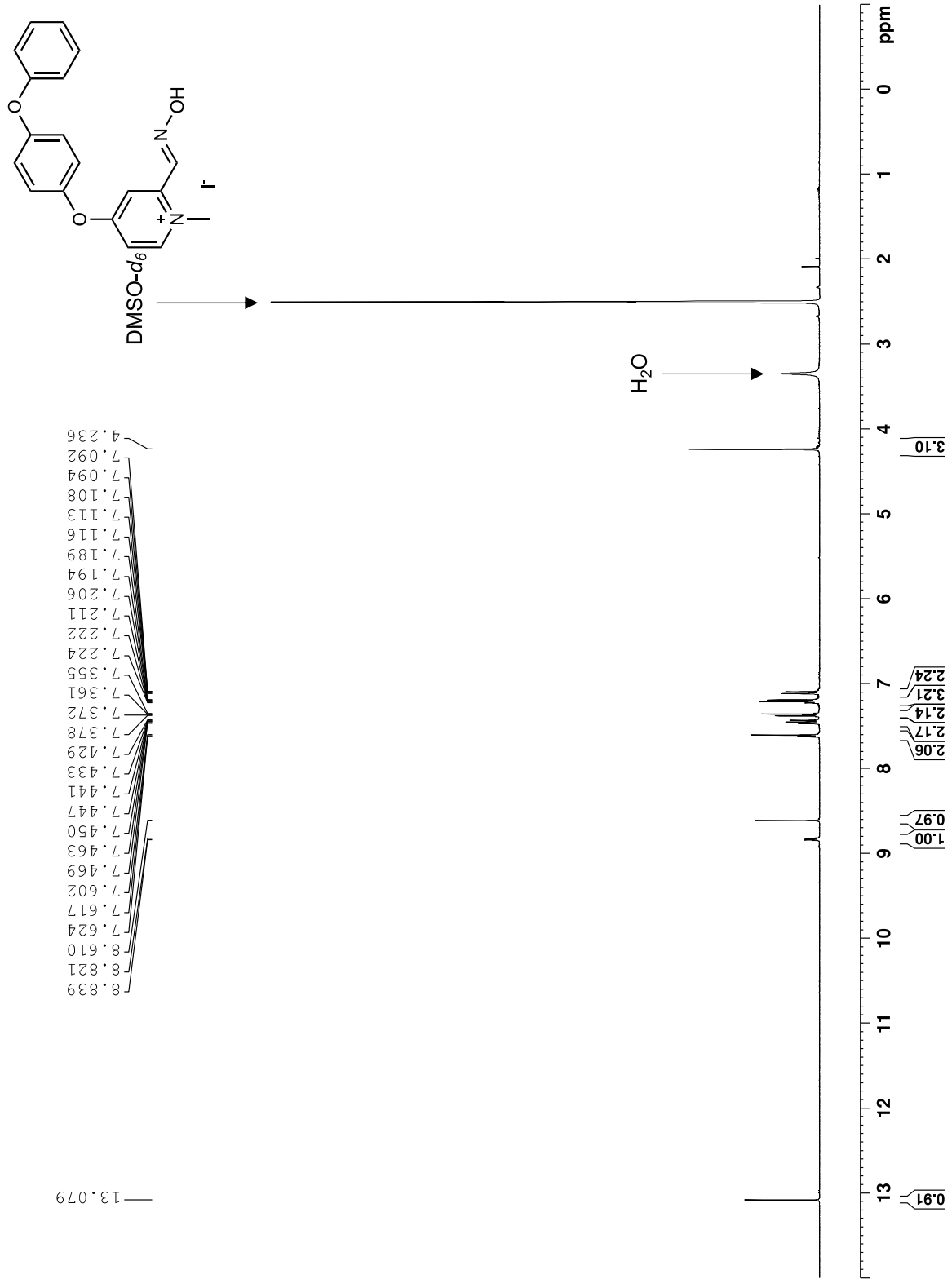

Spectrum 246. ^{1}H NMR of *(E)*-2-((hydroxyimino)methyl)-1-methyl-4-(4-phenoxyphenoxy)pyridin-1-ium iodide (**ADG4234**) (400 MHz, 293 K, DMSO-d_6).

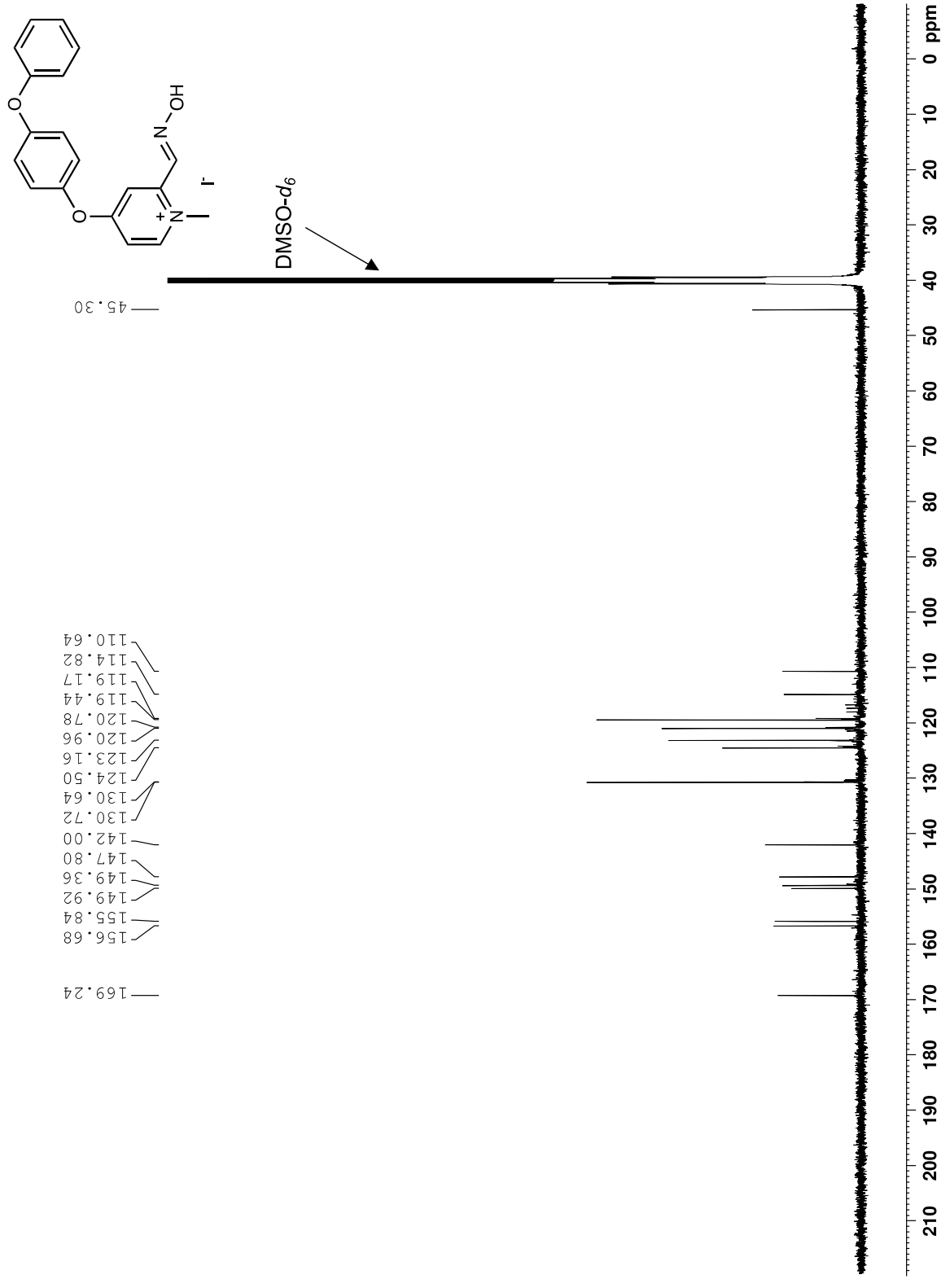

Spectrum 247. ^{13}C NMR of *(E)*-2-((hydroxyimino)methyl)-1-methyl-4-(4-phenoxyphenoxy)pyridin-1-ium iodide (**ADG4234**) (100 MHz, 293 K, DMSO-d_6).

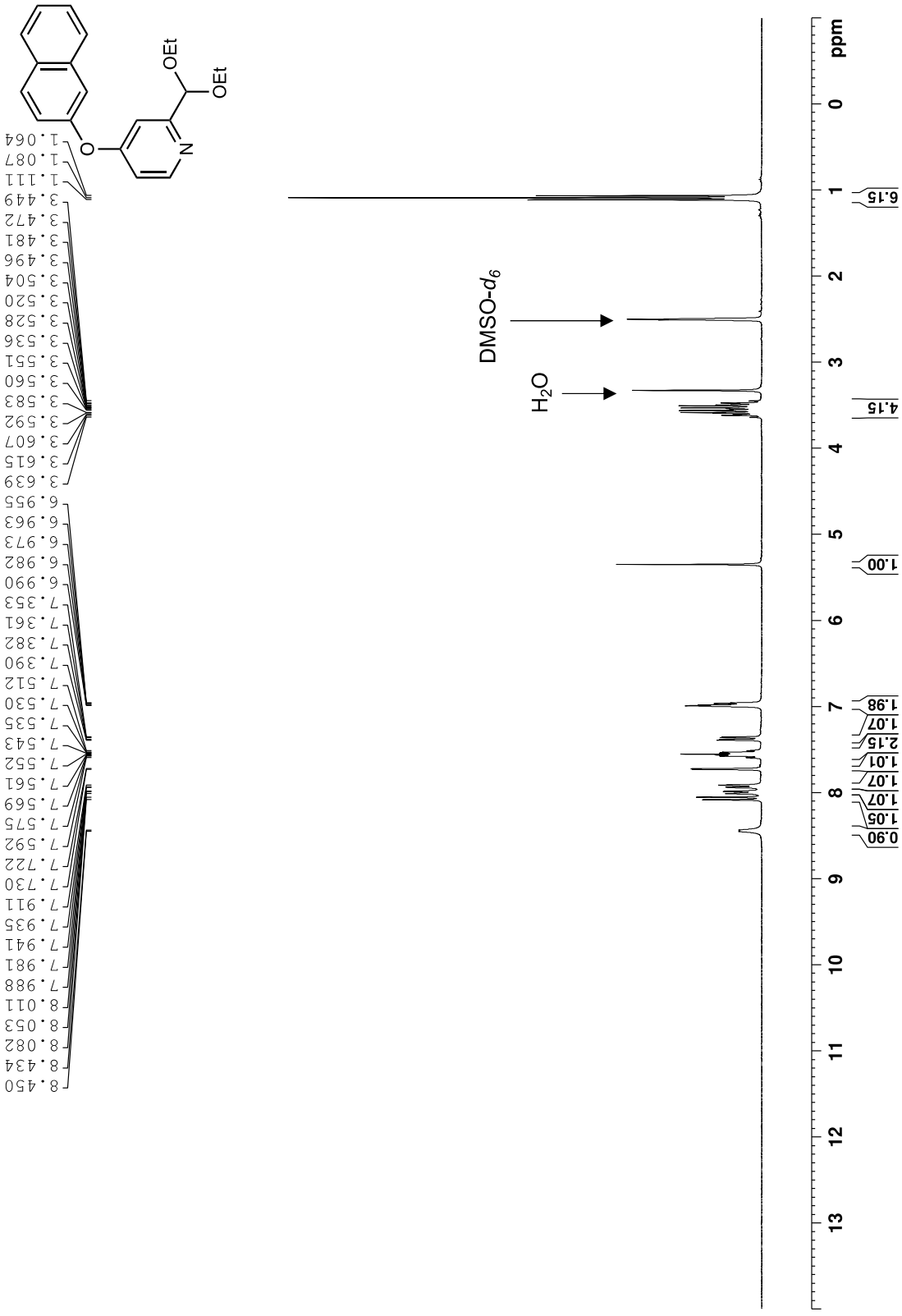

Spectrum 248. ^{1}H NMR of 2-(diethoxymethyl)-4-(naphthalen-2-yloxy)pyridine (300 MHz, 293 K, DMSO-d_6).

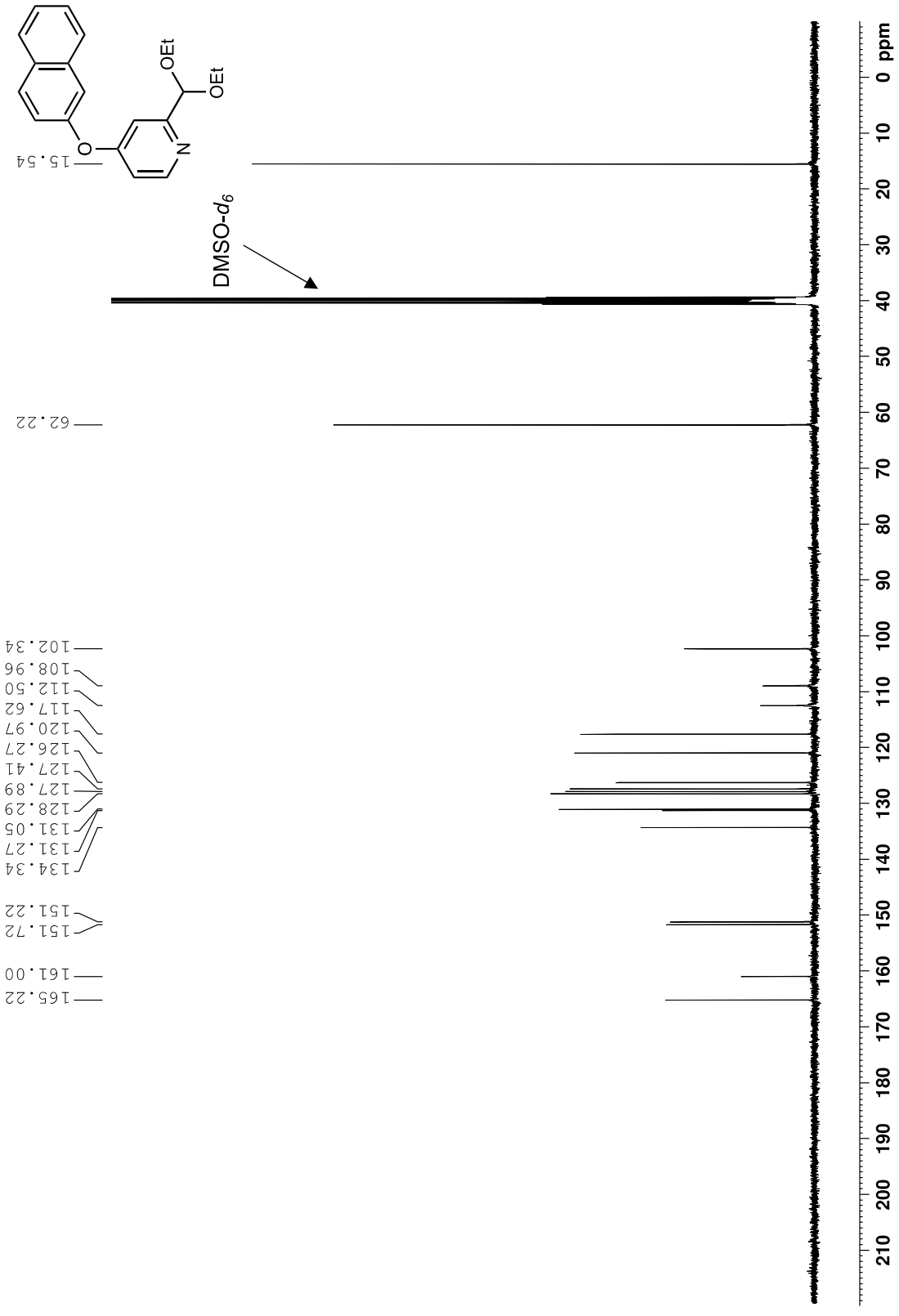

Spectrum 249. ^{13}C NMR of 2-(diethoxymethyl)-4-(naphthalen-2-yloxy)pyridine (100 MHz, 293 K, DMSO-d_6).

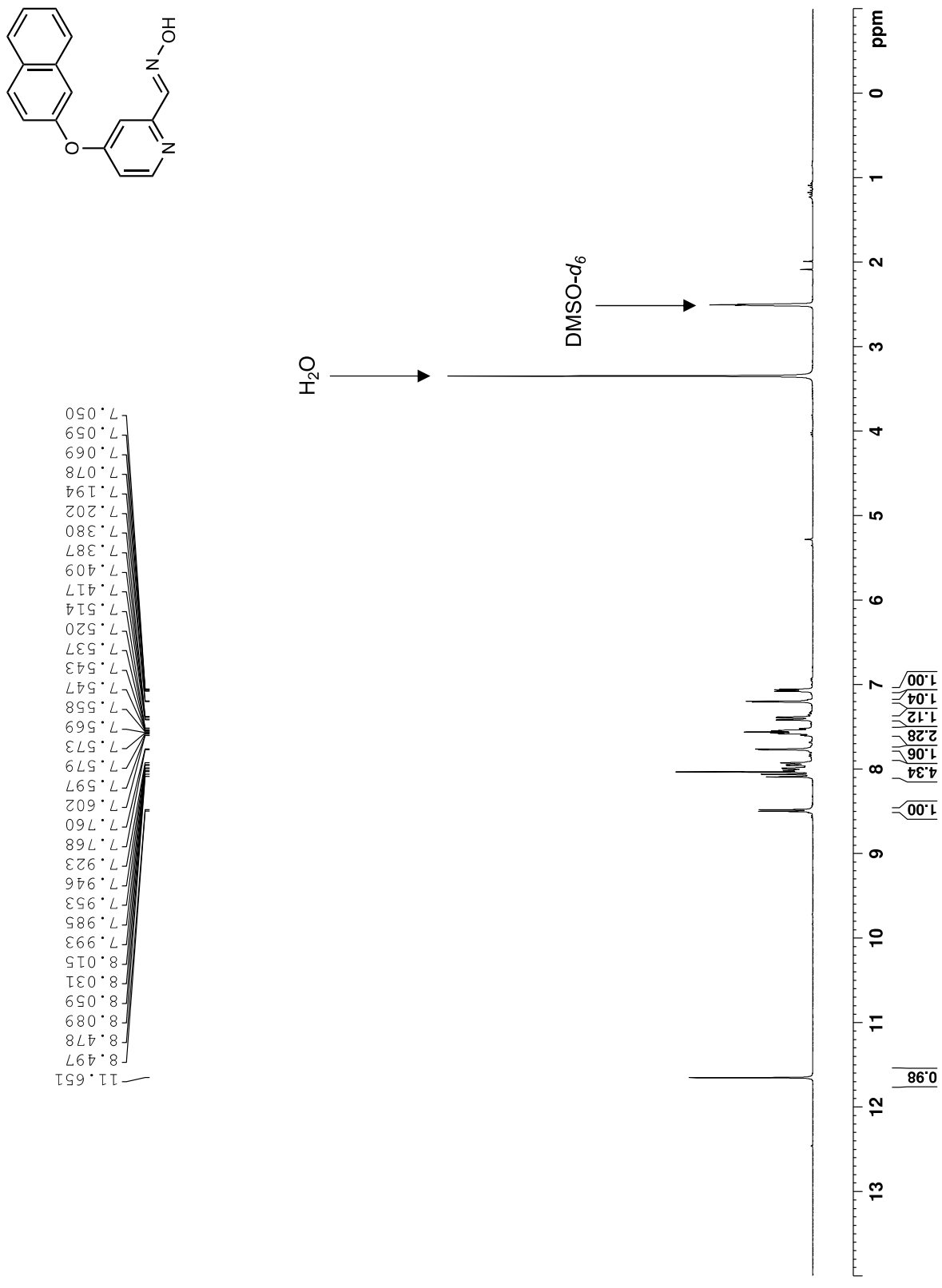

Spectrum 250. ^{1}H NMR of (*E*)-4-(naphthalen-2-yloxy)picolinaldehyde oxime (300 MHz, 293 K, DMSO-d_6).

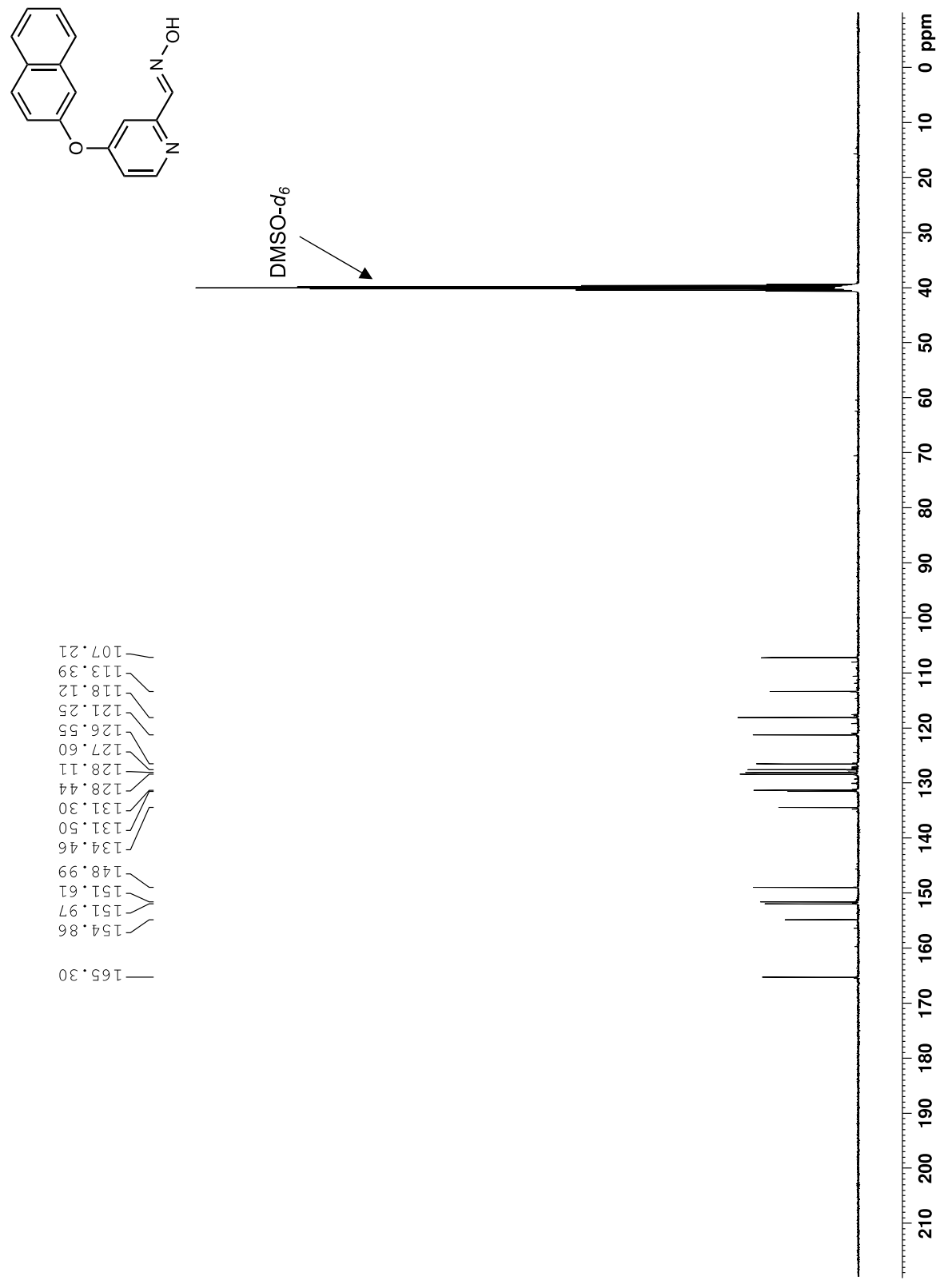

Spectrum 251. ^{13}C NMR of (*E*)-4-(naphthalen-2-yloxy)picolinaldehyde oxime (100 MHz, 293 K, DMSO-d_6).

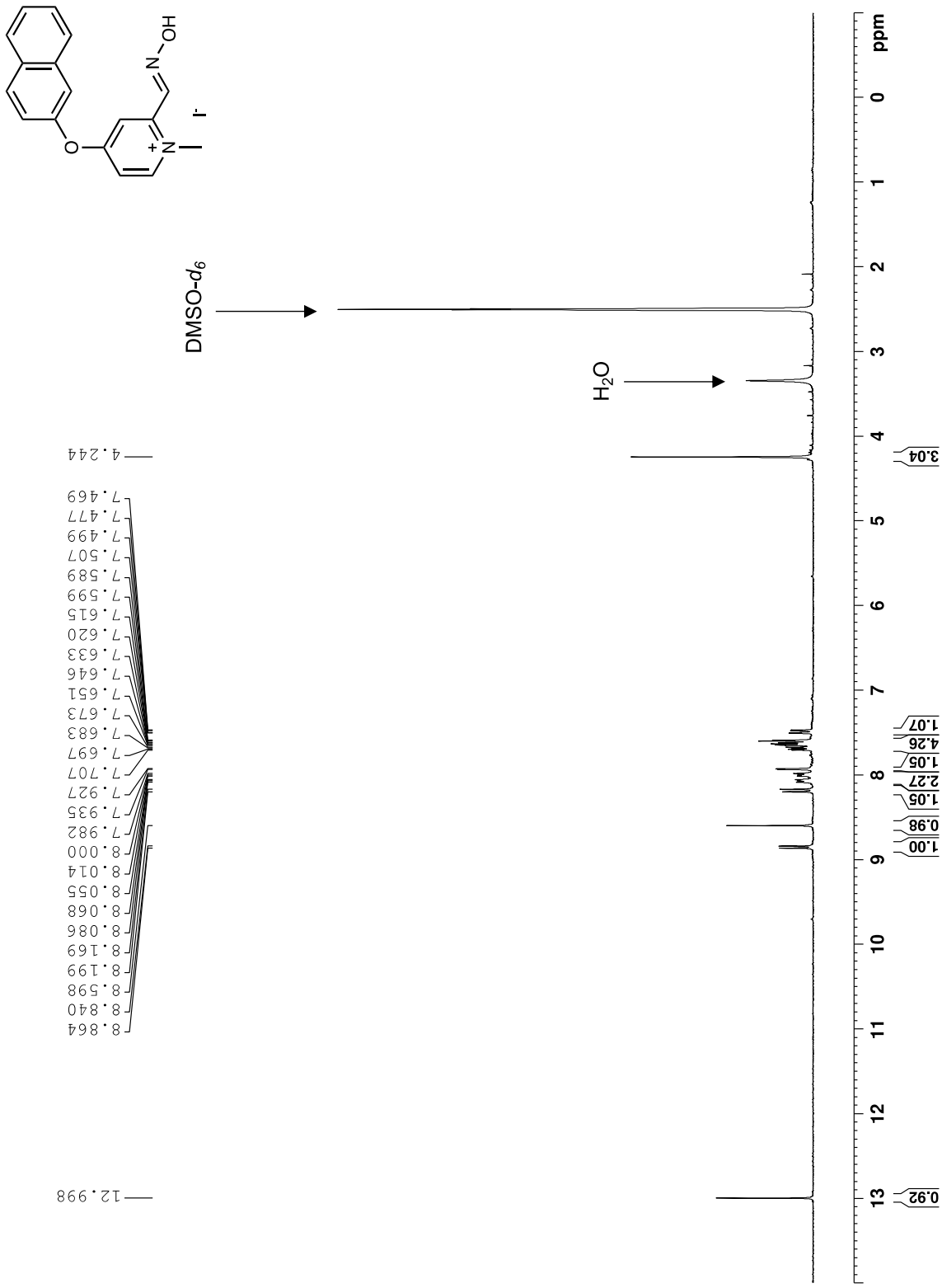

Spectrum 252. ^{1}H NMR of *(E)*-2-((hydroxyimino)methyl)-1-methyl-4-(naphthalen-2-yloxy)pyridin-1-ium iodide (ADG4204) (300 MHz, 293 K, DMSO-d_6).

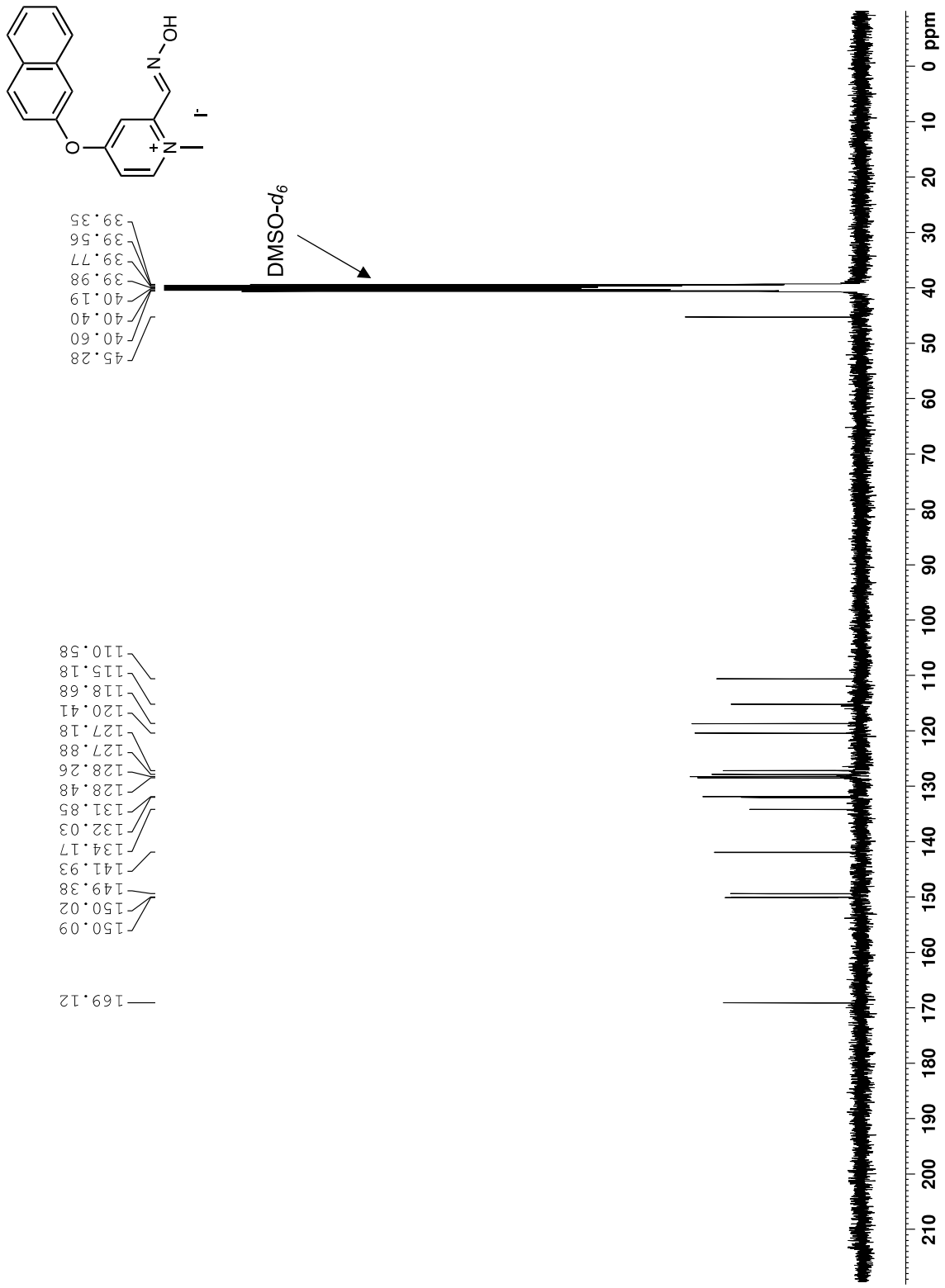

Spectrum 253. ^{13}C NMR of *(E)*-2-((hydroxyimino)methyl)-1-methyl-4-(naphthalen-2-yloxy)pyridin-1-ium iodide (ADG4204) (100 MHz, 293 K, DMSO-d_6).

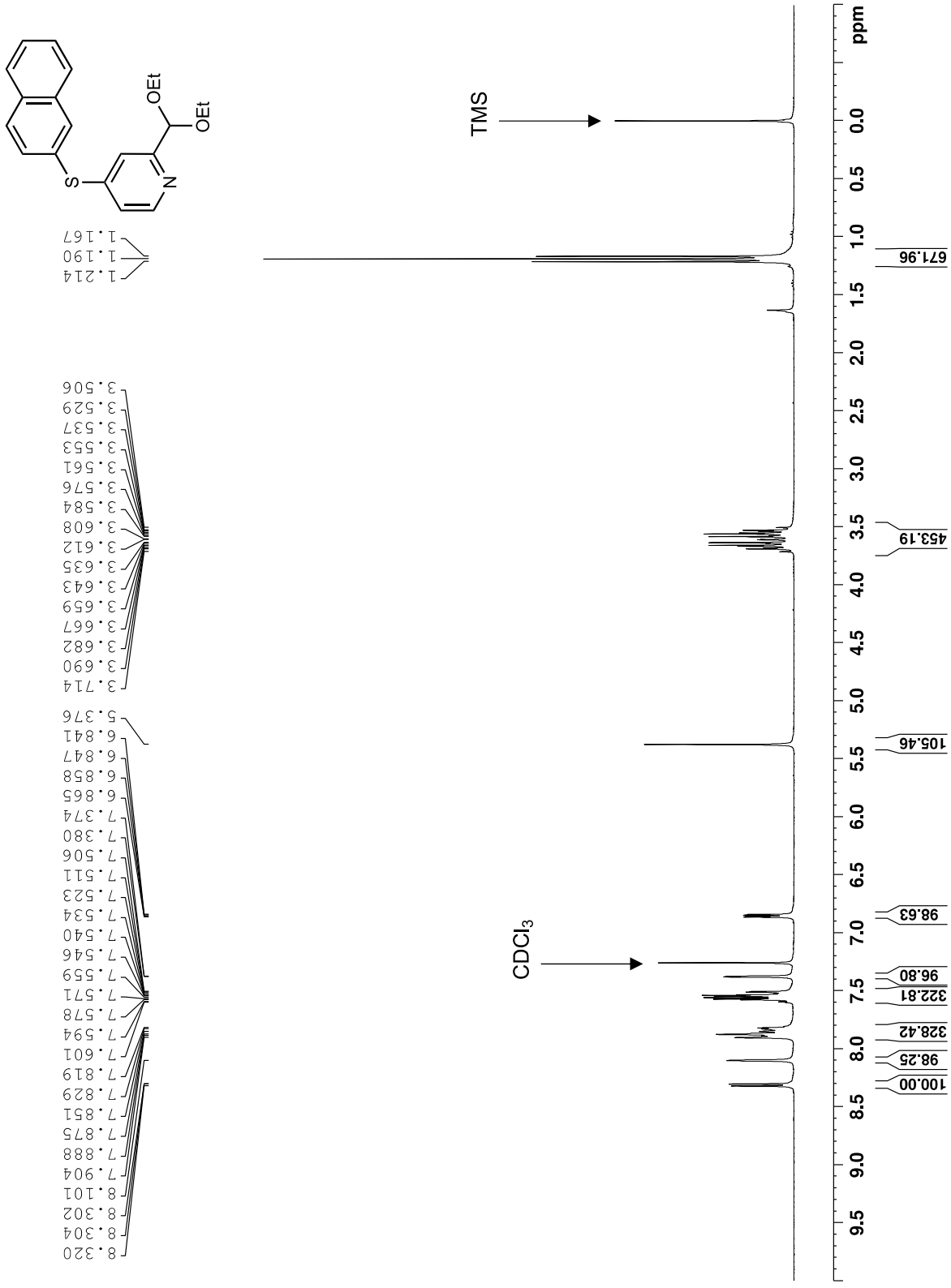

Spectrum 254. ^{1}H NMR of 2-(diethoxymethyl)-4-(naphthalen-2-ylthio)pyridine (300 MHz, 293 K, $CDCl_3$).

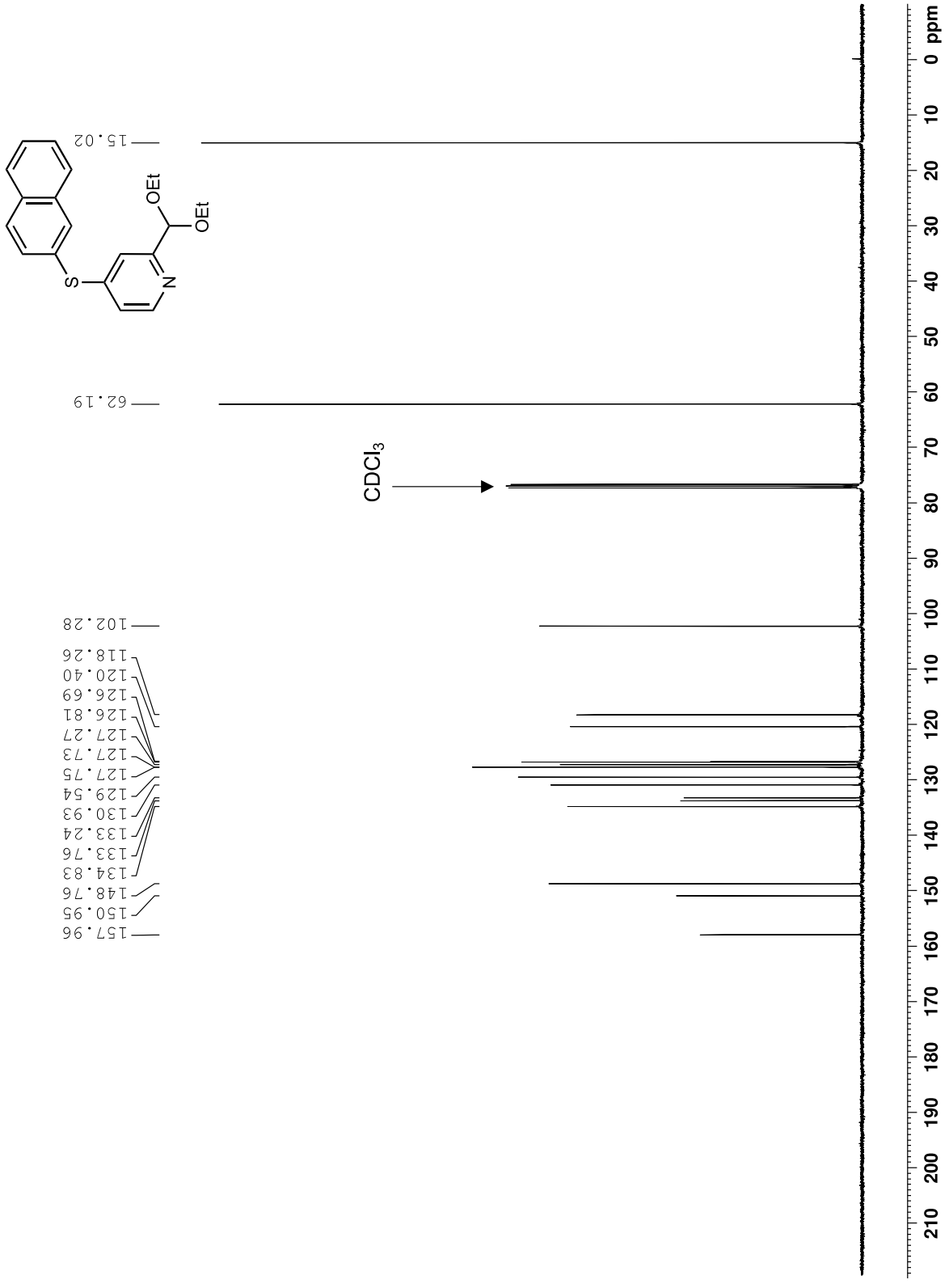

Spectrum 255. ^{13}C NMR of 2-(diethoxymethyl)-4-(naphthalen-2-ylthio)pyridine (100 MHz, 293 K, $CDCl_3$).

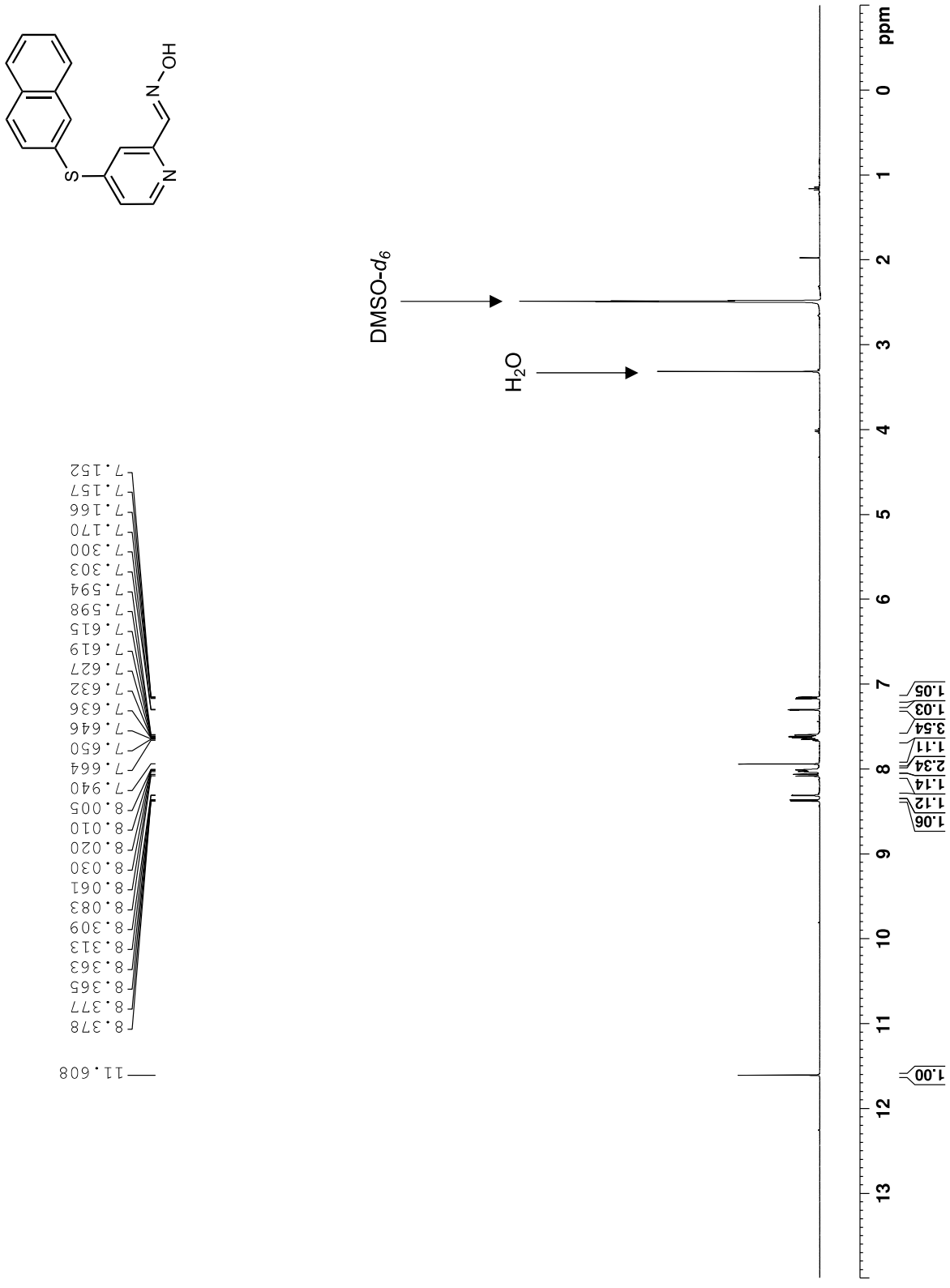

Spectrum 256. ^{1}H NMR of (*E*)-4-(naphthalen-2-ylthio)picolinaldehyde oxime (400 MHz, 293 K, DMSO-d_6).

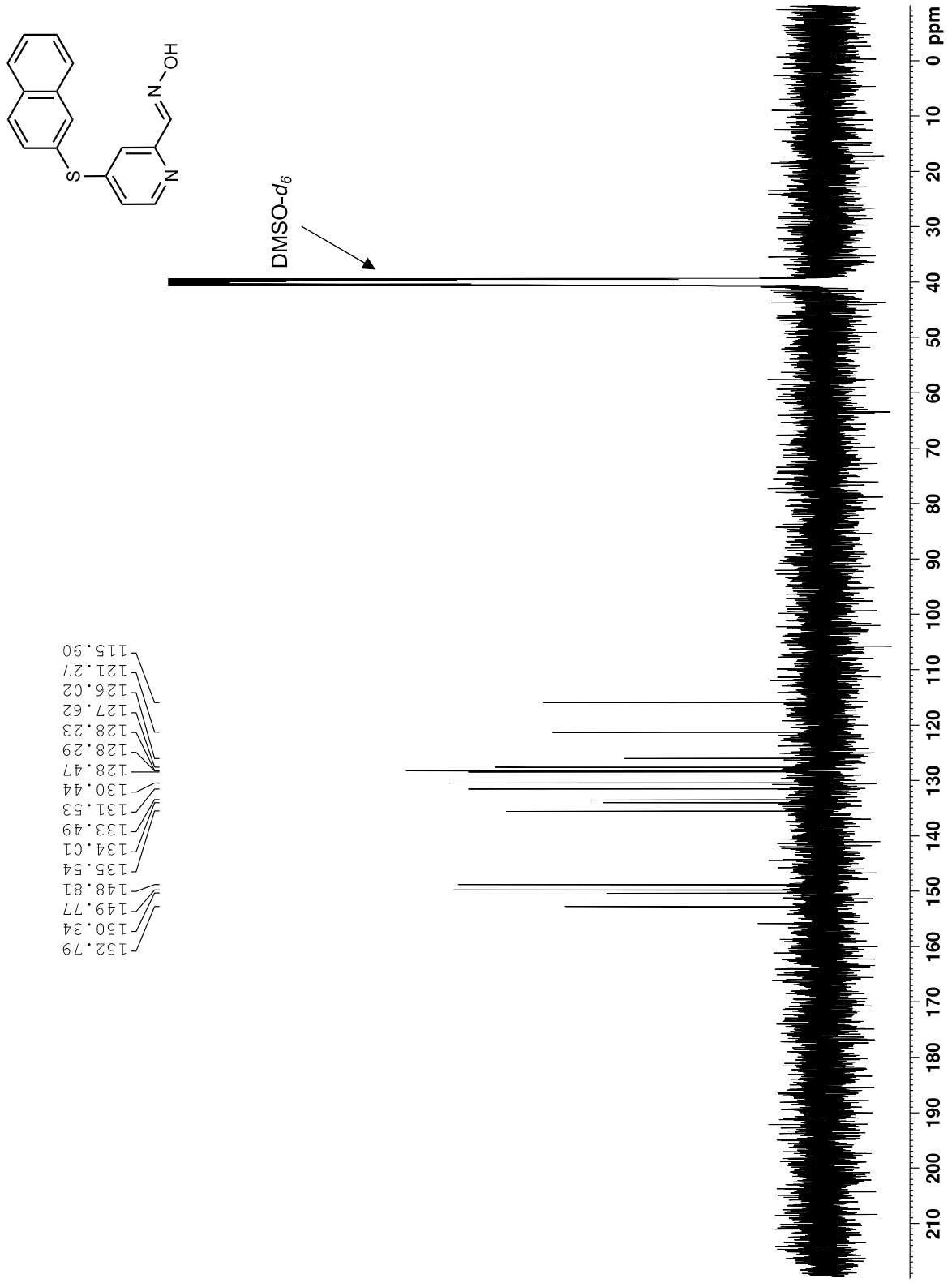

Spectrum 257. ^{13}C NMR of (*E*)-4-(naphthalen-2-ylthio)picolinaldehyde oxime (100 MHz, 293 K, DMSO-d_6).

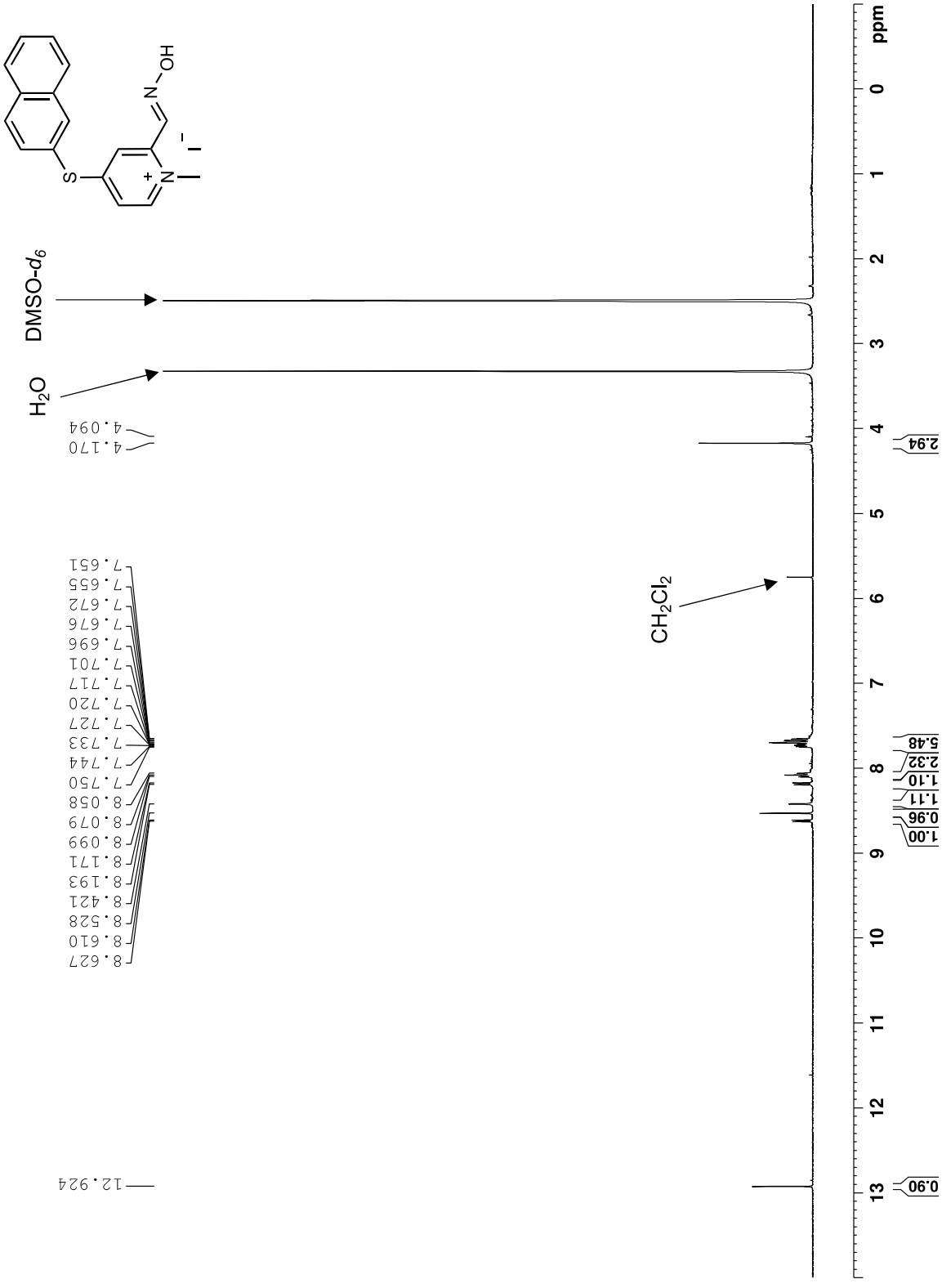

Spectrum 258. ^{1}H NMR of *(E)*-2-((hydroxyimino)methyl)-1-methyl-4-(naphthalen-2-ylthio)pyridin-1-ium iodide (**ADG4072**) (400 MHz, 293 K, DMSO-d_6).

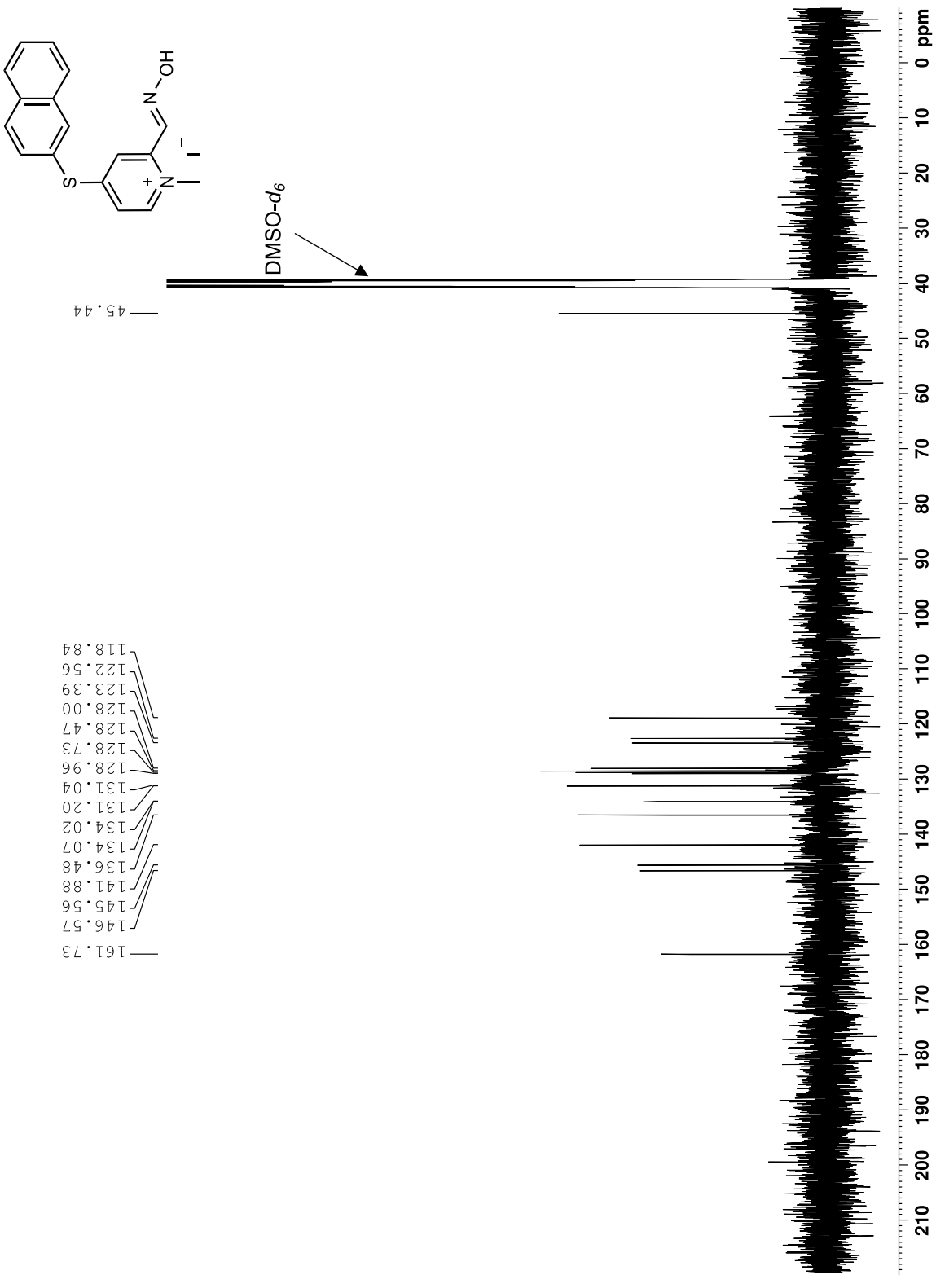

Spectrum 259. ^{13}C NMR of *(E)*-2-((hydroxyimino)methyl)-1-methyl-4-(naphthalen-2-ylthio)pyridin-1-ium iodide (**ADG4072**) (100 MHz, 293 K, DMSO-d_6).

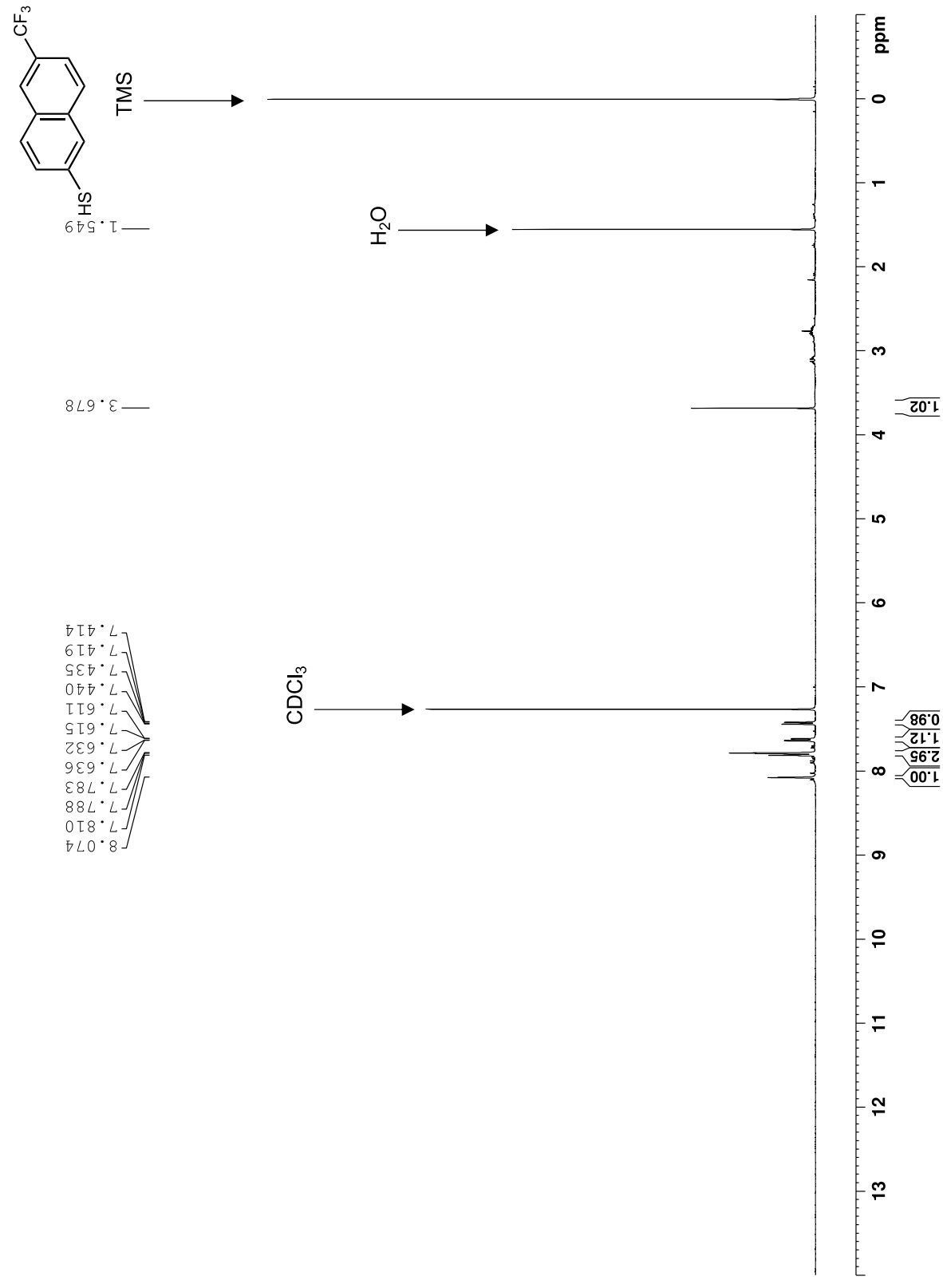

Spectrum 260. ^{1}H NMR of 6-(trifluoromethyl)naphthalene-2-thiol (400 MHz, 293 K, $CDCl_3$).

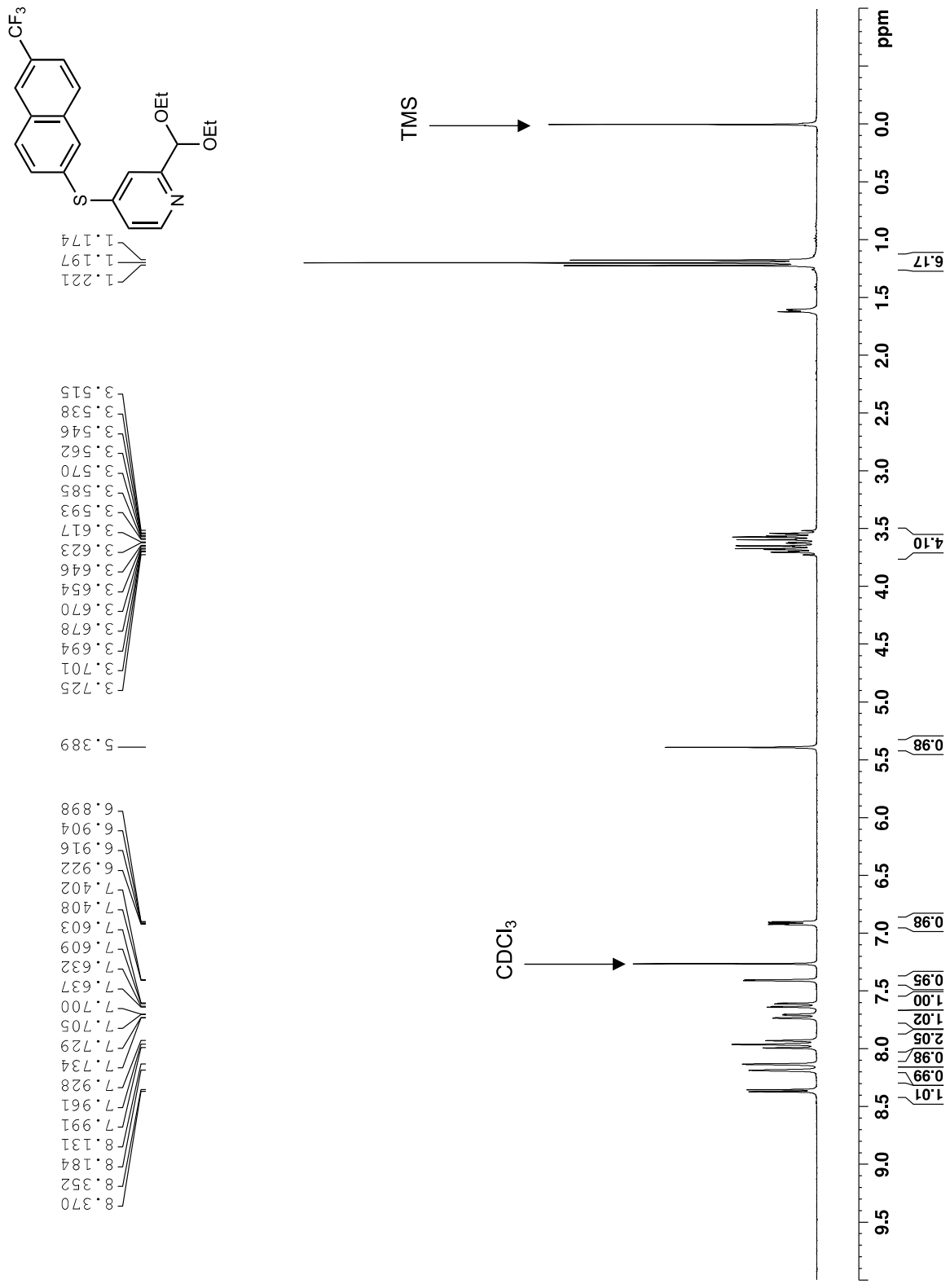

Spectrum 261. ^{1}H NMR of 2-(diethoxymethyl)-4-((6-(trifluoromethyl)naphthalen-2-yl)thio)pyridine (300 MHz, 293 K, $CDCl_3$).

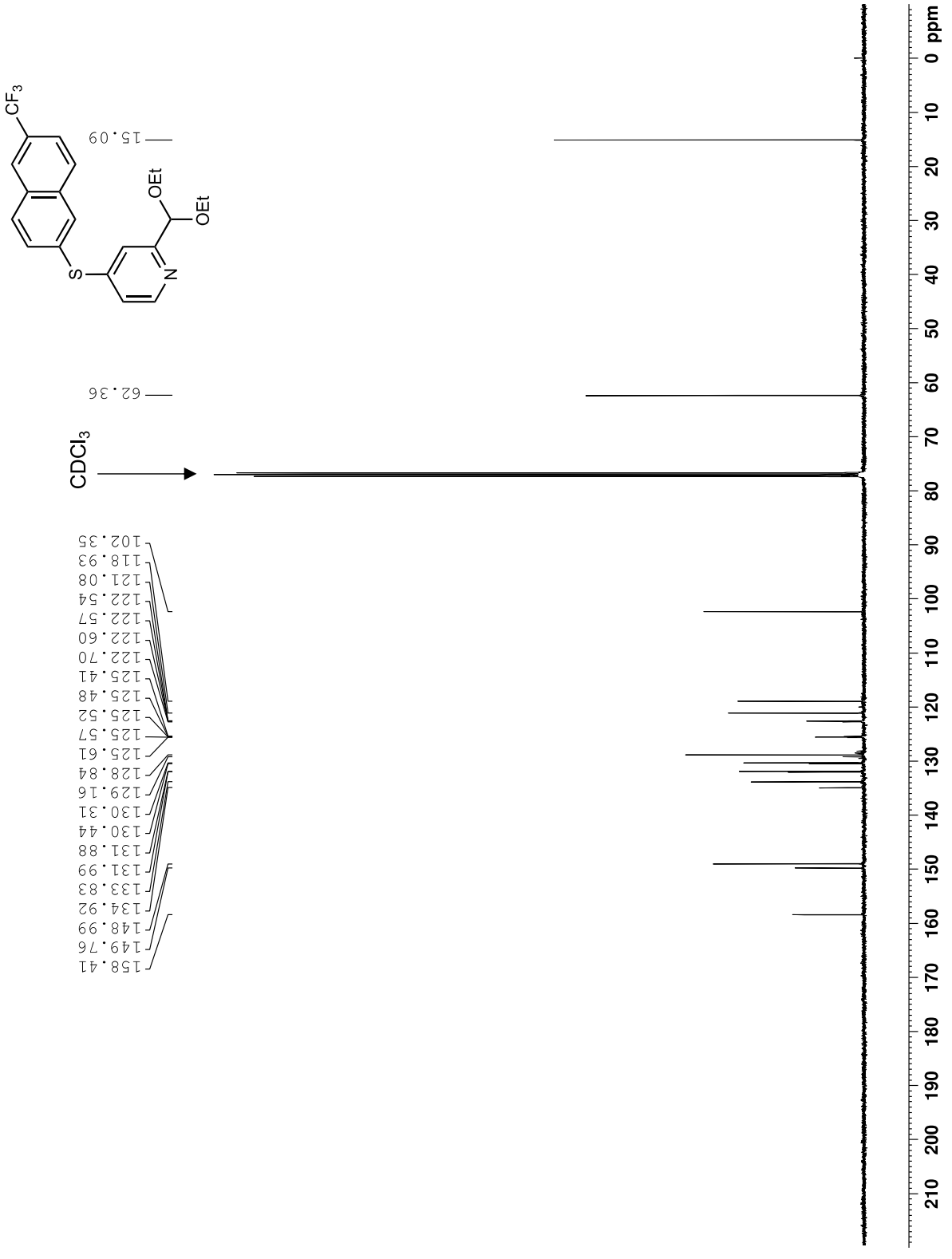

Spectrum 262. ^{13}C NMR of 2-(diethoxymethyl)-4-((6-(trifluoromethyl)naphthalen-2-yl)thio)pyridine (100 MHz, 293 K, $CDCl_3$).

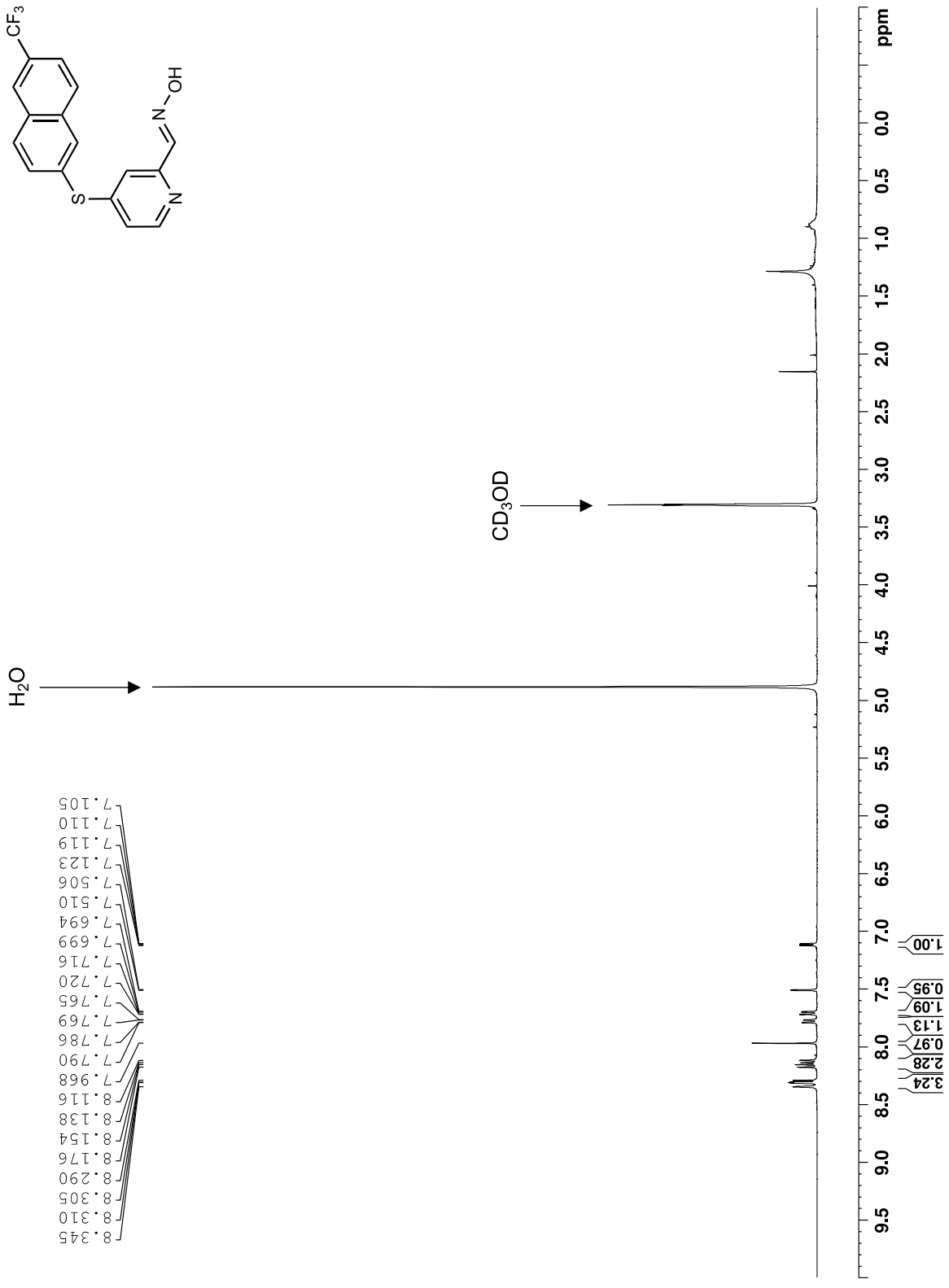

Spectrum 263. ^{1}H NMR of (*E*)-4-((6-(trifluoromethyl)naphthalen-2-yl)thio)picolinaldehyde oxime (400 MHz, 293 K, CD_3OD).

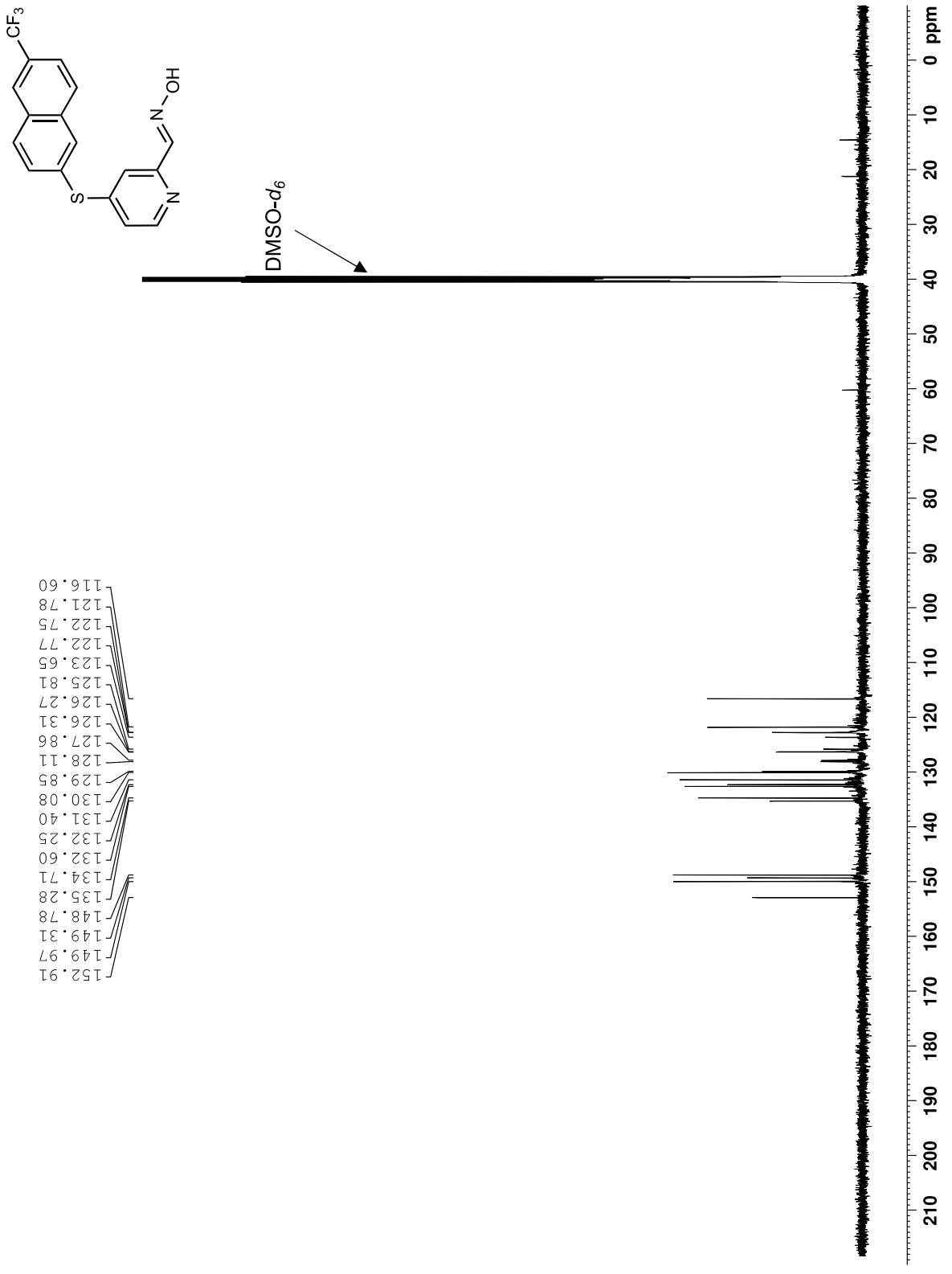

Spectrum 264. ^{13}C NMR of (*E*)-4-((6-(trifluoromethyl)naphthalen-2-yl)thio)picolinaldehyde oxime (125 MHz, 293 K, DMSO-d_6).

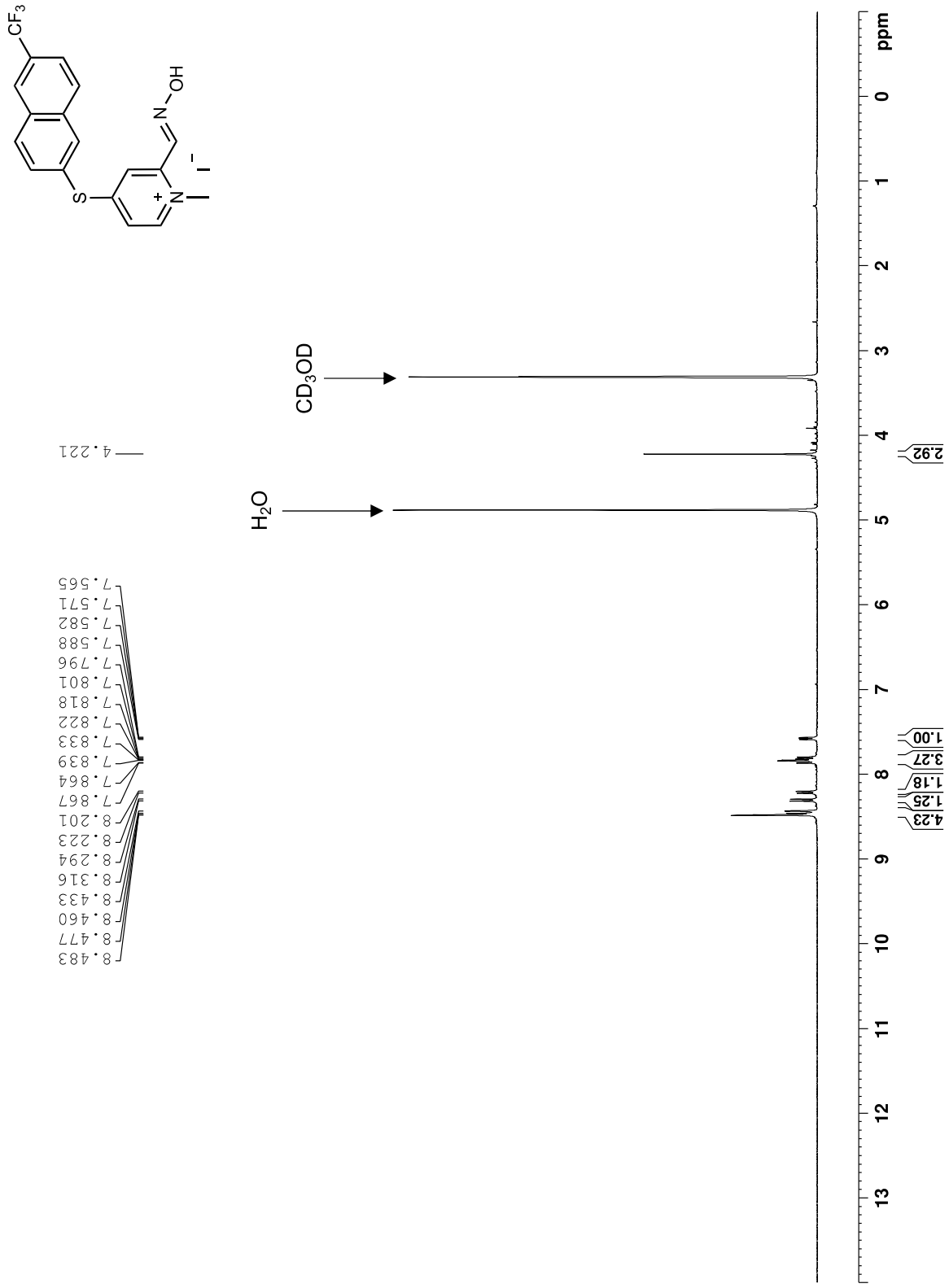

Spectrum 265. ^{1}H NMR of *(E)*-2-((hydroxyimino)methyl)-1-methyl-4-((6-(trifluoromethyl)naphthalen-2-yl)thio)pyridin-1-ium iodide (**ADG4145**) (400 MHz, 293 K, CD_3OD).

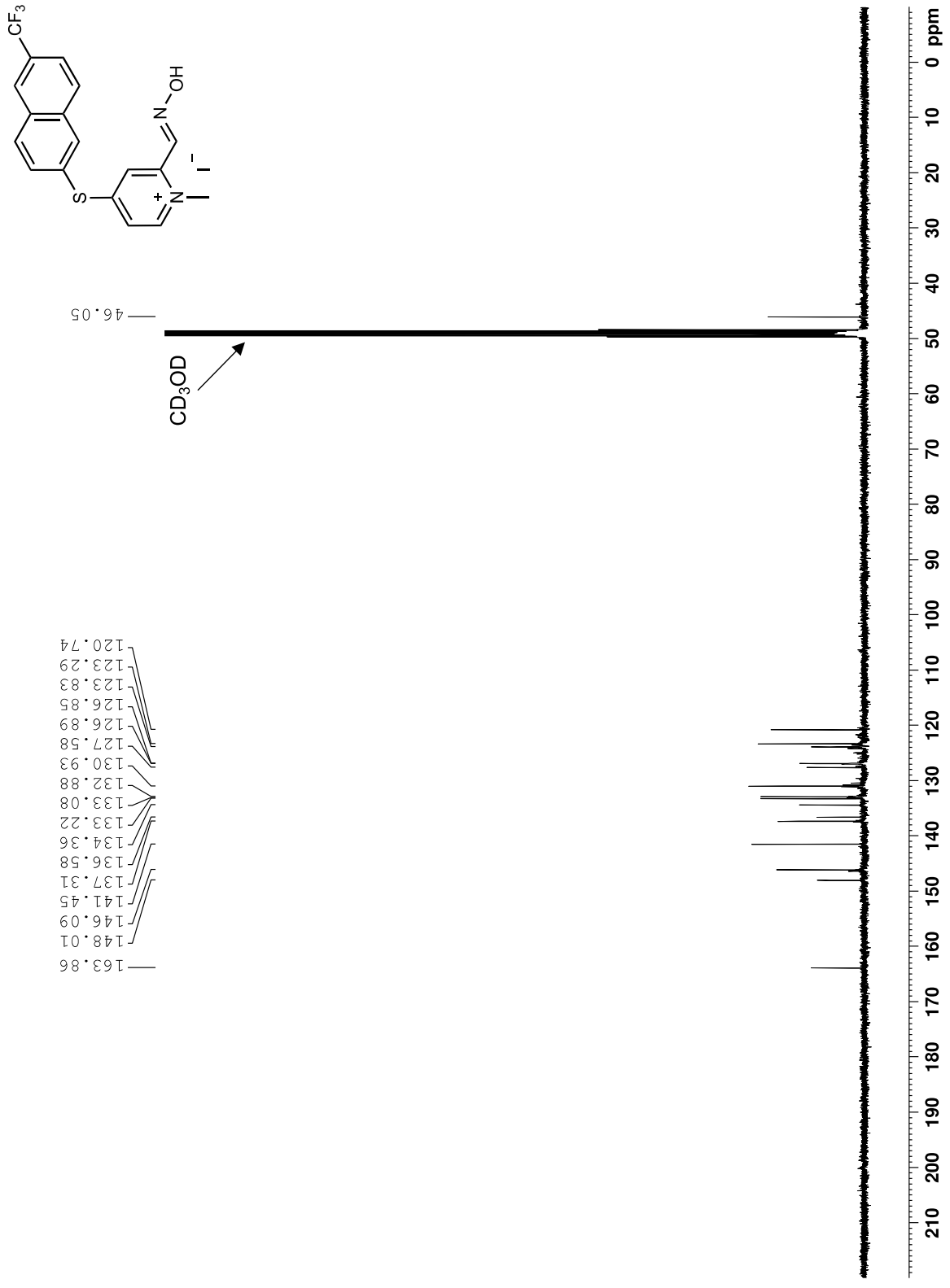

Spectrum 266. ^{13}C NMR of *(E)*-2-((hydroxyimino)methyl)-1-methyl-4-((6-(trifluoromethyl)naphthalen-2-yl)thio)pyridin-1-ium iodide (**ADG4145**) (100 MHz, 293 K, CD_3OD).

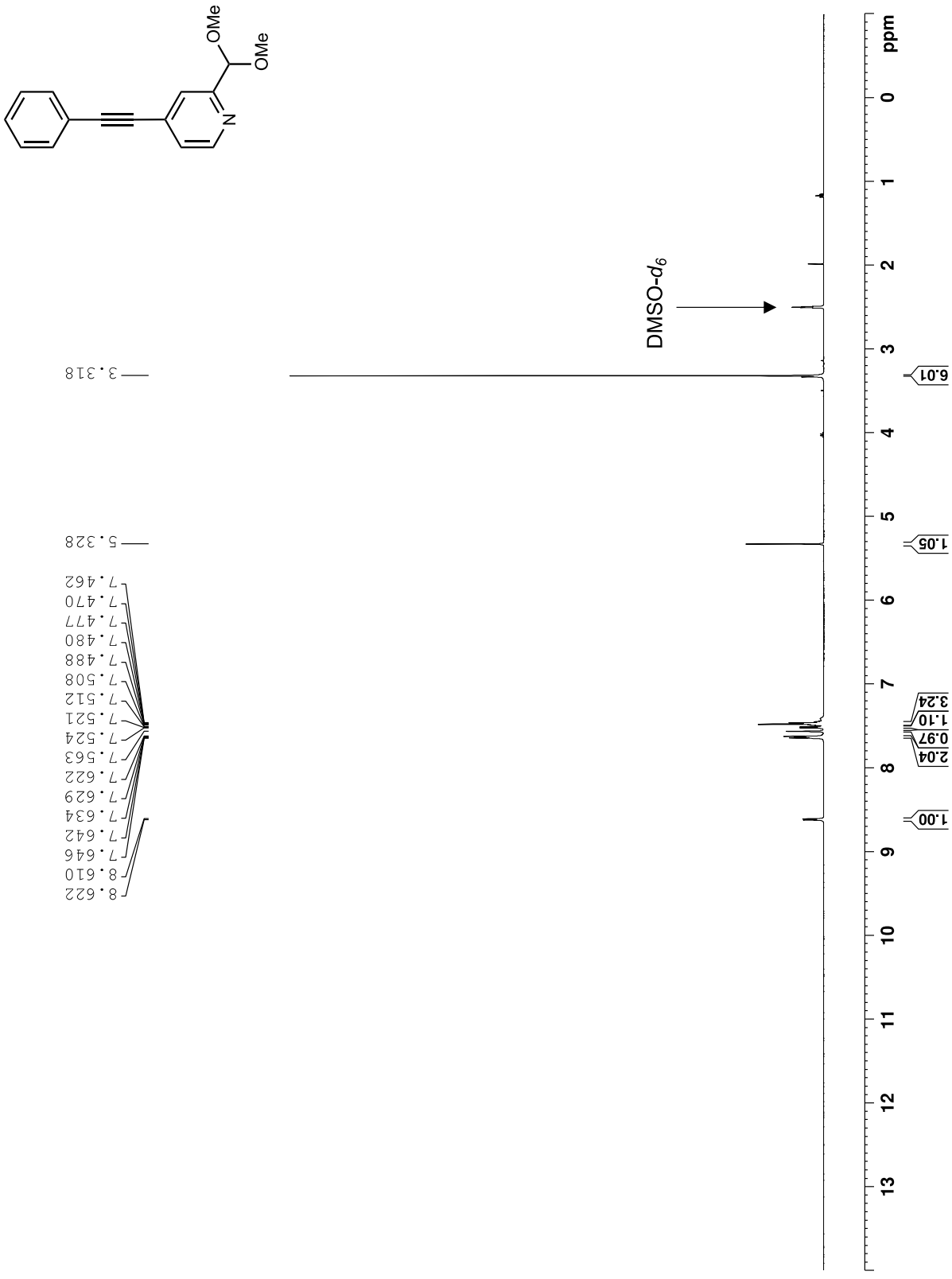

Spectrum 267. ^{1}H NMR for 2-(dimethoxymethyl)-4-(phenylethynyl)pyridine (400 MHz, 293 K, DMSO-d_6).

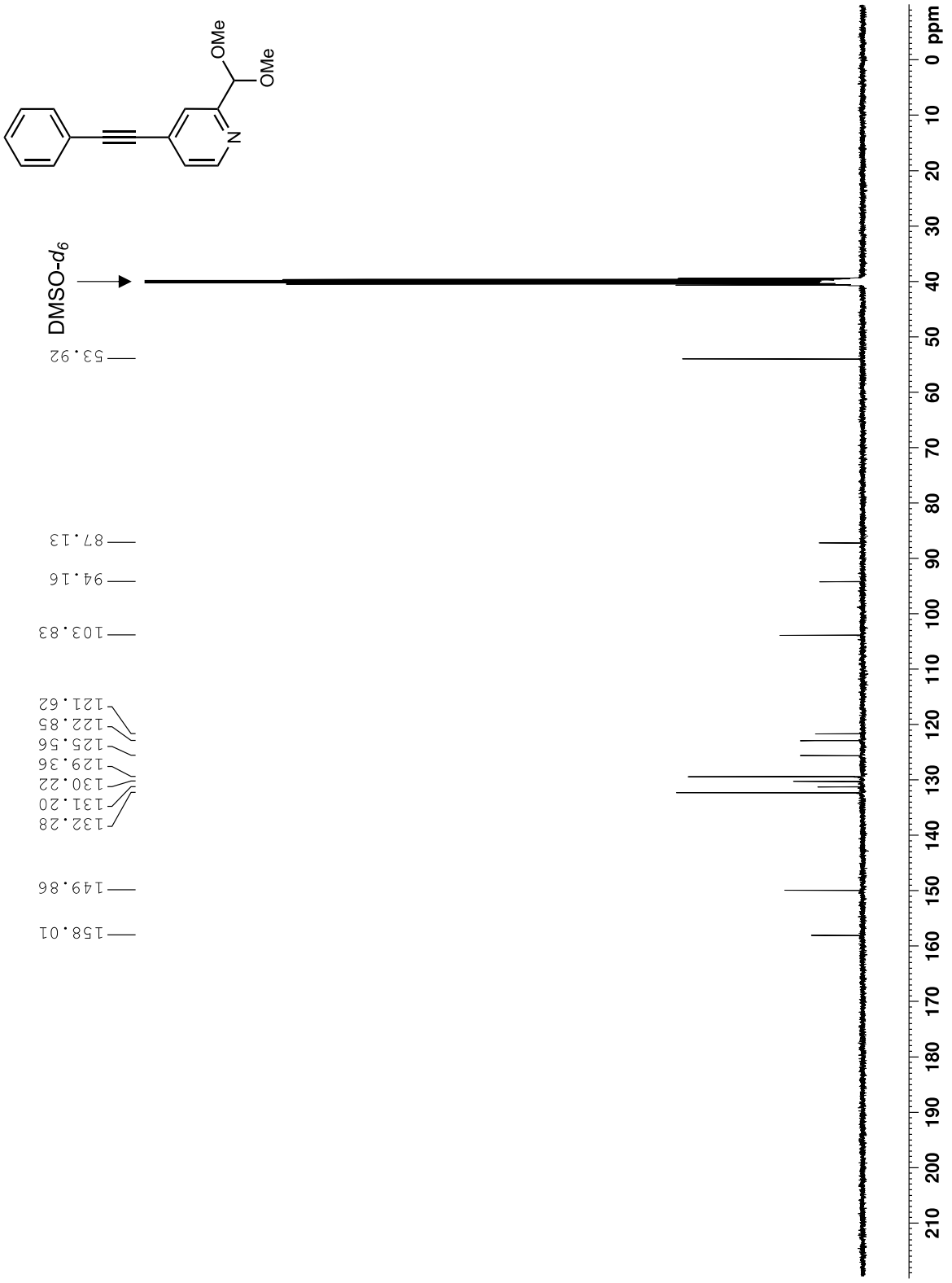

Spectrum 268. ^{13}C NMR for 2-(dimethoxymethyl)-4-(phenylethynyl)pyridine (100 MHz, 293 K, DMSO-d_6).

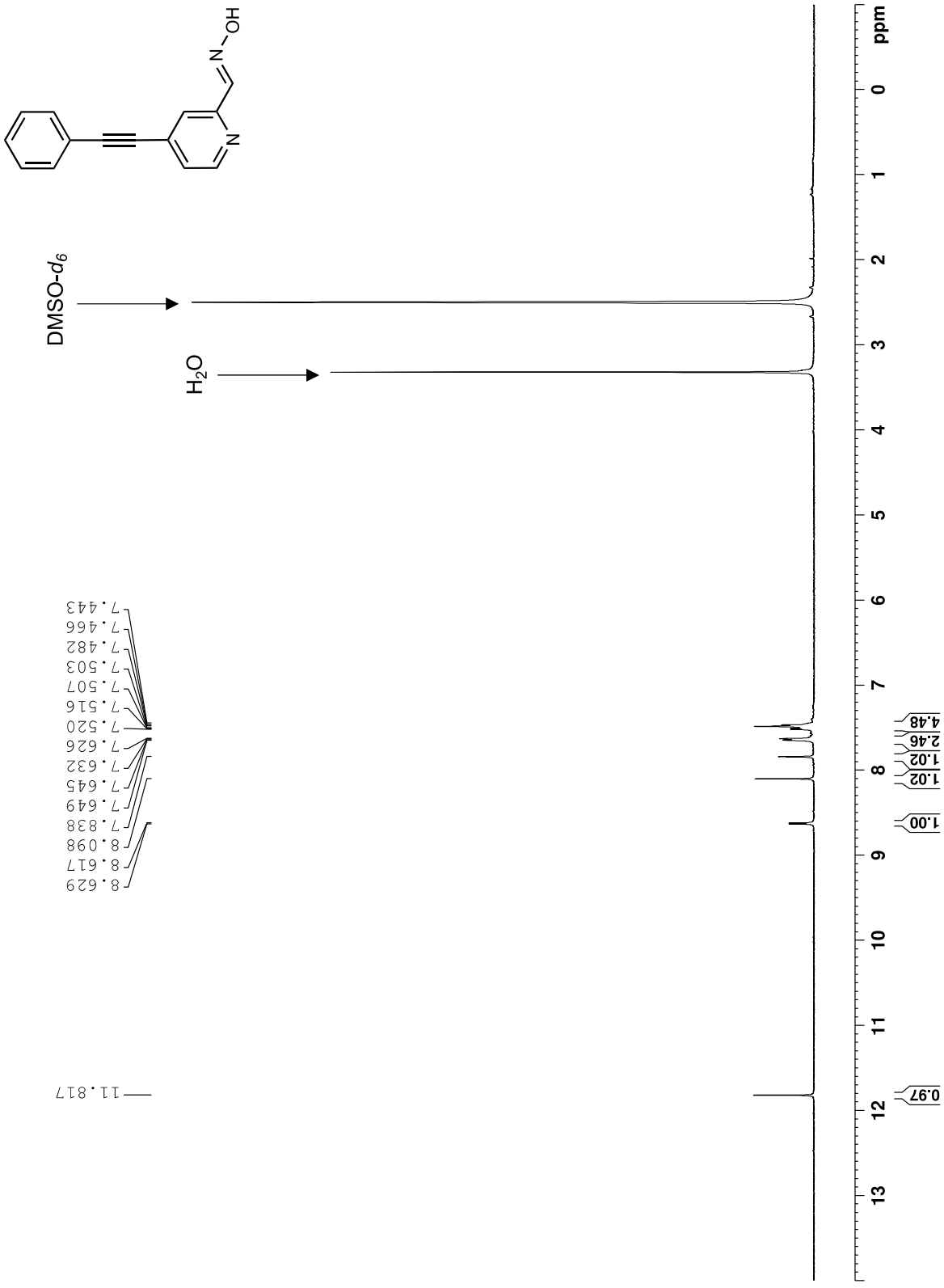

Spectrum 269. ^{1}H NMR for (*E*)-4-(phenylethynyl)picolinaldehyde oxime (400 MHz, 293 K, DMSO-d_6).

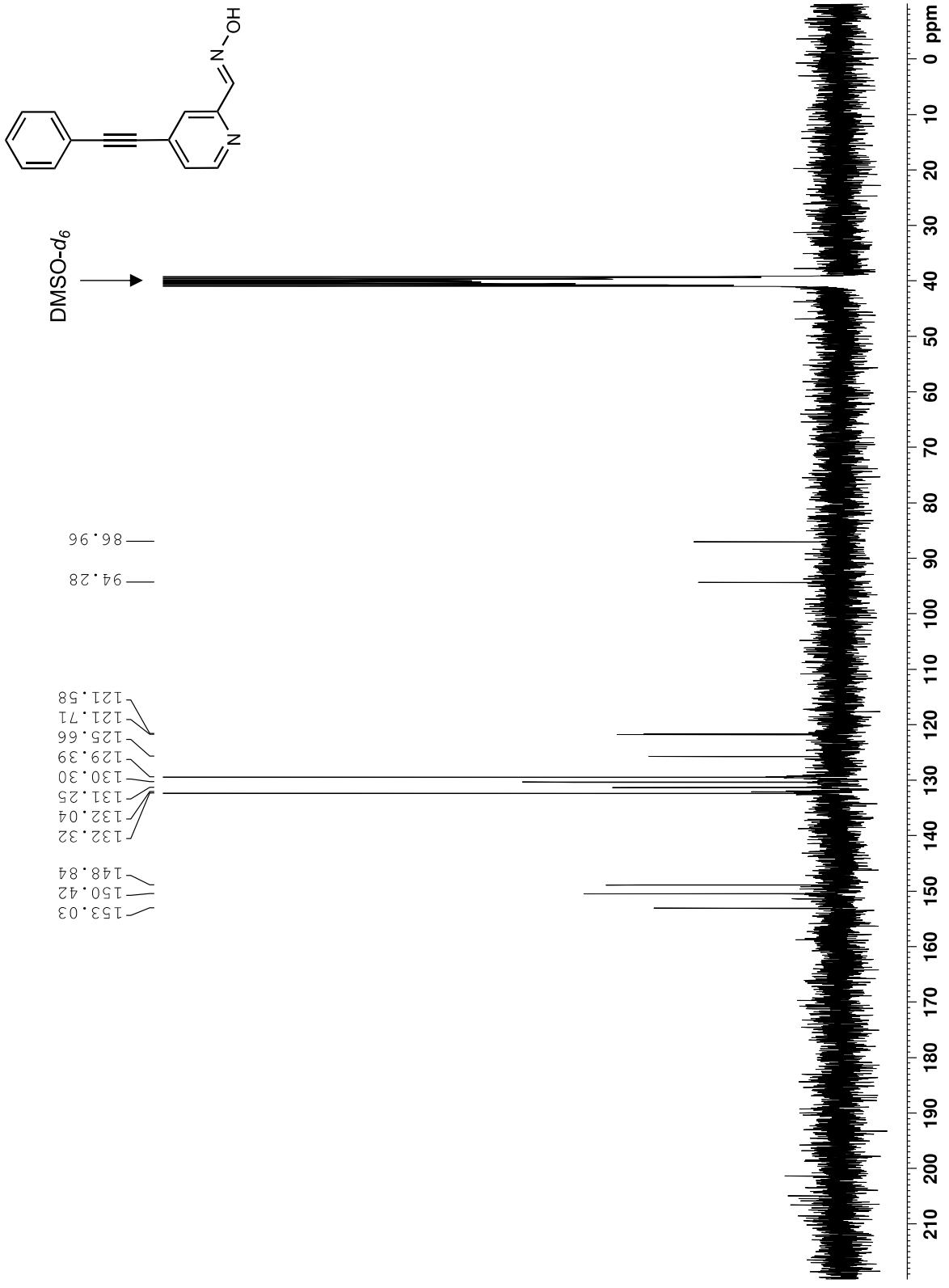

Spectrum 270. ^{13}C NMR for (*E*)-4-(phenylethynyl)picolinaldehyde oxime (75 MHz, 293 K, DMSO-d_6).

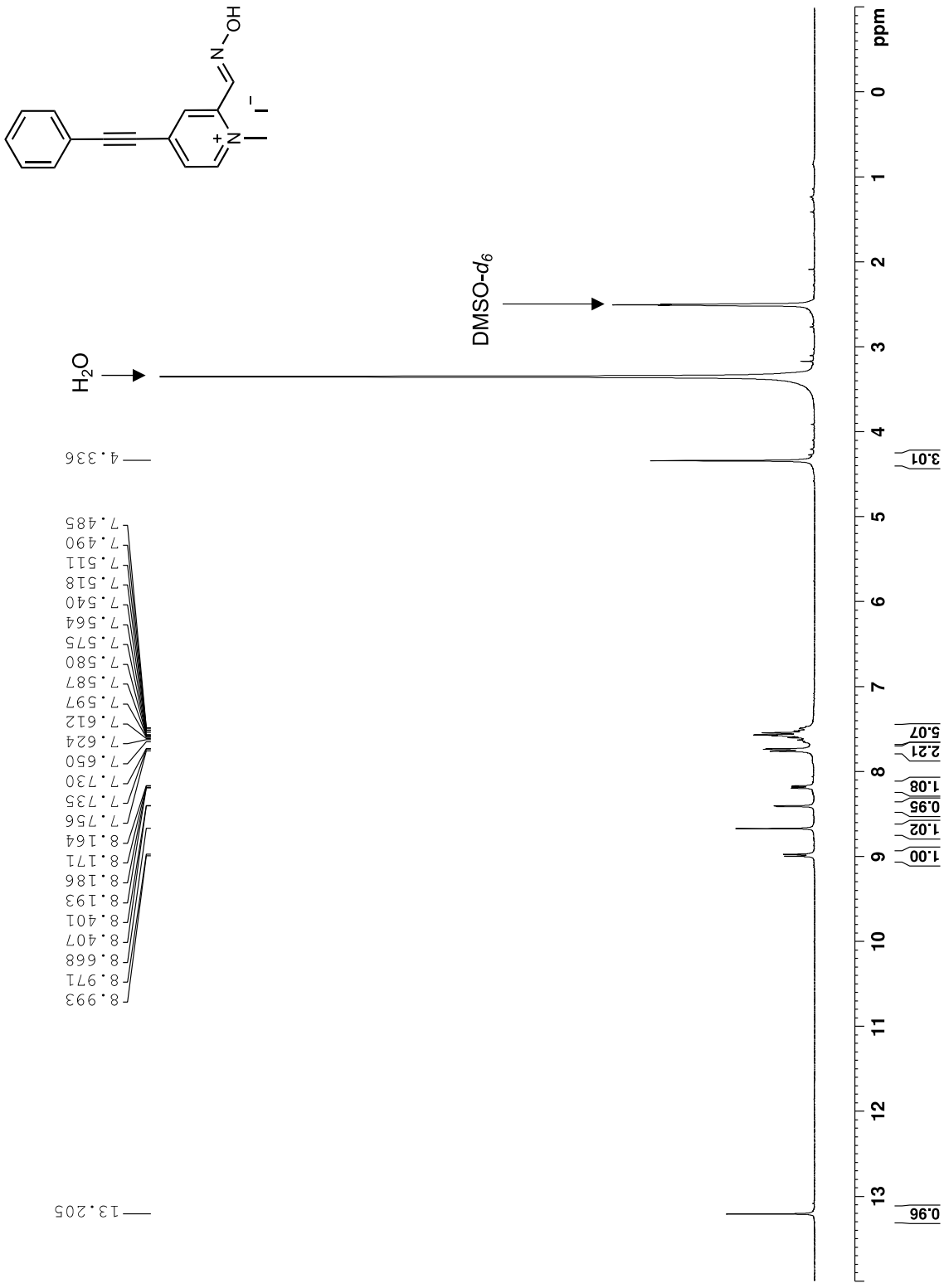

Spectrum 271. ^{1}H NMR for (*E*)-2-[(hydroxyimino)methyl]-1-methyl-4-(phenylethynyl)pyridin-1-ium iodide **(ADG2173)** (300 MHz, 293 K, DMSO-d_6).

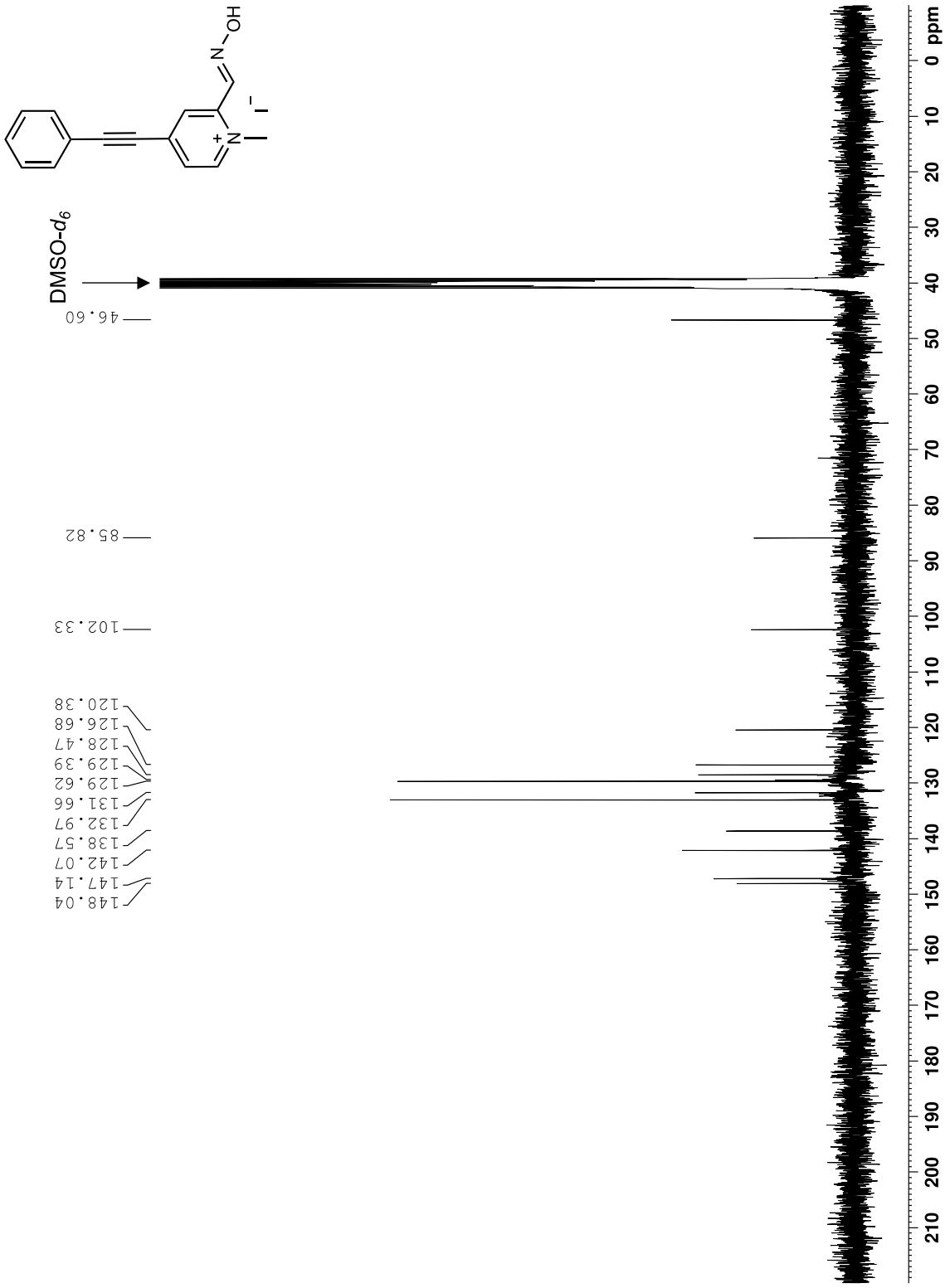

Spectrum 272. ^{13}C NMR for (*E*)-2-[(hydroxyimino)methyl]-1-methyl-4-(phenylethynyl)pyridin-1-ium iodide **(ADG2173)** (75 MHz, 293 K, DMSO-d_6).

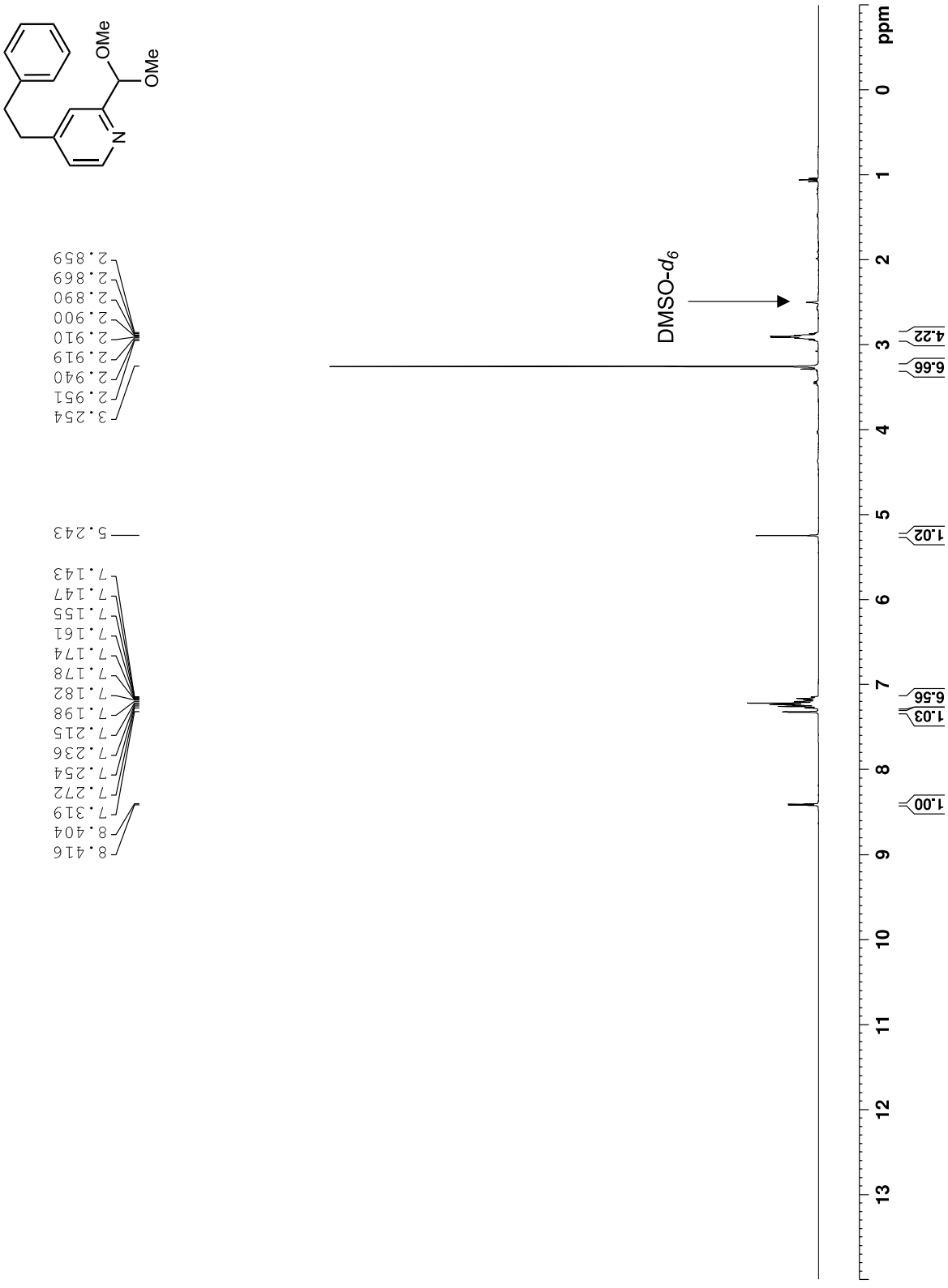

Spectrum 273. [1]H NMR for 2-(dimethoxymethyl)-4-phenethylpyridine (400 MHz, 293 K, DMSO-d_6).

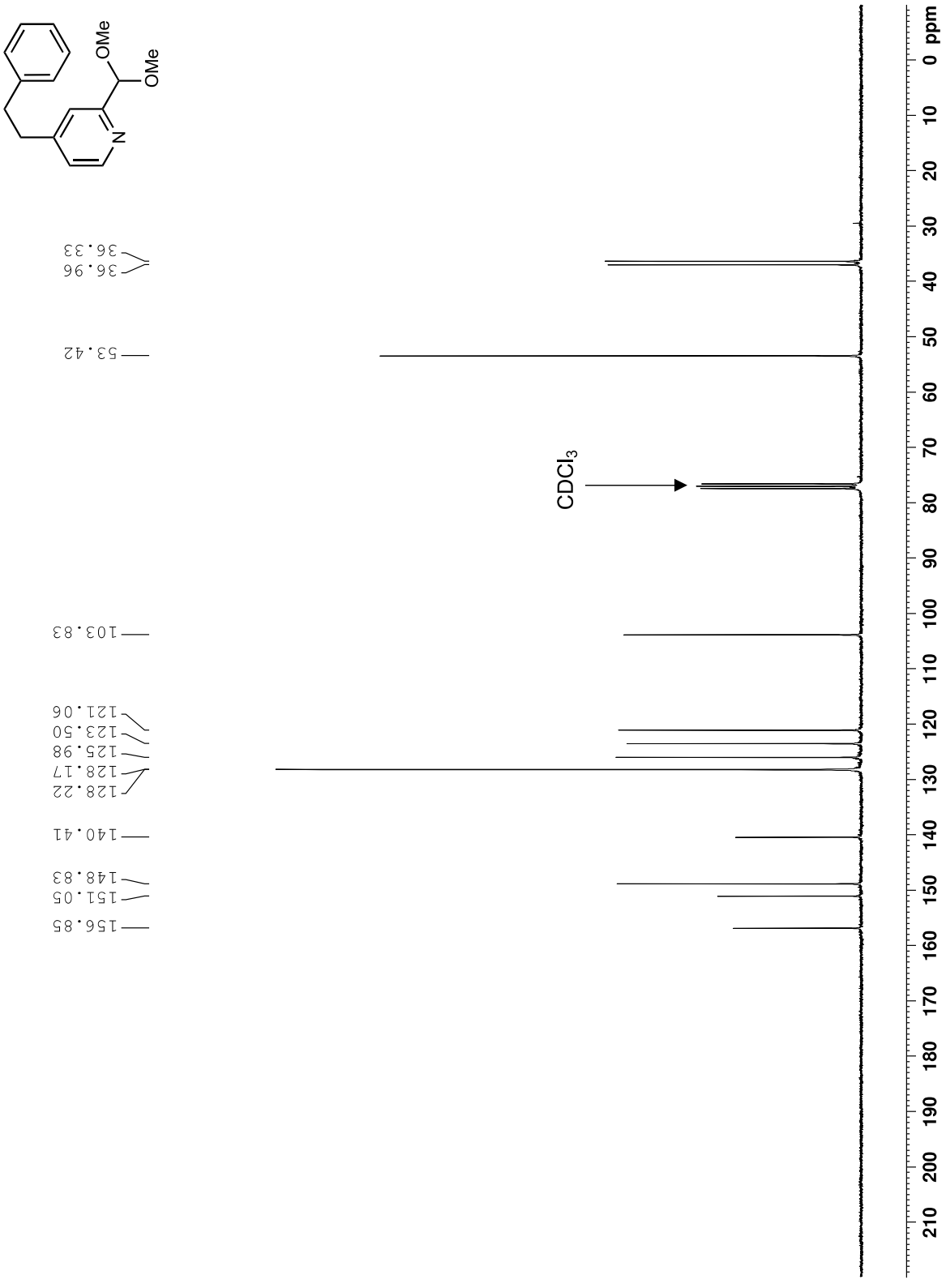

Spectrum 274. ^{13}C NMR for 2-(dimethoxymethyl)-4-phenethylpyridine (75 MHz, 293 K, $CDCl_3$).

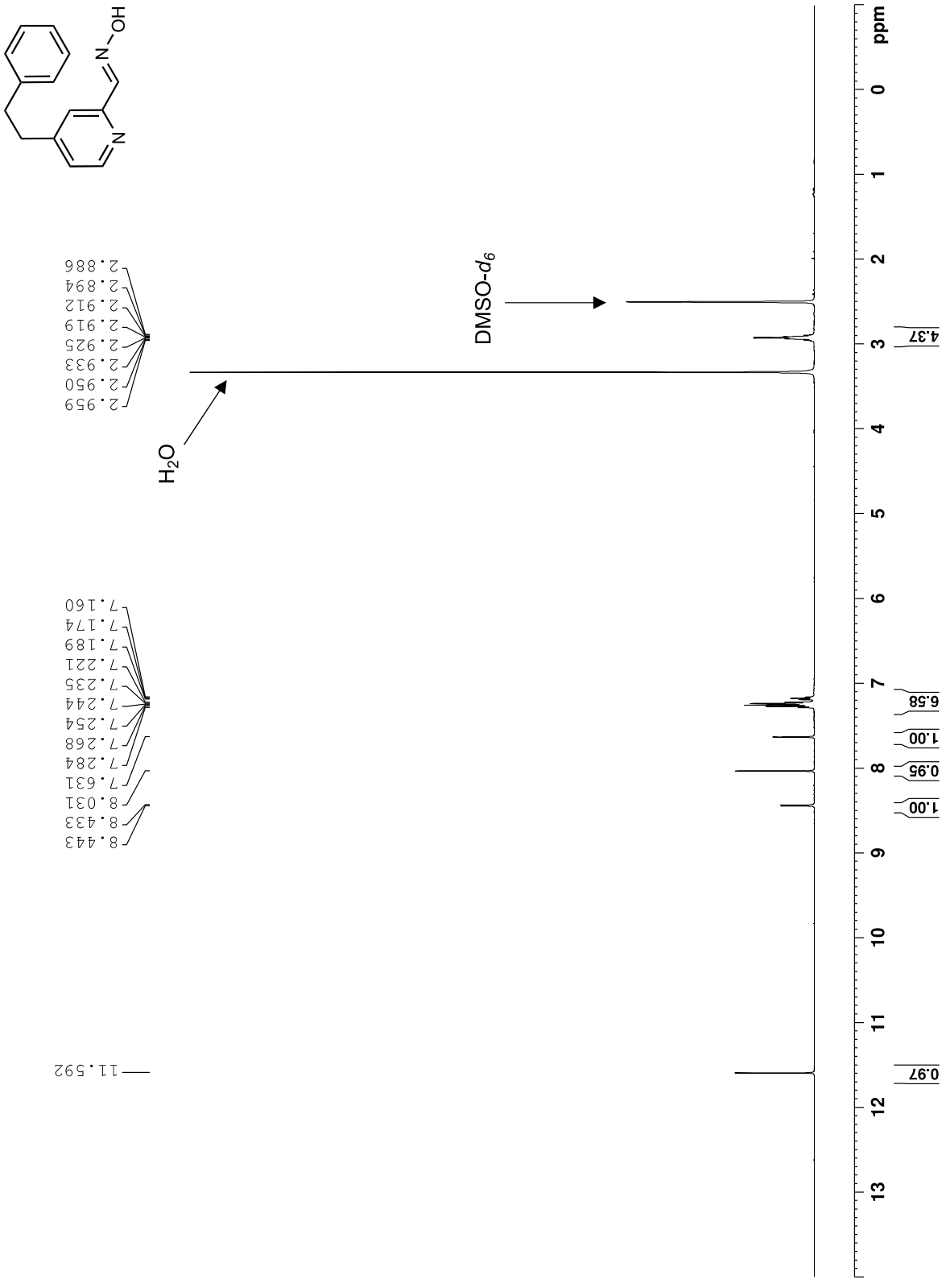

Spectrum 275. ^{1}H NMR for (*E*)-4-phenethylpicolinaldehyde oxime (500 MHz, 293 K, DMSO-d_6).

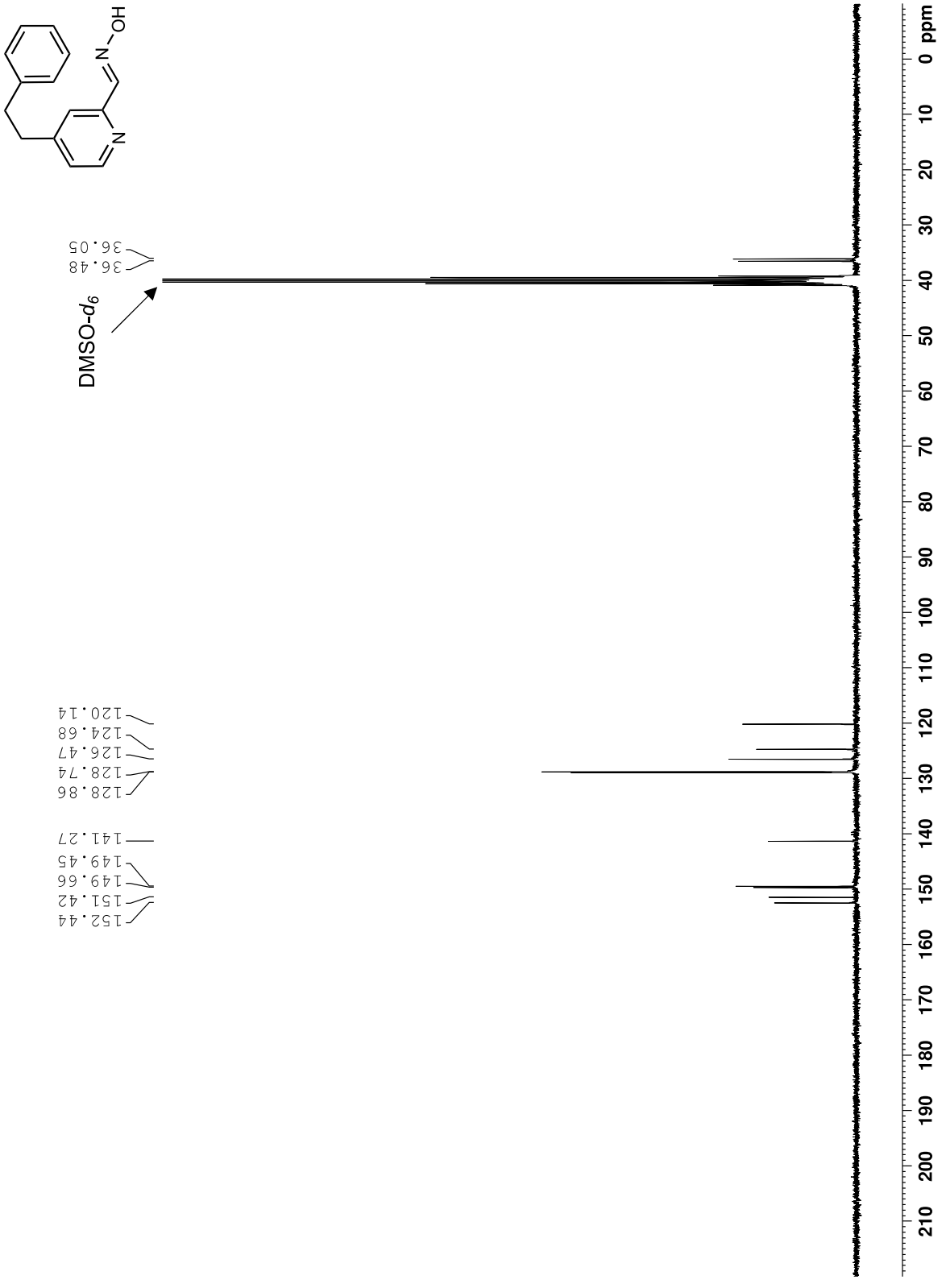

Spectrum 276. ^{13}C NMR for (*E*)-4-phenethylpicolinaldehyde oxime (75 MHz, 293 K, DMSO-d_6).

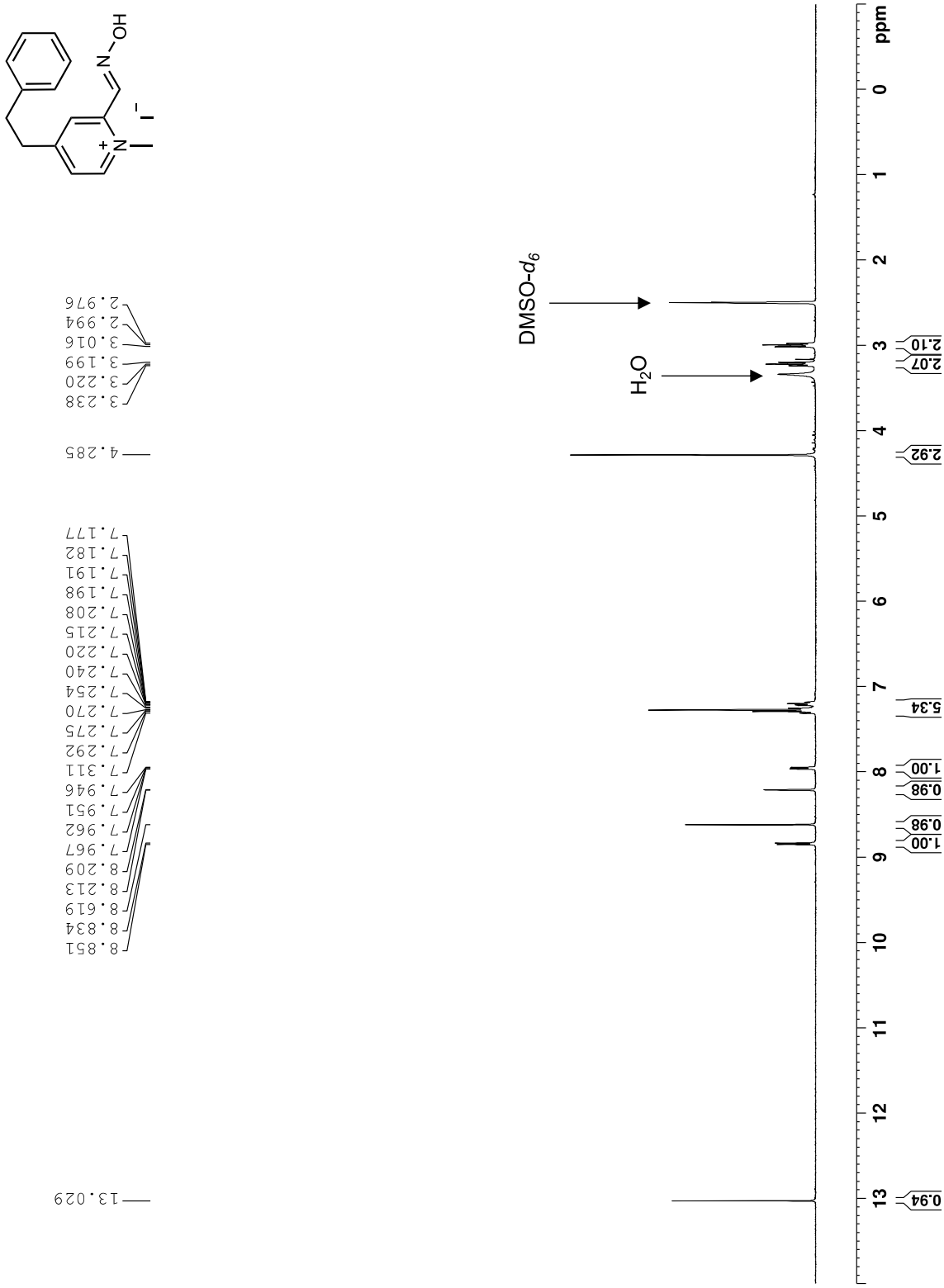

Spectrum 277. ^{1}H NMR for (*E*)-2-((hydroxyimino)methyl)-1-methyl-4-phenethylpyridin-1-ium iodide **(ADG2180)** (400 MHz, 293 K, DMSO-d_6).

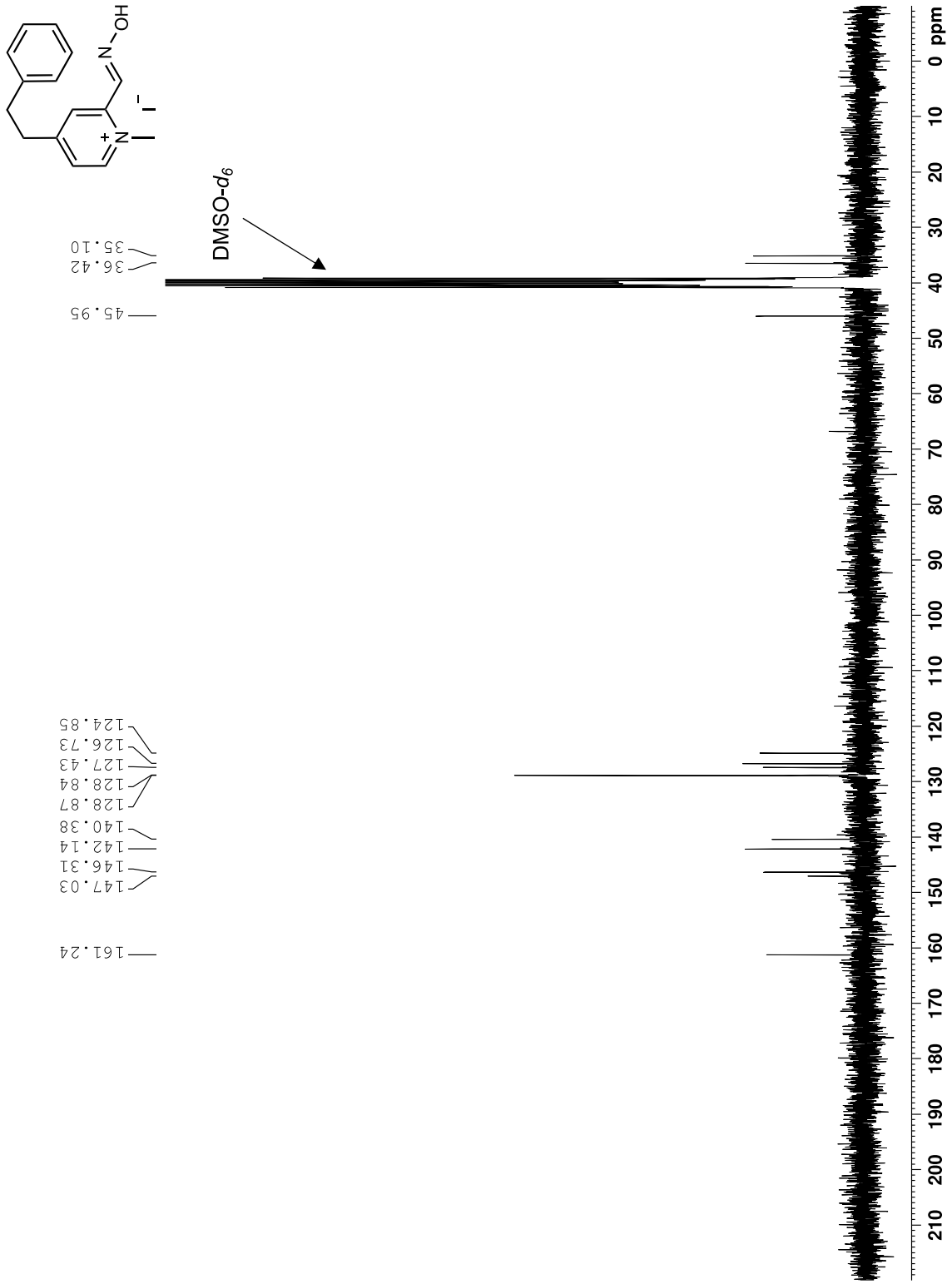

Spectrum 278. ^{13}C NMR for (*E*)-2-((hydroxyimino)methyl)-1-methyl-4-phenethylpyridin-1-ium iodide **(ADG2180)** (75 MHz, 293 K, DMSO-d_6).

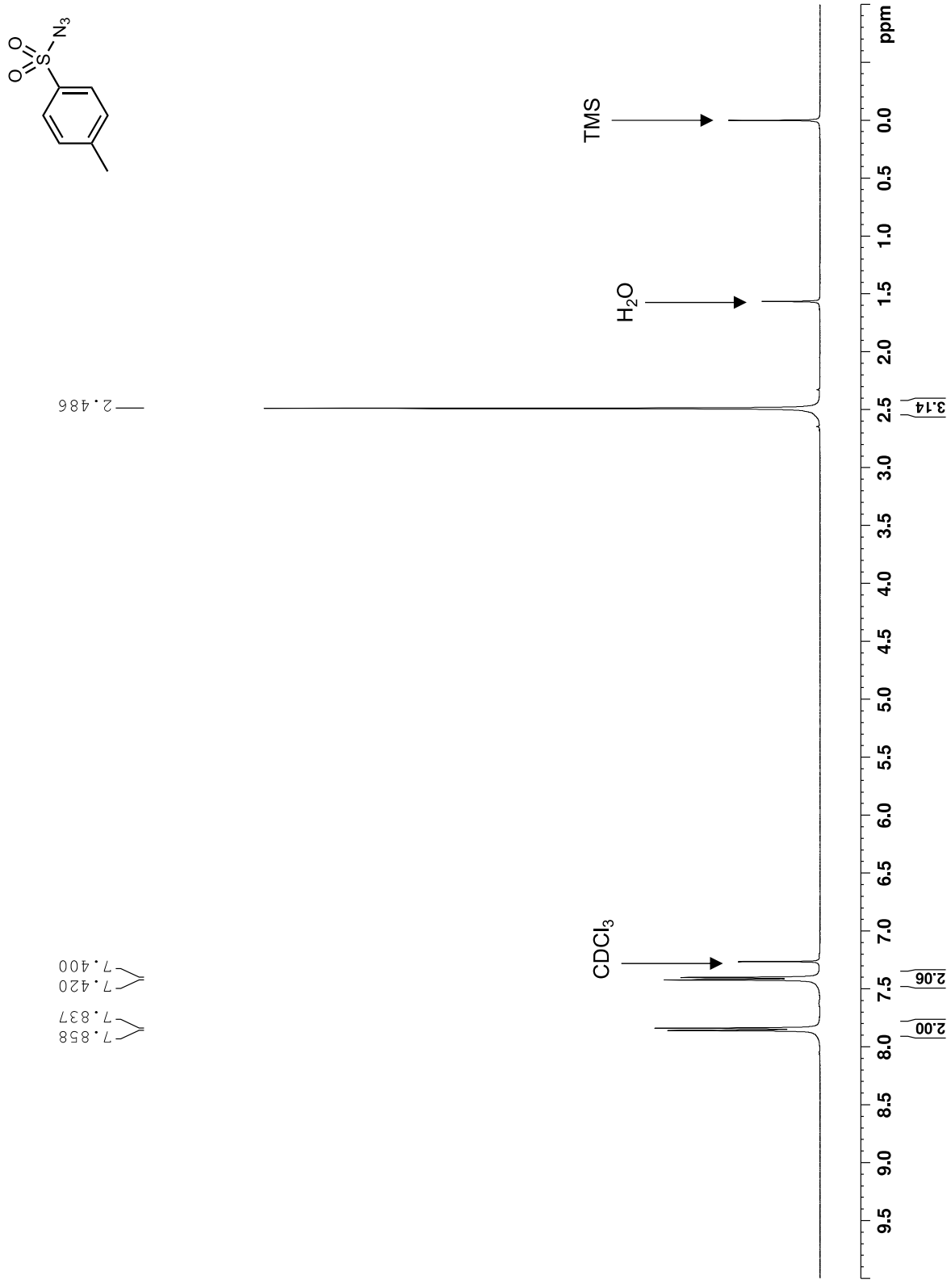

Spectrum 279. ^{1}H NMR of 4-methylbenzenesulfonyl azide (400 MHz, 293 K, $CDCl_3$).

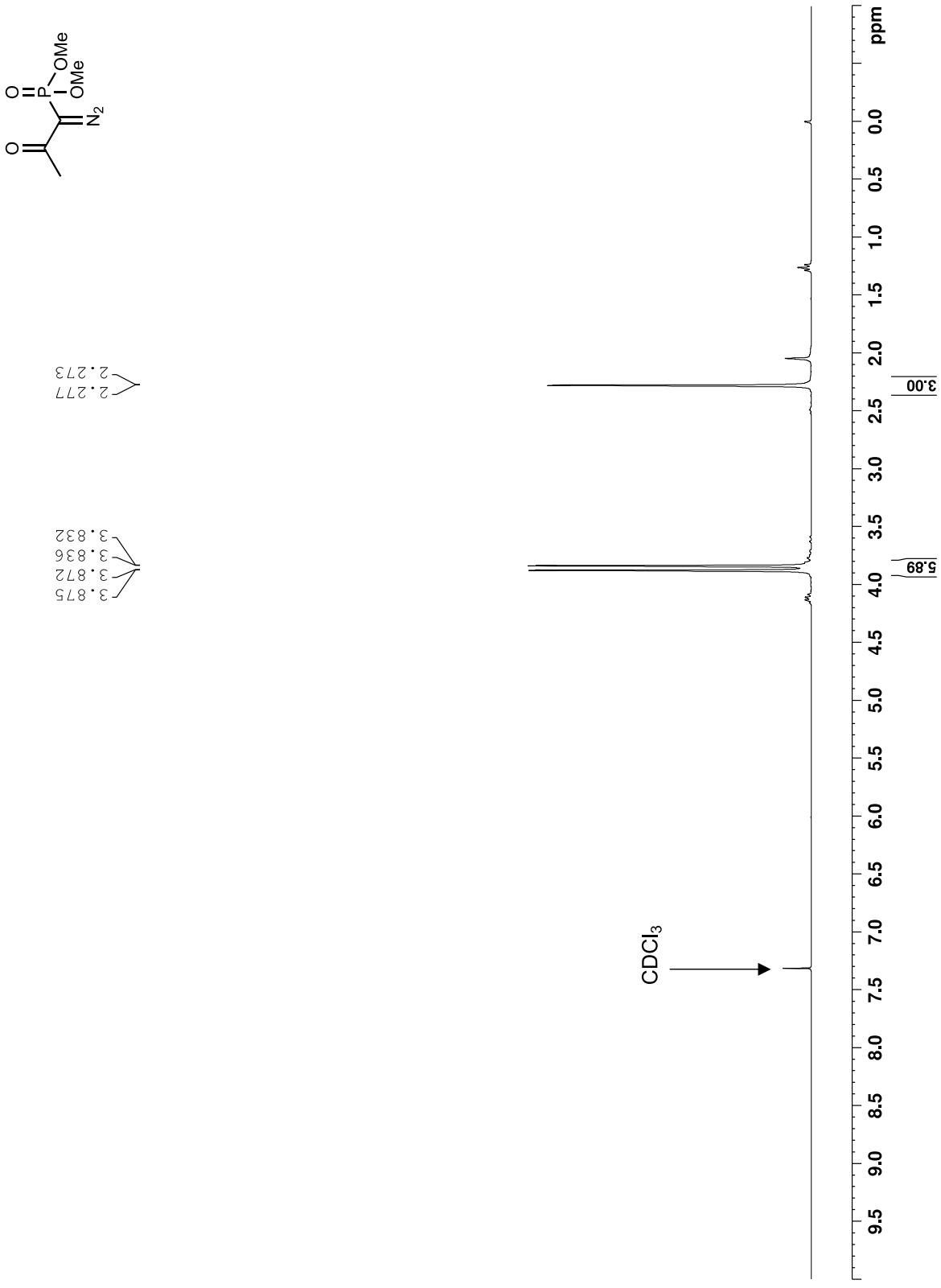

Spectrum 280. ^{1}H NMR of dimethyl (1-diazo-2-oxopropyl)phosphonate (300 MHz, 293 K, $CDCl_3$).

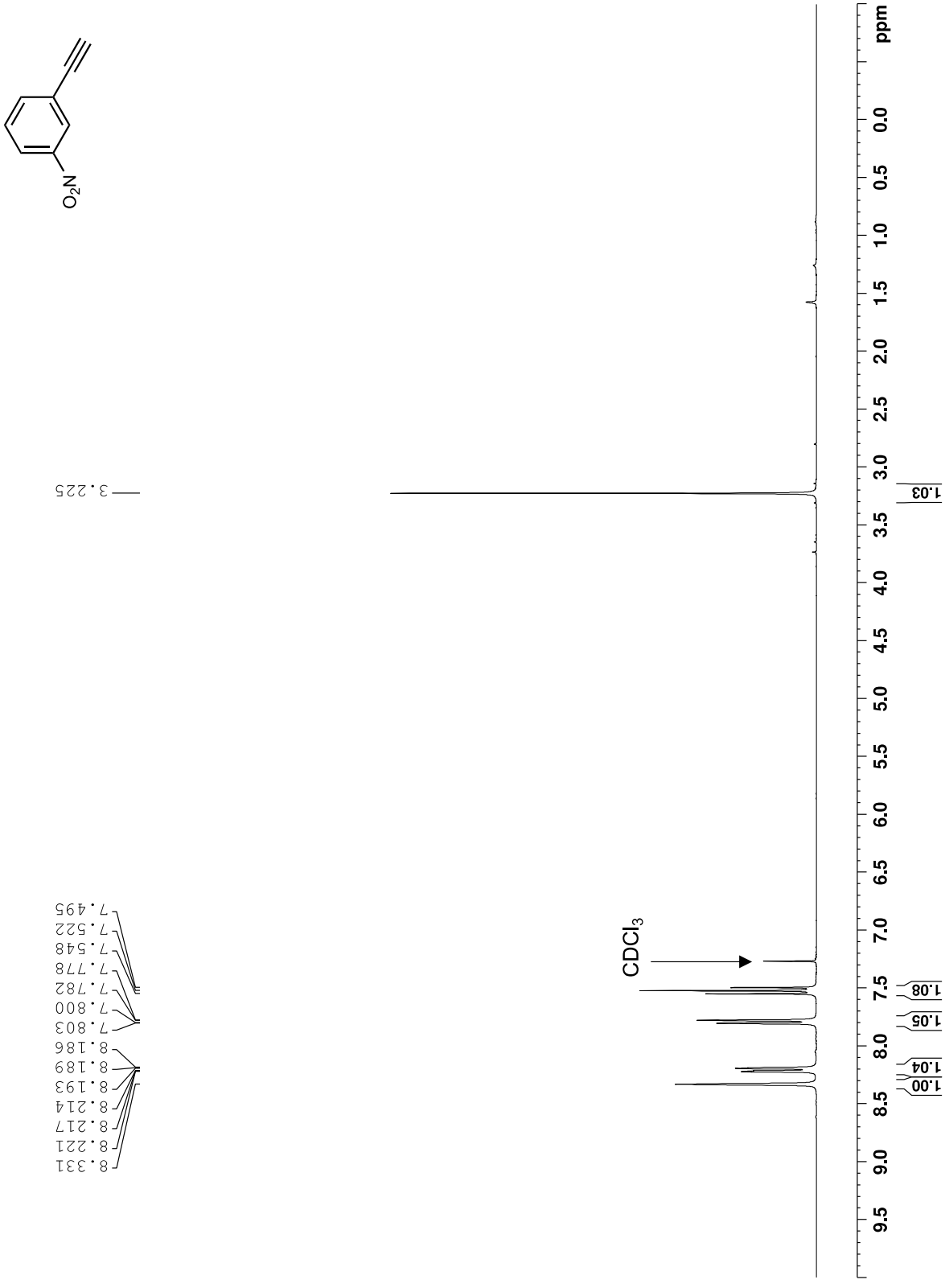

Spectrum 281. ^{1}H NMR of 1-ethynyl-3-nitrobenzene (300 MHz, 293 K, $CDCl_3$).

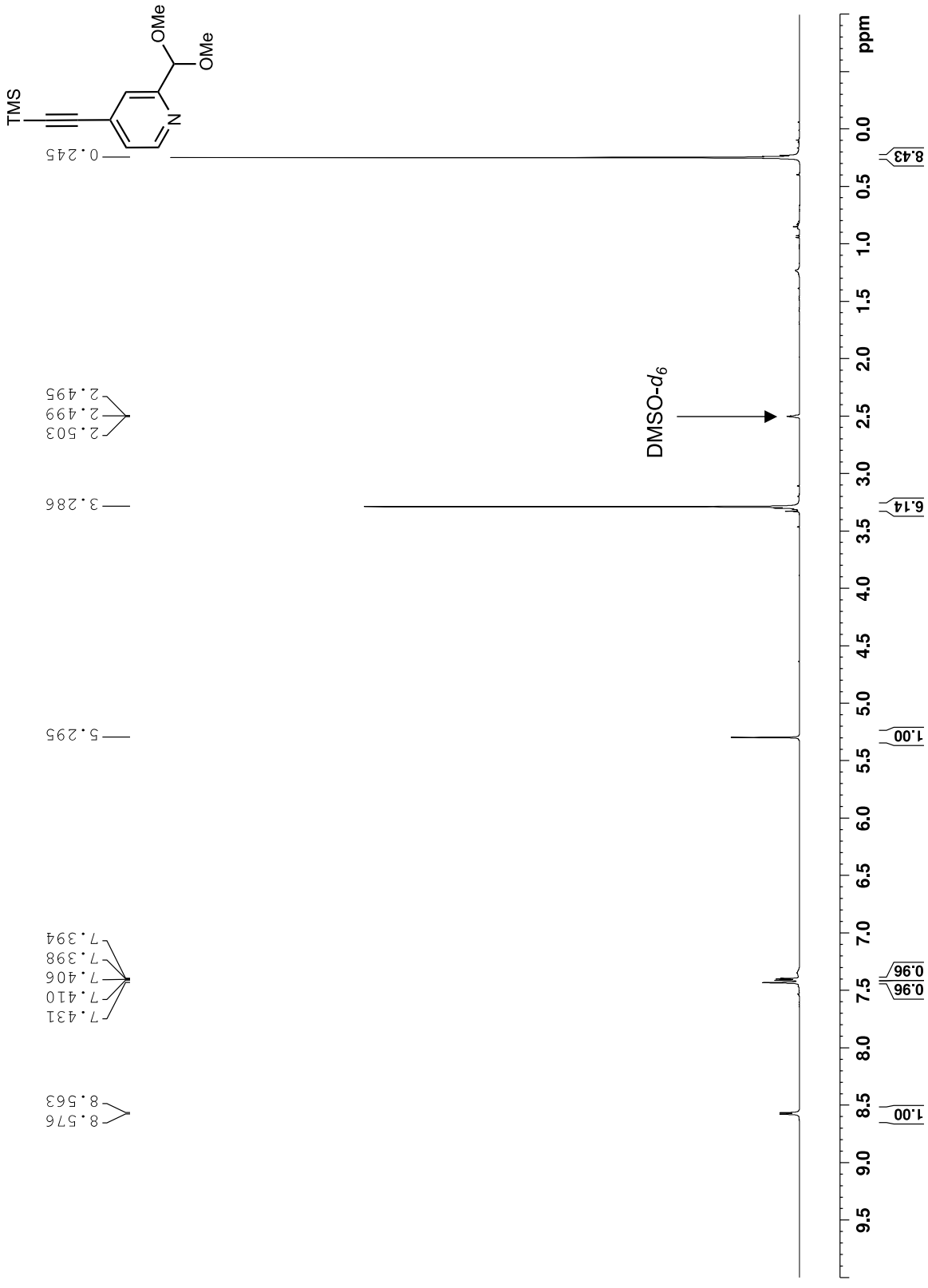

Spectrum 282. ^{1}H NMR of 2-(dimethoxymethyl)-4-((trimethylsilyl)ethynyl)pyridine (400 MHz, 293 K, DMSO-d_6).

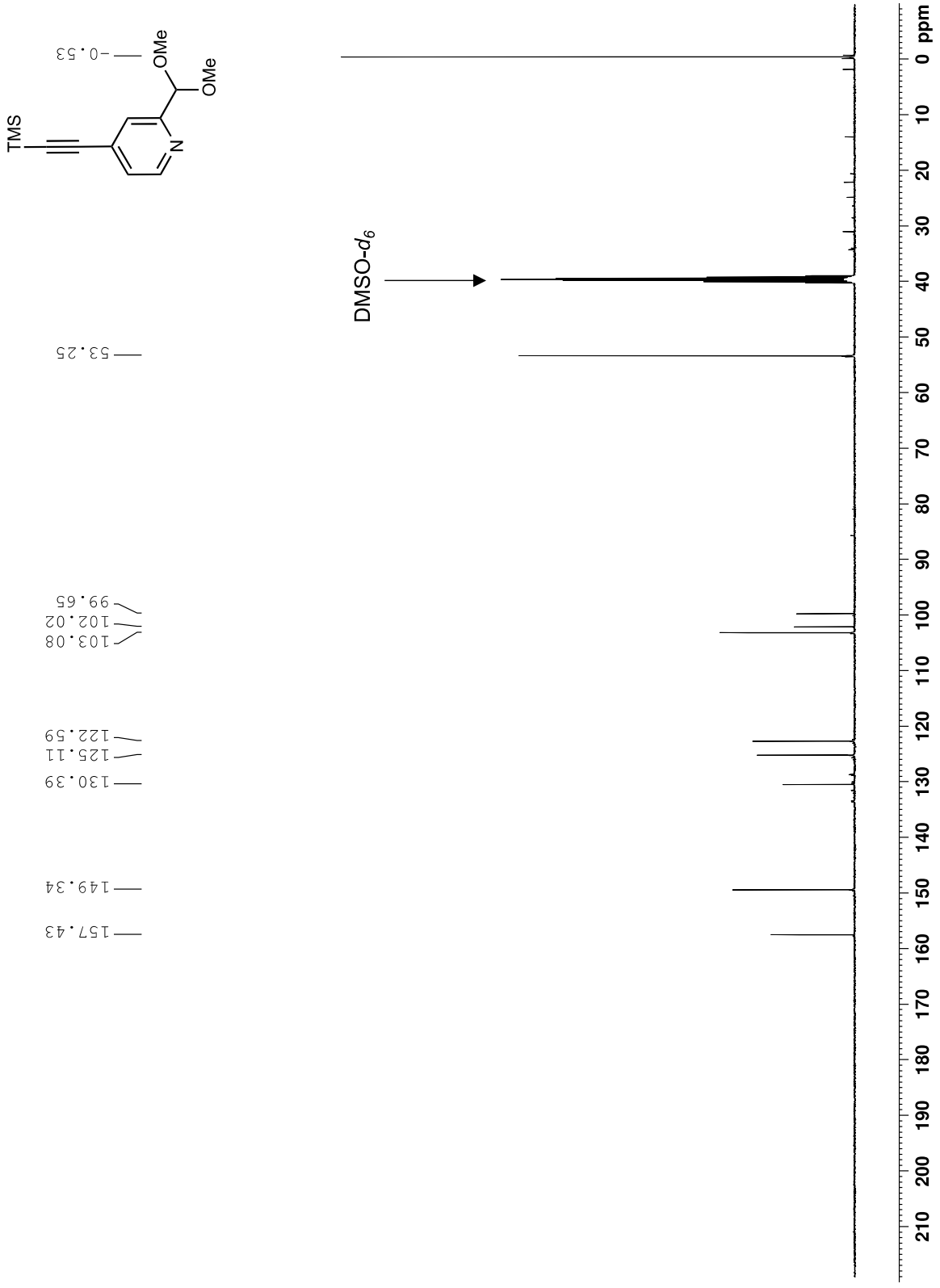

Spectrum 283. ^{13}C NMR of 2-(dimethoxymethyl)-4-((trimethylsilyl)ethynyl)pyridine (100 MHz, 293 K, DMSO-d_6).

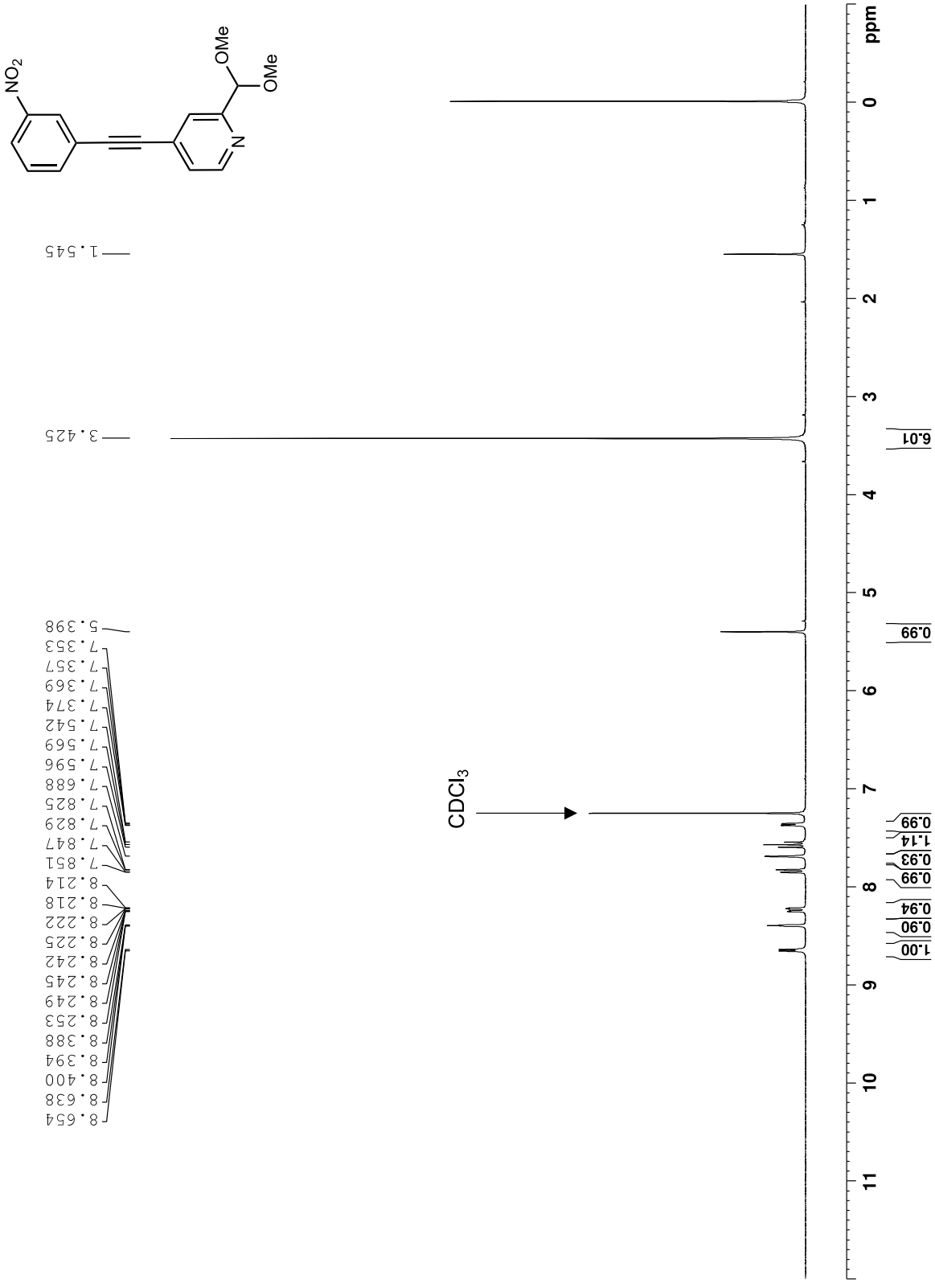

Spectrum 284. ^{1}H NMR of 2-(dimethoxymethyl)-4-((3-nitrophenyl)ethynyl)pyridine (300 MHz, 293 K, $CDCl_3$).

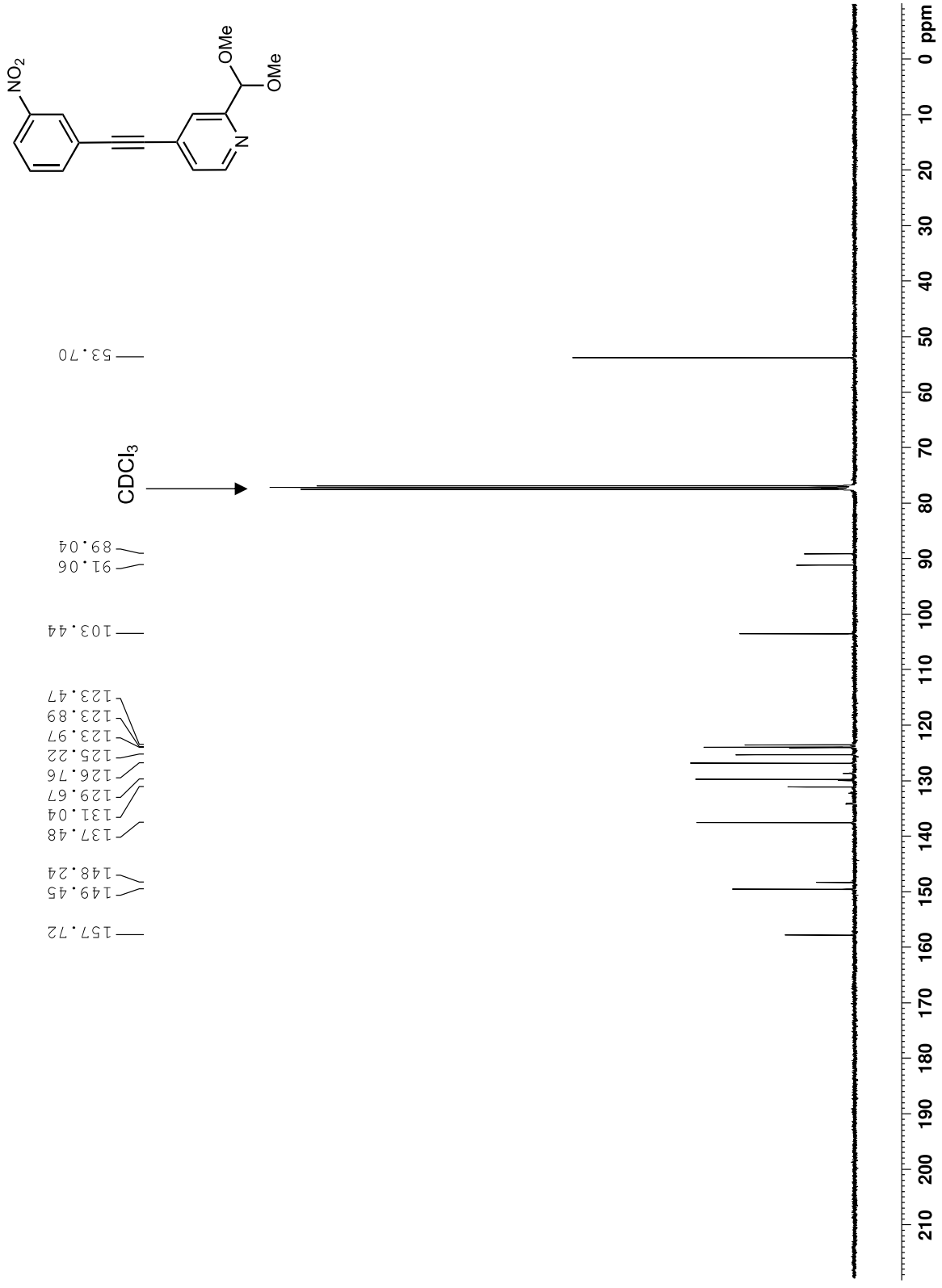

Spectrum 285. ^{13}C NMR of 2-(dimethoxymethyl)-4-((3-nitrophenyl)ethynyl)pyridine (100 MHz, 293 K, $CDCl_3$).

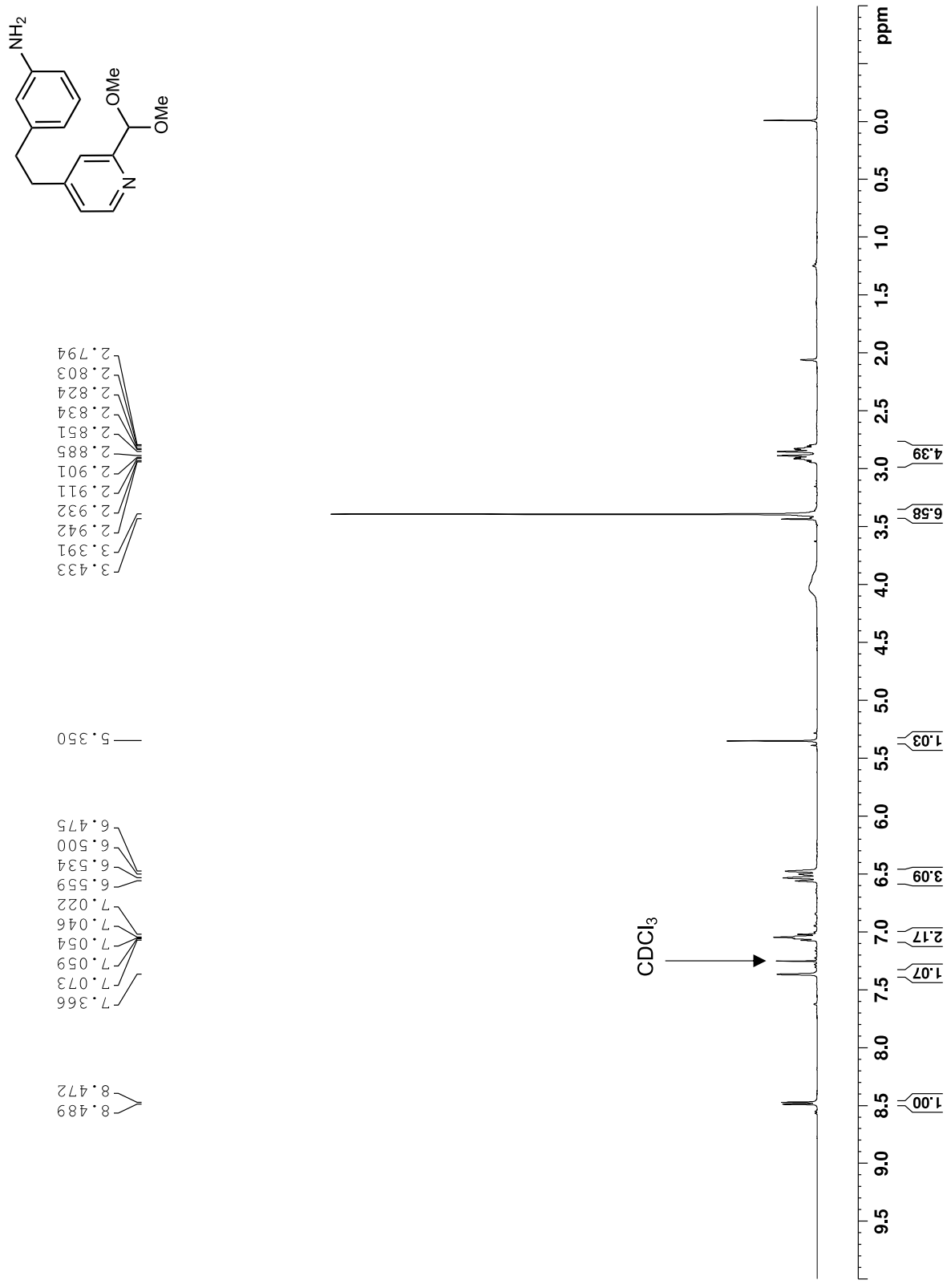

Spectrum 286. ^{1}H NMR of 3-(2-(2-(dimethoxymethyl)pyridin-4-yl)ethyl)aniline (300 MHz, 293 K, $CDCl_3$).

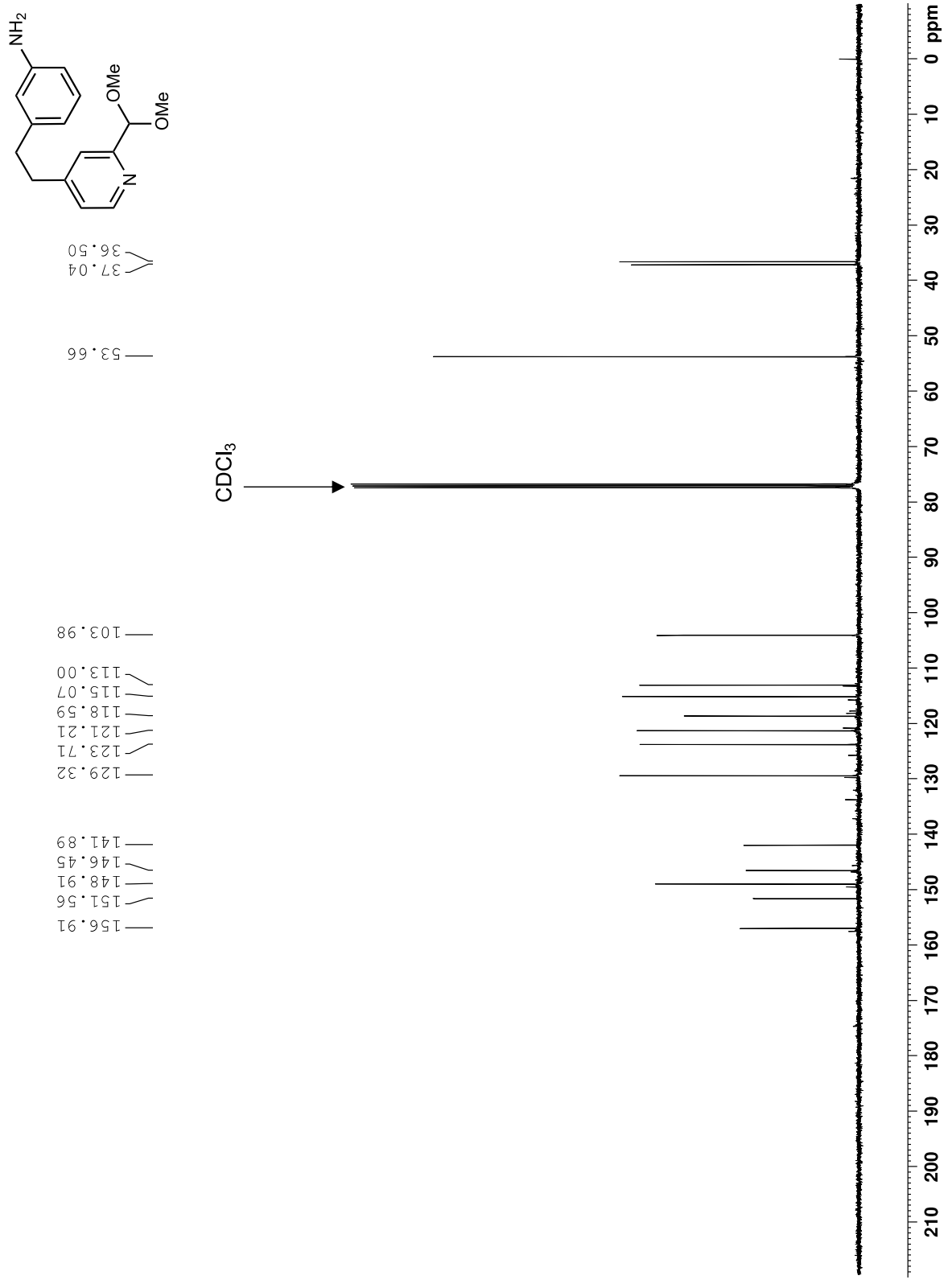

Spectrum 287. ^{13}C NMR of 3-(2-(2-(dimethoxymethyl)pyridin-4-yl)ethyl)aniline (100 MHz, 293 K, $CDCl_3$).

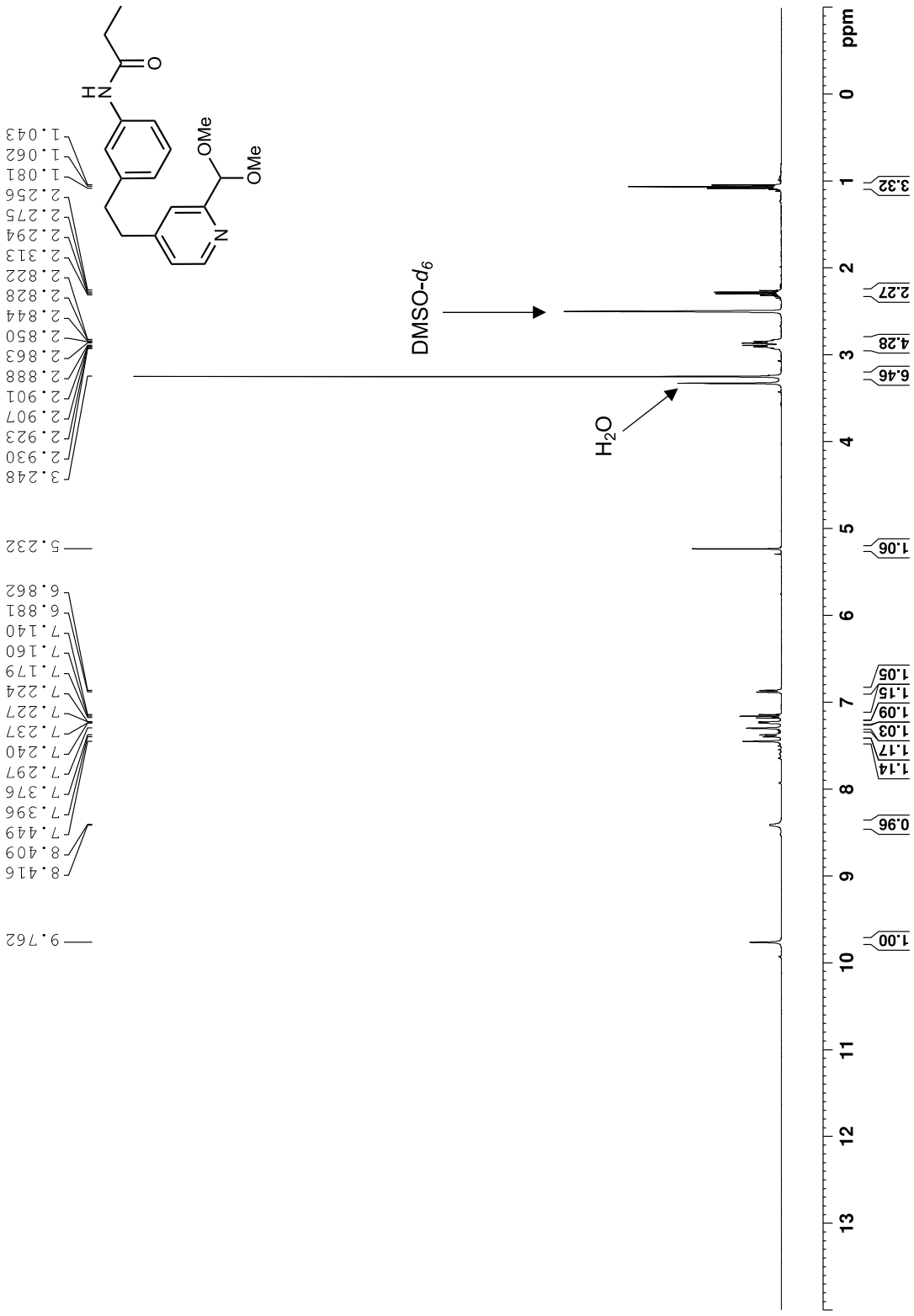

Spectrum 288. ^{1}H NMR of *N*-(3-(2-(2-(dimethoxymethyl)pyridin-4-yl)ethyl)phenyl)propionamide (400 MHz, 293 K, DMSO-d_6).

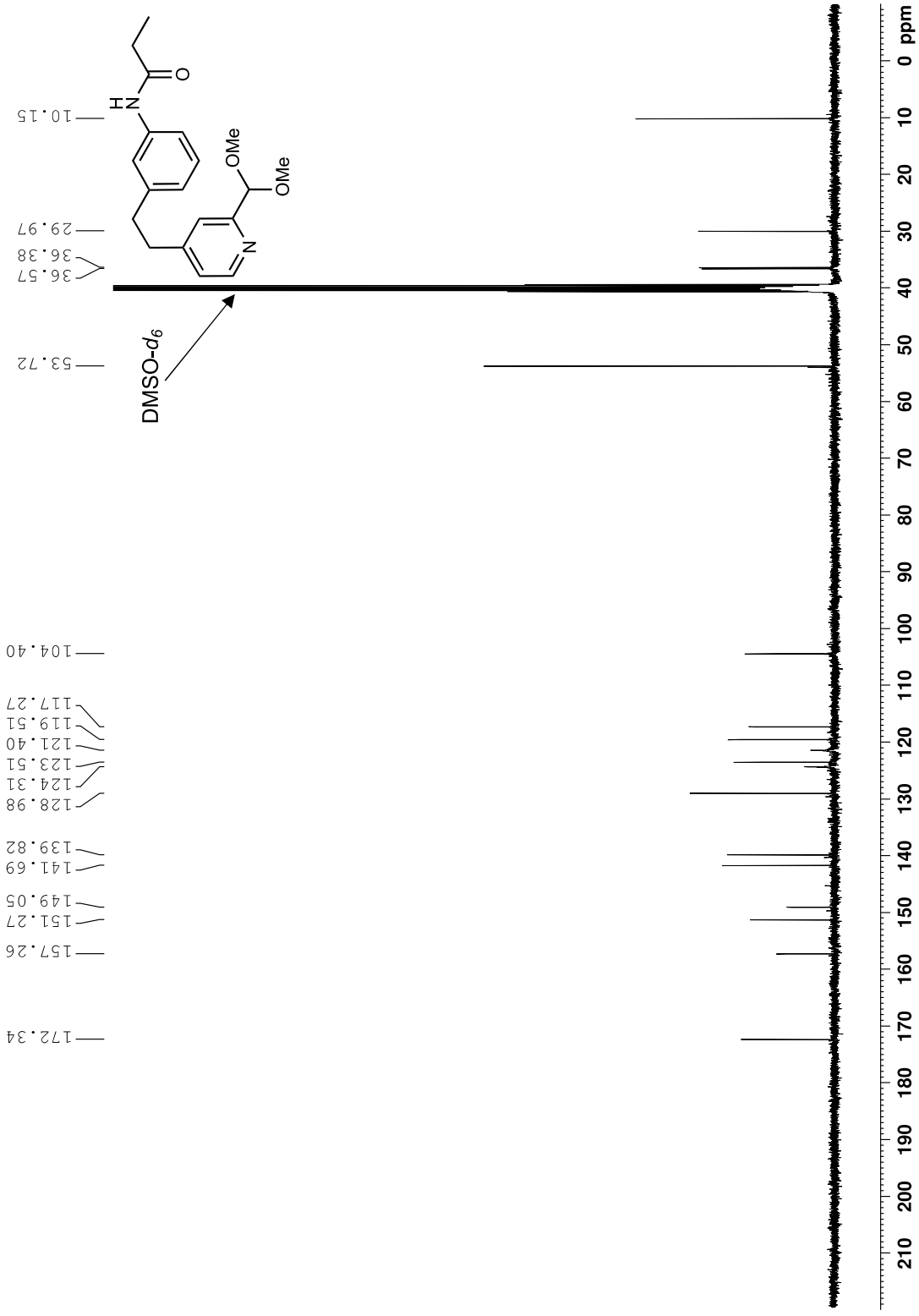

Spectrum 289. ^{13}C NMR of *N*-(3-(2-(2-(dimethoxymethyl)pyridin-4-yl)ethyl)phenyl)propionamide (100 MHz, 293 K, DMSO-d_6).

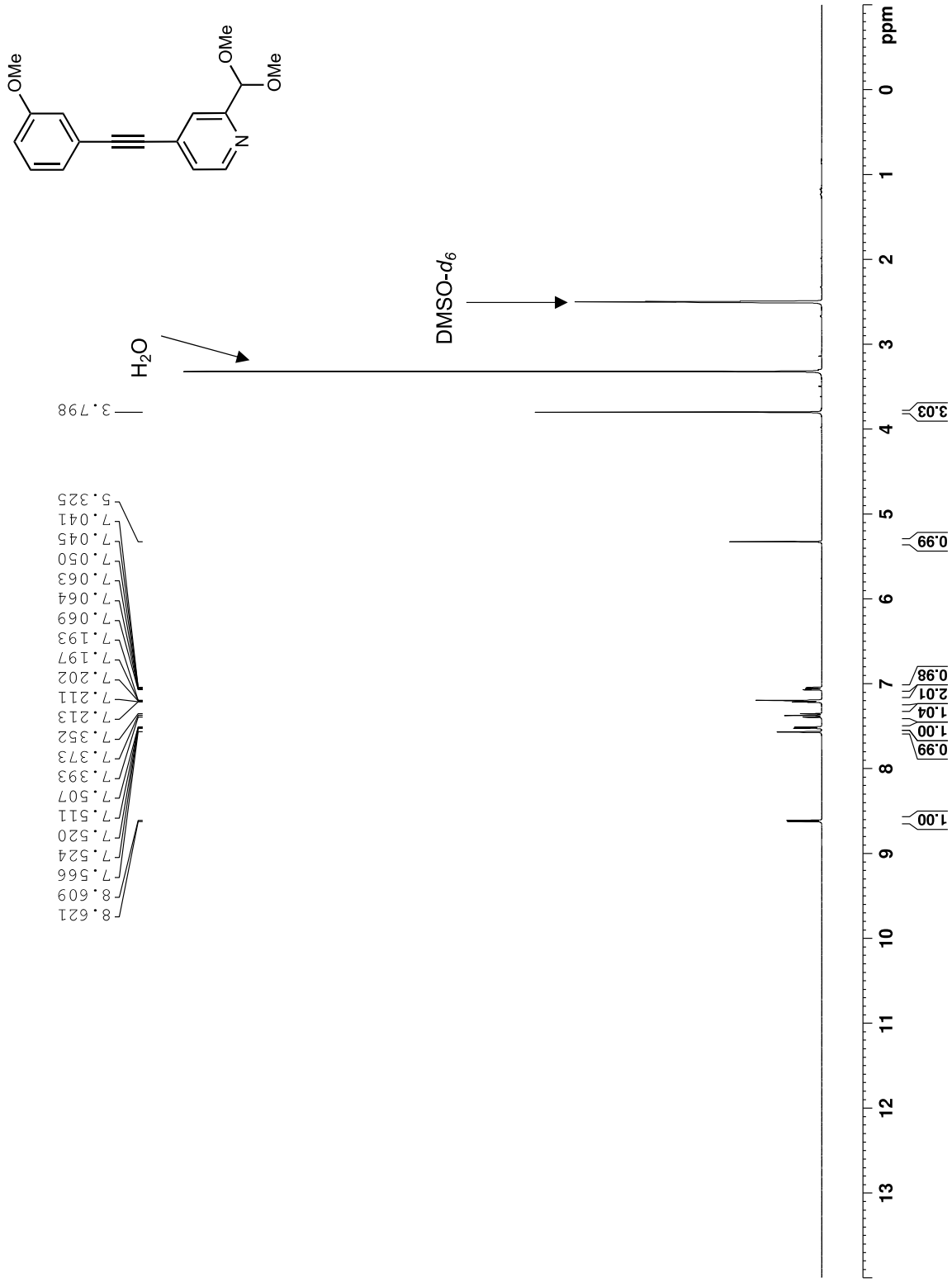

Spectrum 290. ^{1}H NMR for 2-(dimethoxymethyl)-4-((3-methoxyphenyl)ethynyl)pyridine (400 MHz, 293 K, DMSO-d_6).

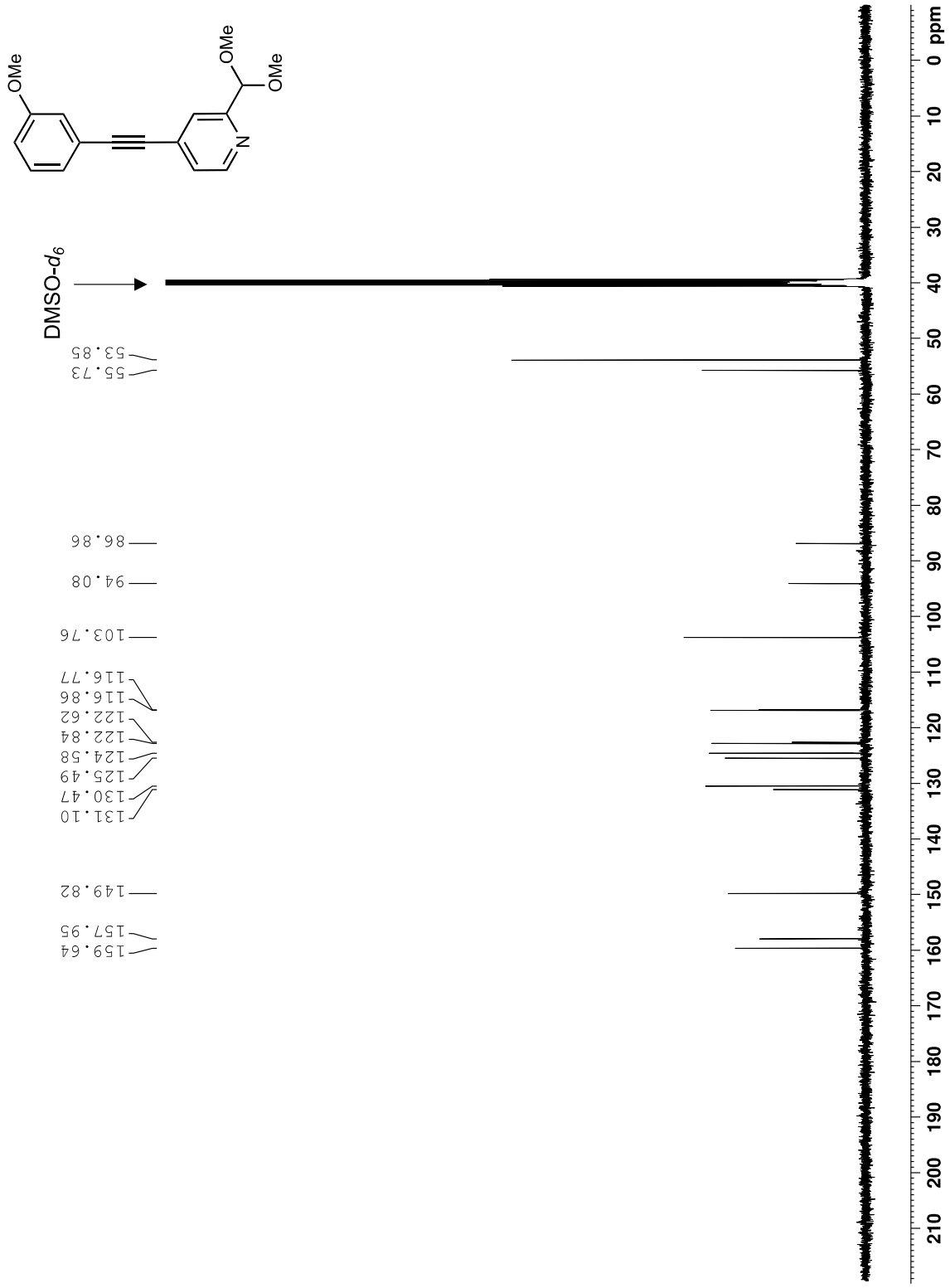

Spectrum 291. ^{13}C NMR for 2-(dimethoxymethyl)-4-((3-methoxyphenyl)ethynyl)pyridine (100 MHz, 293 K, DMSO-d_6).

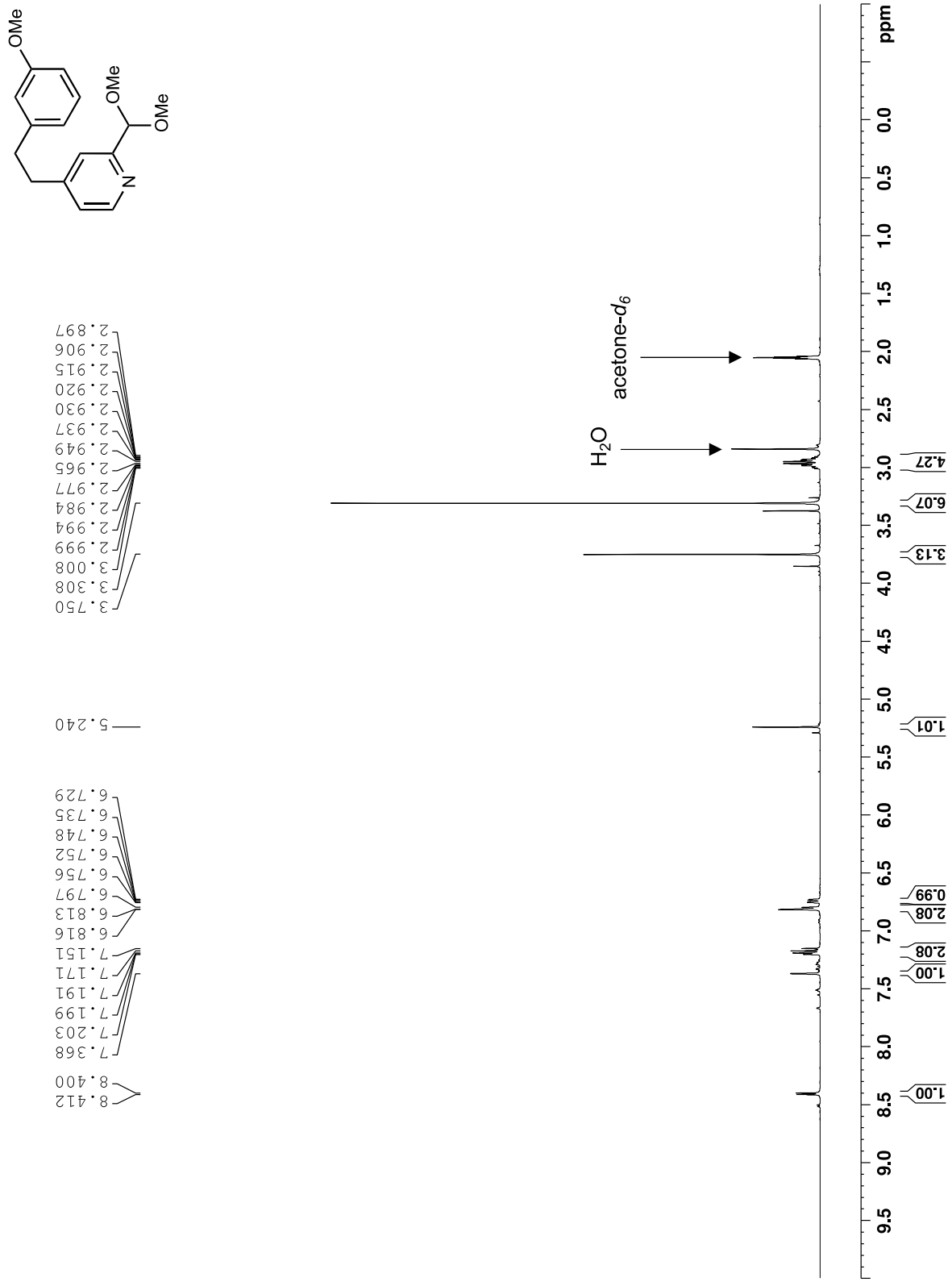

Spectrum 292. ^{1}H NMR for 2-(dimethoxymethyl)-4-(3-methoxyphenethyl)pyridine (400 MHz, 293 K, acetone-d_6).

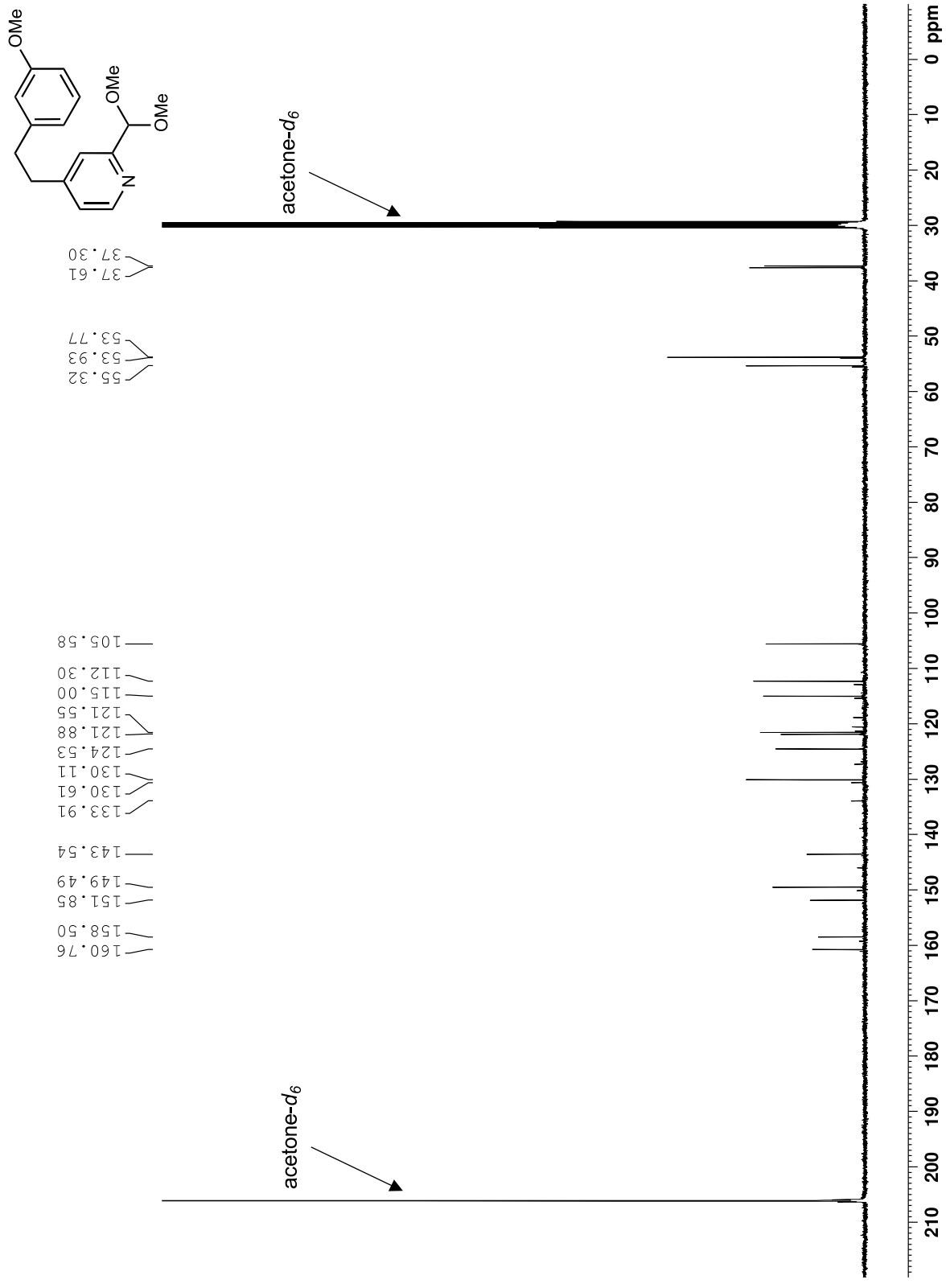

Spectrum 293. ^{13}C NMR for 2-(dimethoxymethyl)-4-(3-methoxyphenethyl)pyridine (100 MHz, 293 K, acetone-d_6).

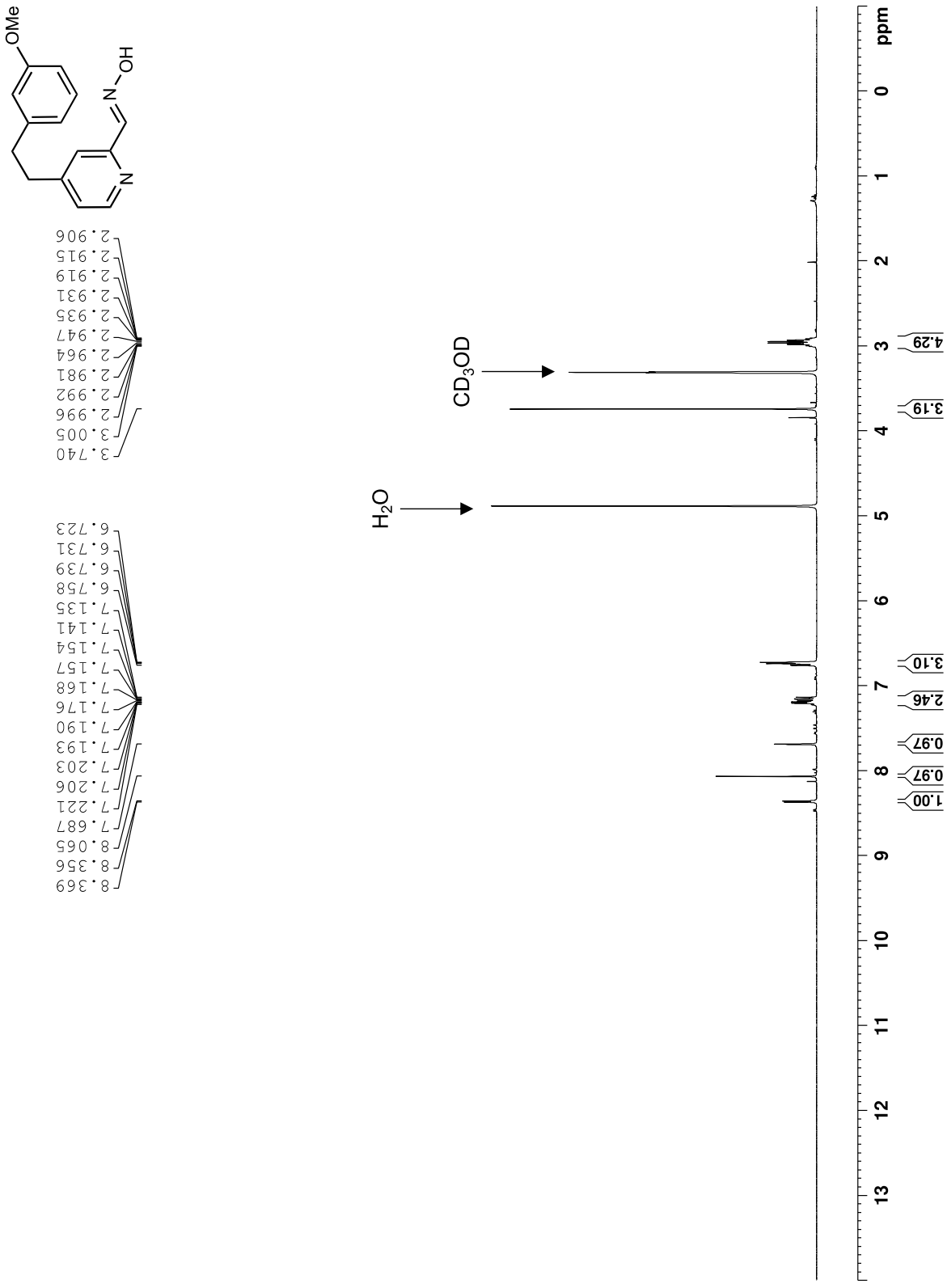

Spectrum 294. ^{1}H NMR for (*E*)-4-(3-methoxyphenethyl)picolinaldehyde oxime (400 MHz, 293 K, CD_3OD).

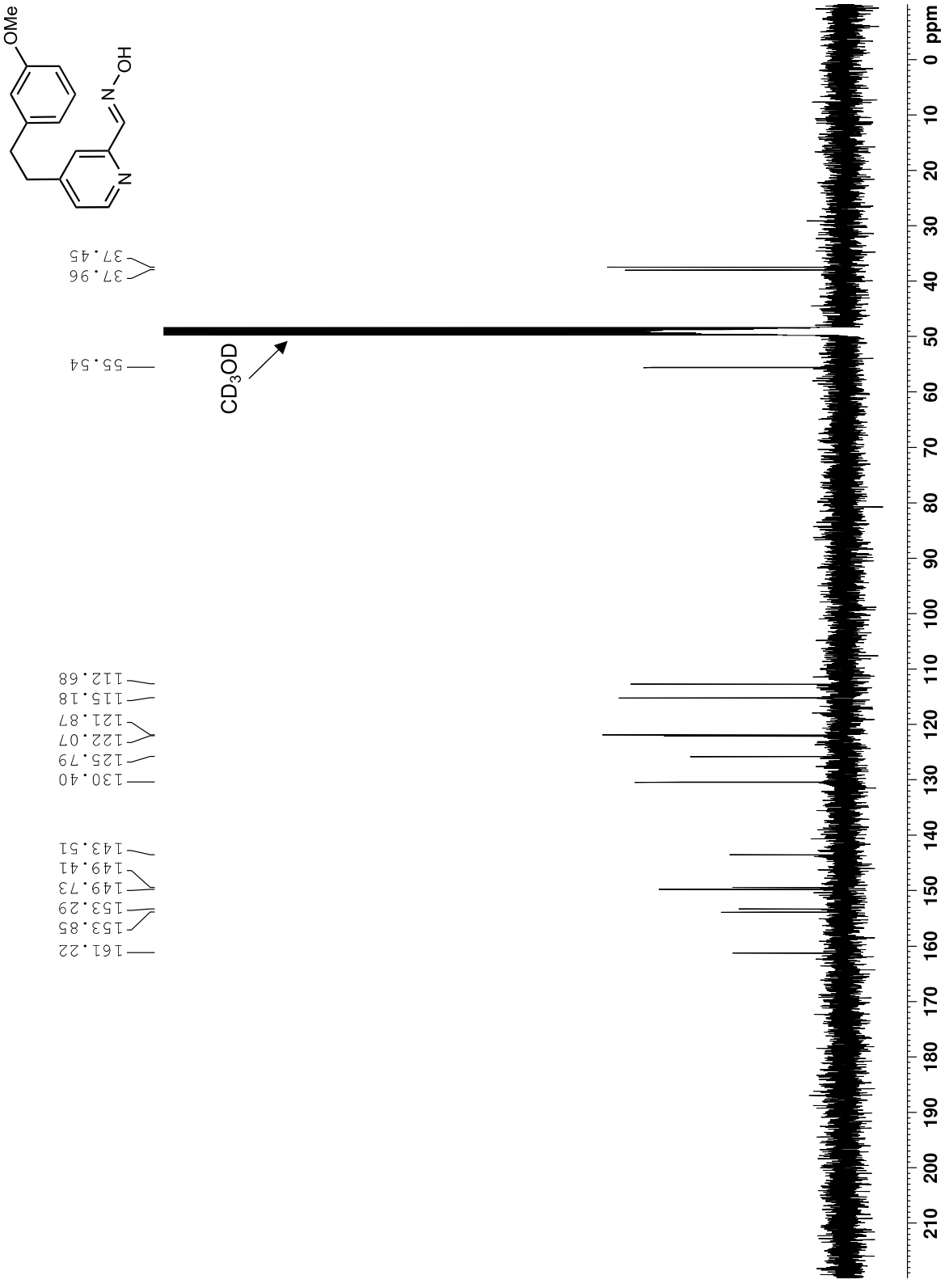

Spectrum 295. ^{13}C NMR for (*E*)-4-(3-methoxyphenethyl)picolinaldehyde oxime (100 MHz, 293 K, CD_3OD).

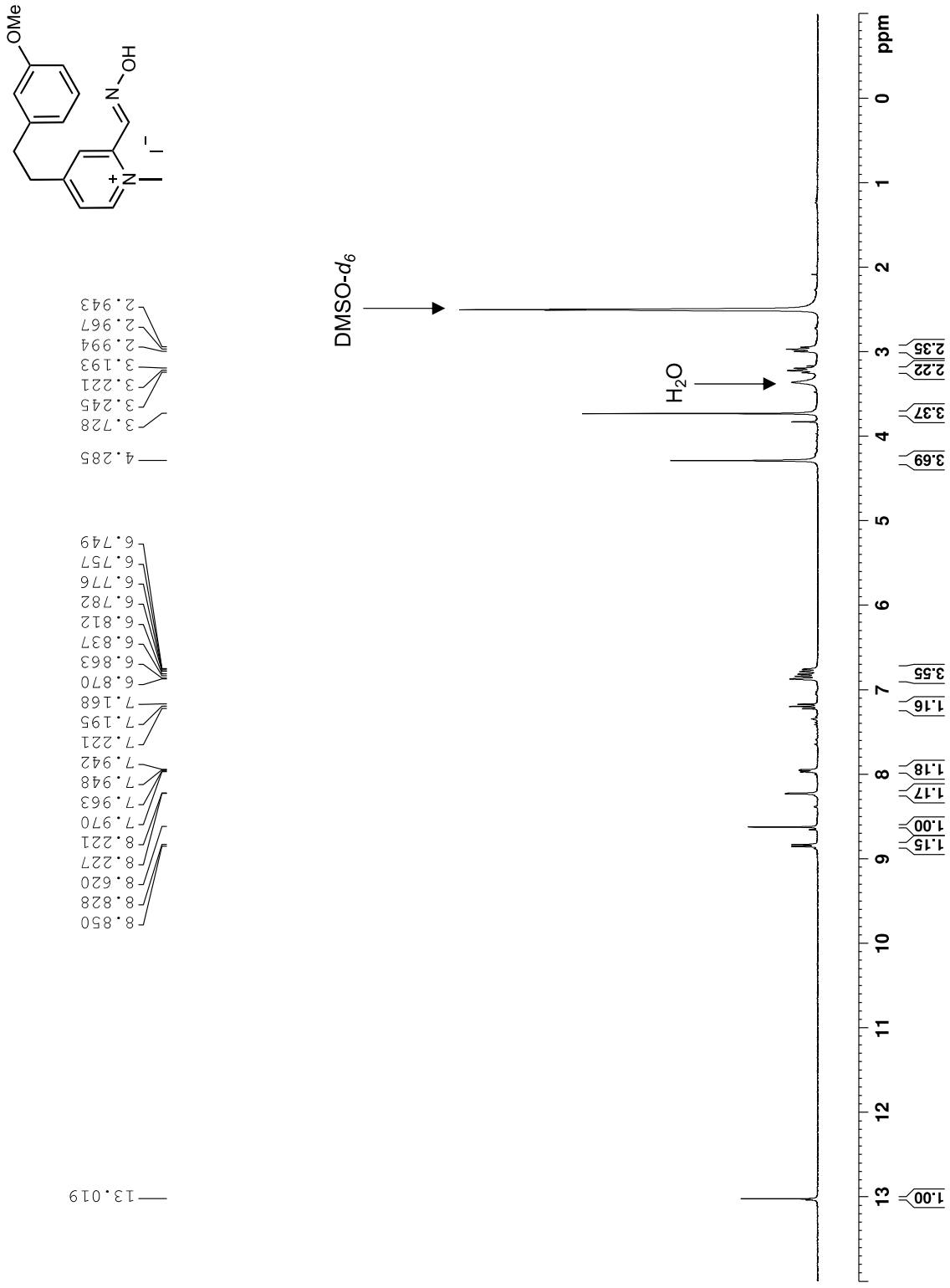

Spectrum 296. ^{1}H NMR for (*E*)-2-((hydroxyimino)methyl)-4-(3-methoxyphenethyl)-1-methylpyridin-1-ium iodide (**ADG4063**) (300 MHz, 293 K, DMSO-d_6).

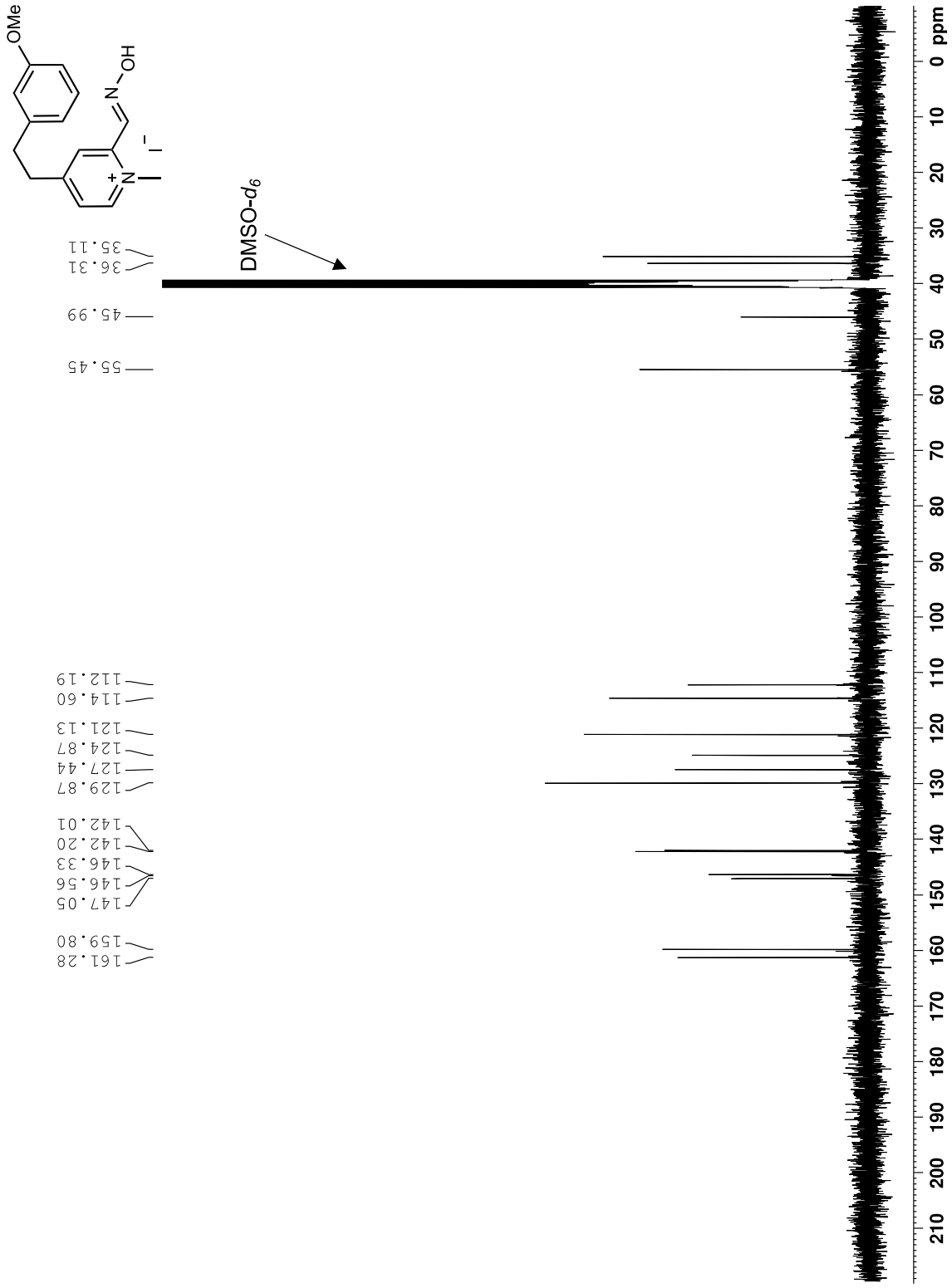

Spectrum 297. ^{13}C NMR for (*E*)-2-((hydroxyimino)methyl)-4-(3-methoxyphenethyl)-1-methylpyridin-1-ium iodide (**ADG4063**) (100 MHz, 293 K, DMSO-d_6).

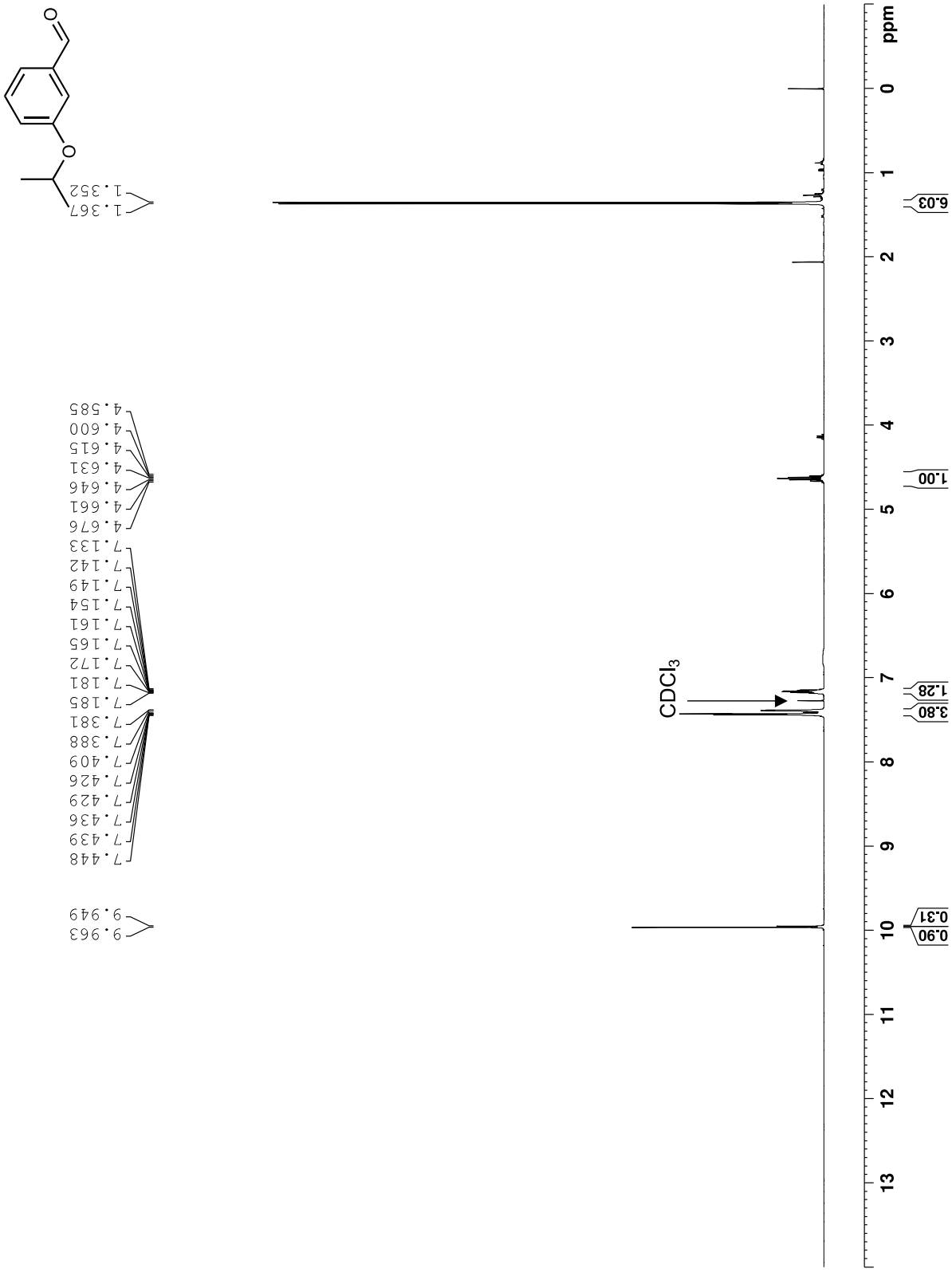

Spectrum 298. ^{1}H NMR of 3-isopropoxybenzaldehyde (400 MHz, 293 K, $CDCl_3$).

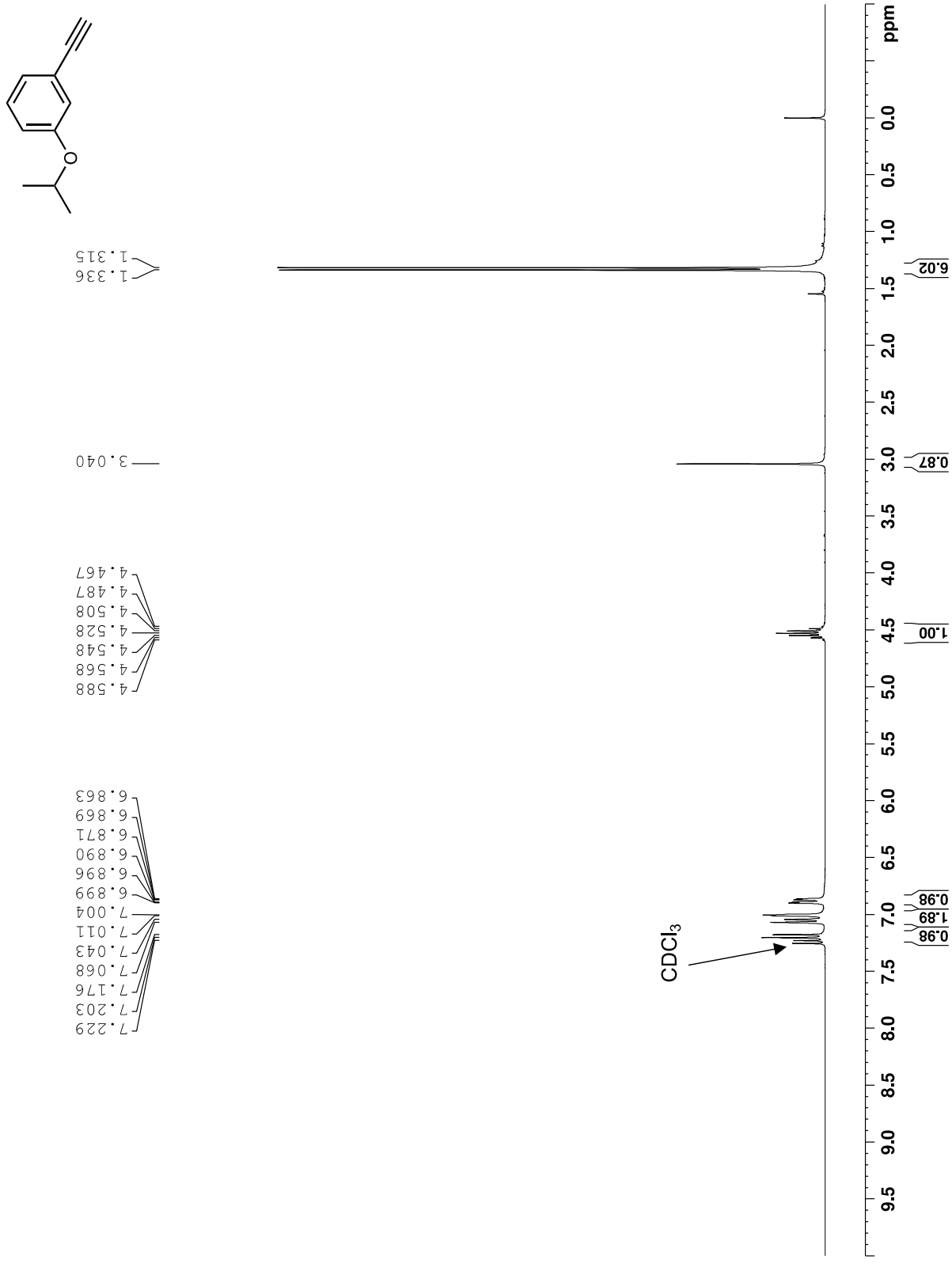

Spectrum 299. ^{1}H NMR for 1-ethynyl-3-isopropoxybenzene (300 MHz, 293 K, $CDCl_3$).

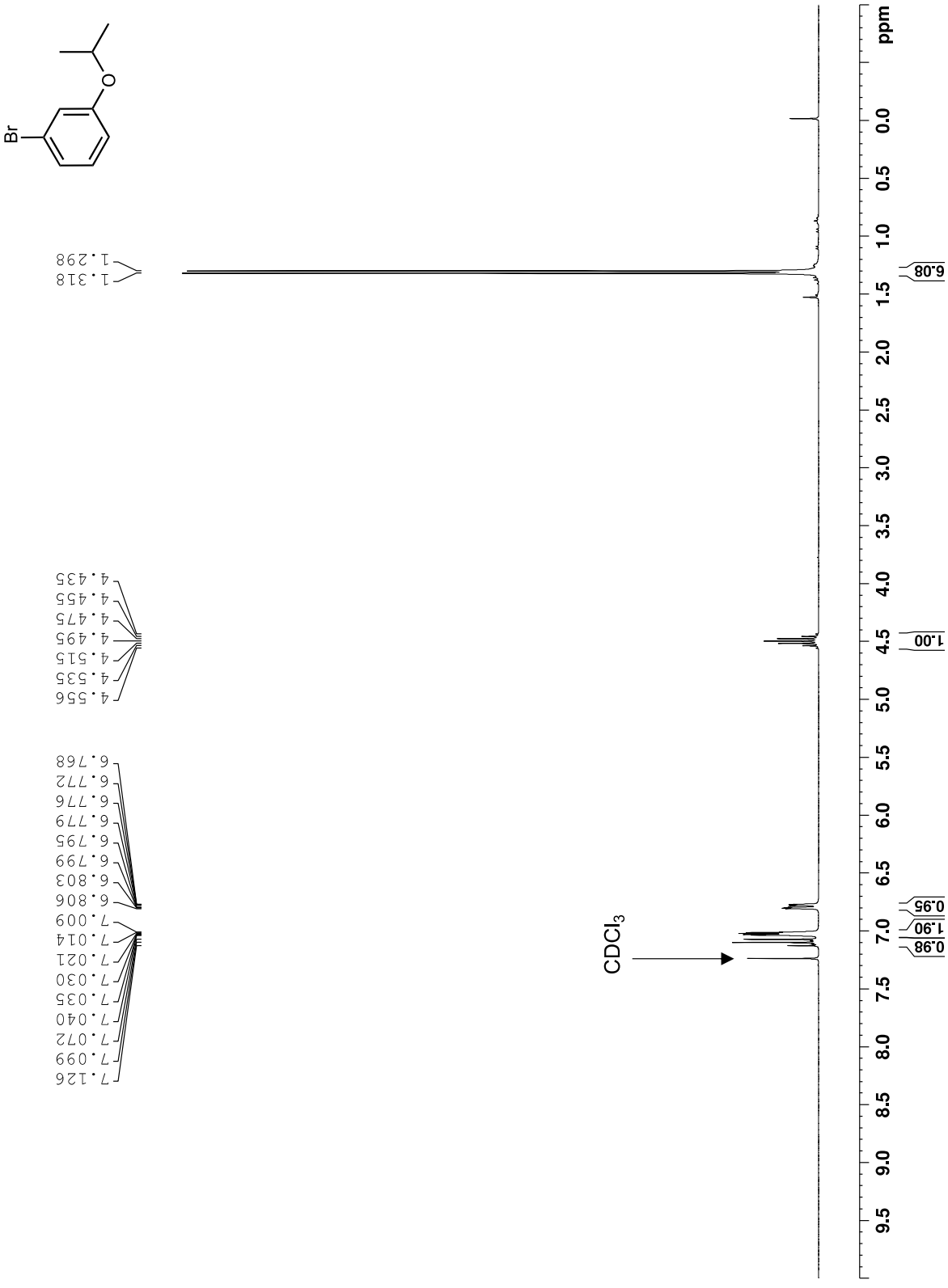

Spectrum 300. ^{1}H NMR for 1-bromo-3-isopropoxybenzene (300 MHz, 293 K, $CDCl_3$).

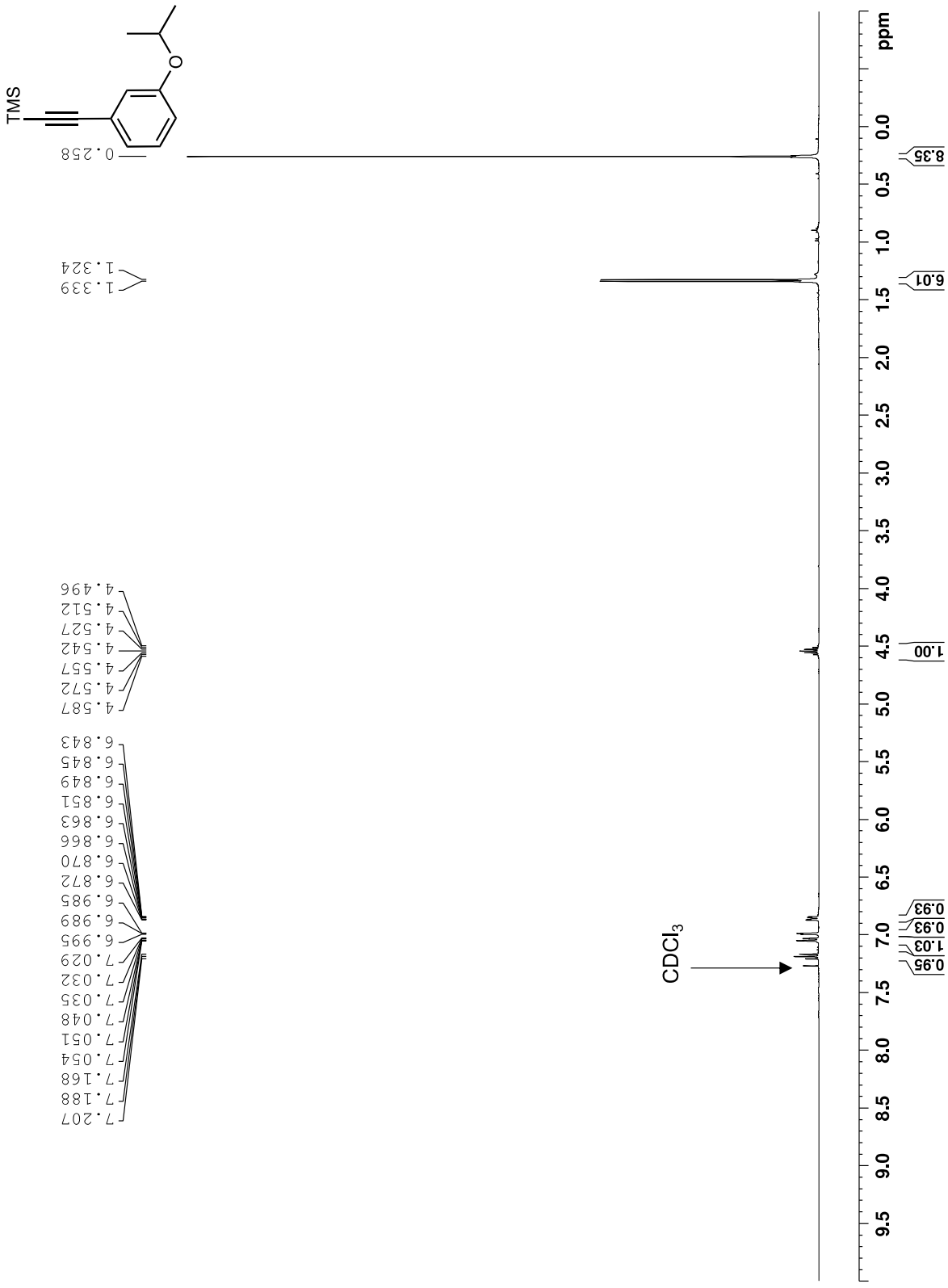

Spectrum 301. ^{1}H NMR for ((3-isopropoxyphenyl)ethynyl)trimethylsilane (400 MHz, 293 K, $CDCl_3$).

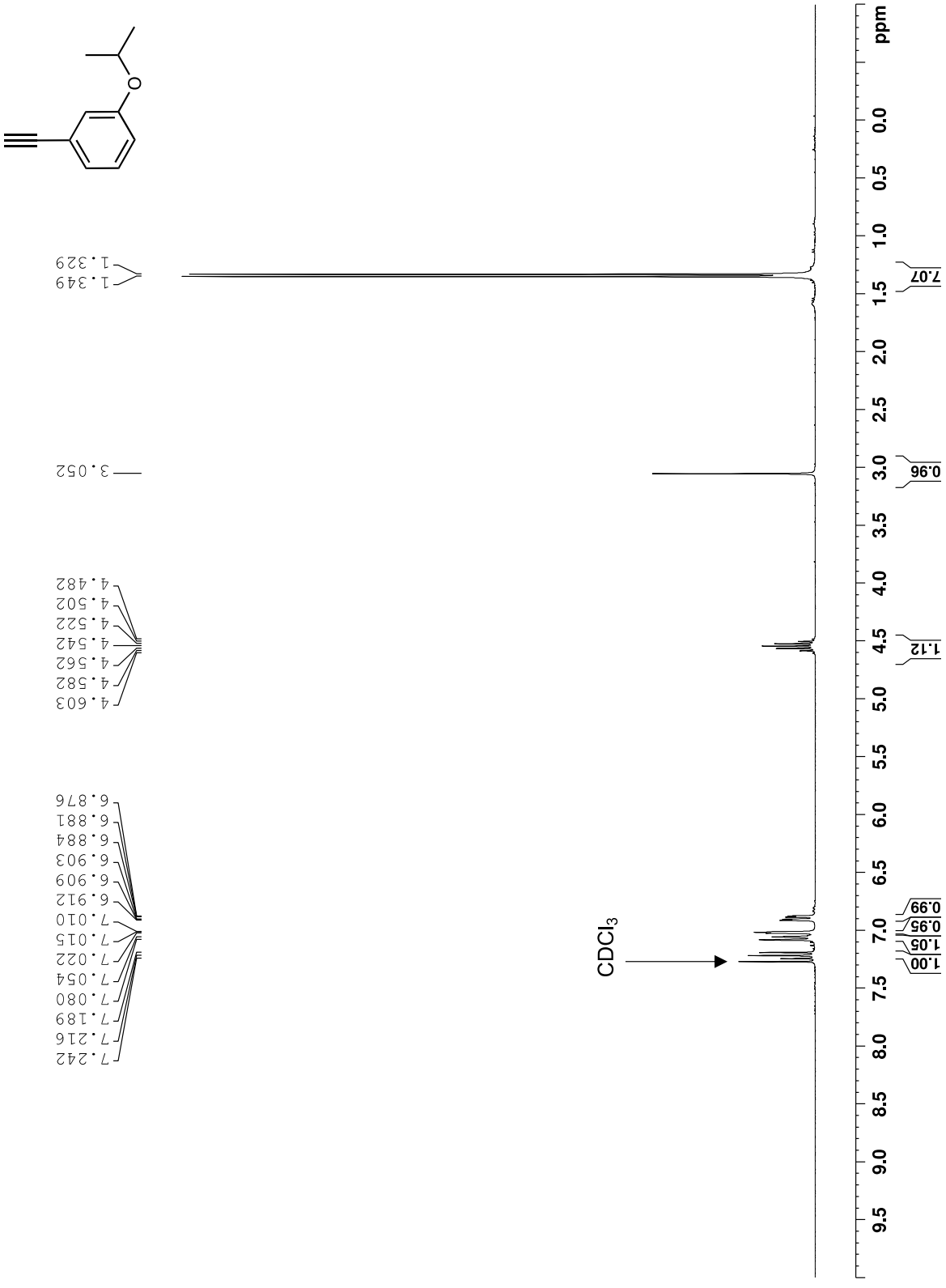

Spectrum 302. ^{1}H NMR for 1-ethynyl-3-isopropoxybenzene (300 MHz, 293 K, $CDCl_3$).

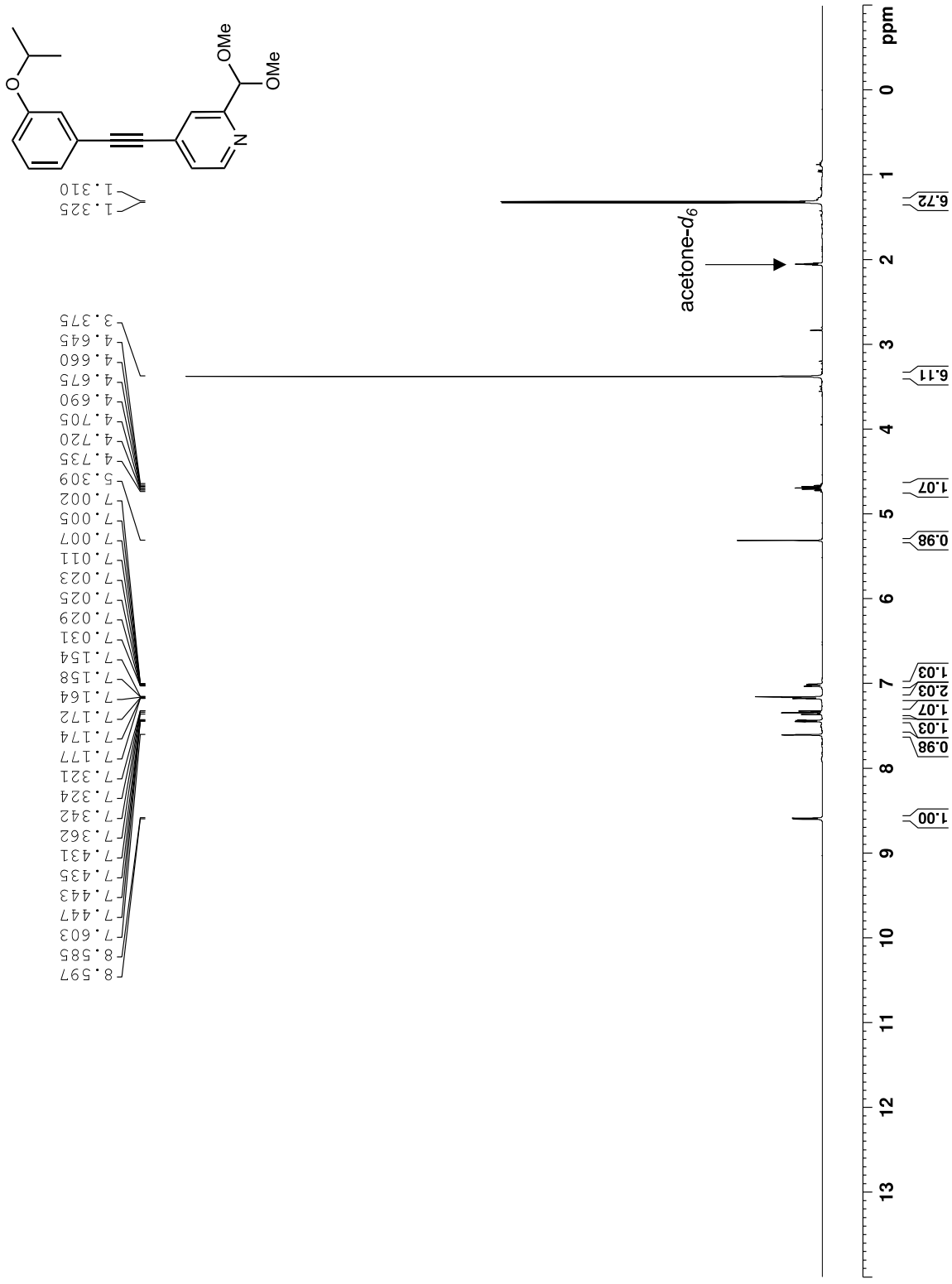

Spectrum 303. ^{1}H NMR for 2-(dimethoxymethyl)-4-((3-isopropoxyphenyl)ethynyl)pyridine (400 MHz, 293 K, acetone-d_6).

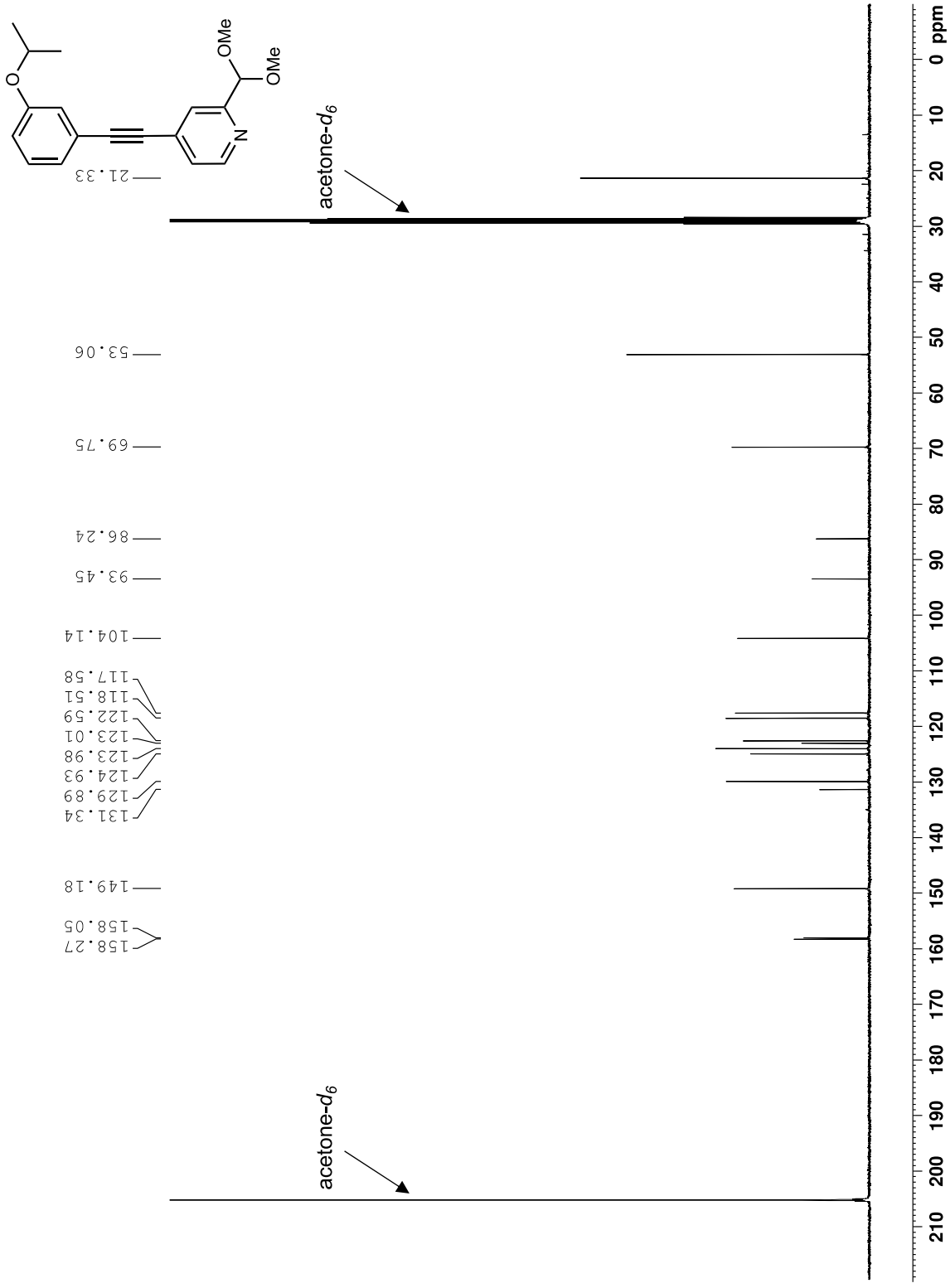

Spectrum 304. ^{13}C NMR for 2-(dimethoxymethyl)-4-((3-isopropoxyphenyl)ethynyl)pyridine (100 MHz, 293 K, acetone-d_6).

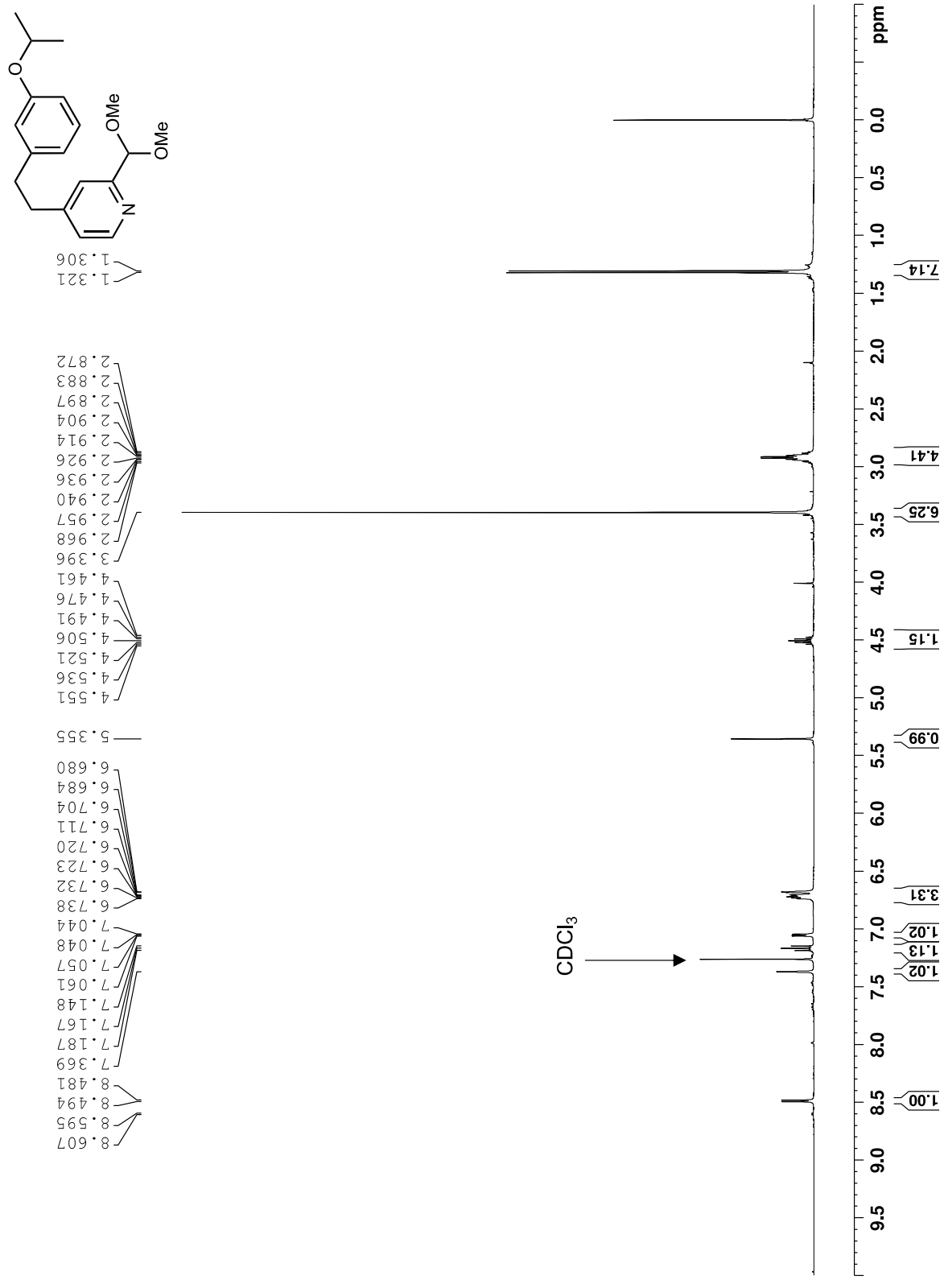

Spectrum 305. ^{1}H NMR for 2-(dimethoxymethyl)-4-(3-isopropoxyphenethyl)pyridine (400 MHz, 293 K, $CDCl_3$).

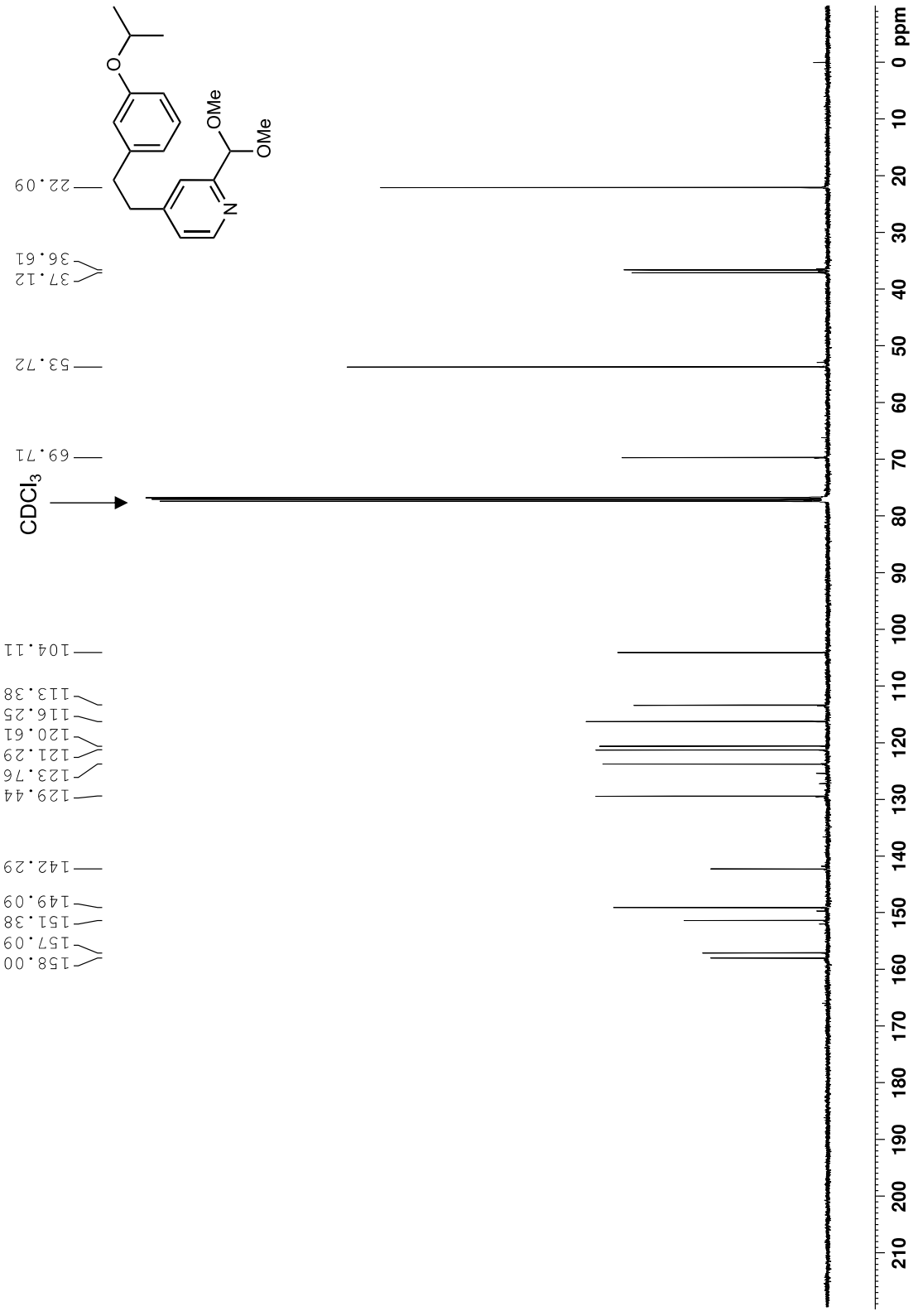

Spectrum 306. ^{13}C NMR for 2-(dimethoxymethyl)-4-(3-isopropoxyphenethyl)pyridine (100 MHz, 293 K, $CDCl_3$).

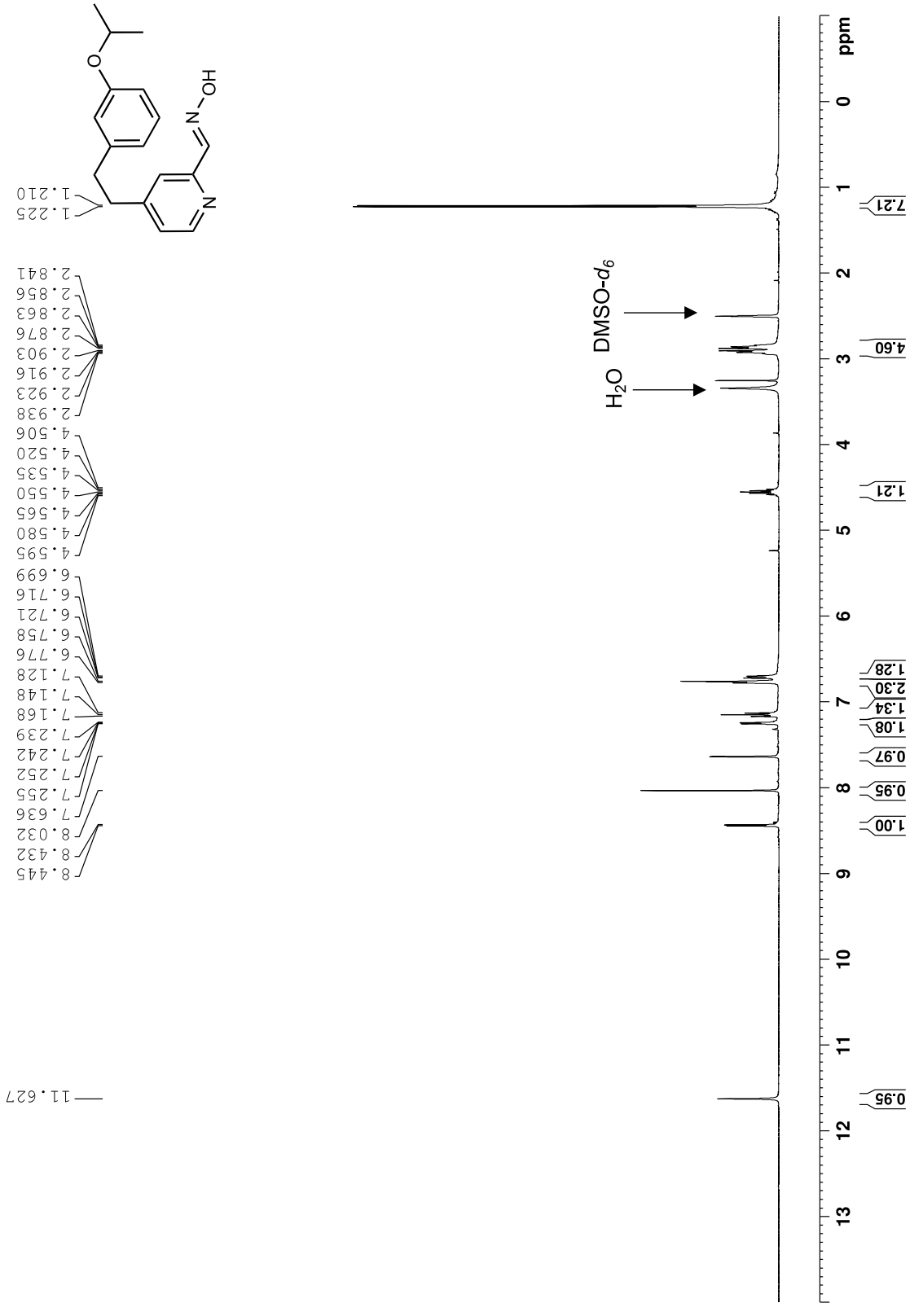

Spectrum 307. ^{1}H NMR for (*E*)-4-(3-isopropoxyphenethyl)picolinaldehyde oxime (400 MHz, 293 K, DMSO-d_6).

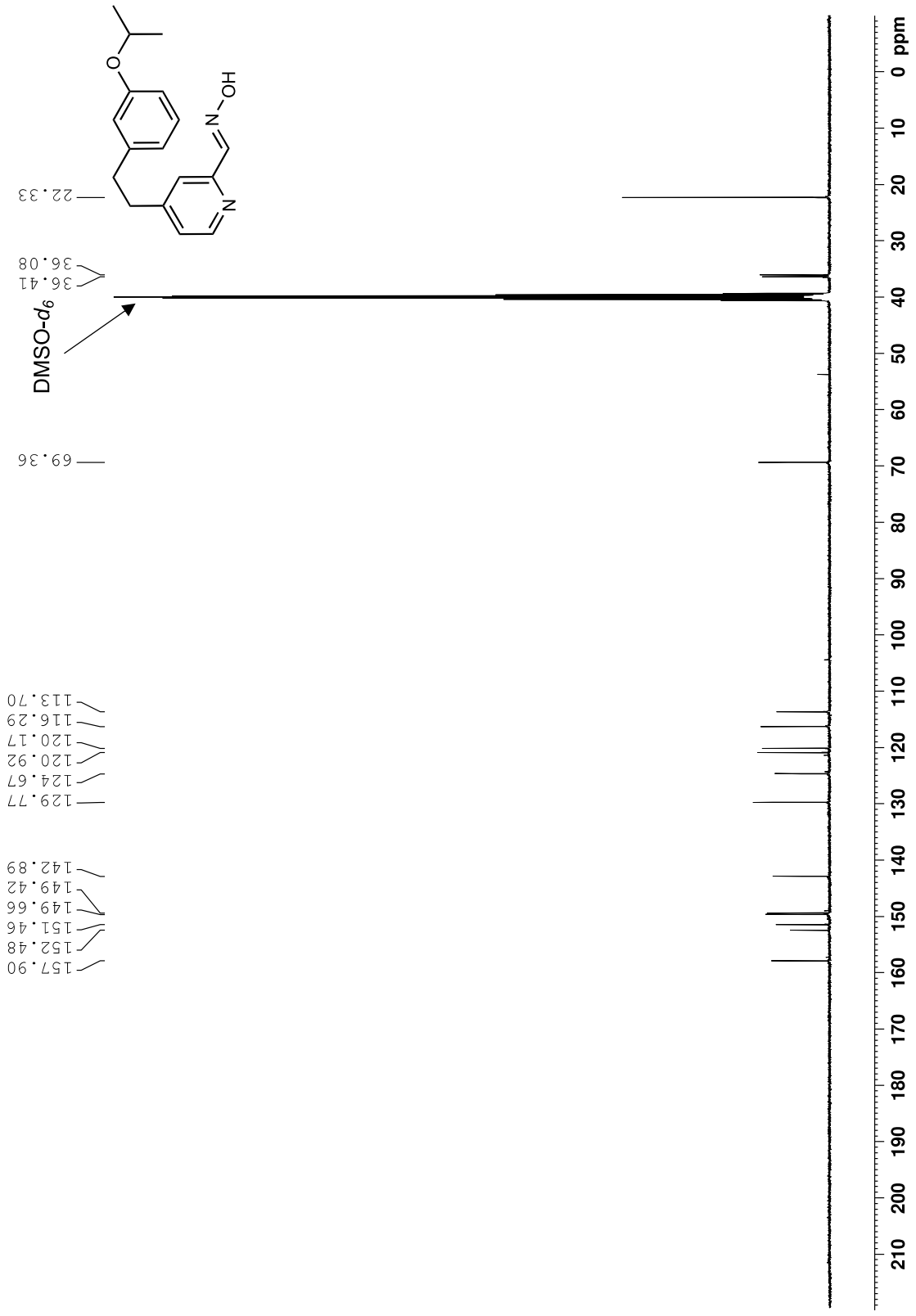

Spectrum 308. ^{13}C NMR for (*E*)-4-(3-isopropoxyphenethyl)picolinaldehyde oxime (100 MHz, 293 K, DMSO-d_6).

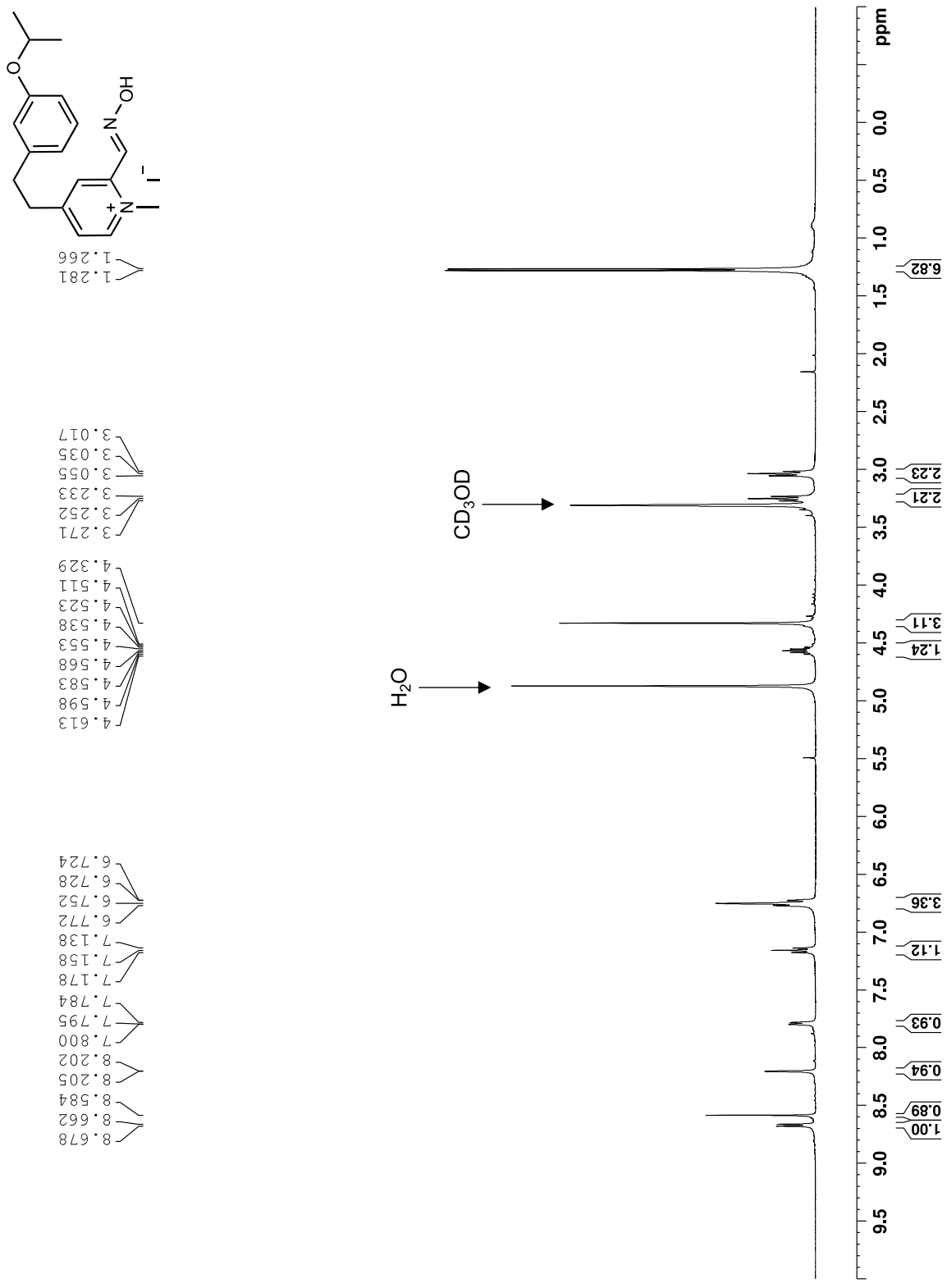

Spectrum 309. ^{1}H NMR for (*E*)-2-((hydroxyimino)methyl)-4-(3-isopropoxyphenethyl)-1-methylpyridin-1-ium iodide (**ADG4111**) (400 MHz, 293 K, CD_3OD).

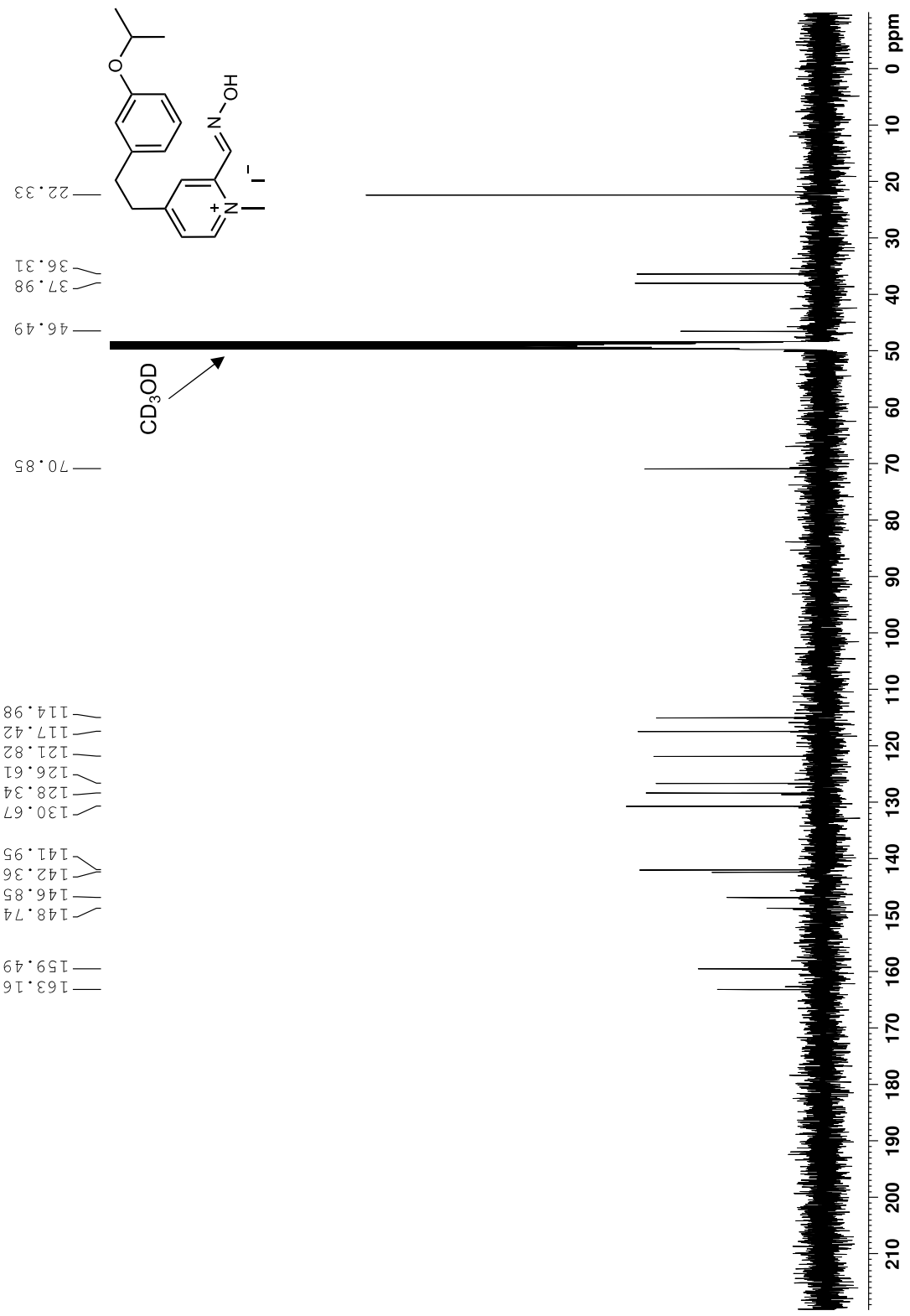

Spectrum 310. ^{13}C NMR for (*E*)-2-((hydroxyimino)methyl)-4-(3-isopropoxyphenethyl)-1-methylpyridin-1-ium iodide (**ADG4111**) (100 MHz, 293 K, CD_3OD).

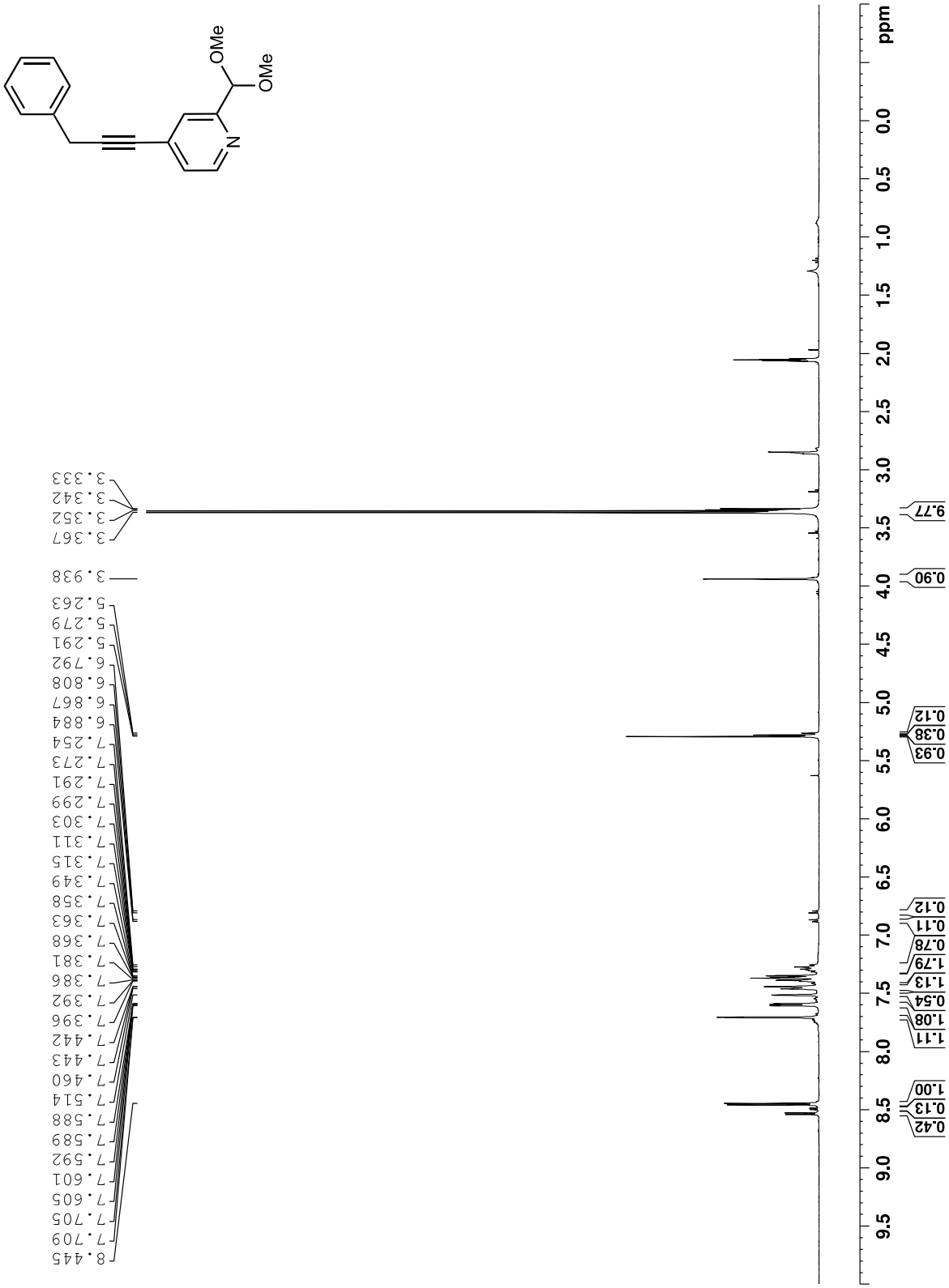

Spectrum 311. ^{1}H NMR for 2-(dimethoxymethyl)-4-(3-phenylprop-1-yn-1-yl)pyridine (400 MHz, 293 K, acetone-d_6).

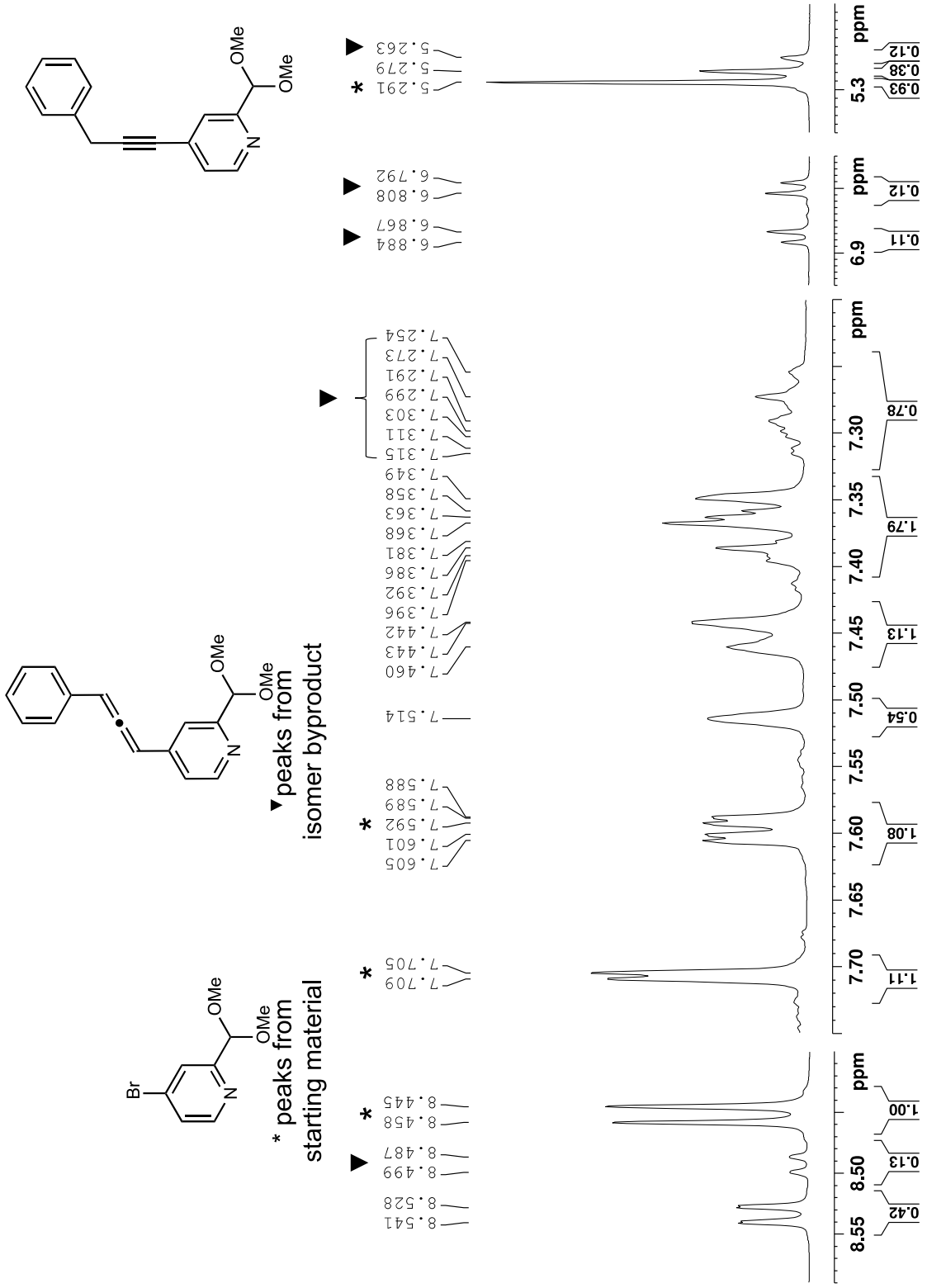

Spectrum 312. Expanded ^{1}H NMR for 2-(dimethoxymethyl)-4-(3-phenylprop-1-yn-1-yl)pyridine (400 MHz, 293 K, acetone-d_6).

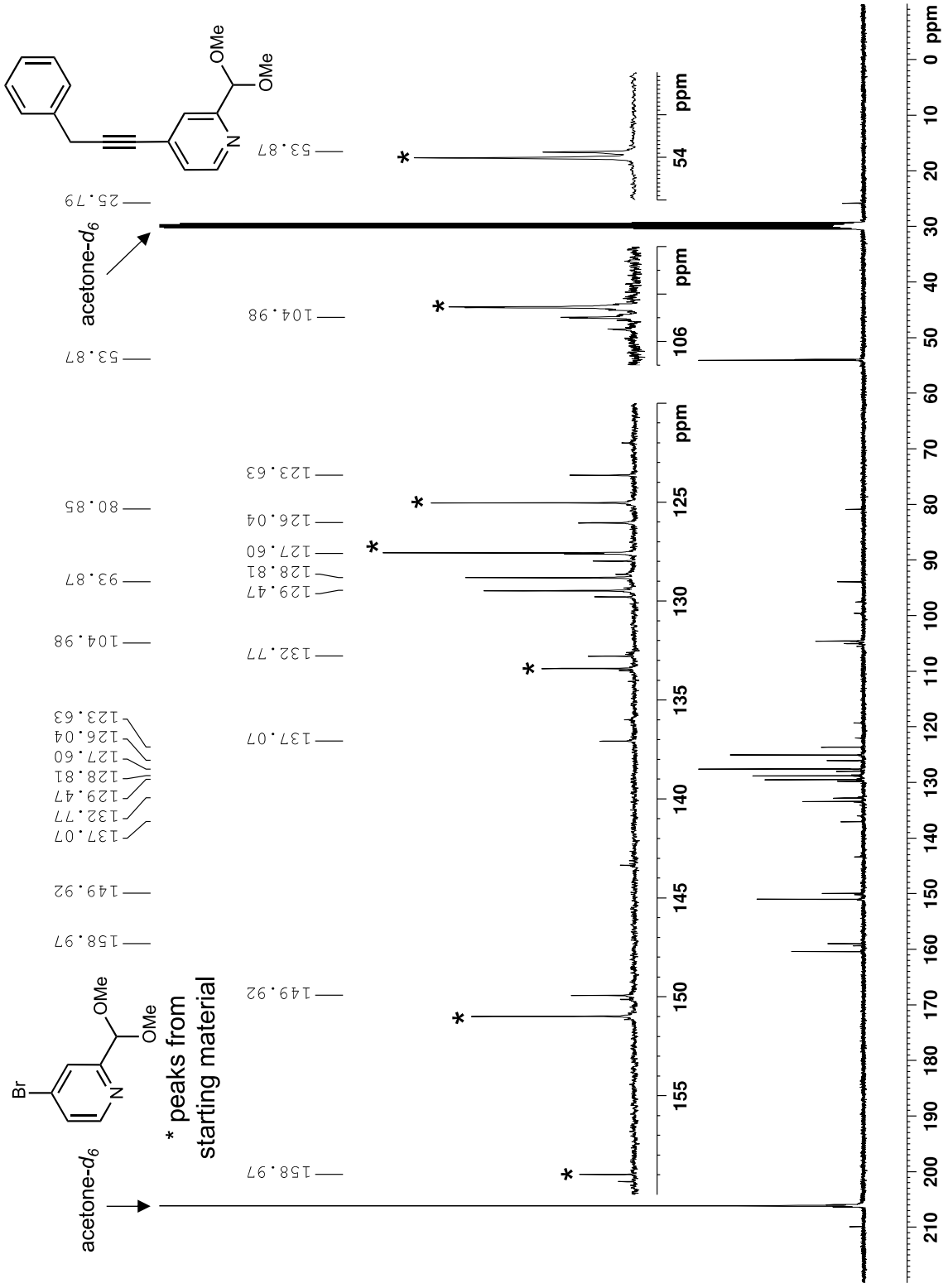

Spectrum 313. ^{13}C NMR for 2-(dimethoxymethyl)-4-(3-phenylprop-1-yn-1-yl)pyridine (100 MHz, 293 K, acetone-d_6).

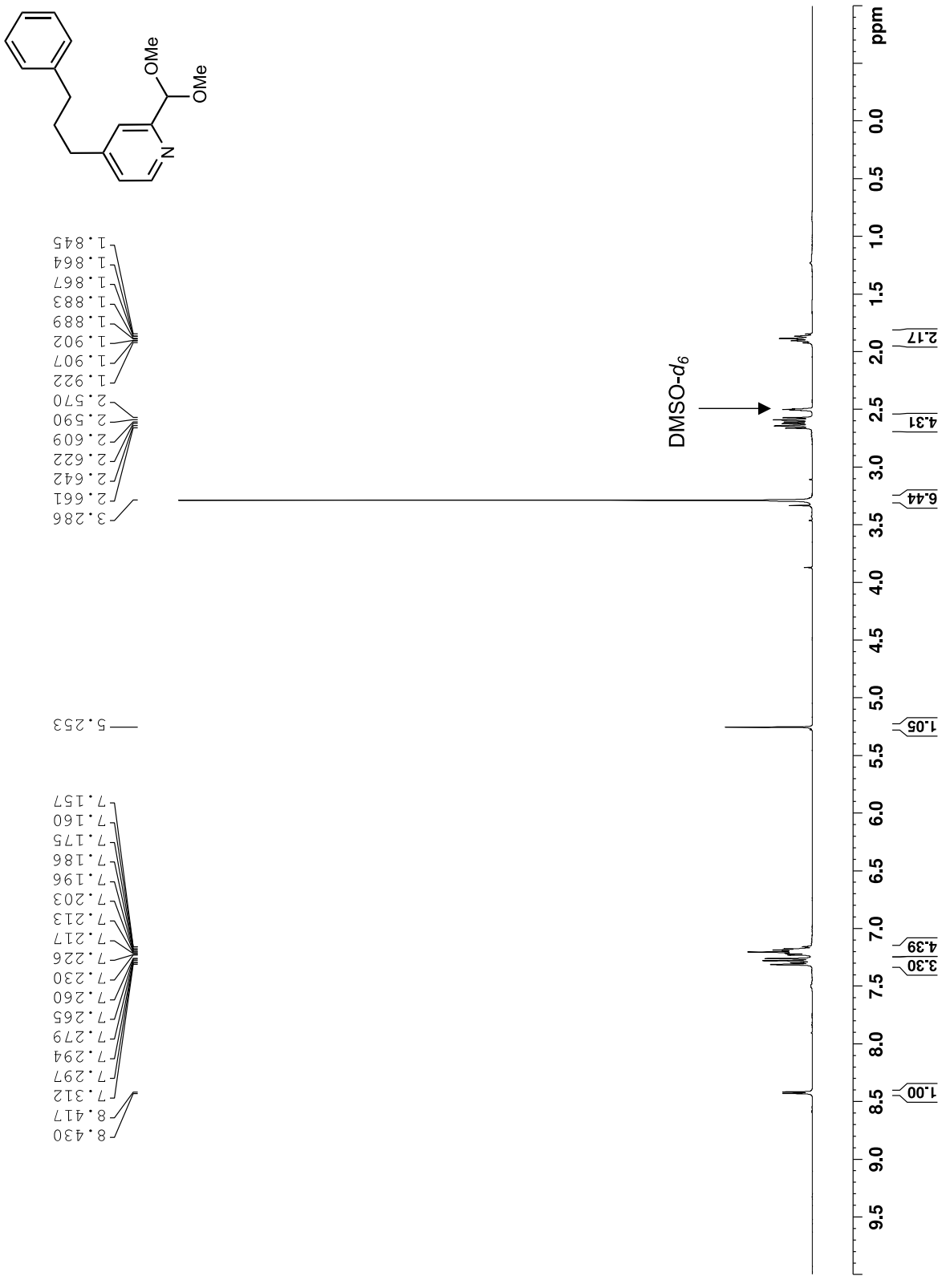

Spectrum 314. ^{1}H NMR for 2-(dimethoxymethyl)-4-(3-phenylpropyl)pyridine (400 MHz, 293 K, DMSO-d_6).

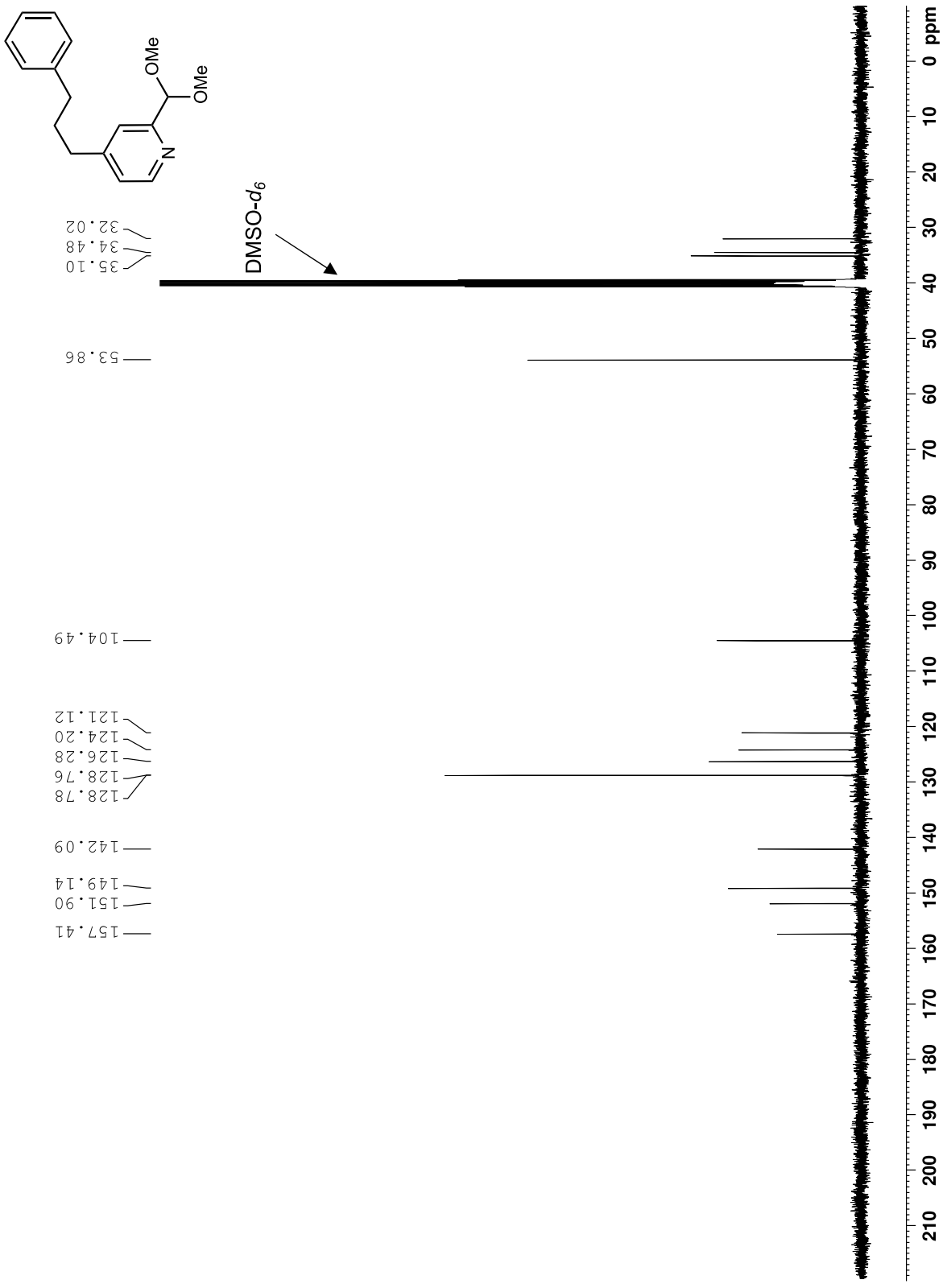

Spectrum 315. ^{13}C NMR for 2-(dimethoxymethyl)-4-(3-phenylpropyl)pyridine (100 MHz, 293 K, DMSO-d_6).

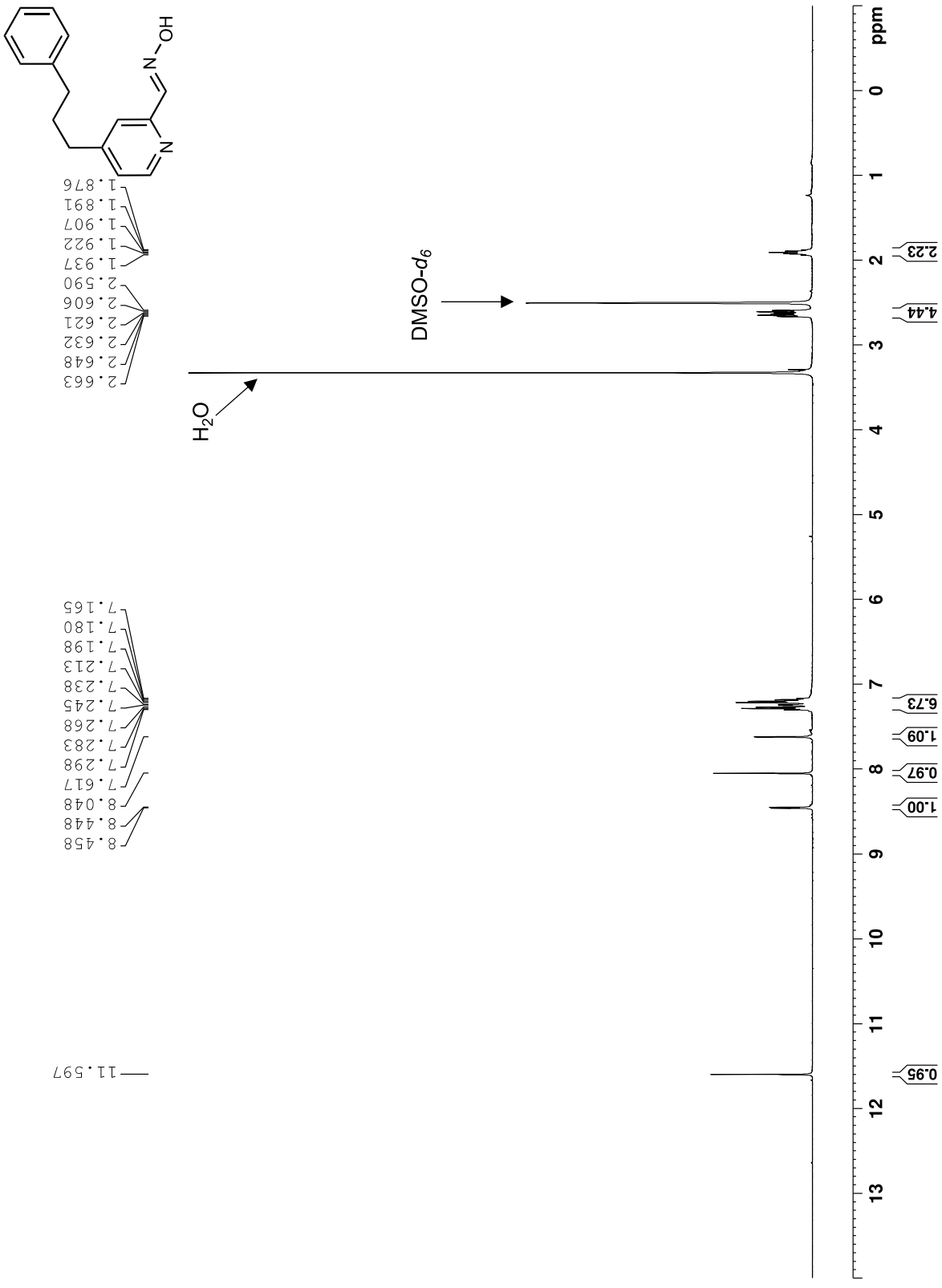

Spectrum 316. ^{1}H NMR for (*E*)-4-(3-phenylpropyl)picolinaldehyde oxime (500 MHz, 293 K, DMSO-d_6).

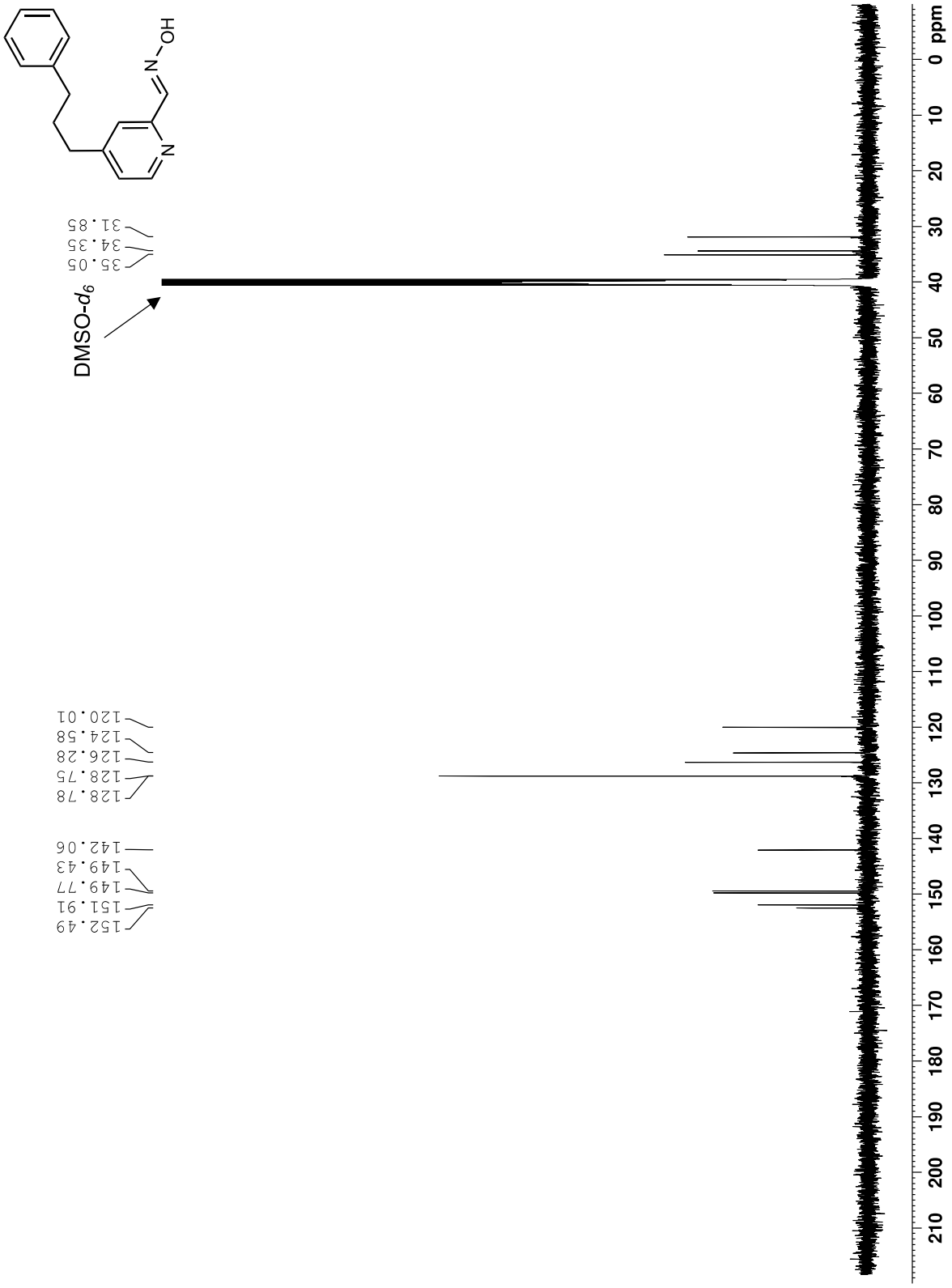

Spectrum 317. ^{13}C NMR for (*E*)-4-(3-phenylpropyl)picolinaldehyde oxime (125 MHz, 293 K, DMSO-d_6).

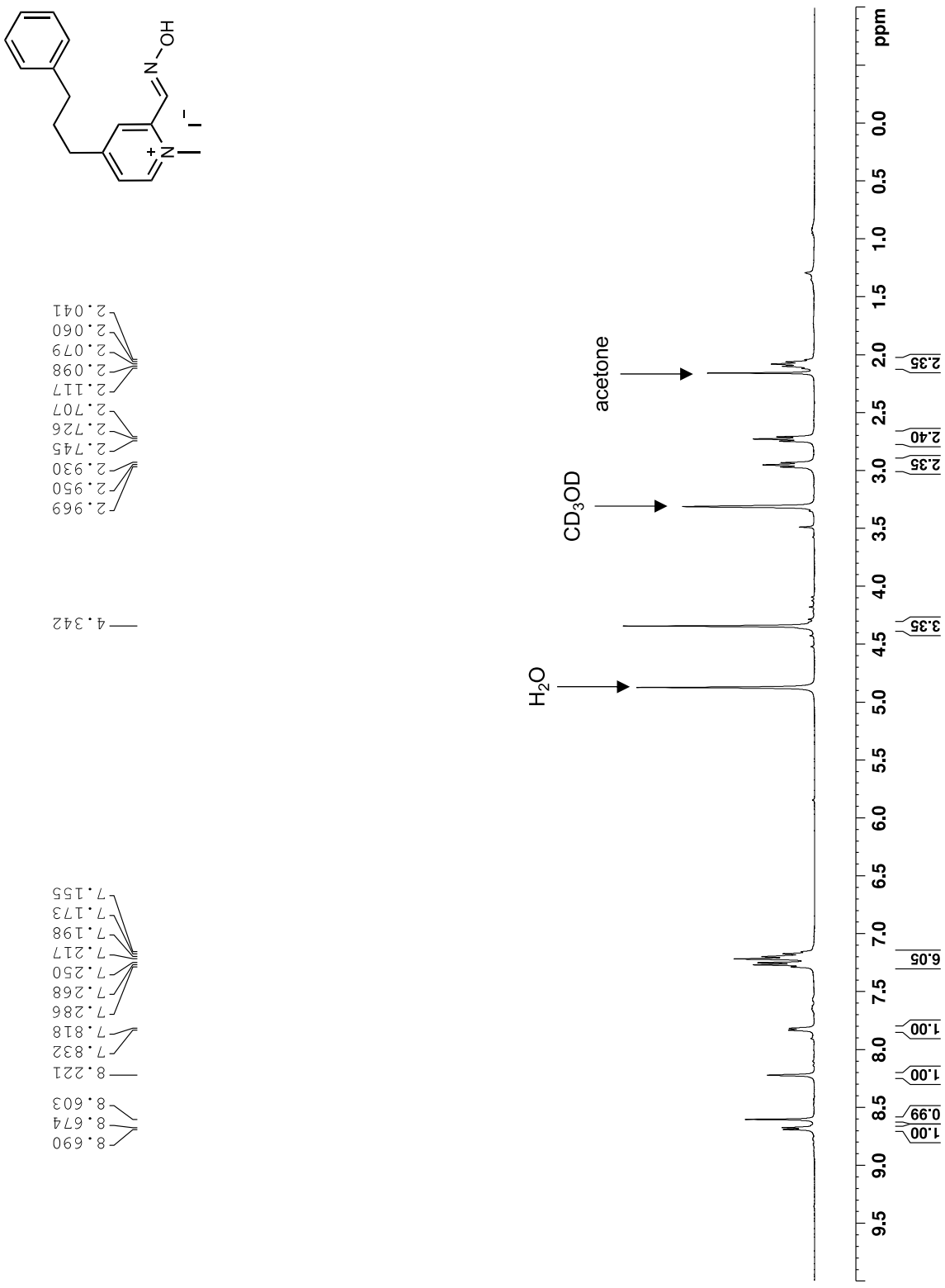

Spectrum 318. ^{1}H NMR for *(E)*-2-((hydroxyimino)methyl)-1-methyl-4-(3-phenylpropyl)pyridin-1-ium (**ADG4300**) (400 MHz, 293 K, CD_3OD).

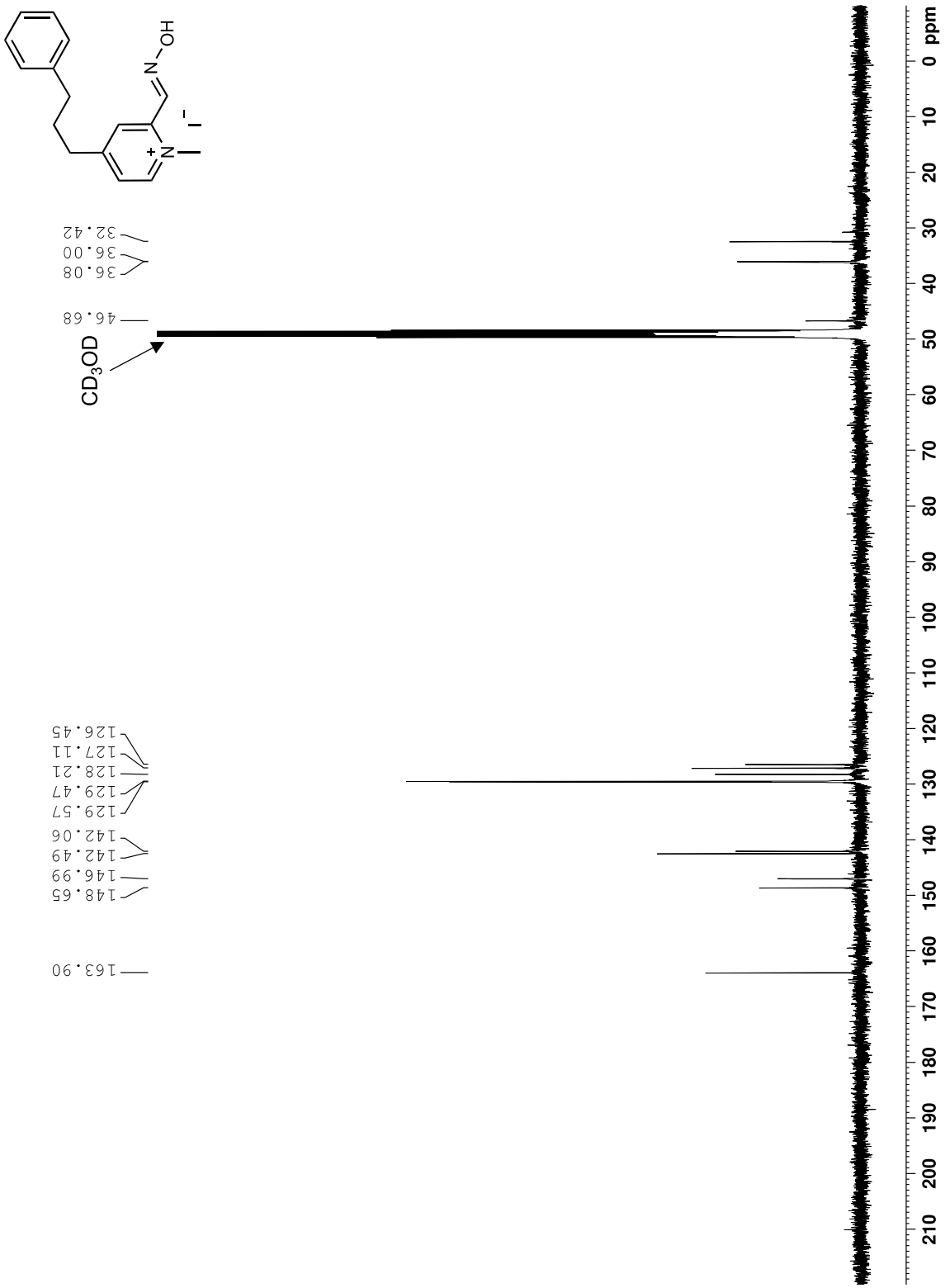

Spectrum 319. ^{13}C NMR for *(E)*-2-((hydroxyimino)methyl)-1-methyl-4-(3-phenylpropyl)pyridin-1-ium (**ADG4300**) (100 MHz, 293 K, CD_3OD).

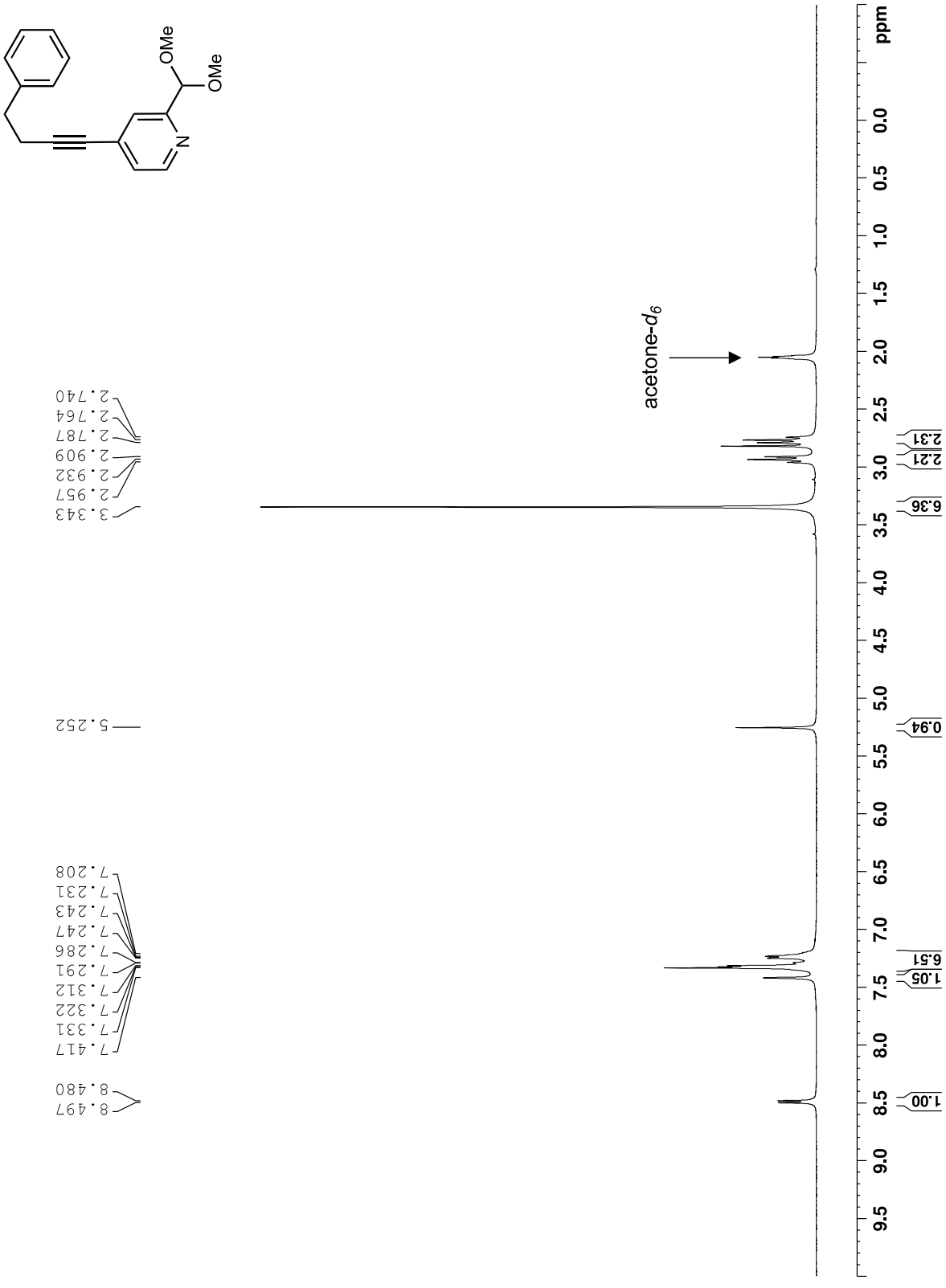

Spectrum 320. ^{1}H NMR for 2-(dimethoxymethyl)-4-(4-phenylbut-1-yn-1-yl)pyridine (300 MHz, 293 K, acetone-d_6).

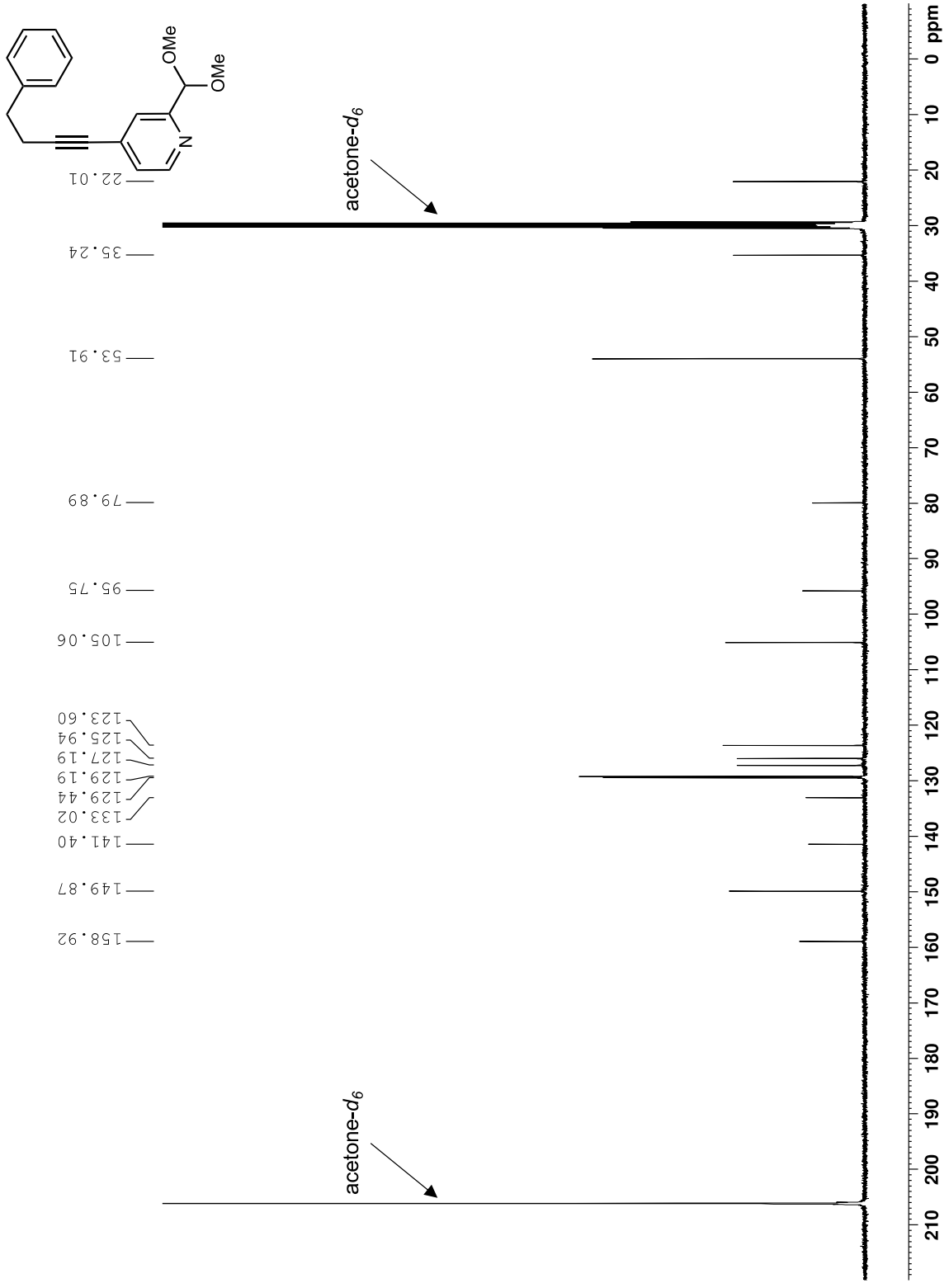

Spectrum 321. ^{13}C NMR for 2-(dimethoxymethyl)-4-(4-phenylbut-1-yn-1-yl)pyridine (100 MHz, 293 K, acetone-d_6).

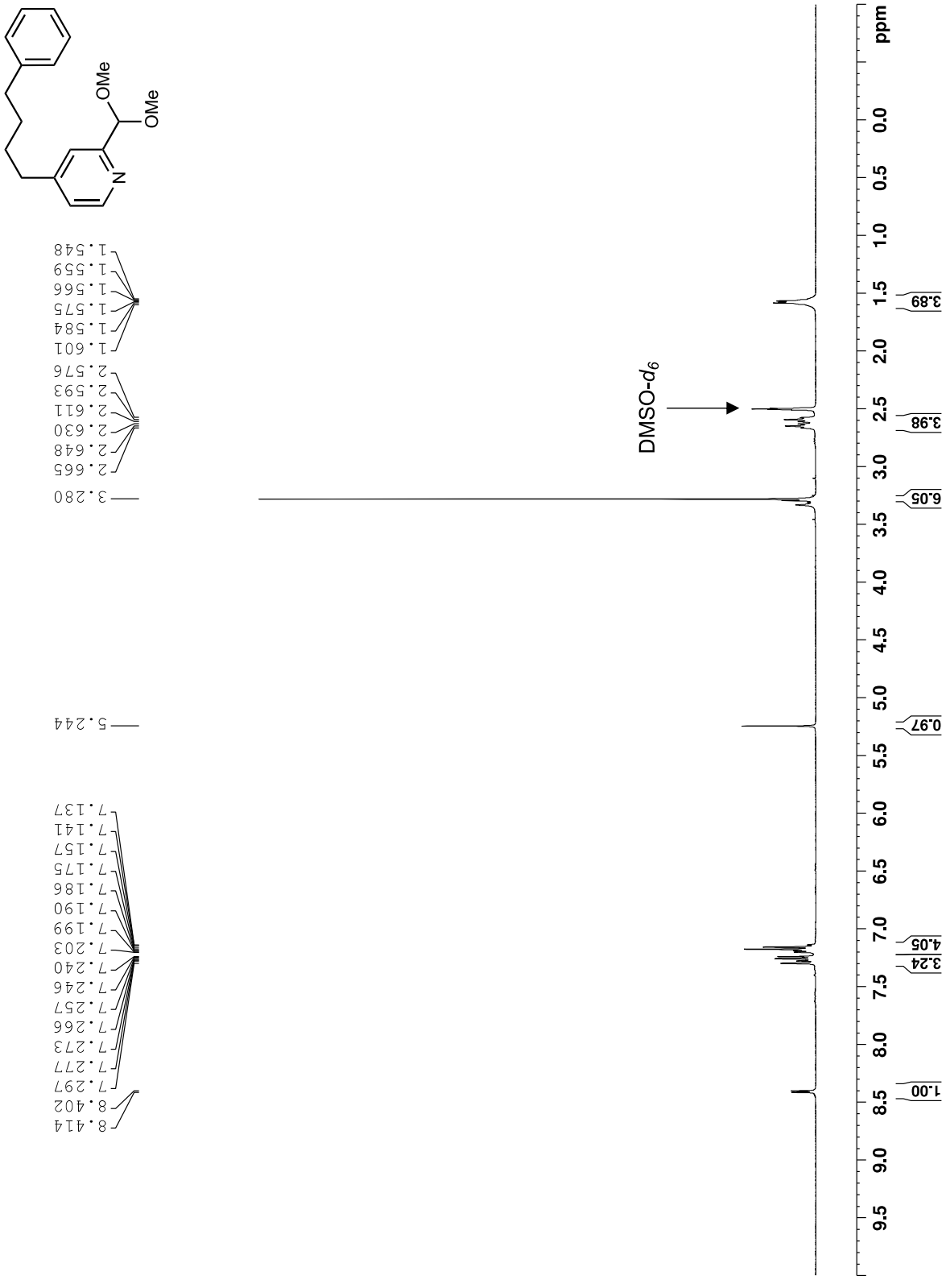

Spectrum 322. ^{1}H NMR for 2-(dimethoxymethyl)-4-(4-phenylbutyl)pyridine (400 MHz, 293 K, DMSO-d_6).

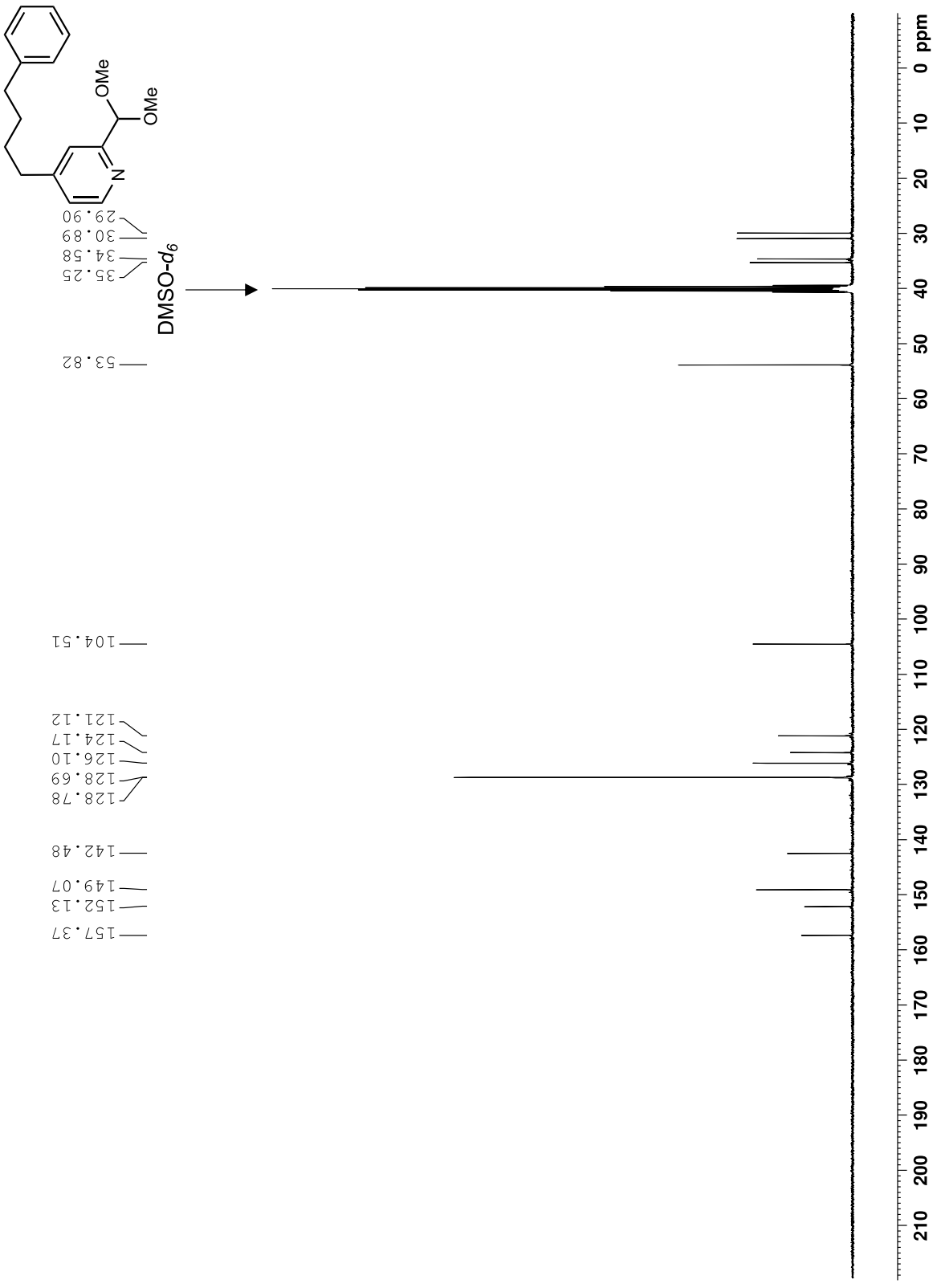

Spectrum 323. ^{13}C NMR for 2-(dimethoxymethyl)-4-(4-phenylbutyl)pyridine (100 MHz, 293 K, DMSO-d_6).

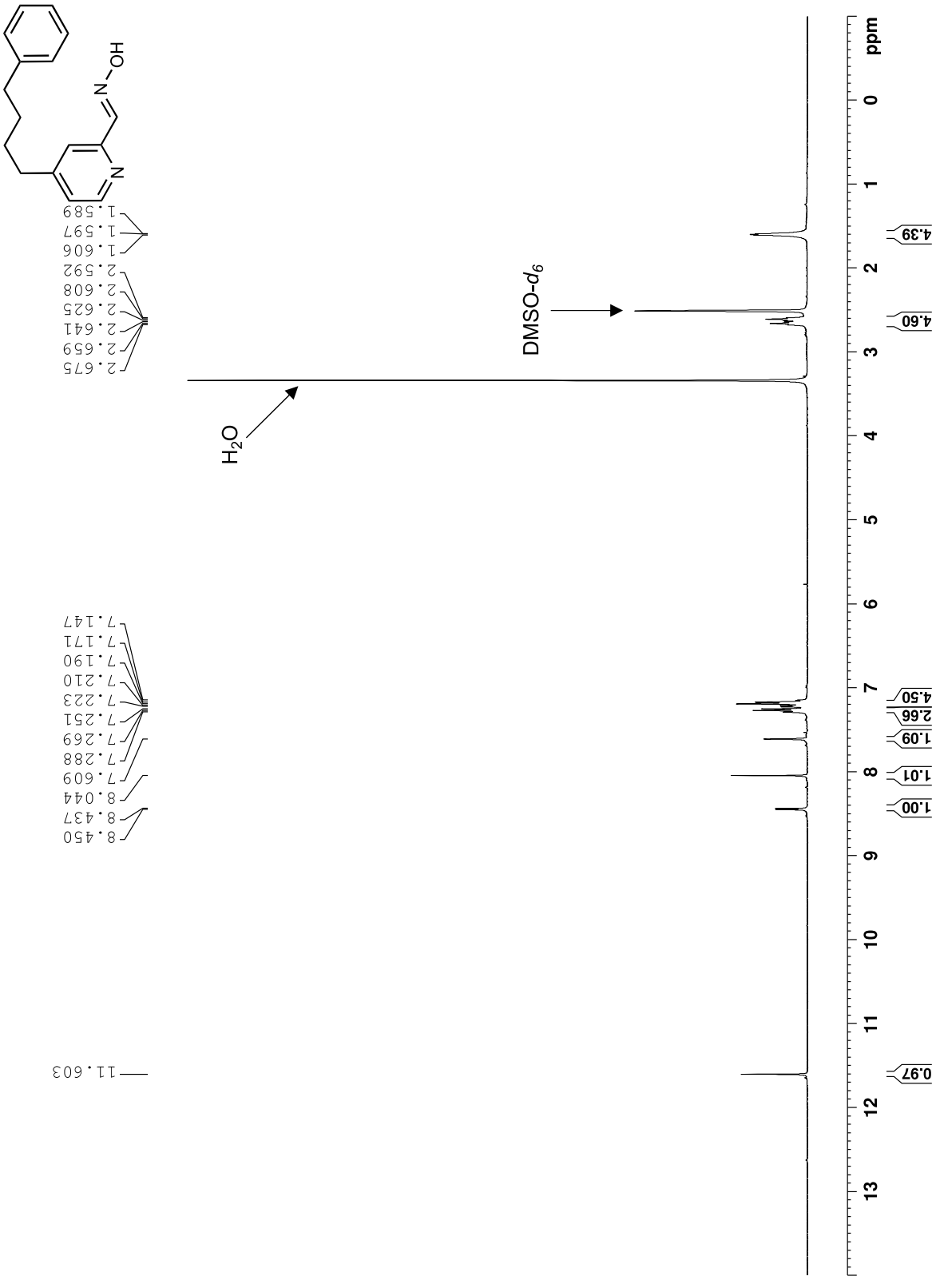

Spectrum 324. ^{1}H NMR for (*E*)-4-(4-phenylbutyl)picolinaldehyde oxime (400 MHz, 293 K, DMSO-d_6).

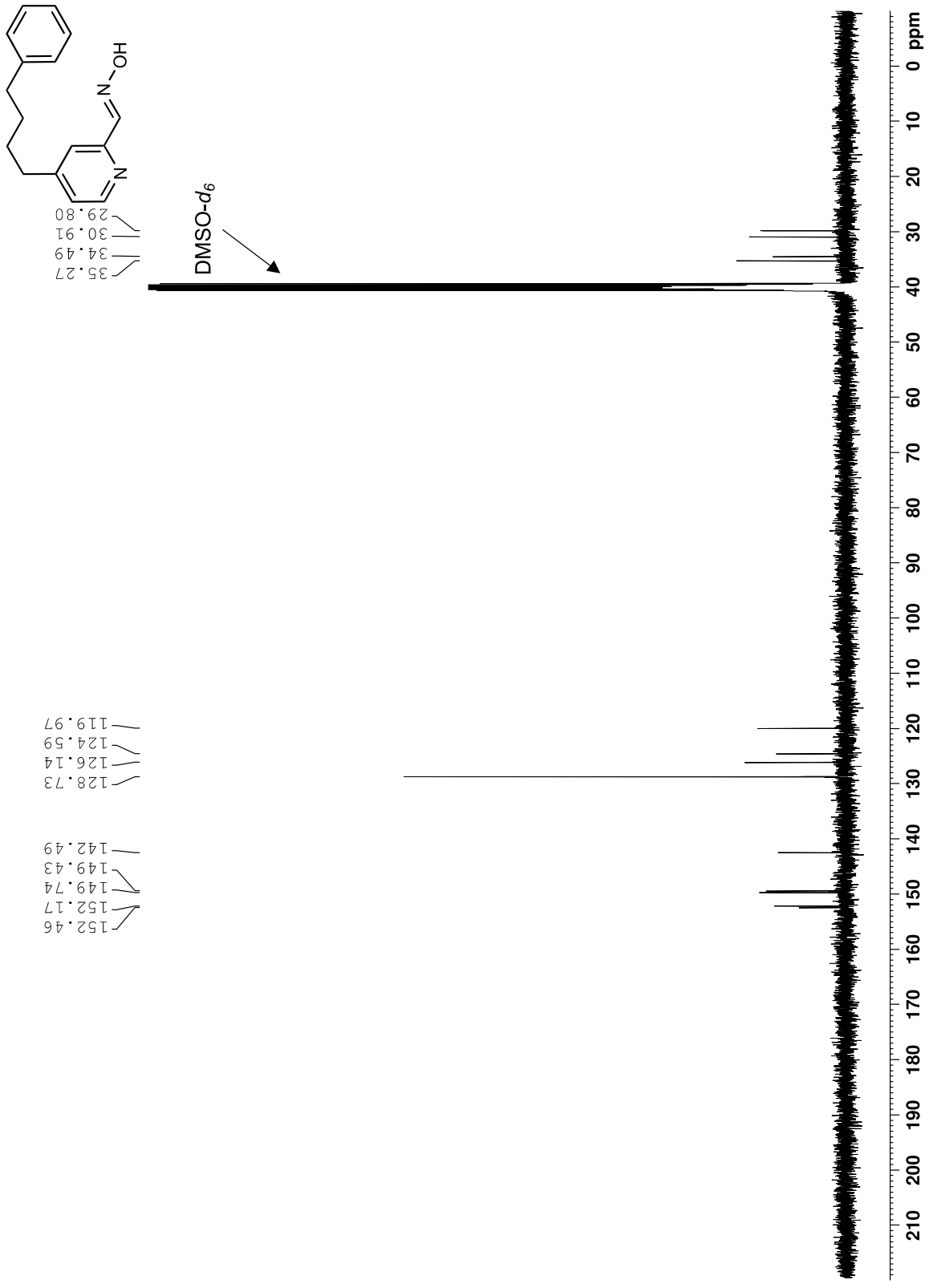

Spectrum 325. ^{13}C NMR for (*E*)-4-(4-phenylbutyl)picolinaldehyde oxime (100 MHz, 293 K, DMSO-d_6).

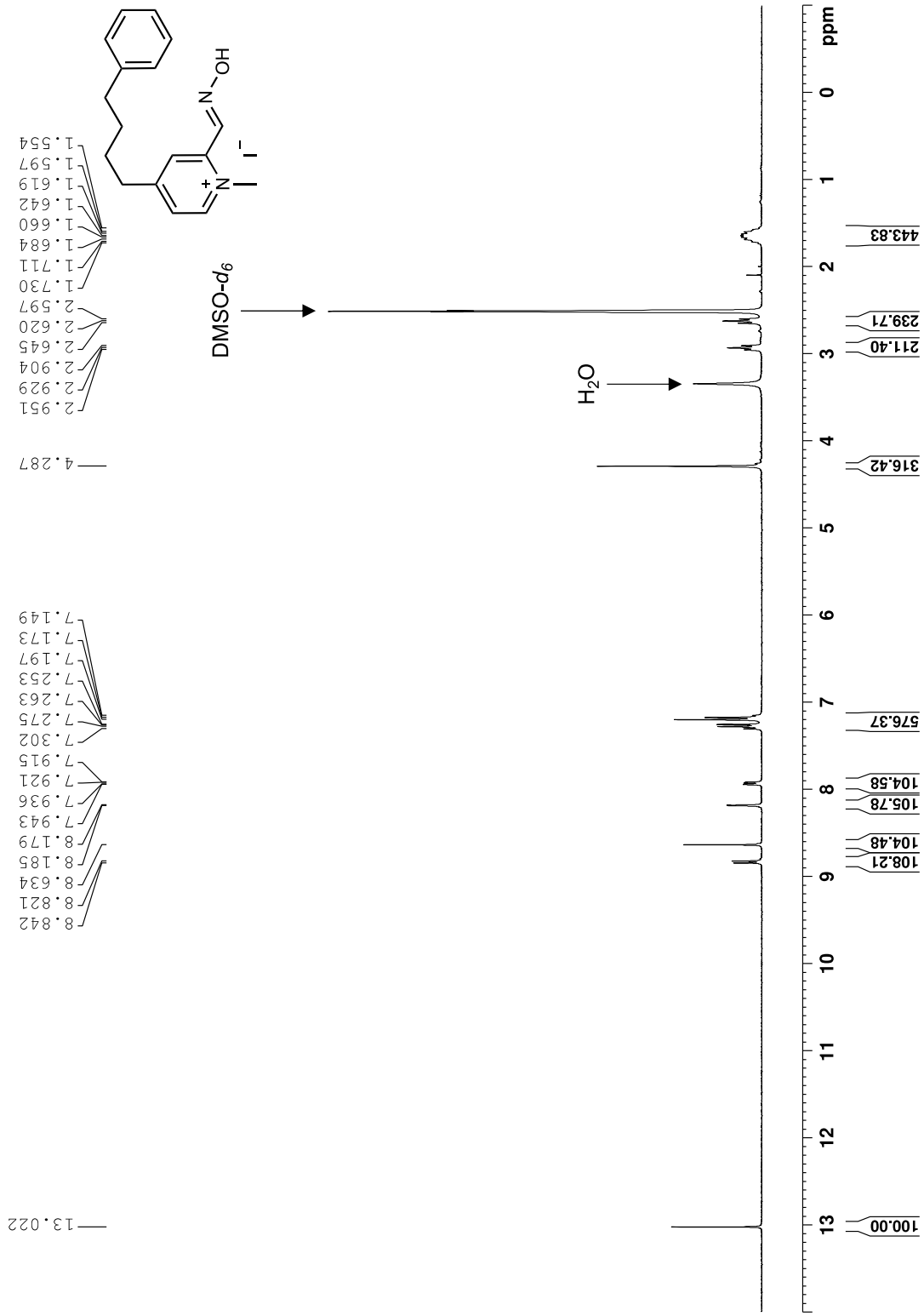

Spectrum 326. ^{1}H NMR for (*E*)-2-((hydroxyimino)methyl)-1-methyl-4-(4-phenylbutyl)pyridin-1-ium iodide (**ADG4244**) (300 MHz, 293 K, DMSO-d_6).

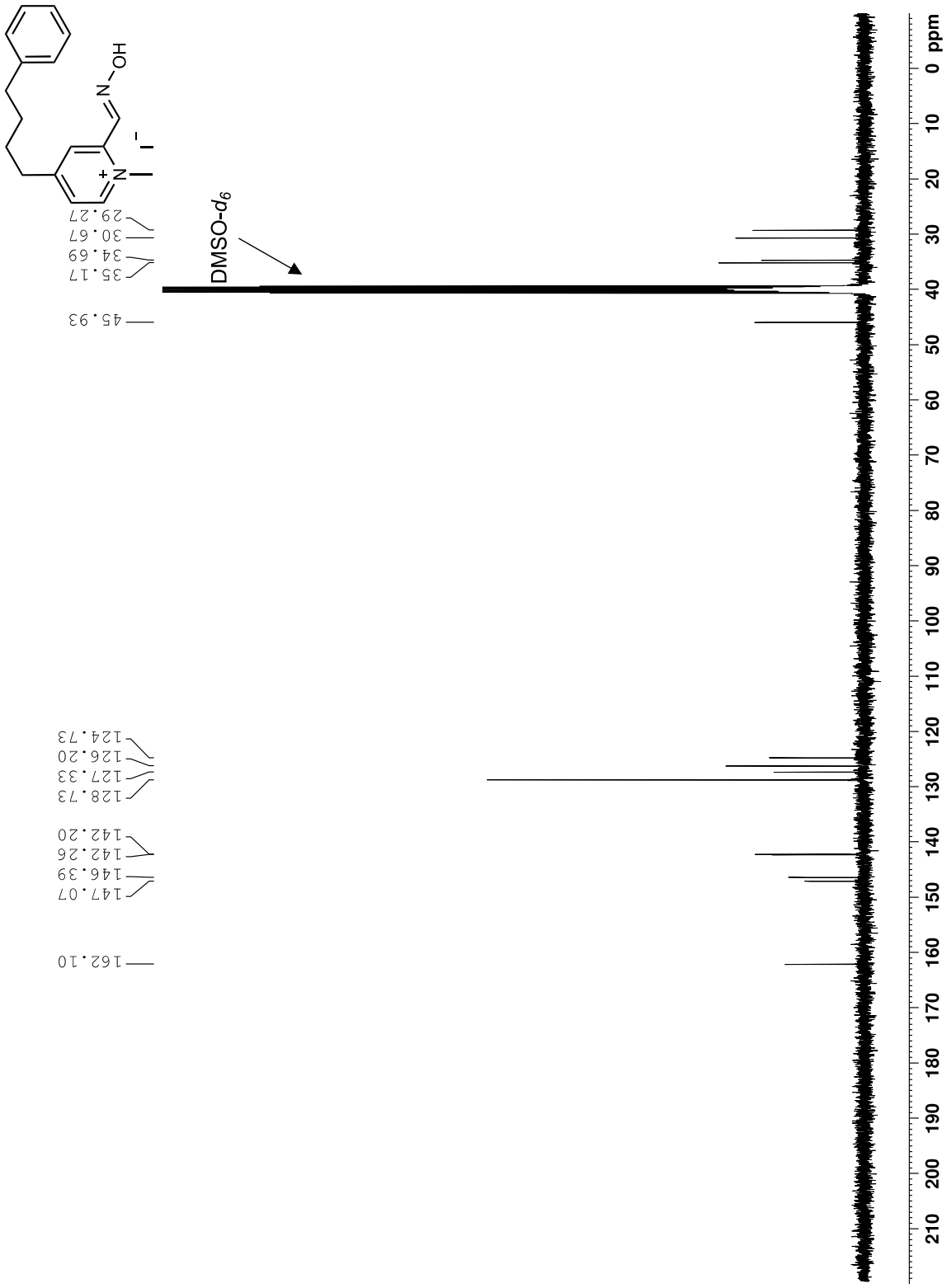

Spectrum 327. ^{13}C NMR for (*E*)-2-((hydroxyimino)methyl)-4-(3-isopropoxyphenethyl)-1-methylpyridin-1-ium iodide (**ADG4244**) (100 MHz, 293 K, DMSO-d_6).

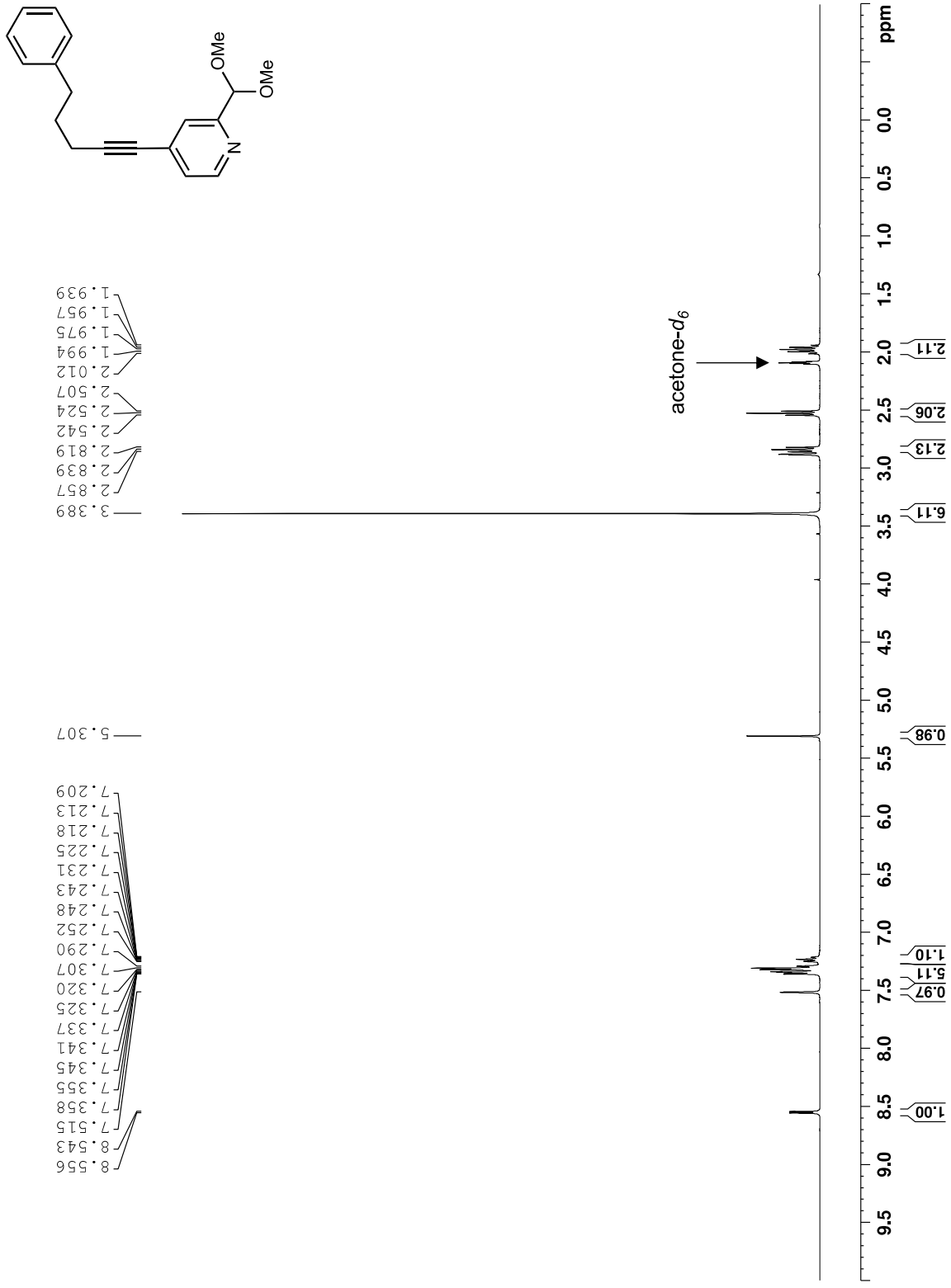

Spectrum 328. ^{1}H NMR for 2-(dimethoxymethyl)-4-(5-phenylpent-1-yn-1-yl)pyridine (400 MHz, 293 K, acetone-d_6).

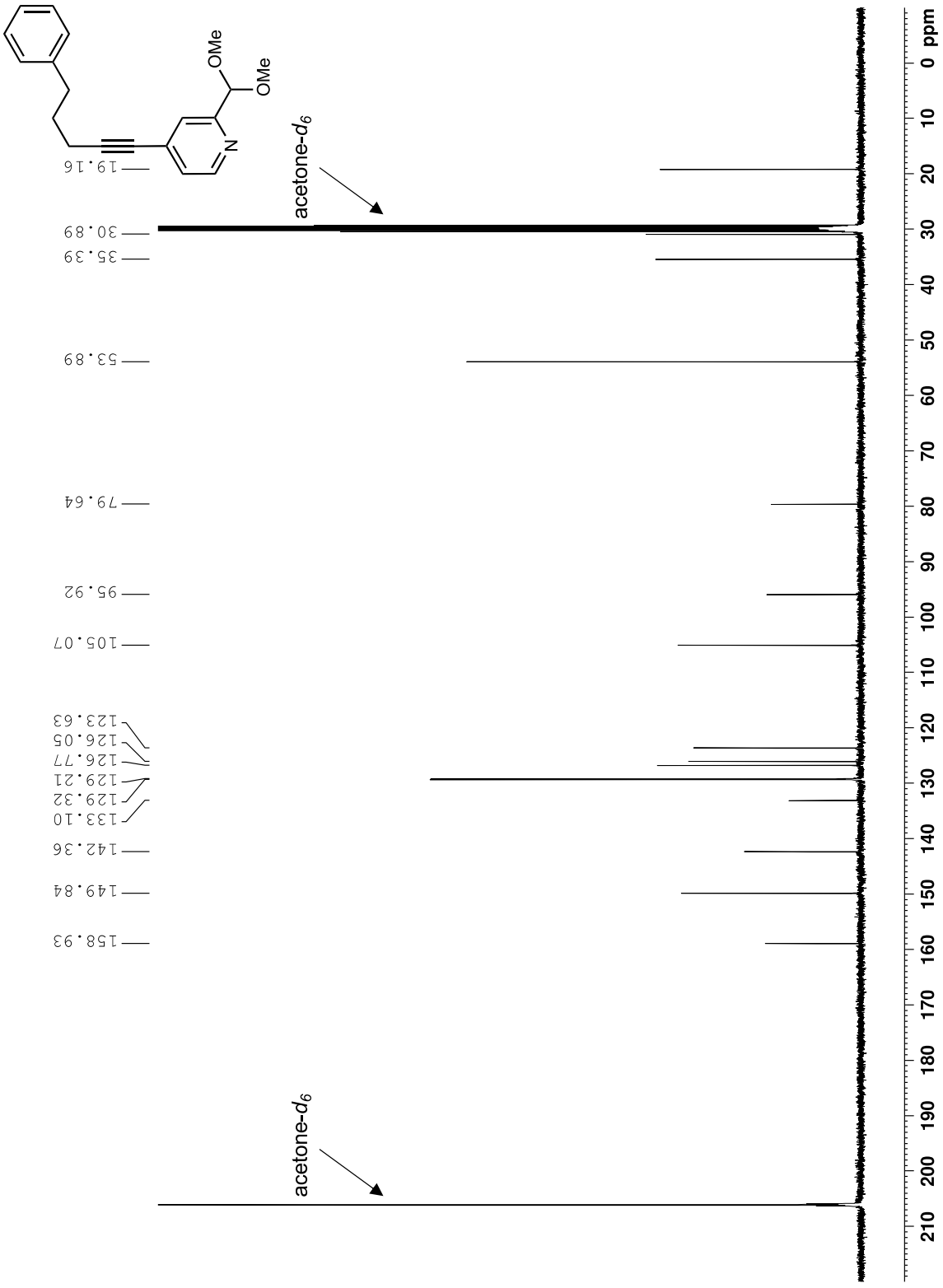

Spectrum 329. ^{13}C NMR for 2-(dimethoxymethyl)-4-(5-phenylpent-1-yn-1-yl)pyridine (100 MHz, 293 K, acetone-d_6).

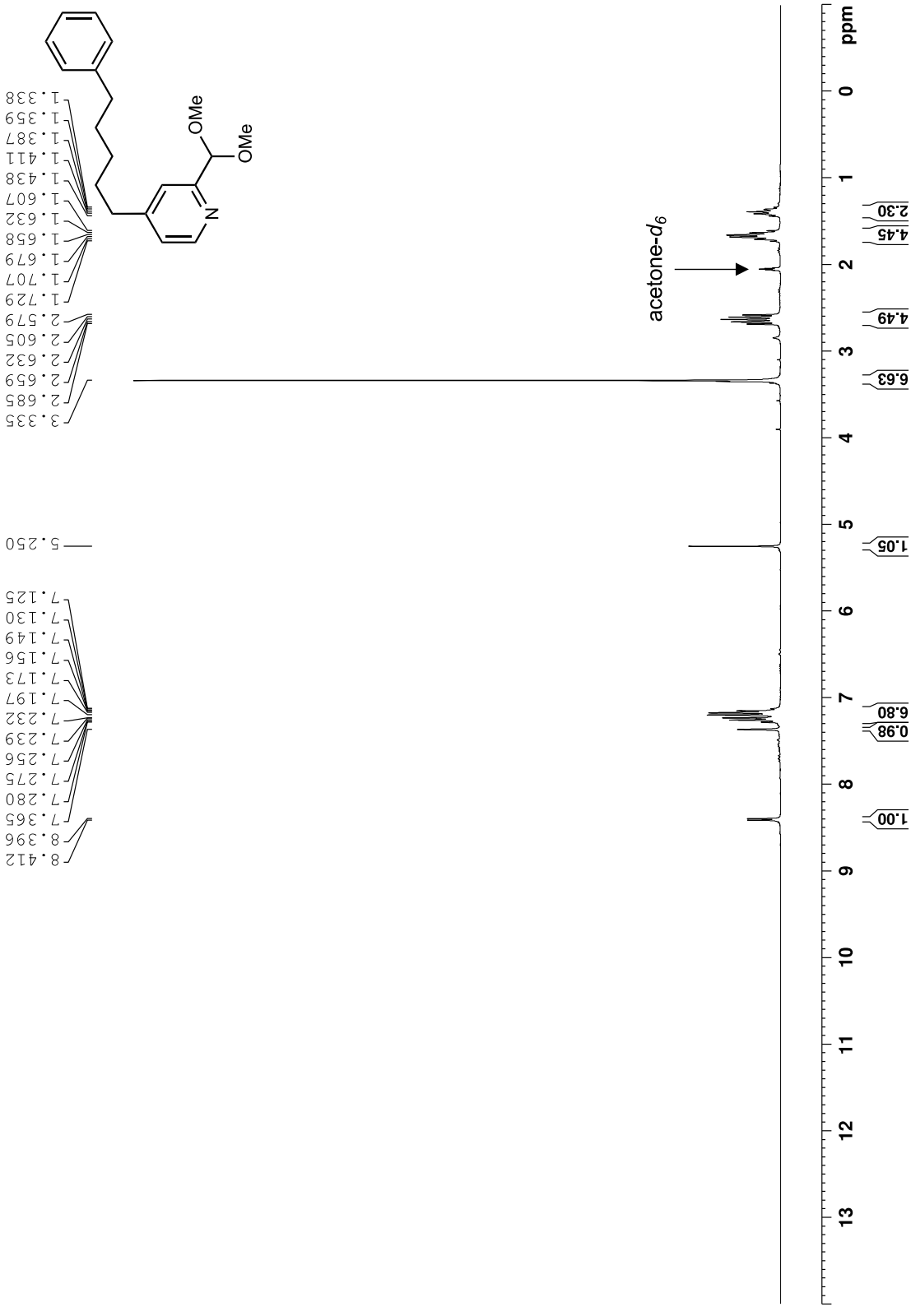

Spectrum 330. ^{1}H NMR for 2-(dimethoxymethyl)-4-(5-phenylpentyl)pyridine (300 MHz, 293 K, acetone-d_6).

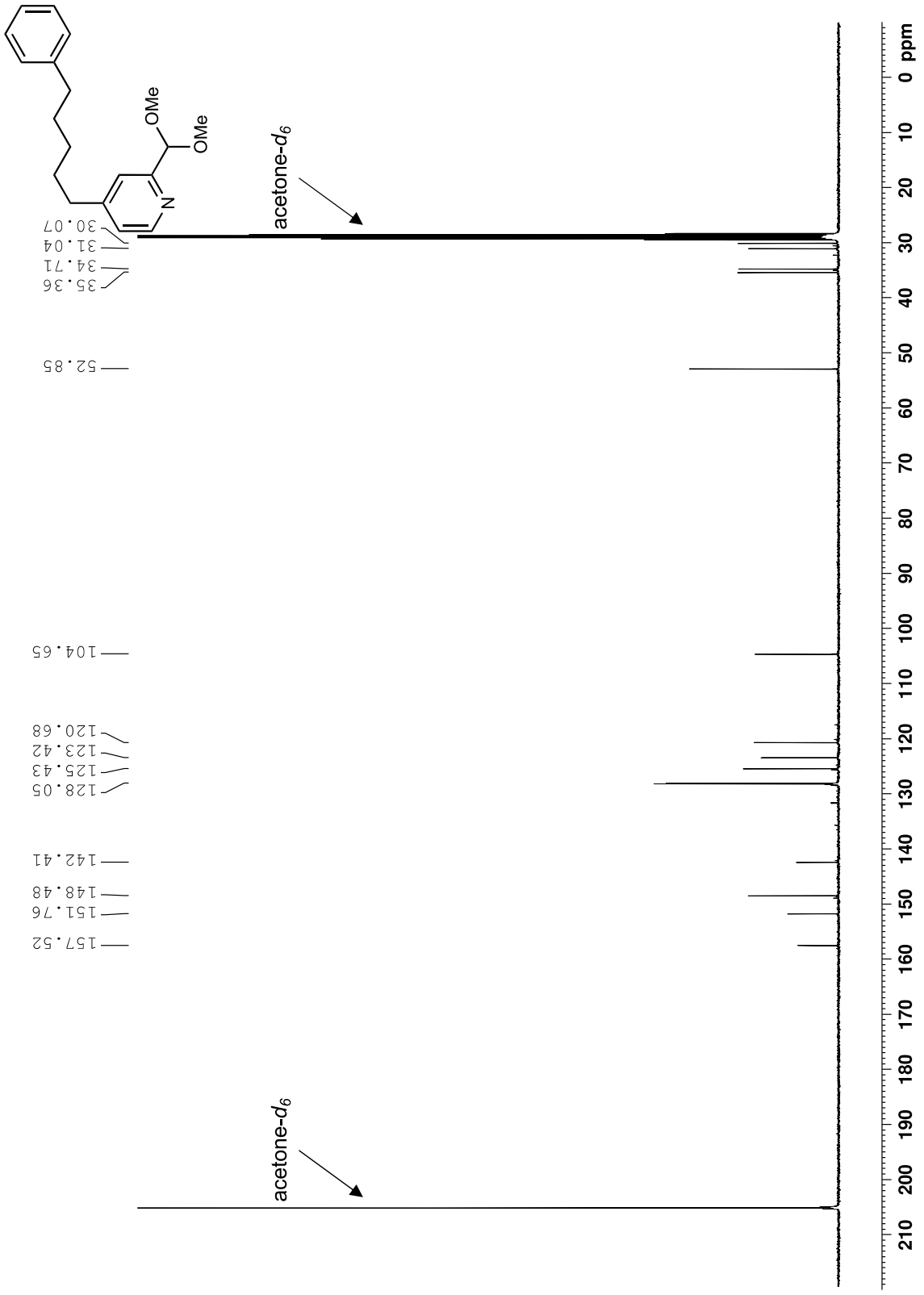

Spectrum 331. ^{13}C NMR for 2-(dimethoxymethyl)-4-(5-phenylpentyl)pyridine (100 MHz, 293 K, acetone-d_6).

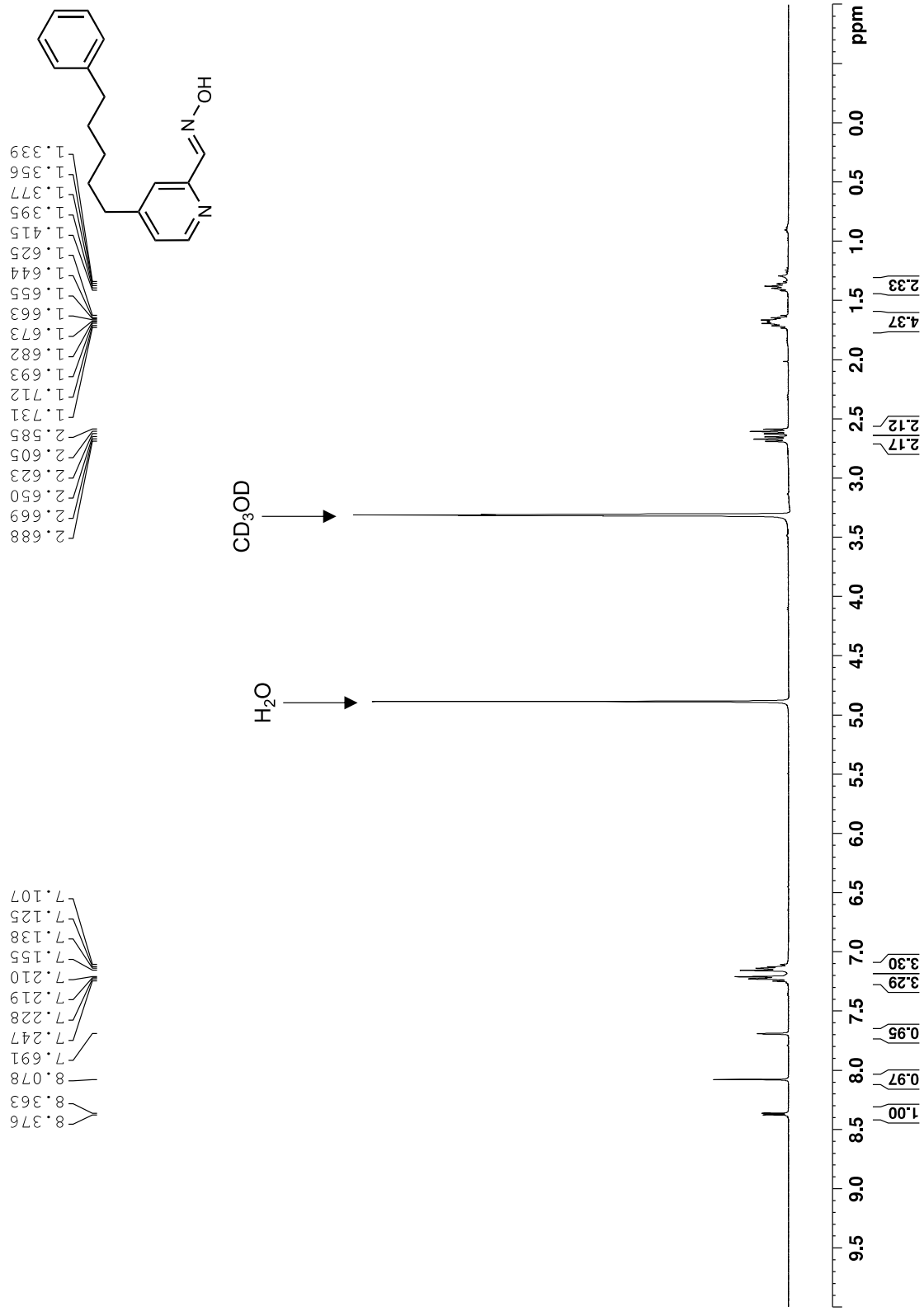

Spectrum 332. ^{1}H NMR for (*E*)-4-(5-phenylpentyl)picolinaldehyde oxime (400 MHz, 293 K, CD_3OD).

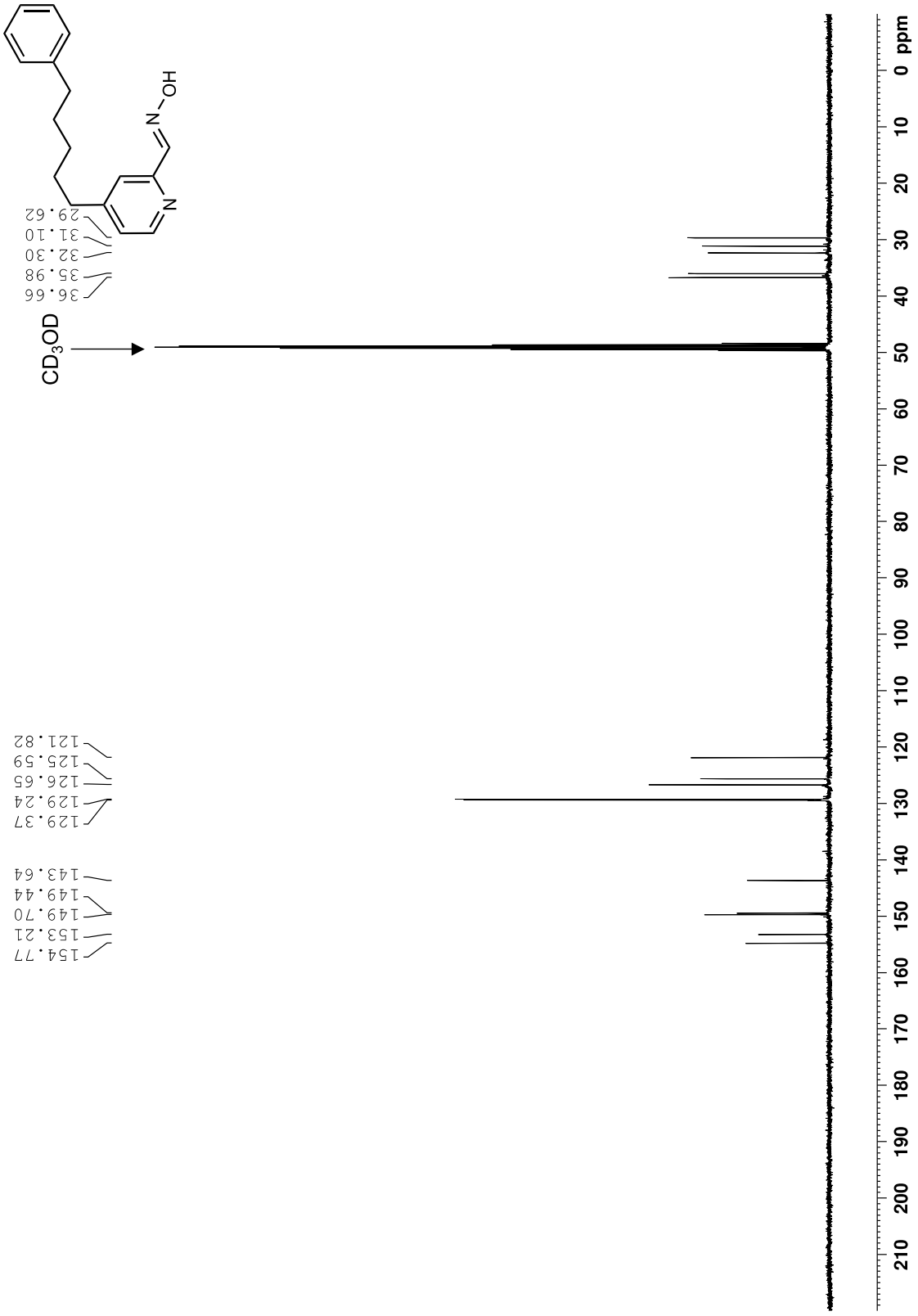

Spectrum 333. ^{13}C NMR for (*E*)-4-(5-phenylpentyl)picolinaldehyde oxime (100 MHz, 293 K, CD_3OD).

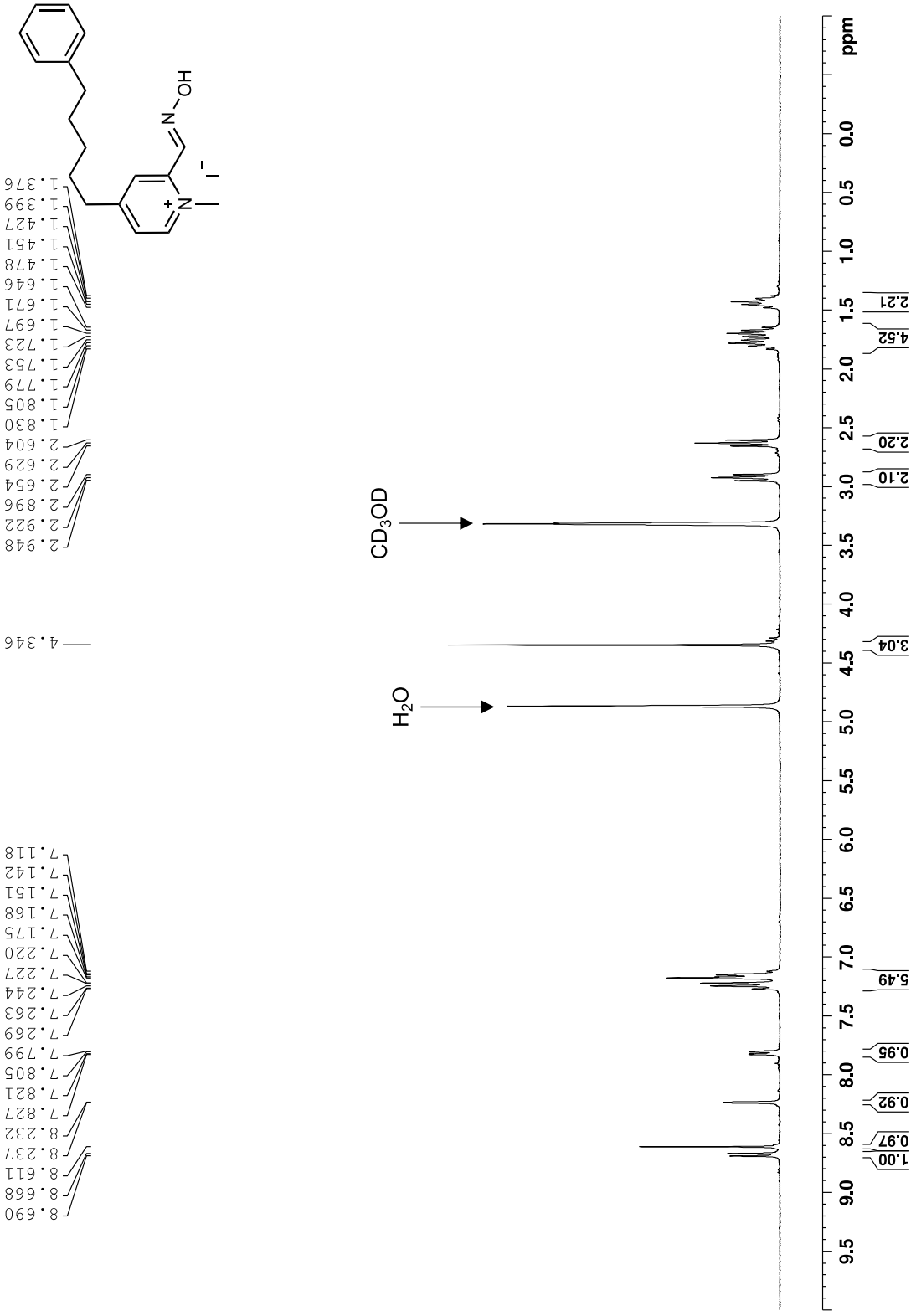

Spectrum 334. ^{1}H NMR for (*E*)-2-((hydroxyimino)methyl)-1-methyl-4-(5-phenylpentyl)pyridin-1-ium iodide (**ADG4282**) (300 MHz, 293 K, CD_3OD).

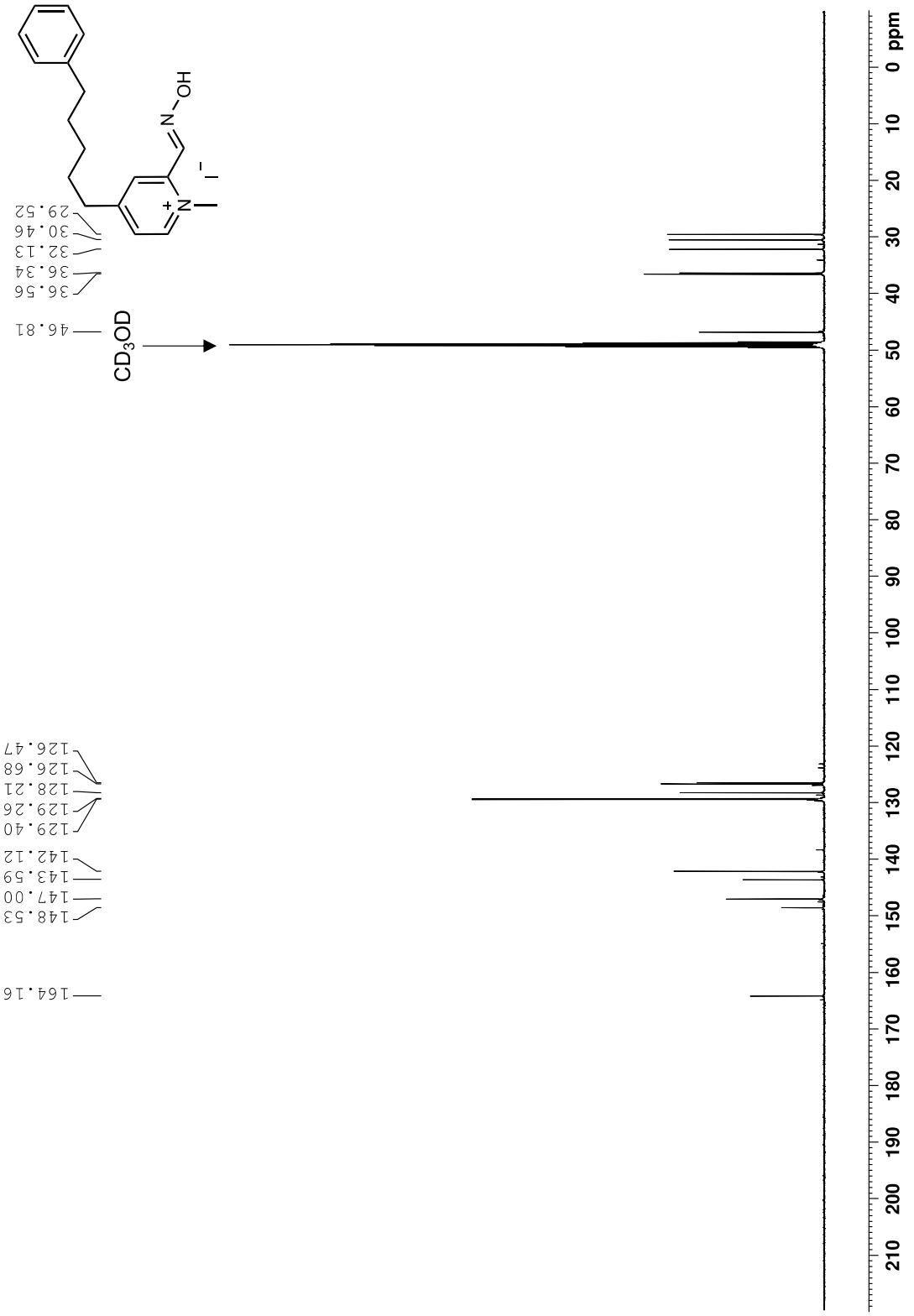

Spectrum 335. ^{13}C NMR for (*E*)-2-((hydroxyimino)methyl)-1-methyl-4-(5-phenylpentyl)pyridin-1-ium iodide (**ADG4282**) (125 MHz, 293 K, CD_3OD).

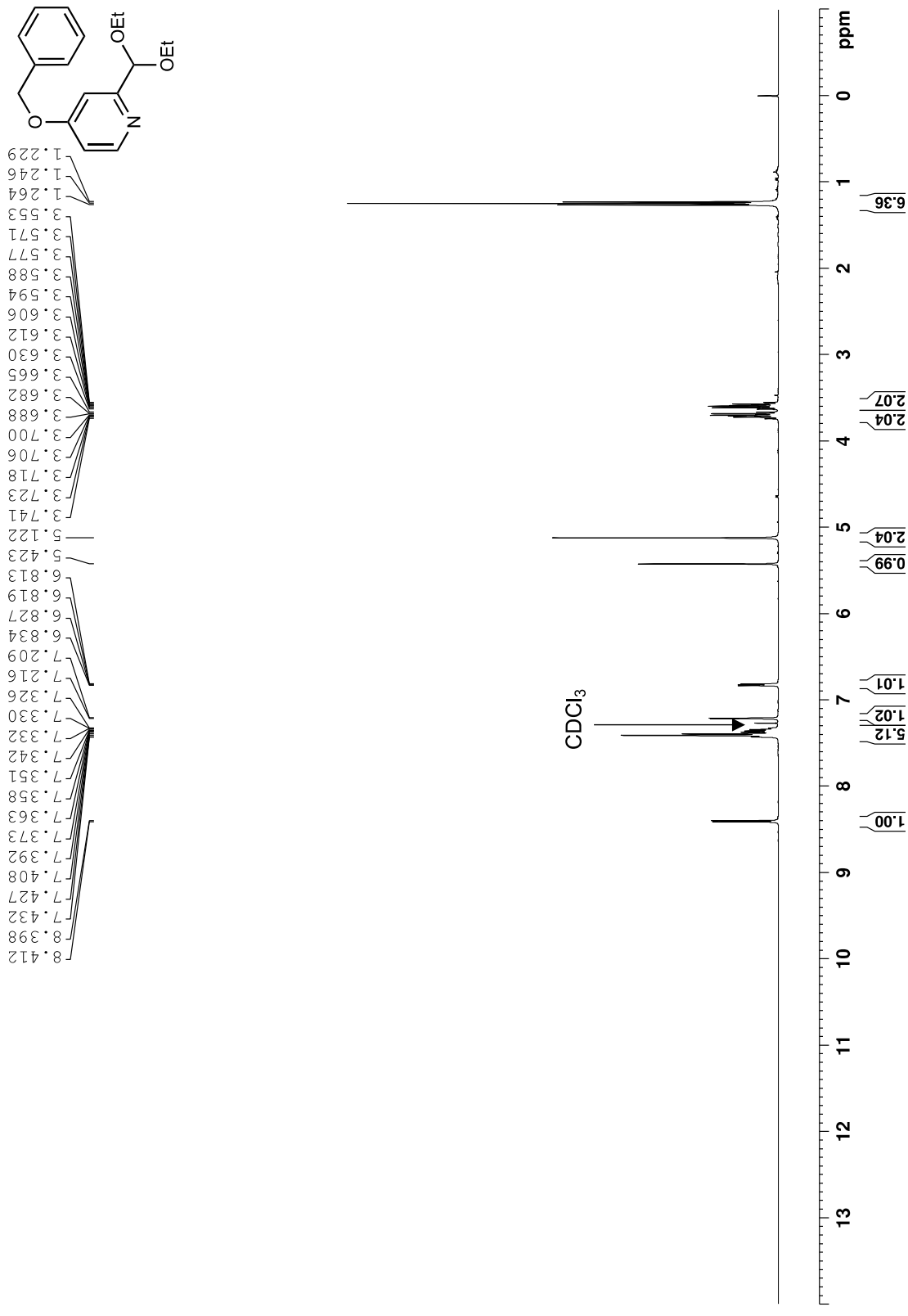

Spectrum 336. ^{1}H NMR for 4-(benzyloxy)-2-(diethoxymethyl)pyridine (400 MHz, 293 K, $CDCl_3$).

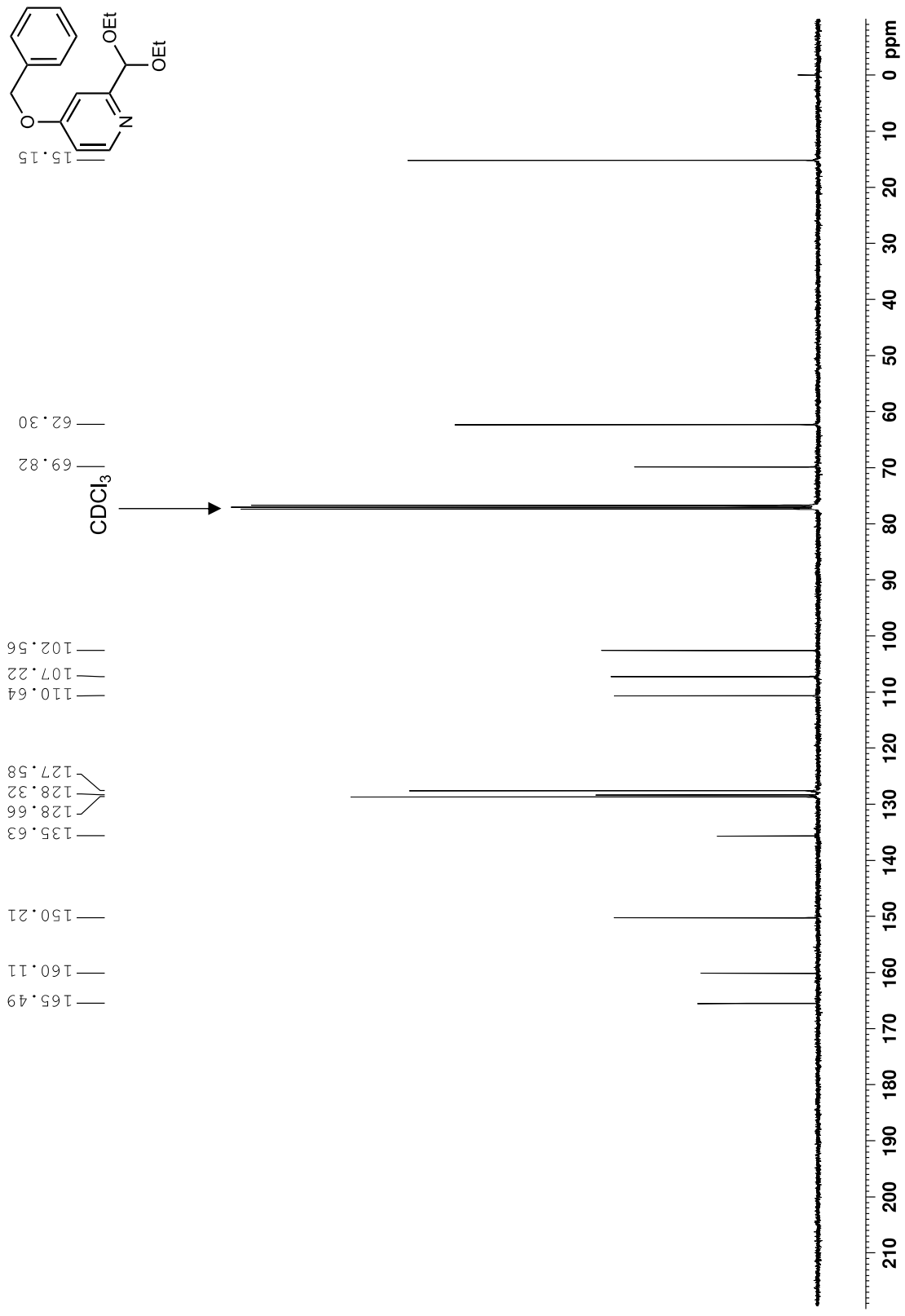

Spectrum 337. ^{13}C NMR for 4-(benzyloxy)-2-(diethoxymethyl)pyridine (100 MHz, 293 K, $CDCl_3$).

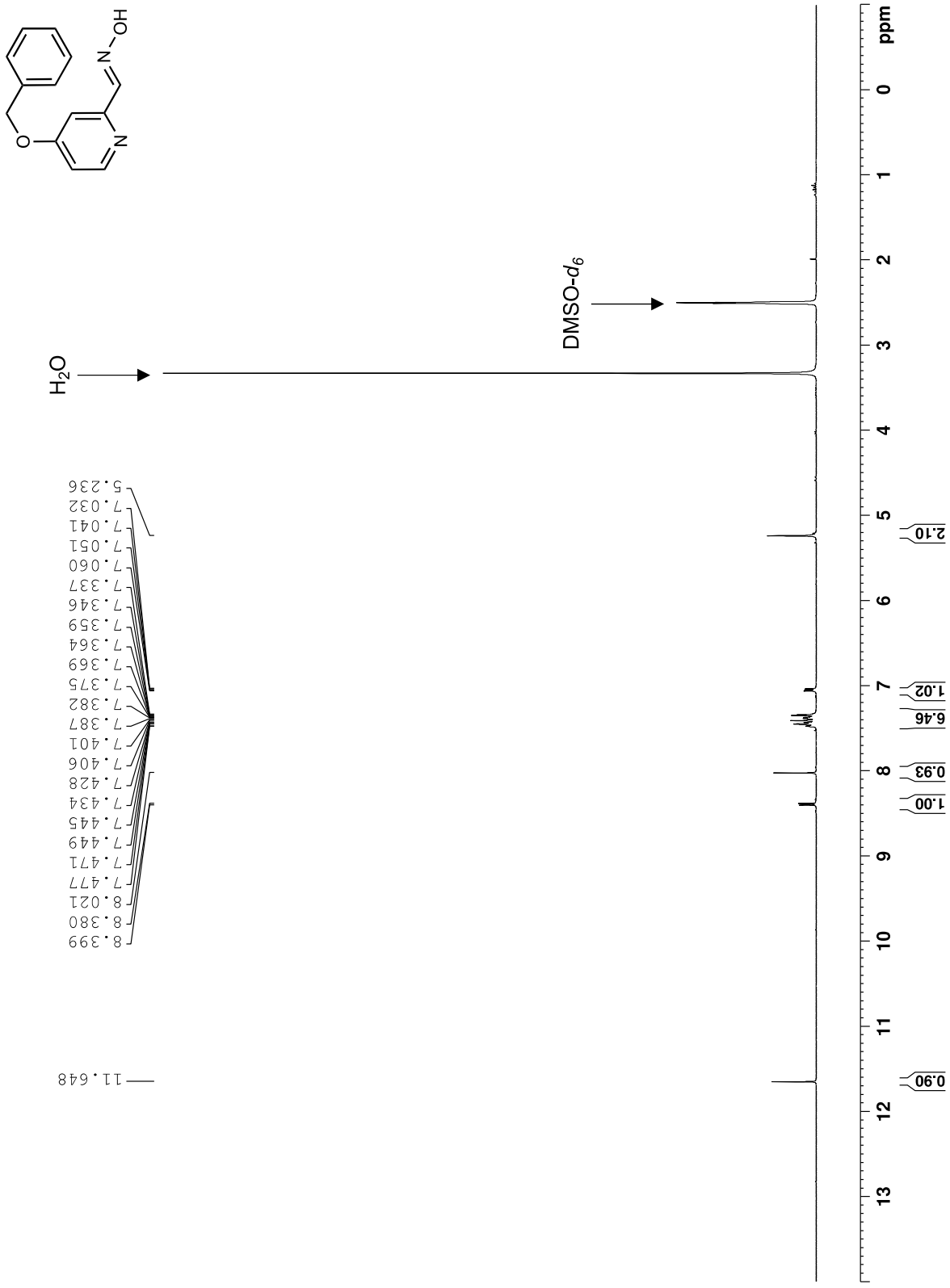

Spectrum 338. [1]H NMR for (*E*)-4-(benzyloxy)picolinaldehyde oxime (300 MHz, 293 K, DMSO-d_6).

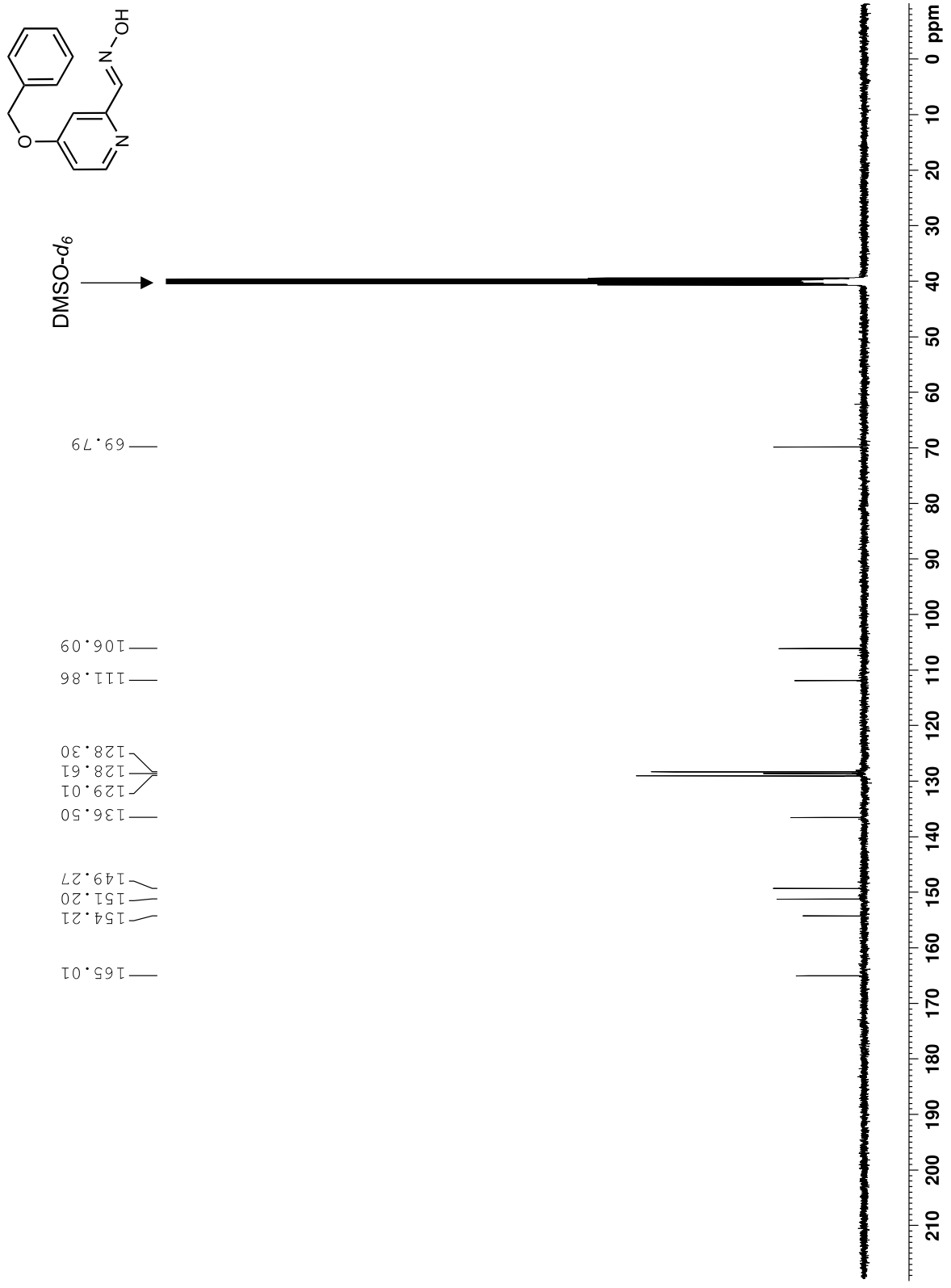

Spectrum 339. ^{13}C NMR for (*E*)-4-(benzyloxy)picolinaldehyde oxime (100 MHz, 293 K, DMSO-d_6).

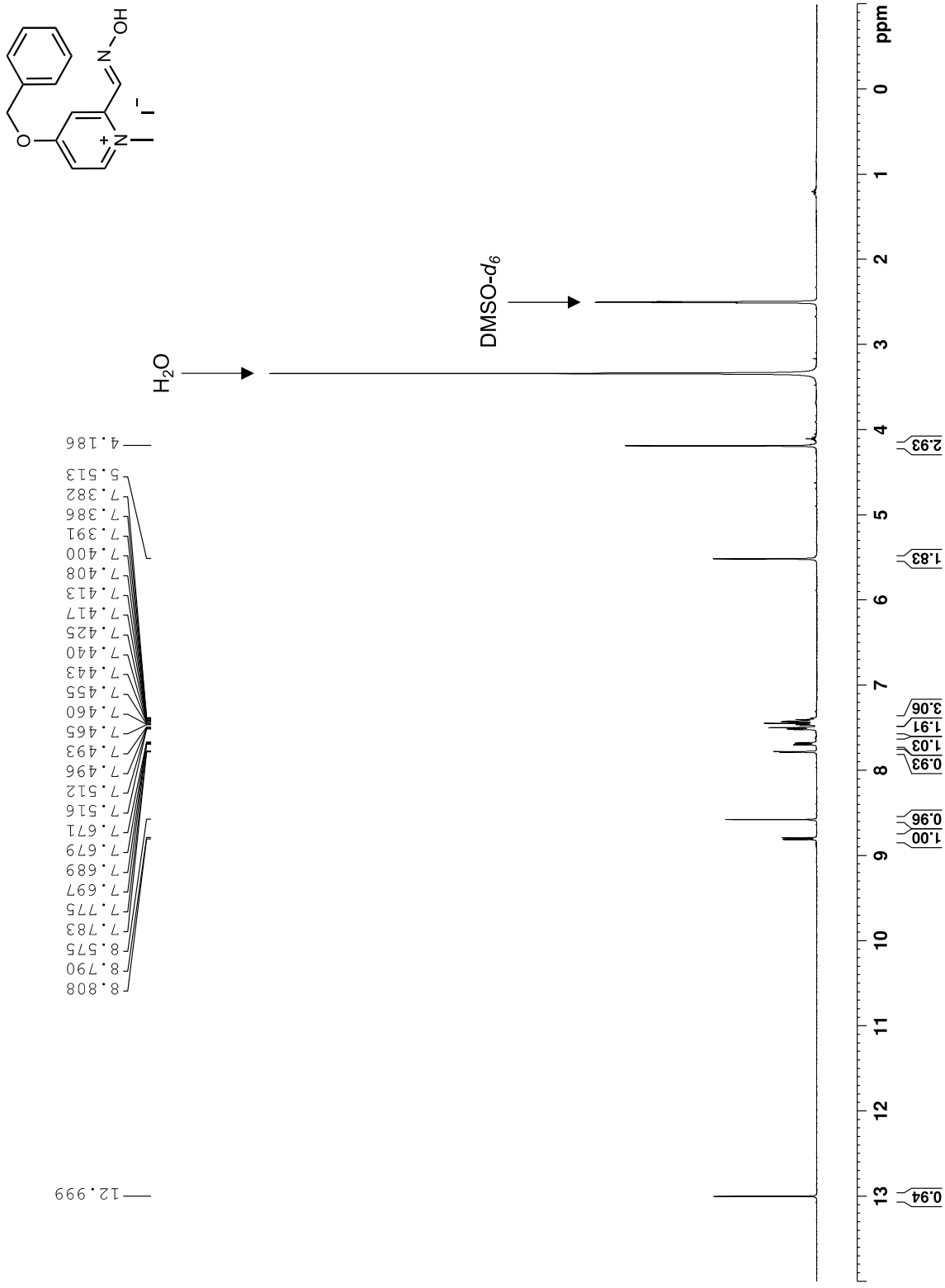

Spectrum 340. ^{1}H NMR for (*E*)-4-(benzyloxy)-2-((hydroxyimino)methyl)-1-methylpyridin-1-ium iodide (**ADG3254**) (400 MHz, 293 K, DMSO-d_6).

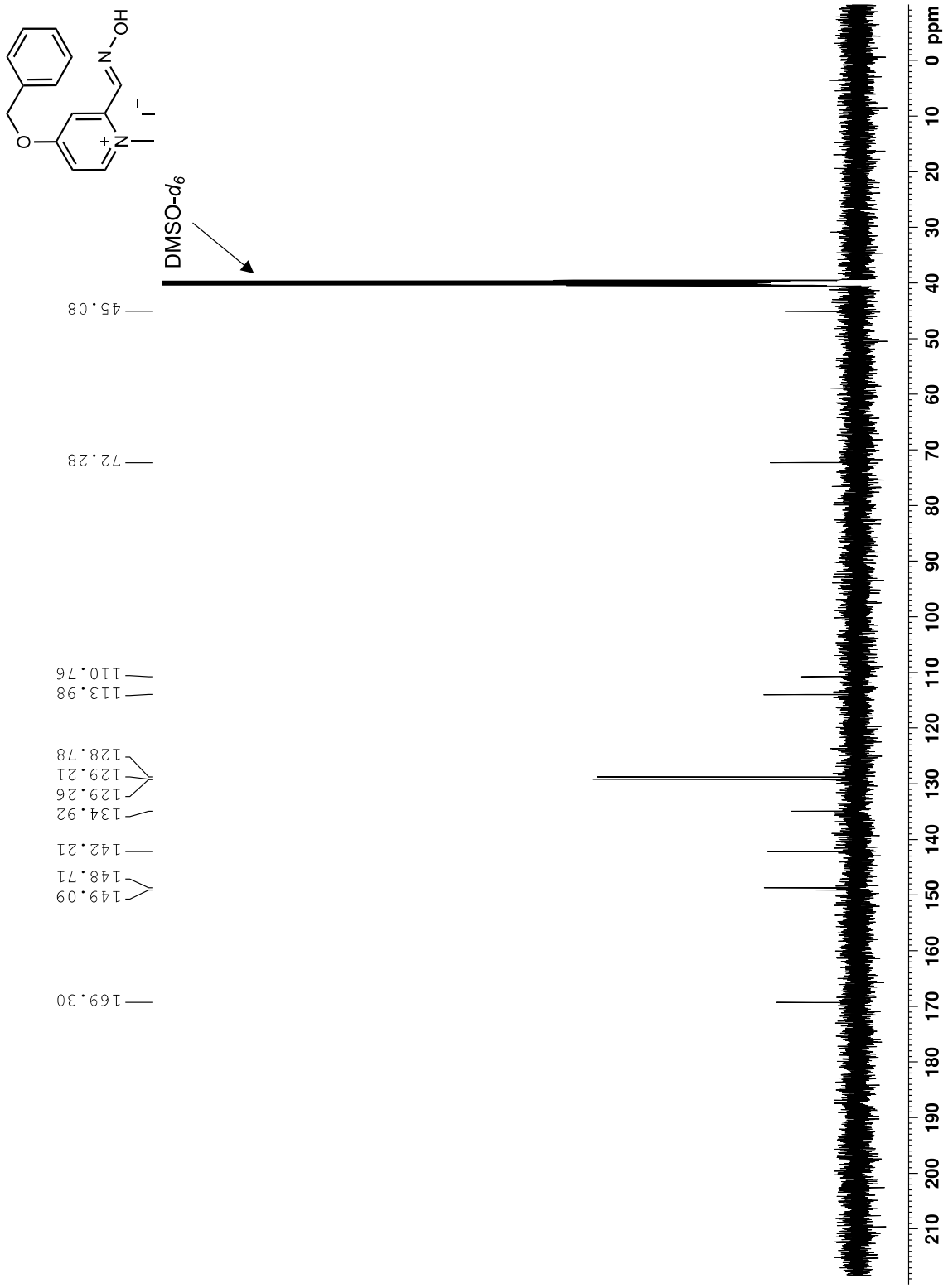

Spectrum 341. ^{13}C NMR for (*E*)-4-(benzyloxy)-2-((hydroxyimino)methyl)-1-methylpyridin-1-ium iodide (**ADG3254**) (125 MHz, 293 K, DMSO-d_6).

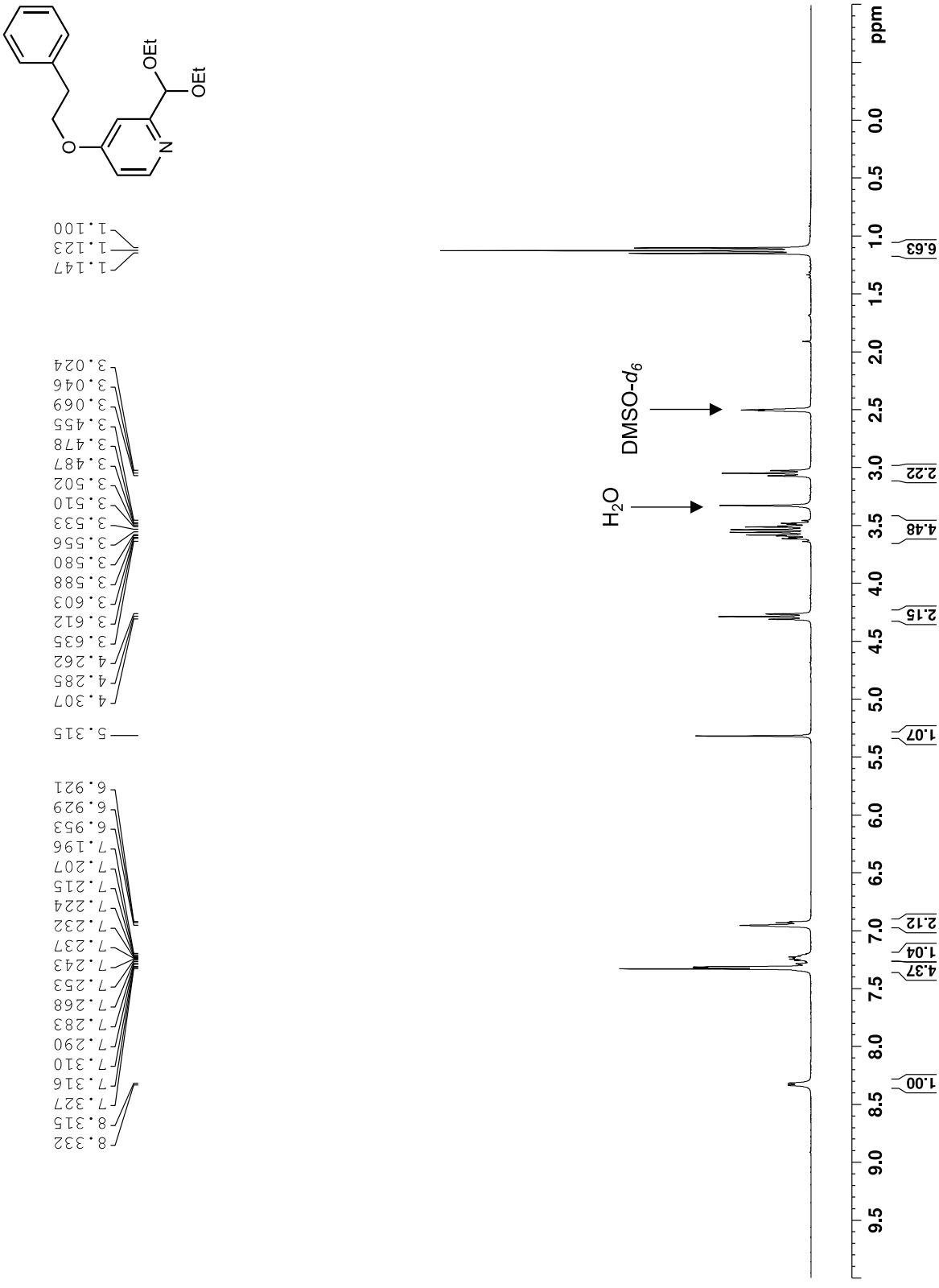

Spectrum 342. ^{1}H NMR for 2-(diethoxymethyl)-4-phenethoxypyridine (300 MHz, 293 K, DMSO-d_6).

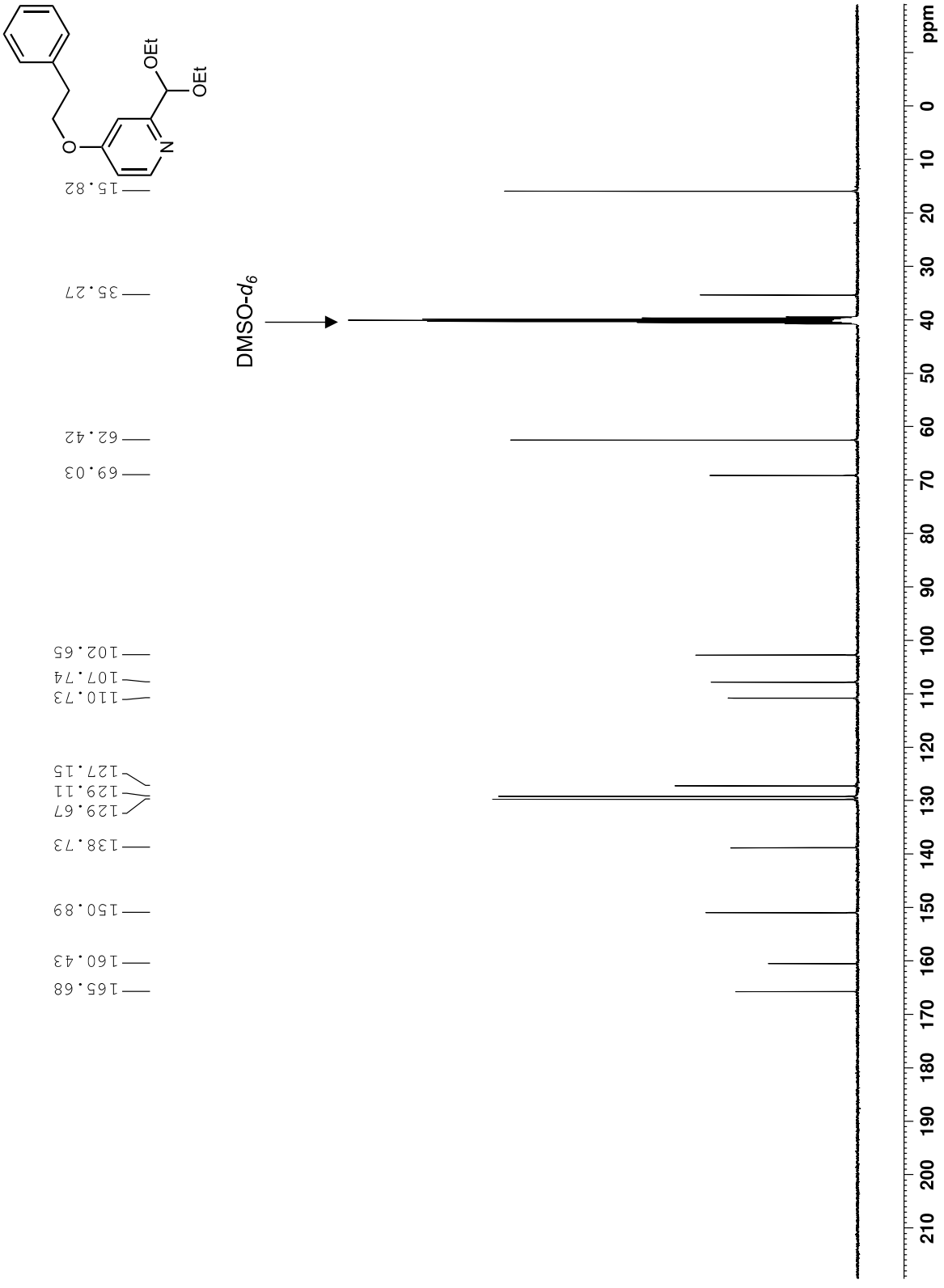

Spectrum 343. ^{13}C NMR for 2-(diethoxymethyl)-4-phenethoxypyridine (100 MHz, 293 K, DMSO-d_6).

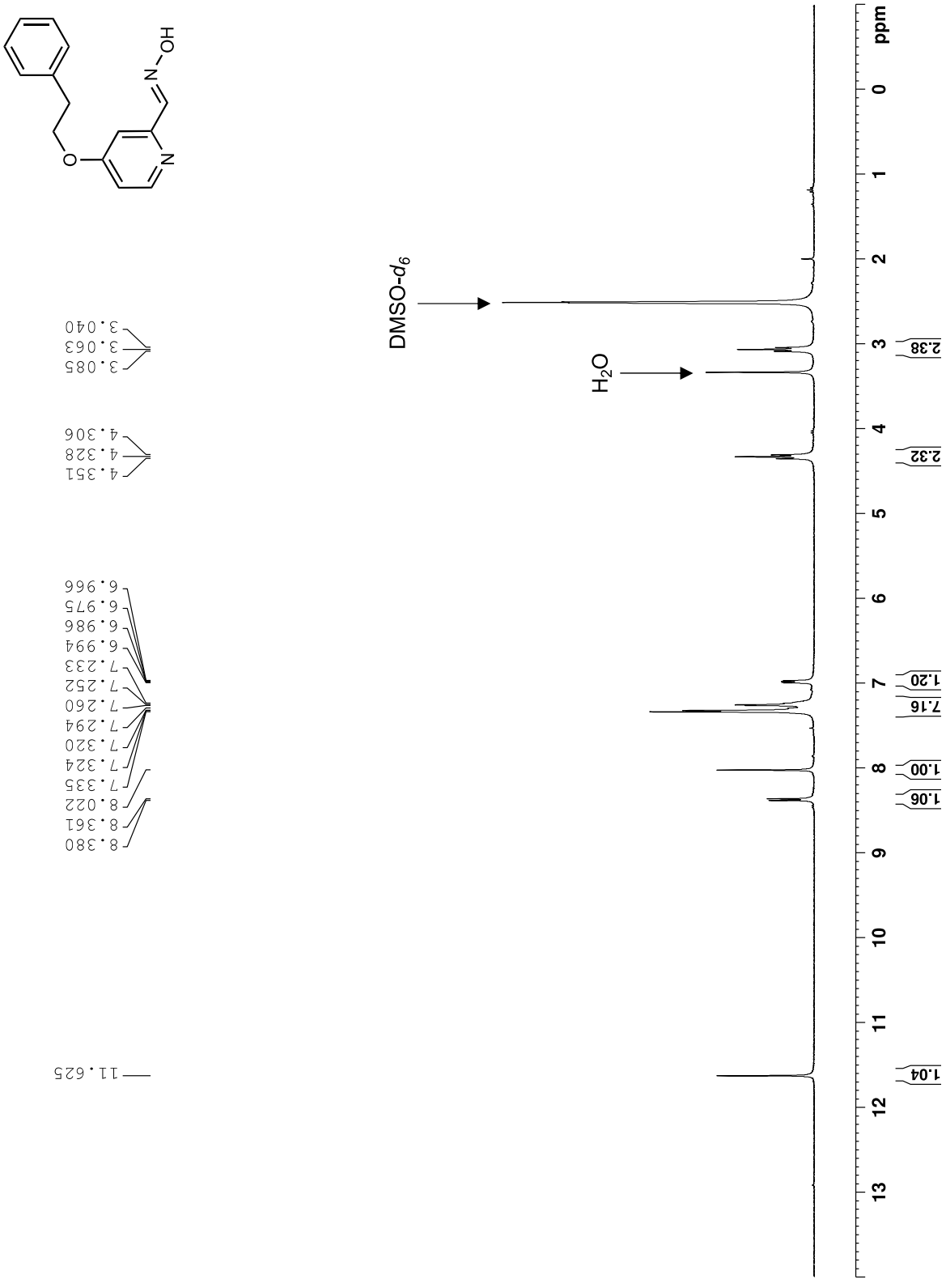

Spectrum 344. ^{1}H NMR for (*E*)-4-phenethoxypicolinaldehyde oxime (300 MHz, 293 K, DMSO-d_6).

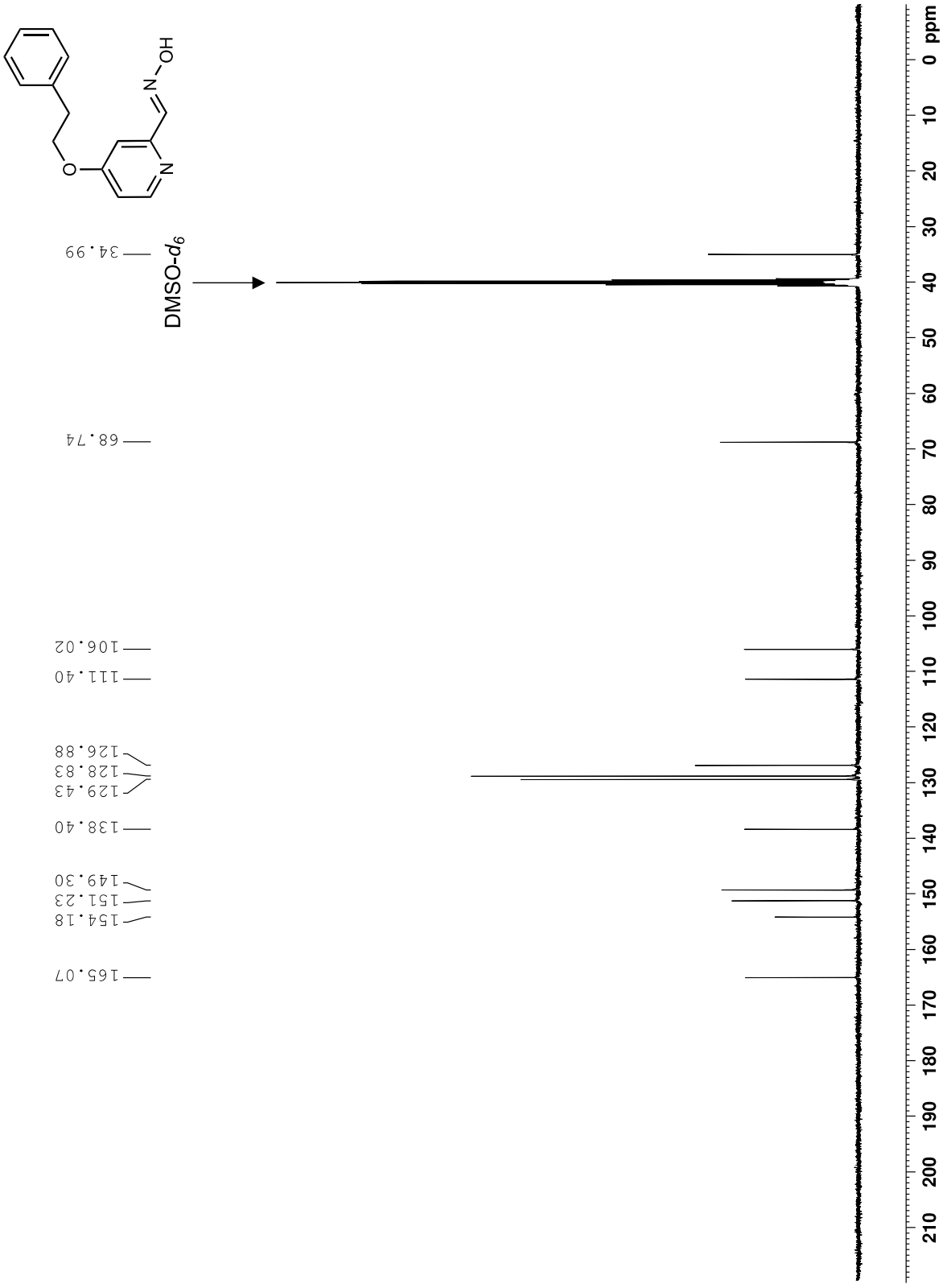

Spectrum 345. ^{13}C NMR for (*E*)-4-phenethoxypicolinaldehyde oxime (100 MHz, 293 K, DMSO-d_6).

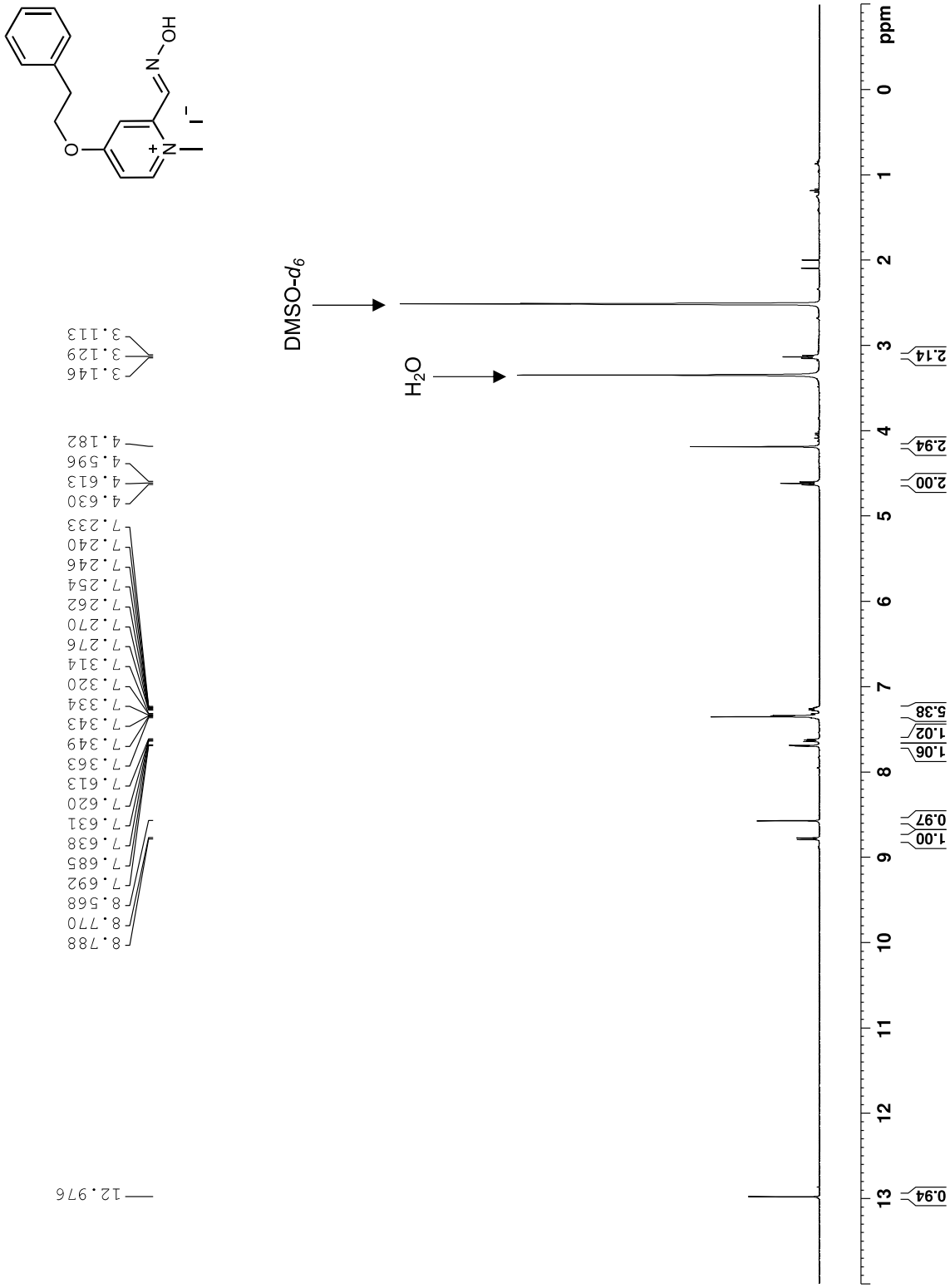

Spectrum 346. ^{1}H NMR for (*E*)-2-((hydroxyimino)methyl)-1-methyl-4-phenethoxypyridin-1-ium iodide (**ADG4250**) (400 MHz, 293 K, DMSO-d_6).

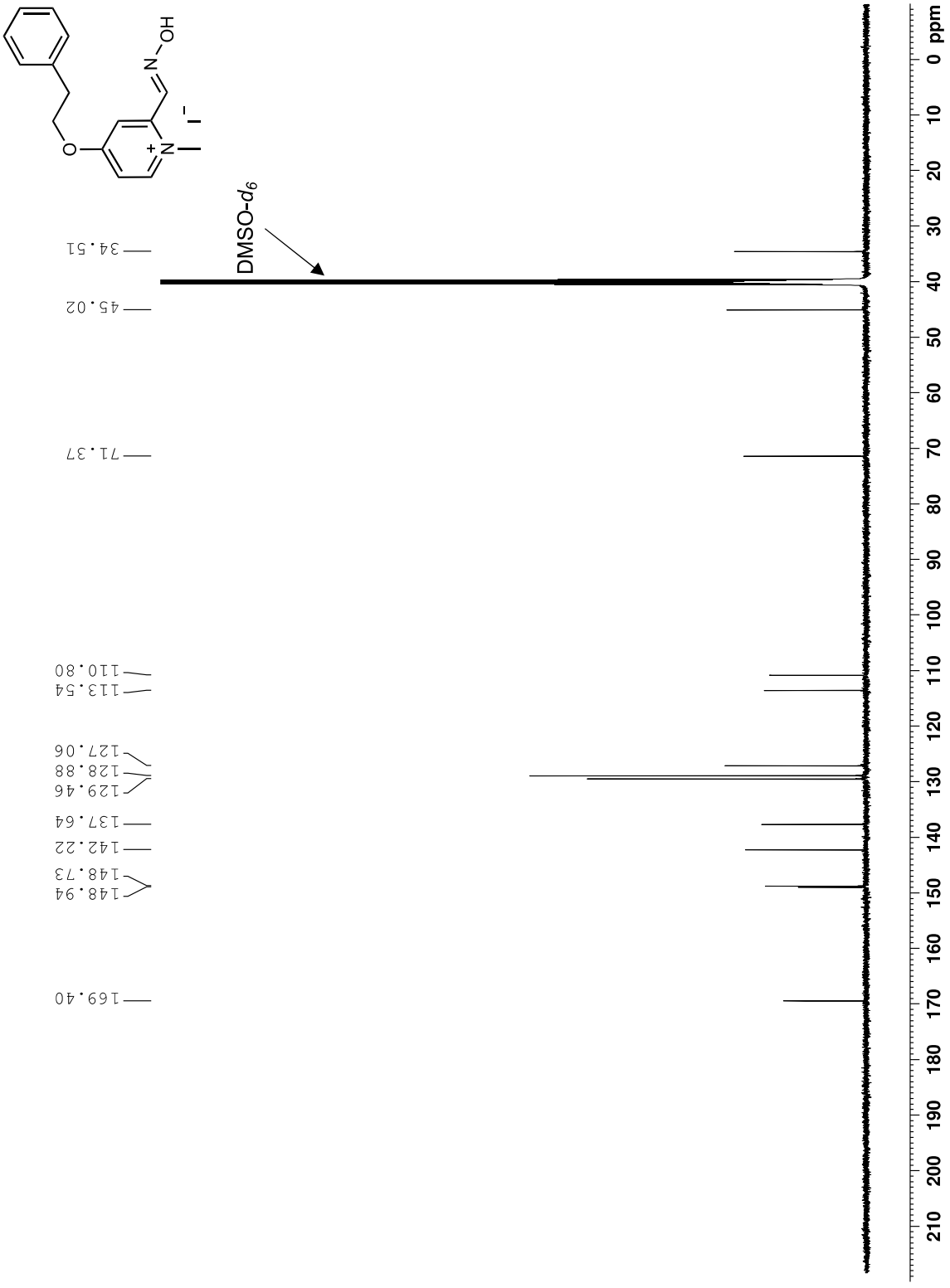

Spectrum 347. ^{13}C NMR for (*E*)-2-((hydroxyimino)methyl)-1-methyl-4-phenethoxypyridin-1-ium iodide (**ADG4250**) (125 MHz, 293 K, DMSO-d_6).

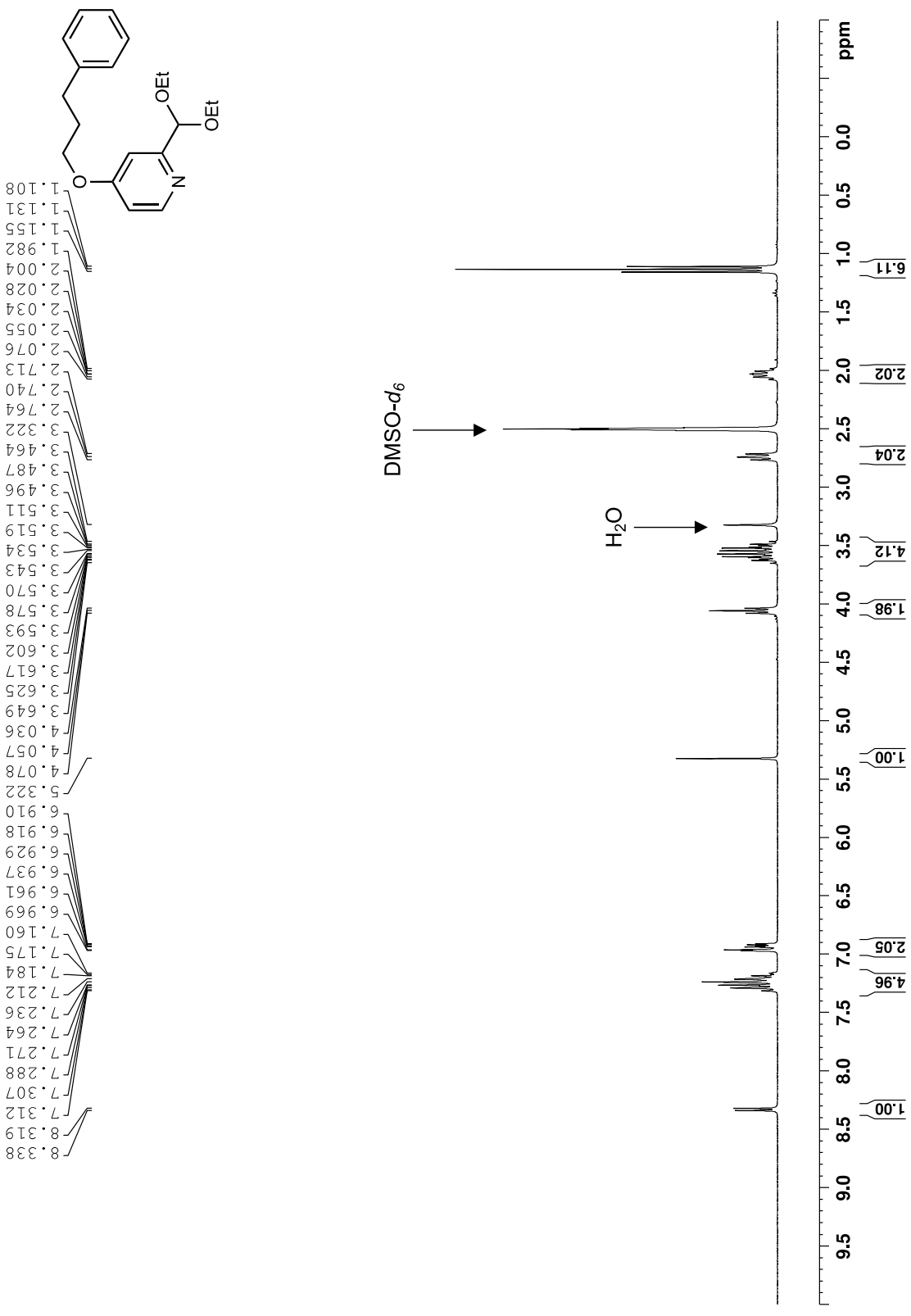

Spectrum 348. ^{1}H NMR for 2-(diethoxymethyl)-4-(3-phenylpropoxy)pyridine (300 MHz, 293 K, DMSO-d_6).

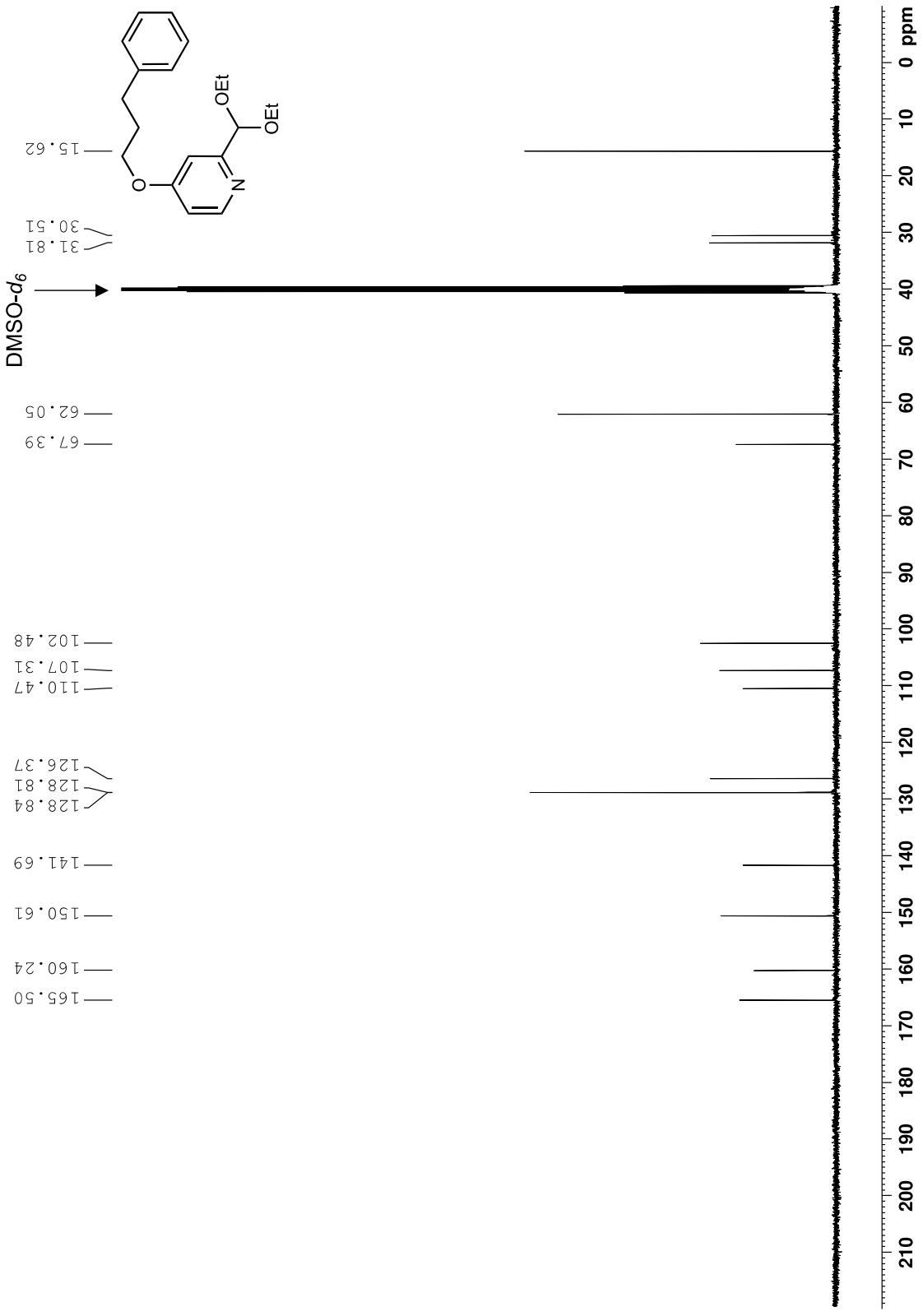

Spectrum 349. ^{13}C NMR for 2-(diethoxymethyl)-4-(3-phenylpropoxy)pyridine (100 MHz, 293 K, DMSO-d_6).

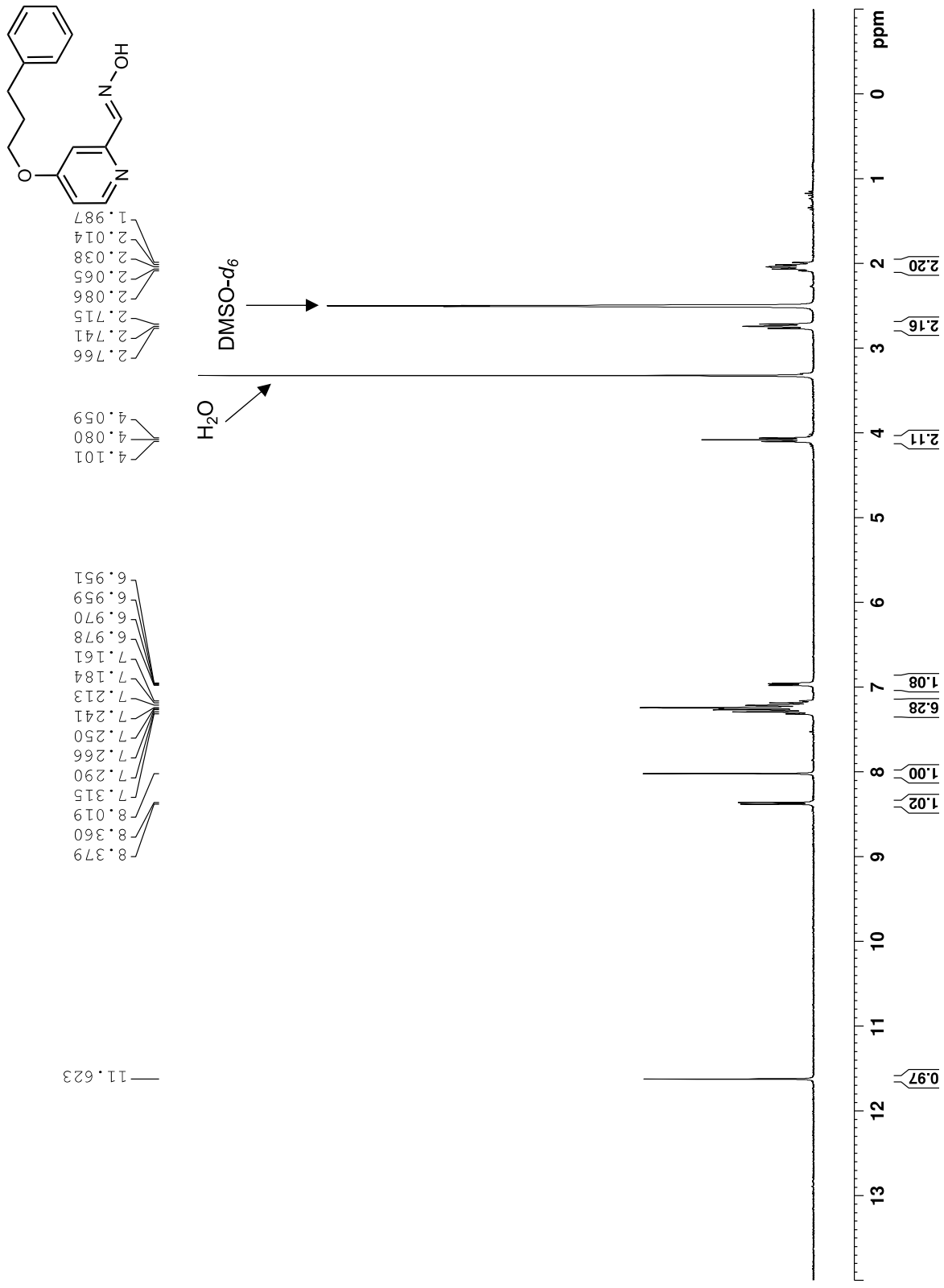

Spectrum 350. ^{1}H NMR for (*E*)-4-(3-phenylpropoxy)picolinaldehyde oxime (300 MHz, 293 K, DMSO-d_6).

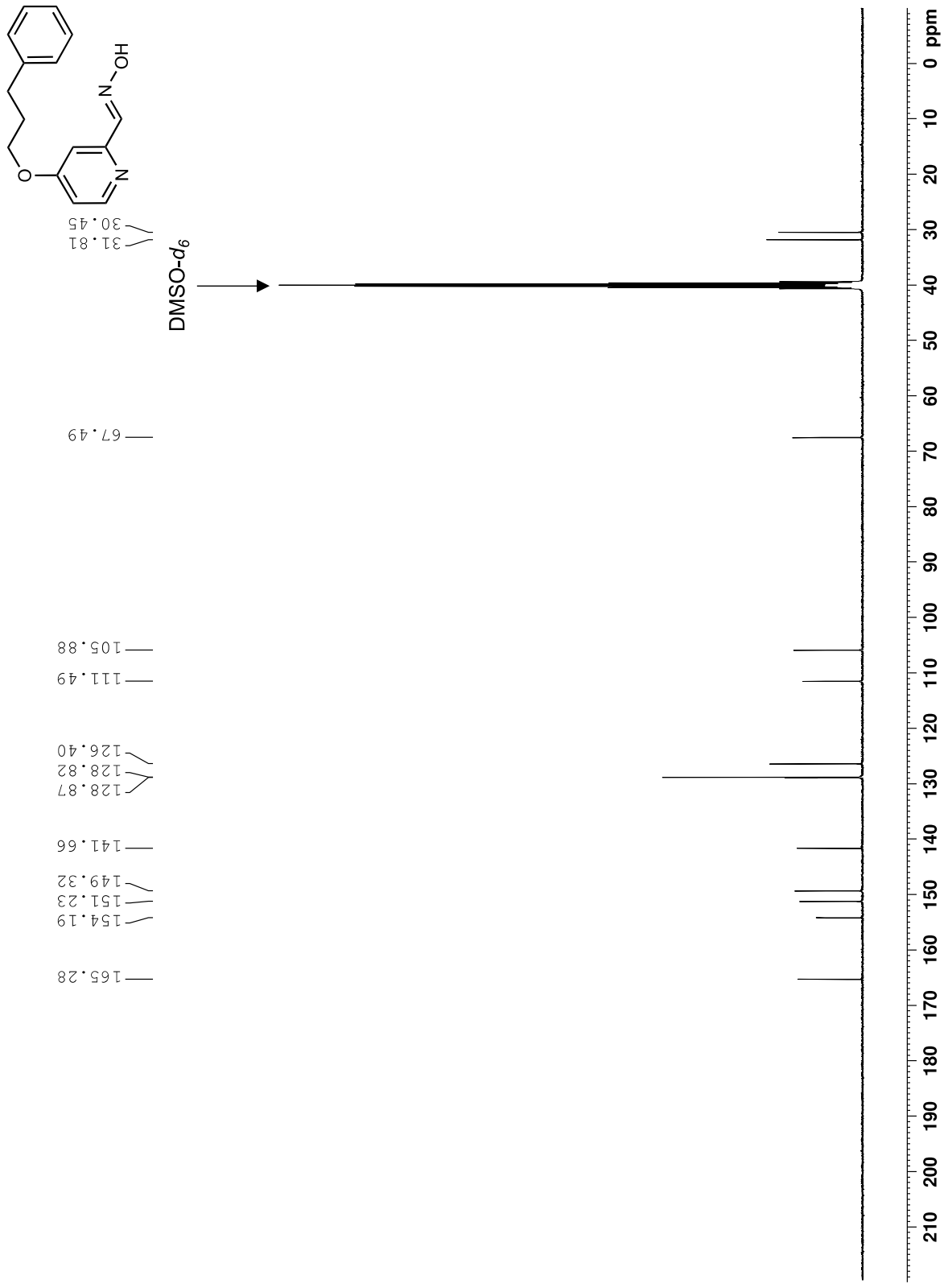

Spectrum 351. ^{13}C NMR for (*E*)-4-(3-phenylpropoxy)picolinaldehyde oxime (100 MHz, 293 K, DMSO-d_6).

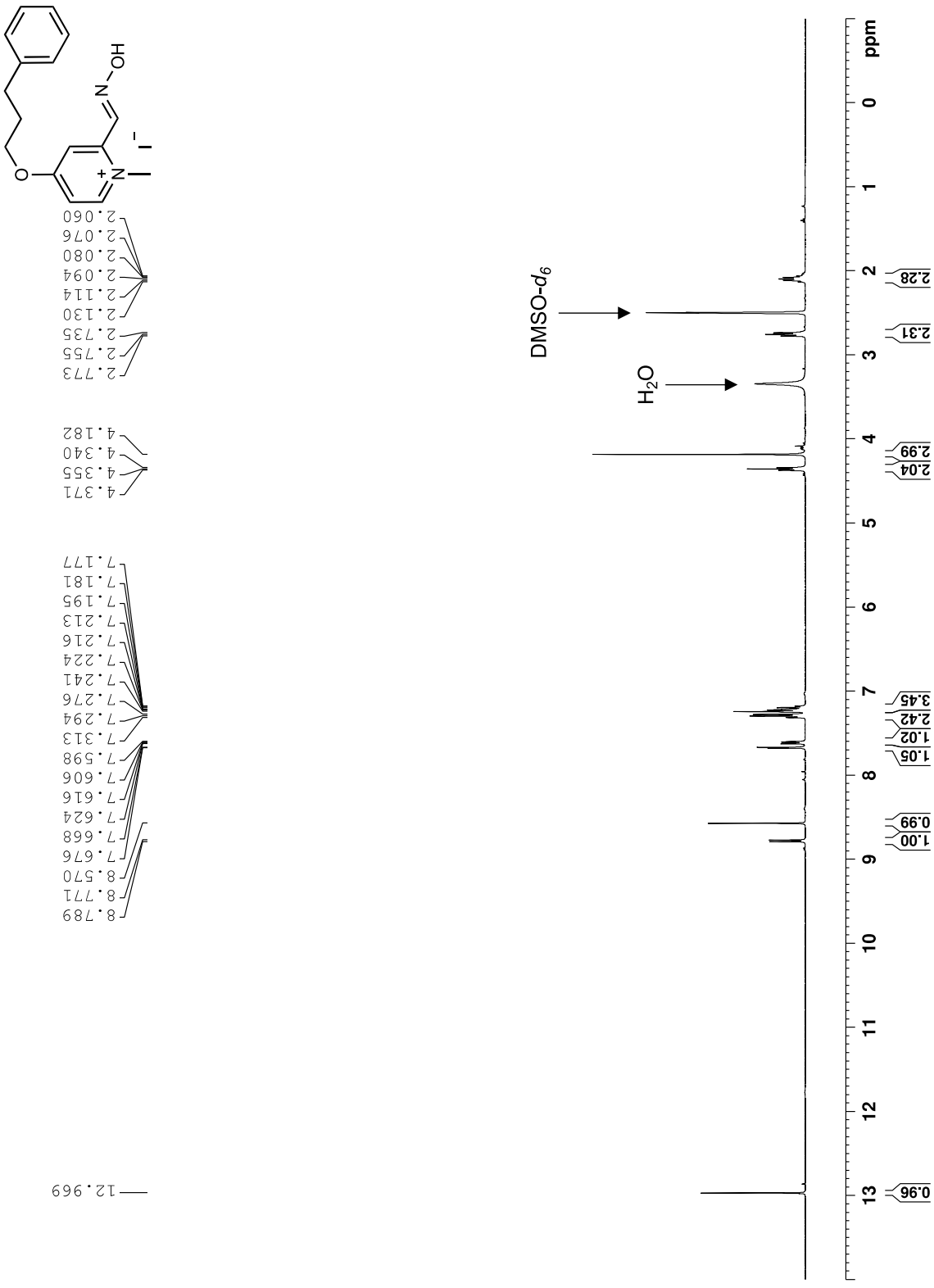

Spectrum 352. ^{1}H NMR for (*E*)-2-((hydroxyimino)methyl)-1-methyl-4-(3-phenylpropoxy)pyridin-1-ium iodide (**ADG4253**) (400 MHz, 293 K, DMSO-d_6).

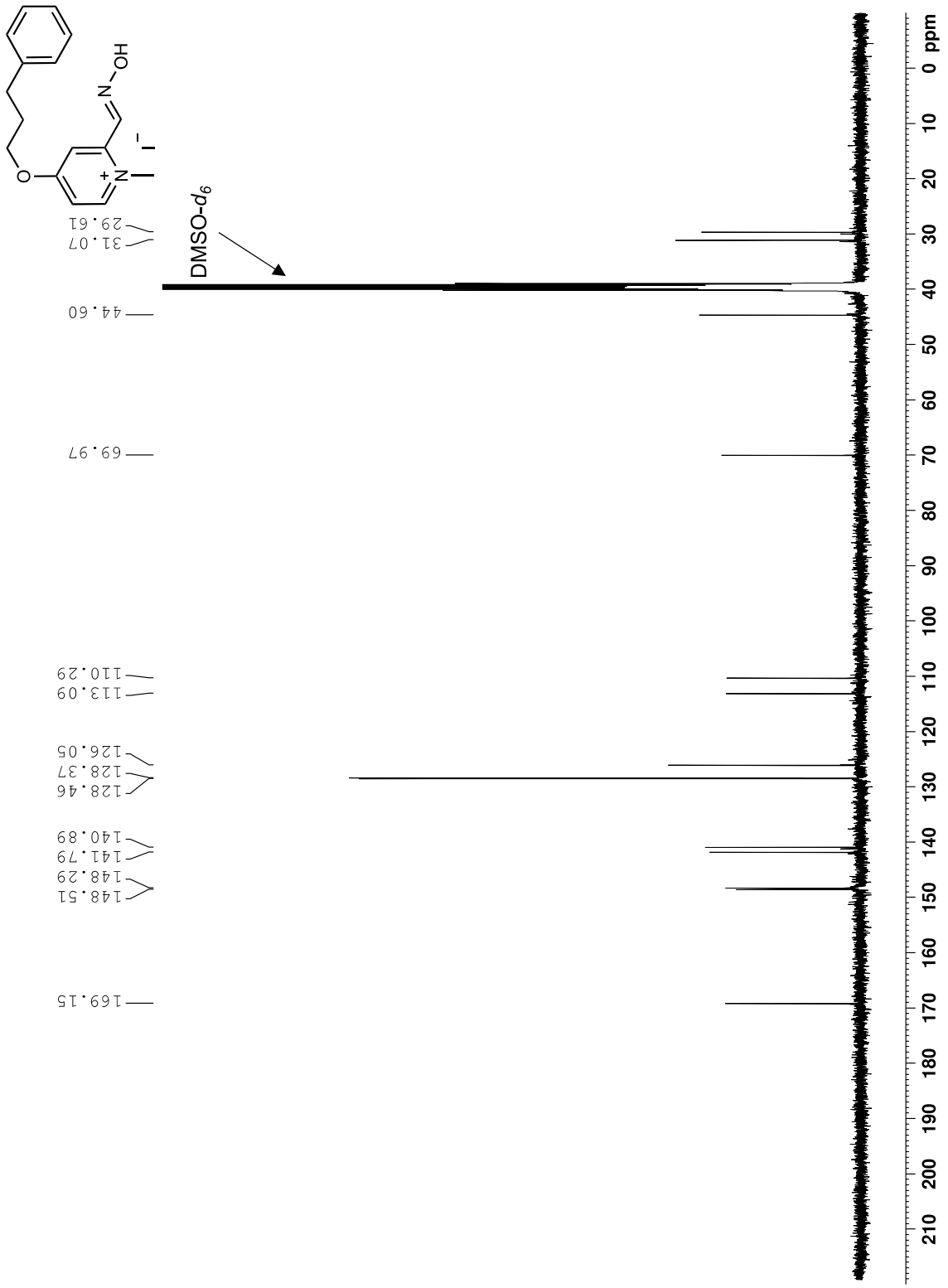

Spectrum 353. ^{13}C NMR for (*E*)-2-((hydroxyimino)methyl)-1-methyl-4-(3-phenylpropoxy)pyridin-1-ium iodide (**ADG4253**) (100 MHz, 293 K, DMSO-d_6).

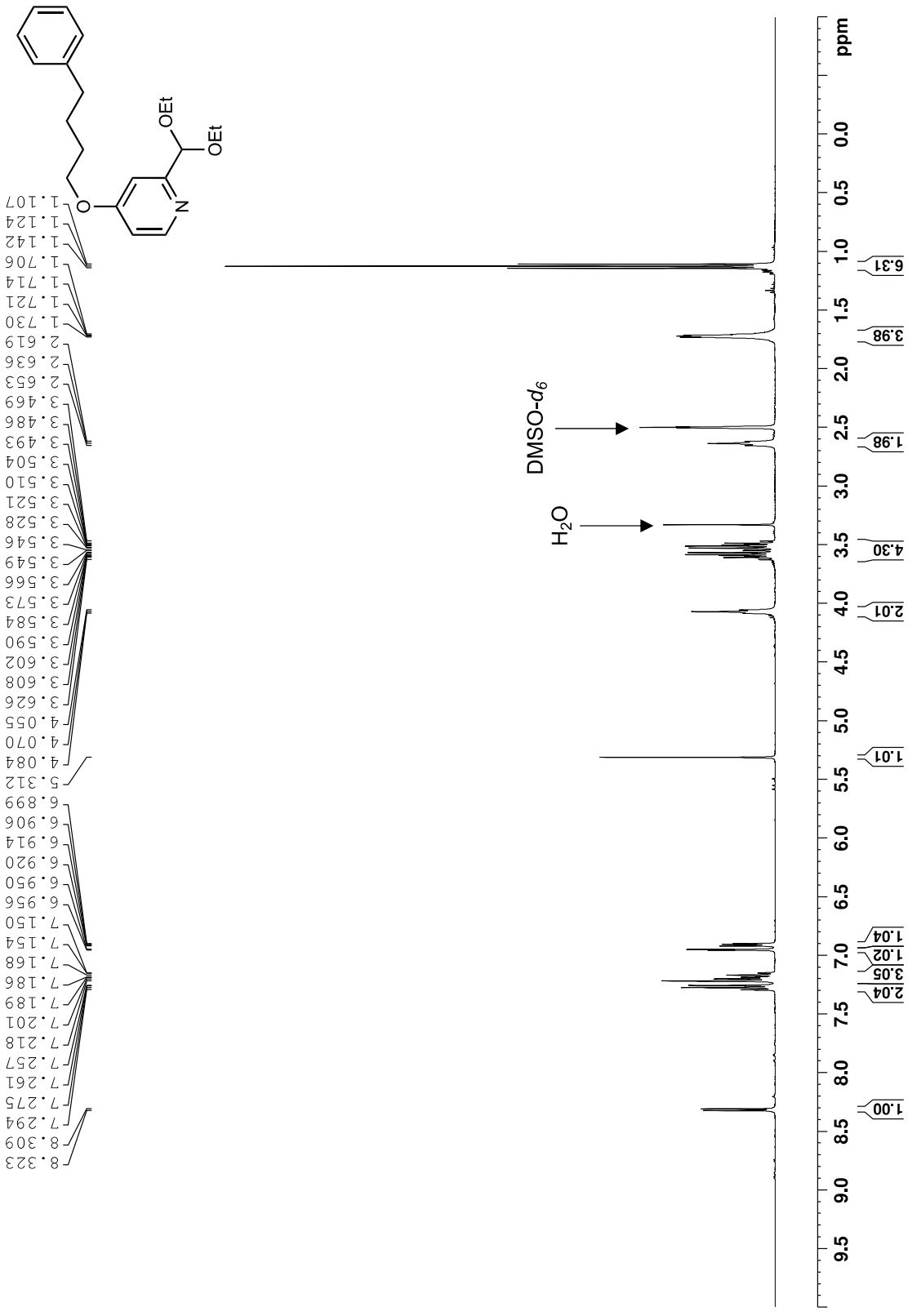

Spectrum 354. [1]H NMR for 2-(diethoxymethyl)-4-(4-phenylbutoxy)pyridine (400 MHz, 293 K, DMSO-d_6).

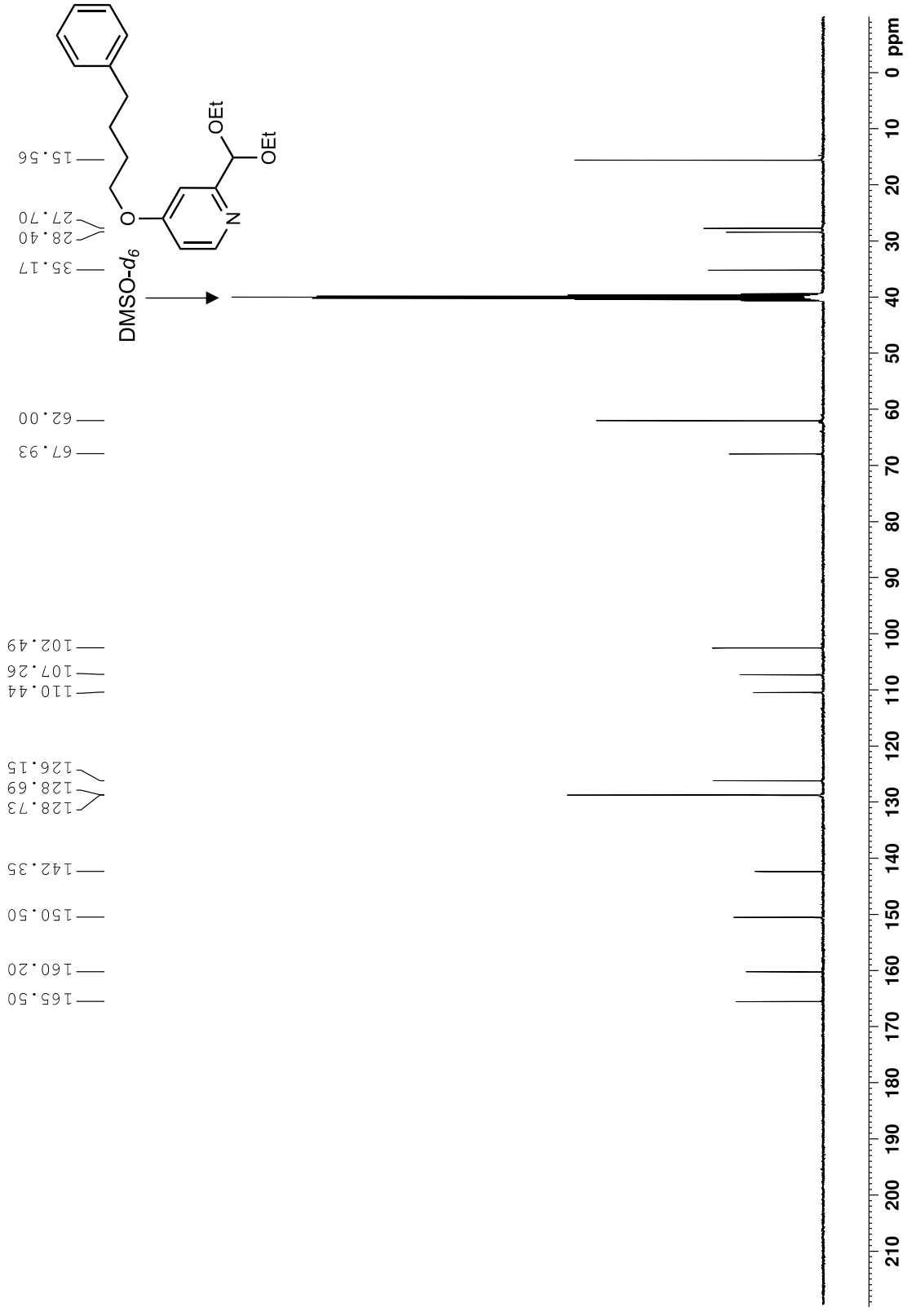

Spectrum 355. ^{13}C NMR for 2-(diethoxymethyl)-4-(4-phenylbutoxy)pyridine (100 MHz, 293 K, DMSO-d_6).

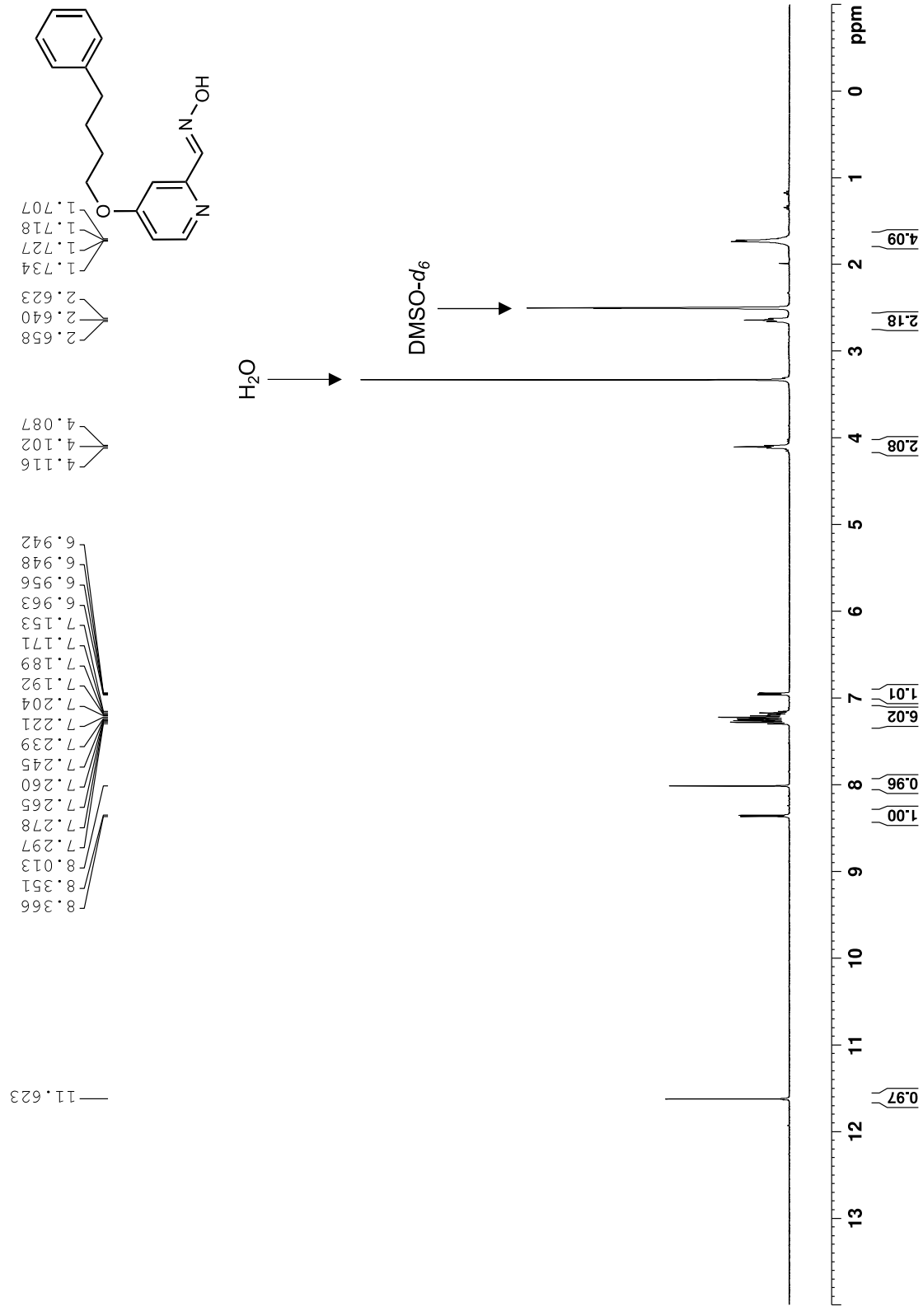

Spectrum 356. ^{1}H NMR for (*E*)-4-(4-phenylbutoxy)picolinaldehyde oxime (400 MHz, 293 K, DMSO-d_6).

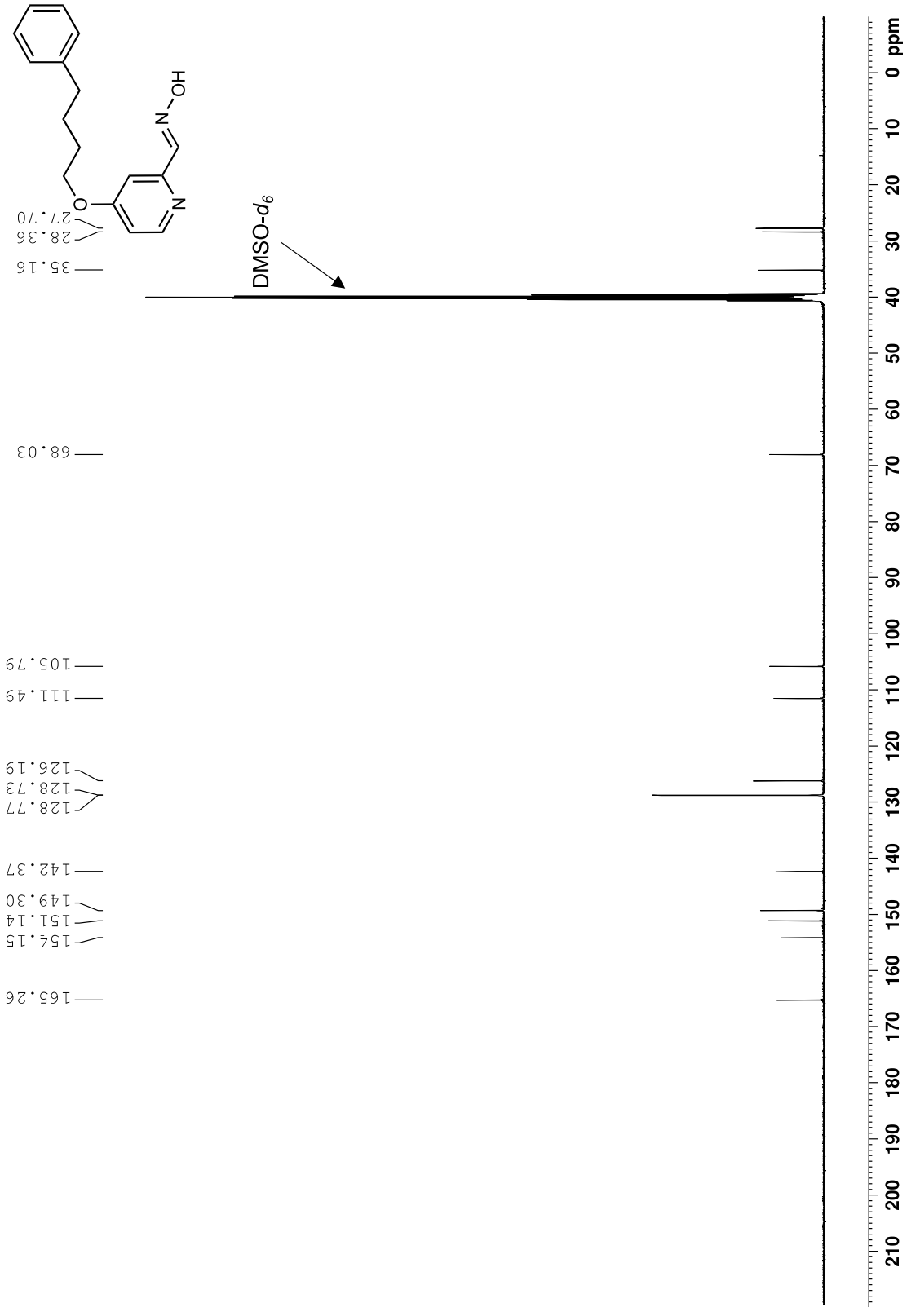

Spectrum 357. ^{13}C NMR for (*E*)-4-(4-phenylbutoxy)picolinaldehyde oxime (100 MHz, 293 K, DMSO-d_6).

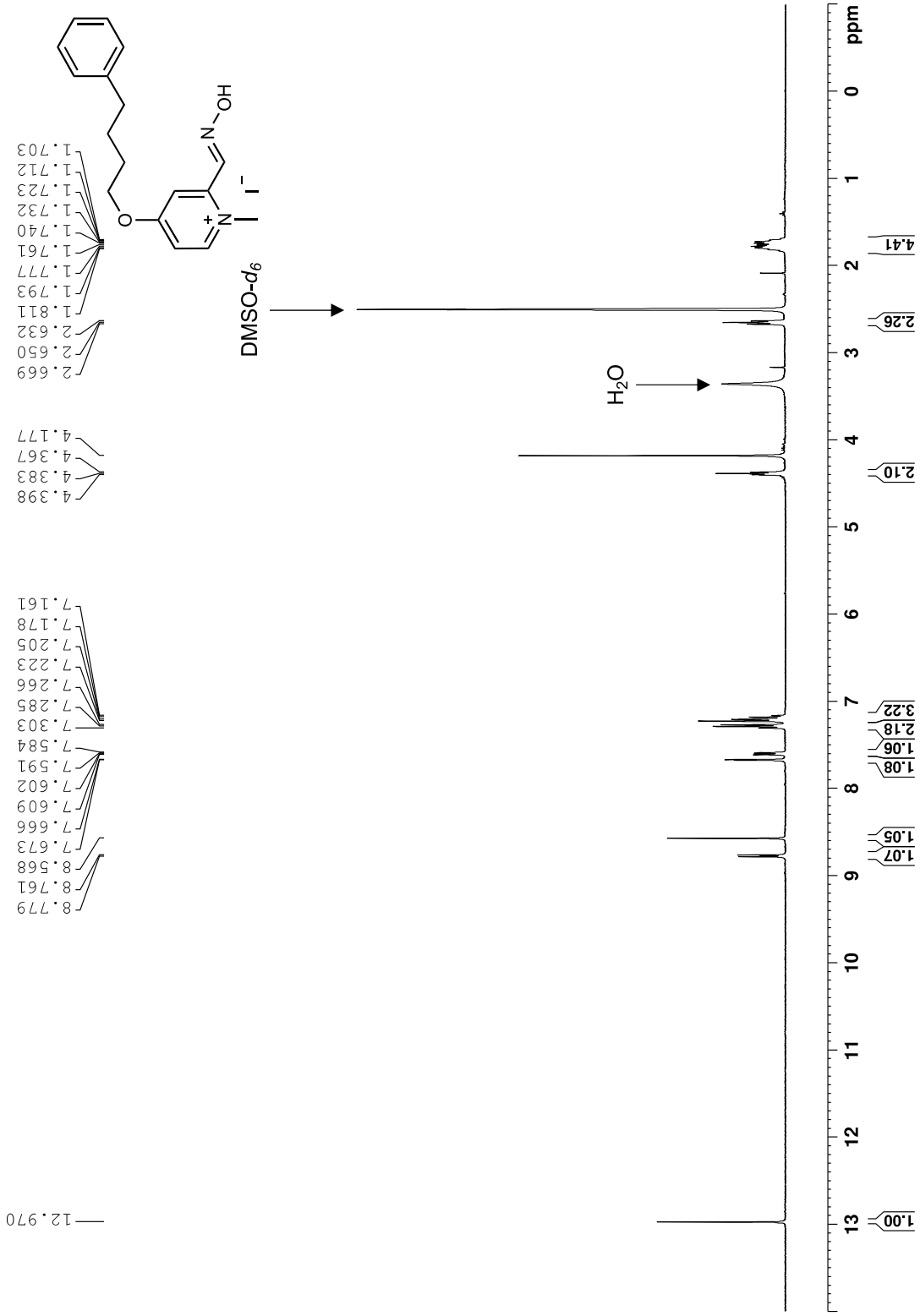

Spectrum 358. ^{1}H NMR for (*E*)-2-((hydroxyimino)methyl)-1-methyl-4-(4-phenylbutoxy)pyridin-1-ium iodide (**ADG4286**) (400 MHz, 293 K, DMSO-d_6).

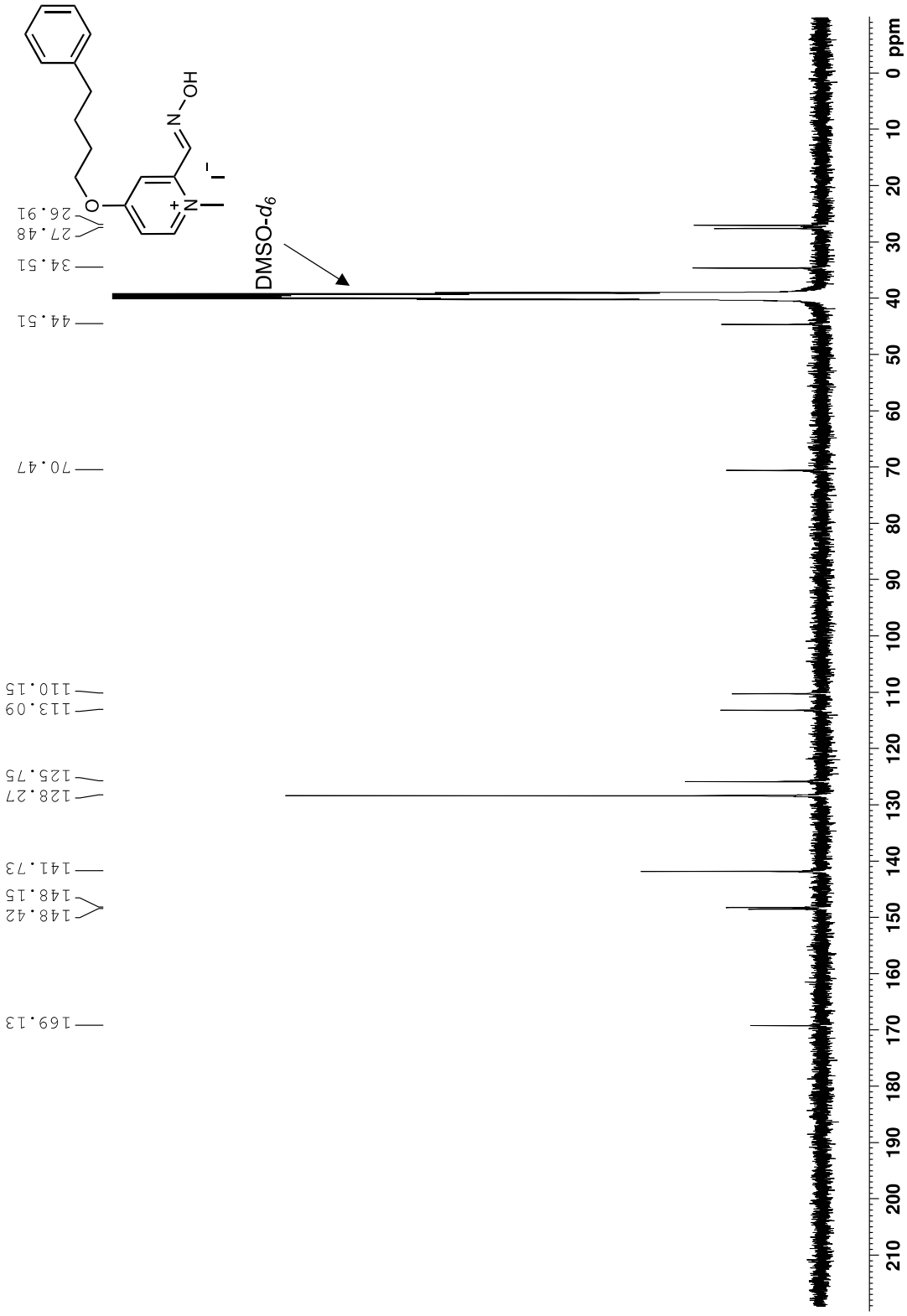

Spectrum 359. ^{13}C NMR for (*E*)-2-((hydroxyimino)methyl)-1-methyl-4-(4-phenylbutoxy)pyridin-1-ium iodide (**ADG4286**) (100 MHz, 293 K, DMSO-d_6).

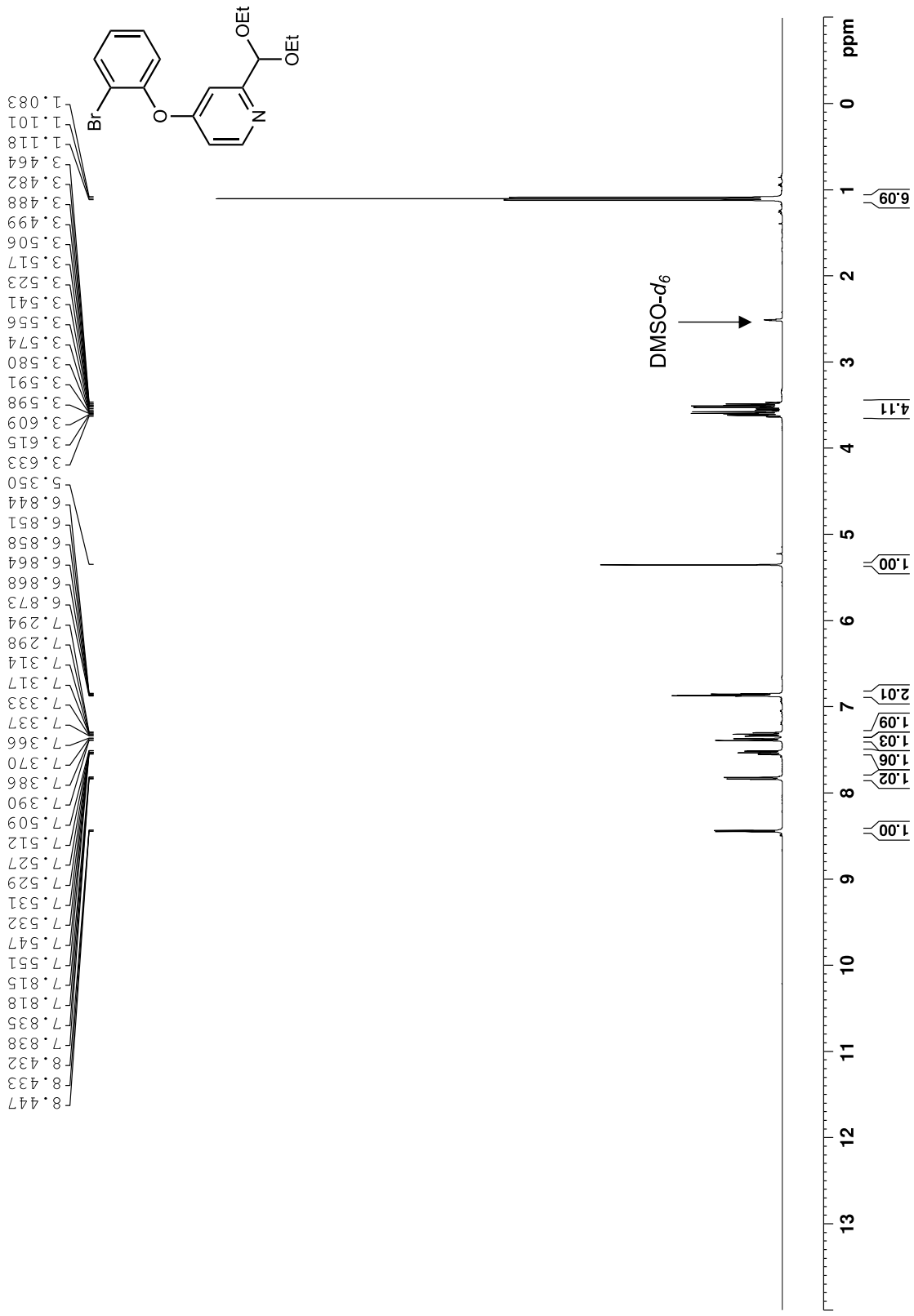

Spectrum 360. ^{1}H NMR for 4-(2-bromophenoxy)-2-(diethoxymethyl)pyridine (400 MHz, 293 K, DMSO-d_6).

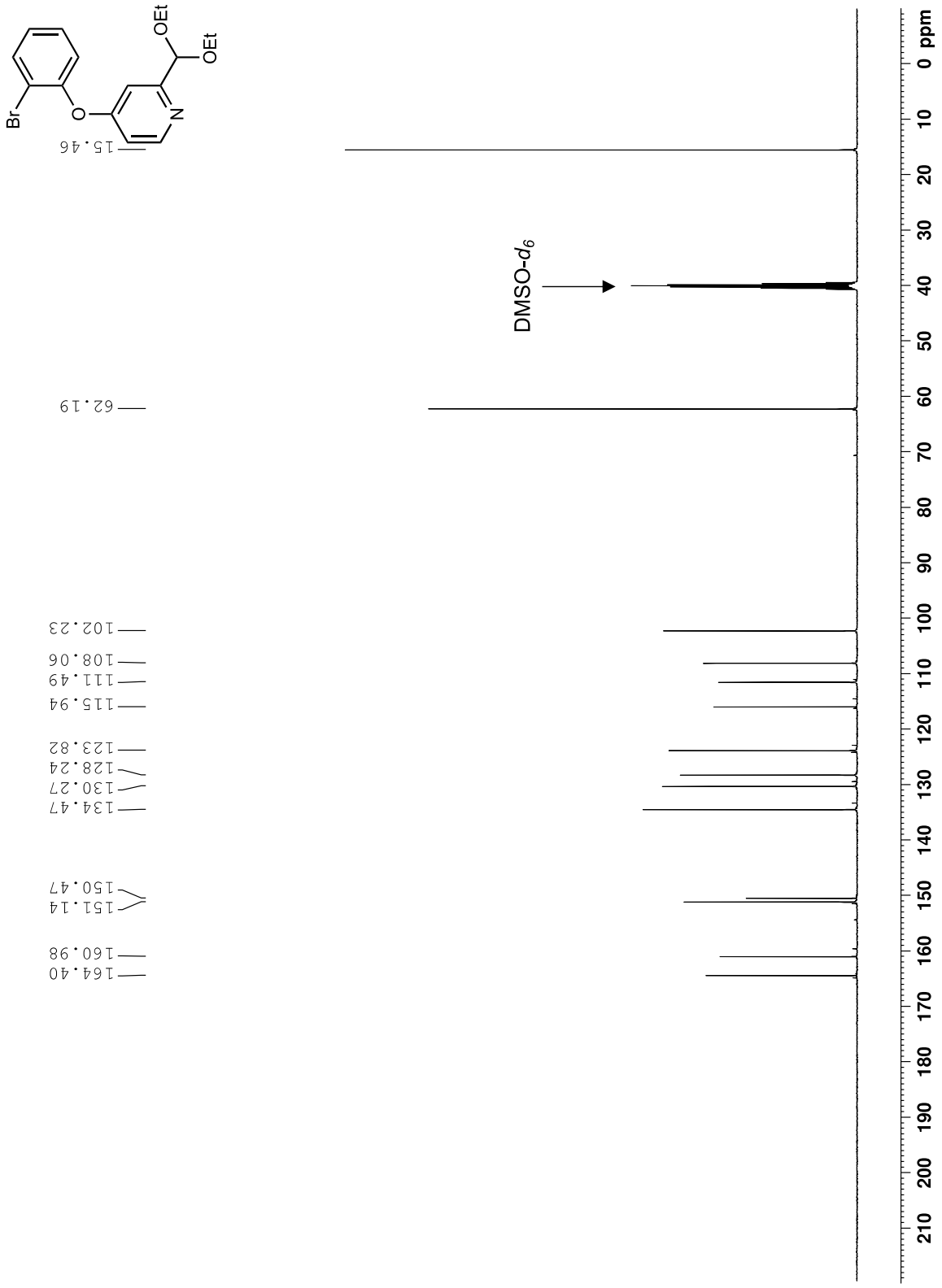

Spectrum 361. ^{13}C NMR for 4-(2-bromophenoxy)-2-(diethoxymethyl)pyridine (100 MHz, 293 K, DMSO-d_6).

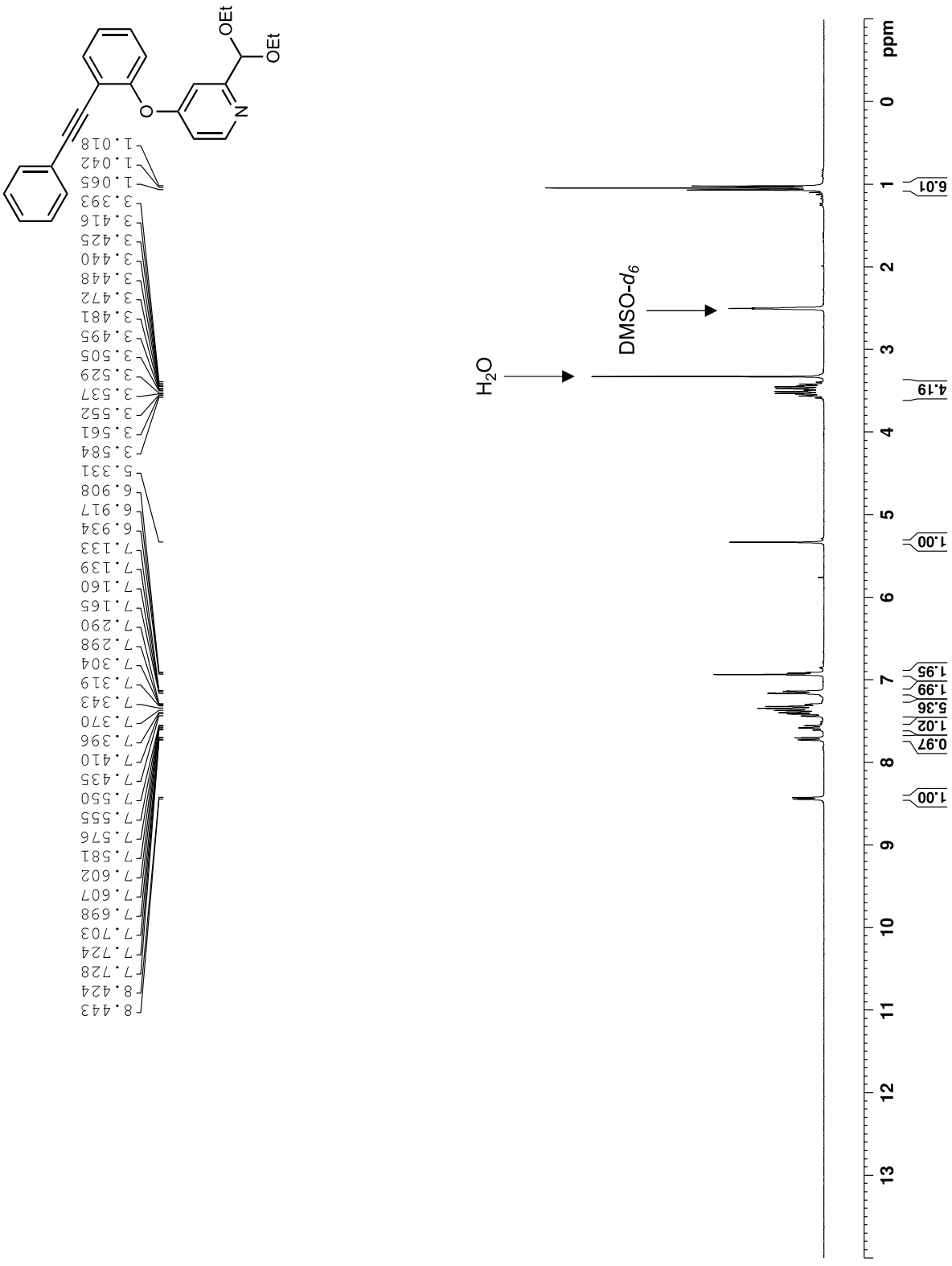

Spectrum 362. ^{1}H NMR for 2-(diethoxymethyl)-4-(2-(phenylethynyl)phenoxy)pyridine (300 MHz, 293 K, DMSO-d_6).

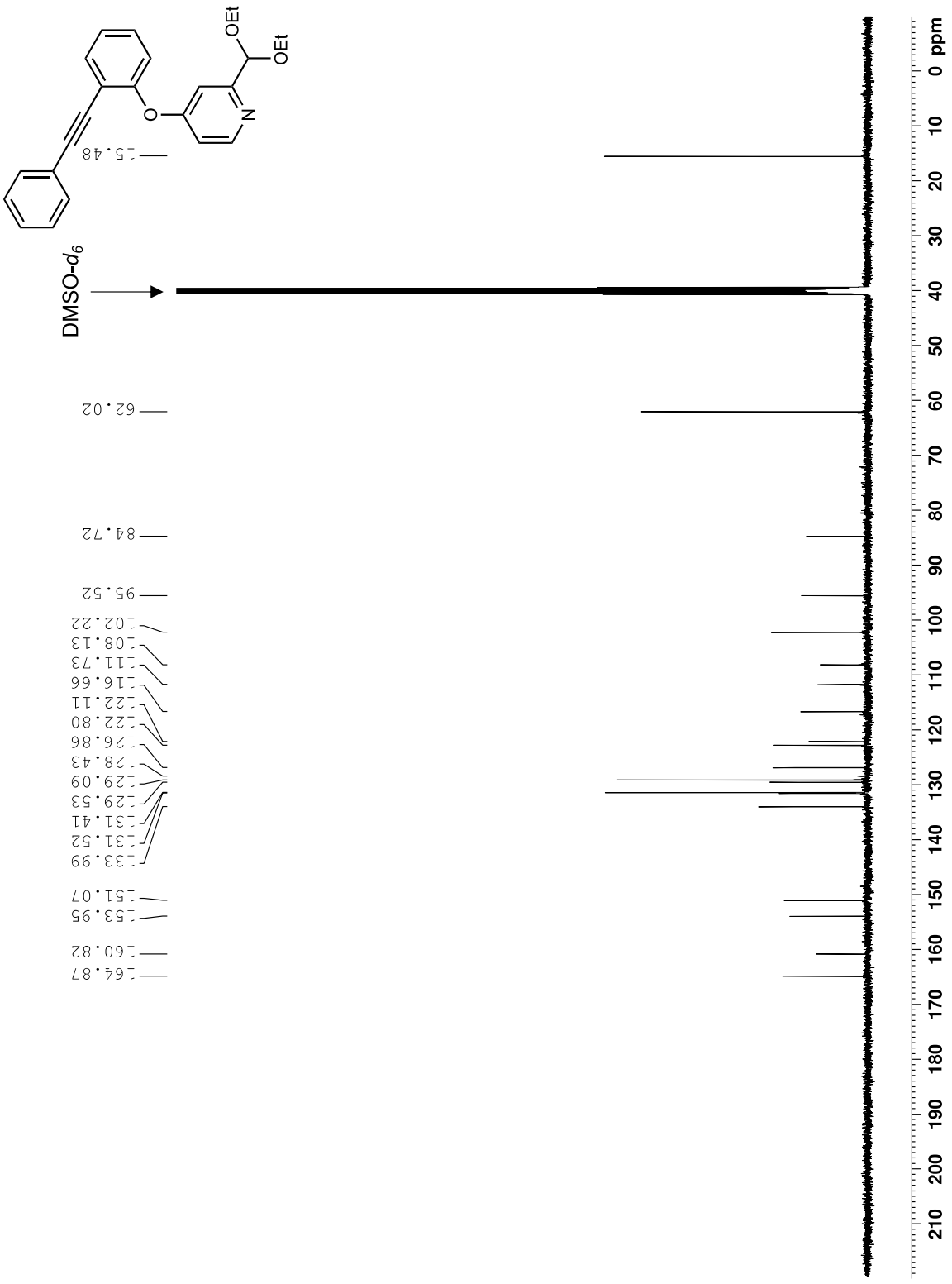

Spectrum 363. ^{13}C NMR for 2-(diethoxymethyl)-4-(2-(phenylethynyl)phenoxy)pyridine (100 MHz, 293 K, DMSO-d_6).

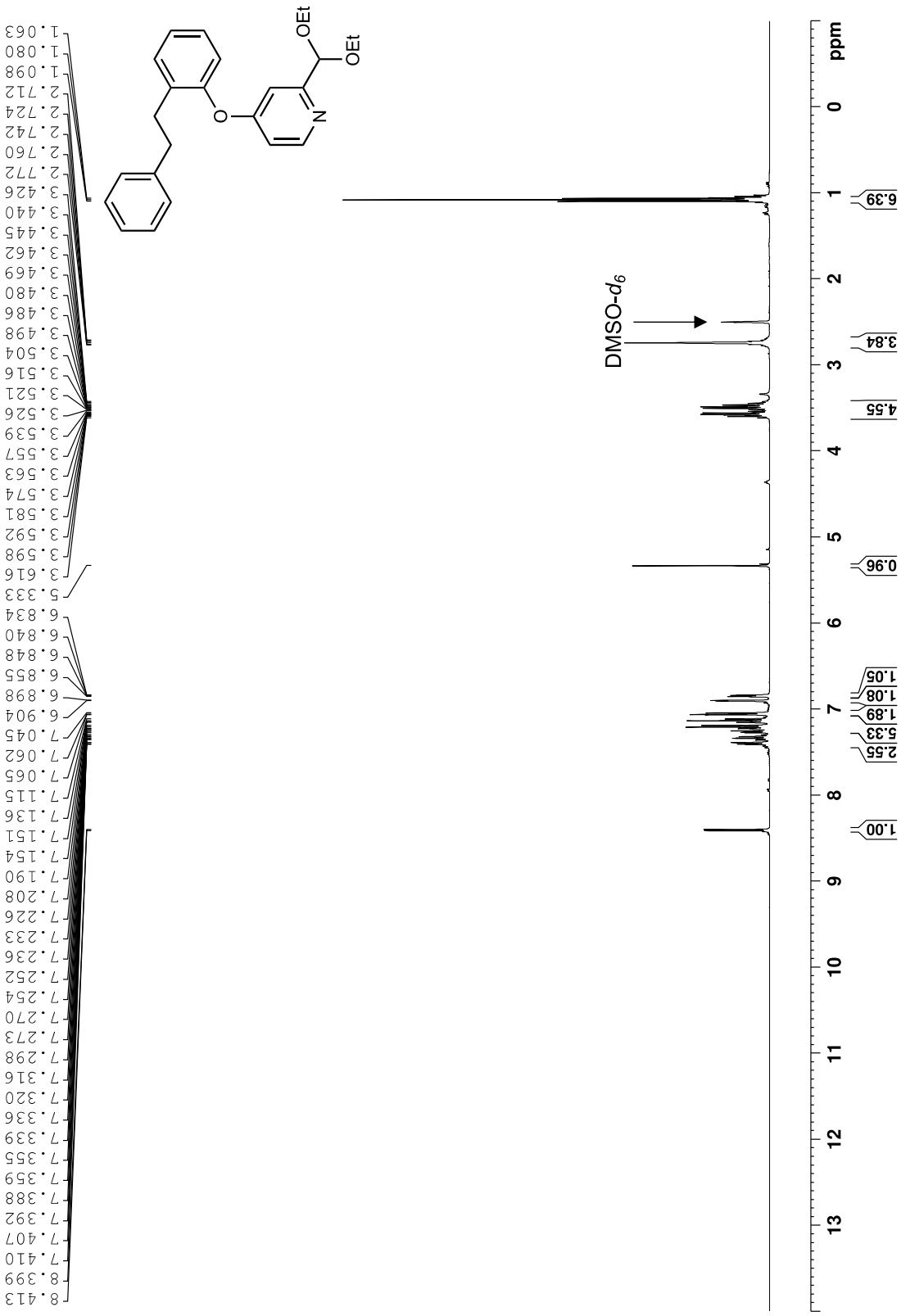

Spectrum 364. ^{1}H NMR for 2-(diethoxymethyl)-4-(2-phenethylphenoxy)pyridine (400 MHz, 293 K, DMSO-d_6).

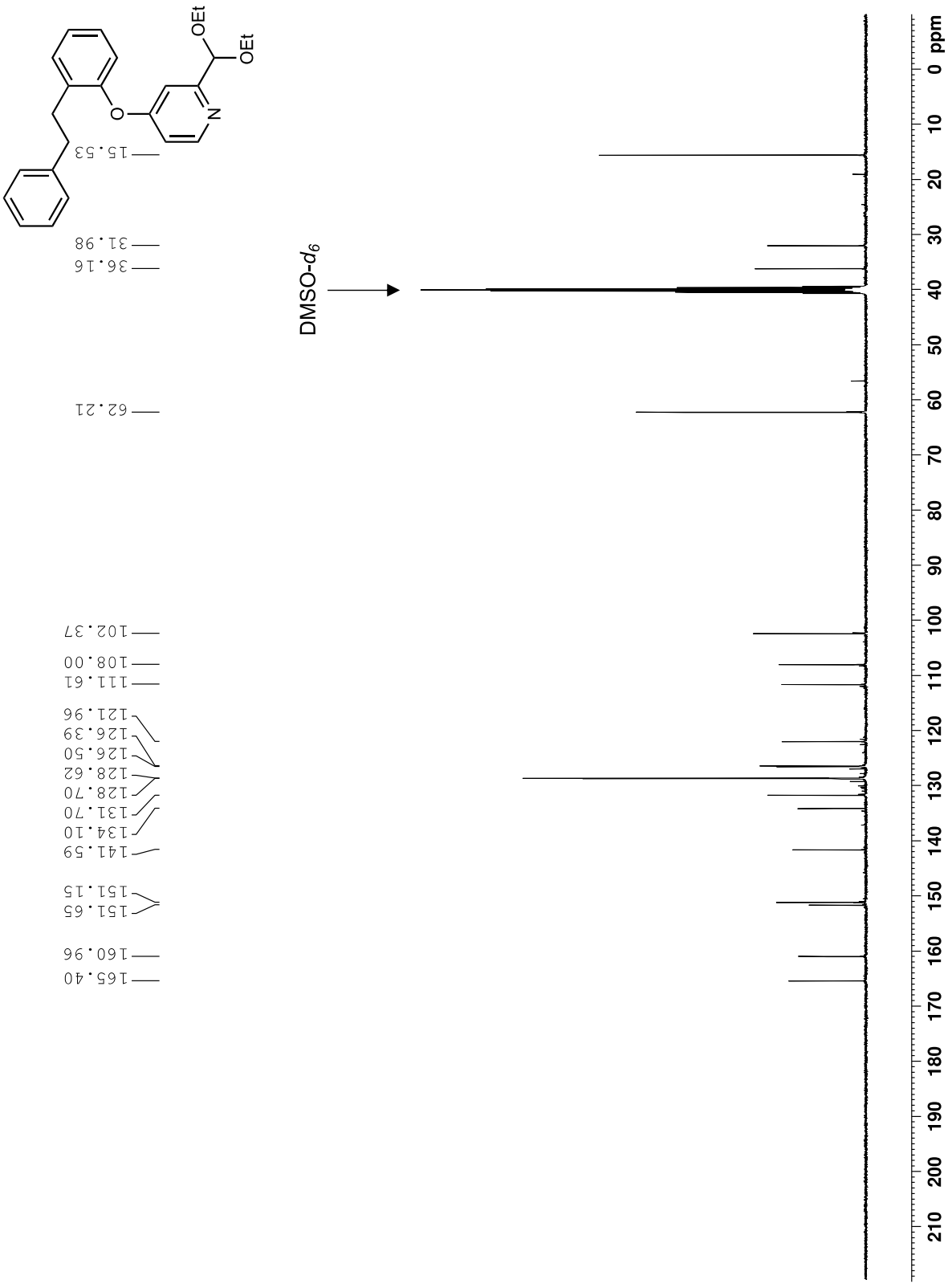

Spectrum 365. ^{13}C NMR for 2-(diethoxymethyl)-4-(2-phenethylphenoxy)pyridine (100 MHz, 293 K, DMSO-d_6).

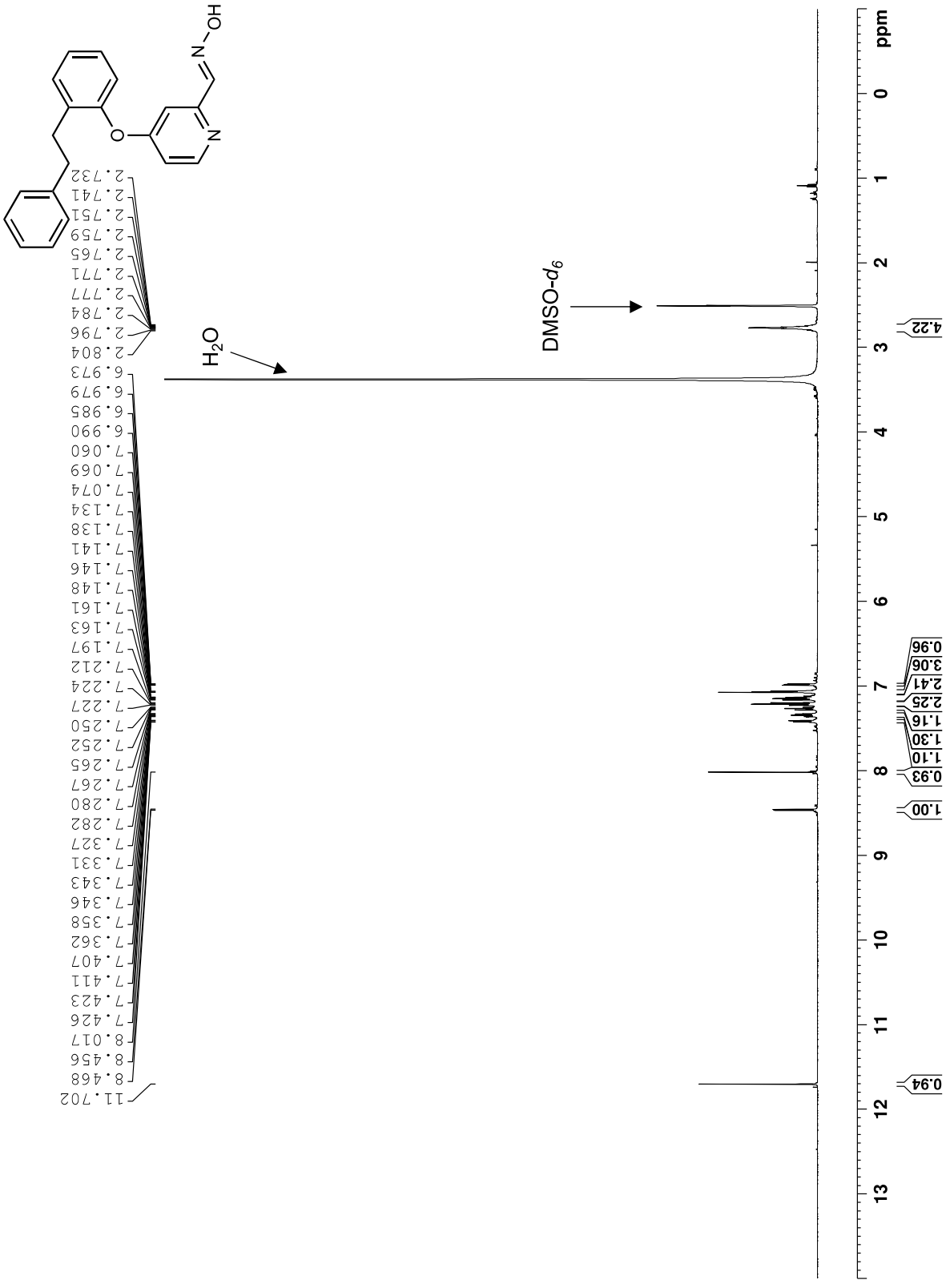

Spectrum 366. ^{1}H NMR for (*E*)-4-(2-phenethylphenoxy)picolinaldehyde oxime (500 MHz, 293 K, DMSO-d_6)).

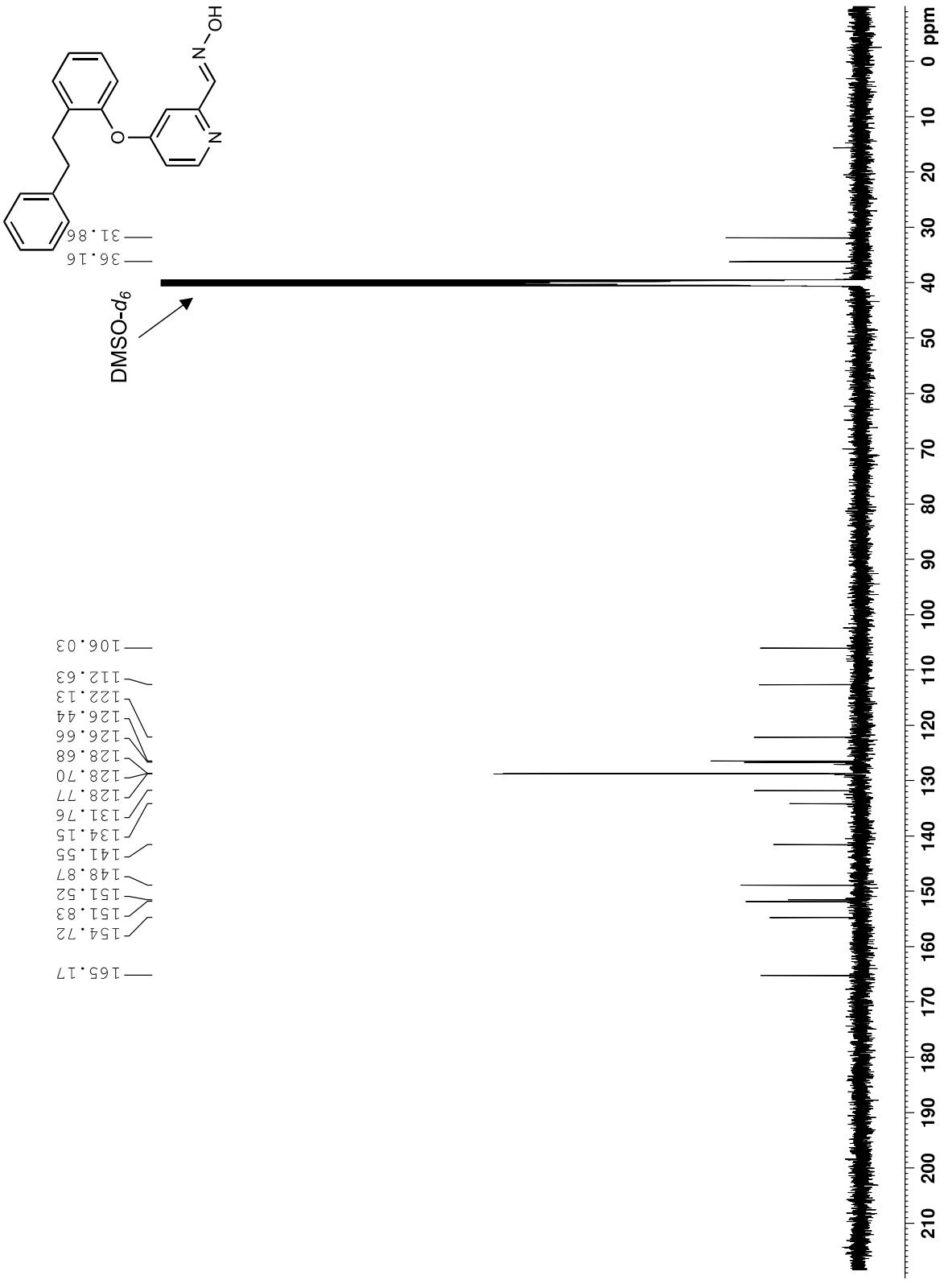

Spectrum 367. ^{13}C NMR for (*E*)-4-(2-phenethylphenoxy)picolinaldehyde oxime (125 MHz, 293 K, DMSO-d_6).

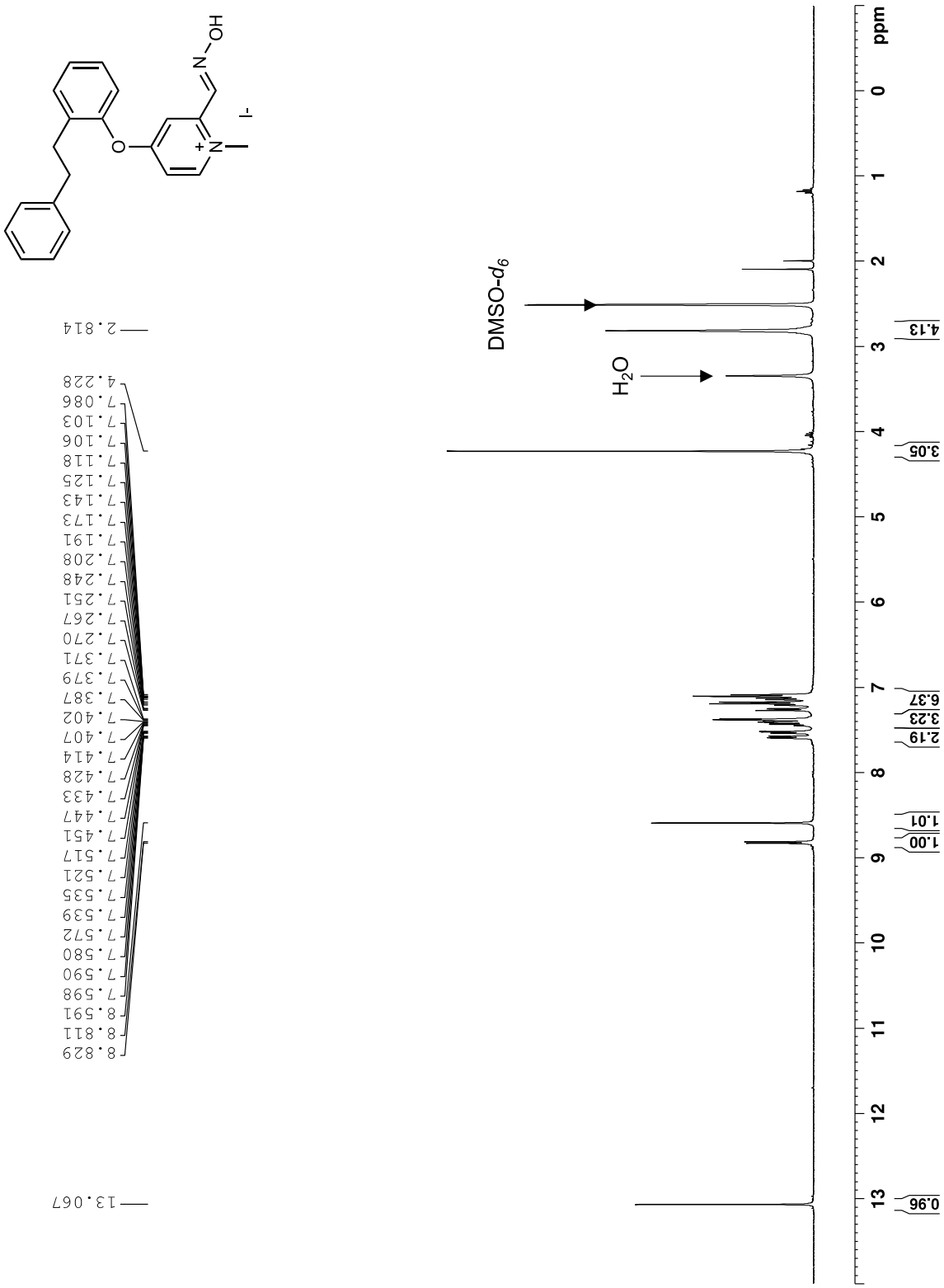

Spectrum 368. ^{1}H NMR for (*E*)-2-((hydroxyimino)methyl)-1-methyl-4-(2-phenethylphenoxy)pyridin-1-ium iodide (**ADG4298**) (400 MHz, 293 K, DMSO-d_6).

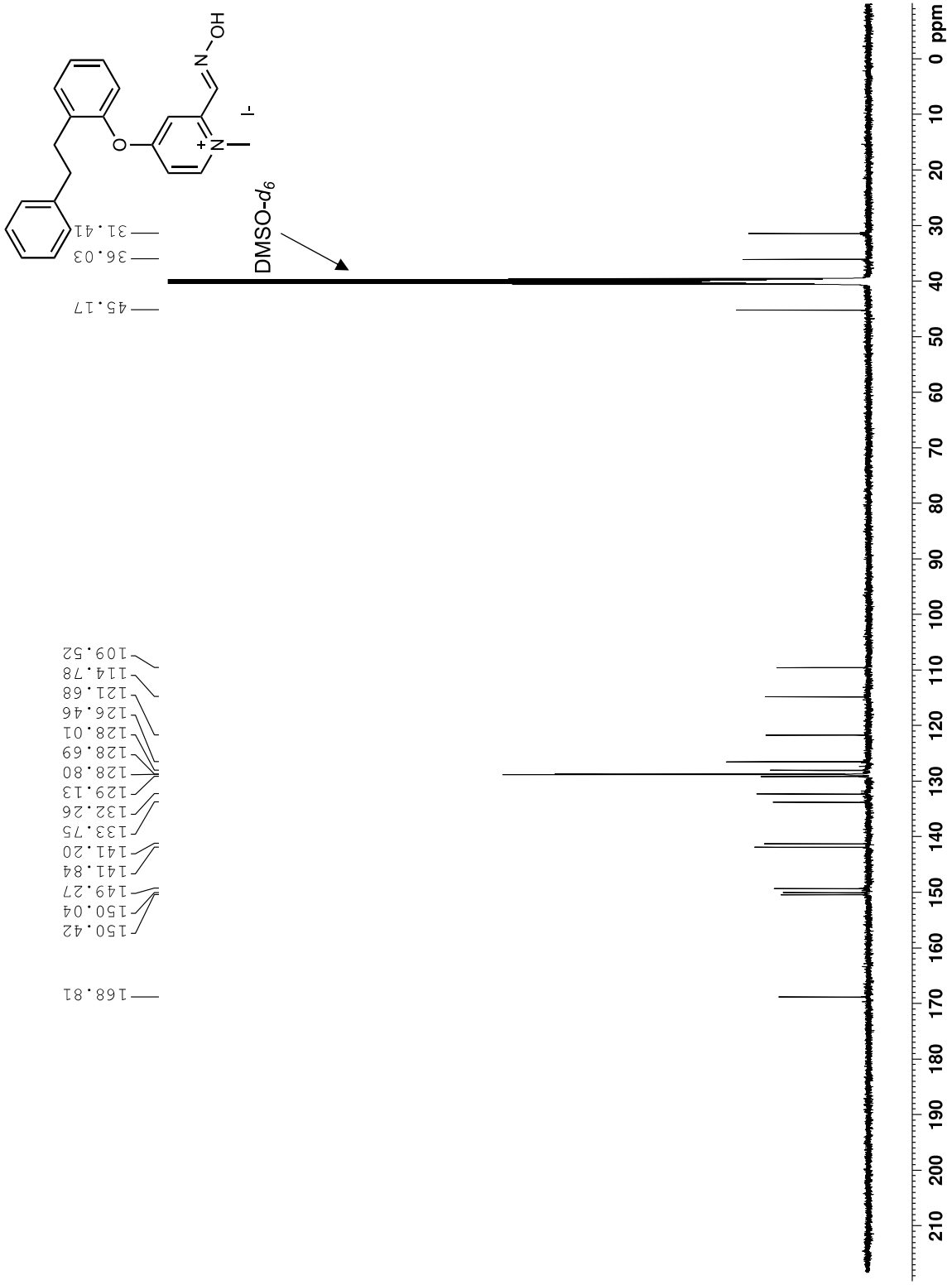

Spectrum 369. ^{13}C NMR for (*E*)-2-((hydroxyimino)methyl)-1-methyl-4-(2-phenethylphenoxy)pyridin-1-ium iodide (**ADG4298**) (125 MHz, 293 K, DMSO-d_6).

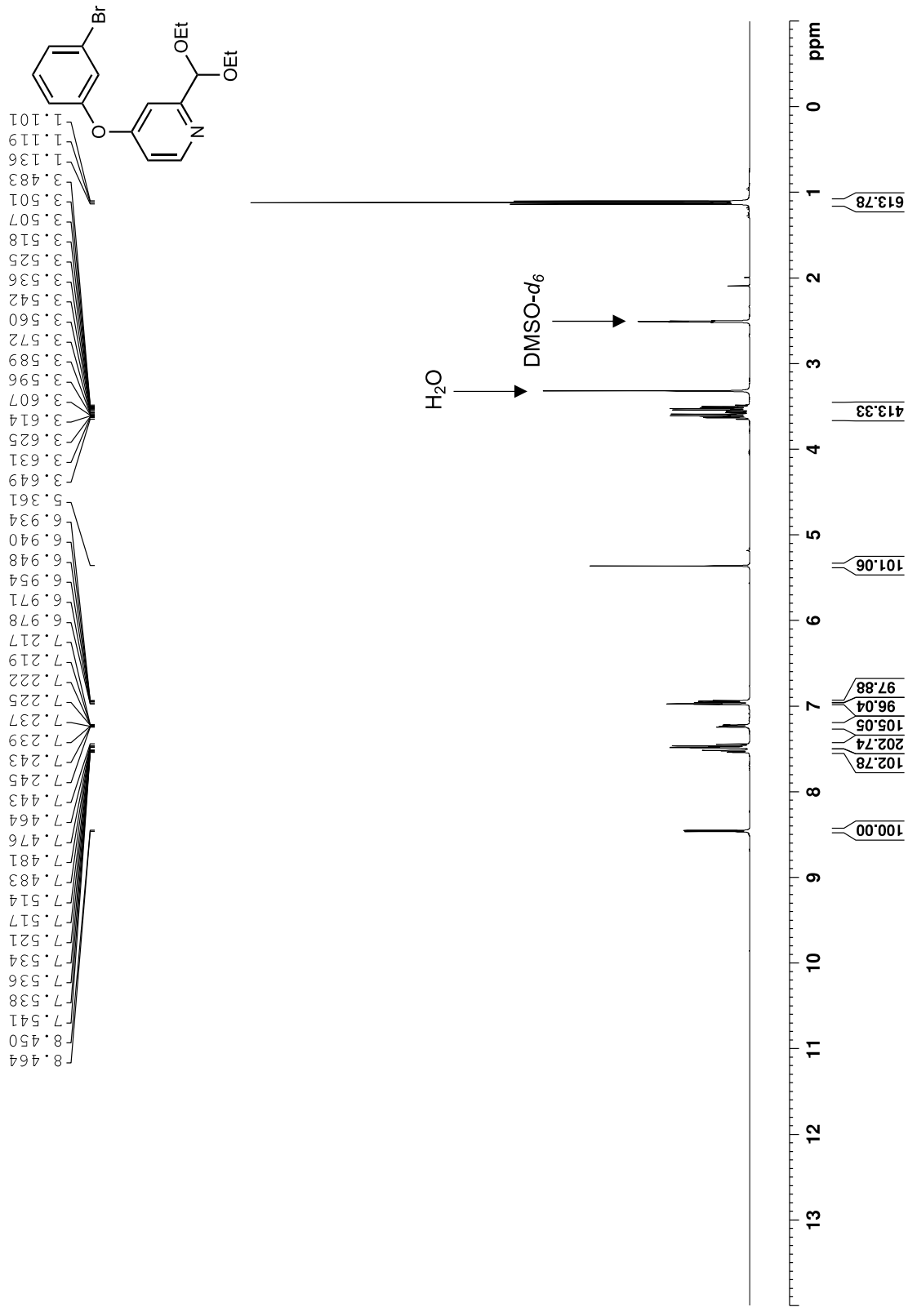

Spectrum 370. ^{1}H NMR for 4-(3-bromophenoxy)-2-(diethoxymethyl)pyridine (400 MHz, 293 K, DMSO-d_6).

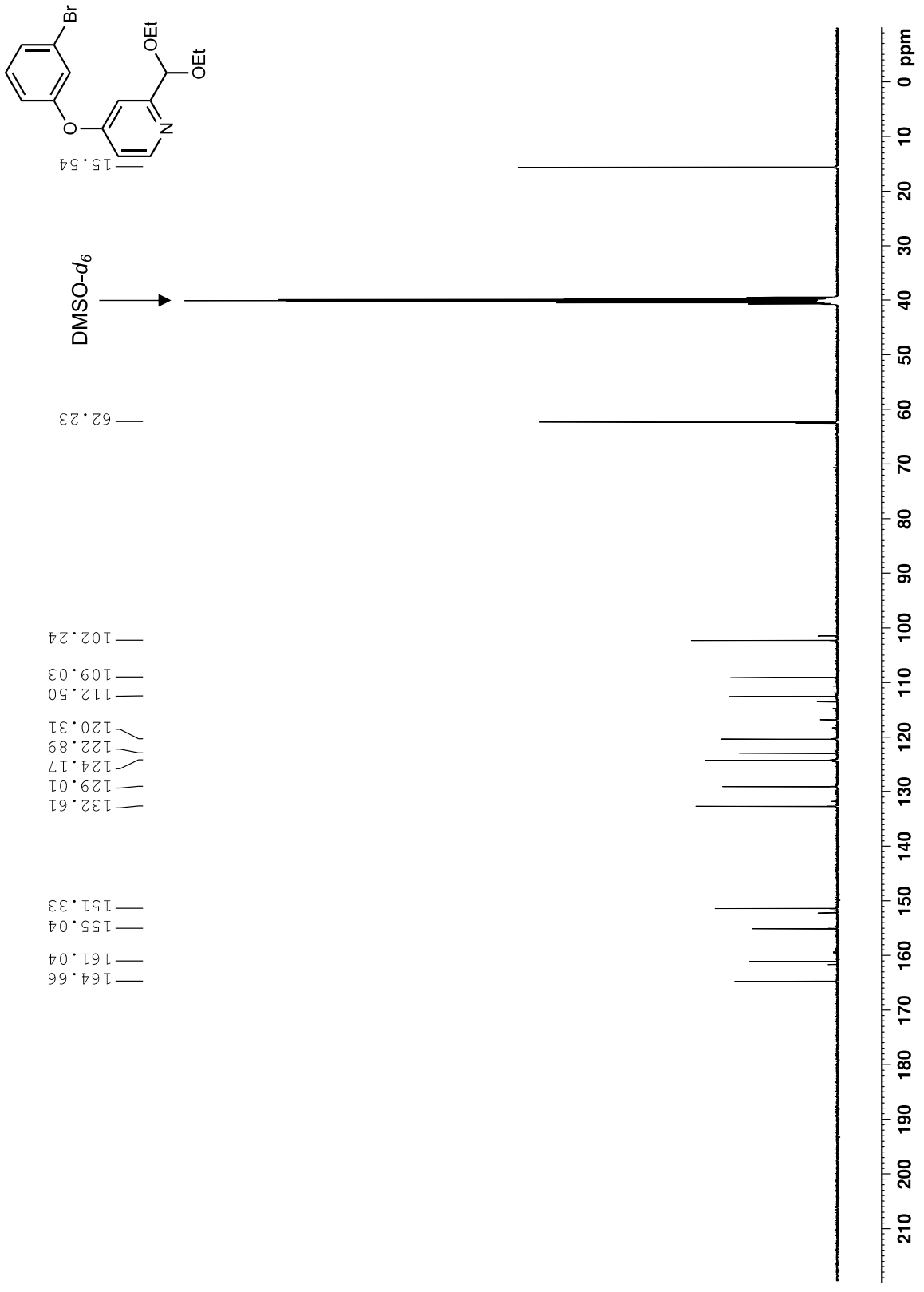

Spectrum 371. ^{13}C NMR for 4-(3-bromophenoxy)-2-(diethoxymethyl)pyridine (100 MHz, 293 K, DMSO-d_6).

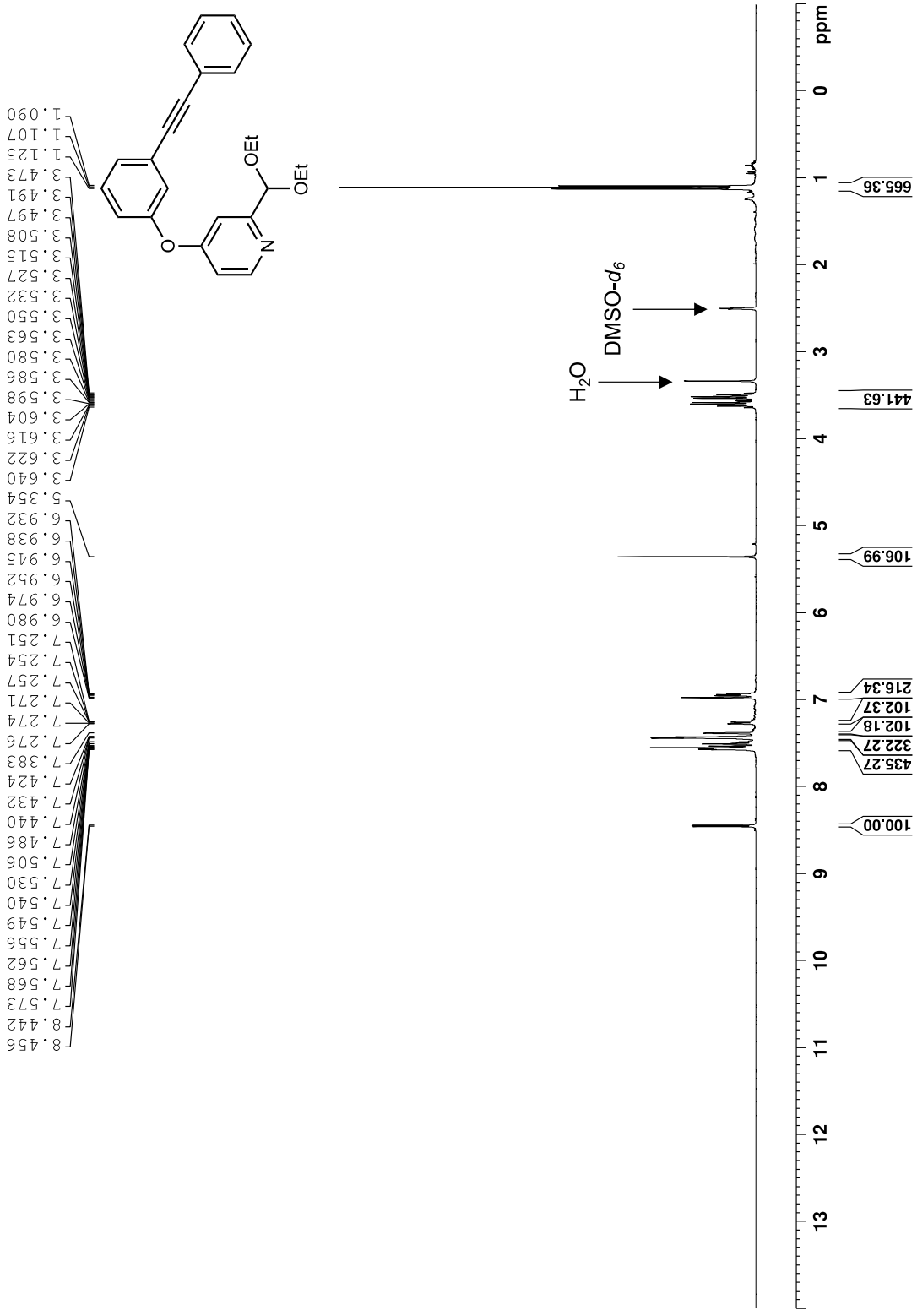

Spectrum 372. ^{1}H NMR for 2-(diethoxymethyl)-4-(2-(phenylethynyl)phenoxy)pyridine (400 MHz, 293 K, DMSO-d_6).

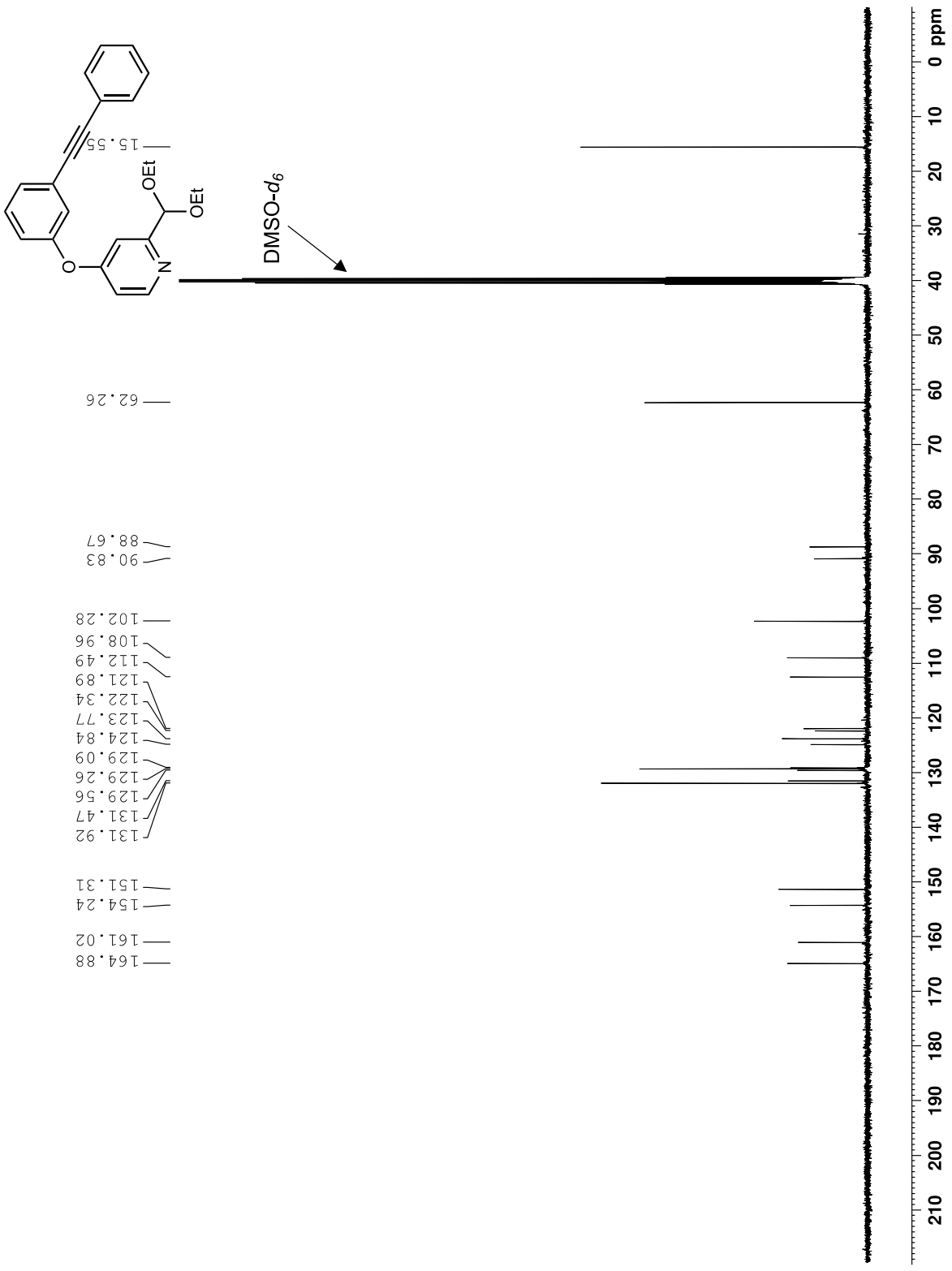

Spectrum 373. ^{13}C NMR for 2-(diethoxymethyl)-4-(2-(phenylethynyl)phenoxy)pyridine (100 MHz, 293 K, DMSO-d_6).

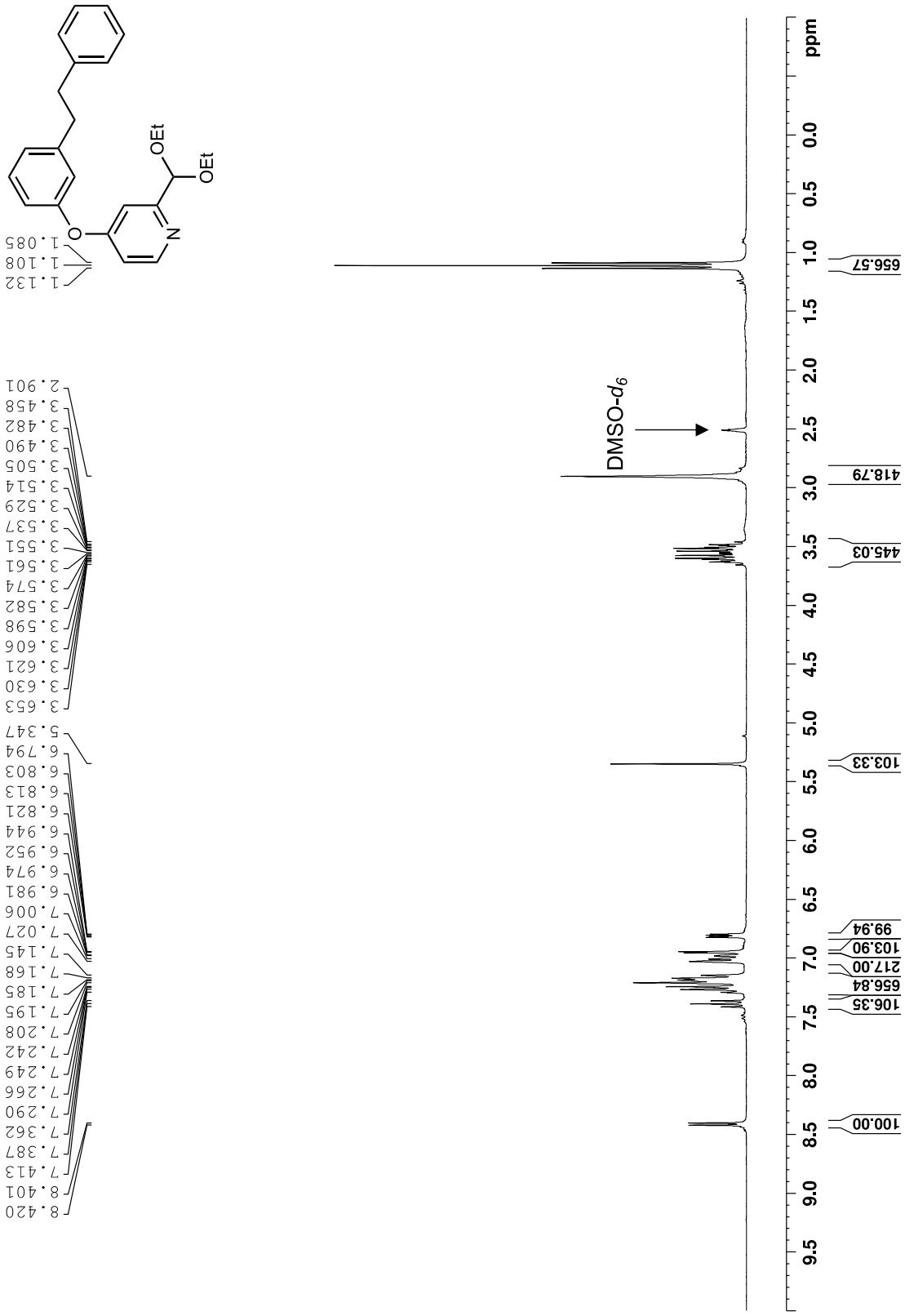

Spectrum 374. ^{1}H NMR for 2-(diethoxymethyl)-4-(3-phenethylphenoxy)pyridine (300 MHz, 293 K, DMSO-d_6).

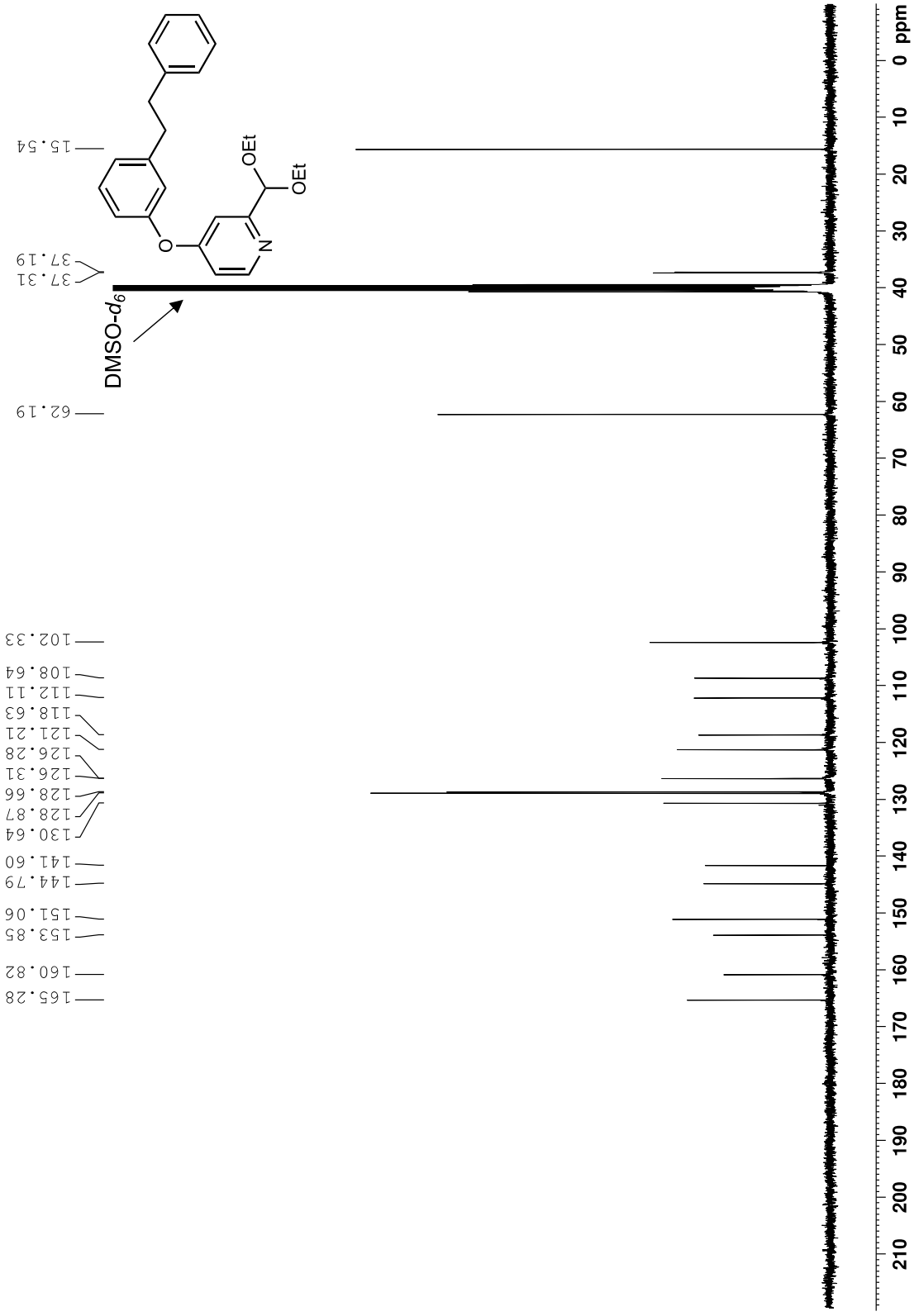

Spectrum 375. ^{13}C NMR for 2-(diethoxymethyl)-4-(3-phenethylphenoxy)pyridine (100 MHz, 293 K, DMSO-d_6).

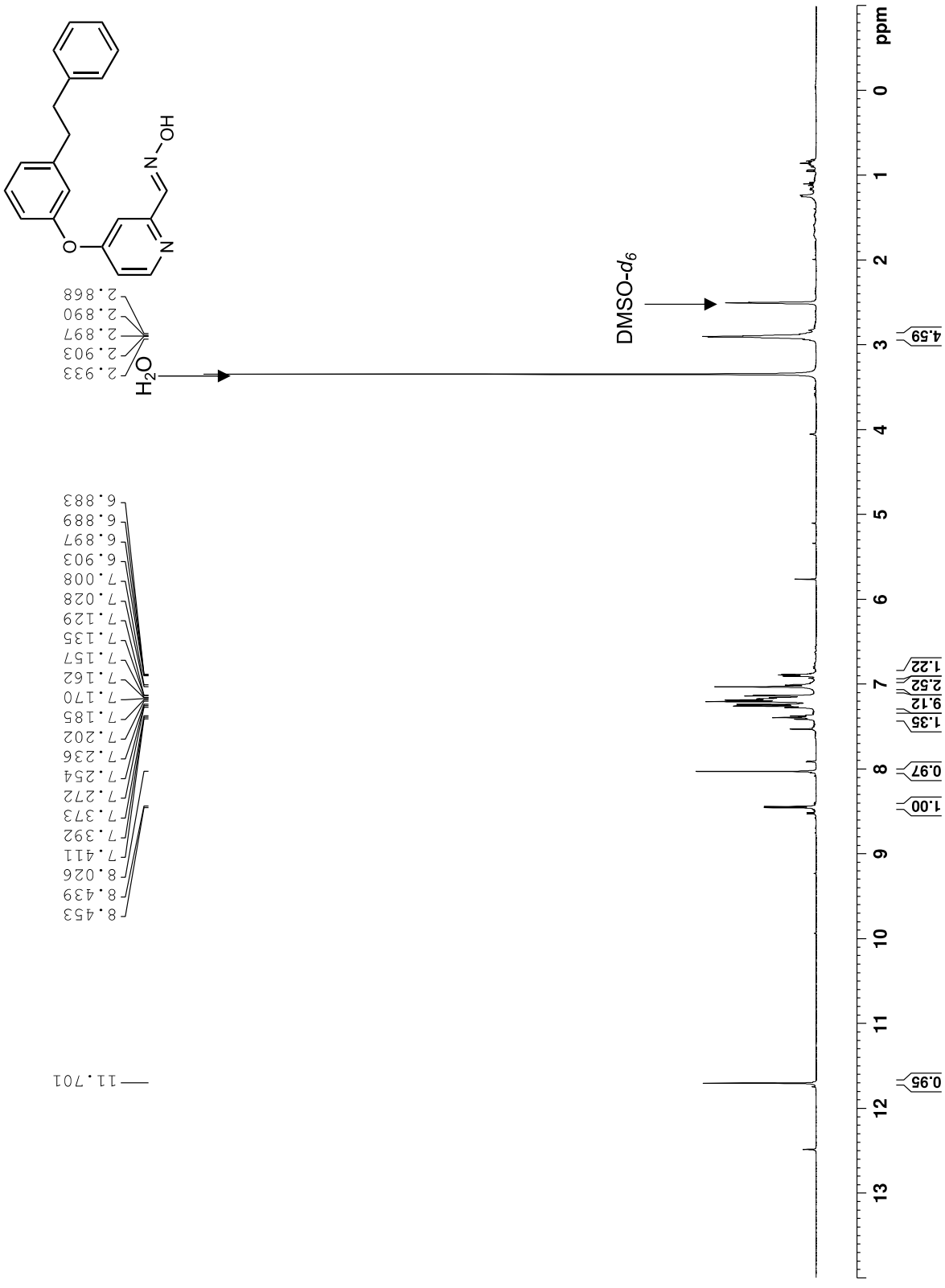

Spectrum 376. ^{1}H NMR for (*E*)-4-(3-phenethylphenoxy)picolinaldehyde oxime (400 MHz, 293 K, DMSO-d_6).

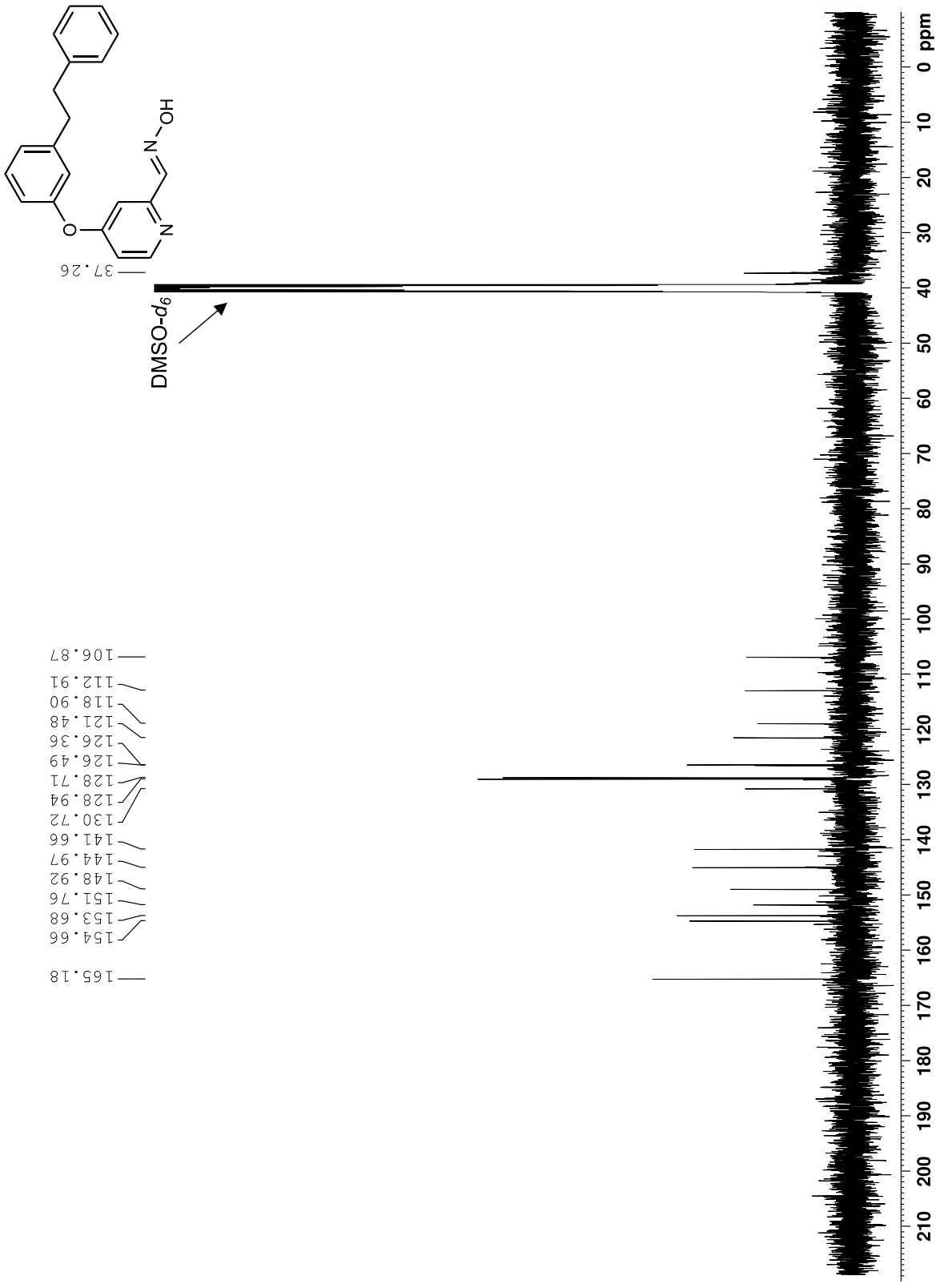

Spectrum 377. ^{13}C NMR for (*E*)-4-(3-phenethylphenoxy)picolinaldehyde oxime (100 MHz, 293 K, DMSO-d_6).

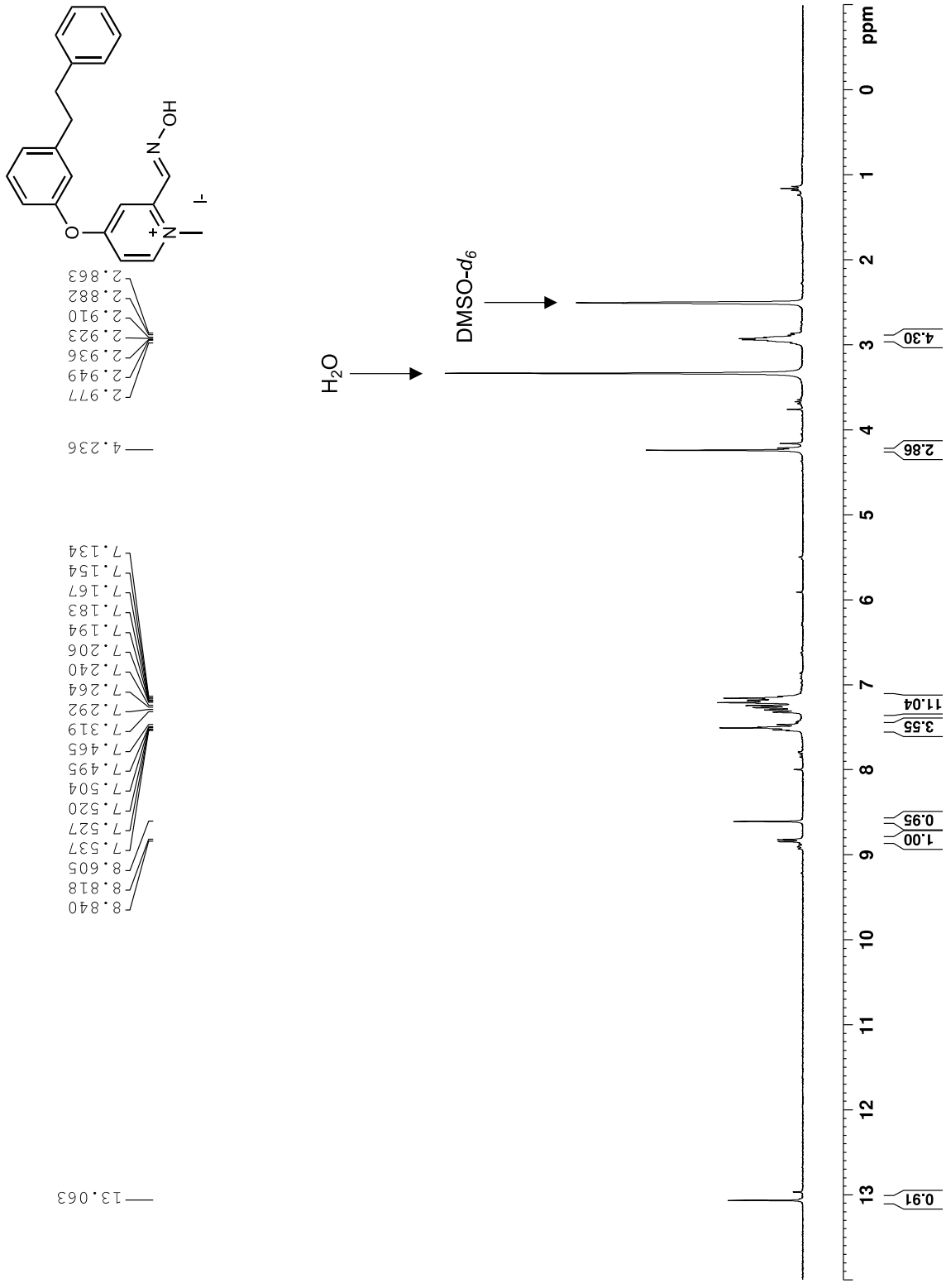

Spectrum 378. ^{1}H NMR for *(E)*-2-((hydroxyimino)methyl)-1-methyl-4-(3-phenethylphenoxy)pyridin-1-ium iodide (**ADG4291)** (300 MHz, 293 K, DMSO-d_6).

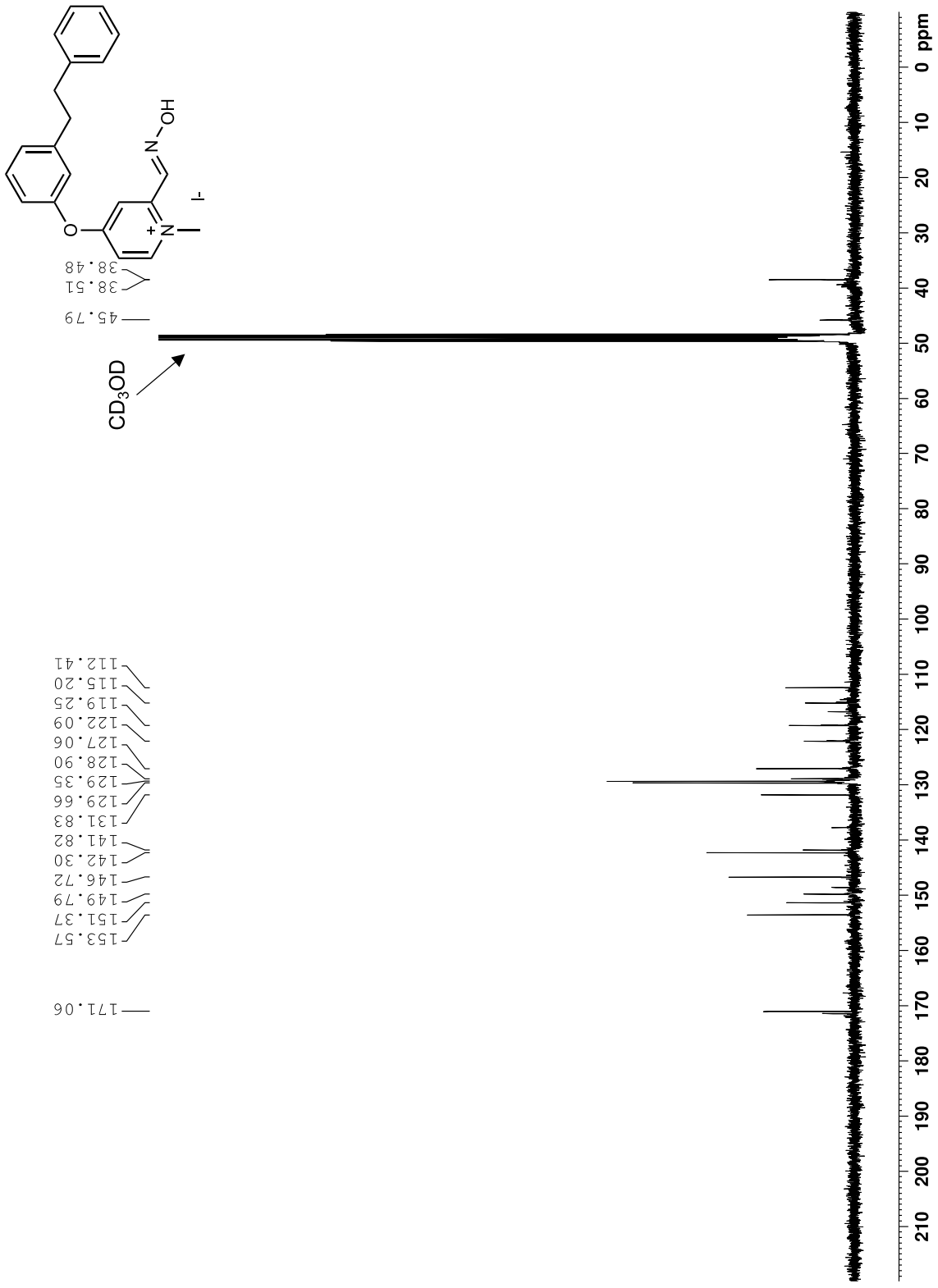

Spectrum 379. ^{13}C NMR for *(E)*-2-((hydroxyimino)methyl)-1-methyl-4-(3-phenethylphenoxy)pyridin-1-ium iodide (**ADG4291)** (100 MHz, 293 K, CD_3OD).

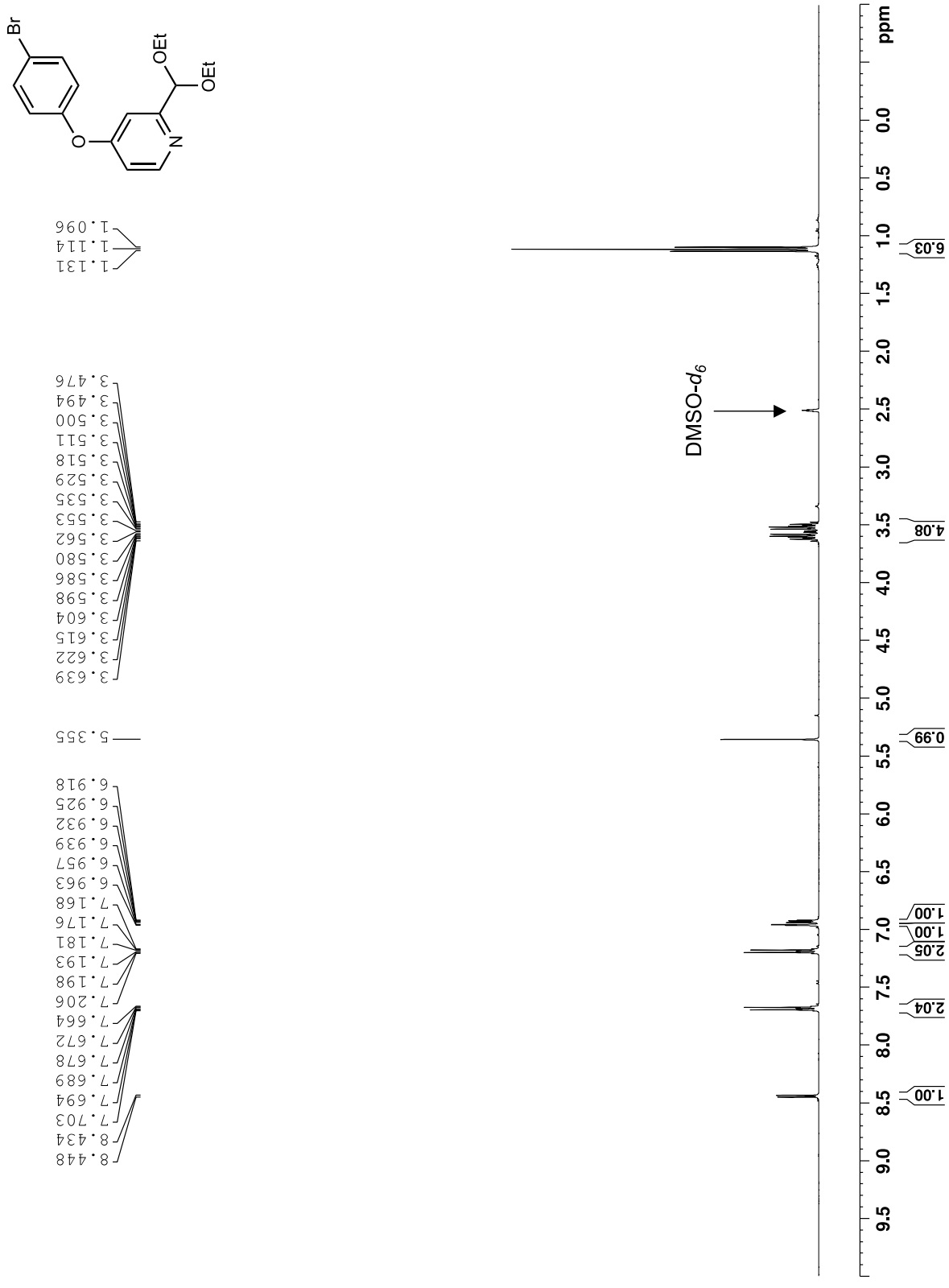

Spectrum 380. ^{1}H NMR for 4-(4-bromophenoxy)-2-(diethoxymethyl)pyridine (400 MHz, 293 K, DMSO-d_6).

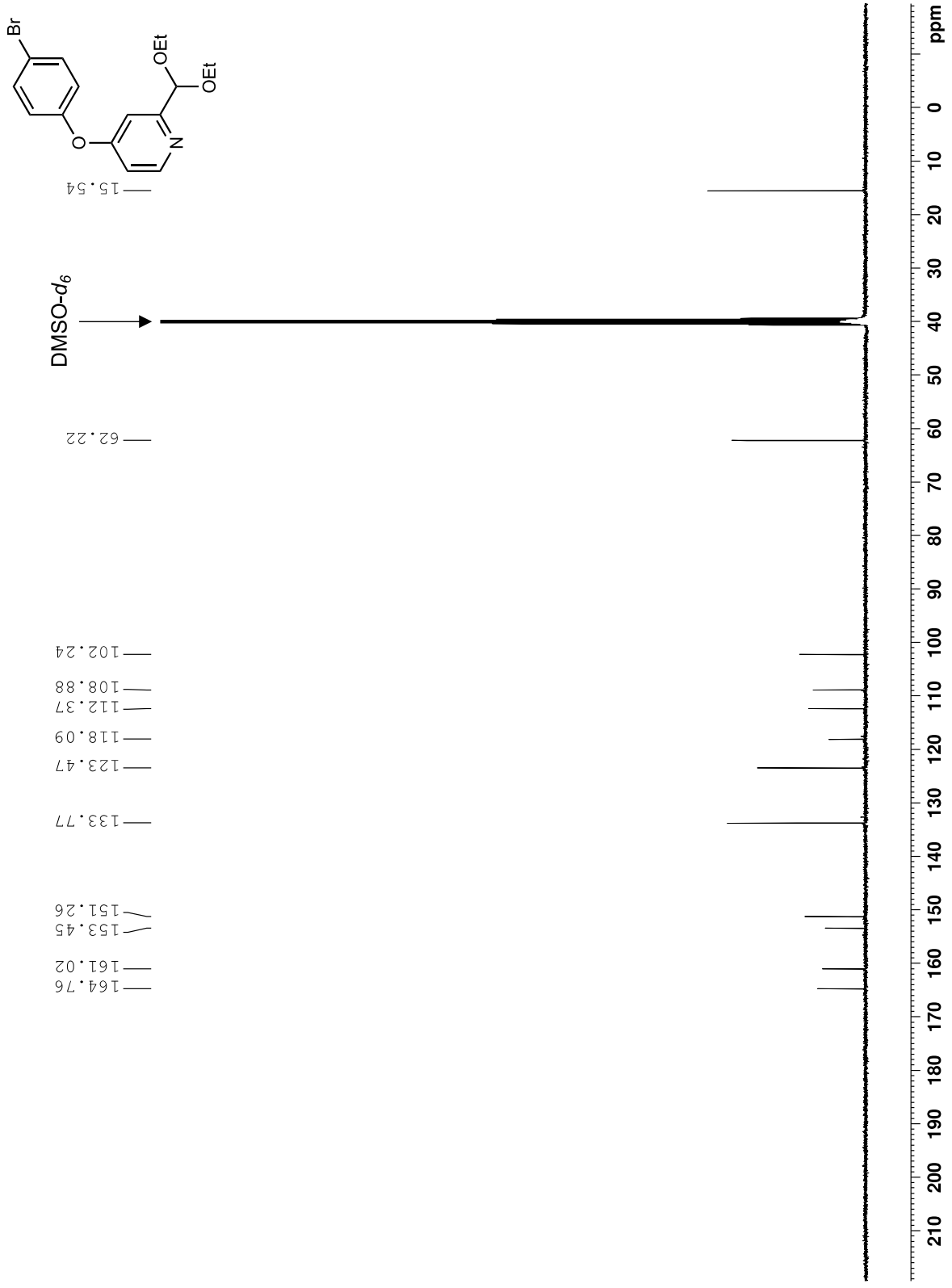

Spectrum 381. ^{13}C NMR for 4-(4-bromophenoxy)-2-(diethoxymethyl)pyridine (100 MHz, 293 K, DMSO-d_6).

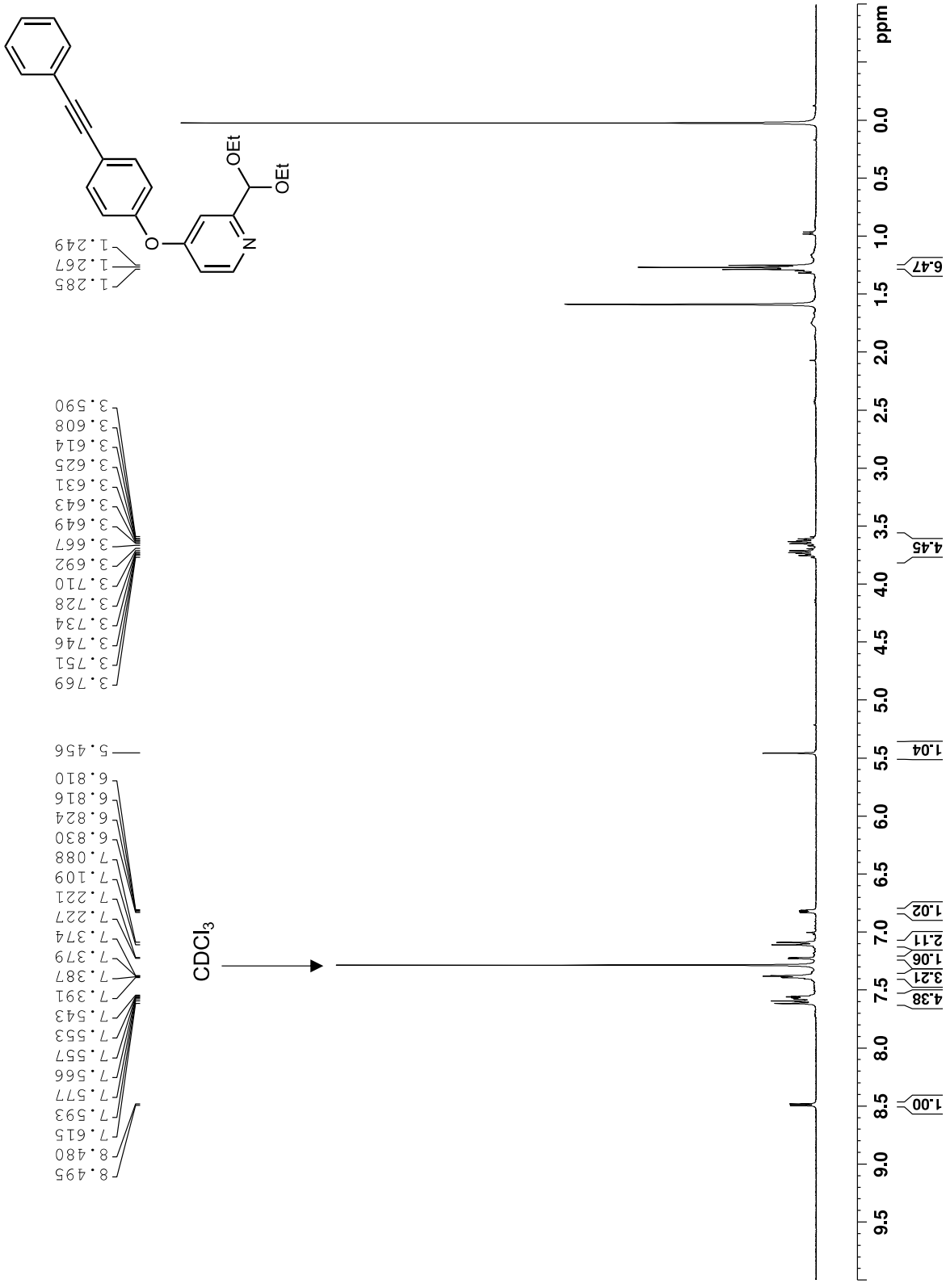

Spectrum 382. ^{1}H NMR for 2-(diethoxymethyl)-4-(4-(phenylethynyl)phenoxy)pyridine (400 MHz, 293 K, $CDCl_3$).

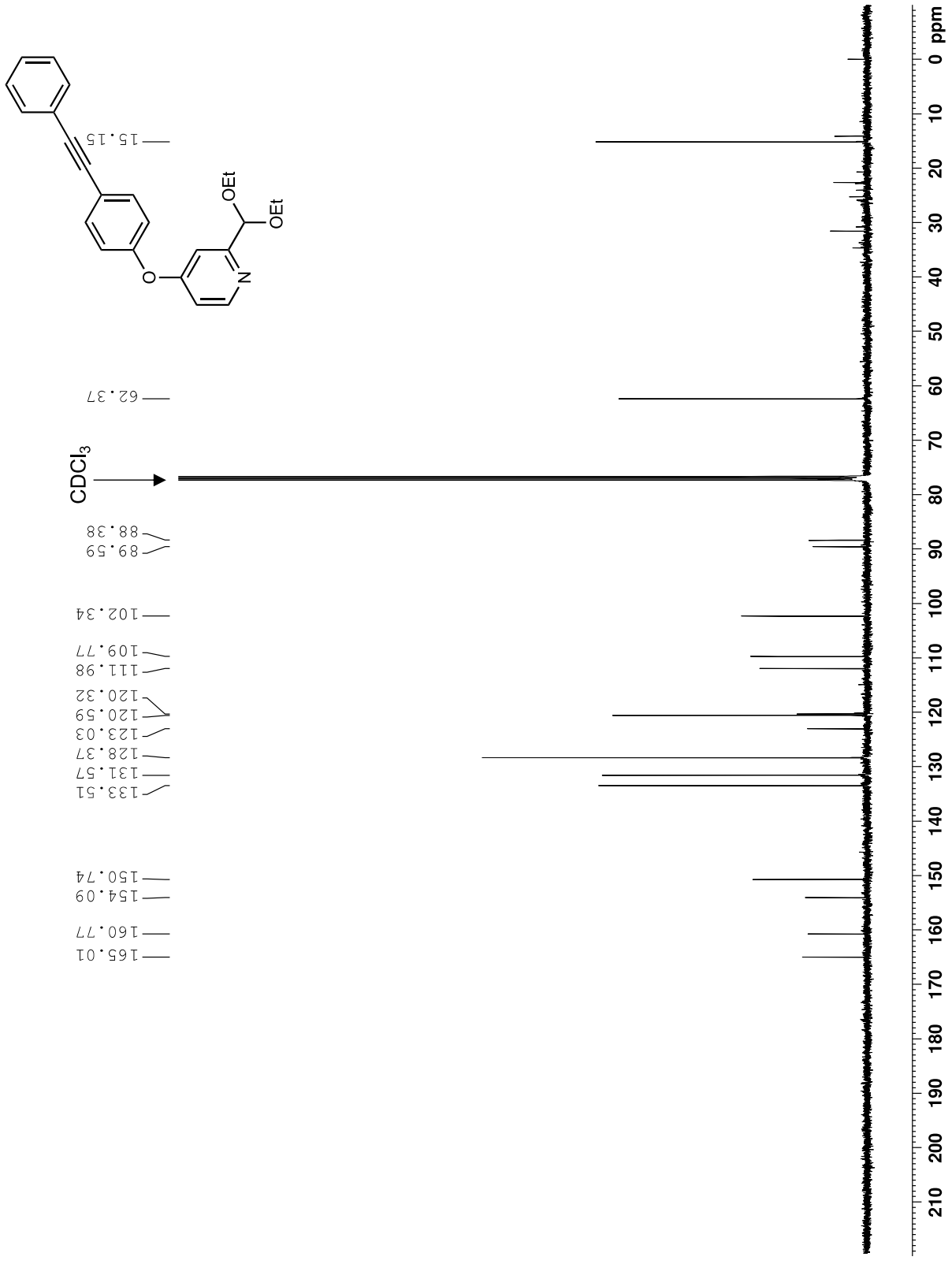

Spectrum 383. ^{13}C NMR for 2-(diethoxymethyl)-4-(4-(phenylethynyl)phenoxy)pyridine (100 MHz, 293 K, $CDCl_3$).

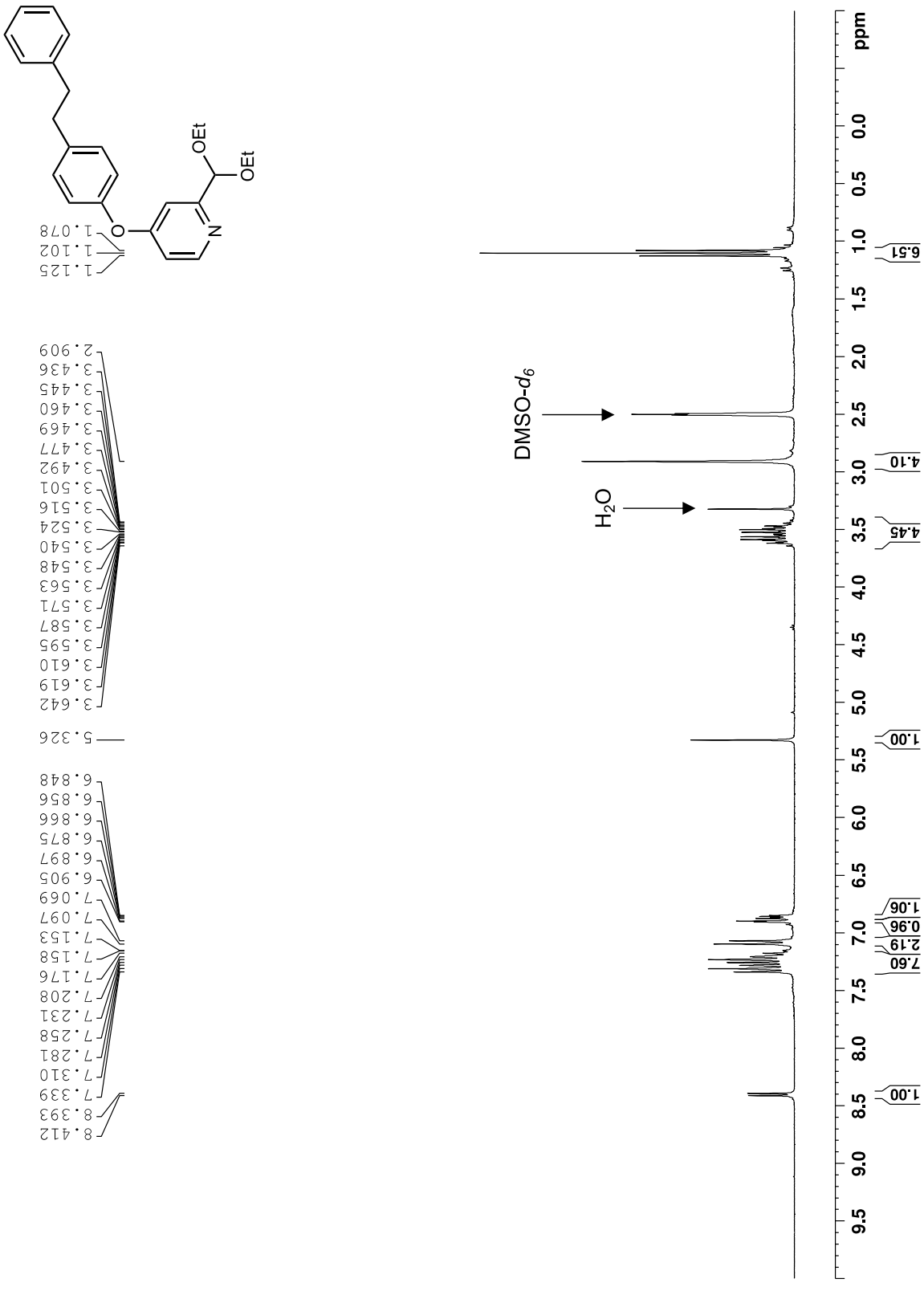

Spectrum 384. [1]H NMR for 2-(diethoxymethyl)-4-(4-phenethylphenoxy)pyridine (300 MHz, 293 K, DMSO-d_6).

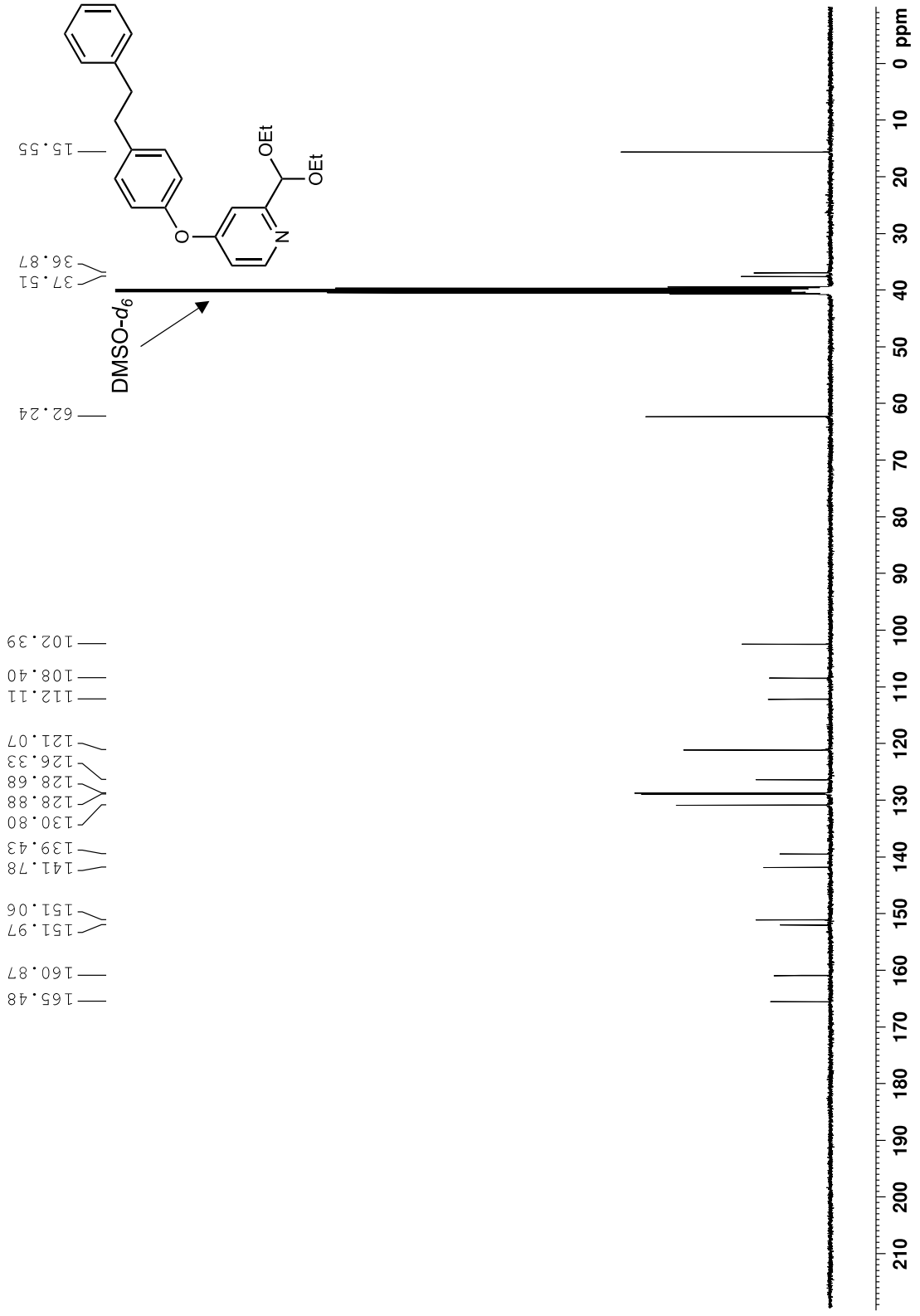

Spectrum 385. ^{13}C NMR for 2-(diethoxymethyl)-4-(4-phenethylphenoxy)pyridine (100 MHz, 293 K, DMSO-d_6).

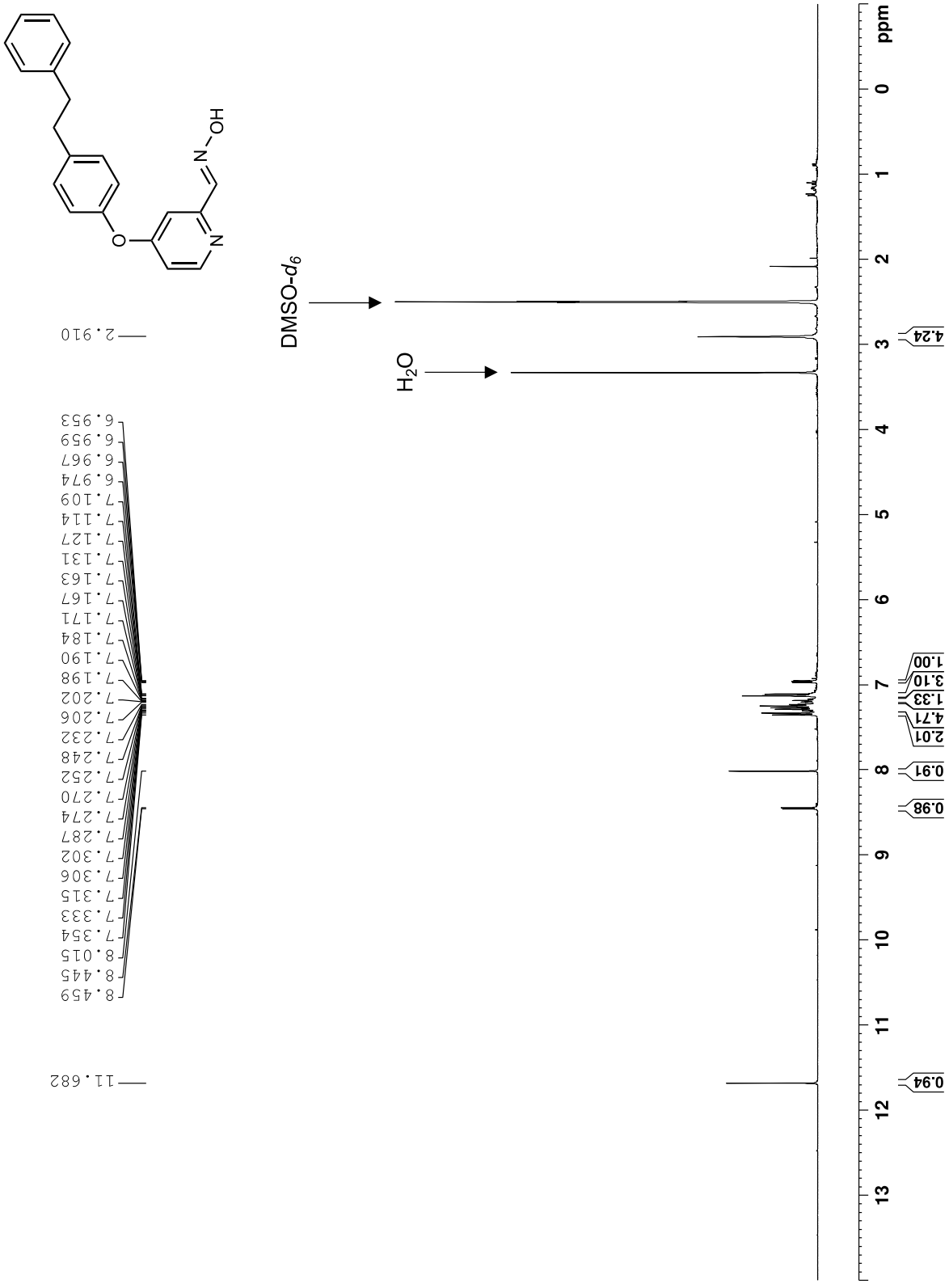

Spectrum 386. ^{1}H NMR for (*E*)-4-(4-phenethylphenoxy)picolinaldehyde oxime (400 MHz, 293 K, DMSO-d_6).

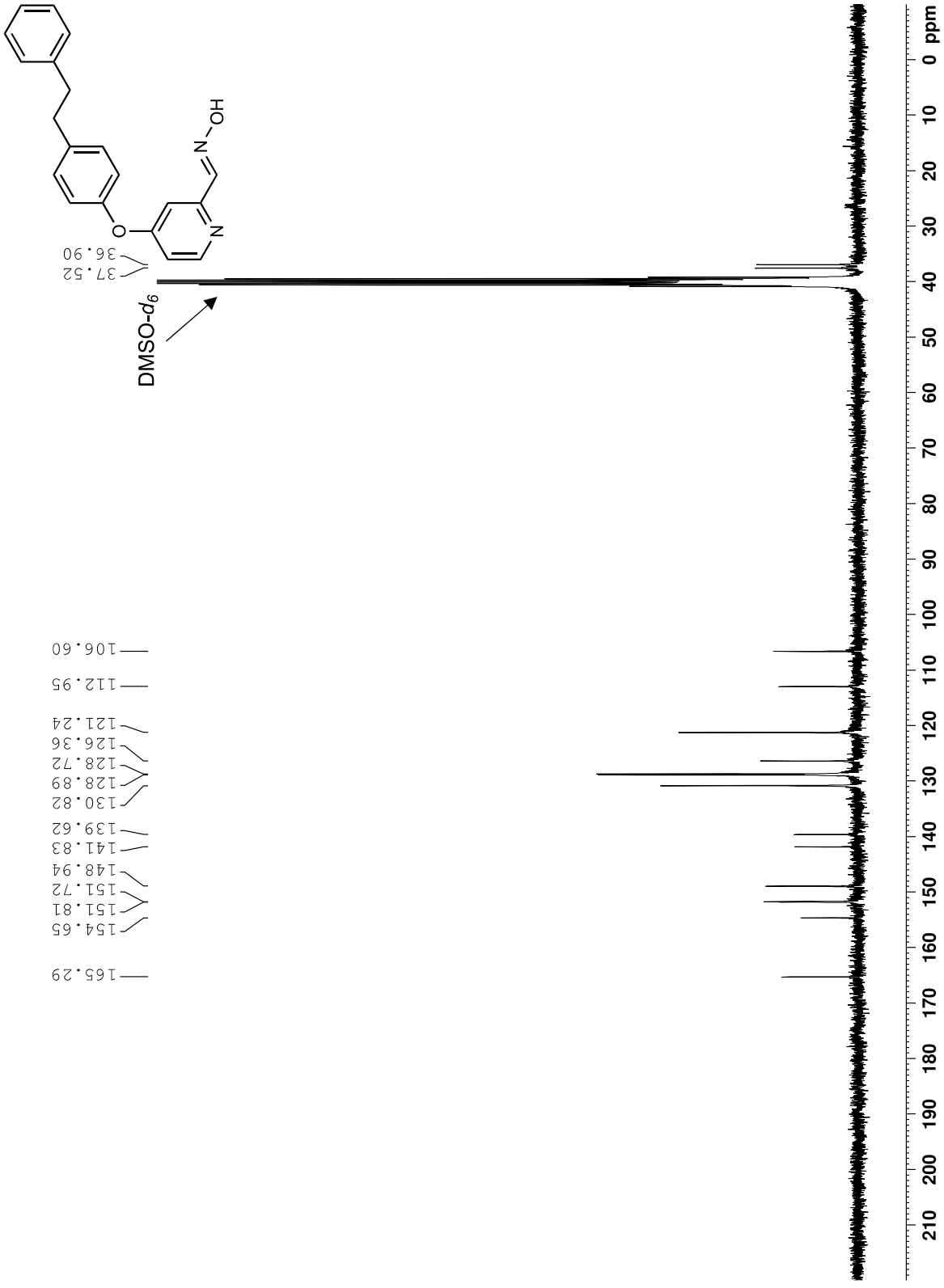

Spectrum 387. ^{13}C NMR for (*E*)-4-(4-phenethylphenoxy)picolinaldehyde oxime (75 MHz, 293 K, DMSO-d_6).

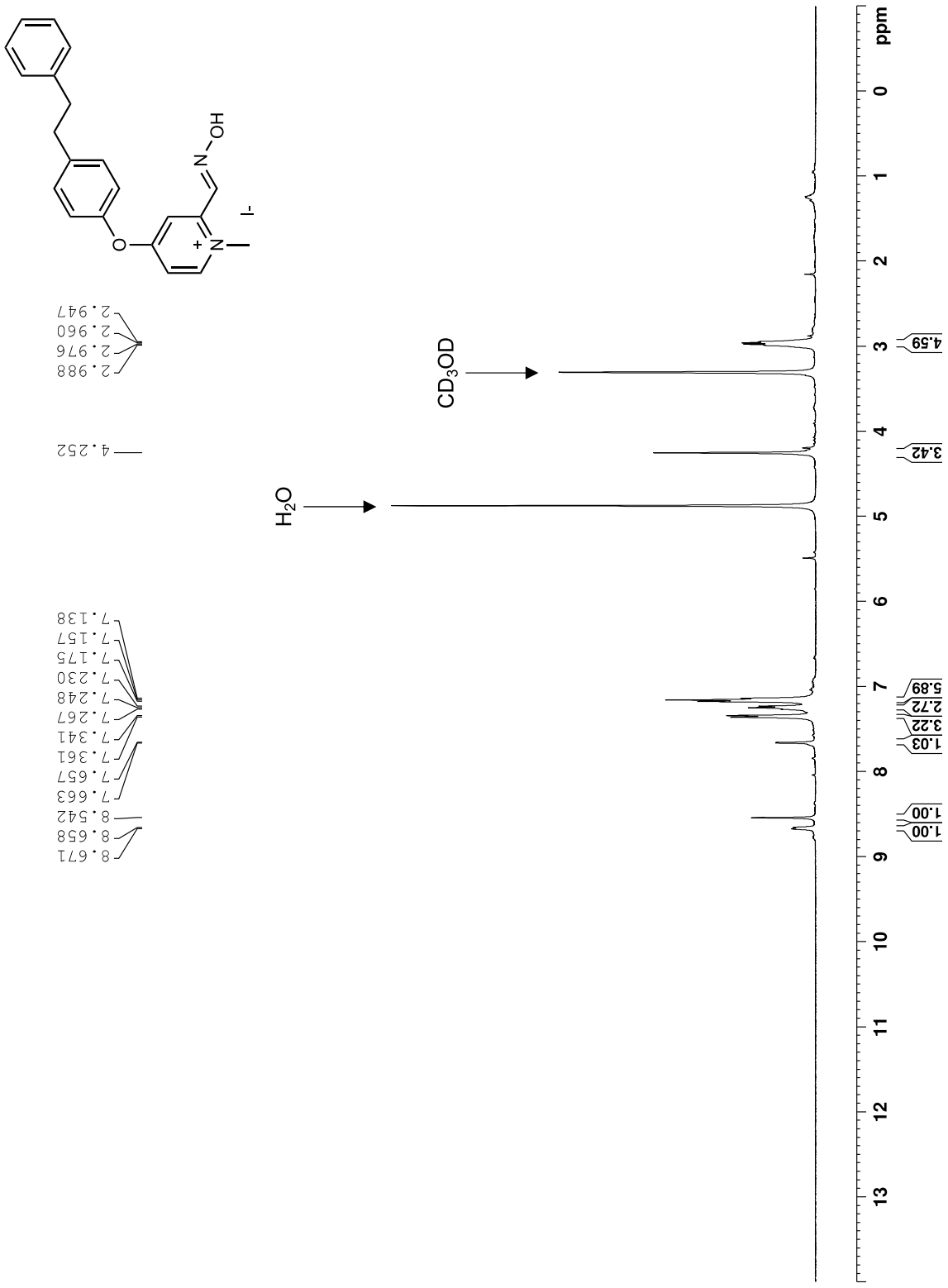

Spectrum 388. ^{1}H NMR for (*E*)-2-((hydroxyimino)methyl)-1-methyl-4-(4-phenethylphenoxy)pyridin-1-ium iodide (**ADG4278**) (400 MHz, 293 K, CD_3OD).

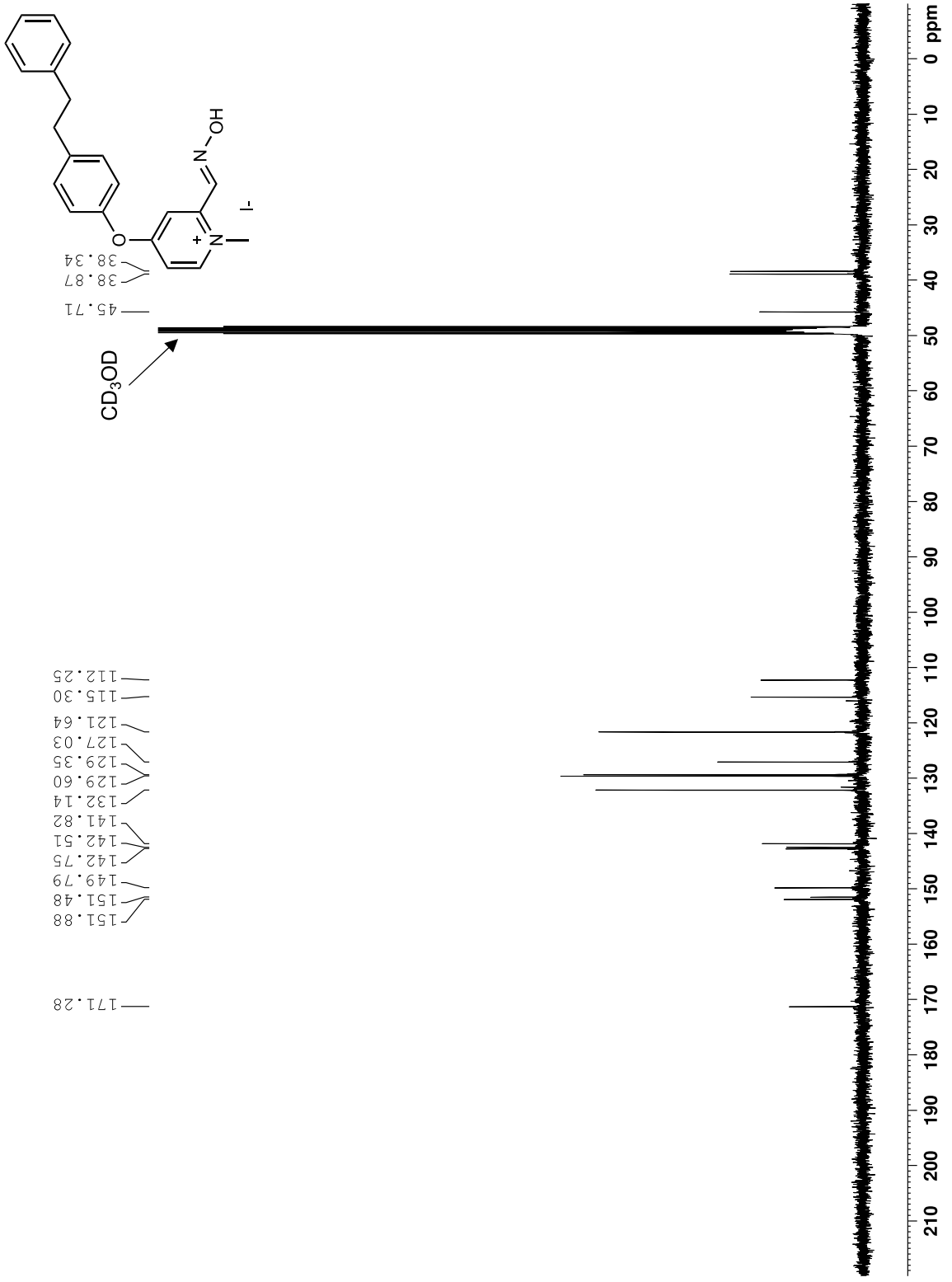

Spectrum 389. ^{13}C NMR for (*E*)-2-((hydroxyimino)methyl)-1-methyl-4-(4-phenethylphenoxy)pyridin-1-ium iodide (**ADG4278**) (100 MHz, 293 K, CD_3OD).

Bibliography

1) Prado, M. A. M.; Reis, R. A. M.; Prado, V. F.; de Mello, M. C.; Gomez, M. V.; de Mello, F. G., Regulation of acetylcholine synthesis and storage. *Neurochem. Int.* **2002,** *41* (5), 291–299.

2) Prado, V. F.; Janickova, H.; Al-Onaizi, M. A.; Prado, M. A. M., Cholinergic circuits in cognitive flexibility. *Neuroscience* **2017,** *345*, 130–141.

3) Mercey, G.; Verdelet, T.; Renou, J.; Kliachyna, M.; Baati, R.; Nachon, F.; Jean, L.; Renard, P.-Y., Reactivators of acetylcholinesterase inhibited by organophosphorus nerve agents. *Acc. Chem. Res.* **2012,** *45* (5), 756–766.

4) Quinn, D. M., Acetylcholinesterase: enzyme structure, reaction dynamics, and virtual transition states. *Chem. Rev.* **1987,** *87* (5), 955–979.

5) Jensen, K. P.; DeVito, E. E.; Yip, S.; Carroll, K. M.; Sofuoglu, M., The cholinergic system as a treatment target for opioid use disorder. *CNS Drugs* **2018,** *32* (11), 981–996.

6) Hampel, H.; Mesulam, M. M.; Cuello, A. C.; Farlow, M. R.; Giacobini, E.; Grossberg, G. T.; Khachaturian, A. S.; Vergallo, A.; Cavedo, E.; Snyder, P. J.; Khachaturian, Z. S., The cholinergic system in the pathophysiology and treatment of Alzheimer's disease. *Brain* **2018,** *141* (7), 1917–1933.

7) Dvir, H.; Silman, I.; Harel, M.; Rosenberry, T. L.; Sussman, J. L., Acetylcholinesterase: from 3D structure to function. *Chem.-Biol. Interact.* **2010,** *187* (1), 10–22.

8) Rothenberg, M. A.; Nachmansohn, D., Studies on cholinesterase: III. purification of the enzyme from electric tissue by fractional ammonium sulfate precipitation. *J. Biol. Chem.* **1947,** *168* (1), 223–231.

9) Leuzinger, W.; Baker, A. L., Acetylcholinesterase, I. large-scale purification, homogeneity, and amino acid analysis. *Proc. Natl. Acad. Sci. U. S. A.* **1967,** *57* (2), 446–451.

10) Schumacher, M.; Camp, S.; Maulet, Y.; Newton, M.; MacPhee-Quigley, K.; Taylor, S. S.; Friedmann, T.; Taylor, P., Primary structure of *Torpedo californica* acetylcholinesterase deduced from its cDNA sequence. *Nature* **1986,** *319* (6052), 407–409.

11) Sussman, J. L.; Harel, M.; Frolow, F.; Oefner, C.; Goldman, A.; Toker, L.; Silman, I., Atomic structure of acetylcholinesterase from *Torpedo californica*: a prototypic acetylcholine-binding protein. *Science* **1991,** *253* (5022), 872–879.

12) Bourne, Y.; Taylor, P.; Marchot, P., Acetylcholinesterase inhibition by fasciculin: crystal structure of the complex. *Cell* **1995,** *83* (3), 503–512.

13) Harel, M.; Kryger, G.; Rosenberry, T. L.; Mallender, W. D.; Lewis, T.; Fletcher, R. J.; Guss, J. M.; Silman, I.; Sussman, J. L., Three-dimensional structures of *Drosophila melanogaster* acetylcholinesterase and of its complexes with two potent inhibitors. *Protein Sci.* **2000,** *9* (6), 1063–1072.

14) Kryger, G.; Giles, K.; Harel, M.; Toker, L.; Velan, B.; Lazar, A.; Kronman, C.; Barak, D.; Ariel, N.; Shafferman, A.; Silman, I.; Sussman, J. L., 3D Structure of a complex of human acetylcholinesterase with fasciculin-II at 2.7 Å resolution. In *Structure and Function of Cholinesterases and Related Proteins*, Doctor, B. P.; Taylor, P.; Quinn, D. M.; Rotundo, R. L.; Gentry, M. K., Eds. Springer US: Boston, MA, 1998; pp 370–370.

15) Pullman, A., Binding sites of acetylcholine in the aromatic gorge leading to the active site of acetylcholinesterase. *Molecular Engineering* **1995,** *5* (1), 11–23.

16) Wilson, I. B.; Ginsburg, S., A powerful reactivator of alkylphosphate-inhibited acetylcholinesterase. *Biochim. Biophys. Acta* **1955,** *18*, 168–170.

17) Zhang, Y.; Kua, J.; McCammon, J. A., Role of the catalytic triad and oxyanion hole in acetylcholinesterase catalysis: an ab initio QM/MM study. *J. Am. Chem. Soc.* **2002,** *124* (35), 10572–10577.

18) Wilson, I. B.; Bergmann, F.; Nachmansohn, D., Acetylcholinesterase: mechanism of the catalysis of acylation reactions. *J. Biol. Chem.* **1950,** *186* (2), 781–790.

19) Rosenberry, T. L., Catalysis by acetylcholinesterase: evidence that the rate-limiting step for acylation with certain substrates precedes general acid-base catalysis. *Proc. Natl. Acad. Sci. U. S. A.* **1975,** *72* (10), 3834–3838.

20) Warshel, A.; Naray-Szabo, G.; Sussman, F.; Hwang, J. K., How do serine proteases really work? *Biochemistry* **1989,** *28* (9), 3629–3637.

21) Fuxreiter, M.; Warshel, A., Origin of the catalytic power of acetylcholinesterase: computer simulation studies. *J. Am. Chem. Soc.* **1998,** *120* (1), 183–194.

22) Topf, M.; Richards, W. G., Theoretical studies on the deacylation step of serine protease catalysis in the gas phase, in solution, and in elastase. *J. Am. Chem. Soc.* **2004,** *126* (44), 14631–14641.

23) Blow, D. M.; Birktoft, J. J.; Hartley, B. S., Role of a buried acid group in the mechanism of action of chymotrypsin. *Nature* **1969,** *221* (5178), 337–340.

24) Zhou, Y.; Wang, S.; Zhang, Y., Catalytic reaction mechanism of acetylcholinesterase determined by Born−Oppenheimer ab initio QM/MM molecular dynamics simulations. *J. Phys. Chem. B* **2010,** *114* (26), 8817–8825.

25) Hans-Jürgen Nolte, T. L. R., Eberhard Neumann, Effective charge on acetylcholinesterase active sites determined from the ionic strength dependence of association rate constants with cationic ligands. *Biochemistry* **1980,** *19* (16), 3705–3711.

26) Froede, H. C.; Wilson, I. B., Direct determination of acetyl-enzyme intermediate in the acetylcholinesterase-catalyzed hydrolysis of acetylcholine and acetylthiocholine. *J. Biol. Chem.* **1984,** *259* (17), 11010–11013.

27) Dougherty, D. A.; Stauffer, D. A., Acetylcholine binding by a synthetic receptor: implications for biological recognition. *Science* **1990,** *250* (4987), 1558–1560.

28) Shafferman, A.; Velan, B.; Ordentlich, A.; Kronman, C.; Grosfeld, H.; Leitner, M.; Flashner, Y.; Cohen, S.; Barak, D.; Ariel, N., Substrate inhibition of acetylcholinesterase: residues affecting signal transduction from the surface to the catalytic center. *The EMBO Journal* **1992,** *11* (10), 3561–3568.

29) Ordentlich, A.; Barak, D.; Kronman, C.; Flashner, Y.; Leitner, M.; Segall, Y.; Ariel, N.; Cohen, S.; Velan, B.; Shafferman, A., Dissection of the human acetylcholinesterase active center determinants of substrate specificity. Identification of residues constituting the anionic site, the hydrophobic site, and the acyl pocket. *J. Biol. Chem.* **1993,** *268* (23), 17083–17095.

30) Weise, C.; Kreienkamp, H. J.; Raba, R.; Pedak, A.; Aaviksaar, A.; Hucho, F., Anionic subsites of the acetylcholinesterase from *Torpedo californica*: affinity labelling with the cationic reagent *N*,*N*-dimethyl-2-phenyl-aziridinium. *The EMBO Journal* **1990,** *9* (12), 3885–3888.

31) Branduardi, D.; Gervasio, F. L.; Cavalli, A.; Recanatini, M.; Parrinello, M., The role of the peripheral anionic site and cation−π interactions in the ligand penetration of the human AChE gorge. *J. Am. Chem. Soc.* **2005,** *127* (25), 9147–9155.

32) Taylor, P.; Radić, Z., The cholinesterases: from genes to proteins. *Annu. Rev. Pharmacol. Toxicol.* **1994,** *34* (1), 281–320.

33) Bourne, Y.; Taylor, P.; Radić, Z.; Marchot, P., Structural insights into ligand interactions at the acetylcholinesterase peripheral anionic site. *The EMBO Journal* **2003,** *22* (1), 1–12.

34) Wiesner, J.; Kříž, Z.; Kuča, K.; Jun, D.; Koča, J., Acetylcholinesterases – the structural similarities and differences. *J. Enzyme Inhib. Med. Chem.* **2007,** *22* (4), 417–424.

35) Fiser, A., Template-Based Protein Structure Modeling. In *Computational Biology*, Fenyö, D., Ed. Humana Press: Totowa, NJ, 2010; pp 73–94.

36) Cavalcante, F. d. A. S.; Simas, B. C. A.; Barcellos, C. M.; de Oliveira, G. M. V.; Sousa, B. R.; Cabral, A. d. M. P.; Kuča, K.; França, C. C. T., Acetylcholinesterase: the “hub” for

neurodegenerative diseases and chemical weapons convention. *Biomolecules* **2020,** *10* (3), 414.

37) Lee, E. C., Clinical manifestations of sarin nerve gas exposure. *JAMA* **2003,** *290* (5), 659–662.

38) Talmage, S. S. W., A. P.; Hauschild, V.; Munro, N. B.; King, J. , Chemical Warfare Agent Degradation and Decontamination *Curr. Org. Chem.* **2007,** *11* (3), 285–298.

39) Macilwain, C., Study proves Iraq used nerve gas. *Nature* **1993,** *363* (6424), 3.

40) Jeyaratnam, J., Acute pesticide poisoning: a major global health problem. *World Health Stat. Q.* **1990,** *43* (3), 139–144.

41) Eto, M., *Organophosphorus Pesticides*. CRC Press: Boca Raton, 2018.

42) Litchfield, M. H., Estimates of acute pesticide poisoning in agricultural workers in less developed countries. *Toxicol. Rev.* **2005,** *24* (4), 271–278.

43) McCauley, L. A., Chapter 6 - Epidemiology of Chemical Warfare Agents. *Handbook of Toxicology of Chemical Warfare Agents (Second Edition)* **2015**, 47–54.

44) *Guidelines for Chemical Warfare Agents in Military Field Drinking Water*. The National Academies Press: Washington, DC, 1995; p 80.

45) Mioduszewski, R.; Manthei, J.; Way, R.; Burnett, D.; Gaviola, B.; Muse, W.; Thomson, S.; Sommerville, D.; Crosier, R., Interaction of exposure concentration and duration in determining acute toxic effects of sarin vapor in rats. *Toxicol. Sci.* **2002,** *66* (2), 176–184.

46) Watson, A.; Opresko, D.; Young, R.; Hauschild, V., Development and application of acute exposure guideline levels (AEGLs) for chemical warfare nerve and sulfur mustard agents. *J. Toxicol. Environ. Health, Pt. B Crit. Rev.* **2006,** *9* (3), 173–263.

47) MacPhee-Quigley, K.; Taylor, P.; Taylor, S., Primary structures of the catalytic subunits from two molecular forms of acetylcholinesterase. A comparison of NH_2-terminal and active center sequences. *J. Biol. Chem.* **1985,** *260* (22), 12185–12189.

48) Millard, C. B.; Kryger, G.; Ordentlich, A.; Greenblatt, H. M.; Harel, M.; Raves, M. L.; Segall, Y.; Barak, D.; Shafferman, A.; Silman, I.; Sussman, J. L., Crystal structures of aged phosphonylated acetylcholinesterase: nerve agent reaction products at the atomic level. *Biochemistry* **1999,** *38* (22), 7032–7039.

49) Millard, C. B.; Koellner, G.; Ordentlich, A.; Shafferman, A.; Silman, I.; Sussman, J. L., Reaction products of acetylcholinesterase and VX reveal a mobile histidine in the catalytic triad. *J. Am. Chem. Soc.* **1999,** *121* (42), 9883–9884.

50) Eddleston, M.; Buckley, N. A.; Eyer, P.; Dawson, A. H., Management of acute organophosphorus pesticide poisoning. *Lancet* **2008,** *371* (9612), 597–607.

51) Acharya, J.; Dubey, D. K.; Srivastava, A. K.; Raza, S. K., *In vitro* reactivation of sarin-inhibited human acetylcholinesterase (AChE) by bis-pyridinium oximes connected by xylene linkers. *Toxicol. In Vitro* **2011,** *25* (1), 251–256.

52) Benschop, H. P.; Keijer, J. H., On the mechanism of ageing of phosphonylated cholinesterases. *Biochimica et Biophysica Acta (BBA) - Enzymology and Biological Oxidation* **1966,** *128* (3), 586–588.

53) Shafferman, A.; Ordentlich, A.; Barak, D.; Stein, D.; Ariel, N.; Velan, B., Aging of phosphylated human acetylcholinesterase: catalytic processes mediated by aromatic and polar residues of the active centre. *Biochem. J.* **1996,** *318* (3), 833–840.

54) Carletti, E.; Li, H.; Li, B.; Ekström, F.; Nicolet, Y.; Loiodice, M.; Gillon, E.; Froment, M. T.; Lockridge, O.; Schopfer, L. M.; Masson, P.; Nachon, F., Aging of cholinesterases phosphylated by tabun proceeds through O-dealkylation. *J. Am. Chem. Soc.* **2008,** *130* (47), 16011–16020.

55) Sirin, G. S.; Zhou, Y.; Lior-Hoffmann, L.; Wang, S.; Zhang, Y., Aging mechanism of soman inhibited acetylcholinesterase. *J. Phys. Chem. B* **2012,** *116* (40), 12199–12207.

56) Chandar, N. B.; Lo, R.; Ganguly, B., Quantum chemical and steered molecular dynamics studies for one pot solution to reactivate aged acetylcholinesterase with alkylator oxime. *Chem.-Biol. Interact.* **2014,** *223*, 58–68.

57) Yoder, R. J.; Zhuang, Q.; Beck, J. M.; Franjesevic, A.; Blanton, T. G.; Sillart, S.; Secor, T.; Guerra, L.; Brown, J. D.; Reid, C.; McElroy, C. A.; Doğan Ekici, Ö.; Callam, C. S.; Hadad, C. M., Study of para-quinone methide precursors toward the realkylation of aged acetylcholinesterase. *ACS Med. Chem. Lett.* **2017,** *8* (6), 622–627.

58) Steinberg, G. M.; Lieske, C. N.; Boldt, R.; Goan, J. C.; Podall, H. E., Model studies for the reactivation of aged phosphonylated acetylcholinesterase. Use of alkylating agents containing nucleophilic groups. *J. Med. Chem.* **1970,** *13* (3), 435–446.

59) Newmark, J., Therapy for acute nerve agent poisoning. *Neurology: Clinical Practice* **2019**, 10.1212/CPJ.0000000000000641.

60) Lorke, D. E., Entry of oximes into the brain: a review *Curr. Med. Chem.* **2008,** *15*, 743–753.

61) Hörnberg, A.; Artursson, E.; Wärme, R.; Pang, Y.-P.; Ekström, F., Crystal structures of oxime-bound fenamiphos-acetylcholinesterases: Reactivation involving flipping of the His447 ring to form a reactive Glu334–His447–oxime triad. *Biochem. Pharmacol.* **2010,** *79* (3), 507–515.

62) Ekström, F. J.; Astot, C.; Pang, Y. P., Novel nerve-agent antidote design based on crystallographic and mass spectrometric analyses of tabun-conjugated acetylcholinesterase in complex with antidotes. *Clin. Pharmacol. Ther.* **2007,** *82* (3), 282–293.

63) Fina, N. J.; Edwards, J. O., The alpha effect. A review. *Int. J. Chem. Kinet.* **1973,** *5* (1), 1-26.

64) Terrier, F.; Rodriguez-Dafonte, P.; Le Guével, E.; Moutiers, G., Revisiting the reactivity of oximate α-nucleophiles with electrophilic phosphorus centers. Relevance to detoxification of sarin, soman and DFP under mild conditions. *Org. Biomol. Chem.* **2006,** *4* (23), 4352–4363.

65) Wang, J.; Gu, J.; Leszczynski, J.; Feliks, M.; Sokalski, W. A., Oxime-induced reactivation of sarin-inhibited AChE: a theoretical mechanisms study. *J. Phys. Chem. B* **2007,** *111* (9), 2404–2408.

66) Ekström, F.; Hörnberg, A.; Artursson, E.; Hammarström, L.-G.; Schneider, G.; Pang, Y.-P., Structure of HI-6•sarin-acetylcholinesterase determined by x-ray crystallography and molecular dynamics simulation: reactivator mechanism and design. *PLoS One* **2009,** *4* (6), e5957–e5957.

67) Taylor, P.; Reiner, E.; Kovarik, Z.; Radić, Z., Application of recombinant DNA methods for production of cholinesterases as organophosphate antidotes and detectors. *Arh. Hig. Rada Toksikol.* **2007,** *58* (3), 339–345.

68) PROTOPAM Chloride (pralidoxime chloride) for Injection U.S. Food and Drug Administration: 2010.

69) Eyer, P., The role of oximes in the management of organophosphorus pesticide poisoning. *Toxicol. Rev.* **2003,** *22* (3), 165–190.

70) Sakurada, K., Pralidoxime iodide (2-PAM) penetrates across the blood-brain barrier. *Neurochem. Res.* **2003,** *28* (9), 1401–1407.

71) Worek, F.; Thiermann, H.; Szinicz, L.; Eyer, P., Kinetic analysis of interactions between human acetylcholinesterase, structurally different organophosphorus compounds and oximes. *Biochem. Pharmacol.* **2004,** *68* (11), 2237–2248.

72) Ballabh, P.; Braun, A.; Nedergaard, M., The blood-brain barrier: an overview: structure, regulation, and clinical implications. *Neurobiol. Dis.* **2004,** *16* (1), 1–13.

73) Pardridge, W. M., Blood-brain barrier delivery. *Drug Discovery Today* **2007,** *12* (1), 54–61.

74) Di, L.; Kerns, E. H., Chapter 10 - Blood-Brain Barrier. In *Drug-Like Properties (Second Edition)*, Di, L.; Kerns, E. H., Eds. Academic Press: Boston, 2016; pp 141–159.

75) Worek, F.; Reiter, G.; Eyer, P.; Szinicz, L., Reactivation kinetics of acetylcholinesterase from different species inhibited by highly toxic organophosphates. *Arch. Toxicol.* **2002,** *76* (9), 523–529.

76) Ellman, G. L.; Courtney, K. D.; Andres, V., Jr.; Feather-Stone, R. M., A new and rapid colorimetric determination of acetylcholinesterase activity. *Biochem. Pharmacol.* **1961,** *7* (2), 88–95.

77) Saint-André, G.; Kliachyna, M.; Kodepelly, S.; Louise-Leriche, L.; Gillon, E.; Renard, P.-Y.; Nachon, F.; Baati, R.; Wagner, A., Design, synthesis and evaluation of new α-nucleophiles for the hydrolysis of organophosphorus nerve agents: application to the reactivation of phosphorylated acetylcholinesterase. *Tetrahedron* **2011,** *67* (34), 6352-6361.

78) Hayashi, I.; Ogihara, K.; Shimizu, K., Reactivity of aromatic o-hydroxy oximes. I. Synthesis and aminolysis of acylglycine esters of aromatic *o*-hydroxy oximes. *Bull. Chem. Soc. Jpn.* **1983,** *56* (8), 2432–2437.

79) Kliachyna, M.; Santoni, G.; Nussbaum, V.; Renou, J.; Sanson, B.; Colletier, J.-P.; Arboléas, M.; Loiodice, M.; Weik, M.; Jean, L.; Renard, P.-Y.; Nachon, F.; Baati, R., Design, synthesis and biological evaluation of novel tetrahydroacridine pyridine- aldoxime and -amidoxime hybrids as efficient uncharged reactivators of nerve agent-inhibited human acetylcholinesterase. *Eur. J. Med. Chem.* **2014,** *78*, 455–467.

80) Renou, J.; Mercey, G.; Verdelet, T.; Păunescu, E.; Gillon, E.; Arboléas, M.; Loiodice, M.; Kliachyna, M.; Baati, R.; Nachon, F.; Jean, L.; Renard, P.-Y., Syntheses and in vitro evaluations of uncharged reactivators for human acetylcholinesterase inhibited by organophosphorus nerve agents. *Chem.-Biol. Interact.* **2013,** *203* (1), 81–84.

81) Timperley, C. M.; Banks, R. E.; Young, I. M.; Haszeldine, R. N., Synthesis of some fluorine-containing pyridinealdoximes of potential use for the treatment of organophosphorus nerve-agent poisoning. *J. Fluorine Chem.* **2011,** *132* (8), 541–547.

82) Goff, D. A.; Koolpe, G. A.; Kelson, A. B.; Vu, H. M.; Taylor, D. L.; Bedford, C. D.; Harris III, R. N.; Mussalam, H.; Koplovitz, I., Quaternary salts of 2-[(hydroxyimino) methyl] imidazole. 4. Effect of various side-chain substituents on therapeutic activity against anticholinesterase intoxication. *J. Med. Chem.* **1991,** *34* (4), 1363–1368.

83) Koolpe, G. A.; Lovejoy, S. M.; Goff, D. A.; Lin, K. Y.; Leung, D. S.; Bedford, C. D.; Harris III, R. N.; Musallam, H.; Koplovitz, I., Quaternary salts of 2-[(hydroxyimino) methyl] imidazole. 5. Structure-activity relationships for side-chain nitro-, sulfone-, amino-, and aminosulfonyl-substituted analogs for therapy against anticholinesterase intoxication. *J. Med. Chem.* **1991,** *34* (4), 1368–1376.

84) Kovarik, Z.; Maček, N.; Sit, R. K.; Radić, Z.; Fokin, V. V.; Barry Sharpless, K.; Taylor, P., Centrally acting oximes in reactivation of tabun-phosphoramidated AChE. *Chem.-Biol. Interact.* **2013,** *203* (1), 77–80.

85) Radić, Z.; Sit, R. K.; Kovarik, Z.; Berend, S.; Garcia, E.; Zhang, L.; Amitai, G.; Green, C.; Radić, B.; Fokin, V. V.; Sharpless, K. B.; Taylor, P., Refinement of structural leads for centrally acting oxime reactivators of phosphylated cholinesterases. *J. Biol. Chem.* **2012,** *287* (15), 11798–11809.

86) Sit, R. K.; Fokin, V. V.; Amitai, G.; Sharpless, K. B.; Taylor, P.; Radić, Z., Imidazole aldoximes effective in assisting butyrylcholinesterase catalysis of organophosphate detoxification. *J. Med. Chem.* **2014,** *57* (4), 1378–1389.

87) Sit, R. K.; Radić, Z.; Gerardi, V.; Zhang, L.; Garcia, E.; Katalinić, M.; Amitai, G.; Kovarik, Z.; Fokin, V. V.; Sharpless, K. B.; Taylor, P., New structural scaffolds for centrally acting oxime reactivators of phosphylated cholinesterases. *J. Biol. Chem.* **2011,** *286* (22), 19422–19430.

88) Musilek, K.; Holas, O.; Misik, J.; Pohanka, M.; Novotny, L.; Dohnal, V.; Opletalova, V.; Kuča, K., Monooxime-monocarbamoyl bispyridinium xylene-linked reactivators of acetylcholinesterase—synthesis, in vitro and toxicity evaluation, and docking studies. *ChemMedChem* **2010,** *5* (2), 247–254.

89) Nurulain, S. M.; Lorke, D. E.; Hasan, M. Y.; Shafiullah, M.; Kuča, K.; Musilek, K.; Petroianu, G. A., Efficacy of eight experimental bispyridinium oximes against paraoxon-induced mortality: comparison with the conventional oximes pralidoxime and obidoxime. *Neurotox. Res.* **2009,** *16* (1), 60.

90) Cabal, J.; Kuča, K.; Kassa, J., Specification of the structure of oximes able to reactivate tabun-inhibited acetylcholinesterase. *Basic Clin. Pharmacol. Toxicol.* **2004,** *95* (2), 81–86.

91) Kuča, K.; Cabal, J.; Jung, Y. S.; Musilek, K.; Soukup, O.; Jun, D.; Pohanka, M.; Musilova, L.; Karasová, J.; Novotný, L.; Hrabinova, M., Reactivation of human brain homogenate cholinesterases inhibited by tabun using newly developed oximes K117 and K127. *Basic Clin. Pharmacol. Toxicol.* **2009,** *105* (3), 207–210.

92) Chambers, J. E.; Chambers, H. W.; Meek, E. C.; Pringle, R. B., Testing of novel brain-penetrating oxime reactivators of acetylcholinesterase inhibited by nerve agent surrogates. *Chem.-Biol. Interact.* **2013,** *203* (1), 135–138.

93) Ohta, H.; Ohmori, T.; Suzuki, S.; Ikegaya, H.; Sakurada, K.; Takatori, T., New safe method for preparation of sarin-exposed human erythrocytes acetylcholinesterase using non-toxic and stable sarin analogue isopropyl *p*-nitrophenyl methylphosphonate and its application to evaluation of nerve agent antidotes. *Pharm. Res.* **2006,** *23* (12), 2827–2833.

94) Okuno, S.; Sakurada, K.; Ohta, H.; Ikegaya, H.; Kazui, Y.; Akutsu, T.; Takatori, T.; Iwadate, K., Blood-brain barrier penetration of novel pyridinealdoxime methiodide (PAM)-type oximes examined by brain microdialysis with LC-MS/MS. *Toxicol. Appl. Pharmacol.* **2008,** *227* (1), 8–15.

95) Wager, T. T.; Hou, X. J.; Verhoest, P. R.; Villalobos, A., Moving beyond rules: The development of a central nervous system multiparameter optimization (CNS MPO) approach to enable alignment of druglike properties. *ACS Chem. Neurosci.* **2010,** *1* (6), 435–449.

96) Wolak, D. J.; Thorne, R. G., Diffusion of macromolecules in the brain: Implications for drug delivery. *Mol. Pharmaceut.* **2013,** *10* (5), 1492–1504.

97) Carpenter, T. S.; Kirshner, D. A.; Lau, E. Y.; Wong, S. E.; Nilmeier, J. P.; Lightstone, F. C., A method to predict blood-brain barrier permeability of drug-like compounds using molecular dynamics simulations. *Biophys J* **2014,** *107* (3), 630–641.

98) Pirrung, M. C.; Liu, Y.; Deng, L.; Halstead, D. K.; Li, Z.; May, J. F.; Wedel, M.; Austin, D. A.; Webster, N. J. G., Methyl scanning: total synthesis of demethylasterriquinone B1 and derivatives for identification of sites of interaction with and isolation of its receptor(s). *J. Am. Chem. Soc.* **2005,** *127* (13), 4609–4624.

99) Limnios, D.; Kokotos, C. G., 2,2,2-Trifluoroacetophenone as an organocatalyst for the oxidation of tertiary amines and azines to *N*-oxides. *Chem. Eur. J.* **2014,** *20* (2), 559–563.

100) Boekelheide, V.; Linn, W. J., Rearrangements of *N*-oxides. A novel synthesis of pyridyl carbinols and aldehydes. *J. Am. Chem. Soc.* **1954,** *76* (5), 1286–1291.

101) Saxena, A.; Viragh, C.; Frazier, D. S.; Kovach, I. M.; Maxwell, D. M.; Lockridge, O.; Doctor, B. P., The pH dependence of dealkylation in soman-inhibited cholinesterases and their mutants: further evidence for a push−pull Mechanism. *Biochemistry* **1998,** *37* (43), 15086–15096.

102) Franklin, M. C.; Rudolph, M. J.; Ginter, C.; Cassidy, M. S.; Cheung, J., Structures of paraoxon-inhibited human acetylcholinesterase reveal perturbations of the acyl loop and the dimer interface. *Proteins: Structure, Function, and Bioinformatics* **2016,** *84* (9), 1246–1256.

103) Bourne, Y.; Radić, Z.; Sulzenbacher, G.; Kim, E.; Taylor, P.; Marchot, P., Substrate and product trafficking through the active center gorge of acetylcholinesterase analyzed by crystallography and equilibrium binding. *J. Biol. Chem.* **2006,** *281* (39), 29256–29267.

104) Feher, M.; Schmidt, J. M., Property distributions: differences between drugs, natural products, and molecules from combinatorial chemistry. *J. Chem. Inf. Comput. Sci.* **2003,** *43* (1), 218–227.

105) Feng, M.; Tang, B.; Liang, S. H.; Jiang, X., Sulfur containing scaffolds in drugs: synthesis and application in medicinal chemistry. *Curr. Top. Med. Chem.* **2016,** *16* (11), 1200–1216.

106) Taylor, R. D.; MacCoss, M.; Lawson, A. D. G., Rings in drugs. *J. Med. Chem.* **2014,** *57* (14), 5845–5859.

107) Ertl, P.; Altmann, E.; McKenna, J. M., The most common functional groups in bioactive molecules and how their popularity has evolved over time. *J. Med. Chem.* **2020,** *63* (15), 8408–8418.

108) Topczewski, J. J.; Lodge, A. M.; Yasapala, S. N.; Payne, M. K.; Keshavarzi, P. M.; Quinn, D. M., Reversible inhibition of human acetylcholinesterase by methoxypyridinium species. *Bioorg. Med. Chem. Lett.* **2013,** *23* (21), 5786–5789.

109) Quinn, D.; Topczewski, J. J. Preparation of methoxypyridinium compounds as alkylating agents for treating organophosphorus poisoning by reactivating aged-AChE adducts. US20140323473A1, 2014.

110) Connon, Stephen J.; Hegarty, Anthony F., Stabilised 2,3-pyridyne reactive intermediates of exceptional dienophilicity. *Eur. J. Org. Chem.* **2004,** *2004* (16), 3477–3483.

111) Comba, P.; Morgen, M.; Wadepohl, H., Tuning of the properties of transition-metal bispidine complexes by variation of the basicity of the aromatic donor groups. *Inorg. Chem.* **2013,** *52* (11), 6481–6501.

112) Choudhury, A. R.; Islam, K.; Kirchner, M. T.; Mehta, G.; Guru Row, T. N., In situ cryocrystallization of diphenyl ether: C−H···π mediated polymorphic forms. *J. Am. Chem. Soc.* **2004,** *126* (39), 12274–12275.

113) Gunbas, G.; Hafezi, N.; Sheppard, W. L.; Olmstead, M. M.; Stoyanova, I. V.; Tham, F. S.; Meyer, M. P.; Mascal, M., Extreme oxatriquinanes and a record C–O bond length. *Nat. Chem.* **2012,** *4* (12), 1018–1023.

114) Nekhoroshev, V. P.; Gubaidullin, R. R.; Yarkova, A. G.; Nekhorosheva, A. V.; Nifant'ev, I. E.; Voronkov, E. O.; Poleshchuk, O. K.; Tarasova, O. I., Transformations of diphenyl sulfide and diphenylamine on aluminum chloride. *Pet. Chem.* **2017,** *57* (3), 272–277.

115) Gillis, E. P.; Eastman, K. J.; Hill, M. D.; Donnelly, D. J.; Meanwell, N. A., Applications of fluorine in medicinal chemistry. *J. Med. Chem.* **2015,** *58* (21), 8315–8359.

116) Shah, P.; Westwell, A. D., The role of fluorine in medicinal chemistry. *J. Enzyme Inhib. Med. Chem.* **2007,** *22* (5), 527–540.

117) Hagmann, W. K., The many roles for fluorine in medicinal chemistry. *J. Med. Chem.* **2008,** *51* (15), 4359–4369.

118) Park, B. K.; Kitteringham, N. R.; O'Neill, P. M., Metabolism of fluorine-containing drugs. *Annu. Rev. Pharmacol. Toxicol.* **2001,** *41* (1), 443-470.

119) Schönherr, H.; Cernak, T., Profound methyl effects in drug discovery and a call for new C–H methylation reactions. *Angew. Chem. Int. Ed.* **2013,** *52* (47), 12256–12267.

120) Barreiro, E. J.; Kümmerle, A. E.; Fraga, C. A. M., The methylation effect in medicinal chemistry. *Chem. Rev.* **2011,** *111* (9), 5215–5246.

121) Nawrozkij, M. B.; Forgione, M.; Yablokov, A. S.; Lucidi, A.; Tomaselli, D.; Patsilinakos, A.; Panella, C.; Hailu, G. S.; Kirillov, I. A.; Badia, R.; Riveira-Muñoz, E.; Crespan, E.; Armijos Rivera, J. I.; Cirilli, R.; Ragno, R.; Esté, J. A.; Maga, G.; Mai, A.; Rotili, D., Effect of α-methoxy substitution on the anti-HIV activity of dihydropyrimidin-4(3*H*)-ones. *J. Med. Chem.* **2019,** *62* (2), 604–621.

122) Knochel, P.; Dohle, W.; Gommermann, N.; Kneisel, F. F.; Kopp, F.; Korn, T.; Sapountzis, I.; Vu, V. A., Highly functionalized organomagnesium reagents prepared through halogen-metal exchange. *Angew. Chem. Int. Ed.* **2003,** *42* (36), 4302–4320.

123) Kansy, M.; Senner, F.; Gubernator, K., Physicochemical high throughput screening: parallel artificial membrane permeation assay in the description of passive absorption processes. *J. Med. Chem.* **1998,** *41* (7), 1007–1010.

124) Zheng, Y.; Chen, X.; Benet, L. Z., Reliability of in vitro and in vivo methods for predicting the effect of P-glycoprotein on the delivery of antidepressants to the brain. *Clin. Pharmacokinet.* **2016,** *55* (2), 143–167.

125) Sonogashira, K.; Tohda, Y.; Hagihara, N., A convenient synthesis of acetylenes: catalytic substitutions of acetylenic hydrogen with bromoalkenes, iodoarenes and bromopyridines. *Tetrahedron Lett.* **1975,** *16* (50), 4467–4470.

126) Ohira, S., Methanolysis of dimethyl (1-diazo-2-oxopropyl) phosphonate: generation of dimethyl (diazomethyl) phosphonate and reaction with carbonyl compounds. *Synth. Commun.* **1989,** *19* (3-4), 561–564.

127) Müller, S. G.; Liepold, B.; Roth, G. J.; Bestmann, H. J., An improved one-pot procedure for the synthesis of alkynes from aldehydes. *Synlett* **1996,** (06), 521–522.

128) Roth, G. J.; Liepold, B.; Müller, S. G.; Bestmann, H. J., Further improvements of the synthesis of alkynes from aldehydes. *Synthesis* **2004,** (1), 59–62.

129) Seyferth, D.; Marmor, R. S., Dimethyl diazomethylphosphonate: its preparation and reactions. *Tetrahedron Lett.* **1970,** *11* (28), 2493–2496.

130) Gilbert, J. C.; Weerasooriya, U., Elaboration of aldehydes and ketones to alkynes: improved methodology. *The Journal of Organic Chemistry* **1979,** *44* (26), 4997–4998.

131) Murata, S.; Iwamura, H., Magnetic interaction between the triplet centers in ethynylenebis(phenylnitrenes) and 1,3-butadiyne-1,4-diylbis(phenylnitrenes). *J. Am. Chem. Soc.* **1991,** *113* (15), 5547–5556.

132) Stephens, R. D.; Castro, C. E., The substitution of aryl iodides with cuprous acetylides. A synthesis of tolanes and heterocyclics. *J. Org. Chem.* **1963,** *28* (12), 3313–3315.

133) Chanteau, S. H.; Tour, J. M., Synthesis of potential molecular electronic devices containing pyridine units. *Tetrahedron Lett.* **2001,** *42* (17), 3057–3060.

134) Durley, R. C.; Grapperhaus, M. L.; Hickory, B. S.; Massa, M. A.; Wang, J. L.; Spangler, D. P.; Mischke, D. A.; Parnas, B. L.; Fobian, Y. M.; Rath, N. P.; Honda, D. D.; Zeng, M.; Connolly, D. T.; Heuvelman, D. M.; Witherbee, B. J.; Melton, M. A.; Glenn, K. C.; Krul, E. S.; Smith, M. E.; Sikorski, J. A., Chiral *N,N*-disubstituted trifluoro-3-amino-2-propanols are potent inhibitors of cholesteryl ester transfer protein. *J. Med. Chem.* **2002,** *45* (18), 3891–3904.

135) Ahn, S. I.; Sei, Y. J.; Park, H.-J.; Kim, J.; Ryu, Y.; Choi, J. J.; Sung, H.-J.; MacDonald, T. J.; Levey, A. I.; Kim, Y., Microengineered human blood–brain barrier platform for understanding nanoparticle transport mechanisms. *Nat. Commun.* **2020,** *11* (1), 175.

136) Lu, T. M.; Houghton, S.; Magdeldin, T.; Durán, J. G. B.; Minotti, A. P.; Snead, A.; Sproul, A.; Nguyen, D.-H. T.; Xiang, J.; Fine, H. A.; Rosenwaks, Z.; Studer, L.; Rafii, S.; Agalliu, D.; Redmond, D.; Lis, R., Pluripotent stem cell-derived epithelium misidentified as brain microvascular endothelium requires ETS factors to acquire vascular fate. *Proc. Natl. Acad. Sci. U. S. A.* **2021,** *118* (8), e2016950118.

137) Kovarik, Z.; Maček Hrvat, N., Efficient detoxification of nerve agents by oxime-assisted reactivation of acetylcholinesterase mutants. *Neuropharmacology* **2020,** *171*, 108111.

138) Cheung, J.; Rudolph, M. J.; Burshteyn, F.; Cassidy, M. S.; Gary, E. N.; Love, J.; Franklin, M. C.; Height, J. J., Structures of human acetylcholinesterase in complex with pharmacologically important ligands. *J. Med. Chem.* **2012,** *55* (22), 10282–10286.

139) Bourne, Y.; Grassi, J.; Bougis, P. E.; Marchot, P., Conformational flexibility of the acetylcholinesterase tetramer suggested by X-ray crystallography. *J. Biol. Chem.* **1999,** *274* (43), 30370–30376.

140) Katz, F. S.; Pecic, S.; Tran, T. H.; Trakht, I.; Schneider, L.; Zhu, Z.; Ton-That, L.; Luzac, M.; Zlatanic, V.; Damera, S.; Macdonald, J.; Landry, D. W.; Tong, L.; Stojanovic, M. N., Discovery of new classes of compounds that reactivate acetylcholinesterase inhibited by organophosphates. *ChemBioChem* **2015,** *16* (15), 2205–2215.

141) Dvir, H.; Jiang, H. L.; Wong, D. M.; Harel, M.; Chetrit, M.; He, X. C.; Jin, G. Y.; Yu, G. L.; Tang, X. C.; Silman, I.; Bai, D. L.; Sussman, J. L., X-ray structures of *Torpedo californica* acetylcholinesterase complexed with (+)-Huperzine A and (-)-huperzine B: Structural evidence for an active site rearrangement. *Biochemistry* **2002,** *41* (35), 10810–10818.

142) Kellogg, G. E.; Abraham, D. J., KEY, LOCK, and LOCKSMITH: Complementary hydropathic map predictions of drug structure from a known receptor-receptor structure from known drugs. *Journal of Molecular Graphics* **1992,** *10* (4), 212–217.

143) Kellogg, G. E.; Semus, S. F.; Abraham, D. J., HINT: A new method of empirical hydrophobic field calculation for CoMFA. *Journal of Computer-Aided Molecular Design* **1991,** *5* (6), 545–552.

144) Kellogg, G. E., HINT, 2.01; eduSoft: Ashland, VA, 1993.

145) Leo, A.; Hansch, C., *Substituent constants for correlation analysis in chemistry and biology*. John Wiley & Sons: 1979.

146) Shrake, A.; Rupley, J. A., Environment and exposure to solvent of protein atoms. Lysozyme and insulin. *J. Mol. Biol.* **1973,** *79* (2), 351–371.

147) Tanga, M. J.; Bupp, J. E.; Tochimoto, T. K., Syntheses of five potential heterocyclic amine food mutagens. *J. Heterocycl. Chem.* **1997,** *34* (3), 717–727.

148) Krinochkin, A. P.; Kopchuk, D. S.; Chepchugov, N. V.; Kovalev, I. S.; Zyryanov, G. V.; Rusinov, V. L.; Chupakhin, O. N., Effect of substituent in pyridine-2-carbaldehydes on their heterocyclization to 1,2,4-triazines and 1,2,4-triazine 4-oxides. *Russ. J. Org. Chem.* **2017,** *53* (7), 963–970.

149) Jones, R. C.; Canty, A. J.; Deverell, J. A.; Gardiner, M. G.; Guijt, R. M.; Rodemann, T.; Smith, J. A.; Tolhurst, V.-A., Supported palladium catalysis using a heteroleptic 2-methylthiomethylpyridine–*N,S*–donor motif for Mizoroki–Heck and Suzuki–Miyaura coupling, including continuous organic monolith in capillary microscale flow-through mode. *Tetrahedron* **2009,** *65* (36), 7474–7481.

150) Walter, E. R. H.; Williams, J. A. G.; Parker, D., Solvent polarity and oxygen sensitivity, rather than viscosity, determine lifetimes of biaryl-sensitised terbium luminescence. *Chem. Commun.* **2017,** *53* (100), 13344–13347.

151) Charoensutthivarakul, S.; David Hong, W.; Leung, S. C.; Gibbons, P. D.; Bedingfield, P. T. P.; Nixon, G. L.; Lawrenson, A. S.; Berry, N. G.; Ward, S. A.; Biagini, G. A.; O'Neill, P. M., 2-Pyridylquinolone antimalarials with improved antimalarial activity and physicochemical properties. *MedChemComm* **2015,** *6* (7), 1252–1259.

152) Cren, S.; Rueedi, G.; Zumbrunn, C. Preparation of antibacterial oxetane-3-yloxy substituted biaromatic derivatives. 2017.

153) Liu, Y.; Kim, J.; Seo, H.; Park, S.; Chae, J., Copper(II)-catalyzed single-step synthesis of aryl thiols from aryl halides and 1,2-ethanedithiol. *Adv. Synth. Catal.* **2015,** *357* (10), 2205–2212.

154) Ghosh, Arun K.; Bischoff, A.; Cappiello, J., Asymmetric total synthesis of the gastroprotective microbial agent AI-77-B. *Eur. J. Org. Chem.* **2003,** *2003* (5), 821–832.

155) Cloutier, M.; Roudias, M.; Paquin, J.-F., Regioselective gold-catalyzed hydration of CF_3- and SF_5-alkynes. *Org. Lett.* **2019,** *21* (10), 3866–3870.

156) Egbertson, M.; McGaughey, G. B.; Pitzenberger, S. M.; Stauffer, S. R.; Coburn, C. A.; Stachel, S. J.; Yang, W.; Barrow, J. C.; Neilson, L. A.; McWherter, M.; Perlow, D.; Fahr, B.; Munshi, S.; Allison, T. J.; Holloway, K.; Selnick, H. G.; Yang, Z.; Swestock, J.; Simon, A. J.; Sankaranarayanan, S.; Colussi, D.; Tugusheva, K.; Lai, M.-T.; Pietrak, B.; Haugabook, S.; Jin, L.; Chen, I. W.; Holahan, M.; Stranieri-Michener, M.; Cook, J. J.; Vacca, J.; Graham, S. L., Methyl-substitution of an iminohydantoin spiropiperidine β-secretase (BACE-1) inhibitor has a profound effect on its potency. *Bioorg. Med. Chem. Lett.* **2015,** *25* (21), 4812–4819.

157) Katsumata, T.; Shiotsuki, M.; Sanda, F.; Sauvage, X.; Delaude, L.; Masuda, T., Polymerization of ortho-substituted phenylacetylenes with well-defined ruthenium-alkylidene catalysts and related metathesis initiators. *Macromol. Chem. Phys.* **2009,** *210* (22), 1891–1902.

158) Keenan, M.; Abbott, M. J.; Alexander, P. W.; Armstrong, T.; Best, W. M.; Berven, B.; Botero, A.; Chaplin, J. H.; Charman, S. A.; Chatelain, E.; von Geldern, T. W.; Kerfoot, M.; Khong, A.; Nguyen, T.; McManus, J. D.; Morizzi, J.; Ryan, E.; Scandale, I.; Thompson, R. A.; Wang, S. Z.; White, K. L., Analogues of fenarimol are potent inhibitors of *Trypanosoma cruzi* and are efficacious in a murine model of Chagas disease. *J. Med. Chem.* **2012,** *55* (9), 4189–4204.